THE 68TH INTERNATIONAL

CONFERENCE FOR STUDENTS OF PHYSICS AND NATURAL SCIENCES

OPEN READINGS

BOOK OF ABSTRACTS | 2025

Vilnius University

VILNIUS UNIVERSITY PRESS

Editors:

Rimantas Naina
Vincentas Adomaitis
Emilijus Maskvytis
Mykolas Žemaitis
Jokūbas Mačiulis
Tautvydas Kairys

Cover and Interior Design:

Goda Grybauskaitė

Vilnius University Press
9 Saulėtekio Av., III Building, LT-10222 Vilnius
info@leidykla.vu.lt, www.leidykla.vu.lt/en/
www.knygynas.vu.lt, www.journals.vu.lt

Bibliographic information is available
on the Lithuanian Integral Library Information System (LIBIS) portal ibiblioteka.lt
ISSN 3030-2463

© Vilnius University, 2025

Dear Participant,

Welcome to the 68th International Conference for Students of Physics and Natural Sciences — Open Readings 2025!

The Open Readings 2025 organizing committee is proud to welcome not only students, but also accomplished scientists from around the world. This conference provides an exceptional platform for you to grow as a researcher by sharing your work, exchanging ideas, and connecting with fellow scientists.

This year's programme features lectures by world-renowned scientists covering a wide array of topics, along with presentations from passionate young researchers like yourselves. We are confident that the conference will offer an enriching and memorable experience.

We encourage you to approach this opportunity with curiosity and creativity. By doing so, you contribute to the spirit of collaboration that drives scientific progress and helps shape a brighter future.

We wish you the best of luck on your scientific journey. May Open Readings 2025 inspire you to carry curiosity and innovation with you throughout your life and career.

Sincerely,
The Open Readings Organizing Committee



Conference Chair

Goda Grybauskaitė, *Faculty of Physics, Vilnius University, SPIE Chapter of Vilnius University*

Organizing Committee

Martynas Keršys, *Faculty of Physics, Vilnius University, SPIE Chapter of Vilnius University*

Eimantas Urniežius, *Faculty of Physics, Vilnius University*

Justas Norkus, *Faculty of Physics, Vilnius University*

Džiugas Krencius, *Faculty of Physics, Vilnius University*

Dominykas Augulis, *Faculty of Physics, Vilnius University*

Goda Mažeikaitė, *Faculty of Physics, Vilnius University, SPIE Chapter of Vilnius University*

Deimantė Juknevičiūtė, *Faculty of Physics, Vilnius University*

Smiltė Gibavičūtė, *Faculty of Physics, Vilnius University*

Laura Grizickaitė, *Faculty of Philology, Vilnius University*

Liudvikas Šegžda, *Faculty of Physics, Vilnius University*

Ieva Rimkevičiūtė, *Faculty of Physics, Vilnius University*

Tautvydas Kairys, *Faculty of Physics, Vilnius University*

Agnė Schoroškaitė, *Faculty of Physics, Vilnius University*

Amelija Rupkutė, *Faculty of Physics, Vilnius University*

Kristupas Bagdonas, *Faculty of Physics, Vilnius University, SPIE Chapter of Vilnius University*

Paulius Daraška, *Faculty of Physics, Vilnius University*

Dominykas Mačiulaitis, *Faculty of Physics, Vilnius University*

Atėnė Dovydėnaitė, *Faculty of Physics, Vilnius University*

Teresė Kreišmonaitė, *Faculty of Physics, Vilnius University, SPIE Chapter of Vilnius University*

Augustas Pupinas, *Faculty of Physics, Vilnius University*

Tomas Latvaitis, *Faculty of Physics, Vilnius University*

Daniel Rodz, *Faculty of Physics, Vilnius University*

Aurėja Ertmanaitė, *Faculty of Physics, Vilnius University*

Ignas Dailidėnas, *Faculty of Physics, Vilnius University, SPIE Chapter of Vilnius University*

Akvilė Sukauskaitė, *Faculty of Physics, Vilnius University*

Vincentas Adomaitis, *Faculty of Physics, Vilnius University, SPIE Chapter of Vilnius University*

Rimantas Naina, *Faculty of Physics, Vilnius University, SPIE Chapter of Vilnius University*

Mykolas Vaitilas, *Faculty of Physics, Vilnius University*

Mykolas Žemaitis, *Faculty of Physics, Vilnius University*

Emilijus Maskvytis, *Faculty of Physics, Vilnius University*

Dovydas Žiūra, *Faculty of Physics, Vilnius University*

Jokūbas Mačiulis, *Faculty of Physics, Vilnius University*

Povilas Užtupys, *Faculty of Physics, Vilnius University*

Pranas Grybauskas, *Life Sciences Center, Vilnius University*

Titas Gagilas, *Faculty of Fundamental Sciences, Vilnius Tech*

Mantas Krejaras, *Faculty of Electronics, Vilnius Tech*

Giedrius Puidokas, *Faculty of Physics, Vilnius University*

Chairmen

Balys Momgaudis, *Laser Research Center, Faculty of Physics, Vilnius University*

Tomas Grinys, *Institute of Photonics and Nanotechnology, Faculty of Physics, Vilnius University*

Julius Vengelis, *Laser Research Center, Faculty of Physics, Vilnius University*

Tadas Malinauskas, *Institute of Photonics and Nanotechnology, Faculty of Physics, Vilnius University*

Arnas Drazdauskas, *Institute of Theoretical Physics and Astronomy, Faculty of Physics, Vilnius University*

Edita Palaimienė, *Institute of Applied Electrodynamics and Telecommunications, Faculty of Physics, Vilnius University*

Aleksejus Kononovičius, *Institute of Theoretical Physics and Astronomy, Faculty of Physics, Vilnius University*

Justinas Jorudas, *Department of Optoelectronics, Center for Physical Sciences and Technology*

Antanas Zinovičius, *Department of Mechatronics, Robotics and Digital Manufacturing, Faculty of Mechanics, Vilnius Tech*

Aistė Zentelytė, *Institute of Biochemistry, Life Sciences Center, Vilnius University*

Saulius Klimašauskas, *Institute of Biotechnology, Life Sciences Center, Vilnius University*

Tadas Matijošius, *Department of Chemical Engineering and Technology, Center for Physical Sciences and Technology*

Dovilė Lengvinaitė, *Institute of Chemical Physics, Faculty of Physics, Vilnius University*

Gintautas Bagdžiūnas, *Institute of Biochemistry, Life Sciences Center, Vilnius University*

Irmantas Kašalynas, *Institute of Applied Electrodynamics and Telecommunications, Faculty of Physics, Vilnius University*

Marius Navickas, *Laser Research Center, Faculty of Physics, Vilnius University*

Lina Grinevičiūtė, *Department of Laser Technologies, Center for Physical Sciences and Technology*

Mikas Vengris, *Laser Research Center, Faculty of Physics, Vilnius University*

Algirdas Mekys, *Institute of Photonics and Nanotechnology, Faculty of Physics, Vilnius University*

Rolandas Tamošiūnas, *Institute of Photonics and Nanotechnology, Faculty of Physics, Vilnius University*

Saulius Miasojedovas, *Institute of Photonics and Nanotechnology, Faculty of Physics, Vilnius University*

Tomas Serevičius, *Institute of Photonics and Nanotechnology, Faculty of Physics, Vilnius University*

Dovydas Banevičius, *Institute of Photonics and Nanotechnology, Faculty of Physics, Vilnius University*

Rokas Žalnėravičius, *Department of Electrochemical Material Science, Center for Physical Sciences and Technology*

Kristijonas Genevičius, *Institute of Chemical Physics, Faculty of Physics, Vilnius University*

Artūras Katelnikovas, *Department of Physical Chemistry, Faculty of Chemistry and Geosciences, Vilnius University*

Dominykas Augulis, *Institute of Photonics and Nanotechnology, Faculty of Physics, Vilnius University*

Tomas Šalkus, *Institute of Applied Electrodynamics and Telecommunications, Faculty of Physics, Vilnius University*

Virginija Dudutienė, *Institute of Biotechnology, Life Sciences Center, Vilnius University*

Žydrūnas Podlipskas, *Institute of Photonics and Nanotechnology, Faculty of Physics, Vilnius University*

Jevgenij Chmeliov, *Institute of Chemical Physics, Faculty of Physics, Vilnius University*

Viktorija Tamulienė, *Laser Research Center, Faculty of Physics, Vilnius University*

Viktoras Masevičius, *Department of Organic Chemistry, Faculty of Chemistry and Geosciences, Vilnius University*

Rimantė Bandzevičiūtė, *Institute of Chemical Physics, Faculty of Physics, Vilnius University*

Steponas Raišys, *Institute of Photonics and Nanotechnology, Faculty of Physics, Vilnius University*

Brigita Abakevičienė, *Institute of Materials Science, Faculty of Mathematics and Natural Sciences, Kaunas University of Technology*

Saulius Bagdonas, *Laser Research Center, Faculty of Physics, Vilnius University*

Lena Golubewa, *Department of Molecular Compound Physics, Center for Physical Sciences and Technology*

Laurynas Dagys, *Institute of Chemical Physics, Faculty of Physics, Vilnius University*

Vytautas Klimavičius, *Institute of Chemical Physics, Faculty of Physics, Vilnius University*

Gerda Jasinevičienė, *Life Sciences Center, Vilnius University*

Marija Ger, *Institute of Biochemistry, Life Sciences Center, Vilnius University*

Marius Butkevičius, *Institute of Biochemistry, Life Sciences Center, Vilnius University*

Gytis Sliaužys, *Institute of Chemical Physics, Faculty of Physics, Vilnius University*

Vaidas Pačebutas, *Department of Optoelectronics, Center for Physical Sciences and Technology*

Veronika Borutinskaite, *Institute of Biochemistry, Life Sciences Center, Vilnius University*

Eglė Lastauskienė, *Institute of Biosciences, Life Sciences Center, Vilnius University*

Rūta Kananavičiūtė, *Institute of Biosciences, Life Sciences Center, Vilnius University*

Irina Buchovec, *Institute of Photonics and Nanotechnology, Faculty of Physics, Vilnius University*

Eimina Dirvelytė, *Institute of Biosciences, Life Sciences Center, Vilnius University*

Neringa Daugelavičienė, *EMBL Partnership Institute, Life Sciences Center, Vilnius University*

Aidas Alaburda, *Institute of Biosciences, Life Sciences Center, Vilnius University*

Mindaugas Zaremba, *Institute of Biotechnology, Life Sciences Center, Vilnius University*

Algirdas Mikalkėnas, *Institute of Biosciences, Life Sciences Centre, Vilnius University*

Neda Jonutytė-Trembo, *Department of Microbiology and Biotechnology, Life Sciences Center, Vilnius University*

Eglė Balčiūnaitė, *Laboratory of Molecular Oncology, National Cancer Institute*

Nina Urbelienė, *Institute of Biochemistry, Life Sciences Center, Vilnius University*

Gabrielė Vasiliauskaitė, *Department of Neurobiology and Biophysics, Life Science Center, Vilnius University*

Lina Davulienė, *Department of Environmental Research, Center for Physical Sciences and Technology*

Ieva Žutautė, *Department of Organic Chemistry, Faculty of Chemistry and Geosciences, Vilnius University*

Rita Bukšnaitienė, *Department of Organic Chemistry, Faculty of Chemistry and Geosciences, Vilnius University*

Virginija Kepeniene, *Department of Catalysis, Center for Physical Sciences and Technology*

Danielis Rutkauskas, *Department of Molecular Compound Physics, Center for Physical Sciences and Technology*

Steigvilė Byčenkienė, *Department of Environmental Research, Center for Physical Sciences and Technology*

Ramūnas Levinas, *Department of Catalysis, Center for Physical Sciences and Technology*

Edita Voitechovič, *Department of Nanoengineering, Center for Physical Sciences and Technology*

Vilmantas Pupkis, *Department of Neurobiology and Biophysics, Life Science Center, Vilnius University*

Rasa Pauliukaitė, *Department of Nanoengineering, Center for Physical Sciences and Technology*

Gražina Petraitytė, *Department of Organic Chemistry, Faculty of Chemistry and Geosciences, Vilnius University*

Dovydas Karoblis, *Department of Inorganic Chemistry, Faculty of Chemistry and Geosciences, Vilnius University*

Milita Vagner, *Department of Inorganic Chemistry, Faculty of Chemistry and Geosciences, Vilnius University*

Albinas Žilinskas, *Institute of Chemistry, Faculty of Chemistry and Geosciences, Vilnius University*

Jelena Dodonova - Vaitkūnienė, *Department of Organic Chemistry, Faculty of Chemistry and Geosciences, Vilnius University*

Edvinas Orentas, *Department of Organic Chemistry, Faculty of Chemistry and Geosciences, Vilnius University*

Renata Butkutė, *Institute of Photonics and Nanotechnology, Faculty of Physics, Vilnius University*

Jokūbas Pimpė, *Laser Research Center, Faculty of Physics, Vilnius University*

Simonas Draukšas, *Institute of Theoretical Physics and Astronomy, Faculty of Physics, Vilnius University*

Jonas Žmuidzinas, *California Institute of Technology, USA*

Programme Committee

Andrius Gelžinis, *Institute of Chemical Physics, Faculty of Physics, Vilnius University*

Andrius Žemaitis, *Department of Laser Technologies, Center for Physical Sciences and Technology*

Brigita Abakevičienė, *Institute of Materials Science, Faculty of Mathematics and Natural Sciences, Kaunas University of Technology*

Danielis Rutkauskas, *Department of Molecular Compound Physics, Center for Physical Sciences and Technology*

Dovydas Banevičius, *Institute of Photonics and Nanotechnology, Faculty of Physics, Vilnius University*

Erikas Atkočaitis, *Laser Research Center, Faculty of Physics, Vilnius University*

Julius Vengelis, *Laser Research Center, Faculty of Physics, Vilnius University*

Kristijonas Genevičius, *Institute of Chemical Physics, Faculty of Physics, Vilnius University*

Laimonas Deveikis, *Institute of Photonics and Nanotechnology, Faculty of Physics, Vilnius University*

Linas Vilčiauskas, *Department of Chemical Engineering and Technology, Center for Physical Sciences and Technology*

Markus Ambrosh, *Institute of Theoretical Physics and Astronomy, Faculty of Physics, Vilnius University*

Mažena Mackoit-Sinkevičienė, *Institute of Theoretical Physics and Astronomy, Faculty of Physics, Vilnius University*

Mindaugas Kamarauskas, *Institute of Chemical Physics, Faculty of Physics, Vilnius University*

Rimantė Bandzevičiūtė, *Institute of Chemical Physics, Faculty of Physics, Vilnius University*

Sergėjus Balčiūnas, *Institute of Applied Electrodynamics and Telecommunications, Faculty of Physics, Vilnius University*

Steponas Raišys, *Institute of Photonics and Nanotechnology, Faculty of Physics, Vilnius University*

Tadas Malinauskas, *Institute of Photonics and Nanotechnology, Faculty of Physics, Vilnius University*

Tomas Čeponis, *Institute of Photonics and Nanotechnology, Faculty of Physics, Vilnius University*

Tomas Šalkus, *Institute of Applied Electrodynamics and Telecommunications, Faculty of Physics, Vilnius University*

Tomas Serevičius, *Institute of Photonics and Nanotechnology, Faculty of Physics, Vilnius University*

Tomas Tamulevičius, *Institute of Materials Science, Faculty of Mathematics and Natural Sciences, Kaunas University of Technology*

Vytautas Klimavičius, *Institute of Chemical Physics, Faculty of Physics, Vilnius University*

Dominykas Augulis, *Institute of Photonics and Nanotechnology, Faculty of Physics, Vilnius University*

Aldona Balčiūnaitė, *Department of Optoelectronics, Center for Physical Sciences and Technology*

Algirdas Mikalkėnas, *Institute of Biosciences, Life Sciences Centre, Vilnius University*

Edvinas Orentas, *Department of Organic Chemistry, Faculty of Chemistry and Geosciences, Vilnius University*

Ieva Matulaitienė, *Department of Organic Chemistry, Center for Physical Sciences and Technology*

Ilja Ignatjev, *Department of Organic Chemistry, Center for Physical Sciences and Technology*

Jurga Būdienė, *Department of Organic Chemistry, Center for Physical Sciences and Technology*

Jurga Juodkazytė, *Department of Chemical Engineering and Technology, Center for Physical Sciences and Technology*

Artūras Katelnikovas, *Institute of Chemistry, Faculty of Chemistry and Geosciences, Vilnius University*

Agnė Kalnaitytė-Vengelienė, *Laser Research Center, Faculty of Physics, Vilnius University*

Aistė Zentelytė, *Institute of Biochemistry, Life Sciences Center, Vilnius University*

Enrika Celitan, *Department of Biochemistry and Molecular Biology, Life Sciences Center, Vilnius University*

Ieva Uogintė, *Department of Environmental Research, SRI Center for Physical Sciences and Technology*

Irena Nedveckytė, *Institute of Biosciences, Life Sciences Centre, Vilnius University*

Irina Buchovec, *Institute of Photonics and Nanotechnology, Faculty of Physics, Vilnius University*

Nina Urbelienė, *Institute of Biochemistry, Life Sciences Center, Vilnius University*

Rūta Kananavičiūtė, *Department of Microbiology and Biotechnology, Life Sciences Centre, Vilnius University*

Veronika Borutinskaite, *Institute of Biochemistry, Life Sciences Center, Vilnius University*

Virginija Kalcienė, *Institute of Biosciences, Life Sciences Center, Vilnius University*

Lena Golubewa, *Department of Molecular Compound Physics, Center for Physical Sciences and Technology*

Laima Čepulytė, *Institute of Biotechnology, Life Sciences Center, Vilnius University*

Gerda Jasinevičienė, *Life Sciences Center, Vilnius University*

Eimina Dirvelytė, *Institute of Biosciences, Life Sciences Center, Vilnius University*

Neringa Daugelavičienė, *EMBL Partnership Institute, Life Sciences Center, Vilnius University*

Simonas Kutanovas, *EMBL Partnership Institute, Life Sciences Center, Vilnius University*

68TH INTERNATIONAL

CONFERENCE FOR STUDENTS OF PHYSICS AND NATURAL SCIENCES

OPEN READINGS 2025

DAY 1 (2025-05-13)

Room: A101 — Opening Ceremony — **9:00-9:15**

Break — **9:15-9:30**

Room: A101 — **ORAL SESSION: O1** — **9:30-10:45**

Laser Physics and Optical Technologies

9:30 Dainius Ratkus: FEMTOSECOND LASER POLISHING AND ABLATION OF SILICON CARBIDE WAFERS
9:45 Saulė Petrauskaitė: UPSCALING AND THE OPTIMIZATION OF ACRYLIC RESINS FOR LASER FABRICATION OF LOW-DENSITY 3D MICROSTRUCTURES
10:00 Tadas Latvys: OPTIMIZED TALBOT INTERFEROMETER DESIGN FOR HIGH-PRECISION LASER INTERFERENCE PATTERNING
10:15 Ieva Baltrukonytė: EVALUATION OF VARIOUS PERIODICALLY POLED NONLINEAR CRYSTALS POLING QUALITY
10:30 Ignas Dailidėnas: OPTICAL SECOND HARMONIC GENERATION IN A PLANAR QUASI-SYMMETRICAL GaN WAVEGUIDE

Session Chair: Balys Momgaudis

Room: D401 — **ORAL SESSION: O2** — **9:30-10:45**

Material Science and Nanotechnology

9:30 Andrea Zelioli: DESIGN OF VERTICAL-EXTERNAL-CAVITY SURFACE-EMITTING LASERS FOR NIR EMISSION
9:45 Aivaras Špokas: DEVELOPMENT OF APPLICATION FOCUSED BISMUTH CONTAINING NIR ELECTRICALLY PUMPED EMITTERS
10:00 Julianija Nikitina: SUBMICRON PERIODIC STRUCTURES IN METAL OXIDE THINFILM VIA LASER ABLATION AND THERMAL OXIDATION
10:15 Helēna Ose: FABRICATION OF SUBMICRON STRUCTURES VIA DOUBLE EXPOSURE UV LITHOGRAPHY
10:30 Artūr Harnik: LASER DIRECT WRITING 3D PRINTING OF LUMINESCENT YAG:Ce MICROSTRUCTURES

Session Chair: Tomas Grinys

Coffee Break — **10:45-11:15**

Room: A101 —  — **Yuqing Jiao | PLENARY TALK** — **Integrated Nanophotonics and its Convergence with Electronics** — **11:15-12:30**

Chair: Renata Butkutė

Lunch Break — **12:30-13:15**

Room: A101 — **ORAL SESSION: O3** — **13:15-14:30**

Laser Physics and Optical Technologies

13:15 Matas Petrėnas: AMPLIFICATION AND SHAPING PECULIARITIES OF SILICON PHOTOMULTIPLIER PULSES
13:30 Augustė Černeckytė: BEYOND 3 μM: HIGH-INTENSITY FEMTOSECOND PULSES FROM OPCPA AND ROTATIONAL SRS
13:45 Ignas Lukošiūnas: THEORETICAL INVESTIGATION OF GUIDED MODE RESONANCE EFFECT IN OPTICAL GAIN CAVITIES
14:00 Tomas Latvys: INFLUENCE OF CONICAL WAVE FORMATION ON SUBNANOSECOND BACKWARD WAVE OPTICAL PARAMETRIC AMPLIFIER
14:15 Indrė Meškėlaitė: DESIGN AND OPTIMIZATION OF PARITY-TIME SYMMETRIC STRUCTURES FOR UNIDIRECTIONAL PROPAGATION OF LIGHT

Session Chair: Julius Vengelis

Room: D401 — **ORAL SESSION: O4** — **13:15-14:30**

Material Science and Nanotechnology

13:15 Aistė Štaupienė: THE EVALUATION OF PHOTOLUMINESCENCE EFFICIENCY OF GaAsBi QUANTUM WELLS
13:30 Seda Türkcan: CARRIER DYNAMICS IN InGaN MQW STRUCTURE WITH VARYING EMISSION WAVELENGTHS
13:45 Karolis Stravinskas: INFLUENCE OF SiC REINFORCEMENT ON MECHANICAL AND THERMAL PROPERTIES OF DMLS MANUFACTURED AlSi10Mg COMPOSITES
14:00 Adam Puchalski: STRAIN ENGINEERING AND FERROELECTRIC BEHAVIOR OF BaTiO3 THIN FILMS: A MOLECULAR DYNAMICS STUDY
14:15 Justina Žemgulytė: DIELECTRIC LOADED HELIX ANTENNAS

Session Chair: Tadas Malinauskas

Coffee Break — **14:30-15:00**

Room: A101 —  — **Clara Saraceno | PLENARY TALK** — **Ultrafast Lasers, Terahertz light and More** — **15:00-16:15**

Chair: Jokūbas Pimpė

Break — **16:15-16:30**

Main hall — **POSTER SESSION: P1** — **16:30-18:00**

Laser Physics and Optical Technologies,
Material Science and Nanotechnology

68TH INTERNATIONAL

CONFERENCE FOR STUDENTS OF PHYSICS AND NATURAL SCIENCES

OPEN READINGS 2025

DAY 2 (2025-05-14)

Room: A101 — **ORAL SESSION: O5** — **9:00-10:30**

Astrophysics and Astronomy

9:00 **Martynas Laužikas**: EX EFFLUXI AD ASTRA: QUANTIFYING ACTIVE GALACTIC NUCLEUS-ENHANCED STAR FORMATION
9:15 **Eimantas Skuodas**: CLEARING THE COSMIC TABLE: HOW BLACK HOLES CLEAR AWAY THEIR MEALS
9:30 **Milda Valytė**: COMPARISON OF SIMULATED AND OBSERVED GALACTIC OUTFLOWS
9:45 **Ugnė Jonauskaitė**: CHEMICAL ANALYSIS OF PLANETARY HOST STARS
10:00 **Vladas Šatas**: RECONSTRUCTION OF 3D ASTEROIDS FROM 2D IMAGES
10:15 **Simas Sviensas**: MINIATIURIZATION FEASABILITY BY USING BISMUTH AS A PROPELLANT FOR A HALL THRUSTER

Session Chair: Arnas Drazdauskas

Room: D401 — **ORAL SESSION: O6** — **9:00-10:30**

Spectroscopy and Imaging

9:00 **Gediminas Usevičius**: ELECTRON PARAMAGNETIC RESONANCE: GOING MICRO FOR MACRO GAINS
9:15 **Tautvydas Taraškevičius**: THE IMPORTANCE OF FOURIER TRANSFORM INFRARED SPECTRA PROCESSING FOR ANALYSIS OF BIOLOGICAL SAMPLES
9:30 **Rokas Lemežis**: ^{35}Cl AND ^{37}Cl SOLID-STATE NMR STUDY OF CALCIUM CHLORAPATITE
9:45 **Hasan SARIGUL**: FDTD MODELLING FOR ELECTROMAGNETIC FIELD ENHANCEMENT IN BOW-TIE ARRAY FOR SERS APPLICATIONS
10:00 **Rodrigas Liudvinavičius**: EXPLORING THE IMPACT OF MICROBUMP ARRAYDIMENSIONS ON HYBRID LATTICE PLASMON RESONANCE QUALITY
10:15 **Vita Petrikaitė**: PLASMONIC COLORS FROM THIN GOLD FILMS WITH A TITANIUM ADHESION LAYER ON A GLASS SUBSTRATE VIA NANOSECOND LASER THERMAL HEATING

Session Chair: Tomas Grinys

Coffee Break — **10:30-11:00**

Room: A101 —  **Ewine van Dishoeck | PLENARY TALK** — **Building Stars, Planets and the Ingredients for Life in Space** — **11:00-12:15**

Chair: Jonas Žmuidzinas

Lunch Break — **12:15-12:30**

Lunch Break — **12:30-13:00**

Room: A101 — **ORAL SESSION: O7** — **13:15-14:15**

Theoretical Physics

13:00 **Luka Baklaga:** JOULE-THIEF RL AGENTS: EXPLOITING AI HARDWARE THERMODYNAMICS TO UNDERMINE CRYPTOGRAPHIC SECURITY
13:15 **Alberts Bilzēns:** NUMERICAL MODELING OF COULOMB INTERACTION EFFECTS ON ELECTRON EMISSION FROM AN ELLIPTICAL QUANTUM DOT
13:30 **Dāvis Gaiziņš:** CHARACTERIZATION OF ELECTROSPUN MAGNETIC MATERIALS IN A ROTATING MAGNETIC FIELD
13:45 **Austėja Jurgaitytė:** PIXEL DETECTOR MODULE QUALITY TESTS FOR THE CMS PHASE-2 UPGRADE BACKWARD WAVE OPTICAL PARAMETRIC AMPLIFIER
14:00 **Eglė Lenkaitytė:** DRELL-YAN PROCESS STUDY USING OPEN DATA FROM THE CERN CMS EXPERIMENT

Session Chair: Aleksejus Kononovičius

Room: D401 — **ORAL SESSION: O8** — **13:15-14:15**

Spectroscopy and Imaging

13:00 **Barbora Škėlaitė:** THz SPECTRA DEPENDENCE ON FREE CARRIER CONCENTRATION IN n-GaAs/GaAs STRUCTURES WITH METASURFACES
13:15 **Ugnė Šilingaitė:** THZ IMAGING OF HIDDEN OBJECTS AND THEIR CLASSIFICATION USING NEURAL NETWORKS
13:30 **Lukas Stacevičius:** INVESTIGATION OF DIVERSE SCATTERING MATERIALS USING DIGITAL TERAHERTZ HOLOGRAPHY
13:45 **Florian Dötzer:** THEORETICAL ANALOGIES AND PRACTICAL DIFFERENCES BETWEEN IMAGING AND LENSLESS INTERFEROMETRIC METHODS
14:00 **Ignas Pocius:** MODELLING AND MICROWAVE COUPLING OF 3.1 GHz EPR RESONATORS

Session Chair: Justinas Jorudas

12:30-13:45

Workshop

'Personal Science Communication Strategy'



Goda Raibytė-Aleksa

Coffee Break — **14:15-14:45**

Room: A101 —  **Laura Šerkšnytė | PLENARY TALK** — **Searching for Antihelium in Our Galaxy from Colliders to Cosmic Ray** — **14:45-16:00**

Chair: Simonas Draukšas

Break — **16:00-16:15**

Main hall — **POSTER SESSION: P2** — **16:15-17:45**

Astrophysics and Astronomy, Theoretical Physics, Spectroscopy and Imaging, Material Science and Nanotechnology, Biochemistry, Biophysics and Biotechnology, Biology, Genetics and Biomedical Sciences, Chemistry and Chemical Physics

68TH INTERNATIONAL

CONFERENCE FOR STUDENTS OF PHYSICS AND NATURAL SCIENCES

OPEN READINGS 2025

DAY 3 (2025-05-15)

Room: A101 **ORAL SESSION: O9** **9:00-10:30**

Biochemistry, Biophysics and Biotechnology

9:00 Džiugas Sabonis: MECHANISMS OF BACTERIAL ANTIPHAGE DEFENSE BY NAD+ BASED INTRACELLULAR SIGNALS
9:15 Barbora Lekešytė: THE PORE-STABILIZING EFFECT OF NISIN WITH NANOSECOND AND MICROSECOND PULSE BURSTS FOR ELECTROCHEMOTHERAPY
9:30 Patricija Daugėlaitė: ANTIPROLIFERATIVE AND EPIGENETIC EFFECTS OF CANNABIDIOL ON ACUTE LYMPHOBLASTIC LEUKEMIA OR LYMPHOMA CELL LINES
9:45 Emilė Pečiukaitytė: DUAL NIR-EXCITABLE NANOCOMPLEX FOR EFFECTIVE PHOTODYNAMIC CANCER THERAPY
10:00 Radvilė Janušauskaitė: INVESTIGATION OF THE LINK BETWEEN ACTION POTENTIAL TRANSMISSION PROPERTIES AND THE ELECTROPHYSIOLOGICAL PARAMETERS OF TANDEM INTERNODAL CELLS OF NITELLOPSIS OBTUSA
10:15 Emīls Šmits: PHYSICS-INFORMED NEURAL NETWORKS FOR ACCURATE SHEAR STRESS MAPPING AT CELL-SUBSTRATE INTERFACES IN ORGAN-ON-A-CHIP SYSTEMS

Session Chair: Antanas Zinovičius

Room: D401 **ORAL SESSION: O10** **9:00-10:30**

Biology, Genetics and Biomedical Sciences

9:00 Karolina Matekonytė: NON-INVASIVE DETECTION OF RENAL CLEAR CELL CARCINOMA USING URINARY METHYLATED DNA AS A BIOMARKER
9:15 Enrika Baronaitė: BREAST ADENOCARCINOMA-DERIVED EXTRACELLULAR VESICLES ARE ASSOCIATED WITH CHANGES IN THE METABOLIC AND BIOENERGETIC FUNCTIONS OF CARDIOVASCULAR SYSTEM CELLS
9:30 Dainius Lukauskas: THE EFFECT OF NOVEL HYDRAZONE DERIVATIVES ON HUMAN LUNG, TRIPLE-NEGATIVE BREAST AND SKIN CANCER CELL 2D AND 3D CULTURES
9:45 Erika Girniūtė: COMPREHENSIVE CHARACTERIZATION OF ORGANOIDS FORMED FROM PATIENT-DERIVED ENDOMETRIUM FOR INFERTILITY RESEARCH
10:00 Girstautė Dabkevičiūtė: DEVELOPMENT AND CHARACTERIZATION OF HYBRID LIPOSOME-EXOSOME NANOPARTICLES FOR TARGETED DRUG DELIVERY IN GLIOBLASTOMA
10:15 Paulina Kazlauskaitė: EXPLORING THE PHYSICOCHEMICAL AND RADIOBIOLOGICAL MECHANISMS OF FLASH RADIOTHERAPY

Session Chair: Aistė Zentelytė

Coffee Break **10:30-11:00**

Room: A101  **Srirang Manohar | PLENARY TALK** **Photoacoustic Imaging: Basics, Technology and Applications in Breast Imaging** **11:00-12:15**

Chair: Saulius Bagdonas

Lunch Break **12:15-13:00**

Room: DA01 **SPECIAL EVENT** **13:15-14:30**

‘Beyond the Visible: Linking Thoughts on Light’

 **Naglis Kardelis**

Dovydas Banevičius 

 **Srirang Manohar**

Benas Ulevičius 

Chair: Laisvūnas Čekavičius

Room: D101 **ORAL SESSION: O11** **13:15-14:15**

Biochemistry, Biophysics and Biotechnology

13:00 AYODEJI AMOBONYE: VALORISATION OF WALNUT SHELL AS A SOURCE OF BIOACTIVE DERIVATIVES: IN SILICO POLYPHENOL OXIDASE INHIBITION AND TOXICITY PREDICTION
13:15 Evelina Lukaitė: ELECTROGENICITY IN PATHOGENIC BACTERIAL BIOFILMS
13:30 Edvard Romanovski: ANALYSIS OF PROTEINS POTENTIALLY INVOLVED IN β-LACTAM RESISTANCE IN OPPORTUNISTIC PATHOGEN STENOTROPHOMONAS MALTOPHILIA
13:45 Rita Banciul: ENHANCING AI-DRIVEN BIOMOLECULAR STRUCTURE PREDICTION WITH VOROMQA-AA: A NEW APPROACH TO ACCURACY ESTIMATION
14:00 Paulius Toliušis: ADAPTATION OF CROFT-SEQ FOR OFF-TARGET DETECTION OF VARIOUS GENOME EDITING TOOLS

Session Chair: Saulius Klimašauskas

Coffee Break **14:15-14:45**

Room: A101  **Zoltán Molnár | PLENARY TALK** **Altered Transient Circuits as an Underlying Cause of Cognitive Dysfunctions** **14:45-16:00**

Chair: Aidas Alabudra

Break **16:00-16:15**

Main hall **POSTER SESSION: P3** **16:15-17:45**

Biochemistry, Biophysics and Biotechnology,
Biology, Genenetics and Biomedical Sciences

68TH INTERNATIONAL

CONFERENCE FOR STUDENTS OF PHYSICS AND NATURAL SCIENCES

OPEN READINGS 2025

DAY 4 (2025-05-16)

Room: A101 — **ORAL SESSION: O12** — **9:00-10:30**

Chemistry and Chemical Physics

9:00 **Agnė Minderytė**: FESTIVE FLARES: HOW BONFIRES AND FIREWORKS SHAPE URBAN AEROSOL OPTICAL PROPERTIES
9:15 **ABDULLAH KHAN**: WHERE MICROPLASTICS MEET PEDESTRIANS: EVALUATING GREEN INFRASTRUCTURES ROLE IN REDUCING TRANSPORT-RELATED POLLUTION
9:30 **Greta Linkaitė**: ECO-FRIENDLY PRODUCTION OF BIPHASIC CALCIUM PHOSPHATE GRANULES: GYPSUM CONVERSION UNDER VARRIED SYNTHESIS CONDITIONS
9:45 **Greta Kasputė**: TRANSILATIONAL APPROACH OF MOLECULAR IMPRINTED POLYMERS INTEGRATION WITH ESSENTIAL OILS
10:00 **Daria Kuchynska**: DETERMINATION OF THE DEGREE OF POLYMERIZATION OF STARCH MODIFIED WITH CITRIC AND LACTIC ACIDS
10:15 **Anastasija Aleksandrovič**: REGENERATION OF TETHERED BILAYER LIPID MEMBRANES FOR REUSABLE BIOSENSORS

Session Chair: Tadas Matijošius

Room: D401 — **ORAL SESSION: O13** — **9:00-10:30**

Materials Science and Nanotechnology

9:15 **Paulius Buidovas**: CATALYTIC METHANE PYROLYSIS OVER CHLORIDE-DERIVED METAL CARBON-SUPPORTED CATALYSTS FOR HYDROGEN PRODUCTION
9:30 **Justas Žuvelis**: EMISSION PROPERTIES OF BISMUTH QUANTUM DOTS IN ANNEALED GaAsBi/AlAs QUANTUM WELLS
9:45 **Ilya Navitski**: MXENES-BASED ELECTROCHEMICAL SENSOR FOR QUICK AND ACCURATE DETERMINATION OF CADMIUM ION CONCENTRATIONIN AQEOUS ENVIRONMENTS
10:00 **Krzysztof Gadomski**: SYNTHESIS AND CHARACTERIZATION OF HIGHLY CONDUCTIVE NANOCRYSTALLIZED ε-$LiVOPO_4$ LIKE GLASSES
10:15 **Maria Vuin**: MODEL OF NONLINEAR PORO-VISCOELASTIC FELT MATERIAL

Session Chair: Dovilė Lengvinaitė

Coffee Break — **10:30-11:00**

Room: A101



Rodolphe Jazzar | PLENARY TALK

Carbon Unleashed: These Carbenes Revolutionizing Material Science and Catalysis

11:00-12:15

Chair: Edvinas Orentas

Lunch Break — **12:15-13:00**

Room: A101 — **ORAL SESSION: O14** — **13:00-14:15**

Chemistry and Chemical Physics

13:00 **Ivan Halimski**: CONCENTRATION QUENCHING OF FLUORESCENCE IN DIFFERENT MOLECULAR SYSTEMS: SIMILARITIES AND DIFFERENCES
13:15 **Sonata Pleskytė**: INFLUENCE OF MICROPLASTIC FILM SIZE ON PHOTOCATALYTIC DEGRADATION OF LDPE USING Ag-TiO_2 NANOMATERIALS
13:30 **Skirmantas Musteikis**: SYNTHESIS AND INVESTIGATION OF CARBAZOLE AND PHENOXAZINE ORGANIC SEMICONDUCTORS
13:45 **Amina Elkady**: MODELING THE STRUCTURE AND NMR SPECTRA OF AMANTADINE ENCAPSULATED IN SUPRAMOLECULAR MATRICES
14:00 **Gabrielė Rankelytė**: IMPACT OF PROTEIN GEOMETRY AND PROTONATION PATTERN ON THE EXCITED STATES OF PIGMENTS IN PHOTOSYNTHETIC COMPLEXES

Session Chair: Gintautas Bagdžiūnas

Room: D401 — **ORAL SESSION: O15** — **13:00-14:15**

Materials Science and Nanotechnology

13:00 **Titas Klepeckas**: ACCEPTOR AGGREGATION IN PM6:Y6 ORGANIC SOLAR CELL BLENDS REVEALED BY SPECTRAL DECOMPOSITION
13:15 **Noor ul ain ahmed**: COMPARATIVE CONDUCTIVITY ANALYSIS OF TRANSPARENT ELECTRODES FOR SOLAR CELLS
13:30 **Daniel Rodz**: SPECTRAL PROPERTIES OF YTTERBIUM SPECIES IN DOPED CESIUM LEAD HALIDE PEROVSKITES
13:45 **Paula Baltaševičiūtė**: CHARGE CARRIER MIGRATION IN 2D/3D PEROVSKITES
14:00 **Zofia Dziekan**: LIQUID CRYSTAL ELASTOMER MICROSCTRUCTURES WITH TUNABLE OPTOMECHANICAL PROPERTIES

Session Chair: Irmantas Kašalynas

Coffee Break — **14:15-14:45**

Room: A101



Ričardas Rotomskis
INTERNATIONAL DAY OF LIGHT SPECIAL LECTURE

Biophotonics at the Faculty of Physics: from Laser Flash to Cancer Theranostic Nanotechnologies

14:45-15:45

Main hall — **POSTER SESSION: P4** — **15:45-17:15**

Chemistry and Chemical Physics

Break — **17:15-17:30**

Room: A101 — **Closing Remarks and Awards** — **17:30-18:15**

Contents

Invited Speakers 41

INTEGRATED NANOPHOTONICS AND ITS CONVERGENCE WITH ELECTRONICS
Yuqing Jiao 42

ULTRAFAST LASERS, TERAHERTZ LIGHT AND MORE
Clara Saraceno 43

BUILDING STARS, PLANETS AND THE INGREDIENTS FOR LIFE IN SPACE
Ewine van Dishoeck 44

SEARCHING FOR ANTIHELIUM IN OUR GALAXY: FROM COLLIDERS TO COSMIC RAY DETECTORS
Laura Šerkšnytė 45

PHOTOACOUSTIC IMAGING: BASICS, TECHNOLOGY AND APPLICATIONS IN BREAST IMAGING
Srirang Manohar 46

ALTERED TRANSIENT CIRCUITS AS AN UNDERLYING CAUSE OF COGNITIVE DYSFUNCTIONS
Zoltán Molnár 47

CARBON UNLEASHED: THESE CARBENES REVOLUTIONIZING MATERIAL SCIENCE AND CATALYSIS
Rodolphe Jazzar 49

Oral Session 1: Laser Physics and Optical Technologies 50

O1-1 FEMTOSECOND LASER POLISHING AND ABLATION OF SILICON CARBIDE WAFERS
Dainius Ratkus, Andrius Žemaitis 51

O1-2 UPSCALING AND THE OPTIMIZATION OF ACRYLIC RESINS FOR LASER FABRICATION OF LOW-DENSITY 3D MICROSTRUCTURES
Saulė Petrauskaitė, Dimitra Ladika, Ioanna Angeliki Petsi, Mangirdas Malinauskas 52

O1-3 OPTIMIZED TALBOT INTERFEROMETER DESIGN FOR HIGH-PRECISION LASER INTERFERENCE PATTERNING
Tadas Latvys, Vytautas Jukna, Darius Gailevičius, Dominyka Stonytė, Domas Paipulas 53

O1-4 EVALUATION OF VARIOUS PERIODICALLY POLED NONLINEAR CRYSTALS POLING QUALITY
Ieva Baltrukonytė, Jokūbas Pimpė, Julius Vengelis 54

O1-5 OPTICAL SECOND HARMONIC GENERATION IN A PLANAR QUASI-SYMMETRICAL GaN WAVEGUIDE STRUCTURE
Ignas Dailidėnas, Roland Tomašiūnas 55

Oral Session 2: Material Science and Nanotechnology 56

O2-1 DESIGN OF VERTICAL-EXTERNAL-CAVITY SURFACE-EMITTING LASERS FOR NIR EMISSION
Andrea Zelioli, Aivaras Špokas, Aistė Štaupienė, Martynas Talaikis, Martynas Skapas, Darius Gailevičius, Artūras Suchodolskis, Aurimas Čerškus, Sandra Stanionytė, Augustas Vaitkevičius, Bronislovas Čechavičius, Evelina Dudutienė, Renata Butkutė 57

O2-2 DEVELOPMENT OF APPLICATION FOCUSED BISMUTH CONTAINING NIR ELECTRICALLY PUMPED EMITTERS
Aivaras Špokas, Andrea Zelioli, Augustas Vaitkevičius, Bronislovas Čechavičius, Evelina Dudutienė, Andrius Bičiūnas, Virginijus Bukauskas, Mindaugas Kamarauskas, Renata Butkutė 58

O2-3 SUBMICRON PERIODIC STRUCTURES IN METAL OXIDE THINFILM VIA LASER ABLATION AND THERMAL OXIDATION
Julianija Nikitina, Simonas Indrišiūnas, Tomas Tolenis, Mindaugas Andrulevičius, Lina Grinevičiūtė . . 59

O2-4 FABRICATION OF SUBMICRON STRUCTURES VIA DOUBLE EXPOSURE UV LITHOGRAPHY
Helena Ose, Edvins Letko 60

O2-5 LASER DIRECT WRITING 3D PRINTING OF LUMINESCENT YAG:Ce MICROSTRUCTURES
A. Harnik, R. Virkėtis, D. Dapšys, D. Ladika, G. Merkininkaitė, S. Šakirzanovas, M. Malinauskas 61

Oral Session 3: Laser Physics and Optical Technologies 62

O3-2 BEYOND 3 µM: HIGH-INTENSITY FEMTOSECOND PULSES FROM OPCPA AND ROTATIONAL SRS
Augustė Černeckytė, Paulius Mackonis, Aleksej Rodin 63

O3-3 THEORETICAL INVESTIGATION OF GUIDED MODE RESONANCE EFFECT IN OPTICAL GAIN CAVITIES
Ignas Lukosiunas, Kestutis Staliunas 64

O3-4 INFLUENCE OF CONICAL WAVE FORMATION ON SUBNANOSECOND BACKWARD WAVE OPTICAL PARAMETRIC AMPLIFIER
Tomas Latvys, Viktorija Tamulienė 65

O3-5 DESIGN AND OPTIMIZATION OF PARITY-TIME SYMMETRIC STRUCTURES FOR UNIDIRECTIONAL PROPAGATION OF LIGHT
Indre Meskelaite, Kestutis Staliunas, Darius Gailevicius 66

Oral Session 4: Material Science and Nanotechnology 67

O4-1 THE EVALUATION OF PHOTOLUMINESCENCE EFFICIENCY OF GaAsBi QUANTUM WELLS
Aistė Štaupienė, Andrea Zelioli, Aivaras Špokas, Bronislovas Čechavičius, Renata Butkutė, Evelina Dudutienė 68

O4-2 CARRIER DYNAMICS IN InGaN MQW STRUCTURE WITH VARYING EMISSION WAVELENGTHS
Seda Türkcan, Kazimieras Nomeika 69

O4-3 INFLUENCE OF SiC REINFORCEMENT ON MECHANICAL AND THERMAL PROPERTIES OF DMLS MANUFACTURED AlSi10Mg COMPOSITES
Karolis Stravinskas, Ričardas Petkus, Ada Steponavičiūtė, Genrik Mordas 70

O4-4 STRAIN ENGINEERING AND FERROELECTRIC BEHAVIOR OF $BaTiO_3$ THIN FILMS: A MOLECULAR DYNAMICS STUDY
Adam Puchalski, Anoop K. Kushwaha, Rajan Khadka, Tomasz K. Pietrzak, Pawel Keblinski 71

O4-5 DIELECTRIC LOADED HELIX ANTENNAS
Justina Žemgulytė, Paulius Ragulis, Romualdas Trusovas, Karolis Ratautas, Žilvinas Kancleris 72

Oral Session 5: Astrophysics and Astronomy 73

O5-1 EX EFFLUXI AD ASTRA: QUANTIFYING ACTIVE GALACTIC NUCLEUS-ENHANCED STAR FORMATION
Martynas Laužikas, Kastytis Zubovas 74

O5-2 CLEARING THE COSMIC TABLE: HOW BLACK HOLES CLEAR AWAY THEIR MEALS
Eimantas Skuodas, Kastytis Zubovas, Matas Tartėnas 75

O5-3 COMPARISON OF SIMULATED AND OBSERVED GALACTIC OUTFLOWS
Milda Valytė, Kastytis Zubovas 76

O5-4 CHEMICAL ANALYSIS OF PLANETARY HOST STARS
Ugnė Jonauskaitė, Edita Stonkutė 77

O5-5 RECONSTRUCTION OF 3D ASTEROIDS FROM 2D IMAGES
Vladas Šatas, Donatas Narbutis 78

O5-6 MINIATIURIZATION FEASABILITY BY USING BISMUTH AS A PROPELLANT FOR A HALL THRUSTER
Simas Sviensas, Jonas Klimantas, Ina Tetsmann 79

Oral Session 6: Spectroscopy and Imaging 80

O6-1 ELECTRON PARAMAGNETIC RESONANCE: GOING MICRO FOR MACRO GAINS
Gediminas Usevičius, Oscar W. Kennedy, Ignas Pocius, Patrick Hogan, Ana Villanueva Ruiz de Temino, Jean-Baptiste Verstraete, Paulina Verbaitytė, G. Antilen Jacob, Mindaugas Kamarauskas, Marius Treideris, Joseph Alexander, Vidmantas Kalendra, Jūras Banys, John J.L. Morton, Mantas Šimėnas 81

O6-2 THE IMPORTANCE OF FOURIER TRANSFORM INFRARED SPECTRA PROCESSING FOR ANALYSIS OF BIOLOGICAL SAMPLES
Tautvydas Taraškevičius, Rimantė Bandzevičiūtė, Vytautas Žėkas, Emilis Gabrielis Byčius, Dovilė Karčiauskaitė 82

O6-3 ^{35}Cl AND ^{37}Cl SOLID-STATE NMR STUDY OF CALCIUM CHLORAPATITE
Rokas Lemežis, Vytautas Klimavičius 83

O6-4 FDTD MODELLING FOR ELECTROMAGNETIC FIELD ENHANCEMENT IN BOW-TIE ARRAY FOR SERS APPLICATIONS
Hasan Sarigul, Tomas Tamulevičius 84

O6-5 EXPLORING THE IMPACT OF MICROBUMP ARRAYDIMENSIONS ON HYBRID LATTICE PLASMON RESONANCE QUALITY
Rodrigas Liudvinavičius, Evaldas Stankevičius 85

O6-6 PLASMONIC COLORS FROM THIN GOLD FILMS WITH A TITANIUM ADHESION LAYER ON A GLASS SUBSTRATE VIA NANOSECOND LASER THERMAL HEATING
Vita Petrikaitė, Evaldas Stankevičius 86

Oral Session 7: Theoretical Physics 87

O7-2 NUMERICAL MODELING OF COULOMB INTERACTION EFFECTS ON ELECTRON EMISSION FROM AN ELLIPTICAL QUANTUM DOT
Alberts Bilzens, Girts Barinovs 88

O7-3 CHARACTERIZATION OF ELECTROSPUN MAGNETIC MATERIALS IN A ROTATING MAGNETIC FIELD
Dāvis Gaiziņš, Jānis Cīmurs, Viesturs Šints, Oksana Petričenko, Roman Viter, Viktor Zabolotnii, Iryna Tepliakova 89

O7-4 PIXEL DETECTOR MODULE QUALITY TESTS FOR THE CMS PHASE-2 UPGRADE
Austėja Jurgaitytė, Marijus Ambrozas 90

O7-5 DRELL-YAN PROCESS STUDY USING OPEN DATA FROM THE CERN CMS EXPERIMENT
Eglė Lenkaitytė, Marijus Ambrozas 91

Oral Session 8: Spectroscopy and Imaging 92

O8-1 THz SPECTRA DEPENDENCE ON FREE CARRIER CONCENTRATION IN n-GaAs/GaAs STRUCTURES WITH METASURFACES
Barbora Škėlaitė, Daniil Pashnev, Vytautas Jakštas, Aivaras Špokas, Ignas Grigelionis 93

O8-2 THZ IMAGING OF HIDDEN OBJECTS AND THEIR CLASSIFICATION USING NEURAL NETWORKS
Ugnė Šilingaitė, Ignas Grigelionis 94

O8-3 INVESTIGATION OF DIVERSE SCATTERING MATERIALS USING DIGITAL TERAHERTZ HOLOGRAPHY
Lukas Stacevičius, Linas Minkevičius, Ignas Grigelionis, Agnieszka Siemion, Rusnė Ivaškevičiūtė-Povilauskienė, Gintaras Valušis . . . 95

O8-4 THEORETICAL ANALOGIES AND PRACTICAL DIFFERENCES BETWEEN IMAGING AND LENSLESS INTERFEROMETRIC METHODS
Florian Dötzer, Marie Mannagottera, Stefan Sinzinger . . . 96

O8-5 MODELLING AND MICROWAVE COUPLING OF 3.1 GHz EPR RESONATORS
Ignas Pocius, Justinas Turčak, Mantas Šimėnas, Jūras Banys . . . 97

Oral Session 9: Biochemistry, Biophysics and Biotechnology 98

O9-1 MECHANISMS OF BACTERIAL ANTIPHAGE DEFENSE BY NAD^+ BASED INTRACELLULAR SIGNALS
Dziugas Sabonis . . . 99

O9-2 THE PORE-STABILIZING EFFECT OF NISIN WITH NANOSECOND AND MICROSECOND PULSE BURSTS FOR ELECTROCHEMOTHERAPY
Barbora Lekešytė, Olga Michel, Julita Kulbacka, Vitalij Novickij . . . 100

O9-3 ANTIPROLIFERATIVE AND EPIGENETIC EFFECTS OF CANNABIDIOL ON ACUTE LYMPHOBLASTIC LEUKEMIA OR LYMPHOMA CELL LINES
Patricija Daugėlaitė, Veronika Borutinskaitė . . . 101

O9-4 DUAL NIR-EXCITABLE NANOCOMPLEX FOR EFFECTIVE PHOTODYNAMIC CANCER THERAPY
Emilė Pečiukaitytė, Simona Steponkienė, Alėja Marija Daugėlaitė, Greta Butkienė, Eglė Ežerskytė, Vaidas Klimkevičius, Vitalijus Karabanovas . . . 102

O9-5 INVESTIGATION OF THE LINK BETWEEN ACTION POTENTIAL TRANSMISSION PROPERTIES AND THE ELECTROPHYSIOLOGICAL PARAMETERS OF TANDEM INTERNODAL CELLS OF NITELLOPSIS OBTUSA
Radvilė Janušauskaitė, Vilmantas Pupkis, Vilma Kisnierienė, Indrė Lapeikaitė . . . 103

O9-6 PHYSICS-INFORMED NEURAL NETWORKS FOR ACCURATE SHEAR STRESS MAPPING AT CELL-SUBSTRATE INTERFACES IN ORGAN-ON-A-CHIP SYSTEMS
Emīls Šmits, Jānis Cīmurs, Viesturs Šints . . . 104

Oral Session 10: Biology, Genetics and Biomedical Sciences 105

O10-1 NON-INVASIVE DETECTION OF RENAL CLEAR CELL CARCINOMA USING URINARY METHYLATED DNA AS A BIOMARKER
Karolina Matekonytė, Raimonda Kubiliūtė, Algirdas Žalimas, Sonata Jarmalaitė . . . 106

O10-2 BREAST ADENOCARCINOMA-DERIVED EXTRACELLULAR VESICLES ARE ASSOCIATED WITH CHANGES IN THE METABOLIC AND BIOENERGETIC FUNCTIONS OF CARDIOVASCULAR SYSTEM CELLS
Enrika Baronaitė, Deimantė Kulakauskienė, Vytenis Keturakis, Zbigniev Balion, Edgaras Stankevičius, Aistė Jekabsone . . . 107

O10-3 THE EFFECT OF NOVEL HYDRAZONE DERIVATIVES ON HUMAN LUNG, TRIPLE-NEGATIVE BREAST AND SKIN CANCER CELL 2D AND 3D CULTURES
Dainius Lukauskas, Aida Šermukšnytė, Ingrida Tumosienė, Kristina Kantminienė, Vilma Petrikaitė . . . 108

O10-4 COMPREHENSIVE CHARACTERIZATION OF ORGANOIDS FORMED FROM PATIENT-DERIVED ENDOMETRIUM FOR INFERTILITY RESEARCH
Erika Girniūtė, Deimantė Žukauskaitė, Rūta Navakauskienė . . . 109

O10-5 DEVELOPMENT AND CHARACTERIZATION OF HYBRID LIPOSOME-EXOSOME NANOPARTICLES FOR TARGETED DRUG DELIVERY IN GLIOBLASTOMA
Girstautė Dabkevičiūtė, Christian Celia, Vilma Petrikaitė . . . 110

O10-6 EXPLORING THE PHYSICOCHEMICAL AND RADIOBIOLOGICAL MECHANISMS OF FLASH RADIOTHERAPY
Paulina Kazlauskaitė, Akvilė Šlėktaitė-Kišonė, Džiugilė Valiukevičiūtė, Marius Burkanas, Aleksandras Cicinas, Mindaugas Džiugelis, Ričardas Rotomskis, Jonas Venius, Rasa Sabaliauskaitė . . . 111

Oral Session 11: Biochemistry, Biophysics and Biotechnology 112

O11-1 VALORISATION OF WALNUT SHELL AS A SOURCE OF BIOACTIVE DERIVATIVES: IN SILICO POLYPHENOL OXIDASE INHIBITION AND TOXICITY PREDICTION
Ayodeji Amobonye, Joana Bendoraitiene, Laura Peciulyte, Ramune Rutkaite 113

O11-2 ELECTROGENICITY IN PATHOGENIC BACTERIAL BIOFILMS
Evelina Lukaitė, Marius Butkevičius, Eglė Malachovskienė, Algimantas Paškevičius, Marius Dagys, Rokas Žalnėravičius 114

O11-3 ANALYSIS OF PROTEINS POTENTIALLY INVOLVED IN β-LACTAM RESISTANCE IN OPPORTUNISTIC PATHOGEN STENOTROPHOMONAS MALTOPHILIA
Edvard Romanovski, Laurita Klimkaitė, Ignas Ragaišis, Julija Armalytė 115

O11-4 ENHANCING AI-DRIVEN BIOMOLECULAR STRUCTURE PREDICTION WITH VOROMQA-AA: A NEW APPROACH TO ACCURACY ESTIMATION
Rita Banciul, Kliment Olechnovič, Justas Dapkūnas 116

O11-5 ADAPTATION OF CROFT-SEQ FOR OFF-TARGET DETECTION OF VARIOUS GENOME EDITING TOOLS
Paulius Toliušis, Gunda Petraitytė, Algirdas Grybauskas, Mindaugas Zaremba 117

Oral Session 12: Chemistry and Chemical Physics 118

O12-1 FESTIVE FLARES: HOW BONFIRES AND FIREWORKS SHAPE URBAN AEROSOL OPTICAL PROPERTIES
Agnė Minderytė, Steigvilė Byčenkienė 119

O12-2 WHERE MICROPLASTICS MEET PEDESTRIANS: EVALUATING GREEN INFRASTRUCTURES ROLE IN REDUCING TRANSPORT-RELATED POLLUTION
Abdullah Khan, Valda Araminienėb, Ieva Uogintė, Iveta Varnagirytė-Kabašinskienė, Valentinas Černiauskas, Valda Gudynaitė-Franckevičienėb, Algis Džiugysc, Edgaras Misiulisc, Steigvilė Byčenkienė . . 120

O12-3 ECO-FRIENDLY PRODUCTION OF BIPHASIC CALCIUM PHOSPHATE GRANULES: GYPSUM CONVERSION UNDER VARRIED SYNTHESIS CONDITIONS
Greta Linkaite, Skirmantas Astramskas, Ruta Raiseliene, dr. Inga Grigoraviciute, dr. Aivaras Kareiva . 121

O12-4 TRANSILATIONAL APPROACH OF MOLECULAR IMPRINTED POLYMERS INTEGRATION WITH ESSENTIAL OILS
Greta Kasputė, Urtė Prentice 122

O12-5 DETERMINATION OF THE DEGREE OF POLYMERIZATION OF STARCH MODIFIED WITH CITRIC AND LACTIC ACIDS
Daria Kuchynska, Olena Ishchenko, Roman Kachan 123

O12-6 REGENERATION OF TETHERED BILAYER LIPID MEMBRANES FOR REUSABLE BIOSENSORS
Anastasija Aleksandrovič, Inga Gabriūnaitė, Aušra Valiūnienė, Gintaras Valinčius 124

Oral Session 13: Materials Science and Nanotechnology 125

O13-2 EMISSION PROPERTIES OF BISMUTH QUANTUM DOTS IN ANNEALED GaAsBi/AlAs QUANTUM WELLS
Justas Žuvelis, E. Dudutienė, S. Stanionytė, M. Skapas, B. Čechavičius, R. Butkutė 126

O13-3 MXENES-BASED ELECTROCHEMICAL SENSOR FOR QUICK AND ACCURATE DETERMINATION OF CADMIUM ION CONCENTRATIONIN AQEOUS ENVIRONMENTS
Ilya Navitski, Šarūnas Žukauskas, Alma Ručinskienė, Ernestas Svirbutavičius, Simonas Ramanavičius, Arūnas Ramanavičius 127

O13-4 SYNTHESIS AND CHARACTERIZATION OF HIGHLY CONDUCTIVE NANOCRYSTALLIZED ε-$LiVOPO_4$ LIKE GLASSES
Krzysztof Gadomski, Viktoriia Vlasenko, Wojciech Grunwald, Sylwester J. Rzoska, Jerzy E. Garbarczyk, Tomasz K. Pietrzak 128

O13-5 MODEL OF NONLINEAR PORO-VISCOELASTIC FELT MATERIAL
Maria Miranda Vuin, Dmitri Kartofelev 129

Oral Session 14: Chemistry and Chemical Physics 130

O14-1 CONCENTRATION QUENCHING OF FLUORESCENCE IN DIFFERENT MOLECULAR SYSTEMS: SIMILARITIES AND DIFFERENCES
Ivan Halimski, Simona Streckaitė, Renata Karpicz, Jevgenij Chmeliov, Andrius Gelzinis, Darius Abramavicius, Leonas Valkunas 131

O14-2 INFLUENCE OF MICROPLASTIC FILM SIZE ON PHOTOCATALYTIC DEGRADATION OF LDPE USING Ag-TiO_2 NANOMATERIALS
Sonata Pleskytė, Ieva Uogintė, Steigvilė Byčenkienė 132

O14-3 SYNTHESIS AND INVESTIGATION OF CARBAZOLE AND PHENOXAZINE ORGANIC SEMICONDUCTORS
Skirmantas Musteikis, Mantas Marčinskas, Tadas Malinauskas 133

O14-4 MODELING THE STRUCTURE AND NMR SPECTRA OF AMANTADINE ENCAPSULATED IN SUPRAMOLECULAR MATRICES
Amina Elkady, Kęstutis Aidas 134

O14-5 IMPACT OF PROTEIN GEOMETRY AND PROTONATION PATTERN ON THE EXCITED STATES OF PIGMENTS IN PHOTOSYNTHETIC COMPLEXES
Gabriele Rankelyte, Jevgenij Chmeliov, Andrius Gelzinis, Leonas Valkunas 135

Oral Session 15: Materials Science and Nanotechnology 136

O15-1 ACCEPTOR AGGREGATION IN PM6:Y6 ORGANIC SOLAR CELL BLENDS REVEALED BY SPECTRAL DECOMPOSITION
Titas Klepeckas, Dr. habil. Vidmantas Gulbinas 137

O15-2 COMPARATIVE CONDUCTIVITY ANALYSIS OF TRANSPARENT ELECTRODES FOR SOLAR CELLS
Noor ul ain ahmed, Patrizia lamberti, Maksim Shundalau, Renata Adami, Maria Sarno, Claudia Cirillo, Vidmantas Gulbina, Martynas Talaikis 138

O15-3 SPECTRAL PROPERTIES OF YTTERBIUM SPECIES IN DOPED CESIUM LEAD HALIDE PEROVSKITES
Daniel Rodz, Simona Steckaitė, Vitalii Boiko, Mariusz Stefanski, Dariusz Hreniak, Vidmantas Gulbinas 139

O15-4 CHARGE CARRIER MIGRATION IN 2D/3D PEROVSKITES
Paula Baltaševičiūtė, Vidas Pakštas, Vidmantas Jašinskas, Vidmantas Gulbinas, Marius Franckevičius 140

O15-5 LIQUID CRYSTAL ELASTOMER MICROSCTRUCTURES WITH TUNABLE OPTOMECHANICAL PROPERTIES
Zofia Dziekan, Mikolaj Rogoz, Piotr Wasylczyk 141

Poster Session 1: Laser Physics and Optical Technologies, Material Science and Nanotechnology 142

P1-1 GLASS SCRIBING WITH BESSEL BEAM USING MHZ BURSTS
Aleksandras Kondratas, Juozas Dudutis, Paulius Gečys 143

P1-2 OPTIMIZATION OF FEMTOSECOND LASER CUTTING PROCESS PARAMETERS FOR POLYMER OF VARIOUS THICKNESSES
Arnas Vyšniauskas, Laimis Zubauskas, Valdemar Stankevič, Paulius Gečys 144

P1-3 NON-OPTICAL CONTACT GLASS WELDING AT DIFFERENT LASER PULSE DURATIONS
Neda Mažeikytė, Edgaras Markauskas, Paulius Gečys 145

P1-4 QUALITY ENHANCEMENT OF CUT GLASS USING A CO_2 LASER
Patricija Šleiniūtė, Laimis Zubauskas, Miglė Mackevičiūtė, Paulius Gečys 146

P1-5 MAXIMIZING CUTTING SPEED OF THIN STAINLESS-STEELSHEETS BY NANOSECOND AND PICOSECOND LASER PULSES
Lukas Brundza, Andrius Žemaitis, Mindaugas Gedvilas 147

P1-6 REDUCTION OF Si REFLECTANCE VIA FEMTOSECOND LASER-PROCESSING
Mantas Mikalkevičius, Andrius Vasiliauskas, Mindaugas Juodėnas, Tomas Tamulevičius, Asta Tamulevičienė 148

P1-9 HUMIDITY-INDUCED STRESS MEASUREMENTS IN NANOSTRUCTURED GLAD COATINGS FOR HIGH LIDT MIRRORS
Adomas Strazdas, Simas Melnikas, Lukas Ramalis 149

P1-10 SELECTIVE LASER ETCHING OF FUSED SILICA USING LOW NUMERICAL APERTURE FOCUSING OPTICS
Rimantas Naina, Valdemar Stankevič 150

P1-11 TRANSPARENT MICROSCALE ELECTRODES FORMED BY LASER-INDUCED METAL DEPOSITION ON GLASS FOR SMART WINDOWS APPLICATION
Dainius Balkauskas, Evaldas Kvietkauskas, Modestas Sadauskas, Viktorija Vrubliauskaitė, Romualdas Trusovas, Karolis Ratautas, Alexandr Belosludtsev 151

P1-12 PULSED LASER DEPOSITION OF NBT-BT THIN FILMS
Eglė Martinaitytė, Vadzim Haronin, Šarūnas Svirskas 152

P1-13 SYNTHESIS AND CHARACTERIZATION OF PALLADIUM NANOPARTICLES VIA LASER ABLATION OF TARGET IN WATER
Amelija Nicytė, Ornela Rakauskaitė, Mantas Mikalkevičius, Toma´š Albert Štefanov, Dejan Prokop, Vrňata Martin, Michal Novotný, Joris More Chevalier, Tomas Tamulevičius 153

P1-14 FABRICATION OF HIGH POROSITY FOAM TARGETS FOR INERTIAL CONFINEMENT FUSION INVESTIGATION
Ioanna-Angeliki Petsi, Saule Petrauskaite, Mangirdas Malinauskas 154

P1-15 INVESTIGATION OF THE PROPERTIES OF A PIEZORESISTIVE SENSOR FABRICATED USING LASER MICROFABRICATION TECHNOLOGIES
Šarūnas Mickus, Romualdas Trusovas, Karolis Ratautas, Justina Žemgulytė, Paulius Ragulis, Modestas Sadauskas, Evaldas Kvietkauskas, Gediminas Račiukaitis 155

P1-16 PECULIARITIES OF THERMAL EFFECT MANAGEMENT IN AN END-PUMPED HIGH AVERAGE POWER BULK YB:YAG LASER AMPLIFIER
Lukas Kamarauskas, Aivaras Kazakevičius, Andrejus Michailovas 156

P1-17 MODELING OF SECOND HARMONIC GENERATION SPECTRA IN CHIRAL TPPS4 NANOTUBES
Eimantas Urniežius, Laura Baliulytė, Darius Abramavičius 157

P1-18 FLUORESCENCE LIFETIME MEASUREMENTS USING THERMAL SOURCE
Evita Spalinskaitė, Vytautas Žičkus, Zigmas Balevičius 158

P1-19 HIGH REPETITION RATE FEMTOSECOND SUPERCONTINUUM GENERATION IN KGW CRYSTAL AND ALL-NORMAL DISPERSION PHOTONIC CRYSTAL FIBER
Simona Armalytė, Jokūbas Pimpė, Julius Vengelis 159

P1-20 DOUBLE FANO RESONANCES IN NANO-MODULATED THIN FILMS FOR FREQUENCY AND ANGULAR FILTERING
Lucciano A. Letelier C., Julianija Nikitina, Lina Grineviciute, Kestutis Staliunas 160

P1-21 IMAGING OF SURFACE ACOUSTIC WAVES AND MEMS WITH PICOMETER DISPLACEMENTS USING HOLOGRAPHIC VIBROMETRY
Florian Dötzer, Johannes May, Marie Mannagottera, Stefan Sinzinger 161

P1-22 NUMERICAL ANALYSIS OF PHOTONIC CRYSTAL WAVEGUIDE LOGICAL CIRCUITS
Andrius Zinkevičius, Ignas Lukošiūnas 162

P1-23 INVESTIGATION OF THE SPATIAL DISTRIBUTION OF THE PHOTOLUMINESCENCE SPECTRAL PROPERTIES OF PLASTIC SCINTILLATING OPTICAL FIBERS USING CONFOCAL MICROSCOPY
Mikas Iršėnas, Augustas Vaitkevičius 163

P1-24 FLEXIBLE SALISBURY SCREEN WITH MICROWAVE METASURFACE FOR ENHANCED ELECTROMAGNETIC ABSORPTION
Augustas Koklevičius, Paulius Ragulis, Žilvinas Kancleris, Audronė Sankauskaitė, Vitalija Rubežienė . 164

P1-26 ANNEALING EFFECTS ON RADIATION-DAMAGED GaN DETECTORS FOR SPACE AND HIGH-ENERGY APPLICATIONS
Mykolas Strigūnas, Jevgenij Pavlov, Tomas Čeponis 165

P1-27 FORMATION AND INVESTIGATION OF GAN SENSORS FOR RECORDING OF IONIZING RADIATION
Jonas Seilius, Vytautas Rumbauskas, Tomas Čeponis, Rokas Dobužinskas 166

P1-28 DISLOCATION REDUCTION IN GaN LAYER GROWN ON PATTERNED SAPPHIRE SUBSTRATE
Karolina German, Tadas Malinauskas, Virginijus Bukauskas, Arūnas Kadys 167

P1-29 SENSOR BASED ON HOT CARRIER EFFECT FOR ELECTROMAGNETIC RADIATION DETECTION
Vladyslav Kyshchun, Yana Faier, Oleksandr Masalskyi, Ihor Zharchenko, Jonas Gradauskas, Aldis Šilėnas, Aurimas Čerškus 168

P1-30 INVESTIGATION OF ANTENNA-COUPLED ALGAN/GAN HIGH ELECTRON MOBILITY TRANSISTORS FOR SUB-THZ WAVES DETECTION
Miroslav Saniuk, Maxim Moscotin, Justinas Jorudas, Irmantas Kašalynas 169

P1-31 TEMPERATURE-DEPENDENT PHOTOLUMINESCENCE OF LOCALIZED CARRIERS IN III-NITRIDE QUANTUM WELLS BY KINETIC MONTE-CARLO SIMULATION
Ralfas Chvainickas, Oleg Kravcov 170

P1-33 TRANSIENT CATHODOLUMINESCENCE IN NITRIDE V-DEFECTS
Gabija Soltanaitė, Žydrūnas Podlipskas, Mantas Migauskas 171

P1-35 INVESTIGATION OF BULK HETEROJUNCTION (BHJ) SOLAR CELLS USING A KINETIC PHOTOCONDUCTIVITY METHOD
Dovilė Vasiliauskaitė, Ernestas Kasparavičius, Vidmantas Gulbinas 172

P1-36 B-SITE MIXING EFFECTS ON PHASE TRANSITIONS AND DIELECTRIC PROPERTIES OF $MAPb_{1-x}Sn_xBr_3$ HYBRID PEROVSKITES
Gabrielius Rimkus, Sergejus Balčiūnas, Hanna R. Petrosova, Olesia I. Kucheriv, Rokas Lemežis, Vytautas Klimavičius, Vidmantas Kalendra, Jūras Banys, Ilýa A. Guralśkiy, Mantas Šimėnas 173

P1-37 INVESTIGATION IF SBSEI THIN FILMS WITH OPEN AND CLOSED ANNEALING VARIATIONS
Deividas Vainauskas, Vidas Pakštas, Rokas Kondrotas 174

P1-38 XRD STUDY OF COPPER-TIN SULPHIDE FILMS ON FTO GLASS
Dominyka Zubrickaitė, Asta Bronušienė, Ingrida Ancutienė 175

P1-39 NEW CARBAZOLE-BASED DERIVATIVES AS HOST MATERIALS FOR VERY EFFICIENT OLEDS
Raminta Beresneviciute, Daiva Tavgeniene, Dovydas Blazevicius, Kuan-Wei Chen, Yu-Hsuan Chen, Saulius Grigalevicius, Chih-Hao Chang 176

P1-40 THE INFLUENCE OF MILLING ON THE GRAIN SIZE OF LEAD-FREE SOLID SOLUTIONS $0.8Na_{0.5}Bi_{0.5}TiO_3$ - $0.2BaTiO_3$.
Ugnius Dominykas Sviackevičius, Artyom Plyushch, Rokas Dobužinskas, Šarūnas Svirskas, Algirdas Selskis, Robertas Grigalaitis, Jūras Banys 177

P1-41 TWO-STAGE SYNTHESIS OF Ca_a Si_b TiO_c COMPOUNDS
Ričardas Kleinauskas, Anatolijus Eisinas, Jolanta Donėlienė 178

P1-42 DESIGN OF A TWISTED DOUBLE DONOR IN CARBAZOLE-METHYLPYRIMIDINE-BASED EMITTERS LEADING TO THE TRIPLE CHARGE-TRANSFER EMISSION
Dovydas Blaževičius, Gintarė Kručaitė, Saulius Grigalevičius, Oleg Dimitriev 179

P1-43 NUMERICAL MODELING OF SELF-ASSEMBLY OF $INDO_4$ MOLECULES ON Ag SURFACES
Jorunas Dobilas, Evaldas E. Tornau 180

P1-44 ETHYL CELLULOSE AS A HOST MATERIAL FOR THERMALLY-ACTIVATED DELAYED FLUORESCENCE EMITTERS
Gintare Krucaite, Daiva Tavgeniene, Saulius Grigalevičius, Alla Bogoslovska, Amjad Ali, Glib Baryshnikov, Petro Smertenko, Mats Fahlman, Andrei Smertenko, Oleg Dimitriev 181

P1-45 INVESTIGATIONS OF PHOTOPHYSICAL PROPERTIES OF DERIVATIVES OF PHENOTHIAZINE AND DIFFERENTLY MODIFIED 3,5-DICYANOPYRIDINE FOR DOWN-CONVERTING WHITE LIGHT-EMITTING DIODES
Lesia Volyniuk, Serhii Melnykov, Pavel Arsenyan, Oleksandr Bezvikonnyi, Dmytro Volyniuk, Pavlo Stakhira, Audrius Bucinskas, Juozas Vidas Grazulevicius 182

P1-46 OVERSHOOT PULSES IN PEROVSKITE LIGHT EMITTING DIODES. THE ROLE OF OPERATION CONDITIONS
Ignas Ledzinskas, Rokas Gegevičius, Vidmantas Gulbinas 183

P1-47 SHORT-RANGE CHARGE TRANSFER ANDBIPOLAR CHARGE TRANSPORT IN DIBENZO{A,C}IMIDAZOPHENAZINE-BASED EMITTER WITH MR-TADF FOR SOLUTION-PROCESSABLE HYPERFLUORESCENT OLEDs
Hamisu Aliyu Mohammed, Matas Guzauskas, Viktorija Andruleviciene, Dmytro Volyniuk, Woon Kai Lin, Azhar Ariffin, Juozas Vidas Grazulevicius 184

P1-48 VIS-TO-UV PHOTON UPCONVERSION IN THIN FILMS EMPLOYING MR-TADF SENSITIZER
Džiugas Krencius, Naglis Vasarevičius, Manvydas Dapkevičius, Justas Lekavičius, Steponas Raišys, Karolis Kazlauskas 185

P1-49 PHENANTHRO(9,10-d)HAVING ELECTROACTIVE DERIVATIVES AS HOST MATERIALS FOR OLEDs
Daiva Tavgeniene, Dovydas Blazevicius, Saulius Grigalevicius, Gintare Krucaite, Karolis Kazlauskas, Dovydas Banevicius, Vygintas Jankauskas, Egidijus Kamarauskas 186

P1-50 NOVEL HOST MATERIALS FOR STABLE BLUE THERMALLY ACTIVATED DELAYED FLUORESCENCE OLEDS
Domantas Berenis, Rita Butkutė, Gediminas Kreiza, Giedrius Puidokas, Vaida Jašinskaitė-Koženiauskienė, Karolis Kazlauskas 187

P1-52 APPLICATION OF A DIBENZOFURAN-BASED HOST WITH HIGH TRIPLET ENERGY FOR THIRD-GENERATION BLUE ORGANIC LIGHT-EMITTING DIODES
Kristupas Bagdonas, Goda Grybauskaitė, Gediminas Kreiza, Edvinas Orentas, Eigirdas Skuodis, Karolis Kazlauskas, Dovydas Banevičius 188

P1-54 NOVEL HOLE-TRANSPORTING MATERIALS WITH HIGH HOLE MOBILITY FOR EFFICIENT AND STABLE RED OLEDS
Melika Ghasemi, Mariia Stanitska, Svetlana Sargsyan, Dmytro Volyniuk, Rasa Keruckienė, Juozas Vidas Gražulevičius 189

P1-55 DONOR-ACCEPTOR-DONOR TYPE FLUORESCENT EMITTERS WITH BENZOTHIADIAZOLE CORES AS PROMISING MATERIALS FOR OLEDS
Svetlana Sargsyan, Rasa Keruckiene, Ehsan Ullah Rashid, Matas Guzauskasa, Dmytro Volyniuk, Viktorija Andruleviciene, Juozas Vidas Grazulevičius 190

P1-56 IMIDAZOLE AND FLUORENE DERIVATIVES AS HIGHLY EFFICIENT FLUORESCENT LIGHT SOURCES: SYNTHESIS AND INVESTIGATION
Mohamed Abdella, Guzauskas Matas, Jurate Simokaitiene, Juozas Vidas Grazulevicius 191

P1-57 SYNTHESIS AND STUDIES OF LONG-WAVELENGTH ABSORBING ORGANIC SEMICONDUCTORS FOR OPTOELECTRONICS
Khushdeep Kaur, Rita Butkutė, Oleksandr Bezvikonnyi, Dmytro Volyniuk, Juozas Vidas Gražulevičius . 192

P1-58 ELECTROCHEMICAL SENSOR FOR SALICYLIC ACID BASED ON A MOLECULARLY IMPRINTED POLYMER
Gabrielė Slaboševičiūtė, Ernestas Brazys, Vilma Ratautaitė 193

P1-60 THE FORMATION AND ELECTROCHEMICAL EVALUATION OF POLYMERIC NANOCOMPOSITES BASED ON GLUCOSE OXIDASE AND GOLD NANOCOMPOUNDS
Natalija German, Almira Ramanaviciene, Arunas Ramanavicius 194

P1-61 THE ELECTROCHEMICAL EVALUATION OF GLUCOSE BIOSENSOR BASED ON INCORPORATING PLATINUM NANOSTRUCTURES, GLUCOSE OXIDASE, AND POLYMERIZED 1,10-PHENANTHROLINE-5,6-DIONE
Gustė Jakučiūnaitė, Natalija German 195

P1-62 PLASMONIC METASURAFCE FOR ENHANCED HER KINETICS BY PHOTOELECTROCHEMICAL WATER SPLITTING.
Muhammad Haris, Klaudijus Midveris, Syeda Ammara Shabbir, Gvidas Klyvis, Mindaugas Juodėnas, Tomas Tamulevičius, Asta Tamulevičienė, Hamid latif, Sigitas Tamulevičius 196

P1-63 VISUAL RECOGNITION FOR MICRO-ACCURACY IN SECM RESEARCH
Rokas Bagdonas, Simonas Jurkynas, Inga Morkvėnaitė-Vilkončienė, Andrius Dzedzickis 197

P1-64 Co/β ZEOLITE FOR ORR IN ALKALINE MEDIA
Kristina Radinović, Jadranka Milikić, Ana Nastasić, Katarina Rondović, Ljiljana Damjanović-Vasilić, Aldona Balčiūnaitė, Vladislav Rac, Rastko Vasilić 198

P1-65 Ni/β ZEOLITE FOR OER IN ALKALINE MEDIA
Jadranka Milikić, Ana Nastasić, Kristina Radinović, Katarina Rondović, Ljiljana Damjanović-Vasilić, Aldona Balčiūnaitė, Vladislav Rac, Rastko Vasilić 199

P1-66 CHARACTERIZATION OF FIBROUS MICROPLASTIC EMITTED FROM VIRGIN AND RECYCLED POLYESTER FABRICS
Ugnė Gliaudelytė 200

P1-67 IMPACT OF HEXAMETHYLDISILAZANE ON BEETROOT POWDER BYPRODUCTS AND POLYMER INTERACTION: PROPERTIES AND INTERFACIAL DYNAMICS
khadija ramzan 201

P1-68 The Influence of Industrial Tea Waste Ash on Mechanical Properties of Natural Rubber Materials
Jelena Lubura Stošić, Oskar Bera, Dario Balaban, Teodora Vukša, Siniša Simić 202

P1-69 DEVELOPMENT OF A CAPSAICIN-BASED DRUG DELIVERY SYSTEM
Felix Lücke, Šarūnas Žukauskas, Arūnas Ramanavičius, Almira Ramanavičienė 203

P1-70 SYNTHESIS AN NANOCRYSTALLISATION OF Na_{2+x} $VFe_2(PO_4)_{3-x}(SiO_4)_x$ ALLUAUDITE-TYPE GLASSES
Martyna Jankowska, Krzysztof Gadomski, Maciej Nowagiel, Tomasz K. Pietrzak, Lauren Blanc, Linda Nazar 204

P1-71 PHYTOHYDROGELS WITH THE ADDITION OF STARCH AND MODIFIED STARCH
Kolomiiets Viktoriia, Irina Liashok, Viktoriia Plavan, Olena Kryukova, Viacheslav Shvets 205

P1-73 PHOTOPHYSICAL STUDY OF PURINE BASED MOLECULES FOR METAL ION SENSING
Jana Jermak, Kamilė Boguševičienė, Justina Jovaišaite, Irina Novosjolova, Maris Turks, Gediminas Jonušauskas, Gediminas Kreiza, Huang-Tsung Chang, Saulius Juršėnas 206

P1-75 DESIGNING THERMORESPONSIVE POLY(N-ISOPROPYLACRYLAMIDE) COPOLYMERS FOR BIOMEDICINE VIA ONE-POT MICROWAVE-ASSISTED SYNTHESIS
Marija Krstić, Nina Jokić, Ivan Ristić 207

P1-77 Ni/β ZEOLITE FOR ORR IN ALKALINE MEDIA
Ana Nastasić, Jadranka Milikić, Kristina Radinović, Katarina Rondović, Ljiljana Damjanović-Vasilić, Aldona Balčiūnaitė, Vladislav Rac, Rastko Vasilić 208

P1-78 PREPARATION OF Sm3+ IONS DOPED MgAl2O4 BY SOL-GEL POLYACRYLAMIDE SYNTHESIS
Pranga Prava Mandal, Dovydas Karoblis, Aivaras Kareiva 209

P1-79 SAMARIUM AND GADOLINIUM DOPED CERIA NANOPOWDERS FOR INTERMEDIATE TEMPERATURE SOLID OXIDE FUEL CELLS
Augustinas Zinkus, Mantas Sriubas, Brigita Abakevičienė 210

P1-80 ENHANCING ELECTRON TRANSFER EFFICIENCY IN MICROBIAL FUELCELLS THROUGH GOLD NANOPARTICLE MODIFICATION OF SACCHAROMYCES CEREVISIAE
Teresė Kondrotaitė, Antanas Zinovičius, Domas Pirštelis, Inga Morkvėnaitė-Vilkončienė 211

P1-81 ENHANCING T7 DNA POLYMERASE IMMOBILIZATION FOR REUSABLE BIOSENSORS
Julija Sarvutiene, Deivis Plaušinaitis, Arunas Ramanavicius, Urte Prentice 212

P1-82 SIMULTANEOUS IN SITU DIELECTRIC AND CRYSTALLOGRAPHIC TEMPERATURE DEPENDENT MEASUREMENTS.
Kaspars Jaundzems, Reinis Ignatans 213

P1-83 HYBRID PLASMONIC-PHOTONIC MODES OF NANOPARTICLE ARRAYS IN HIGH REFRACTIVE INDEX THIN-FILM MEDIA
Klaudijus Midveris, Gvidas Klyvis, Mindaugas Juodenas, Joel Henzie, Tomas Klinavicius, Andrius Vasiliauskas, Asta Tamuleviciene, Tomas Tamulevicius 214

P1-84 LOW-FREQUENCY NOISE CHARACTERISTICS OF GRAPHENE/h-BN/Si JUNCTIONS
Ingrida Pliaterytė, Justinas Glemža, Šarūnas Meškinis, Rimantas Gudaitis, Šarūnas Jankauskas, Asta Guobienė, Andrius Vasiliauskas, Sandra Pralgauskaitė, Jonas Matukas 215

P1-85 ANALYSIS OF ELECTROMAGNETIC PROPERTIES IN VARIOUS 3D-PRINTED COMPOSITES
J. Varnyte, E. Palaimiene, J. Macutkevic, P. Blyweert, J. Banys, A. Celzard 216

P1-86 DEFECT SPECTROSCOPY IN PROTON IRRADIATED SILICON LOW GAIN AVALANCHE DETECTORS
Margarita Biveinytė, Tomas Čeponis, Laimonas Deveikis 217

P1-87 SPECTROSCOPY OF RADIATION-INDUCED DEFECTS IN p-TYPE Si AND SiGe ALLOYS
Gertrūda Pociūtė, Tomas Čeponis, Jevgenij Pavlov 218

P1-88 DEPTH-DEPENDENT OPTICAL PROPERTIES OF InGaAs QUANTUM STRUCTURES EXPLORED BY VARIABLE EXCITATION ENERGY
Kipras Mažeika, Augustas Vaitkevičius, Andrea Zelioili, Aivaras Špokas, Renata Butkutė 219

P1-89 ADSORPTION PERFORMANCE OF MXENES FOR AZURE A AND METHYLENE BLUE: pH-DEPENDENT BEHAVIOUR AND KINETIC INSIGHTS
Germantė Paulikaitė, Simonas Ramanavičius, Šarūnas Žukauskas, Martynas Talaikis, Gediminas Niaura, Oleksiy Gogotsi 220

P1-91 APPLICATION OF FIBERGLASS COMPOSITES TO PRODUCE COMPLEX GEOMETRIC PARTS
Agnius Paneckas, Urte Cigane, Justas Ciganas 221

P1-92 DETERMINATION OF ETCHING PARAMETERS FOR STRUCTURAL TEXTILES TO IMPROVE ADHESION TO INORGANIC SEMICONDUCTORS
Evaldas Sutkus, Valentina Krylova 222

P1-93 ENHANCED PHYSICAL PROPERTIES OF PVB/ZNO-T/NAPT NANOCOMPOSITE COATINGS: DEVELOPMENT AND CHARACTERIZATION
Mindaugas Ilickas, Asta Guobienė, Simas Račkauskas, Brigita Abakevičienė 223

P1-94 DESIGN AND OPTIMIZATION OF HYBRID LIPID-POLYMERIC NANOPARTICLES FORTARGETED DRUG DELIVERY IN CARDIOVASCULAR DISEASES
Ugnė Žulpaitė, Vilma Petrikaitė 224

P1-95 OPTIMIZATION OF PREPARATION PARAMETERS OF PHOSPHATE BONDED CERAMICS
Žygimantas Logminas, Artyom Plyshch, Šarūnas Svirskas, Algirdas Selskis, Jūras Banys 225

P1-96 GOLD NANOCOMPOUNDS MEDIATED CADMIUM ION DETECTION BASED ON GLUCOSE OXIDASE INHIBITION
Katazyna Blazevic, Natalija German, Benediktas Brasiunas, Asta Kausaite-Minkstimiene, Almira Ramanaviciene 226

P1-97 DETERMINATION OF BAND ALIGNMENTS IN ANTIMONY SELENIDE AND TITANIUM OXIDE HETEROJUNCTIONS BY ULTRAVIOLET PHOTOELECTRON SPECTROSCOPY
Gerarda Jocytė, Rokas Kondrotas, Jurgis Pilipavičius, Vidas Pakštas 227

P1-98 EMISSIVE TAGS BASED ON PHENOXATHIIN CONTAINING DONOR-ACCEPTOR TYPE COMPOUNDS WITH ENHANCED ROOM TEMPERATURE PHOSPHORESCENCE
Lukas Dvylys, Rasa Keruckiene, Lesia Volyniuk, Dmytro Volyniuk, Juozas V. Grazulevicius 228

P1-99 PLATFORM FOR NV CENTER SPIN DYNAMICS
Vakaris Šilys, Julius Janušonis, Tadas Paulauskas 229

Poster Session 2: Astrophysics and Astronomy, Theoretical Physics, Spectroscopy and Imaging, Material Science and Nanotechnology, Biochemistry, Biophysics and Biotechnology, Biology, Genetics and Biomedical Sciences, Chemistry and Chemical Physics **230**

P2-1 IMAGINARY SYNTHETIC MAGNETIC FIELD
Saulius Alminas, Domantas Burba, Gediminas Juzeliūnas, Tomas Babelis, Ian B. Spielman 231

P2-2 ANALOGIES BETWEEN QUANTUM AND CLASSICAL SYSTEMS
Justina Vaičaitytė, Andrius Gelžinis, Leonas Valkūnas 232

P2-3 QUANTUM MANY-BODY PHASES IN SUBWAVELENGTH BRICK WALL LATTICE
D. Viarbitski, D. Burba, G. Juzeliunas, G. Žlabys 233

P2-4 SINGLE PHOTON EMITTERS IN HEXAGONAL BORON NITRIDE FOR QUANTUM COMMUNICATIONS
Ifra Bibi, Viktorija Nargelienė, Vakaris Šilys, Julius Janušonis, Vitalij Kovalevskij, Tadas Paulauskas . . 234

P2-5 DEVELOPMENT OF THZ METALENS AND APPLICATIONFOR BEAM SHAPING AND IMAGING
Karolis Redeckas, Kasparas Stanaitis, Vladislovas Čižas, Rusnė Ivaškevičiute-Povilauskienė, Linas Minkevičius 235

P2-6 RADIATION-INDUCED DEFECT STUDIES IN p-TYPE PIN AND LGAD DETECTORS
Faustina Kiaušaitė, Tomas Čeponis, Jevgenij Pavlov 236

P2-7 PRECISION THz SPECTROSCOPY OF METHANOL: JPL-BASED THEORETICAL MODELING FOR ENHANCED SPECTRAL ANALYSIS AND REMOTE SENSING
Patricija Ivanauskaitė, Dovilė Čibiraitė-Lukenskienė 237

P2-8 OPTIMIZATION OF THZ IMAGING SYSTEMS USING 3D-PRINTED HIGH-IMPACT POLYSTYRENE LENSES
Kasparas Stanaitis, Karolis Redeckas, Vladislovas Čižas, Ignas Grigelionis, Linas Minkevičius 238

P2-9 SOLID STATE NMR STUDY OF IMMOBILIZED POLYMERS
Emilis Čiupaila, Dr. Vaidas Klimkevičius, Dr. Vytautas Klimavičius 239

P2-10 NMR RELAXATION STUDY OF FUMARIC ACID AND ITS ISOTOPOMERS
Adomas Valeika 240

P2-12 ESEEM and HYSCORE spectroscopy: Unlocking the secrets of spin-nuclear interaction
Giedrė Kuktaitė, Gediminas Usevičius, Mantas Šimėnas, Jūras Banys 241

P2-13 METHANE DETECTION FROM NATURAL AND INDUSTRIAL SOURCES BY MEASURING MIR ABSORPTION
Jonas Jeffrey Haist, Vilius Žalėnas, Laurynas Butkus, Artūras Plukis 242

P2-14 PROSPECTS OF CVD DIAMOND-BASED SUBSTRATES: E-CARS SPECTROSCOPY AND IMAGING
Paulius Rindzevičius, Mariam Quarshie, Sergei Malykhin, Andrej Dementjev 243

P2-15 STRUCTURAL ANALYSIS OF BUTYRIC ACID USING MATRIX ISOLATION INFRARED SPECTROSCOPY AND THEORETICAL CALCULATIONS
Klaudija Pukalskaite, Jogile Macyte 244

P2-16 DYNAMIC FULL-FIELD OPTICAL COHERENCE MICROSCOPY OF BIOMEDICAL TISSUE
Erikas Tarvydas, Austėja Trečiokaitė, Karolis Adomavičius, Urtė Neniškytė, Egidijus Auksorius 245

P2-17 PROTOTYPE SYSTEM OF HYPERSPECTRAL IMAGING BASED ON LEDs
Agnė Urbonaitė, Pranciškus Vitta 246

P2-18 FULL FIELD OPTICAL COHERENCE TOMOGRAPHY IN VIVO RETINAL IMAGING WITH OPTIMIZED BEAM SPLITTER AND REDUCED COHERENCE NOISE
Austėja Trečiokaite, Erikas Tarvydas, Karolis Adomavičius, Egidijus Auksorius 247

P2-19 STUDY OF ELECTRON ACCELERATION IN STRONG INFRARED RADIATION FIELDS FOR SELECT PARAMETERS
Džiugas Vyšniauskas, Artūras Plukis, Janina Grinevičiūtė 248

P2-20 EFFECT OF PEG SUBSTITUENT LENGTH ON CELLULAR UPTAKE OF UPCONVERTING NANOPARTICLES
Aleja Marija Daugelaite, Egle Ezerskyte, Kristina Bolgova, Edvin Parafjanovic, Arturas Katelnikovas, Vitalijus Karabanovas, Greta Butkiene, Vaidas Klimkevicius 249

P2-21 CONCENTRATION QUENCHING IN SOLUTIONS OF CHLOROHYLL A MOLECULES
Vilius Čirgelis, Simona Streckaitė, Jevgenij Chmeliov, Leonas Valkūnas, Andrius Gelžinis 250

P2-22 DEVELOPMENT OF A PHOTODYNAMIC ANTIMICROBIAL IRRADIATION PROTOTYPE AND FUTURE PHOTOSENSITIZER STUDIES
Tomas Krupavičius, Pranciškus Vitta, Irina Buchovec 251

P2-23 INFLUENCE OF THE MEDIUM ON THE SPECTROSCOPIC PROPERTIES AND PHOTOSTABILITY OF MG-CHLOROPHYLLIN
Marija Kalnaityte, Rasa Miliukaitė, Danielė Gedminaitė, Agnė Kalnaitytė - Vengelienė, Saulius Bagdonas 252

P2-24 EFFECT OF QUANTUM DOTS ON THE PHOTOSTABILITY OF THE SPECTROSCOPIC PROPERTIES OF MG-CHLOROPHYLLIN
Aistė Krasauskaitė, Marija Kalnaitytė, Saulius Bagdonas, Agnė Kalnaitytė - Vengelienė 253

P2-25 INVESTIGATION OF $TPPS_4$ AGGREGATION USING SPECTROSCOPY AND ATOMIC FORCE MICROSCOPY
Greta Tamoliūnaitė, Vilius Poderys, Ričardas Rotomskis 254

P2-26 COMPLEXATION OF $TPPS_4$ WITH POLYVINYL ALCOHOL POLYMER IN AQUA AND POLYMER MATRIX
Simona Pusvaškytė, Greta Tamoliūnaitė, Skaistė Talanovaitė, Vilius Poderys, Ričardas Rotomskis . . . 255

P2-27 ENVIRONMENTAL BEHAVIOR AND BIOCOMPATIBILITY OF UPCONVERTING NANOPARTICLES IN FRESH WATER
Augustas Morkvėnas, Vilius Poderys, Danguolė Montvydienė, Jūratė Karosienė, Vitalijus Karabanovas, Živilė Jurgelėnė 256

P2-28 TUNNELING EFFECTS IN MANGANITE NANOSTRUCTURES IN THE PRESENCE OF STRONG MAGNETIC FIELDS
Dariuš Antonovič, Vilius Vertelis, Skirmantas Keršulis, Nerija Žurauskienė 257

P2-29 DEVELOPMENT OF UPCONVERTING CORE-SHELL-SHELL NANOPARTICLES WITH MULTIWAVELENGTH EMISSION FOR THERANOSTIC APPLICATIONS
Egle Ezerskyte, Arturas Katelnikovas, Vaidas Klimkevicius 258

P2-30 PREPARATION AND FUNCTIONALIZATION OF GOLD NANORODS FOR BIOCONJUGATION APPLICATIONS
Tymofii Omelchenko, Marina Sapauskiene, Veronika Zahorodna, Oleksiy Gogotsi, Almira Ramanaviciene, Anton Popov 259

P2-31 ELECTROCHEMICAL GLUCOSE BIOSENSORS BASED ON GOLD NANORODS
Marina Sapauskiene, Viktorija Lisyte, Almira Ramanaviciene, Anton Popov 260

P2-32 NOVEL TITANIUM SUBOXIDE AND CORE-SHELL NANOSTRUCTURES FOR PHOTOCATALYTIC WASTEWATER TREATMENT
Aswathi Raveendran, Simonas Ramanavicius, Germante Paulikaite, Agne Sukoviene, Arunas Jagminas 261

P2-33 SYNTHESIS AND CHARACTERIZATION OF NIOBIUM NANOPARTICLES: A COMPARATIVE STUDY OF TWO METHODS
MUHAMMAD USMAN KHALID, Wanessa De Melo, Monika Kirsnytė, Arunas Stirke 262

P2-34 RESISTIVITY AND LOW FREQUENCY NOISE OF HYBRID COMPOSITES WITH CARBON NANOTUBES AND CARBONIZED NICKEL
Frydrichas Mireckas, Sandra Pralgauskaitė, Jan Macutkevič 263

P2-35 PRODUCTION OF CELLULOSE-GRAPHENE OXIDE (CO-GO) NANOCOMPOSITES FOR THE EXTRACTION OF NANOPLASTICS FROM FRESH WATER
Mahrosh Javed, Galina Lujaniene, Sergej Semcuk, Vidas Pakstas, Ausra Selskiene, Algirdas Selskis, Kestutis Mazeika, Martynas Talaikis 264

P2-36 EFFECTS OF NANOSECOND PULSES DELIVERED AT ULTRA-HIGH FREQUENCY ON MITOCHONDRIAL DEPOLARIZATION, ROS, CELL PERMEABILIZATION AND CELL VIABILITY
Paulina Malakauskaitė, Vytautas Kašėta, Vitalij Novickij 265

P2-37 STUDIES OF THE SPATIAL STRUCTURE OF $TPPS_4$ AGGREGATES USING ATOMIC FORCE MICROSCOPY
Teresė Kreišmontaitė, Greta Tamoliūnaitė, Vilius Poderys, Ričardas Rotomskis 266

P2-38 CHLOROPHYLLIN-CHITOSAN COMPLEX STOICHIOMETRY ANALYSIS FOR ANTIMICROBIAL PHOTODYNAMIC INACTIVATION
Gabrielė Vasiliauskaitė, Irina Buchovec 267

P2-39 EVALUATING PHOTOPHYSICAL PROPERTIES OF RIBOFLAVIN, MAGNESIUM CHLOROPHYLLIN AND THEIR MIXTURE IN SOLUTION
Urtė Mitrofanaitė, Irina Buchovec 268

P2-40 PROTONATION DYNAMICS OF TPPS CORE: IMPACT OF THE NUMBER OF SULFONATE SUBSTITUENTS
Skaistė Talanovaitė, Vilius Poderys, Ričardas Rotomskis 269

P2-41 SPECTROSCOPIC STUDY OF OXIDATIVE STRESS IN GREEN MACROALGA NITELLOPSIS OBTUSA
Aušrinė Navickaitė, Viltė Mickytė, Vilmantas Pupkis, Saulius Bagdonas, Vilma Kisnierienė 270

P2-42 RIBOFLAVIN-BASED PHOTODYNAMIC INACTIVATION FOR CONTROLLING THE PLANT PATHOGEN PSEUDOMONAS SYRINGAE
Fausta Guzauskaite, Irina Buhovec 271

P2-45 INFLUENCE OF THE PGLX PROTEIN MUTATIONS ON THE BREX PROTECTION
Justė Adomaitytė, Tomas Šinkūnas 272

P2-46 NATURAL COLORANTS FROM BEETROOT WASTE
Indrė Bernatavičiūtė, Rūta Gruškienė, Jolanta Sereikaitė 273

P2-47 APPLICATION OF MFC IN AGRICULTURAL SAMPLES USING E.MELILOTI
Agnė Boguševičė, Tomas Mockaitis, Inga Morkvėnaitė-Vilkončienė 274

P2-48 INTEGRATING ARTIFICIAL INTELLIGENCE, MOLECULAR DYNAMICS, AND DFT TO INVESTIGATE MONOAMINE OXIDASE INHIBITION
Augustas Markevičius, Gintautas Bagdžiūnas 275

P2-49 ORGAN-SPECIFIC STABLE CARBON ISOTOPIC COMPOSITION ($\delta^{13}C$) AND CARBON CONTENT DYNAMICS IN VACCINIUM MYRTILLUS L. (EUROPEAN BLUEBERRY)
Aistė Tuzinaitė, Anita Elizabeth Clarke, dr. Andrius Garbaras, dr. Radvilė Rimgailė-Voicik 276

P2-50 EFFECTS OF QUANTUM DOTS ON AUTOFLUORESCENCE AND PHOTOSYNTHETIC PARAMETERS OF MICROALGAE
Danielė Gedminaitė, Rasa Miliukaitė, Martyna Petkutė, Agnė Kalnaitytė-Vengelienė 277

P2-51 STRUCTURAL INSIGHTS INTO S100A9 AND S100A8 PROTEINS VIA DEER SPECTROSCOPY
Aiste Pestenyte, Gediminas Usevicius, Darius Sulskis, Ieva Baronaite, Vytautas Smirnovas, Juras Banys, Mantas Simenas 278

P2-52 LOW-TEMPERATURE SYNTHESIS OF MAGNESIUM WHITLOCKITE FROM AMORPHOUS CALCIUM PHOSPHATE
Gabriele Egle Budzyte, Greta Linkaite, Aleksej Zarkov, Aivaras Kareiva, Inga Grigoraviciute 279

P2-53 CELL SPHEROIDS AS A TOOL FOR INVESTIGATION IN MATERIAL ENGINEERING
Valdemaras Milkus, Greta Leonavičienė, Suji Kim, Linas Mažutis 280

P2-54 DEOXYGENATION OF TTA-UC SOLUTIONS BY EFFICIENT OXYGEN SCAVENGING
Dominykas Likas, Steponas Raišys 281

P2-55 ACHIEVING LONG-LASTING ROOM-TEMPERATURE PHOSPHORESCENCE IN PHENOTHIAZINE DERIVATIVES
Vilius Stankevičius, Jonas Žurauskas, Paulius Vaickūnas, Steponas Raišys, Edvinas Orentas, Karolis Kazlauskas . . . 282

P2-56 INVESTIGATION OF CONDUCTIVE POLYMER BASED DRUG DELIVERY SYSTEMS
Elena Nedzinskaitė, Felix Lücke, Šarūnas Žukauskas, Arūnas Ramanavičius, Almira Ramanavičienė . 283

P2-57 CO-PRECIPITATION SYNTHESIS AND CHARACTERISATION OF Mg/Al-LAYERED DOUBLE HYDROXIDES (LDH)
Gabija Navašinskaitė, Denis Sokol, Gabrielė Klydžiūtė, Aivaras Kareiva . . . 284

P2-58 TRIMETALLIC CoMoW ELECTROCATALYSTS FOR HYDROGEN GENERATION
Raminta Šakickaitė, Zita Sukackienė, Loreta Tamašauskaitė-Tamašiūnaitė . . . 285

P2-59 INVESTIGATION OF SUPERCAPACITIVE BEHAVIOR OF COPPER-OXIDE BASED NANOSTRUCTURED FILMS
Gintautas Jonkus, Henrikas Cesiulis, Ramunas Levinas, Natalia Tsyntsaru . . . 286

P2-60 FABRICATION OF MODIFIED HEXAGONAL BORON NITRIDE 3D PHOTOCATALYSTS BY COMBINING STEREOLITHOGRAPHY AND PYROLYSIS
Robertas Virkėtis, Vaidas Klimkevičius, Greta Merkininkaitė, Simas Šakirzanovas . . . 287

P2-62 SYNTHESIS AND INVESTIGATION OF AROMATIC ELECTRON-TRANSPORTING PHOSPHINE OXIDE COMPOUNDS
Andrius Stankus, Mantas Marčinskas . . . 288

P2-63 $GdPO_4$:Cr^{3+} AND VPO_4:Cr^{3+} SYNTHESIS BY SOLID-STATE REACTION
Miglė Minalgaitė, Ramūnas Skaudžius . . . 289

P2-64 SYNTHESIS AND APPLICATION OF ISOTHIOURONIUM MOIETY CONTAINING CARBOXYLIC OR PHOSPHONIC ACIDS IN PEROVSKITE SOLAR CELLS
Justina Mikučiūnaitė, Kasparas Rakštys . . . 290

P2-66 INVESTIGATION OF ZINC HEXACYANOFERRATE FOR AQUEOUS ZINC ION BATTERIES
Dovilė Škarnulytė, Jurgis Pilipavičius, Linas Vilčiauskas . . . 291

P2-67 IMPACT OF CAPSULAR POLYSACCHARIDES ON ACINETOBACTER BAUMANNII SURVIVAL UNDER ANTIBIOTIC-INDUCED STRESS
Dominykas Grigorjevas, Jūratė Skerniškytė . . . 292

P2-68 PHENOTYPIC CHARACTERIZATION OF ACTINOBACTERIA ISOLATED FROM APHIDS ADELGES (APHRASTASIA) PECTINATAE (HEMIPTERA: ADELGIDAE)
Gustė Tamošiūnaitė, Jekaterina Havelka, Nomeda Kuisienė . . . 293

P2-69 MUTATIONAL ANALYSIS OF A NOVEL BACTERIAL DEFENSE SYSTEM
Vakarė Gavėnaitė, Tomas Šinkūnas, Inga Songailienė . . . 294

P2-70 INACTIVATION OF THE OPPORTUNISTIC PATHOGEN STENOTROPHOMONAS MALTOPHILIA BY 5-AMINOLEVULINIC ACID-BASED PHOTODYNAMIC THERAPY
Gabija Gervinskytė, Irina Buchovec . . . 295

P2-71 STRUCTURAL INVESTIGATION OF A BACTERIAL ANTI-PHAGE SYSTEM
Miglė Paulikaitė, Monika Jasnauskaitė, Dr. Patrick Pausch . . . 296

P2-73 MOLECULAR MECHANISMS DIFFERENTLY AFFECTING THE ATRIAL CELLS UNDER NORMOXIA AND HYPOXIA
Liepa Gedvilaitė, Dr. Rokas Mikšiūnas, Dr. Daiva Bironaitė . . . 297

P2-75 PHENOLOXIDASE ACTIVITY OF MICROSCOPICFUNGI FOUND IN OLD-GROWTH FORESTS: DIVERSITY AND LIGNIN DEGRADATION POTENTIAL
Ieva Sokė, Dovydas Petlinskas, Daiva Burokienė . . . 298

P2-76 EXPLORING GENETIC BIOMARKERS IN PLASMA SAMPLES FROM CLEAR CELL RENAL CELL CARCINOMA PATIENTS
Milda Urbonaitė, Ieva Vaicekauskaitė, Algirdas Žalimas, Rasa Sabaliauskaitė . . . 299

P2-78 STUDY OF POTENTIAL NEW DRUG COMBINATIONS FOR TREATMENT OF ENDOMETRIAL CANCER CELLS
Aistė Jarašūnaitė, Veronika Viktorija Borutinskaitė 300

P2-79 ELECTROCHEMICAL INVESTIGATION OF CHO CELLS WITH VARIOUS REDOX MEDIATORS
Domantas Barkauskas, Tomas Mockaitis, Inga Morkvėnaitė- Vilkončienė, Ingrida Bružaitė 301

P2-80 REDOX PROPERTIES OF CHLOROBACULUM TEPIDUM FERREDOXIN:NADP$^+$ OXIDOREDUCTASE: POTENTIOMETRIC CHARACTERISTICS AND REACTIONS WITH PROOXIDANT XENOBIOTICS
Dominykas Laibakojis, Daisuke Seo, Mindaugas Lesanavičius, Narimantas Čėnas 302

P2-81 APPLICATION OF MICROFLUIDIC TECHNOLOGY TO α-SYNUCLEIN LIQUID-LIQUID PHASE SEPARATION STUDY
Saulė Rapalytė, Dominykas Veiveris, Karolis Goda, Mantas Žiaunys, Vytautas Smirnovas, Darius Šulskis 303

P2-83 WILD BEES AND WASPS (HYMENOPTERA: ACULEATA) IN RESTORED INLAND SAND DUNES IN SOUTHEASTERN LITHUANIA
Dominykas Slančiauskas 304

P2-84 HYMENOPTERA (INSECTA) IN LARGE DIAMETER DEAD TREE TRUNKS OF DECIDUOUS TREE SPECIES IN LITHUANIA
Simonas Slančiauskas 305

P2-85 RESEARCH OF MULTIENZYMATIC FLAVIN ADENINE DINUCLEOTIDE BIOSENSOR PLATFORM
Agnė Vanagaitė, Eimantas Ramonas 306

P2-86 MOLECULARLY IMPRINTED POLYMER BASED BIOSENSOR FOR SELECTIVE DETECTION OF THE SARS-COV-2 SPIKE PROTEIN.
Artem Yerniiazov, Sharunas Zukauskas, Arunas Ramanavicius 307

P2-87 ANALYSIS OF DOPED BARIUM BORATE
Marius Dzvinka, Martynas Misevičius 308

P2-88 BISMUTH SULFIDE THIN FILM SYNTHESIS AND DEPOSITION ON FTO GLASS
Aistis Melnikas, Skirma Žalenkienė 309

P2-90 INVESTIGATION OF TIME-OF-FLIGHT RELIABILITY IN EVALUATING BIMOLECULAR RECOMBINATION IN BULK HETEROJUNCTION DEVICES
Martynas Stonkus, Kristijonas Genevičius, Romualdas Jonas Čepas 310

P2-91 MOLTEN SALT SYNTHESIS AND INVESTIGATION OF RADIOCHROMIC BARIUM APATITE
Simona Bendziute, Aleksej Zarkov 311

P2-94 EPR INVESTIGATION OF ENCAPSULATED ATOMIC HYDROGEN IN POSS CAGES FOR QUANTUM TECHNOLOGIES
Justinas Turčak, Gediminas Usevičius, Vidmantas Kalendra, Jūras Banys, George Mitrikas, Mantas Šimėnas 312

P2-95 IMPACT OF STARTING MATERIALS AND Ba^{2+} DOPING CONCENTRATION ON THE MICROSTRUCTURE AND PHASE FORMATION OF $La_2Mo_2O_9$
Ugnė Vazgelevičiūtė, Artūras Žalga, Giedrė Gaidamavičienė 313

P2-96 SUBSTRATE SPECIFICITY STUDY OF AI-GENERATED BOS TAURUS TERMINAL DEOXYNUCLEOTIDE TRANSFERASE VARIANTS
Simona Lukšytė, Roberta Statkevičiūtė, Andrius Burdulis, Taisija Dėmčėnko, Linas Zakrys, Skaistė Valinskytė, Rolandas Meškys 314

P2-97 INFLUENCE OF PROCESS CONDITIONS ON THE PYROLYTIC CONVERSION OF PLASTICS: FOCUS ON THE REACTION KINETICS AND PRODUCT DISTRIBUTION
Ieva Kiminaitė, Simon Schuler, Clara Leonie Brigitte Eckert, Vilmantė Kudelytė 315

P2-99 VIBRATIONAL SPECTROSCOPY STUDY OF ANCHOR MOLECULE STRUCTURE FOR MODEL LIPID MEMBRANES
Kamilla Kalmykova, Vaidas Pudžaitis, Martynas Talaikis 316

Poster Session 3: Biochemistry, Biophysics and Biotechnology, Biology, Genenetics and Biomedical Sciences 317

P3-1 THE EFFECT OF NOVEL HYDRAZONE DERIVATIVES ON HUMAN BRAIN, TRIPLE–NEGATIVE BREAST, AND SKIN CANCER CELL LINES
Tomas Ragauskas, Juozas Kiltinavičius, Ingrida Tumosienė, Kristina Kantminienė, Vilma Petrikaitė . . 318

P3-2 STUDY OF INNATE RESISTANCE OF HUMAN COLORECTAL CANCER CELLS
Ieva Norkaitytė, Eglė Žalytė 319

P3-3 POTENTIAL BIOMARKERS FOR PREDICTING PROGNOSIS AND TREATMENT RESPONSE IN TRIPLE-NEGATIVE BREAST CANCER (TNBC)
Domas Stitilis, Adomas Vasiliauskas, Linas Kunigenas, Monika Drobniene, Egle Strainiene, Kestutis Suziedelis 320

P3-4 MOLECULAR AND MORPHOLOGICAL DETECTION OF SARCOCYSTIS HALIETI IN MUSCLES OF RAPTORS FROM LITHUANIA
Evelina Juozaitytė-Ngugu, Tautvilė Šukytė, Dalius Butkauskas, Petras Prakas 321

P3-5 P62 PROMOTES COLORECTAL CANCER CELL SURVIVAL AND CHEMORESISTANCE
Guoda Vaitiekaitė, Andrius Jasinevičius, Aušra Sasnauskienė, Vilmantė Žitkutė 322

P3-6 SCREENING FOR NOVEL ENZYMES USING MODIFIED PURINES
Daniil Kaminskyi, Ieva Petkevičiūtė, Jaunius Urbonavičius, Daiva Tauraitė 323

P3-7 DESIGN AND MOLECULAR DOCKING STUDIES OF PYRIDINE-1,2,4-TRIAZOLE-3-THIONE DERIVATIVES AS POTENTIAL ANTICANCER DRUG CANDIDATES
Aida Šermukšnytė, Maryna Stasevych, Olena Komarovska-Porokhnyavets, Viktor Zvarych, Juozas Kiltinavičius, Simona Talačkaitė, Ingrida Tumosienė, Kristina Kantminienė 324

P3-8 HETEROLOGOUS EXPRESSION OF A CLASS II LANTHIPEPTIDE FROM PAENIBACILLUS SP. 23TSA30-6 STRAIN IN LACTOCOCCUS LACTIS
Kamilė Pozniakaitė, Nomeda Kuisienė, Rūta Kananavičiūtė 325

P3-9 SYNTHESIS OF RECOMBINANT APIS MELLIFERA ALLERGENS API M 7 AND APIM 10 IN ESCHERICHIA COLI
Aistis Navickas, Laima Čepulytė, Vytautas Rudokas, Rasa Petraitytė-Burneikienė 326

P3-10 PRODUCTION AND FUNCTIONAL ANALYSIS OF CYSTEINE-MUTATED RECOMBINANT HUMAN MITOCHONDRIAL CARBONIC ANHYDRASES CAVA AND CAVB
Austėja Frederaitė, Tautvydas Kojis, Aurelija Mickevičiūtė, Lina Baranauskienė 327

P3-11 DEVELOPMENT OF A RAPID METHOD FOR FUNCTIONAL SELECTION OF URETHANASES FROM METAGENOMIC LIBRARIES
Kristupas Volbikas, Nina Urbelienė, Rolandas Meškys 328

P3-12 APPLICATION OF SYNTHESISED GLUCOSE-6-ESTERS FOR DETERMINATION OF ESTERASE ACTIVITY
Gustė Pikturnaitė, Marius Butkevičius 329

P3-13 BIOCOMPATIBILITY EVALUATION OF POLYCAPROLACTONE-MXENE SCAFFOLDS USING HUMAN UMBILICAL VEIN ENDOTHELIAL CELLS
Rusnė Uzielaitė, Rokas Mikšiūnas, Simonas Ramanavičius, Antanas Zinovičius, Inga Morkvėnaitė-Vilkončienė, Maksym Pogorielov, Viktoriia Korniienko, Arūnas Ramanavičius 330

P3-14 ANALYSIS OF CANCER CELL MIGRATION ON COLLAGEN SCAFFOLDS
Jorė Rutkauskaitė, Ilona Uzielienė, Tadas Jelinskas, Martynas Gavutis, Alėja Marija Daugėlaitė, Džiugas Jurgutis, Ričardas Rotomskis 331

P3-15 MODIFICATION OF COLLAGEN BY REPLACING PROLINE OR HYDROXYPROLINE WITH A 2-AZABICYCLOALKANE FRAGMENT
Volodymyr Lyakh, Radosław Gaida, Elżbieta Wojaczyńska 332

P3-16 INFLUENCE OF CELL SHAPE ON MICROVISCOSITY OF LIPID DROPLETS AND PLASMA MEMBRANE IN MESENCHYMAL STEM CELLS
Jekaterina Skibickaja, Džiugas Jurgutis, Airina Mazėtytė-Godienė, Martynas Gavutis, Jelena Dodonova-Vaitkūnienė, Ramūnas Valiokas, Vitalijus Karabanovas 333

P3-17 ASSOCIATIONS OF MIR-146A-5P AND MIR-31-5P WITH NEUROINFLAMMATORY DISEASES
Ugnė Zubrickaitė, Edita Kuncevičienė, Laura Šauklytė, Evelina Gružauskienė, Paulina Vaitkienė 334

P3-18 DETERMINATION OF QUANTITATIVE COMPOSITION OF PHLORIDZIN AND CHLOROGENIC ACID IN ORNAMENTAL APPLE FRUIT SAMPLES
Samanta Petrauskaitė, Darius Ryliškis, Mindaugas Liaudanskas, Valdimaras Janulis 335

P3-19 STRUCTURE OF MOLLUSC COMMUNITIES OF IN THE SITES OF VERTIGO MOULINSIANA (DUPUY, 1849)
Guoda Petraitytė, Benediktas Jukonis, Jekaterina Havelka, Grita Skujienė 336

P3-20 LINE-1 PROMOTER ORF2 EXPRESSION AS A PREDICTIVE BIOMARKER FOR DIAGNOSING SERRATED ADENOMAS IN MALES
Rima Miknaite, Ryte Rynkeviciene, Inga Kildusiene, Auguste Kaceniene, Kestutis Suziedelis, Giedre Smailyte 337

P3-21 GENETIC MAPPING OF BARLEY TWEAKY SPIKE MUTATION
Miglė Remeikytė, Vėjūnė Pukenytė, Virginija Vaitkūnienė, Sigita Jurkonienė, Raimondas Šiukšta 338

P3-22 EPITRANSCRIPTOMIC MODIFICATIONS AS THERAPEUTIC TARGETS IN GLIOMA
Kamilė Milkintaitė, Urbanavičiūtė-Orentė Rūta 339

P3-23 DETECTION OF MEASLES VIRUS ANTIBODIES USING ENZYME-LINKED IMMUNOSORBENT ASSAY
Justina Dagytė, Indrė Lipatova, Algimantas Paulauskas 340

P3-24 REPROGRAMMING STRATEGIES: COMPARING THE EFFECTIVENESS OF MONOLAYER AND NEUROSPHERE TECHNIQUES IN MESENCHYMAL STEM CELLS DEDIFFERENTIATION INTO NEURAL STEM CELLS
Greta Žvinakytė, Vitoldas Šalašidi, Giedrius Steponaitis 341

P3-25 UNLOCKING THE ANTIOXIDANT POTENTIAL OF GREEN WASTE THROUGH SOLID-STATE KOMBUCHA FERMENTATION
Taisa Vashkevich, Vilma Kaškonienė, Audrius Sigitas Maruška 342

P3-26 MICROBIAL DIVERSITY IN FERMENTED FOOD SYSTEMS USING SHOTGUN METAGENOMIC ANALYSIS WITH SEABUCKTHORN SECONDARY RAW MATERIALS
Juozas Girtas, Ingrida Mažeikienė, Antanas Šarkinas, Karolina Almonaitytė 343

P3-30 IDENTIFICATIONOF BIOFILM FORMATION FACTORS IN CLINICAL METHICILLIN RESISTANT STAPHYLOCOCCUSAUREUS (MRSA) ISOLATES
Dorota Demjanko, Agnė Kirkliauskienė, Greta Vizujė, Jolanta Miciulevičienė, Tatjana Kirtiklienė 344

P3-31 SEARCH AND ANALYSIS OF PYRETHROID-DEGRADING MICROBIAL LIPOLYTICENZYMES
Ugnė Rickevičiūtė, Alisa Gricajeva 345

P3-32 SYNTHESIS,CHARACTERIZATION, AND PROPERTY PREDICTION OF 1-(5-CHLOROPYRIDIN-2-YL)-N-(4-SUBSTITUTED BENZYLIDENE)-5-OXOPYRROLIDINE-3-CARBOHYDRAZIDES
Simona Talačkaitė, Aida Šermukšnytė, Kristina Kantminienė, Ilona Jonuškienė, Ingrida Tumosienė . . 346

P3-33 MULTIPLEXED EPIGENETIC PROFILING WITH Mx-TOP: A NOVEL METHOD FOR CHROMATIN AND DNA MODIFICATION ANALYSIS
Kotryna Kvederavičiūtė, Kotryna Skardžiūtė, Inga Pečiulienė, Janina Ličytė, Milda Narmontė, Saulius Klimašauskas, Edita Kriukienė 347

P3-34 CONSTRUCTION OF BACTERIOPHAGE GENOMIC DNA FRAGMENT LIBRARIES
Miglė Plioplytė, Jonas Juozapaitis, Giedrius Sasnauskas 348

P3-35 INTERACTION SURFACES WITHIN THE TYPE I-F CRISPR-CAS EFFECTOR COMPLEX
Toma Liegutė, Inga Songailienė, Tomas Šinkūnas 349

P3-36 HETEROLOGOUS EXPRESSION OF GRTB, A PREDICTED COLLAGEN-LIKE PROTEIN OF GRANULICELLA TUNDRICOLA MP5ACTX9T
Rosita Kavaliauskaitė, Rūta Kananavičiūtė . . . 350

P3-37 STUDY OF TYPE IV-A2 CRISPR-CAS SYSTEMS
Gintarė Žvejytė, Rimvydė Čepaitė, Patrick Pausch . . . 351

P3-38 DEVELOPMENT OF HYPOALLERGENIC VARIANTS OF COMMON MUGWORT ALLERGEN COMPONENT ART V 3
Eva Kupetytė, Laima Čepulytė, Rasa Petraitytė-Burneikienė . . . 352

P3-39 THE SPECIFICITY OF THE STREPTOCOCCUS PNEUMONIAE TOXIN PNEUMOLYSIN FOR LIPID BILAYER COMPOSITION
Adelė Unikauskaitė, Tadas Ragliauskas . . . 353

P3-40 SINGLE-CELL HIGH-THROUGHPUT RT-PCR ANALYSIS OF PFA FIXED PROKARYOTIC SAMPLES
Laura Kuliešytė, Greta Leonavičienė, Linas Mažutis . . . 354

P3-41 OLOKUN - A NOVEL PROKARYOTIC ANTIPHAGE DEFENSE SYSTEM
Vincentas Raudys, Viktorija Rainytė, Edvinas Jurgelaitis, Paulius Toliušis, Mindaugas Zaremba . . . 355

P3-42 DEVELOPMENT OF THE BACTERIAL AMIDOHYDROLASE YQFB TO IMPROVE ITS BIOTHERAPEUTIC APPLICATIONS
Kamilė Dzisevič, Viktorija Preitakaitė, Rolandas Meškys . . . 356

P3-43 SINGLE-CELL ISOLATION USING SEMI-PERMEABLE CAPSULES: MARKER GENE DETECTION AND CELL CULTIVATION ANALYSIS
Aina El Ravvas, Linas Mažutis . . . 357

P3-44 RECOMBINANT β-CARBONIC ANHYDRASE PROTEINS PRODUCTION
Eglė Lukauskaitė, Tautvydas Kojis, Justinas Babinskas, Ieva Gaubė, Lina Baranauskienė, Inga Matijošytė 358

P3-45 EXPANDING THE ARSENAL: FIRST PEEK AT A NOVEL TYPE III CRISPR-CAS EFFECTOR
Marija Duchovskyte, Dalia Smalakyte, Irmantas Mogila, Gintautas Tamulaitis . . . 359

P3-46 DISASSEMBLY AND REASSEMBLY OF L-A VIRUS-LIKE PARTICLES PURIFIED FROM SACCHAROMYCES CEREVISIAE
Kamilė Vaišaitė, Enrika Celitan, Saulius Serva . . . 360

P3-47 SYNTHESIS OF RECOMBINANT ARTEMISIA VULGARIS ALLERGEN ART V 3 IN DIFFERENT YEAST EXPRESSION SYSTEMS
Emilija Dobrovolskytė, Laima Čepulytė, Paulius Lukas Tamošiūnas, Rasa Petraitytė-Burneikienė . . . 361

P3-48 CLONING, EXPRESSION AND FUNCTIONAL ANALYSIS OF RECOMBINANT LIPOXYGENASE
Vytautė Blekaitytė, Dovilė Daunoraitė, Inga Matijošytė . . . 362

P3-49 BIOCHEMICAL CHARACTERIZATION OF ARGONAUTE PROTEINS XAUSPARDA AND EAESPARDA CONTAINING NUCLEASE EFFECTOR DOMAIN
Edvinas Jurgelaitis, Arunas Silanskas, Mindaugas Zaremba . . . 363

P3-50 CHARACTERIZATION OF HYBRID CLASS 1 AND CLASS 2 CRISPR-CAS SYSTEMS
Brigita Duchovska, Tomas Šinkūnas, Tautvydas Karvelis . . . 364

P3-52 STUDY OF SPLIT pAGOS AND THE ACTIVITY OF THEIR ASSOCIATED HEPN EFFECTORS IN E. COLI
Rokas Bružaitis, Edvardas Golovinas, Mindaugas Zaremba . . . 365

P3-53 OPTIC NEURITIS: EXPLORING GENETIC ASSOCIATIONS OF EXOC3L1 AND TNF IN THE LITHUANIAN POPULATION
Auguste Simanonyte, Rusne Lapienyte, Kriste Kaikaryte, Rasa Liutkeviciene . . . 366

P3-54 STUDIES ON ANTIOXIDANT ACTIVITY AND PHYTOCHEMICAL COMPOUNDS IN FLAX (LINUM USITATISSIMUM L.) CALLUS CULTURES IN VITRO
Judita Zeiderytė . . . 367

P3-55 ASSOCIATIONS BETWEEN COPY NUMBER VARIATIONS OF α-AMYLASE AND TEETH LOSS IN INDIVIDUALS WITH INTELLECTUAL DISABILITY
Neringa Meilutė, Indrė Stankevičienė, Kristina Daniūnaitė . . . 368

P3-56 DNA ISOLATION FROM HERBARIUM SPECIMENS: A COMPARISON OF DIFFERENT METHODS
Viktorija Dolotova, Jurgita Butkuvienė . . . 369

P3-57 HEAVY METAL BIOACCUMULATION CAPACITY IN PROTOZOA - TETRAHYMENA TERMOPHILA
Mindaugas Matijūnas, Remigijus Ivanauskas . . . 370

P3-58 EXPLORING ENZYMATIC POLYURETHANE DEGRADATION BY A URETHANE BOND HYDROLYSING ENZYME FROM LYSINIBACILLUS SP.
Eglė Gečaitė, Jokūbas Krutkevičius, Inga Matijošytė . . . 371

P3-59 FORMULATION OF BIOMIMETIC LIPID BASED NANOPARTICLES FOR CRISPR/CAS9 DELIVERY
Kamilė Bužinskytė, Evelina Jankaitytė, Rima Budvytytė . . . 372

P3-60 SCREENING AND CHARACTERIZATION OF PSYCHROPHYLIC XYLANOLYTIC BACTERIA
Kamilia Mikelevič, Nomeda Kuisienė . . . 373

P3-61 THE IMPACT OF DIFFERENT ORIGINS AND CONCENTRATIONS MICROPLASTICS ON SOIL AND BUCKWHEAT (FAGOPYRUMESCULENTUM L.) CARBON AND NITROGEN
S. Dreskinienė, M. Vilkienė, K. Barčauskaitė . . . 374

P3-62 SERCH, PURIFICATION AND ANALYSIS OF PYRETHROIDS-DEGRADING AND OTHER BIOTECHNOLOGICALLY APPLICABLE LIPOLYTIC ENZYMES
Jūratė Udraitė, Ugnė Rickevičiūtė, Alisa Gricajeva . . . 375

P3-63 CYANOPHAGE-INDUCED TRANSCRIPTIONAL CHANGES IN RAPHIDIOPSIS RACIBORSKII
Vaiva Slatkevičiūtė, Barbara Klimczak, Gediminas Azlbutas, Adam Antosiak, Petras Venckus, Hanna Zkukava, Natalija Kazlauskienė, Sarit Avrani, Dariusz Dziga, Sigitas Šulčius . . . 376

P3-64 REMOTE SENSING ANALYSIS OF VEGETATION COVER DYNAMICS AS AN INDICATOR OF EVOLUTIONARY TRENDS OF THE SUKHA SPIT (KINBURN PENINSULA, BLACK SEA, UKRAINE)
Yuliia Shevchuk, Oleksiy Davydov . . . 377

P3-65 REGULATION OF LARGE TERMINASESUBUNIT NUCLEASE ACTIVITY BY THE PORTAL PROTEIN IN NOVEL JUMBO PHAGE KLEB27-3
Miglė Šarpilo, Ayush Kumar Ganguli, Algirdas Toleikis . . . 378

P3-66 FUNCTIONAL ANALYSIS OF SMALL REGULATORY RNA SLLM1238 IN LACTOCOCCUS LACTIS
Naglis Mykolas Pakštys, Oskaras Safinas, Kotryna Kvederavičiūtė, Milda Mickutė, Janina Ličytė, Giedrius Vilkaitis . . . 379

P3-67 HIGH-THROUGHPUT KINETIC PROFILING OF RNA-GUIDED NUCLEASES FOR PRECISION GENOME EDITING
Marius Vinogradovas, Gytis Druteika, Lina Krikščikaitė, Arūnas Šilanskas, Tautvydas Karvelis, Stephen Knox Jones Jr. . . . 380

P3-68 CHARACTERIZATION OF A NOVEL PROTEIN OF THE BACTERIAL ANTIVIRAL DEFENSE SYSTEM THOERIS
Ugnė Andrijauskaitė, Arūnas Šilanskas, Giedrė Tamulaitienė . . . 381

P3-69 STUDY OF INTERACTION BETWEEN SHORT PAGOS AND RNA CHAPERONE HFQ USING NAD^+ DETECTION
Jokūbas Šiaučiūnas, Evelina Zagorskaitė, Edvinas Jurgelaitis, Mindaugas Zaremba . . . 382

P3-70 UNCOVERING NEW PROKARYOTIC ANTIVIRAL DEFENSE SYSTEMS: PD-T4-1, PD-T7-1, AZACA AND MOKOSH I
Viktorija Rainytė, Paulius Toliušis, Mindaugas Zaremba . . . 383

P3-71 COMPREHENSIVE ANALYSIS OF M6A AND M5C RNA METHYLATION PROFILES IN GLIOMAS
Samanta Tamašuitytė, Rūta Urbanavičiūtė-Orentė . . . 384

P3-72 CHARACTERIZATION OF DesR-DEPENDED VANILLIC AND SYRINGIC ACIDS-INDUCIBLE SYSTEM FROM SPHINGOBIUM SP.SYK-6
Miglė Loveikytė, Naglis Malys, Ernesta Augustienė . . . 385

P3-73 EXPLORING SOYBEAN-MICROORGANISM INTERACTIONS THROUGH STABLE ISOTOPE ANALYSIS
Raminta Skipitytė, Rūta Barisevičiūtė, Monika Toleikienė . . . 386

P3-74 DETERMINATION OF QUANTITATIVE COMPOSITION OF α-AMYRIN AND MASLINIC ACID IN PRUNUS DOMESTICA L. FRUIT SAMPLES
Augustė Adomaitytė, Mindaugas Liaudanskas, Rima Šedbarė, Juozas Lanauskas, Darius Kviklys, Jonas Viškelis, Pranas Viškelis, Valdimaras Janulis 387

P3-75 BIOCONTROL CAPABILITIES OF ENDOPHYTIC FUNGI DERIVED FROM SCOTS PINE AGAINST NEEDLE CAST
Milana Šilanskienė, Dorotėja Vaitiekūnaitė, Vaida Sirgedaitė-Šėžienė 388

P3-76 DIVERSITY OF INSECTS (INSECTA) IN DECAYING DEAD WOOD PARTIALLY SUBMERGED IN WATER
Austėja Černiauskaitė, Virginija Podėnienė, Jekaterina Havelka 389

P3-77 DETERMINATION OF QUALITATIVEAND QUANTITATIVE COMPOSITION OF PHENOLIC COMPOUNDS IN RAPESEED HONEY SAMPLES
Ernesta Zaksaitė, Mindaugas Liaudanskas, Sonata Trumbeckaitė, Vaidotas Žvikas 390

P3-78 ENVIRONMENTAL IMPLICATIONS OF DIVERSE RHIZOSPHERIC COMMUNITIES OF BACTERIA FOR NATURAL WEED SUPPRESSION ALONGSIDE CROP GROWTH STIMULATION
Tasawar Abbas 391

P3-79 EFFECT OF AGING ON THE STRUCTURAL PARAMETERS OF A BIODEGRADABLE SENSOR MADE FROM SEAWEED
Ujjawal Malani, Uldis Zaimis, Jurate Jolanta Petroniene, Andrius Dzedzickis, Vytautas Bucinskas . . . 392

P3-80 THE EFFECT OF LACTICASEIBACILLUS CASEI CELL-FREE SUPERNATANT ON DECIDUALIZATION OF ENDOMETRIUM STROMAL CELLS
Saulė Dominyka Bučiūnaitė, Elvina Valatkaitė, Rūta Navakauskienė 393

P3-81 TIME-DEPENDENT EFFECTS ON MITOCHONDRIAL FUNCTIONS INDUCED BY PSORIASIS-LIKE INFLAMMATION IN HUMAN KERATINOCYTES AND FIBROBLASTS
Martyna Uldukytė, Gabrielė Kulkovienė, Ramunė Morkūnienė, Aistė Jekabsone 394

P3-82 MATERNAL HIGH-FAT DIET EFFECT ON THE OFFSPRINGS RETINAL INFLAMMATORY RESPONSE
Patricija Čepauskytė, Gintarė Urbonaitė, Neda Ieva Biliūtė, Guoda Laurinavičiūtė, Urtė Neniškytė . . . 395

P3-83 MICROGRAVITY AND YEAST RESISTANCE TO MANDELIC ACID: EXPLORING THE CONNECTION WITH TELOMERE LENGTH
Ugnė Juodviršytė, Eglė Lastauskienė 396

P3-84 INVESTIGATION OF THE EFFECTS OF TRANSCRANIAL MAGNETIC STIMULATION IN A DIFFERENTIATED SH-SY5Y CELL MODEL
Deimilė Asipavičiūtė, Aistė Zentelytė, Vladas Valiulis, Rūta Navakauskienė, Giedrė Valiulienė 397

P3-85 RESEARCH OF ANEXIN A4 INFLUENCE ON PLASMA MEMBRAIN PERMABILIZATION DYNAMICS AND CELL VIABILITY AFTER ELECTROPORATION
Augustinas Andziuslis, Baltramiejus Jakštys, Saulius Šatkauskas 398

P3-86 OXIDATION AND CROSS-INTERACTIONS AS KEY MODULATORS OF S100A1 PROTEIN AGGREGATION
Viktorija Karalkevičiūtė, Ieva Baronaitė, Vytautas Smirnovas, Darius Šulskis 399

P3-87 PRODUCTION OF THEORETICAL TTV CAPSID PROTEIN IN E. COLI
Gabija Klimavičiūtė, Uršulė Simonaitytė, Martynas Simanavičius 400

P3-88 ELECTROCHEMICAL ANALYSIS OF ENSIFER MELILOTI USING DIVERSE REDOX MEDIATORS FOR MFC APPLICATIONS
Asta Bubnelytė, Tomas Mockaitis, Ingrida Bružaitė, Inga Morkvėnaitė-Vilkončienė 401

P3-89 ISOLATION AND PURIFICATION OF ASCORBATE OXIDASE FROM THE APPLE.
Patrycija Kostiukevič, Jolanta Sereikaitė 402

P3-90 STUDY OF XYLOSE TRANSPORT IN MODIFIED OGATAEA POLYMORPHA YEAST DURING ALCOHOLIC FERMENTATION
Tomas Stanevičius, Tomas Nenartavičius, Andryi Sibirny, Rimantas Daugelavičius 403

P3-91 THE POTENTIAL OF WASTE VEGETABLE OIL IN GHANA FOR BIODIESEL PRODUCTION
Felix Nkansah Buabeng 404

P3-92 PHYSICOCHEMICAL PROPERTIES OF NISIN AND K2 TOXIN-LOADED FUCOIDAN PARTICLES
Aistė Galinskaitė, Rūta Gruškienė, Tatjana Kavleiskaja, Jolanta Sereikaitė . . . 405

P3-93 THE INFLUENCE OF THE MEDIUM PH ON THE EFFICIENCY OF NYSTATIN ON CANDIDA YEAST
Eglė Vansevičiūtė, Tomas Stanevičius, Rimantas Daugelavičius . . . 406

P3-94 PROTEOLYTIC STABILITY OF NISIN DELIVERY SYSTEMS AGAINST PROTEASE FROM RHIZOPUS CHINENSIS
Agnė Česnulevičiūtė, Rūta Gruškienė . . . 407

P3-95 ENGINEERING YEAST SURFACE DISPLAY SYSTEM FOR EXPRESSION OF ESTERASE FROM GEOBACILLUS STEAROTHERMOPHILUS
Viktorija Kurpickaja, Arūnė Verbickaitė, Rasa Petraitytė-Burneikienė . . . 408

P3-96 SYNTHESIS OF HYDRAZONES FROM 3-(4-ETHOXYPHENYL)AMINOPROPANEHYDRAZIDE AND EVALUATION OF THEIR BIOLOGICAL ACTIVITY IN SILICO
Juozas Kiltinavičius, Aida Šermukšnytė, Kristina Kantminienė, Ilona Jonuškienė, Ingrida Tumosienė . . 409

P3-97 CYTOTOXICITY OF ANTIBACTERIAL TUNGSTEN TRIOXIDE NANOPARTICLE-COATED TEXTILES ON HUMAN UMBILICAL VEIN ENDOTHELIAL CELLS (HUVEC) IN VITRO
Laura Kairytė, Raminta Rodaitė, Agnė Giedraitienė, Modestas Ružauskas, Rita Šiugždinienė, Šarūnas Varnagiris, Darius Milčius . . . 410

P3-98 INVESTIGATION OF INFLAMMATORY RESPONSE PATHWAY - INFLAMMASOME ACTIVATION
Viltė Mataraitė, Milda Norkienė, Asta Lučiūnaitė . . . 411

P3-99 EVALUATION OF PHYTOCHEMICALS AND BIOACTIVITY IN BROCCOLI (BRASSICA OLERACEA VAR. ITALICA) CALLUS CULTURES IN VITRO
Paulina Lukošiūtė . . . 412

Poster Session 4: Chemistry and Chemical Physics 413

P4-1 EXPLORING THE SYNTHESIS OF NOVEL BENZIMIDAZOTHIAZINES AS POTENTIAL AMYLOID AGGREGATION MODULATORS
Urtė Milerytė, Rita Bukšnaitienė, Ieva Žutautė . . . 414

P4-2 SYNTHESIS AND BIOLOGICAL EVALUATION OF NOVEL SULFANILAMIDE DERIVATIVES
Valdas Vainauskas, Vytautas Mickevičius, Birutė Grybaitė . . . 415

P4-3 SYNTHESIS AND BIOLOGICAL ACTIVITY OF 2-SUBSTITUTED-N-HETEROARYLACETAMIDES
Gabrielė Juraitytė, Austėja Šakalytė, Algirdas Šačkus, Ingrida Šatkauskienė, Vida Malinauskienė . . . 416

P4-4 SYNTHESIS OF POTENTIAL PROLIFERATING CELL NUCLEAR ANTIGEN INHIBITORS
Simona Jonušienė, Mantas Jonušis, Denis Sokol . . . 417

P4-5 5-HETEROARYL-1,3,4-OXADIAZOL-2-THIOLS:SYNTHESIS, ALKYLATION, ACYLATION AND BIOTESTING
Roberta Kuneikytė, Ieva Bartkevičiūtė, Algirdas Šačkus, Vilija Kederienė, Vida Malinauskienė, Asta Žukauskaitė . . . 418

P4-6 SYNTHESIS AND INVESTIGATION OF CONDENSED SYSTEMS WITH PYRAZOLE SCAFFOLD
Povilas Viltrakis, Eglė Arbačiauskienė, Algirdas Šačkus, Vilija Kederienė . . . 419

P4-7 SYNTHESIS OF NEW 4-PHENYL-1-(3,4,5-TRIMETHOXYPHENYL)-1H-IMIDAZOLE-2-THIOLDERIVATIVES
B. Grybaitė, A. Starkauskaitė, V. Mickevičius . . . 420

P4-8 SYNTHESIS OF PHOSPHORUS-CONTAINING POLYESTERS OF L-GLUTAMIC ACID AND THEIR COMPLEXES WITH ANTIBIOTICS
Yaryna Kuryshchuk, Diana Varchuk, Zoriana Nadashkevych, Anna Stasiuk . . . 421

P4-9 SYNTHESIS OF NEW 3-SUBSTITUDED-6-BROMOBENZOXAZOLIN-2-ONE DERIVATIVES
Monika Bertašiūtė, Vytautas Mickevičius, Birutė Grybaitė . . . 422

P4-10 SYNTHESIS OF TARGETED 4-(7H-IMIDAZO(2,1-b)(1,3)THIAZIN-5-YL)ANILINE DERIVATES
Polina Pylskaja, Martyna Paulauskaitė, Ieva Žutautė . . . 423

P4-11 SYNTHESIS AND MODIFICATION OF ETHYL 2-(2-(-7H-IMIDAZO(2,1-b)(1,3)THIAZIN-5-YL)PHENOXY)ACETATE FOR AMYLOID AGGREGATION INHIBITION
Fausta Kairytė, Indrė Misiūnaitė-Vaškevičienė, Ieva Žutautė 424

P4-12 SYNTHESIS OF A NEW GENERATIONOF HSP90 INHIBITORS CONTAINING A BENZIMIDAZOLE-RESORCINOL MOIETY
Vilius Petraška, Ieva Žutautė, Algirdas Brukštus 425

P4-13 SYNTHESIS OF NEW 1-(NAPHTHALEN-1-YL)-4-PHENYL-1H-IMIDAZOLE-2-THIOL DERIVATIVES
Aistė Starkauskaitė, Birutė Grybaitė, Vytautas Mickevičius 426

P4-14 COMPUTATIONAL STUDY OF ELECTRONIC SPECTRA AND STRUCTURE OF RETINOIDS
Julius Ažukas, Žyginta Murnikova, Kęstutis Aidas 427

P4-15 SYNTHESIS OF MODULAR AND FUNCTIONALIZABLE SUPRAMOLECULAR CAVITANDS
Nojus Radzevičius, Eivydas Trioška, Edvinas Orentas 428

P4-16 STUDY OF THE OPTICAL PROPERTIES OF THE COMPLEX OF CARBON-BASED QUANTUM DOTS AND COMPOUNDS WITH ANTICANCER PROPERTIES
Martynas Zalieckas, Nikita Belko, Hanna Maltanava, Polina Kuzhir, Renata Karpicz 429

P4-17 ACOST-EFFECTIVE NiZn/Ti EIECTROCATALYST FOR EFFICIENT HYDROGEN EVOLUTION AND OXYGEN EVOLUTION REACTIONS
Tripura Ganti, Aldona Balčiūnaitė, Jūrate Vaičiūnienė, Loreta Tamašauskaitė-Tamašiūnaitė, Eugenijus Norkus 430

P4-18 NICKEL COBALT CATALYSTS FOR HYDROGEN GENERATION
Gitana Valeckytė, Zita Sukackienė, Jūratė Vaičiūnienė, Loreta Tamašauskaitė-Tamašiūnaitė, Eugenijus Norkus 431

P4-19 NON-PRECIOUS METAL ELECTROCATALYSTS FOR THE OVERALLWATER SPLITTING: SYNTHESIS, CHARACTERIZATION AND PROPERTIES
Huma Amber, Aldona Balčiūnaitė, Loreta Tamašauskaitė-Tamašiūnaitė, Jūratė Vaičiūnienė, Eugenijus Norkus 432

P4-20 APPLICATION OF FLEXIBLE NICKEL-IRON CATALYSTS FOR WATER SPLITTING REACTIONS
Dmytro Shyshkin, Loreta Tamasauskaite-Tamasiunaite, Aldona Balciunaite 433

P4-21 ADVANCED 3D BIMETALLIC NICKEL-IRON/TITANIUM BIFUNCTIONAL ELECTROCATALYSTS FOR EFFECTIVE HYDROGEN EVOLUTION REACTION IN ACIDIC MEDIA
Shahid Nawaz, Aldona Balčiūnaitė, Loreta Tamašauskaitė-Tamašiūnaitė, Eugenijus Norkus 434

P4-22 A COMPARATIVE STUDY OF HYDROGEN EVOLUTION REACTION PERFORMANCE BY NON-NOBLE TRANSITION METAL-BASED 3D ELECTROCATALYSTS TOWARDS ALKALINE WATER SPLITTING
Sukomol Barua, Aldona Balčiūnaitė, Jūratė Vaičiūnienė, Loreta Tamašauskaitė-Tamašiūnaitė, Eugenijus Norkus 435

P4-23 SUSTAINABLE NICKEL-DOPED NITROGEN-ENRICHED BIOMASS-DERIVEDCARBON CATALYSTS FOR HYDRAZINE FUEL CELLS
Virginija Ulevičienė, Aldona Balčiūnaitė, Daina Upskuvienė, Galina Dobele, Aleksandrs Volperts, Ance Plavniece, Aivars Zhurinsh, Loreta Tamašauskaitė-Tamašiūnaitė, Eugenijus Norkus 436

P4-24 CATHODE CATALYST SELECTION FOR ENHANCING OXYGEN REDUCTION REACTION OF FUEL CELLS: GR/Cu, Co_3 O_4-NC/GR/Cu, AND Co_3O_4-Cr_2O_3-NC/GR/Cu
Karina Vjūnova, Loreta Tamašauskaitė-Tamašiūnaitė 437

P4-25 SYNTHESIS OF PHENOTHIAZINE DERIVATIVES EXHIBITING VERY LONG ROOM TEMPERATURE PHOSPHORESCENCE
Paulius Vaickūnas, Jonas Žurauskas, Vilius Stankevičius, Steponas Raišys, Karolis Kazlauskas, Edvinas Orentas 438

P4-26 INVESTIGATION OF CHROMIUM EMISSION IN THE NIR REGION OF YAG AND YLuAG BY CHANGING Cr^{3+} CONTENT IN THE HOST MATRIX
Nerija Ričkutė, Greta Inkrataitė 439

P4-27 SPECTROSCOPIC STUDY OF FREE-BASE MESO-TETRAPHENYLPORPHYRIN AND HEXAGONAL BORON NITRIDE VAN DER WAALS COMPLEX
Jelizaveta Fedotova, Ivan Halimski, Martynas Talaikis, Renata Karpicz, Jevgenij Chmeliov, Patrizia Lamberti, Maksim Shundalau 440

P4-28 LUMINESCENT PROPERTIES OF RARE-EARTH DOPED $NaAlGeO_4$ PHOSPHORS
Gabija Janušauskaitė, Martynas Misevičius 441

P4-29 SYNTHESIS AND PROPERTIES OF (9-FLUORENYLIDENE)MALONONITRILE DERIVATIVES AS ELECTRON TRANSPORTING MATERIALS
Julius Petrulevičius, Marytė Daškevičienė, Giedrė Bubnienė, Giedrius Juška, Vygintas Jankauskas, Vytautas Getautis 442

P4-30 SYNTHESIS AND OPTICAL PROPERTIES OF Mn^{5+} -DOPED $Sr_5(PO_4)_3F$
Jonas Stadulis, Arturas Katelnikovas, Aleksej Zarkov 443

P4-31 THE SOL-GEL SYNTHESIS AND CHARACTERIZATION OF $Y_{2.97-x}Na_xTb_{0.03}Al_5O_{12}$ garnets
Diana Vistorskaja, Arturas Katelnikovas, Gintautas Tamulaitis, Aivaras Kareiva 444

P4-32 CHARACTERIZATION OF OPTICAL AND MECHANICAL PROPERTIES OF $Ti_3C_2T_x$ MXENE THIN FILMS
Miglė Stančiauskaitė, Justina Anulytė, Simonas Ramanavičius, Ernesta Bužavaite-Vertelienė, Zigmas Balevičius, Ieva Plikusienė 445

P4-33 PHYSICAL AND CHEMICAL CHARACTERISTICS OF MICROPLASTIC PARTICLES IN LITHUANIANS SCHOOLS PREMISES
Tomas Stonkus, Ieva Uogintė, Steigvilė Byčenkienė 446

P4-34 POTENTIAL APPLICATION OF BUCKWHEAT HULL FOR EFFICIENT BIOSORPTION OF CADMIUM FROM AQEUOUS MEDIA: AN INSIGHT INTO THE SORPTION KINETIC, EQUILIBRIUM AND THERMODYNAMIC STUDIES
Tayyab Tahir, Rūta Druteikienė, Zita Žukauskaitė, Jūratė Vaičiūnienė 447

P4-35 A MACHINE LEARNING FRAMEWORK FOR AIR POLLUTION MODELING USING SATELLITE DATA AND URBAN SPATIAL FEATURES IN VILNIUS
Mehri Davtalab, Steigvilė Byčenkienė 448

P4-36 SOURCE APPORTIONMENT OF AEROSOL PARTICLES BY POSITIVE MATRIX FACTORIZATION IN URBAN BACKGROUND ENVIRONMENT (VILNIUS, LITHUANIA)
Viachaslau Alifirenka, Vitalij Kovalevskij, Mindaugas Gaspariūnas, Mindaugas Bernatonis, Steigvilė Byčenkienė 449

P4-37 SYNTHESIS AND APPLICATION OF $Ti_3C_2T_X$ MXENES FOR DRINKING WATER QUALITY ASSESSMENT
Kristina Sobol, Almira Ramanaviciene, Simonas Ramanavicius 450

P4-38 EXPLORING THE INFLUENCE OF BIOMASS BURNING ON ATMOSPHERIC AEROSOLS THROUGH ISOTOPIC ANALYSIS
Durre Nayab Habib, Andrius Garbaras, Agnė Mašalaitė-Nalivaikė 451

P4-39 STUDY ON THE KINETICS AND ISOTHERMS OF SORPTION OF MICROPLASTICS AND LIGNIN NANOMATERIALS
Austėja Burbulytė, Ieva Uogintė 452

P4-40 REMOVAL OF MICROPLASTICS FROM WATER USING A CATIONIC STARCH FLOCCULANT
Klaudija Cerkaite, Joana Bendoraitiene 453

P4-41 APPLICATION OF MAGNETIC BIOPOLYMERS FOR WATER PURIFICATION RADIONUCLIDES AND HEAVY METALS
Sergej Šemčuk, Galina Lujanienė, Kęstutis Jokšas, Karina Kuzborskaja, Vidas Pakštas, Kęstutis Mažeika, Martynas Talaikis, Jonas Mažeika, Živilė Jurgelėnė 454

P4-42 THE IMPACT OF ISOPROPANOL TREATED SPENT COFFEE GROUNDS ON VARIOUS PROPERTIES OF BUILDING GYPSUM
Neringa Matutytė, Nora Kybartienė 455

P4-43 ONE-POT APTES GRAFTED SILICA SYNTHESIS AND MODIFICATION WITH AGNP
Gerardas Laurinavičius, Vilius Poškus 456

P4-44 ASSUMPTIONS FOR MODELING NITROGEN BIOFERTILIZER GRANULATION
Dovilė Oksaitė, Rasa Šlinkšienė 457

P4-45 THE USE OF COFFEE SILVERSKIN PARTICLES AS FILLERS IN CELLULOSE ACETATE BASED BIOPLASTICS
Laurynas Lukomskis, Laura Peciulyte, Ramune Rutkaite 458

P4-46 INFLUENCE OF RAW MATERIAL ORIGIN ON THE CONCENTRATION OF NITROGEN, PHOSPHORUS AND POTASSIUM IN BULK ORGANIC FERTILIZERS
Gabija Aleksaitytė, Odeta Pocienė, Rasa Šlinkšienė 459

P4-47 LIQUID NITROGEN-CALCIUM-MAGNESIUM FERTILIZER WITHEXTRACT FROM BIODEGRADABLE MATERIALS
Eglė Didžiulytė, Rasa Šlinkšienė 460

P4-48 SYNTHESIS ANDSTUDY OF THE PROPERTIES OF POLYMER HYDROGEL AS A COMPONENT OF FIRE-RESISTANT POLYMER-MINERAL (HYBRID) HYDROGEL
Diana Varchuk, Serhiy Tsykunkov, Olha Maikovych, Nataliya Nosova, Serhiy Varvarenko 461

P4-49 APPLICATION AND OPTIMIZATION OF LIQUIDCHROMATOGRAPHY METHOD FOR THE STUDY OF CORDYCEPIN AND ITS DERIVATIVES
Ąžuolas Ivickas, Evaldas Naujalis, Simonas Balčiūnas 462

P4-50 OPTIMIZATION OF SOLID-PHASE EXTRACTION FOR THE ANALYSIS OF SEDATIVE-HYPNOTIC DRUGS IN BIOLOGICAL SAMPLES
Nerijus Karlonas 463

P4-52 STUDY OF WUPyV VIRUS-LIKE PARTICLES IMMUNE COMPLEX FORMATION WITH MONOCLONAL ANTIBODIES BY SPECTROSCOPIC ELLIPSOMETRY AND QUARTZ CRYSTAL MICROBALANCE WITH DISSIPATION
Silvija Juciutė, Asta Lučiūnaitė, Vincentas Mačiulis, Ieva Plikusienė 464

P4-53 EFFECT OF ELECTRODE POTENTIAL ON ELECTROCHEMICAL IMPEDANCE SPECTRA OF TETHERED-BILAYER LIPID MEMBRANES ON FLUORINE-DOPED TIN OXIDE
Narvydas Dėnas, Kipras Eigminas, Aušra Valiūnienė 465

P4-54 MICROFLUIDIC CHIP FABRICATION FOR THE DEVELOPMENT OF A NERVE-ON-CHIP MODEL
Kamilė Kasperavičiūtė, Arūnas Stirkė, Wanessa Melo, Eivydas Andriukonis 466

P4-55 DEVELOPMENT AND INVESTIGATION OF IN-SITU NMR PROBE
Aurimas Dubauskas, Jurgis Pilipavičius, Linas Vilčiauskas, Vytautas Klimavičius 467

P4-56 SHROOM CLUES: WHAT STABLE ISOTOPES REVEAL ABOUT FUNGI
Justina Stonytė, Aistė Tuzinaitė, Giedrė Keen Motuzaitė Matuzevičiūtė, Rasa Pauliukaitė 468

P4-57 SURFACE PLASMON RESONANCE IMMUNOSENSOR FOR DETECTION OF SARS-COV-2 ANTI-RBD ANTIBODIES
Agne Giniunaite, Almira Ramanaviciene, Asta Kausaite-Minkstimiene 469

P4-58 ELECTROCHEMICAL FORMATION AND EVALUATION OF POLYPYRROLE LAYER FOR DEVELOPMENT OF MOLECULARLY IMPRINTED POLYMER
Domas Pirstelis, Ernestas Brazys, Vilma Ratautaite, Arunas Ramanavicius 470

P4-59 PEI-DERIVED LASER-INDUCED GRAPHENE FOR ZINC ELECTROCHEMICAL SENSING: EFFECT OF LASER WAVELENGTH ON MORPHOLOGY AND ELECTROCHEMICAL PERFORMANCE
Pamela Rivera, Šarūnas Mickus, Aivaras Sartanavičius, Romualdas Trusovas, Rasa Pauliukaite 471

P4-60 Au-MXENE HETEROSTRUCTURE FOR THE COLORIMETRIC SENSING OF BIOMOLECULES
Saqib Ali, Veronika Zahorodna, Oleksiy Gogotsi, Arunas Ramanavicius, Simonas Ramanavicius 472

P4-61 DEVELOPMENT OF GLUCOSE BIOSENSORS USING GLUCOSE OXIDASE AND NANOPARTICLE-MODIFIED ELEKCRTRODES
Rugilė Blauzdžiūnaitė, Antanas Zinovičius 473

P4-62 APPLICATION OF PtCo NANOZYMES IN THE DEVELOPMENT OF AN AMPEROMETRIC GLUCOSE BIOSENSOR
Aistė Krikštaponytė, Asta Kaušaitė-Minkštimienė 474

P4-63 DOSY INVESTIGATION OF BIOACTIVE IONIC LIQUIDS
Lukas Mikalauskas, Vytautas Klimavičius 475

P4-64 SYNTHESIS OF NEW IMIDAZOLE-2-THIOLES CONTAINING CARBAZOLYL MOIETY
Tomas Tutkus, Birutė Sapijanskaitė-Banevič 476

P4-65 MAGNETIC-CONTROLLED HYDROGELS BASED ON POLYESTER-TYPE PSEUDO-POLYAMINOACIDS
Yuliia Kyrychuk, Roman Taras, Volodymyr Samaryk, Yaryna Kuryshchuk 477

P4-66 SYNTHESIS AND CHARACTERIZATION OF CROSS-LINKED COPOLYMERS BASED ON DEXTRIN AND POLY(N-ISOPROPYLACRYLAMIDE)
Emilija Morkvėnaitė, Miglė Savickė, Dovilė Liudvinavičiūtė, Ramunė Rutkaitė 478

P4-67 THE CREATION OF POROUS HYDROGELS USING PEROXIDES
Yuliia Cherkas, Nataliia Bukartyk, Solomiia Kapatsila, Serhiy Tsykunkov, Volodymyr Samaryk 479

P4-68 EFFECT OF CALCIUM IONS STRUCTURING METHODS ON THE PHYSICAL AND MECHANICAL PROPERTIES OF ALGINATE HYDROGELS
Solomiia Kapatsila, Yuliia Kyrychuk, Yuliia Cherkas, Volodymyr Samaryk 480

P4-69 PREPARATION AND INVESTIGATION OF ARTHROSPIRA PLATENSIS EXTRACT ENCAPSULATED IN MODIFIED STARCH USING DIFFERENT TECHNIQUES
Dovilė Liudvinavičiūtė, Vesta Navikaitė-Šnipaitienė, Vaida Kitrytė-Syrpa, Michail Syrpas, Ramunė Rutkaitė 481

P4-70 DEVELOPMENT OF BIOACTIVE 3D-PRINTED POLYLACTIC ACID AND HYDROXYAPATITE SCAFFOLDS FOR BONE TISSUE ENGINEERING
Jokūbas Lukošiūnas, Martyna Sabaitė, Odeta Baniukaitienė 482

P4-71 SYNTHESIS OF 6-CHLORORESORCINOLS MODIFIED WITH CYCLIC AMINES AND AMIDES IN THE FOURTH POSITION
Ugnius Popovas, Ieva Žutautė 483

P4-72 MODIFICATION OF CORN STARCH VIA SUCCINYLATION AND ACETYLATION
Muhammad Nasif, Ayodeji Amobonye, Joana Bendoraitiene, Laura Peciulyte, Remo Merijs Meri, Shu-Kai Yeh, Ramune Rutkaite 484

P4-73 PHOTOREDOX MANIFOLD FOR DEHYDROGENATIVE COUPLING USING PROTONS AS THE SOLE OXIDANTS
Jonas Žurauskas, Paulius Vaickūnas, Gustautas Snarskis, Gediminas Kreiza, Steponas Raišys, Mantas Šimėnas, Vidmantas Kalendra, Kęstutis Zakarauskas, Barbara Chatinovska, Karolis Kazlauskas, Edvinas Orentas 485

P4-74 ELECTRON-DEFICIENT PHOSPHINE LIGANDS FOR PALLADIUM CATALYSED C-N CROSS-COUPLING REACTIONS
Jonas Paukštys, Tomas Paškevičius, Linas Labanauskas 486

P4-75 INVESTIGATION OF ELECTROPHILIC CYCLIZATION REACTIONS OF 2-ALKENYLTHIOIMIDAZOLES
Martyna Paulauskaitė, Ieva Žutautė 487

P4-76 INVESTIGATION OF SYNTHETIC PATHWAYS FOR REZORCINOL COMPOUNDS WITH SULFUR-CONTAINING NITROGEN HETEROCYCLES
Gabija Griškonytė, Ieva Žutautė, Rita Bukšnaitienė, Algirdas Brukštus 488

P4-77 SYNTHESIS OF N-(2,4-DIFLUOROPHENYL)-β-ALANINE DERIVATIVES AND INVESTIGATION OF THEIR PROPERTIES
Guoda Pranaitytė, Birutė Grybaitė, Vytautas Mickevičius 489

P4-78 EFFICIENT TWO-STEP SYNTHESIS OF NOVEL IMIDAZOPYRAZOLOOXAZEPINES
Agnė Užupytė, Algirdas Šačkus, Eglė Arbačiauskienė 490

P4-79 FORMATION OF PHOSPOENOLPYRUVATE UNDER PREBIOTIC CONDITIONS
Kajetan Sołtysiak, Rafał Szabla 491

P4-80 TAILORING THE PROPERTIES OF LANTHANUM-DOPED SrSnO3 LAYERS: THE ROLE OF GAS FLOW RATES
Mindaugas Voznikas, Milita Vagner, Tomas Murauskas, Virgaudas Kubilius, Valentina Plaušinaitienė . 492

P4-81 IMPORTANCE OF DRYING SPEED AND SHRINKAGE COEFFICIENT IN THE SYNTHESIS OF CRACK-FREE SILICA XEROGELS VIA THE SOL-GEL METHOD
Austėja Šernaitė, Greta Inkrataitė, Ramūnas Skaudžius 493

P4-82 INTERMOLECULAR STRUCTURE ANALYSIS OF CHOLINE TRYPTOPHANATE IONIC LIQUID USING MD AND QM/MM SIMULATIONS
Jonas Vaitiekūnas, Lukas Mikalauskas, Vytautas Klimavičius, Einaras Sipavičius, Kęstutis Aidas . . . 494

P4-83 SYNTHESIS OF REDOX-ACTIVE SUPRAMOLECULAR CAPSULE
Gabija Sergejevaitė, Domantas Valčeckas, Edvinas Orentas 495

P4-84 LAYERED DOUBLE HYDROXIDES: INVESTIGATING SYNTHESIS KINETICS AND THEIR BIOMEDICAL APPLICATIONS
Neringa Gailiūtė, Denis Sokol 496

P4-85 MANGANESE COATINGS: TEMPERATURE INFLUENCE ON ELETROCHEMICAL DEPOSITION
Vasaris Statkevičius, Nerita Žmuidzinavičienė, Egidijus Griškonis 497

P4-86 GROWTH OF YB:CALGO CRYSTAL BY OPTICAL FLOATING ZONE METHOD
Domantas Černius, Monika Skruodienė, Anatolijs Šarakovskis, Ekaterina Pomjakushina, Ramūnas Skaudžius 498

P4-87 FORMATION OF CARBONATED HYDROXYAPATITE UNDER HYDROTHERMAL CONDITIONS
Lidija Turilinaitė, Gabrielė Šarapajevaitė, Tadas Dambrauskas 499

P4-88 INFLUENCE OF CU^{2+} IONSON THE FORMATION OF HYDROXYAPATITE UNDER DIFFERENT SYNTHESIS METHODS
Monika Tiskute, Kęstutis Baltakys, Tadas Dambrauskas 500

P4-89 COMPUTATIONAL STUDY OF NMR SPECTRA AND STRUCTURAL PROPERTIES OF TETRAPEPTIDE IN IONIC LIQUID MIXTURES WITH WATER
Amina Elkady, Žyginta Murnikova, Kęstutis Aidas 501

P4-90 BIOSYNTHESIS OF SILVER NANOPARTICLES VIA MEDUSOMYCES GISEVII FERMENTATION WITH TILIA CORDATA EXTRACT: ANTIMICROBIAL, ANTIOXIDANT PROPERTIES AND PHYTOCHEMICAL ANALYSIS.
Urte Raubyte, Aiste Balciunaitiene, Mindaugas Liaudanskas, Jonas Viskelis 502

P4-91 IMPROVEMENTS OF THE POLYMERS REPRESENTATION IN COD USING QUOTIENT GRAPHS
Yaroslav Rozdobudko, Andrius Merkys, Antanas Vaitkus, Saulius Gražulis 503

P4-92 MACHINE LEARNING FORCE FIELD PARAMETRIZATION AND APPLICATIONS FOR PHOSPHORIC ACID BASED SYSTEMS
Gabrielius Mockus, Deimantas Šmigelskas, Rokas Šilkinis, Linas Vilčiauskas 504

P4-93 GOLD-NICKEL-RHENIUM-PHOSPHORUS CATALYSTS FOR EFFICIENT SODIUM BOROHYDRIDE OXIDATION
Eimantas Kiseliovas, Aušrinė Zabielaitė, Aldona Balčiūnaitė, Jūratė Vaičiūnienė, Loreta Tamašauskaitė-Tamašiūnaitė 505

P4-94 SEASONAL CHANGES IN THE VOLATILE PROFILE OF SCOTS PINE (PINUS SYLVESTRIS) NEEDLE EXTRACTS: HYDRODISTILLATION VS. SUPERCRITICAL CO_2 EXTRACTION
Jokūbas Kojelis, Laura Jūrienė, Renata Baranauskienė, Ramutė Maždžierienė, Petras Rimantas Venskutonis 506

P4-95 EFFICIENT RECOVERY OF ANTIOXIDANT-RICH EXTRACTS FROM BOGBEAN (MENYANTHES TRIFOLIATA L.) LEAVES
Julija Ginkutė, Marius Užupis, Michail Syrpas, Vaida Kitrytė-Syrpa 507

P4-96 MECHANICALLY FRACTIONATED BLACK CURRANT SEEDS AND SKINS AS A VALUABLE SOURCE OF BIOACTIVE COMPOUNDS
Laura Jūrienė, Milda Pukalskienė 508

P4-97 ANTIOXIDANT ACTIVITY OF DIOSCOREA CAUCASICA AND DIOSCOREA NIPPONICA LEAVES AND ROOTS EXTRACTS OBTAINED BY DIFFERENT EXTRACTION METHODS
Laura Jūrienė, Jovita Jovaišaitė, Petras Rimantas Venskutonis 509

P4-98 SYNTHESIS AND INVESTIGATION OF PHOTOPOLYMERS BASED ON NATURAL OIL AND GLYCEROL DERIVATIVES
Vilte Šereikaite, Aukse Navaruckiene, Aistis Lapinskas, Jolita Ostrauskaite 510

P4-99 ORGANIC DYES AS SELF-ASSEMBLED MONOLAYERS FOR PHOTOVOLTAIC DEVICES
Milda Žitinevičiūtė, Matas Steponaitis 511

P4-100 ELECTROCHEMICAL BEHAVIOUR OF ZIRCONIUM THIN FILMS ON STAINLESS STEEL IN HER
R. Jurgelionytė, I. Barauskienė, G. Laukaitis, E. Valatka 512

P4-101 SYNTHESIS AND INVESTIGATION OF SELF-ASSEMBLED MONOLAYER BENZIMIDAZOLE DERIVATIVES
Gabija Linkaitė, dr. Mantas Marčinskas 513

P4-102 FACILE AND LOW-COST DESIGN ALTERNATIVE OF SPIRO-OMETAD AS SEMICONDUCTOR FOR EFFICIENT PEROVSKITE SOLAR CELLS
Šarūnė Daškevičiūtė, Yi Zhang, Kasparas Rakštys, Marytė Daškevičienė, Vygintas Jankauskas, Mohammad Khaja Nazeeruddin, Vytautas Getautis 514

P4-103 BRANCHEDFLUORENYLIDENE DERIVATIVES WITH LOW IONIZATION POTENTIALS AS HOLE-TRANSPORTINGMATERIALS FOR PEROVSKITE SOLAR CELLS
Aistė Jegorovė, Jianxing Xia, Matas Steponaitis, Marytė Daškevičienė, Vygintas Jankauskas, Alytis Gruodis, Egidijus Kamarauskas, Mohammad Khaja Nazeeruddin, Vytautas Getautis 515

Invited Speakers

INTEGRATED NANOPHOTONICS AND ITS CONVERGENCE WITH ELECTRONICS

Yuqing Jiao[1]

[1] Institure for Photonic Integration (IPI), Eindhoven University of Technology, The Netherlands
y.jiao@tue.nl

Photonic integrated circuit (PIC) technology powers up wide applications from communication and computing to sensing and precision metrology. In this talk, I will start with an introduction to the PIC concept, materials and principles, then discuss the recent advancement of PIC technology and particularly the latest research at TU Eindhoven. I will introduce our InP-based nanophotonics technology and showcase how this next-gen PIC technology can empower AI and quantum applications, as well as enable a convergence of photonics and electronics into a single chip technology. Finally I will share our vision on the future scaling of the PIC technology, especially in speed, energy efficiency and integration density.

The talk will cover the nanophotonic integrated circuit platform “IMOS” developed at TU Eindhoven. The technology is based on a thin membrane made of InP material. With enhanced optical confinement, the technology holds the promise to drive the future scaling in density, speed and efficiency. The technology also enables seamless 3D integration with electronics wafers. This enables co-design of photonics and electronics and can unleash performance enhancement that was not achievable when designing the two chips separately.

About the Invited Speaker

Yuqing Jiao is an Associate Professor at the Eindhoven University of Technology and leads a research group in the Institute of Photonic Integration. He specializes in heterogeneous photonic integration technologies, focusing on III-V and III-N integration on Si/SiN circuits and exploring new materials for emerging photonic applications. Dr. Jiao has co-authored over 70 journal articles, 150 conference papers, and holds four patents. He is a senior member of IEEE, a board member of the IEEE Photonics Society Benelux Chapter, and has delivered invited talks at major conferences such as OFC, CLEO, and Photonics West.



ULTRAFAST LASERS, TERAHERTZ LIGHT AND MORE

Clara Saraceno[1]

[1]Faculty of Physics and Astronomy, Ruhr University Bochum, Germany
clara.saraceno@ruhr-uni-bochum.de

Ultrafast lasers are coherent light sources producing pulses with femtosecond duration (10-15s) and - during this short time - to generate powers routinely exceeding the gigawatt (10^9 W) level. To put these parameters into perspective: a femtosecond is to a second what a hair width is to the distance between the earth and the sun; and a gigawatt is the equivalent power produced by 1000 nuclear power plants – and this can be nowadays routinely achieved at the table-top of most ultrafast laser labs. The correspondingly extremely high intensities reachable in these very short timescales are comparable to the forces binding atoms to electrons and are thus an incredibly powerful tool to understand and modify the properties and processes involved in all states of matter spanning all states, liquid, solid, gas, and plasma, and all scales, nano, meso, and macro.

This makes the application fields of ultrafast lasers extremely wide: they allow us on the one hand to process and functionalize virtually any material; and on the other hand, to understand the dynamics of the smallest bricks of our universe. They also enable us to reach extreme pressure and temperature conditions comparable to those present in stars, and to routinely access material nonlinearities to generate inaccessible “colors” in our spectrum - from X-rays to terahertz (THz). In this presentation, we will give an overview of the immense possibilities open by lasers and more particularly ultrafast lasers. We will focus on the generation of powerful Terahertz light, and its applications in spectroscopy – one example of areas currently fueled by advances in laser technology- and will present future directions and challenges in laser sources.

About the Invited Speaker

Clara Saraceno is a Full Professor at Ruhr University Bochum, Germany. Her current main research thrusts include high-power ultrafast lasers and Terahertz science and technology. Prof. Saraceno has received numerous recognitions for her recent research, including the SPIE Harold E. Edgerton Award for high-speed optics and the International Fellowship Award from the Leibniz Institute for Crystal Growth. Prof. Saraceno is a Fellow of Optica (2022) and a strong advocate for women in STEM.



BUILDING STARS, PLANETS AND THE INGREDIENTS FOR LIFE IN SPACE

Ewine F. van Dishoeck[1]

[1]Leiden Observatory, Leiden University, the Netherlands
ewine@strw.leidenuniv.nl

Thousands of planets have been discovered around stars other than our Sun. But how and where are these exo-planets born, and why are they so different from those in our own solar system? Which ingredients are available to build them? Thanks to powerful new telescopes, including the James Webb Space Telescope and the Atacama Large Millimeter Array, astronomers can now zoom in to planetary construction sites and study their composition. Water and a surprisingly rich variety of organic materials are found near forming stars and planets. How are these molecules made under the extreme conditions in space and can they be delivered to new planets to form the basis for life elsewhere in the universe?

About the Invited Speaker

Ewine van Dishoeck is a professor of molecular astrophysics at Leiden University, the Netherlands. The work of her group innovatively unites the world of chemistry with that of physics and astronomy. She has been heavily involved in the planning of major new telescopes, and has been fortunate to receive many awards, including the 2018 Kavli Prize for Astrophysics, as well as membership of several academies. From 2018 to 2021, Ewine served as the President of the International Astronomical Union (IAU).



SEARCHING FOR ANTIHELIUM IN OUR GALAXY: FROM COLLIDERS TO COSMIC RAY DETECTORS

Laura Šerkšnytė[1]

[1]CERN, ALICE Collaboration, Switzerland
laura.serksnyte@cern.ch

CERN is best known for its groundbreaking discoveries in particle physics, from the Higgs boson to precision tests of the Standard Model. But beyond the search for fundamental particles, the experiments at the Large Hadron Collider (LHC) also offer unique insights into the broader mysteries of the Universe. ALICE, designed to study the properties of the quark-gluon plasma, has become a versatile laboratory for exploring a wide range of phenomena, including the production and interactions of light antinuclei. Among them, antihelium-3 is particularly intriguing—not only is it produced in high-energy nuclear collisions, but it could also act as a messenger from the depths of the galaxy, carrying potential signatures of exotic astrophysical processes.

One of the most exciting possibilities is that antihelium nuclei might originate from dark matter annihilation or decay. While cosmic rays can also produce such antinuclei through interactions with interstellar matter, theoretical models suggest that at low energies, a dark matter signal would be dominant. Detecting even a few antihelium nuclei in space could provide groundbreaking evidence for physics beyond the Standard Model. However, to interpret such observations, we must first understand how these antinuclei are produced and propagate through the Galaxy, surviving interactions with interstellar gas. This is where experiments like ALICE play a crucial role—by measuring how antihelium is created and how it interacts with ordinary matter, we provide the essential input needed to model cosmic-ray transport and distinguish between conventional astrophysical sources and potential dark matter signatures.

By bridging collider physics with astrophysical questions, ALICE continues to push the boundaries of our understanding, making it a powerful tool for exploring the universe in unexpected ways.

About the Invited Speaker

Laura Šerkšnytė is a Research Fellow at CERN, contributing to the ALICE experiment at the Large Hadron Collider. Her research focuses on light antinuclei, including antideuterons and antihelium, as tools for detecting dark matter and particle interactions in proton-proton collisions. The scientist's groundbreaking work, published in Nature Physics, earned her the André Mischke Award in 2021. Dr. Šerkšnytė also developed innovative methods to study three-baryon systems, advancing the understanding of neutron star matter. She was awarded Summa Cum Laude for her PhD and the 2024 Excellence Cluster ORIGINS Award.



PHOTOACOUSTIC IMAGING: BASICS, TECHNOLOGY AND APPLICATIONS IN BREAST IMAGING

Srirang Manohar[1]

[1] 1Multi-Modality Medical Imaging (M3I) Group, Faculty of Science and Technology, University of Twente, the Netherlands
s.manohar@utwente.nl

Photoacoustic (PA) imaging, is a non-invasive imaging modality that relies on optical absorption of tissue constituents for contrast. In PA, nanosecond laser pulses are used to illuminate the tissue. The light gets absorbed at locations where there is especially blood present. The absorbed optical energy is converted into heat leading to thermoelastic expansion which produces ultrasound waves which are detected. PA tomography is interesting for imaging dominantly blood vessels which is important functional and physiological information in living tissues.

We present the technology behind a hybrid photoacoustic-ultrasound (PA-US) tomographic imaging system, PAM3 developed within a European consortium. The system employs a hemispherical geometry with an imaging bowl filled with water into which the breast is positioned. The bowl has 512 ultrasound transducers distributed on its inside surface. Forty optical fibre bundles terminate at the inner surface of the bowl, distributed to illuminate the breast homogenously for photoacoustic excitation. In addition to functioning in reception mode for photoacoustic imaging, the transducers can be used in emission mode for ultrasound transmission imaging. During a measurement, the imaging bowl and its contents rotate around the breast, which is immobilized in a transparent cup, to acquire multiple projections. The reconstruction of PA CT images was performed using an iterative model-based optimisation framework. The sound speed reconstructions were implemented using a similar approach, sometimes called Full Waveform Inversion.

We conclude by demonstrating the functionalities of the imaging system and its imaging capability on healthy volunteers and breast cancer patients. From the multispectral photoacoustic (PA) mode, we obtain angiographic breast structures in 3D throughout the breast, and provide a measure for the blood oxygen saturation. From the ultrasound (US) mode, the sound speed images serve to improve the accuracy of the PA reconstruction, and also provide morphological information which helps interpretation of the PA images. We touch upon future studies that we aim perform using this system.

About the Invited Speaker

Prof. Srirang Manohar is a Professor and Chair of Multi-Modality Medical Imaging (M3I) at the University of Twente, specializing in non-invasive diagnostic technologies like photoacoustic and ultrasound imaging. He has led PAMMOTH, a European project to develop a radiation-free and real-time breast cancer diagnostic device. His research also targets thyroid issues, prostate cancer, and rheumatoid arthritis. Prof. Manohar combines innovative technology development with early clinical applications to improve diagnostic and therapeutic outcomes globally.



ALTERED TRANSIENT CIRCUITS AS AN UNDERLYING CAUSE OF COGNITIVE DYSFUNCTIONS

Zoltán Molnár[1]

[1]Department of Physiology, Anatomy and Genetics, University of Oxford, United Kingdom
zoltan.molnar@dpag.ox.ac.uk

The lowermost cell layer of the cerebral cortex that contains interstitial white matter cells in humans has great clinical relevance. These neurons are very abundant during development and express higher proportions of susceptibility genes linked to human cognitive disorders than any other cortical layer and their distribution is known to be altered in schizophrenia and autism [1]-[4]. Despite these clinical links, our current knowledge on the adult layer 6b is limited. These cells are the remnants of the subplate cells that are present in large numbers and play key role in the formation of cortical circuits but a large fraction of them die during postnatal development. The adult population that remains in all mammals to form interstitial white matter cells in human or layer 6b in mouse display unique conserved gene expression and connectivity. Members of my laboratory recently identified intracortical and thalamic projections from a subpopulation of layer 6b cells that might regulate both cortical and thalamic arousal of cortical areas that are involved in higher cortical functions [5]. We study their input and output using combined anatomical, genetic, and physiological approaches. Selected cortical areas, relevant for sensory perception, arousal, and sleep (V1, S1, M1, prefrontal cortex) are studied using genetic and chemogenetic methods. Our data suggest that 6b is not just a developmental remnant cell population in the adult, but a layer that plays a key role in cortical state control, integrating and modulating information processing and alterations of this circuit could lead to disturbance of information processing, anxiety and sleep disorders.

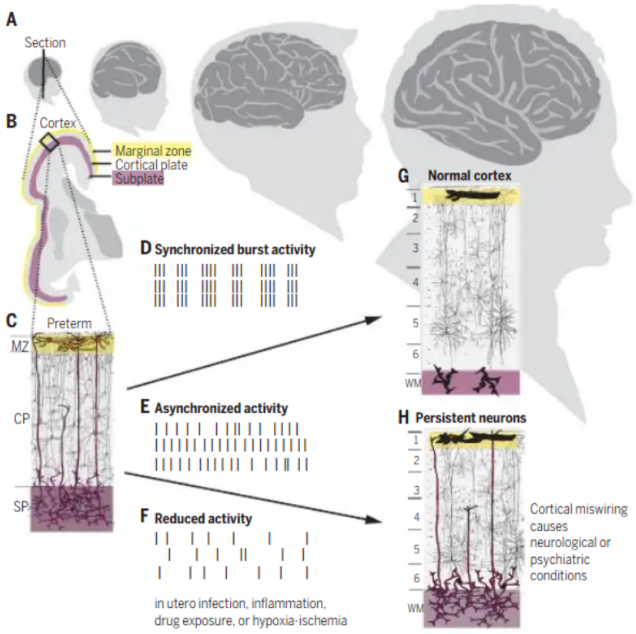


Fig. 1. Early spontaneous synchronized neuronal activity sculpts cortical architecture.

[1] M. Hoerder-Suabedissen et al., *Proc. Natl. Acad. Sci. U.S.A.*, vol. 110, no. 9, pp. 3555–3560, 2013.
[2] T. E. Bakken et al., *Nature*, vol. 535, no. 7612, pp. 367–375, 2016.
[3] Z. Molnár et al., *J. Anat.*, vol. 235, pp. 432–451, 2019.

About the Invited Speaker

Zoltán Molnár is a Professor of Developmental Neuroscience at the University of Oxford. His research focuses on the early development of the mammalian cerebral cortex, particularly the role of transient subplate neurons in the specialization of cortical areas. Prof. Molnár's findings in fundamental developmental biology also contribute to the understanding of the origins and pathomechanisms of developmental conditions such as autism and schizophrenia.



CARBON UNLEASHED: THESE CARBENES REVOLUTIONIZING MATERIAL SCIENCE AND CATALYSIS

Rodolphe Jazzar[1]

[1]1UCSD-CNRS Joint Research Laboratory, Department of Chemistry and Biochemistry, University of California San Diego, United States
rodolphe.jazzar@cnrs.fr

Since their conceptual introduction in the mid-20th century, carbenes (compounds featuring a neutral, divalent carbon center) have evolved from theoretical curiosities into indispensable tools across multiple disciplines. Once considered too reactive for isolation, advances in spectroscopy and synthetic methodology have uncovered a remarkable diversity of stable and transient carbene species. From their presence in interstellar environments to their role in modifying surfaces at the atomic level, carbenes continue to challenge our understanding of chemical bonding and reactivity.

In catalysis, carbenes have had a transformative impact, particularly as ligands for transition metals and main-group elements. Their ability to fine-tune electronic and steric properties has led to breakthroughs in selective transformations, small-molecule activation, and nanocluster stabilization. More recently, their use as surface anchors has bridged the gap between homogeneous and heterogeneous catalysis, offering unprecedented control over reactivity at solid interfaces.

Together, we will trace the journey of carbenes from elusive intermediates to powerful molecular architects, highlighting their expanding role in modern chemistry and materials science. With ongoing advancements in computational design and synthetic control, the future promises even more exotic carbene structures with applications that extend beyond traditional paradigms, reshaping the frontiers of chemical innovation.

About the Invited Speaker

Rodolphe F. Jazzar is a professor in the Chemistry Department at the University of California, San Diego, and a CNRS Research Director. His groundbreaking work focuses on the intricate processes underpinning fundamental chemical transformations. By combining experimental and computational methods, his team aims to provide a deeper understanding of these transformations, ultimately enabling the development of novel catalysts and materials with transformative applications in energy, synthesis, and nanotechnology. In 2023, Dr. Jazzar was awarded the prestigious J.M. Lehn Award for excellence in organic chemistry, recognizing his transformative contributions to modern science.



Oral Session 1

Laser Physics and Optical Technologies

Chair: Dr. B. Momgaudis

FEMTOSECOND LASER POLISHING AND ABLATION OF SILICON CARBIDE WAFERS

Dainius Ratkus[1], Andrius Žemaitis[2]

[1]Department of Laser Technologies (LTS), Center for Physical Sciences and Technology (FTMC), Savanorių Ave. 231, 02300 Vilnius, Lithuania
dainius.ratkus@ftmc.lt

Silicon carbide (SiC) has become a critical material in the fabrication of SiC wafers for electronic applications, especially power semiconductor applications, due to its exceptional thermal resistance, extended operational lifespan, and high energy efficiency. One of the key steps in SiC wafer fabrication is chemical mechanical polishing (CMP). However, CMP has several drawbacks, including high cost, low material removal rate, contamination risk, and environmental and chemical waste concerns.

Laser polishing is an alternative technique for reducing surface roughness by inducing molten and re-solidified layers. It is environmentally friendly as it does not require chemicals, pads, or slurries. Therefore, laser polishing could minimize costs and errors when smoothing the surface of such materials.

In this research, a thorough investigation of SiC wafer polishing and ablation using a femtosecond GHz burst laser (Carbide, Light Conversion). This study aimed to optimize laser processing parameters to achieve the lowest possible surface roughness and the highest ablation efficiency. For this task, smart optimisation techniques were employed allowing to find the optimal laser fluence for the highest ablation efficiency and reach the surface roughness below the initial one [1, 2].

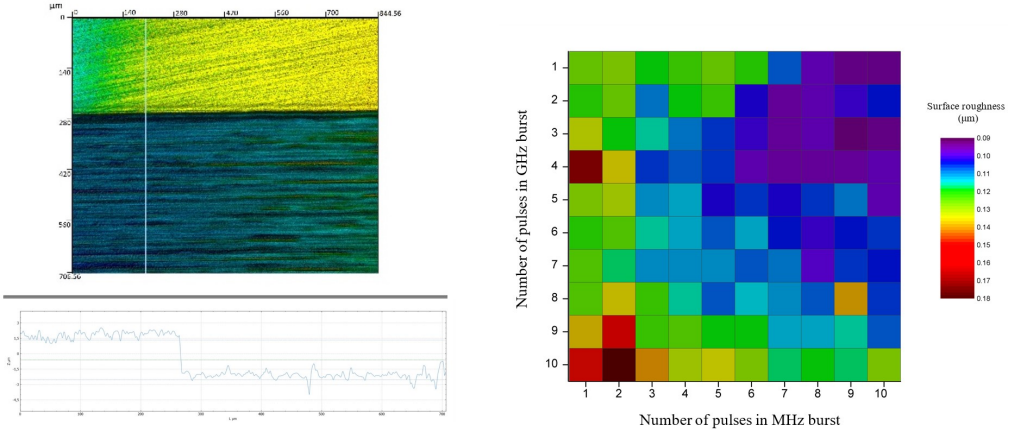


Fig. 1. Profilometeric image of half-ablated SiC surface (left); surface roughness of laser ablated SiC versus number of pulses in MHz and GHz bursts, scan speed 500 mm/s, line spacing 10 µm, laser fluence 0.84 J/cm^2 (right).

[1] [1] A. Žemaitis, U. Gudauskytė, S. Steponavičiūtė, P. Gečys, and M. Gedvilas, The ultrafast burst laser ablation of metals: Speed and quality come together, Opt. Laser Technol., 180, (2025), doi: 10.1016/j.optlastec.2024.111458.

[2] A. Žemaitis, P. Gečys, and M. Gedvilas, Efficient Ablation, further GHz Burst Polishing, and Surface Texturing by Ultrafast Laser, Adv. Eng. Mater., 26(21), p. 2302262, (2024), doi: https://doi.org/10.1002/adem.202302262.

UPSCALING AND THE OPTIMIZATION OF ACRYLIC RESINS FOR LASER FABRICATION OF LOW-DENSITY 3D MICROSTRUCTURES

Saulė Petrauskaitė[1], Dimitra Ladika[1], Ioanna Angeliki Petsi[1], Mangirdas Malinauskas[1]

[1]Laser Research Center, Faculty of Physics, Vilnius University, Lithuania
saule.petrauskaite@ff.stud.vu.lt

Two-photon Lithography (TPL) is an additive manufacturing technique that enables the production of high-precision 3D micro-/ nanoscale structures with features exceeding the diffraction limit of light. TPL relies on two-photon absorption, in which two photons are absorbed simultaneously to trigger localized polymerization in the resin [1]. Thus, absorption occurs only in a limited focused volume when the light intensity exceeds a certain threshold. This unique property allows for precise control of the fabrication process and the creation of complex 3D geometries. Particularly in this study, TPL is employed to create low-density, highly porous microstructures, called foams, for the application in Inertial Confinement Fusion (ICF), which is a potential method of generating energy by using high-power lasers to compress a fuel capsule. In laser-plasma interactions, low-density foams are commonly used as targets because they can transform into large-volume homogeneous plasmas. Foam targets quickly transition from solid to uniform plasma under intense radiation, while their low density enables precise control of plasma conditions for tailored experiments [2].

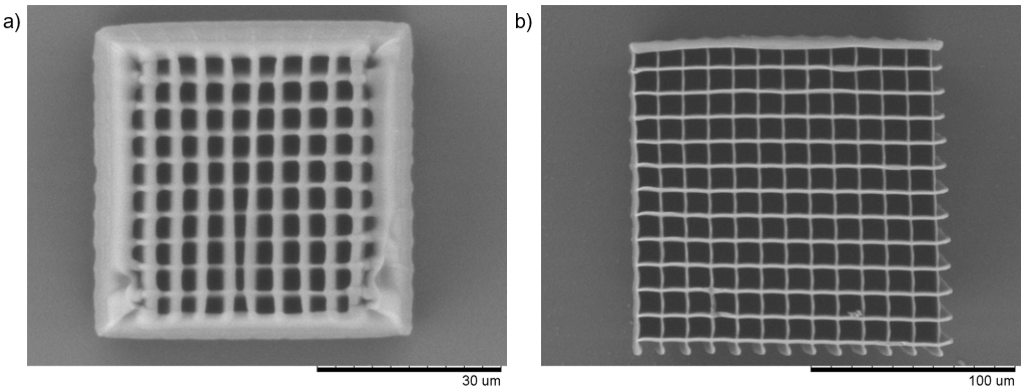


Fig. 1. Scanning electron microscope images of TPL-made foam structures using the same woodpile model. a) PETA60/PETTA40 with 0.5% of Thioxanthen-9-one concentration with power 220 mW and scanning velocity 10 mm/s/ b) DPEPA material with 3 molar % of DMPA with power of 70 mW and scanning velocity 10 mm/s.

To form low-density ordered micro-structured foams using TPL, it is important to select suitable resins with optimal photosensitivity, high polymerization rate, low shrinkage and suitable mechanical properties. To be used in ICF experiments, foams have a few requirements, mainly that foams must be composed exclusively of light elements (hydrogen, carbon, and oxygen) to maintain a homogeneous environment during ICF experiments, ensuring that the structural components are not heavier than elements in air. For this purpose, acrylic resins are employed consisting of H, C, and O, particularly the commercially available PETA, PETTA and DPEPA materials as well as photoinitiators such as Irgacure 369, Thioxanthone and DMPA. This study investigates the optimal combination of acrylic resins and photoinitiators, along with their concentrations, to produce low-density foams via TPL (Fig. 1), specifically designed for future ICF applications. From Fig.1, it is observed that the DPEPA material delivers significantly improved results, enabling the fabrication of much larger structures with higher resolution.

[1] Wang, H., Zhang, W., Ladika, D., et al. Two-Photon Polymerization Lithography for optics and Photonics: Fundamentals, materials, technologies, and applications. Advanced Functional Materials, 33(39), 2214211, 2023.
[2] Tikhonchuk, V., Gu, Y. J., Klimo, O., Limpouch, J., & Weber, S. Studies of laser-plasma interaction physics with low-density targets for direct-drive inertial confinement schemes. Matter and Radiation at Extremes, 4(4), 045402, 2019.

OPTIMIZED TALBOT INTERFEROMETER DESIGN FOR HIGH-PRECISION LASER INTERFERENCE PATTERNING

Tadas Latvys[1], Vytautas Jukna[1], Darius Gailevičius[1], Dominyka Stonytė[1], Domas Paipulas[1]

[1]Laser Research Center, Faculty of Physics, Vilnius University, Lithuania
tadas.latvys@ff.vu.lt

Direct laser interference patterning (DLIP) enables the fabrication of sub-micrometer periodic structures without post-processing, finding applications in photonics, electronics, medicine, and tribology [1]. To minimize thermal defects and enhance precision, fs-UV pulses are used. However, the use of broadband femtosecond UV pulses introduces spatio-temporal effects in interferometer designs, reducing fluence and degrading pattern quality.

This study investigates the performance of a compact Talbot interferometer (Fig. 1a), consisting of a lens, holographic beam splitter, and two parallel mirrors, in minimizing these effects. Using the Kostenbauder matrix formalism [2,3], three lens configurations were analyzed: a spherical lens and two cylindrical lenses with perpendicular orientations. By incorporating laser and interferometer parameters, we determined which lens minimizes pulse front and phase tilt effects, which can impact pulse overlap and interference contrast.

Results show that both spherical and parallel-axis cylindrical lenses cause significant pulse front and phase tilts (Fig. 1b), leading to increased pulse duration. The latter also led to insufficient fluence, preventing patterning of (100) crystalline silicon, even at maximum laser power. In contrast, In contrast, a perpendicular-axis cylindrical lens exhibited minimal pulse distortions (Fig. 1c) and ensured optimal pulse overlap and high interference contrast and minimal pulse duration increase.

These findings demonstrate that selecting an appropriate lens configuration in Talbot interferometers is crucial for achieving high-precision DLIP.

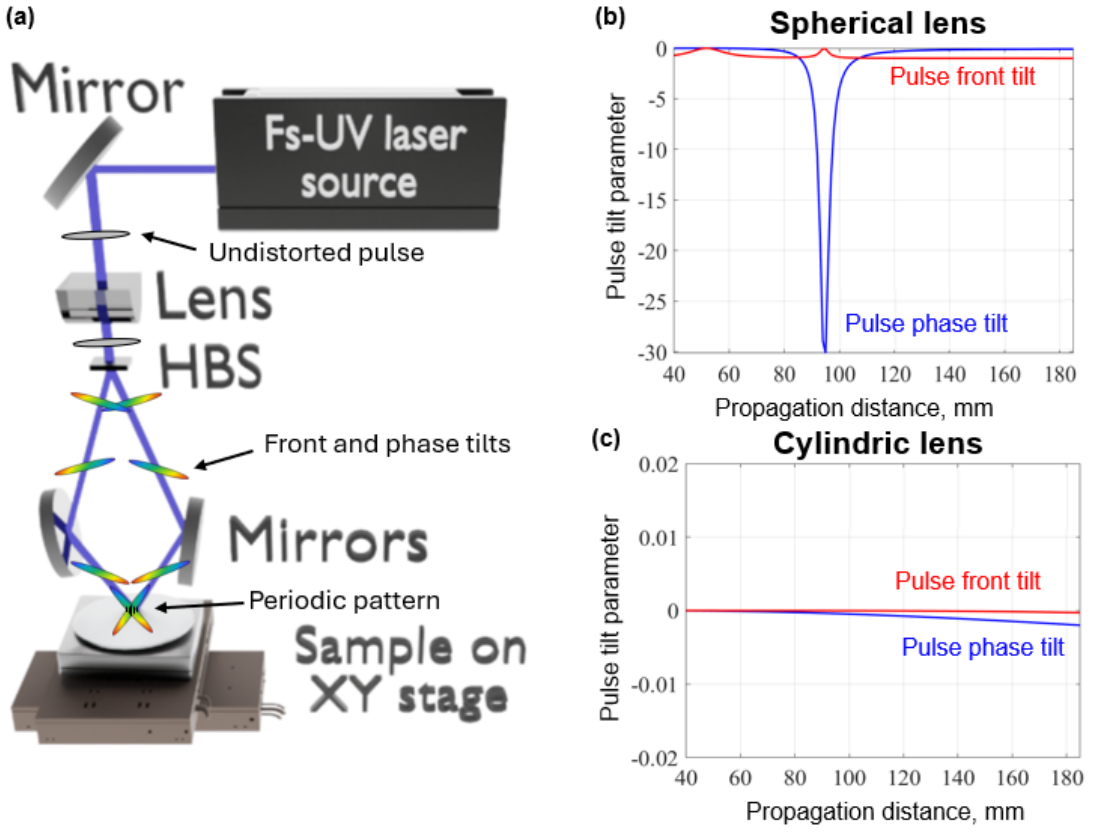


Fig. 1. Optical setup of the Talbot interferometer (a) and the calculated pulse front tilts for spherical (b) and cylindrical (c) lenses.

[1] Wang, H., Deng, D., Zhai, Z. & Yao, Y. Laser-processed functional surface structures for multi-functional applications-a review. J. Manuf. Process. 116, 247–283 (2024).
[2] Kostenbauder, A. G. Ray-pulse matrices: a rational treatment for dispersive optical systems. IEEE J. Quantum Electron. 26, 1148–1157 (1990).
[3] Ouellette, F. & Li, J. Performance comparison of phase mask interferometers for writing fiber Bragg gratings with femtosecond pulses. OSA Contin. 2, 1215 (2019).

EVALUATION OF VARIOUS PERIODICALLY POLED NONLINEAR CRYSTALS POLING QUALITY

Ieva Baltrukonytė[1], Jokūbas Pimpė[1], Julius Vengelis[1]

[1]Vilnius University
ieva.baltrukonyte@ff.stud.vu.lt

Periodically poled (PP) crystals play a crucial role in nonlinear optics, enabling efficient quasi-phase matching (QPM). The most reliable fabrication method of PP crystals is electric field poling, where a patterned photoresist with a specified duty cycle, period and grating type (single, multi, fan-out) is applied to the crystal c-faces. A strong electric field causes domain inversion resulting in the stable periodically poled domains (gratings) and effective nonlinearity inverses its sign after each coherence length, enabling efficient nonlinear optical interactions through the highest nonlinear optical susceptibility tensor elements, efficient parametric light generation, second harmonic and THz radiation generation [1].

Poling process is prone to defects like inhomogeneity of domain period and the 50/50 duty cycle in the whole grating volume. Various methods, including second harmonic microscopy, confocal microscopy, scanning electron microscopy, near-field microscopy can visualize domain structures but are time-consuming and visualize only small parts of domain structure [2]. Therefore, there are diffraction-based methods like applying a weak electric field to the PP crystals and exposing it to laser light creates diffraction patterns which carries information about domain period, duty cycle [3]. Such method also has drawbacks which may change diffraction pattern intensities: imaging lens aberrations, CCD camera sensitivity. Multi-pass resonator-based OPO scans provide domain homogeneity data but with low resolution [4].

This work presents results of various PP nonlinear crystals' poling quality evaluation using a simple and non-destructive method that was recently demonstrated in Laser Research Center [5]. The method is based on 2D scan of the PP crystal in direction perpendicular to pump beam and the measurement of parametric light generated during nonlinear process in a single pass optical OPG setup. In this way we can observe efficiency of nonlinear frequency conversion process at each crystal entrance aperture point. The result of such scan is quality homogeneity "map" which directly corresponds to domain homogeneity for all the gratings of the crystal. We constructed a universal, compact and portable optical setup, so measurements of poling quality can be performed in different laboratories with different laser sources. The scanning is performed with motorized translation stages that allow accurate scanning step (1.25μm) and the errors due to crystal physical shape are minimal as the beam passes through the crystal only a single time. The generated parametric light (signal wave) is measured with pyroelectric power sensor, so measurement is relatively fast. The quality of various condition and manufacturer crystals was estimated and compared.

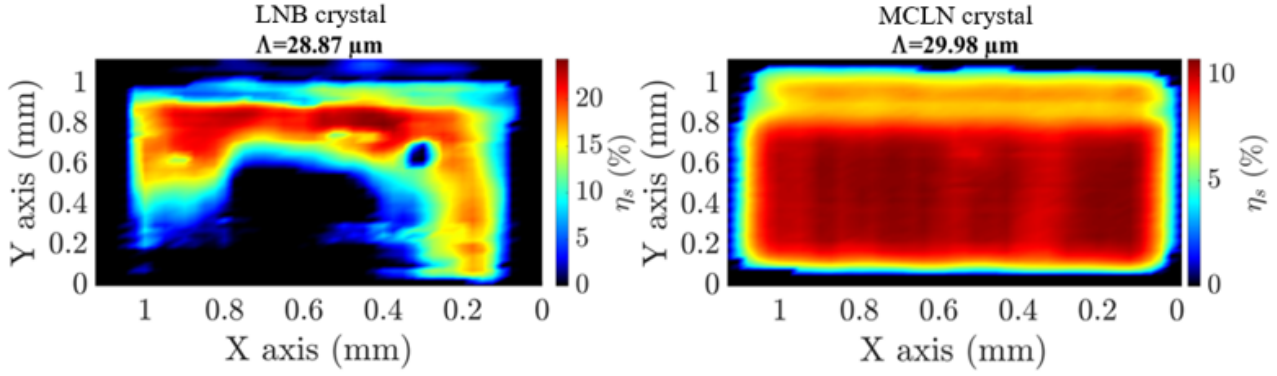


Fig. 1. Signal wave conversion efficiency distribution directly related to poling quality.

[1] S. Hayashi, K. Nawata, T. Taira, J.-i. Shikata, K. Kawase, H. Minamide, Ultrabright continuously tunable terahertz-wave generation at room temperature, Sci. Rep. 4 (1) (2014) 1–5.
[2] K. Pandiyan, Y.-S. Kang, H.-H. Lim, B.-J. Kim, O. Prakash, M.-S. Cha, Poling quality evaluation of periodically poled lithium niobate using diffraction method, J. Opt. Soc. Korea 12 (3) (2008) 205–209.
[3] M. Müller, E. Soergel, K. Buse, C. Langrock, and M. Fejer, Investigation of periodically poled lithium niobate crystals by light di raction, Journal of Applied Physics 97(4), 044102 (2005).
[4] H. Karlsson, Fabrication of periodically poled crystals from the KTP family and their applications in nonlinear optics, Doctoral dissertation. ISSN 0280-316X, Stockholm (1999).
[5] J. Banys, J. Pimpė, O. Balachninaitė, V. Jarutis, J. Vengelis, Non-destructive periodic poling quality evaluation of MgO:PPLN and Rb:PPKTP crystals based on crystal translation and parametric light generation, Optik 277, 170686 (2023).

OPTICAL SECOND HARMONIC GENERATION IN A PLANAR QUASI-SYMMETRICAL GaN WAVEGUIDE STRUCTURE

Ignas Dailidėnas[1], Roland Tomašiūnas[1]

[1] Institute of Photonics and Nanotechnology, Vilnius University, Saulėtekio al. 3, LT-10257 Vilnius, Lithuania
ignas.dailidenas@ff.vu.lt

Efficient second-harmonic generation (SHG) approaches often rely on periodic poling structures, which can be complex to fabricate. We present a novel quasi-symmetric GaN waveguide optimized for green light SHG, utilizing modal phase matching. Our design incorporates a complex GaN-based multilayered planar waveguide structure with GaN polarity inversion in the core fabricated via metal-organic chemical vapor deposition (MOCVD) [1].

The core of this waveguide is structured to enhance optical mode overlap by using Ga-polar and N-polar GaN layers. The resulting waveguide comprises a **507 nm Ga-polar** and **91 nm N-polar GaN** sandwich, separated by a **20 nm** atomic layer deposition (ALD) of $\mathbf{Al_2O_3}$. From the sapphire substrate, it is separated by a 420 nm AlGaN cladding layer. Additionally, a TiO_2 layer is deposited on the waveguide core to improve mode confinement.

For SHG experiments, a picosecond laser and the end-fire coupling method were utilized. The observed SHG spectrum exhibited a peak at **1108 nm**, accompanied by periodic peaks separated by **20 nm**. These peaks are attributed to modal interference involving both transverse magnetic (TM) and transverse electric (TE) modes. Currently, we are advancing in detecting SHG directed perpendicular to the waveguide surface, as theoretically predicted.

This waveguide structure shows promise for tunable SHG applications. However, further research and fine-tuning are necessary to optimize its performance.

Acknowledgements

This research has been carried out in the framework of the „Universities' Excellence Initiative" programme by the Ministry of Education, Science and Sports of the Republic of Lithuania under the agreement with the Research Council of Lithuania (project No. S-A-UEI-23-6).

[1] R.Tomašiūnas, D.Kezys, M.Kolenda, I.Dailidėnas, A.Kadys, I.Reklaitis, S.Melnikas, L.Grineviciūtė, R.Petruškevčius, V.Vaičaitis, A.Tarre, K.Kukli. Green light second-harmonic generation in a planar quasi-symmetrical GaN waveguide structure. IEEE Proc., Tu.D7.2, 2024. DOI: 10.1109/ICTON62926.2024.10647764R.Tomašiūnas, D.Kezys, M.Kolenda, I.Dailidėnas, A.Kadys, I.Reklaitis, S.Melnikas, L.Grineviciūtė, R.Petruškevčius, V.Vaičaitis, A.Tarre, K.Kukli. Green light second-harmonic generation in a planar quasi-symmetrical GaN waveguide structure. IEEE Proc., Tu.D7.2, 2024. DOI: 10.1109/ICTON62926.2024.10647764

ORAL SESSION 2

Material Science and Nanotechnology

Chair: Dr. T. Grinys

DESIGN OF VERTICAL-EXTERNAL-CAVITY SURFACE-EMITTING LASERS FOR NIR EMISSION

Andrea Zelioli[1], Aivaras Špokas[1,2], Aistė Štaupienė[1,2], Martynas Talaikis[1], Martynas Skapas[1], Darius Gailevičius[3], Artūras Suchodolskis[1], Aurimas Čerškus[1], Sandra Stanionytė[1], Augustas Vaitkevičius[1,2], Bronislovas Čechavičius[1], Evelina Dudutienė[1], Renata Butkutė[1,2]

[1]State research institute Center for Physical Sciences and Technology, Saulėtekio al. 3, Vilnius, Lithuania
[2]Institute of Photonics and Nanotechnology, Vilnius University, Saulėtekio al. 3, Vilnius, Lithuania
[3]Laser research center, Vilnius University, Saulėtekio av. 10, Vilnius, Lithuania
andrea.zelioli@ftmc.com

Vertical-External-Cavity Surface-Emitting Lasers (VECSELs) offer a flexible alternative to conventional Vertical-Cavity Surface-Emitting Lasers (VCSELs) by substituting the top distributed Bragg reflector (DBR) with an external coupler, which facilitates efficient optical pumping and provides easier access to the cavity. This architecture supports a higher output power potential, with the principal constraint of it being thermal management [1, 2].

In this study, we designed and fabricated two VECSEL chips engineered for emission in the NIR. One device with InGaAs multiple quantum wells (MQWs) in the gain region, whereas the second chip employs GaAsBi MQWs. The integration of bismuth into the GaAs lattice accelerates bandgap reduction relative to indium, while simultaneously enhancing temperature stability and increasing the spin–orbit split-off energy, thereby mitigating non-radiative Auger recombination and rendering GaAsBi an attractive material for long-wavelength optoelectronic applications. A sketch of such structure is presented in Figure 1 on the left, the chip can be divided in two main components, a DBR and the gain region plus window layers. Our work was focused on the optimization of the design and grown of both of these parts.

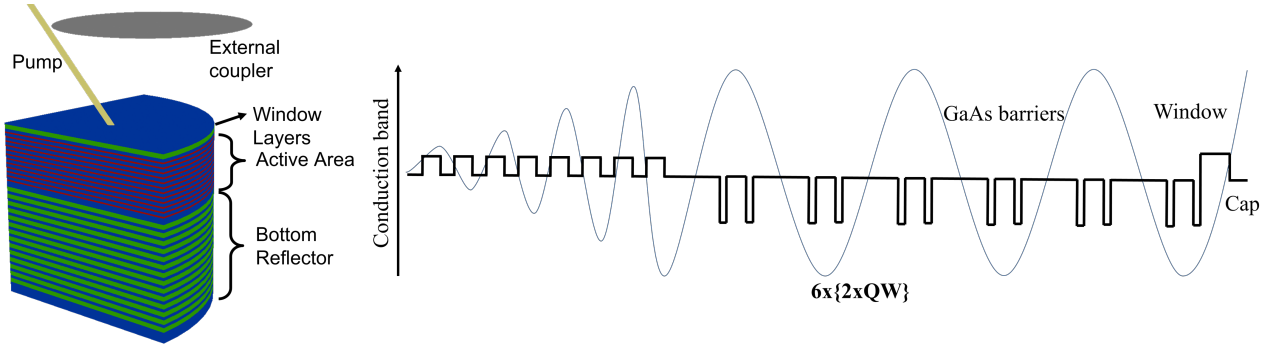


Fig. 1. On the left the sketch of a VECSEL structure, while on the right the conduction band of the chip, with the standing wave shown in blue

Both structures were grown by solid-source molecular beam epitaxy using a Veeco GENxplor system. A DBR composed of 30 AlAs/GaAs periods was designed to center the MQW emission within the photonic stopband. To reduce overall chip thickness and improve heat dissipation, a gain region featuring 12 quantum wells with alternating barrier thicknesses was implemented, the barrier dimensions were optimized so that the antinodes of the lasing standing wave coincide with the QW positions, thereby enhancing emission coupling, the conduction band of the full structure is presented in Figure 1 on the right, in blue the laser standing wave is shown.

Specifically, the InGaAs-based chip utilized QWs 5.7 nm thick (with 20% indium) separated by 98 nm barriers and capped with 7 nm barriers, whereas the GaAsBi device featured 5.5 nm QWs (with 8% bismuth) interleaved with barriers of 7 nm and 150 nm. Lasing was demonstrated at 976 nm from a 500 µm-diameter region in the InGaAs/GaAs device, and notably, lasing at 1070 nm was observed in the GaAsBi/GaAs device representing the first reported instance of lasing from a GaAsBi-based VECSEL.

Acknowledgements
This research was funded by the Research Council of Lithuania (LMTLT), agreement No. [S-LT-TW-24-8].

[1] Muszalski Jan, et al., "VECSELs emitting at 976nm designed for second harmonic generation in the blue wavelength region", Proc. SPIE 8702, Laser Technology 2012: Progress in Lasers, 87020A (2013).
[2] Jacquemet Mathieu, et al., "Single-frequency cw vertical external cavity surface emitting semiconductor laser at 1003 nm and 501 nm by intracavity frequency doubling", Applied Physics B, 86(3), 503-510 (2007).

DEVELOPMENT OF APPLICATION FOCUSED BISMUTH CONTAINING NIR ELECTRICALLY PUMPED EMITTERS

Aivaras Špokas[1,2], Andrea Zelioli[1], Augustas Vaitkevičius[1,2], Bronislovas Čechavičius[1], Evelina Dudutienė[1], Andrius Bičiūnas[1], Virginijus Bukauskas[1], Mindaugas Kamarauskas[1], Renata Butkutė[1,2]

[1]Center for Physical Sciences and Technology, Vilnius, Lithuania
[2]Institute of Photonics and Nanotechnology, Vilnius University, Vilnius, Lithuania
aivaras.spokas@ftmc.lt

Near Infrared (NIR) spectral region has a plethora of different everyday applications. Due to its high penetration depth into soft tissue, it can be used in both sensing (e.g. pulse oximetry) and treatment of humans. Furthermore, all modern communications also rely on semiconductor lasers with emission at 1300 and 1550 nm. Finally, this spectral region has a well-developed detector technology based on classical semiconductor materials (Si, Ge, InGaAs). Despite this the emitters working in this region struggle with temperature stability and due to their narrow bandgap are prone to large Auger recombination losses. More than two decades ago GaAsBi was proposed as an attractive NIR material. It has a large bandgap reduction of up to 88 meV per 1% of As being replaced by Bi in the GaAs lattice [1]. Moreover, it possesses a temperature insensitive emission spectrum, with stable room temperature operation [2, 3]. Finally, it has been showcased that the strong effect of bismuth incorporation on the valence band of the material induces a large increase of the spin-orbit split-off energy, which at 10.5 % of Bi content becomes larger than the bandgap, meaning that one of the major non-radiative Auger loss mechanisms becomes suppressed [4]. Despite these properties being direct solutions to the main drawbacks of current NIR emitters, the success of GaAsBi is limited by its complicated growth and defectiveness, stemming from the low growth temperature (< 420 °C) and stochiometric As to Ga ratio, contrary to the classic approach in growth of AIII-BV at a group V overpressure.

This work focuses on the MBE growth optimization of the GaAsBi active region design and fabrication of electrically pumped diode emitters. Initially, growth and characterization of GaAsBi multiple rectangular quantum well (RQW) test structures was carried out to determine the optimal growth regime and clarify the influence of parameters on the optical quality of the quantum structures. This was followed by the fabrication of laser diode (LD) and LED structures. Structures were grown with different layer designs and dopant profiles, some were additionally buffered by AlAs sacrificial layers, allowing for the removal of the substrate and bonding onto different platforms (e.g. SiC or InP). The characterization of LEDs revealed the spectral stability in a wide temperature range from 30 to 300 K, with the central emission wavelength shifting from 1035 to 1060 nm. Rapid thermal annealing was shown to have a positive influence on the LED active region quality. LDs with lasing lines in the range from 1000 nm to 1140 nm were grown and processed. The output peak power of GaAsBi 3xRQW based semiconductor microlasers reached up to 10 mW.

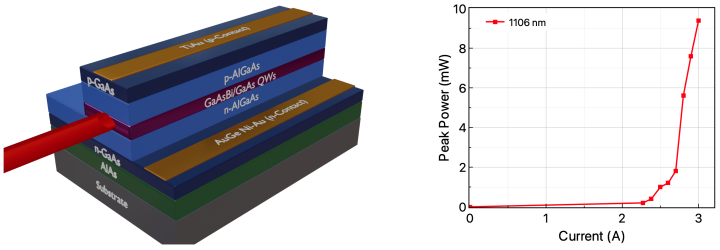


Fig. 1. (Left) Schematic of an FP edge emitting LD. (Right) Injection current – output power characteristics of a 3xRQW GaAsBi/GaAs LD (pulsed excitation 50 ns at 1 kHz).

Acknowledgements

The work (“Apvalkalinio p - AlGaAs sluoksnio technologijos vystymas lazerinių diodų integracijai ant Si platformos”) was supported by the Research Council of Lithuania under agreement no. P-ST-24-170

[1] S. Francoeur, M. J. Seong, A. Mascarenhas, S. Tixier, M. Adamcyk, and T. Tiedje, “Band gap of GaAs1-xBix, 0<x<3.6%,” Appl. Phys. Lett., 82, 3874–3876 (2003).
[2] Y. Tominaga, K. Oe, and M. Yoshimoto, “Low temperature dependence of oscillation wavelength in GaAs1-xBix laser by photo-pumping,” Appl. Phys. Exp., 3, 062201 (2010).
[3] 3. P. Ludewig, N. Knaub, N. Hossain, S. Reinhard, L. Nattermann, I. P. Marko, S. R. Jin, K. Hild, S. Chatterjee, W. Stolz, S. J. Sweeney, K. Volz, “Electrical injection Ga(AsBi)/(AlGa)As single quantum well laser”, Appl. Phys. Lett. 102 (24): 242115. (2013).
[4] K. Alberi, O. D. Dubon, W. Walukiewicz, K. M. Yu, K. Bertulis, and A. Krotkus, “Valence band anticrossing in GaBixAs1-x,” Appl. Phys. Lett., 91, 10–13 (2007).

SUBMICRON PERIODIC STRUCTURES IN METAL OXIDE THINFILM VIA LASER ABLATION AND THERMAL OXIDATION

Julianija Nikitina[1], Simonas Indrišiūnas[1], Tomas Tolenis[2], Mindaugas Andrulevičius[3], Lina Grinevičiūtė[1]

[1]Department of Laser Technologies, Center for Physical Sciences and Technology, Vilnius, Lithuania
[2]ELI Beamlines Facility, Extreme Light Infrastructure ERIC, Dolní Bŕežany, Czech Republic
[3]Institute of Materials Science, Kaunas University of Technology, Kaunas, Lithuania
julianija.nikitina@ftmc.lt

Periodic structures, featuring periodic modulation of optical constants, exhibit polarization control, spectral and angular selectivity of light, and thus were found extremely useful for laser radiation manipulation. However, fabrication technologies of periodic structures have to face strict requirements for laser optics, especially for high-power systems. Despite a sub-micrometer scale of periodicity required for visible and infrared spectral region applications, the next significant criteria are optical transparency and durability, which require a completely inorganic composition of all constituent materials. Polymers are quite easily processed and can be transparent in the target spectral regions, but they exhibit lower optical resistance compared with fully inorganic materials such as metal oxides [1]. Although direct patterning the latter while striving for sufficiently low surface roughness is a non-trivial task, especially if sub-micrometric periodicity is required. To get around a direct patterning of metal oxides, a metallic thin film deposited on a glass can be structured. Subsequent annealing at elevated temperatures promotes a metal oxidation reaction, resulting in a fully inorganic, transparent periodic structure. Several structuring techniques capable of submicron surface patterning have been described in the literature, including lithography, ion beam etching and ultrashort laser processing. Among these, only the latter can circumvent the complexities associated with other techniques, such as contamination during manufacturing, time-consuming and expensive large-scale production. Based on this, ultrashort laser processing, specifically Direct Laser Interference Patterning (DLIP), was chosen for this study.

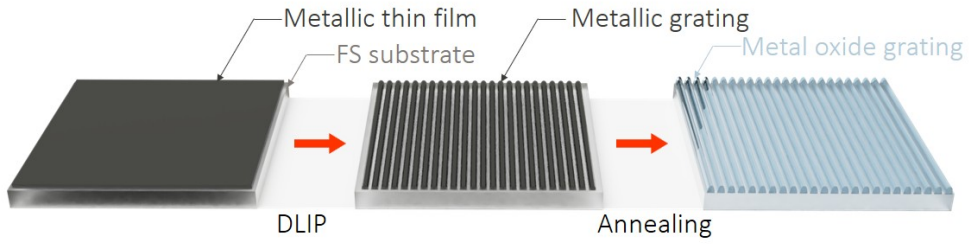


Fig. 1. Fig. 1 Fabrication steps of submicron periodic surface structure in metal oxide thin film, including Direct Laser Interference patterning (DLIP) of metallic layer and thermal oxidation.

In this work [2], we present a two-step method for the fabrication of submicron metal oxide periodic structure (Fig.1), avoiding complexities of direct structuring of dielectric materials. A linear surface pattern with a spatial periodicity of 750 nm was fabricated in pure tantalum metal thin film via the DLIP technique, followed by annealing to form the tantalum oxide periodic structure. To achieve this, prior investigation of non-patterned metallic thin films annealing was done in search of appropriate oxidation parameters. The fabricated structures were characterized in terms of composition, surface morphology, and optical properties, demonstrating the capabilities of the proposed method.

Acknowledgements

This work was supported by the PerFIN project from the Research Council of Lithuania (LMTLT), agreement No S-MIP-22–80.

[1] A. Žukauskas, et al., 'Effect of the photoinitiator presence and exposure conditions on laser-induced damage threshold of ORMOSIL (SZ2080)', Optical Materials, vol. 39, 2015, doi: 10.1016/J.OPTMAT.2014.11.031.
[2] J. Nikitina, et al., 'Submicron periodic structures in metal oxide coating via laser ablation and thermal oxidation', Applied Surface Science Advances, vol. 24, December, 2024, doi: 10.1016/j.apsadv.2024.100660.

FABRICATION OF SUBMICRON STRUCTURES VIA DOUBLE EXPOSURE UV LITHOGRAPHY

Helena Ose[1,2], Edvins Letko[2]

[1]Faculty of Science and Technology, University of Latvia, Jelgavas iela 3, Riga, LV-1004
[2]Institute of Solid State Physics, University of Latvia, Ķengaraga iela 8, Riga, LV-1063
helena.ose@cfi.lu.lv

Keywords: ring resonators, double-exposure UV lithography, SU-8.

Ring resonators are essential components in biosensors, optical sensor systems, integrated circuits, and telecommunication devices, as well as in enhancing laser coherence. Their fabrication requires high precision, typically achieved using electron beam lithography (EBL). However, EBL is slow and complex, prompting interest in UV lithography as a faster, more accessible alternative. Conventional UV lithography faces challenges due to diffraction effects, limiting feature sizes to approximately 1 µm when using a 375 nm wavelength source. Creating small gaps is particularly difficult, as closely spaced structures tend to merge due to optical diffraction. This research explores a double-exposure UV lithography method to fabricate submicron ring resonators using SU-8, aiming to achieve gap sizes as small as 20–100 nm. To enhance alignment precision, metalized markers were used for overlaying the two lithographic exposures. The fabricated structures were analyzed using a scanning electron microscope (SEM) to evaluate gap profiles and tested for optical resonance by coupling laser light into the resonators. Additionally, COMSOL modeling was performed to optimize the ring resonator design and predict expected optical behavior. Achieving submicron structures using UV lithography would represent a significant advancement, offering a faster and more scalable alternative to traditional EBL-based fabrication. This method has the potential to simplify production while maintaining the precision needed for photonic applications.

LASER DIRECT WRITING 3D PRINTING OF LUMINESCENT YAG:Ce MICROSTRUCTURES

A. Harnik[1], R. Virkėtis[2], D. Dapšys[1], D. Ladika[1], G. Merkininkaitė[2], S. Šakirzanovas[2], M. Malinauskas[1]

[1]Laser Research Center, Faculty of Physics, Vilnius University, Saulėtekio Ave. 10, LT- 10223, Vilnius, Lithuania
[2]Institute of Chemistry, Faculty of Chemistry and Geosciences, Vilnius University, LT- 03225, Naugarduko Str. 24, Vilnius, Lithuania
arturas.harnik@ff.vu.lt

Yttrium aliuminium garnet (YAG) has been a laser gain medium for over 60 years [1]. Czochralski synthesis method has been used as the primary production method of YAG monocrystals [2]. While polycrystalline YAG has a higher number of synthesis methods available for its production [3,4], none of them are suitable for the fabrication of complex 3D YAG microstructures. This work aims to show that two-photon polymerization laser 3D printing [5] can produce polycrystalline 3D luminescent YAG:Ce microstructures via the post-processing calcination step [6,7].

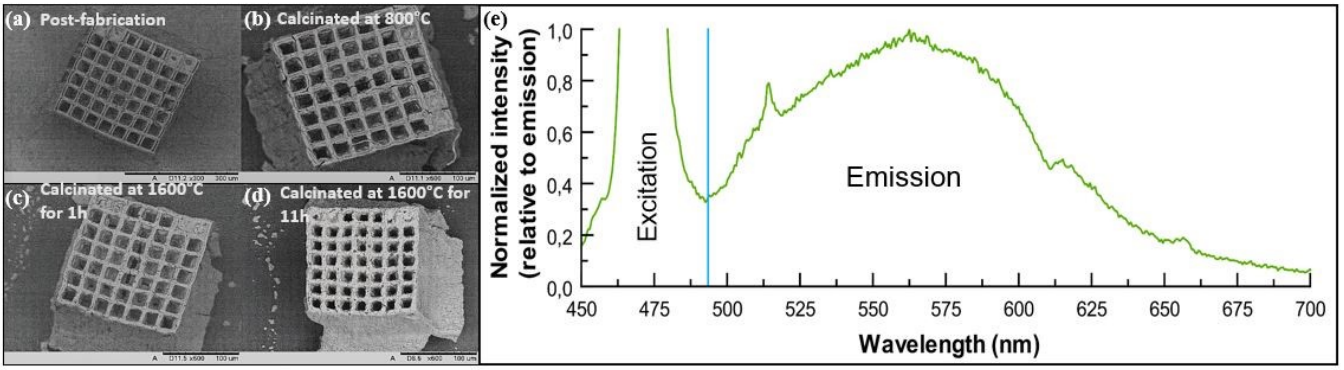


Fig. 1. Laser 3D micro-printed YAG:Ce microstructures (a) post-fabrication, (b) heated at 800 °C, (c) heated at 1600 °C for 1 h, (d) 11 h and (e) emission spectra of YAG:Ce 2% 3D microstructured sample when excited at 470 nm wavelength.

YAG and YAG:Ce precursor 3D objects were produced by a Laser Nanofactory (UAB Femtika) femtosecond laser lithography workstation and using two-photon polymerization 3D printing method for enhanced resolution. 517 nm irradiation wavelength laser of 144 fs pulses was used for the fabrication of 3D microstructures. To study and determine the most optimal production parameters for these materials, 3D arrays of woodpile structures were printed by changing exposure power (intensity) and fabrication time (scanning velocity). After the fabrication, polymerized YAG/YAG:Ce precursor samples were immersed in ethanol to dissolve unpolymerized resin. Afterward, samples were heated first at 800 °C to remove all of the organic matter and later at 1600 °C to produce pure YAG/YAG:Ce. The temperature necessary for the first heating step was determined using the thermogravimetric analysis method. The purity of the calcinated YAG/YAG:Ce samples was also estimated using the single crystal X-ray diffraction analysis method. This was done by obtaining X-ray diffraction data - Debye Scherrer rings, and integrating that data using Bruker Apex 3 software. Finally, luminescence measurements of YAG:Ce were carried out, showing the dependence of Ce concentration on luminescence intensity.

Acknowledgements

This research has been carried out in the framework of the ”Universities‘ Excellence Initiative” program by the Ministry of Education, Science and Sports of the Republic of Lithuania under the agreement with the Research Council of Lithuania (project No. S-A-UEI-23-6) and was funded by Vilnius University Research Promotion Fund (project No. MSF-JM-10/2024).

[1] Zac, “Is It Time To Invest In A Cutera YAG Laser?“, laserresell„ May 16 2022, https://laserresell.com/buying-usedequipment/cutera-yag-laser/, (Accessed: 27 June 2024).
[2] Ikesue, A., Aung, Y. L., and Lupei, V., [Ceramic Lasers], Cambridge University Press (2013).
[3] B. Bettes and Yi Xie, “Synthesis and processing of transparent polycrystalline doped yttrium aluminum garnet: a review”, Mater. Res. Lett., 11-1, 1-20 (2023).
[4] A. Towata, H. J. Hwang, M. Yasuoka, M. Sando and K. Niihara, “Preparation of polycrystalline YAG/alumina composite fibers and YAG fiber by sol–gel method”, Composites, A 32 (8), 1127-1131 (2001).
[5] G. Zyla and M. Farsari, “Frontiers of Laser-Based 3D Printing: A Perspective on Multi-Photon Lithography“, Laser Photonics Rev., 18-7, 2301312 (2024).
[6] G. Merkininkaitė, E. Aleksandravičius, M. Malinauskas, D. Gailevičius and S. Šakirzanovas, „Laser additive manufacturing of Si/ZrO2 tunable crystalline phase 3D nanostructures”, Opto-Electron Adv., 5, 210077 (2022).
[7] A. Harnik and et al., „Laser 3D micro-/nano-structurization of luminescent materials“, Appl. Mater. Today, IN REVIEW (2025).

ORAL SESSION 3

Laser Physics and Optical Technologies

Chair: Dr. J. Vengelis

BEYOND 3 µM: HIGH-INTENSITY FEMTOSECOND PULSES FROM OPCPA AND ROTATIONAL SRS

Augustė Černeckytė[1], Paulius Mackonis[1], Aleksej Rodin[1]

[1]Solid State Lasers Laboratory, Department of Laser Technologies, Center for Physical Sciences and Technology
auguste.cerneckyte@ftmc.lt

Sources of intense femtosecond laser radiation in the wavelength range of 1.8 – 3 µm are in demand for generating THz and attosecond X-ray pulses [1], particle acceleration and remote sensing, biological imaging, medicine, and material processing by direct excitation of phonon modes. Several approaches to delivering intense ultrashort laser pulses in the wavelength range greater than 2 µm have been explored. The most advanced sources have been shown to be primarily based on optical parametric chirped pulse amplification (OPCPA), operating in the degeneracy range when pumped by a single-picosecond lasers near 1 µm.

We demonstrate a compact and cost-effective mid-IR laser source driven by 1.3 ps pulses from a Yb-rod laser operating at 1030 nm. Broadband supercontinuum (SC) seed pulses in the wavelength range 1050 – 2400 nm obtained in a 130 mm long YAG crystal were amplified in a three-stage collinear OPCPA, and then both the signal and idler pulses were focused into a hydrogen cell to extend the OPCPA coverage beyond 3 µm by the high-order cascade rotational stimulated rotational Raman scattering (SRS). During the experiments, the pressure, cell length, spectral mismatch between the signal and idler pulses, and the chirp induced in the SC pulses were optimized. A modified two-stage four-pass Yb-rod chirped pulse amplifier [2] with a record gain of 10 million was used as the pump source for both SC and BiBO-based OPCPA (Fig. 1 left). Compared to the previous implementation [3] the dispersion of SC seed pulse has been varied using an acousto-optic programmable dispersive filter (AOPDF).

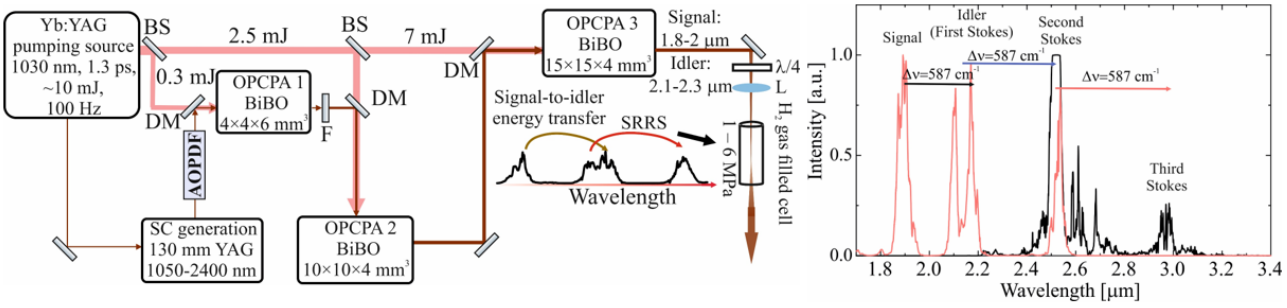


Fig. 1. Experimental setup for investigation of transient rotational SRS in compressed hydrogen – left: DM – dichroic mirrors; BS – beam splitters; λ/4 – quarter-wave retardation plate; L – focusing lens; AOPDF – acousto-optic programmable dispersive filter. Normalized output spectra from a 63 cm (red line) and 43 cm (red and black line) cell at 6 MPa hydrogen pressure – right.

With a total energy contained in the incident signal and idler pulses of 1.5 mJ and a hydrogen pressure of 6 MPa, a third-order rotational Stokes pulse was observed at a wavelength beyond 3 µm (Fig. 1). The transient cascade rotational SRS in compressed hydrogen provides a Stokes pulse energy of over 70 µJ at 2.6 µm with a conversion efficiency of 11% after optimization of the signal and idler spectra, the chirp induced in the signal pulses, and the cell length. Positively chirped broadband SC seed pulses contribute to the extension of the SRS spectral bandwidth to longer wavelengths compared to negatively chirped ones. Although the possibility of third-order Stokes generation at a wavelength of 3 µm has been demonstrated, to improve the SRS conversion efficiency it is necessary to use another SC seed covering the range of 2.5 – 3.5 µm. This possibility was also demonstrated when pumping the YAG rod near 2 µm.

Thus, the generation of high-order Stokes pulses via transient rotational SRS in compressed hydrogen was investigated using sub-picosecond signal and idler pulses in the short-wave infrared spectral range. This new approach to generating intense femtosecond pulses, combining OPCPA with transient rotational SRS, now already provides spectral extension from 2 µm to 3.1 µm.

[1] P. Agostini and L. F. DiMauro, “The physics of attosecond light pulses,” Rep. Prog. Phys. 67, 813–855 (2004).
[2] P. Mackonis and A. M. Rodin, “Laser with 1.2 ps, 20 mJ pulses at 100 Hz based on CPA with a low doping level Yb:YAG rods for seeding and pumping of OPCPA,” Opt. Express 28, 1261–1268 (2020).
[3] A. Petrulenas, P. Mackonis, and A. M. Rodin, “High-efficiency bismuth borate-based optical parametric chirped pulse amplifier with ~2.1 mJ, 38 fs output pulses at ~2150 nm,” High Power Laser Sci. 11 (2023).

THEORETICAL INVESTIGATION OF GUIDED MODE RESONANCE EFFECT IN OPTICAL GAIN CAVITIES

Ignas Lukosiunas[1], Kestutis Staliunas[1,2,3]

[1]Vilnius University, Laser Research Center, Sauletekio Ave. 10, Vilnius, Lithuania
[2]ICREA, Passeig Lluís Companys 23, 08010, Barcelona, Spain
[3]UPC, Dep. de Fisica, Rambla Sant Nebridi 22, 08222, Terrassa (Barcelona), Spain
ignas.lukosiunas@ff.vu.lt

The guided mode resonance (GMR) is an effect introduced by R. Magnusson in thin modulated films which is characterized by narrow-band reflection and transmission properties, high resonance quality factors as well as its applications for spatial filtering in laser systems, polarization filters, and angular dispersion control [1]. Such universal devices are broadly studied, however, only as passive filters that exhibit no optical gain. Structures with optical gain are capable of enchancing the transmitted and reflected radiation via introduced imaginary refractive index, where the imaginary part corresponds to the exponential amplification of guided mode's amplitude.The concept of enhanced radiation via incorporating gain is illustrated in Fig. 1.

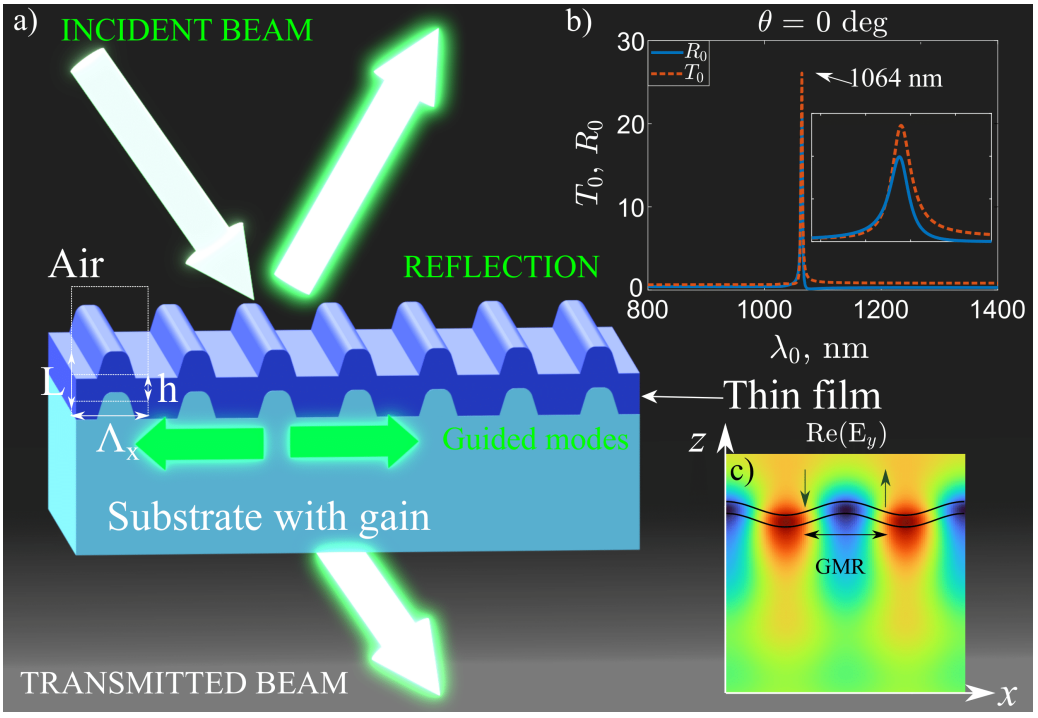


Fig. 1. The concept of an active meta-mirror: a) the incident beam couples into the waveguiding mode of the thin film. Backcoupling results in substantial increase of the reflected ant transmitted radiation. b). Reflection/transmission dependence on the wavelength by crossing the resonance. c) the field distribution in the thin film.

The gain material itself is introduced as a perovskite with imaginary refractive index capable of exponential amplification of diffraction efficiencies [2]. With proper optimization algorithms and numerical tools [3], the device geometry can be tuned to achieve high resonance quality factors and optimal coupling between incident radiation, excited guided modes and the radiation itself, thus maximizing the reflection and transmission coefficient values. Such structures can be used as angle sensitive amplifiers, low-pass amplifiers in laser systems. In this work we apply genetic optimization algorithm with 2D RCWA method to achieve device designs which exhibit enchanced gain via GMR effect. We also expand on the analytical model which we use to quantitavely explain the behavior and characteristics of the achieved results.

[1] S. S. Wang and R. Magnusson, "Theory and applications of guided-mode resonance filters," Appl. Opt. 32, 2606-2613 (1993)
[2] A. Liu et al, "Metal Halide Perovskites toward Electrically Pumped Lasers". Laser Photonics Rev 2022, 16, 2200189.
[3] M. G. Moharam and T. K. Gaylord, "Rigorous coupled-wave analysis of planar-grating diffraction," J. Opt. Soc. Am. 71, 811-818 (1981)

INFLUENCE OF CONICAL WAVE FORMATION ON SUBNANOSECOND BACKWARD WAVE OPTICAL PARAMETRIC AMPLIFIER

Tomas Latvys[1], Viktorija Tamulienė[1]

[1]Laser Reasearch Center
tomas.latvys@ff.stud.vu.lt

A backward wave optical parametric oscillator (BWOPO) converts pump radiation into longer-wavelength signal and idler waves propagating in opposite directions, enabling mirrorless oscillation. Unlike conventional optical parametric generators and amplifiers, BWOPOs produce much narrower spectral widths and maintain stable wavelengths despite temperature changes [1]. Developing a model for BWOPOs is essential for optimizing design parameters, predicting performance, and understanding nonlinear dynamics without costly experiments. However, existing models are exclusively one-dimensional (1D), limiting their ability to capture spatial effects and more complex interactions [2,3]. Here, we propose a three dimensional (3D) model for a BWOPO in a periodically poled $KTiOPO_4$ (PPKTP) crystal pumped by subnanosecond pulses from a Nd:YAG microlaser.

To model this system, we use three-wave coupling equations that account for beam diffraction, temporal walk-off, nonlinear coupling, and both linear and two-photon absorption. By numerically solving them using the split-step method, we can track the evolution of wave amplitudes throughout the interaction region.

As shown in Fig. 1a, the 3D model enables us to visualize smooth and well-structured temporal profiles of the pump and generated pulses, closely resembling real experimental results. In contrast, the 1D simulation (Fig. 1b) exhibits highly oscillatory behaviour. The presence of off-axis components in the 3D model leads to the formation of ring-shaped beams (Fig. 1c), which become hidden when the beam profile is time-integrated (Fig. 1d). Our analysis reveals that this ring-shaped structure originates from X-wave formation within the nonlinear crystal. The sign of an X-wave's propagation velocity is determined by the wavelengths of the generated waves, allowing it to travel either toward the crystal's end or its front.

In conclusion, the proposed BWOPO model surpasses the limitations of previous 1D approaches and effectively demonstrates X-wave formation as a distinctive feature.

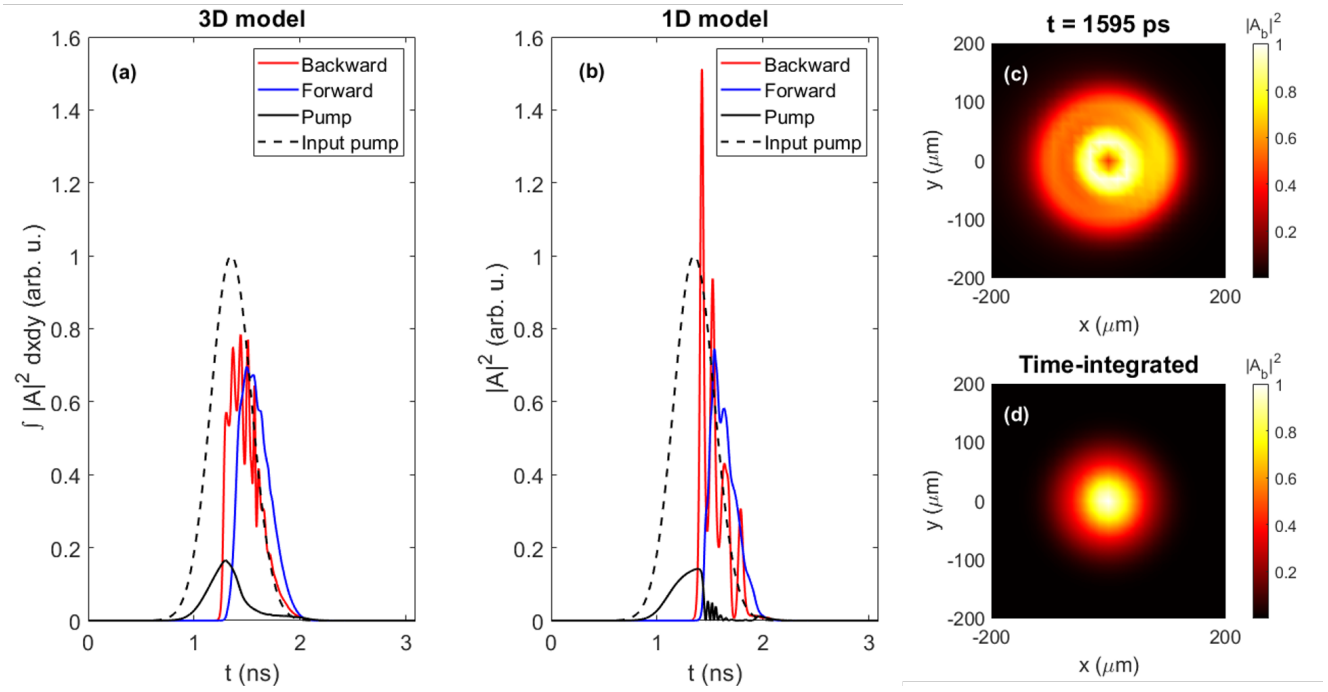


Fig. 1. Fig 1. Output temporal profiles of pump and generated pulses for (a) 3D and (b) 1D simulations. Spatial profiles of the backward wave at (c) t = 1595 ps and (d) integrated over time. Pump wavelength: 532 nm, pulse energy: E_p= 0.1 mJ.

[1] C. Canalias, V. Pasiskevicius, Mirrorless optical parametric oscillator, Nature Photonics 1, 459-462 (2007).
[2] C. E. Minor, R. S. Cudney, Mirrorless optical parametric oscillation in bulk PPLN and PPLT: a feasibility study, Appl. Phys. B 123, 38 (2017).
[3] C. Montes, B. Gay-Para, M. De Micheli, P. Aschieri, Mirrorless optical parametric oscillators with stitching faults: backward downconversion efficiency and coherence gain versus stochastic pump bandwidth, J. Opt. Soc. Am. B 31, 3186-3192 (2014).

DESIGN AND OPTIMIZATION OF PARITY-TIME SYMMETRIC STRUCTURES FOR UNIDIRECTIONAL PROPAGATION OF LIGHT

Indre Meskelaite[1], Kestutis Staliunas[1,2,3], Darius Gailevicius[1]

[1]Vilnius University, Faculty of Physics, Laser Research Center, Sauletekio Ave. 10, 10223, Vilnius, Lithuania
[2]ICREA, Passeig Lluís Companys 23, 08010, Barcelona, Spain
[3]UPC, Dep. de Fisica, Rambla Sant Nebridi 22, 08222, Terrassa (Barcelona), Spain
indre.meskelaite@ff.stud.vu.lt

As the demand for computational power continues to grow, conventional electronic computing systems face technological, economic, and environmental challenges. In response to this, with recent advances in photonics technology, optical computing emerges as a viable alternative, offering higher speeds and lower power consumption. One particularly promising approach to optical computing is the optical neural network (ONN), a hardware-based implementation of an artificial neural network (ANN) that employs different optical devices to perform the required functions [1].

In this work, as our first step toward demonstrating an ONN, we focus on developing an optical waveguide capable of unidirectional light propagation. The unidirectionality is achieved through a specially designed structure that adheres to the parity-time (PT) symmetry requirement of non-Hermitian photonics [2]. In particular, to fulfill this condition, both the real and imaginary components of the structure's effective refractive index must be periodically modulated and phase-shifted by $\pi/4$ relative to each other. A schematic representation of a few examples of the possible structure designs is provided in Fig. 1(a). In this work, we present the numerical investigation, encompassing the design and optimization, of such structures, as well as the exploration of different material systems that best suit our fabrication capabilities and foreseen applications.

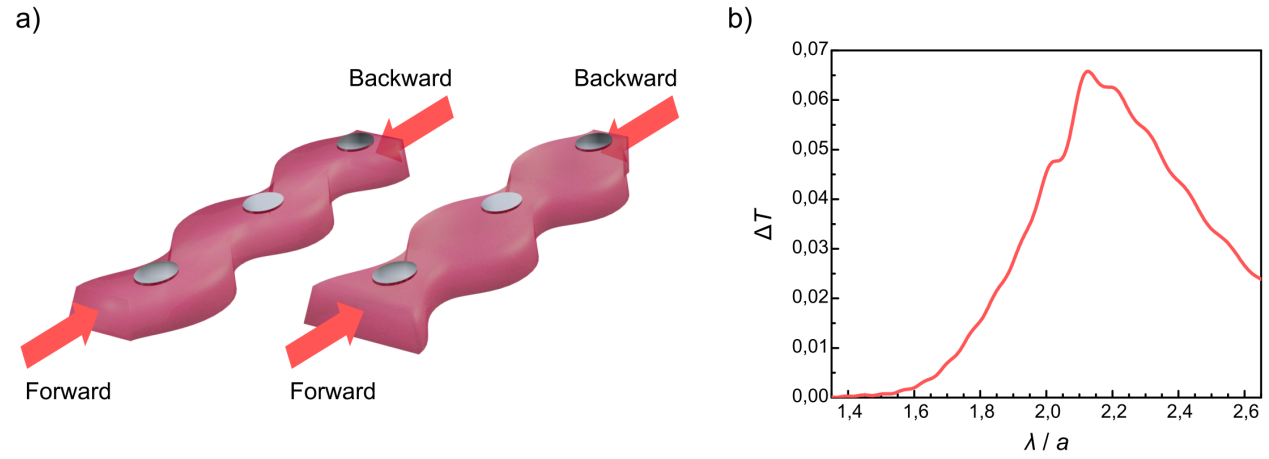


Fig. 1. PT-symmetric structures for unidirectional light propagation. (a) Two examples of the possible structure designs: a periodically modulated dielectric waveguide with metallic islands periodically deposited on top. (b) The difference between the forward- and backward-injected light transmission as a function of the wavelength normalized to the modulation period.

The results of an initial numerical study of such a PT-symmetric structure (left structure in Fig. 1(a)) already indicate that the difference ΔT between the transmission of the forward- and backward-injected light is present for certain wavelength λ and modulation period a ratios even for a non-optimized design (see Fig. 1(b)). Consequently, with careful further optimization of the structure design and an appropriate choice of the material system, an increase in ΔT is expected.

[1] B. J. Shastri et al., "Photonics for artificial intelligence and neuromorphic computing," Nature Photonics, vol. 15, no. 2, pp. 102–114, Jan. 2021, doi: https://doi.org/10.1038/s41566-020-00754-y.
[2] Y. Huang, Y. Shen, C. Min, S. Fan, and Georgios Veronis, "Unidirectional reflectionless light propagation at exceptional points," Nanophotonics, vol. 6, no. 5, pp. 977–996, May 2017, doi: https://doi.org/10.1515/nanoph-2017-0019.

ORAL SESSION 4

Material Science and Nanotechnology

Chair: Dr. T. Malinauskas

THE EVALUATION OF PHOTOLUMINESCENCE EFFICIENCY OF GaAsBi QUANTUM WELLS

Aistė Štaupienė[1], Andrea Zelioli[1], Aivaras Špokas[1], Bronislovas Čechavičius[1], Renata Butkutė[1], Evelina Dudutienė[1]

[1]SRI Center for Physical Sciences and Technology, Saulėtekio av. 3, Vilnius, Lithuania
aiste.staupiene@ftmc.lt

GaAsBi quantum well (QW) structures have gained significant interest as potential active media for opto-electronic devices operating in the near-infrared (NIR) region. One of the key advantages of GaAsBi is its strong bandgap redshift with increasing Bi content, as well as its enhanced spin-orbit splitting, which can suppress Auger recombination and inter-valence band absorption. Additionally, GaAsBi exhibits reduced temperature sensitivity, enabling tunable laser operation on a well-developed GaAs platform without the need for additional cooling [1-3].

However, the growth of GaAsBi quantum structures is challenging, as it requires low growth temperatures in order to incorporate large Bi atoms into the GaAs lattice. This leads to a high point defect density, resulting in a significant reduction in GaAsBi luminescence intensity and emission efficiency. Therefore, optimizing the growth conditions to enhance the quality of GaAsBi is crucial for developing efficient NIR sources, necessitating precise efficiency measurements, which help to fine-tune growth conditions and improve material quality.

This study focuses on developing a reliable method for calculating internal quantum efficiency (IQE) of GaAsBi quantum structures. A comprehensive analysis of carrier recombination processes was conducted using absolute IQE measurements with an integrating sphere and our newly developed ABB* method [4], which includes contribution from trap-assisted Auger-Meitner non-radiative recombination (TAAR) (see fig. 1). The acquired IQE values for different quantum structures highlighted the detrimental effect of low growth temperatures and Bi content on material quality and photoluminescence (PL) emission.

We show a simple analysis method to not only calculate the IQE but also evaluate the relative carrier recombination ratios. This work facilitates a direct comparison of samples even across different research laboratories and provides valuable insights into both radiative and non-radiative recombination mechanisms. These findings contribute to the optimization of GaAsBi growth processes, paving the way for enhanced optoelectronic device performance in the NIR region.

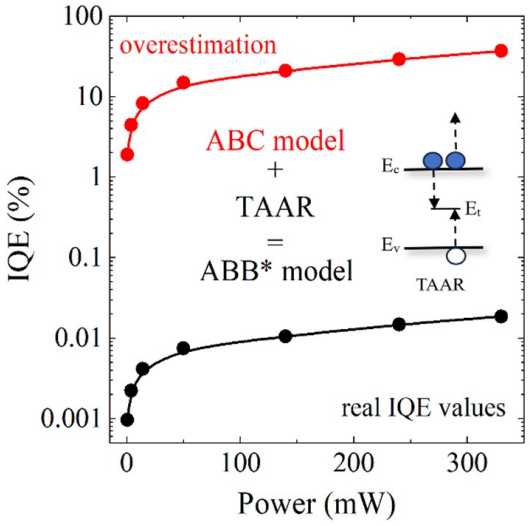


Fig. 1. Calculated emission efficiencies of GaAsBi/GaAs multiple quantum well structure employing the ABC and modified ABB* methods.

Acknowledgements

This joint Lithuania-Taiwan project has received funding from Research Council of Lithuania under contract no. S-LT-TW-24-8.

[1] T. Fuyuki et al., Appl. Phys. Lett., 103, 202105 (2013)R. D. Richards et al. Phys. Stat. Sol. (B) 259(2), 2100330 (2022).
[2] K. Alberi et al., Appl. Phys. Lett. 91, 051909 (2007).
[3] R. D. Richards et al. Phys. Stat. Sol. (B) 259(2), 2100330 (2022).
[4] A. Staupiene et al. Appl. Phys. Lett. 125, 221102 (2024).

CARRIER DYNAMICS IN InGaN MQW STRUCTURE WITH VARYING EMISSION WAVELENGTHS

Seda Türkcan[1], Kazimieras Nomeika[1]

[1] Institute of Photonics and Nanotechnology, Vilnius University
seda.turkcan@ff.stud.vu.lt

InGaN is a semiconductor extensively used in optoelectronic applications, including LEDs and laser diodes due to its high mobility, good internal quantum efficiencies and tunable bandgap. To this day, nitride-based light emitting devices face challenges such as efficiency drop at high carrier densities and reduction in internal quantum efficiency in the green wavelength region, known as the ”green gap”, which hinders the production of high-efficiency green light devices. Despite these challenges, InGaN remains as a leading candidate for covering the entire visible spectrum, making it critical to study the effects of variations in indium content and QW width on these structures. In this study, we investigate the non-equilibrium carrier dynamics of an InGaN MQW sample with spatial variations in indium content, using light-induced transient grating and time-integrated photoluminescence techniques. By analyzing lifetime, diffusivity, and diffusion length properties, we establish their relationship with internal quantum efficiency and model the carrier dynamics with a modified ABC model. This study reveals how carrier dynamics in InGaN QWs change with varying emission wavelengths with variations in indium content and QW width, while keeping other factors constant. Our findings show a decreasing trend in the recombination rates of different channels at longer wavelengths.

INFLUENCE OF SiC REINFORCEMENT ON MECHANICAL AND THERMAL PROPERTIES OF DMLS MANUFACTURED AlSi10Mg COMPOSITES

Karolis Stravinskas[1], Ričardas Petkus[1], Ada Steponavičiūtė[1], Genrik Mordas[1]

[1]Center for Physical Sciences and Technology, Department of Laser Technologies, Vilnius, Lithuania
karolis.stravinskas@ftmc.lt

This study investigates the effect of 10% Silicon Carbide (SiC) reinforcement on the mechanical and thermal properties of AlSi10Mg made by Direct Metal Laser Sintering (DMLS). The research optimised laser energy density to study the effect on density, hardness, surface roughness, tensile strength and thermal behaviour. A comparison between unreinforced AlSi10Mg and SiC reinforced AlSi10Mg shows the complex interactions between laser processing parameters, thermal conductivity and phase stability. The introduction of SiC changes the material's response to laser energy, affecting melt pool dynamics, solidification behaviour and residual stress formation. The results show SiC reinforcement improves hardness and wear resistance but increases thermal stresses, so process control is required to avoid defects like porosity, microcracking and SiC decomposition. The composite also has a change in optimal process parameters due to thermal conductivity, laser absorption and powder bed packing density compared to base alloy. These results highlight the need to balance laser power, scan speed and hatch spacing to get defect free structure with desired mechanical and thermal properties. This study provides insights into the role of SiC in Metal Matrix Composites (MMCs) and practical guidelines to refine DMLS parameters to get the best combination of strength, hardness, ductility and thermal stability in SiC reinforced AlSi10Mg parts. The results contribute to the understanding of MMCs for high performance applications in aerospace, automotive and thermal management systems.

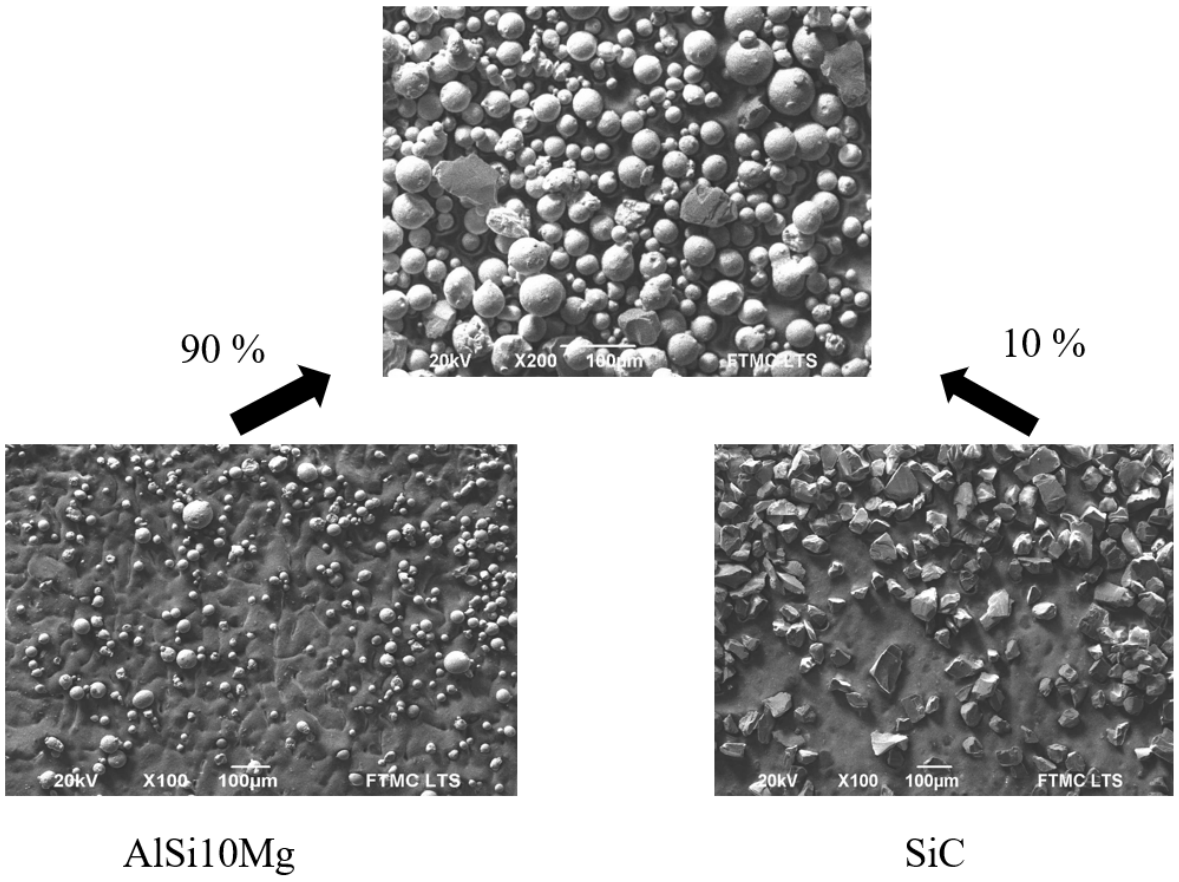


Fig. 1. SEM images of powders used for DMLS: AlSi10Mg and SiC

STRAIN ENGINEERING AND FERROELECTRIC BEHAVIOR OF $BaTiO_3$ THIN FILMS: A MOLECULAR DYNAMICS STUDY

Adam Puchalski[1], Anoop K. Kushwaha[2], Rajan Khadka[2], Tomasz K. Pietrzak[1], Pawel Keblinski[2]

[1]Faculty of Physics, Warsaw University of Technology, Poland
[2]Department of Materials Science and Engineering, Rensselaer Polytechnic Institute, USA
adam.puchalski.stud@pw.edu.pl

Low-dimensional perovskite-structured ferroelectrics display spontaneous polarization, piezoelectric and pyroelectric effects as well as large dielectric constants. They are candidates for numerous applications, such as ferroelectric memory (FeRAM), microsensors and micro- and nano-scale capacitors [1]. In these applications the properties of the devices are heavily dependent on the thickness of the ferroelectric layers, especially when approaching the scale of single atomic layers where the spontaneous polarization and hysteresis loop change considerably [2]. Barium titanate (BTO) is a model ferroelectric and researching it can provide insights into the mechanisms responsible for the thickness-dependance of ferroelectric properties [3].

This work is a continuation of the study [2], where vacuum-suspended BTO thin films were simulated using molecular dynamics package LAMMPS [4] and a core-shell model. The results showed that in thin films with thickness around 12 nm, in-plane polarized films exhibit a clear hysteresis loop, while out-of-plane polarized ones already exhibit other effects without a clear hysteresis loop.

The aim of this study is to expand of the previous results by including the effects of strain, which occurs in real devices, where ferroelectric layers are deposited on a substrate with a different lattice constant. One approach to simulating these effects is simulating a film, where the first few layers are fixed in place and the rest of the film relaxes on a ”stiff” base. This method shows, that the out-of-plane polarization of layers close to the base differs from the one for the suspended film and resembles it for layers further away. Other methods for simulating the substrate, such as applying additional external forces are also investigated.

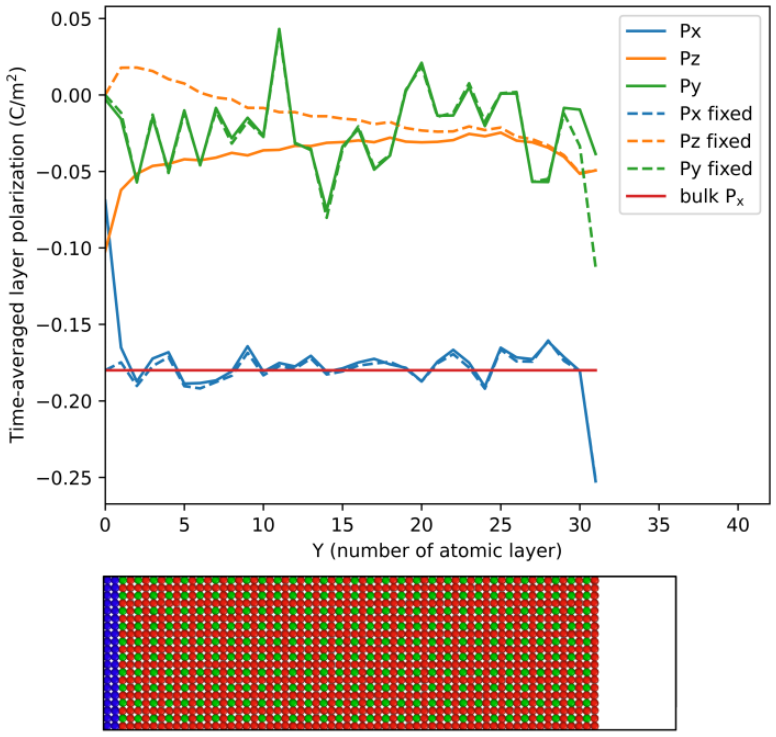


Fig. 1. The preliminary results of a polarization profile of a 12 nm film on a single fixed layer. z is the out-of-plane direction, the film is polarized in-plane. The structure below shows the fixed layers in blue, green represents barium, red oxygen and grey titanium.

[1] N. Setter, D. Damjanovic, L. Eng, et al.: Ferroelectric Thin Films: Review of Materials, Properties, and Applications, Journal of Applied Physics 100 (2006) 051606.
[2] A. K. Kushwaha, R. Khadka, P. Keblinski, Surface-Induced effects in ferroelectric BaTiO3 thin films, Surfaces and Interfaces 56 (2025) 2468-0230
[3] R. Khadka, P. Keblinski: Molecular dynamics study of domain switching dynamics in KNbO3 and BaTiO3. Journal of Materials Science 57 (2022) 12929–12946
[4] Aidan P. Thompson et al. LAMMPS - a flexible simulation tool for particle-based materials modeling at the atomic, meso, and continuum scales, Computer Physics Communications 271 (2022) 0010-4655

DIELECTRIC LOADED HELIX ANTENNAS

Justina Žemgulytė[1], Paulius Ragulis[1], Romualdas Trusovas[2], Karolis Ratautas[2], Žilvinas Kancleris[1]

[1]Department of Physical Technologies, Center for Physical Sciences and Technology, Lithuania
[2]Department of Laser Technologies, Center for Physical Sciences and Technology, Lithuania
justina.zemgulyte@ftmc.lt

Axial-mode helix antennas, where the circumference of the helix is approximately equal to the operating wavelength, are highly valued for their directional radiation patterns, high gain, and wide operational bandwidth. Dielectric loading is a well-established technique for antenna miniaturization, as it effectively slows wave propagation and reduces the physical size of the structure. However, the effects of dielectric loading on the radiation characteristics, efficiency, and bandwidth of helix antennas have not been thoroughly investigated.

We investigated dielectric loaded helix antenna in order to observe how the insertion of a dielectric material affects the operational frequency of the helix. During the work it was discovered that increasing the dielectric permittivity of the material inside the helix not only reduces the antenna dimensions, but also degrades the antenna's gain, axial ratio, and radiation characteristics. We hypothesize that this degradation results from a suboptimal pitch angle. In a helix antenna interaction between turns allows for constructive interference of the radiated waves along the axis of the helix. When the electromagnetic field is disturbed by the inserted dielectric material, it is likely that the optimal pitch angle also changes. To investigate the dependence of the optimal pitch angle on the dielectric permittivity of the inserted material, we performed electromagnetic simulations in CST Studio. In the picture (Fig. 1) we see electric field in y0z plane radiated by the helix antenna at different conditions. We observe that, at the optimal pitch angle and frequency (Fig. 1 A, B), the fields generated by each winding interfere constructively, producing a directional beam with high gain. However, under non-ideal conditions the running wave pattern is disrupted, and the fields from each winding interfere destructively, leading to scattered radiation.

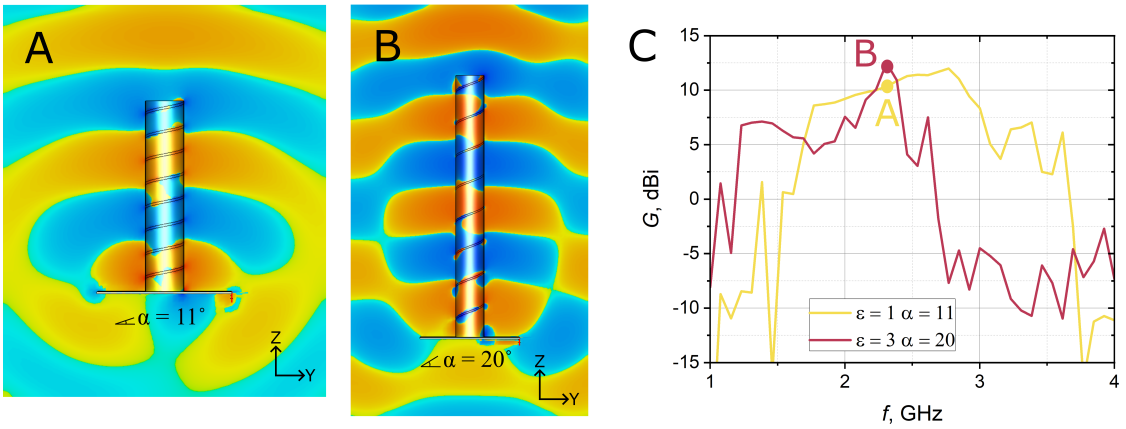


Fig. 1. Electromagnetic fields at points of interest, A - ε =1; α = 11˚ f = 2.33 GHz, B - ε =3; α = 20˚ f = 2.33 GHz, C – antenna gain dependence on frequency

To further investigate this phenomenon, we analyse fields and currents induced by helix under varying conditions to confirm the optimal parameters for constructive interference along the helix axis. To confirm our findings, we manufactured dielectric loaded helix antenna using a novel SSAIL (selective surface activation by laser) technique, that allows growing metallization on wide range of dielectric materials. Antennas are measured, and their results are compared to simulated data.

Reducing helix size using high dielectric permittivity dielectrics without degrading radiation characteristics would make it highly suitable for a wide range of telecommunications applications or space communication systems where weight, size, and performance are critical constraints.

ORAL SESSION 5

Astrophysics and Astronomy

Chair: Dr. A. Drazdauskas

EX EFFLUXI AD ASTRA: QUANTIFYING ACTIVE GALACTIC NUCLEUS-ENHANCED STAR FORMATION

Martynas Laužikas[1], Kastytis Zubovas[1,2]

[1]Center for Physical Sciences and Technology, Vilnius, Lithuania
[2]Astronomical Observatory, Vilnius University, Vilnius, Lithuania
martynas.lauzikas@ftmc.lt

By now, it is well established that most massive galaxies host a supermassive black hole at their centres. Occasionally an interstellar gas cloud intersects its sphere of gravitational influence; then, a hot accretion disc forms and often launches a relativistic particle wind - an active galactic nucleus (AGN) phase begins. Active nuclei flicker in bursts lasting several hundred thousand years, followed by quiescent intervals. Cumulative energy released by the nuclear activity is well above the gravitational binding energy of the galactic bulges. This indicates the coupling of AGN-released energy to surrounding gas must be inefficient, although capable of altering the star formation rates as inferred from the observed black hole mass-stellar velocity dispersion relation [1]. A successful model [2] has been developed in which the relation forms primarily by AGN wind-driven outflow interaction with the surrounding gas. Fast outflows (>500 km/s) simply remove the gas from the bulge, quenching star formation. On the other hand, the effect of slower outflows is debated. There is observational evidence and numerical simulations [3] to support the possibility of positive feedback, i.e. star formation enhancement, but it is limited to slow, warm-to-hot outflows below 200 km/s.

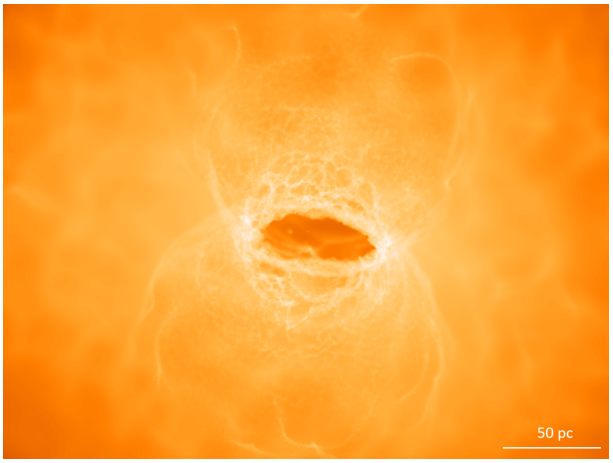


Fig. 1. Density map of expanding outflow. A short burst of nuclear activity creates a 50 pc wide central cavity surrounded by layers of multiphase gas.

We aim to further constrain the conditions required for positive feedback to manifest. We use numerical simulations to investigate the formation and propagation of an AGN-driven outflow in a realistic environment. We utilise the SPH/N-body code Gadget3 supplemented with an AGN-wind-based feedback prescription and a simplified radiative transfer. We model the evolution of a 600-pc-wide region composed of a turbulent gas shell distributed approximately isothermally, evolving in a rotating isothermal potential, with a SMBH embedded in the centre (see Fig.1). We track the propagation of a multiphase outflow created by a single Eddington-limited AGN episode. As it expands through the initially spherical approximately isothermal gas shell, the outflow both enhances star formation in the galactic disc and forms stars itself as it fragments. On the other hand, the long-term effect is negative as the outflow expels large amounts of gas. I will detail the relative importance of negative and positive feedback and their impact on the radial and velocity distributions of the stellar population.

Observations so far have provided only limited evidence of positive AGN feedback, but this should change with upcoming surveys. Our results can be used to reconstruct recent galactic activity from observed AGN-enhanced star formation, or provide insights into the contribution of positive AGN feedback to the scatter of the M-sigma relation.

[1] Ferrarese, F. & Merritt, D. (2000), The Astrophysical Journal, 539, L9-L12
[2] King, A. & Pounds, K. (2015), Annual Review of Astronomy and Astrophysics, 53, 115
[3] Laužikas, M. & Zubovas, K. (2024), Astronomy&Astrophysics, 690, A396

CLEARING THE COSMIC TABLE: HOW BLACK HOLES CLEAR AWAY THEIR MEALS

Eimantas Skuodas[1], Kastytis Zubovas[2], Matas Tartėnas[3]

[1]Institute of Theoretical Physics and Astronomy, Vilnius University, Lithuania
[2]Fundamental research division, Vilnius University, Lithuania
eimantas.skuodas@ff.stud.vu.lt

Supermassive black holes (SMBHs) at galactic centers significantly influence their environment through gravitational forces and energetic feedback mechanisms. Active galactic nuclei (AGN) outflows interact with surrounding gas structures, affecting galaxy evolution. Understanding these interactions is crucial for modeling large-scale astrophysical processes. This study aims to determine how AGN with different luminosities influence the evolution of inhomogeneous gas clouds, with a focus on mass outflow rates, momentum transfer, and energy transport.

We conducted smoothed particle hydrodynamics (SPH) simulations using the GADGET-3 code, incorporating SPHS modifications [1] for enhanced resolution. The models included different AGN luminosities and initial turbulence conditions to assess their impact on outflow characteristics. Higher AGN luminosities accelerate gas ejection and increase fragmentation of gas clouds. Enhanced mass transport and kinetic energy transfer were observed at elevated luminosities, aligning with theoretical expectations [2]. However, cooling of the outflowing gas reduced outflow efficiency, leading to deviations from analytical predictions.

The findings highlight the importance of cooling effects in AGN-driven outflows, suggesting that theoretical models must incorporate these mechanisms for accurate predictions. Moreover, our results indicate that AGN luminosity plays a crucial role in shaping outflow dynamics, with higher luminosities leading to accelerated gas ejection and increased fragmentation. Future studies should explore additional environmental factors, including the impact of AGN luminosity variations.

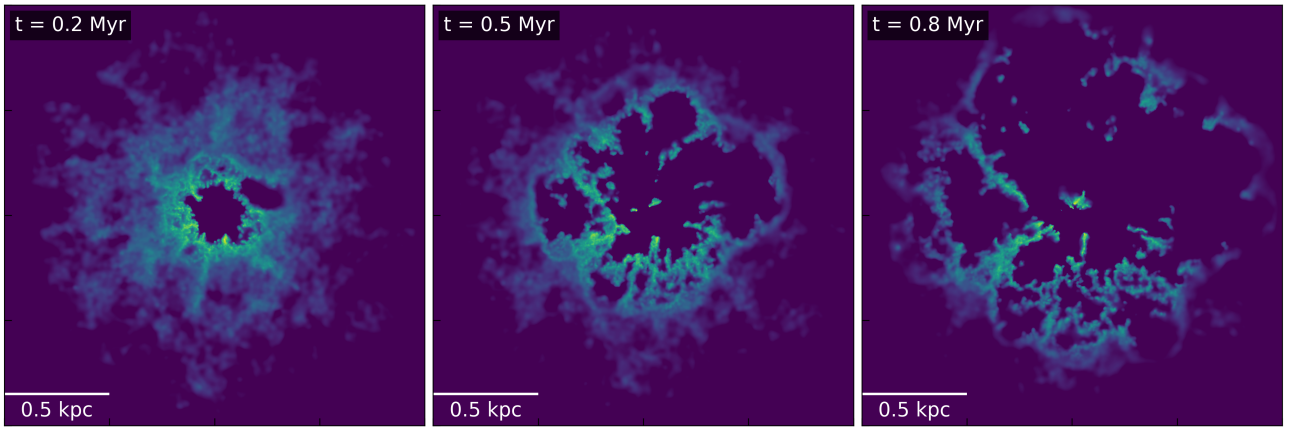


Fig. 1. Gas density around an $L_{\rm AGN} = L_{\rm Edd}$ AGN integrated through a 0.1 kpc thick slice. The maps, arranged from left to right, are ordered by increasing time: $t = 0.2$ Myr, $t = 0.5$, and $t = 0.8$. Brighter colors indicate higher gas densities.

[1] J. I. Read, T. Hayfield, MNRAS 422, 3037 (2012)
[2] K. Zubovas, A. King, ApJ 745, L34 (2012)

COMPARISON OF SIMULATED AND OBSERVED GALACTIC OUTFLOWS

Milda Valytė[1,2], Kastytis Zubovas[1,2]

[1]Institute of Theoretical Physics and Astronomy, VU
[2]Fundamental Research division, Center for Physical Sciences and Technology, Vilnius
milda.valyte@ftmc.lt

Active galactic nuclei (AGN) are sources of immense radiation that can profoundly influence the evolution of their host galaxies. AGN-driven outflows influence the interstellar medium and regulate star formation. To better understand the mechanisms driving these outflows, it is important to comprehend how parameters of the host galaxy, such as star formation rate (SFR), stellar mass ($M_\star$) and AGN luminosity ($L_{\rm AGN}$), relate to key characteristics of galactic outflows, including mass transfer rate, velocity, energy and momentum rates across different cosmic epochs.

In this study, we analyze data from the high resolution, cosmological, hydrodynamical IllustrisTNG50 simulation [1], which is run with the moving-mesh code AREPO, and select AGN-driven outflows using criteria such as gas velocities and AGN luminosity. We compare these estimated outflow and galactic parameters with observational data [2] and the semi-analytical MAGNOFIT model [3], which is used to generate large-scale outflows, to assess consistency between theoretical predictions and simulated results. Our analysis shows a strong connection between outflow velocity and galaxy stellar mass, which agrees with observational findings. Figure 1 indicates that massive galaxies exhibit more energetic outflows, which can be explained by the relationship between a galaxy's stellar mass and its black hole. It is also known that more massive galaxies typically have higher star formation rates.

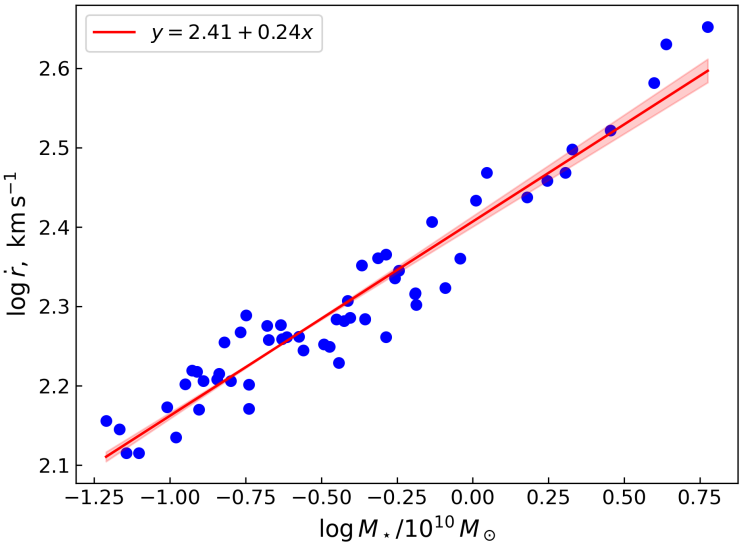


Fig. 1. The relationship between outflow velocity and galaxy stellar mass.

In our study, we find that $M_\star$, SFR and $L_{\rm AGN}$ are closely related to the outflow velocity, so we describe the overall dependence by a single polynomial equation:

$$\log\left(\frac{\dot{r}}{\mathrm{km\,s^{-1}}}\right) = 0,72\log\left(895,91\frac{\mathrm{SFR}}{M_\odot\,\mathrm{yr^{-1}}} + 170,52\frac{L_{\rm AGN}}{10^{43}\,\mathrm{erg\,s^{-1}}}\right) - 0,40\log\left(\frac{M_\star}{10^{10}M_\odot}\right) \quad (1)$$

Our results show reasonable agreement with observational data, particulary in the relation between outflow velocity and galaxy stellar mass. However, some discrepancies remain, suggesting that additional physical processes may need to be considered in numerical cosmological simulations to produce realistic galactic outflows.

[1] Nelson, D., "The IllustrisTNG simulations: public data release", Computational Astrophysics and Cosmology, vol. 6, no. 1, Art. no. 2, Springer, 2019.
[2] Fluetsch, A., "Cold molecular outflows in the local Universe and their feedback effect on galaxies", Monthly Notices of the Royal Astronomical Society, vol. 483, no. 4, OUP, pp. 4586–4614, 2019.
[3] Zubovas, K., Bialopetravičius, J., and Kazlauskaitė, M., "Determining active galactic nucleus luminosity histories using present-day outflow properties: a neural network-based approach", Monthly Notices of the Royal Astronomical Society, vol. 515, no. 2, OUP, pp. 1705–1722, 2022

CHEMICAL ANALYSIS OF PLANETARY HOST STARS

Ugnė Jonauskaitė[1], Edita Stonkutė[1]

[1] Institute of Theoretical Physics and Astronomy, Faculty of Physics, Vilnius University
ugne.jonauskaite@ff.stud.vu.lt

As of February 2025, there are around 5800 confirmed exoplanets detected in the Milky Way, and the number is constantly growing. In addition, the accuracy of determined planetary physical and orbital parameters is also improving.

Thanks to a large amount of available data about exoplanets and their stars it is now possible to investigate the distributions of various planetary physical and orbital parameters, as well as their correlations with the parameters of their stars and the chemical abundances of elements in their atmospheres. For example, in a study by Petigura et al., 2018 [1] it has been found that while massive planets are usually found orbiting stars with higher metallicities, that correlation isn't as prominent in terrestrial planets, indicating that stellar metallicity might play a role in determining the compositions of planets that form around a star.

A large amount of exoplanets have been detected around stars like the Sun. Solar twin and analogue stars have similar physical parameters (effective temperature, surface gravity) to the Sun and are assumed to have similar evolutionary histories. Because of this, they are useful when analysing various stellar chemical abundance trends.

Using spectra from the Vilnius University Echelle Spectrograph (VUES), I have determined the chemical abundances of alpha- and iron-group elements for 28 solar twins and analogues with confirmed exoplanets. I looked for potential correlations between the chemical compositions of planetary host stars and the parameters of the planets orbiting them. In this poster, I will present my findings.

[1] A. Petigura, G. W. Marcy, J. N. Winn, et al., "The California-Kepler Survey. IV. Metal-rich Stars Host a Greater Diversity of Planets", 155, 89 (2018)

RECONSTRUCTION OF 3D ASTEROIDS FROM 2D IMAGES

Vladas Šatas[1], Donatas Narbutis[1]

[1]Institute of Theoretical Physics and Astronomy, Faculty of Physics, Vilnius University, Lithuania
vladas.satas@ff.stud.vu.lt

Reconstructing three-dimensional (3D) objects from two-dimensional (2D) images is a crucial technique in computational vision, particularly in astrophysics, where it enables accurate shape modeling of celestial bodies from observational data [1]. This work explores high-fidelity 3D asteroid reconstruction using synthetic image data generated in Blender and processed with COLMAP structure-from-motion and multi-view stereo techniques [2, 3]. The primary objective of this research is to gain a comprehensive understanding of the 3D reconstruction pipeline while assessing the influence of various parameters – such as the number of images, resolution, sampling iterations, and model texture – on the reconstruction quality.

In the study, asteroid models were procedurally created in Blender [4] using a node-based approach with Perlin noise to introduce realistic surface irregularities. Multiple image sets were rendered from different viewpoints under controlled lighting and camera positioning. These images were then processed using COLMAP to reconstruct 3D models, which were subsequently compared against the original Blender model using CloudCompare [5] to assess accuracy via the cloud-to-cloud distance method.

The analysis revealed that surface texture plays a significant role in reconstruction quality. Specifically, a textured surface with high-frequency random noise patterns yielded the most accurate results, while smooth or homogeneous textures led to greater reconstruction errors. The optimal reconstruction was achieved using a dataset of 64 images at full resolution with 128 sampling iterations, resulting in the lowest deviation from the original model. These findings highlight the importance of texture detail and image quality in 3D shape recovery.

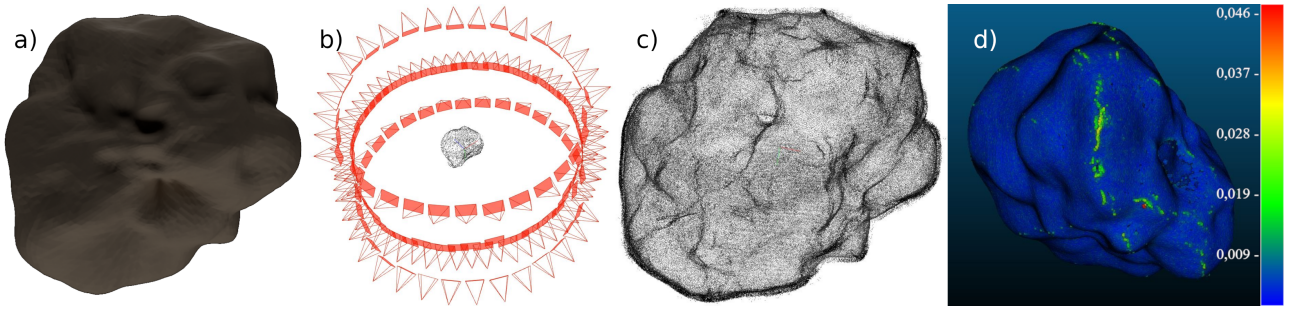


Fig. 1. a) An asteroid model created in Blender (1.79 km × 2.29 km × 2.3 km); b) COLMAP calculated camera positions with reconstructed asteroid model in the middle; c) dense point cloud of the reconstructed asteroid (∼350 000 points); d) accuracy error visualisation highlighting reconstruction deviations, in kilometers.

[1] W. Steffen, et al., Shape: A 3D Modeling Tool for Astrophysics, IEEE Transactions on Visualization and Computer Graphics, vol. 17, no. 4, pp. 454–465, 2011.
[2] R. Hartley and A. Zisserman, Multiple View Geometry in Computer Vision, 2nd ed. Cambridge, 2003
[3] L. Schönberger et al., COLMAP - structure-from-motion and multi-view stereo. https://colmap.github.io, 2016
[4] Blender Development Team, Blender (version 4.3). https://www. blender.org, 2024
[5] CloudCompare (version 2.13.2), http://www.cloudcompare.org, 2024

MINIATIURIZATION FEASABILITY BY USING BISMUTH AS A PROPELLANT FOR A HALL THRUSTER

Simas Sviensas[1], Jonas Klimantas[2], Ina Tetsmann[1]

[1]Departament of Mechanical and Materials engineering, faculty of Mechanics, Vilnius Gediminas Technical University
[2]UAB UVIRESO
simas.sviensas@stud.vilniustech.lt

Electric propulsion systems, such as Hall Effect Thrusters (HET), are widely used in space missions due to their high efficiency and performance, replacing chemical thrusters, which are highly limited by their operating time and working principles. Thus, manufacturers are seeking to maximize payload space and lower costs—driving research into miniaturization. Traditional xenon propellant, stored in large pressurized tanks, is costly and limited on Earth, prompting the search for alternatives[1].

In this particular study, we analyze how miniaturization of HET is possible through using pure bismuth as a novel propellant, it's sustainability for use in future space missions and determine miniatiurization's implications for the thruster.

To find out if bismuth can be a feasible option for use in miniaturized propulsion systems, which might seem like a daunting task at first due to the sheer number of processes involved, two different software tools were used in combination to compile a numerical model of HET. The model was simplified to reduce computational time while maintaining the essential physical processes. Thermal simulations were conducted to analyze temperature changes during ionization. Using CST Studio Suite, heat loss data from electron and ion collisions was imported into Solidworks FLOW/THERMAL, where direct solar heating, thermal loads, and radiation were applied for representative results. Literature investigation on the implications of miniaturization[2] was combined with numerical studies, and a verdict on feasibility was provided.

Gained data shows that most of the heat losses caused by wall collisions occur in the inner channel of the 250 W HET, meaning that this zone will be prone to the most erosion - notable point of failure in HETs[3]. Thermal simulations reveal that the inner channel edges of the engine heat up to around 650 °C and inner magnetic cores up to 350 °C after just one hour from a "cold start". At such temperatures, soft iron cores will approach their Curie temperature of 770 °C and lose their magnetic abilities, instantly compromising the operation of the HET[4]. This is mainly caused by the additional mechanisms required to vaporize bismuth (according to calculations, 50-100 watts of heating power is required). Optimizing these mechanisms and utilizing parasitic heat losses could eliminate the need for pressurized tanks, saving up to 33% of payload space - enabling a miniaturized, sustainable propulsion system.

From this study, considering the demand for space sustainability and miniaturization from a growing number of satellites in LEO and despite higher operational temperatures with Bi, its cost-effectiveness, space savings, better thrust-to-power ratio, and availability as a resource on Earth, demand it's recognition as a viable propellant for the future.

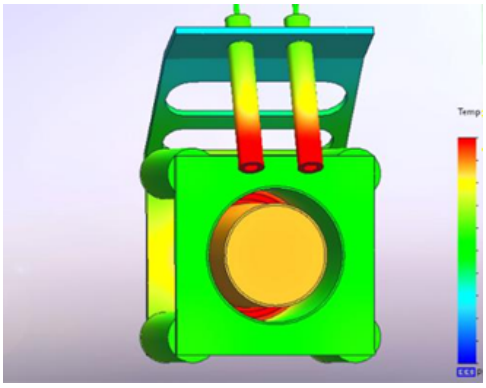


Fig. 1. Thermal results visualization

[1] Tirila, V.-G., Demairé, A., & Ryan, C. N. (2023). Review of alternative propellants in Hall thrusters. Acta Astronautica, 212, 284–306.
[2] Käthe Dannenmayer. (2012).Scaling laws and electron properties in Hall effect thrusters. Université d'Orléans.
[3] Yim, J. T., Keidar, M., & Boyd, I. D. (2006). An investigation of factors involved in Hall thruster wall erosion modeling. 42nd AIAA/ASME/SAE/ASEE Joint Propulsion Conference & Exhibit.
[4] Jacek & Bourdain, Loic. (2017). Thermal stability of the krypton Hall effect thruster. Nukleonika. 62. 9-15. 10.1515/nuka-2017-0002.

ORAL SESSION 6

Spectroscopy and Imaging

Chair: Dr. E. Palaimienė

ELECTRON PARAMAGNETIC RESONANCE: GOING MICRO FOR MACRO GAINS

Gediminas Usevičius[1], Oscar W. Kennedy[2], Ignas Pocius[1], Patrick Hogan[2], Ana Villanueva Ruiz de Temino[2], Jean-Baptiste Verstraete[2], Paulina Verbaitytė[1], G. Antilen Jacob[2], Mindaugas Kamarauskas[3], Marius Treideris[3], Joseph Alexander[2], Vidmantas Kalendra[1], Jūras Banys[1], John J.L. Morton[2,4], Mantas Šimėnas[1]

[1]Faculty of Physics, Vilnius University, Sauletekio 3, LT-10257 Vilnius, Lithuania
[2]London Centre for Nanotechnology, University College London, London WC1H 0AH, UK
[3]Center for Physical Sciences and Technology, Sauletekio 3, LT-10257 Vilnius, Lithuania
[4]Dept. of Electronic \& Electrical Engineering, University College London, London WC1E 7JE, UK
gediminas.usevicius@ff.vu.lt

The increasing demand of quantum technologies and a need to study minute amount samples has not surpassed electron paramagnetic resonance (EPR) spectroscopy [1]. 3D resonators with few μL mode volumes rarely do the job when studying only tens of billion spins. Thus, in recent years microresonators of various geomteries have been desgined and used to study systems previously unfeasible to do so [2,3]. However, their application remained very limited due to requiring very specific instrumental setups and samples. Here, I present our approach which employs planar spiral-shaped microresonators of 7 nL mode volumes fabricated from Yttrium Barium Copper Oxide (YBCO) high-temperature superconductor. A significant 3500-fold increase in the spin number sensitivity over commercial 3D resonators has been achieved which is fully compatible with conventional instrumentation and typical sample conditions. Our approach significantly advances the applicability of superconducting microresonators as versatile and readily applicable tools for high sensitivity EPR.

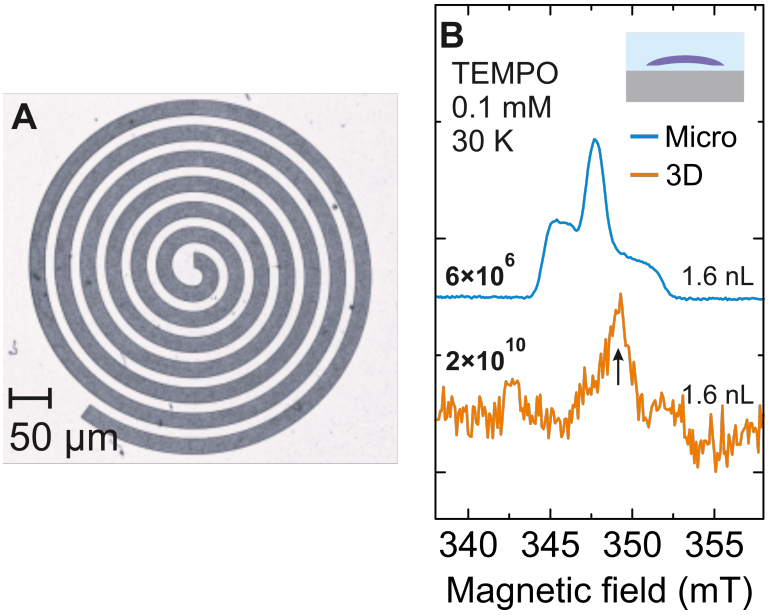


Fig. 1. (A) Fabricated planar YBCO spiral microwave microresonator on a sapphire substrate.(B) Echo-detected field sweep spectra of a 0.1 mM TEMPO sample obtained at 30 K using the spiral microresonator (1.6 nL sample volume) (blue) and a measurement of the same sample obtained using the Bruker MD5 resonator and the same measurement time are presented (orange) for comparison yielding only the impurity signal of the sapphire ring (arrows). The determined spin-number sensitivities (spins/G/$\sqrt{\text{Hz}}$) are indicated above the measured spectra.

[1] D. Goldfarb and S. Stoll, EPR Spectroscopy: Fundamentals and Methods, eMagRes Books. Wiley, 2018.
[2] Y. Twig, E. Suhovoy, and A. Blank, “Sensitive surface loop-gap microresonators for electron spin resonance,” Rev. Sci. Instrum., vol. 81, p. 104703, 2010.
[3] A. Bienfait et al., “Reaching the quantum limit of sensitivity in electron spin resonance,” Nat. Nanotechnol., vol. 11, pp. 253–257, 2016.

THE IMPORTANCE OF FOURIER TRANSFORM INFRARED SPECTRA PROCESSING FOR ANALYSIS OF BIOLOGICAL SAMPLES

Tautvydas Taraškevičius[1], Rimantė Bandzevičiūtė[1], Vytautas Žėkas[2], Emilis Gabrielis Byčius[2], Dovilė Karčiauskaitė[2]

[1]Institute of Chemical Physics, Vilnius University, Saulėtekio av. 3, 10257 Vilnius, Lithuania
[2]Department of Physiology, Biochemistry, Microbiology and Laboratory Medicine, Institute of Biomedical Sciences, Faculty of Medicine, Vilnius University, M. K. Čiurlionio st. 21, 03101 Vilnius, Lithuania
tautvydas.taraskevicius@ff.stud.vu.lt

Fourier transform infrared (FTIR) spectroscopy is a versatile vibrational spectroscopy method with great potential for applications in biological and medical research. Its main advantages are the relative ease of use, rapid acquisition of spectra, non-destructivity and non-specificity. However, the accuracy of the technique is hampered by unwanted phenomena introducing deviations of the spectra. This necessitates the application of preprocessing techniques, such as baseline correction and spectra normalization. The goal of this study is to evaluate the impact spectra preprocessing has on infrared spectra classification models based on a case study, as well to identify good practices in FTIR spectra analysis of biological samples.

FTIR spectra of blood derived extracellular vesicles (EVs) from healthy individuals and post myocardial infarction patients were used as a case study. The vesicle samples were prepared at the Vilnius University Faculty of Medicine laboratories. A total of 84 FTIR spectra were used in the analysis, 26 of which were from EVs of infarction patients. The spectra were preprocessed using various techniques and outputted to supervised and unsupervised classification models with the objective of differentiating between vesicles and evaluating the classification accuracy. For unsupervised models, k-means clustering and hierarchical cluster analysis (HCA) were used. For supervised models, logistic regression with and without principal component analysis (PCA) was used. The supervised models were trained and tested using 5-fold cross-validation.

Based on the results of the models (Fig. 1), the following observations were made. First, baseline correction and spectra normalization are vital for cluster analysis. Second, supervised models tend to perform better if the spectral data have their standard deviations normalized to 1. Furthermore, standard deviation normalization also increased the amount of principal components required to achieve a high explained variance. It should be noted that each spectral dataset has its own optimal data processing procedure that usually has to be found by comparing several methods.

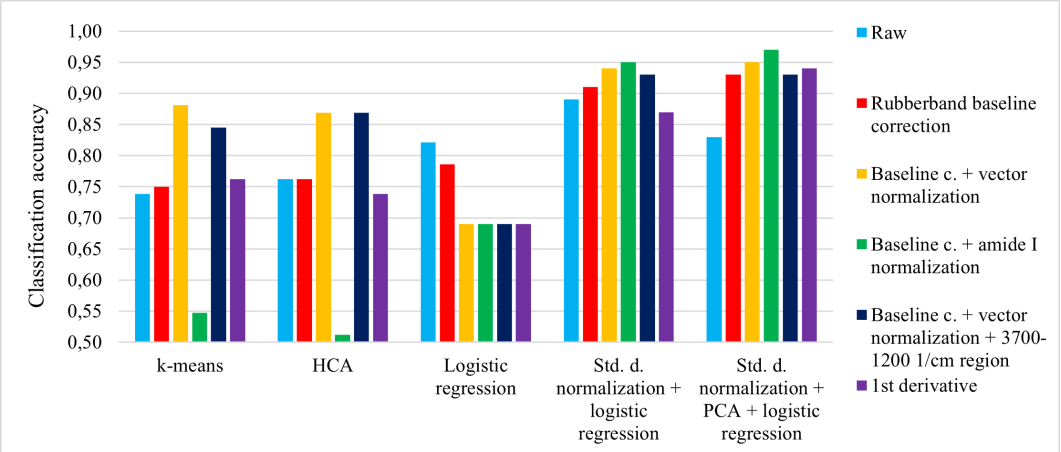


Fig. 1. The classification accuracy of extracellular vesicle FTIR spectra preprocessed using various techniques for each of the classification models used in this study.

^{35}Cl AND ^{37}Cl SOLID-STATE NMR STUDY OF CALCIUM CHLORAPATITE

Rokas Lemežis[1], Vytautas Klimavičius[1]

[1]Institute of Chemical Physics, Faculty of Physics, Vilnius University, Vilnius, Lithuania
rokas.lemezis@ff.stud.vu.lt

Calcium phosphates (CaPs) are a family of materials used for various applications such as bone regeneration [1], catalysis, development of optical materials (LED), etc. CaPs are used in phosphorus-based LEDs for light conversion from higher to lower energies. Properties such as thermal stability, doping capabilities and photoluminescent properties are necessary for CaPs application in LED development [2].

In this study solid-state nuclear magnetic resonance (ssNMR) was used to characterize calcium chlorapatite ($Ca_5(PO_4)_3Cl$, ClAp) samples with varying structural phases. ClAp samples were synthesized using molten salt synthesis method. Varying ratio of molten salts and treatment temperature we can control morphology of the samples. Furthermore, ssNMR of quadrupolar nuclei lets us probe the electronic environment at the site of nucleus of investigation. In this case, ^{35}Cl and ^{37}Cl ssNMR is used to determine number structural phases present in the samples and their dependance on synthesis parameters.

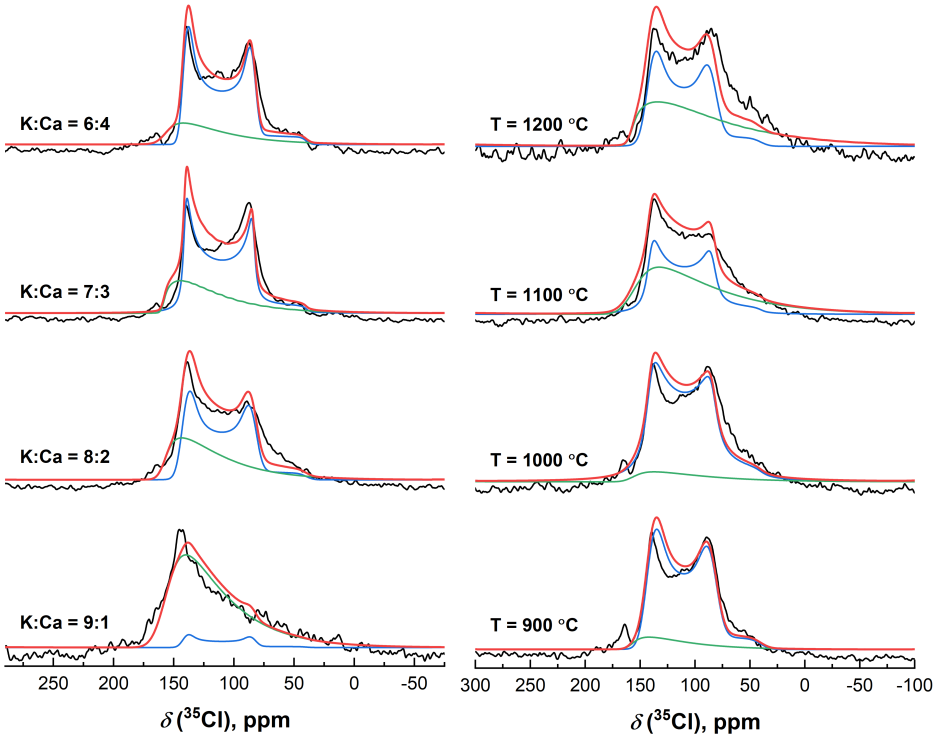


Fig. 1. ^{35}Cl MAS NMR spectra of ClAp synthesized with (left) different molar proportions of molten salts (K:Ca = 9:1; 8:2; 7:3; 6:4, T = 750 °C, ACP:flux = 1:2, t = 5 h) and (right) varying treatment temperatures (T = 900; 1000; 1100; 1200 °C, K:Ca = 6:4, ACP:flux = 1:10, t = 5h).

It was found that the calcium chlorapatite samples contain crystalline and glassy type structural phases. Controlling the ratio of KCl and $CaCl_2$ molten salts during synthesis influences formation of structural phases (increasing $CaCl_2$ concentration increases concentration of crystalline phase). In contrast, treatment temperature used during synthesis influences disorder factor of glassy type structure (higher temperatures corelate with wider distribution of chlorine environments of glass structural phase).

[1] W. Habraken, P. Habibovic, M. Epple, and M. Bohner, “Calcium phosphates in biomedical applications: materials for the future?,” Materials Today, vol. 19, no. 2, pp. 69–87, Mar. 2016.

[2] Z. Zhang, J. Wang, M. Zhang, Q. Zhang, and Q. Su, “The energy transfer from Eu2+ to Tb3+ in calcium chlorapatite phosphor and its potential application in LEDs,” Appl. Phys. B, vol. 91, no. 3, pp. 529–537, Jun. 2008.

FDTD MODELLING FOR ELECTROMAGNETIC FIELD ENHANCEMENT IN BOW-TIE ARRAY FOR SERS APPLICATIONS

Hasan Sarigul[1], Tomas Tamulevičius[1,2]

[1]Department of Physics, Kaunas University of Technology, Studentų St. 50, Kaunas, LT-51368, Lithuania
[2]Institute of Materials Science, Kaunas University of Technology, K. Baršausko St. 59, LT-51423, Kaunas, Lithuania
hasan.sarigul@ktu.lt

Surface-enhanced Raman Scattering (SERS) serves high-sensitivity technique for low-concentration and label-free detection of the fingerprint spectrum. SERS-based analyte sensing is attributed to the local electromagnetic (EM) field concentration, termed hotspots, that occur due to the gaps and edges between noble metal nanostructures [1]. Structures with nano-size gaps such as bow-tie geometries attract considerable attention from researchers as they can enhance EM fields significantly via plasmon coupling effects [2,3].

Since the SERS performance of noble metals is highly dependent on their geometry, we simulated the EM near fields in gold bow-tie triangle arrays employing the finite-difference time-domain (FDTD) method which is an effective computational method for examining nanostructures. The optical behavior of the edge sharpness and tip-to-tip gap parameters of the gold bow-tie triangle arrays were investigated. For the periodicity properties of the simulation region, boundary conditions were chosen as anti-symmetric for the X direction, symmetric for the Y direction, and perfectly matched layer (PML) for the Z direction. A 5 nm mesh was used for FDTD simulations the adjustments were made for the 785 nm resonant wavelengths. Optimization studies from sharp tips to 50 nm radius tips and nanogaps ranging from 0 to 200 nm showed that bow-tie structure with small nanogaps 5 nm, 10 nm, and 15 nm could enhance the incoming EM field intensity and SERS enhancement factor of approximately by up to 2.3 x 10^3 and 3.9×10^5, respectively. It was found that the gold bow-tie triangle array exhibits excellent SERS performance and significantly increases the EM field and SERS enhancement factor.

Acknowledgements
This work was supported by the Research Council of Lithuania (RCL) (Project no.: S-PD-24-115).

[1] T. Gao et al., ACS Nano, vol. 18, no. 32, pp. 21593–21606,(2024).
[2] O. S. J. Hagger et al., Mater. Adv., vol. 4, no. 15, pp. 3239–3245, (2023).
[3] N. Khinevich et al., Sensors and Actuators B: Chemical, vol. 394, 134418, (2023).

EXPLORING THE IMPACT OF MICROBUMP ARRAYDIMENSIONS ON HYBRID LATTICE PLASMON RESONANCE QUALITY

Rodrigas Liudvinavičius[1], Evaldas Stankevičius[1]

[1]Center for Physical Sciences and Technology, Laser Technology Department
rodrigas.liudvinavicius@ftmc.lt

In recent years, the field of nanotechnology has gained increasing attention due to the successful application of nanostructures in sensor fabrication and the development of new optical devices [1]. Among the successful nanodevices, metal nanostructures, especially those made of noble metals like gold, play a significant role. These materials exhibit unique and strong plasmonic properties that describe the interaction between light and nanostructures. The fabrication of plasmonic nanostructures is often done using electron beam and focused ion beam lithographic methods. However, these methods have limitations in terms of pattern resolution and production cost. Recent advancements in laser-based techniques, such as laser direct writing (LDW) on metal surfaces, emerge as an alternative, offering cost-effectiveness and the ability to control structure parameters directly. The study focuses on the formation of microbumps using LDW, taking advantage of gold's elastic and yield strength properties. Despite the advantages, there is a challenge in achieving a strong optical response for hybridized plasmonic modes [2]. The study discusses methods to enhance the response, such as reducing the period and increasing the array size. However, limitations arise, and finding the right balance between these parameters is crucial for optimizing the optical response in plasmonic arrays during measurements.

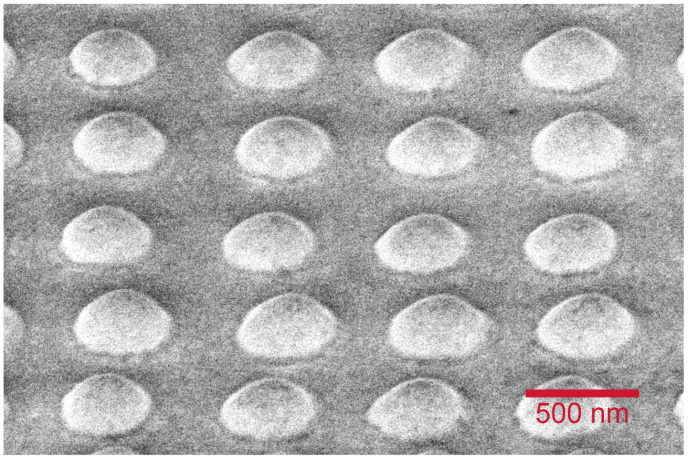


Fig. 1. Fig. 1. SEM micrograph of fabricated bumps array in a thin gold film 50 nm. Microstructures were formed using a single-shot laser pulse with 0.4 nJ energy. Periodicity between bumps is 650 nm.

In this work, an investigation of the influence of the array size on the quality parameters of plasmonic excitation will be presented. The analysis includes considerations of measurement improvements achieved with additional aperture-limiting diaphragms for measuring beams.

Acknowledgements

The authors acknowledge the Research Council of Lithuania (LMT, Lithuania) for the received funding under project No. S-MIP-23-32.

[1] K. Yang, et al., Metallic Plasmonic Array Structures: Principles, Fabrications, Properties, and Applications. Adv. Mater. 33(50), pp. 2007988 (2021).
[2] E. Stankevičius, et al., Direct Laser Writing for the Formation of Large-Scale Gold Microbumps Arrays Generating Hybrid Lattice Plasmon Polaritons in Vis–NIR Range, Adv. Opt. Mater. 9, 2100027 (2021).
[3] R. Liudvinavicius, et al., Titanium adhesion layer influence on the formation of hybrid lattice plasmon structures via laser-direct writing, Optics & Laser Technology, Volume 175, 2024.

PLASMONIC COLORS FROM THIN GOLD FILMS WITH A TITANIUM ADHESION LAYER ON A GLASS SUBSTRATE VIA NANOSECOND LASER THERMAL HEATING

Vita Petrikaitė[1], Evaldas Stankevičius[1]

[1]Department of Laser Technologies, Center for Physical Sciences and Technology, Vilnius, Lithuania
vita.petrikaite@ftmc.lt

Conventional synthetic dyes exhibit a wide color spectrum but often release toxic and non-biodegradable chemicals, contributing to environmental harm [1]. Plasmonic nanostructures, particularly gold nanoparticles, offer a sustainable alternative due to their size-dependent optical properties, but gold thin films generally exhibit a limited color range due to morphological constraints [2]. This study aims to overcome the inherent limitations of gold thin films and expand the range of achievable plasmonic colors by introducing a titanium (Ti) adhesion layer beneath the gold film, modified by laser-induced thermal heating processing. This method aims to improve both the diversity of plasmonic colors and the adhesion properties of the film [3] and to provide environmentally friendly and durable alternatives for anti-counterfeiting [4], high-resolution printing, photonic devices, and decorative applications [5].

Gold nanoparticles were generated on glass substrates with Ti underlayers using a nanosecond pulsed laser operating at a 532 nm wavelength. A systematic investigation was carried out by varying the pulse energy (3.5-38.5 µJ), scan speed (1-500 mm/s), repetition rate (0.5-100 kHz), and hatch spacing (25-75 µm) to optimize the laser parameters for plasmonic color formation. The Ti underlayer was found to significantly influence the morphology of the gold film, promoting the formation of smaller islands during laser-induced dewetting. This morphological change broadened the achievable color range, including hues beyond the limited palette of gold thin films. The results demonstrated improved adhesion and enhanced color diversity. Introducing a Ti adhesion layer with laser thermal processing offers a scalable and cost-effective method for producing tunable, high-resolution plasmonic colors.

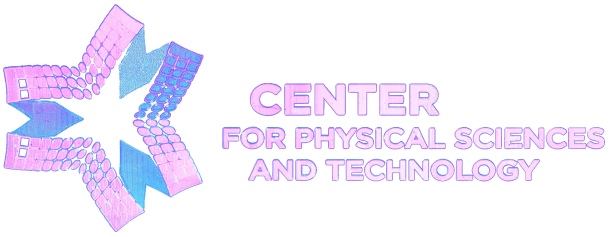


Fig. 1. Optical microscopy picture of the laser-generated plasmonic image of Center for Physical Sciences and Technology logo.

[1] J. Lin, W. Ye, M. Xie, et al. Environmental impacts and remediation of dye-containing wastewater. Nat Rev Earth Environ 4, 785–803 (2023).
[2] V. Petrikaitė, G. Niaura, E. Stankevičius, et al. Hybrid gold-silver nanoparticles synthesis on a glass substrate using a nanosecond laser-induced dewetting of thin bimetallic films and their application in SERS. Opt Laser Technol., 168, 109956 (2024).
[3] R. Liudvinavičius, A. Selskis, E. Stankevičius. Titanium adhesion layer influence on the formation of hybrid lattice plasmon structures via laser-direct writing. Optics & Laser Technology, 175, 110807 (2024).
[4] V. Caligiuri, A. Patra, M. De Santo, et al. Hybrid plasmonic/photonic nanoscale strategy for multilevel anticounterfeit labels. ACS applied materials & interfaces, 13(41), 49172-49183 (2021).
[5] M. Song, D. Wang, S. Peana, et al. Colors with plasmonic nanostructures: A full-spectrum review. Applied physics reviews, 6(4) (2019).

ORAL SESSION 7

Theoretical Physics

Chair: Dr. A. Kononovičius

NUMERICAL MODELING OF COULOMB INTERACTION EFFECTS ON ELECTRON EMISSION FROM AN ELLIPTICAL QUANTUM DOT

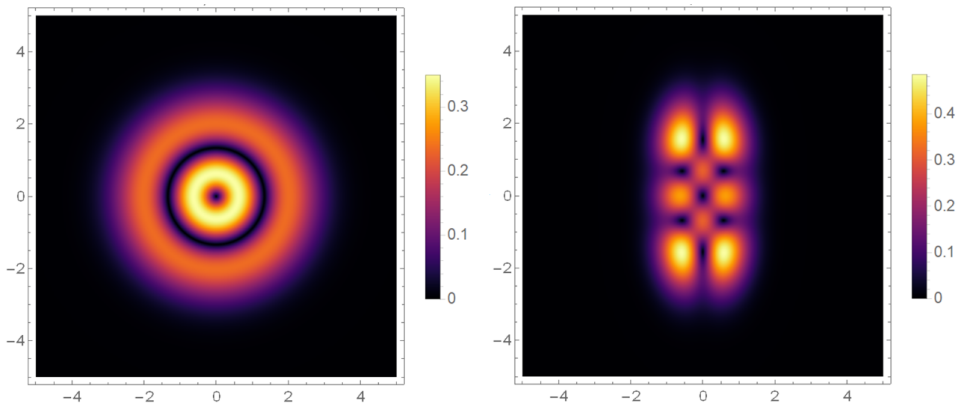
Alberts Bilzens[1], Girts Barinovs[1]

[1]Department of Theoretical Physics, Nanoelectronics Theory Group, University of Latvia, Latvia
alberts.bilzens@lu.lv

Electron pumps generate precisely quantized currents, a cornerstone for establishing fundamental current standards and for applications requiring high-fidelity electron manipulation. They are essential for achieving high precision in quantum metrology, yet their performance is often limited by uncertainties in electron emission dynamics. In this work, we focus on both one- and two-electron systems confined in an elliptical quantum dot subjected to a strong magnetic field. Focusing initially on the one-electron scenario (fig. 1, isotropic and anisotropic case for a given wavefunction) , this study explores more complex conditions, such as where two electrons with Coulomb interaction may be emitted simultaneously.

Our objective was to develop and validate a robust numerical model that not only yields accurate energy eigenvalues and wavefunctions but also serves as a benchmark for parameter tuning. To this end, we employ an analytical approach to calculate Hamiltonian matrix elements — avoiding the need for traditional numerical integration [1]. The acquired analytical wavefunctions for one-electron system [2] provide crucial insights into how parameters influence numerical results and their precision, thereby guiding the optimal configuration for the electron pump for different purposes.

The presented approach enables the characterization of both one-electron and two-electron with Coulomb interaction emission and suggests pathways either to increase the accuracy of electron pumps for metrological applications by eliminating two-electron emission or to maximize two-electron quasiparticle emission for entangled particle sources in quantum computing applications.



(a) Isotropic potential (b) Anisotropic potential

Fig. 1. *Absolute values of one-electron wavefunction $\psi_{1,2}$ for isotropic and anisotropic potentials with applied magnetic field*

[1] H. J. Korsch and M. Glück, European Journal of Physics, vol. 23, no. 4, p. 413, Jun. 2002. doi: 10.1088/0143- 0807/23/4/305.
[2] J. Kyriakidis and S. J. Penney, "Coherent rotations of a single spin-based qubit in a single quantum dot at fixed zeeman energy," Phys. Rev. B, vol. 71, p. 125 332, 12 Mar. 2005. doi: 10.1103/PhysRevB.71.125332.

CHARACTERIZATION OF ELECTROSPUN MAGNETIC MATERIALS IN A ROTATING MAGNETIC FIELD

Dāvis Gaiziņš[1], Jānis Cīmurs[1], Viesturs Šints[1], Oksana Petričenko[1], Roman Viter[1], Viktor Zabolotnii[1], Iryna Tepliakova[1]

[1]Department of Physics, Faculty of Science and Technology, University of Latvia, Riga, Latvia
davisgaizins043@inbox.lv

The research is mainly focused on determining the properties of electrospun polymer fibers with encapsulated magnetic particles in a rotating magnetic field.

To do this superparamagnetic particles were obtained chemically by coprecipitation method. A solution was prepared by dissolving polyacrylonitrile fibers in dimethylformamide and adding magnetic nanoparticles. The solution was then pumped through a needle into a spinning camera with a voltage applied between the solution in the needle and the walls of the camera, and then dried. The result was electrospun fibers containing magnetic particles.

The fibers are immersed in a fluid and are then subjected to an ultrasound treatment to obtain finer strands of the fibers. The resulting sample was placed in a rotating magnetic field under a microsope for further investigation.

The microscope is connected to a camera with an overhead view of the solution of particles and fluid. The sample is placed into a magnetic coil system where a three-dimensional time dependant magnetic field can be generated which surrounds the sample when it is under the microscope. The behavior of these magnetic particles under the influence of a rotating magnetic field is then filmed at different magnetic field rotation frequencies and strengths. The smallest magnetic field rotation frequency at which a particle in the fluid can no longer follow the magnetic field is the critical frequency. For frequencies above critical the particles show back and forth rotation without completing a full rotation. The critical frequency can be obtained by the angle the particle lags behind the magnetic field for frequencies below critical and by the mean rotation of the particle for frequencies above critical. The critical frequency allows us to relate the magnetic and hydrodynamic properties of each particle. The critical frequency is obtained in the fluid to obtain the magnetic properties of the material. When the magnetic properties are obtained, the particles are used as magnetic probes to obtain viscoelastic properties of the fluid.

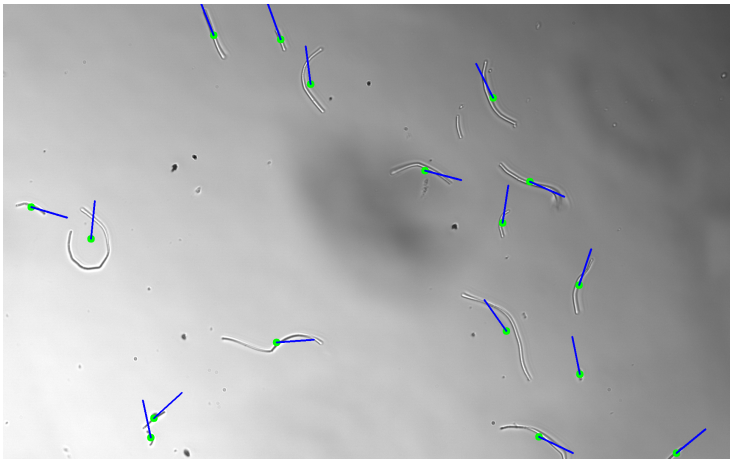


Fig. 1. Center of mass and orientation of particles

The data from the filmed videos of the particles is obtained using an image processing algorithm which is written in Python code. It detects the center of mass coordinates, orientation, surface area and length of the particles within each frame of the video. The center of mass of the particle is determined using moments obtained by an OpenCV function. The orientations of particles are determined by using moments and creating a covariation matrix for each particle and determining the eigenvector of this matrix corresponding to the major axis. This vector does not change orientation with respect to the particle as long as it does not change its shape. And the length of a particle along its trajectory is determined using skeletonization of particles in the image.

PIXEL DETECTOR MODULE QUALITY TESTS FOR THE CMS PHASE-2 UPGRADE

Austėja Jurgaitytė[1], Marijus Ambrozas[1]

[1]Experimental Nuclear and Particle Physics Center, Faculty of Physics, Vilnius University, Lithuania
austeja.jurgaityte@ff.vu.lt

The Large Hadron Collider (LHC), located at CERN, is currently the world's largest and most powerful particle accelerator, with the circumference of its ring tunnel being approximately 27 kilometers [1]. Two beams of particles, sped up to achieve up to the record energy of 6.8 TeV per beam [2], travel inside the LHC, regularly colliding at four designated particle collision points. Particle detectors are stationed at each collision point, with Compact Muon Solenoid (CMS) – a general purpose detector – being one of them [1].

After Run 3 ends in July 2026, LHC will go into Long Shutdown 3 during which it will be significantly upgraded. This project is called the High-Luminosity Large Hadron Collider (HL-LHC) and is scheduled to be finished by 2030 [3]. After the upgrade, it is planned that the LHC will run at a center-of-mass energy of 14 TeV and its instantaneous peak luminosity will increase roughly by a factor of 5 to 7.5 compared to its current nominal luminosity [1, 4]. This means that there will be a lot more particle collisions, which will significantly increase the potential of observing interesting physics phenomena. However, the levels of radiation will also rise, necessitating robustness upgrades to both the collider and the detectors.

Together with the LHC, CMS will also be upgraded to maximise the efficiency of the luminosity increase. This is the CMS Phase-2 Upgrade project, which will notably improve on the detector granularity, the trigger system and the detector's resistance to decay from radiation. To help reach these goals, the silicon tracking system, which is the closest to the collision point and receives the most radiation, will have to be fully replaced. The system itself will be composed of the Inner Tracker, based on silicon pixel modules, and the Outer Tracker, consisting of silicon strip and macro-pixel modules [4].

The pixel module is the building block of the Inner Tracker. Its main components are the sensors, bump-bonded to the readout chips, which are wire-bonded to the module readout. It is planned that the Inner Tracker will consist of modules with two or four readout chips, as shown in Fig. 1 [4].

The current iteration of pixel chips, called the CROCv2, is entering the production phase and has to be tested to guarantee the compliance to the high integrity standards. This testing chain has to calibrate the module and test for dead pixels, noise levels, readout latency and other parameters. In this presentation, we will present our performed testing procedures and the results observed with the current production modules.

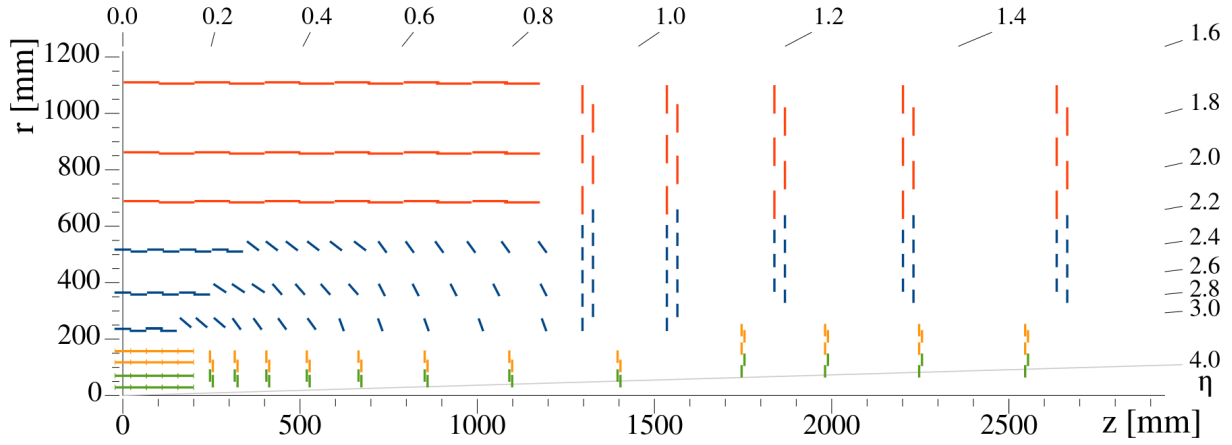


Fig. 1. Scheme of a quarter of the Phase-2 CMS tracking system in r-z view. The Inner Tracker pixel modules with two readout chips are shown in green, while yellow is used for the four chip modules [4].

[1] L. Evans and P. Bryant, "LHC Machine," Journal of Instrumentation, vol. 3, no. 08, p. S08001, Aug. 2008. [Online]. DOI: 10.1088/1748-0221/3/08/S08001.

[2] F.F. Van der Veken, A. Abramov, G. Azzopardi, G. Broggi, R. Bruce, R. Cai, M. D'Andrea, K. A. Dewhurst, A. Frasca, P. Hermes, B. Lindstrom, D. Mirarchi, S. Redaelli, F. Ziliotto, and D. Demetriadou, "Collimation performance of the 400MJ LHC beam at 6.8 TeV," JACoW IPAC, vol. 2023, pp. TUPM119, 2023. [Online]. DOI: 10.18429/JACoW-IPAC2023-TUPM119.

[3] M. Lamont, "Updated schedule for CERN's accelerators," CERN News, Oct. 2024, [Online]. Available: https://home.cern/news/opinion/accelerators/updated- schedule-cerns-accelerators.

[4] CMS Collaboration, "The Phase-2 Upgrade of the CMS Tracker," CERN, Geneva, Tech. Rep. CERN-LHCC-2017-009, CMS-TDR-014, Jul. 2017. [Online]. DOI: 10.17181/CERN.QZ28.FLHW.

DRELL-YAN PROCESS STUDY USING OPEN DATA FROM THE CERN CMS EXPERIMENT

Eglė Lenkaitytė[1], Marijus Ambrozas[1]

[1] Institute of Theoretical Physics and Astronomy, Faculty of Physics, Vilnius University
egle.lenkaityte@ff.stud.vu.lt

The research in elementary particle physics conducted at CERN significantly contributes to our understanding of the world around us. In the Large Hadron Collider (LHC), high-energy protons are collided, and the newly formed particles provide information about fundamental laws of nature and the structure of the Universe. The LHC accelerates protons to nearly the speed of light, and they are smashed together at four collision points, one of which is the Compact Muon Solenoid (CMS) detector. Experiments conducted in the CMS detector not only search for new particles but also refine existing knowledge. One important process under investigation is the Drell-Yan process, first described in 1970 by physicists Sidney David Drell and Tung-Mow Yan [1]. This remains an active, although well-studied, area of research that helps refine the structure of hadrons and parton distribution functions, which are crucial theoretical tools for modeling particle collisions and testing Standard Model predictions. The process describes the creation of a lepton pair from the annihilation of a high-energy quark and antiquark. This study focuses on the Drell-Yan process, where a pair of muons is created via a Z boson.

During this study, statistical properties of the muon pair and the originating particle were calculated, including transverse momentum, energy, pseudorapidity, azimuthal angle, and mass. The obtained results were visualized using histograms. The data for this study was taken from the CERN open data portal. The data originates from experiments conducted in 2016 but was only made publicly available in 2024. Calculations were performed using all 13 TeV proton collision events that contained at least two high-energy muons. More details about the study will be provided during the presentation. By providing open access to experimental data, CERN allows non-staff members to explore particle physics and enables researchers and students worldwide to contribute to data analysis and promote science.

[1] S. D. Drell, T. M. Yan. Massive Lepton Pair Production in Hadron Hadron Collisions at High-Energies, Phys. Rev. Lett. 25 316-320, 1970. DOI:10.1103/Phys RevLett.25.316

ORAL SESSION 8

Spectroscopy and Imaging

Chair: Dr. J. Jorudas

THz SPECTRA DEPENDENCE ON FREE CARRIER CONCENTRATION IN n-GaAs/GaAs STRUCTURES WITH METASURFACES

Barbora Škėlaitė[1,2], Daniil Pashnev[1], Vytautas Jakštas[3], Aivaras Špokas[1,2], Ignas Grigelionis[1]

[1]Center for Physical Sciences and Technology, Department of Optoelectronics, Saulėtekis ave. 3, Vilnius, Lithuania
[2]Vilnius University, Institute of Photonics and Nanotechnology, Saulėtekis ave. 3, Vilnius, Lithuania
[3]Center for Physical Sciences and Technology, Department of Physical Technologies, Saulėtekis ave. 3, Vilnius, Lithuania
barbora.skelaite@ftmc.lt

Terahertz (THz) frequency range of the electromagnetic (EM) wave spectrum is known for unique properties, such as the ability to pass through dielectric materials that are non-transparent to visible light (paper, wood, textile), that have various applications [1, 2]. Currently available THz sources are cost ineffective, either suffer from limited operating frequency range or require cryogenic temperatures, and contain intricate inner structure that results in complex manufacturing processes [3]. As an alternative, thermal sources providing broad-band thermal radiation specifically tailored to narrow emission lines of desired frequency could be used, allowing for the mitigation of the above-mentioned limitations. In this work, the *n*-GaAs/GaAs-based semiconductor structures with specially designed metasurfaces for narrow (selective) THz emission are investigated. The metasurface was etched into the top *n*-GaAs layer structured as a periodic array of rectangle-shaped metacells with side lengths ranging from 14 µm to 23 µm to form pillar-like structures. Three samples with different electron concentrations in metasurface layers were fabricated.

Reflectance of samples equipped with metasurfaces were investigated both theoretically and experimentally. Reflection spectra (Fig. 1) were measured at normal incident angle by commercial THz time-domain system (Teravil, T-SPEC 800), with flat gold plate as a reference. It was observed that by changing electron concentration of the *n*-GaAs layers the resonance frequency can be tuned. Resonant frequency of structures with electron concentration of 1×10^{18} cm^{-3} reached 1.82 THz for *s*- and 1.46 THz for *p*-polarization and for structures with 2.1×10^{18} cm^{-3} electron concentration the frequency of the first harmonic reached 1.97 THz and 1.49 THz for *s*- and *p*- polarization, respectively.

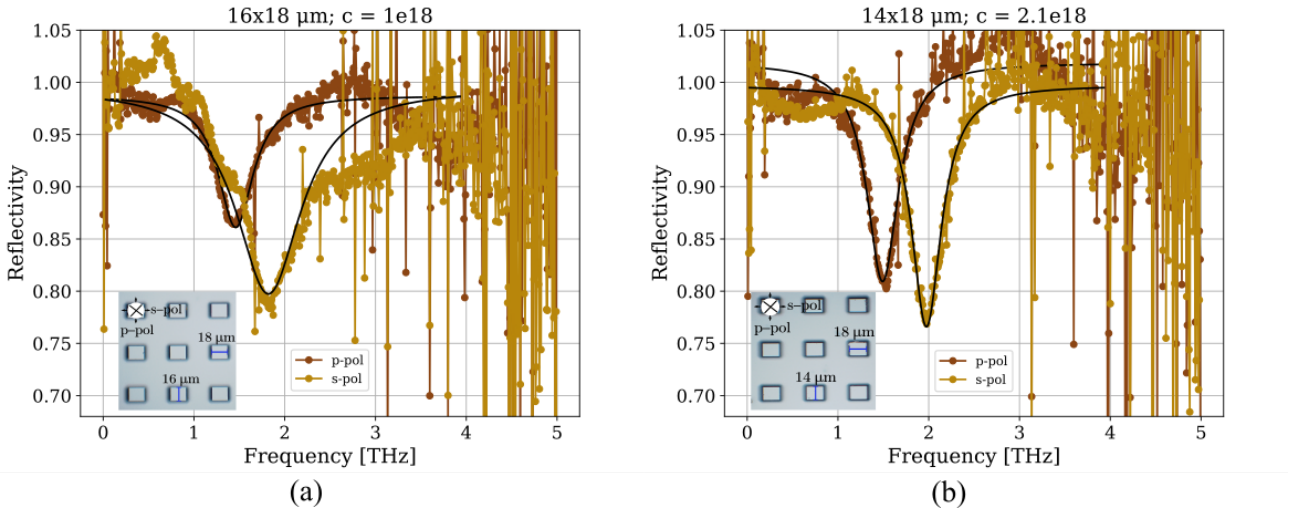


Fig. 1. Experimentally measured reflectivity spectra of *n*-GaAs/GaAs structures with rectangular metacells, where the electron concentration of the *n*-GaAs layers were (a) 1×10^{18} cm^{-3} and (b) 2.1×10^{18} cm^{-3}. Measurements were performed for rectangular metacells of dimensions (a) 16 µm × 18 µm and (b) 14 µm × 18 µm. The black lines indicate the Lorentzian fit and inserts reveal microscopic photos of the fabricated structures and geometry of the investigated metacells.

[1] M. Bauer et al., 'Antenna-coupled field-effect transistors for multi-spectral terahertz imaging up to 4.25 THz', Opt. Express, vol. 22, no. 16, pp. 19235–19241, Aug. 2014.
[2] J. Li et al., 'Rapid sensing of hidden objects and defects using a single-pixel diffractive terahertz sensor', Nature communications, vol. 14, no. 1, p. 6791, 2023.
[3] A. Leitenstorfer et al., 'The 2023 terahertz science and technology roadmap', Journal of Physics D: Applied Physics, vol. 56, no. 22, p. 223001, Apr. 2023.

THZ IMAGING OF HIDDEN OBJECTS AND THEIR CLASSIFICATION USING NEURAL NETWORKS

Ugnė Šilingaitė[1,2], Ignas Grigelionis[1]

[1]Center for Physical Sciences and Technology
[2]Vilnius University
ugnsili@gmail.com

Machine learning models have recently made various breakthroughs in solving computer vision tasks and have a high accuracy in object classification problems [1], thus can be applied to terahertz (THz) images. However, THz images are often plagued with the problem of low spatial resolution due to the limited hardware capabilities and long imaging times, thus there are no available datasets which would be suitable for neural network training. The goal of our work is to create a dataset containing THz images of different objects and use that dataset to train Convolution neural network models to detect and classify the objects in the dataset. Raster method was used to get 152 images, which were used for training and testing of the models.

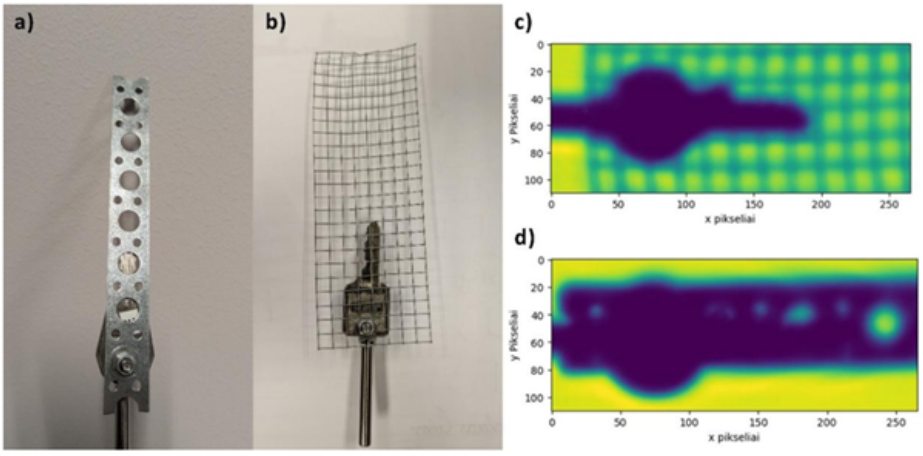


Fig. 1. a) Example of a key hidden behind a metal plate in visible light, b) a key hidden behind a metal mesh in visible light, c) THz image of a key hidden behind a metal mesh, d) THz image of a key hidden behind a metal plate.

In this work we trained a simple Convolutional neural network model for object classification and reached 95% overall accuracy. U-Net [2] model was also trained for object detection and reached 0,91 Dice coefficient on training data.

[1] HASSAN, Aya, Moatamed REFAAT, and Ashraf HEMEIDA. Image classification based deep learning: A Review. Aswan University Journal of Sciences and Technology [online]. 2022, 2(1), 11–35 [viewed 17 February 2025]. ISSN 2735-3095. Available from: doi:10.21608/aujst.2022.259887

[2] RONNEBERGER, Olaf, Philipp FISCHER, and Thomas BROX. U-Net: Convolutional Networks for Biomedical Image Segmentation. In: Lecture Notes in Computer Science [online]. Cham: Springer International Publishing, 2015, pp. 234–241 [viewed 17 February 2025]. ISBN 9783319245737. Available from: doi:10.1007/978-3-319-24574-4_28

INVESTIGATION OF DIVERSE SCATTERING MATERIALS USING DIGITAL TERAHERTZ HOLOGRAPHY

Lukas Stacevičius[1,2], Linas Minkevičius[1], Ignas Grigelionis[1], Agnieszka Siemion[3], Rusnė Ivaškevičiūtė-Povilauskienė[1], Gintaras Valušis[1]

[1]Center for Physical Sciences and Technology, Department of Optoelectronics, 10257 Vilnius, Lithuania
[2]Vilnius University, Faculty of Physics, 10222 Vilnius, Lithuania
[3]Warsaw University of Technology, Faculty of Physics, 00-662 Warsaw, Poland
lukas.stacevicius@ftmc.lt

Terahertz (THz) radiation has attracted a great scientific interest due to its ability to penetrate materials that are opaque to visible light [1]. However, conventional imaging cannot resolve low-absorbing materials, which require the employment of coherent recording methods. Digital holography [2], a rapidly advancing imaging technique, has been explored for its high sensitivity and potential to distinguish transparent, weakly absorbing materials, giving insight into light scattering effects.

In this work we have investigated diverse scattering materials by numerically evaluating their scattering properties and performing digital holography at 600 GHz frequency. Investigated samples consisted of four different materials, such as sugar, soda, coffee and polymer called TX-151 (see inset in Fig.1(a)). Substances were sifted and divided into different categories by grain sizes: less than 125 µm; 125-250 µm; 250-500 µm and 500-1000 µm.

Since the sizes of investigated grains are comparable to the wavelength of used THz radiation, Mie scattering properties of investigated materials were evaluated, using the discrete dipole approximation (DDA) method [3] for non-spherical particles. The extinction, scattering, and absorption properties were evaluated, where the highest extinction efficiency of 2.12 was found for sugar grains within the 250-500 µm size range, correlating with the lowest value in the hologram reconstruction of amplitude distribution. Moreover, scattered light intensity dependence on scattering angle was evaluated for each material, shown in Fig.1(a). The values of scattered light intensity of different substances matched the experimental recordings, with the least transmitted light corresponding to the highest scattering.

In the reconstructed hologram image shown in Fig.1(c), the signal amplitudes of different materials were better resolved compared to direct imaging (see Fig.1(b)), with an intensity difference of 0.81 compared to 0.65, respectively. It was demonstrated that digital THz holography technique enables a more effective evaluation of various scattering materials compared to conventional THz imaging methods.

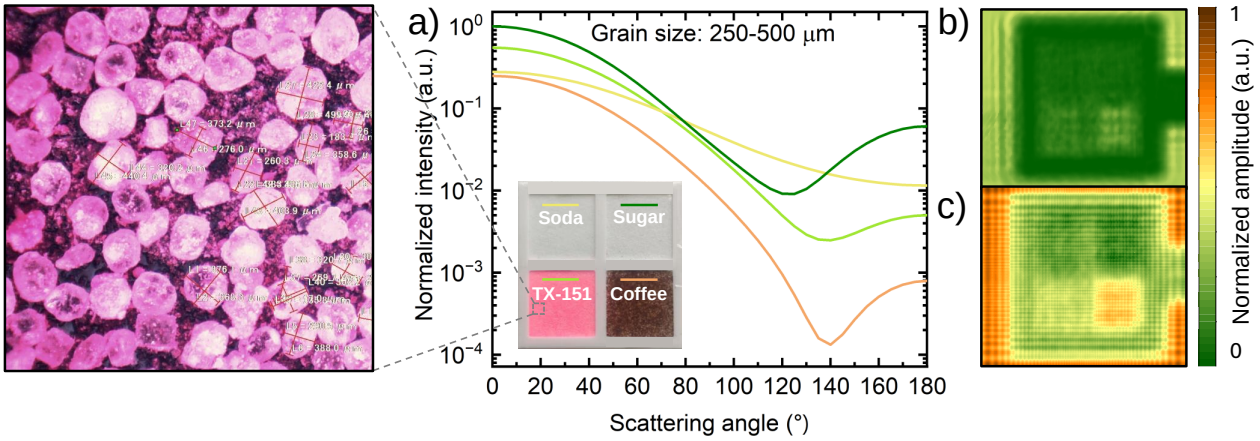


Fig. 1. Normalized intensity dependence on scattering angle for different materials, with the y-axis in logarithmic scale (a). Image of the investigated samples is depicted in the inset of this graph. The enlarged picture of TX-151 material is depicted on the left side of the graph. Amplitude distribution of investigated sample using direct THz imaging (b) and reconstructed amplitude distribution obtained using THz holography (c). The color scale is normalized to the maximum value.

[1] Mittleman D. M., Optics Express, vol. 26, no. 8, pp. 9417–9431 (2018).
[2] Sheridan J. T. et al., J. Opt., vol. 22, 123002 (2020).
[3] Draine B. T. et al., J. Opt. Soc. Am. A., vol. 11, no. 4, pp. 1491-1499 (1994).

THEORETICAL ANALOGIES AND PRACTICAL DIFFERENCES BETWEEN IMAGING AND LENSLESS INTERFEROMETRIC METHODS

Florian Dötzer[1], Marie Mannagottera[1], Stefan Sinzinger[1]

[1]Optical Engineering Group, Department of Mechanical Engineering, TU Ilmenau, Germany
florian.doetzer@tu-ilmenau.de

Interferometry is ubiquitous in dimensional measurement as it constitutes an extremely sensitive and highly versatile metrological tool. Depending on the configuration, it can be used for the characterization of surface topologies, distances or vibrations. Many of these applications require spatially resolved measurements. This can either be achieved by classical imaging of the object to the detector using an objective lens or by a lensless (or non-imaging) holographic setup. Accordingly, either an image of the object plane or its farfield distribution is superimposed with the reference beam and thereby characterized. Both methods can also be implemented in off-axis-configuration, which sacrifices some spatial resolution to enable single-shot measurements instead of the sequential phase shifting required for an inline-configuration. Apart from the required post-processing, imaging and lensless methods thus offer identical performance in theory. In practice however, depending on the properties of the measurement object, one method may lead to a more efficient use of the detector than the other. Fig. 1 illustrates this idea by an example.

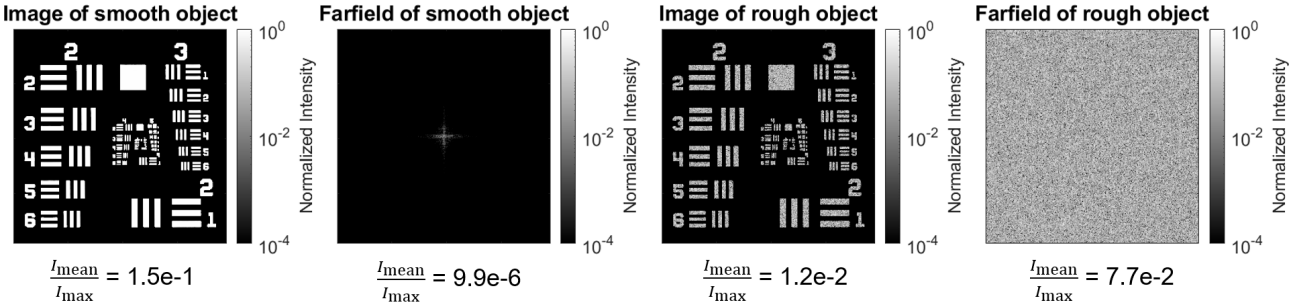


Fig. 1. Simulated intensity distributions (normalized to the respective maximum value) for images and farfield distributions of a plane wave, reflected/scattered from an optically smooth/rough USAF target.

If the surface of the object is assumed to be smooth, the image of the object directly resembles the object itself. The farfield distribution on the other hand shows a diffraction pattern, mostly spread into the vertical and horizontal direction according to the two most prominent orientations found in the object. The intensity is thus distributed very unevenly and most regions are illuminated only weakly while the center of the frame is strongly pronounced. The ratio between the mean intensity across the whole frame and the maximum value constitutes a measure of homogeneity and amounts to only 9.9e-6 in this case. The limited dynamic range of the detector is used very inefficiently for most pixels, as a large portion of the frame is basically black if the image is not supposed to be overexposed in the center. For the imaging system, a ratio of 1.5e-1 is obtained instead and thus makes use of the detector more efficiently for this specific object. For an object with the same USAF reflectivity distribution, but an optically rough surface, the intensity ratio for the imaging system is deteriorated by speckle noise to a value of now 1.2e-2. The spatially homogeneous far field distribution across the whole frame partially compensates for the speckle noise and the calculated intensity ratio of 7.7e-2 indicates that the lensless system operates more efficiently for this object. In our contribution, we present a more thorough theoretical investigation as well as real-world examples encountered in a holographic vibrometry laboratory setup.

MODELLING AND MICROWAVE COUPLING OF 3.1 GHz EPR RESONATORS

Ignas Pocius[1], Justinas Turčak[1], Mantas Šimėnas[1], Jūras Banys[1]

[1]Faculty of Physics, Vilnius University, Lithuania
ignas.pocius@ff.vu.lt

Electron paramagnetic resonance (EPR) spectroscopy is a widely used technique for studying paramagnetic centres in materials ranging from solids to proteins. The method is based on the quantum nature of the electron spin, which causes splitting of its energy levels in the magnetic field. The essence of EPR spectroscopy is the excitation of the quantum transitions between these levels and the detection of the microwave absorption using microwave resonators [1,2].

Here, we use CST Microwave Studio computational electromagnetics tool to simulate microwave coupling of a 3.1 GHz microwave resonator for EPR studies of spin qubits in ^{171}Yb:$CaWO_4$. Two loop-gap microresonator designs and various ways of microwave coupling were investigated (Fig. 1). We also explore how the microwave magnetic field homogeneity in the central loop of the microresonator depends on the number of outer loops. We compare our simulation results with the experimental observations and further discuss the best microwave coupling geometries.

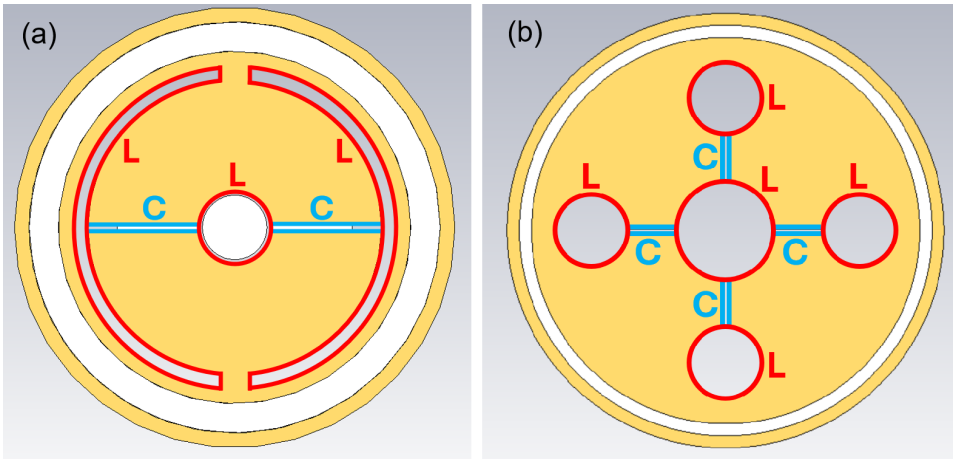


Fig. 1. Geometry of a 3.1 GHz (a) three-loop two-gap (b) five-loop four-gap resonator with an outer copper shield and a PTFE dielectric ring between them. (a) parts of the resonator geometry generating the inductance (L) and capacitance (C)

[1] A. Lund, M. Shiotani, and S. Shimada, Principles and applications of ESR spectroscopy. Springer Netherlands, 2011
[2] J. R. B. A. Weil, Basic Principles of Paramagnetic Resonance, ch. 1, 1–35. John Wiley & Sons, Ltd, 2006

ORAL SESSION 9

Biochemistry, Biophysics and Biotechnology

Chair: Dr. A. Zinovičius

MECHANISMS OF BACTERIAL ANTIPHAGE DEFENSE BY NAD$^+$ BASED INTRACELLULAR SIGNALS

Dziugas Sabonis[1]

[1]Institute of Biotechnology, Life Sciences Center, Vilnius University, Vilnius, Lithuania
dziugas.sabonis@gmc.vu.lt

In nature, bacteria are in constant danger posed by viruses that infect them, named bacteriophages (phages). This caused bacteria to evolve genetic elements called defense systems, to protect them against phage predation. In addition to the well-known gene and genome “scissors” - restriction-modification and CRISPR-Cas systems - more than 100 different bacterial antiviral defense systems have recently been discovered[1]. Many of these systems are based on two module composition: a sensor which recognizes phage infection and an effector which halts the phage cycle, commonly by exerting a toxic effect to the bacterial cell. Thoeris is a two module bacterial defense system consisting of a sensor ThsB homologous to the TIR (Toll/interleukin-1 receptor)-domain and an effector, ThsA protein[2]. ThsB recognizes a phage infection and synthesizes a unique signaling molecule which is then bound by the ThsA effector, exerting a toxic effect[3]. Based on the domain composition of ThsA proteins Thoeris systems are classified into types: type I (SIR2-STALD)[4] and type II (TM-Macro)[5].

Structural (cryo-EM, x-ray crystallography) and functional (enzyme assays, spectroscopy, biological assays) techniques were used to decipher the mechanism of action of Thoeris type I and type II systems. It was shown that type I ThsB’ uses NAD$^+$ as a substrate to produce 1’’-3’-gcADPR signaling molecule, which is then bound by STALD domain of type I ThsA protein. This causes conformational changes in ThsA protein and subsequent oligomerization into filaments. This action activates ThsA NADase activity via SIR2 domain, which depletes cellular NAD$^+$ and halts the phage cycle.

For type II system it was shown that ThsB uses amino acid histidine and NAD$^+$ as substrates to produce a signaling molecule His-ADPR. This signaling molecule is then bound by the Macro domain of type II ThsA protein and causes its oligomerization. This points to a possible membrane disruption mechanism via its transmembrane domains to halt the phage cycle.

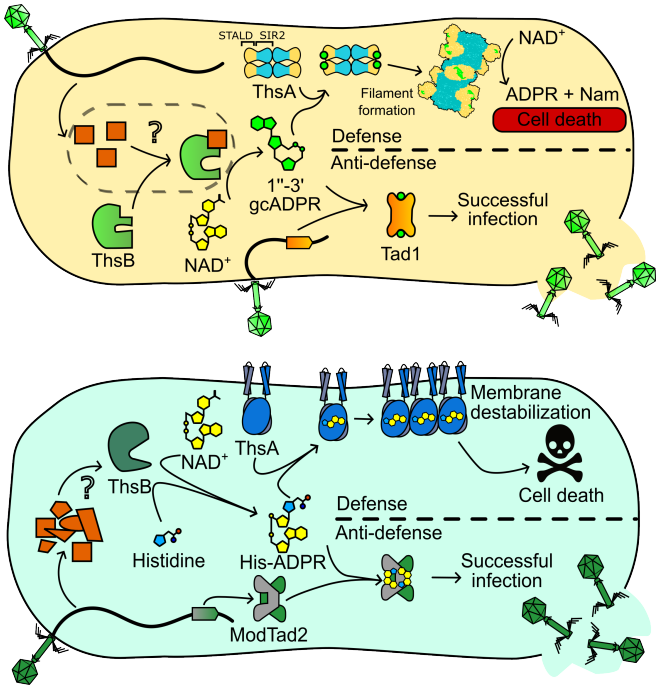


Fig. 1. Suggested mechanisms for Thoeris systems type I and type II.

[1] H. Georjon and A. Bernheim, ‘The highly diverse antiphage defence systems of bacteria’, Nat Rev Microbiol, vol. 21, no. 10, pp. 686–700, Oct. 2023
[2] S. Doron et al., ‘Systematic discovery of antiphage defense systems in the microbial pangenome’, Science, vol. 359, no. 6379, p. eaar4120, Mar. 2018
[3] G. Ofir et al., ‘Antiviral activity of bacterial TIR domains via immune signalling molecules’, Nature, vol. 600, no. 7887, Art. no. 7887, Dec. 2021
[4] G. Tamulaitiene et al., ‘Activation of Thoeris antiviral system via SIR2 effector filament assembly’, Nature, vol. 627, no. 8003, pp. 431–436, Mar. 2024
[5] D. Sabonis et al., ‘TIR domains produce histidine-ADPR conjugates as immune signaling molecules in bacteria’, Jan. 03, 2024, bioRxiv.

THE PORE-STABILIZING EFFECT OF NISIN WITH NANOSECOND AND MICROSECOND PULSE BURSTS FOR ELECTROCHEMOTHERAPY

Barbora Lekešytė[1,2], Olga Michel[1,3], Julita Kulbacka[1,3], Vitalij Novickij[1,2]

[1]State Research Institute Centre for Innovative Medicine, Department of Immunology and Bioelectrochemistry, Vilnius, Lithuania
[2]Vilnius Gediminas Technical University, Faculty of Electronics, Vilnius, Lithuania
[3]Wrocław Medical University, Department of Molecular and Cellular Biology, Wrocław, Poland
barbora.lekesyte@imcentras.lt

Electrochemotherapy (ECT) is a technique that uses a pulsed electric field (PEF) to improve the transmembrane delivery of chemotherapeutic drugs. This process relies on creating hydrophilic pores in the cell membrane via electroporation. Consequently, managing the density, stability, and size of these pores is essential for ensuring effective drug administration. Nisin is a naturally occurring peptide known for its antibacterial properties, which can facilitate the aggregation of proteins at the edges of pores, possibly influencing pore resealing. Moreover, studies have demonstrated that nisin can boost the effectiveness of chemotherapy across a range of cancer cell lines, indicating it might offer synergistic anticancer benefits. The possibility of nisin enhancing drug delivery through changes in pore induction or resealing, along with its potential additional anticancer effects, raises optimism for its therapeutic use alongside ECT. However, the impact of nisin in the context of ECT has not yet been explored.

Consequently, the primary objective of this study is to collect experimental evidence that illustrates nisin's ability to influence pores created in the membranes of a cancer cells through electroporation. In this study, we combine electrochemotherapy using microsecond: 0.6–1.5 kV/cm × 100 µs × 8 (1 Hz) and nanosecond: 6 kV/cm × 300 ns × 100 (1, 10, 100 kHz and 1 MHz) electric field pulses. These electric field pulses were performed on a murine 4T1 cell line. Our findings indicate that nisin has a substantial impact on electroporation. The synergistic effects, which include enhanced permeabilization and molecular electrotransfer, become particularly profound with a higher pulse burst frequency. Furthermore, nisin lowers the permeabilization thresholds, influences the resealing of pores, and demonstrates anticancer effects comparable to those of traditional electrochemotherapy. Notably, nisin exerted no toxicity in breast cancer cells, which offers confidence in its potential use alongside electrochemotherapy.

Acknowledgments: The research was supported by the Research Council of Lithuania, Grant Nr. S-PD-24-123.

Keywords: nanosecond pulses, nisin, pores, 4T1, drug delivery, permeabilization, resealing, electrochemotherapy

ANTIPROLIFERATIVE AND EPIGENETIC EFFECTS OF CANNABIDIOL ON ACUTE LYMPHOBLASTIC LEUKEMIA OR LYMPHOMA CELL LINES

Patricija Daugėlaitė[1,2], Veronika Borutinskaitė[1,2]

[1]Vilnius University
[2]Life sciences center
patricija.daugelaite@chgf.stud.vu.lt

Acute lymphoblastic leukemia (ALL) and lymphoma are aggressive hematological malignancies originating from immature lymphoid cells. These disorders are characterized by rapid uncontrolled proliferation and impaired differentiation, leading to disruption of normal hematopoiesis and immune function. Despite significant advancements in treatment strategies, including chemotherapy, immunotherapy, and targeted therapies, relapse and resistance remain major clinical challenges [1]. Investigating alternative therapies for ALL and lymphoma is crucial because they may offer new, less toxic treatment options for patients who experience severe side effects from conventional therapies. Additionally, exploring these alternatives could lead to novel mechanisms of action that improve treatment outcomes and enhance patients' quality of life.

In this study, ALL and lymphoma cells were treated with CBD to evaluate its therapeutic effects. ALL and lymphoma cell lines Jurkat, UoC-B6, RAJI, NALM-6, REH, and SU-DHL-4 were treated with 16 μM CBD. Cell viability and apoptosis were evaluated using trypan blue exclusion for live/dead cell counting and propidium iodide (PI) staining analyzed by flow cytometry to assess apoptosis. RT-qPCR was performed to quantify gene expression levels of target genes. Results demonstrated that CBD treatment significantly increased cell apoptosis, upregulateds immune-regulatory genes such as TNFα and IL-6, and downregulated epigenetic regulators DNMT1 and HDAC1 in ALL and lymphoma cells. The downregulation of epigenetic regulatory enzymes DNA methyltransferase 1 (DNMT1) and histone deacetylase 1 (HDAC1) implicates epigenetic modulation as a mechanism underlying CBD's anti-proliferative effects. Further gene expression analysis revealed upregulation of pro-inflammatory cytokines, tumor necrosis factor-alpha (TNFα) and interleukin-6 (IL-6), suggesting activation of immune-modulatory pathways.

These findings suggest a multifaceted mechanism of action for CBD, modulating both proliferation and epigenetic regulation. Our results highlight the need for further research into CBD as an alternative or adjunct therapy for ALL, aiming to improve patient outcomes by reducing chemotherapy-related side effects and overcoming drug resistance. Exploring novel treatment strategies such as CBD-based therapies may offer new hope for patients with refractory or relapsed disease.

[1] T. Terwilliger and M. Abdul-Hay, "Acute lymphoblastic leukemia: a comprehensive review and 2017 update," Blood Cancer Journal, vol. 7, e577, June 2017. [Online]. Available: https://pubmed.ncbi.nlm.nih.gov/. [Accessed January 26, 2025]

DUAL NIR-EXCITABLE NANOCOMPLEX FOR EFFECTIVE PHOTODYNAMIC CANCER THERAPY

Emilė Pečiukaitytė[1,2], Simona Steponkienė[1], Alėja Marija Daugėlaitė[1,3], Greta Butkienė[1], Eglė Ežerskytė[1,3], Vaidas Klimkevičius[1,3], Vitalijus Karabanovas[1,4]

[1]Biomedical Physics Laboratory, National Cancer Institute, Vilnius, Lithuania
[2]Life Sciences Center, Vilnius University, Vilnius, Lithuania
[3]Institute of Chemistry, Vilnius University, Vilnius, Lithuania
[4]Department of Chemistry and Bioengineering, Vilnius Gediminas Technical University, Vilnius, Lithuania
emile.peciukaityte@nvi.lt

According to the European Commission, cancer was the second largest cause of death in the EU in 2021, with 1.1 million deaths annually [1]. Current cancer therapeutic approaches are not always as effective or long-lasting as expected, highlighting the need for more precise and efficient alternatives with minimal side effects. One such approach is photodynamic therapy (PDT), which uses photosensitizers (PS), compounds that become active only when exposed to light. PS-induced phototoxic reactions occur only in illuminated areas, reducing unwanted side effects. However, PS molecules are prone to photobleaching. Additionally, their activation typically depends on a red light, which has limited tissue penetration, complicating the treatment of deep-seated tumors. To solve these issues and enhance PS functionality, nanoparticles can be introduced as energy donors, thus shifting PS excitation to near-infrared (NIR) [2]. This study focuses on developing a therapeutic nanocomplex of PS Chlorin e6 (Ce6) loaded into the phospholipid/polyethylene glycol coating of upconverting nanoparticles (UCNP) for NIR-activated PDT.

Firstly, the surface of $NaGdF_4:Yb^{3+}$, Er^{3+}@$NaGdF_4:Yb^{3+}$, Nd^{3+} UCNPs were modified with 3 different mixtures of phosphatidylcholine and phosphoethanolamine-polyethylene glycol phospholipids (PLs). Ce6 encapsulation was achieved by mixing surface-coated UCNPs with concentrated Ce6 solution and washing excess Ce6 afterwards. The singlet oxygen generation efficiency of UCNPs-PLs-Ce6 was evaluated upon illumination with 980 nm and 808 nm lasers, using a singlet oxygen sensor green probe. Accumulation, cytotoxicity, and in vitro PDT were performed in colon cancer cell lines DLD-1 and HCT116.

The obtained spectroscopic data and average luminescence decay confirmed donor-acceptor pair formation and energy transfer between UCNPs and Ce6. Quantitative evaluation of singlet oxygen demonstrated the high effectiveness of UCNPs-PLs-Ce6, highlighting its promising therapeutic potential. Furthermore, a comparative study revealed significantly better photostability of Ce6 within the nanocomplex. In contrast, free Ce6 photobleached and degraded. Cellular studies showed UCNPs-PLs-Ce6 accumulation in the perinuclear region with maintained nanocomplex stability inside the cells. *In vitro* PDT upon 980 nm and 808 nm laser irradiation decreased cancer cell viability. Irradiation by 808 nm laser was continuously performed, while 980 nm laser needed fractionation in time due to thermal heating.

Overall, a therapeutic nanocomplex with extended PDT activation light from red to NIR and enhanced Ce6 photostability was developed. Photostable Ce6 enables improved therapeutic effects *in vitro*, while 808 nm laser light enables deeper tissue penetration and elimination of photothermal effects. This study not only contributes to fundamental knowledge but also demonstrates the potential of nano complexes in novel cancer therapy.

Acknowledgements

This project has received funding from the Research Council of Lithuania (LMTLT), agreement No. S-MIP-22-31 and No. P-ST-24-258.

[1] Eurostat, “Cancer statistics,” European Commission, [Online]. Available: https://ec.europa.eu/eurostat/statistics-explained/index.php?title=Cancer_statistics. Accessed: Feb. 14, 2025.

[2] A. Skripka et al., “Decoupling Theranostics with Rare Earth Doped Nanoparticles,” Advanced Functional Materials, vol. 29, no. 12. Wiley, Jan. 02, 2019. doi: 10.1002/adfm.201807105.

INVESTIGATION OF THE LINK BETWEEN ACTION POTENTIAL TRANSMISSION PROPERTIES AND THE ELECTROPHYSIOLOGICAL PARAMETERS OF TANDEM INTERNODAL CELLS OF NITELLOPSIS OBTUSA

Radvilė Janušauskaitė[1], Vilmantas Pupkis[1], Vilma Kisnierienė[1], Indrė Lapeikaitė[1]

[1]Vilnius University
radvile.asar@gmail.com

The study of membrane excitability has primarily been shaped by investigations in animal cells, but the significant role of electrical excitation in plants has been recognized almost simultaneously. For a long time, it was believed that action potentials (APs) served similar functions in both plant and animal systems, a theory supported by the similarities observed in excitations between plant cells, like Nitella, and nerve cells, such as squid giant axons. In plants, environmental factors such as fluctuations in temperature, mechanical stimuli, and various signaling molecules—can trigger the generation of APs. Once an electrical signal is generated in response to a stimulus, it is transmitted to other regions of the plant, helping to coordinate cellular adaptations. This process influences essential physiological functions such as respiration and photosynthesis.

Among the many signaling molecules that can modulate AP parameters, glutamate (Glu) is one of the most universal. Previous studies have shown that Glu alters various AP parameters in Characean internodal cells. However, it remains unclear whether these changes affect the propagation and transmission characteristics of APs. Additionally, under standard environmental conditions, it is still unknown whether Characean macroalgae exhibit a directional disparity in AP transmission and which electrophysiological parameters influence the probability and velocity of AP transmission between internodal cells. To address these questions, this study aims to examine the link between AP transmission properties and the electrophysiological parameters of tandem internodal cells in Nitellopsis obtusa. The research employed the two-electrode current-clamp technique, with intracellular glass electrodes inserted into both basal and apical cells of each tandem (internodal cell-multicellular node-internodal cell). Three APs were elicited in one cell every 5 minutes by gradually increasing the direct current until the excitation threshold was reached. The membrane potential was consistently recorded in both cells. The protocol was repeated bidirectionally, first in a control solution (APW') and then in a solution containing Glu dissolved in APW'.

The results revealed that, under standard conditions, the probability and velocity of AP transmission between internodal cells of N.obtusa were higher in the basal direction compared to the apical direction. In control conditions, a hyperpolarized excitation threshold, prolonged repolarization, and a depolarized resting potential were associated with a higher probability of transmission. Additionally, transmission velocity positively correlated with AP amplitude and the reduced difference between the membrane resting potential and the excitation threshold. Exposure of the entire tandem to 1 mM glutamate for 30 minutes resulted in a significant decrease in the percentage of transmitted APs between adjacent internodal cells and reduced the transmission velocity.

PHYSICS-INFORMED NEURAL NETWORKS FOR ACCURATE SHEAR STRESS MAPPING AT CELL-SUBSTRATE INTERFACES IN ORGAN-ON-A-CHIP SYSTEMS

Emīls Šmits[1], Jānis Cīmurs[1], Viesturs Šints[1]

[1]MMML lab, Department of Physics, Faculty of Science and Technology, University of Latvia
es18211@edu.lu.lv

Accurate measurement of shear stress at the cell–substrate interface is crucial for understanding cell behavior in organ-on-a-chip (OOC) systems, where mechanical forces regulate processes such as cell alignment and differentiation. Precision of traditional methods heavily depend on the spatial resolution of Particle Image Velocimetry (PIV) measurements and are further compromised by noise inherent in PIV data, which amplifies uncertainties in local shear stress estimation [1].

In this work, we address the inverse problem of reconstructing a continuous flow field from sparse 2D PIV data using Physics-Informed Neural Networks (PINNs) [2]. By embedding the Navier–Stokes equations and incorporating a power-law formulation of the medium's non-Newtonian rheology directly into the loss function, our approach captures the complex fluid behavior while enforcing physical constraints during neural network training. The main goal of our research is to define the cell–substrate boundary and compute local shear stress with high spatial resolution and precision.

Using well-defined simulations with known ground truth, we demonstrate that our technique provides improved boundary detection compared to conventional image processing methods and generates shear stress maps that accurately capture the medium's detailed rheological behavior. Moreover, our PINN-based approach exhibits robustness to noise in PIV measurements, resulting in more reliable flow reconstructions. These refined maps support more informed microfluidic device design and enhance the evaluation of in vitro models for biomedical research.

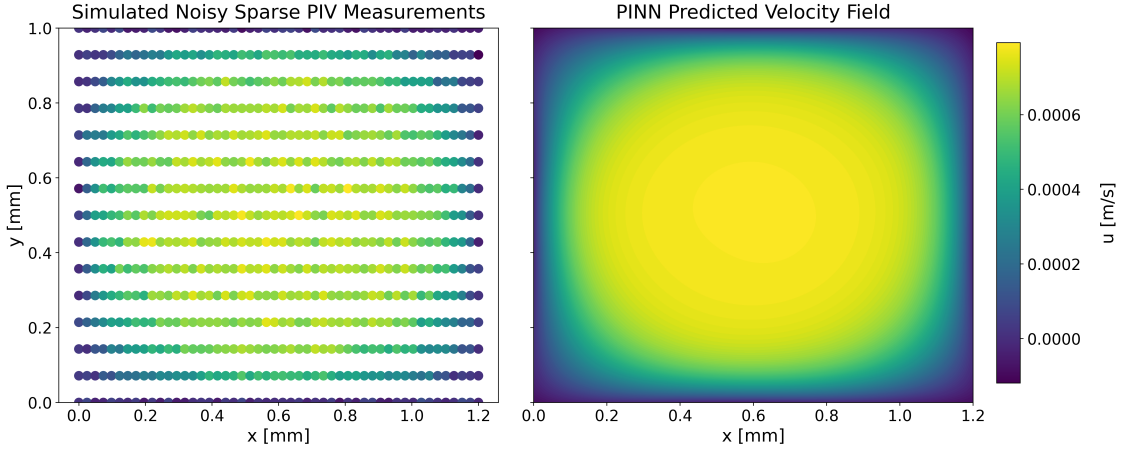


Fig. 1. Comparison between a simulated sparse and noisy PIV dataset (left) and the PINN-predicted continuous velocity field (right). Colors indicate velocity magnitude (in m/s)

[1] V. Šints et al., 'Physical model of serum supplemented medium flow in organ-on-a-chip systems', 2024, arXiv. doi: 10.48550/ARXIV.2409.13650.

[2] M. Mahmoudabadbozchelou, G. Em. Karniadakis, and S. Jamali, 'nn-PINNs: Non-Newtonian physics-informed neural networks for complex fluid modeling', Soft Matter, vol. 18, no. 1. Royal Society of Chemistry (RSC), pp. 172–185, 2022. doi: 10.1039/d1sm01298c.

ORAL SESSION 10

Biology, Genetics and Biomedical Sciences

Chair: Dr. A. Zentelytė

NON-INVASIVE DETECTION OF RENAL CLEAR CELL CARCINOMA USING URINARY METHYLATED DNA AS A BIOMARKER

Karolina Matekonytė[1], Raimonda Kubiliūtė[1,2], Algirdas Žalimas[1,2], Sonata Jarmalaitė[1]

[1]Life sciences center, Vilnius University, Lithuania
[2]National Cancer Institute, Vilnius, Lithuania
karolina.matekonyte@gmc.stud.vu.lt

Renal clear cell carcinoma is a type of kidney cancer, known for being diagnosed mostly accidentally because of its largely asymptomatic nature. Detection in later stages contributes to worse treatment outcomes for patients. The currently available diagnostic tools for this cancer include biopsies and medical imaging, methods that are either invasive or lacking in their prognostic capabilities. Our current research focuses on potential non-invasive biomarkers that could provide diagnostic and prognostic information about the disease.

DNA methylation, a naturally occurring process, one of many corrupted as cancer develops, has been explored as a biomarker in our laboratory before by using Agilent Human DNA Methylation 1 × 244K Microarrays. Our current work seeks to look at the methylation of selected genes' regulatory sequences in urine sediments of patients and asymptomatic controls using quantitative methylation-specific PCR.

The results have been analyzed using t-test and ROC curve analysis methods. Methylation levels at the regulatory regions of all selected genes were found to be significantly higher in urine sediments of renal clear cell carcinoma patients, compared to asymptomatic controls. All of them also had significant diagnostic potential, and one was distinguished as a potential prognostic biomarker with a significantly higher methylation level in the case of a higher tumor stage.

All in all, our investigation of methylated DNA sequences as non-invasive biomarkers for renal clear cell carcinoma showed significant diagnostic and prognostic potential.

BREAST ADENOCARCINOMA-DERIVED EXTRACELLULAR VESICLES ARE ASSOCIATED WITH CHANGES IN THE METABOLIC AND BIOENERGETIC FUNCTIONS OF CARDIOVASCULAR SYSTEM CELLS

Enrika Baronaitė[1], Deimantė Kulakauskienė[1], Vytenis Keturakis[1], Zbigniev Balion[1], Edgaras Stankevičius[1], Aistė Jekabsone[1]

[1]Preclinical Research Laboratory for Medicinal Products, Institute of Cardiology, Lithuanian University of Health Sciences, Kaunas, LT-50162, Lithuania
enrikabaronaite@gmail.com

Breast cancer is one of the most diagnosed tumours in the world, and it is localised close to heart tissue [1]. Extracellular vesicles (EVs) secreted by cancer, which are rich in oncoproteins and oncogenic factors, play a crucial role in tumor growth and spread [2]. Cancer cells produce these vesicles in significantly larger quantities than healthy cells [3]. EVs can easily cross biological barriers and reach any part of the body, including the heart, making it easier for them to transmit oncogenic material to healthy cells [4]. It is known that EVs can influence the function, viability, and morphology of vascular cells, but there is still a lack of information on their effects on cardiomyocytes [4]. Cardio-oncology is a new branch of science that explores the relationship between oncological and cardiovascular diseases [5]. However, there is still a lack of studies investigating the connection between these pathologies through cancer-secreted EVs [5]. For this reason, the aim of this work was to determine the effects of the extracellular vesicles secreted by the breast cancer on the function and viability of cardiovascular system cells.

EVs were purified from human breast adenocarcinoma MCF-7 cell conditioned media using centrifugation and polymer precipitation methods. EVs was characterised by size using dynamic light scattering method and nanoparticle tracking analysis, by total protein using Bradford assay and by total RNA using TRIzol reagent. To examine the effect of breast cancer EVs on the cardiovascular system we affected primary Wistar rat cardiomyocytes and human umbilical cord vascular endothelial cells HUVEC with MCF-7 EVs. The viability of affected cells was estimated by PrestoBlue assay and bioenergetic changes in mitochondria were detected using the Seahorse XFp analyser. Statistical analysis and visualisation were made with GraphPad 10 program.

We determined that both size MCF-7 EVs (small and large) inhibit HUVEC viability, migration and bioenergetics processes, however large EVs induced a higher-level inhibition of metabolism and mitochondrial respiration in cardiomyocytes.

The obtained results suggests that both size MCF-7 EVs inhibit HUVEC and cardiomyocytes functions and viability. Large EVs had a greater inhibitory effect on cardiomyocytes function and bioenergetic processes than small EVs. HUVEC functions was inhibited equally by EVs of both sizes. It is possible that such inhibition of cardiovascular system cells indicates that cancer-derived EVs promote inflammatory processes and oxidative stress within the cells, which can lead to functional changes in mitochondria, thereby inhibiting cellular respiration and energy production.

[1] M. Arnold et al., “Current and future burden of breast cancer: Global statistics for 2020 and 2040,” Breast, vol. 66, pp. 15–23, Dec. 2022
[2] J. W. Clancy and C. D’Souza-Schorey, “Tumor-Derived Extracellular Vesicles: Multifunctional Entities in the Tumor Microenvironment,” Annual Review of Pathology: Mechanisms of Disease, vol. 18, no. 1, Oct. 2022
[3] X. Zhou, Y. Jia, C. Mao, and S. Liu, “Small extracellular vesicles: Non-negligible vesicles in tumor progression, diagnosis, and therapy,” Cancer letters, vol. 580, p. 216481, Jan. 2024
[4] Y. Xu, K. Feng, H. Zhao, L. Di, L. Wang, and R. Wang, “Tumor-derived extracellular vesicles as messengers of natural products in cancer treatment,” Theranostics, vol. 12, no. 4, pp. 1683–1714, 2022
[5] D. Cardinale et al., “Cardiac biomarkers in the field of cardio-oncology,” European Heart Journal. Acute Cardiovascular Care, vol. 11, no. 11, pp. e1–e2, Oct. 2022

THE EFFECT OF NOVEL HYDRAZONE DERIVATIVES ON HUMAN LUNG, TRIPLE-NEGATIVE BREAST AND SKIN CANCER CELL 2D AND 3D CULTURES

Dainius Lukauskas[1], Aida Šermukšnytė[2], Ingrida Tumosienė[2], Kristina Kantminienė[3], Vilma Petrikaitė[1,4]

[1]Department of Drug Targets Histopathology, Institute of Cardiology, Lithuanian University of Health Sciences, Lithuania
[2]Department of Organic Chemistry, Faculty of Chemical Technology, Kaunas University of Technology, Lithuania
[3]Department of Physical and Inorganic Chemistry, Faculty of Chemical Technology, Kaunas University of Technology, Lithuania
[4]Life Sciences Center, Institute of Biotechnology, Vilnius University, Lithuania
dainius.lukauskas@chgf.stud.vu.lt

Cancer remains one of the leading causes of death worldwide, with lung, breast, and skin cancers being among the types with the highest incidence rates [1]. Lung cancer accounts for 18.7% of all new cancer mortality cases and is the most prevalent type worldwide [1]. Triple-negative breast cancer accounts for 12-17% of all new breast cancer cases and is associated with an adverse prognosis [2]. Although melanoma represents only 1% of skin cancer incidence, it accounts for over 80% of all skin cancer deaths [3,4]. Targeted therapies have demonstrated significant therapeutic potential in both standalone and combination cancer treatments [5]. In this study, we evaluate the anticancer activity of newly synthesized potential kinase inhibitors — hydrazone derivatives — in lung adenocarcinoma cell line A549, triple-negative breast cancer cell line MDA-MB-231, and melanoma cell line IGR39.

The impact on cell viability of 14 novel hydrazone derivatives, bearing substitutes pyridine and 1,2,4-triazole moieties, was screened using the MTT assay at 50 µM compound concentration. Selected compounds with significant cytotoxic activity were further studied to establish their EC_{50} values. Based on determined values, compounds IT160, IT164, IT165, IT166, IT167, and IT168 were identified as promising candidates for further evaluation. The most potent compound, IT168, demonstrated an EC_{50} profile closest to that of the reference compound sunitinib, a clinically approved kinase inhibitor, with compound IT168 EC_{50} value being approximately 4 µM (sunitinib 2 µM) to the cancerous cell lines and approximately 5 µM (sunitinib 8 µM) to non-cancerous human fibroblasts (HF).

Following EC_{50} determination, we assessed selected compounds for their effect on cell migration using the wound healing assay at 50% and 10% of their corresponding EC_{50} values. Only sunitinib exhibited statistically significant inhibition of migration across the used cell lines.

Additionally, we evaluated the impact on three-dimensional (3D) cell culture growth and cell viability, revealing that compound 168 significantly reduced cell viability in A549 cell line spheroids at a fixed 5 µM concentration, albeit with lower efficacy than sunitinib. Despite the lack of substantial effects on migration or spheroid growth, the results from cell viability assays suggest potential applications in combination therapy and they aid in further compound structural optimization.

In conclusion, compounds IT160, IT164, IT165, IT166, IT167, and IT168 exhibited notable anticancer activity in 2D cultures, with compound IT168 showing the most promising results in the A549 cell line 3D models. Further studies are necessary to explore their mechanisms of action and potential therapeutic applications.

[1] F. Bray et al., “Global cancer statistics 2022: GLOBOCAN estimates of incidence and mortality worldwide for 36 cancers in 185 countries,” CA. Cancer J. Clin., vol. 74, no. 3, pp. 229–263, 2024, doi: 10.3322/caac.21834.
[2] W. D. Foulkes, I. E. Smith, and J. S. Reis-Filho, “Triple-Negative Breast Cancer,” N. Engl. J. Med., vol. 363, no. 20, pp. 1938–1948, Nov. 2010, doi: 10.1056/NEJMra1001389.
[3] Surveillance, Epidemiology, and End Results (SEER) Program (www.seer.cancer.gov) SEER*Stat Database: Incidence - SEER Research Data, 8 Registries, Nov 2023 Sub (1975-2021), National Cancer Institute, DCCPS, Surveillance Research Program, released April 2024, based on the November 2023 submission.
[4] K. Saginala, A. Barsouk, J. S. Aluru, P. Rawla, and A. Barsouk, “Epidemiology of Melanoma,” Med. Sci., vol. 9, no. 4, Art. no. 4, Dec. 2021, doi: 10.3390/medsci9040063.
[5] Y. T. Lee, Y. J. Tan, and C. E. Oon, “Molecular targeted therapy: Treating cancer with specificity,” Eur. J. Pharmacol., vol. 834, pp. 188–196, Sep. 2018, doi: 10.1016/j.ejphar.2018.07.034.

COMPREHENSIVE CHARACTERIZATION OF ORGANOIDS FORMED FROM PATIENT-DERIVED ENDOMETRIUM FOR INFERTILITY RESEARCH

Erika Girniūtė[1], Deimantė Žukauskaitė[1], Rūta Navakauskienė[1]

[1]Department of Molecular Cell Biology, Institute of Biochemistry, Life Sciences Center, Vilnius University, Lithuania
erika.girniute@gmc.stud.vu.lt

In vitro 3D cell culture systems, termed organoids, are currently extensively used model systems that compared with 2D monolayer cell cultures, more closely resemble architectural and functional characteristics of tissues *in vivo* [1]. Human endometrium, the inner lining of the uterus, has long been a subject of cell biology research to study pregnancy-related physiology and gynecological problems. Despite that, studies regarding topics such as trophoblast implantation and invasion have been limited due to the absence of appropriate research models [2]. Human endometrial organoids have been reported fairly recently and this field of study still requires more work to improve current models since they have the potential to be used in patient-specific pregnancy and gynecological disease studies [3].

In this work, we aimed to construct patient-derived endometrial organoids that model endometrium *in vitro* and characterize their structural as well as functional properties. For organoid construction, endometrial epithelial cell clusters were cultured in a commercial extracellular matrix solution, which serves as a scaffold for 3D structure formation, in addition to an organoid culturing medium containing specific signaling factors. Self-assembling organoids were cultured and passaged after 5-7 days, and the formed organoids were assessed by microscopy along with immunofluorescence of marker proteins.

Our results demonstrate that when cultured in extracellular matrix mimicking conditions, endometrial epithelial cells from *ex vivo* samples self-assemble into 3D spherical structures. They can be passaged while maintaining their morphology and structural properties. We observed that organoids express glandular epithelium-specific structural proteins (EpCAM, Cytokeratin, etc.) as well as functional proteins, such as MUC1, at different levels.

Overall, our study presents the construction of patient-specific endometrial organoids that reproduce tissue-defining characteristics and function and can thus be applied to various physiological and pathological research experiments *in vitro*.

[1] Liu, Y., Sun, Y., & Cheng, S. (2024). Advances in the use of organoids in endometrial diseases. International Journal of Gynecology & Obstetrics.

[2] Shibata, S., Endo, S., Nagai, L. A., H. Kobayashi, E., Oike, A., Kobayashi, N., ... & Arima, T. (2024). Modeling embryo-endometrial interface recapitulating human embryo implantation. Science advances, 10(8), eadi4819.

[3] Li, Y., Qin, M., Liu, N., & Zhang, C. (2025). Organoid development and applications in gynecological cancers: the new stage of tumor treatment. Journal of Nanobiotechnology, 23(1), 20.

DEVELOPMENT AND CHARACTERIZATION OF HYBRID LIPOSOME-EXOSOME NANOPARTICLES FOR TARGETED DRUG DELIVERY IN GLIOBLASTOMA

Girstautė Dabkevičiūtė[1], Christian Celia[2], Vilma Petrikaitė[1,3]

[1]Life Sciences Center, Institute of Biotechnology, Vilnius University, Lithuania
[2]Department of Pharmacy, University of Chieti - Pescara "G. d'Annunzio", Italy
[3]Laboratory of Drug Targets Histopathology, Institute of Cardiology, Lithuanian University of Health Sciences, Lithuania
girstaute.dabkeviciute@bti.stud.vu.lt

Glioblastoma (GBM) is the most aggressive brain malignancy in adults [1]. The complex microenvironment of GBM presents significant obstacles to traditional drug delivery methods, prompting the exploration of nanoparticles (NPs). The fusion of liposomes (LPs) and exosomes (EXOs) is considered a promising strategy to enhance drug carrier biocompatibility, targeting properties, and cellular uptake [2]. The goal of our research was to synthesize and characterize hybrid NPs for the delivery of doxorubicin (DOX) to GBM cells.

Two LP formulations, F1 and F2, were prepared via the thin layer evaporation method, each with distinct lipid molar ratios: 6:3:1 for DPPC:CHOL:DSPEmPEG2000 in F1 and 7:4:6:1 for DPPC:DPPS:CHOL:DSPEmPEG2000 in F2. Lipid films were hydrated with either a PBS solution (10 mM, pH 7.4), ammonium sulphate solution (250 mM, pH 5.5), or M_0 macrophage-derived EXOs in PBS, following extrusion through membrane filters. For loaded LPs, DOX was entrapped using a pH gradient and remote loading procedure, with entrapment efficiency (EE%) determined by fluorescence. Size, polydispersity index (PdI), and zeta potential (ZP) were assessed using dynamic light scattering. Long-term stability of all NPs at 4 °C was evaluated weekly for a month. The short-term stability of empty LPs and the drug release of loaded LPs in DMEM with 10% FBS at different pH levels were assessed under stirring at 37 °C for 72 hours.

The average size of F1, F2, M_0-F1 and M_0-F2 NPs was below 152 nm, while loaded LPs increased in diameter by up to 20 nm. The PdI of all NPs was < 0.2. ZP of empty NPs was −13.2 ± 1.2 mV (F1), −23.4 ± 1.9 mV (F2), -36.4 ± 3.9 mV (M_0-F1), and -24.6 ± 2.4 mV (M_0-F2), while DOX loading altered ZP from 6 to 13 mV. F1, F2, DOX-F2, M_0-F1 and M_0-F2 remained stable at 4 °C for a month. However, the PdI of DOX-F1 slightly increased in the third week. Empty LPs remained stable in stressful conditions for 72 hours. The EE% of F2 LPs was 40% higher compared to F1. Finally, DOX was released more rapidly from F2 NPs at pH 5.5, increasing selectivity for the tumor microenvironment.

Overall, the F2 liposomal formulation showed promising characteristics for developing hybrid nanocarriers, making M_0-F2 NPs a strong candidate for surface modifications and further *in vitro* studies.

[1] S. Bahadur, A. K. Sahu, P. Baghel, and S. Saha, "Current promising treatment strategy for glioblastoma multiform: A review," Oncology Reviews, vol. 13, no. 2, Jul. 2019

[2] D. N. Moholkar, Raghuram Kandimalla, R. C. Gupta, and Farrukh Aqil, "Advances in lipid-based carriers for cancer therapeutics: Liposomes, exosomes and hybrid exosomes," Cancer letters, vol. 565, pp. 216220–216220, Jul. 2023

EXPLORING THE PHYSICOCHEMICAL AND RADIOBIOLOGICAL MECHANISMS OF FLASH RADIOTHERAPY

Paulina Kazlauskaitė[1,2,3], Akvilė Šlėktaitė-Kišonė[2,4], Džiugilė Valiukevičiūtė[4], Marius Burkanas[4], Aleksandras Cicinas[4], Mindaugas Džiugelis[2,4], Ričardas Rotomskis[2], Jonas Venius[2,4], Rasa Sabaliauskaitė[1,5]

[1]National Cancer Institute, Laboratory of Genetic Diagnostics, 08406 Vilnius, Lithuania
[2]National Cancer Institute, Biomedical Physics Laboratory, 08406 Vilnius, Lithuania
[3]Institute of Biomedical Sciences, Faculty of Medicine, Vilnius University, 08661 Vilnius, Lithuania
[4]National Cancer Center, Medical Physics Department, 08406 Vilnius, Lithuania
[5]Institute of Biosciences, Life Sciences Center, Vilnius University, 10257 Vilnius, Lithuania
paulina.kazlauskaite@mf.stud.vu.lt

Radiotherapy (RT) is used in approximately 50% of cancer patients [1]. While highly effective, its potential is limited by toxicity to healthy cells, restricting doses that can be safely administered [2]. To address this issue, research has focused on studying the unique radiobiological responses at ultrahigh dose rates, known as FLASH-RT [3]. Recent studies show that FLASH-RT reduces damage to healthy tissues while maintaining tumor control, making it a promising alternative to conventional RT (CONV-RT) [4]. However, the molecular mechanisms underlying distinct responses to FLASH and CONV irradiation remain insufficiently understood. Therefore, the aim of this study was to compare the effects of FLASH-RT and CONV-RT on reactive oxygen species (ROS) production in water and intracellular environment-mimicking solutions, as well as their impact on miRNAs expression and cell viability in prostate cancer and normal colon 3D spheroids.

All samples were irradiated using a clinical linear accelerator modified to achieve the required dose rates for FLASH-RT. Water and Bovine Serum Albumin (BSA)-enriched solutions received 10, 15, and 20 Gy doses, and ROS production was measured *via* fluorescence spectroscopy. Prostate cancer (C4-2) and normal colon (CRL-1541) cell spheroids were irradiated with 17 Gy doses. MiRNA-21-5p, miRNA-29a-3p, and miRNA-222-3p levels were measured at 12, 24, 48, and 72 hours post-RT using reverse transcription quantitative PCR with expression determined relative to untreated controls using the $2^{-\Delta\Delta Ct}$ method. Cell viability was assessed on days 1, 4, 7, and 11 post-RT using the XTT assay, with results expressed as a percentage relative to untreated controls.

FLASH-RT produced notably lower ROS levels compared to CONV-RT in both water ($\sim$3 times) and BSA-enriched ($\sim$1.8 times) solutions. At 24 hours post-RT, there were no differences in miRNAs expression between CONV-RT and FLASH-RT in either cell line. By 72 hours, CRL-1541 cells showed significant downregulation of the studied miRNAs following CONV-RT compared to FLASH-RT, while no significant differences were found between two treatments in C4-2 cells. Additionally, CONV-RT significantly reduced cell viability compared to FLASH-RT on day one post-RT in CRL-1541 cells, whereas no significant differences in FLASH-RT and CONV-RT treatment effects were observed in C4-2 cells.

The results suggest FLASH-RT reduces ROS production, minimizing ROS effects on cell damage. Distinct miRNA expression and cell viability patterns suggest differing mechanisms between FLASH-RT and CONV-RT in healthy and cancerous cells. Notably, miRNAs expression at 72 hours post-RT and cell viability on day one post-RT reveal that while FLASH-RT affects cancer cells similarly to CONV-RT, it shows unique protective effects on normal cells. These findings suggest that FLASH-RT may selectively spare healthy cells, highlighting the need for further investigation.

Acknowledgements

This study was supported by the National Cancer Institute Research Fund and the Research Council of Lithuania (LMTLT), agreement No. S-MIP-24-134.

[1] Delaney, G., Jacob, S., Featherstone, C., & Barton, M. (2005). The role of radiotherapy in cancer treatment. Cancer, 104(6), 1129–1137. https://doi.org/10.1002/cncr.21324

[2] Barnett, G. C., West, C. M. L., Dunning, A. M., Elliott, R. M., Coles, C. E., Pharoah, P. D. P., & Burnet, N. G. (2009). Normal tissue reactions to radiotherapy: towards tailoring treatment dose by genotype. Nature Reviews. Cancer, 9(2), 134–142. https://doi.org/10.1038/nrc2587

[3] Friedl, A. A., Prise, K. M., Butterworth, K. T., Montay-Gruel, P., & Favaudon, V. (2021). Radiobiology of the FLASH effect. Medical Physics, 49(3), 1993–2013. https://doi.org/10.1002/mp.15184

[4] Favaudon, V., Caplier, L., Monceau, V., Pouzoulet, F., Sayarath, M., Fouillade, C., Poupon, M., Brito, I., Hupé, P., Bourhis, J., Hall, J., Fontaine, J., & Vozenin, M. (2014). Ultrahigh dose-rate FLASH irradiation increases the differential response between normal and tumor tissue in mice. Science Translational Medicine, 6(245). https://doi.org/10.1126/scitranslmed.3008973

ORAL SESSION 11

Biochemistry, Biophysics and Biotechnology

Chair: Dr. S. Klimašauskas

VALORISATION OF WALNUT SHELL AS A SOURCE OF BIOACTIVE DERIVATIVES: IN SILICO POLYPHENOL OXIDASE INHIBITION AND TOXICITY PREDICTION

Ayodeji Amobonye[1], Joana Bendoraitiene[1], Laura Peciulyte[1], Ramune Rutkaite[1]

[1]Department of Polymer Chemistry and Technology, Kaunas University of Technology, Lithuania
ayodeji.amobonye@ktu.lt

Waste valorisation has been identified as key component of global sustainability, UN sustainable development goals and the bioeconomy [1, 2]. In this context, walnut shell (WNS), an agro-waste which accounts for more than half of the total weight of the nut and potentially could be explored as a source of bioactive ingredients in food processing/packaging technologies. In this study, phenolic-rich methanolic extract was obtained from WNS via microwave assisted extraction [3] and its bioactivity was assessed. The antioxidant activity assays demonstrated that extract has IC50 of 203.91 mg/mL, 102.48 mg/mL and 71.52 µg/mL, against ABTS•+, DPPH• and O2•– radicals, respectively, as well as FRAP value of 629. 33 µmol Fe (II)/g. In addition, the IC50 of extract against mushroom tyrosinase was found to be 512.46 µg/mL. LC-MS and GC-MS analyses revealed a total of 53 phenolic and non-phenolic compounds in the WNS extract which were docked against mushroom tyrosinase. Molecular docking analysis indicated better binding interactions between the WNS compounds, chlorogenic acid (-9.3 kcal/mol), 3-O-p-coumaroylquinic acid (-9 kcal/mol), betulin (-8.9 kcal/mol) when compared to epigallocatechin gallate (-8.2 kcal/mol) and butylated hydroxytoluene (-6.5 kcal/mol), which are well known food preservatives. Furthermore, the WNS compounds evaluated were observed to be relatively non-toxic based on their predicted LD50, pLC50 and pIGC50 values as well as their predicted pharmacokinetic properties. These results underscore the significance of WNS as a renewable bioresource for high-value applications, however, more work is required to demonstrate its potential within food related applications.

Acknowledgements
This project was funded by the Research Council of Lithuania (LMTLT), agreement No S-PD-24-33.

[1] A. S. Matharu et al. Bioresour. Technol. vol. l, no. 215, pp. 123-130, (2016).
[2] B. Segers et al. RSC Sustain. vol. 2, pp 3730-3749, (2024).
[3] A. A. B. Mokaizh, et al., J. Ind. Eng. Chem. vol. 142, pp. 321-328, (2025).

ELECTROGENICITY IN PATHOGENIC BACTERIAL BIOFILMS

Evelina Lukaitė[1], Marius Butkevičius[2], Eglė Malachovskienė[3], Algimantas Paškevičius[3], Marius Dagys[2], Rokas Žalnėravičius[1,2]

[1]Department of Electrochemical Materials Science, Center of Physical and Technological Sciences, Saulėtekio av. 3, Vilnius, Lithuania
[2]Department of Bioanalysis, Life Sciences Center, Vilnius University, Saulėtekio av. 7, Vilnius, Lithuania
[3]Laboratory of Biodeterioration Research, Nature Research Centre, Akademijos 2, Vilnius, Lithuania
evelina.lukaite@ftmc.lt

Biofilms are implicated in approximately 80% of all chronic infections. Their prevalence in conditions such as chronic wounds, catheter-associated infections and pneumonia underscores the necessity for effective detection methods to manage these infections properly [1]-[2]. Electrochemical techniques can provide quick results, often within minutes to hours, compared to the days required by traditional culture methods [3]. Identifying biofilm presence can inform treatment decisions and improve patient outcomes [4]. This work seeks to determine the electrogenic characteristics of bacterial biofilms from Gram-positive species *S. haemolyticus, E. faecalis* and Gram-negative species *P.aeruginosa, S. maltophilia*.

To monitor biofilm growth, we used open circuit potential (OCP), chronoamperometry and optical density (OD) measurements. A carbon cloth (CC) and Ag/AgCl 3M KCl were used as working and reference electrodes, respectively, as presented in the schematic illustration (Fig. 1). Depending on the bacteria, the OCP shifted from 100-50 mV to −200 - −300 mV in a bacterial solution, indicating that bioelectrochemical coupling had occurred. We observed the negative potential shifts by mediated electron transfer (MET), which connects bacterial metabolism to the electrode surface. Amperometry further confirmed the bacteria's ability to transfer electrons through MET and direct electron transfer (DET) mechanisms. In agreement with OCP and OD results, the current-time dependence highlights the extracellular electron transfer (EET) mechanism across different stages of biofilm development and bacterial growth, including the lag, log and stationary phases.

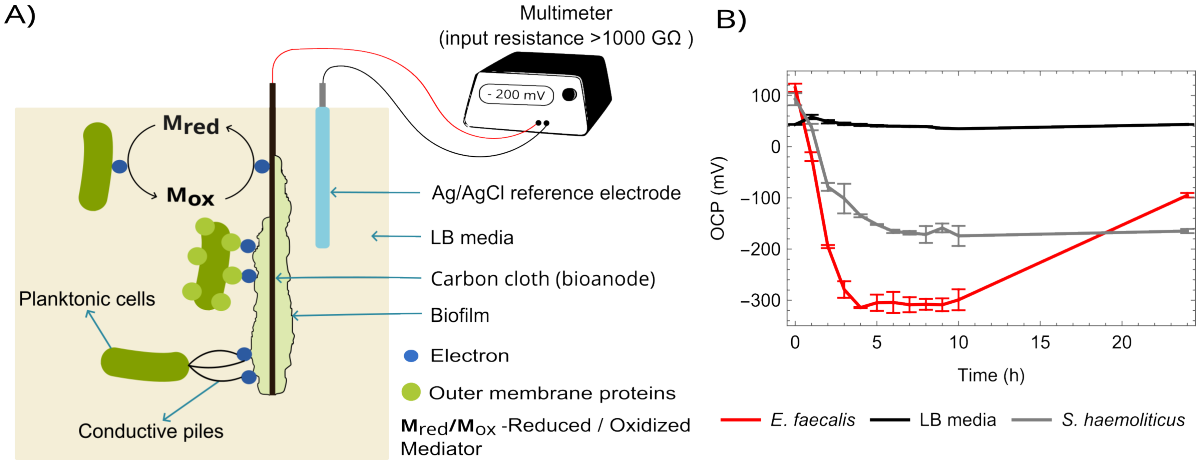


Fig. 1. A) Open circuit potential measurement scheme B) Example of OCP changes with bacteria's

This study shows that *E. faecalis* had the most negative OCP (-303 mV) and the highest current density (435 nA/cm^2), whereas *S. haemolyticus* demonstrated the lowest electroactivity with an OCP of -165 mV and a current density of 120 nA/cm^2. Gram-negative bacteria exhibited stable OCP and steady currents, reflecting consistent bioelectrochemical activity. These results highlight the potential of electrochemical methods for rapid detection and analysis of biofilm-related infections.

[1] N. Aoyama et al., 'AC Electromagnetic Field Controls the Biofilms on the Glass Surface by Escherichia coli & Staphylococcus epidermidis Inhibition Effect', Materials, vol. 16, no. 21, p. 7051, Nov. 2023, doi: 10.3390/ma16217051.
[2] M. Jamal, U. Tasneem, T. Hussain, and S. Andleeb, 'Bacterial Biofilm: Its Composition, Formation and Role in Human Infections', Res. Rev. J. Microbiol. Biotechnol., vol. 4, pp. 1–14, Jul. 2015.
[3] P. Thirabowonkitphithan et al., 'Electrogenicity of microbial biofilms of medically relevant microorganisms: potentiometric, amperometric and wireless detection', Biosens. Bioelectron., vol. 246, p. 115892, Feb. 2024, doi: 10.1016/j.bios.2023.115892.
[4] A. Schulze, F. Mitterer, J. P. Pombo, and S. Schild, 'Biofilms by bacterial human pathogens: Clinical relevance - development, composition and regulation - therapeutical strategies', Microb. Cell, vol. 8, no. 2, pp. 28–56, Feb. 2021, doi: 10.15698/mic2021.02.741.

ANALYSIS OF PROTEINS POTENTIALLY INVOLVED IN β-LACTAM RESISTANCE IN OPPORTUNISTIC PATHOGEN STENOTROPHOMONAS MALTOPHILIA

Edvard Romanovski[1], Laurita Klimkaitė[1], Ignas Ragaišis[1], Julija Armalytė[1]

[1]Institute of Biosciences, Department of Biochemistry and Molecular Biology, Life Sciences Center, Vilnius University
edvard.romanovski@gmc.stud.vu.lt

The rise of bacterial resistance to antibiotics is a growing global health crisis. World Health Organization estimated that by 2050 antibiotic resistance could lead to as many as 10 million deaths annually due to infections that are no longer treatable [1]. Multidrug resistant pathogens, such as *Stenotrophomonas maltophilia*, present a particular challenge due to their resistance to multiple antibiotics. Gram-negative opportunistic pathogen *S. maltophilia* has been rapidly acquiring resistance, making infections progressively more difficult to treat, while the mechanisms underlying its antibiotic resistance remain understudied. *S. maltophilia* is known to exhibit resistance to various antibiotics, including β-lactams, which are among the most clinically significant antibiotics [2]. Although *S. maltophilia* resistance to β-lactam antibiotics is well-documented, only two β-lactamases, L1 (a metallo-β-lactamase) and L2 (a class A serine β-lactamase), have been researched and characterized as enzymes that confer resistance by degrading β-lactam antibiotics [3]. We previously identified that β-lactam resistant *S. maltophilia* SM3 isolate codes 10 additional proteins that are homologous to known β-lactamases, suggesting that these proteins may also contribute to the β-lactam resistance.

The aim of this study was to evaluate whether the 10 β-lactamase homologous proteins identified in *S. maltophilia* contribute to β-lactam resistance. To achieve this, a bioinformatic analysis using the Beta-Lactamase DataBase was performed to identify and compare the sequences of analysed proteins to verified β-lactamases from various bacterial species [4]. Then the genes encoding these homologous proteins were cloned into expression plasmids for functional analysis. The enzymatic activity was assessed in an *Escherichia coli* expression strain using the nitrocefin assay, a standard method for detecting β-lactamase activity. Additionally, the role of these proteins in antibiotic resistance will be assessed by performing a minimum inhibitory concentration analysis.

The bioinformatic analysis revealed that all the proteins examined shared homology with known β-lactamases, with sequence identities ranging from 24.8% to 29.5%. This level of homology is considered sufficient to support further investigation into their potential as functional β-lactamases [5]. The nitrocefin assay, validated with the well-characterized L1 β-lactamase, was successfully applied to three of the homologous proteins. The remaining putative β-lactamases will be evaluated using the same approach with the nitrocefin assay, and additional evaluation methods will be employed to further explore their contribution to β-lactam resistance.

[1] M. Talaat et al., “Increasing Antimicrobial Resistance in World Health Organization Eastern Mediterranean Region, 2017-2019,” Emerg Infect Dis, vol. 28, no. 4, pp. 717–724, Apr. 2022, doi: 10.3201/eid2804.211975.

[2] M. S. Said, E. Tirthani, and E. Lesho, “Stenotrophomonas Maltophilia,” in StatPearls, Treasure Island (FL): StatPearls Publishing, 2025. Accessed: Feb. 16, 2025. [Online]. Available: http://www.ncbi.nlm.nih.gov/books/NBK572123/

[3] P. S. Mercuri et al., “Clonal diversity and metallo-beta-lactamase production in clinical isolates of Stenotrophomonas maltophilia,” Microb Drug Resist, vol. 8, no. 3, pp. 193–200, 2002, doi: 10.1089/107662902760326904.

[4] T. Naas et al., “Beta-lactamase database (BLDB) - structure and function,” J Enzyme Inhib Med Chem, vol. 32, no. 1, pp. 917–919, Dec. 2017, doi: 10.1080/14756366.2017.1344235.

[5] W. R. Pearson, “An Introduction to Sequence Similarity (‘Homology’) Searching,” Curr Protoc Bioinformatics, vol. 0 3, p. 10.1002/0471250953.bi0301s42, Jun. 2013, doi: 10.1002/0471250953.bi0301s42.

ENHANCING AI-DRIVEN BIOMOLECULAR STRUCTURE PREDICTION WITH VOROMQA-AA: A NEW APPROACH TO ACCURACY ESTIMATION

Rita Banciul[1], Kliment Olechnovič[1,2], Justas Dapkūnas[1]

[1]Institute of Biotechnology, Life Sciences Center, Vilnius University
[2]CNRS Laboratoire Jean Kuntzmann, Grenoble
rita.banciul@gmc.vu.lt

All cellular processes from energy production to cell division and signal transduction are based on interactions between proteins, nucleic acids, and other molecules. The structures of the resulting biomolecular complexes directly affect how they function. Therefore, knowing the three-dimensional arrangement is crucial for understanding fundamental biological processes, as well as designing biomolecules for therapeutic and industrial applications.

Recent advances in deep learning-based modeling have significantly improved the accuracy and accessibility of protein structure prediction. However, predictions for nucleic acids, ligands, and their complexes with proteins remain less reliable, having lower accuracy and less certain confidence metrics. While methods like AlphaFold and RoseTTAFold represent major progress, they function as black-box models, offering little transparency into their decision-making [1]. This lack of interpretability makes it difficult to assess reliability, identify errors, and fully trust their predictions, posing challenges for applications requiring high structural accuracy. Furthermore, multiple biomolecular modeling methods are available, each generating several structure models of varying accuracy, thus selecting the most reliable prediction becomes a major challenge.

To address both issues, structure quality assessment tools are essential. Previously, we developed VoroMQA [2], a quality assessment method for protein structures. However, with the release of methods capable of predicting biomolecular complexes including proteins, nucleic acids, ligands, and ions [3], there is an increasing need for accuracy estimation methods of broader scope.

Here, we present the development of VoroMQA-aa (VoroMQA all-atom), an advanced quality assessment tool capable of evaluating a broad range of macromolecular structures, including proteins, nucleic acids, and their complexes with ligands and ions. VoroMQA-aa is a knowledge-based statistical potential that utilizes contact areas derived from Voronoi tessellation to assess structure quality. To train this potential, we utilized a large dataset of experimentally determined structures. Due to the limited availability of structures containing nucleic acids, ligands, and ions, we adopted a novel training approach. Instead of relying on a clustered subset of reference structures, we incorporated all available structures, using clustering data to account for similarity of sequences and interaction interfaces. This strategy enhances the robustness and generalizability of VoroMQA-aa across diverse biomolecular systems.

VoroMQA-aa bridges the gap between AI-driven structure prediction and reliable model selection as well as interpretation, providing deeper insights into biomolecular interactions and functions.

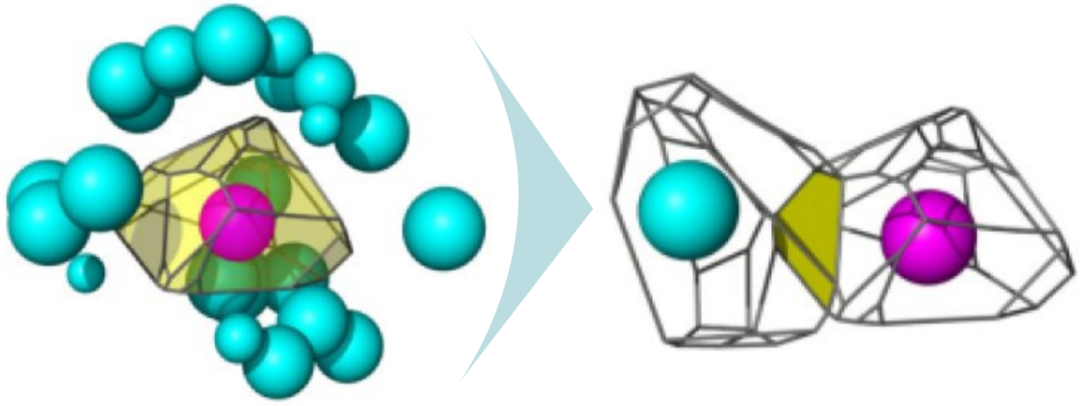


Fig. 1. Constructing contact area of two atoms by Voronoi tessellation.

[1] von Eschenbach, W.J. (2021). Transparency and the Black Box Problem: Why We Do Not Trust AI. Philos. Technol. 34, 1607–1622.
[2] Olechnovič, K., Venclovas, Č. (2017). VoroMQA: Assessment of protein structure quality using interatomic contact areas. Proteins, 85(6), 1131–1145.
[3] Abramson, J., et al. (2024). Accurate structure prediction of biomolecular interactions with AlphaFold 3. Nature, 630, 493–500.

ADAPTATION OF CROFT-SEQ FOR OFF-TARGET DETECTION OF VARIOUS GENOME EDITING TOOLS

Paulius Toliušis[1], Gunda Petraitytė[2], Algirdas Grybauskas[1], Mindaugas Zaremba[1]

[1]Institute of Biotechnology, Life Sciences Center, Vilnius University, Lithuania
[2]Institute of Biomedical Sciences, Faculty of Medicine, Vilnius University, Lithuania
paulius.toliusis@bti.vu.lt

Programmable genome editing nucleases, such as CRISPR-Cas9, have attracted significant scientific interest due to their immense potential for gene editing and the treatment of human genetic diseases. The successful development of these tools is crucial for both fundamental and clinical applications to ensure that genome editing tools are reliable and safe. Because of their ability to easily target specific DNA sites, these nucleases enable precise and rapid genome editing. Although these nucleases are designed to cut their intended target site (on-target), they often tend to also cut DNA sequences similar to the target site (off-targets). This can lead to harmful gene mutations or chromosomal rearrangements, potentially causing cancerous transformations or even cell death. To address these issues, a variety of methods have been developed to detect off-target sites of Cas9 nucleases both in vitro and in vivo [1]. However, the vast majority of these methods are specifically designed to detect double-strand DNA breaks caused by genome editing nucleases like CRISPR-Cas9, which leave “blunt” DNA ends after cutting. Only a few methods have been developed and adapted for other genome editing tools (non-Cas9), such as Cas12 or base editors, for detecting off-targets in vitro [2, 3]. However, these methods are often expensive, complex and have relatively low sensitivity. Therefore, the ability to detect off-target sequences of various genome editing tools would enable the improvement and selection of more suitable and safer tools for genome editing.

Recently, we have developed a sensitive, simple, fast, and cost-effective CRISPR-Cas9 off-target detection method called CROFT-Seq [4], which, in many aspects, rivals or even outperforms other well-known in vitro off-target detection methods, such as SITE-Seq [5] and CIRCLE-Seq [6]. In this research, we will aim to employ and modify existing CROFT-Seq method by incorporating additional enzymes and experimental stages for detecting off-target sites of various genome editing tools, such as Cas12 and base editors. Additionally, we will modify the bioinformatics algorithm of the CROFT-Seq off-target site analysis to make it suitable for identifying off-target sequences of different genome editing tools. Furthermore, we will perform genome editing of HEK293T cells in vivo and validate wether potential off-target sites identified in vitro are also cleaved during genome editing in living cells. Comparing in vitro off-target sequences with those validated in vivo will allow us to draw significant conclusions regarding the accuracy and sensitivity of the developed methods. With the advancement of the robotics industry, there is a growing demand for adapting off-target detection methods to robotic systems. Therefore, as part of this project, we will also aim to adapt the modified CROFT-Seq methods for use with the Opentrons OT-2 robotic system.

[1] Guo, C.; Ma, X.; Gao, F.; Guo, Y. Off-Target Effects in CRISPR/Cas9 Gene Editing. Front Bioeng Biotechnol 2023, 11, 1143157. https://doi.org/10.3389/fbioe.2023.1143157.

[2] Liang, P.; Xie, X.; Zhi, S.; Sun, H.; Zhang, X.; Chen, Y.; Chen, Y.; Xiong, Y.; Ma, W.; Liu, D.; Huang, J.; Songyang, Z. Genome-Wide Profiling of Adenine Base Editor Specificity by EndoV-Seq. Nat Commun 2019, 10 (1), 67. https://doi.org/10.1038/s41467-018-07988-z.

[3] Kim, D.; Lim, K.; Kim, S.-T.; Yoon, S.; Kim, K.; Ryu, S.-M.; Kim, J.-S. Genome-Wide Target Specificities of CRISPR RNA-Guided Programmable Deaminases. Nat Biotechnol 2017, 35 (5), 475–480. https://doi.org/10.1038/nbt.3852.

[4] Zaremba, M.; Toliusis, P.; Karvelis, T.; Sasnauskas, G.; Sinkunas, T.; Grybauskas, A.; Silanskas, A.; Zagorskaitė, E. CRISPR Nuclease Off-Target Detection by Sequencing (CROFT-Seq). US Patent App: 18/326,486; EP Patent App: EP23176409.3; JP Patent App: 2023-090453.

[5] Cameron, P.; Fuller, C. K.; Donohoue, P. D.; Jones, B. N.; Thompson, M. S.; Carter, M. M.; Gradia, S.; Vidal, B.; Garner, E.; Slorach, E. M.; Lau, E.; Banh, L. M.; Lied, A. M.; Edwards, L. S.; Settle, A. H.; Capurso, D.; Llaca, V.; Deschamps, S.; Cigan, M.; Young, J. K.; May, A. P. Mapping the Genomic Landscape of CRISPR–Cas9 Cleavage. Nat Methods 2017, 14 (6), 600–606. https://doi.org/10.1038/nmeth.4284.

[6] Tsai, S. Q.; Nguyen, N. T.; Malagon-Lopez, J.; Topkar, V. V.; Aryee, M. J.; Joung, J. K. CIRCLE-Seq: A Highly Sensitive in Vitro Screen for Genome-Wide CRISPR-Cas9 Nuclease off-Targets. Nat Methods 2017, 14 (6), 607–614. https://doi.org/10.1038/nmeth.4278.

ORAL SESSION 12

Chemistry and Chemical Physics

Chair: Dr. T. Matijošius

FESTIVE FLARES: HOW BONFIRES AND FIREWORKS SHAPE URBAN AEROSOL OPTICAL PROPERTIES

Agnė Minderytė[1], Steigvilė Byčenkienė[1]

[1]Center for Physical Sciences and Technology, Department of Environmental Research
agne.minderyte@ftmc.lt

Aerosol particles interact with light primarily through scattering or absorption, processes influenced by their chemical composition which depends on the source. Sulfate and nitrate, for example, are well-known contributors to light scattering. Even though there are numerous studies on aerosol particles originating from fireworks or biomass burning, a consensus on the strength of the radiative effect of the carbonaceous aerosols has not been reached. This case study examines how two major events - a nationwide bonfire-burning celebration during Midsummer and fireworks on New Year's Eve – impact aerosol black carbon (BC) mass concentration and optical properties at an urban background site in Vilnius. Aerosol light-absorption (at waveleghts 370, 470, 520, 590, 660, 880, 950 nm) and equivalent BC mass concentration (eBC) (at 880 nm) were measured using an Aethalometer (AE33, Magee Scientific), aerosol scattering properties (at waveleghts 450, 550, 700 nm) were measured using a Nephelometer (TSI model 3563). The analysis focused on changes in aerosol BC source contributions, absorption and scattering Ångström exponents (AAE and SAE), and single scattering albedo (SSA) during two specific periods: 15th December (2021) to 28th February (2022) and 1st June to 18th August (2022).

On the night of 23rd June, during the Midsummer celebration, a 3-fold increase in the total BC mass concentration was observed. The extensive bonfire burning resulted in a 7-fold increase in BC_{BB} (BC from biomass burning) compared to the season average. This high BC_{BB} contribution enhanced aerosol light absorption, reducing the SSA by 12%, which indicates an increased warming effect on the atmosphere. During New Year's Eve, the BC mass concentration doubled compared to the cold season average. Due to increase in light-absorbing aerosol concentration, the SSA decreased by 17%. This multi-parameter investigation highlights two short-term, high-pollution events, providing a deeper understanding of biomass-burning-related aerosols and their impact on atmospheric radiative transfer.

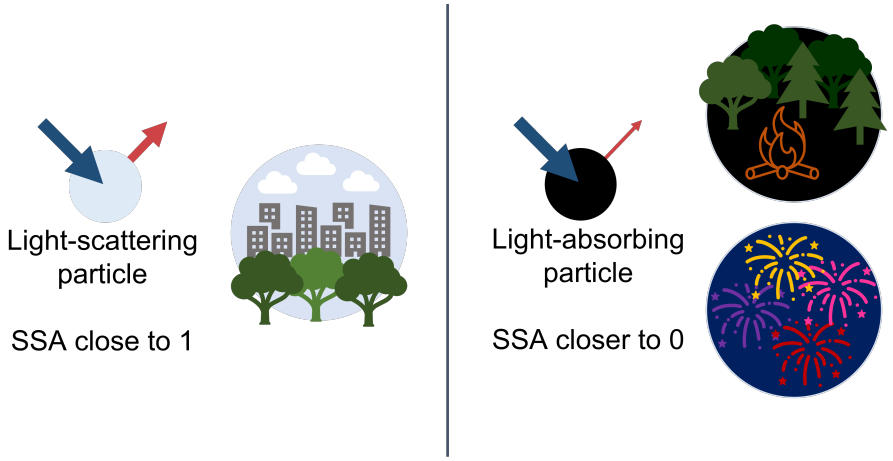


Fig. 1. Schematic visualising of characteristic single scattering albedo (SSA) values during normal ambient conditions and during special events with bonfires or fireworks. (Created by the author)

WHERE MICROPLASTICS MEET PEDESTRIANS: EVALUATING GREEN INFRASTRUCTURES ROLE IN REDUCING TRANSPORT-RELATED POLLUTION

Abdullah Khan[1], Valda Araminienėb[2], Ieva Uogintė[1], Iveta Varnagirytė-Kabašinskienė[2], Valentinas Černiauskas[2], Valda Gudynaitė-Franckevičienėb[2], Algis Džiugysc[3], Edgaras Misiulisc[3], Steigvilė Byčenkienė[1]

[1]SRI Center for Physical Sciences and Technology (FTMC), Saulėtekio Ave. 3, Vilnius, Lithuania
[2]Lithuanian Research Centre for Agriculture and Forestry (LAMMC), Instituto av. 1, Akademija, Kėdainiai distr., Lithuania
[3]Lithuanian Energy Institute (LEI), Breslaujos str. 3, Kaunas, Lithuania
abdullahkkhan44@gmail.com

As cities grapple with the invisible threat of airborne microplastics (MPs), non-exhaust emissions, especially tire wear particles (TWPs)—are becoming significant contributors to urban air pollution. While vehicular emissions regulations have successfully reduced exhaust pollutants, non-exhaust emissions remain a significant challenge. Urban Green infrastructure (UGI), often valued for its aesthetic and ecological functions, has yet to be fully explored for its potential to reduce MP exposure. This study investigates the role of a Thuja occidentalis hedge in Kaunas, Lithuania, as a natural barrier against traffic-induced MPs. Over a year-long sampling campaign (June 2023–April 2024), passive deposition was conducted at four distances from the hedge (-1 m, 0 m, +1 m, +2 m), with additional sampling in the hedge's absence to establish an experimental-control comparison. Optical microscope analysis revealed distinct size and shape distributions, while micro-FTIR spectroscopy confirmed the dominant presence of PE and PP in the collected MPs. MP concentrations peaked in spring (5.95 particles/cm^2/day) at the roadside (-1m). Most MPs were fragments (91.38%), with polyethylene (PE) as the dominant polymer (43.04%), followed by polypropylene (PP) (15.11%). The hedge demonstrated remarkable efficiency in capturing MPs, particularly in summer, with removal rates of 64.5% for total MPs, 64.3% for fragments, and 71.4% for fibers. The hedge effectively trapped larger MPs (>50 µm). This study highlights the untapped potential of UGI as an active defender against transport-related MP pollution in the urban environment, advocating for its strategic incorporation into urban design to enhance public health protection.

ECO-FRIENDLY PRODUCTION OF BIPHASIC CALCIUM PHOSPHATE GRANULES: GYPSUM CONVERSION UNDER VARRIED SYNTHESIS CONDITIONS

Greta Linkaite[1], Skirmantas Astramskas[1], Ruta Raiseliene[1], dr. Inga Grigoraviciute[1], dr. Aivaras Kareiva[1]

[1] Faculty of Chemistry and Geosciences, Vilnius University
greta.linkaite@chgf.stud.vu.lt

In recent decades, increasing life expectancy and an ageing population have posed new challenges to a number of medical issues, including bone degeneration and related pathologies, prompting the search for innovative hard tissue reconstruction methods. Hard tissues of human body mainly consist of calcium phosphate (CP) nanocrystals, dominated by two major phases- nonstoichiometric hydroxyapatite and magnesium whitlockite (Mg-WH), embedded within a collagen matrix [1-2]. While monophasic CP can be and are used as bone implants, recent research shows that multiphase CP composites exhibit a better biological response than traditional single-phase CP materials [3]. CP composites preserve the biocompatibility, osteoconductivity and osteoinductivity of the constituent CP phases, and also allow for the adjustment of key characteristics of the implant, such as biodegradability and mechanical durability, to meet specific clinical requirements by adjusting the ratio between different phases.

This study focuses on the development of biphasic calcium phosphate (BCP) granules composed of magnesium whitlockite and carbonate hydroxyapatite, designed to closely mimic the natural composition of bone and enhance biocompatibility for implant applications. The granules were synthesized from an environmentally friendly gypsum precursor at low temperatures through dissolution-precipitation reactions under static and rotational conditions. By varying synthesis dynamics, the study examines its impact on the phase composition, structure, and morphology of the final product. Various analytical techniques, including XRD, FTIR, and ICP-OES, were used to examine material composition, while SEM and BET analysis assessed surface properties. Synthesized BCP pellets with different CHA and Mg-WH ratios exhibited variations in structure, composition, and surface characteristics based on synthesis conditions. XRD, FTIR, and ICP-OES revealed that higher Mg^{2+} concentrations used in the synthesis process influenced phase composition, while BET analysis showed that increasing Mg-WH content reduced surface area and porosity.

[1] N.Reznikov, Fractal-Like Hierarchical Organization of Bone Begins at Nanoscale (Science, 2018)
[2] H.Cheng, Synergistic Interplay Between the Two Major Bone Minerals Hydroxyapatite and Whitlockite Nanoparticles for Osteogenic Differentiation of Mesenchymal Stem Cells (Acta Biomater,2018)
[3] J.M.Bouler, Biphasic Calcium Phosphate Ceramics for Bone Reconstruction (Acta Biomater, 2017)

TRANSILATIONAL APPROACH OF MOLECULAR IMPRINTED POLYMERS INTEGRATION WITH ESSENTIAL OILS

Greta Kasputė[1,2], Urtė Prentice[1,2,3]

[1]State Research Institute Centre for Innovative Medicine, Santariskiu St. 5, LT-08410, Vilnius, Lithuania.
[2]Department of Nanotechnology, State Research Institute Center for Physical Sciences and Technology (FTMC), Sauletekio Av. 3, LT-10257 Vilnius, Lithuania.
[3]Department of Physical Chemistry, Institute of Chemistry, Faculty of Chemistry and Geosciences, Vilnius University, Naugarduko St. 24, LT-03225 Vilnius, Lithuania.
greta.kaspute@ftmc.lt

Molecularly imprinted polymer (MIP) technologies hold great promise not only as sensors for detecting specific molecules but also for the controlled release of drugs and active compounds in precise concentrations. This dual functionality is important in advancing targeted and efficient drug delivery systems. Research into MIPs and their adsorption/desorption mechanisms is therefore critical. In this context, geraniol - a component of essential oils (EOs) - is incorporated into studies to evaluate adsorption kinetics and explore its therapeutic potential. Geraniol is rich of biological effects such as anti-inflammatory, antioxidant or antitumor. However, there is lack of information about this molecule effectiveness, delivery and safety. Essential oils (EOs) are naturally derived mixtures with some therapeutic applications. However, traditional delivery of therapeutics systems still struggles with issues such as instability, low bioavailability, uncontrolled release of active compounds, and rapid degradation. Integrating EOs into MIP-based delivery systems addresses these challenges by enhancing stability, enabling controlled release, and providing targeted delivery. Molecular imprinting techniques, including covalent, non-covalent, and semi-covalent imprinting, allow for the creation of highly selective binding cavities, significantly improving the efficacy and therapeutic benefits of EOs.[1] Innovative treatment strategies are especially critical for rare diseases such as Duchenne muscular dystrophy (DMD), where personalised and adjusted treatment is important with specifics of therapeutics used. Current therapies, like corticosteroids, are often accompanied by severe side effects, underscoring the need for safer, more effective alternatives. Nutraceuticals, including herbal extracts and EOs, present a promising avenue for novel drug delivery systems. Combining EOs with MIP technology offers the potential for improved drug formulations, enhancing precision, safety, and therapeutic efficacy.[2] By leveraging controlled release and targeted action, EO-based active component delivery systems may provide better muscle function and mental health outcomes in DMD patients. While preliminary research indicates promise, further studies are essential to validate the potential of EO-based MIP systems in addressing therapeutic needs for DMD and other conditions.

[1] G. Kaspute, A. Ramanavicius, U. Prentice, Molecular Imprinting Technology for Advanced Delivery of Essential Oils. Polymers 2024, 16, 2441. https://doi.org/10.3390/polym16172441
[2] G. Kaspute, B.D. Arunagiri, R. Alexander, A. Ramanavicius, U. Samukaite-Bubniene, Development of Essential Oil Delivery Systems by 'Click Chemistry' Methods: Possible Ways to Manage Duchenne Muscular Dystrophy. Materials 2023, 16, 6537. https://doi.org/10.3390/ma16196537

DETERMINATION OF THE DEGREE OF POLYMERIZATION OF STARCH MODIFIED WITH CITRIC AND LACTIC ACIDS

Daria Kuchynska[1], Olena Ishchenko[1], Roman Kachan[1]

[1]Kyiv National University of Technologies and Design
dkuchinska@gmail.com

Starch modification is a significant research area in food technology and materials science. Acid treatment is a promising method that alters starch structure and properties, though its mechanisms require further study [1]. This study aimed to determine the effects of citric and lactic acid concentrations and treatment duration on the degree of polymerization (DP) of potato starch. Samples were treated with citric (1 mol/L, 0.5 mol/L) and lactic acid (1 mol/L, 0.5 mol/L) solutions for 1.5, 2.0, 2.5 hours at 60 °C. After 24-hour settling, titration with 0.1 N NaOH was performed. DP was assessed viscometrically after dissolution in cadexomer, and predictive equations based on time (τ) and concentration (C) were developed: Citric acid: DP = 149.86 - 20.07·τ - 37·C; Lactic acid: DP = 209.33 - 23·τ - 76.67·C

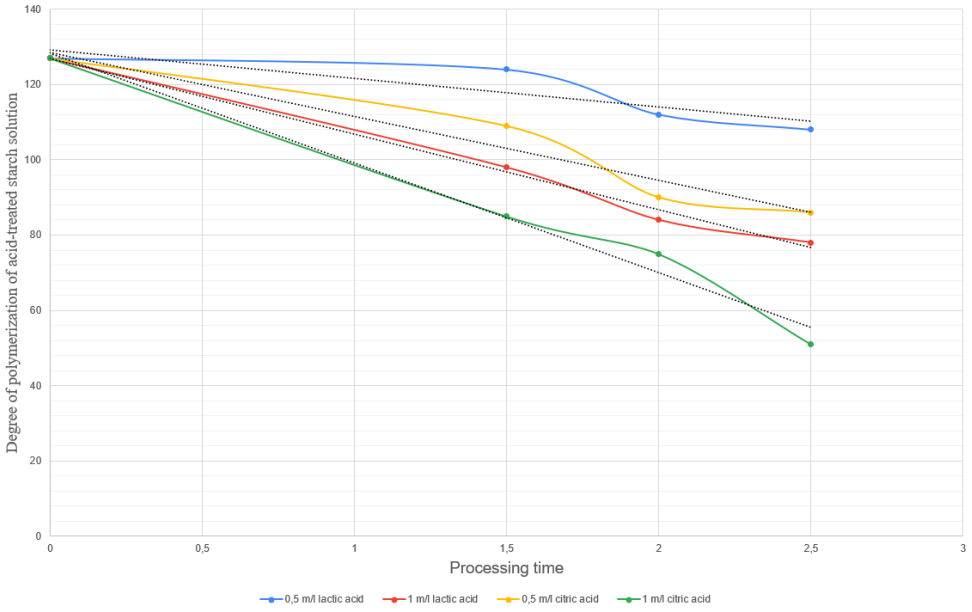


Fig. 1. Fig 1.The graph of the dependence of the degree of polymerization on time and treatment concentration

Results showed that DP decreased from 127 to 51 with citric acid and from 127 to 78 with lactic acid. The interaction of carboxyl groups with the polysaccharide matrix influenced polymerization: citric acid (three carboxyl groups) formed ester bonds, promoting a network structure, while lactic acid (one carboxyl group) facilitated hydrolysis, shortening polymer chains [2]. Carboxyl groups initially present in the solution integrate into the starch structure, participating in branching and hydrolysis. As a result, fewer free polymer fragments remain in the solution, leading to a lower degree of polymerization. Analysis of the treatment solutions confirmed a decrease in carboxyl group concentration, indicating their incorporation into the starch structure. DP strongly depended on acid type, concentration, and treatment duration. Citric acid enhanced structural stability, whereas lactic acid led to greater chain cleavage. These findings enable precise control over starch properties for specific applications [3].

[1] Gerezgiher, A & Szabó, T. (2022). Crosslinking of Starch Using Citric Acid. Journal of Physics: Conference Series. 2315. 012036. 10.1088/1742-6596/2315/1/012036.
[2] Ishchenko, O., Kuchynska, D., Plavan, V. & Ostrauskaitė, J. Wound Dressings Films Based on the Citric Acid Modified Starch. The 10th International Conference on Advanced Materials and Systems (ICAMS 2024), 2024, Sciendo, pp. 101-106.
[3] Mohd Adnan, Ahmad Faris, Nishida Haruo, Shirai Yoshihito. (2008). Evaluation of kinetics parameters for poly(L-lactic acid) hydrolysis under high-pressure steam. Polymer Degradation and Stability. 93. 1053-1058. 10.1016/j.polymdegradstab.2008.03.022.

REGENERATION OF TETHERED BILAYER LIPID MEMBRANES FOR REUSABLE BIOSENSORS

Anastasija Aleksandrovič[1], Inga Gabriūnaitė[2], Aušra Valiūnienė[1], Gintaras Valinčius[3]

[1]Center for Physical Sciences and Technology
[2]Vilnius University
[3]Unaffiliated scientist
anastasija.aleksandrovic@ftmc.lt

Tethered phospholipid membranes (tBLMs) on conductive surfaces modified with self-assembled monolayers (SAMs) are increasingly studied for biosensor development. While gold is commonly used for these biosensors, its poor membrane regeneration and high cost make it less desirable. Metal oxides as substrates for tBLM formation offer a potential alternative due to their lower cost and the possibility of membrane regeneration.

This study investigates tBLMs of varying compositions formed on fluorine-doped tin oxide (FTO) surfaces modified with different silane compounds. The focus is on the interaction between the membranes and proteins, and the conditions necessary for membrane regeneration after protein incorporation. Since phospholipids are soluble in many alcohols while proteins are not, the primary objective was to determine the optimal conditions for removing both the phospholipid membrane and the protein from the surface. Ideally, after removing the protein-affected bilayer, the SAM-modified FTO surface would remain intact, allowing for repeated membrane formation. This work explores how regeneration efficiency is affected by the conditions used for the removal of tBLM with incorporated proteins.

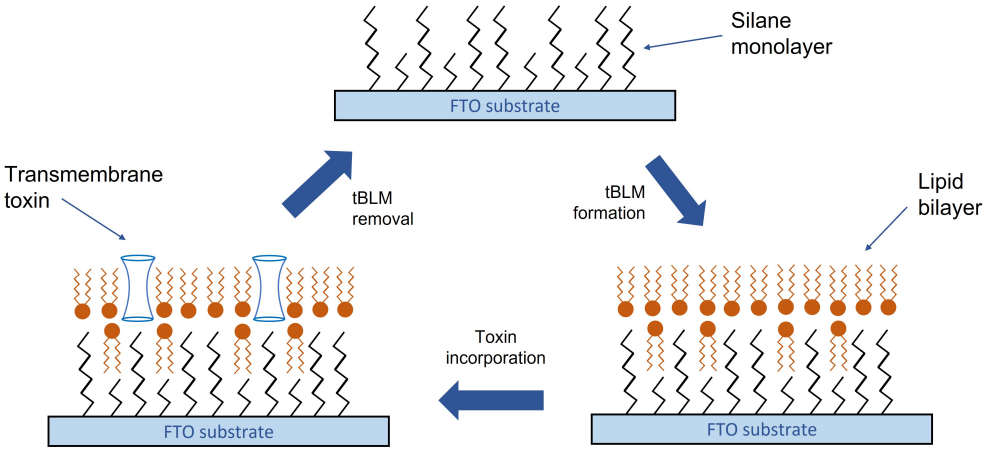


Fig. 1. Scheme of tBLM regeneration process

ORAL SESSION 13

Material Science and Nanotechnology

Chair: Dr. D. Lengvinaitė

EMISSION PROPERTIES OF BISMUTH QUANTUM DOTS IN ANNEALED GaAsBi/AlAs QUANTUM WELLS

Justas Žuvelis[1], E. Dudutienė[1], S. Stanionytė[2], M. Skapas[2], B. Čechavičius[1], R. Butkutė[1]

[1]Center for Physical Sciences and Technology, Department of Optoelectronics, Saulėtekio av. 3, Vilnius, Lithuania
[2]Center for Physical Sciences and Technology, Department of Characterization of Materials Structure, Saulėtekio av. 3, Vilnius, Lithuania
justas.zuvelis@ftmc.lt

Semiconductor quantum dots (QDs) have attracted considerable research interest in recent years due to their distinct properties. These nanostructures have shown a number of advantages over bulk and quantum well structures, which are commonly used as gain media in photonic applications [1]. Given the growing interest, bismuth (Bi) QDs have emerged as a promising candidate for optoelectronic devices operating in the near-infrared (NIR). The formation of Bi QDs was first described by Luna et al. [2], where GaAsBi was subjected to post-growth thermal annealing. While bulk Bi is semimetallic, theoretical estimates predicted that Bi nanoparticles become semiconducting at diameters below 16 nm [3]. Emission from Bi QDs in the wavelength range of 1300–1500 nm was reported in the same work, however, no further optical studies of Bi QDs have been conducted.

In this work, we present a comprehensive photoluminescence (PL) study of Bi QDs to understand how growth and annealing conditions impact their optical properties. Various GaAsBi/AlAs quantum well (QW) heterostructures with thicknesses of 4 and 10 nm were deposited by molecular beam epitaxy at substrate temperatures ranging from 165 to 330 °C. A rapid thermal annealing (RTA) oven was used for post-growth annealing at temperatures above 650 °C. It was demonstrated that after thermal treatment a broad band centered around 0.9 eV, related to emission from Bi QDs, emerged in the room temperature PL spectra. The bismuth nanocrystal peak for the 10 nm-thick GaAsBi/AlAs QW structures was redshifted when compared to that of the 4 nm, indicating that larger QDs form in wider QWs. Temperature-dependent measurements in the 3-300 K range revealed good thermal stability of the Bi QDs band gap (Fig. 1a). Moreover, excitation-dependent PL measurements at room temperature (Fig. 1b) suggested that Bi clusters exhibit strong carrier confinement effects, comparable to quantum dots grown by the Stranski-Krastanov method [4].

These findings imply that with further optimization of growth and annealing conditions, GaAsBi QWs containing bismuth QDs could be a promising material for devices operating in the NIR spectral range.

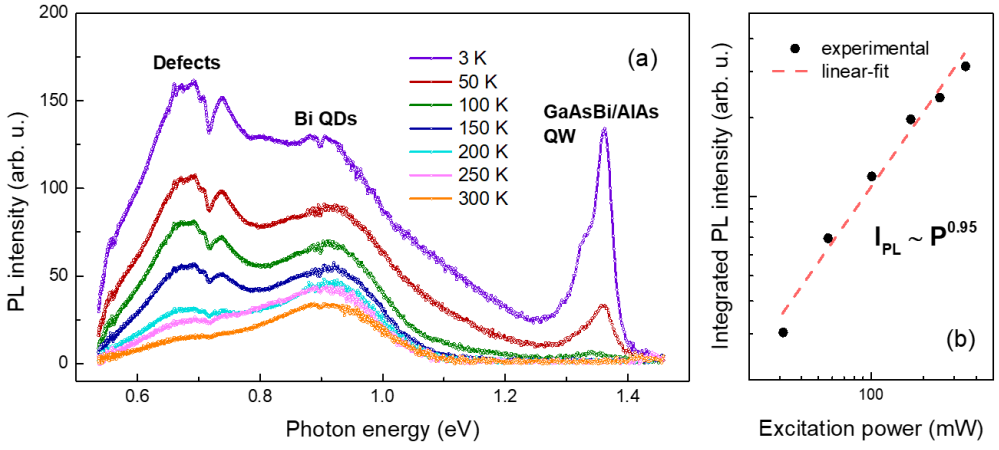


Fig. 1. (a) Temperature-dependent photoluminescence spectra of a 5×GaAsBi/AlAs QW structure with a QW thickness of 4 nm, annealed in the RTA oven at 750 °C for 3 min. (b) Integrated PL intensity of Bi QDs as a function of excitation power in a double logarithmic scale at room temperature, with a fit to the power law function.

Acknowledgements
This work has received funding from the Research Council of Lithuania (LMTLT), agreement No S-MIP-24-99.

[1] S. Chen et al., "Electrically pumped continuous-wave 1.3 μm InAs/GaAs quantum dot lasers monolithically grown on on-axis Si (001) substrates", Optics Express 25(5):4632, February 2017.
[2] E. Luna et al., "Formation and phase transformation of Bi-containing QD-like clusters in annealed GaAsBi", Nanotechnology 25(20):205605, April 2014.
[3] R. Butkutė et al., "Bismuth Quantum Dots in Annealed GaAsBi/AlAs Quantum Wells", Nanoscale Research Letters 12(1):436, December 2017.
[4] Xian(Ann) Hu et al., "Photoluminescence of InAs/GaAs quantum dots under direct two-photon excitation", Scientific Reports 10(1):10930, July 2020.

MXENES-BASED ELECTROCHEMICAL SENSOR FOR QUICK AND ACCURATE DETERMINATION OF CADMIUM ION CONCENTRATIONIN AQEOUS ENVIRONMENTS

Ilya Navitski[1], Šarūnas Žukauskas[1], Alma Ručinskienė[1], Ernestas Svirbutavičius[2], Simonas Ramanavičius[1], Arūnas Ramanavičius[2]

[1]State Research Institute Center for Physical Sciences and Technology (FTMC), Sauletekio Av. 3, LT-10257 Vilnius, Lithuania
[2]Institute of Chemistry, Faculty of Chemistry and Geosciences, Vilnius University (VU), Naugarduko g. 24, LT-03225 Lithuania
ilya.navitski@ftmc.lt

Environmental contamination by cadmium is widespread due to its industrial applications, including semiconductors, industrial batteries, and electroplating. Although efforts are underway to phase out cadmium, many of these applications still lack viable alternatives. In addition, insufficient or lax decontamination standards often lead to waste that pollutes water sources, creating a direct route for cadmium to enter the human body. Once inside, cadmium can damage vital biological systems and functions, highlighting the need for reliable detection methods. Electrochemical sensors are well suited to this task, offering high precision, ease of fabrication, and low production costs [1]. Among the potential materials for such sensors, MXenes, two-dimensional titanium carbide nanostructures, show great promise [2]. Here, we present an MXene-based sensor for the accurate detection of cadmium ions in various water samples.

The sensor was prepared by drop-casting a mixture of MXenes and Nafion onto a glassy carbon electrode (GCE). We evaluated its sensitivity, selectivity, and limit of detection (LOD) using differential pulse voltammetry. Measurements were carried out at different temperatures and across a range of pH values (3.5–5.5) in an acetic buffer solution to determine how these conditions affect sensor performance.

Results showed that sensor performance depends on both temperature and pH. More acidic conditions (pH 3.5–4.0) yielded higher sensitivity but a narrower operating range compared to less acidic environments. We selected pH 4.5 as an optimal balance between working range and sensitivity. At this pH, the sensor demonstrated an operating range of 1.03–27.53 µM, with an LOD of 0.82 µM and a sensitivity of 5.36 µA/(µM·cm^2). In the presence of other heavy metal ions, the sensor was notably selective for cadmium (Fig. 1A), detecting only lead in addition to cadmium. The lead signal was approximately twice that of cadmium, suggesting MXenes have a higher affinity for lead. Nonetheless, the sensor maintained excellent accuracy for cadmium detection in real-world water samples (Fig. 1B).

Overall, the GCE/MXene–Nafion sensor exhibited high sensitivity, selectivity, and stability (up to three weeks), and its operating range and sensitivity can be tuned by adjusting the pH. This makes the sensor a promising tool for monitoring cadmium pollution, particularly in industrial settings.

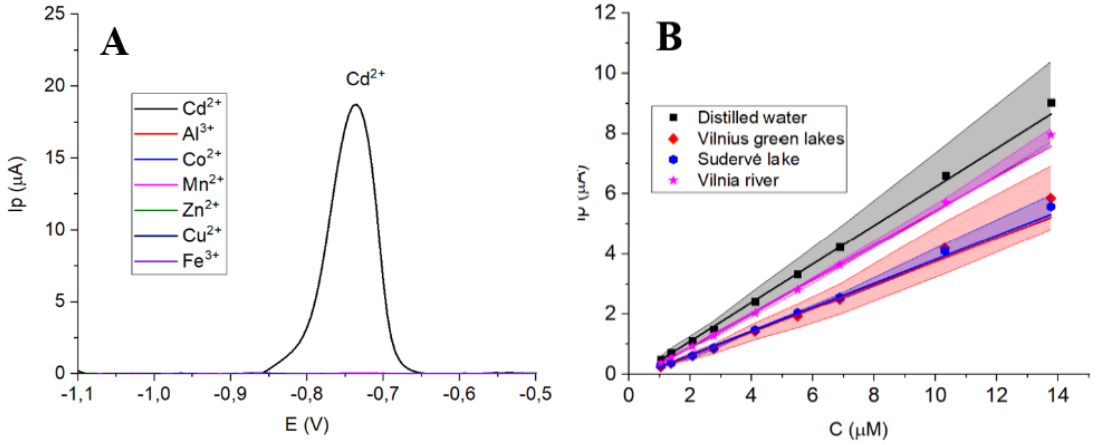


Fig. 1. Differential pulse voltammograms of sensor performance to different ions presence in the solution (A) and sensor's performance in different aquatic environments (B).

[1] S. Zukauskas et al., "Electrochemical real-time sensor for the detection of Pb(II) ions based on Ti3C2Tx MXene," The Science of The Total Environment, vol. 950, pp. 175190–175190, Jul. 2024, doi: https://doi.org/10.1016/j.scitotenv.2024.175190.
[2] Ilya Navitski, Agne Ramanaviciute, Simonas Ramanavicius, Maksym Pogorielov, and Arunas Ramanavicius, "MXene-Based Chemo-Sensors and Other Sensing Devices," Nanomaterials, vol. 14, no. 5, pp. 447–447, Feb. 2024, doi: https://doi.org/10.3390/nano14050447.

SYNTHESIS AND CHARACTERIZATION OF HIGHLY CONDUCTIVE NANOCRYSTALLIZED ε-LiVOPO$_4$ LIKE GLASSES

Krzysztof Gadomski[1], Viktoriia Vlasenko[1], Wojciech Grunwald[1], Sylwester J. Rzoska[2], Jerzy E. Garbarczyk[1], Tomasz K. Pietrzak[1]

[1]Faculty of Physics, Warsaw University of Technology, Poland
[2]Institute of High Pressure Physics of the Polish Academy of Sciences, Poland
krzysztof.gadomski2.dokt@pw.edu.pl

In recent decades, significant developments have been observed in mobile electronics as well as renewable energy sources. For each of these applications, it is required that electrochemical cells exhibit the best possible performance parameters. Unfortunately, one of the main factors limiting the potential of contemporary electrochemical batteries is the low electrical conductivity of the cathode material, which impacts both the value and retention of gravimetric capacity under high discharge currents.

Vanadate-phosphates are a broad group of materials that have been studied for years for use as a cathode in lithium-ion cells. One of the more promising materials investigated in recent years is the triclinic phase ε-LiVOPO$_4$. For example, M. S. Whittingham's group showed that a test cell based on a cathode of ε-LiVOPO$_4$ has a gravimetric capacity of about 200 mAh/g at a discharge current of C/10, and this capacity decreases to 100-150 mAh/g with a 20-fold increase in discharge current (to 2C current) [1]. Other experimental works [2] show that the capacity of such cells decreases by about 25% after 50 charge-discharge cycles. This indicates that the technology for producing this material is still imperfect. One method to improve the properties of such materials is the thermal nanocrystallization of glasses [3]. This method has previously been used to increase conductivity in materials such as LiFePO$_4$ [4] or 90 V_2O_5 ·10 P_2O_5 [5].

Therefore, in this work we aimed at obtaining a glassy analog of LiVOPO$_4$ using the melt-quenching method. Thermal analysis was used to investigate the thermal stability of the pristine glass and identify temperatures of glass transition and crystallization. The process of nanocrystallization was observed in-situ by high-temperature X-ray diffractometry in inert gas flow – confirming appearance of the desired LiVOPO$_4$ phase. The maximum temperature of thermal nanocrystallization was optimized to increase the electrical conductivity as much as possible, namely to at least 10^{-6} S/cm at room temperature.

Acknowledgements

This work was supported by the National Science Centre (NCN, Poland) through OPUS-23 grant no. 2022/45/B/ST5/04005.

[1] Yong Shi et al.: Electrochemical Performance of Nanosized Disordered LiVOPO4. American Chemical Society. 3 (2018) 7310-7323
[2] Zishan Ahsan et al.: Enhanced stability and electrochemical properties of lanthanum and cerium co-modified LiVOPO4 cathode materials for Li-ion batteries. Journal of Rare Earths 41 (2023) 1590-1596
[3] T.K. Pietrzak, M. Wasiucionek, J.E. Garbarczyk: Towards Higher Electric Conductivity and Wider Phase Stability Range via Nanostructured Glass-Ceramics Processing. Nanomaterials 11 (2021) 1321
[4] Krzysztof Gadomski et al.: Synthesis and electrical properties of glassy and nanocrystalline LiFePO4. Journal of Non-Crystalline Solids 625 (2024) 122771
[5] Tomasz K. Pietrzak et al.: Highly Conductive 90V2O5·10P2O5 Nanocrystalline Cathode Materials for Lithium-ion Batteries. Procedia Engineering 98 (2014) 28-35

MODEL OF NONLINEAR PORO-VISCOELASTIC FELT MATERIAL

Maria Miranda Vuin[1], Dmitri Kartofelev[1]

[1]Tallinn University of Technology, School of Science, Department of Cybernetics, Laboratory of Solid Mechanics, Tallinn, Estonia
maria.vuin@taltech.ee

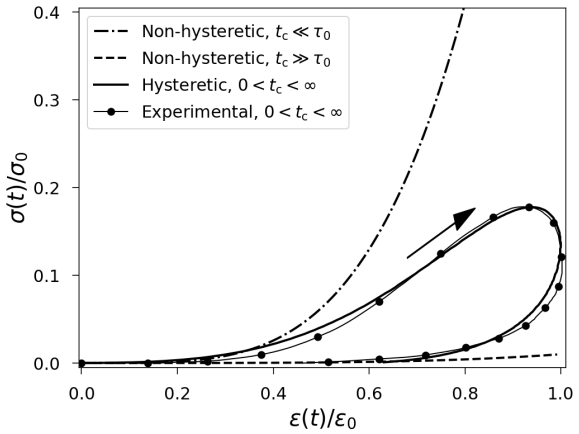


Fig. 1. Typical dynamic stress-strain curves and loops describing the felt material. The arrow indicates the direction of the material loading.

Felt is produced through a process called felting. In this process, fibers are intertwined through heat, moisture, and pressure, resulting in a randomly oriented structure. The structure allows felt to be used in several industries, such as automotive and aeronautical, because of its noise reduction, damping, and shock absorption properties. The governing equation describing wave propagation in felt is derived from the 1D equation of motion

$$\rho \frac{\partial^2 u}{\partial t^2} = \frac{\partial \sigma}{\partial x}, \tag{1}$$

where ρ is the density, $u(x,t)$ is the displacement, and σ is the stress. The experimentally confirmed constitutive relation is the following:

$$\sigma(\varepsilon) = E_\mathrm{d}\left[\varepsilon^p(t) - \frac{\gamma}{\tau_0}\int_0^t \varepsilon^p(\xi)\exp\left(\frac{\xi - t}{\tau_0}\right)\mathrm{d}\xi\right], \tag{2}$$

where E_d is the dynamic Young's modulus, $\varepsilon = \partial u/\partial x$ is the strain, $p \geq 1$, $p \in \mathbb{R}$ is the exponent introducing the nonlinearity, $0 \leq \gamma < 1$ is the hereditary amplitude, and τ_0 is the relaxation time [1, 2, 3, 4].

To understand the felt material, it is essential to understand the hysteresis loop dynamics in the force-compression tests. Examples of the measured and fitted stress-strain curves are shown in Fig. 1. It can be seen that in the general case for $0 < t_\mathrm{c} < \infty$, the loading and unloading branches do not follow the same path. The hysteresis loop means that felt is a material with memory. Analysis of (2) shows that under a rapid material loading-unloading cycle lasting for $t = t_\mathrm{c} \ll \tau_0$, and for a slow loading-unloading cycle $t = t_\mathrm{c} \gg \tau_0$ constitutive equation (2) takes the following forms, respectively:

$$\sigma(\varepsilon) = E_\mathrm{d}\varepsilon^p(t), \qquad \sigma(\varepsilon) = E_\mathrm{s}\varepsilon^p(t), \tag{3}$$

where $E_\mathrm{s} = E_\mathrm{d}(1-\gamma)$ is the static Young's modulus. The material loading and unloading curves for these limiting cases (3) follow the same path in both loading directions, as shown in Fig. 1.

A dispersion analysis conducted on model (1) reveals the existence of a band gap (BG) and a negative group velocity (NGV). Both properties are surprising for a material that is composed of randomly oriented elastic fibers. It can be shown that for realistic parameter values the BG and NGV influence only low-frequency wave components. For valid parameter values, there are no dispersive effects driven by NGV [4]. The presented model sheds light on the acoustics of fibrous and porous materials in general.

Acknowledgements
This work was supported by the Estonian Research Council (PRG1227).

[1] Yu. N. Rabotnov, Elements of Hereditary Solid Mechanics, MIR Publishers, Moscow, USSR, 1980.
[2] A. Stulov, "Experimental and computational studies of piano hammers," Acta Acust united Ac, 91(6), (2005), pp. 1086–1097.
[3] D. Kartofelev, A. Stulov, "Propagation of deformation waves in wool felt," Acta Mech., 225, (2014), pp. 3103– 3113.
[4] D. Kartofelev, A. Stulov, "Wave propagation and dispersion in microstructured wool felt," Wave Motion 57, (2015), pp. 23–33.

ORAL SESSION 14

Chemistry and Chemical Physics

Chair: Dr. G. Bagdžiūnas

CONCENTRATION QUENCHING OF FLUORESCENCE IN DIFFERENT MOLECULAR SYSTEMS: SIMILARITIES AND DIFFERENCES

Ivan Halimski[1], Simona Streckaitė[1], Renata Karpicz[1], Jevgenij Chmeliov[1,2], Andrius Gelzinis[1,2], Darius Abramavicius[2], Leonas Valkunas[1]

[1]Department of Molecular Compound Physics, Center for Physical Sciences and Technology, Lithuania
[2]Institute of Chemical Physics, Faculty of Physics, Vilnius University, Lithuania
ivan.halimski@ftmc.lt

Fluorescence (FL) concentration quenching (CQ) is a phenomenon that occurs when the FL quantum yield decreases with increasing molecular concentration [1, 2]. It is observed for different systems ranging from synthetic dyes to chlorophylls in both solutions and thin films. In spite of the fact that CQ is a well-known phenomenon, its origin is not completely understood. Most frequently, it is attributed to excitation migration processes from fluorescent species to non-fluorescent ones, whose number increases with increasing concentration.

CQ results in loss of energy and is harmful for photovoltaic applications, but can be useful for biosensing applications. Therefore, it is important to i) understand and ii) control the phenomenon. One of the most effective tools for analyzing CQ is time-resolved fluorescence, which provides information on possible excitation transfer processes [1].

In this work we provide deep analysis of CQ in trans-stilbene (TS) thin films [2] and free-base and zinc phthalocyanines ([Zn]TTBPc) solutions and thin films. CQ in Pcs occurs due to Förster resonant energy transfer between monomeric species (which act as donors) and non-fluorescent aggregates (acceptor species), whose number increases with increasing concentration. To describe CQ dynamics in Pcs we apply stretched-exponential fit of FL time decay and simple model, where donor is surrounded by infinite number of acceptors (see 'stretched' and 'DAC' fits on Fig. 1 a, b). CQ in TS occurs due to smooth transition of optical properties from monomeric to crystallite with concentration increase. We apply global analysis of FL decay via non-negative matrix factorization (see Fig. 1 c) to show, that small aggregates of TS, which are formed in thin films at high concentrations, have faster (260 ps) FL lifetime compared to those of monomers (710 ps) and monocrystals (1.6 ns).

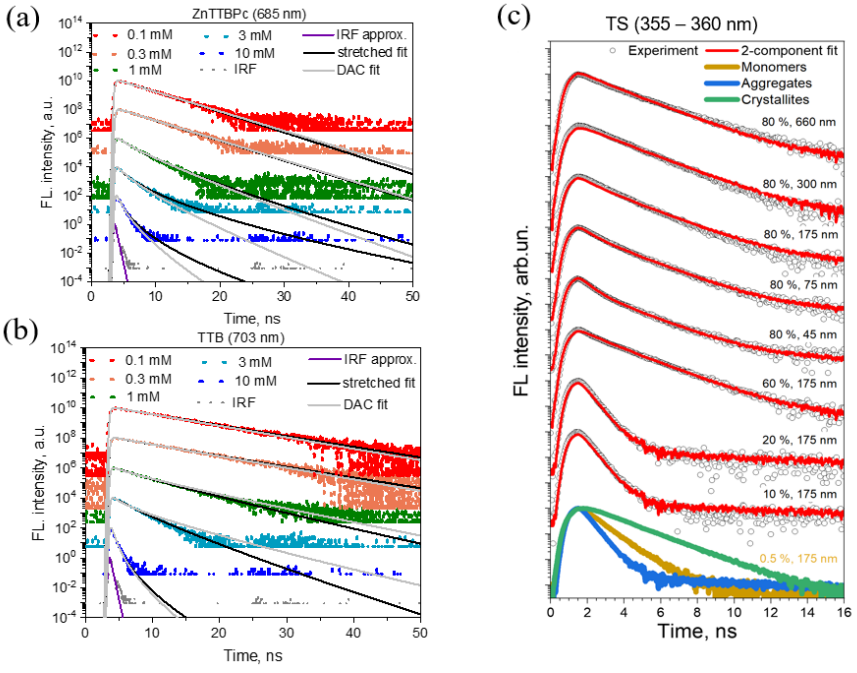


Fig. 1. Fluorescence decay of a) ZnTTBPc and b) TTBPc solutions, and c) trans-stilbene thin films [2].

We support our analysis with steady-state absorption and fluorescence. These techniques applied together is an effective tool to analyze CQ dynamics.

[1] S. Barysitė et al., J. Phys. Chem. B 128, 4887 – 4897, 2024.
[2] I. Halimski et.al., Phys. Chem. Chem. Phys. 26, 23692 – 23702, 2024.

INFLUENCE OF MICROPLASTIC FILM SIZE ON PHOTOCATALYTIC DEGRADATION OF LDPE USING Ag-TiO_2 NANOMATERIALS

Sonata Pleskytė[1], Ieva Uogintė[1], Steigvilė Byčenkienė[1]

[1]Center for Physical Sciences and Technology (FTMC), Department of Environmental Research, Saulėtekio Ave. 3, LT – 10257, Vilnius, Lithuania
sonata.pleskyte@ftmc.lt

Excessive plastic use in domestic, industrial, and agricultural sectors provides new environmental challenges. In particular, polyethylene (PE) is one of the most widely used plastics in the world, with more than 100 million tons produced annually [1]. According to the reports, more than 80% of agricultural films is made from low-density polyethylene (LDPE) [2]. Once microplastics enter the environment, they can accumulate or be transferred through different ecosystems and eventually reach human body. Thus, attention has been focused on advanced technologies for the degradation of microplastics, such as photocatalytic, chemical, and biological methods. Among these methods, photocatalytic degradation stands out as the most promising approach for the degradation of microplastics. TiO_2 nanoparticles are widely applicable for degrading organic pollutants due to their high photoactivity and stability. However, TiO_2 initiated degradation of LDPE is often limited by the rapid recombination of electron-hole pairs. Therefore, in this study, Ag-TiO_2 nanomaterials were proposed as more photoactive alternatives for the degradation of LDPE films. Moreover, since the effectiveness of microplastic degradation is dependent on the properties of the particles, the influence of microplastic size on its degradation was also evaluated.

Ag-TiO_2 nanomaterials with different amount of Ag were synthesized using the photoreduction method. Black LDPE microplastic films with a size of 1×1 mm and 3×3 mm were used. The reaction was carried out in a closed UV chamber under UV-A irradiation in an aqueous medium. A higher Ag concentration in Ag-TiO_2 nanocomposites enhanced the degradation efficiency of LDPE films by up to 35%. LDPE films with a size of 1×1 mm exhibited a higher degradation efficiency (9.4%) after 960 minutes compared to 3×3 mm films (6.18%). A carbonyl group peak at 1725 cm^{-1} was observed after 120 minutes of UV irradiation for the 1×1 mm film, while it appeared only after 360 minutes for the 3×3 mm film. The obtained results suggested that size of microplastics is a crucial parameter, with photocatalytic performance being more efficient for smaller size LDPE microplastic films.

[1] Plastics – the Fast Facts, 2024. https://plasticseurope.org/knowledge-hub/plastics-the-fast-facts-2024/ (accessed: 13-02-2025).
[2] L. Ramos, G. Berenstein, E. A. Hughes, A. Zalts, and J. M. Montserrat, “Polyethylene film incorporation into the horticultural soil of small periurban production units in Argentina,” Science of the Total Environment, vol. 523, pp. 74–81, Aug. 2015, doi: 10.1016/j.scitotenv.2015.03.142.

SYNTHESIS AND INVESTIGATION OF CARBAZOLE AND PHENOXAZINE ORGANIC SEMICONDUCTORS

Skirmantas Musteikis[1], Mantas Marčinskas[1], Tadas Malinauskas[1]

[1]Department of Organic Chemistry, Kaunas University of Technology, Lithuania
skirmantas.musteikis@ktu.lt

As more attention and investment goes into solar energy, researchers are trying to develop better alternatives to the currently most widely used silicon-based solar cells. Silicon solar cells have high manufacturing and energy costs, hence a new more cost-effective technology is required. One of the best candidates is perovskite-based solar cells. These can be produced more cheaply using simpler manufacturing methods and the end product has comparable power conversion efficiency (PCE) [1].

For perovskite solar cells to work efficiently it is necessary to have layers that separate positive and negative charges, which are being generated in the perovskite light absorber, so they do not recombine [2]. Materials that carry positive charges, called hole transporting materials (HTMs), typically limit solar cells' efficiency. Currently one of the most perspective HMTs are those able to form a self-assembled monolayer (SAM). Solar cells with SAM hole transporting materials tend to have higher efficiency, lower HTM consumption and can be used for the manufacture of silicon/perovskite tandems to reach even higher PCE.

SAM forming HTMs are organic molecules, therefore it is possible to easily modify them to be more compatible with the perovskite layer. In this work, we demonstrate, how HTMs can be adapted to perovskites of different compositions, by modifying chemical structure. Using carbazole-based HTM in lead-based perovskites we have achieved high – 20.9% PCE. By changing carbazole to phenoxazine derivative we have achieved relatively high 7.7% efficiency in tin-based perovskite devices.

In summary, this research shows that by modifying central fragments of hole transporting materials, we can adapt them to different perovskite formulations and achieve improved efficiencies, thus making perovskite solar cell technology more viable for commercial use.

[1] Khatoon, S., et al. Materials Science for Energy Technologies, 6: 437-459 (2023).
[2] Liu, S. et al., Nature, 15, 27, (2023).

MODELING THE STRUCTURE AND NMR SPECTRA OF AMANTADINE ENCAPSULATED IN SUPRAMOLECULAR MATRICES

Amina Elkady[1], Kęstutis Aidas[2]

[1]Institute of Chemistry, Faculty of Chemistry and Geosciences, Vilnius University
[2]Institute of Chemical Physics, Faculty of Physics, Vilnius University
amina.elkady@chgf.stud.vu.lt

Cavitands (or synthetic receptors) are supramolecular compounds with an enclosed cavity capable of binding small molecules—an attribute that makes them promising for diagnostic applications in biological fluids. Experiments reveal that carbohydrate-based cavitands selectively encapsulate certain alkylammonium compounds, such as drug amantadine, shifting its 1H NMR signals into the negative region (relative to tetramethylsilane) [1]. This distinct spectral shift highlights the potential of cavitands for metabolomic analyses.

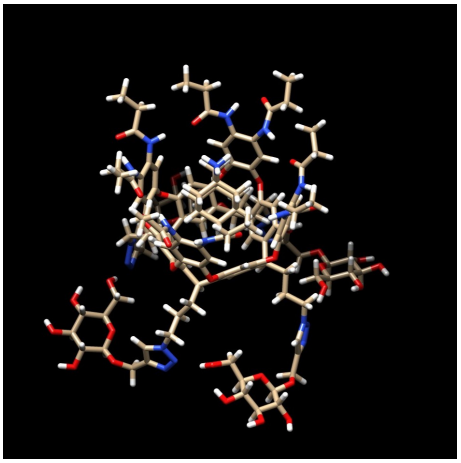


Fig. 1. tetrakis-β-D-glucosyl cavitand–protonated amantadine complex

In this project, the tetrakis-β-D-glucosyl cavitand–protonated amantadine complex is investigated using classical molecular dynamics (MD) simulations, combined with hybrid quantum mechanics/molecular mechanics (QM/MM) methods. Classical MD allows exploration of large-scale molecular behavior under defined thermodynamic conditions, while QM/MM calculations accurately capture electronic effects crucial for NMR shielding. By averaging over configurations from the MD trajectory, temperature-dependent influences are also included. Moreover, the computed NMR spectrum shows good agreement with experimental data, confirming the reliability of this modeling approach. This integrated approach advances our understanding of cavitand–drug interactions and underpins future applications of synthetic cavitands in biomedical diagnostics.

Acknowledgements

This study was supported by the Research Council of Lithuania. Computations were performed on resources provided by the High-Performance Computing Center “HPC Saulėtekis” at Vilnius University, Lithuania.

[1] D. A. Ryan & J. Rebek, ”1H NMR detection of small molecules in human urine with a deep cavitand synthetic receptor”, Analyst,138, 1008-1010 (2013)

IMPACT OF PROTEIN GEOMETRY AND PROTONATION PATTERN ON THE EXCITED STATES OF PIGMENTS IN PHOTOSYNTHETIC COMPLEXES

Gabriele Rankelyte[1], Jevgenij Chmeliov[1,2], Andrius Gelzinis[1,2], Leonas Valkunas[1,2]

[1]Department of Molecular Compound Physics, Centre for Physical Sciences and Technology, Vilnius, Lithuania
[2]Institute of Chemical Physics, Faculty of Physics, Vilnius University, Lithuania
gabriele.rankelyte@ftmc.lt

Photosynthesis is one of the most important processes on Earth. The most efficient organisms that carry out photosynthesis are land plants or higher plants. In the thylakoid membrane of chloroplasts there are two systems that carry out photosynthesis – Photosystem I (PSI) and Photosystem II (PSII), both with their own light harvesting complexes – LHCI and LHCII. PSI is the most efficient light-to-energy conversion apparatus where almost all light, absorbed by the light harvesting antenna LHCI, is converted to chemical energy [1] through the series of reactions and energy transactions. In plants, light harvesting antenna of PSI is composed of four species of LHCI complexes. They all have very similar structure; however, their spectral properties are different. The excitation dynamics in LHCI is highly affected by the charge-transfer (CT) states that occur between the pigments(chlorophylls and/or carotenoids). Known charge-transfer sites in LHCI do not completely explain the spectral properties of this antenna suggesting the presence of more CT states. The energy of these states is of course affected by the surrounding environment (pigments and the protein). Therefore, it is necessary to account for the environment to model light-harvesting complexes properly. In our work, we investigated the LHCI of PSI complex structure [2] (Fig. 1), freely available at Protein Data Bank (PDB ID: 5L8R). Properties of the excited states of the pigments were calculated using "VU HPC" Saulėtekis supercomputer. Charge-density coupling method [3] was used to evaluate excited state energy shifts, caused by the electrostatic environment. The results obtained while working with 5L8R structure were compared to the results of our previous study [4], where the object of the research was Lhca4 sub-complex structure in lower resolution. Our most recent findings demonstrate the sensitivity of pigment excited state properties to changes in the surrounding environmental geometry. Besides the geometry, amino acids can change their protonation state as well affecting the charge distribution within the protein chain and the contribution of each part to the shift of the pigment energies.

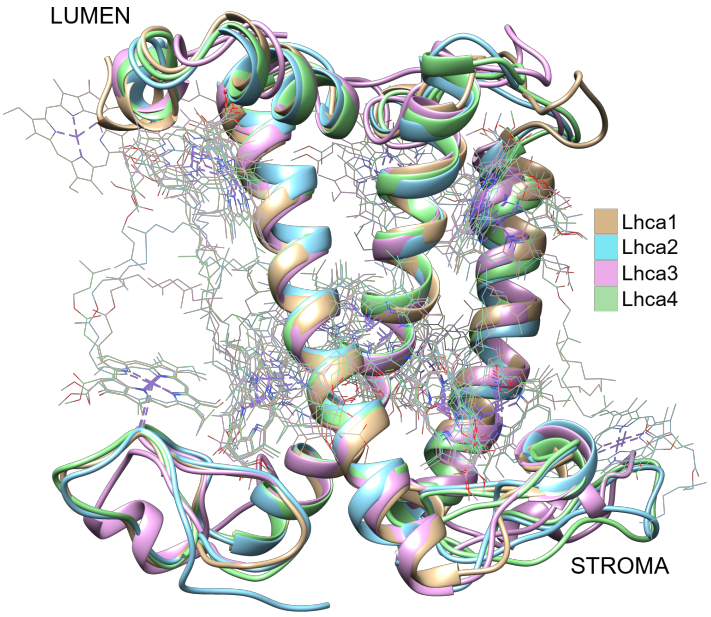


Fig. 1. Lhca1-Lhca4 sub-complexes of LHCI, matched on top of each other (PDB ID: 5L8R, chains 1-4).

[1] R. Croce, H. van Amerongen, Light-harvesting in Photosystem I, Photosynth. Res. 116, 153-166 (2013).
[2] Y. Mazor, A. Borovikova, I. Caspy, N. Nelson, Structure of the Plant Photosystem I Supercomplex at 2.6 Å Resolution, Nat. Plants, 3, 17014-17014 (2017).
[3] T. Renger, F. Müh, Understanding Photosynthetic Light-harvesting: a Bottom Up Theoretical Approach, Phys. Chem. Chem. Phys. 15, 3348-3371 (2013).
[4] G. Rankelytė, A. Gelzinis, B. Robert, L. Valkunas & J. Chmeliov, Environment-dependent chlorophyll–chlorophyll charge transfer states in Lhca4 pigment–protein complex, Front. Plant Sci. 15, 1412750 (2024).

ORAL SESSION 15

Material Science and Nanotechnology

Chair: Dr. I. Kašalynas

ACCEPTOR AGGREGATION IN PM6:Y6 ORGANIC SOLAR CELL BLENDS REVEALED BY SPECTRAL DECOMPOSITION

Titas Klepeckas[1], Dr. habil. Vidmantas Gulbinas[1]

[1]Department of Molecular Compound Physics, Center for Physical Sciences and Technology, Lithuania
titas.klepeckas@ff.stud.vu.lt

Recent advances in organic solar cells (OSCs) have been driven by the development of novel material systems, with PM6:Y6 blends emerging as promising candidates due to their power conversion efficiencies (PCEs) approaching 20%[1]. Although these efficiencies are impressive, certified OSC devices have recently surpassed this benchmark[2]. A major challenge limiting further performance improvements in PM6:Y6 systems is the incomplete understanding of the mechanisms underlying free charge carrier generation. One hypothesis suggests that free charge carriers are generated via energy cascades within the acceptor phase, where delocalized electrons migrate toward well-ordered aggregated domains, ultimately facilitating efficient charge separation[3]. This cascade mechanism may reduce recombination losses and enhance overall device performance.

In this study, we examine the role of acceptor aggregation in modulating exciton dissociation and charge separation in PM6:Y6 devices by employing spectral decomposition of the acceptor absorption spectra using Franck-Condon component analysis. Inspired by recent work from the Danie Khoh group[4], our method deconvolutes the complex absorption spectra of Y6 into distinct vibrational components, thereby distinguishing between aggregated and non-aggregated states. We observe that specific Franck–Condon vibrational progressions correlate with different molecular arrangements: well-ordered, aggregated Y6 domains exhibit red-shifted spectral features, whereas disordered regions display blue-shifted signatures.

By systematically varying the blend stoichiometry and thermal annealing conditions, we correlate the degree of Y6 aggregation with changes in the optical absorption profile and subsequent photocurrent generation. Our results indicate that a moderate degree of aggregation promotes exciton delocalization and enhances free charge carrier generation, thus facilitating more efficient charge separation at the donor-acceptor interface. In contrast, both excessive and insufficient aggregation lead to the formation of quasi-stable delocalized states or increased non-radiative recombination losses. Furthermore, time-resolved fluorescence measurements support the conclusion that aggregate formation modulates the local electronic environment, influencing the energy offset between excitonic and charge-transfer states.

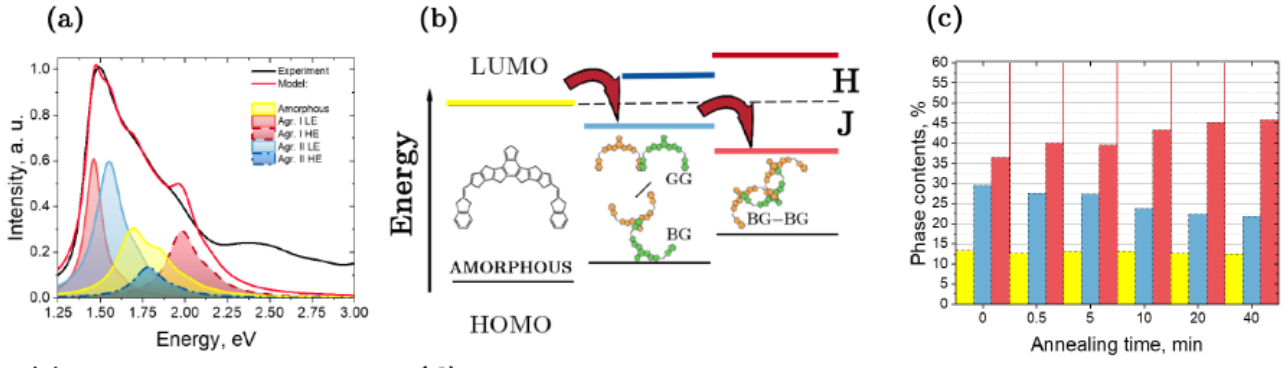


Fig. 1. (a) Pristine acceptor absorption deconvolution. (b) Schematic of HOMO/LUMO levels in amorphous and aggregated phases, showing π-π interactions between acceptor cores (B) and end groups (G) with red arrows indicating electron energy cascades (adapted from Ref. [3]). (c) Relative intensities from the deconvoluted acceptor-rich blend absorption.

[1] Shoaee, S. et. al. What We Have Learnt from PM6:Y6. Adv. Mater. 2023, 35 (32), 2302005.
[2] Chen, Chen, et al. "Molecular interaction induced dual fibrils towards organic solar cells with certified efficiency over 20%." Nature Communications 15.1 (2024): 6865.
[3] Natsuda, Shin-ichiro, et al. "Cascaded energy landscape as a key driver for slow yet efficient charge separation with small energy offset in organic solar cells." Energy & Environmental Science 15.4 (2022): 1545-1555.
[4] Kroh, Daniel, et al. "Identifying the signatures of intermolecular interactions in blends of PM6 with Y6 and N4 using absorption spectroscopy." Advanced Functional Materials 32.44 (2022): 2205711.

COMPARATIVE CONDUCTIVITY ANALYSIS OF TRANSPARENT ELECTRODES FOR SOLAR CELLS

Noor ul ain ahmed[1], Patrizia lamberti[1,3], Maksim Shundalau[1], Renata Adami[2,3], Maria Sarno[2,3], Claudia Cirillo[2,3], Vidmantas Gulbina[4], Martynas Talaikis[4]

[1]Department of Information and Electrical Engineering and Applied Mathematics, University of Salerno, Fisciano (SA), Italy
[2]Department of Physics "E.R. Caianiello" (DF), University of Salerno, Fisciano (SA), Italy
[3]Interdepartmental Centre Research Centre for NANOMAterials and nanoTEchnology (NANO_MATES), Fisciano (SA), Italy
[4]Center for Physical Sciences and Technology, Vilnius, Lithuania
nahmed@unisa.it

Electrodes play a crucial role in the efficiency, stability and overall performance of next-generation optoelectronic devices, particularly solar cells [1]. Transparent electrodes on the top of solar cells can enhance power conversion efficiency by maximizing the light absorption and facilitates the efficient charge collection [2]. This study provides a comparison of graphene-based electrodes with ITO and hybrid ITO/graphene materials in terms of electrical conductivity. A detailed analysis would be conducted to evaluate charge transport behavior and nanoscale electrical properties. The graphene electrodes are prepared by cold wall chemical vapor deposition method and are experimentally verified by Raman spectroscopy. ITO electrodes are commercially obtained and used as a base for hybrid ITO/graphene electrodes. The results provide insights into the feasibility of referring a material as a superior transparent electrode, highlighting its advantages and limitations compared to conventional materials. This work contributes to optimizing electrodes selection for applications in solar cells, displays, and flexible electronics.

Acknowledgements

This work was partially supported by the EU under the Italian National Recovery and Resilience Plan (NRRP) of NextGenerationEU, Project Title UPWARD CUP E53D23014490001 - Grant Assignment Decree No. 1383 of 01/09/2023, by partnership on "Telecommunications of the Future" (PE00000001 - program "RESTART") and from the Horizon Europe MSCA programme under FLORIN project (GA n° 101086142).

[1] Xiao, J.; Shi, C.; Zhou, C.; Zhang, D.; Li, Y.; Chen, Q. Contact Engineering: Electrode Materials for Highly Efficient and Stable Perovskite Solar Cells.; 2017.

[2] Xu, Y.; Wang, J.; Sun, L.; Huang, H.; Han, J.; Huang, H.; Zhai, L.; Zou, C. Top Transparent Electrodes for Fabricating Semitransparent Organic and Perovskite Solar Cells. J. Mater. Chem. C 2021, 9, 9102–9123, doi:10.1039/D1TC02413B.

SPECTRAL PROPERTIES OF YTTERBIUM SPECIES IN DOPED CESIUM LEAD HALIDE PEROVSKITES

Daniel Rodz[1], Simona Steckaitė[1], Vitalii Boiko[2], Mariusz Stefanski[2], Dariusz Hreniak[2], Vidmantas Gulbinas[1]

[1]Department of Molecular Compound Physics, Center for Physical Sciences and Technology, Vilnius, Lithuania.
[2]Institute of Low Temperature and Structure Research, Polish Academy of Sciences, 50-422 Wroclaw, Poland
daniel.rodz@ftmc.lt

Perovskites have been shown to be a promising material in photovoltaics, where single junction perovskite solar cells have reached efficiencies of 26.1% [1]. $CsPbCl_3$ perovskites doped with Yb^{3+} ions are capable of quantum cutting (QC), where one perovskite exciton is converted into two ytterbium excitations [2]. This phenomenon can be used in luminescent solar converters to efficiently turn ultraviolet light into near infrared light, which has been shown to increase commercial solar cell efficiency [3]. The main problem holding back commercial use of these materials is the toxic and hard to scale methods of synthesis, primarily hot injection methods [4]. We used a modified facile mechanosynthesis method [5], where only simple grinding and annealing are required to synthesize perovskite powders. We are exploring energy transfer mechanisms between the perovskite and Yb^{3+} ions by applying steady state and time resolved spectroscopy methods.

We investigate low temperature photoluminescence (PL) spectra of $CsPb_{1-1.5x}Yb_xCl_3$ dopped with different Yb^{3+} concentrations, where two ytterbium species with different optical properties should form: dimers and monomers [6]. Dimers are two adjacent Yb^{3+} ions in the perovskite that can undergo QC, while monomers are solitary Yb^{3+} ions that cannot undergo QC and probably are not incorporated into the perovskite lattice. By mathematically manipulating Yb doped perovskite PL spectra excited at two different wavelengths, 375 and 940 nm, we derived PL spectrum for each of the Yb species (fig. 1A). Mathematical methods were used to approximate perovskite dopped with different Yb^{3+} concentrations PL upon 375 nm excitation from the obtained dimer and monomer spectra (fig. 1B). The proportion of monomers increases with Yb^{3+} concentration (fig. 1B), which suggests that at higher concentrations Yb^{3+} ions are not as efficiently incorporated into the lattice or energy is being transferred from the dimers to monomers. At low concentrations we observe more Yb^{3+} dimers due to optimal ion concentration for the incorporation into the lattice and low migration limited quenching. The differences in intensities of 976 nm peak (fig. 1B), are attributed to reabsorption by the monomers. Further experiments are being conducted using perovskite quantum dots, which should create different ratios of species. This would allow more precise identification of their characteristics.

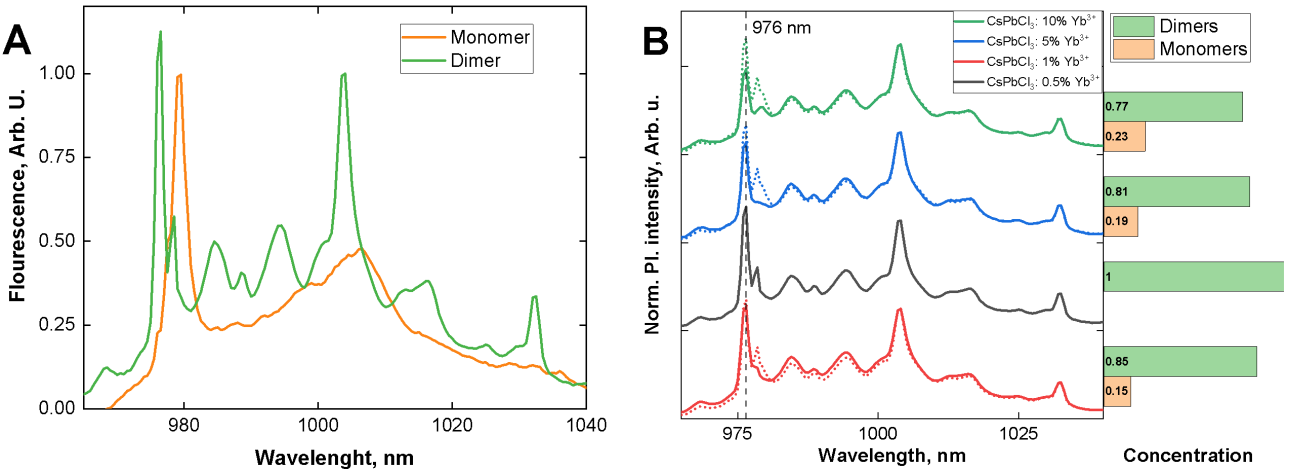


Fig. 1. (A) PL spectra of dimeric and monomeric Yb species in the perovskite powders mathematically obtained from the experimental data measured at 80 K, upon 375 nm excitation. (B) Perovskite PL at 80 K, upon 375 nm excitation (solid) and approximation made from mathematically obtained monomer and dimer spectra (dotted). Bar graphs show at what proportions dimer and monomer spectra were added.

[1] Z. Liang, et al. Nature 2023, 624, 557.
[2] X. Luo, et al. Nano Lett. 2019, 19, 338.
[3] D. M. Kroupa, et al. ACS En. Lett. 2018, 3, 2390.
[4] N. Ding, et al. Nano Energy, 2020, 78, 105278
[5] S. Streckaitė, et al. J. Mat. Chem. 2023, 11, 15463.
[6] S. Streckaitė, et al. J. Mat. Chem. 2024, 12, 11995.

CHARGE CARRIER MIGRATION IN 2D/3D PEROVSKITES

Paula Baltaševičiūtė[1,2], Vidas Pakštas[1], Vidmantas Jašinskas[1], Vidmantas Gulbinas[1], Marius Franckevičius[1]

[1]Department of Molecular Compound Physics, Center for Physical Sciences and Technology, Lithuania
[2]Institute of Photonics and Nanotechnology, Vilnius University, Lithuania
paula.baltaseviciute@ftmc.lt

Perovskites emerged in the scientific world because of their attractive optoelectrical properties with promising applications in solar cells, LEDs and photodetectors. Depending on the application field, these material properties can be changed by simply adjusting their composition [1-2]. This lets perovskites exist in diverse structural forms, including 3D, 2D, quasi-2D, each exhibiting unique charge carrier dynamics relevant to devices performance. Two distinct processes in perovskite materials can be distinguished: charge carrier migration and excitation energy migration [3]. Understanding which one is dominant in material is crucial both for fundamental knowledge and for educated design and optimization of devices [2]. This study investigates the effects of dimensionality on charge carrier migration as the perovskite structure transitions from fully 3D to quasi-2D and 2D configurations.

There were five different perovskites. By changing the ratio of smaller and bigger organic cations (PEA^+ and FA^+) in perovskite lattice, we analyzed which migration mechanism takes place using photoluminescence at different temperatures and pump-probe experiments. In purely 2D perovskite (low *n* Ruddlesden–Popper phase) stable excitons form in 2D materials even at room temperature. The absence of additional peaks or spectral changes suggests that photo-excitations recombine where they are generated rather than migrating to distinct lower-energy sites. Quasi-2D perovskites (a mixture of phases with different layer number *n*) show that the emission is dominated by the lowest-bandgap (largest-*n*) domains, which appear as the most red-shifted PL band. Therefore, cooling inhibits the funneling process, so excitons/carriers become “trapped” in the higher-bandgap domains and radiatively recombine there, instead of all funneling into the lowest-bandgap sites. This is observed as distinct PL peaks corresponding to *n = 1, 2, 3,* etc. By comparing 2D, quasi-2D, and 3D cases, we see a continuum: from tightly bound excitons that stay put (2D), to hybrid systems where carriers relocate to favorable sites (quasi-2D), to 3D free carriers moving in a uniform lattice.

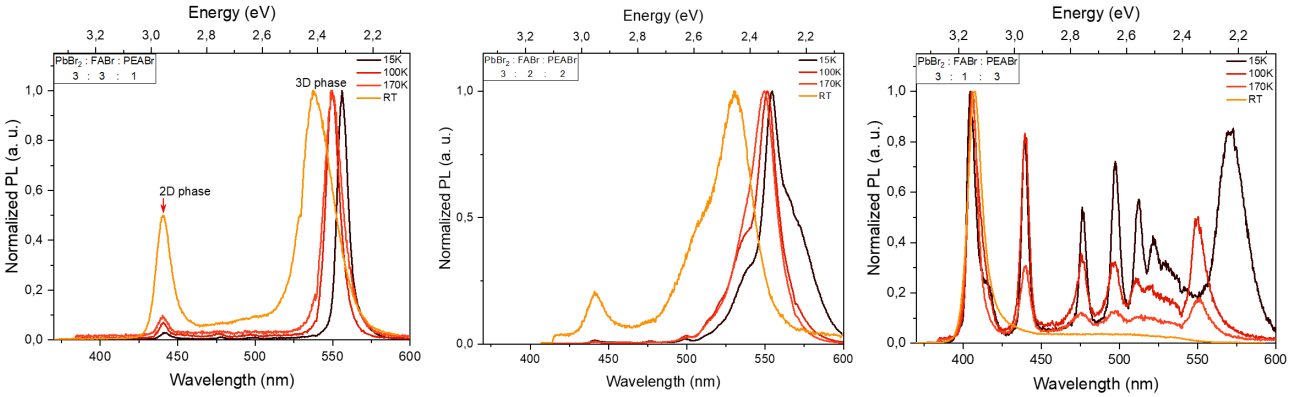


Fig. 1. PL spectra of perovskite thin films with different A cation ratios at various temperatures.

In conclusion, charge migration is the dominant mechanism in quasi-2D and 3D perovskites, whereas 2D perovskites primarily exhibit localized exciton recombination. Unlike 3D or 2D perovskites, quasi-2D structures funnel charge carriers efficiently, leading to higher radiative recombination efficiency, which is crucial for LEDs and other optoelectronic applications.

[1] Azhar Fakharuddin et al., Nature Electronics, Volume 5, Issue 4, Pages 203–216 (2022).
[2] Giulia Grancini et al., Nature Reviews Materials, Volume 3, Issue 7, Pages 270–290 (2018).
[3] Azhar Fakharuddin et al., Advanced Functional Materials, Volume 31, Issue 32, Article Number 2010076 (2021).

LIQUID CRYSTAL ELASTOMER MICROSCTRUCTURES WITH TUNABLE OPTOMECHANICAL PROPERTIES

Zofia Dziekan[1], Mikolaj Rogoz[1], Piotr Wasylczyk[1]

[1]Faculty of Physics, University of Warsaw, Pasteura 5, 02-093 Warsaw, Poland
zu.dziekan@student.uw.edu.pl

Liquid crystal elastomers (LCEs) are smart materials that combine the orientational order of liquid crystals with the elasticity of elastomers, allowing them to undergo reversible deformations in response to stimuli such as heat, light, or electric fields. Their actuation - bending, twisting, or shrinking - can be programmed during the fabrication stage, by aligning liquid crystal molecules before polymerization, making them ideal for applications in soft robotics and micromotors [1].

Conventional methods for controlling LC alignment, such as surface alignment through rubbing or using external fields, offer limited spatial control over molecular alignment [2]. To overcome these constraints, we explore direct laser writing (DLW), a high-precision, two-photon lithography technique that enables the fabrication of intricate 3D micro- and nanostructures via selective resist photopolymerization. While DLW has been used to create LCE microstructures, previous implementations have relied on additional alignment techniques (e.g. rubbing or photopatterning), to create anisotropic material.

Our research demonstrates that line-by-line laser scanning during polymerization can directly control LC molecule orientation, likely due to interactions between polymerized regions and neighboring LC molecules. This enables the fabrication of LCE microstructures with customized birefringence patterns and reversible deformation capabilities (Fig. 1). Notably, this method allows fabrication on challenging surfaces, such as the end face of an optical fiber. Additionally, it provides greater control over local molecular alignment, enabling the creation of complex director patterns without requiring additional processing steps. This direct-writing approach expands the possibilities for integrating LCEs into micro-optical and micro-mechanical systems with precise structural and functional customization.

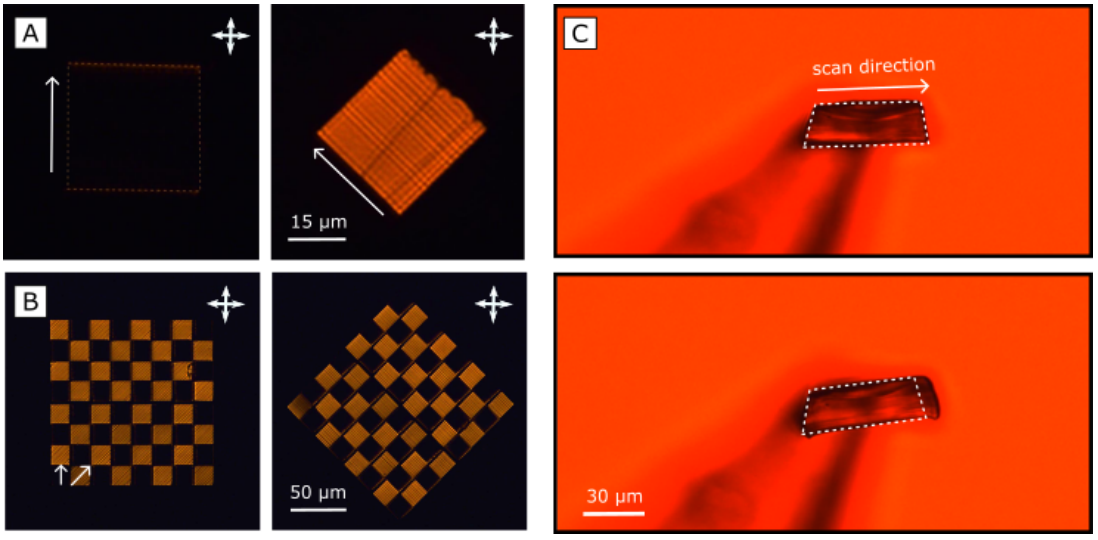


Fig. 1. (A) LCE square and (B) checkered pattern fabricated using DLW. Images were taken with the sample placed between crossed linear polarizers. (C) Thermal deformation of an LCE µ-cuboid heated with laser light. Arrows indicate the direction of the laser scan and corresponding material elongation.

Acknowledgements

This work was supported by the Polish Ministry of Science and Higher Education under the program Perły Nauki (project No. PN/01/0158/2022).

[1] M. Rogóż et al., "From light-powered motors, to micro-grippers, to crawling caterpillars, snails and beyond—light-responsive oriented polymers in action," Materials, vol. 15, no. 22, p. 8214, 2022

[2] J. Zhao, L. Zhang, and J. Hu, "Varied alignment methods and versatile actuations for liquid crystal elastomers: A review," Adv. Intell. Syst., vol. 4, no. 3, p. 2100065, 2021

Poster Session 1

Laser Physics and Optical Technologies Material Science and Nanotechnology

GLASS SCRIBING WITH BESSEL BEAM USING MHZ BURSTS

Aleksandras Kondratas[1], Juozas Dudutis[1], Paulius Gečys[1]

[1]Center for Physical Sciences and Technology, Savanoriu ave. 231, LT-02300, Vilnius, Lithuania
aleksandras.kondratas@ftmc.lt

Bessel beams are categorised under non-diffractive beams. They can be formed using a conical prism (axicon). The resulting interference of the optical waves creates a Bessel beam which can have a larger depth of focus compared to Gaussian beam [1], self-healing property [2], and higher resistance to spherical aberrations [3]. Bessel beams are used in optical trapping, superresolution imaging, material processing, and in other applications [1]. Such beams are attractive for glass scribing due to the ability to vary the depth of focus by changing the diameter of incoming Gaussian beam or using different half cone angles of the Bessel beam facilitating the formation of elongated modifications. Additionally, transverse direction of the modifications can be controlled with asymmetrical beams, so that cracks align with the direction of scribing, which increases scanning speed, decreases separation stress and side wall roughness [4].

Increasing the number of laser pulses in the MHz regime has been shown to produce longer transverse cracks [5]. These larger cracks help to increase scribing speed. Furthermore, the ability to control crack direction through polarisation has recently been demonstrated using a loosely focused Gaussian beam and burst regimes [6]. Investigating this phenomenon with other types of laser beams is of particular interest.

In this study, scanning speed, burst energy, linear and circular polarisation effects on transverse crack formation were investigated scribing 1 mm thickness soda-lime glass samples with Bessel beam. Ultrashort pulse laser FemtoLux 30 from Ekspla was used for the experiment operating in MHz burst regime. Separation stress was measured by breaking samples with a four-point bending setup. Roughness of the samples was measured with a confocal profilometer.

Optimal scribing speeds and burst energies were found which resulted in lowest separation stress or roughness for polarisation aligned with scribing direction, perpendicular to it, and for circular polarisation. Fig. 1 shows how cracks align in the scribing direction when polarisation is parallel to it and sidewall images by optical microscopy. When using low burst energies crack formation angle corresponds to linear polarisation angle.

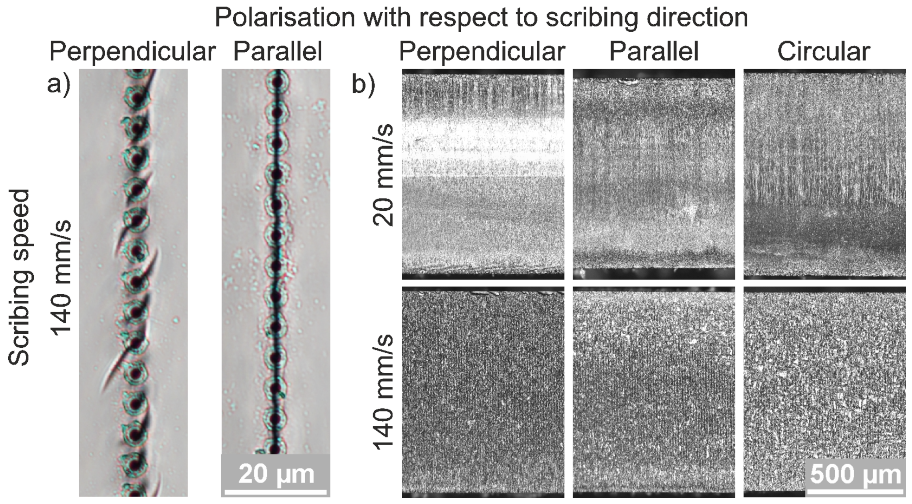


Fig. 1. Samples scribed with different polarisations and scribing speeds. a) Top surface of scribed lines and b) sidewall surfaces of the separated areas. When the polarisation is parallel it corresponds to the scribing direction.

[1] S. N. Khonina, N. L. Kazanskiy, S. V. Karpeev et al., Bessel Beam: Significance and Applications—A Progressive Review, Micromachines (Basel), Vol. 11, Issue 11, p. 997, 2020
[2] X. Chu, Analytical study on the self-healing property of Bessel beam, The European Physical Journal, Vol. 66, Issue 10, pp. 1–5, 2012
[3] M. Kaiser, S. Nolte, J. Hellstern et al., High-quality tailored-edge cleaving using aberration-corrected Bessel-like beams, Optics Letters, Vol. 43, Issue 13, pp. 3164-3167, 2018
[4] J. Dudutis, J. Pipiras, G. Račiukaitis et al., Transversal and axial modulation of axicon-generated Bessel beams using amplitude and phase masks for glass processing applications, Opt Express, Vol. 30, Issue 2, pp. 1860–1874, 2022
[5] F. Hendricks, V. V. Matylitsky, M. Domke et al., Time-resolved study of femtosecond laser induced micro-modifications inside transparent brittle materials, Proc. SPIE, Vol. 9740, pp. 162–169, 2016
[6] M. Mackevičiūtė, J. Dudutis, and P. Gečys, A comparative study on MHz and GHz bursts addressing the polarization-based control of laser-induced modifications in fused silica, Opt Laser Technol, Vol. 181, p. 111289, 2025

OPTIMIZATION OF FEMTOSECOND LASER CUTTING PROCESS PARAMETERS FOR POLYMER OF VARIOUS THICKNESSES

Arnas Vyšniauskas[1,2], Laimis Zubauskas[1], Valdemar Stankevič[1,2], Paulius Gečys[1]

[1]Center for physical sciences and technology (FTMC), Savanorių Ave. 231, LT-02300, Vilnius, Lithuania
[2]Akoneer, Ltd, Mokslininkų 6B, LT-08412, Vilnius, Lithuania
arnas.vysniauskas@ftmc.lt

This research focuses on using femtosecond laser pulses for polymer cutting process optimization. As polymers consist of very large molecules and are sensitive to heat or can easily be damaged, cutting technique with ultrashort pulse lasers could heavily influence wider application in the future. Polymers are getting more and more attention as a versatile material for biomedical, micro-optics and other applications where specific polymer properties are needed. During polymer cutting with femtosecond laser pulses better quality can be achieved avoiding heat affected zones (HAZ) due to indirect lattice heating, thus benefiting from “cold” ablation. We demonstrate cutting various thickness polyamide (PI), polyethylene (PET) and polycarbonate (PC) films. During experiments laser parameters such as pulse repetition rate, average power and pulse overlap were optimized to achieve high-quality cuts and avoid HAZ. As a result, process parameters were optimized for each polymer cutting with ultrashort pulse laser.

NON-OPTICAL CONTACT GLASS WELDING AT DIFFERENT LASER PULSE DURATIONS

Neda Mažeikytė[1], Edgaras Markauskas[1], Paulius Gečys[1]

[1]Center for Physical Sciences and Technology (FTMC), Department of Laser Technologies (LTS), Savanoriu Ave. 231, 02300 Vilnius, Lithuania
neda.mazeikyte@ftmc.lt

Laser-based glass welding offers significant advantages over soldering and adhesive bonding by producing durable joints without creep, outgassing, or aging [1]. Femtosecond (fs) pulses achieve high weld strength and quality due to strong non-linear absorption. While widely used in optical contact welding, their application in non-optical contact welding remains limited, with most studies relying on picosecond pulses [2,3]. The major limitation of fs pulses comes from larger beam spot sizes typically used in non-optical contact welding, significantly increasing the Rayleigh range inside the glass. This, in turn, increases non-linear absorption above the focal plane, reducing the energy reaching the weld area and typically causing either insufficient weld formation or thermal stress-induced cracking. The femtosecond laser bursts address this issue by distributing high pulse energy across multiple sub-pulses while maintaining the same energy in the burst. This approach reduces non-linear absorption outside the focal plane, enabling more efficient energy delivery to the welding area.

This study investigated non-optical contact welding of soda-lime glass plates using single-pulses and MHz bursts of an ultrashort pulsed laser. The laser operated at a 1030 nm wavelength, with pulse durations ranging from 176 fs to 10 ps. Weld quality was evaluated using an optical microscope and a surface profiler, while longitudinal tensile tests were used to determine weld strength. Weld strength and quality were compared between different pulse durations.

Figure 1 presents the results obtained with 10 ps duration pulses. Increasing the number of sub-pulses within the burst increased the weld strength, reaching a maximum strength at 13 sub-pulses. The highest strength was 30% higher than that of single-pulse welding. Optical microscope analysis revealed that glass fracturing inside the welding area increased with sub-pulse numbers.

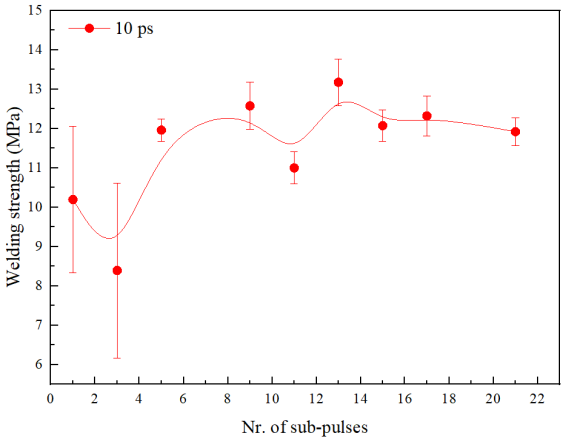


Fig. 1. Weld strength dependence on the number of sub-pulses within the burst for 10 ps pulses.

[1] Zhang, J., et al. The effect of gap on the quality of glass-to-glass welding using a picosecond laser. Optics and Lasers in Engineering, vol. 134, pp. 106248 (2020).
[2] Richter, S., et al. Bonding of glass with femtosecond laser pulses at high repetition rates. Applied Physics. vol. 103, pp. 257–261 (2011).
[3] Lipat'eva, T. O., et al. Precision Laser Welding of Silica Glass with Iron-Nickel Alloy. Glass and Ceramics. vol. 77, pp. 435 – 437 (2021).

QUALITY ENHANCEMENT OF CUT GLASS USING A CO_2 LASER

Patricija Šleiniūtė[1], Laimis Zubauskas[1], Miglė Mackevičiūtė[1], Paulius Gečys[1]

[1]Center for Physical Science and Technology (FTMC), Savanorių Ave. 231, Vilnius, Lithuania
patricija.sleiniute@ftmc.lt

Laser-based glass-cutting techniques play a critical role in the precision processing of transparent materials, including various types of glasses. Specifically, an effective material removal mechanism in bottom-up laser cutting provides accurate cuts at high processing rates [1, 2]. However, this results in reduced cut quality and the flexural strength of the cut pieces [3].

In this work, soda-lime glass (SLG) and fused silica glass (FS) samples were cut using a Carbide 40 (from Light Conversion) femtosecond laser in a BiBurst (GHz burst in MHz burst) regime to utilize the full laser glass cutting potential. A CO_2 laser was used to enhance the cut sidewall quality by peeling [4] or polishing [5] defected glass layer for SLG and FS samples respectively.

After conducting quality enhancement experiments, an experimentally generated map of soda-lime glass peeling showed that successful peeling can be achieved in a narrow laser energy dose window from 11.56 ± 1.37 to 17.92 ± 3.22 J/cm2. Furthermore, due to the removed defective layer, the peeling process increased the cut glass strip strength by up to 2.4 times. Moreover, by remelting the defective layer of fused silica with the laser polishing technique, the strength of the samples increased by up to 2.6 times.

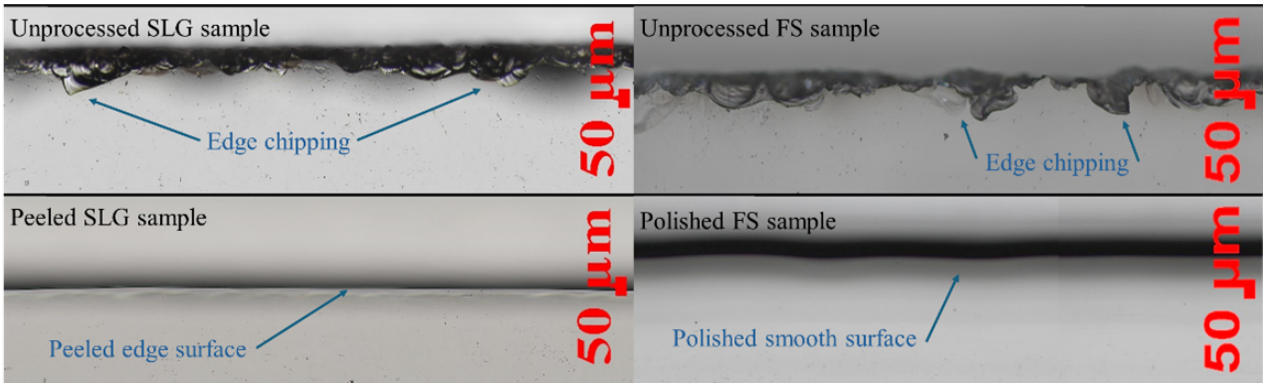


Fig. 1. Optical images of surface chipping of soda-lime glass (SLG) strips (left) and fused silica glass (FS) (right) before and after quality enhancement with a CO_2 laser.

[1] M. Mackevičiūtė, J. Dudutis, and P. Gečys, Fast and efficient bottom-up cutting of soda-lime glass using GHz bursts of short laser pulses, Optics and Lasers in Engineering, Vol. 183, 108490, (2024).
[2] P. Gečys, J. Dudutis, G. Račiukaitis, Nanosecond laser processing of soda-lime glass, Journal of Micro/Nanoengineering, Vol.10, pp. 254-258, (2015).
[3] J. Dudutis, L. Zubauskas, E. Daknys, E. Markauskas, R. Gvozdaitė, G. Račiukaitis, and P. Gečys, Quality and flexural strengthof laser-cut glass: classical top-down ablation versus water-assisted and bottom-up machining, Optics Express, Vol. 30(3), pp. 4564-4582, (2022).
[4] T.C. Chiu et al., On the mechanics of laser peeling for ultra-thin glasses, Engineering Fracture Mechanics, Vol. 163, pp. 236-247, (2016).
[5] L. Zubauskas, E. Markauskas, A. Vyšniauskas, V. Stankevič, and P. Gečys, Comparative analysis of microlens array formation in fused silica glass by laser: Femtosecond versus picosecond pulses, Journal of Science: Advanced Materials and Devices, Vol. 9(4), 100804, (2024).

MAXIMIZING CUTTING SPEED OF THIN STAINLESS-STEELSHEETS BY NANOSECOND AND PICOSECOND LASER PULSES

Lukas Brundza[1], Andrius Žemaitis[1], Mindaugas Gedvilas[1]

[1]Department of Laser Technologies (LTS), Center for Physical Sciences and Technology (FTMC), Savanorių Ave. 231, 02300 Vilnius, Lithuania
lukas.brundza@ff.stud.vu.lt

In recent years, nanosecond and picosecond lasers have demonstrated remarkable capabilities in the laser processing of metals with minimal thermal effects, high efficiency, and precision [1]. However, despite numerous advancements in ablation efficiency optimization [2-9], optimizing the cutting speed of thin sheets remains a challenge, even though recent theoretical progress has been reported [10]. Maximizing laser cutting speed is crucial for industrial applications, as it directly impacts manufacturing efficiency, energy consumption, and overall production costs.

This study aims to investigate the key factors influencing the laser cutting speed of thin metal sheets using nanosecond and picosecond pulses, including laser parameters and process optimization strategies. By systematically analyzing the effects of peak laser fluence controlled by focal positioning, we seek to establish optimal conditions for enhancing cutting speed. Additionally, a comparative analysis was conducted to determine the advantages and disadvantages of nanosecond versus picosecond lasers in cutting thin stainless-steel sheets. Laser irradiation with a central wavelength of 1064 nm, controllable pulse durations of 4.5 ns or 13 ps, and a repetition rate of 400 kHz was used in the experiments. We determined that the maximum cutting speeds were 28 mm/s for nanosecond pulses at an average laser power of 38 W and 14 mm/s for picosecond pulses at an average laser power of 44 W for stainless steel sheets with a thickness of 0.3 mm at certain optimal fluence values using a slightly defocused Gaussian beam. The beam size optimization theoretical approach was adopted from [10] to explain the experimental data. These results will be valuable for industries requiring high-precision microfabrication, such as electronics, automotive, and medical device manufacturing, where speed and accuracy are most critical.

[1] Žemaitis et al., Opt Lasers Eng 176, 108046 (2024).
[2] Račiukaitis et al., J Laser Micro Nanoen 4, 186 (2009.
[3] Žemaitis et al., Sci Rep 8, 17376 (2018).
[4] Žemaitis et al., Opt Lasers Eng 114, 83 (2019).
[5] Žemaitis et al., Sci Rep 9, 12280 (2019).
[6] Gaidys et al., Appl Surf Sci 483, 962 (2019).
[7] Žemaitis et al., Opt Express 29, 7641 (2021).
[8] Žemaitis et al., Sci Rep 14, 5614 (2024).
[9] Žemaitis et al., Opt Laser Technol 180, 111458 (2025).
[10] Du et al., Opt Express 31, 9750 (2023).

REDUCTION OF Si REFLECTANCE VIA FEMTOSECOND LASER-PROCESSING

Mantas Mikalkevičius[1], Andrius Vasiliauskas[1], Mindaugas Juodėnas[1], Tomas Tamulevičius[1,2], Asta Tamulevičienė[1,2]

[1]Institute of Materials Science of Kaunas University of Technology, K. Baršausko Str. 59, LT-51423, Kaunas, Lithuani
[2]Department of Physics of Kaunas University of Technology, Studentų Str. 50, LT-51368, Kaunas, Lithuania
mantas.mikalkevicius@ktu.lt

Crystalline silicon (c-Si) solar cells are very popular due to their low cost and relatively good efficiency. However, the reduction of optical losses which are mainly attributed to reflectance is still one of the technological challenges in achieving higher efficiencies [1].

In this work, a 200 nm chrome thin film was deposited on a polished Si wafer by e-beam evaporation technique. The purpose of chrome film was to act as a mask for the reactive-ion etching process of the silicon substrate. Then, laser-induced periodic surface structures (LIPSS) were imposed on the surface via femtosecond laser Pharos (Ligh conversion), at 200 kHz and 1030 nm wavelength. Fluence varied in range from 147 to 245 mJ/cm^2. Then, quazi-periodic structures were thinned down in chromium etchant (Sigma Aldrich) solution for 40 s to expose the silicon surface. Later, the inductively coupled deep reactive-ion etching process was applied to transfer a grating-like structure mask from chrome into the crystalline silicon substrate. Lastly, we used the same chromium etchant to completely remove the chrome mask.

Reflectance measurements in UV-Vis-NIR with integrating sphere were performed for pristine and laser-treated surfaces. The 28 % reflectance of the pristine Si wafer was reduced by 23 and 20 % by applying 147 mJ/cm^2 and 172 mJ/cm^2 fluence irradiation and imposing the LIPSS (Figure 1). An even bigger drop in reflectance was obtained when 196, 220, and 245 mJ/cm^2 fluence was used, where it went below 2 %.

Our work shows that LIPSS in chrome thin film can be used as a mask for silicon etching and formed structures greatly reduce reflectance.

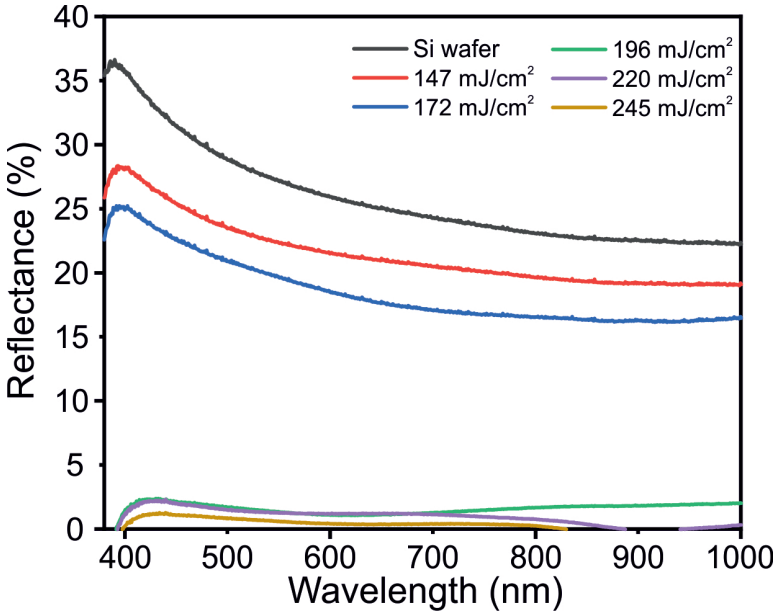


Fig. 1. Reflectance spectra of Si wafer and grating-like structures formed in the silicon substrate depending on laser fluence used for LIPSS formation

[1] Kato, S., Kurokawa, Y., & Soga, T. (2022). Enhancement of reflectance reduction of solar cells by a silicon nanoparticle layer on a textured silicon substrate. Results in Optics, 9, 100296. https://doi.org/10.1016/j.rio.2022.100296

HUMIDITY-INDUCED STRESS MEASUREMENTS IN NANOSTRUCTURED GLAD COATINGS FOR HIGH LIDT MIRRORS

Adomas Strazdas[1], Simas Melnikas[1], Lukas Ramalis[1]

[1]Center for Physical Sciences and Technology, Savanoriu Ave. 231, LT-02300 Vilnius, Lithuania
adomas.strazdas@ftmc.lt

Optical components are essential in laser systems used to direct and control laser-generated radiation. Demands for optical elements, including mirrors, are rapidly increasing, therefore making such elements a weakest link when it comes to laser-induced damage threshold (LIDT). To gain benefits in optical resistivity or spectral performance, a fairly new method is developed using nanostructured thin films coated by GLancing Angle Deposition (GLAD) method. Conventional titanium oxide mirrors with low LIDT can be enhanced by depositing an additional “upgrade” [1] coating to improve LIDT. In order to achieve this, environmental stability measurements are investigated.

The aim of this study was to investigate the dependence of the nanostructured coating stress on humidity. The upgrade 5-layer coating consists of 2 porous silica layers with low refractive index deposited at substrate tilt angle of 70° and 3 dense hafnia (deposited at 0°) with high refractive index. Porous films tend to absorb water and can induce some instabilities depending on humidity in the environment. Water molecule movement changes the intrinsic stress values of the film a considerable amount, and may lead to coating cracking.

To test this hypothesis, a gas isolating chamber was constructed around an interferometer to measure the stress induced surface curvature of porous coatings under different humidity values. At first you insert the porous film, measure the peak-to-valley values, and start introducing nitrogen gas, to lower the humidity. To get higher humidity a container with a water salt mixture [2] was placed inside to create a more humid atmosphere. The measurements were carried out at several different levels of humidity. Highest and lowest achieved humidity was about 5 rh% and 79 rh% respectively.

The obtained results demonstrate that as we decrease the humidity the stress increases. The peak-to-valley values changed from 0.625 λ to 1.202λ (see Figure 1), as humidity was lowered to 5rh%. This change indicates that by having a higher humidity the power value may go down, and if the humidity is changed aggressively, it may lead to cracking of the coating.

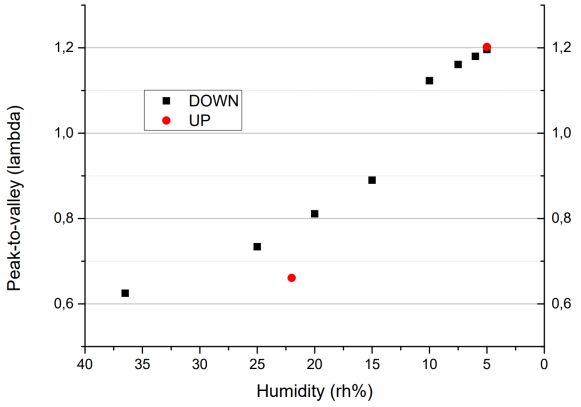


Fig. 1. Dependence of peak-to-valley values of humidity as humidity decreases (DOWN) and recovers (UP).

All in all, we coated GLAD coatings on titanium/silicon mirrors which had low intrinsic stress. Afterwards it was discovered that the stress was dependent on humidity, and a lot of problems arose. If these issues were dealt with, such developed coatings could be of major use as they are aimed to be applied in ultrafast laser systems.

[1] Grineviciutė L., et al., Optics and laser technology, Vol. 129 (2020)
[2] Greenspan L., Journal of research,Vol. 81A, 89-96 (1977)

SELECTIVE LASER ETCHING OF FUSED SILICA USING LOW NUMERICAL APERTURE FOCUSING OPTICS

Rimantas Naina[1], Valdemar Stankevič[1]

[1]Department of Laser Technologies, Center for Physical Sciences and Technology
rimantas.naina@ftmc.lt

Femtosecond laser induced selective etching (FLISE) is a subtractive microfabrication technique which allows for the formation of 3D structures in transparent materials with resolution as small as a few microns. The maximum height (depth) of structures which can be fabricated is limited by the choice of focusing optics. By using low numerical aperture (NA) objectives structures with heights of over a centimeter can be written.

For structures written using a low NA objective we investigate how different writing parameters affect etching selectivity and quality. Our goal is to find parameters that give a high etching rate while keeping good etching quality. Modification shapes are examined as well since it has previously been shown that low NA objectives can produce circularly shaped modifications [1].

Etching rates are determined by writing lines at a depth of 100 µm in fused silica with a CARBIDE (Light Conversion) laser system (setup shown in fig. 1 a) using different writing parameters: energy, repetition rate, pulse duration, pulse density, burst mode. The NA of our setup is 0.22. The fused silica samples are etched in 80 °C KOH for an hour before measuring the etched out channel lengths with an optical microscope (fig. 1 b). Simple 3D structures are also written at the surface to check for crack formation.

We observe that the use of GHz and MHz bursts can highly increase etching rates. The effect is most prominent for lines written using short pulse durations (400 fs) where no etching was achieved when using single pulses but etching was observed for lines written with GHz or MHz bursts. For longer pulse durations this effect becomes less noticeable and for pulse durations over 2 ps the maximum etching rates are the same for lines written with and without burst mode. By writing simple 3D structures we determine that good etching quality can be achieved with pulse durations of about 1-2 ps. The use of MHz or GHz bursts of 2 or 3 pulses can help reduce crack formation in this regime. We also find a writing regime with 200-400 fs pulse durations and the use of MHz bursts with 10 pulses where no cracks were observed in the etched structures. For longer pulses up to 10 ps we observe an increase in cracking as well as the formation of circularly shaped modifications.

Our results show that by using pulse bursts etching rates can be increased and etching can be achieved even with short pulse durations. By using these shorter pulses crack formation can be reduced.

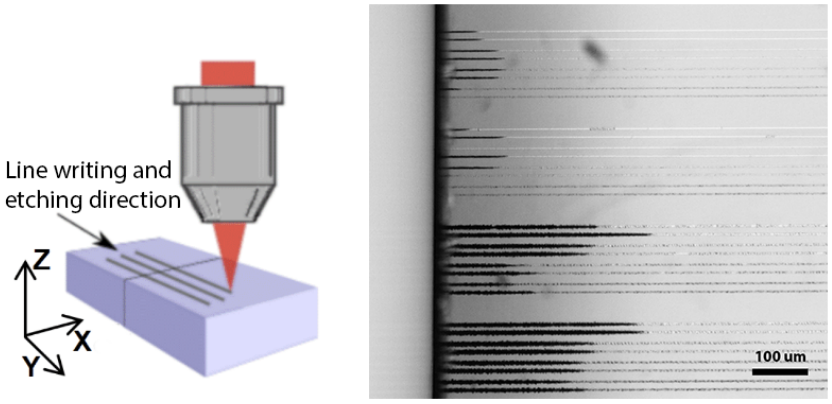


Fig. 1. Measurement of etching speeds. (a) Experimental setup [2] (b) Example of lines written with different parameters after 1 h of etching in KOH

[1] P. Wang et al., “2 Three-dimensional laser printing of macro-scale glass 3 objects at a micro-scale resolution,” 2019.
[2] A. Butkutė et al., “Optimization of selective laser etching (SLE) for glass micromechanical structure fabrication,” Opt. Express, vol. 29, no. 15, p. 23487, Jul. 2021, doi: 10.1364/OE.430623.

TRANSPARENT MICROSCALE ELECTRODES FORMED BY LASER-INDUCED METAL DEPOSITION ON GLASS FOR SMART WINDOWS APPLICATION

Dainius Balkauskas[1], Evaldas Kvietkauskas[1], Modestas Sadauskas[1], Viktorija Vrubliauskaitė[1], Romualdas Trusovas[1], Karolis Ratautas[1], Alexandr Belosludtsev[1]

[1]Center for Physical Sciences and Technology (FTMC)
dainius.balkauskas@ftmc.lt

Windows are part of any building architecture which lets the light in and creates connection with nature, surrounding environment. During sunny days, a lot of UV and infrared light comes into building. European Directive 2018/844 states that buildings are responsible for 36% of greenhouse gas emissions and that 50% of final energy consumption in the European Union is related to the use of heating, ventilation and air conditioning systems. Therefore, new technologies that can reduce energy consumption are necessary. Electrochromic materials have the unique property of changing the transmittance of light when an electric current is applied. Windows based on these materials will be able to dynamically regulate the entry of ultraviolet and infrared light into buildings, thus improving comfort and reducing energy costs. Transparent conductive electrodes are very import part of smart windows. We demonstrate a cost-efficient and large-scalable method of transparent microscale metal electrodes fabrication on a glass using laser-induced metal deposition technology. The novel electrodes are effective conductive layers, presenting a promising alternative to rare, brittle, and expensive Indium Tin Oxide (ITO). In our study, we discussed not only electrode formation technique, but also compared various electrodes' designs. Furthermore, the optimized copper electrode design was tested in a real multilayer smart window structure and proove that such electrodes can work with different electrochromic coatings.

PULSED LASER DEPOSITION OF NBT-BT THIN FILMS

Eglė Martinaitytė[1], Vadzim Haronin[1], Šarūnas Svirskas[1]

[1]Faculty of Physics, Vilnius University, Vilnius, Lithuania
egle.martinaityte@ff.stud.vu.lt

Ferroelectric thin films are widely used in capacitors, sensors, actuators and piezoelectric microelectromechanical systems (piezoMEMS) due to their excellent dielectric and piezoelectric properties [1]. Many of these applications rely on lead-based materials for their high performance [2]. However, the environmental and health risks associated with lead have induced the search for lead-free alternatives. One of the promising candidates is $0.8Na_{0.5}Bi_{0.5}TiO_3$-$0.2BaTiO_3$ (NBT-BT) [3], though achieving high-quality thin films with controlled properties remains challenging. This study aims to optimize the deposition parameters of NBT-BT thin films grown using pulsed laser deposition (PLD) to obtain homogeneous and non-conductive materials.

NBT-BT thin films were deposited on $Pt/TiO_2/SiO_2/Si$ substrates using a KrF excimer laser (wavelength: 248 nm, fluence: 1.5 J/cm^2) at different substrate temperature, deposition distance and process pressure, as detailed in Table 1. Structural and morphological characteristics were analyzed using scanning electron microscopy (SEM) and X-ray diffraction (XRD). Dielectric properties were measured using an LCR meter to examine ferroelectric properties. The obtained results indicate that deposition parameters significantly influence crystallinity, grain size, and film uniformity which can be seen in Fig. 1. A well-defined perovskite phase was observed under optimized conditions.

These findings highlight the importance of parameter control in PLD for fabricating high-quality NBT-BT films on silicon and platinum substrates. The study provides insights into optimizing deposition conditions for improved film uniformity and electrical properties, contributing to the advancement of lead-free ferroelectric materials for future usage in electronic devices.

Table 1. Deposition parameters.

Sample	Temperature, °C	Process Pressure, mbar	Distance, mm
B1	600	0.3	55
B2	600	0.3	75
B3	600	0.3	95
B4	550	0.3	55
B5	650	0.3	55
B6	600	0.06	55

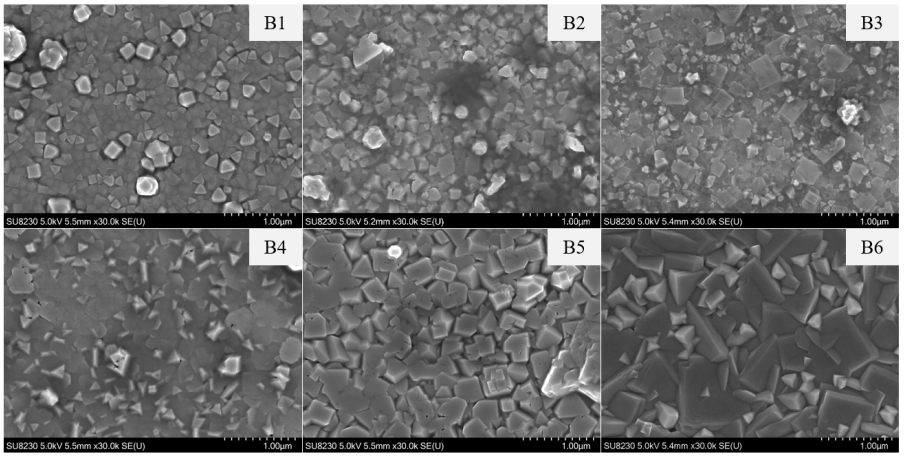


Fig. 1. SEM pictures for each deposited film.

[1] N. Setter et al.,"Ferroelectric thin films: Review of materials, properties, and applications," Journal of Applied Physics 100, 051606 (2006).
[2] X. Wang et al., "Ultra-high piezoelectric performance by rational tuning of heterovalent-ion doping in lead-free piezoelectric ceramics," Nano Energy 101, (2022).
[3] S. K. Patri, R. N. P. Choudhary, "Dielectric materials : introduction, research and applications," Nova Science, pp. 59-61, (2009).

SYNTHESIS AND CHARACTERIZATION OF PALLADIUM NANOPARTICLES VIA LASER ABLATION OF TARGET IN WATER

Amelija Nicytė[1], Ornela Rakauskaitė[1], Mantas Mikalkevičius[2], Toma´š Albert Štefanov[3], Dejan Prokop[4,5], Vrňata Martin[4], Michal Novotný[3,5], Joris More Chevalier[5], Tomas Tamulevičius[1,2]

[1]Faculty of Mathematics and Natural Sciences, Kaunas University of Technology, Lithuania
[2]Institute of Materials Science of Kaunas University of Technology, Lithuania
[3]Department of Physics and Measuring Technique, University of Chemistry and Technology, Czech Republic
[4]Faculty of Mathematics and Physics Charles University in Prague, Czech Republic
[5]Institute of Physics of the Czech Academy of Sciences, Czech Republic
ornela.rakauskaite@ktu.edu

Palladium (Pd) nanoparticles (NPs) have gained significant attention due to their unique physical and chemical properties, such as enhanced catalytic activity and excellent electronic conductivity. These characteristics make Pd NPs particularly suitable for applications in sensors, where high sensitivity and rapid response times are required [1].

In this work, we performed the Pd NP photophysical synthesis employing a Yb:KGW femtosecond pulsed laser and micromachining system [2]. The palladium target was submerged in deionized water with a 2 mm layer covering its surface. A 1030 nm wavelength femtosecond laser with 1.9 µJ pulse energy and 0.6 J/cm^2 fluence at a 200 kHz repetition rate was used for ablation. The beam focused to a 20 µm spot, scanned at 20 mm/s speed with a galvanometric scanner over a 2 mm × 2 mm area with 30 µm y-direction steps. Elemental composition analysis of the synthesized nanoparticles was conducted using energy-dispersive X-ray spectroscopy (EDS). The sample analysis confirmed the formation of high-purity Pd nanoparticles.

SEM micrographs of the dried Pd NPs on crystalline silicon substrate revealed that the mean diameter is 20 nm and the broad size distributions follow a log-normal distribution, which is characteristic for NPs produced via metal target laser ablation in liquid.

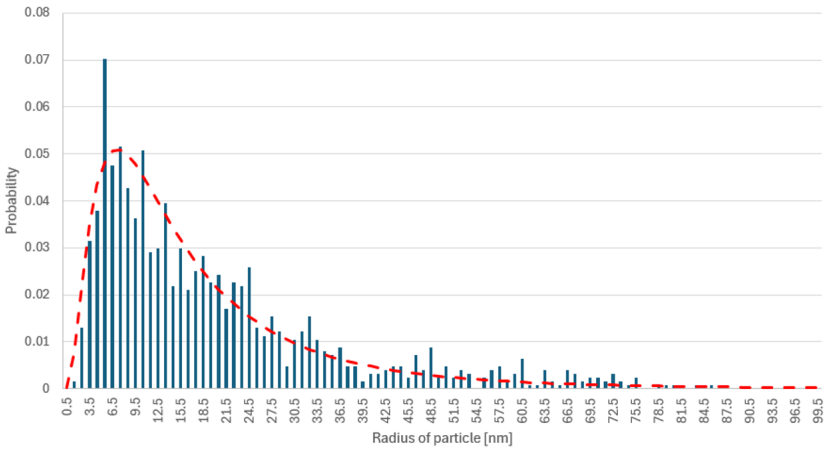


Fig. 1. Probability density function (PDF) of Pd NPs synthesized using a fs-laser. The red dashed line indicates the fitted log-normal distribution.

The research was carried out within joint research project between the Lithuanian and Czech academies – “HAMLET”.

[1] Mohazzab., et al., Stainless steel mesh-GO/Pd NPs: Catalytic applications of Suzuki–Miyaura and Stille coupling reactions in eco-friendly media. Green Chemistry, 21 (2019) 3319-3327
[2] Peckus D., et al., Optimization of process parameters for the photophysical synthesis of colloidal Ag, Au, and Cu nanoparticles using femtosecond laser ablation in water, Optical Materials, 161 (2025) 116796

FABRICATION OF HIGH POROSITY FOAM TARGETS FOR INERTIAL CONFINEMENT FUSION INVESTIGATION

Ioanna-Angeliki Petsi[1,2,3], Saule Petrauskaite[1,2], Mangirdas Malinauskas[1,2]

[1]Vilnius University
[2]Laser Research Center
[3]University of Patras
petsiioannaangeliki@gmail.com

Inertial Confinement Fusion (ICF) is a fusion energy approach that uses intense laser or X-ray pulses to rapidly compress and heat a tiny fuel capsule, creating the extreme conditions needed for nuclear fusion. It has the potential to provide an almost limitless, clean, and sustainable source of energy, with possible applications in energy production, nuclear research, astrophysics, high-energy physics, and theoretical space propulsion.

Micro-foam targets are used in ICF experiments and must have high porosity, be composed of light elements (with carbon as the heaviest), and maintain uniform density. Various manufacturing methods can produce these foam targets, including 3D printing, carbon-based aerogels, and polymerization of foams. Among these, laser polymerization is the most promising, as it offers the highest resolution and precise control over the target's density.

The main goal of this work was to use a femtosecond laser to fabricate high-porosity woodpile foams from acrylate materials (Pentaerythritol triacrylate and Pentaerythritol tetraacrylate), optimizing both the laser writing speed and power. This study marks the first time a green laser has been used on these materials. After fabrication, the woodpile structures were integrated into a 3D-printed holder, for investigation for ICF, which will take place in ABC group of ENEA center in Frascati.

Figure 1 presents the process of integrating the foams into the holder. First, the woodpiles were fabricated. Next, the porosity was increased, and a thin wall was added around the woodpile to enhance rigidity. A 3D-printed holder was then created. Finally, the woodpile was mechanically inserted into the holder.

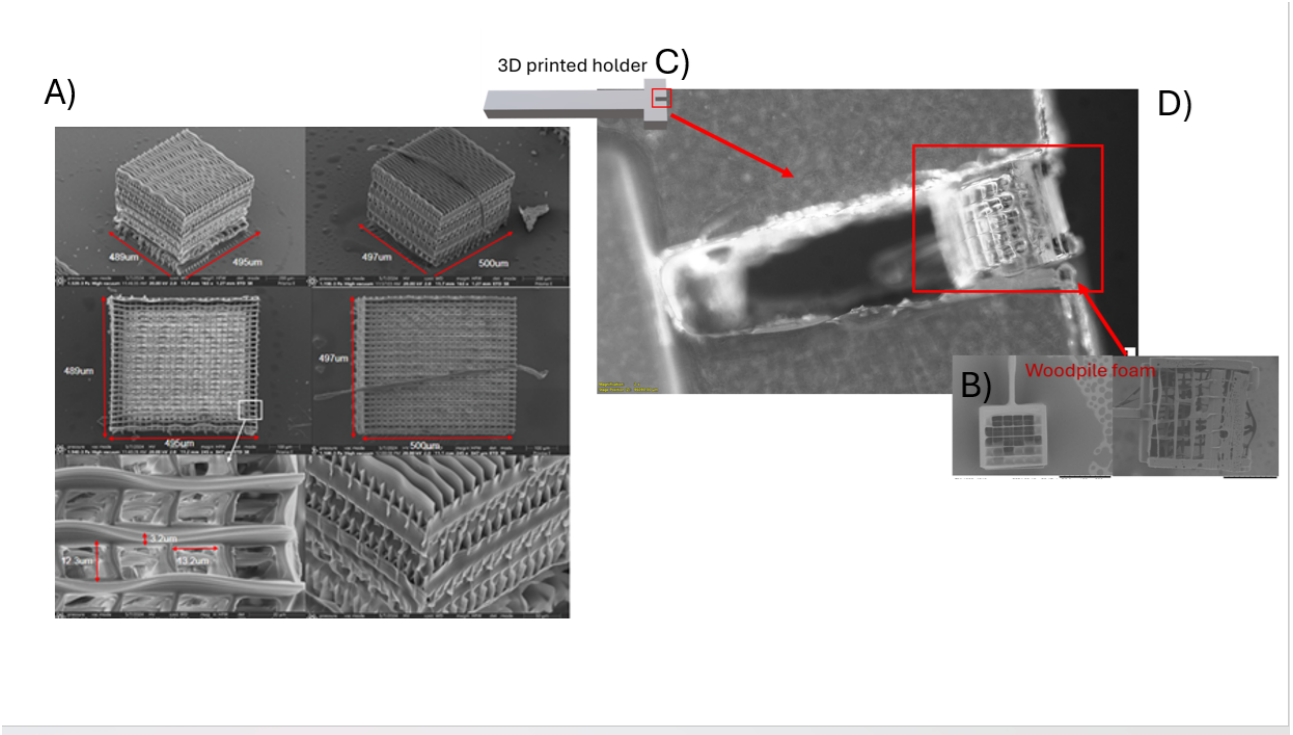


Fig. 1. (A) Scanning electron microscope image of a woodpile foam with a laser writing speed of 50 µm/s and a writing power of 50 mW. (B) Woodpile foam with a thin wall for added rigidity. (C) 3D-printed holder (STL file). (D) Woodpile integrated into the holder.

INVESTIGATION OF THE PROPERTIES OF A PIEZORESISTIVE SENSOR FABRICATED USING LASER MICROFABRICATION TECHNOLOGIES

Šarūnas Mickus[1], Romualdas Trusovas[1], Karolis Ratautas[1], Justina Žemgulytė[2], Paulius Ragulis[2], Modestas Sadauskas[1], Evaldas Kvietkauskas[1], Gediminas Račiukaitis[1]

[1]Department of Laser Technologies, Center for Physical Sciences and Technology, Lithuania
[2]Department of Physical Technologies, Center for Physical Sciences and Technology, Lithuania
sarunas.mickus@ftmc.lt

Our daily lives are packed with many integrated, functional, and miniaturized devices, the demand for which has increased significantly in recent years. Among the most widely used electromechanical sensors are piezoresistive, a type of pressure sensor based on the piezoresistive effect. This effect describes how the electrical resistance of a material changes when it is subjected to a mechanical load. Piezoresistive sensors are widely studied due to their excellent sensitivity, simple design and durability. Their advantages are their relatively low cost of production, the possibility of obtaining different sensitivities and the wide range of measured pressures.

The integration of flexible dielectric materials is a necessary factor for the development of flexible and miniaturized electronics. To achieve this integration, it is necessary to develop technologies to create electrically conductive zones on the surface of dielectrics. The effective use of such materials requires technologies that allow the localization of such zones with high precision.

In this work, widely used engineering polymers polyimide (PI) and polyetherimide (PEI) are investigated. PI and PEI are high-temperature polymers with outstanding thermal and dimensional stability, chemical resistance, and good electrical properties. These polymers are widely used in aerospace, automotive and consumer products. [1] However, further research into selective surface metallization and electrically conductive zone formation technologies is needed for their successful application in integrated electronics. Selective surface activation induced by laser (SSAIL) has been chosen as the metallization technology to form conductive copper traces. As a possible technology for forming sensitive areas of the sensor, laser-induced graphene (LIG) technology was chosen.

It has been experimentally demonstrated that a 3.3 kΩ piezoresistive sensor with a LIG layer on a polyimide surface can be fabricated by combining different laser technologies (Fig. 1). Such a methodology has great potential and can be used as one of the alternative and sustainable solutions for the production of flexible sensors with integrated electronics. However, further research is still necessary to improve the stability, repeatability, and efficiency of the resistance response of the LIG layer. The properties of the junction between graphene and copper also need to be improved to minimize the junction resistance. For this purpose, further optimization of the LIG process will be carried out by tuning the laser process parameters, exploring different designs, and further analysis of the contact formation between copper and graphene.

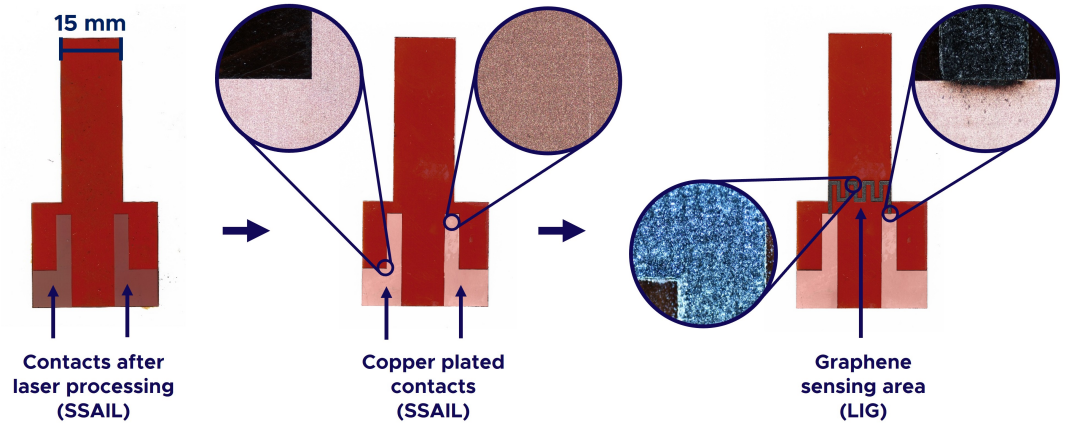


Fig. 1. The main steps for producing a piezoresistive sensor. The circles show microscope images of different parts of the sensor.

[1] Y. Houeix et al., "Laser-synthesis of conductive carbon-based materials from two flexible commercial substrates: A comparison," Appl. Surf. Sci., vol. 634, 2023.

PECULIARITIES OF THERMAL EFFECT MANAGEMENT IN AN END-PUMPED HIGH AVERAGE POWER BULK YB:YAG LASER AMPLIFIER

Lukas Kamarauskas[1,2], Aivaras Kazakevičius[1,3], Andrejus Michailovas[1,3]

[1]UAB Ekspla, Savanorių ave. 237, LT-02300 Vilnius, Lithuania
[2]Faculty of Physics, Vilnius University, Saulėtekio al. 10, LT-10223 Vilnius, Lithuania
[3]National Center for Physical Sciences and Technology, Savanorių ave. 231, LT-02300 Vilnius, Lithuania
lukas.kamarauskas@ff.stud.vu.lt

Ultra-short pulsed lasers featuring high average power and energy good quality beams are widely used for pumping optical parametric chirped pulse amplifiers (OPCPA), generation of X-ray radiation or material processing utilizing interference patterning and many other. Yb:YAG has a range of properties suitable for high-power diode-pumped solid-state (DPSS) lasers, such as low quantum defect, high heat conductivity, long fluorescence lifetime, high tensile strength, etc. These properties allow Yb:YAG based lasers to reliably generate powerful good quality beams [1]. Amplification of laser beams using isotropic materials, such as YAG or laser glasses suffers from thermal effects, such as thermal lensing, birefringence and depolarization which are most prevalent in high intensity lasers. These effects can degrade beam parameters and cause undesired losses. A classical end-pumped rod-type amplifier configuration offers high optical to optical amplification efficiency but greatly suffers from thermal effects and as a result requires extra steps to achieve required beam parameters [2]. In this work the thermal effects and methods to control them in high average power end pumped rod type Yb:YAG laser amplifiers are discussed and resultant beam parameters are investigated in our high repetition rate hybrid laser system.

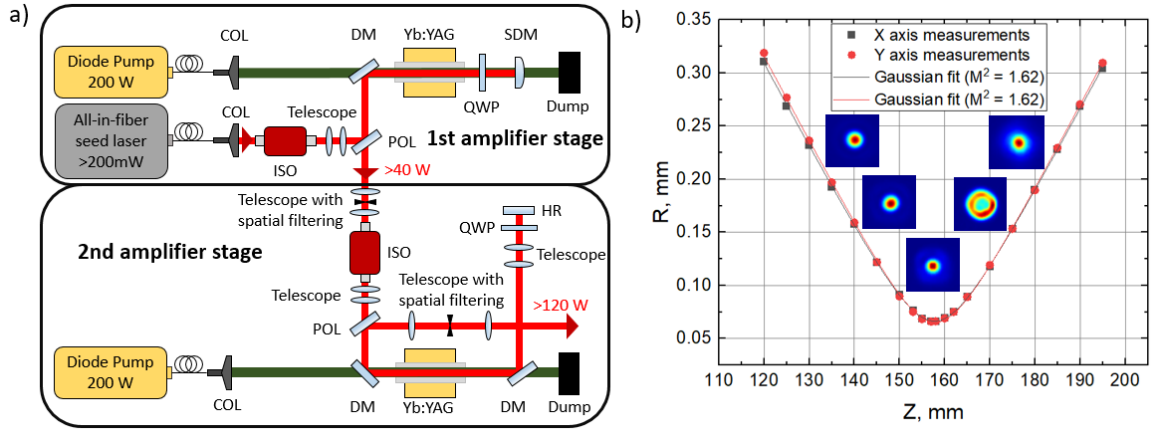


Fig. 1. a) Schematic of a two-stage end-pumped double-pass Yb:YAG rod amplifier. COL – colimating optics, ISO – optical isolator, HR – high reflectivity mirror, POL – thin-film polarizer, DM – dichroic mirror, QWP – quarter wave plate, SDM – spherical dichroic mirror. b) Beam quality measurement results for the second amplifier stage. Insets – qualitative comparison of the system output beam profile evolution after focusing lens. Profile size is scaled for convenience.

A master oscillator power amplifier (MOPA) laser system, which consists of a fiber seed source and two stages of free-space end-pumped double-pass Yb:YAG rod amplifiers was investigated. The system produced 100 ps stretched pulses at >120 W average power and 100 kHz – 1 MHz pulse repetition rates. The depolarization losses (7-8 %) in the laser system were quite moderate. The output beam profile was affected primarily by gain saturation, which resulted in a reduced beam quality parameter, M2 ≈ 1.6 (Fig. 1.). A spatial filtering scheme was employed to significantly improve the beam quality reaching almost the diffraction limit (M2 ≈ 1.05) at the cost of the moderate losses of 10.7 %. It is apparent that increased thermal load on the active medium, has a significant influence on the beam parameters. At high pumping power depolarization can cause severe losses and in addition degrade the beam profile further highlighting the importance of depolarization compensation.

[1] Solid-State Laser Engineering, vol. 1. in Springer Series in Optical Sciences, vol. 1. New York, NY: Springer New York, 2006. doi: 10.1007/0-387-29338-8.
[2] L. Veselis, R. Burokas, O. Ulčinas, T. Gertus, K. Michailovas, and A. Michailovas, "Depolarization compensation with a spatially variable wave plate in a 116 W, 441 fs, 1 MHz Yb:YAG double-pass laser amplifier," Appl. Opt., vol. 60, no. 24, p. 7164, Aug. 2021, doi: 10.1364/AO.432573.

MODELING OF SECOND HARMONIC GENERATION SPECTRA IN CHIRAL TPPS4 NANOTUBES

Eimantas Urniežius[1], Laura Baliulytė[1], Darius Abramavičius[1]

[1]Vilnius University, Faculty of Physics, Institute of Chemical Physics, Saulėtekio al. 3, LT-10257 Vilnius
eimantas.urniezius@ff.vu.lt

Second harmonic generation (SHG) plays a crucial role in modern nonlinear optics, with applications spanning nonlinear photonics and material science. Organic molecular aggregates, owing to their distinct morphology, are promising candidates for nonlinear optical applications. One such aggregate is formed by zwitterionic meso-tetra(4-sulfonatophenyl) porphyrin (TPPS4), which self-assembles into chiral nanotubes under acidic conditions (pH ≤ 4). In this study, we model the nonlinear optical properties of TPPS4 nanotubes using quantum chemistry methods.

We construct two chiral nanotube models — one with clockwise and the other with counterclockwise chirality — and compute their SHG responses using our in-house quantum chemistry package, QCFP. Density functional theory (DFT) calculations, performed using CAM-B3LYP 6-311G(d,p) in water (PCM), reveal significant differences in dipole moments between the Z1 and Z2 TPPS4 monomers in both ground and excited states. These dipole moments are then used to evaluate the SHG response of each nanotube. Calculated SHG response spectra indicate that intensity varies with the polarization and propagation direction of the incident wave. Our findings also suggest that chirality plays a role in the strength of the SHG response. These findings enhance our understanding of the nonlinear optical behavior of TPPS4 aggregates and highlight their potential for applications in tunable photonic devices.

[1] S. M. Vlaming, Ramūnas Augulis, Marc, J. Knoester, and P.H.M. van Loosdrecht, “Exciton Spectra and the Microscopic Structure of Self-Assembled Porphyrin Nanotubes,” vol. 113, no. 8, pp. 2273–2283, Feb. 2009, doi: https://doi.org/10.1021/jp808235c.

[2] G. Schifino, M. Fortino, L. M. Scolaro, and A. Pietropaolo, “Chiral self-organization of the TPPS4 porphyrin assisted by molecular rotations,” Molecular Systems Design & Engineering, vol. 8, no. 12, pp. 1512–1519, 2023, doi: https://doi.org/10.1039/d3me00072a.

FLUORESCENCE LIFETIME MEASUREMENTS USING THERMAL SOURCE

Evita Spalinskaitė[1], Vytautas Žičkus[1,2], Zigmas Balevičius[1]

[1]Plasmonics and Nanophotonics Lab., Department of Laser Technologies, Center for Physical Sciences and Technology, Saulėtekio av. 3, LT-10257 Vilnius, Lithuania
[2]School of Physics and Astronomy, University of Glasgow, Glasgow G12 8QQ, United Kingdom
evita.spalinskaite@ftmc.lt

Fluorescence lifetime measurements are widely used in exploring various biological environments, revealing changes in pH, temperature, and viscosity among other parameters [1]. Measurements are typically performed with time-correlated single photon counting (TCSPC) methods, which are limited to 100's of picoseconds lifetime resolution due to limitations of electrical hardware [2]. Recently, Fluorescence lifetime Hong-Ou-Mandel sensing (FLHOM) method [2], where temporal resolution is limited by optical properties of light, overcomes the limitations of standard technique. Here, we introduce a low-cost version of the FLHOM method, by replacing a coherent reference source with a thermal source.

We used Allura Red fluorescent dye, with a nominal lifetime of $\sim$1.6 ps [2], as a reference source to probe the lifetime of a 4-DASPI dye in a Mach-Zehnder interferometer set up. Secondly, we deconvolved the measured second-order correlation function and recovered fluorescence lifetime of 5.6 ps, in agreement with previous findings [2]. We measured a reduced interference visibility around 6.5% due to intrinsically bunched nature of thermal light. In conclusion, integrating fluorescent dye as a reference thermal source reduces the complexity and cost of the experimental system. Despite marginal reduction in achievable lifetime resolution, the method opens opportunities to measure ultrashort fluorescence lifetime.

[1] Datta R., Heaster T. M., Sharick J. T., et al., Fluorescence lifetime imaging microscopy: fundamentals and advances in instrumentation, analysis, and applications, J. Biomed. Opt. 25(7), 071203 (2020)
[2] Lyons, A., Zickus, V., Álvarez-Mendoza, R. et al., Fluorescence lifetime Hong-Ou-Mandel sensing. Nat Commun 14, 8005 (2023)

HIGH REPETITION RATE FEMTOSECOND SUPERCONTINUUM GENERATION IN KGW CRYSTAL AND ALL-NORMAL DISPERSION PHOTONIC CRYSTAL FIBER

Simona Armalytė[1], Jokūbas Pimpė[1], Julius Vengelis[1]

[1]Laser Research Center, Faculty of Physics, Vilnius University, Saulėtekio av. 10, Vilnius, Lithuania
simona.armalyte@ff.stud.vu.lt

In recent decades, significant progress has been made in the development of ultrashort laser systems with high average power. These laser systems, which operate at high repetition rates (around tens MHz) while maintaining substantial average power, have enabled new applications. These applications span from fundamental scientific research, including spectroscopy, high harmonic generation, and nonlinear microscopy, to precise material processing in manufacturing [1]. As a result, amplification stages are essential for these laser systems. For this purpose, a unique fiber chirped pulse amplification (FCPA) system based on ytterbium-doped large mode area photonic crystal fiber rod amplifier has been developed at the Laser Research Centre of Vilnius University, generating 114 fs pulses with a repetition rate of 76 MHz and an output power of 71 W [2, 3]. Most applications require a tunable wavelength laser source, and therefore a parametric amplifier with supercontinuum (SC) seed will be designed for this laser system. Although continuum generation is already a widely studied phenomenon in most bulk crystals and fibers [4], there are almost no continua demonstrated with such a combination of pump conditions.

The aim of this study was to investigate and compare supercontinuum generated in 10 mm long KGW crystal and in a 2 m long all-normal dispersion photonic crystal fiber (ANDi-PCF). The SC generated in both cases showed similar spectrum broadening and temporal coherence. The recorded maximum SC spectrum covers wavelengths in the 680 nm – 1220 nm range (evaluated at the 10−6 intensity level) in KGW crystal and 670 – 1450 nm range (evaluated at the 10−3 intensity level) in ANDi-PCF case (Fig. 1). The SC generated in the KGW crystal demonstrated better temporal stability and simplicity of the setup and therefore has more potential for application in parametric amplification.

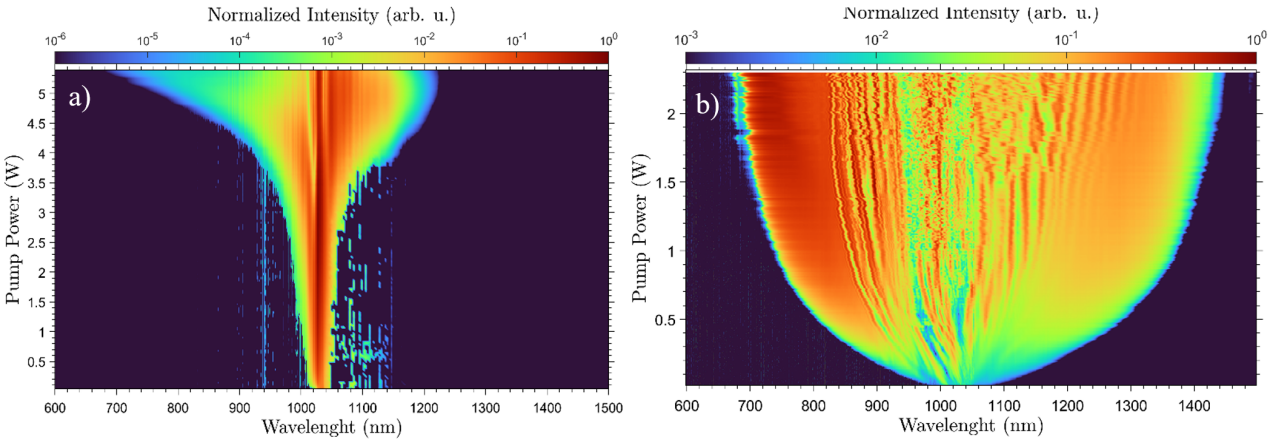


Fig. 1. The evolution of the output spectrum as a function of average pump power in the KGW crystal (a) and ANDi-PCF (b).

[1] C. Saraceno, F. Emaury, A. Diebold, I. Graumann, M. Golling, U. Keller, Trends in high-power ultrafast lasers, Proc. SPIE 9835, 98350 (2016).
[2] J. Pimpė, J. Banys, S. Armalytė, V. Jarutis, J. Vengelis, Development of fiber rod type high repetition rate and average power femtosecond laser system based on FCPA, 'Optica Laser Congress and Exhibition 2024', October 20 – 24, 2024, Osaka, Japan.
[3] J. Pimpė, J. Banys, S. Armalytė, V. Jarutis, J. Vengelis, Development of fiber rod based high repetition rate and average output power laser system using pre-chirp managed nonlinear amplification, 'EPS-QEOD Europhoton 2024', August 25 – 30, 2024, Vilnius, Lithuania.
[4] V. Marčiulionytė, J. Banys, J. Vengelis, R. Grigutis, G. Tamošauskas, and A. Dubietis, "Low-threshold supercontinuum generation in a homogeneous bulk material at 76 MHz pulse repetition rate," Opt Lett, 48(17), 4609, (2023).

DOUBLE FANO RESONANCES IN NANO-MODULATED THIN FILMS FOR FREQUENCY AND ANGULAR FILTERING

Lucciano A. Letelier C.[1], Julianija Nikitina[1], Lina Grineviciute[1], Kestutis Staliunas[2,3,4]

[1]Center for Physical Sciences and Technology (FTMC), Savanoriu Ave. 231, LT-02300 Vilnius, Lithuania
[2]Vilnius University, Faculty of Physics, Laser Research Center, Sauletekio Ave. 10, Vilnius, Lithuania
[3]ICREA, Passeig Lluís Companys 23, 08010, Barcelona, Spain
[4]UPC, Departamento de Fisica, Rambla Sant Nebridi 22, 08222, Terrassa (Barcelona) Spain
lucciano.letelier@ftmc.lt

Fano resonances in periodically nano-modulated thin films are known to produce narrow bandgaps in both frequency and angular domains [1,2]. At resonance, the incident wave couples to the planar waveguiding mode of the film, resulting in zero transmission and 100% reflection [3]. The bandwidth of these resonances is proportional to the coupling coefficient between the incident radiation and the waveguiding mode. In this work, we demonstrate that combining two closely spaced resonances can create extremely narrow high-pass bands in transmission, with a theoretically tunable passband width that can approach zero in wavelength-angle space.

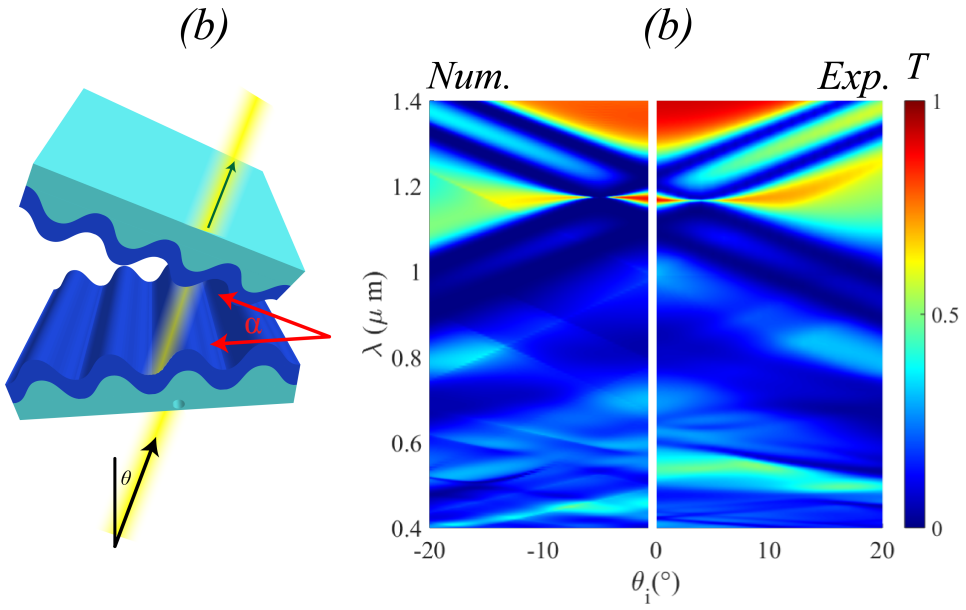


Fig. 1. Frequency and Angular Filtering. (a) Schematic of the double-tilted grating structure. (b) Comparison of transmission maps from numerical simulations and experimental results.

Using these principles, we fabricate single-layer gratings and experimentally measure their transmission characteristics. By tilting two identical filter structures at a small angle relative to each other, obtaining a high-pass window in the angle-wavelength domain. This approach enables control over the spectral and angular properties of the transmitted light by changing the tilted angle, offering potential applications in compact optical system.

Acknowledgements
This work has received funding from the Research Council of Lithuania (LMTLT), agreement no. S-LT-TW-24-9.

[1] L. Grineviciute, J. Nikitina, C. Babayigit, and K. Staliunas, \textit{Appl. Phys. Lett.} \textbf{118}, 131114 (2021).
[2] L. Grineviciutė, C. Babayigit, D. Gailevičius, E. Bor, M. Turduev, V. Purlys, T. Tolenis, H. Kurt, and K. Staliunas, \textit{Applied Surface Science} \textbf{481}, 353 (2019).
[3] L. Lukosiunas, L. Grineviciute, J. Nikitina, et al., \textit{Phys. Rev. A} \textbf{107}, L061501 (2023).

IMAGING OF SURFACE ACOUSTIC WAVES AND MEMS WITH PICOMETER DISPLACEMENTS USING HOLOGRAPHIC VIBROMETRY

Florian Dötzer[1], Johannes May[1], Marie Mannagottera[1], Stefan Sinzinger[1]

[1]Optical Engineering Group, Department of Mechanical Engineering, TU Ilmenau, Germany
florian.doetzer@tu-ilmenau.de

Holographic vibrometry is an interferometric method for the fast and spatially resolved characterization of surface vibrations on the nano- and picoscale [1]. Similar to laser Doppler vibromery (LDV), it exploits the Doppler shift light experiences when it is reflected from a moving object. It allows for a full-field measurement instead of relying on a point-by-point scanning process and thus offers very fast measurements. This is crucial when measurements are to be performed in production or quality control.
In the following, we assume light with frequency f_L which is reflected from an object surface harmonically vibrating with frequency f_{obj} and displacement amplitude $\hat{z}_{obj}$. This corresponds to a harmonic phase modulation which generates sidebands at $f_L \pm m \cdot f_{obj}$ as illustrated in equation (1) using the Jacobi Anger identity. The object displacement is thus encoded in the amplitude factors of the different spectral components which are given by the Bessel functions J_m.

$$e^{i2\pi f_L t} \cdot e^{i\frac{4\pi\hat{z}_{obj}}{\lambda}\sin(2\pi f_{obj}t)} = \sum_m J_m\left(\frac{4\pi\hat{z}_{obj}}{\lambda}\right) \cdot e^{i(2\pi(f_L+mf_{obj})t)}, \quad m \in Z \tag{1}$$

For displacements smaller than ≈ 10 nm, J_0 is close to unity and $J_n \approx 0$ for $n \geq 2$ but J_1 is approximately proportional to the displacement $\hat{z}_{obj}$. By recording a hologram of this spectral component at $f_L \pm f_{obj}$ and reconstructing its image in the object plane by numerical Fresnel backpropagation, the spatial distribution of the sideband amplitude and thus the vibration displacement across the object's surface is obtained.
In practice, this is achieved by shifting the frequency of the light in the reference arm by $\Delta f = f_{obj}$ using acousto-optic modulators, such that it matches the frequency of the sideband. A frequency shift of $\Delta f = f_{obj} + f_b$ leads to a beat frequency f_b between the reference arm and the first sideband in the object arm. If a sequence of images is recorded, narrow-band filtering can be employed in the frequency domain to boost the SNR according to the working principle of a lock-in amplifier.

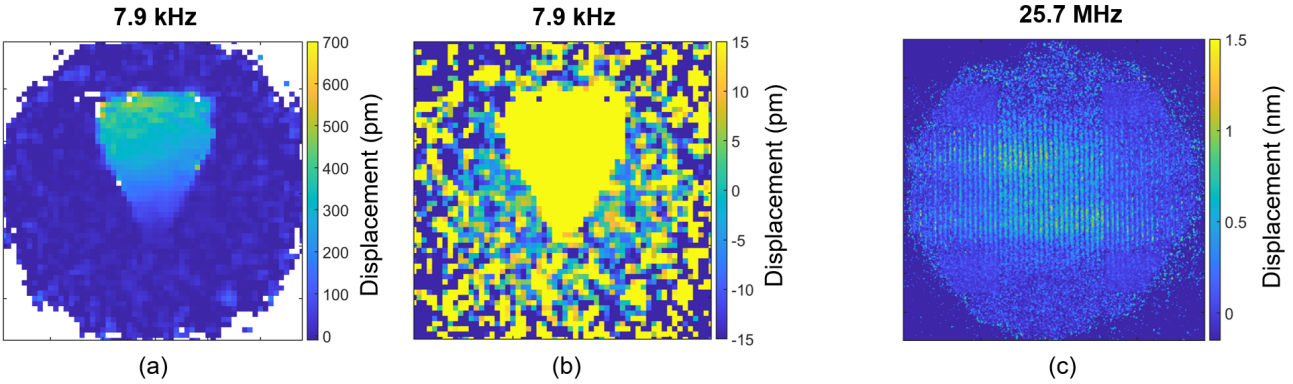


Fig. 1. Vibration displacement of a MEMS cantilever (a), magnified colorbar to assess noise floor (b) and vibration displacement of a surface acoustic wave.

We present measurement results of a MEMS cantilever at its resonance in the kHz-regime, shown in Fig 1 (a-b). At 100 fps, 12800 frames were recorded in just above 2 min, resulting in a noise floor on the order of 10 pm. A measurement of a standing surface acoustic wave field between two interdigital transducers at 25.7 MHz is shown in (c). It was reconstructed from 400 frames, corresponding to a measurement time of 10 s at 40 fps. Similar measurements using LDV can take up to several days [2].

Acknowledgements

We sincerely express our gratitude to Prof. Dr. Claudia Lenk and Dr. Jörg König for providing us with the MEMS- and SAW-samples, respectively.

[1] N. Verrier et al., Full Field Holographic Vibrometry at Ultimate Limits, New Techniques in Digital Holography, 255-293 (2015)
[2] R. Weser et al., Three-dimensional heating and patterning dynamics of particles in microscale acoustic tweezers, Lab on a Chip (2022)

NUMERICAL ANALYSIS OF PHOTONIC CRYSTAL WAVEGUIDE LOGICAL CIRCUITS

Andrius Zinkevičius[1], Ignas Lukošiūnas[2]

[1]Vilnius University
[2]Laser Research Center
andrius.zinkevicius@ff.stud.vu.lt

Photonic crystals (PhCs) are materials with periodically varying dielectric permittivity distributions. Under the right conditions, such devices can have photonic band gaps which prohibit electromagnetic wave propagation of certain frequency and polarization [1]. Such features make PhCs as waveguides – not only can very high transmittance quality be controlled [2], but light can be contained even with very sharp bends present in the waveguide channels [3]. For this reason, very small and intricate light guiding devices can be realized which makes them great for making photonic logical elements, that can work 5-10 times faster than top of the line electronic counter parts while using a fraction of the power (clock rates can reach values of 12.5 GHz [4], compared to approximately 3 GHz that moder GPU's provide while using power in the order of microwatts [5]). In this work we present a photonic logical element design, with silicon waveguide channels, which is based on a ring resonator. All numerical simulations have been caried out using finite difference frequency domain method in Academic MATLAB Environment. Similar devices with air waveguiding channels have already been proposed [6], but they lack confinement since there is no total internal reflection and lead to a diverging wave.

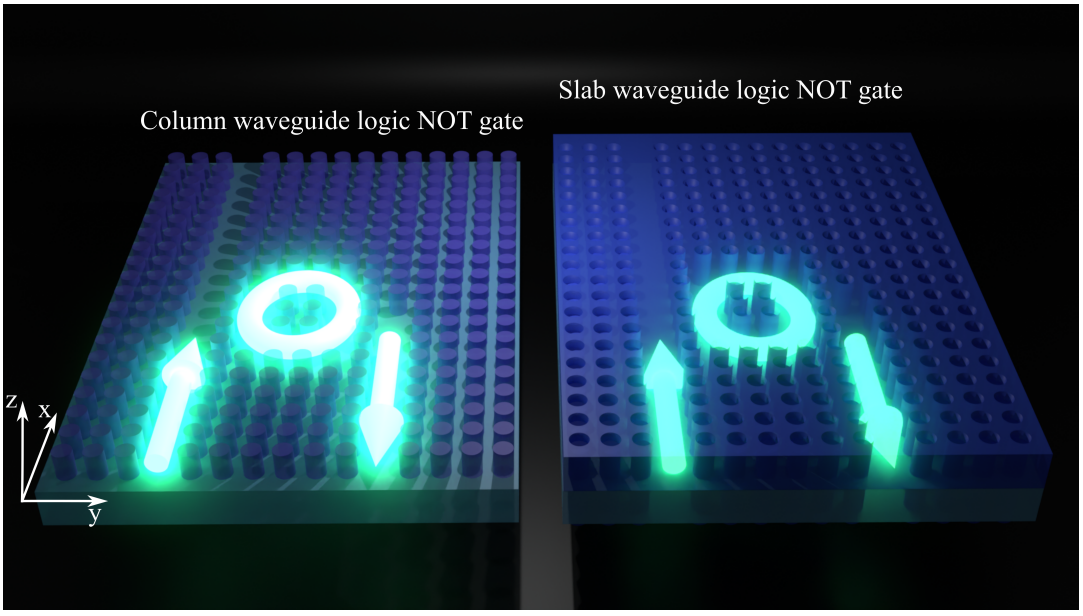


Fig. 1. Column waveguide (left) and slab waveguide (right) logical NOT gate concepts.

[1] Cersonsky, R.K., Antonaglia, J., Dice, B.D. et al. The diversity of three-dimensional photonic crystals. Nat Commun 12, 2543 (2021). https://doi.org/10.1038/s41467-021-22809-6.
[2] Zhipeng Ma, Yuanjian Wan, Yu Zhang, and Jian Wang, "Broadband lateral leakage suppression for TM polarization empowered by slab-photonic-crystal-modified ridge waveguide," Opt. Express 32, 31730-31740 (2024).
[3] Liu, G.; Wang, F.; Gao, Y.; Jia, B.; Guan, X.; Lu, P.; Song, H. Topology Optimization of Low-Loss Z-Bend 2D Photonic Crystal Waveguide. Photonics 2023, 10, 202. https://doi.org/10.3390/photonics10020202.
[4] Luis Pedraza Caballero, Michelle L. Povinelli, Jhonattan C. Ramirez, Paulo S. S. Guimarães, and Omar P. Vilela Neto, "Photonic crystal integrated logic gates and circuits," Opt. Express 30, 1976-1993 (2022).
[5] M.A. Butt, S.N. Khonina, N.L. Kazanskiy, Recent advances in photonic crystal optical devices: A review, Optics & Laser Technology,Volume 142, 2021, 107265, ISSN 0030-3992, https://doi.org/10.1016/j.optlastec.2021.107265.
[6] Jeevan Jot Singh, Divya Dhawan, Neena Gupta, 2D photonic crystal hexagonal ring resonator-based all-optical logic gates, Optics & Laser Technology, Volume 165, 2023, 109624, ISSN 0030-3992, https://doi.org/10.1016/j.optlastec.2023.109624.

INVESTIGATION OF THE SPATIAL DISTRIBUTION OF THE PHOTOLUMINESCENCE SPECTRAL PROPERTIES OF PLASTIC SCINTILLATING OPTICAL FIBERS USING CONFOCAL MICROSCOPY

Mikas Iršėnas[1], Augustas Vaitkevičius[1]

[1]Vilniaus University, Institute of Photonics and Nanotechnology, Saulėtekio al. 3 Vilnius
mikas.irsenas@ff.stud.vu.lt

Plastic scintillating optical fibers have gained attention in high energy particle tracking detectors due to their flexibility, ease of fabrication, low cost, good light output, good timing and insensitivity to magnetic fields. They are employed in major experiments such as the Large Hadron Collider beauty (LHCb) experiment, where they are the central component of SciFi detector [1].

The aim of this study is to investigate distribution of various spectral properties across the cross-section of plastic scintillating optical fibers. Assessing the homogeneity of these fibers is important for ensuring uniform signal formation and accurate particle detection needed for tracking detectors application.

Two different plastic scintillating optical fibers (Kuraray) were analyzed: 78MJ and 3HF, with luminescence peaks at 450 nm and 520 nm, respectively. They are 250 μm in diameter, with structure consisting of core with activator and spectral shifter luminophores, inner polymethyl-methacrylate (PMMA) cladding and outer fluorinated polymer cladding [2].

The uniformity of samples was analyzed by investigating the spatial distribution of different photoluminescence parameters. The investigation was performed using the WITec Alpha 300S scanning confocal microscopy system coupled with a 405 nm excitation laser. Measurements were performed across the entire fiber cross-section and separately on the core center, side and cladding, using objectives with different magnifications and numerical apertures.

The measurements showed higher uniformity in 78MJ optical fiber with both core center and sides scintillating at 470 nm while cladding showed 450 nm peaks. In contrast, the 3HF fiber displayed greater spectral variation, with the core center scintillating at 460 nm and sides showing second peak at 540 nm. Also more localized peaks of 470, 530 and 450 nm were detected. 3HF fiber cladding showed peak at 500 nm. These results will be used for further research and serve as a reference for comparison with radiation-exposed plastic optical fibers.

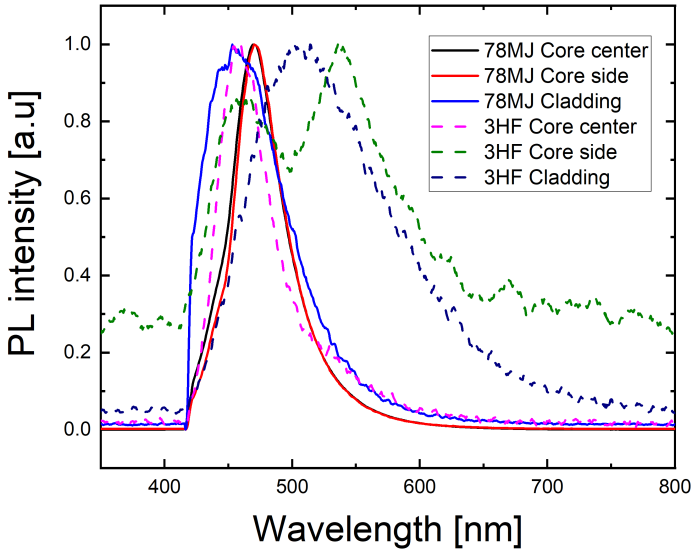


Fig. 1. Photoluminescence spectras of two different optical fibers (78MJ and 3HF) measured at core center, core side and cladding

[1] P. Hopchev, “SciFi: A large Scintillating Fibre Tracker for LHCb,” arXiv.org, 2017. https://arxiv.org/abs/1710.08325 (accessed Feb. 16, 2025).

[2] A. Bravar and Y. Demets, “Timing properties of blue-emitting scintillating fibers,” Journal of Instrumentation, vol. 17, no. 12, pp. P12020–P12020, Dec. 2022

FLEXIBLE SALISBURY SCREEN WITH MICROWAVE METASURFACE FOR ENHANCED ELECTROMAGNETIC ABSORPTION

Augustas Koklevičius[1], Paulius Ragulis[1], Žilvinas Kancleris[1], Audronė Sankauskaitė[2], Vitalija Rubežienė[2]

[1]Department of Physical Technologies, Center for Physical Sciences and Technology, Lithuania
[2]Department of Textile Technologies, Center for Physical Sciences and Technology, Lithuania
augustas.koklevicius@ftmc.lt

The need to reduce electromagnetic (EM) reflection is essential for applications in stealth technology, absorbing high power EM radiation for protection and minimal visibility to detection systems. Traditional metallic microwave metasurfaces are constrained by their rigidity, weight, and thickness. Recent studies have shown that flexible metasurfaces on textile substrates can provide effective absorption while maintaining adaptability to curved surfaces, making them suitable for applications where a substantial contribution to shielding should come from absorption [1, 2].

This study presents a flexible Salisbury screen design with metasurface [Fig. 1 (A)], aimed at reducing EM wave reflections in microwave range. The structure [Fig. 2 (B)] consists of a textile substrate fully coated with conductive paste containing PEDOT:PSS, followed by a thick non-conductive textile layer and a second textile layer coated with a metasurface made from the same paste. Reflections in structure are minimized because of destructive interference, significantly improving the overall absorption at targeted frequencies. The dimensions of the metasurface unit cell and gap size between layers are selected in such a way that their resonant frequencies would match, maximizing destructive interference for effective reflection reduction. The metasurface array consisted of 13×13 mm conductive squares arranged in a 26 mm period and a fully coated structure. The surface resistivities of layers ranged from 40 Ω/sq to 300 Ω/sq. The gaps between the layers varied from 3 mm to 9 mm. The fabric thickness was considered to be H=0.1 mm, with a dielectric permittivity of ε=1.6, and the conductive polymer thickness was h=0.01 mm.

The shielding efficiency of each individual layer was measured to assess the conductivity, quality, and performance of each layer. Experimental results were compared with CST Studio simulations to determine surface conductivity and identify the most effective layer configurations for reflection reduction. Using the conductivity values and CST simulation results, the optimal layer configurations were modeled and further optimized for improved performance. Figure 3 (C) shows the shielding effectiveness (SE) of two samples compared with simulations, highlighting the resonance effects of the metasurface and Salisbury screen.

The combination of conductive textile layers with metasurfaces reduced transmission and reflections at specific frequencies, enhancing stealth potential. The results demonstrate that the proposed flexible structure offers a compact and effective solution for minimizing electromagnetic signatures in various environments.

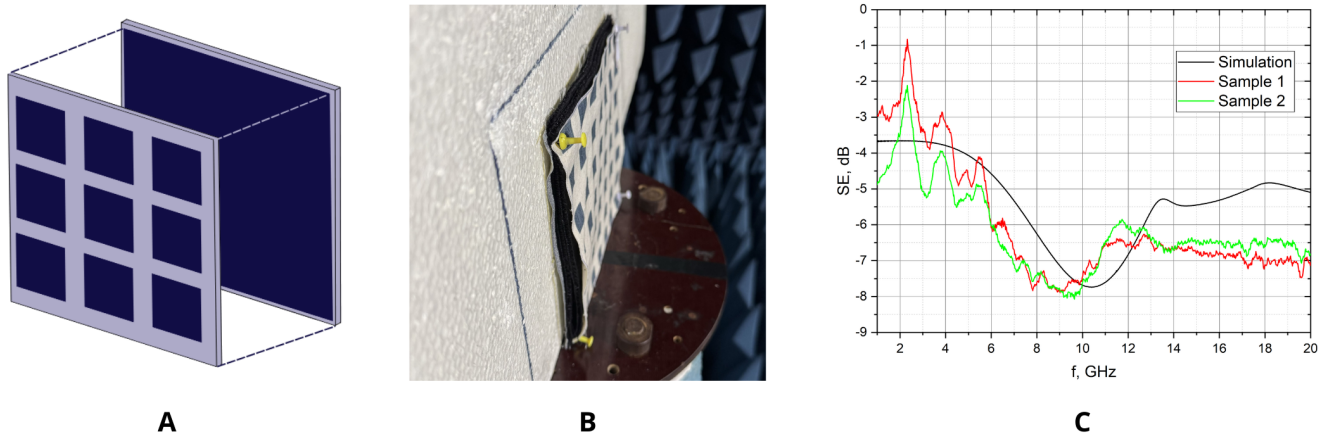


Fig. 1. Proposed structure (A). Produced Salisbury screen structure with metasurface on top (B). Measured shielding effectiveness (SE) for different layer configurations (C).

[1] Y. Zhou et al., "Flexible and lightweight metamaterials for microwave absorption," Mater. Des., vol. 160, pp. 30–39, 2018. doi:10.1016/j.matdes.2018.09.045.
[2] X. Liu et al., "Textile-based flexible metasurfaces for electromagnetic wave absorption," Mater. Sci. Eng. B, vol. 281, 2022. doi:10.1016/j.mseb.2022.115739.

ANNEALING EFFECTS ON RADIATION-DAMAGED GaN DETECTORS FOR SPACE AND HIGH-ENERGY APPLICATIONS

Mykolas Strigūnas[1], Jevgenij Pavlov[1], Tomas Čeponis[1]

[1] Institute of Photonics and Nanotechnology, Vilnius University, Vilnius, Lithuania
mykolas.strigunas@ff.stud.vu.lt

Gallium Nitride (GaN) is a wide-direct-bandgap semiconductor material widely utilized in high-voltage electronics, space applications, and medical diagnostic equipment due to its excellent radiation hardness and thermal stability [1-3]. The dual response capability of GaN makes it an attractive candidate for radiation monitoring and high-energy physics experiments, such as ALICE and CMS detectors at CERN [4]. A crucial advantage of GaN-based devices is their potential for optoelectronic characteristic recovery after exposure to radiation, enabling annealing-based restoration instead of costly device replacements. This is particularly beneficial for applications in extreme environments such as space, nuclear reactors, and particle accelerators, where radiation damage can degrade detector performance over time.

In this study, various optical and electrical characterization techniques were employed to investigate the isochronal annealing effects on proton-irradiated metal-organic chemical vapor deposition (MOCVD) GaN. Figure 1a presents the microwave photoconductivity (MW-PC) signal for pristine and irradiated samples during annealing, while Figure 1b displays the time-integrated photoluminescence (TI-PL) spectra for the same samples.

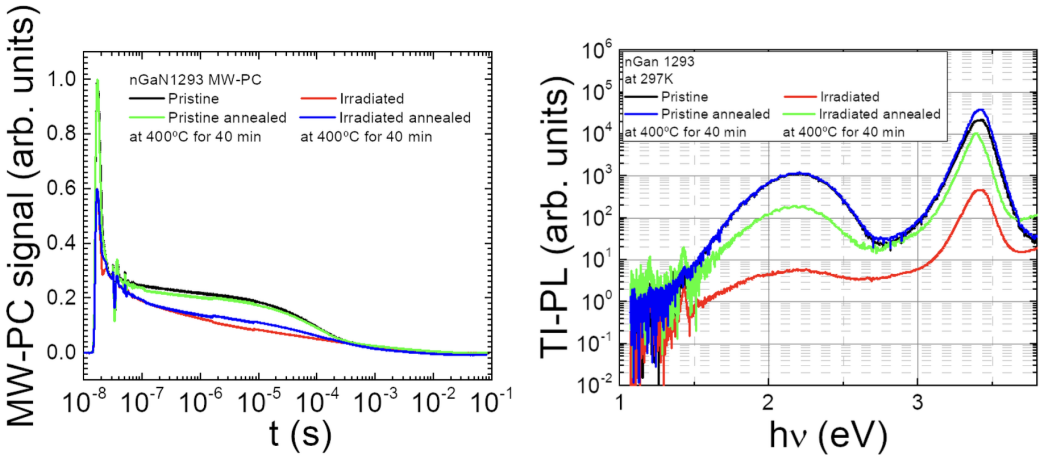


Fig. 1. (a) MW-PC signal of pristine and irradiated MOCVD GaN. (b) TI-PL spectra of pristine and irradiated samples.

The results reveal significant changes in carrier lifetime and luminescence band characteristics following annealing, demonstrating the material's potential for self-healing under controlled thermal treatment. These findings indicate that GaN detectors can regain their operational efficiency in radiation-rich environments, enhancing their longevity and reducing maintenance costs in space missions, nuclear facilities, and high-energy physics experiments. The results of this study will be presented at the conference, providing new insights into optimizing GaN-based detectors for extreme operational conditions.

[1] T. Ceponis, M. Burkanas, A. Cicinas, L. Deveikis, J. Pavlov, V. Rumbauskas, J. Venius, E. Gaubas, Combined techniques for recovery of radiation damaged detectors, Materials Science in Semiconductor Processing, 2023, 107863
[2] M. A. Reshchikov, D. O. Demchenko, D. Ye, O. Andrieiev, M. Vorobiov, K. Grabianska, M. Zajac, P. Nita, M. Iwinska, M. Bockowski, B. McEwen, F. Shahedipour-Sandvik, The effect of annealing on photoluminescence from defects in ammonothermal GaN. J. Appl. Phys. 2022; 131 (3): 035704.
[3] T. Ceponis, K. Badokas, L. Deveikis, J. Pavlov,V. Rumbauskas, V. Kovalevskij, S. Stanionyte, G. Tamulaitis and E. Gaubas, Evolution of Scintillation and Electrical Characteristics of AlGaN Double- Response Sensors During Proton Irradiation, Sensors 2019, 19, 3388
[4] J. Wang, P., Mulligan; L. Brillson, L. R. Cao. Review of using gallium nitride for ionizing radiation detection. Appl. Phys. Rev. 2025, 2, 031102

FORMATION AND INVESTIGATION OF GAN SENSORS FOR RECORDING OF IONIZING RADIATION

Jonas Seilius[1], Vytautas Rumbauskas[1], Tomas Čeponis[1], Rokas Dobužinskas[2]

[1]Institute of Photonics and Nanotechnology, Vilnius University, Saulėtekio av. 3, LT-10257, Vilnius, Lithuania
[2]Institute of Chemical Physics, Vilnius University, Saulėtekio av. 3, LT-10257, Vilnius, Lithuania
jonas.seilius@ff.stud.vu.lt

The rapid development of technology requires reliable and high-quality sensors capable of operating in extreme conditions, such as exposure to ionizing radiation. This radiation can originate from natural sources like cosmic rays, radionuclides in the Earth's crust, or radon, as well as artificial sources such as nuclear power plants, medical equipment, and scientific facilities.

Due to its high radiation resistance, gallium nitride (GaN) is being extensively studied for ionizing radiation detection. GaN exhibits superior properties, such as a wide bandgap, high thermal stability, and excellent radiation hardness. These qualities make it a promising candidate for developing sensors in particle physics, astronomy, and nuclear science [1,2].

During investigation, the tube voltage (20kV to 60kV) and current were varied.The study involved two types of samples. The first group consisted of three GaN LED structures (811, 807, 886) grown by Metal-Organic Chemical Vapor Deposition (MOCVD) at the Vilnius University Nitride Technology Group. The second group included two commercial Schottky photodiodes: GUV B (AlGaN-based) and GUV C (AlN-based). One of them (GUV B) showed no signal. The recorded values were grouped by tube voltage and plotted on a logarithmic scale.

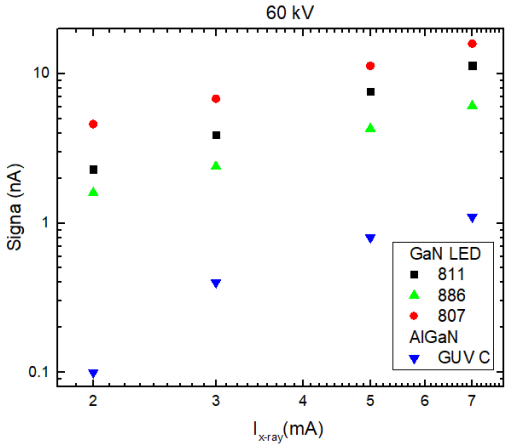


Fig. 1. Short-circuit current dependence on X-ray tube current at 60 kV voltage

The sensor response to varying X-ray intensity shows that GaN LED 807 provided the highest signal, which is linear on a double logarithmic scale. In contrast, GUV C data points were more scattered due to its weak and noisy signal. The stronger response of GaN LED 807 may result from a thinner pGaN layer, reducing charge carrier recombination. As expected, Schottky diodes were less sensitive to X-rays, and no signal was detected from GUV B due to damaged electrical contacts.

GaN LED 807 showed the highest X-ray sensitivity, with a linear response on a double logarithmic scale, suggesting reduced carrier recombination due to its thinner p-GaN layer. GUV C's broader signal dispersion indicates higher noise and lower sensitivity, while the absence of response from GUV B is attributed to electrical contact failure.

[1] Sandupatla, A., Arulkumaran, S., Ing, N. G., Nitta, S., Kennedy, J., & Amano, H. Vertical GaN-on-GaN Schottky diodes as α-particle radiation sensors. Micromachines, 11(5), 519. (2020).
[2] Geng, X., Xia, X., Liu, J., Cui, X., Sun, Z., Huang, H., ... & Liang, H.. Charge transport mechanism of self-powered GaN pin α-particle detector. Superlattices and Microstructures, 143, 106563. (2020).

DISLOCATION REDUCTION IN GaN LAYER GROWN ON PATTERNED SAPPHIRE SUBSTRATE

Karolina German[1], Tadas Malinauskas[1], Virginijus Bukauskas[2], Arūnas Kadys[1]

[1]Institute of Photonics and Nanotechnology, Faculty of Physics, Vilnius University, Saulėtekio av. 3, 10257, Vilnius
[2]Center for Physical Sciences and Technology, Saulėtekio av. 3, 10257, Vilnius
karolina.german@ff.stud.vu.lt

Gallium nitride (GaN) is a III-V group semiconductor with a direct bandgap of 3,4 eV. Incorporating elements like indium (In) or aluminum (Al) allows tuning the bandgap from 0,7 eV (InN) to 6,2 eV (AlN), covering light absorption spectra from infrared to ultraviolet, including visible wavelengths [1]. Due to tunable bandgaps, nitrides are used in ultraviolet, blue, red, and green LEDs, as well as violet laser diodes. GaN operates at temperatures up to 600 $^{\circ}\mathrm{C}$ and is resistant to radiation (protons, neutrons, gamma, and alpha particles), making it suitable for space and high-energy particle detectors [2]. With a mechanical strength of 12 GPa and thermal conductivity of 1,3 $\div$ 2,1 W/cmK [3], GaN is highly robust.

GaN layers are grown on substrates such as sapphire ($\mathrm{Al_2O_3}$), silicon (Si), or silicon carbide (SiC). SiC offers minimal lattice mismatch (3,5 $\%$) but it is expensive, while sapphire is more cost-effective despite higher lattice mismatch (16 $\%$).

Growing GaN on sapphire can introduce defects, reducing carrier mobility and inducing cracks due to thermal expansion differences. Techniques to minimize defects include dual-step growth, dielectric layer masks, and patterned sapphire substrates (PSS). PSS involves forming structures like cones or pyramids on the substrate, guiding initial GaN island formation and improving layer quality [4].

During the practical work, we successfully optimized the growth process of monocrystalline GaN layers at different stages on patterned sapphire substrates (PSS) using MOVPE. We investigated the influence of growth temperature on the surface morphology and crystalline structure of the GaN layer. By reducing the dislocation density, we improved the quality of the GaN crystal. The obtained results confirm that the continuous GaN layer grown on PSS is suitable for further technological research and will be used to achieve the objectives of ongoing projects.

Keywords: MOVPE, GaN, dislocation density, PSS.

[1] S. Gnanaeswaran, Study of energy band diagrams of group III-Nitride heterostructures, 2003.
[2] A. Y. Polyakoc et al, Radiation effects in GaN matterials and devices, Journal of Materials Chemistry, 2012.
[3] F. Roccaforte and M. Leszczynski, Introduction to gallium nitride properties and applications, 2020.
[4] Lin Shang et al, The effect of nucleation layer thickness on the structural evolution and crystal quality of bulk GaN grown by a two-step process on cone-patterned sapphire substrate, Journal of Crystal Growth, 2016.

SENSOR BASED ON HOT CARRIER EFFECT FOR ELECTROMAGNETIC RADIATION DETECTION

Vladyslav Kyshchun[1], Yana Faier[1], Oleksandr Masalskyi[1,2], Ihor Zharchenko[1,2], Jonas Gradauskas[1,2], Aldis Šilėnas[2], Aurimas Čerškus[1,2]

[1]Department of Physics, Vilnius Gediminas Technical University, Lithuania
[2]Laboratory of Electronic Processes, Center for Physical Sciences and Technology, Lithuania
oleksandr.masalskyi@ftmc.lt

Carrier heating process in semiconductors is a result of intraband absorption, so-called below band gap absorption and interband absorption of photons with energy much larger than the band gap of a semiconductor. This nature of hot carrier effect gives reasons to discuss the controversial place of it in photovoltaics. On the one side, hot carrier photocurrent across a p-n junction suppresses classical photocurrent caused by electron-hole pair generation and thereby decreases the efficiency of solar cells because these currents have opposite polarities [1]. On the other side, since the hot carrier photocurrent current goes from the intraband absorption of photons, this phenomenon can be used to develop detectors of electromagnetic radiation of photons having energy below the band gap of the absorber. This study presents GaAs/AlGaAs ratchet sensor based on the hot carrier effect (Fig. 1) [2]. The detector was fabricated on an n-type GaAs wafer with two layers of graded gap GaAs-$Al_{0.2}Ga_{0.8}As$ grown by liquid phase epitaxy. The sensor was illuminated with pulsed (17 ns) laser radiation of up to 10 MW/cm^2 light intensity of 1.064 μm wavelength with corresponding photon energy 1.17 eV which is lower than the width of the GaAs band gap (1.42 eV). The photoresponse was recorded at 300 and 80 K temperatures and depicted in Fig 1.

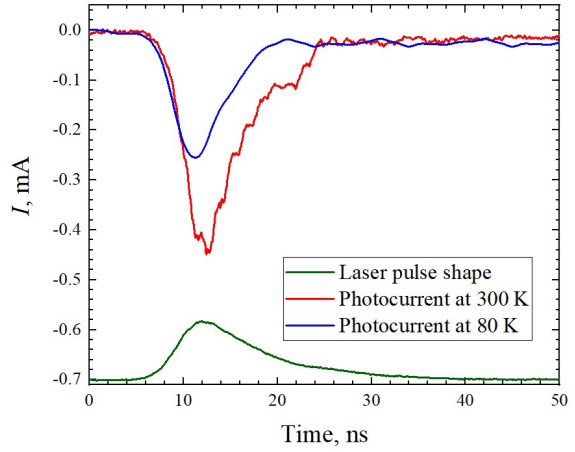


Fig. 1. Photocurrent induced across the ratchet-based sensor under pulsed laser illumination of 1.064 μm at 7.5 MW/cm^2 light intensity. Red and blue lines indicate photocurrent at 300 K and 80 K, respectively; the green line shows laser pulse shape in arb. u.

The sensor is fast, it gives information about the ns-long laser pulse shape since photoresponse pulse completely follows the laser signal shape [3]. Also, the results show that the developed sensor has linear current-power dependence at both temperatures. Finally, the observed decrease in the detected photocurrents at 80 K compared to 300 K first of all is attributed to the absorption coefficient of GaAs decreasing with temperature.

In conclusion, the ratchet-based GaAs/AlGaAs structure showed itself as a possible novel type of electromagnetic sensor operating based on the hot carrier effect. The band structure of the device is weakly dependent on the temperature, which makes it possible to use the sensor in a wide range of temperatures. To increase the voltage sensitivity, the number of active graded gap layers should be increased. Expected, that the sensor's response time can reach the picoseconds scale, since the energy relaxation time of hot carriers is about 1 ps in semiconductors. Linear dependence of the output photocurrent on light intensity provides and simplifies an approach for setting the fitting function of the sensors. All these features make this device highly advantageous for a wide range of industrial applications.

[1] J. Gradauskas, S. Ašmontas, A. Sužiedėlis et al., Influence of hot carrier and thermal components on photovoltage formation across the p-n junction, Appl. Sci. 10, 1-8 (2020).
[2] J. Gradauskas, S. Ašmontas, A. Sužiedėlis et al., Reketinis plataus spektro spinduliuotės jutiklis. (Patent, Lithuania 2023).
[3] O. Masalskyi, Investigation and application of hot carrier phenomenon in photovoltaics (Doctoral thesis, Lithuania 2023)

INVESTIGATION OF ANTENNA-COUPLED ALGAN/GAN HIGH ELECTRON MOBILITY TRANSISTORS FOR SUB-THZ WAVES DETECTION

Miroslav Saniuk[1], Maxim Moscotin[1], Justinas Jorudas[1], Irmantas Kašalynas[1]

[1]Terahertz Photonics Laboratory, Department of Optoelectronics, Center for Physical Sciences and Technology (FTMC), Vilnius, Lithuania
miroslav.saniuk@ftmc.lt

Terahertz (THz) radiation is an electromagnetic field oscillations with frequencies in the range from 300 GHz to 10 THz (λ = 1 mm - λ = 30 µm). Such electromagnetic radiation can effectively penetrate materials that are opaque to visible light, but unlike X-rays, THz radiation is non-ionizing, making it safe for human health. In comparison to microwave radiation, THz waves offer superior spatial resolution, making them highly useful in imaging applications. These properties make THz radiation useful in various fields, including security, spectroscopy, medicine, and telecommunications. However, the development of cost-effective and high-speed detection methods for terahertz radiation remains a significant scientific challenge.

To address this problem, new semiconductor sensors for THz radiation are being developed, operating on the principle of plasma wave excitation in the channel of a high-electron-mobility transistor (HEMT) with a two-dimensional electron gas (2DEG) [1]. These sensors can function in either a resonant regime, where a narrow responsivity peak with high values is achieved, or a non-resonant regime, which provides the lower responsivity values but with the wider responsivity peak. To create a sensor capable of operating in both detection regimes, EdgeFET-type HEMTs have been proposed [2]. In this transistor geometry, the channel length is significantly larger than its width ($L_{CH} >> W_{CH}$), and two bow-tie antennas are connected to the transistor electrodes. The first set of bow-tie antenna elements is connected to the channel electrodes, forming an ohmic coupling (S-D). The second set of antenna elements consists of two gate electrodes, symmetrically positioned relative to the channel and connected through the AlGaN barrier, forming a capacitive coupling (G-G). This transistor geometry enables control of the channel width by applying a gate voltage, allowing switching between resonant and non-resonant operation modes.

In this work, the responsivity of modified AlGaN/GaN EdgeFETs with different channel lengths (21 µm, 13.5 µm, and 9 µm) to 150 GHz and 300 GHz radiation was investigated in a non-resonant regime. The results showed that the transistors responsivity at 150 GHz increases as the channel length decreases. Additionally, capacitive coupling (G-G) was found to provide higher responsivity values than ohmic coupling (S-D). When comparing sensor performance at different frequencies, the responsivity in ohmic mode (S-D) at 300 GHz was up to 5 times higher than at 150 GHz, whereas capacitive coupling (G-G) resulted in the lowest responsivity values.

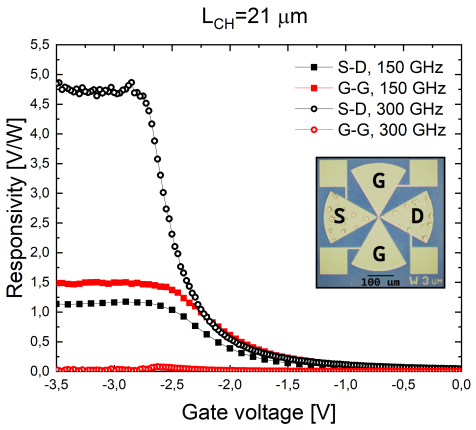


Fig. 1. Responsivity of M-EdgeFET with 21 µm channel length to 150 and 300 GHz radiation as a function of gate voltage using ohmic (S-D) and capacitive (G-G) coupling.

[1] M. Dyakonov and M. Shur, Plasma wave electronics: novel terahertz devices using two di mensional electron fluid, IEEE Transactions on Electron Devices, 1996, 43, 1640–1645.
[2] P. Sai, D. B. But, I. Yahniuk, et al., Algan/gan field effect transistor with two lateral Schottky barrier gates towards resonant detection in sub-mm range, Semiconductor Science and Technology, jan 2019, 34, 024002.

TEMPERATURE-DEPENDENT PHOTOLUMINESCENCE OF LOCALIZED CARRIERS IN III-NITRIDE QUANTUM WELLS BY KINETIC MONTE-CARLO SIMULATION

Ralfas Chvainickas[1], Oleg Kravcov[1]

[1]Institute of Photonics and Nanotechnology, Faculty of Physics, Vilnius University, Saulėtekio av. 3, LT-10257, Vilnius, Lithuania
ralfas.chvainickas@ff.stud.vu.lt

Nitrides are compounds consisting of nitrogen and electropositive elements, commonly used in electronic and optoelectronic applications due to their strong covalent bonding and thermal stability. Temperature - dependent photoluminescence of localized carriers in quantum wells is influenced by disorder, which comes from alloy fluctuations, interface roughness and potential variations that create localized states affecting localized carrier dynamics. It affects the spectral peak position, producing an S - shaped shift, and the linewidth, resulting in a W - shaped broadening. Typically, it is simulated using Monte - Carlo algorithm to investigate exciton energy redistribution among localized states via hopping. The results help clarify experimental observations and reveal how localized carriers behave in disordered quantum wells.

To investigate the temperature-dependent photoluminescence of localized carriers in disordered III - nitride quantum wells, we employed a computational approach using Python 3 to model exciton dynamics under varying conditions. The study focused on the spectral peak position, full width at half maximum (FWHM), photoluminescence intensity, and internal quantum efficiency (IQE), analysing their dependence on temperature, carrier density, and localization parameters. Kinetic Monte - Carlo (KMC) simulations were utilized to capture localized carriers energy redistribution among localized states through hopping mechanisms. The simulated results will be compared with experimental measurements, enabling a comprehensive understanding of the interplay between disorder-induced localization effects and recombination dynamics.

[1] S. D. Baranovskii, R. Eichmann, and P. Thomas, ”Optical spectra in quantum wells are in many cases strongly influenced by disorder...,” Phys. Rev. B, vol. 58, no. 19, pp. 13081–13087, 1998.

TRANSIENT CATHODOLUMINESCENCE IN NITRIDE V-DEFECTS

Gabija Soltanaitė[1], Žydrūnas Podlipskas[1], Mantas Migauskas[1]

[1]Vilnius university
gabija.soltanaite@ff.vu.lt

Carrier recombination and diffusion in nitride materials have been extensively studied on a macroscopic scale and linked to various sample characteristics, including quantum well width, alloy composition, dislocation density, and overall efficiency. However, the precise mechanisms by which V-defect size, morphology, and local environment affect carrier diffusion and recombination remain unclear. With the rise of high-precision micro-scale optoelectronics, where defect impact is most pronounced, it is crucial to analyze these defects at the nanoscale and in real time.

This study aims to provide an up-close examination of V-defects, which naturally form in InGaN, by employing time-resolved cathodoluminescence (TRCL) to obtain transient nanoscale CL profiles of dislocation-induced defects, enabling a deeper understanding of carrier behavior within and around them. The main objective is to profile transient times and cathodoluminescence intensity in relation to defect size. Transient times were extracted by capturing luminescence decay both in areas unaffected by the defect and along the defect's geometry on the same axis. First, a broad-area CL and SEM scans of the sample were performed. Then, measurements of similarly sized defects within InGaN samples were conducted, capturing intensity and time variations, along with CL maps and SEM images of individual defects. After data processing, the extracted parameters were used to visualize profiles of individual defects and defect groups of similar sizes. Depending on size and other potential factors, V-defects are known to influence sample properties in a dual way. The results reveal that larger defects enhance carrier diffusion length, but at the same time, they introduce non-radiative recombination channels, reducing overall efficiency. In some cases, however, V-defects have been observed to screen dislocations, mitigating their negative effects on non-radiative recombination.

By analyzing measured transient times and intensity trends—such as intensity drop and faster transients—defect profiles were evaluated based on two key factors: [1] the depth of the profile, reflecting the contrast of each parameter inside and outside the defect, and [2] luminescence variations across the defect structure. For future work, full TRCL maps would enable a more detailed analysis of carrier lifetime and luminescence intensity by capturing decay dynamics and intensity variations fully in a selected area of the sample. Resolving carrier dynamics at the defect level would offer advances for defect-engineered optoelectronics, key insights for optimizing micro-LEDs, quantum wells, and next-generation GaN-based devices.

[1] Kim, M. K., Choi, S., Lee, J. H., Park, C. H., Chung, T. H., Baek, J. H., & Cho, Y. H. (2017). Investigating carrier localization and transfer in InGaN/GaN quantum wells with V-pits using near-field scanning optical microscopy and correlation analysis. Scientific Reports, 7. https://doi.org/10.1038/srep42221

[2] Sheen, M. H., Kim, S. D., Lee, J. H., Shim, J. I., & Kim, Y. W. (2015). V-pits as Barriers to Diffusion of Carriers in InGaN/GaN Quantum Wells. Journal of Electronic Materials, 44(11), 4134–4138. https://doi.org/10.1007/s11664-015-3994-z

INVESTIGATION OF BULK HETEROJUNCTION (BHJ) SOLAR CELLS USING A KINETIC PHOTOCONDUCTIVITY METHOD

Dovilė Vasiliauskaitė[1,2], Ernestas Kasparavičius[2], Vidmantas Gulbinas[2]

[1]Vilnius University
[2]Center for Physical Sciences and Technology
dovile.vasiliauskaite@ff.stud.vu.lt

In recent decades, renewable energy sources, such as wind, solar, and hydroelectric power, have garnered immense interest in various scientific and technological areas of research, with solar power being one of the most promising fields. Rapid advancements in the power conversion efficiency of organic solar cells, from 2% to 19.19% [1, 2] in just over fifteen years of research, have shown the conceivable possibility of replacing silicon-based photovoltaic (PV) devices with cheaper polymer-based alternatives. Key factors in such a possible transition are the unique properties of organic solar cells. The manufacturing costs of polymer-based devices are significantly lower compared to traditional silicon PVs, they are less dependent on finite natural resources, and they are generally less eco-toxic [3, 4]. Additionally, polymer-based devices can be flexible and transparent, with their color modifiable and adjustable, allowing for a plethora of aesthetic and functional organic PV device options [5].

This work investigates the charge carrier dynamics of organic bulk-heterojunction solar cells based on a D18:Y6 donor/acceptor blend, with different hole-transporting layers (HTLs) composed of PEDOT:PSS, PTAA (hole-transporting materials), 2PACz, and MeO-2PACz (self-assembling monolayers). Charge carrier lifetimes of classical inverted ITO/HTL/D18:Y6/PMMA/Ag and modified inverted ITO/HTL/D18:Y6 organic solar cells were investigated by applying the kinetic photoconductivity method and varying the excitation conditions of the samples. The charge carrier dynamics of both cell structures were compared. The results showed that PEDOT:PSS and PTAA performed best as the hole-transporting layers in classical inverted solar cells, while only PTAA showed a significant effect in modified inverted cells. Additionally, the results demonstrated that the modified inverted structure is a suitable alternative for investigations of charge carrier dynamics in organic solar cells.

[1] Ricardo A. Marques Lameirinhas, João Paulo N. Torres and João P. de Melo Cunha, A Photovoltaic Technology Review: History, Fundamentals and Applications, Energ. 15(5), 1823, 2022.
[2] Luye Cao, Hengyuan Zhang, Xiaoyang Du, Hui Lin, Caijun Zheng, Gang Yang, Min Deng, Xiaopeng Xu, Silu Tao, Qiang Peng, Highly electronegative additives suppress energetic disorder to realize 19.19 % efficiency binary organic solar cells, Nan. Energ. 129, 110016, 2024
[3] Elina Buitrago, Anna Maria Novello, Thierry Meyer, Third-Generation Solar Cells: Toxicity and Risk of Exposure, Helv. Chim. Act. 103, 9, 2020.
[4] Miles Krebs-Moberg, Mandy Pitz, Tiara L. Dorsette, Shabbir H. Gheewala, Third generation of photovoltaic panels: A life cycle assessment, Ren. Energ. 164, 556-563, 2021.
[5] Christoph J. Brabec, Andreas Distler, Xiaoyan Du, Hans-Joachim Egelhaaf, Jens Hauch, Thomas Heumueller, Ning Li, Material Strategies to Accelerate OPV Technology Toward a GW Technology, Adv. Energ. Mat. 10, 43, 2001864, 2020.

B-SITE MIXING EFFECTS ON PHASE TRANSITIONS AND DIELECTRIC PROPERTIES OF $MAPb_{1-x}Sn_xBr_3$ HYBRID PEROVSKITES

Gabrielius Rimkus[1], Sergejus Balčiūnas[1], Hanna R. Petrosova[3], Olesia I. Kucheriv[3], Rokas Lemežis[2], Vytautas Klimavičius[2], Vidmantas Kalendra[1], Jūras Banys[1], Il'ya A. Gural'skiy[3], Mantas Šimėnas[1]

[1]Faculty of Physics, Vilnius University, Saulėtekio 3, LT-10257 Vilnius, Lithuania
[2]Institute of Chemical Physics, Vilnius University, Saulėtekio 3, LT-10257 Vilnius, Lithuania
[3]Department of Chemistry, Taras Shevchenko National University of Kyiv, Kyiv 01601, Ukraine
gabrielius.rimkus@ff.stud.vu.lt

Ion mixing is a powerful strategy for tuning the performance and stability of hybrid perovskite-based photovoltaic devices. While A- and X-site mixing have been extensively studied, the effects of B-site mixing on the structural and dynamic properties of MA-based perovskites remain less explored [1].

In this study, the structural and dynamic properties of mixed lead–tin halide perovskites $MAPb_{1-x}Sn_xBr_3$ are primarily investigated using broadband dielectric spectroscopy. Complementary experiments, including differential scanning calorimetry and nuclear quadrupole resonance, performed by colleagues, enabled the mapping of the temperature–composition phase diagram. The results indicate that B-site mixing slightly stabilizes the cubic phase, although its influence on structural phase transitions is less pronounced compared to A- and X-site mixing.

Dielectric measurements further reveal that B-site mixing increases the number of dynamically active MA cations in the low-temperature phase, substantially disrupting the long-range ordering of the organic sublattice and suggesting the formation of a glassy phase [2]. Additionally, the increased activation energy in mixed compounds indicates that B-site mixing raises the reorientation barrier of MA cations.

These findings provide insights into the complex interplay between structural and dynamic properties in mixed-metal perovskites, contributing to their potential optimization for photovoltaic applications.

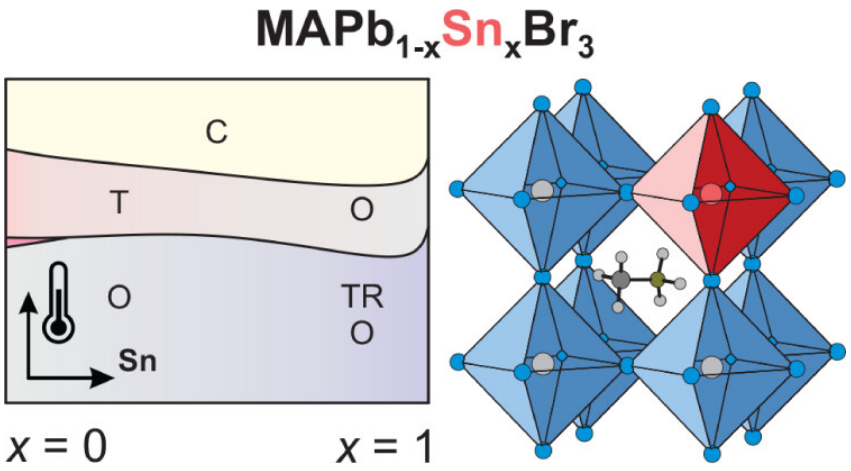


Fig. 1. Temperature–composition phase diagram (left) of mixed $MAPb_{1-x}Sn_xBr_3$ perovskites. Abbreviations: C = cubic, T = tetragonal, O = orthorhombic, TR = triclinic. Structural representation of the perovskite framework (right), with blue octahedra representing $PbBr_6$ and red octahedra indicating $SnBr_6$ units.

[1] M. Šimėnas, et al. Phase Transitions and Dynamics in Mixed Three- and Low-Dimensional Lead Halide Perovskites. Chem. Rev 2024, 124, 2281–2326.
[2] G. Rimkus, et al. B-Site Mixing Effects in Hybrid Perovskites: Phase Transitions and Dielectric Response of MAPb1-xSnxBr3. Chem. Mater 2024, 36, 7397–7405.

INVESTIGATION IF SBSEI THIN FILMS WITH OPEN AND CLOSED ANNEALING VARIATIONS

Deividas Vainauskas[1], Vidas Pakštas[1], Rokas Kondrotas[1]

[1]Department of Characterization of Materials Structure, State research institute Center for Physical Sciences and Technology, Sauletekio av. 3, Vilnius, Lithuania
deividas.vainauskas@ftmc.lt

Recently, antimony selenoiodide (SbSeI), one of the chalcohalide semiconductors that belongs to V-VI-VII class materials has been the subject of growing interest for applications, such as, X-ray and γ-ray detection, photocatalysis, solar cells, and in other optoelectronic devices. SbSeI enjoys additional benefits compared to other PV thin film systems, including the earth abundant and low toxicity chemical composition, high thermodynamic stability and large absorption coefficient (up to 10^5 cm^{-1}). Although SbSeI has very promising properties, there are few studies where this material has been used as an absorber layer in solar cells and reported power conversion efficiency was low 4,1 % [1]. One of the key challenges in synthesizing SbSeI thin film absorbers for PV application, is its tendency to form porous needle-like structure [2].

Because of quasi-1-dimensional crystalline structure of SbSeI, it has a preferred growth direction along [001] axis resulting in rod-shaped grain growth. The goal of this study was to find synthesis approach that could allow to obtain continuous, uniform and compact SbSeI thin films morphology.

In this study we used a two-stage synthesis route where the first precursor layers were deposited and then followed by annealing step. SbSeI precursors films were deposited under vacuum by thermal evaporation method. Thin films deposition parameters, such as evaporation power, distance from source to substrate and source boat geometry were optimized for synthesis of compact, uniform, continuous precursor films. For the crystallization stage, annealing under N_2 atmosphere was performed with temperatures ranging from 150 ^{o}C up to 300 ^{o}C to achieve crystalline, compact SbSeI thin film with molar ratio near 1:1:1. Two annealing configurations were explored: a) open space and b) closed space. Structural properties of SbSeI thin films were characterized by XRD (θ-θ, Bragg-Brentano geometry), SEM and EDX methods.

In terms of precursor film homogeneity and uniformity in thickness, we found that optimal distance between source and sample was 5 cm. Also we found that precursor film composition was dependent on the evaporation power and under optimal conditions near-stoichiometric molar composition was obtained in open configuration, but at higher substrate temperatures SbSeI starts to decompose and Sb_2Se_3 phase is present. On contrary, annealing with closed configuration resulted in a stable SbSeI phase even up to 300 ^{o}C. Using a two-stage synthesis route we were able to achieve uniform, compact and high crystalline quality SbSeI thin films.

[1] Nie, Riming, et al. ”Efficient and stable antimony selenoiodide solar cells.” Advanced Science 8.8 (2021): 2003172.
[2] Caño, Ivan, et al. ”SbSeI and SbSeBr micro-columnar solar cells by a novel high pressure-based synthesis process.” Journal of Materials Chemistry A 11.33 (2023): 17616-17627.

XRD STUDY OF COPPER-TIN SULPHIDE FILMS ON FTO GLASS

Dominyka Zubrickaitė[1], Asta Bronušienė[1], Ingrida Ancutienė[1]

[1]Department of Physical and Inorganic Chemistry of Kaunas University of Technology
dominyka.zubrickaite@ktu.edu

Various tin sulfides are chalcogenide semiconductor materials that have attracted great interest due to their abundant, inexpensive, and non-toxic elements, as well as their suitable optical and electrical properties for use as photovoltaic absorbers [1]. The ternary Cu-Sn-S system includes stable compounds such as Cu_2SnS_3, Cu_3SnS_4, and Cu_4SnS_4 [1]. Cu_2SnS_3 is the most studied compound in this system and has been successfully applied in thin-film solar cells. Additionally, Cu_4SnS_4 has demonstrated photovoltaic properties in thin-film devices with an efficiency of 2.34% [1]. The aim of this work was to synthesize copper-tin sulphide films on FTO glass by sequential ion adsorption and reaction (SILAR) method and characterize the films using XRD analysis. For the deposition of tin sulphide films, each sample was prepared in the following steps: firstly, the cleaned FTO substrate was immersed into a cationic precursor (0.1 M $SnCl_2$ and citric acid solution) for 30s and the tin ions on the top of the substrate were adsorbed, secondly, a sample was immersed in an anionic precursor (0.1 M Na_2S solution) for 30s. During this step sulphide ions react with tin ions adsorbed on the top and form tin sulphide films. To remove loosely bound ions, the samples were washed in distilled water for 20s after immersions in the cationic and anionic precursors. In this study 20, 30,40 SILAR cycles were carried out. Then the samples were modified with solutions (0.1 M) of copper (II) and copper (II/I) ions, carried out with solutions of copper (II) sulphate or copper(II) sulphate with hydroquinone, for different durations (10; 20; 30 minutes). Then, the samples were annealed at 200 °C to increase the crystallinity of obtained films. X-ray diffraction analysis of the copper-tin sulphide films on the FTO glass slides was carried out using a Bruker AXS D8 Advance X-ray diffractometer. The X-ray diffractograms of the films were analysed using the Search Match software package. X-ray diffraction analysis identified SnS, Sn_2S_3, Sn_3S_4, anilite, djurleite, digenite and mixed copper tin sulphide phases Cu_4SnS_4 and $Cu_2Sn_3S_8$. From the RSDA analysis it can be concluded that the number of cycles, the duration of treatment with copper (II) salt solution and the use of hydroquinone, and annealing temperature affects the deposited layers.

[1] ROBLES, V. et al. Copper tin sulfide (CuxSnSy) thin films evaporated with x = 3,4 atomic ratios: Influence of the substrate temperature and the subsequent annealing in sulfur. Materials Research Bulletin, 2016, Vol. 83

NEW CARBAZOLE-BASED DERIVATIVES AS HOST MATERIALS FOR VERY EFFICIENT OLEDS

Raminta Beresneviciute[1], Daiva Tavgeniene[1], Dovydas Blazevicius[1], Kuan-Wei Chen[2], Yu-Hsuan Chen[2], Saulius Grigalevicius[1], Chih-Hao Chang[2]

[1]Department of Polymer Chemistry and Technology, Kaunas University of Technology, Kaunas, Lithuania
[2]Department of Electrical Engineering, Yuan Ze University, Taiwan
raminta.beresneviciute@ktu.lt

Over the past decade, organic light-emitting diodes (OLEDs) have been widely tested in next-generation electronic devices due to potential applications in full-color flat-panel displays and solid-state lighting. Compared with traditional liquid crystal display, OLEDs have many unique features, such as high contrast, wide viewing angle, low driving voltage, flexibility, fast response, and lightweight [1-3]. Organic electroactive materials are extensively synthesized and studied as components of the mentioned devices. Here, we present new carbazole-based derivatives with carbazole rings as electron-donating fragments and pyridinyl fragments as electron acceptors. The structures of materials **HM1-HM4** are shown in Figure 1.

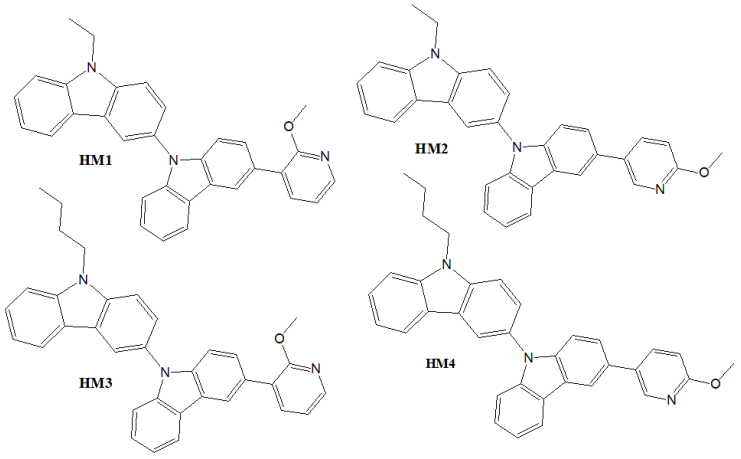


Fig. 1. The structures of materials **HM1-HM4**

The electroactive derivatives demonstrated suitable thermal, film forming and optoelectronic properties as potential host materials for green-emitting phosphorescent $Ir(ppy)_2$ guest and were applied for preparation of the efficient devices. The objective materials have very high thermal stabilities (temperatures of 5% weight loss 371-387 ^{o}C) and can form amorphous layers, also having rather high glass transition temperatures in the region of 89-97 ^{o}C. Triplet energy gaps of the four compounds were about 2.7-2.8 eV, making them appropriate for use as host materials in green phosphorescent OLEDs with $Ir(ppy)_3$ guest. Also, a composite host system incorporating a synthesized **HM** host and bis-4,6-(3,5-di-3-pyridylphenyl)-2-methylpyrimidine was developed to enhance hole and electron transport within the emitting layer. Notably, the device using 9-(9-butylcarbazol-3-yl)-3-(2-methoxypyridin-3-yl)carbazole (**HM2**) host outperformed the other devices, achieving peak efficiencies of 16.9% (58.3 cd/A and 65.0 lm/W) with maximum luminance exceeding 241100 cd/m^2. Finally, these results confirm that the specific molecular and device architecture designs are effective, providing new ways for developing efficient emitting layers of the OLED devices in future.

Acknowledgements

We gratefully acknowledge the funding support from the Research Council of Lithuania (grant No. S-MIP-22-84) and from the National Science and Technology Council of Taiwan, under the grant number (MOST 111-2221-E-155-012-MY2 and NSTC 112-2923-E-155-002-MY4).

[1] H. W. Chen, J. H. Lee, B. Y. Lin, S. Chen, S. T. Wu. Liquid crystal display and organic light-emitting diode display: present status and future perspectives (Light. Sci. Appl., 2018;7:17168)
[2] X. Wu, X. Yan, Y. Chen, W. Zhu, P. T. Chou. Advances in organic materials for chiral luminescence-based OLEDs. (Trends. Chem., 2023;5:734-47)
[3] I. Siddiqui, S. Kumar, Y. F. Tsai, P. Gautam, K. Shahnawaz, K. Kesavan, et. al. Status and challenges of blue OLEDs: A review. (Nanomaterials 2023;13:2521)

THE INFLUENCE OF MILLING ON THE GRAIN SIZE OF LEAD-FREE SOLID SOLUTIONS $0.8Na_{0.5}$ $Bi_{0.5}TiO_3$ - $0.2BaTiO_3$.

Ugnius Dominykas Sviackevičius[1], Artyom Plyushch[1], Rokas Dobužinskas[1], Šarūnas Svirskas[1], Algirdas Selskis[2], Robertas Grigalaitis[1], Jūras Banys[1]

[1]Faculty of physics, Vilnius university, Saulėtekio 9, LT-10222, Vilnius, Lithuania
[2]Center for Physical Sciences and Technology, Saulėtekio 3, LT-10257 Vilnius, Lithuania
dominykas.sviackevicius@ff.vu.lt

Piezoelectric ceramics play an important role in electronics as actuators, sensors, resonators and ultrasonic transducers. However, most conventional piezoelectrics contain lead, posing environmental and health hazards. Increasing interest in lead-free alternatives is driven by the Restriction of Hazardous Substances (RoHS) directive, which limits the use of lead-based materials. Among the most promising lead-free ferroelectric ceramics is the $(1-x)(Na_{1/2}Bi_{1/2}TiO_3) - x(BaTiO_3)$ family. This research aims to synthesize the $0.8Na_{1/2}Bi_{1/2}TiO_3 - 0.2BaTiO_3$ via the solid-state reaction method and to investigate the effect of varying milling durations on the mean grain size of powders, in order to optimize its microstructural and functional properties.

Commercially available Na_2CO_3, Bi_2O_3, TiO_2, and $BaCO_3$ (Sigma-Aldrich) were weighed and milled with the planetary mill in isopropyl alcohol for 24 hours. The mixture was then calcined at 900 °C for 4 h, milled again, pressed into 8 mm diameter pellets, and sintered at 1200 °C for 4 hours. X-ray diffraction analysis confirmed the formation of the perovskite phase and its purity. Dielectric measurements exhibited a characteristic sharp peak (see Figure 1) at a temperature of 537K, while piezoelectric and ferroelectric properties are promising in comparison to those presented in the literature.

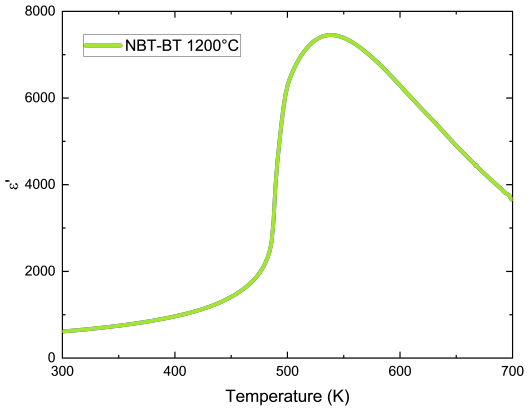


Fig. 1. Dielectric constant dependence on temperature.

TWO-STAGE SYNTHESIS OF Ca_a Si_b TiO_c COMPOUNDS

Ričardas Kleinauskas[1], Anatolijus Eisinas[1], Jolanta Donėlienė[2,3]

[1]Department of Silicate Technology, Kaunas University of Technology, Lithuania
[2]Applied Research Institute for Prospective Technologies, Vilnius, Lithuania
[3]Public Institute "Perspektyvinių technologijų taikomųjų tyrimų institutas", Vilnius, Lithuania
ricardas.kleinauskas@ktu.lt

Due to their high thermal resistence, biological compatibility and modifiable optical properties, $Ca_aSi_bTiO_c$ compounds are widely used in bioceramics, glazes [1], semiconductors and photocatalytic materials [2]. $Ca_aSi_bTiO_c$ compounds are produced by high temperature (1200-1400 °C) solid phase sintering of crystalline raw materials (CaO, SiO_2, TiO_2) [3]. In contrast, the use of initial dissolved organic (Ca/Si/Ti) salts and sol-gel synthesis can reduce the synthesis temperature to 1000 °C. However, the application of this method is limited by expensive raw materials and high solvent consumption. Therefore, this work proposes to synthesize (sol-gel) an amorphous TiO_2 additive, study its influence on the formation of calcium silicate hydrates under hydrothermal synthesis conditions and their crystalisation into $Ca_aSi_bTiO_c$ compounds during sintering. It is assumed that, unlike its crystalline forms, amorphous TiO_2 can intercalate into calcium silicate hydrates' lattice and that hydrothermal curing will lead to formation of purer $Ca_aSi_bTiO_c$ phases at lower sintering temperatures.

In this work, amorphous titanium dioxide was prepared in accordance to our earlier experiments [4]. Two base samples were prepared by mixing amorphous TiO_2, amorphous SiO_2 and CaO equal to molar ratio of 1. One of the samples was then mixed with H_2O to reach the water/solid ratio of 10. The hydrothermal synthesis was performed under saturated steam pressure of 15 bar at a temperature of 200 °C for 4 hours. After treatment, synthesis products were filtered, dried and sieved (<80 μm). Both raw crystaline and hydrothermally cured mixtures were then calcinated at temperatures of 900-1200 °C for 1 hour. Synthesis products were characterized by XRD and STA instrumental methods.

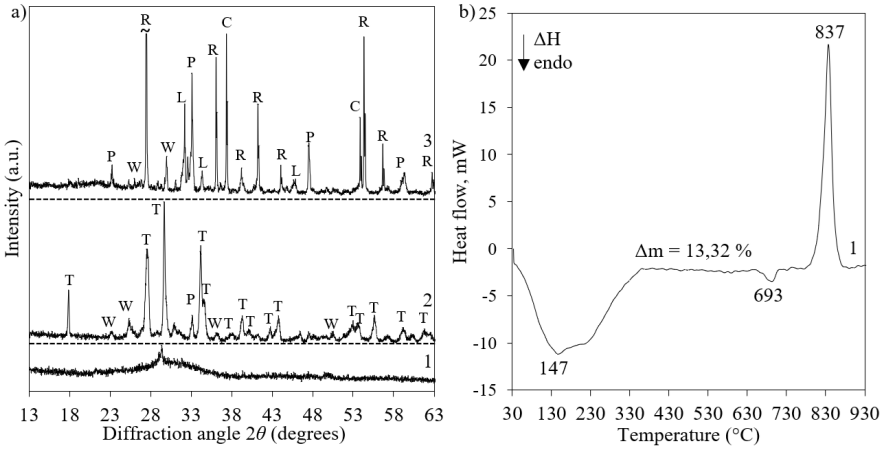


Fig. 1. a) XRD and b) DSC patterns of 1) hydrothermally cured and uncalcinated; 2) hydrothermally cured and 3) dry CaO-SiO_2-TiO_2 mixtures after calcination in 2) 900 and 3) 1200 °C. Indexes – T – titanite; W – wollastonite; P – $CaTiO_3$; L – larnite; R – rutille; C - lime

The most important aspect of two-stage preparation method is the formation of homogenous amorphous CaO-SiO_2-TiO_2-H_2O compounds (I stage) **(Fig 1. a. 1)**, which promote the formation of dominant $Ca_aSi_bTiO_c$ compounds during calcination (II stage) **(Fig 1. a. 2)** at low temperatures **(Fig 1. b; 800-880 °C)**. Meanwhile after calcination of dry sample, it was determined that crystaline CaO-SiO_2-TiO_2 mixture did not form $Ca_aSi_bTiO_c$ compounds, as secondary phases rutille, lime and calcium silicates (larnite and wollastonite) are dominant in the synthesis products **(Fig 1. a. 3)**.

[1] L. Zhihong, et al. High-solar-reflectance building ceramic tiles based on titanite (CaTiSiO5) glaze. Solar Energy, 153, 623-627, (2017).
[2] H. Shouqiang, et al. CaF2-based near-infrared photocatalyst using the multifunctional CaTiO3 precursors as the calcium source. ACS Applied Materials & Interfaces, 7.36: 20170-20178, (2015).
[3] L. Yangzi, et al. Synthesis of sphene by TiO2 combined with CaCO3 and SiO2 in solid phase and its application as ceramic opacifier. Chemical Physics, 575: 112076, (2023).
[4] J. Doneliene, et al. Effect of Precursor Nature and Sol-Gel Synthesis Conditions on TiO2 Aerogel's Structure. Molecules, 26, 5090, (2021).

DESIGN OF A TWISTED DOUBLE DONOR IN CARBAZOLE-METHYLPYRIMIDINE-BASED EMITTERS LEADING TO THE TRIPLE CHARGE-TRANSFER EMISSION

Dovydas Blaževičius[1], Gintarė Kručaitė[1], Saulius Grigalevičius[1], Oleg Dimitriev[2]

[1]Department of Polymer Chemistry and Technology, Faculty of Chemical Technology, Kaunas University of Technology, Lithuania
[2]V.E. Lashkaryov Institute of Semiconductor Physics, NAS of Ukraine, Ukraine
dovydas.blazevicius@ktu.lt

The advantages that organic light emitting diode (OLED) based technologies offer in terms of brightness, viewing angle, contrast ratio, production cost, etc. are not rivalled by liquid crystal-based displays. In this study we present novel methylpyrimidine-carbazole derivatives and influence of complication of donor arm structure to emissive properties. Thermally activated delayed fluorescence (TADF) is a now well-known emission mechanism which make it theoretically possible to achieve 100% internal quantum efficiency.Novel D2-D1-A-D1-D2 emitters with the donor arm composed of a double twisted donor-donor moieties provide additional routes for charge-transfer (CT) emission. Here we show that a structural complication of the donor arm by additional donor moiety, i.e., from D-A-D to D2-D1-A-D1-D2 yields a transition from a dual to triple CT band with corresponding red shift and increasing contribution of the low-energy emission components. The observed relationship between complexity of the donor moiety and multicomponent CT emission band in various D-A-D structures provides a clue for design of thermally activated delayed fluorescence emitters with controllable emission properties. Figure 1 depicts photoluminescence spectra, chemical structures and HOMO-LUMO distribution of new compounds.

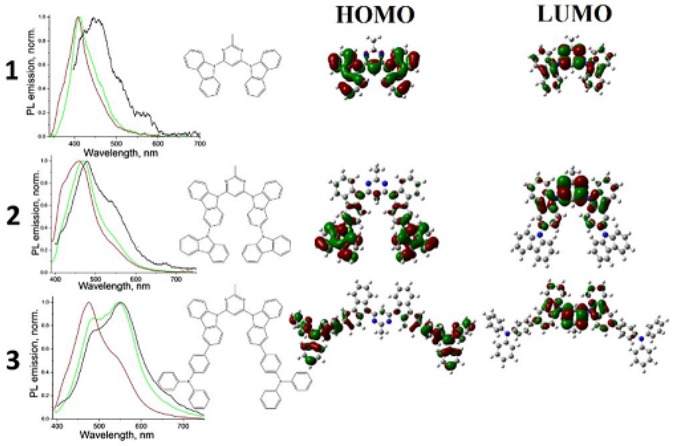


Fig. 1. PL emission spectra (green - chloroform, brown – THF, black - acetone solutions, all 10-5 M), chemical structures, HOMO and LUMO distribution

Comparison of PL emission spectra of 1, 2, and 3 in the same solvent further elucidates the difference related to the dye complexity. Specifically, in chloroform, the relative contribution of the LE emission component in terms of the integral of the first Gaussian in the spectra of 1, 2, and 3 constitutes 51:2:0, respectively, whereas the relative contribution ratio of CT1 component is 21:82:62, respectively. For CT2, the ratio is 0:18:60, respectively. That is, the compound 1 does not possess the CT2 emission, while the compound 3 losses the LE emission, respectively. In conclusion, complication of the donor arm in the twisted D-A-D compounds leads to increasing twisting disorder and, as a consequence, to appearance of additional charge-transfer routes from the different donor moieties. This is displayed as appearance of additional emission components and broadening of the PL emission spectra. The observed relationship between complexity of the donor moiety and multicomponent CT emission band in the D-A-D structures suggests new design principles of thermally activated delayed fluorescence emitters with controllable emission properties.

Acknowledgements

This work was financially supported by the Research Council of Lithuania (Grant No. S-LU-24-7) and Ministry of Education and Science of Ukraine (project M/54-2024) and in part by the Knut and Alice Wallenberg Foundation (KAW) through the Wallenberg Wood Science Center.

NUMERICAL MODELING OF SELF-ASSEMBLY OF $INDO_4$ MOLECULES ON Ag SURFACES

Jorunas Dobilas[1,2], Evaldas E. Tornau[2]

[1]Department of Functional Materials and Electronics, Center for Physical Science and Technology, Lithuania
[2]Faculty of Physics, Vilnius University, Lithuania
jorunas.dobilas@ftmc.lt

Self-assembly of organic molecules on graphite and metal surfaces into highly ordered nanostructures is one of the most interesting processes of modern physics and chemistry. Self-assembled nanolayers are nowadays used in different biological, medical applications and nanoelectronics [1].

Recently, the self-assembly of s-indacene-1,3,5,7(2H,6H)-tetrone (also known as $INDO_4$) on metallic surfaces was explored by scanning tunneling microscopy (STM) [2]. $INDO_4$ molecules can form a variety of brick wall, pin wheel and honeycomb (HON) structures on Ag(100), (111) and (110) and Cu(111) metal surfaces. These molecules can also build centered HON structures, including a special system on Ag(111), where the central molecule of the hexagon is degenerate and acts as a ”molecular switch”. Degeneracy of this ordered structure makes it very interesting from both experimental and theoretical points of view.

Different numerical methods are used to simulate the processes of molecular self-assembly, density functional theory (DFT), molecular dynamics or Monte Carlo methods being among the most popular ones.

We proposed a discrete interaction model to describe the ordering of centered HON structures of $INDO_4$ on Ag. Utilizing STM observations and DFT calculations, we introduced four different intermolecular interaction potentials in our model for $INDO_4$/Ag(100) and solved it by using the Monte Carlo (Metropolis) method (see Fig. 1). To describe the degeneracy of $INDO_4$/Ag(111) we modified the model by studying the ordering of molecular clusters, instead of individual molecules. This allowed us to demonstrate the degeneracy of the central molecule in HON phase. In addition, we performed DFT calculations to investigate the expansion of centered HON structure and evaluate the interaction potentials.

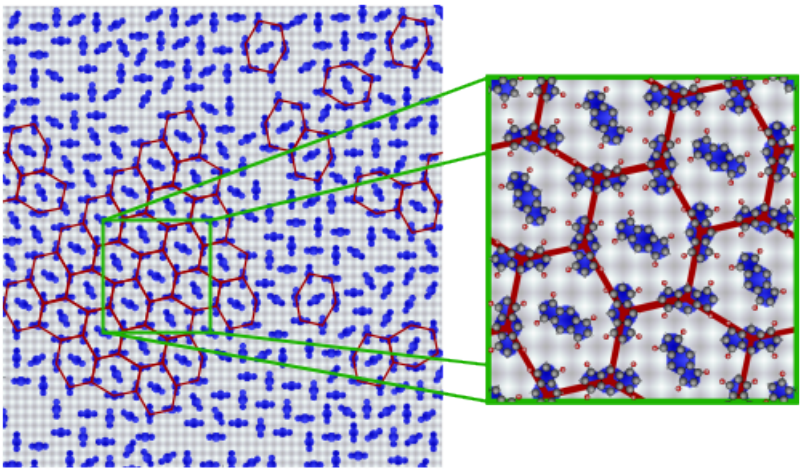


Fig. 1. Generated honeycomb phase cluster from $INDO_4$ molecules on Ag(100) surface using Metropolis algorithm. All discrete interaction energies are set equal. Zoomed in section shows the placement of molecules.

[1] Joachim, Christian, Jim K. Gimzewski, and Arieh Aviram. ”Electronics using hybrid-molecular and mono-molecular devices.” Nature 408.6812 (2000): 541-548.
[2] Kalashnyk, Nataliya, and Sylvain Clair. ”Self-Accommodating honeycomb networks from supramolecular self-assembly of s-indacene-tetrone on silver surfaces.” Langmuir 38.3 (2022): 1067-1071.

ETHYL CELLULOSE AS A HOST MATERIAL FOR THERMALLY-ACTIVATED DELAYED FLUORESCENCE EMITTERS

Gintare Krucaite[1], Daiva Tavgeniene[1], Saulius Grigalevičius[1], Alla Bogoslovska[2], Amjad Ali[3], Glib Baryshnikov[3], Petro Smertenko[2], Mats Fahlman[3], Andrei Smertenko[4], Oleg Dimitriev[2,3]

[1]Department of Polymer Chemistry and Technology, Kaunas University of Technology, Radvilenuplentas 19, Kaunas, LT50254, Lithuania
[2]V. Lashkaryov Institute of Semiconductor Physics, NAS of Ukraine, Pr. Nauki 41, Kyiv03028
[3]Laboratory of Organic Electronics and Wallenberg Wood Science Center, Linköping University, Norrköping 60174, Sweden
[4]Institute of Biological Chemistry, Washington State University, Pullman, WA 99164-7411, USA
gintare.krucaite@ktu.lt

Thermally-activated delayed fluorescence (TADF) emitters are typically used in OLEDs by doping them into a host matrix to prevent emission losses caused by aggregation, concentration quenching, and unwanted excimer emission.TADF molecules that are constructed of donor and acceptor moieties separated by a single chemical bond or a flexible bridge can easily provide soft twisted states, leading to a wide range of shapes and hence CT energies even at room temperature [1, 2, 3]. While small molecules are usually chosen for the host matrix design, polymers could offer better solution processing and lower production costs for light-emitting structures. In this study, we demonstrate that ethyl cellulose (EC), an environmentally friendly polymer, can serve as a host matrix for specific TADF molecules, enabling the preparation of high-quality films through solution processing. We found that the photoluminescence (PL) quantum yield of composite samples using the EC matrix is enhanced by about ten times compared to neat solid-state films of the same dyes. Our PL emission spectroscopy and fluorescence microscopy studies on two pairs of donor-acceptor-donor molecules—each pair having the same donor units but different sulfonyl or carbonyl acceptor groups—revealed distinct morphologies and complex emission bands. The emission color was determined by the interplay of emission components in the multicomponent charge-transfer band. Neat dye films showed aggregated species with red-shifted charge-transfer emission, while guest-host systems exhibited smooth morphology with brighter, more even, and blue-shifted emission. The enhanced PL emission in composite films is attributed to a model where emitter molecules are frozen in the polymer matrix, adopting a restricted twisting disorder. In contrast, the PL emission in neat dye films is weakened due to a more free molecular twisting. We suggest that the specific interface between EC and emitter molecules facilitates specific intermolecular packing and suppresses intramolecular twisting upon photoexcitation, leading to a dominant locally excited state and a resulting blue shift in the emission spectrum.

Acknowledgements

This work was supported by the Research Council of Lithuania (Grant No. S-LU-24-7) and bilateral Ukraine-Lithuania project (M/54-2024).

[1] Lauteslager, X. Y., van Stokkum, I. H., van Ramesdonk, H. J., Brouwer, A. M., & Verhoeven, J. W. (1999). Conformational Dynamics of Semiflexibly Bridged Donor– Acceptor Systems Studied with a Streak Camera and Spectrotemporal Parametrization of Fluorescence. The Journal of Physical Chemistry A, 103(6), 653-659.

[2] Tanaka, H., Shizu, K., Nakanotani, H., & Adachi, C. (2014). Dual intramolecular charge-transfer fluorescence derived from a phenothiazine-triphenyltriazine derivative. The Journal of Physical Chemistry C, 118(29), 15985-15994.

[3] Rodríguez-Cortés, L. A., Hernández, F. J., Rodríguez, M., Toscano, R. A., Jiménez-Sánchez, A., Crespo-Otero, R., & Rodríguez-Molina, B. (2023). Conformational emissive states in dual-state emitters with benzotriazole acceptors. Matter, 6(4), 1140-1159.

INVESTIGATIONS OF PHOTOPHYSICAL PROPERTIES OF DERIVATIVES OF PHENOTHIAZINE AND DIFFERENTLY MODIFIED 3,5-DICYANOPYRIDINE FOR DOWN-CONVERTING WHITE LIGHT-EMITTING DIODES

Lesia Volyniuk[1], Serhii Melnykov[2], Pavel Arsenyan[3], Oleksandr Bezvikonnyi[1], Dmytro Volyniuk[1], Pavlo Stakhira[2], Audrius Bucinskas[1], Juozas Vidas Grazulevicius[1]

[1]Department of Polymer Chemistry and Technology, Kaunas University of Technology, K. Barsausko g. 59, 51423, Kaunas, Lithuania
[2]Department of Electronic Engineering, Lviv Polytechnic National University, Stepan Bandera st. 12, 79013, Lviv, Ukraine
[3]Latvian Institute of Organic Synthesis, Aizkraukles 21, LV-1006, Riga
lesia.volyniuk@ktu.lt

Single-molecular white organic emitters are highly desirable for down-converting white light-emitting diodes (WLEDs) [1]. However, most reported organic compounds generally emit one colour, and the few examples of single-molecular white emitters exhibit low photoluminescence quantum yields (PLQYs), subpar colour quality, or complex molecular structures that hinder their practical applications [2]. For instance, we previously reported a single molecule white light emitter showing CIE 1931 coordinates of (0.26, 0.31) and PLQY of 33% [3]. Considering the low quality of the white light from existing emitters, there remains a need to develop novel single-molecular white emitters with high PLQYs, stable colour coordinates, and colour rendering index (CRI) values, as well as simple structures that can be easily incorporated into solid films. In this work, we investigated the photophysical properties of three newly developed derivatives of phenothiazine and 3,5-dicyanopyridine aiming to obtain single-molecular white emitters for WLEDs. Powders of phenothiazine and 3,5-dicyanopyridine derivatives were investigated before and after they underwent different external stimuli, including grounding, solvent-fuming, heating and melting. The target compounds exhibit attractive mechanochromic properties, facilitating the tuning of emissions from deep blue to red. Their mechanochromic properties were elucidated by various conformational states that enable single-molecule white emissions with PLQYs of 9.63%. Derivatives of phenothiazine and 3,5-dicyanopyridine were used as emitters in down-converting WLEDs. In the best case, fabricated WLEDs were characterised by power efficiency of 6.1 lm/W and white emission with CRI of 78 and CIE 1931 coordinates (0.34, 0.32).

Acknowledgements

This work is supported by Horizon Europe, the European Union's framework programme for research and innovation (R&I) for 2021-2027, project HELIOS, grant agreement No 101155017.

[1] M. Zhang et al., Efficient single-molecular white-light emission for iridium-based photoluminescent and electroluminescent white OLEDs,(Cell Rep Phys Sci, vol. 4, no. 12,p. 101684, Dec. 2023).
[2] Z. He et al., White light emission from a single organic molecule with dual phosphorescence at room temperature(Nature Communications , vol. 8, no. 1, pp. 1–8, Sep. 2017).
[3] F. Khan, L. Volyniuk, M. Ghasemi, D. Volyniuk, J. V. Grazulevicius, and R. Misra, "Efficient monomolecular white emission of phenothiazine boronic ester derivatives with room temperature phosphorescence(J Mater Chem C Mater, vol. 10, no. 28, pp. 10347–10355, Jun. 2022).

OVERSHOOT PULSES IN PEROVSKITE LIGHT EMITTING DIODES. THE ROLE OF OPERATION CONDITIONS

Ignas Ledzinskas[1,2], Rokas Gegevičius[1], Vidmantas Gulbinas[1]

[1]Department of Molecular Compound Physics, Center for Physical Sciences and Technology
[2]Faculty of Physics, Vilnius University
ignas.ledzinskas@ff.stud.vu.lt

Hybrid perovskite light-emitting diodes (PeLEDs) are a promising new technology for the development of next-generation light sources. They are characterized by high photoluminescence (PL) and electroluminescence (EL) efficiency, which is now above 30%. In some applications, PeLEDs are expected to operate in pulsed mode. Generation of light pulses with sufficiently high intensity requires high power electrical pumping, which poses significant problems for electrical pumping and leads to deterioration of PeLED performance, its degradation or even damage. PeLEDs operating in a non-conventional regime based on the so-called overshoot effect enable generation of short, high intensity, perfectly electrically synchronizable optical pulses by using relatively low-power electrical pumping.

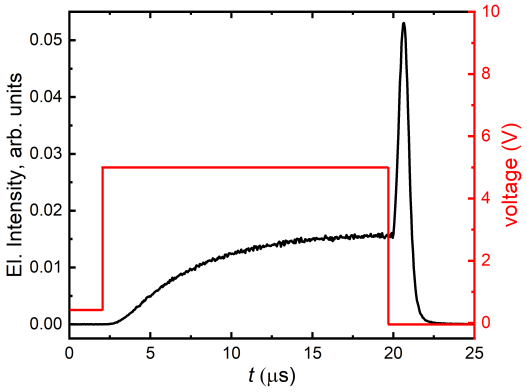


Fig. 1. Electroluminescence overshoot transient after application of rectangular voltage pulse (red).

Here we demonstrate overshoot pulse generation by Formamidinium lead iodide (FAPI) PeLEDs and analyse their formation dependencies on temperature and time-shape of varying voltage electrical pumping pulses. The overshoot pulse intensity and shape are determined not only by the voltage and duration of pump pulses, but also on the offset voltage applied between pump pulses and negative voltage pulses applied immediately after the pump pulse termination. Intensity of overshoot pulses strongly increases at temperatures below 200 K. We demonstrate that redistribution of mobile ions affecting electric field strength and its spatial distribution along the perovskite layer thickness is mainly responsible for the unusual overshoot pulse generation properties. Mathematical modelling of the electroluminescence dynamics enables to reproduce the electroluminescence dynamics and reveals two PeLED operation regimes enabling or disabling overshoot pulse generation.

SHORT-RANGE CHARGE TRANSFER ANDBIPOLAR CHARGE TRANSPORT IN DIBENZO{A,C}IMIDAZOPHENAZINE-BASED EMITTER WITH MR-TADF FOR SOLUTION-PROCESSABLE HYPERFLUORESCENT OLEDs

Hamisu Aliyu Mohammed[1], Matas Guzauskas[1], Viktorija Andruleviciene[1], Dmytro Volyniuk[1], Woon Kai Lin[2], Azhar Ariffin[3], Juozas Vidas Grazulevicius[1]

[1]Department of Polymer Chemistry and Technology, Kaunas University of Technology.
[2]Low Dimensional Material Research Centre, Department of Physics, University Malaya, Kuala Lumpur, Malaysia.
[3]Department of Chemistry, University Malaya, Kuala Lumpur, Malaysia.
hammoh@ktu.lt

We present a novel approach to the emitters exhibiting multiple resonance-induced thermally activated delayed fluorescence (MR-TADF), addressing the challenges of the synthesis of pure-color emitters with efficient triplet harvesting. Building upon our recently reported acceptor, 11,13-dihydro-12H-dibenzo[a,c]imidazo[4,5-i]phenazin-12-one (BIPO) with a small modification, we developed a new derivative, which integrates the BIPO core with a 5H-dibenzo[b,f]azepine donor unit. The synthesized compounds exhibit highly efficient narrowband photoluminescence (PL) with full width at half-maximum (FWHM) as low as 35 nm and photoluminescence quantum yields of their solutions reaching more than 75% and solid matrix approaching 100%. Notably, the synthesized compound demonstrates short-range charge-transfer emission, enabling efficient MR-TADF despite a relatively large experimental singlet-triplet energy gap. The MR-TADF mechanism was thoroughly investigated through temperature-dependent steady-state luminescence spectroscopy, time-resolved luminescence spectroscopy, and theoretical calculations, revealing the involvement of higher-lying triplet states that facilitate reverse intersystem crossing. Time-of-flight studies of the solid films of the newly synthesized compound underscore the bipolar charge transport properties. Hole and electron mobilities exceeded 1×10^{-4} $cm^2/V{\cdot}s$ under high electric fields. Furthermore, the newly synthesized emitter performs well in solution-processed hyperfluorescent organic light-emitting diodes, achieving external quantum efficiency of 5.7% and sky-blue emission with a narrow FWHM of 53 nm. These findings highlight the synthesized derivative of BIPO and 5H-dibenzo[b,f]azepine as a promising candidate for the next-generation pure-color, energy-efficient OLEDs.

VIS-TO-UV PHOTON UPCONVERSION IN THIN FILMS EMPLOYING MR-TADF SENSITIZER

Džiugas Krencius[1], Naglis Vasarevičius[1], Manvydas Dapkevičius[1], Justas Lekavičius[1], Steponas Raišys[1], Karolis Kazlauskas[1]

[1]Institute of Photonics and Nanotechnology, Faculty of Physics, Vilnius University, Lithuania
dziugas.krencius@vu.ff.lt

Triplet-triplet annihilation based light upconversion (UC) into the UV region is a process in which an organic molecular system, composed of a sensitizer and an annihilator, absorbs low-energy visible photons and via triplet annihilation converts them into higher-energy UV photons. Some of the areas where this process can be applied are photocatalysis [1], hydrogen generation by water splitting [2] and germicidal purification of contaminated water [3]. The majority of UC studies are focused on light conversion in solutions, whereas for broader practical applications thin films (solid phase) are required.

The aim of this study is to assess photophysical properties of UV annihilators, choose a suitable sensitizer by considering the energy levels of molecules, and optimize the annihilator concentrations to achieve high UC quantum yield (UCQY). The annihilators researched in this work are 2,5-diphenylfuran (PPF), 2,5-diphenyloxazole (PPO), 2,5-bis(3,5-di-tert- butylphenyl)furan (tB-PPF), and 2-Phenylbenzimidazole (2PB). The quantum yields were determined using an absolute measurement approach with an integrating sphere. The singlet and triplet exciton lifetimes, used to calculate the efficiency of inter- and intra-molecular transitions, were measured by time correlated single photon counting (TCSPC) and time-resolved phosphorescence spectroscopy with time-gated detection.

Thin film samples were prepared with annihilator concentrations ranging from 0.1% to 100% in a poly(methyl methacrylate) (PMMA) matrix. The 2PB and tB-PPF had low fluorescence quantum yield (FLQY), rendering these annihilators unsuitable for UC systems. In contrast, the FLQY of PPF and PPO reached 60% and 74% respectively. At high concentrations PPO exhibited a smaller spectral red shift, making it the most suitable for UC among the four annihilators.

A MR-TADF sensitizer (BNCzPTZ) was utilized for these UC systems, where the best performing film comprising of 25 %wt PPO and 0.1 %wt BNCzPTZ in a PMMA matrix achieved UCQY of 0.7%. Triplet energy transfer reached high efficiency of 97%. However, UCQY was limited by significantly lower FLQY (only 15% in this sample), and intersystem crossing efficiency (73%).

UCQY could be further improved by optimizing the sensitizer concentration. It is expected that the lower BNCzPTZ concentration would result in higher FLQY in the UC films due to reduced Förster resonance energy transfer back to sensitizer.

[1] S.-Y. Hwang, D. Song, E.-J. Seo, F. Hollmann, Y. You, and J.-B. Park, “Triplet–triplet annihilation-based photon-upconversion to broaden the wavelength spectrum for photobiocatalysis,” Scientific Reports, vol. 12, no. 1, p. 9397, Jun. 2022, doi: https://doi.org/10.1038/s41598-022-13406-8.

[2] E. Madbak et al., “Utilising triplet–triplet annihilation upconversion for overall photocatalytic water splitting,” Chemical Communications, vol. 61, no. 1, pp. 157–160, 2025, doi: https://doi.org/10.1039/d4cc03961k.

[3] Christoph Kerzig and O. S. Wenger, “Sensitized triplet–triplet annihilation upconversion in water and its application to photochemical transformations,” Chemical Science, vol. 9, no. 32, pp. 6670–6678, Jan. 2018, doi: https://doi.org/10.1039/c8sc01829d.

PHENANTHRO(9,10-d)HAVING ELECTROACTIVE DERIVATIVES AS HOST MATERIALS FOR OLEDs

Daiva Tavgeniene[1], Dovydas Blazevicius[1], Saulius Grigalevicius[1], Gintare Krucaite[1], Karolis Kazlauskas[2], Dovydas Banevicius[2], Vygintas Jankauskas[3], Egidijus Kamarauskas[3]

[1]Department of Polymer Chemistry and Technology, Faculty of Chemical Technology, Kaunas University of Technology, Kaunas, Lithuania
[2]Institute of Photonics and Nanotechnology, Faculty of Physics, Vilnius University, Vilnius, Lithuania
[3]Institute of Chemical Physics, Faculty of Physics, Vilnius University, Vilnius, Lithuania
daiva.tavgeniene@ktu.lt

Organic light emitting (OLED) technology keeps advancing significantly in areas like solid-state lighting and display innovations [1, 2]. In the past decade, the development of unconventional display forms has been a key challenge in materials science, electrical engineering, and mechanical engineering, driven by their potential for diverse applications with outstanding features like ultra-lightweight design, unbreakable durability, and flexibility [3, 4].

Third generation, purely organic TADF emitters get a lot of attention as a potential replacement of the expensive phosphorescent emitters because of their ability to use 100% excitons for light emission without the need of noble metal emitters [5, 6]. Here, we demonstrate synthesis and properties of the new electroactive compounds, which have promising properties to be used as host materials for TADF based emitters.

The synthesis and full characterization of newly developed bipolar phenanthro[9,10-d]imidazole-based compounds are reported. The new derivatives deminstrated very high thermal stability and they formed amorphous layers with glass transition temperatures of 73-167 ºC. The electron photoemission spectra of the layers showed ionization potentials in the range of 5.39-5.59 eV. Hole drift mobility in thin layers of some derivatives exceed 2.8 × 10^{-5} $cm^2V^{-1}s^{-1}$ at high electric fields at room temperature. The new derivatives were tested as hosts in OLEDs for commercial red TADF based emitter: 7,10-bis(4-(diphenylamino)phenyl)-2,3-dicyanopyrazino-phenanthrene (TPA-DCPP). The OLED device with 9-(2-ethylhexyl)-3-(1-phenylphenanthro[9,10-d]imidazol-2-yl)carbazole host exhibited superior performance with rather low turn on voltage of 3.5 V, maximum brightness of about 1000 cd/m^2 and peak efficiency exceeding 5.6%. The characteristics are better than those of a similar device using the well-known commercial host material: 4,4′-bis(9-carbazolyl)-1,1′-biphenyl (CBP).

Acknowledgements
We gratefully acknowledge the funding support from the Research Council of Lithuania (grant No. S-MIP-22-84).

[1] Yoshida H, Nakatani S, Inoue T, Usui Y, Ohtsuka F. Mura-free G8.5 220ppi inkjet printing technology for OLED and QLED display panels. J Soc Inf Display 2024;32:255-6.
[2] Baumgarten S, Hoberg T, Lohmann T, Mazinani B, Walter P, Koutsonas A. Fullfield and extrafoveal visual evoked potentials in healthy eyes: reference data for a curved OLED display. Doc Ophthalmol 2022;145:247-62.
[3] Song H, Song YJ, Hong J, Kang KS, Yu S, Cho HE, Kim JH, Lee SM. Water stable and matrix addressable OLED fiber textiles for wearable displays with large emission area. npj Flex Electron. 2022;6:66.
[4] Donaldson L. First 3D-printed flexible OLED display demonstrated. Mater Today 2022;53:3-4.
[5] Kumar A, Lee W, Lee T, Jung H, Yoo S, Lee MH. Triarylboron-based TADF emitters with perfluoro substituents: high-efficiency OLEDs with a power efficiency over 100 lm W−1. J Mater Chem C 2020;8:4253-63.
[6] Uoyama H, Goushi K, Shizu K, Nomura H, Adachi C. Highly efficient organic light-emitting diodes from delayed fluorescence. Nature 2012;492:234-8.

NOVEL HOST MATERIALS FOR STABLE BLUE THERMALLY ACTIVATED DELAYED FLUORESCENCE OLEDS

Domantas Berenis[1], Rita Butkutė[2], Gediminas Kreiza[1], Giedrius Puidokas[1], Vaida Jašinskaitė-Koženiauskienė[2], Karolis Kazlauskas[1]

[1]Institute of Photonics and Nanotechnology, Vilnius University, Saulėtekio av. 3 LT-10257, Vilnius, Lithuania
[2]Department of Polymer Chemistry and Technology, Kaunas University of Technology, Radvilėnų rd. 19, LT-50254 Kaunas, Lithuania
domantas.berenis@ff.stud.vu.lt

Organic light-emitting diode (OLED) technology has been established in the display sector due to its ease of fabrication and high energy efficiency. Current OLED displays employ low-efficiency fluorescent or expensive heavy metal-containing phosphorescent emitters. In recent years, thermally activated delayed fluorescence (TADF) materials have emerged as a promising alternative to currently utilized purely organic emitters, achieving 100% internal quantum efficiency [1]. However, developing stable and efficient blue OLEDs presents challenges due to high-energy exciton transitions, leading to increased degradation pathways. Host materials are vital in optimizing device performance by facilitating efficient energy transfer and suppressing undesirable intermolecular interactions. Therefore, engineering a proper host material for the emissive layer of blue TADF OLEDs is an essential step for the advancement of this technology.

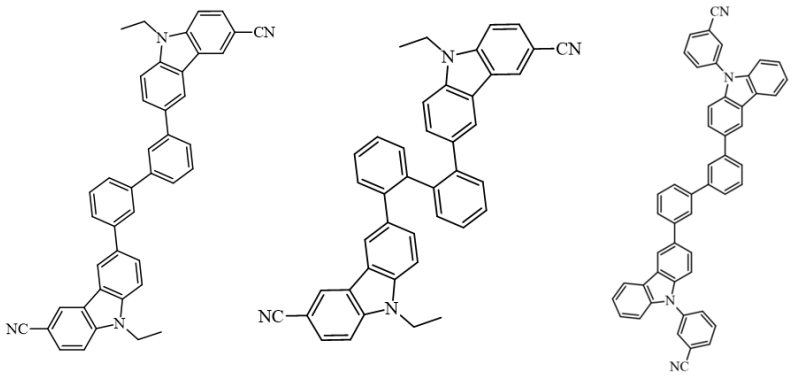


Fig. 1. Molecular structures of studied host materials.

In this work, we introduce and investigate three novel carbazole-based OLED host materials (Fig. 1). New molecules were designed to avoid relatively weak C-N bonds, which are known for exhibiting one of the lowest bond dissociation energies in a typical structure [2,3]. Additionally, cyano substituents were added to enhance electron transfer character. Photophysical and electrochemical studies of novel hosts, as well as the performance of blue OLED devices, are presented. Novel hosts exhibit significantly high singlet and triplet excited state energies and ambipolar charge transfer properties, enabling their successful utilization in OLED fabrication.

[1] H. Uoyama, et al., Nature, vol. 492, no. 7428, pp. 234–238 (2012)
[2] A. S. D. Sandanayaka, et. al., J. Phys. Chem. C, 119 (42), 23845-23851 (2015).
[3] M. Hong, et. al., Chemistry of Materials 2016 28 (16), 5791-5798 (2016).

APPLICATION OF A DIBENZOFURAN-BASED HOST WITH HIGH TRIPLET ENERGY FOR THIRD-GENERATION BLUE ORGANIC LIGHT-EMITTING DIODES

Kristupas Bagdonas[1], Goda Grybauskaitė[1], Gediminas Kreiza[1], Edvinas Orentas[2], Eigirdas Skuodis[1], Karolis Kazlauskas[1], Dovydas Banevičius[1]

[1]Vilnius University, Institute of Photonics and Nanotechnology, Saulėtekio al. 3, Vilnius
[2]Vilnius University, Department of Organic Chemistry, Naugarduko g. 24, Vilnius
kristupas.bagdonas@ff.stud.vu.lt

In recent years, thermally activated delayed fluorescence (TADF) has become a well-established mechanism for achieving an internal quantum efficiency of 100% in organic light-emitting diodes (OLEDs)[1]. However, for efficient device performance, emitter molecules must be doped into a suitable matrix. This matrix material should facilitate uniform charge carrier distribution and stabilize the emitter, thereby minimizing the risks of aggregation and degradation. To prevent excitation transfer from the emitter back to the matrix, compounds with a high triplet energy level are necessary[2].

The aim of this research was to investigate **4-[2-(2-dibenzofuran-4-ylphenyl)phenyl]dibenzofuran** and its applicability as an OLED host. The material's energy structure was obtained from absorption and emission measurements and cyclic voltammetry. Optimal emitter-host concentration was determined from the highest photoluminescence quantum yield (PLQY). Fabricated OLED devices were electro-optically characterized to determine their efficiency and stability properties.

The compound was determined to have a triplet energy of 2.88eV, making it suitable for hosting the **DMeCzIPN** emitter. The optimal emitter concentration in the host was found to be 20%, which resulted in the highest measured PLQY of 66.3%. OLEDs were fabricated using the vacuum deposition method. The devices exhibited a turn-on voltage of 2.6V and achieved a luminance of $32400\,\mathrm{cd/m^2}$ at a current density of $332\,\mathrm{mA/cm^2}$. The OLEDs demonstrated an external quantum efficiency of up to 8%, with an efficiency decrease of 0.34% within the commercially relevant brightness range of $100\,\mathrm{cd/m^2}$ to $1000\,\mathrm{cd/m^2}$. Under constant current operation, the devices required 245 hours and 2.5 hours to degrade to half of their original brightness at initial luminance levels of $100\,\mathrm{cd/m^2}$ and $1000\,\mathrm{cd/m^2}$, respectively.

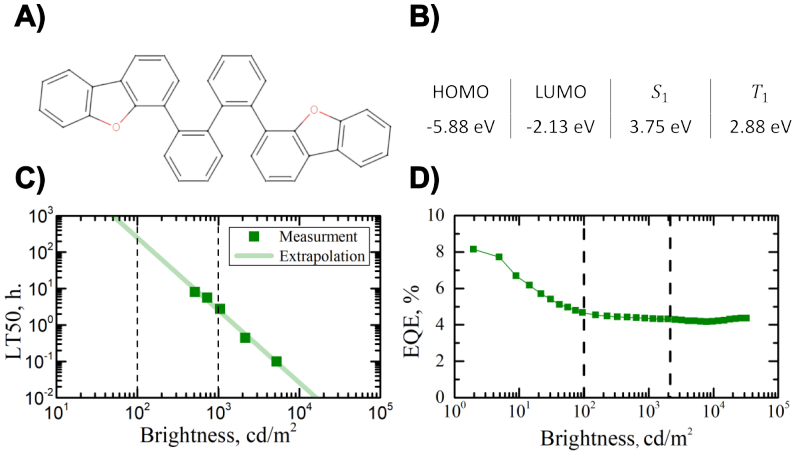


Fig. 1. A) Host material chemical structure, B) Host material molecular energy level values, C) OLED stability graph, D) OLED efficiency graph.

[1] Yang X. Advances in High-Efficiency Blue OLED Materials. Photonics 11, 864 (2024).
[2] Youn K. M. et al. High triplet energy bipolar host materials with the combination of dibenzofuran and benziimidazobenzoimidazole moieties for blue thermally activated delayed fluorescence emitter. J. Mater. Chem. C 8, 13811–13818 (2020)

NOVEL HOLE-TRANSPORTING MATERIALS WITH HIGH HOLE MOBILITY FOR EFFICIENT AND STABLE RED OLEDS

Melika Ghasemi[1], Mariia Stanitska[1], Svetlana Sargsyan[1], Dmytro Volyniuk[1], Rasa Keruckienė[1], Juozas Vidas Gražulevičius[1]

[1]Department of Polymer Chemistry and Technology, Kaunas University of Technology, K. Baršausko St. 59, LT-51423 Kaunas, Lithuania
melika.ghasemi@ktu.edu

Organic light-emitting diodes (OLEDs) have gained significant attention due to their flexibility, high efficiency, and low manufacturing cost [1]. This technology has been widely implemented in display and solid-state lighting applications [2]. To achieve highly efficient devices, a multilayered structure is recommended. One approach for improving efficiency is the incorporation of a hole transporting layer (HTL), which reduces the energy barrier for the excitons, enhances hole transportation and recombination within the emissive layer, and prevents charge accumulation [3]. An ideal hole transporting material should exhibit high thermal and morphological stability, an optimal highest occupied molecular orbital energy level, and compatibility with adjacent layers to minimize interfacial defects [4]. In this study a series of novel metal-free organic compounds featuring carbazole and dibenzofuran moieties were meticulously designed, synthesized, and characterized for their potential as HTLs for OLEDs. Photophysical studies revealed that all the compounds exhibit room-temperature phosphorescence in an inert matrix, along with excellent thermal stability, with decomposition temperature ($T_{d-5\%}$) exceeding 400 ^{o}C and glass transition above 100 ^{o}C. The hole transporting capabilities of the compounds were determined to be 2.28 × 10^{-4} cm^2/Vs and 2.34 × 10^{-4} cm^2/Vs at an electric field of 5× 10^5 V/cm, confirming their suitability as HTLs for OLED applications. The compounds were tested as the HTLs in red phosphorescent OLEDs, resulting in external quantum efficiency of 18.2% and a low turn on voltage of 4.39V, with negligible difference compared to the reference device.

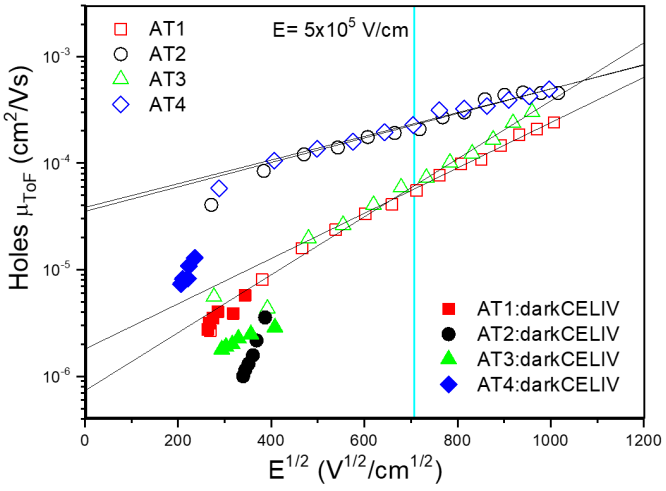


Fig. 1. Hole mobility as a function of electric field.

Acknowledgements
This research was supported by the Research Council of Lithuania (Project “COLED” No P-MIP-24-81).

[1] Y. Zhao, J. Su, W. Zou, Y. Wu, C. Zhang, and M. Shao, “Influence of MoO3’s blend in hole transporting layer on the performance of Alq3-based OLEDs,” Next Materials, vol. 6, p. 100426, Jan. 2025, doi: 10.1016/J.NXMATE.2024.100426.
[2] H. Sasabe and J. Kido, “Development of high performance OLEDs for general lighting,” J Mater Chem C Mater, vol. 1, no. 9, pp. 1699–1707, Feb. 2013, doi: 10.1039/C2TC00584K.
[3] G. Krucaite, D. Tavgeniene, Z. Xie, X. Lin, B. Zhang, and S. Grigalevicius, “Polyethers containing 4-(carbazol-2-yl)-7-arylbenzo[c]-1,2,5-thiadiazole chromophores as solution processed materials for hole transporting layers of OLEDs,” Opt Mater (Amst), vol. 76, pp. 63–68, Feb. 2018, doi: 10.1016/J.OPTMAT.2017.12.028.
[4] S. S. Reddy et al., “Highly Efficient Organic Hole Transporting Materials for Perovskite and Organic Solar Cells with Long-Term Stability,” Advanced Materials, vol. 28, no. 4, pp. 686–693, Jan. 2016, doi: 10.1002/ADMA.201503729.

DONOR-ACCEPTOR-DONOR TYPE FLUORESCENT EMITTERS WITH BENZOTHIADIAZOLE CORES AS PROMISING MATERIALS FOR OLEDS

Svetlana Sargsyan[1], Rasa Keruckiene[1], Ehsan Ullah Rashid[1], Matas Guzauskasa[1], Dmytro Volyniuk[1], Viktorija Andruleviciene[1], Juozas Vidas Grazulevičius[1]

[1]Department of Polymer Chemistry and Technology, Faculty of Chemical Technology, Kaunas University of Technology, K. Baršausko st. 59, LT-51423, Kaunas, Lithuania.
svetlana.sargsyan@ktu.edu

Over the past few decades, organic light-emitting diodes (OLEDs) have gained significant attention for their potential in solid-state lightingand flat-panel displays, due to their flexibility, cost-effectiveness, and high efficiency [1]. The development of novel organic emitters has become crucial to meet the growing demand for high-performance OLEDs in next-generation lighting and display technologies. The benzothiadiazole electron-withdrawing moiety, is commonly utilised in the design of organic emitters due to its rigid planar structure, which enhances emission performance [2]. Herein, we present the design and synthetic strategy for two novel compounds, synthesized through a straightforward, cost-effective single-step nucleophilic substitution reaction between the benzothiadiazole group and two different donors, 3,6-diphenyl-9H-carbazole and 10H-phenoxazine. Thermal, electrochemical, and photophysical properties of benzothiadiazole-based compounds are reported. Both compounds exhibit high temperatures of the onsets of thermal degradation and a high glass transition temperature, as well as optimum ionization potentials (IP). Photoluminescence (PL) studies revealed exceptionally high quantum yields. Time-of-flight charge mobility analysis confirmed the bipolar charge transporting properties of both the compounds, highlighting their potential as efficient electron- and hole-transporting materials. Considering the optimum IP and PL high emission quantum yields, they have the potential to be applied in OLEDs.

Keywords: OLEDs, benzothiadiazole, D-A-D-type fluorescence.

[1] Michael Y. Wong etc. Purely Organic Thermally Activated Delayed Fluorescence Materials for Organic Light-Emitting Diodes. Advanced Materials, 2017.

[2] Shipan Xu a etc. Design of donor-acceptor-acceptor (D-A-A′)-type fluorescence emitters based on benzothiadiazole with the hybridized local and charge-transfer (HLCT) excited state feature for green to deep-red emitting OLEDs. Organic Electronics, February 2025.

IMIDAZOLE AND FLUORENE DERIVATIVES AS HIGHLY EFFICIENT FLUORESCENT LIGHT SOURCES: SYNTHESIS AND INVESTIGATION

Mohamed Abdella[1], Guzauskas Matas[1], Jurate Simokaitiene[1], Juozas Vidas Grazulevicius[1]

[1]Department of Polymer Chemistry and Technology, Kaunas University of Technology
mohamed.abdella@ktu.edu

The use of organic light-emitting diodes (OLEDs) in diverse flat-panel display technologies, including smartphones and large-screen televisions, has attracted considerable attention [1]. OLEDs provide several benefits, such as simplified development, rapid response time, extensive viewing angles, little energy usage, compatibility with flexible plastic substrates, and a variety of form factors appropriate for different display kinds [2]. The incorporation of imidazole derivatives as acceptors with fluorene as a donor may facilitate efficient charge transfer, perhaps enhancing the singlet exciton yield. The compounds of imidazole and fluorene are anticipated to serve as effective deep blue luminophores. Moreover, the addition of sterically large substituents at the C-9 position of the fluorene moiety diminishes the overlap of frontier molecular orbitals and electron exchange with adjacent molecules, thereby facilitating the maintenance of a high photoluminescence quantum yield in the solid state. [1, 3].

This work included the synthesis and examination of several derivatives of imidazole and fluorene-based compounds as prospective materials for blue OLEDs. The thermal and photophysical analysis of these materials indicated that the synthesized compounds exhibited high-intensity emission with brief emission lifetimes ranging from 1.54 to 7.63 ns, positioning them as attractive candidates for rapid-response OLEDs. Furthermore, they exhibited significant thermal stability and formed molecular glasses with elevated glass transition temperatures of 130°.

[1] G. Chen, Z. Qiu, J. H. Tan, W. C. Chen, P. Zhou, L. Xing, S. Ji, Y. Qin, Z. Zhao, Y. Huo, Dye. Pigment. 2021, 184, 108754.
[2] J. M. Ha, S. H. Hur, A. Pathak, J.-E. Jeong, H. Y. Woo, NPG Asia Mater. 2021, 13, 53.
[3] C. Du, T. Lu, Z. Cheng, Y. Chang, H. Liu, J. Wang, L. Wan, Y. Lv, P. Lu, J. Mater. Chem. C 2022, 10, 14186.

SYNTHESIS AND STUDIES OF LONG-WAVELENGTH ABSORBING ORGANIC SEMICONDUCTORS FOR OPTOELECTRONICS

Khushdeep Kaur[1], Rita Butkutė[1], Oleksandr Bezvikonnyi[1], Dmytro Volyniuk[1], Juozas Vidas Gražulevičius[1]

[1]Department of Polymer Chemistry and Technology, Kaunas University of Technology, K. Barsausko st. 59, 51423, Kaunas, Lithuania
khushdeep.kaur@ktu.edu

Owing to the unique ability of organic semiconductors exhibiting absorption in long-wavelength regions of visible spectrum to capture low-energy photons, they play a crucial role in advancement of next-generation optoelectronic devices such as high-efficiency solar cells, photodetectors, biomedical imaging, and optical communication devices.1Additionally, such materials are suitable for night vision in security and surveillance which helps to improve sensitivity towards low light conditions. Carbazole moiety is frequently used as an electron-donating group in the design of π-conjugated molecules owing to the hole-transporting capabilities, optical properties, thermal and chemical stability, and easy structural modification of carbazole derivatives. 2 Also, the strong electron acceptors, 1,1,2,2-tetracyanoethylene (TCNE) and 7,7,8,8-tetracyanoquinodimethane (TCNQ) are highly reactive toward electron-rich alkynes.2,3 Taking into account, the increased demand for the development of organic semiconductors exhibiting absorption in long-wavelength regions of the visible spectrum, we designed novel materials containing 9-ethyl carbazole as donor unit appended with strong acceptor units i.e. TCNQ and TCNE. The synthesis of the designed compounds was successfully furnished using two step synthetic schemes followed by structural characterization using NMR and mass spectrometry. The photophysical, electrochemical and theoretical analysis of the synthesized compounds was carried out and the structure-property relationship was established. Conclusively, the newly synthesized materials can be suitable for photonic and optical devices particularly for organic photodetectors.

Acknowledgements
This project has received funding from the Research Council of Lithuania (LMTLT), agreement No S-MIP-22-78.

[1] 1. Michinobu, T., & Diederich, F. The [2+2] Cycloaddition-Retroelectrocyclization (CA-RE) Click Reaction: Facile Access to Molecular and Polymeric Push-Pull Chromophores. Angewandte Chemie International Edition, 57(14), 2018, 3552–3577. https://doi:10.1002/anie.20171160
[2] 2. Pankaj Kumar Gupta, Faizal Khan, and Rajneesh Misra. NIR-Absorbing 1,1,4,4-Tetracyanobuta-1,3-diene- and Dicyanoquinodimethane-Functionalized Donor–Acceptor Phenothiazine Derivatives: Synthesis and Characterization. J. Org. Chem. 2023, 88, 14308−14322. https://doi.org/10.1021/acs.joc.3c01029.
[3] 3. Qingyuan Li, Yunlong Guo, and Yunqi Liu. Exploration of Near-Infrared Organic Photodetectors. Chemistry of Materials 2019 31 (17), 6359-6379. https://10.1021/acs.chemmater.9b00966.

ELECTROCHEMICAL SENSOR FOR SALICYLIC ACID BASED ON A MOLECULARLY IMPRINTED POLYMER

Gabrielė Slaboševičiūtė[1,2], Ernestas Brazys[1,3], Vilma Ratautaitė[1]

[1]Department of Nanotechnology, State Research Institute Center for Physical Sciences and Technology (FTMC), Sauletekio Ave. 3, Vilnius LT-10257, Lithuania
[2]Department of Chemistry and Bioengineering, Faculty of Fundamental Sciences, Vilnius Tech, Sauletekio Ave. 11, Vilnius LT-10223, Lithuania
[3]Department of Physical Chemistry, Institute of Chemistry, Faculty of Chemistry and Geosciences, Vilnius University (VU), Naugarduko str. 24, Vilnius LT-03225, Lithuania
gabriele.slaboseviciute@ftmc.lt

Salicylic acid and its derivatives are used in the pharmaceutical industry to synthesise medical drugs, and its intermediates are used to manufacture dyes, agrochemicals and perfumery products. Salicylic acid is also commonly encountered in the food industry as a preservative in milk and milk products to increase shelf life. However, it is illegal to do so since it may have adverse effects on human health. Salicylic acid impairs the digestibility of milk or may cause gastric irritation, bleeding, diarrhea and even death, especially in young infants, who are extremely sensitive to such irritants. The addition of small quantities of salicylic acid to milk either to improve its keeping quality or to delay its spoilage has been a problem for regulatory bodies from the early history of dairying [1]. Therefore, creating a valid, quick and easy-to-use system that could help detect and quantify this substance in various food samples is essential. A molecularly imprinted biosensor fits this criteria and could be an excellent tool for salicylic acid detection in milk samples. This study presents some aspects of molecularly imprinted biosensor development.

The typical molecular imprinting procedure consists of a few steps: 1) self-assembly of monomer, crosslinker, and template molecules to create pre-polymerization complexes; 2) chemical or electrochemical polymerisation; 3) removal of the template molecules from the obtained polymer, which generates the binding sites in the structure of the polymer, which are specific or complementary to the template molecules [2,3]. This characteristic is helpful for the development of sensors for specific detection.

Two methods have been used to synthesise the polymer required for the sensor: chemical and electrochemical. During chemical synthesis, the polymerisation of aniline was initiated with ammonium persulphate. The synthesised aniline polymer with molecularly imprinted salicylic acid (MIP) was used for spectrophotometric measurements to determine the interaction of the polymer with the template. The electrochemical synthesis was carried out in a three-electrode electrochemical cell (working electrode (WE) - indium tin oxide coated glass (ITO), counter electrode (CE) - platinum grid, reference electrode (RE) - Ag/AgCl $_{3MKCl}$) by electrochemical pulse technique. To improve the adhesion of the polymer to the surface of the working electrode, ITO was activated with trisodium citrate before polymer deposition. The interaction of the MIP-coated ITO with salicylic acid was further investigated by cyclic voltammetry (CV), electrochemical impedance spectroscopy (EIS) and square wave voltammetry (SWV).

[1] P. Singh, N. Gandhi, “Milk Preservatives and Adulterants: Processing, Regulatory and Safety Issues”, Food Reviews International, vol. 31, pp. 236–261, 2015. https://doi.org/10.1080/87559129.2014.994818.
[2] K. Haupt, A. V. Linares, M. Bompart, B.T.S. Bui, Molecularly Imprinted Polymers, Springer, Berlin, Heidelberg, 2011. https://doi.org/10.1007/128_2011_307.
[3] E. Brazys, V. Ratautaite, E. Mohsenzadeh, R. Boguzaite, A. Ramanaviciute, A. Ramanavicius, “Formation of molecularly imprinted polymers: Strategies applied for the removal of protein template (review)”, Advances in Colloid and Interface Science, vol. 337, pp. 103386, 2025. https://doi.org/10.1016/J.CIS.2024.103386.

THE FORMATION AND ELECTROCHEMICAL EVALUATION OF POLYMERIC NANOCOMPOSITES BASED ON GLUCOSE OXIDASE AND GOLD NANOCOMPOUNDS

Natalija German[1], Almira Ramanaviciene[1], Arunas Ramanavicius[2]

[1]Department of Immunology and Bioelectrochemistry, State Research Institute Centre for Innovative Medicine, Vilnius, Lithuania
[2]Department of Physical Chemistry, Faculty of Chemistry and Geosciences, Vilnius University, Vilnius, Lithuania
natalija.german@imcentras.lt

The development of glucose biosensors has great significance in the diagnosis and control of diabetes mellitus, which is considered a worldwide public health problem, which increases the risk of heart disease, kidney failure, blindness, postoperative and wound infections [1]. Major fundamental and nanotechnological advances opened new horizons for the application of nanomaterials and hybrid composites in bioanalytical chemistry [2]. Gold nanocompounds are usually used as connectors between the surface of an electrode and the red-ox center of glucose oxidase (GOx) [3]. The incorporation of gold nanoparticles (AuNPs) within polymers is an important aspect in the synthesis of conductive composites. Biosensors based on the GOx, AuNPs and modified by a polymeric layer have found promising applications in glucose sensing during clinical analysis and for food processing [2].

The main aim of the present study was to evaluate some characteristics of a glucose biosensor based on polyaniline (PANI) and polypyrrole (Ppy), with embedded GOx and 6 nm size AuNPs or gold-nanoclusters formed from chloroaurate ions ($AuCl_4^-$) (PANI/AuNPs$_{(6nm)}$-GOx, PANI/AuNPs($AuCl_4^-$)-GOx, Ppy/AuNPs$_{(6nm)}$-GOx and Ppy/AuNPs($AuCl_4^-$)-GOx) nanocomposites. Cyclic voltammetry (CV) was applied for the investigation of analytical characteristics of the glucose biosensor and for the evaluation of these modified electrodes in the determination of glucose in real serum samples in the presence of some interfering materials. The scheme of polymeric nanocomposites's formation and electrochemical investigations is presented in Fig. 1. It was investigated that the relationship between log I_{pa} and log v registered from CV anodic peaks in the presence of glucose was linear and the electrochemical reaction was controlled by the diffusion. The glucose biosensor based on GR modified by Ppy/AuNPs($AuCl_4^-$)-GOx nanocomposites was characterized by high sensitivity (4.31 mA mM cm^{-2}) and good stability (the half-life period of 19 days). The GR electrode modified by Ppy/AuNPs($AuCl_4^-$)-GOx nanocomposites was suitable for the determination of glucose in the sample of human blood serum in the presence of interfering species with the recoveries in the range of 93.6–94.8%.

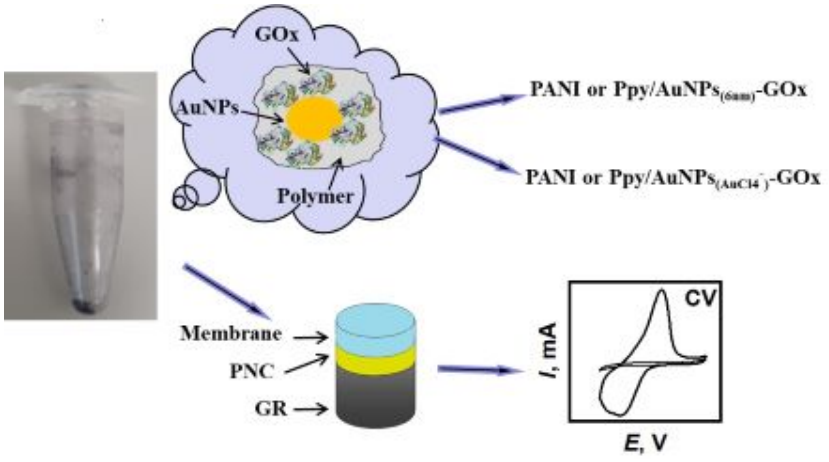


Fig. 1. The scheme of polymeric nanocomposites' formation, followed by investigations using CV.

Acknowledgements
This research was funded by the Research Council of Lithuania, a grant No. S-MIP-20-18

[1] M. Labib, E.H. Sargent, S.O. Kelley, Electrochemical methods for the analysis of clinically relevant biomolecules, Chemical Reviews 116, 9001–9090 (2016)
[2] H. Li, D. Du, C. Zhu, G. Yang, Y. Lin, Electrochemical sensors and biosensors based on nanomaterials and nanostructures, Analytical Chemistry 87, 230–249 (2014)
[3] H.R. Luckarift, D. Ivnitski, R. Rincón, P. Atanassov, G.R. Johnson, Glucose oxidase catalyzed self-assembly of bioelectroactive gold nanostructure, Electroanalysis 22, 784–792 (2010)

THE ELECTROCHEMICAL EVALUATION OF GLUCOSE BIOSENSOR BASED ON INCORPORATING PLATINUM NANOSTRUCTURES, GLUCOSE OXIDASE, AND POLYMERIZED 1,10-PHENANTHROLINE-5,6-DIONE

Gustė Jakučiūnaitė[1], Natalija German[2,3]

[1]Department of Analytical and Environmental Chemistry, Faculty of Chemistry and Geosciences, Vilnius University, Vilnius, Lithuania
[2]Department of Immunology and Bioelectrochemistry, State Research Institute Centre for Innovative Medicine, Vilnius, Lithuania
[3]Department of Chemistry and Bioengineering, Faculty of Fundamental Sciences, Vilnius Gediminas Technical University Vilnius Tech, Vilnius, Lithuania
guste.jakuciunaite@chgf.stud.vu.lt

Electrochemical biosensors are widely recognized today as highly sensitive and efficient tools for detecting various substances. They play a significant role in disease diagnosis and enable identifying a wide range of targets, spanning pharmaceutical and clinical fields to industrial, food, and environmental sectors [1]. Electrochemical biosensors incorporating glucose oxidase (GOx) are among the most effective tools for glucose measurement, offering high selectivity, sensitivity, and low detection limits. Developing a second-generation glucose sensor requires a mediator to facilitate electron transfer between the enzyme and the electrode through oxidation-reduction reactions. Polymerized mediator, 1,10-phenanthroline-5,6-dione (pPD), plays a crucial role in improving overall sensor performance, ensuring higher sensitivity, stability, and reliability in glucose detection. Due to their unique structural, optical, and catalytic properties, platinum nanostructures (PtNS) exhibit remarkable catalytic activity and are widely used in electrochemical analysis. They are universally recognized for their outstanding ability to catalyze the oxidation and reduction of hydrogen peroxide, attributed to their high active surface area and favourable latent planes compared to bulk metals. Additionally, their biological compatibility makes them highly attractive for the development of oxidase-based sensors [2]. In this study, the main aim to highlight the importance of all chemical compounds in developing an optimal system for creating a biosensor that can be widely used in today's industry. The modification's process of electrode's surface is shown in Figure 1. Analysing the cyclic voltammograms provides information about the increased current when pPD is added, proving that pPD enhances the system's conductivity. GOx likely facilitates electron transfer, as it is an enzyme capable of catalyzing redox reactions. When these components work together, a synergetic effect is observed, ensuring excellent reversibility of oxidation and reduction processes. The presented calibration curves correspond to hyperbolic functions and follow Michaelis-Menten kinetics. The depicted dependencies illustrate the CE/PtNS/GOx/pPD system (ΔI_{max} = 42.2 $\pm$ 2.8 μA; 6.64%; K_M = 230 mmol/L). This study demonstrates that the incorporation of pPD, GOx, and PtNS significantly improves the performance of glucose biosensors. The findings suggest that further optimization is needed to enhance long-term stability for practical applications in glucose monitoring.

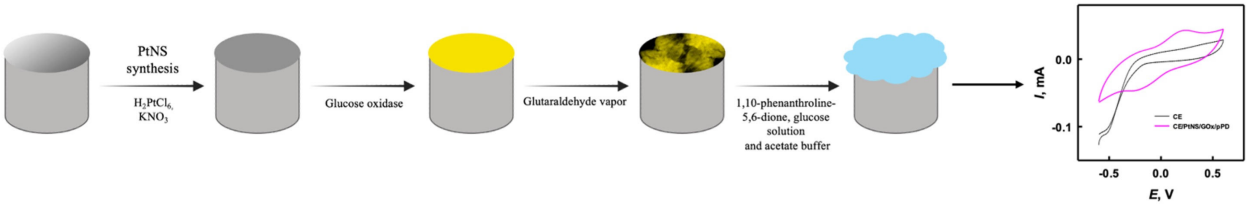


Fig. 1. A schematic visualization of an electrode modification process, featuring cyclic voltammograms.

[1] P. K. Kalambate et al., "Electrochemical (bio) sensors go green," Biosensors and Bioelectronics, vol. 163, p. 112270, May 2020, doi: 10.1016/j.bios.2020.112270.
[2] H. Teymourian, A. Barfidokht, and J. Wang, "Electrochemical glucose sensors in diabetes management: an updated review (2010–2020)," Chemical Society Reviews, vol. 49, no. 21, pp. 7671–7709, Jan. 2020, doi: 10.1039/d0cs00304b.

PLASMONIC METASURAFCE FOR ENHANCED HER KINETICS BY PHOTOELECTROCHEMICAL WATER SPLITTING.

Muhammad Haris[1], Klaudijus Midveris[1], Syeda Ammara Shabbir[2], Gvidas Klyvis[1], Mindaugas Juodėnas[1], Tomas Tamulevičius[1], Asta Tamulevičienė[1], Hamid latif[2], Sigitas Tamulevičius[1]

[1]Institute of Materials Science, Kaunas University of Technology, LT, 51423, Kaunas,
[2]Department of Physics, Forman Christian College (A Chartered University), Lahore, 54600, Pakistan,
muhammad.haris@ktu.edu

Hydrogen evolution reaction (HER) kinetics under solar light context has been enhanced by heterostructure photocatalysts assembled from plasmonic nanoparticles (NPs) coupled with semiconductors. Plasmonic Heterostructures manifested HER photocatalytic efficiency greater than solitary semiconductors because plasmonic NPs magnify the absorption wavelengths through their localized surface plasmons resonance (LSPR) within the visible–IR sweep. Nevertheless, these regimes exhibit major hinders of poor charge mobility from the Schottky junction, diminishing and limiting their noteworthy employment. On the contrary, the Plasmonic metasurface is a quintessential route for an undeviating metamorphosis of solar light to green hydrogen. It's an exquisite technique to magnify the quantum tunneling to adjacent RGO shielding barrier via the creation of hot spots and thermionic emission, through and over the feeble metal-metal junction (Ohmic junction). This approach could be considered to attain intensified hydrogen evolution kinetics at the onset potential of 0VRHE. According to the estimated computational assumptions, an explicit transmittance peak has been observed at 608 nm to produce Plasmonic lattice resonance or coupling by accompanying diffractive modes of a periodic array (SLR) and LSPR of single nanoparticles to enhance near-field coupling. In the visible region, this attribute can be employed to achieve almost 70%-80% HER kinetics compared to the complete solar spectrum, conversely, as solitary, at a specific wavelength corresponds to Plasmonic lattice coupling (608 nm), efficiency could be 20% to 30%[1-3].

Acknowledgements

This project has received funding from the Research Council of Lithuania (LMTLT), agreement no S-ST-24-10 (Water Splitting Enhancement by Plasmonic Nanomaterials (FORESAIL))

[1] Kravets, V. G., Kabashin, A. V., Barnes, W. L., & Grigorenko, A. N. (2018). Plasmonic surface lattice resonances: a review of properties and applications. Chemical reviews, 118(12), 5912-5951

[2] Bin-Alam, M. S., Reshef, O., Mamchur, Y., Alam, M. Z., Carlow, G., Upham, J., ... & Dolgaleva, K. (2021). Ultra-high-Q resonances in plasmonic metasurfaces. Nature communications, 12(1), 974.

[3] Guo, R., Chen, L., Yan, Z., Ma, R., Feng, S., & Deng, S. (2024). High-Quality Resonances from Plasmonic Nanoparticle Lattices under Normal Incidence. The Journal of Physical Chemistry C, 128(27), 11298-11305.

VISUAL RECOGNITION FOR MICRO-ACCURACY IN SECM RESEARCH

Rokas Bagdonas[1], Simonas Jurkynas[1], Inga Morkvėnaitė-Vilkončienė[1], Andrius Dzedzickis[1]

[1]Vilnius Gediminas Technical University
rokas.bagdonas@vilniustech.lt

This work investigates the performance accuracy of uniquely developed scanning electrochemical microscopy (SECM) devices and their errors in acceleration, which can negatively affect the accuracy of measurements. Scanning electrochemical microscopy (SECM) is a broader class of scanning probe microscopy (SPM) technique used to measure the local electrochemical behavior of liquid-solid, liquid-gas, and liquid-liquid interfaces. In this work, an image recognition technique is developed to provide the SECM operator with real-time information on the accuracy of the electrode movement. Using the MATLAB software environment and integrated image recognition algorithms, the methodology processes the digital microscope image, allowing accurate determination of the electrode position and possible errors.

The methodology's effectiveness was evaluated by performing tests on fixed reference samples, whose precise dimensions and location allowed an accurate measurement of the errors of the SECM device. The results showed that the methodology allows an accurate estimation of the displacement errors and the creation of a map of the expected errors. This allows not only a preliminary evaluation of the accuracy of the SECM device, but also a dynamic monitoring of possible undetected errors during experiments.

The main conclusion is that this methodology can be applied to both one-off and commercialized SECM devices, improving their accuracy and smoothness. A major advantage of the methodology is its ease of use. It does not require modification of the SECM device, as it builds on existing components such as the digital microscope. The only possible modification required is the addition of a comparison scale to the sample holder, but experiments have shown that the technique works without it. In future studies, the system can be enhanced to improve the accuracy of detection of organic sample shapes.

Co/β ZEOLITE FOR ORR IN ALKALINE MEDIA

Kristina Radinović[1], Jadranka Milikić[1], Ana Nastasić[2], Katarina Rondović[1], Ljiljana Damjanović-Vasilić[1], Aldona Balčiūnaitė[3], Vladislav Rac[4], Rastko Vasilić[5]

[1]University of Belgrade, Faculty of Physical Chemistry, Studentski trg 12-16, 11158 Belgrade, Serbia
[2]Department of Nuclear and Plasma Physics, Vinča Institute of Nuclear Sciences – National Institute of the Republic of Serbia, University of Belgrade, P.O. Box 522, 11001 Belgrade, Serbia
[3]Center for Physical Sciences and Technology, Saulėtekio Ave. 3, Vilnius LT-10257, Lithuania
[4]Faculty of Agriculture, Department of Chemistry, University of Belgrade, Nemanjina 6, 11080 Zemun, Serbia
[5]University of Belgrade, Faculty of Physics, Studentski trg 12-16, 11000 Belgrade, Serbia
kikaftm@gmail.com

Zeolites, also known as crystalline aluminosilicates, are characterized by their large specific surface area, porosity, and easy incorporation of cations, which makes them attractive materials for use in electrocatalysis [1,2]. Therefore, this group of materials can be used for the oxygen reduction reaction (ORR) as there is a trend of the world transitioning to green energy sources in an increasingly demanding effort to protect the environment [3,4].

In this work, β zeolite was synthesized in combination with the transition metal cobalt (Co), and as such was tested for activity towards ORR. Namely, the electrocatalytic activity was tested in N_2- and O_2- saturated 1 M KOH solution at 20 mV s^{-1}, using cyclic voltammetry (CV).

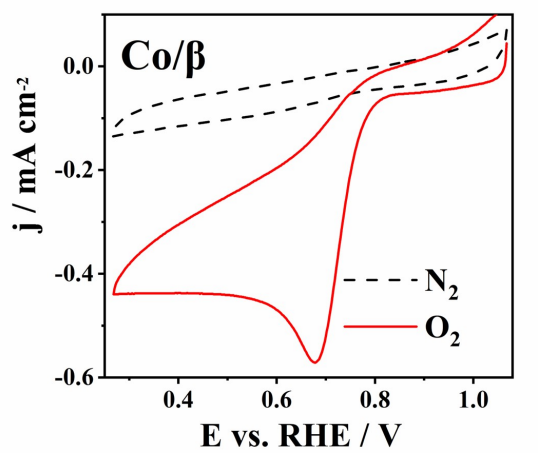


Fig. 1. CVs (cathodic scan) of Co/β at 20 mV s^{-1} in N_2- and O_2- saturated 1 M KOH solution.

As can be seen from **Fig. 1**, a clearly defined characteristic peak for ORR is observed at a potential of 0.68 V with a current density of about -0.60 mA cm^{-2}. On the other hand, the current density in N_2 was about -0.06 mA cm^{-2}, confirming the activity of Co/β zeolite for ORR, which further implies that the synthesized zeolite may represent a potentially good catalyst for application in fuel cells and batteries.

[1] J. Milikić, S. Stojanović, L. Damjanović-Vasilić, R. Vasilić, L. Rakočević, S. Lazarević, B. Šljukić, Porous cerium-zeolite bifunctional ORR/OER electrocatalysts in alkaline media, J. Electroanal. Chem. 944 (2023). https://doi.org/10.1016/j.jelechem.2023.117668
[2] J. Milikić, S. Stojanović, L. Damjanović-Vasilić, R. Vasilić, B. Šljukić, Efficient bifunctional cerium-zeolite electrocatalysts for oxygen evolution and oxygen reduction reactions in alkaline media, Synth. Met. 292 (2023) 1–10. https://doi.org/10.1016/j.synthmet.2022.117231.
[3] J. Milikić, A. Nastasić, M. Martins, C.A.C. Sequeira, B. Šljukić, Air Cathodes and Bifunctional Oxygen Electrocatalysts for Aqueous Metal–Air Batteries, Batteries. 9 (2023) 394. https://doi.org/10.3390/batteries9080394.
[4] K. Radinović, D. Mladenović, J. Milikić, M. Alsaiari, F.A. Harraz, D.M.F. Santos, B. Šljukić, Tuning Electrocatalytic Activity of Gold Silver Nanoparticles on Reduced Graphene Oxide for Oxygen Reduction Reaction, J. Electrochem. Soc. 169 (2022) 054501. https://doi.org/10.1149/1945-7111/ac67b7.

Ni/β ZEOLITE FOR OER IN ALKALINE MEDIA

Jadranka Milikić[1], Ana Nastasić[2], Kristina Radinović[1], Katarina Rondović[1], Ljiljana Damjanović-Vasilić[1], Aldona Balčiūnaitė[3], Vladislav Rac[4], Rastko Vasilić[5]

[1]University of Belgrade, Faculty of Physical Chemistry, Studentski trg 12-16, 11158 Belgrade, Serbia
[2]Department of Nuclear and Plasma Physics, Vinča Institute of Nuclear Sciences – National Institute of the Republic of Serbia, University of Belgrade, P.O. Box 522, 11001 Belgrade, Serbia
[3]Center for Physical Sciences and Technology, Saulėtekio Ave. 3, Vilnius LT-10257, Lithuania
[4]Faculty of Agriculture, Department of Chemistry, University of Belgrade, Nemanjina 6, 11080 Zemun, Serbia
[5]University of Belgrade, Faculty of Physics, Studentski trg 12-16, 11000 Belgrade, Serbia
jadrankamilikic87@gmail.com

Rechargeable metal-air batteries (MABs) present the most attractive electrochemical devices with charging by oxygen evolution reaction (OER) and discharging by oxygen reduction reaction (ORR). Namely, MAB performances strongly depend on the OER/ORR activity of the examined electrocatalyst. It is well known that RuO_2/IrO_2 and Pt are the most active for the catalysis of OER and ORR, respectively. The high price and scarcity of them limited their electrochemical applications [1-3].

Zeolite is the most attractive porous crystalline solid with many applications in different areas because of its unique structure [3,4]. Zeolite β (BEA structural type) as a three-dimensional intersecting channel system was ionically exchanged with Ni and calcinated at high temperature to prepare Ni/β zeolite [4]. Crystalline structure and morphology of the Ni/β was done by X-ray powder diffraction analysis (XRD) and scanning electron microscopy with energy dispersive spectroscopy (SEM-EDS), respectively.

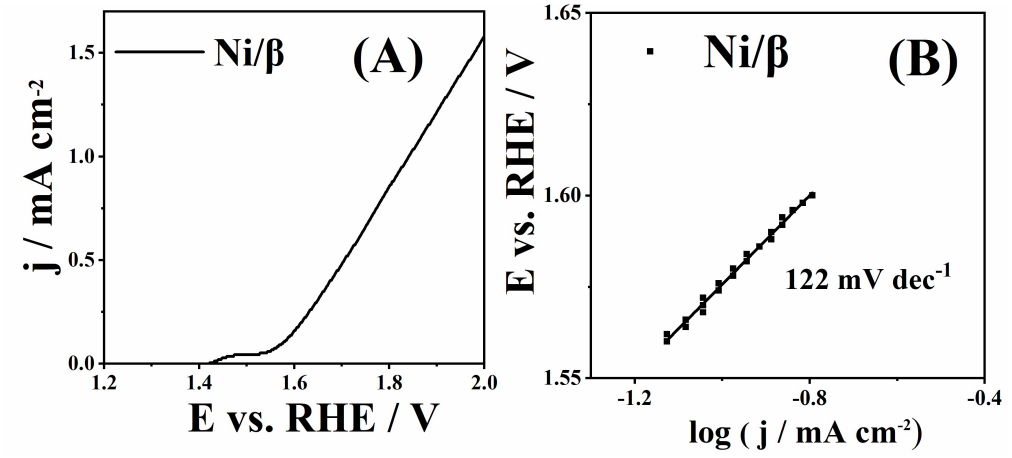


Fig. 1. OER polarization curves of Ni/β at 20 mV s^{-1} and 1200 rpm (A), with the corresponding Tafel plots (B).

Here we present an examination of Ni/β zeolite as an electrocatalyst for OER in alkaline media. Namely, Ni/β shows OER activity with a Tafel slope of 122 mV dec^{-1} and a current density of 1.5 mA cm^{-2} at 2 V. This behavior is comparable with other OER zeolite electrocatalysts where Ce-β cal showed 114 mV dec^{-1} [4]. Ni/β could be combined with nano-structured carbon structure to improve potential application levels in MABs.

[1] J. Milikić, A. Nastasić, M. Martins et al., Air Cathodes and Bifunctional Oxygen Electrocatalysts for Aqueous Metal–Air Batteries, Batteries 9, 1-24 (2023).
[2] J. Milikić, A. Nastasić, S. Knežević et al., Efficient nano-size ZnM/rGO (M = Ni, Cu, and Fe) electrocatalysts for oxygen electrode reactions in alkaline media, International Journal of Hydrogen Energy 97, 247-258 (2025).
[3] J. Milikić, S. Stojanović, L. Damjanović-Vasilić et al., Porous cerium-zeolite bifunctional ORR/OER electrocatalysts in alkaline media, Journal of Electroanalytical Chemistry 944, 117668 (2023).
[4] J. Milikić, S. Stojanović, L. Damjanović-Vasilić et al., Efficient bifunctional cerium-zeolite electrocatalysts for oxygen evolution and oxygen reduction reaction in alkaline media, Synthetic Metals 292, 117231 (2023)..

CHARACTERIZATION OF FIBROUS MICROPLASTIC EMITTED FROM VIRGIN AND RECYCLED POLYESTER FABRICS

Ugnė Gliaudelytė[1]

[1]Department of Production Engineering, Kaunas University of Technology, Lithuania
ugne.gliaudelyte@ktu.edu

Fiber-shaped microplastics, often referred to as *fibrous microplastic*, are plastic particles with a length higher than 300 nm and lower than 15 mm and with a diameter to length ratio higher than 3 [1]. It was found that recycled synthetic fibers release more fibrous microplastics than virgin fibers, because they are more prone to breakage due to their uneven surfaces and lower break and tensile strengths [2, 3]. These results started raising questions about whether recycled fibers are a more sustainable choice. However, the morphological differences in microplastics also play a significant role in their mitigation. In this paper, a simple methodology was used to collect, analyze and compare the quantity and the morphological differences between virgin and recycled polyester fibrous microplastics emitted into the water during washing.

Two black interlock knitted polyester fabrics with filament yarns used in women's sportswear were selected: F1 composition – 100 % virgin polyester, mass per unit area – 120.0 ± 5 g/m^2, thickness – 0.600 ± 0.05 mm, course density – 19.0 ± 0.5 cm^{-1}, wale density – 23.0 ± 0.5 cm^{-1}; F2: composition – 100 % recycled polyester, mass per unit area – 100.0 ± 5 g/m^2, thickness – 0.490 ± 0.05 mm, course density – 24.0 ± 0.5 cm^{-1}, wale density – 33.0 ± 0.5 cm^{-1}. Three samples of each fabric were washed five times in water with liquid detergent. Wastewater was collected after each wash and filtered through filters. Filters were weighed before and after filtration. Image analysis was performed using light microscope *Lumenera INFINITY* and *ImageJ* software to assess fibrous microplastics number, length, and shape.

Results confirmed that amounts of fibrous microplastic after each wash from both fabrics were similar and differences were statistically insignificant, but fibrous microplastics from recycled polyester fabrics were longer than fibrous microplastics from the virgin polyester fabric. These findings suggest that assessing fibrous microplastic morphology is important when implementing microplastic mitigations strategies, because fewer but longer particles are easier to mitigate than higher amounts of shorter particles.

[1] ISO 4484-2:2023. Textiles and textile products—microplastics from textile sources—part 2: qualitative and quantitative analysis of microplastics. [Accessed: February 16, 2025]
[2] Yuksekkaya ME, Celep G, Dogan G, et al. A comparative study of physical properties of yarns and fabrics produced from virgin and recycled fibers. J Eng Fibers Fabr 2016; 11: 155892501601100209. [Accessed: February 16, 2025]
[3] Uyanık S. A study on the suitability of which yarn number to use for recycled polyester fiber. J Text Inst 2019; 110: 1012–1031.

IMPACT OF HEXAMETHYLDISILAZANE ON BEETROOT POWDER BYPRODUCTS AND POLYMER INTERACTION: PROPERTIES AND INTERFACIAL DYNAMICS

khadija ramzan[1]

[1]Lithuanian center for agriculture and forestry science
khadija.ramzan@lammc.lt

Polydimethylsiloxanes (PMDSs) are most used polymer in siloxane elastomer. However, because of an intrinsic weak connection between PDMS chains, these polymers exhibit poor mechanical strength and tear resistance, which limits their application. To enhance their properties many fillers including pigments from fruit and vegetable waste, have been studied as a sustainable reinforcement. Because of their low price, accessibility, and environmental benefits, natural reinforcements have become more and more popular in recent years, spurred by environmental concerns. The aim of this study is to incorporate the coarse powdered beetroot waste (BWP) before and after silylation into PDMS and to investigate the effect of silylating agent on the properties of composites. In this study BWP was incorporated into single component poly(dimethylsiloxane) (PDMS) macromolecular matrix at different concentrations (5%, 10%, 15%, and 20%) before and after silylation with hexamethyldisilazane (HMDS) by a mixing process to develop a bioelastomer composites with tuneable properties. Hexamethyldisilazane (HMDS) is a silylating agent was used to modify the fillers and to investigate its effect for hydrophobicity, thermal stability, and reinforcement effects. The color of beetroot powder changed from red to dark brownish after silylation, indicating chemical modifications. The results showed that hydrophobicization improved the surface wettability by up to 20%. This implies that the material's surface became more hydrophobic. From SEM analysis the obtained composite with the beetroot powder shows strong adhesion at the interface (the area where different materials meet). This suggests that the pigment might play a role in improving the interaction between the composite material and any surface it adheres to, possibly enhancing the mechanical properties. Tensile strength in PDMS/beetrootHMDS 20% inceraese 35 % compare with pure PDMS. In addition to improving the interfacial adhesion between the filler and silicone composites, silylation promotes the network's densification of materials. Keywords: Silylation, hexamethyldisilazane (HMDS), polydimethylsiloxane (PDMS), bioelastomer composites, natural fillers, sustainable materials.

[1] Ahmad, D., Van Den Boogaert, I., Miller, J., Presswell, R., & Jouhara, H. (2018). Hydrophilic and hydrophobic materials and their applications. Energy Sources, Part A: Recovery, Utilization, and Environmental Effects, 40(22), 2686-2725.

[2] Jankauskaitė, V., Balčiūnaitienė, A., Alexandrova, R., Buškuvienė, N., & Žukienė, K. (2020). Effect of cellulose microfiber silylation procedures on the properties and antibacterial activity of polydimethylsiloxane. Coatings, 10(6), 567.

The Influence of Industrial Tea Waste Ash on Mechanical Properties of Natural Rubber Materials

Jelena Lubura Stošić[1], Oskar Bera[1], Dario Balaban[1,2], Teodora Vukša[1], Siniša Simić[1]

[1]University of Novi Sad, Faculty of Technology Novi Sad, Bulevar cara Lazara 1, 21000 Novi Sad, Serbia
[2]University of East Sarajevo, Faculty of Technology Zvornik, Karakaj 34A, 75400 Zvornik, Republic of Srpska, Bosnia and Herzegovina
jelenalubura@uns.ac.rs

Tea demand is rising rapidly worldwide and is expected to keep growing in the next decade. To keep up with the increasing demand for tea, global production is increasing, leading to the accumulation of vast amounts of tea waste, which causes significant environmental challenges. As a result, there is a strong research focus on finding sustainable ways to repurpose this waste, and make a valuable product through circular economy. One promising approach is the incorporation of tea waste ash into rubber products, providing a solution to both the environmental challenges of tea waste and the industry's need for eco-friendly materials. Rubber products are widely used in numerous applications, particularly where their high elasticity is essential. The rubber industry is increasingly pursuing renewable alternatives, driven by its heavy reliance on fossil fuels and the fast-rising demand for energy. Tea waste, a type of lignocellulosic biomass, can be burned and the resulting ash utilized in rubber products. In this research, the different tea waste, green tea (*camellia sinensis*), hibiscus (*rosa sinensis*) and lemongrass (*melissa officinalis*), were burned in a furnace with circulating air at 800 °C in order to obtain ash for natural rubber composites. The obtained tea waste ash, with varying contents of 2.5 and 5 phr, was incorporated into the natural rubber mixture using a standard commercial recipe and then vulcanized at 150 °C during 15 minutes. Mechanical properties (hardness, elongation at break, tensile strength) were tested, revealing that 2.5 phr of tea waste ash, regardless of the tea type, can be added without significantly affecting the product's mechanical properties. Furthermore, the sample containing 2.5 phr of lemongrass waste ash did not impact the mechanical properties of final natural rubber product. The results of this study demonstrated that a small amount of tea waste ash can be incorporated into natural rubber composites without significantly affecting the mechanical properties of the rubber products. Utilizing herbal ash offers significant advantages, as it repurposes waste into a valuable resource, enhancing the circular economy. Additionally, it allows the rubber industry to meet stringent environmental protection requirements.

Acknowledgements

The authors would like to acknowledge the Ministry of Science, Technological Development and Innovation of Republic of Serbia for their financial support, Project No. 451-03-65/2024-03/200134.

DEVELOPMENT OF A CAPSAICIN-BASED DRUG DELIVERY SYSTEM

Felix Lücke[1], Šarūnas Žukauskas[1,3], Arūnas Ramanavičius[1,2], Almira Ramanavičienė[2,3]

[1]Centre for Physical Sciences and Technology
[2]Vilnius University
[3]State Research Institute Centre for Innovative Medicine
felix.luecke@ftmc.lt

Treatment for chronic pain consists of opioids and NSAIDs, which can cause health issues on their own.[1] The topical application of capsaicin is a promising milder alternative. However, due to concerns about the effectiveness and associated risks of long-term use of capsaicin [2-4], a polymer-based drug delivery system (DDS) may help address these issues. Our objective was to design and explore a polymer-based drug delivery system for the topical application of capsaicin.

To achieve this goal, we first extracted capsaicin from chili peppers using vegetable oil. The oil infused with capsaicin (CapOil) was then embedded into a polypyrrole (PPy) matrix, which was further fused together and stabilized with polyaniline (PANI).

Capsaicin was released from the produced system using chronoamperometry. The release characteristics of the system were analyzed with spectrometry, Chrono Amperometry (CA) and Pulsed Chrono Amperometry (PCA).

We were able to design a functioning DDS system based on a polymer matrix with inserted capsaicin.

The ratio of polymer to analyte was optimized to 30vol% of CapOil. The best release potential was determined to be 1.75V. A long-term PCA measurement showed that the system reacts predictable to applied potential after an initial 10min delay. Based on these findings we were able to design and build a prototype (see Figure 1).

The gathered results show that a polymer-based DDS in combination with capsaicin is viable. With further research these systems could be developed into a product.

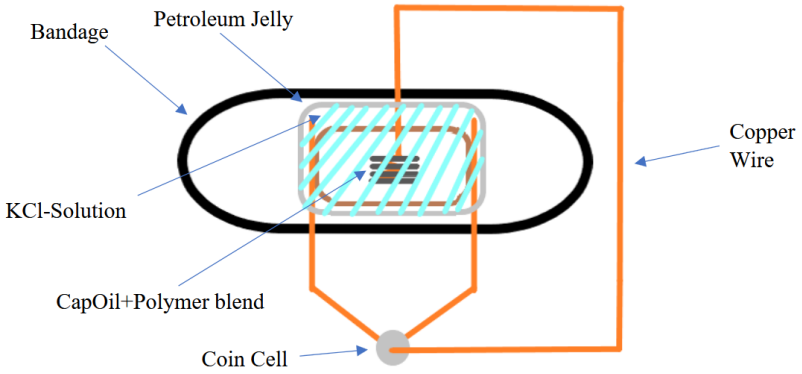


Fig. 1. Schematic of the prototype

Acknowledgements

This project has received funding from the Research Council of Lithuania (LMTLT), project No P-PD-24-159.

[1] 1. Mills SEE, Nicolson KP, Smith BH (2019) Chronic pain: a review of its epidemiology and associated factors in population-based studies. BJA: British Journal of Anaesthesia 123:e273. https://doi.org/10.1016/J.BJA.2019.03.023

[2] 2. Mason L, Moore RA, Derry S, Edwards JE, McQuay HJ (2004) Systematic review of topical capsaicin for the treatment of chronic pain. BMJ : British Medical Journal 328:991. https://doi.org/10.1136/BMJ.38042.506748.EE

[3] 3. Rollyson WD, Stover CA, Brown KC, Perry HE, Stevenson CD, McNees CA, Ball JG, Valentovic MA, Dasgupta P (2014) Bioavailability of capsaicin and its implications for drug delivery. J Control Release 0:96. https://doi.org/10.1016/J.JCONREL.2014.09.027

[4] 4. Arora V, Campbell JN, Chung MK (2021) Fight fire with fire: Neurobiology of capsaicin-induced analgesia for chronic pain. Pharmacol Ther 220

SYNTHESIS AN NANOCRYSTALLISATION OF Na_{2+x} $VFe_2(PO_4)_{3-x}(SiO_4)_x$ ALLUAUDITE-TYPE GLASSES

Martyna Jankowska[1], Krzysztof Gadomski[1], Maciej Nowagiel[1], Tomasz K. Pietrzak[1], Lauren Blanc[2], Linda Nazar[2]

[1]Faculty of Physics, Warsaw University of Technology, Poland
[2]Department of Chemistry and the Waterloo Institute for Nanotechnology, University of Waterloo, Ontario, ON, Canada
martyna.jankowska.stud@pw.edu.pl

Last few decades, intensive development of batteries has been observed. Right now, they are used almost everywhere: in electric cars, smartphones, and even to stabilize power output from renewable power sources. In the last case, sodium-ion batteries (NIBs) are expected to be a sustainable and cheap alternative to lithium ones [1].

Alluaudites, first described by Fisher in 1955 [2], are among the prospective cathode materials for NIBs, with a theoretical gravimetric capacity close to 170 mAh/g [3]. However, poor electrical conductivity is one of the main obstacles to their implementation. Our previous studies on amorphous analogues of selected cathode materials show a significant increase in electrical conductivity as a result of their thermal nanocrystallisation due to the occurrence of the preferable conditions for the polaron hopping mechanism [5].

In our previous research, we studied alluaudite-like materials with a nominal composition of $Na_2Fe_3(PO_4)_3$, $Na_2Fe_2V(PO_4)_3$, and $Na_2FeMnV(PO_4)_3$ [4]. We observed a significant (5 orders of magnitude) and irreversible increase in the conductivity, resulting in nanomaterials with (25 °C) ≈ 1 mS/cm. We also elaborated optimal synthesis conditions to obtain alluaudite-like nanomaterials with maximum possible phase purity [6]. We performed electrochemical characterisation of the most prospective samples in prototype sodium cells. Their average performance, however, did not reflect the superior electrical conductivity of the active material.

Therefore, in this work, we decided to synthesise $Na_2Fe_2V(PO_4)_3$ alluaudite-like glass with an addition of silicon dioxide. It is expected that SiO_4 tetrahedra might change the ion transport landscape in nanocrystalline materials and, consequently, improve their electrochemical performance. Here, we present the thermal (DSC), structural (XRD) and electrical (impedance spectroscopy) properties of our novel nanomaterials.

[1] V. Palomares et al., Energy & Environmental Science 5 (2012), 5884–5901
[2] D.J. Fisher, American Mineralogist 40 (1955), 1100–1109.
[3] K. Trad et al., Chemistry of Materials 22 (2010), 5554–5562.
[4] A.E. Chamryga et al., Journal of Non-Crystalline Solids 526 (2019), 119721.
[5] T.K. Pietrzak et al., Materials Science and Engineering B 213 (2016), 140–147.
[6] M. Nowagiel et al., Materials 14(17) (2021), 4997.

PHYTOHYDROGELS WITH THE ADDITION OF STARCH AND MODIFIED STARCH

Kolomiiets Viktoriia[1], Irina Liashok[1], Viktoriia Plavan[1], Olena Kryukova[1], Viacheslav Shvets[1]

[1]Kyiv National University of Technology and Design
lyashok.io@knutd.com.ua

Oral diseases are a pressing health problem worldwide. Their characteristic features are infections caused by microorganisms, inflammatory processes and tissue degradation. Hydrogels, due to their unique characteristics, have gained great importance in modern dentistry [1]. Their three-dimensional structure, high water content, biocompatibility and various biological properties make them suitable for use as drug delivery systems, antimicrobial agents, matrices for tissue regeneration and biosensors. Due to the resistance of many microorganisms to synthetic drugs, the use of dosage forms with plant extracts is relevant [2].

The work investigated the possibility of obtaining PVA hydrogels based on aqueous extracts of nettle, chamomile and oak bark by cryostructuring with the addition of starch (St) and carboxymethylated starch (CMS) in a 1:1 ratio. It is known that PVA forms a spatial structure of hydrogels upon thawing, and St and CMS upon freezing. It was found that all the studied phytohydrogels form stable structures, which were studied for their sorption properties in relation to the action of distilled water and physiological NaCl solution [3, 4]. All hydrogels reach an equilibrium value of the degree of sorption within 3-4 hours. The value of the equilibrium degree of sorption depending on the composition and type of plant extract is shown in the Figure 1.

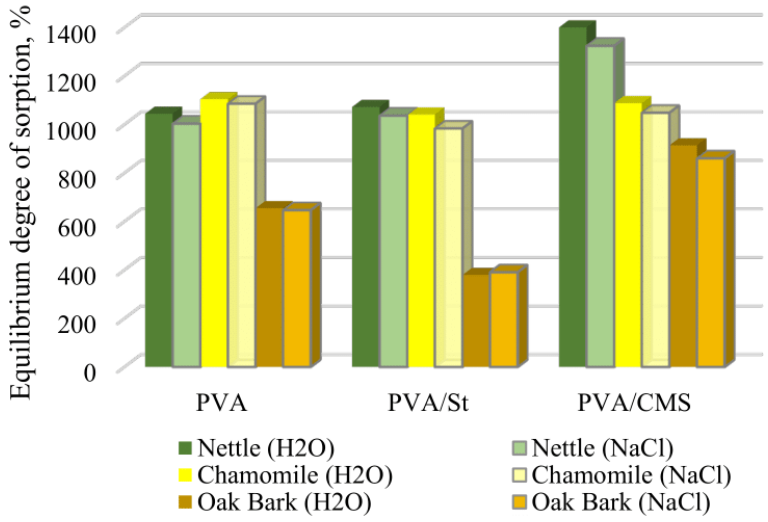


Fig. 1. Dependence of the equilibrium degree of sorption of PVA hydrogels based on aqueous extracts of nettle, chamomile, and oak bark with the addition of starch or carboxymethylated starch.

It was found that the addition of CMS increases the equilibrium degree of sorption for samples based on nettle extract and oak bark by 1.47 and 1.39 times, respectively. For hydrogels based on chamomile extract, the equilibrium degree of sorption decreases with the addition of St by 1.06 times, and with the addition of CMS by 1.01 times. Thus, taking into account the values of the equilibrium degrees of sorption, it is advisable to continue research in the direction of determining the nature of the release of active ingredients of plant extracts to establish the effectiveness of the use of hydrogels in dentistry.

[1] W. Chen, C. Zhang, S. Peng, Y. Lin, and Z. Ye, “Hydrogels in Dental Medicine,” Adv. Therap., vol. 7, p. 2300128, 2023. doi: 10.1002/adtp.202300128.
[2] A. I. Lopes, M. M. Pintado, and F. K. Tavaria, “Plant-Based Films and Hydrogels for Wound Healing,” Microorganisms, vol. 12, no. 3, p. 438, 2024. doi: 10.3390/microorganisms12030438.
[3] I. Liashok, O. Kriukova, V. Shvets, M. Kychuzhynets, and V. Halahan, “Physical properties of hydrogels and pva films based on aqueous nettle extract,” Herald of Khmelnytskyi National University. Technical Sciences, vol. 343, no. 6(1), pp. 412–417, 2024. doi: 10.31891/2307-5732-2024-343-6-61.
[4] I. O. Liashok, V. P. Plavan, O. A. Kriukova, M. M. Polushkin, V. V. Shvets, and Ya. S. Shapovalova, “Influence of polysaccharides on physical properties of pva films and hydrogels based on aqueous extract of the medicinal chamomile (Matricaria Chamomilla),” Technologies and Engineering, no. 5(22), pp. 101–109, 2024. doi: 10.30857/2786-5371.2024.5.10.

PHOTOPHYSICAL STUDY OF PURINE BASED MOLECULES FOR METAL ION SENSING

Jana Jermak[1], Kamilė Boguševičienė[1], Justina Jovaišaite[1], Irina Novosjolova[2], Maris Turks[2], Gediminas Jonušauskas[3], Gediminas Kreiza[1], Huang-Tsung Chang[4], Saulius Juršėnas[1]

[1]Institute of Photonics and Nanotechnology, Faculty of Physics, Vilnius University, Lithuania
[2]Institute of Technology of Organic Chemistry, Faculty of Materials Science and Applied Chemistry, Riga Technical University, Latvia
[3]Laboratoire Ondes et Matière d'Aquitaine, Bordeaux University, France
[4]Department of Biomedical Sciences, College of Medicine, Chang Gung University, Taoyuan, Taiwan
jana.jermak@ff.stud.vu.lt

Purine is a nitrogen-containing aromatic compound with a fused pyrimidine-imidazole ring structure which plays a crucial role in forming essential biological molecules: DNA, RNA. Current applications of purines are mainly focused on therapeutic and pharmaceutical areas for instance, anti-cancer therapy, antiviral drugs and bio-stimulation (caffeine) [1]. Beyond medical applications, purine-based derivatives with molecular D – A – D‘ structure show significant potential in metal ion sensing [2]. This important property of the purine compounds allows for the extension of application areas to use purine-based derivatives in environmental monitoring and chemical analysis.

Four purine derivatives (AIB – 137, AIB – 188, ZiK – 740, ZiK – 772) with two donor groups of different strength at positions C2 and C6 were under investigation for metal ion sensing purpose. Several characterization techniques were used, including steady-state absorption and fluorescence. Compounds of the AIB type were compared based on their efficacy in detecting tin (II) using acetonitrile as a solvent. The replacement of carbon atoms with oxygen in the carbon chains resulted in increased water solubility of ZiK type molecules. It was observed, that these purine derivatives are highly sensitive for silver (II) ions. Relatively more polar ZiK – 740 showed great potential for metal ion sensing inside living cells, which facilitates their use in biomedical applications.

[1] A. Kovaļovs, I. N.. 1,2,3-Triazoles as leaving groups in purine chemistry: a three-step synthesis of N6-substituted-2-triazolyl-adenine nucleosides and photophysical properties thereof. Tetrahedron Lett., 54(8), 850–853. (2013)
[2] J. Jovaisaite, D. C.. Proof of principle of a purine D–A–D’ ligand based ratiometric chemical sensor harnessing complexation induced intermolecular PET. Phys. Chem. Chem. Phys., 22, 26502. (2020)

DESIGNING THERMORESPONSIVE POLY(N-ISOPROPYLACRYLAMIDE) COPOLYMERS FOR BIOMEDICINE VIA ONE-POT MICROWAVE-ASSISTED SYNTHESIS

Marija Krstić[1], Nina Jokić[1], Ivan Ristić[1]

[1]University of Novi Sad, Faculty of Technology Novi Sad, Bulevar cara Lazara 1, 21000 Novi Sad, Serbia
mkostic607@gmail.com

Poly(N-isopropylacrylamide) (PNIPAM) is a thermoresponsive polymer widely studied for its lower critical solution temperature (LCST) of 32°C, making it suitable biomedical applications. The aim of this work is to synthesize PNIPAM-based copolymers with an adjusted LCST of 37°C, ideal for biomedical applications, through an innovative one-pot microwave-assisted polymerization process. Copolymers were synthesized using comonomers such as methyl methacrylate (MMA), acrylic acid (AAc), acrylamide (AAm), maleic anhydride (MA), and styrene (St), with comonomer concentrations ranged from 5 wt% to 20 wt%. Structural, thermal and mechanical characterization of the obtained copolymers was carried out using Fourier-transform infrared spectroscopy (FTIR), differential scanning calorimetry (DSC) and dynamic-mechanical analysis (DMA). Results showed significant LCST tunability based on comonomer type and concentration. Copolymers with MMA displayed stable LCSTs at ∼33°C across all concentrations. AAc-based copolymers, as well as MA-based copolymers, achieved LCSTs of 34–35°C, while Aam-based copolymers demonstrated precise control, with LCSTs ranging from 36°C (5 wt% AAm) to 39°C (10 wt% AAm), achieving the desired 37°C with the addition of 6 wt% AAm. Conversely, copolymers with St exhibited a substantial decrease in LCST to 21°C, reflecting the hydrophobic influence of styrene. FTIR confirmed successful copolymerization, while DSC and DMA analyses provided insights into thermal transitions and mechanical properties, respectively. This study highlights the potential of microwave synthesis in tailoring PNIPAM-based thermosensitive films for biomedicine via copolymerization, with precise LCST adjustments enabling advanced applications in wound dressing and drug delivery.

Acknowledgements

Authors would like to thank the NATO SPS program, project G6031-"Wearable Smart Patches for Multimodal Wound Healing - DRESWOUTRE" for financial support.

Ni/β ZEOLITE FOR ORR IN ALKALINE MEDIA

Ana Nastasić[1], Jadranka Milikić[2], Kristina Radinović[2], Katarina Rondović[2], Ljiljana Damjanović-Vasilić[2], Aldona Balčiūnaitė[3], Vladislav Rac[4], Rastko Vasilić[5]

[1]Department of Nuclear and Plasma Physics, Vinča Institute of Nuclear Sciences – National Institute of the Republic of Serbia, University of Belgrade, P.O. Box 522, 11001 Belgrade, Serbia
[2]University of Belgrade, Faculty of Physical Chemistry, Studentski trg 12-16, 11158 Belgrade, Serbia
[3]Center for Physical Sciences and Technology, Saulėtekio Ave. 3, Vilnius LT-10257, Lithuania
[4]Faculty of Agriculture, Department of Chemistry, University of Belgrade, Nemanjina 6, 11080 Zemun, Serbia
[5]University of Belgrade, Faculty of Physics, Studentski trg 12-16, 11000 Belgrade, Serbia
ana.nastasic@vin.bg.ac.rs

The development of novel, efficient enough, more stable and low-cost electrocatalysts for the oxygen reduction reaction (ORR) is one of the crucial obstacles to the commercialization of fuel cells and metal-air batteries, i.e. the world's transition to green zero-carbon energy sources and solving the energy supply problem [1,2]. Crystalline aluminosilicates, better known as zeolites, have a unique structure that makes them suitable as active matrix in electrocatalysis, namely: exceptional ion exchange capacity, high adsorption, and large specific surface area [3-5].

Herein, β zeolite was combined with the transition metal nickel (Ni) that shows promising stability and activity in the field of electrocatalysis. The electrocatalytic activity of the obtained material (Ni/β) towards ORR was examined in N_2- and O_2- saturated 1 M KOH solution by cyclic voltammetry (CV) (**Fig. 1**).

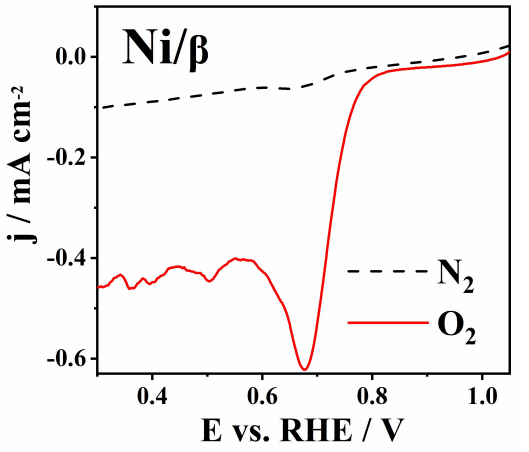


Fig. 1. CVs (cathodic scan) of Ni/β at 20 mV s^{-1} in N_2- and O_2- saturated 1 M KOH solution

A characteristic ORR peak was observed at a potential of 0.68 V vs. RHE in an O_2- saturated solution. Slightly more than ten times higher current density at this potential in an O_2- saturated solution, compared to the current density observed in a N_2- saturated solution, leads to the conclusion that Ni/β zeolite is active towards the ORR and that it could be potentially good replacement for costly benchmark platinum-based electrocatalysts.

Acknowledgements

A.N. acknowledge support provided by the Vinča Institute of Nuclear Sciences, through Contract No. 451-03-136/2025-03/ 200017 with the Ministry of Science, Technological Development, and Innovation of the Republic of Serbia.

[1] J. Milikić, A. Nastasić, M. Martins et al., Air Cathodes and Bifunctional Oxygen Electrocatalysts for Aqueous Metal–Air Batteries, Batteries 9, 1-24 (2023).
[2] J. Milikić, A. Nastasić, S. Knežević et al., Efficient nano-size ZnM/rGO (M = Ni, Cu, and Fe) electrocatalysts for oxygen electrode reactions in alkaline media, International Journal of Hydrogen Energy 97, 247-258 (2025).
[3] J. Milikić, S. Stojanović, L. Damjanović-Vasilić et al., Porous cerium-zeolite bifunctional ORR/OER electrocatalysts in alkaline media, Journal of Electroanalytical Chemistry 944, 117668 (2023).
[4] J. Milikić, S. Stojanović, L. Damjanović-Vasilić et al., Efficient bifunctional cerium-zeolite electrocatalysts for oxygen evolution and oxygen reduction reaction in alkaline media, Synthetic Metals 292, 117231 (2023).
[5] X. Wei, Y. Li, Z. Hua et al., One-Pot Synthesized Nickel-Doped Hierarchically Porous Beta Zeolite for Enhanced Methanol Electrocatalytic Oxidation Activity, ChemCatChem 12, 6285-6290 (2020).

PREPARATION OF Sm3+ IONS DOPED MgAl2O4 BY SOL-GEL POLYACRYLAMIDE SYNTHESIS

Pranga Prava Mandal[1], Dovydas Karoblis[2], Aivaras Kareiva[3]

[1]Institute of Chemistry, Vilnius University, Naugarduko 24, LT-03225, Vilnius, Lithuania
prava.mandal@chgf.stud.vu.lt

Luminescence is a spontaneous emission of radiation from an electronically excited species not in thermal equilibrium with its environment. Luminescent materials can absorb energy and then emit that energy as photons of light [1]. This is known as excitation and emission. Luminescent materials are composed of a different matrix and an activator (usually transition element or lanthanide). Many different classes of materials can be used as matrices, including perovskites, pyrochlores, spinels, etc. WIn our experiment we are using MgAl2O4 spinel material as a matrix. While many different lanthanide ions, like Eu3+ [2], Ho3+ [3], have already been doped into the magnesium aluminate structure, there is no work regarding the Sm3+ substitution for this spinel. In this work, we investigated the possible Sm3+ ions doping into the MgAl2O4 system.

MgAl2O4 spinel was prepared by sol-gel polyacrylamide synthesis route. As this method uses acrylamide, which during the polymerization reaction forms a polymer carcass, restricting the growth of the particles. We have prepared phase pure MgAl2O4 compounds in the broad temperature range from 700 °C up to 1200 °C with relatively short annealing time of 2 h. When we tried the doping of small concentration of Sm3+ ions, there was a formation of MgO as an impurity phase. The final compounds were analyzed by different techniques, including X-ray diffraction, scanning electron microscopy (SEM) FT-IR spectroscopy. SEM results showed that with the increasing temperature the particle size increased. FTIR graphs showed the formation of spinel structure as well as that at the lower temperature (700 °C), there were additional peaks which could possibly be for Mg-O-C due to incomplete combustion.

[1] Amol Nande, … S.J. Dhoble, in Functional Materials from Carbon, Inorganic, and Organic Sources, 2023.
[2] I. E. Kolesnikov, E. V. Golyeva, A. V. Kurochkin, M. Mikhailov, Structural and luminescence properties of MgAl2O4:Eu3+ nanopowders, Journal of Alloys and Compounds, 654 (2016) 32-38.
[3] S. N. Manjula, M. Chandrasekhar, M. R. Anil Kumar, V. Bhoomika, N. Raghavendra, M. N. Somashekar, C. R. Ravikumar, H. Nagabhushana, Studies on photoluminescence, electrochemical sensors, and photocatalysis using Ho3+-doped MgAl2O4 nanophosphors, Journal of the Iranian Chemical Society, 21.5 (2024) 1245-1257.

SAMARIUM AND GADOLINIUM DOPED CERIA NANOPOWDERS FOR INTERMEDIATE TEMPERATURE SOLID OXIDE FUEL CELLS

Augustinas Zinkus[1,2], Mantas Sriubas[1,2], Brigita Abakevičienė[1,2]

[1]Institute of Materials Science, Kaunas University of Technology, K. Baršausko st. 59, 51423 Kaunas, Lithuania
[2]Department of Physics, Kaunas University of Technology, Studentų st. 50, 51368 Kaunas, Lithuania
augustinas.zinkus@ktu.lt

New advances in hydrogen fuel cells technology play a significant role in addressing environmental problems, caused by traditional (combustion) methods of electrical energy generation. Solid oxide fuel cells (SOFCs) are capable of directly transforming chemical energy into electricity with high efficiency, fuel flexibility and low environmental impact, offering clean energy conversion [1, 2]. The electrolyte is fundamental to the operation of SOFC, as it serves to separate the fuel at the anode from the oxidant at the cathode. To achieve high efficiency, the electrolyte must possess high oxygen ion conductivity, minimal electronic conductivity and chemical stability under operational conditions [3]. However, using traditional electrolytes, such as yttria-stabilized zirconia (YSZ), these properties are only observed at high temperatures (800-1000 °C), which leads to material degradation and reduced longevity [4]. The previous research studies indicate that ceria-based electrolytes, especially co-doped with rare earth elements - samarium (Sm^{3+}) and gadolinium (Gd^{3+}), enhance oxygen ion conductivity and maintains high efficiency at intermediate temperatures (500-700 °C).

This research focuses on samarium and gadolinium co-doped ceria (SGDC), as an alternative electrolyte material. SGDC nanopowders with stoichiometric formula ($Ce_{0.825}Sm_{0.0875}Gd_{0.0875}O_{2-\delta}$) were synthesized using co-precipitation synthesis method. The XRD results of co-doped ceria nanopowders confirmed fluorite-type cubic structure (Fig. 1 a)). Calculated crystallite sizes and lattice parameters of SGDC nanopowders as a function of temperature are plotted in Fig. 1 b). The average lattice parameter is 542.9 pm and crystallite size is 23.2 nm at higher calcination temperatures. The morphological properties of the pressed ceramic pellets were examined using scanning electron microscopy (SEM). The impedance spectroscopy (IS) showed an increase in the total resistance of ceramics.

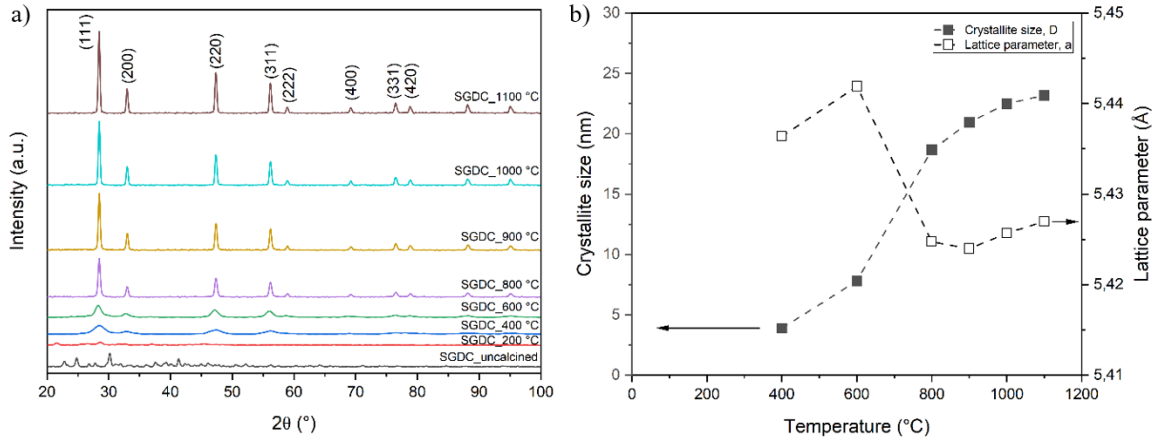


Fig. 1. a) XRD patterns of SGDC nanopowders and b) plot of the crystallite size *D* and lattice parameter *a* vs. calcination temperatures

Acknowledgements

The research was funded by project No. S-MIP-24-8/2025 of the funding programme by the Research Council of Lithuania (LMT).

[1] R.-A. Felseghi, E. Carcadea, M. S. Raboaca, C. N. TRUFIN, and C. Filote, "Hydrogen Fuel Cell Technology for the Sustainable Future of Stationary Applications," Energies, vol. 12, no. 23, p. 4593, Dec. 2019, doi: https://doi.org/10.3390/en12234593
[2] M. K. Singla, P. Nijhawan, and A. S. Oberoi, "Hydrogen fuel and fuel cell technology for 61a cleaner future: 61a review," Environmental Science and Pollution Research, vol. 28, no. 28, Feb. 2021, doi: https://doi.org/10.1007/s11356-020-12231-8
[3] M. Singh, D. Zappa, and E. Comini, "Solid oxide fuel cell: Decade of progress, future perspectives and challenges," International Journal of Hydrogen Energy, vol. 46, no. 54, pp. 27643–27674, Aug. 2021, doi: https://doi.org/10.1016/j.ijhydene.2021.06.020
[4] S. Hussain and L. Yangping, "Review of solid oxide fuel cell materials: cathode, anode, and electrolyte," Energy Transitions, Oct. 2020, doi: https://doi.org/10.1007/s41825-020-00029-8

ENHANCING ELECTRON TRANSFER EFFICIENCY IN MICROBIAL FUELCELLS THROUGH GOLD NANOPARTICLE MODIFICATION OF SACCHAROMYCES CEREVISIAE

Teresė Kondrotaitė[1], Antanas Zinovičius[1,2], Domas Pirštelis[2], Inga Morkvėnaitė-Vilkončienė[1,2]

[1]Vilnius Tech
[2]State Research Institute Centre for Physical Sciences and Technology
terese.kondrotaite@vilniustech.lt

This study investigates the microbial fuel cell (MFC) performance through the modification of Saccharomyces cerevisiae with gold nanoparticles (AuNPs) and polypyrrole (PPy). The yeast:AuNP-modified electrodes generated the highest median current of 2.57 nA, significantly outperforming the yeast:PPy-modified (0.82 nA) electrodes. Power density measurements further confirmed the superior performance of the yeast:AuNP-modified electrodes, showcasing a notable improvement in current densities and power outputs. Yeast:AuNP-modified graphite electrodes produced a higher power density of 22.8 mW/m2, albeit with a lower current density, compared to electrodes modified solely with yeast which produced a power density of 5.7 mW/m2. These findings highlight the potential of AuNPs in significantly enhancing the electrochemical performance of yeast-based MFCs, providing a promising approach for the development of more efficient bioelectrochemical systems.

ENHANCING T7 DNA POLYMERASE IMMOBILIZATION FOR REUSABLE BIOSENSORS

Julija Sarvutiene[1], Deivis Plaušinaitis[2], Arunas Ramanavicius[1,2], Urte Prentice[1,2]

[1]Center for Physical Sciences and Technology
[2]Vilnius University, Department of Physical Chemistry, Faculty of Chemistry and Geoscience, Naugarduko str. 24, LT-03225 Vilnius, Lithuania
urte.bubniene@gmail.com

The immobilization of DNA-modifying enzymes onto solid surfaces is a complex yet essential task in biotechnology, especially for reusable biosensors for DNA analysis [1]. One of the unique challenges in immobilizing these enzymes is their structural sensitivity and the risk of denaturation, distinguishing them from more robust industrial enzymes that can function effectively while attached to solid supports. This study focuses on enhancing the reusability of T7 DNA polymerase by optimizing its immobilization process for sustainable biotechnological applications. DNA-modifying enzymes often require precise conditions, such as specific ion concentrations (e.g., Mg^{2+} for polymerases) and stable temperatures [2]. To monitor the real-time immobilization of T7 DNA polymerase and evaluate the analytical signals produced during enzymatic activity, we employed quartz crystal microbalance (QCM) technology. QCM does not require additional labeling, which reduces potential interference and helps maintain enzyme activity. It can detect mass changes at the nanogram level, making it ideal for monitoring thin molecular layers and facilitating targeted DNA detection. We explored covalent attachment strategies using self-assembled monolayers of different thiol compositions on a gold-based QCM sensor (QSense-disk) to enhance enzyme stability and functionality. Additionally, we implemented an active-site protection strategy [2,3] for exonucleases to reduce the risk of inactivation. Our findings demonstrate that effective immobilization allows DNA detection while preserving enzyme functionality, paving the way for cost-effective, reusable biosensors. These results underscore the potential of immobilized DNA-modifying enzymes in real-time, label-free biosensing technologies, offering significant advantages [4,5] for continuous DNA analysis and sustainable biotechnological applications.

[1] Dronina, J., Bubniene, U. S. & Ramanavicius, A. The application of DNA polymerases and Cas9 as representative of DNA-modifying enzymes group in DNA sensor design (review). Biosensors and Bioelectronics 112867 (2020) doi:10.1016/j.bios.2020.112867
[2] Dronina, J., Plausinaitis D., Bubniene, U. S., Ramanavicius, A. Real-time-flow and label-free assessment of T7 DNA polymerase immobilization. Materials Today Nano. 100232 (2022)
[3] Lim, G., Hwang, H. J. & Kim, J. H. Protected immobilization of Taq DNA polymerase by active site masking on self-assembled monolayers of ω-functionalized thiols. Analytical Biochemistry 419, 205–210 (2011).
[4] Dronina, J., Bubniene, U. S., Ramanavicius, A. Towards application of CRISPR-Cpf1 in the design of modern viral DNA detection tools (Review). Journal of Nanobiotechnology. 41 (2022)
[5] Dronina, J., Bubniene, U. S., Ramanavicius, A. Advances and Insights in the Diagnosis of Viral Infections. Journal of Nanobiotechnology. 348 (2021)

SIMULTANEOUS IN SITU DIELECTRIC AND CRYSTALLOGRAPHIC TEMPERATURE DEPENDENT MEASUREMENTS.

Kaspars Jaundzems[1], Reinis Ignatans[1]

[1] Institute of Solid State Physics, University of Latvia
jaun.kaspars@gmail.com

The dielectric and crystallographic measurements of various materials using X-ray diffraction (XRD) methods, accompanied by an inductance, capacitance, resistance (LCR) meter, can be of great use for studying and modifying these materials. Performing these measurements independently has the chance to produce unexpected errors or lead to false conclusions.

In this work, the electrical infrastructure and software needed for these measurements were developed in order to obtain the XRD pattern and capacitance of materials under varying temperatures. From the capacitance data, it is possible to gain information on other properties of the material, such as its dielectric constant and polarization.

This system was tested on barium titanate ($BaTiO_3$), which has been extensively studied. This ceramic was chosen for its multiple structural phase transitions at different temperatures, in turn changing its dielectric constant. The results are well aligned with prior research indicating to the effectiveness of the system.

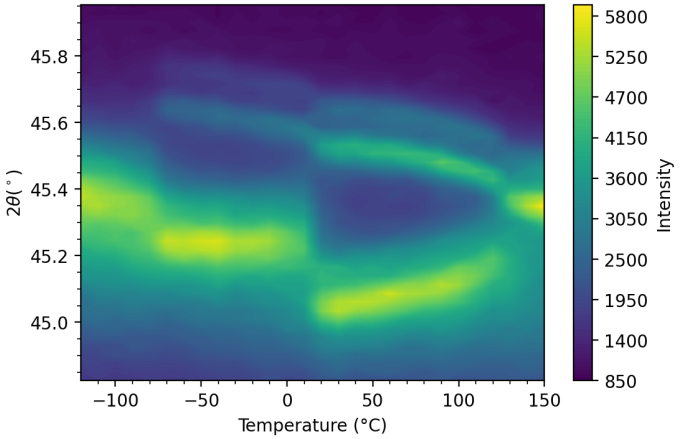


Fig. 1. Splitting of the (200) XRD peak of barium titanate with changing temperature, indicating a structural phase transition

HYBRID PLASMONIC-PHOTONIC MODES OF NANOPARTICLE ARRAYS IN HIGH REFRACTIVE INDEX THIN-FILM MEDIA

Klaudijus Midveris[1], Gvidas Klyvis[1], Mindaugas Juodenas[1], Joel Henzie[3], Tomas Klinavicius[1], Andrius Vasiliauskas[1], Asta Tamuleviciene[1,2], Tomas Tamulevicius[1,2]

[1]Institute of Materials Science, Kaunas University of Technology, Lithuania
[2]Department of Physics, Kaunas University of Technology, Lithuania
[3]Research Center for Materials Nanoarchitectonics, National Institute for Materials Science, Japan.
klaudijus.midveris@ktu.lt

One of the most studied methods for producing hydrogen is photoelectrochemical (PEC) water splitting, which uses solar energy and semiconductors that are abundant in the Earth's crust [1]. The efficiency of the H_2 evolution process under solar illumination has been greatly enhanced using heterostructure photocatalysts made of semiconductor materials, coupled with plasmonic noble metal nanoparticles (NPs) carrying localized surface plasmon resonances (LSPR). The NPs expand the light optical wavelength absorption capacity of wide bandgap semiconductors through the excitations of the conduction band electrons at the metal-semiconductor interface. Additionally, periodic arrangements of NPs allow for guidance of 1^{st} order diffraction orders into the thin-film semiconductor, introducing guided modes, further enhancing light absorption characteristics. Achieving critical coupling between the LSPR of individual particles, in-plane propagation of diffraction orders and their sustainment through guided modes in the surrounding thin film media allows the steady state absorption to be maximized under energy conservation [2]. This work investigates the light trapping and extinction capacity of periodic Ag cuboctahedra/thin film TiO_2 heterostructures through the experimental and computational evaluation (Fig. 1) of sustained hybrid plasmonic and photonic surface lattice resonances (SLRs), that show orders of magnitude stronger localized electromagnetic fields with respect to disordered arrangements of analogous particles [3].

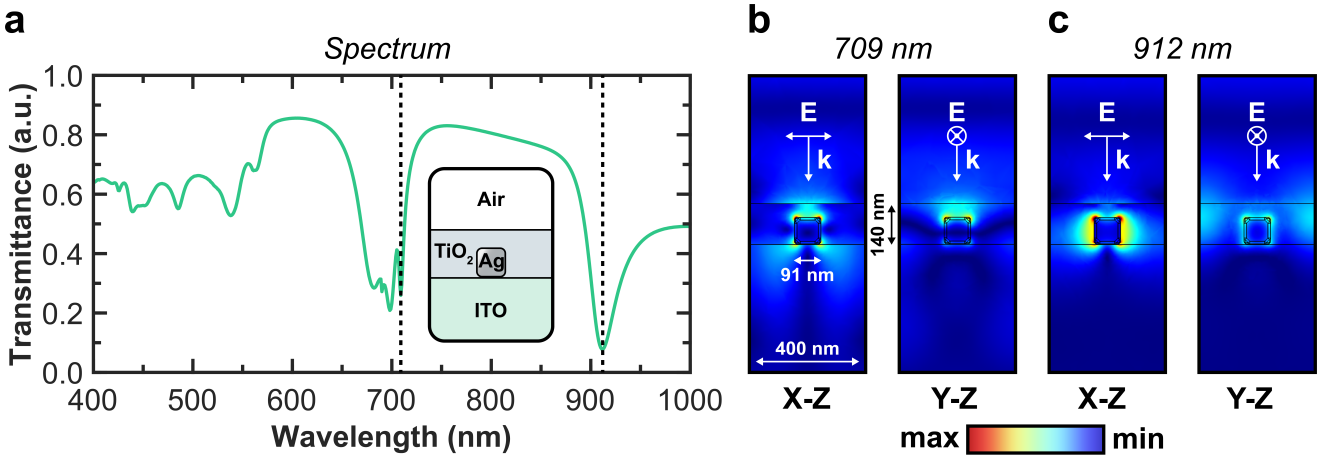


Fig. 1. Finite-Element-Method simulated transmittance spectrum of periodic Ag cuboctahedra/thin-film TiO_2/ITO heterostructure depicted in the inset (a), with the electric near-field enhancement distribution at resonant wavelengths of 709 nm (b) and 912 nm (c). The pitch of the NP array was 400 nm.

Acknowledgements
The work was supported by the Research Council of Lithuania (LMT) project No. S-MIP-23-93.

[1] ZHOU, Peng, NAVID, Ishtiaque Ahmed, MA, Yongjin, XIAO, Yixin, WANG, Ping, YE, Zhengwei, ZHOU, Baowen, SUN, Kai and MI, Zetian. Solar-to-hydrogen efficiency of more than 9% in photocatalytic water splitting. Nature 2023.
[2] TSE, Joshua T. Y., MURAI, Shunsuke, TANAKA, Katsuhisa. Resonant Critical Coupling of Surface Lattice Resonances with a Fluorescent Absorptive Thin Film. J. Phys. Chem. C 2023.
[3] JUODENAS, Mindaugas, TAMULEVIČIUS, Tomas, HENZIE, Joel, ERTS, Donats and TAMULEVIČIUS, Sigitas. Surface Lattice Resonances in Self-Assembled Arrays of Monodisperse Ag Cuboctahedra. ACS Nano 2019.

LOW-FREQUENCY NOISE CHARACTERISTICS OF GRAPHENE/h-BN/Si JUNCTIONS

Ingrida Pliaterytė[1], Justinas Glemža[1], Šarūnas Meškinis[2], Rimantas Gudaitis[2], Šarūnas Jankauskas[2], Asta Guobienė[2], Andrius Vasiliauskas[2], Sandra Pralgauskaitė[1], Jonas Matukas[1]

[1]Institute of Applied Electrodynamics and Telecommunications, Vilnius University, Vilnius, Lithuania
[2]Institute of Materials Science, Kaunas University of Technology, Kaunas, Lithuania
ingrida.pliateryte@ff.stud.vu.lt

Widely studied for its exceptional electrical, thermal and optical properties, graphene is a promising material for electronic and optoelectronic device applications. Among these, graphene-Si Schottky junctions are actively researched for their potential use as solar cells, gas sensors, photodetectors and barristors [1]. However, the graphene-Si junction presents unresolved challenges including large variation of the ideality factor (~1-30) and limited performance due to graphene-Si interface defects such as dangling bonds at Si surface [2]. In effort to mitigate the latter problem passivating insulator layer is introduced between Si and graphene, with hexagonal boron nitride (h-BN) being well-suited due to its close lattice match to graphene [3]. To investigate such junctions low-frequency noise measurements are employed as they have proven to be a sensitive tool for assessing device quality, defectiveness and reliability and provide insight into underlying physical processes. The aim of this work is to investigate the low-frequency noise characteristics of graphene/h-BN/n-Si(100) junctions for evaluation of their overall performance and its dependence on h-BN layer thickness.

Graphene/h-BN/n-Si(100) junctions with different h-BN layer thicknesses (0-15 nm) were investigated. Graphene was directly synthesized on the substrate using microwave plasma-enhanced chemical vapor deposition (PECVD). Electrical noise characteristics were measured in the 10 Hz – 100 kHz frequency range at forward and reverse bias. In all investigated samples $1/f$ or $1/f^{\alpha}$-type fluctuations were observed with "white" spectrum part of thermal noise at low bias (Fig. 1). Several samples are distinguished by Lorentzian type spectra (samples 3 and 4 in Fig. 1), which are attributed to charge carrier capture and emission processes with distinct relaxation times. Samples with higher resistance showed higher noise intensity while samples with the greatest h-BN layer thickness (15 nm) are characterized by lower noise intensity.

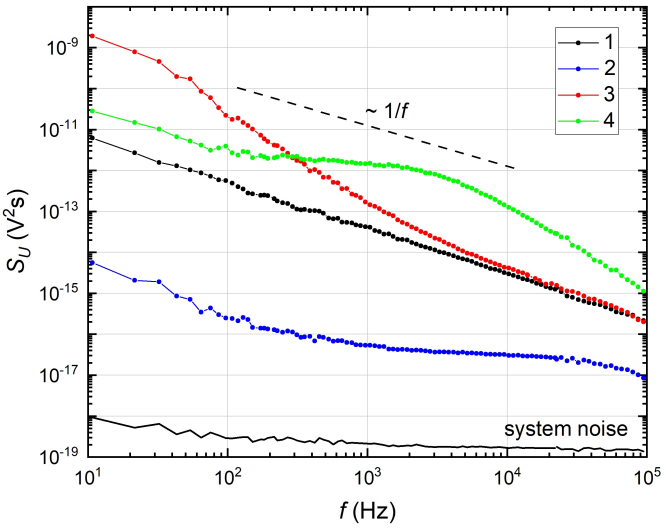


Fig. 1. Noise spectra with different types of observed electrical fluctuations in graphene/h-BN/n-Si(100) junctions with h-BN layer thickness of 3 nm at 0.5 mA (1), 15 nm at 0.005 mA (2), 0 nm at 0.095 mA (3) and 5 nm at 0.075 mA (4).

[1] An, Y. et al., "Forward-bias diode parameters, electronic noise, and photoresponse of graphene/silicon Schottky junctions with an interfacial native oxide layer", J. Appl. Phys., vol. 118, no. 11, p. 114307, (2015).
[2] Wong, H. et al., "Effects of silicon surface defects on the graphene/silicon Schottky characteristics", Results in Physics, vol. 29, p. 104744, (2021).
[3] Wang, C. et al., "Temperature dependent device characteristics of graphene/h-BN/Si heterojunction", Semicond. Sci. Technol., vol. 35, p. 075020, (2020).

ANALYSIS OF ELECTROMAGNETIC PROPERTIES IN VARIOUS 3D-PRINTED COMPOSITES

J. Varnyte[1], E. Palaimiene[1], J. Macutkevic[1], P. Blyweert[2], J. Banys[1], A. Celzard[2]

[1]Institute of Applied Electrodynamics and Telecommunications, Vilnius University, Sauletekio av. 3, LT-10257 Vilnius, Lithuania
[2]Université de Lorraine, CNRS, IJL, F-88000 Epinal, France
juta.varnyte@ff.stud.vu.lt

Electromagnetic radiation (EM) emitted by various devices can affect other devices in their path, reducing their efficiency or even causing damage. EM shielding materials help prevent this. These materials, known as absorbers, act as barriers to the propagating radiation [1]. A material's absorption increases with more electric and magnetic dipoles. Materials with high dielectric permittivity are the source of these dielectric dipoles [2]. Standard-filled materials require significant amounts of resources. Therefore, various structured materials are being developed. This approach aims to reduce resource consumption and lower production costs.

The objective of this study is to investigate the electromagnetic radiation absorption of composite materials with different concentrations of carbon nanotubes (1.3 wt % and 1.8 wt %) and barium titanate ($BaTiO_3$) (10 % and 20 %) across a broad frequency range. Additionally, it evaluates how the absorption coefficient depends on the 3D structure of the composite material.

Figure 1 presents the measured dependence of the absorption coefficient on frequency for samples with different structures and compositions. The best absorption is observed in composites containing barium titanate additives. At the highest concentration (20 %), the highest absorption coefficient values (0.3 – 0.7) were recorded. In a filled plate, the absorption coefficient reaches up to 70 %. As the EM frequency increases, the HREA structure also exhibits rapidly rising values, with absorption increasing from 40 % to 60 %. The poorest absorption (30 % – 40 %) is observed in BH-structured samples containing barium titanate. It was determined that the most minor changes in absorption properties compared to the filled plate occur when using the HREA structure.

Even at low concentrations (1.3 wt % and 1.8 wt %), carbon nanotubes used as polymer composite fillers enhance electromagnetic radiation absorption. Increasing the $BaTiO_3$ concentration further improves shielding properties. While the 3D structure significantly influences the material's interaction with electromagnetic radiation, greater attention should be given to its composition to develop the most effective absorber for practical applications.

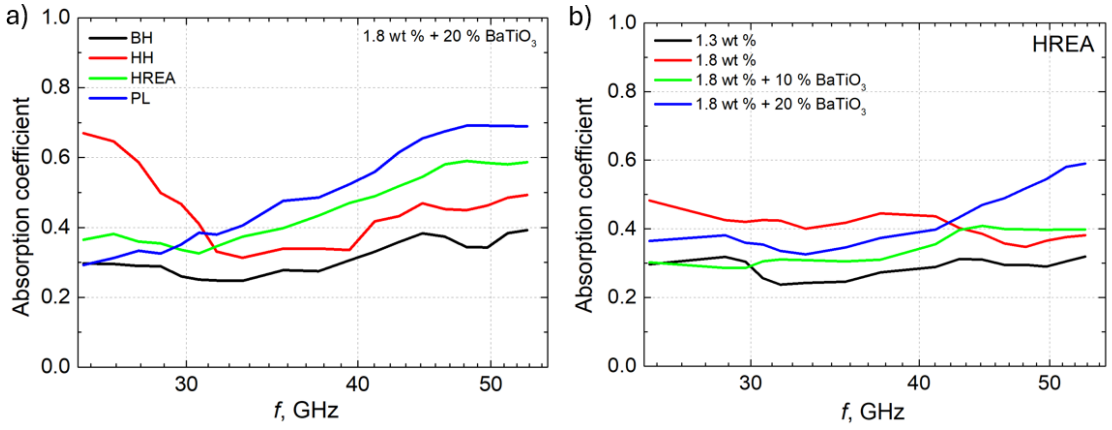


Fig. 1. Dependence of the absorption coefficient on frequency in a) composites with 1.8 wt % carbon nanotubes and 20 % barium titanate fillers and b) HREA 3D-structured samples with different concentrations.

[1] M. Nasreen Taj, B. Daruka Prasad et al., PANI-molybdate nanocomposites: Structural, morphological and dielectric properties for the effective electromagnetic interference (EMI) shielding applications in X-band, Applied Surface Science Advances, 7, 100203 (2022). https://doi.org/10.1016/j.apsadv.2021.100203

[2] Y. Tao, P. Li, S. Q. Shi, Effects of Carbonization Temperature and Component Ratio on Electromagnetic Interference Shielding Effectiveness of Woodceramics. Materials, 9(7):540 (2016). https://doi.org/10.3390/ma9070540

DEFECT SPECTROSCOPY IN PROTON IRRADIATED SILICON LOW GAIN AVALANCHE DETECTORS

Margarita Biveinytė[1], Tomas Čeponis[1], Laimonas Deveikis[1]

[1]Vilnius University, Institute of Photonics and Nanotechnology
margarita.biveinyte@ff.stud.vu.lt

Over the past few years, Low Gain Avalanche Detectors (LGADs) have demonstrated outstanding performance in detecting high-energy particles. They have been selected as the technology of choice for the timing detectors in the upcoming ATLAS and CMS upgrades of the High-Luminosity Large Hadron Collider (HL-LHC) [1]. Although LGADs exhibit good timing resolution and signal-to-noise (S/N) ratio when detecting high-energy charged particles due to the avalanche multiplication mechanism in the gain layer, they also suffer from radiation-induced performance degradation, which leads to the deterioration of silicon sensors' functional characteristics caused by electrically active defects within the bandgap of the material and acceptor removal effect in the gain layer [2]. Therefore, characterizing particle sensors before and after irradiation is essential to predict variations in their parameters under ionizing radiation, assess radiation hardness, develop new structures, and explore alternative applications.

In highly irradiated sensors, defect densities can be comparable to or even higher than the dopant concentration. As a result, sensitive analytical techniques for determining deep-level parameters, such as Capacitance Deep Level Transient Spectroscopy (C-DLTS), become ineffective. C-DLTS measurements with LGAD sensors have shown unreliable spectra due to strong capacitance drop [3]. For this reason, optical excitation technique such as photoionization spectroscopy can be employed. The photoionization spectroscopy method was chosen for defects identification, which allows the determination of defect levels or their complexes in a material based on their activation (absorption) energies even with high defect densities.

In this study, two sets of LGADs produced by Hamamatsu Photonics (HPK) [4] and Centro Nacional de Microelectrónica (CNM) [5] with an active area of 1.3×1.3 mm^2 were investigated in collaboration with CERN. The samples were irradiated with high energy protons (24 GeV) with fluences in the range of 10^{12} – 10^{16} p/cm^2. Activation energies and types of irradiation induced electrically active defects will be presented and discussed.

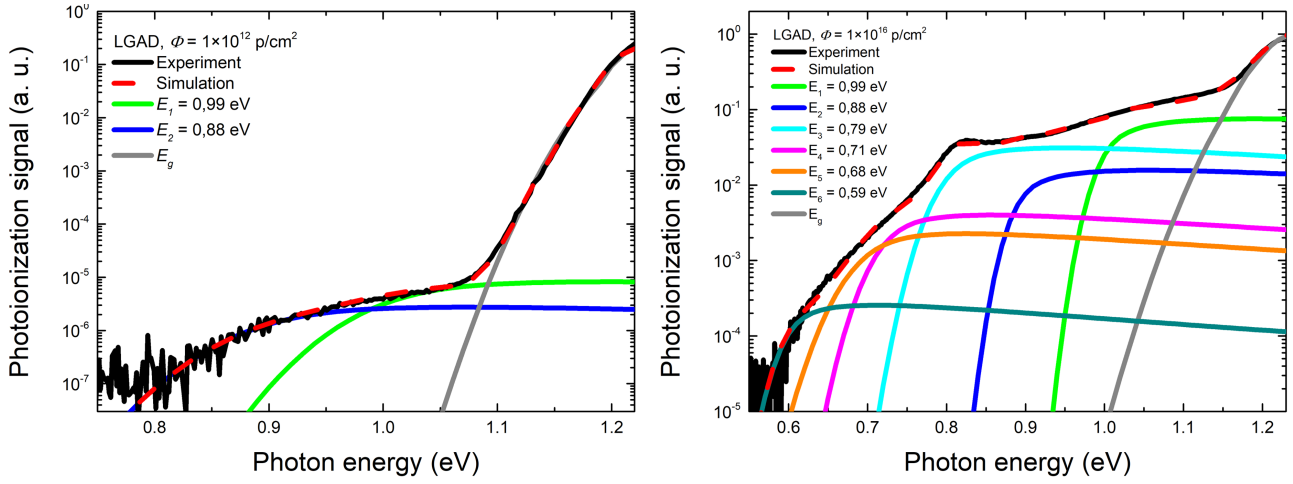


Fig. 1. Experimentally measured and simulated photoionization spectra of LGADs irradiated with different proton fluences.

[1] E. Currás, M. Fernández, M. Moll, Gain suppression mechanism observed in Low Gain Avalanche Detectors (2021).
[2] M. Moll, Displacement damage in silicon detectors for high energy physics. IEEE Transactions on Nuclear Science 65, 1561-1582 (2018).
[3] A. Himmerlich, N. Castello-Mor et al., Defect characterization studies on irradiated boron-doped silicon pad diodes and Low Gain Avalanche Detectors. Nuclear Instruments and Methods in Physics Research Section A 1048 (2023).
[4] https://www.hamamatsu.com/jp/en.html (last checked 2025-01-29).
[5] https://www.cnm.es/ (last checked 2025-01-29).

SPECTROSCOPY OF RADIATION-INDUCED DEFECTS IN p-TYPE Si AND SiGe ALLOYS

Gertrūda Pociūtė[1], Tomas Čeponis[1], Jevgenij Pavlov[1]

[1]Institute of Photonics and Nanotechnology, Vilnius University, Saulėtekio av. 3, LT-10257, Vilnius, Lithuania
gertruda.pociute@ff.stud.vu.lt

Radiation-induced transformations of boron dopant in p-type silicon (Si) lead to the “acceptor removal”, which degrades the performance of particle detectors [1]. The effect arises due to the transformation of substitutional lattice site boron (B_s) into interstitial (B_i) boron under irradiation. The subsequent migration of B_i and its interaction with interstitial oxygen impurity (O_i) in the Si crystal result in the formation of the interstitial boron–interstitial oxygen complex (B_iO_i), further altering the material properties. Alternative materials, such as silicon-germanium (SiGe), are being researched to mitigate these issues. SiGe alloys are promising materials for applications in photovoltaics, space technology, and high-frequency heterojunction bipolar transistors operating in the near-THz range [2]. Recent studies suggest their potential use in lithium-ion battery anodes [3] and microelectronic/optoelectronic devices, including high-speed temperature sensors, Hall-effect transducers, and γ-ray detectors [4,5]. In this work, p-type silicon (Si) and SiGe diodes with different Ge contents irradiated with 5,5 MeV electrons were studied. Capacitance deep-level transient spectroscopy (C-DLTS) and photoionization spectroscopy (PIS) were used to observe radiation-induced defects in SiGe detectors.

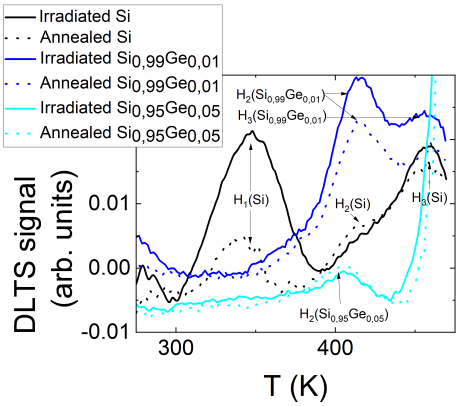


Fig. 1. The DLTS spectra of majority carrier traps in irradiated and annealed Si, $Si_{0,99}Ge_{0,01}$ ir $Si_{0,95}Ge_{0,05}$ diodes.

The DLTS spectra were measured in the 15–475 K temperature range. The spectra of the majority carrier traps were recorded at a reverse bias voltage of -5 V (U_R) and injection pulses of 200 ms duration (tp) at -0.1 V (U_P) (Fig.1). The spectra of the minority carrier traps were also investigated at reverse bias voltage (U_R) of -1 V and injection pulses of 200 ms duration (tp) at 2 V (U_P).

The results of this study, highlighting the radiation-induced defect dynamics in p-type Si and SiGe diodes with varying Ge contents and their evolution under annealing, will be presented and discussed in detail.

[1] J. Pavlov, T. Čeponis, K. Pukas, L. Makarenko, E. Gaubas, 5.5 MeV Electron Irradiation-Induced Transformation of Minority Carrier Traps in p-Type Si and Si1−xGex Alloys, Materials, 15 (2022). DOI: 10.3390/ma15051861.
[2] Y. Yang, S. Liu, X. Bian, J. Feng, Y. An, C. Yuan, Morphology- and Porosity-Tunable Synthesis of 3D Nanoporous SiGe Alloy as a High-Performance Lithium-Ion Battery Anode, ACS Nano, (2018). DOI: 10.1021/acsnano.8b00426.
[3] Yonenaga, I. Reference Module in Materials Science and Materials Engineering (Elsevier: Amsterdam, 2016).
[4] G. Kissinger, S. Pizzini, Silicon, Germanium, and Their Alloys: Growth, Defects, Impurities, and (CRC Press: Boca Raton, 2015).

DEPTH-DEPENDENT OPTICAL PROPERTIES OF InGaAs QUANTUM STRUCTURES EXPLORED BY VARIABLE EXCITATION ENERGY

Kipras Mažeika[1], Augustas Vaitkevičius[1,2], Andrea Zelioili[2], Aivaras Špokas[1,2], Renata Butkutė[1,2]

[1]Vilnius University, Institute of Photonics and Nanotechnology, Saulėtekio al. 3, Vilnius
[2]State research institute Center for Physical Sciences and Technology, Saulėtekio al. 3, Vilnius
kipras.mazeika@ff.stud.vu.lt

Indium gallium arsenide (InGaAs), a III-V group semiconductor alloy of indium arsenide (InAs) and gallium arsenide (GaAs), is valued for its tunable bandgap, high electron mobility, and enhanced quantum confinement effects [1-2]. These properties make it crucial for applications in photonics, high-speed electronics, and telecommunications [3-6]. The main drawback of the material is that the lattice mismatch between InGaAs and its GaAs substrate causes strain and defects like dislocations [7], which degrade performance by reducing carrier mobility and affecting optical properties [8]. In order to address this challenge, the growth parameters have to be optimized. In this work the InGaAs quantum structures were studied by performing photoluminescence (PL) measurements at different wavelengths to assess how growth parameters affect their structural properties.

Four InGaAs samples with varying In content (from 18% up to 26%) and structural features (barrier thicknesses) were grown by molecular-beam epitaxy (MBE) and investigated using a confocal microscope system. PL measurements using lasers with 405 nm and 662 nm wavelengths probed the structures at different depths to examine emission characteristics and assess material homogeneity.

The study found that emission maps differed significantly based on excitation wavelength due to variations in penetration depth. Defects visible with shorter excitation wavelengths were undetectable with longer wavelengths (Fig. 1). The results showed that indium content influences spectral properties, with higher indium levels leading to broader, red-shifted spectra under longer wavelength excitation. However, inconsistencies were observed under 405 nm excitation, likely due to limited penetration depth and noise.

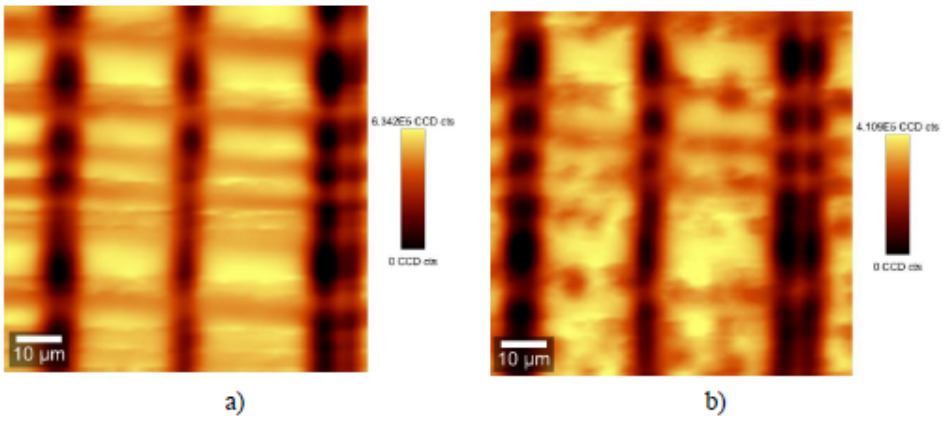


Fig. 1. PL intensity maps for $In_{0.26}Ga_{0.74}As$ sample obtained with (a) 662 nm excitation wavelength, (b) 405 nm excitation wavelength.

The obtained results suggest that indium content has direct impact on the spectral width and shift of the material's emission spectra. In addition, linking the features observed with different excitation wavelengths with the structural properties requires accurately determining absorption coefficients at energies significantly above the band gap.

[1] J. Katcki et al., "Formation of Dislocations in InGaAs/GaAs Heterostructures," phys. stat. sol. (a), vol. 171, no. 1, pp. 275–282, 1999,
[2] J. Wang et al., "Effect of localized states on the optical properties in InGaAs/GaAs multiple quantum wells grown by MOCVD," Photonics and Nanostructures - Fundamentals and Applications, vol. 51, p. 101047, 2022.
[3] K. C. Hsu et al., "Optical and electrical characteristics of GaAs/InGaAs quantum-well device," Journal of Alloys and Compounds, vol. 471, no. 1–2, pp. 567–569, 2009.
[4] X. Chen, et al., "MOCVD Growth and Thermal Stability Analysis of 1.2 mm InGaAs/GaAs Multi Quantum Well Structure". Journal of Alloys and Compounds, vol. 922, p. 166173, 2022.
[5] D. Gregušová et al., "Properties of InGaAs/GaAs metal-oxide-semiconductor heterostructure field-effect transistors modified by surface treatment," Applied Surface Science, vol. 395, pp. 140–144, 2017.
[6] T. Kikkawa, et al., "AlGaAs/GaAs and AlGaAs/InGaAs/GaAs High Electron Mobility Transistors Grown by Metalorganic Vapor Phase Epitaxy Using Tertiarybutylarsine," Japan Journal of Applied Physics, vol. 30, no. 10A, p. L1718, 1991.
[7] J. W. Matthews et al., "Defects in epitaxial multilayers," Journal of Crystal Growth, vol. 27, pp. 118–125, 1974.
[8] Ł. Gelczuk, et al., "Deep traps and optical properties of partially strain-relaxed InGaAs/GaAs heterostructures," Materials Science and Engineering: B, vol. 147, no. 2–3, pp. 166–170, 2008.

ADSORPTION PERFORMANCE OF MXENES FOR AZURE A AND METHYLENE BLUE: pH-DEPENDENT BEHAVIOUR AND KINETIC INSIGHTS

Germantė Paulikaitė[1], Simonas Ramanavičius[1], Šarūnas Žukauskas[2], Martynas Talaikis[3], Gediminas Niaura[3], Oleksiy Gogotsi[4]

[1]Center for Physical Sciences and Technology, Department of Electrochemical Material Science, Nanostructures Laboratory
[2]Center for Physical Sciences and Technology, Department of Nanotechnology, Bioanalysis Laboratory
[3]Center for Physical Sciences and Technology, Department of Organic Chemistry, Nanostructures Laboratory
[4]Materials Research Center, Krzhizhanovskogo street, 3, 03680, Kyiv, Ukraine
germante.paulikaite@ftmc.lt

This study looks over the perspective of MXenes, a novel class of two-dimensional materials, for the effective removal of organic contaminants. MXenes are characterized by their high surface area, excellent conductivity, unique surface chemistry, and strong adsorption capabilities. These materials are synthesized by adapting selective etching of aluminum layers from MAX-phase precursors, resulting in a layered structure suitable for various applications, e.g., surface-enhanced Raman spectroscopy [1], electrochemical sensors for water quality monitoring [2]. In this study, the adsorption performance of MXenes in removing organic pollutants, specifically Methylene Blue and Azure A, from aqueous solutions across a pH range from 4 to 6, was investigated. Initial results indicate that MXenes pose significant potential for dye adsorption due to their large active surface area. The adsorption efficiency and adsorption coefficients of MXenes were evaluated and calculated for both dyes under different pH conditions. Additionally, kinetic studies reveal that MXenes facilitate rapid adsorption, and regeneration studies indicate MXenes' reusability capabilities. The primary results indicate that MXenes could serve as a sustainable and highly efficient adsorbent for vast organic pollutant removal.

Acknowledgements
This project received funding from the Research Council of Lithuania (LMTLT), agreement No. S-MIP-24-14 .

[1] Adomavičiute-Grabusove S, Ramanavičius S, Popov A, Šablinskas V, Gogotsi O, Ramanavicius A. Selective enhancement of SERS spectral bands of salicylic acid adsorbate on 2D Ti3C2Tx-based MXene film. Chemosensors 2021;9:223. https://doi.org/10.3390/ijms21239224
[2] Ramanavičius S, Ramanavičius A. Progress and Insights in the Application of MXenes as New 2D Nano-Materials Suitable for Biosensors and Biofuel Cell Design. Int J Mol Sci 2020;21. https://doi.org/10.3390/ijms21239224

APPLICATION OF FIBERGLASS COMPOSITES TO PRODUCE COMPLEX GEOMETRIC PARTS

Agnius Paneckas[1], Urte Cigane[1], Justas Ciganas[1]

[1]Siauliai State Higher Education Institution
agnius.paneckas@stud.svako.lt

Fiberglass is widely used in the production of different parts to achieve the lightness of the structures without losing strength [1]. In order to create a part with complex geometry, the problem arises that it is necessary to produce larger workpieces, which must be subsequently processed by milling or using other technologies. In this work, a new technology is proposed to avoid further processing of the parts. The idea of the technology is to cut the fiberglass fabric to the required dimensions before curing and then, after precise positioning, cure it with ultraviolet (UV) resin. This process is repeated until the geometry of the required dimensions is obtained.

In this investigation, the fabrication of the composite and the analysis of its mechanical properties were included. Fiberglass and UV resin were used to create the composite. The UV resin was the same as that used for stereolithography (SLA) 3D printers. The fiberglass was cut according to the sample geometry of the ISO 527 standard 'dog bone'. Each layer was covered with UV resin and a new layer of fiberglass was added. The total height of the composite was 3 mm and there were 14 layers of fiberglass inside. The composite was cured with UV light.

Tensile results showed that the addition of UV resin to the fiberglass fabric increased the strength of the sample by 5.7 times. It is worth highlighting that the increase in strength was in one direction, so this should be taken into account when designing products. The tested composite was further analysed with a scanning electron microscope (SEM). After the analysis, it was determined that the UV resin was evenly distributed throughout the composite and filled the air gaps.

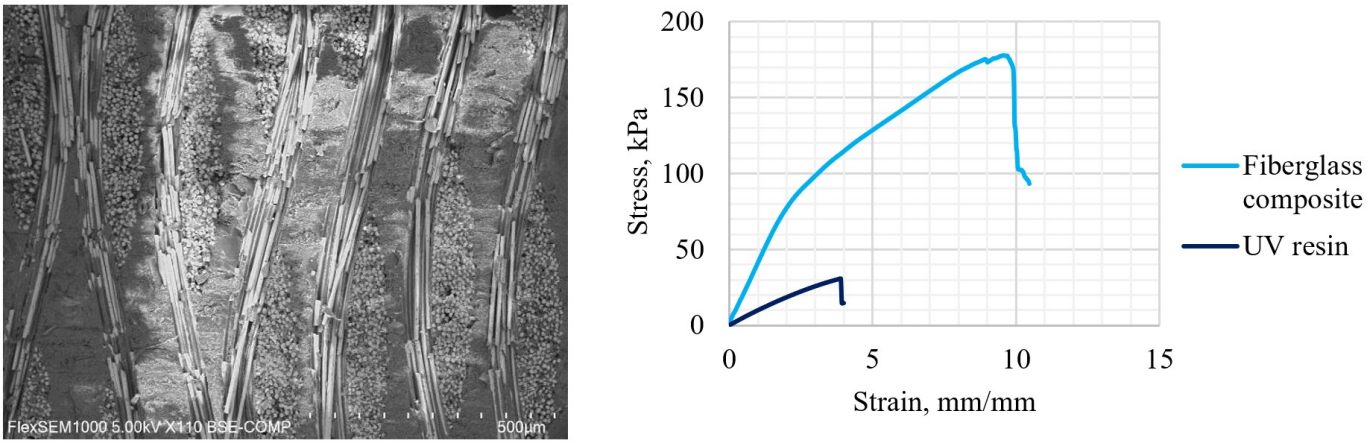


Fig. 1. SEM image of fiberglass composite and results of tensile test

The results of the study led to the conclusion that the technology for producing complex geometry parts using fiberglass composite provides an opportunity to increase the strength of parts. The data obtained will be used in further development of production technology.

[1] Săftoiu, G.V., Constantin, C., Nicoară, A., Pelin, G., Ficai, D. and Ficai, A. (2024) Glass Fibre-Reinforced Composite Materials Used in the Aeronautical Transport Sector: A Critical Circular Economy Point of View. Sustainability, 16, 4632. https://doi.org/10.3390/su16114632

DETERMINATION OF ETCHING PARAMETERS FOR STRUCTURAL TEXTILES TO IMPROVE ADHESION TO INORGANIC SEMICONDUCTORS

Evaldas Sutkus[1], Valentina Krylova[1]

[1]Kaunas University of Technology
evaldas.sutkus@ktu.edu

Solar energy is one of the most promising ways to generate electricity through photovoltaic conversion in solar cells. Currently, the most widely used silicon solar cells, while widely available, have significant limitations: they are material-intensive to manufacture, very brittle, and exhibit reduced efficiency at elevated temperatures [1]. To address these challenges, hybrid organic-inorganic materials have emerged as a potential alternative. In particular, the integration of structural textiles with inorganic semiconductors offers a route to more efficient and flexible solar cells due to their excellent optical and electrical properties, including high theoretical efficiency, robust thermodynamic stability, low toxicity and low-cost fabrication [2, 3].

This study focuses on evaluating the optimisation of etching parameters to improve the surface compatibility of structural textiles and inorganic semiconductors.

In order to determine the appropriate etching parameters, the process was evaluated by monitoring the appearance of hydroxyl groups on the surface after treatment in the etching solution consisting of acid and oxidant [4]. Samples of several commercially available structural textiles were treated in this solution for 2, 4 or 6 hours at a temperature of 70-100 °C. The samples were then rinsed with hot water, distilled water, dried and the attenuated total reflection Fourier transform infrared (ATR-FTIR) spectra recorded. After etching to determine the degree of etching required to ensure adhesion of the deposited semiconductor layer to the as-prepared samples, a very simple, inexpensive and economically reproducible SILAR method was used to deposit Ag_2S thin films at room temperature [5].

It was found that optimal surface modification was achieved when -OH groups were formed, as observed in the ATR-FTIR spectra (Fig. 1). This suggests increased surface hydrophilicity, which is expected to improve the adhesion of the deposited Ag_2S layer.

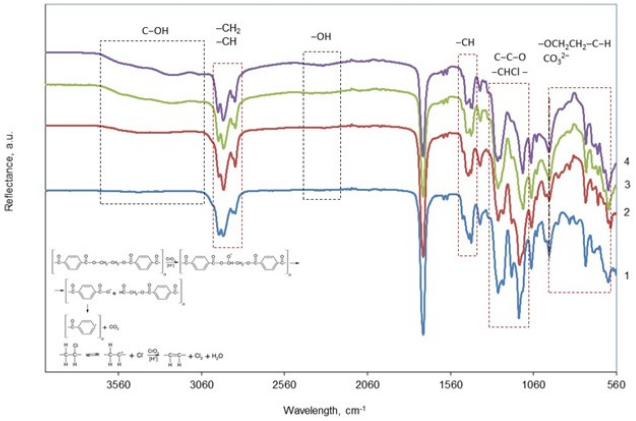


Fig. 1. ATR-FTIR spectra of unetched (1) and etched PET/PVC samples treated at 70±1 °C for different times (h): 2– 2; 3 – 4; 4 – 6.

Successful deposition of Ag_2S thin films on appropriately treated polymer substrates could pave the way for the development of flexible, efficient, and cost-effective hybrid solar cells. Future work will focus on optimizing the deposition of Ag_2S thin films and evaluation of the ability to use them for solar cells.

[1] Oni, A.M., Mohsin, A.S.M., Rahman, M.M., & Hossain Bhuian, M.B., Energy Rep. 11 (2024) 3345-3366.
[2] Dong, W., Fu, J., Yang, J., Ren, S., Zhu, H., Wang, Y., Hao, J., Zhang, Y., & Zheng, Z., J. Mater. Chem. C. 11 (2023) 16842-16858
[3] Hussain, N.A., Latif, L.A., & Mohamad, H.J., Indones. J. Electr. Eng. Comput. Sci. 31 (2023) 692-699.
[4] Alaburdaite, R., Krylova V. Polym. Degrad. Stab. 211 (2023) 1-14.
[5] Geremew, T., J. 3D Print. Appl. 1 (2022) 1-24.

ENHANCED PHYSICAL PROPERTIES OF PVB/ZNO-T/NAPT NANOCOMPOSITE COATINGS: DEVELOPMENT AND CHARACTERIZATION

Mindaugas Ilickas[1], Asta Guobienė[1], Simas Račkauskas[1], Brigita Abakevičienė[1,2]

[1]Institute of Materials Science, Kaunas University of Technology, K. Baršausko St. 59, 51423 Kaunas, Lithuania
[2]Department of Physics, Kaunas University of Technology, Studentų St. 50, 51368 Kaunas, Lithuania
mindaugas.ilickas@ktu.edu

The COVID-19 pandemic highlighted the link between hygiene, lifestyle, and microorganism spread, highlighting the need for durable biocide-resistant coatings. Antimicrobials, such as biocides and antibiotics, are crucial for infection control, but antimicrobial resistance, identified by the WHO as a global threat, could cause 10 million deaths annually by 2050 [1]. Zinc oxide (ZnO) and 2-mercaptopyridine N-oxide sodium salt (NaPT) are approved for safe antimicrobial use. Among ZnO structures, tetrapods (ZnO-T) are unique, with four nanorods joined at a central core [2].

This study developed durable PVB/ZnO-T/NaPT nanocomposite coatings and evaluated their physical properties on quartz glass. ZnO-T sizes were controlled by centrifugation (0-5000 rpm, S_0-S_5), and NaPT concentrations ranged from 0.1% to 10%. Physical properties were evaluated using XRD, UV-Vis's spectroscopy, and water contact angle (CA) analysis.

X-ray diffraction analysis of ZnO-T powders revealed a reduction in crystallite size with increasing centrifugation speed, decreasing from 42 nm at 0 rpm (S_0) to 30 nm at 5000 rpm (S_5). UV-Vis-NIR spectroscopy confirmed the successful formation of the PVB/ZnO-T/NaPT nanocomposite (see Fig. 1). The spectral properties demonstrated characteristic features of both ZnO-T and NaPT, indicative of their effective incorporation into the nanocomposite. Water contact angle (CA) analysis showed that smaller ZnO-T particle sizes enhanced the hydrophobicity of the coatings, with the CA increasing from 84° for PVB-ZnO-TS_0 to 98° for PVB-ZnO-TS_5. Similarly, coatings with higher NaPT concentrations exhibited improved hydrophobicity, with CA rising from 72° for PVB-0.1NaPT to 86° for PVB-10NaPT. However, when the PVB/ZnO-T/NaPT nanocomposite was formed, smaller ZnO-T sizes resulted in a decrease in CA. This research underscores the importance of optimising coating formation processes to improve the physical properties of the resulting coating surfaces.

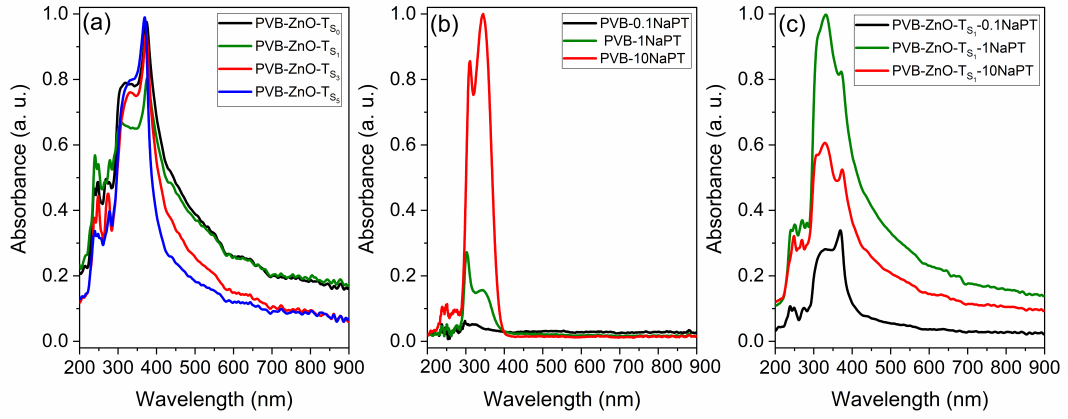


Fig. 1. UV-Vis's spectra of the analysed coatings: (a) PVB coatings incorporating ZnO-T particles of varying sizes; (b) PVB coatings containing different concentrations of NaPT; (c) PVB coatings incorporating ZnO-TS_1 particles combined with varying concentrations of NaPT

[1] K.W.K. Tang, B.C. Millar, J.E. Moore, Antimicrobial Resistance (AMR), Br J Biomed Sci 80 (2023).
[2] M. Ilickas, S. Rackauskas et al., ZnO tetrapod morphology influence on UV sensing properties, Nanotechnology 35 (2024).

DESIGN AND OPTIMIZATION OF HYBRID LIPID-POLYMERIC NANOPARTICLES FORTARGETED DRUG DELIVERY IN CARDIOVASCULAR DISEASES

Ugnė Žulpaitė[1], Vilma Petrikaitė[1,2]

[1]Laboratory of Drug Targets Histopathology, Institute of Cardiology, Lithuanian University of Health Sciences, Kaunas, Lithuania
[2]Institute of Biotechnology, Life Sciences Center, Vilnius University, Vilnius, Lithuania
ugne.zulpaite@lsmu.lt

Coronary heart disease (CHD), also known as ischemic heart disease (IHD), is a condition characterized by restricted blood flow to the heart muscle due to partial narrowing or complete blockage of the coronary arteries [1]. The coronary arteries are essential for maintaining heart health by ensuring a continuous blood supply. This blood delivers oxygen and vital nutrients to the myocardium, supporting proper heart function. Insufficient blood supply leads to severe complications, including myocardial necrosis and subsequent scarring, ultimately contributing to high morbidity and mortality worldwide, with approximately 18 million deaths annually [2]. Early diagnosis and effective therapeutic strategies are critical to mitigating disease progression. Nanoparticles have emerged as a promising approach for IHD management, offering advanced solutions for targeted drug delivery [3], imaging [4] and tissue regeneration[5]. Research has demonstrated that nanoparticle-based formulations can enhance the visualization of damaged myocardium while also improving the pharmacokinetic, physical and chemical properties of incorporated cardiological drugs in vivo. Our study aimed to optimize hybrid lipid-polymeric nanoparticles (HLPN) by varying lipid-to-polymer ratios (1:10, 1:5, 1:3, 2:5, 1:2, 3:5, 2:3, 3:4, 4:5, 1:1). Following synthesis, the most effective formulations, identified based on their physicochemical properties, were loaded with curcumin.

Poly(lactic-co-glycolic acid), cholesterol and 1,2-distearoyl-sn-glycero-3-phosphoethanolamine-N-[methoxy(polyethylene glycol)-2000] were used for the synthesis of HLPN. The size, polydispersity index (PdI) and zeta potential of nanoparticles were evaluated using the dynamic light scattering method. The colloidal stability of selected HLPN was determined in a cell growth medium for 72 hours. Curcumin entrapment in HLPN was measured by fluorescence spectroscopy and the entrapment efficiency was calculated based on the measured values.

After synthesis, nanoparticles with sizes up to 150 nm were selected, and four different formulations (1:3, 1:2, 2:3, 1:1) were chosen for further experiments. Stability tests showed that the 1:1 formulation was characterized by a variation of PdI, and in the 2:3 formulation, there was a significant increase in particle size. The most stable formulations were the 1:2 and 1:3. When curcumin was incorporated into the 1:2 and 1:3 nanoparticles, the 1:3 formulation, with a higher polymer content, showed a greater curcumin entrapment efficiency of 64 %, compared to 55 % for the 1:2 formulation.

In conclusion, the 1:3 nanoparticle formulation was the most suitable for further studies, showing enhanced stability and curcumin entrapment efficiency.

[1] Khan, Moien AB, et al., Global epidemiology of ischemic heart disease: results from the global burden of disease study. Cureus 12.7 (2020).
[2] Mouli, Manoj, et al., Ischemia Heart Disease: Current Diagnosis, Treatment Methods, and Genetic Research. Hacettepe University Journal of the Faculty of Pharmacy 44.4: 373-389 (2024).
[3] Xue, Xiaomei, et al., Delivery of microRNA-1 inhibitor by dendrimer-based nanovector: An early targeting therapy for myocardial infarction in mice. Nanomedicine: Nanotechnology, Biology and Medicine 14.2: 619-631 (2018).
[4] Xue, Yugang, et al., Engineered macrophage membrane-enveloped nanomedicine for ameliorating myocardial infarction in a mouse model. Bioengineering & Translational Medicine 6.2: e10197 (2021).
[5] Zheng, Yuanyuan, et al., MnO nanoparticles with potential application in magnetic resonance imaging and drug delivery for myocardial infarction. International journal of nanomedicine 6177-6188(2018).

OPTIMIZATION OF PREPARATION PARAMETERS OF PHOSPHATE BONDED CERAMICS

Žygimantas Logminas[1], Artyom Plyshch[1], Šarūnas Svirskas[1], Algirdas Selskis[2], Jūras Banys[1]

[1]Faculty of Physics, Vilnius University, Sauletekio al. 9, LT-10222 Vilnius, Lithuania
[2]Center for Physical Sciences and Technology, Saulėtekio al. 3, LT-10257 Vilnius, Lithuania.
zygimantas.logminas@ff.vu.lt

Ceramics play a huge part in nowadays life due to wide range of applications – from dielectrics in capacitors to piezocalipers, memory elements, and sensors. Phosphate-bonded ceramics (PBCs) are perspective alternative to conventional ones or produced by means of complicated and energy-intensive methods as spark plasma sintering or hot pressing. PBCs are eco-friendly, demonstrate outstanding thermal, chemical and mechanical stability. One of sufficient drawbacks of such ceramics is relatively lower density in comparison to their conventionally made counterparts. In this report, we research and ways to improve the properties of these ceramics by means of optimization of the preparation technique.

The phosphate binder was prepared by dissolving AlPO4 in water until the density of this mixture reached 1,40 g/cm2. 1,5 g of barium titanate where homogenized with 8,5 % of binder and pressed into pellets under 86,7 MPa, 173,3 MPa, 260,2 MPa, 347 MPa, 520 MPa, and 693,9 MPa. Two series of samples were produced – one with mean grain sizes of 700 nm and one with 300 nm. Afterwards, the produced tablets were left to cure for 24h and heated up in a furnace at 300 C for 1h. In order to explore the planar distribution of density (or dielectric permitivitty), one side the tablet was coated fully with silver contact via vapor deposition and on the other side a constellation of co-radial contacts was applied (see fig. 1).

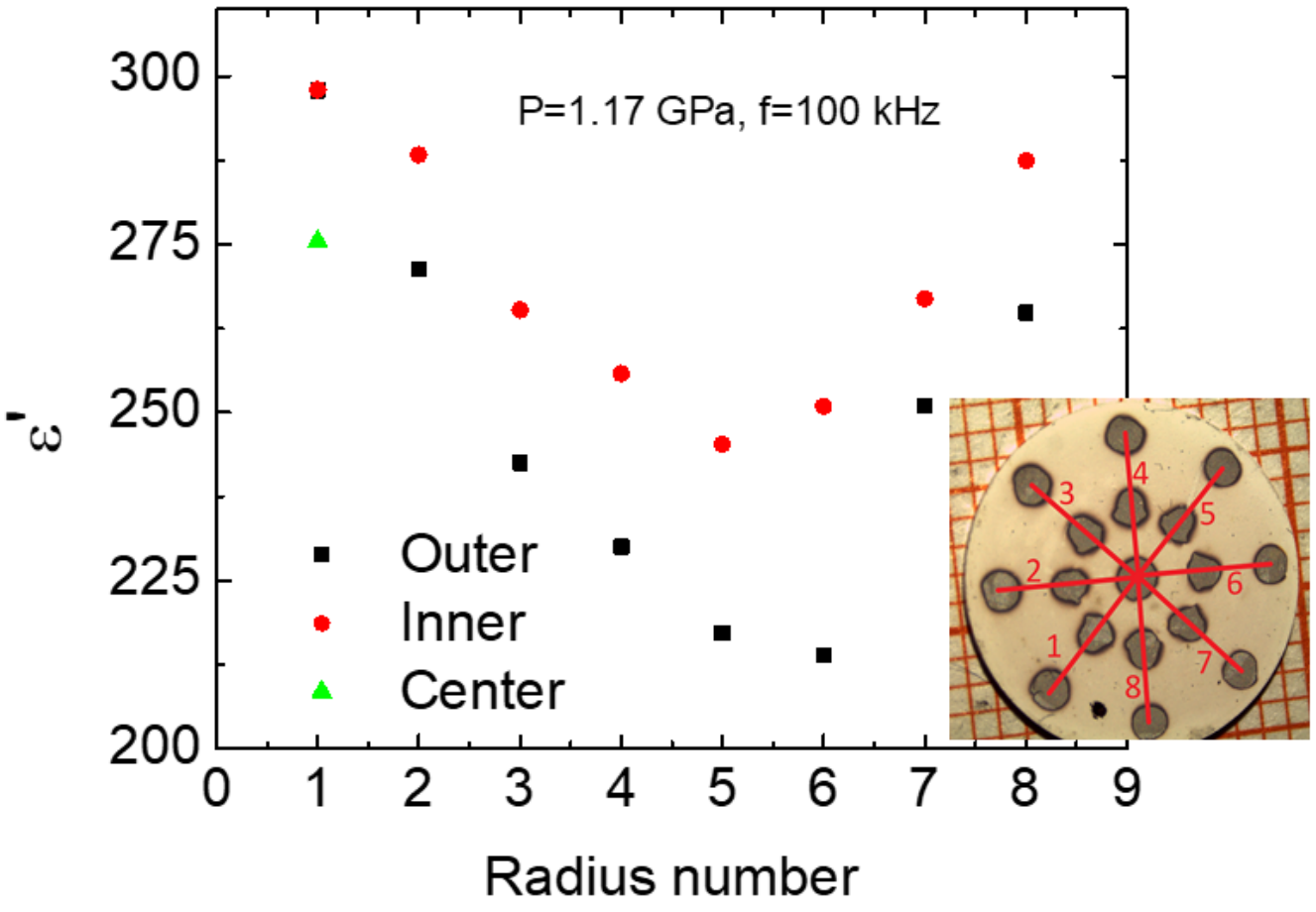


Fig. 1. Fig. 1. Dependance of tablet‘s dielectric permitivitty and it‘s location on the tablet. The X axis depicts radius number. The colors depict whether the contact is on the inner or outer ring

GOLD NANOCOMPOUNDS MEDIATED CADMIUM ION DETECTION BASED ON GLUCOSE OXIDASE INHIBITION

Katazyna Blazevic[1], Natalija German[2], Benediktas Brasiunas[1], Asta Kausaite-Minkstimiene[1,2], Almira Ramanaviciene[1,2]

[1]NanoTechnas - Center of Nanotechnology and Materials Science, Institute of Chemistry, Faculty of Chemistry and Geosciences, Vilnius University, Naugarduko str. 24, LT-03225 Vilnius, Lithuania
[2]Department of Immunology and Bioelectrochemistry, State Research Institute Centre for Innovative Medicine, Santariskiu str. 5, LT-08406 Vilnius, Lithuania
katazyna.blazevic@chgf.vu.lt

Cadmium is a highly toxic heavy metal that poses significant risks to human health and the environment and, therefore, requires rapid and reliable detection [1,2]. The main goal of his study is to develop and evaluate an electrochemical biosensor capable of detecting Cd^{2+} ions by inhibiting the glucose oxidase (GOx) activity. The effect of gold nanoparticles (AuNPs) and dendritic nanostructures (DAuNSs) on enzyme inhibition by the Cd^{2+} ions in the presence of a soluble redox mediator, phenazine methosulfate (PMS), is investigated.

Our approach involves modifying a graphite rod (GR) electrode with DAuNSs via electrochemical deposition and then immobilizing GOx on the electrode surface. We investigated the influence of the applied constant potential and the hydrogen tetrachloroaurate(III) concentration on the formed DAuNSs' morphology and the glucose biosensor's analytical signal. The obtained results were compared with glucose biosensors based on electrodes without nanoparticles (GR/GOx) and modified with 13 nm AuNPs and GOx (GR/AuNPs/GOx). We observed that Cd^{2+} causes a decrease in GOx activity in all cases, which can be registered as a reduced electrochemical signal. However, the highest impact of Cd^{2+} on the electrochemical signal of the developed biosensor was observed using electrode modified with DAuNSs and GOx (GR/DAuNSs/GOx). These findings suggest that DAuNSs improve glucose biosensors' performance and offer an efficient approach for monitoring contamination by Cd^{2+} of the environment and biological samples. These findings can be applied to the sensitive detection of other toxic metal ions.

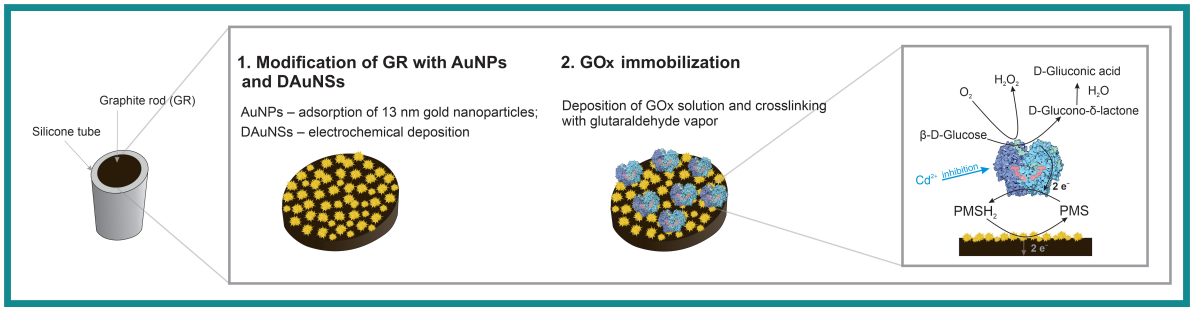


Fig. 1. Scheme of glucose biosensor development and inhibition of GOx by Cd^{2+} ions.

Acknowledgements

This research has received funding from the Research Council of Lithuania (LMTLT), agreement No. S-MIP-24-7.

[1] L. Anchidin-Norocel, G. Gutt, E. Tataranu, and S. Amariei, "Electrochemical sensors and biosensors : effective tools for detecting heavy metals in water and food with possible implications for children ' s health," Int. J. Electrochem. Sci., vol. 19, no. February, 2024, doi: 10.1016/j.ijoes.2024.100643

[2] B. Li et al., "Recent advance of nanomaterials modified electrochemical sensors in the detection of heavy metal ions in food and water," Food Chem., vol. 440, no. June 2023, p. 138213, 2024, doi: 10.1016/j.foodchem.2023.138213

DETERMINATION OF BAND ALIGNMENTS IN ANTIMONY SELENIDE AND TITANIUM OXIDE HETEROJUNCTIONS BY ULTRAVIOLET PHOTOELECTRON SPECTROSCOPY

Gerarda Jocytė[1], Rokas Kondrotas[1], Jurgis Pilipavičius[1], Vidas Pakštas[1]

[1]Center for Physical Sciences and Technology, Department of Characterisation of Materials Structure, Vilnius, Lithuania
gerarda.jocyte@ftmc.lt

Thin-film solar cells have the potential to become the future of solar energy, as their production requires fewer materials, and their efficiency is rapidly approaching that of currently used solar cells. One of the materials used in the fabrication of thin-film solar cells is antimony selenide (Sb_2Se_3) [1]. This semiconductor, characterized by a one-dimensional crystalline structure, has a band gap of approximately 1.2 eV, an absorption coefficient exceeding 10^4 cm^{-1}, and electron mobility in monocrystals ranging from 10 to 40 $cm^2V^{-1}s^{-1}$. Due to its structural properties, the electrical characteristics of the semiconductor's surface vary depending on the grain orientation, which may influence charge transport in Sb_2Se_3 heterojunctions [2,3]. In this work, we aim to investigate how ionization potential changes with Sb_2Se_3 grain orientation and how it affects the charge carrier transfer.

To determine the energy band alignment in the heterojunction with titanium oxide (TiO_2), X-ray photoelectron spectroscopy (XPS) and ultraviolet photoelectron spectroscopy (UPS) were utilised. Three Sb_2Se_3 samples with different grain orientations were studied: (hkl) with l ≠ 0, (hk0), and (120). The XPS method, together with Ar etching, was used to identify chemical elements and to get rid of contaminants. UPS was utilised to analyse valence electron spectra, from which semiconductor ionization energy (E_I) corresponding to the valence band maximum (VBM) was determined. The energy band structure was developed using the obtained VBM values and the literature-reported Sb_2Se_3 band gap (E_g). E_I and E_g of TiO_2 were taken from the literature and were used to illustrate band alignment in the heterojunction.

The calculated VBM positions for the (hk0) and (120) samples were very similar (approximately 5.3 eV), while for the (hkl) orientation, where l ≠ 0, the value was 5.1 eV. By constructing the heterojunction energy band diagram, the conduction band minimum (CBM) positions of Sb_2Se_3 were determined. For the (hk0) orientation, the CBM offset in the heterojunction was -0.16 eV, whereas for (hkl) with l ≠ 0, the offset was +0.05 eV. This suggested that charge carrier transfer across the TiO_2/Sb_2Se_3 (hkl, l≠0) heterojunction is more favourable than in TiO_2/Sb_2Se_3 (hk0) because of lower energetic barrier for electrons. As such, higher Sb_2Se_3 solar cell performance usually observed in thin films with (hkl, l≠0) grain orientation originates not only because of higher carrier mobility, but also because of more efficient charge carrier transfer across the heterojunction.

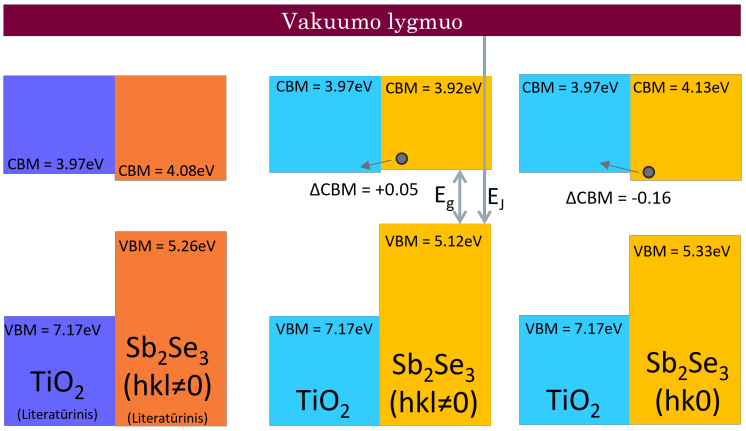


Fig. 1. Band alignment illustration based on values measured with UPS.

[1] C. Chen, K. Li, and J. Tang, Ten years of sb2se3 thin film solar cells, Solar RRL, 2022, 6, 2200094.
[2] Mamta, Y. Singh, K. Maurya, and V. Singh, A review on properties, applications, and depo sition techniques of antimony selenide, Solar Energy Materials and Solar Cells, 2021, 230, 111223.
[3] J. Lin, A. Mahmood, G. Chen, et al., Crystallographic orientation control and defect passiva tion for high-efficient antimony selenide thin-film solar cells, Materials Today Physics, 2022, 27, 100772.

EMISSIVE TAGS BASED ON PHENOXATHIIN CONTAINING DONOR-ACCEPTOR TYPE COMPOUNDS WITH ENHANCED ROOM TEMPERATURE PHOSPHORESCENCE

Lukas Dvylys[1], Rasa Keruckiene[1], Lesia Volyniuk[1], Dmytro Volyniuk[1], Juozas V. Grazulevicius[1]

[1]Department of Polymer Chemistry and Technology, Kaunas University of Technology, Lithuania
lukas.dvylys@ktu.edu

Recent studies have highlighted the potential of organic room-temperature phosphorescence (RTP) materials for applications such as bioimaging, organic light-emitting diodes (OLEDs), dynamic light therapy, data encryption, and anti-counterfeiting [1]. Organic metal-free RTP compounds offer numerous advantages over inorganic or metal-based complexes and nanodot-based RTP systems, including lower cost and toxicity, extended emission lifetimes and tunable emission [2, 3]. The development of organic RTP materials was previously limited by their crystalline nature. Advances in amorphous polymer matrices and intermolecular interactions have overcome these challenges, enabling the development of programmable luminescent tags (PLTs) for flexible information storage [4, 5]. The long emission lifetime of RTP materials makes them unsuitable for OLED displays [6]. However, this characteristic allows their use in electronics-free thin-film information storage systems and wavelength-tracking sensors [7]. One type of such devices are emissive tags, which require long-lived luminescence and can be used for anticounterfeiting, labeling, and data exchange [8].

Phenoxathiin is still scarcely used as an electron donor. It was selected due to its distinctive structure, which includes oxygen and sulfur atoms [9]. This moiety is expected to enhance spin–orbit coupling, promoting intersystem crossing from the singlet to the triplet state, which is essential process for phosphorescence. Additionally, the presence of n orbitals within the phenoxathiin ring system may contribute to triplet state stabilization, while its rigid structure could minimize nonradiative decay, both of which are crucial for efficient RTP [10].

In this study, we report the synthesis, thermal, and photophysical properties, as well as the theoretical study of three new electron-accepting quinoxaline derivatives and three phenoxathiine containing donor–acceptor type compounds, as potential candidates for emissive tag fabrication.

Acknowledgements
This project has received funding from the Research Council of Lithuania (LMTLT), agreement No S-MIP-23-50.

[1] Q. Zhou, C. Yang, Y. Zhao. Chem., 2023, vol. 9, pp. 2446–2480.
[2] Q. Zhang, S. Xu, L. Zhang, L. Yang, C. Jiang. Adv. Sci., 2024, vol. 11, 2400781.
[3] J. Yang, M. Fang, Z. Li. Acc Mater Res, 2021, vol. 2, pp. 644–654.
[4] X. Guo, et al. Small, 2024, vol. 20, 2303464.
[5] M. Gmelch, et al. Adv. Sci., 2021, vol. 8, 2102104.
[6] Y. Zhang, S.R. Forrest. Phys. Rev. Lett., 2012, vol. 108, 267404.
[7] M. Gmelch, et al. Adv. Sci., 2021, vol. 8, 2102104.
[8] H. Thomas, et al. Adv. Mater, 2024, vol. 36, 2310674.
[9] M. Li, et al. Chem. Comm., 2019, vol. 55, pp. 7215–7218.
[10] F. Liao, et al. Dyes Pigm., 2021, vol. 193, 109505.

PLATFORM FOR NV CENTER SPIN DYNAMICS

Vakaris Šilys[1], Julius Janušonis[1], Tadas Paulauskas[1]

[1]Center for Physical Sciences and Technology, Vilnius, Lithuania
vakaris.silys@ftmc.lt

Nitrogen-vacancy (NV) centers in diamond have become a key platform for precision sensing of magnetic fields at ambient conditions, offering tunable control and readout of spin states [1-2]. In this work, we compare the coherence properties of NV centers in both bulk diamond and microdiamond samples, examining their performance in DC and AC magnetic field sensing under various pulse sequences—including Ramsey interferometry and dynamic decoupling. By systematically evaluating optically detected magnetic resonance (ODMR), Rabi oscillations, and T_1 and T_2 relaxation times, we identify how different sample forms and control protocols impact sensing sensitivity and coherence.

Our scanning confocal microscopy measurement platform integrates single-photon counting with microwave pulse shaping, pico-second laser excitation and charge dynamics analysis module, thereby enabling optimization of time-resolved control and readout of NV spin states. We demonstrate optimized bulk and single defect ODMR signals, Rabi oscillations, as well as T_1 and T_2 decay profiles. We further show how tailored pulse sequences, such as dynamical decoupling, can enhance sensitivity to both DC and AC magnetic fields across several experimental scenarios.

These results highlight the adaptability and effectiveness of NV-based sensors, with potential applications ranging from fundamental quantum research to nanoscale magnetic imaging. Future work will focus on developing a compact room-temperature operated quantum sensing and information processing platform.

[1] C. L. Degen, F. Reinhard, and P. Cappellaro, “Quantum sensing,” Rev. Mod. Phys. 89, 035002 (2017).
[2] M. W. Doherty, N. B. Manson, P. Delaney, F. Jelezko, J. Wrachtrup, and L. C. L. Hollenberg, “The nitrogen-vacancy colour centre in diamond,” Phys. Rep. 528, 1–45 (2013).

POSTER SESSION 2

Astrophysics and Astronomy
Theoretical Physics
Spectroscopy and Imaging
Material Science and Nanotechnology
Biochemistry, Biophysics and Biotechnology
Biology, Genetics and Biomedical Sciences
Chemistry and Chemical Physics

IMAGINARY SYNTHETIC MAGNETIC FIELD

Saulius Alminas[1], Domantas Burba[1], Gediminas Juzeliūnas[1], Tomas Babelis[1], Ian B. Spielman[2]

[1]Institute of Theoretical Physics and Astronomy, Vilnius University, Lithuania
[2]National Institute of Standards and Technology, Gaithersburg, USA
saulius.alminas@ff.vu.lt

The study of charged particles in magnetic field has been a fundamental topic in condensed matter physics, underlying phenomena such as Landau levels and the quantum Hall effect. In the traditional Hermitian system Landau levels arise from the interaction between a charged particle and a real-valued magnetic field which induces cyclotron motion and discrete Landau levels. Recently, these ideas have been extended into non-Hermitian systems, in which certain phenomena is emerge such as non-Hermitian skin effect (NHSE), where eigenstates accumulate at system boundaries [2]. Additionally, a recent study [1] introduced a two-dimensional non-Hermitian lattice model subjected to an imaginary magnetic field revealing unique topological and spectral properties of non-Hermitian systems.

Here we analyze the effect of imaginary vector potential on Landau problem and explore how non-Hermitian nature of the system modifies energy spectrum. In particular, we investigate how the non-Hermitian nature of the system and imaginary magnetic field alters Landau levels, leading to complex energy spectrum, altering the conventional understanding of Landau quantization. This sets a stage for further investigation into non-Hermitian physics.

[1] Ozawa, T., Hayata, T. Two-dimensional lattice with an imaginary magnetic field. Phys. Rev. B 109, 085113 (2024).
[2] Zhao, E., Wang, Z., He, C. et al. Two-dimensional non-Hermitian skin effect in an ultracold Fermi gas. Nature 637, 565–573 (2025).

ANALOGIES BETWEEN QUANTUM AND CLASSICAL SYSTEMS

Justina Vaičaitytė[1,2], Andrius Gelžinis[1,2], Leonas Valkūnas[2]

[1]Vilnius University, Faculty of Physics
[2]Center for Physical Sciences and Technology, Department of Molecular Compounds Physics
justina.vaicaityte@ff.stud.vu.lt

Quantum mechanics can describe phenomena that occur in microscopic systems. However, sometimes those phenomena can be equivalently described in a classical way. Thus, some quantum systems can be analyzed using classical systems instead. An example of such classical system could be a set of coupled classical oscillators. Skinner [1] has shown that *N* - level quantum system dynamics can be exactly modelled using at most N^2-1 coordinates of classical coupled oscillators.

In this work we investigate few-level quantum systems. One of such systems is a dimer (two-level system), characterized by excitation energies ε_1 and ε_2, and interaction energy J. Using the Liouville space and density operator formalism we obtain 2 equations for time-dependent quantities q_{12} and b, which are the real part of the coherence and the difference of populations, respectively:

$$\begin{cases} \ddot{q}_{12} = -\xi^2 q_{12} - J\xi b; \\ \ddot{b} = -4J\xi q_{12} - 4J^2 b. \end{cases} \tag{1}$$

Here $\xi = \varepsilon_2 - \varepsilon_1$. We find that this system can be described equivalently using a classical system, composed of two beads that are connected to each other and the ceiling with springs and can move along y direction only (see Fig. 1). The parameters of this classical system can be expressed in terms of ξ and J in such a way that the dynamics of the classical system reproduce quantum system dynamics.

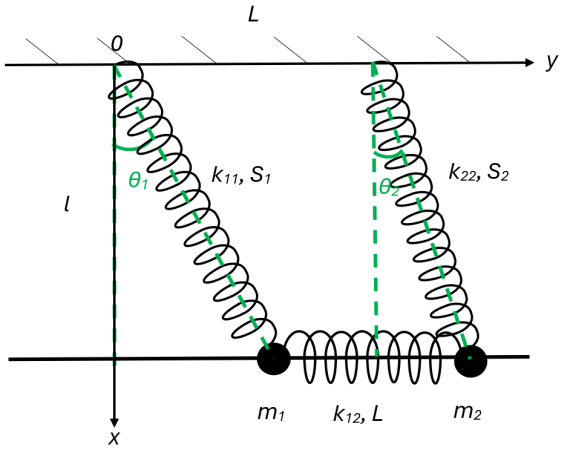


Fig. 1. Classical system composed of two beads of masses m_1 and m_2 connected to each other with a spring of stiffness k_{12} and length L, and the ceiling with springs of stiffness k_{11} and k_{22}, and lengths S_1 and S_2. The distance between the beads and the ceiling is l.

If a quantum effect can be described using mathematically equivalent classical equations, then the effect's nature might not be entirely quantum. This raises fundamental questions about the importance of quantumness in seemingly purely quantum systems. Thus it is important to study the differences between quantum and classical systems. In the future, among other things, we plan to investigate more complicated quantum systems that are also described by the density operator. Density operator formalism is more general than wave function formalism as it allows one to consider open quantum systems as well, which is one of the goals of our work.

[1] T. E. Skinner, Exact mapping of the quantum states in arbitrary n-level systems to the positions of classical coupled oscillators, Physical Review A 88, 012110 (2013).

QUANTUM MANY-BODY PHASES IN SUBWAVELENGTH BRICK WALL LATTICE

D. Viarbitski[1], D. Burba[1], G. Juzeliunas[1], G. Žlabys[2]

[1]Institute of Theoretical Physics and Astronomy, Vilnius University, Sauletekio 3, Vilnius, Lithuania
[2]Okinawa Institute of Science and Technology Graduate University, Okinawa, Japan
dzmitry.viarbitski@ff.vu.lt

The study of quantum many-body systems has led to the discovery of numerous exotic quantum phases of matter, driven by the interplay between particle interactions, quantum fluctuations, and symmetry breaking. Among these, pair superfluids [1] and supersolids are particularly fascinating, as they represent different manifestations of quantum coherence and collective behavior in strongly correlated systems. In this paper, we propose a state-dependent lattice [2] for ultracold bosons based on a particular tripod atom-light coupling scheme [3]. We show that it manifests an extended Bose-Hubbard model and we explore the emergence of novel quantum phases, chief among them (pair) superfluids, supersolids, and Mott insulators.

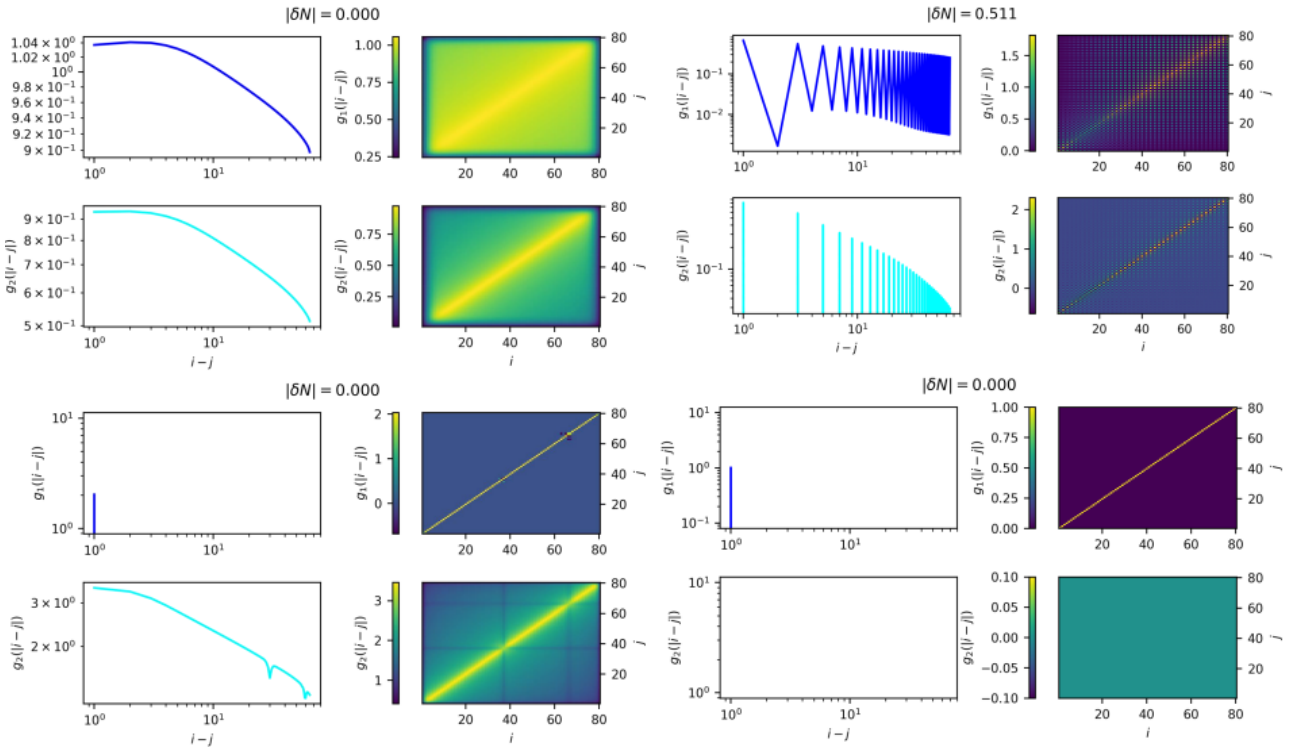


Fig. 1. Bottom-right (MI): Quantities for following p-band parameters in canonical ensemble: J1 = J2 = 0, g0 = 1.0, gx = 0, gz = 0, G000 = 1.0, G011 = −G001 = 0.5, Npart = Nlat , Nlat = 80, boson-dim= 6 Top-right (SS): Quantities for following p-band parameters in canonical ensemble: J1 = $-0.1/\sqrt{10}$, J2 = 0.1, g0= 0.5, gx = −0.5, gz = 0.05, G000 = 1, G011 = −G001 = 0.5, Npart = Nlat , Nlat = 80, boson-dim= 6. Top-left (SF): Quantities for following p-band parameters in canonical ensemble: J1 = J2 = 0, g0 = 1.0, gx = 0, gz = 1.0, G000 = 1, G011 = −G001 = 0.5, Npart = Nlat , Nlat = 80, boson-dim= 6. Bottom-left (PSF): Quantities for following p-band parameters in canonical ensemble: J1 = J2 = 0, g0 = 0.1, gx = 1.0, gz = 0, G000 = 1, G011 = −G001 = 0.5, Npart = 2Nlat , Nlat = 80, boson-dim= 6.

[1] X.-F. Zhou, Y.-S. Zhang, and G.-C. Guo, Phys. Rev. A 80,013605 (2009)
[2] M. Eckholt and J. J. García-Ripoll, New Journal of Physics 11, 093028 (2009)
[3] E. Gvozdiovas, P. Račkauskas, and G. Juzeliunas, SciPost Phys. 11, 100 (2021)

SINGLE PHOTON EMITTERS IN HEXAGONAL BORON NITRIDE FOR QUANTUM COMMUNICATIONS

Ifra Bibi[1], Viktorija Nargelienė[1], Vakaris Šilys[1], Julius Janušonis[1], Vitalij Kovalevskij[1], Tadas Paulauskas[1]

[1]Center for Physical Sciences and Technology, Saulėtekio al. 3, 10257 Vilnius, Lithuania
ifra.bibi@ftmc.lt

Hexagonal boron nitride (hBN) has garnered as significant attention as a platform for room-temperature operating single-photon sources (SPS). However, early research has been primarily focused on identifying a variety SPS and there has been comparatively little effort to engineer emitters to work as building blocks of quantum communications [1-2]. Herein, we report on the controlled creation of visible-spectrum emitters in hBN through implantation of different dopants. hBN flakes were first mechanically exfoliated on suitable substrates and were subjected to optimized protocols for defect generation using high-temperature annealing, chemical, and plasma processing. We employed ion beam irradiation using several species, including silicon, titanium, and aluminum to induce defects in mechanically exfoliated hBN. Single-photon emission properties from atomic defects in hBN flakes were characterized using scanning confocal photoluminescence microscopy, second-order correlation (Hanbury Brown and Twiss) measurements, lifetime measurements, while spin properties of the defects were examined using optically detected magnetic resonance. These results provide crucial insights for the development of robust quantum key distribution systems and pave the way for integrating hBN-based SPSs into real-world quantum communication architectures.

[1] Esmann, M., Wein, S. C., Antón-Solanas, C. (2024). Solid-State Single-Photon Sources: Recent Advances for Novel Quantum Materials. Advanced Functional Materials, 2315936.

[2] Boretti, A., Blackledge, J., Castelletto, S. (2025). Advancing hexagonal boron nitride single photon sources: A strategic roadmap for quantum applications. Materials Science in Semiconductor Processing, 185, 108932

DEVELOPMENT OF THZ METALENS AND APPLICATIONFOR BEAM SHAPING AND IMAGING

Karolis Redeckas[1,2], Kasparas Stanaitis[1,2], Vladislovas Čižas[1], Rusnė Ivaškevičiute-Povilauskienė[1], Linas Minkevičius[1,2]

[1]Center for Physical Science and Technology
[2]Vilnius University
karolis.redeckas@ftmc.lt

Terahertz (THz) radiation, spanning frequencies from 100 GHz to 10 THz, has low non-ionizing energy and can penetrate various dielectric materials [1]. This property makes it valuable in fields like security screening, quality control in manufacturing, imaging, and bio-fabric analysis [2]. Traditionally, these applications have depended on large, costly lenses or mirrors to control beam propagation, limiting their practicality. A promising approach to miniaturizing these systems is the use of metalenses. These lenses integrate a phase profile with metaatoms—subwavelength geometric structures like split-ring resonators—to manipulate phase delay and polarization rotation effectively.

This research covers numerical simulations conducted to determine the appropriate complementary split-ring resonators (CSRR) metaatoms for integration into a 253 GHz metalens design. Non-paraxial and axicon metalenses were created with F=30 mm focal length and d=60mm focal depth, respectively. Both lenses were designed with 2 and 4 subzones and evaluated numerically. Results led to the selection of two metalenses for physical fabrication by laser ablation method.

Firstly, the non-paraxial and axicon metalenses focusing performance was experimentally evaluated (Fig. 1). Then applied in direct imaging setup, where USAF 1951 resolution evaluation target was used. System with focusing non-paraxial metalens achieve high: 0.63λ resolution, while focusing with axicon metalens reaches 0.85λ resolution and allows to position target not so precisely or even cover focusing element.

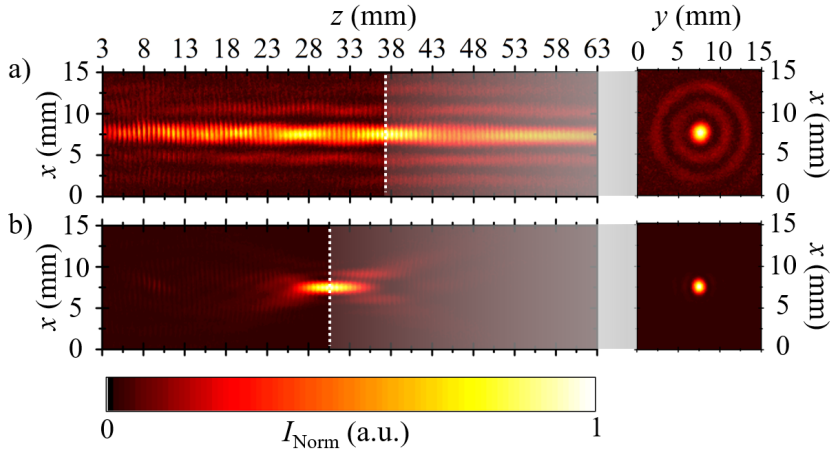


Fig. 1. Bessel beam shaped by axicon metalens a); Gaussian beam shaped by non-paraxial metalens b).

Acknowledgements
Research was funded by Lithuanian Science Council, project number: P-ST-24-54

[1] Nagatsuma, T. (2011). Terahertz technologies: present and future. IEICE Electronics Express, 8, 1127- 1142.
[2] Mittleman, D. M. (2018). Twenty years of terahertz imaging. Optics Express, 26, 9417-9431.

RADIATION-INDUCED DEFECT STUDIES IN p-TYPE PIN AND LGAD DETECTORS

Faustina Kiaušaitė[1], Tomas Čeponis[1], Jevgenij Pavlov[1]

[1]Institute of Photonics and Nanotechnology, Vilnius University, Saulėtekio av. 3, LT-10257, Vilnius, Lithuania
faustina.kiausaite@ff.stud.vu.lt

Low Gain Avalanche Detector (LGAD) is the perspective technology used in ATLAS and CMS detectors due to their high-precision timing performance. However, their highly boron-doped gain layer is susceptible to radiation-induced deactivation of boron dopants, known as the Acceptor Removal Effect [1]. Understanding boron-associated deep-level defects is crucial for ensuring the reliable operation of these detectors in harsh radiation environments.

In this study, Deep Level Transient Spectroscopy (DLTS) and Minority Carrier Deep Level Transient Spectroscopy (MC-DLTS) were performed on p-type LGAD and PIN detector samples irradiated with 26 GeV protons at a fluence of 1×10^{12} cm^{-2}. Trap analysis was conducted using correlation functions, Laplace transformation, and literature references [2–4]. The DLTS spectra revealed up to seven hole traps (H), as shown in Figure 1a, while the MC-DLTS spectra exhibited up to four electron traps (E), as shown in Figure 1b.

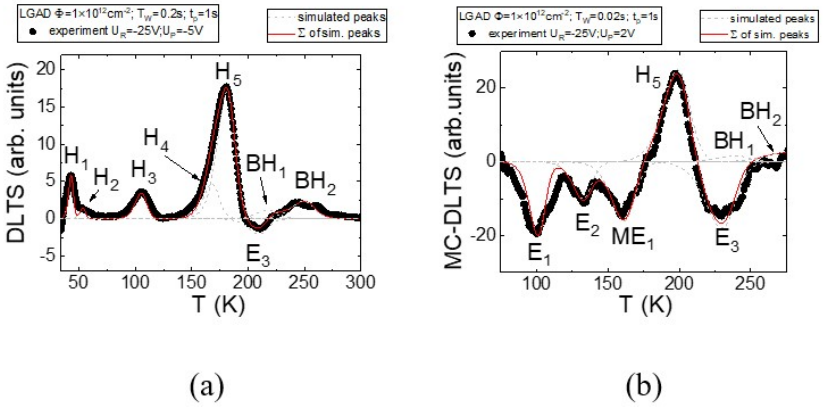


Fig. 1. (a) the DLT and (b) the MC-DLT spectra recorded on the irradiated LGAD sample.

ME_1 trap is a metastable defect, and it can disappear after forward current (electron injection) and BH_1 and BH_2 traps can appear. After annealing, this process is backward, which means that the metastable ME_1 trap (negative-U center) is connected with BH_1 and BH_2 traps, and they all belong to the same DBH defect. Boron atoms take part in the formation of the DBH defect [4]. The traps of E_1 and E_3 are usually not represented in the MC-DLT spectrum of p-type Si diode (it is more common for n-type Si majority traps). Still, they can be “highlighted” in p-type semiconductors by using optical Minority Carrier Transient Spectroscopy [5]. In our case, we have several layered structures (LGAD), which can pull minority carriers from another layer.

While previous DLTS studies have focused on PIN diodes, the application of DLTS to LGADs provides new insights into the formation of radiation-induced defects in these p-type structures. This research enhances our understanding of carrier recombination processes in avalanche diode layers, contributing to the development of more radiation-tolerant detectors.

[1] A. Himmerlich, N. Castello-Mor, E. C. Rivera, Y. Gurimskaya, V. Maulerova-Subert, M. Moll, I. Pintilie, E. Fretwurst, C. Liao, J. Schwandt. Defect characterization studies on irradiated boron-doped silicon pad diodes and Low Gain Avalanche Detectors. Nuclear Inst. And Methods in physics Reseach, A 2023, 1048, 167977.

[2] T. Ceponis; S. Lastovskii; L. Makarenko; J. Pavlov; K. Pukas; E. Gaubas. Study of radiation-induced defects in p-Type Si1-xGex diodes before and after annealing. Materials 2020, 13, 5684.

[3] J. Pavlov; T. Ceponis; K. Pukas; L. Makarenko; E. Gaubas. 5.5 MeV electron irradiation-induce transformation of minority carrier traps in p-type Si and Si1-xGex alloys. Materials 2022, 15, 1861.

[4] L.F. Makarenko; S.B. Lastovski; H. S. Yakushevich; E. Gaubas; J. Pavlov; V.V. Kozlovski; M. Moll; I. Pintilie. Formation of a bistable interstitial complex in irradiated p-type silicon. Phys. Status Solidi A 2019, 216, 1900354.

[5] P. Blood; J.W. Orton. The electrical characterization of semiconductors: majority carriers and electron states. Academic Press Inc.: San Diego, CA, USA, 1992.

PRECISION THz SPECTROSCOPY OF METHANOL: JPL-BASED THEORETICAL MODELING FOR ENHANCED SPECTRAL ANALYSIS AND REMOTE SENSING

Patricija Ivanauskaitė[1,2], Dovilė Čibiraitė-Lukenskienė[1]

[1]Department of Optoelectronics, Center for Physical Sciences and Technology (FTMC), Lithuania
[2]Faculty of Physics, Vilnius University, Vilnius, Lithuania
patricija.ivanauskaite@ftmc.lt

Terahertz (THz) radiation (0.1–10 THz) [1], has garnered significant attention for applications in atmospheric monitoring, industrial exhaust analysis, environmental sensing, and biomedical diagnostics, necessitating scalable, high-precision spectroscopic solutions.

This study focuses on THz methanol spectroscopy and the application of a theoretical model, which applies broadening to discrete spectral data taken from the Jet Propulsion Laboratory (JPL) molecular spectroscopy database [2]. The resulting spectrum, modelled under specific conditions, serves as a reference for comparing experimental data and assessing the performance of a 0.25 THz emitter-detector pair. These findings contribute to advancing THz technology and improving spectroscopic methodologies.

Modelling utilized JPL data, renowned for extensive THz-range spectral information, to predict methanol's absorption line widths and its broadening mechanisms. As a key atmospheric trace constituent, methanol exhibits well-defined absorption features, making it an ideal reference for THz spectroscopy under higher stratosphere pressure conditions (<1 mbar). The spectral line broadening under investigation consists of Gaussian (Doppler, due to thermal motion) and Lorentzian (collisional/pressure) broadenings, both of which combine to form the Voigt profile [3]. Accurate modelling of these broadening effects is crucial for precise spectral analysis, reliable atmospheric sensing and understanding of dynamic energy exchange in the stratosphere for better climate change predictions. A Python-based computational approach was employed, overlaying the modelled Voigt profile onto reference spectra to refine Voigt profile parameters by optimizing spectral fits against reference methanol spectra at 134 mTorr and 298 K over 1.480 – 1.495 THz range [4].

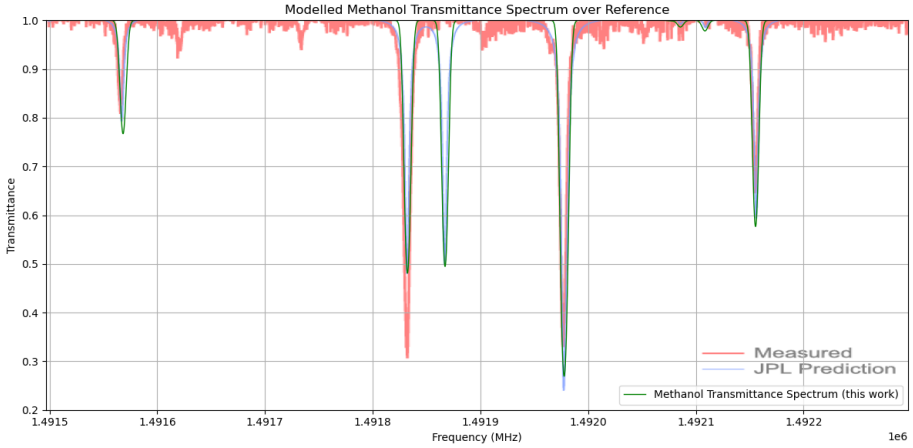


Fig. 1. Modelled Voigt profile fit to reference methanol spectra at 134 mTorr and 298 K [4].

Future experimental validation will refine methanol spectroscopy using field-effect transistor-based THz spectroscopy under varying pressure conditions in a gas cell and applied gate voltages on a designed tunable 252 - 256 GHz source. This will allow a direct comparison between the experimental data and modelled spectra based on data extracted from the JPL database. The goal of the experiments will be to refine the measurement method to reach the highest possible spectral resolution.

[1] Wilke, I. "Terahertz Spectroscopy Applications." Encyclopedia of Spectroscopy and Spectrometry, Elsevier, 2017, pp. 427–31, https://doi.org/10.1016/b978-0-12-409547-2.12094-3.
[2] "JPL Molecular Spectroscopy." Nasa.gov, 2017, https://spec.jpl.nasa.gov/.
[3] Hanson, Ronald K., et al. "Spectral Lineshapes." Springer EBooks, Springer Nature, Oct. 2015, pp. 131–48, https://doi.org/10.1007/978-3-319-23252-2_8.
[4] Slocum, D.M., Xu, L.-H., Giles, R.H. and Goyette, T.M. (2015). Retrieval of methanol absorption parameters at terahertz frequencies using multispectral fitting. Journal of Molecular Spectroscopy, [online] 318, pp.12–25. https://doi.org/10.1016/j.jms.2015.09.008.

OPTIMIZATION OF THZ IMAGING SYSTEMS USING 3D-PRINTED HIGH-IMPACT POLYSTYRENE LENSES

Kasparas Stanaitis[1,2], Karolis Redeckas[1,2], Vladislovas Čižas[1], Ignas Grigelionis[1], Linas Minkevičius[1]

[1]Department of Optoelectronics, Center for Physical Sciences and Technology, Vilnius, Lithuania
[2]Faculty of Physics, Vilnius University, Vilnius, Lithuania
kasparas.stanaitis@ftmc.lt

Optical imaging systems are widely used in commercial and scientific fields, such as medicine, security, material analysis, and quality control [1]. These systems often rely on high-energy radiation, like X-rays, which have significant drawbacks, such as ionizing effects and high costs. Terahertz (THz) imaging offers a safer alternative, using non-destructive radiation that can still penetrate most dielectrics.

This study investigates the arrangement of optical components in THz imaging systems, focusing on Gaussian, Bessel, and Airy beam-forming lenses. These lenses were fabricated using extrusion 3D printing with High Impact Polystyrene filament, which offers suitable optical properties for the THz range [2]. The positions of the lenses were systematically adjusted to focus and collect light onto a resolution imaging sample (USAF1951) (Fig. 1.). Seven images with different lens combinations were recorded (Fig. 1). For each combination, the Modulation Transfer Function (MTF) was evaluated to assess the system's contrast, and the Mean Square Error (MSE) was used to compare imaging quality [3]. The contrast data helped identify the optimal conditions for achieving the highest resolution.

The results show that the types and positions of lenses play a crucial role in THz imaging. The combination of classical Gauss-Gauss lenses provided the highest quality imaging but was highly sensitive to misalignment. In contrast, the Bessel lens for light collection proved to be optimal, as it significantly reduced the sensitivity to system alignment.

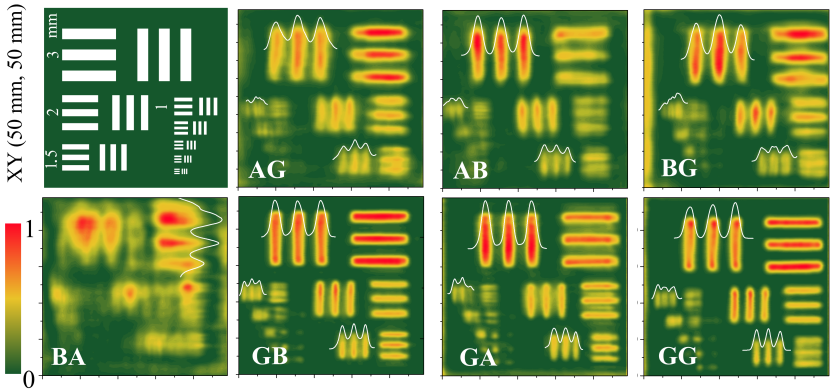


Fig. 1. Top left – modified USAF 1951 resolution target for image quality evaluation, numbers correspond to slit width in mm. Other images are THz imaging results of USAF targets by using different lens compositions. First letter – focusing lens, second – collecting lens (G - Gaussian, B - Bessel, A - Airy).

[1] Valušis, G., Lisauskas, A., Yuan, H., Knap, W., & Roskos, H. G., Roadmap of terahertz imaging 2021 (Sensors, 21(12), 4092, 2021)
[2] Stanaitis, K., Redeckas, K., Bielevičiūtė, A., Bernatonis, M., Jokubauskis, D., Čizas, V., & Minkevičius, L., Study of the low-cost HIPS and paraffin-based terahertz optical components (Lithuanian Journal of Physics, 63(4), 2023)
[3] Stanaitis, K., Čižas, V., Bielevičiūtė, A., Grigelionis, I., & Minkevičius, L., High-impact polystyrene structured light components for terahertz imaging applications (Sensors, 25(1), 131, 2024).

SOLID STATE NMR STUDY OF IMMOBILIZED POLYMERS

Emilis Čiupaila[1], Dr. Vaidas Klimkevičius[2], Dr. Vytautas Klimavičius[3]

[1]Vilnius University
[2]Institute of Chemical Physics
[3]Institute of Chemistry
emilis.ciupaila@ff.stud.vu.lt

Polymers containing catechol functional groups, inspired by marine mussel adhesive proteins, have attracted significant interest for their potential applications as bio-inspired adhesives and composite materials. In this study, the structural interactions between poly(N-catechol dimethyl acrylamide) (PDMAA) and fumed silica (SiO_2) were investigated using solid-state nuclear magnetic resonance (NMR) spectroscopy to determine the nature of their bonding interactions. Solid-state NMR techniques, including 13C CP-MAS, 29Si MAS, and 29Si CP-MAS, were employed to analyze PDMAA-SiO_2 composites synthesized under acidic, neutral, and basic conditions. The 13C CP-MAS spectra confirmed the presence of PDMAA within the composites, identifying characteristic chemical shifts corresponding to key functional groups, while the 29Si MAS and 29Si CP-MAS spectra showed no significant shifts or new peaks indicative of covalent bond formation. The Q2, Q3, and Q4 silicon environments presented by the presence of similar peaks throughout all studied samples. Tn groups indicating -Si-R signals were not observed, suggesting the absence of covalent bond formation between silica and the polymer. These results indicate that the interaction between PDMAA and SiO_2 is non-covalent, likely mediated through hydrogen bonding, providing insights into the structural characteristics of PDMAA-SiO_2 composites for adhesive material development.

NMR RELAXATION STUDY OF FUMARIC ACID AND ITS ISOTOPOMERS

Adomas Valeika[1]

[1]Vilnius University, Faculty of Physics, Institute of Chemical Physics
adomas.valeika@ff.stud.vu.lt

Nuclear magnetic resonance (NMR) is a multipurpose tool for observing chemical and biological processes. Its non-invasive nature allows for materials analysis in various external conditions. Generally, a strong magnetic field with a magnitude of more than 1 Tesla is used to achieve good signal strength and high resolution.

In medical applications of magnetic resonance contrast agents are often used to facilitate higher image contrast for better analysis. Contrast agents work by having a quicker longitudinal relaxation time T_1 which results in higher image contrast. Currently a new contrast agent – fumaric acid, is gaining attention and shows potential. By looking into fumaric acid and its isotopomers the aim is to find desirable isotopomer which has a short relaxation time. Short relaxation time is essential for contrast agents in magnetic resonance imaging. This means that extensive research is required to fully understand this material and its properties in various external conditions[1].

In this work I will discuss the properties of longitudinal relaxation time T_1 of fumaric acid in different temperatures and different external magnetic fields. It was observed that ^{1}H relaxation times were similar but isotopomers with ^{13}C displayed more complex data. Such information would allow for careful evaluation of the potential use in medicine.

[1] V. Balevičius, L. Kimtys, G. A. Misiūnas. Magnetinio rezonanso spektroskopija, 2000.

ESEEM and HYSCORE spectroscopy: Unlocking the secrets of spin-nuclear interaction

Giedrė Kuktaitė[1], Gediminas Usevičius[2], Mantas Šimėnas[3], Jūras Banys[4]

[1]Vilnius University
giedre.kuktaite@ff.stud.vu.lt

Electron Spin Echo Envelope Modulation (ESEEM) and Hyperfine Sublevel Correlation (HYSCORE) spectroscopies are advanced (Electron Paramagnetic Resonance) EPR techniques designed to probe spin-nuclear interactions in paramagnetic systems. ESEEM relies on the modulation of electron spin echo signals caused by hyperfine interactions between electron spins and nearby nuclear spins. By applying a sequence of microwave pulses, the resulting oscillations in echo intensity reveal complex nuclear interactions, enhancing sensitivity and enabling the study of weak spin systems. HYSCORE, using a three-pulse sequence, generates a 2D correlation spectrum that provides detailed insights into hyperfine couplings between electron and nuclear spins, offering high resolution for systems with multiple interacting nuclei. Together, ESEEM and HYSCORE offer valuable tools for investigating the local environments of paramagnetic centers, providing crucial structural and dynamic information for a wide range of scientific applications. Here, we will discuss these techniques and their application to study various materials at Vilnius University.

[1] Dikanov, S. A., & Tsvetkov, Y. Electron Spin Echo Envelope Modulation (ESEEM) Spectroscopy (1992).
[2]

METHANE DETECTION FROM NATURAL AND INDUSTRIAL SOURCES BY MEASURING MIR ABSORPTION

Jonas Jeffrey Haist[1,2], Vilius Žalėnas[1], Laurynas Butkus[1], Artūras Plukis[1]

[1]Center for Physical Sciences and Technology
[2]Vilnius University
jonas.haist@ftmc.lt

Methane is a potent greenhouse gas and developing new methods to measure the emittance of methane from various natural and industrial sources is most important, in addition to being able to detect methane gas leaks from pipelines and natural gas pipes near and in homes, preventing wasting of the gas and uneccesary emissions. This study employed the use of a 3270nm 15mW NanoPlus Distributed Feedback (DFB) laser with an alternating power output around the given frequency achieved by a 100Hz triangle wave signal oscillating from 0mV to 250mV, which is from a signal generator is sent to the laser control module. As the current supplied to the laser varies, the emitted wavelength also changes up to 9 nm. This is enough to move the wavelength in and out of the absorption range, which is visible by a local distortion in the triangle signal. The different absorption lines of methane and water vapor allow to distinguish between the two molecules. The laser wavelength was also manipulated via changing the temperature of the thermoelectric cooler, combined with current variation, this allows to modify the laser wavelength by as much as 16 nm, enough to investigate multiple methane and water vapor absorption lines.

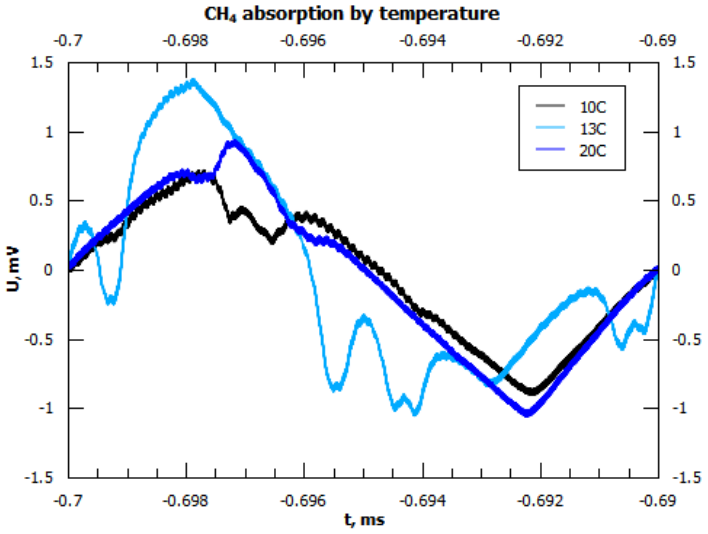


Fig. 1. Response signal under different conditions

The optimal laser temperature for detection of methane and water vapor was determined by shifting the temperature of the laser and observing the distortions of the triangle wave. Note – only the most prolific methane absorption examples have been graphed. The selected laser temperature for further studies is 13 °C, which was chosen for its drastically distorted triangle wave signal (Fig. 1) Calibration was performed in a cuvette with varying pressures and concentrations of methane gas. Using the following equation $U = U_0(1 - e^{-n \bullet \sigma \bullet L})$, the concentration n of methane can be calculated from the size of the distortion of the detected triangle wave. Calibration using a known concentration of CH_4 in a cuvette was performed at various pressures and concentrations. It was discovered that the lowest reliably detectable concentration for 1 meter of optical path was 100 ppm.

The experiment setup was moved outside and measurements were attempted above a grey water sewage access well. Control measurements were run with the manhole cover lowered, which showed clear water vapor absorption and demonstrated the system's ability to work in an outdoor environment. Methane was not detected with the cover removed, even as multiple measurements were repeated. As the optical path for the system outside was 5 meters, this indicates the CH_4 concentration was below 20 ppm.

[1] [1] Vurgaftman, I et al. (2015). Interband cascade lasers. Journal of Physics D: Applied Physics. 48.123001
[2] [2] Du, Zhenhui et al. (2019). Mid-Infrared Tunable Laser-Based Broadband Fingerprint Absorption Spectroscopy for Trace Gas Sensing: A Review. Applied Sciences. 9. 338.
[3] [3] Gardiner, Tracy et al. (2010). A lightweight near-infrared spectrometer for the detection of trace atmospheric species. Review of Scientific Instruments. 81. 083102
[4] [4] Myhre, G. et al. 2013: Anthropogenic and Natural Radiative Forcing. In: Climate Change 2013: The Physical Science Basis. Contribution of Working Group I to the Fifth Assessment Report of the Intergovernmental Panel on Climate Change

PROSPECTS OF CVD DIAMOND-BASED SUBSTRATES: E-CARS SPECTROSCOPY AND IMAGING

Paulius Rindzevičius[1,2], Mariam Quarshie[3], Sergei Malykhin[3], Andrej Dementjev[1]

[1]Department of Molecular Compound Physics, Center for Physical Sciences and Technology, Lithuania
[2]Faculty of Physics, Vilnius University, Lithuania
[3]Department of Physics and Mathematics, Faculty of Science, Forestry and Technology, University of Eastern Finland, Finland
paulius.rindzevicius@ff.stud.vu.lt

Coherent anti-Stokes Raman scattering (CARS) is a third-order nonlinear process that is often used for vibrational imaging and spectroscopy [1]. CARS allows fast chemically specific imaging of certain vibrational modes without any need for labels. However, in most cases CARS signal contains a strong non-resonant background and it's difficult to extract true vibrational information from measured spectra [2]. CARS microscopy can be employed for investigating diamond [3], which has no non-resonant background and has an intense line at 1332 cm^{-1}, which is a frequency of C-C vibrational mode in diamond crystal lattice. Besides that, NV color centers in diamond can be used in electric and magnetic fields quantum sensing [4], while SiV and GeV color centers can be used in temperature sensing [5, 6]. In this work, epi-detection CARS experiments were conducted on various diamond-based substrates with metal structures.

CARS images were taken and spectra were measured using 5 different laser powers, starting from the lowest to avoid sample degradation. The main sample is a substrate with diamond microneedles in Si base. It was compared with other samples that are similar diamond-based substrates, but with 5 nm metal films or different metal nanostructures on diamond surface. Au, Ag, Cu, Ti and Ni were used. Diamond-based substrate without metal structures show a 1332 cm^{-1} line in CARS spectra. Diamond line's intensity dependence on laser power is cubic, which confirms a third-order nonlinear nature of the observed process. Background intensity dependence on laser power is close to quadratic – it is a result of other, linear and second-order processes (for example, two photon excitement fluorescence, TPEF). Au, Ag and Cu nanostructures are often used in SERS and SEIRA spectroscopy [7], but this work shows that Au and Ti structures can be used to enhance CARS signal as well. 5 nm Au film and Au nanoparticles on flat diamond surface degrade from high laser intensity, but Au nanoparticles deposited in nanoholes on diamond surface enhance diamond CARS signal because of plasmonic effects. Diamond-based substrate with rough Ti film has great signal enhancement properties and we propose similar plasmonic mechanism for this enhancement since flat metal surfaces don't enhance CARS signal in conducted experiments. Comparison of diamond resonant line intensity dependence on laser power using various diamond-based substrates is presented in fig. 1. Diamond-based substrates with other metals (Ni, Cu, Ag) degrade from high laser power in these experiments. The obtained results reveal that Au and Ti nanostructures can enhance diamond CARS signal.

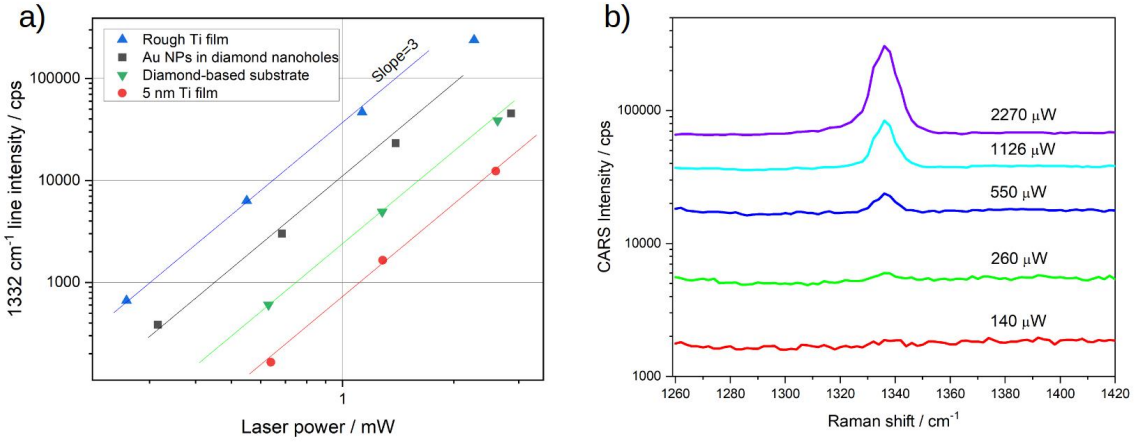


Fig. 1. (a) Dependence of intensity of diamond Raman line (1332 cm^{-1}) on laser power for diamond films covered with various metals, (b) measured CARS spectra of diamond-based substrate with rough Ti film

[1] MUKAMEL, S. Principles of Nonlinear Optical Spectroscopy. Oxford University Press. 1995.
[2] EL-DIASTY, F. Coherent anti-Stokes Raman scattering: Spectroscopy and microscopy. Vibrational Spectroscopy. 2011. Vol. 55, p. 1-35.
[3] DEMENTJEV, A. et al. Polarisation CARS microscopy of diamond needles. Appl. Phys. Lett. 2024. Vol. 124.
[4] DOLDE, F. et al. Electric-field sensing using single diamond spins. Nature physics. 2011. Vol. 7, p. 459-463.
[5] NGUYEN, C. T. et al. All-optical nanoscale thermometry with silicon-vacancy centers in diamond. Appl. Phys. Lett. 2018. Vol. 112.
[6] FAN, J.-W. et al. Germanium-Vacancy Color Center in Diamond as a Temperature Sensor. ACS Photonics. 2018. Vol. 5, p. 765-770.
[7] AROCA, R. Surface Enhanced Vibrational Spectroscopy. Wiley-WHC. 2006.

STRUCTURAL ANALYSIS OF BUTYRIC ACID USING MATRIX ISOLATION INFRARED SPECTROSCOPY AND THEORETICAL CALCULATIONS

Klaudija Pukalskaite[1], Jogile Macyte[1]

[1] Institute of Chemical Physics, Vilnius University, Sauletekio av. 3, 10257 Vilnius, Lithuania
klaudija.pukalskaite@ff.stud.vu.lt

Butyric acid ($C_4H_8O_2$) is a short-chain carboxylic acid that exhibits several conformers due to the rotational flexibility of its alkyl chain and carboxyl group. These conformers may have slightly different physicochemical properties, influencing their reactivity and interactions in various environments [1]. Understanding the structural and energetic differences between these conformers is essential for applications in chemical and biological systems [2,3]. The main goal of this work is to conduct conformational analysis of butyric acid. To accomplish this goal, high-level quantum chemical calculations and low-temperature matrix isolation infrared absorption spectroscopy in different matrices were used.

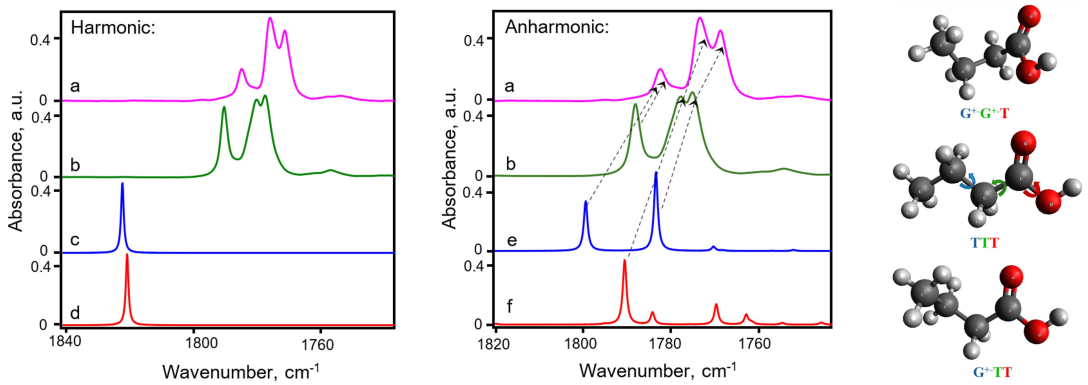


Fig.1. Infrared absorption spectra of butyric acid: (a) experimental in argon matrix, (b) experimental in neon matrix, (c) calculated TTT (harmonic), (d) calculated G±TT (harmonic), (e) calculated TTT (anharmonic), (f) calculated G±TT (anharmonic). Calculated band intensities were scaled to the experimental bands using the same factor for the all calculated spectra.

Geometry optimization and vibrational frequency calculations of possible butyric acid conformers were performed using Density Functional Theory (DFT) with the B3LYP functional and the ab initio Møller-Plesset perturbation theory (MP2), both using the cc-pVTZ basis set. Vibrational frequencies were calculated using both harmonic and anharmonic methods. Theoretical calculations identified three stable conformers of butyric acid; however, only two were experimentally observed in argon and neon matrices. Anharmonic calculations facilitated the identification of Fermi resonance bands in experimental spectra and enabled a more precise assignment of spectral bands in the C=O region. The results are presented in Fig. 1. However, in MP2 calculations, the stability order shifts when Gibbs energy is considered in energy estimations, ultimately identifying TTT as the most stable conformed.

Acknowledgements

Authors are thankful for the provided computational time at High Performance Computing Center “VU HPC Saulėtekis” at Physics Faculty of Vilnius University.

[1] I. Goldberg and J. S. Rokem, ”Organic and Fatty Acid Production, Microbial,” in Encyclopedia of Microbiology, 3rd ed., M. Schaechter, Ed. Academic Press, 2009, pp. 421–442. doi: 10.1016/B978-012373944-5.00156-5.

[2] Z. Xu and L. Jiang, ”3.20 - Butyric Acid,” in Comprehensive Biotechnology, 2nd ed., M. Moo-Young, Ed. Academic Press, 2011, pp. 207–215. doi: 10.1016/B978-0-08-088504-9.00181-1.

[3] M. Dwidar, J.-Y. Park, R. J. Mitchell, and B.-I. Sang, ”The Future of Butyric Acid in Industry,” The Scientific World Journal, vol. 2012, pp. 1–10, Jan. 2012, doi: 10.1100/2012/471417.

DYNAMIC FULL-FIELD OPTICAL COHERENCE MICROSCOPY OF BIOMEDICAL TISSUE

Erikas Tarvydas[1,2], Austėja Trečiokaitė[1,2], Karolis Adomavičius[1], Urtė Neniškytė[3], Egidijus Auksorius[1]

[1]Department of Optoelectronics, Center for Physical Sciences and Technology, Vilnius, Lithuania
[2]Faculty of Physics, Vilnius University, Vilnius, Lithuania
[3]Life Sciences Center, Vilnius University, Vilnius, Lithuania
erikas.tarvydas@ftmc.lt

Optical coherence tomography (OCT) is an interferometric imaging technique commonly used for visualizing various ex vivo and in vivo biomedical samples. The axial resolution of an OCT system is mainly dictated by the spectral width (and consequently the coherence length) of the light source and lateral resolution by the numerical aperture of the objective lens. Full-field (FF-) OCT can achieve resolution better than 1 μm because it allows use of high-NA objectives and broadband light sources [1,2].

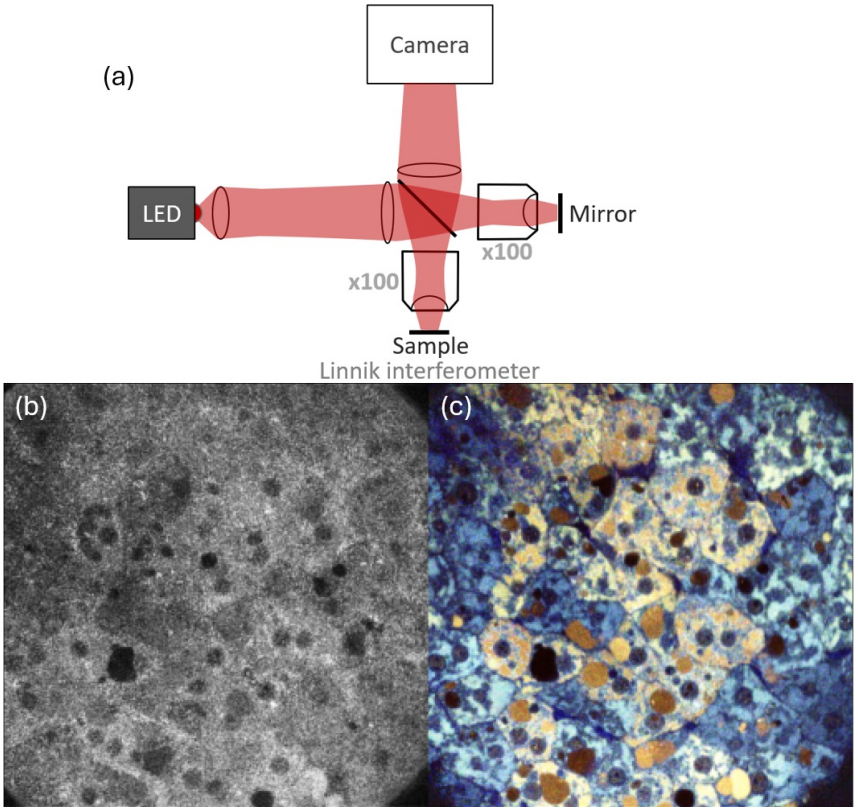


Fig. 1. Principle schematics of high-resolution FF-OCT system (a), comparison between regular (b) and dynamic FF-OCT (c) images of mouse liver.

High-resolution FF-OCT system, shown in Figure. 1.a, can image deep in tissue, featuring Linnik interferometer with two identical high NA immersion objectives, a powerful spatially incoherent white light source and a specialized camera. The system also includes a piezo actuator to enable phase shifting that is necessary to extract OCT images.

Figure 1.b shows a regular FF-OCT image of mouse liver acquired through phase-shifting, wheras Figure 1.c shows dynamic FF-OCT image derived by analyzing vibrations in the acquired interferometric images. As seen in these images, the dynamic FF-OCT provides more detailed images, with clearer cell walls and distinct structures of hepatic tissue. This imaging technique enables the visualization of different cells without the need for specific preparation methods, such as dyes or other modifications commonly required in other imaging techniques.

[1] Dubois, A., Grieve, K., Moneron, G., Lecaque, R., Vabre, L., & Boccara, C. (2004). Ultrahigh-resolution full-field optical coherence tomography. Applied Optics, 43(14), 2874. https://doi.org/10.1364/ao.43.002874
[2] Monfort, T., Azzollini, S., Brogard, J., Clémençon, M., Slembrouck-Brec, A., Forster, V., Picaud, S., Goureau, O., Reichman, S., Thouvenin, O., & Grieve, K. (2023). Dynamic full-field optical coherence tomography module adapted to commercial microscopes allows longitudinal in vitro cell culture study. Communications Biology, 6(1). https://doi.org/10.1038/s42003-023-05378-w
[3] Trečiokaitė, A., Adomavičius, K., & Auksorius, E. (2024). Time-domain full-field optical coherence tomography with a digital defocus correction. Optics Letters, 49(10), 2605. https://doi.org/10.1364/ol.520911

PROTOTYPE SYSTEM OF HYPERSPECTRAL IMAGING BASED ON LEDs

Agnė Urbonaitė[1], Pranciškus Vitta[1]

[1] Institute of Photonics and Nanotechnology, Faculty of Physics, Vilnius University, Lithuania
agne.urbonaite@ff.stud.vu.lt

Personal documents, such as passports, IDs, and driver's licenses, are extremely important in the political, social, and economic aspects of life because they allow to determine a person's identity. Counterfeiting documents enables a variety of crimes: from underage drinking to financial crimes, human trafficking, and terrorism. Therefore, there is a need for tools that allow to determine a document's authenticity confidently . One possibility is hyperspectral imaging (HSI), which is already used in many different fields, where a non-invasive analysis is required. Unfortunately, HSI systems are bulky, expensive, and difficult to operate.

In this work, we present a slightly different approach to hyperspectral imaging in which a standard smartphone camera in combination with a multicolour illumination system is applied. Such a system would be affordable, user-friendly, and portable for document examiners while ensuring proper document authentication. Furthermore, this system could be adapted to be used in other fields that take advantage of HSI. The aim of the work was to develop an MCU-controlled multicolour flash prototype. In the process, sensitivity curves and other camera properties of a commercial smartphone were investigated. Moreover, an enhanced colour discrimination algorithm was developed and tested on different samples. DNG filetype data analysis tools were employed and tailored for automated data analysis and hyperspectral imaging.

To conclude, we have developed a prototype hyperspectral imaging system based on LEDs which can be used for document authentication and other fields of potential applications such as medical diagnostics.

FULL FIELD OPTICAL COHERENCE TOMOGRAPHY IN VIVO RETINAL IMAGING WITH OPTIMIZED BEAM SPLITTER AND REDUCED COHERENCE NOISE

Austėja Trečiokaite[1,2], Erikas Tarvydas[1,2], Karolis Adomavičius[1], Egidijus Auksorius[1]

[1]Department of Optoelectronics, Center for Physical Sciences and Technology, Vilnius, Lithuania
[2]Laser Research center, Department of Physics, Vilnius University, Vilnius, Lithuania
austeja.treciokaite@ftmc.lt

Full Field Optical Coherence Tomography (FF-OCT) is one of the most upcoming methods for in vivo imaging, but there is always a need to improve imaging speed, depth and quality. Fourier Domain (FD-) FF-OCT is most used for retinal imaging due to its speed and innate possibility to digitally correct aberrations [1]. Usually, interferometers for this kind of imaging are based on symmetrical, 50/50 beam splitters, thus by default losing over a half of the overall light and most importantly – more than half of the signal, since intensity of light that can be sent to an eye safely is limited.

Also, even with an increace of signal, coherent light sources are known to produce images of lesser quality due to inherent coherence noice, that presents it self in a form of speckles in OCT images [2].

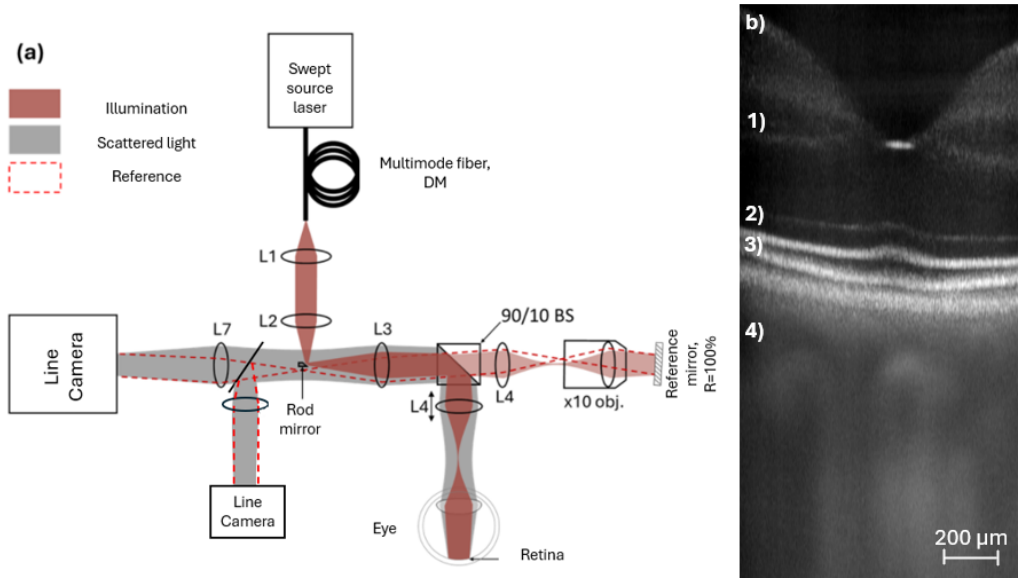


Fig. 1. The principal imaging system is shown (a), acquired in vivo retinal image showing various retinal layers (1 – nerve cell layer, 2 -external limiting membrane , 3 – photoreceptors, 4 – choroidal stroma)(b).

Due to these reasons, the goal of this work is to optimize beam splitting ratios for FF-OCT in Fourier FF-OCT and reduce spatial coherence of a laser in order to improve imaging Signal to Noise Ratio (SNR). We used 90/10 cube beam splitter for FD-OCT imaging in order to improve SNR and a deformable membrane was utilised for laser coupling as a means to distort spatial coherence of a laser beam, before inputing in the system (Figure 1. a). As a result, it was shown that asymmetric, high throughput beam splitter configurations increase FD-FF-OCT systems' SNR by 2,5 times and that reduced spatial coherence visibly increaces the quality of in vivo retinal images (Figure 1. b).

[1] Borycki, D., Auksorius, E., Węgrzyn, P., & Wojtkowski, M. (2020). Computational aberration correction in spatiotemporal optical coherence (STOC) imaging. Optics Letters, 45(6), 1293. https://doi.org/10.1364/ol.384796
[2] Auksorius, E., Borycki, D., & Wojtkowski, M. (2019b). Crosstalk-free volumetric in vivo imaging of a human retina with Fourier-domain full-field optical coherence tomography. Biomedical Optics Express, 10(12), 6390. https://doi.org/10.1364/boe.10.006390

STUDY OF ELECTRON ACCELERATION IN STRONG INFRARED RADIATION FIELDS FOR SELECT PARAMETERS

Džiugas Vyšniauskas[1,2], Artūras Plukis[1], Janina Grinevičiūtė[1]

[1]Center for Physical Sciences and Technology, Vilnius, Lithuania
[2]Institute of Chemical Physics, Vilnius University, Lithuania
dziugas.vysniauskas@ftmc.lt

Space requirements, expenses and complex structures of radio frequency linear accelerators present drawbacks to their usefulness. Dielectric laser accelerators (DLA) rely on charged particle acceleration in a high electromagnetic field caused by laser pulse interaction with dielectric microstructures. In theory, this provides accelerations in the gigavolts per meter (GV/m) range [1], which would be a significant improvement over established technologies that have accelerating fields generally in the tens of megavolts per meter (MV/m) range. In this work, fused silica (SiO_2) and Si microstructures are computationally explored as the basis for a physical experiment optimization.

To carry out the calculations, an infinite three-dimensional lattice of cylindrical elements was constructed (Fig. 1) to interact with a 2 μm and 100 fs laser pulse. Using "MEEP" libraries [2], the time evolution of the electric field was obtained by solving Maxwell's equations through the finite-difference time-domain (FDTD) method. The outcome data were subsequently inputted into a particle tracking program, where the acceleration of the electrons was calculated for different input energies, times and injection coordinates.

It was found that the gradient developed in the silicon (384 MeV/m) microstructure promotes a more efficient acceleration of electrons in comparison to fused silica (151 MeV/m). With further calculations on the localization of the electron introduction, it was found that electrons with maximum acceleration are located near the surface of the microstructure. In experiments with several cells, electron acceleration was found to take place primarily in the first two cells. As the electrons' velocities rise it causes a phase mismatch (Fig. 2) relative to both the laser pulse and to the lattice constant leading to deceleration.

The results obtained suggest that electrons experience maximum acceleration in silicon structures when they are injected along the microstructure surface (561 MeV/m). This acceleration is effective for a maximum of two cells (6 acceleration periods) beyond this, the experimental setup must be readjusted to accommodate the new acceleration conditions.

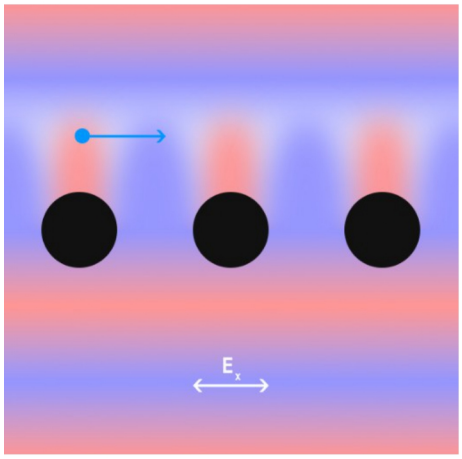


Fig. 1. Two-dimensional scheme of electron acceleration in a lattice of cylindrical elements.

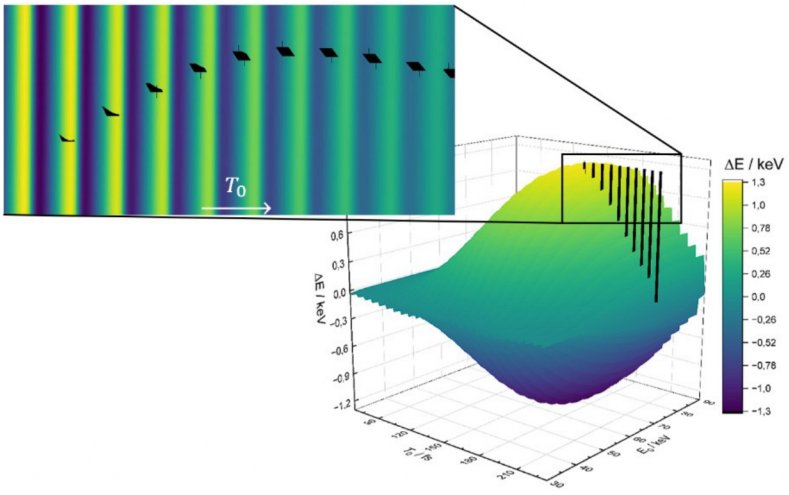


Fig. 2. Electron positions on the acceleration surface for 10 lattice periods.

[1] X. Mei et al, Ultrafast Science, 3:0050 (2023)
[2] A. Oskooi et al, Computer Physics Communications, Vol. 181, pp. 687-702 (2010)

EFFECT OF PEG SUBSTITUENT LENGTH ON CELLULAR UPTAKE OF UPCONVERTING NANOPARTICLES

Aleja Marija Daugelaite[1,2], Egle Ezerskyte[1,2], Kristina Bolgova[2], Edvin Parafjanovic[2], Arturas Katelnikovas[2], Vitalijus Karabanovas[1,3], Greta Butkiene[1], Vaidas Klimkevicius[1,2]

[1]Biomedical Physics Laboratory of National Cancer Institute, Vilnius, Lithuania
[2]Institute of Chemistry, Faculty of Chemistry and Geosciences, Vilnius University, Vilnius, Lithuania
[3]Department of Chemistry and Bioengineering, Vilnius Gediminas Technical University, Vilnius, Lithuania
aleja.daugelaite@nvi.lt

Upconverting nanoparticles (UCNPs) are a unique class of luminescent nanomaterials capable of converting near-infrared (NIR) excitation energy into visible and ultraviolet emission. This property is particularly beneficial for biomedical imaging, as UCNPs can be excited by NIR light within a biological imaging window (750-1300 nm), where tissue absorption and scattering are minimal. This enables deeper tissue penetration than conventional fluorophores that are excited with visible or ultraviolet light [1]. However, a significant challenge in biomedical applications of nanoparticles is their limited accumulation and penetration in certain organs or tumors. To achieve prolonged circulation in the bloodstream and reduce rapid clearance by the mononuclear phagocyte system, surface functionalization strategies such as polyethylene glycol (PEG) coating are commonly used. PEGylation enhances the nanoparticles' hydrophilicity, reduces protein adsorption, and minimizes immune recognition, thereby improving their biocompatibility and systemic retention for *in vivo* imaging and therapeutic applications [2].

In this study, core-shell UCNPs with the chemical composition $NaGdF_4:Yb^{3+},Er^{3+}@NaGdF_4:Yb^{3+},Nd^{3+}$, were synthesized according to the previously described procedure [3]. The surfaces of these nanoparticles were functionalized using custom-designed brush-type copolymers p(DMAm-*co*-OEG_XMA). These copolymers incorporate oligoethylene glycol chains of varying lengths (x = 5, 9, 19) on the UCNP surface.

This study aimed to investigate how the length of PEG substituents affects the cellular uptake of UCNPs. Emission intensity measurements indicated that these modified UCNPs demonstrate long-term stability in aqueous and cell culture media. The intracellular accumulation of UCNPs using laser scanning confocal microscopy and spectrometry was used to evaluate their applicability on different cancer cell lines derived from distinct localizations (breast and prostate cancer) and skin-derived mesenchymal stem cells (S-MSCs). The study revealed that all modified UCNPs exhibited similar uptake behavior in cell monolayers. The accumulation studies were also conducted on cellular spheroids to bring the study closer to the *in vivo* environment. The results indicated that UCNPs accumulate on the surface layers of the spheroids regardless of the length of the PEG substituent. Additional biocompatibility tests confirmed that UCNPs are biocompatible and exhibited no toxicity within the investigated cells. All these findings concluded that functionalized UCNPs are promising biocompatible agents for bioimaging.

Acknowledgements
This project has received funding from the Research Council of Lithuania (LMTLT), agreement No [S-MIP-23-5].

[1] Wilhelm, S. ACS Nano 11, 10644–10653 (2017).
[2] Mitchell, M.J., et al. Nat Rev Drug Discov 20, 101–124 (2021).
[3] Ezerskyte, E. et al., ACS Appl. Nano Mater. 7, 6185–6195 (2024).

CONCENTRATION QUENCHING IN SOLUTIONS OF CHLOROHYLL A MOLECULES

Vilius Čirgelis[1,2], Simona Streckaitė[2], Jevgenij Chmeliov[1,2], Leonas Valkūnas[2], Andrius Gelžinis[1,2]

[1]Physics Faculty, Vilnius University, Lithuania
[2]Center for Physical Sciences and Technology, Lithuania
vilius.cirgelis@ftmc.lt

Most organic fluorophores in low-concentration solutions exhibit a photoluminescence quantum yield (PL QY) close to 1, whereas at higher molecular concentrations, PL QY significantly decreases [1]. This reduction in fluorescence QY with increasing concentration is known as concentration quenching. Since concentration quenching can negatively impact system or instrument performance, understanding its underlying physical mechanisms is crucial [2]. In organometallic compounds like chlorophyll (Chl), this phenomenon is particularly intriguing due to its relevance in photosynthetic complexes. However, a definitive model explaining concentration quenching has yet to be established.

This study aimed to investigate the effects of concentration on Chl-a molecules in solvents of different polarity. To achieve this, absorption (Abs) and fluorescence (FL) spectra, along with fluorescence decay kinetics and PL QY were measured. Chl-a solutions were prepared by dissolving the molecules in toluene (Tol), dimethyl sulfoxide (DMSO), ethanol (EtOH).

Spectral properties of Chl-a solutions strongly depend on solvent properties. In nonpolar Tol, Chl-a spectral changes are the most significant: with increasing concentration Qy (665 nm) Abs band gets wider. In FL, formation of a new 705 nm FL band is observed, which relative intensity increases with concentration. In aprotic polar DMSO, Chl-a Abs spectra changes are observed only for the highest 25 mM concentration, where Qy band shifts to shorter wavelengths - this may indicate H type aggregate formation. In FL spectra, with increasing concentration, 705 nm band formation is observed, however its relative intensity is 3 times lower than in Tol solutions. In protic polar EtOH, Chl-a spectra does not depend on concentration. For Chl-a molecules in all investigated solvents, the decrease of FL intensity with increasing concentration is observed. For concentrations higher than 1 mM, the average FL lifetime decreases, indicating that concentration quenching is present in solutions.

[1] B. Zhang et al. Chemistry of Materials 29, 19, (2017) pp 8395-8403.
[2] Dae Hyun Ahn et al. Nature Photonics, 13, (2019) pp 540-546.

DEVELOPMENT OF A PHOTODYNAMIC ANTIMICROBIAL IRRADIATION PROTOTYPE AND FUTURE PHOTOSENSITIZER STUDIES

Tomas Krupavičius[1], Pranciškus Vitta[1], Irina Buchovec[1]

[1] Institute of Photonics and Nanotechnology, Faculty of Physics, Vilnius University, Lithuania
tomas.kupavicius@ff.stud.vu.lt

Modern agricultural and food industries rely on chemical protection technologies such as bactericides, fungicides, and insecticides to maintain high productivity. Without these treatments, global agricultural output could decrease by approximately 45%, leading to food shortages. [1] However, excessive chemical use poses environmental and health risks, prompting efforts to develop eco-friendly alternatives. One promising approach is antimicrobial photodynamic inactivation (API), which utilizes light and photosensitizers (PS) to selectively inactivate pathogens while minimizing ecological harm.

This study investigates the development and application of an LED-based irradiation prototype for API experiments, designed to enable controlled photodynamic studies on PS solutions, microbial cultures, and PS-treated samples. The prototype was developed during a professional internship at the Institute of Photonics and Nanotechnology, Vilnius University. [2] The project aimed to design a reliable prototype for API research. The initial prototype was equipped with near-UV (402 nm), blue (440 nm), and white LEDs, where near-UV corresponds to the first absorption maximum (Soret band) of magnesium (Mg-Chl) and copper (Cu-Chl) chlorophyllins.

During this project, the prototype was optimized by replacing white LEDs with red LEDs (650 nm) to match the absorption maximum (Q band) of Mg-Chl and Cu-Chl. Additionally, heat dissipation improvements were implemented to enhance system stability. Furthermore, an STM32 microcontroller was programmed to allow precise control of LED intensity, and calibration procedures were refined to ensure accurate and reproducible light exposure.

Challenges encountered during development included thermal damage during LED replacement and compatibility issues with the control software, which were successfully resolved through hardware modifications and software adjustments. The optimized prototype was used to investigate the photophysical properties of Mg-Chl and Cu-Chl under near-UV (402 nm) (Soret band) and red (650 nm) (Q band) light. The experiments helped evaluate the dependence of both photosensitizers' excitation efficiency on sample positioning and applied irradiation intensity, which, in turn, could contribute to enhancing API effectiveness. Additional details on the project and preliminary results will be presented during the poster session.

Keywords: antimicrobial photodynamic inactivation, photosensitizer, chlorophyllin, irradiation prototype, LED calibration, microcontroller programming.

[1] Sharma, A., Kumar, V., Shahzad, B. et al. Worldwide pesticide usage and its impacts on ecosystem. SN Appl. Sci. 1, 1446 (2019). https://doi.org/10.1007/s42452-019-1485-1

[2] Buchovec, I., Klimkaitė, L., Sužiedėlienė, E., & Bagdonas, S. (2022). Inactivation of Opportunistic Pathogens Acinetobacter baumannii and Stenotrophomonas maltophilia by Antimicrobial Photodynamic Therapy. Microorganisms, 10(3), 506. https://doi.org/10.3390/microorganisms10030506

INFLUENCE OF THE MEDIUM ON THE SPECTROSCOPIC PROPERTIES AND PHOTOSTABILITY OF MG-CHLOROPHYLLIN

Marija Kalnaityte[1], Rasa Miliukaitė[1], Danielė Gedminaitė[1], Agnė Kalnaitytė - Vengelienė[1], Saulius Bagdonas[1]

[1]Laser Research Center, Faculty of Physics, Vilnius University, Saulėtekio av. 9, III bld., Vilnius, Lithuania
marija.kalnaityte@ff.stud.vu.lt

Chlorophyllins, which have antioxidant, antimicrobial and anti-inflammatory effects, are not only used as food dyes, but can also be used in photodynamic therapy. Illuminated magnesium chlorophyllin (Chl) has a dual effect on the microenvironment, acting as a photosensitizer and antioxidant [1], which depends on surrounding medium.

In this work, we investigated the changes in optical density (OD) and fluorescence (FL) of magnesium chlorophyllin (4 - 15 µM), as well as the photostability, in various media: distilled water (DW), phosphate buffer (PB, pH 6 - 7), tris(hydroxymethyl)aminomethane buffer (TRIS, pH 6.0 - 7.3), modified Wilkins–Chalgren medium (MWC, pH 7.6), in the presence of $CuCl_2$ or bovine serum albumin (BSA, 10 µM). Spectroscopic measurements of 1 ml samples were performed in 4x10 mm cuvettes. Between measurements, samples were stored in Eppendorf tubes (1.5 ml) at room temperature in the dark. During photostability experiments, an area of approximately 1 cm^2 of the samples in the cuvettes was irradiated with a violet light LED (404 ± 9 nm (FWHM), 30 mW/cm^2). The total dose (18 J/cm^2) was collected in intervals of 1.8 J/cm^2 (from 0 J/cm^2 to 5.4 J/cm^2), 3.6 J/cm^2 (up to 12.6 J/cm^2) and 5.4 J/cm^2. The samples were mixed after irradiation before each measurement.

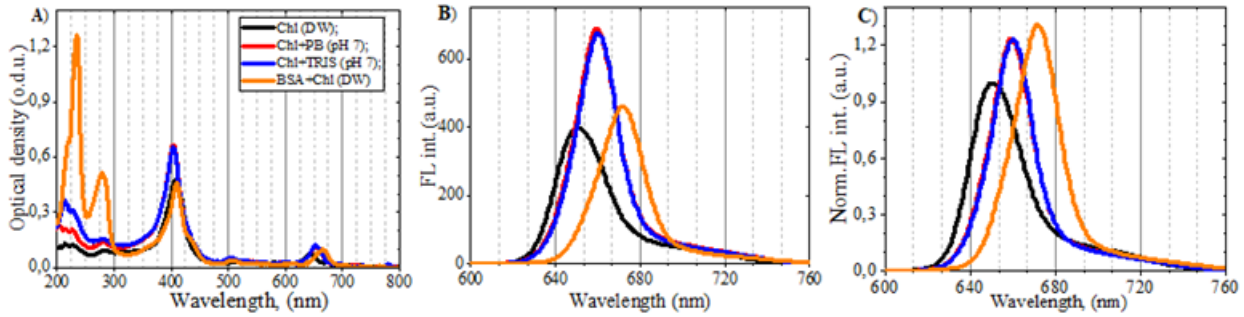


Fig.1 Initial spectra of optical density (A) and FL intensity of magnesium Chl (C = 10 µM) in different media) and in the presence of BSA (B). The FL spectra normalized to the absorbance at excitation wavelength (C). λ_{ex}=405 nm, excitation and emission slits 6 and 2.5.

The initial spectra of magnesium Chl changed significantly in different media (PB and TRIS) when measured at pH 7, and with addition of the protein, compared to DW (Fig. 1 A). A bathochromic 10 nm shift of the FL band was recorded in TRIS and PB media, and a 22 nm shift – with BSA (Fig. 1 B). After normalization of the FL spectrum, it was found that regardless of the chemical type of the buffer or presence of BSA, the FL intensity increased relatively compared to Chl in DW medium (Fig. 1 C). However, with a 2.5 times higher concentration of one type of cation (Cu^{2+})in Chl solutions, the FL intensity decreased more than 10 times compared to DW. Spectroscopic changes of Chl occurring in distilled water and BSA solution immediately after irradiation with a violet diode and after 24 hours were also analyzed.

[1] C. Pucci, C. Martinelli, A. Degl'Innocenti, A. Desii, D. De Pasquale, G. Ciofani, "Light-Activated Biomedical Applications of Chlorophyll Derivatives", Macromolecular Bioscience, Volume 21, Issue 9, (2021)

EFFECT OF QUANTUM DOTS ON THE PHOTOSTABILITY OF THE SPECTROSCOPIC PROPERTIES OF MG-CHLOROPHYLLIN

Aistė Krasauskaitė[1], Marija Kalnaitytė[1], Saulius Bagdonas[1], Agnė Kalnaitytė - Vengelienė[1]

[1]Laser Research Center, Faculty of Physics, Vilnius University, Lithuania
aiste.krasauskaite@ff.stud.vu.lt

Magnesium chlorophyllin (Chl) is known as a semi-synthetic compound derived from chlorophyll, the green pigment. When exposed to light, Chl can act as a photosensitizer (PS) and has potential applications in medicine [1]. Additionally, studies have shown that this compound can function as an antioxidant in cancer cells [2]. Quantum dots (QD) can work together with photosensitizers and be used in medical diagnostics and therapy [3]. However, light is required to excite both PS and QD, so it is also important to evaluate their photostability. Whether photoexcited Chl will act as a PS or an antioxidant depends on the medium, in particular, on QD composition and/or structure.

The aim of this study was to investigate how QD of different compositions (CdTe-COOH (570 nm, PlasmaChem GmbH, Germany) , CuInZnS/ZnS-COOH (550 nm, Nanooptical materials, USA)) affect the spectroscopic properties of Mg-chlorophyllin, specifically optical density (OD) and fluorescence (FL), under irradiation. The concentrations of QDs were selected based on their fluorescence intensity to enable tracking of spectral changes over time. Samples of Mg-chlorophyllin with QDs in distilled water were irradiated at a distance of 8 cm using a 405 nm wavelength diode with a power of 30 mW/cm^2. The irradiation was applied on a 4x10 mm cuvette to a 1 cm^2 sample area. Changes in OD and FL were observed by increasing the irradiation doses, ranging from 1.8 J/cm^2 to 72 J/cm^2.

CuInZnS/ZnS-COOH QDs induced a greater bathochromic shift in the OD spectrum peak (from 645 nm to 655 nm) in distilled water immediately after sample preparation, while CdTe-COOH QDs shifted this peak to 647 nm (Fig. 1a). In the presence of QD, Chl FL peak shifted from 652 nm to 660nm or to 655 nm, respectively (Fig. 1b). In the absence of QDs, light exposure caused a decrease in Chl OD and FL intensity without any spectral shifts. The effect of light on Chl FL varied depending on the composition of the QDs in the medium. Under 18 J/cm^2 irradiation dose, CuInZnS/ZnS-COOH QDs caused a decrease in FL intensity and a further red shift of Chl FL band, whereas in the presence of CdTe-COOH QDs, no shift was observed.

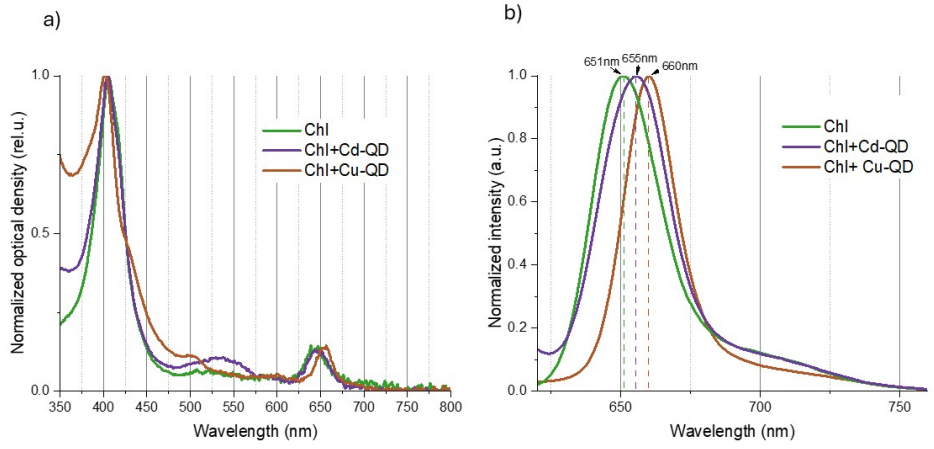


Fig. 1. Initial Chl optical density (a) and fluorescence (b) spectra, with and without quantum dots in the medium. Fluorescence is excited by light with a wavelength of 405 nm.

[1] C. Jiang, F. Scholle, F. Jin, Q. Wei, Q. Wang, ir R. Ghiladi, „Chlorophyllin as a Photosensitizer in Photodynamic Antimicrobial Material“, 2023 m. doi: 10.21203/rs.3.rs-2964210/v1.

[2] M. Ozcan, D. Aydemir, M. Bacanlı, H. G. Anlar, N. N. Ulusu, ir Y. Aksoy, „Protective Effects of Antioxidant Chlorophyllin in Chemically Induced Breast Cancer Model In vivo“, Biol. Trace Elem. Res., t. 199, nr. 12, p. 4475–4488,2021, doi: 10.1007/s12011-021-02585-6.

[3] S. Alizadeh Nobari ir kt., „Emerging trends in quantum dot-based photosensitizers for enhanced photodynamic therapy in cancer treatment“, J. Pharm. Investig., t. 55, nr. 1, p. 55–90, 2025, doi: 10.1007/s40005-024-00698-3.

INVESTIGATION OF $TPPS_4$ AGGREGATION USING SPECTROSCOPY AND ATOMIC FORCE MICROSCOPY

Greta Tamoliūnaitė[1], Vilius Poderys[1], Ričardas Rotomskis[1,2]

[1]Biomedical Physics Laboratory, National Cancer Institute P. Baublio St. 3b, LT-08406 Vilnius, Lithuania
[2]Biophotonics Group of Laser Research Centre, Vilnius University Saulėtekio Ave. 9, LT-10222 Vilnius, Lithuania
greta.tamoliunaite@gmc.stud.vu.lt

Compounds that can self-assemble into controlled aggregate structures could be used as a guided building block and are interesting research objects. Organic and inorganic aggregates are inseparable from supramolecular chemistry, where they can lead to formation of complex structures [1]. 5,10,15,20-Tetrakis(4-sulfonatophenyl)porphyrin ($TPPS_4$) is an organic compound composed of four pyrrole rings and four sulfonatophenyl substituent groups at its *Meso*-positions. $TPPS_4$ is one of the porphyrin ring derivatives that can readily self-assemble into different types of aggregates, dependent on the environmental conditions [2]. This characteristic causes interest in their potential use in supramolecular assemblies.

Changes in concentration and pH in aqueous $TPPS_4$ solutions can induce aggregation processes. In an acidic environment, the central part of $TPPS_4$ is protonated by two protons. At pH≈1 additionally two SO_3- groups are protonated and a zwitterion is formed. This leads to the formation of electrostatic interactions between the positively charged porphyrin ring and the negatively charged side SO_3- groups. As a result, so-called Jelly-type aggregates (J-aggregates) are formed. These aggregates possess interesting optical properties and spatial characteristics and are intensively studied.

The aim of our studies was to determine whether the elimination of electrostatic interactions between two $TPPS_4$ molecules will change the spatial structure of the aggregates and what type of aggregation would occur. At pH=7 the central part of the porphyrin ring is neutral and the total charge of the $TPPS_4$ molecule is (-4) due to the 4 negatively charged SO_3- groups. At pH=-1 both the central part of the porphyrin ring and the four SO_3- groups are protonated and the charge of the $TPPS_4$ molecule is (+2), but the electrostatic interaction between the two $TPPS_4$ molecules does not occur.

Our spectroscopic investigations show that at pH=7, upon increase of $TPPS_4$ concentration, Soret absorption band remains at 414 nm while Q bands shifts to the red spectral region, indicating the novel aggregate formation, that can be imaged by AFM. When the pH is reduced to -1, $TPPS_4$ aggregates are formed as the concentration increases, but their optical and spatial properties differ from J-aggregates. AFM images give no similarity to J-aggregates and show another novel type of aggregates.

Our studies of optical and spatial properties of $TPPS_4$ aggregation at neutral and extreme acidic pH shown that $TPPS_4$ molecules can form more aggregate types. Different interactions are a driving forces to form these aggregates. Ability to form various types of multimolecular aggregate structures is particularly useful in creating various nano-size optoelectronic devices.



Fig. 1. $TPPS_4$ aggregates at pH=-1

[1] Otsuki, J. Supramolecular approach towards light-harvesting materials based on porphyrins and chlorophylls. J. Mater. Chem. A. 6, 6710-6753 (2018). https://doi.org/10.1039/C7TA11274B
[2] Pleckaitis, M., Habach, F., Kontenis, L. et al. Structure and principles of self-assembly of giant “sea urchin” type sulfonatophenyl porphine aggregates. Nano Res. 15, 5527–5537 (2022). https://doi.org/10.1007/s12274-021-4048-x

COMPLEXATION OF $TPPS_4$ WITH POLYVINYL ALCOHOL POLYMER IN AQUA AND POLYMER MATRIX

Simona Pusvaškytė[1], Greta Tamoliūnaitė[1], Skaistė Talanovaitė[1], Vilius Poderys[1], Ričardas Rotomskis[1,2]

[1]Biomedical Physics Laboratory of National Cancer Institute, Baublio 3B, LT-08406, Vilnius, Lithuania
[2]Biophotonics Group of Laser Research Centre, Vilnius University, Saulėtekio 9, c.3, LT-10222, Vilnius, Lithuania
simona.pusvaskyte@gmc.stud.vu.lt

Recent advancements in supramolecular chemistry have expanded the understanding of porphyrin self-assembly, leading to the development of functional materials with promising electro-optical properties for biomedical sensor applications [1]. To harness these properties effectively, stabilization of specific molecular forms or self-assembled structures is crucial. One approach to achieving this is the immobilization of porphyrins within polymer matrices, such as polymer films [2], which provide enhanced stability and controlled organization of the porphyrin molecules.

This work presents the results of the determination of interaction of 5,10,15,20-Tetrakis(4-sulfonatophenyl)porphyrin ($TPPS_4$) with polyvinyl alcohol polymer (PVA) in aqua and immobilized in polymer matrix. $TPPS_4$ tetra sodium salt and poly (vinyl alcohol) stock solutions were made by dissolving $TPPS_4$ and PVA polymer powder separately in deionized water at different pH in the region from pH = -1 to pH = 7.

When PVA ($c = 5 \cdot 10^{-4}$ M) is added to the monomeric $TPPS_4$ solution ($c = 1 \cdot 10^{-6}$ M) at pH = 7, the Soret band, which has a maximum at 414 nm, shifts to 418 nm. Additionally, a complex transformation of the Q bands occur. This indicates that a $TPPS_4$ monomer and PVA complex was formed. Its spectral properties did not change over time, meaning that formed $TPPS_4$-PVA complex was stable in neutral aqueous media.

When monomeric $TPPS_4$ aqueous solution ($c = 1 \cdot 10^{-6}$ M) is acidified (pH = 3), the core of the $TPPS_4$ is protonated. Consequently, Soret band shifts from 414 to 434 nm, and instead of four Q bands, two Q bands remain with maxima at 595 nm and 645 nm. When PVA ($c = 5 \cdot 10^{-4}$M) is added to an acidified $TPPS_4$ aqueous solution, no spectral changes are observed.

More complicated spectral changes were detected when PVA ($c = 4 \cdot 10^{-5}$ M) is added to the $TPPS_4$ solution ($c = 1.4 \cdot 10^{-4}$ M). J- aggregates are present in this sample and additional bands with maxima at 490 nm and 709 nm are formed. The addition of PVA reduces the intensity of J-aggregate bands and a complex transformation of the Soret bands occur, suggesting that addition of PVA brakes down $TPPS_4$ J-aggregates.

These findings imply that PVA interacts with $TPPS_4$ in aqueous solution and stable complex is formed, possible interaction points are presented in Figure 1. Moreover PVA significantly influences stability of J-aggregates.

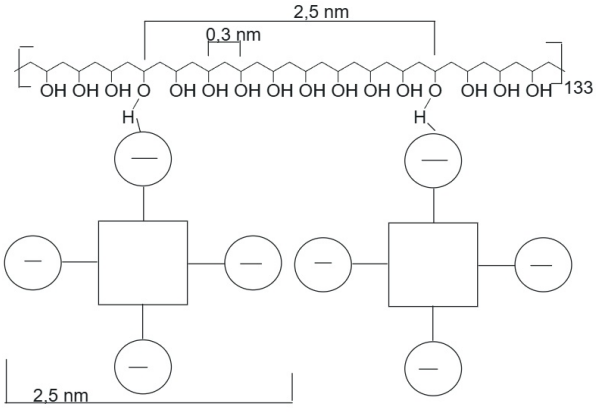


Fig. 1. Possible interaction between $TPPS_4$ and PVA polymer.

[1] P. Dutta, R. Rai, S. Pandey. Effect of Ionic Liquid on J-Aggregation of meso-Tetrakis(4-sulfonatophenyl)porphyrin within Aqueous Mixtures of Poly(ethylene glycol). J. Phys. Chem. B, 115, 1520-6106 (2011). https://doi.org/10.1021/jp112263s
[2] M. Teodorescu, M. Bercea, S. Morariu. Biomaterials of PVA and PVP in medical and pharmaceutical applications: Perspectives and challenges. Biotechnology Advances, 37, 0734-9750 (2019). https://doi.org/10.1016/j.biotechadv.2018.11.008

ENVIRONMENTAL BEHAVIOR AND BIOCOMPATIBILITY OF UPCONVERTING NANOPARTICLES IN FRESH WATER

Augustas Morkvėnas[1,2], Vilius Poderys[1], Danguolė Montvydienė[2], Jūratė Karosienė[2], Vitalijus Karabanovas[1,2], Živilė Jurgelėnė[2]

[1]Biomedical Physics Laboratory, National Cancer Institute, Baublio 3b, LT-08406, Vilnius, Lithuania
[2]Department of Chemistry and Bioengineering, Vilnius Gediminas Technical University, Sauletekio Ave. 11, LT-10223 Vilnius, Lithuania
[3]State Scientific Research Institute Nature Research Centre, Akademijos str. 2, Vilnius, Lithuania
augustas.morkvenas@nvi.lt

Upconverting nanoparticles (UCNPs) have gained significant attention in bioimaging and sensing due to their ability to convert near-infrared light into visible emissions. This unique property allows for deep tissue imaging, reduced photobleaching, and high sensitivity in detection applications[1],[2],[3]. However, their potential ecological impact remains unclear, particularly in aquatic environments, where their interactions with organisms could influence whole ecosystem dynamics.

Algae plays a key role in nutrient cycling in aquatic ecosystem and serves as a bioindicator of water quality. Their rapid growth, high surface-area-to-volume ratio, and sensitivity to environmental changes make them ideal model organisms for investigation of the potential toxicity of nanomaterials[4]. In this study, we investigated the stability of $NaYF_4$:Yb^{3+},Er^{3+} UCNPs, localization of UCNPs in green microalgae *Desmodesmus communis* and potential toxicity. This study used two media: an algae growth media (MWC) and water from the river Neris. UCNPs were tested at concentrations ranging from 2.5 to 100 µg/mL. Confocal laser scanning microscopy (CLSM) was employed to analyze nanoparticle uptake and localization in algae. UCNPs were excited with a 980 nm laser, while algae autofluorescence was excited using a 404 nm laser. Additional optical characterization included absorbance spectroscopy, fluorescence measurements (at 480 nm excitation), upconversion emission spectra (at 980 nm excitation), and emission decay kinetics.

Our results showed that UCNPs emission signals were more intense and nanoparticles were more colloidaly stable in the river Neris water than in MWC. MWC media is a balanced algae growth media rich in nutrients and ions. The ionic strength of MWC media is approximately 5 times higher than that of the river Neris water. This might be one of the factors causing faster aggregation of UCNPs in MWC media. Microbiological investigation of Neris water and MWC media showed that bacteria content in Neris water was 10,000 times higher (although water was filtered through a 0.2 µm filter) than in MWC media. CLSM imaging also confirmed that the river Neris water had much more bacteria compared to MWC media. The results also demonstrated that UCNPs did not localize inside *D. communis* cells. However, we observed that UCNPs interacted with bacteria.

Algae growth (evaluated using the absorbance of chlorophyll band) in MWC media followed an exponential curve, whereas in the river Neris water, it was linear and much slower (after 4 days, chlorophyll concentration was 4 times smaller). However, there were no significant differences in samples with different UCNPs concentrations in both cases. Different algae growth rates might be caused by fewer nutrients in the river Neris water.

Our findings suggest that UCNPs do not bioaccumulate in freshwater microalgae, but further research is needed to assess long-term aquatic toxicity.

Acknowledgements

This work was supported by the Research Council of Lithuania, agreement No [S-MIP-24-92] “Effects of rare earth metals-based nanoparticles on aquatic organism: correlation between nanotoxicity and physico-chemical properties”.

[1] E. Ezerskyte et al., “Biocompatible Upconverting Nanoprobes for Dual-Modal Imaging and Temperature Sensing,” ACS Appl. Nano Mater., vol. 7, no. 6, pp. 6185–6195, Mar. 2024, doi: 10.1021/acsanm.3c06111.
[2] A. Fatima, Md. W. Ahmad, A. K. A. Al Saidi, A. Choudhury, Y. Chang, and G. H. Lee, “Recent Advances in Gadolinium Based Contrast Agents for Bioimaging Applications,” Nanomaterials, vol. 11, no. 9, p. 2449, Sep. 2021, doi: 10.3390/nano11092449.
[3] F. Wang and X. Liu, “Recent advances in the chemistry of lanthanide-doped upconversion nanocrystals,” Chem. Soc. Rev., vol. 38, no. 4, p. 976, 2009, doi: 10.1039/b809132n.
[4] F. Wang et al., “Effects of Nanoparticles on Algae: Adsorption, Distribution, Ecotoxicity and Fate,” Applied Sciences, vol. 9, no. 8, Art. no. 8, Jan. 2019, doi: 10.3390/app9081534.

TUNNELING EFFECTS IN MANGANITE NANOSTRUCTURES IN THE PRESENCE OF STRONG MAGNETIC FIELDS

Dariuš Antonovič[1], Vilius Vertelis[1], Skirmantas Keršulis[1], Nerija Žurauskienė[1]

[1]Center for Physical Sciences and Technology, Department of Functional Materials and Electronics, Saulėtekio av. 3, LT-10257, Vilnius, Lithuania
darius.antonovic@ftmc.lt

Magnetic tunnel junctions (MTJs) are increasingly used in applications such as magnetic field sensors, hard drive read heads and non-volatile memory circuits [1]. While most MTJs are fabricated by growing layers with a controlled insulator barrier thickness, they also can be formed naturally in polycrystalline manganite films, in which the grain boundaries (GBs) act as barriers. At low magnetic field strengths (<100 mT) the resistance of such films can be drastically decreased due to the spin-polarized tunneling of charge carriers through the disordered GBs. This effect is known as low-field magnetoresistance (LFMR) [2] and could be used for magnetoresistive sensor applications. At higher magnetic field strengths, the colossal MR effect occurs due to the alignment of the magnetic moments of the Mn ions. This effect does not achieve saturation even at magnetic field strengths of tens of teslas, which is important for the development of high magnetic field sensors [3]. Apart from the magnetoresistive effect, polycrystalline manganite films also exhibit negative electroresistance (ER) since the electric potential can align the energy levels between the magnetic layers separated by the insulating barrier. Therefore, for device applications, it is essential to understand the charge carrier transport mechanisms occurring in the GBs between crystallites.

In this study, we explore the electrical conductivity behavior of vertically aligned La-Ca(Sr)-Mn-O nanocolumn films with disordered GBs while under the influence of synchronized strong pulsed electric and magnetic fields. Nanosecond electric field pulses were employed to analyze the intrinsic properties of the junctions without introducing adverse thermal effects. The pulsed magnetic fields enabled the investigation of the combined magnetic and electric properties under semi-stationary conditions, with fields reaching up to 20 T. It was demonstrated that with increasing electric field strengths the inelastic tunneling through two or more localized states in the GBs becomes dominant and that tunneling behavior is dependent on both the magnetic field and temperature.

[1] Zheng C. et. al., Magnetoresistive sensor development roadmap (non-recording applications), IEEE Trans. Magn., 2019, 55, 0800130.
[2] Lee S. et al., Intergrain magnetoresistance via second-order tunneling in perovskite manganites, Phys. Rev. Lett., 1999, 82, 4508–4511.
[3] Stankevič T. et al., Pulsed magnetic field measurement system based on colossal magnetoresistance-B-scalar sensors for railgun investigation, Rev. Sci. Instrum, 2014, 85, 044704.

DEVELOPMENT OF UPCONVERTING CORE-SHELL-SHELL NANOPARTICLES WITH MULTIWAVELENGTH EMISSION FOR THERANOSTIC APPLICATIONS

Egle Ezerskyte[1], Arturas Katelnikovas[1], Vaidas Klimkevicius[1]

[1]Faculty of Chemistry and Geosciences, Institute of Chemistry, Vilnius University
egle.ezerskyte@chgf.vu.lt

Developing new theranostic tools or enhancing existing ones is exceptionally relevant, as oncological diseases remain among the most pressing global health challenges. The rapid advancements in nanochemistry over the recent decades have enabled the creation of multifunctional nanoparticles, which can serve both diagnostic and therapeutic purposes, with precise optimization of their physicochemical properties. Upconverting nanoparticles (UCNPs) are particularly noteworthy because they are excited using near-infrared (NIR) radiation, penetrating biological tissues efficiently without causing damage. By carefully tailoring their chemical composition, UCNPs can exhibit multicolor luminescence, making them highly versatile for bioimaging, photodynamic therapy, light-controlled chemotherapy, etc.

This study focuses on synthesizing and comprehensively characterizing core-shell-shell structured nanoparticles based on the $NaGdF_4$ matrix. The core of these UCNPs is doped with Tb^{3+} and Eu^{3+}, the inner shell –with Yb^{3+} and Tm^{3+}, and the outer shell –with Yb^{3+} and Nd^{3+} (see Fig. 1.). A key objective is to optimize the molar ratio of Tb^{3+} and Eu^{3+} in the core, as the $Tb^{3+} \rightarrow Eu^{3+}$ energy transfer directly influences the nature and intensity of luminescence in the green-to-red spectral range, which is critical for both diagnostic and therapeutic applications. By fine-tuning the chemical composition, these nanoparticles can be efficiently excited by ultraviolet and near-infrared radiation. The strategic selection of lanthanides ensures that the emission spectra span ultraviolet, visible, and near-infrared regions, highlighting the strong potential of these UCNPs for multifunctional theranostic applications.

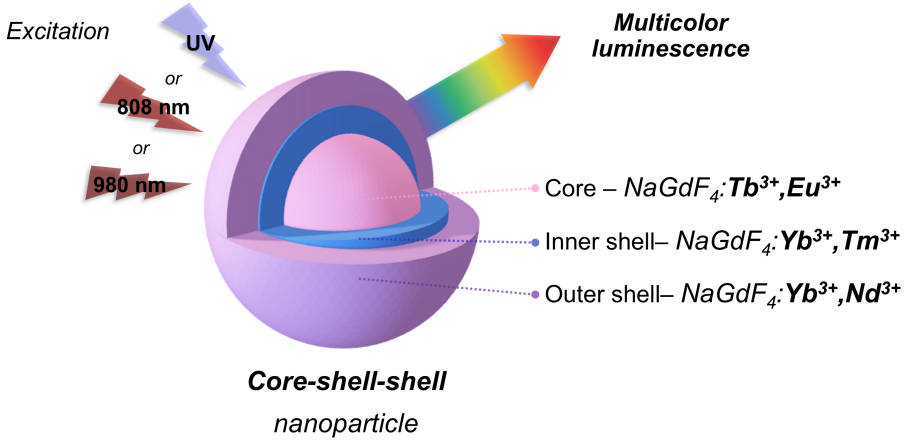


Fig. 1. Principal scheme of core-shell-shell nanoparticle.

This presentation will describe the synthesis and post-synthesis treatment of core-shell-shell structured UCNPs. Additionally, it will provide an in-depth analysis of their structural and optical properties, an evaluation of their optical and colloidal stability in aqueous and biological media, and their preliminary biocompatibility.

Acknowledgements
This project has received funding from the Research Council of Lithuania (LMTLT), agreement No [S-MIP-23-5].

PREPARATION AND FUNCTIONALIZATION OF GOLD NANORODS FOR BIOCONJUGATION APPLICATIONS

Tymofii Omelchenko[1], Marina Sapauskiene[1], Veronika Zahorodna[1], Oleksiy Gogotsi[1], Almira Ramanaviciene[1], Anton Popov[1]

[1]NanoTechnas - Center of Nanotechnology and Materials Science, Faculty of Chemistry and Geosciences, Vilnius University, Lithuania
tymofii.omelchenko@chgf.stud.vu.lt

Gold nanorods (AuNRs) are of great interest in research because of their unique optical and chemical properties in adjustable aspect ratios, and the ease of surface modification. They are particularly valuable in biosensing, bioimaging, and disease diagnosis and detection.[1] A critical challenge in their application is ensuring stable and efficient bioconjugation while preserving their structural integrity and functionality. Traditional functionalization methods often suffer from aggregation, poor biomolecule attachment, or loss of optical properties. A key challenge in their application is ensuring stable and efficient bioconjugation while maintaining structural integrity and functionality. Conventional functionalization methods often encounter issues such as aggregation, poor biomolecule attachment, and loss of optical properties.[2] This study aims to develop an optimized method for synthesizing and functionalizing AuNRs for further bioconjugation. AnNRs with varying aspect ratios were successfully synthesized through a seed-mediated growth method by adjusting the concentration of silver nitrate and systematically varying $AgNO_3$ concentrations. Moreover, the synthesis of AuNRs with a high aspect ratio was performed. These nanorods exhibited longitudinal surface plasmon resonance (LSPR) peaks in the 1000 1200 nm range. The increase in aspect ratio was observed through SEM and UV-Vis spectroscopy, showing a progressive elongation of the nanorods with controlled size distribution. The surface modification methods were applied to get AuNRs composites with MXenes and/or polymers. Fabricated materials were characterized using UV-Vis spectroscopy. The scanning electron microscopy (SEM) analysis was used to examine their morphology and size distribution. The findings indicate that optimizing surface functionalization can enhance the use of AuNRs in bioconjugation, making them more used for biomedical applications.

Acknowledgements

This project has received funding from the European Union's Horizon Europe Framework Programme under grant agreement No. 101131147.

[1] Meng, L., Zhang, J., Li, H., Zhao, W., & Zhao, T. (2019). Preparation and progress in application of gold nanorods. Journal of Nanomaterials, 2019, Article 4925702.

[2] Vedhanayagam, M., Andra, S., Muthalagu, M., & Sreeram, K. J. (2022). Influence of functionalized gold nanorods on the structure of cytochrome-C: An effective bio-nanoconjugate for biomedical applications. Inorganic Chemistry Communications, 146, 110182.

ELECTROCHEMICAL GLUCOSE BIOSENSORS BASED ON GOLD NANORODS

Marina Sapauskiene[1], Viktorija Lisyte[1], Almira Ramanaviciene[1], Anton Popov[1]

[1]NanoTechnas - Center of Nanotechnology and Materials Science, Institute of Chemistry, Faculty of Chemistry and Geosciences, Vilnius University, Naugarduko St. 24, LT-03225 Vilnius, Lithuania
marina.sidorova@chgf.stud.vu.lt

Gold nanorods (AuNRs) have attracted great interest in electrochemical biosensing due to their large surface area and excellent conductivity, which improve electron transfer and sensitivity in sensor applications. In this study, AuNRs were synthesised using two different methods to develop electrochemical glucose biosensors. The structural and morphological properties of AuNRs were analysed by scanning electron microscopy (SEM), while their optical properties were evaluated by UV-Vis spectroscopy. Electrochemical characterisation of the AuNR-modified electrodes was performed using cyclic voltammetry to determine the electroactive surface area, and chronoamperometric measurements were performed to evaluate the sensitivity of the sensor to glucose. Selectivity tests were performed to evaluate the response of the sensor in the presence of interfering substances.

The results showed that AuNR-modified electrodes exhibited improved sensitivity and selectivity in glucose detection. A clear correlation was observed between the properties of the synthesised AuNRs and the performance of the biosensor, highlighting the importance of material properties in sensor optimisation. These results contribute to the further development of AuNR-based electrochemical biosensors for accurate and reliable glucose monitoring, with potential applications in medical diagnostics and biotechnology.

NOVEL TITANIUM SUBOXIDE AND CORE-SHELL NANOSTRUCTURES FOR PHOTOCATALYTIC WASTEWATER TREATMENT

Aswathi Raveendran[1], Simonas Ramanavicius[1], Germante Paulikaite[2], Agne Sukoviene[3], Arunas Jagminas[4]

[1]Department of Electrochemical Material Science, State Research Institute Center for Physical Sciences and Technology (FTMC), Sauletekio av. 3, LT-10257 Vilnius, Lithuania
aswathi.raveendran@ftmc.lt

The contamination of water bodies with organic pollutants has become a pressing global environmental issue, posing severe risks to ecosystems and human health. Organic compounds, such as industrial dyes, pharmaceuticals, pesticides, and petrochemicals, are highly stable and resistant to conventional wastewater treatment methods, leading to their persistent accumulation in aquatic environments [1]. Among various remediation techniques, photocatalytic decomposition has emerged as a highly effective and environmentally friendly approach, utilizing semiconductor materials to harness solar energy and degrade organic pollutants into harmless byproducts. This method offers advantages such as complete mineralization of contaminants, low energy consumption, and the potential for large-scale applications.

Titanium suboxides (Ti_nnO_{2n-1}) have shown great promise due to their tunable bandgap, superior conductivity, and enhanced charge carrier dynamics, which improve photocatalytic efficiency under visible light illumination [2]. Recent studies from our group highlight that these materials demonstrate superior photocatalytic degradation of organic pollutants compared to traditional titanium dioxide (TiO_2) [3]. Additionally, core-shell nanostructures have emerged as an innovative strategy to further enhance photocatalytic performance. These structures, consisting of a photocatalytic core and a functional shell, offer improved charge separation, reduced recombination rates, and enhanced surface reactivity, leading to significantly higher pollutant degradation rates. By engineering core-shell architectures with synergistic material combinations, researchers have developed nanostructures that operate efficiently under visible light, making them highly attractive for wastewater treatment applications [4].

In this work, we explore the recent trends in the synthesis and design of titanium suboxides and core-shell nanostructures for photocatalytic wastewater treatment. We discuss their physicochemical properties, band structure engineering, and mechanisms that enhance photocatalytic activity. Our study demonstrates that both titanium suboxide materials and core-shell nanostructures exhibit significant potential for next-generation wastewater treatment technologies due to their improved charge transport, visible-light responsiveness, and superior degradation efficiency. These advancements pave the way for the development of highly efficient and sustainable photocatalytic systems for environmental remediation.

[1] A. Sukoviene, S. Ali, A. Jagminas, and S. Ramanavicius, "Magnetic Cobalt and Other Types of Ferrite Nanoparticles: Synthesis Aspects and Novel Strategies for Application in Wastewater Treatment (Review)," Applied Sciences, vol. 15, no. 2, p. 857, 2025.

[2] A. Jagminas, S. Ramanavičius, V. Jasulaitienė, and M. Šimėnas, "Hydrothermal synthesis and characterization of nanostructured titanium monoxide films," RSC Advances, vol. 9, no. 68, pp. 39877–39885, 2019.

[3] S. Ramanavicius and A. Jagminas, "Synthesis, Characterisation, and Applications of TiO and Other Black Titania Nanostructures Species (Review)," Crystals, vol. 14, no. 7, p. 647, 2024.

[4] T. Sabirovas, S. Ramanavicius, A. Naujokaitis, G. Niaura, and A. Jagminas, "Design and Characterization of Nanostructured Titanium Monoxide Films Decorated with Polyaniline Species," Coatings, vol. 12, no. 11, p. 1615, 2022.

SYNTHESIS AND CHARACTERIZATION OF NIOBIUM NANOPARTICLES: A COMPARATIVE STUDY OF TWO METHODS

MUHAMMAD USMAN KHALID[1], Wanessa De Melo[4], Monika Kirsnytė[2], Arunas Stirke[3]

[1]FTMC
[2]Vilnius University
wanessa.melo@ftmc.lt

Niobium-based nanoparticles have gained significant attention due to their unique physicochemical properties and potential applications in various fields. In this study, two different synthesis routes were employed to prepare niobium nanoparticles: (1) ammonium niobate(V) oxalate hydrate dissolved in distilled water, with pH adjusted to 7 and 9 using aqueous ammonia and precipitation induced by hydrogen peroxide, and (2) niobium pentoxide dissolved in hydrofluoric acid and deionized water, followed by pH tuning between 7 and 9. The synthesized nanoparticles were washed with distilled water and ethanol, dried at 100 °C for 2–3 hours, and calcined at 450 °C for 1–2 hours. A comparative characterization of the resulting samples was conducted using X-ray diffraction (XRD), Fourier-transform infrared spectroscopy (FTIR), scanning electron microscopy (SEM), transmission electron microscopy (TEM), energy-dispersive X-ray spectroscopy (EDX), and dynamic light scattering (DLS). The study aims to evaluate the influence of precursor selection, pH variation, and processing conditions on particle morphology, crystallinity, and elemental composition. The findings provide insights into the structural and chemical differences between the two synthesis routes, contributing to the optimization of niobium nanoparticle production for various technological applications.

RESISTIVITY AND LOW FREQUENCY NOISE OF HYBRID COMPOSITES WITH CARBON NANOTUBES AND CARBONIZED NICKEL

Frydrichas Mireckas[1], Sandra Pralgauskaitė[1], Jan Macutkevič[1]

[1] Institute of Applied Electrodynamics and Telecommunications, Faculty of Physics, Vilnius University, Lithuania
frydrichas.mireckas@ff.vu.lt

Carbon nanoparticle composites have garnered notable scientific and industrial interest due to a wide range of filler particle options and their corresponding electrical, thermal, and mechanical properties. However, agglomeration of filler particles remains a crucial technological consideration for the applicability of these materials, as it depends on the type and amount of fillers [1].

Low frequency noise measurement enables the investigation of electrical characteristics, as well as the quality of composite materials, since a greater presence of structural defects typically results in higher noise level [2]. For applications in electronics, $1/f$ noise is particularly significant due to the limit it imposes on the sensitivity and selectivity of electrical sensors [3].

Resistivity and low frequency (10 Hz – 20 kHz) noise characteristics of hybrid epoxy composites with multi-walled carbon nanotubes (MWCNTs) and carbonized nickel (Ni@C) were investigated at room temperature and in the temperature range of (75–365) K. Composites were prepared via dispersion of epoxy and different concentrations of MWCNTs (0, 0.09 vol.%) and Ni@C (0, 0.025, 0.2, 5, 15, 25, and 30 vol.%).

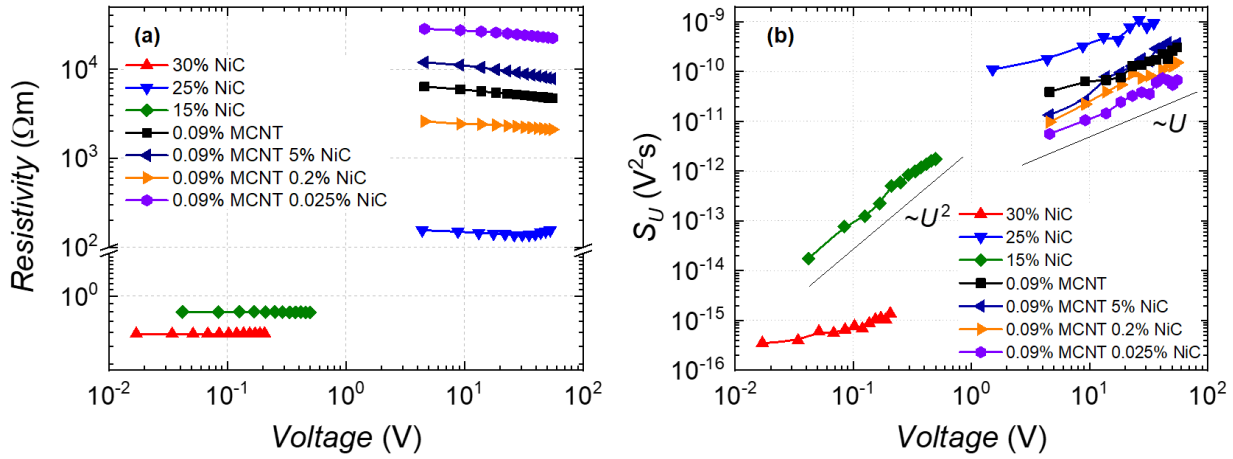


Fig. 1. (a) Resistivity dependence on voltage; (b) voltage noise spectral density dependence on voltage (room temperature, 86 Hz).

The resistivity of the composites is almost independent of voltage (Fig. 1a). Lowest resistivity is observed in composites with 30 vol.% and 15 vol.% Ni@C. In contrast, the 25 vol.% Ni@C composite resistivity is much higher than other single-filler composites. This could be due to increased agglomeration in this composite. The resistivity of hybrid MWCNT/Ni@C composites is generally determined by the MWCNT content and shows no clear dependence on Ni@C concentration.

Low frequency noise spectra are primarily of $1/f$ type. In the proportionality of voltage fluctuation spectral density to voltage $S_U \sim U^b$, exponent b is close to 1 for most of the studied composite samples. This is indicative of an increased contribution of tunneling processes to the conductivity in the composite (Fig. 1b).

[1] V. Choudhary et al., Carbon nanotubes and their composites (Syntheses and Applications of Carbon Nanotubes and Their Composites, IntechOpen, 2013)
[2] S. Pralgauskaitė et al., Resistivity and low-frequency noise characteristics of epoxy-carbon composites (Journal of Applied Physics, vol. 121(11), 2017
[3] A.A. Balandin, Low-frequency 1/f noise in graphene devices (Nature Nanotechnology, vol. 8(8), 2013)

PRODUCTION OF CELLULOSE-GRAPHENE OXIDE (CO-GO) NANOCOMPOSITES FOR THE EXTRACTION OF NANOPLASTICS FROM FRESH WATER

Mahrosh Javed[1], Galina Lujaniene[1], Sergej Semcuk[1], Vidas Pakstas[2], Ausra Selskiene[2], Algirdas Selskis[2], Kestutis Mazeika[3], Martynas Talaikis[4]

[1]Center for Physical Sciences and Technology, Department of Environmental Research Sauletekio av. 3, 10257 Vilnius, Lithuania
[2]Center for Physical Sciences and Technology, Department of Characterisation of Materials Structure Sauletekio av. 3, LT-10257 Vilnius, Lithuania
[3]Center for Physical Sciences and Technology, Department of Nuclear Research Savanorių ave. 231, LT-02300 Vilnius, Lithuania
[4]Center for Physical Sciences and Technology, Department of Organic Chemistry Sauletekio av. 3, 10257 Vilnius, Lithuania
mahrosh.javed@ftmc.lt

Water is a vital component of environment and an essential part of living beings, but the quality of water has been a problem for humans since the beginning of time. Pollution of water systems is mainly the result of industrialization, agriculture and domestic, transport and chemical activities in the environment [1-3]. As urbanization increased, so did the need for alternative, non-renewable resources for domestic and industrial applications, leading to the emergence of the polymer industry. However, the advantage of plastics in terms of easy accessibility, low prices and multiple applications in every household and in almost all walks of life also comes at the cost of overuse and improper disposal in the environment, which leads to the destruction of the polymer structure at the micro and nanoscale, resulting in the release of nanoplastics (NPs) in the environment. These plastic particles are detected in the environment [4] and in the cells of various living organisms [5], raising concerns about potential toxicity in living cells. Therefore, the development of novel materials that are ecologically safe to remove pollutants from freshwater is one of the most important and growing concerns of the 21st century. Various techniques are already used to remove pollutants from freshwater, but adsorption has proven to be a useful technique for water treatment with low cost and good efficacy. Cellulose (CO) is an inexpensive, biodegradable, abundant, non-toxic material that has a high adsorption capacity due to the hydroxyl groups (-OH) present on its surface that form adsorption sites. In addition, graphene oxide (GO), which has various functional groups such as hydroxyl, carbonyl, carboxyl, and epoxy groups, is a good adsorbent. In this study, a synthesized cellulose-graphene oxide (CO-GO) nanocomposite was used to remove polyethylene (PE) and polystyrene (PS) NPs prepared by nanoprecipitation. GO was prepared by a modified Hummer‘s method. The CO-GO nanocomposite was prepared by mixing cellulose and GO solutions with the addition of glutaraldehyde as a crosslinking agent. The PE-NPs and PS-NPs were prepared by separately dissolving polyethylene and polystyrene in trifluoroacetic acid. Both solutions were then mixed with polyvinyl alcohol and stirred continuously until the NPs had formed and stabilized. The solution was centrifuged to separate the NPs and dried. The CO-GO nanocomposite was used in adsorption experiments with PE-NPs and PS-NPs. TEM, SEM, FT-IR, Raman spectroscopy, and XRD methods were used to characterize the CO-GO nanocomposites. The characterization results show that the nanocomposites were synthesized and pretested for the adsorption of nanoplastics. TEM, SEM, FT-IR, Raman spectroscopy and XRD methods were used to estimate the changes that occurred during the adsorption process.

[1] Zaynab, M., et al., Journal of King Saud University-Science, 34(1): p. 101653 (2022).
[2] Faust, S.D. and O.M. Aly, Chemistry of water treatment: CRC press (2018).
[3] Hung, Y.-T., et al., MDPI. p. 330 (2021).
[4] Wibuloutai, J., et al., Water Supply, 23(6): p. 2267-2282 (2023).
[5] Rahman, A., et al., Science of the Total Environment, 757: p. 143872 (2021).

EFFECTS OF NANOSECOND PULSES DELIVERED AT ULTRA-HIGH FREQUENCY ON MITOCHONDRIAL DEPOLARIZATION, ROS, CELL PERMEABILIZATION AND CELL VIABILITY

Paulina Malakauskaitė[1,2], Vytautas Kašėta[3], Vitalij Novickij[1,2]

[1]State Research Institute Centre for Innovative Medicine, Department of Immunology and Bioelectrochemistry, Vilnius, Lithuania
[2]Vilnius Gediminas Technical University, Faculty of Electronics, Vilnius, Lithuania
[3]State Research Institute Centre for Innovative Medicine, Department of Stem Cell Biology, Vilnius, Lithuania
vitalij.novickij@imcentras.lt

It is theoretically predicted that ultrashort nanosecond pulses could be utilized to permeabilize intracellular membranes, including mitochondria [1]. Such a phenomenon would have high applicability in cancer treatment context and could be employed for shifting toward immunogenic cell death as well as induction of immune response [2]. However, currently there is a lack of experimental evidence on the interaction of pulsed electric fields with mitochondria and their function. In this study, for the first time, we characterize the effects of ultra-high repetition frequency (1–5 MHz) nanosecond pulses (6–18 kV/cm, 100 and 300 ns) in the context of mitochondrial depolarization (Tetramethylrhodamine, methyl ester (TMRM)), ROS generation (MitoSOX), cell plasma membrane permeabilization (YO-PRO-1) and cell viability. As a reference, standard microsecond range parametric protocols were used (100 µs × 8 pulses). Our pilot data indicate that depending on the pulse repetition frequency, the efficiency of electroporation can be modulated, i.e., the higher is the frequency, the higher is the permeabilization. Also, the oxidation level has a dose-dependent scaling with pulse burst amplitude, while 100 ns pulses induce significantly lower oxidation than 300 ns pulses. In the context of TMRM fluorescence, our data indicate that treatment of cells with pulsed electric fields induces mitochondrial depolarization, however, the selectivity of the phenomenon is questionable and requires further research. Importantly, the results of our study show that boosting the pulse repetition frequency towards 5 MHz significantly improves the effects of 100 ns pulses, i.e., the protocols cause effective electroporation even in fields, which are considered sub-threshold for this pulse duration range. Therefore, derivation of new and more effective protocols for electroporation-based procedures can be performed without the increase of the energy input.

[1] [1] T. Kotnik, G. Pucihar, M. Reberšek, D. Miklavčič, L.M. Mir, Role of pulse shape in cell membrane electropermeabilization, Biochimica et Biophysica Acta (BBA)-Biomembranes 1614 (2003) 193–200.
[2] [2] S.J. Beebe, N.M. Sain, W. Ren, Induction of cell death mechanisms and apoptosis by nanosecond pulsed electric fields (nsPEFs), Cells 2 (2013) 136–162.

STUDIES OF THE SPATIAL STRUCTURE OF $TPPS_4$ AGGREGATES USING ATOMIC FORCE MICROSCOPY

Teresė Kreišmontaitė[1,2], Greta Tamoliūnaitė[1], Vilius Poderys[1], Ričardas Rotomskis[1,2]

[1]Biomedical Physics Laboratory, National Cancer Institute P. Baublio St. 3b, LT-08406 Vilnius, Lithuania
[2]Biophotonics Group of Laser Research Centre, Vilnius University Sauletekio Ave. 9, LT-10222 Vilnius, Lithuania
terese.kreismontaite@stud.ff.vu.lt

The adsorption of molecules or nanostructures on solid surfaces is one of the fundamental processes for the development of molecular-based nanodevices. Atomic force microscopy (AFM) is a microscopic technique with extremely high lateral resolution for surface imaging. AFM imaging technique was used to reveal $TPPS_4$ aggregate geometric structures, ranging from roughly spherical to highly irregular structures with dimensions in the nanometer scale.

Here we focused our investigation on the adsorption of the $TPPS_4$ aggregates deposited onto hydrophilic mica substrate. 5,10,15,20-Tetrakis(4-sulfonatophenyl) porphyrin ($TPPS_4$) solutions, containing aggregates, were deposited onto mica substrates, dried and/or spin-coated, and then imaged using AFM.

Images of the aggregates deposited on mica substrate are presented in Figure 1> $TPPS_4$ aggregates consisting of individual rods and bundles of rods (A - pH=3) and complex layers (B - pH=7) are seen in the image. The single aggregate rods have a remarkably uniform height, and roads appear to be the basis buildings blocks for longer bundled aggregates [1].

Our prior spectroscopic and AFM investigations [2] showed different aggregation patterns are observed when samples are prepared using $TPPS_4$ solutions of different pH values.

Studies on the spatial properties of $TPPS_4$ aggregates formed in solutions allowed us to visualize result of aggregation processes in different pH environments. Interestingly the formation of aggregates in neutral media was observed in spectral measurements but was not observed by AFM. Such structures offer significant potential for the development and fabrication of diverse nanoscale optoelectronic devices.

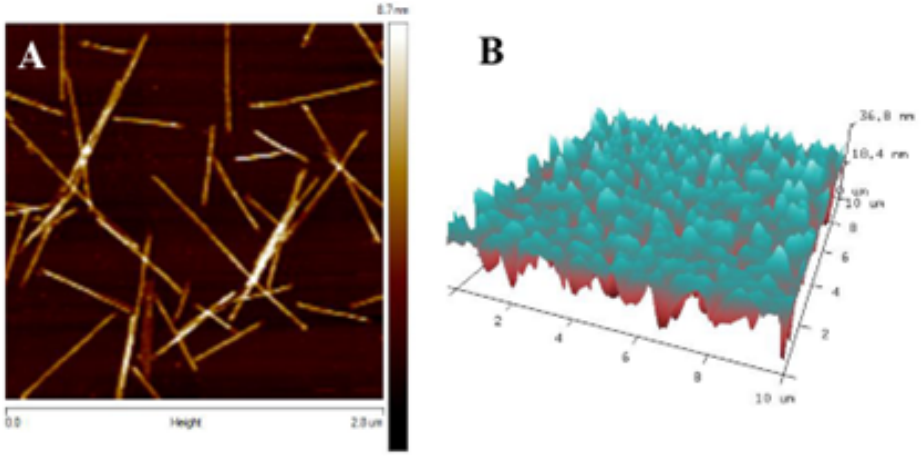


Fig. 1. A - AFM image of $TPPS_4$ aggregates deposited on mica (sample prepared using $TPPS_4$ c=5e-4 mol/l, pH=3 aqueous solution); B - AFM image of $TPPS_4$ aggregates deposited on mica (sample prepared using $TPPS_4$ c=6e-3 mol/l, pH=7 aqueous solution).

[1] A.D. Schwab, D.E. Smith, C.S. Rich, E.R. Young, W.F. Smith, J.C. de Paula, Porphyrin nanorods., J. Phys. Chem. B. 107, 11339-11345, (2003).
[2] G. Tamoliūnaitė, V. Poderys, R. Rotomskis, Spectral and Spatial Characteristics of TPPS4 Aggregates [Conference presentation]., IEEE-NAP 2024, Riga, Latvia, (2024, September 8-12).

CHLOROPHYLLIN-CHITOSAN COMPLEX STOICHIOMETRY ANALYSIS FOR ANTIMICROBIAL PHOTODYNAMIC INACTIVATION

Gabrielė Vasiliauskaitė[1], Irina Buchovec[1]

[1] Institute of Photonics and Nanotechnology, Faculty of Physics, Vilnius University, Saulėtekio av. 3, Vilnius, Lithuania
gabriele.vasiliauskaite@ff.vu.lt

Antimicrobial photodynamic inactivation (API) is a promising approach for combating drug- and pesticides-resistant pathogens, by generating reactive oxygen species (ROS) using photosensitizer (PS), light and molecular oxygen [1]. Chlorophyllin (Chl) is a water-soluble chlorophyll derivative, that exhibits photosensitizing properties, however, its anionic nature limits efficient penetration into bacterial cells, preventing intracellular ROS production. Non-toxic, natural, and cationic Chitosan (CHS) overcomes this limitation by enhancing cellular uptake due to its positive charge and intrinsic antimicrobial properties [2]. This study aims to investigate the molecular interaction dynamics and binding ratio between magnesium (Mg) Chl, copper (Cu) Chl, and chitosan (CHS) using Job plot analysis. Understanding the stoichiometry of these complexes (Fig.1) will provide insights into their self-assembly, stability, and potential aggregation, which are crucial factors directly affecting their antimicrobial photodynamic efficiency.

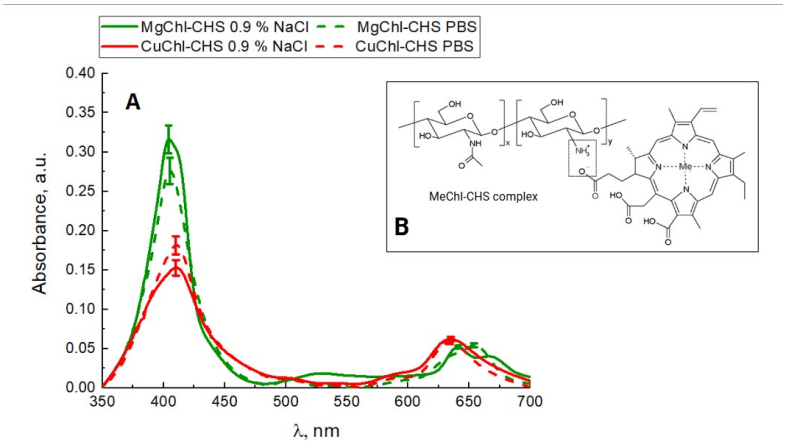


Fig. 1. A) Absorbtion spectra of 0.001 % MgChl- 0.1% CHS and 0.001 % CuChl- 0.1% CHS in 0.9 % NaCl and PBS solutions when molar fraction ratio is 7.4:2.6 and 7.1:2.9 respectively and B) Chl-CHS complex formula. *Me – metal (Mg/Cu).

First, 0.05 % (w/v) Chl and 1.25 % (w/v) CHS stock solutions were prepared for Job plot analysis. These solutions were diluted using 0.9 % NaCl and phosphate buffered saline (PBS) solution to create 1 % (w/v) CHS and 0.01 % (w/v) Chl stock solutions. In the Job plot analysis, the total concentration of the complex was kept constant while varying the molar fraction of Chl (χ_{Chl}). Job plot analysis was used to determine the Chl-CHS binding ratio by measuring absorbance changes at $\sim$ 404 nm across varying χ_{Chl}. The molar fraction χ_{Chl} was calculated using Equation (1):

$$\chi_{Chl} = \frac{n(Chl)}{n(Chl)+n(CHS)} \quad (1)$$

The Job plot analysis of CuChl-CHS and MgChl-CHS complexes revealed that both complexes have the highest absorbance shift at χ_{Chl} 0.9 which indicate a 9:1 Chl:CHS binding ratio in both 0.9% NaCl and PBS solutions suggesting that complexes at this ratio have the most stable bond. However, the high binding ratio observed (9:1) may suggest the possibility of aggregation, cooperative binding, or the presence of multi-binding site systems that can influence API efficiency.

For further investigation, it is important to examine how the binding ratio influences ROS production, which in turn influences API efficiency.

[1] Hamblin, M.R. Antimicrobial photodynamic inactivation: A bright new technique to kill resistant microbes (Current Opinion in Microbiology, 2016)

[2] I. Buchovec, et al. Effective photosensitization-based inactivation of Gram (–) food pathogens and molds using the chlorophyllin–chitosan complex: towards photoactive edible coatings to preserve strawberries (Photochemical and Photobiological Sciences, 2016)

EVALUATING PHOTOPHYSICAL PROPERTIES OF RIBOFLAVIN, MAGNESIUM CHLOROPHYLLIN AND THEIR MIXTURE IN SOLUTION

Urtė Mitrofanaitė[1], Irina Buchovec[2]

[1]Institute of Biosciences, Life Sciences Center, Vilnius University, Saulėtekis ave. 7, LT-10257, Vilnius, Lithuania.
[2]Institute of Photonics and Nanotechnology, Faculty of Physics, Vilnius University.
urte.mitrofanaite@gmc.stud.vu.lt

Foodborne pathogens pose a significant risk to public health, and the growing concern over antibiotic-resistant bacteria necessitates the development of alternative food safety strategies. Antimicrobial photodynamic inactivation (API) is a promising alternative to chemical disinfectants that is less likely to induce resistance. API relies on three components: a photosensitizer (PS), molecular oxygen, and light at a specific PS absorption wavelength [1]. Upon photoexcitation, the PS can undergo either a Type I or Type II reaction (Fig.1), generating reactive oxygen species (ROS) that induce microbial inactivation. API effectiveness depends on PS properties such as absorption, aggregation, and stability [2]. This study aims to analyze and compare the photophysical properties of natural PSs – magnesium chlorophyllin (MgChl), riboflavin (RF), and their mixture (RF/MgChl) in solution – to optimize API performance.

To evaluate the photophysical properties of RF/MgChl, separate stock solutions (0.15 mM) of RF and Mg-Chl were prepared in distilled water. RF was dissolved under continuous stirring at 50°C for 3 hours to ensure complete solubilization and stability, whereas MgChl was stirred only 5 minutes at room temperature. For the RF/MgChl mixture, appropriate volumes of RF and MgChl stock solutions were combined and diluted in phosphate-buffered saline (PBS) to obtain final working concentrations of 0.0075 mM, 0.015 mM, 0.03 mM.

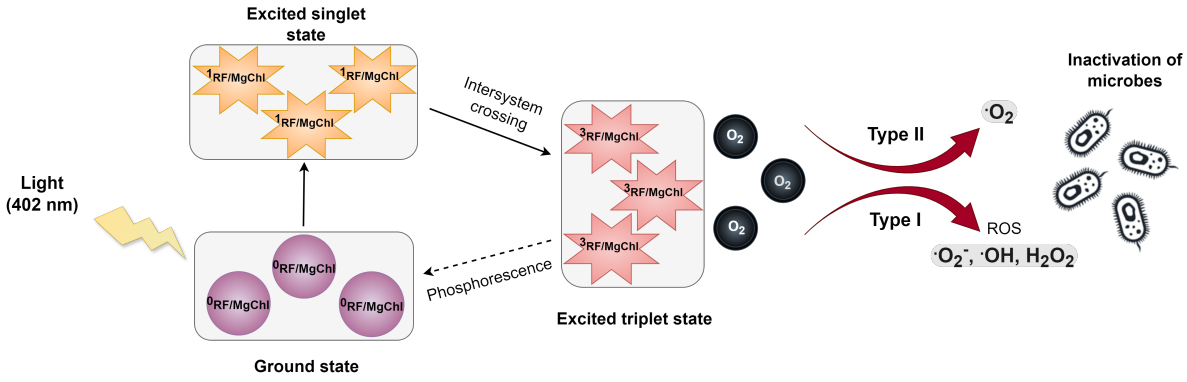


Fig. 1. Model illustrating API using a mixture of RF and MgChl (RF/MgChl) for increased ROS production, leading to enhanced inactivation of microbes.

Spectrophotometric measurements were conducted to determine the absorption wavelengths of separate PS solutions and their mixture. Additionally, particle size distribution was analyzed to assess solution stability, as PS aggregation can impact API efficiency. Triton X-100, a known aggregate-disrupting agent, was used to the extent of PS aggregation and its effect on photophysical properties.

Spectrophotometric analysis showed that MgChl and RF exhibit distinct absorption maxima within the visible-light spectra: 402nm (MgChl) and 440nm (RF). Particle size distribution measurements revealed that MgChl solutions contain larger aggregates (300-5560 nm), whereas RF particles remain below 400 nm. The RF/MgChl mixture displayed intermediate properties, indicating potential aggregation interactions between the two PS. The larger MgChl aggregates suggest a potential reduction in photoactivity and ROS generation, which may influence API efficiency.

Further research will focus on fluorescence and photostability studies to determine the long-term effectiveness of RF, MgChl, and RF/Mg-Chl in API applications. Investigating light-induced degradation and ROS generation efficiency will provide deeper insights into optimizing PS mixtures for enhanced API performance.

[1] Buchovec, I., et al., (2022). Inactivation of opportunistic pathogens Acinetobacter baumannii and Stenotrophomonas maltophilia by antimicrobial photodynamic therapy. Microorganisms, 10(3), 506.
[2] Buchovec, I., et al., (2022). Application of antimicrobial photodynamic therapy for inactivation of Acinetobacter baumannii biofilms. International Journal of Molecular Sciences, 24(1), 722.

PROTONATION DYNAMICS OF TPPS CORE: IMPACT OF THE NUMBER OF SULFONATE SUBSTITUENTS

Skaistė Talanovaitė[1], Vilius Poderys[1], Ričardas Rotomskis[1,2]

[1]Biomedical Physics Laboratory of National Cancer Institute, Baublio 3B, LT-08406, Vilnius, Lithuania
[2]Biophotonics Group of Laser Research Centre, Vilnius University, Saulėtekio 9, c.3, LT-10222, Vilnius, Lithuania
skaiste.talanovaite@gmc.stud.vu.lt

Supramolecular organization of π-conjugated molecules is an attractive way to create functional materials by amplifying the effects of the inherent molecular functionality. Among various π-conjugated molecules TPPS are especially interesting because they have characteristic bands in the visible region, making their supramolecular polymers fascinating candidates for practical electro-optical materials. Over the years, many porphyrin-based supramolecular materials have been created by tuning structures of their building blocks (monomers), especially by varying the peripheral groups attached to the porphyrin core. The number of peripheral SO_3^- groups influences properties of TPPS molecules that can change their practical applications [1]. Here we report differences in protonation process of the porphyrin centre that is affected by number of SO_3^- groups in TPPS molecules– 5,10,15,20-tetrakis(4-sulfonatophenyl)porphyrin ($TPPS_4$), 5,10,15-tris(4-sulfonatophenyl)-20-phenylporphyrin ($TPPS_3$) and 5,10-bis(4-sulfonatophenyl)-15,20-diphenylporphyrin ($TPPS_{2a}$).

In this study absorbance spectra of $TPPS_4$, $TPPS_3$, $TPPS_{2a}$ was continuously measured during titration with hydrochloric acid and sodium hydroxide. Bi-directional titration experiments were performed: from pH=3 to pH=7 (using NaOH) and from pH=7 to pH=3 (using HCl). Changes of absorbance intensity of 434 nm Soret band upon titration was used for determination of pK_a values. Upon acidic titration Soret band shifts from 414 nm (not protonated form) to 434 nm (protonated form). Middle point of this change indicates pK_a value– pH at which concentrations of free base and protonated forms are identical. We determined following pK_a values: pK_a=4.9 for $TPPS_4$, pK_a=4.8 for $TPPS_3$ and pK_a=4 for $TPPS_{2a}$. This difference of pK_a is likely caused by different net charge and different charge distribution of $TPPS_4$, $TPPS_3$ and $TPPS_{2a}$. $TPPS_4$ acquires biggest net charge (-4) which is created by four SO_3^- groups. Bigger negative net charge at the periphery of molecule might cause electron density redistribution and lead to more favourable conditions for protonation of the porphin core.

The acquired results indicate that higher number of peripheral SO_3^- groups favours protonation of the core of TPPS at higher pH value, at lower H^+ concentrations. This also leads to formation of supramolecular TPPS assemblies at higher pH values via ionic interaction between protonated porphyrin core with negatively charged SO_3^-.

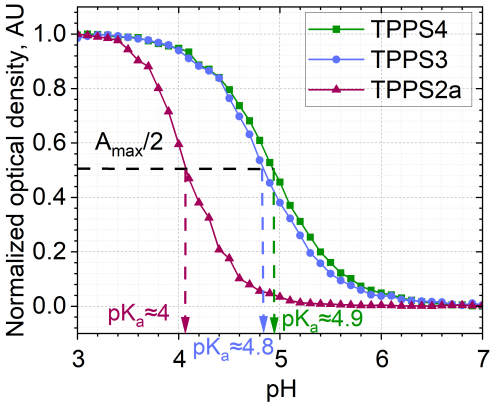


Fig. 1. Dependence of Soret band (434 nm diprotonated form) optical density on pH in $TPPS_4$, $TPPS_3$ and $TPPS_{2a}$ solutions and determination of pK_a values ($c=10^{-6}$ M, l=5 cm).

[1] V. Poderys, A. Selskis, R. Rotomskis, "The polar sulfonic groups influence on structure of self-assembled tetrapyrrolic molecules," vol. 97-98, pp. 221-224, 2004.

SPECTROSCOPIC STUDY OF OXIDATIVE STRESS IN GREEN MACROALGA NITELLOPSIS OBTUSA

Aušrinė Navickaitė[1], Viltė Mickytė[1], Vilmantas Pupkis[1], Saulius Bagdonas[2], Vilma Kisnierienė[1]

[1]Department of Neurobiology and Biophysics, Life Sciences Center, Vilnius University, Lithuania
[2]Laser Research Center, Faculty of Physics, Vilnius University, Lithuania
ausrine.navickaite@gmc.stud.vu.lt

Due to an increasingly changing environment, plants are constantly exposed to adverse environmental conditions that can impair photosynthesis and lead to the overproduction of reactive oxygen species (ROS). This complex phenomenon is known as oxidative stress and can cause significant damage to cellular structures, including chloroplasts, thereby affecting plant growth and development [1]. Implementing early non-invasive detection techniques could assist in the development of innovative strategies to mitigate the effects of adverse environmental conditions and enhance plant resilience.

The effect of ROS was evaluated at the single cell level, employing internodal cells of green macroalga *Nitellopsis obtusa*. Microscopic images were taken to visualize the possible damage of externally applied H_2O_2 (250 µM and 500 µM) on the chlorophyll layer of algal cells after 24 h incubation. In addition, changes in the concentrations of carotenoids and chlorophylls in cell extracts were evaluated via absorption spectroscopy. Photosynthetic processes of intact algal cells after 6 h incubation in H_2O_2 were monitored via pulse-amplitude-modulated (PAM) fluorometry, using blue LED light (445 nm) for excitation.

Microscopic images showed that H_2O_2 damaged the chloroplast layers of algal cells after prolonged exposure (24 h) (Fig. 1). Spectroscopic analysis revealed that H_2O_2 at a concentration of 500 µM caused a reduction in chlorophyll content over 24 h, while both applied concentrations (250 µM and 500 µM) resulted in a significant decrease in carotenoid concentration ($p < 0.05$, Kruskal–Wallis test). Fluorometry showed that the quantum yield of PSII (Y(II)), a measure of photosynthetic efficiency, was lower in both groups studied compared to the values registered in control cells ($p < 0.05$, Kruskal–Wallis test).

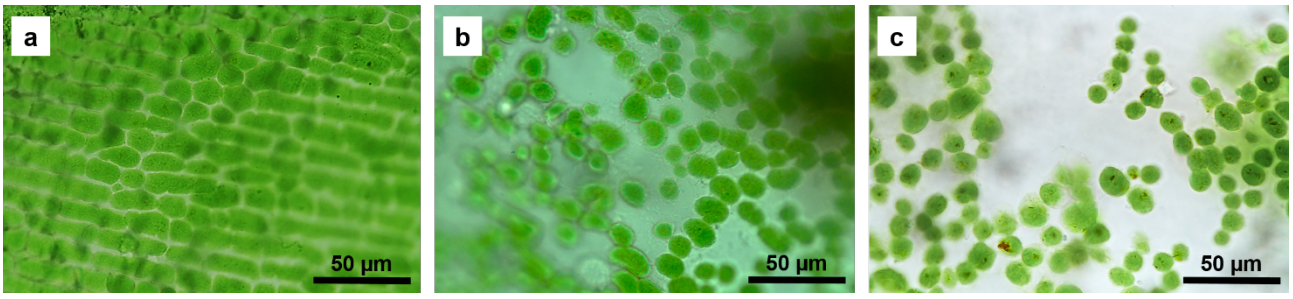


Fig. 1. Microscopic images (40x) of the chloroplast layers of different *Nitellopsis obtusa* cells before (a) and after exposure to 250 µM (b) or 500 µM (c) H_2O_2 for 24 h

The study conducted shows that H_2O_2 (250 µM and 500 µM) causes oxidative stress in algal cells, as indicated by a decrease in carotenoid concentrations, which have antioxidant properties [2]. The effects studied were detected in viable cells using non-invasive techniques, suggesting that the applied methods may be applicable for early detection of physiological stress in plants or for detection of lower, environmentally relevant concentrations of ROS.

[1] Møller, I. M., Jensen, P. E., Hansson, A. (2007) Oxidative modifications to cellular components in plants. Annu Rev Plant Biol, 58, 459-81
[2] Stahl, W., & Sies, H. (2003). Antioxidant activity of carotenoids. Mol Aspects Med, 24(6), 345–351.

RIBOFLAVIN-BASED PHOTODYNAMIC INACTIVATION FOR CONTROLLING THE PLANT PATHOGEN PSEUDOMONAS SYRINGAE

Fausta Guzauskaite[1], Irina Buhovec[2]

[1]Institute of Biosciences, Life Science Center, Vilnius University, Sauletekis Ave. 7, LT-10257, Vilnius, Lithuania
[2]Insitutute of Photonics and Nanotechnology, Faculty of Physics, Vilnius University, Sauletekis Ave. 3, LT-10257, Vilnius, Lithuania
fausta.guzauskaite@gmc.stud.vu.lt

Pseudomonas syringae is a plant pathogen that infects a wide range of crops, including tomatoes, wheat, beans, peas, beetroot, and apples, leading to significant agricultural losses. The global demand for food is projected to increase by 61% by 2050. Traditional plant protection methods, such as chemical and biological treatments, face limitations, including pathogen resistance and environmental concerns. Therefore, there is an urgent need for ecologically friendly and effective alternatives [1]. Antimicrobial photodynamic inactivation (API) is a promising approach that relies on a photosensitizer (PS), light, and molecular oxygen to generate reactive oxygen species (ROS), which induces oxidative damage and microbial inactivation [2]. The choice of PS plays a crucial role in determining API effectiveness, as different compounds vary in their absorption properties, ROS generation efficiency, and antimicrobial activity. Among natural PS, riboflavin (RF), a naturally occurring vitamin B_2, has shown potential for API applications. Upon light activation, RF produces ROS capable of inactivating microbial cells [3].

This study investigates the potential of RF-based API (RF-API) as a novel approach for controlling *P. syringae*. To assess its effectiveness, *P. syringae* cultures were exposed to varying RF concentrations and different irradiation doses. Bacterial viability was evaluated using colony-forming unit (CFU) counting and spectrophotometric measurements of metabolic activity. Additionally, the study examined how the preincubation period, defined as the time bacterial cells were incubated at 28 °C in the dark before irradiation, influences RF-API effectiveness.

This study aims to determine the optimal RF concentration and irradiation dose required for effective *P. syringae* inactivation. Moreover, the impact of preincubation conditions on API efficiency was investigated, providing insights into how pre-treatment conditions influence bacterial susceptibility. These are the first studies to examine the susceptibility of *P. syringae* to RF-API, contributing to the advancement of photodynamic antimicrobial strategies in plant pathogen control. The findings will provide insights into the feasibility of RF-API as a sustainable alternative for agricultural applications. The results and their implications will be presented in the poster session.

Keywords: *Pseudomonas syringae*, Antimicrobial Photodynamic Inactivation (API), riboflavin, plant pathogen

[1] R. Sands, „Patterns of Global Food Consumption Exprected to Shoft in Next Quarter Century as Population, Incomes Rise,“ USDA, 2024.
[2] A. G. L. K. a. P. V. Irina Buchovec, „Antimicrobial Photoinactivation Approach Based on Natural Agents for Control of Bacteria Biofilms in Spacecraft,“ Intenrational Jourlan of Molecular Sciences, 2020.
[3] V. K. C. P. P. C. W. F. L. C. W. L. R. B. S. K. C. T. Y. L. Nuratiqah Farah, „Riboflavin as a promising antimicrobial agent?,“ ScienceDirect, 2022.

INFLUENCE OF THE PGLX PROTEIN MUTATIONS ON THE BREX PROTECTION

Justė Adomaitytė[1], Tomas Šinkūnas[1]

[1]Department of Protein – DNA Interactions, Institute of Biotechnology, Life Sciences Center, Vilnius
juste.adomaityte@gmc.stud.vu.lt

The ongoing co-evolution and co-adaptation of bacteria and bacteriophages has led to the development of antiviral defense systems that are encoded in regions of the bacterial genome called defense islands [1]. One of the bacterial antiviral defense systems is BREX (Bacteriophage Exclusion). It is present in about 10 % of prokaryotic genomes. This system inhibits bacteriophage replication by an unknown mechanism of action [2].

Type 1 BREX system consists of a cassette of 6 protein-coding genes: *brxA, brxB, brxC, pglZ, brxL, pglX*. The *pglX* gene encodes the m6A DNA methyltransferase, which methylates specific sequences in the host genome to distinguish itself from foreign DNA [2]. Bacteriophages can evade BREX protection by encoding protein inhibitors. The Ocr protein encoded by the T7 bacteriophage binds specifically to the PglX protein in a way that mimics the double-stranded helix of DNA and blocks BREX protection [3]. In this study, we analyse the influence of PglX mutations on BREX activity and its inhibition.

[1] K. S. Makarova, Y. I. Wolf, S. Snir, and E. V. Koonin, “Defense islands in bacterial and archaeal genomes and prediction of novel defense systems,” J Bacteriol, vol. 193, no. 21, pp. 6039–6056, Nov. 2011

[2] T. Goldfarb et al., “BREX is a novel phage resistance system widespread in microbial genomes,” EMBO J, vol. 34, no. 2, pp. 169–183, Jan. 2015

[3] A. Isaev et al., “Phage T7 DNA mimic protein Ocr is a potent inhibitor of BREX defence,” Nucleic Acids Res, vol. 48, no. 10, pp. 5397–5406, Jun. 2020

NATURAL COLORANTS FROM BEETROOT WASTE

Indrė Bernatavičiūtė[1], Rūta Gruškienė[1], Jolanta Sereikaitė[1]

[1]Department of Chemistry and Bioengineering, Vilnius Gediminas Technical University, Vilnius, Lithuania
indre.bernataviciute@stud.vilniustech.lt

In the industrial sector, vegetable residual materials have received attention in the production of bio-colorants. Betalain pigments extracted from red beetroots Beta vulgaris provide a natural alternative to synthetic red dyes. These pigments have been successfully used in commercial food coloring primarily due to their natural and non-toxic properties, rich color, and hydrophilic properties [1]. Second of all, medically, they have antiviral, antimicrobial, and antioxidant properties and have many health benefits such as maintaining good blood pressure, better athletic performance abilities, digestive health, brain function, anti-inflammation, and even anti-cancer properties. Betalains are derivatives of betalamic acid and can be classified into two groups: red-violet betacyanins and yellow betaxanthins [2].

Betalains are hydrophilic compounds that accumulate, mainly in the vacuoles of the epidermal tissues of plants that synthesize these pigments. Extracting them from cell vacuoles requires optimal extraction methods to get as much product as possible. These natural pigments are usually obtained from plants by using certain solvents or mechanical extraction methods. When plant tissues are exposed to those solvents – it helps to facilitate the diffusion of pigments into the extraction solution. Mechanical disintegration of tissues involves the destruction of cell wall material and other cellular components to release the desired product [3].

The aim of this work was to optimize betalain extraction conditions from Cylindra beetroot waste. First, beetroot pomace was obtained from cleanly washed beets and freeze-dried. After that, the obtained powder was dispersed in different solvents with various ratios, using several methods and dissolution times. Six solvents were used (water, 20%, 50%, 80% ethanol, and 0.44% or 0.88% ascorbic acid), which were mixed with lyophilized beetroot powder in two ratios - 1:20 and 1:50. In addition, three types of extraction methods were performed: 1) vertical rotation that was carried out for 30, 60, and 120 minutes at 60 rpm speed, 2) ultrasonic disintegration performed for 10 and 20 minutes and 3) homogenization at different speed range – 10000 or 16000 rpm for 1 and 2 minutes.

The best results were obtained performing vertical rotation for 1 hour with two solvents – 0,88% ascorbic acid and 20% ethanol at 1:20 ratio. These extraction conditions helped to obtain the best betalain yield.

[1] Attia G., Moussa M., Sheashea E. Characterization of red pigment extracted from red beet (Beta Vulgaris L.) and its potential uses as antioxidant and natural food colorants. Egyptian Journal of Agricultural Research, 2013, 91(3): 1095-1110.

[2] Masih, D., Singh, N., & Singh, A. Red beetroot : A source of natural colourant and antioxidants : A review.Journal of Pharmacognosy and Phytochemistry, 8(4): 162-166.

[3] Castro-Enríquez D.D., Montaño-Leyva B., Del Toro-Sánchez C.L., Juaréz-Onofre J.E., Carvajal-Millan E., Burruel-Ibarra S.E., Tapia-Hernández J.A., Barreras-Urbina C.G., Rodríguez-Félix F. Stabilization of betalains by encapsulation: A review. The Journal of Food Science and Technology, 57(5):1587-1600.

APPLICATION OF MFC IN AGRICULTURAL SAMPLES USING E.MELILOTI

Agnė Boguševičė[1], Tomas Mockaitis[1], Inga Morkvėnaitė-Vilkončienė[1]

[1]Center for Physical Sciences and Technology, Department of Nanotechology Saulėtekio av. 3, LT-10257 Vilnius, Lithuania
agne.bogusevice@ftmc.lt

Microbial fuel cells (MFCs) have emerged as a promising bioelectrochemical technology for sustainable energy generation and environmental protection. By utilizing electrochemically active microorganisms, MFCs convert organic matter, including biomass and waste, into electricity [1]. Additionally, certain organic pollutants can serve as electron donors or acceptors, enabling simultaneous energy production and pollutant removal. While oxygen is commonly used as an electron acceptor due to its high oxidation potential and availability, ongoing research explores alternative acceptors to enhance system efficiency [2]. As the global shift toward renewable energy becomes imperative due to the environmental impact of fossil fuels, MFCs offer a dual benefit of clean energy generation and waste treatment. This technology holds significant potential for addressing energy demands while contributing to a more sustainable future [3].

The symbiosis between *E. meliloti* and legumes enables nitrogen fixation, initiated by plant-released betaines and flavonoids that attract the bacteria to root hairs. *E. meliloti* secretes nod factors, forming infection threads and bacteroids in root nodules [4]. Nitrogen fixation occurs only in the endosymbiotic state, with leghemoglobin regulating oxygen for nitrogenase activity [5].

This study explores the application of *E. meliloti* in MFCs and examines charge transfer mechanisms between bacteria and electrodes in real agricultural samples. The process is enhanced by various quinone mediators acting as lipophilic redox mediators, aiming to improve electron transfer efficiency and overall MFC performance.

[1] Ramanavicius, S.; Ramanavicius, A. Charge Transfer and Biocompatibility Aspects in Conducting Polymer-Based Enzymatic Biosensors and Biofuel Cells. Nanomaterials 2021, 11, 1–22. https://doi.org/10.3390/nano11020371

[2] Reinikovaite, V.; Zukauskas, S.; Zalneravicius, R.; Ratautaite, V.; Ramanavicius, S.; Bucinskas, V.; Vilkiene, M.; Ramanavicius, A.; Samukaite-Bubniene, U. Assessment of Rhizobium anhuiense Bacteria as a Potential Biocatalyst for Microbial Biofuel Cell Design. Biosensors 2023, 13, 66. https://doi.org/10.3390/bios13010066

[3] Rozene, J.; Morkvenaite-Vilkonciene, I.; Bruzaite, I.; Dzedzickis, A.; Ramanavicius, A. Yeast-based microbial biofuel cell me-diated by 9,10-phenantrenequinone. Electrochim Acta 2021, 373, doi: 10.1016/j.electacta.2021.137918

[4] Bendinskaite, S., Bruzaite, I., Rožėnė, J., Mockaitis, T., Morkvenaite-Vilkonciene, I., Ramanaviciene, A., Zinovicius, A., & Ramanavicius, A. (2024). Microbial Fuel Cell Based on Ensifer meliloti. Journal of the Electrochemical Society, 171(10) https://doi.org/10.1149/1945-7111/ad8037

[5] Nyangau EO, Abe H, Nakayasu Y, Umetsu M, Watanabe M, Tada C. Iron azaphthalocyanine electrocatalysts for enhancing oxygen reduction reactions under neutral conditions and power density in microbial fuel cells. Bioresour Technol Rep 2023, https://doi.org/10.1016/j.biteb.2023.101565

INTEGRATING ARTIFICIAL INTELLIGENCE, MOLECULAR DYNAMICS, AND DFT TO INVESTIGATE MONOAMINE OXIDASE INHIBITION

Augustas Markevičius[1], Gintautas Bagdžiūnas[2]

[1]Group of Supramolecular Analysis and Bioelectronics, Institute of Biochemistry at Life Sciences Centre, Vilnius University, Saulėtekio av. 7, LT-10257, Vilnius, Lithuania
augustas.markevicius@chgf.stud.vu.lt

Monoamine neurotransmitters, including catecholamines and indoles, are metabolized by monoamine oxidase (MAO), an enzyme existing in two isoforms: MAO-A and MAO-B. These isoforms exhibit distinct substrate specificities and tissue distribution. [1], [2] MAO inhibitors are widely prescribed as antidepressants for major depressive disorder, schizophrenia, and other neurological and psychiatric conditions. [3]

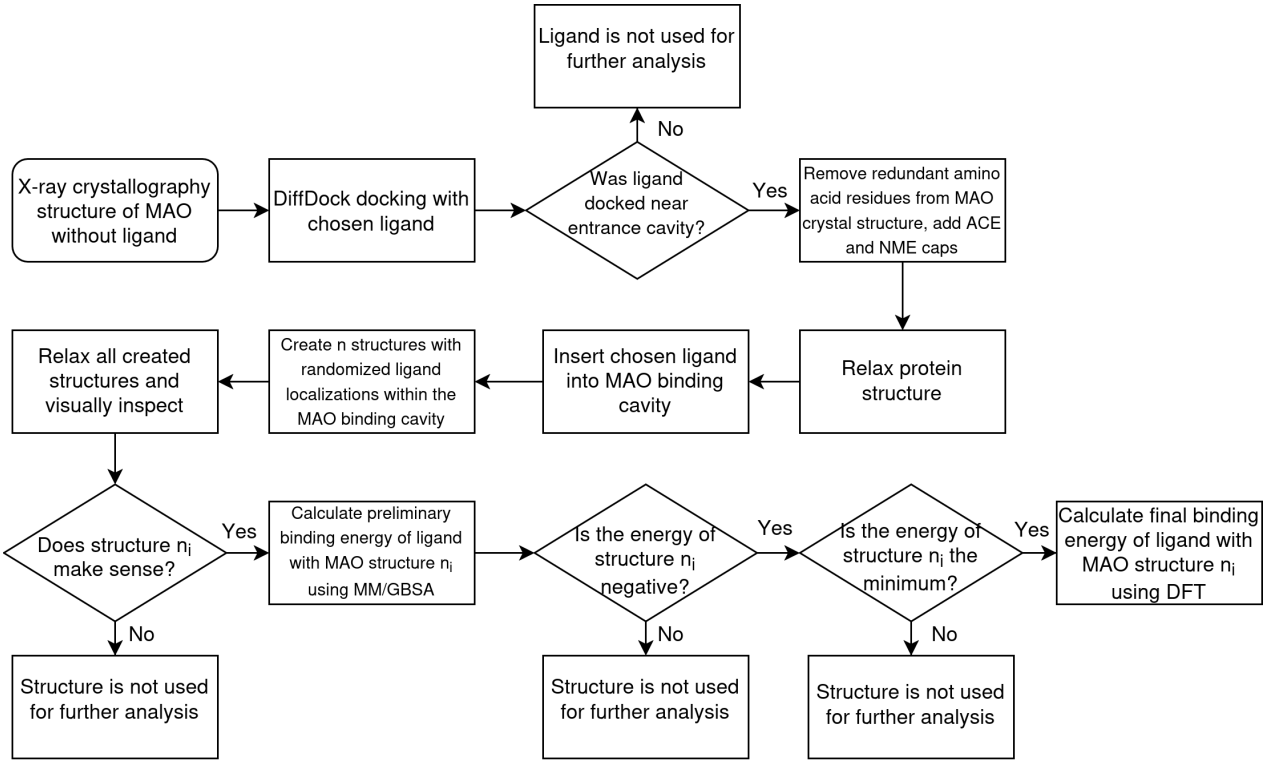


Fig. 1. The workflow for modeling the enzyme-ligand complex.

This study investigates the structures, biocatalytic mechanisms, and inhibitor interactions of human MAO-A and MAO-B using X-ray crystallography data and published literature. We generated theoretical models of the enzyme active sites bound to non-covalent inhibitors (Fig 1). These models were compared with available substrate-enzyme intermediate structures. Employing artificial intelligence, molecular dynamics, and density functional theory (DFT) calculations, we determined the structures and energetic parameters of the active site-inhibitor complexes. This work aims to facilitate the more rapid and reliable prediction of novel antidepressant drugs.

[1] Edmondson, D. E., Mattevi, A., Binda, C., Li, M., & Hubalek, F. (2004). Structure and mechanism of monoamine oxidase. Current Medicinal Chemistry, 11(15), 1983–1993. https://doi.org/10.2174/0929867043364784

[2] Jahng, J. W., Houpt, T. A., Wessel, T. C., Chen, K., Shih, J. C., & Joh, T. H. (1997). Localization of monoamine oxidase A and B mRNA in the rat brain by in situ hybridization. Synapse, 25(1), 30–36. https://doi.org/10.1002/(sici)1098-2396(199701)25:1

[3] Duarte, P., Cuadrado, A., & León, R. (2020). Monoamine oxidase inhibitors: From classic to new clinical approaches. Handbook of Experimental Pharmacology, 229–259. https://doi.org/10.1007/164_2020_384

ORGAN-SPECIFIC STABLE CARBON ISOTOPIC COMPOSITION ($\delta^{13}C$) AND CARBON CONTENT DYNAMICS IN VACCINIUM MYRTILLUS L. (EUROPEAN BLUEBERRY)

Aistė Tuzinaitė[1,2], Anita Elizabeth Clarke[1], dr. Andrius Garbaras[2], dr. Radvilė Rimgailė-Voicik[1]

[1]Vilnius University Life Sciences Center Institute of Biosciences
[2]Center for Physical Sciences and Technology
aiste.tuzinaite@gmc.stud.vu.lt

European blueberry (*Vaccinium myrtillus* L.) shrubs are key components of forest understory, playing an essential role in soil formation processes and contributing to habitat stability [1,2]. Given its ecological significance, understanding the carbon cycling of *V. myrtillus* is crucial. Stable carbon isotopes are widely used in plant ecology to assess plant-environment interactions and provide valuable insights into plant carbon dynamics and the role of plants in the carbon biogeochemical cycle [3]. However, research employing stable carbon isotopes to study blueberry ecophysiology remains scarce.

This study examines organ-specific stable carbon isotope composition ($\delta^{13}C$) and carbon content (C %) dynamics in *V. myrtillus*. Plant samples were collected in August of 2021 along the eastern shore of Lake Gėla in Nemenčinė Forest, Vilnius District. A total of 25 specimens were collected and transported to the laboratory, where they were dried, separated by organs (roots, dry stems, green stems, and leaves), and ground into a fine powder. $\delta^{13}C$ values and carbon content were measured using elemental analysis–isotope ratio mass spectrometry (EA-IRMS).

The results showed that blueberry carbon content was the lowest in leaves and the highest in stems. The lowest $\delta^{13}C$ values were found in roots, while the highest were in stems. These results indicated that stems of *V. myrtillus* serve as the carbon sinks at the whole-plant level. However, no statistically significant correlation was observed between carbon content and $\delta^{13}C$ values, indicating no direct relationship between these parameters. Our study enhances the understanding of carbon dynamics in blueberry shrubs, providing new insights into the ecophysiology of *V. myrtillus* and its functioning in forest ecosystems.

[1] H. A. McCullough, "Plant succession on fallen logs in a virgin spruce-fir forest," *Ecology*, vol. 29, no. 4, pp. 508-513, 1948.
[2] E. Cázares, J. M. Trappe, and A. Jumpponen, "Mycorrhiza-plant colonization patterns on a subalpine glacier forefront as a model system of primary succession," *Mycorrhiza*, vol. 15, pp. 405-416, 2005.
[3] B. Fry, *Stable Isotope Ecology*, vol. 521, p. 318. New York, NY, USA: Springer, 2006.

EFFECTS OF QUANTUM DOTS ON AUTOFLUORESCENCE AND PHOTOSYNTHETIC PARAMETERS OF MICROALGAE

Danielė Gedminaitė[1], Rasa Miliukaitė[1], Martyna Petkutė[1], Agnė Kalnaitytė-Vengelienė[1]

[1]Laser Research Center, Faculty of Physics, Vilnius University, Lithuania
daniele.gedminaite@ff.stud.vu.lt

Green freshwater microalgae, commonly found in lakes, are easily cultivated and highly sensitive to environmental changes, making them excellent bioindicators. Their autofluorescence (AF) enables a safe, non-invasive monitoring of pollutants-induced effects in algae.

Quantum dots (QDs), which are becoming widely industrialized, are nanoscale semiconductor particles with unique optical properties, including bright photoluminescence (PL) which depends on their composition and structure. Their interactions with biological systems depend on the QDs optical properties [1] as well as the biological systems themselves and their environmental conditions. Determining the conditions on which the effect of QDs on microalgae photosynthetic parameters depend will not only help explain the contradictory results presented in the literature but also aid and provide insights into their effects and help in the future by recognizing those same effects.

This study analyzes the effects of three types of QDs – CdTe, CdSe/ZnS, and CuInZnS/ZnS – on autofluorescence and photosynthetic parameters of freshwater microalgae (Scenedesmus sp. and Desmodesmus sp.) by means of pulse amplitude modulation (PAM) fluorometry. Triplicate samples were placed in 96-well dishes (0.3 ml per well) and maintained at 20 ± 1 °C under a white LED light (6W, 8000K) with a 12-hour light/12-hour dark cycle. Illumination was provided by 13 or 34 µmol photons/m^{2}s intensity.

Our study showed that the effects of QDs on photosynthetic parameters of algae depend on their chemical composition. CdTe and CdSe/ZnS QDs did not cause significant changes of measured parameters compared to the control samples, suggesting minimal impact of QDs on algae. In contrast, the CuInZnS/ZnS QDs had a more pronounced effect on algae. However, NPQ parameter varied depending on the algae species: NPQ values increased after 24 hours with QDs in the Desmodesmus sp. samples compared to Scenedesmus sp. (Fig.1). For the same algae species, the effect of QDs varies depending on their growth and lighting conditions: Scenedesmus sp. grown under lower light and transferred to higher light without adaptation showed the most significant decrease in non-photochemical quenching.

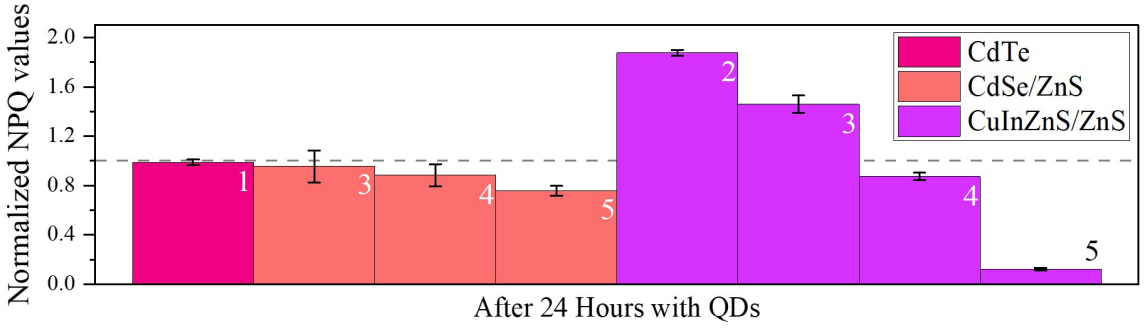


Fig. 1. Normalized average NPQ values after 24 hours in microalgae samples with QDs. The values are normalized to the NPQ values in algae sample without QDs. Different algae species were exposed with different QDs at different light conditions: 1 - Scenedesmus sp. algae at 13 µmol photons/m^{2}s, 2 - Desmodesmus sp. algae at 13 µmol photons/m^{2}s, 3 - Desmodesmus sp. algae at 34 µmol photons/m^{2}s is, 4 – Scenedesmus sp. at 34 µmol photons/m^{2}s, 5 – Scenedesmus sp. at 34 µmol photons/m^{2}s, but without photoadaptation from lower light intensity.

[1] OH, Eunkeu, et al. Meta-analysis of cellular toxicity for cadmium-containing quantum dots. Nature nanotechnology, 2016, 11.5: 479-486.

STRUCTURAL INSIGHTS INTO S100A9 AND S100A8 PROTEINS VIA DEER SPECTROSCOPY

Aiste Pestenyte[1], Gediminas Usevicius[1], Darius Sulskis[2], Ieva Baronaite[2], Vytautas Smirnovas[2], Juras Banys[1], Mantas Simenas[1]

[1]Faculty of Physics, Vilnius University, Saulėtekio al. 3, Vilnius, Lithuania
[2]Sector of Amyloid Research, Institute of Biotechnology, Life Sciences Centre, Vilnius University, Vilnius, Lithuania
aiste.pestenyte@ff.stud.vu.lt

Double electron-electron resonance (DEER) spectroscopy is a powerful and widely used method in structural biology, providing insights into the structural and dynamic properties of biomolecules such as proteins, RNA, and DNA [1]. This pulsed electron paramagnetic resonance (EPR) technique enables the measurement of nanoscale distances between unpaired electron spins by employing microwave pulses at different frequencies. One electron spin is detected while the other is excited, allowing for the observation of dipolar interactions throughout the experiment (Fig. 1) [2]. Since many biomolecules lack unpaired electrons, DEER spectroscopy utilizes site-directed spin labeling (SDSL) to introduce spin labels, enabling structural investigations that are not constrained by crystallization requirements or molecular weight limitations [1].

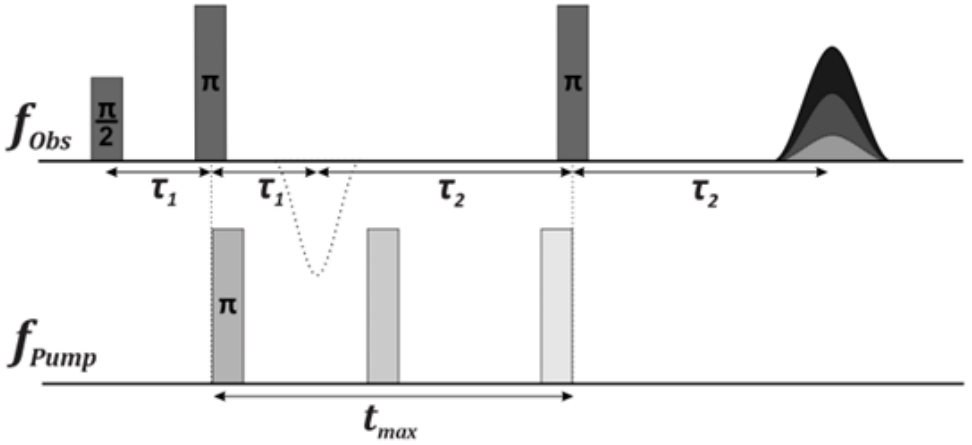


Fig. 1. Microwave pulse sequence of the DEER experiment.

In this study, DEER spectroscopy was used to examine the calcium-binding proteins S100A8 and S100A9, which are associated with neurodegenerative disorders such as Alzheimer's and Parkinson's diseases. Using nitroxide radical spin labels, we measured the distance distributions between labeled cysteine residues, revealing key structural and dynamic properties of these proteins. Our findings demonstrate the potential of DEER spectroscopy for studying protein conformational changes, interactions, and functional mechanisms, further contributing to the understanding of their role in disease-related processes.

[1] Indra D. et al., Use of electron paramagnetic resonance to solve biochemical problems, Biochemistry 2013, 52, 35, 5967−5984
[2] Jeschke G. DEER distance measurements on proteins. Annual review of physical chemistry. 2012 May 5;63:419-46.

LOW-TEMPERATURE SYNTHESIS OF MAGNESIUM WHITLOCKITE FROM AMORPHOUS CALCIUM PHOSPHATE

Gabriele Egle Budzyte[1], Greta Linkaite[1], Aleksej Zarkov[1], Aivaras Kareiva[1], Inga Grigoraviciute[1]

[1]Institute of Chemistry, Vilnius University, Naugarduko 24, LT-03225 Vilnius, Lithuania
egle.budzyte@chgf.vu.lt

One subclass of ceramic biomaterials is calcium phosphates (CPs). These minerals are found in biological tissues, where they form the main component of bones and teeth. CPs exhibit excellent biological properties, promote osteogenesis, and have a chemical composition and structure similar to the inorganic part of natural bone. Magnesium whitlockite (Mg-WH, $Ca_{18}Mg_2(HPO_4)_2(PO_4)_{12}$) is a CP in which calcium is partially replaced by magnesium, and it also occurs in biological tissues. Compared to widely used clinical materials such as hydroxyapatite ($Ca_{10}(PO_4)_6(OH)_2$) or tricalcium phosphate ($Ca_3(PO_4)_2$), Mg-WH stands out for its higher corrosion resistance, plays a crucial role in bone defect healing, and promotes osteogenic differentiation. The use of synthetic Mg-WH in medicine is limited, primarily due to challenges associated with its synthesis. The excellent biological properties of synthetic Mg-WH, along with the ability to control its synthesis process, enable the development of materials with optimized mechanical, chemical, and biological properties, making Mg-WH a promising alternative to traditional biomaterials. Amorphous calcium phosphate (ACP), which has a non-crystalline structure and is therefore highly reactive, is an important member of the CP family and can serve as a precursor for synthesizing other phosphate-based materials, such as Mg-WH. In this study, Mg-WH was synthesized using ACP as a precursor. In a medium composed of a mixture of $(NH_4)H_2PO_4$, $(NH_4)_2HPO_4$, and $Mg(CH_3COO)_2$ solutions (pH = 5.98), ACP dissolves, eventually leading to the precipitation of Mg-WH. The study examines the effects of various synthesis parameters, such as reaction duration, Mg ion concentration, and medium composition, on the composition of the synthesized products. The crystallinity, phase purity, and morphology of the synthesized samples were evaluated using XRD, FTIR, and SEM.

CELL SPHEROIDS AS A TOOL FOR INVESTIGATION IN MATERIAL ENGINEERING

Valdemaras Milkus[1], Greta Leonavičienė[2], Suji Kim[1], Linas Mažutis[1]

[1]Single-cell analysis sector, Life Sciences center, Vilnius University, Vilnius, Lithuania.
[2]Atrandi Biosciences, UAB, Vytenio g. 18, Vilnius, Lithuania.
valdemaras.milkus@bti.vu.lt

It was noticed long ago that some cells in suspension can arrange themselves into nearly perfect spherical 3D clusters. In the last decade the 3D cell spheroids became a powerful tool for analysis. Unlike the usual 2D monolayer cell cultures, the spheroids can mimic the cell-cell and not only cell-environment interactions. This way the spheroids are used for drug-delivery and screening or tumor research. However, the spheroids formed in a suspension are irregular with poor preparation efficiency [1]. Droplet microfluidics helps us to isolate single cells or molecules into water droplets of constant volume in carrier oil phase. More recent applications allow us to produce the droplets which can be later crosslinked into polymer capsules. Coupling the single cell encapsulation, cultivation and the shell permeability allows for cell division and growth [2].

Cell spheroids were grown from the single cells encapsulated into the droplets. The droplets were produced in a microfluidic PDMS-glass chip. The chips are replicated from a silicon-SU8 mold produced by using a soft-litho-graphy method. Using the polymer of high molecular weight (Dextran 500K) we assure a consistent encapsulation of one cell per capsule. Adjusting the flow rates of oil and water phases (Dextran and gelatine) we get the capsules of 60μm in diameter. Two water phases separate to form a gelatine-shell and liquid dextran-saturated core. After crosslinking the cells within the capsules are taken into the cell-growth media for further incubation. Since pore size is too small for Dextran molecule to pass, the polymer is kept inside the capsule adjusting to the osmotic equilibrium. The cell-growth media can reach the cells allowing them to multiply. Eventually the spheroid occupies the volume of capsule and proceeds to grow by deforming a shell (Figure 1). Contrary to other works, here we do not find apoptotic cells [3].

We find the growth of spheroid-radius follows different power-law before and after spheroid confluence. We expect it to be the result of cell compression and rearrangement. This allows us to estimate the bulk modulus of the spheroid- an analog to the Young's modulus. The Young's modulus for the empty capsule was estimated from the relative deformation with an osmotic pressure.

We take the balance of the elastic energy of the shell deformation and the energy created by spheroid. Then we find the pressure created by spheroid over the time of growth. There's no pressure change until confluence. In later stages there are elastic and plastic (permanent) deformations. Overall, the curve is similar to stress-strain curve for any bulk material. This way the growing spheroids might give an insight into the mechanical stability of capsules.

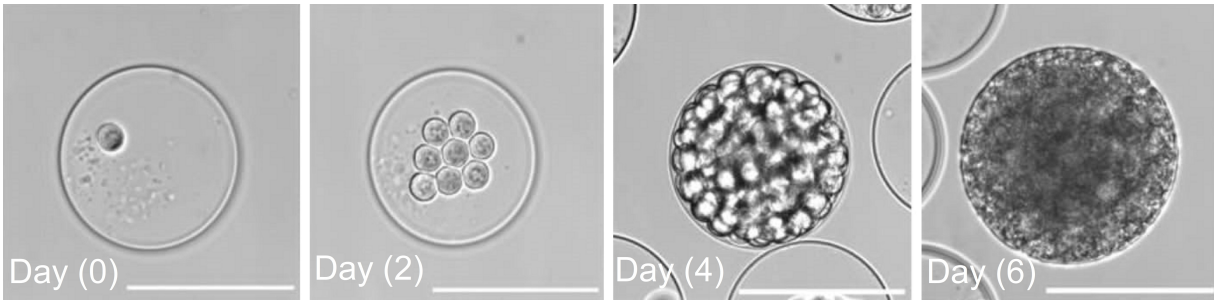


Fig. 1. Pictures of the growing cell-spheroid inside the gelatine capsule. Scale bar 60μm.

[1] Shen, H.; Cai, S.; Wu, C.; Yang, W.; Yu, H.; Liu, L. Micromachines 2021, 12, 96.
[2] Leonaviciene G., Leonavicius K., Meskys R., and Mazutis L., Lab Chip, 2020, 20, 4052.
[3] Alessandri K. et al. PNAS 2013 Sep 10;110(37):14843-8. doi: 10.1073/pnas.1309482110. Epub 2013 Aug 26. PMID: 23980147; PMCID: PMC3773746.

DEOXYGENATION OF TTA-UC SOLUTIONS BY EFFICIENT OXYGEN SCAVENGING

Dominykas Likas[1], Steponas Raišys[1]

[1] Institute of Photonics and Nanotechnology, Faculty of Physics, Vilnius University, Vilnius, Lithuania
dominykas.likas@ff.stud.vu.lt

Triplet-triplet annihilation upconversion (TTA-UC) is a process in which two photons are converted into one of higher energy. Therefore, it is attractive for multiple applications such as drug activation, sensing, photovoltaics and others.[1] TTA-UC relies on the long lifetime of triplet excitons for efficient energy transfer from sensitizer to annihilator and frequent intermolecular interaction between triplet excitons of annihilator. In the solution state, under ambient conditions, dissolved molecular oxygen caused a major measurement problem because it strongly quenches the triplet states, limiting the evaluation of intrinsic photophysical parameters. Several techniques could be used to prevent oxygen quenching, including solution bubbling with inert gases, such as nitrogen, which physically replaces dissolved oxygen in the solvent, or the freeze-pump-thaw method, where the solution is frozen with liquid nitrogen, trapping dissolved gasses inside. After vacuuming and heating a frozen solution, gaseous oxygen is removed.

Although these methods effectively remove oxygen, they require relatively sophisticated technological equipment and are time-consuming. Another way to prevent oxygen quenching is by using oxygen scavengers. After quenching the triplet state, molecular oxygen becomes excited and forms reactive singlet oxygen, which, in the presence of oxygen scavenges, effectively reacts, resulting in the stable form of oxidized scavengers. In this way, oxygen concentration is reduced in the solution.

In this study, various oxygen scavengers were tested, including common organic solvents such as THF, 2-methyltetrahydrofuran, DMSO or sulphur-based scavengers[2] such as dimethylsulfide, trithiane and others. It has been observed that DMSO removes oxygen the most efficiently, however, DMSO, due to its large dipole moment, is particularly suitable solvent for polar molecules. Therefore, alternative scavenging materials, even less efficient, are very attractive.

[1] J. Zhao, W. Wu, J. Sun, S. Guo, Triplet Photosensitizers: From Molecular Design To Applications, Chem. Soc. Rev.,2013, 42, 5323.
[2] D. Dzebo, K. Moth-Poulsen, B. Albinsson, Robust Triplet–Triplet Annihilation Photon Upconversion By Efficient Oxygen Scavenging, Journal of Photochemical & Photobiological Sciences, Photochem. Photobiol. Sci., 2017, 16, 1327.

ACHIEVING LONG-LASTING ROOM-TEMPERATURE PHOSPHORESCENCE IN PHENOTHIAZINE DERIVATIVES

Vilius Stankevičius[1], Jonas Žurauskas[2], Paulius Vaickūnas[2], Steponas Raišys[1], Edvinas Orentas[2], Karolis Kazlauskas[1]

[1]Institute of Photonics and Nanotechnology, Vilnius University, Vilnius, Lithuania
[2]Department of Organic Chemistry, Vilnius University, Vilnius, Lithuania
vilius.stankevicius@ff.stud.vu.lt

Room temperature phosphorescence (RTP) has great potential to be used for various applications in sensing, data encryption, anti-counterfeiting, bioimaging and microcrack detection owing to their unique photophysical properties [1]. Typically, RTP emission is achieved in inorganic material-based systems, including rare earth metals, which are associated with high processing costs, poor biocompatibility, etc. Recently, the focus has shifted to organic RTP systems due to their tunability of emission wavelength, low cost and ease of processing.

For practical applications, RTPs must be efficient and have a long phosphorescence lifetime, which is in principle a challenging task, since promoting intersystem crossing for high-yield triplet generation usually shortens their lifetime [2], [3]. A necessary rigid environment for RTP can be ensured by the crystalline structure of the emitter, however, creating doped polymer RTP systems, as opposed to relying solely on crystal systems, offers a promising approach to enhance the practical applicability of the phenomenon [1]. Consequently, it is necessary to identify and understand the limiting factors of the processes involved in RTP to improve the photophysical properties and application potential of RTP systems.

In this work, dozens of new phenothiazine 5,5-dioxide based RTP emitters have been synthesized, and their RTP properties have been investigated in both their crystal form and doped polymer films. It has been demonstrated that phenothiazine derivatives with broader conjugation (with –Ph or -pCNPh substituents at 3rd and 7th positions) frequently exhibited longer phosphorescence lifetime and higher quantum yield than those with narrower conjugation. Thus, the presence of larger substituents is associated with a decrease in non-radiative decay. Furthermore, it was found that doping the more rigid polymer, polyacrylic acid (PAA), with phenothiazine derivatives can further enhance phosphorescence properties compared to the polymethylmethacrylate (PMMA) matrix. In PAA films, 40% photoluminescence (PL) efficiency was achieved, half of which was phosphorescence, while in PMMA films emission quantum yield was lower, at around 30%. In the polymer films, phosphorescence lifetimes up to 0.7 s were achieved.

[1] Y. Wang, J. Yang, M. Fang, Y. Gong, J. Ren, L. Tu, B. Z. Tang, Z. Li, New Phenothiazine Derivatives That Exhibit Photoinduced Room-Temperature Phosphorescence. Adv. Funct. Mater. 2021, 31, 2101719. DOI: 10.1002/adfm.202101719
[2] H. Ma, Q. Peng, Z. An, W. Huang, Z. Shuai, Efficient and Long-Lived Room-Temperature Organic Phosphorescence: Theoretical Descriptors for Molecular Designs, J. Am. Chem. Soc., 2019 141 (2), 1010-1015. DOI: 10.1021/jacs.8b11224
[3] J. Jovaišaitė, S. Kirschner, S. Raišys, G. Kreiza, P. Baronas, S. Juršėnas, M. Wagner, Diboraanthracene-Doped Polymer Systems for Colour-Tuneable Room-Temperature Organic Afterglow, Angew. Chem. Int. Ed. 2023, 62, e202215071. DOI: 10.1002/anie.202215071

INVESTIGATION OF CONDUCTIVE POLYMER BASED DRUG DELIVERY SYSTEMS

Elena Nedzinskaitė[1], Felix Lücke[1], Šarūnas Žukauskas[1,3], Arūnas Ramanavičius[1,2], Almira Ramanavičienė[2,3]

[1]Centre for Physical Sciences and Technology
[2]Vilnius University
[3]State Research Institute Centre for Innovative Medicine
elena.nedzinskaite@ftmc.lt

Controlled drug delivery is an important research topic in both academia and industry because of its impact on pharmacokinetics and patient compliance. Traditional drug administration does not always ensure targeted delivery, potentially causing undesired side effects. To address this, drug delivery systems are being developed to enable targeted and controlled drug release in response to external stimuli. Our primary goal was to explore the opportunities of using conductive polymers (CP) as carriers for non-steroidal anti-inflammatory drug (NSAIDs), and to develop a controllable drug delivery system for NSAIDs that regulates both its concentration and release time. In this work we focused on employing conductive polymer matrices as a platform for controlled drug release.

To make this system we first electrochemically deposited CP matrix on platinum electrode using potentiometric detection and cyclic voltammetry methods in a solution of CP with NSAIDS and electrolyte. To release the embedded NSAIDs form the CP overoxidation potential over time was applied. Release of NSAIDs was monitored with UV-Vis spectrophotometry where we used the electrolyte as the reference.

The potential applications of this system could be utilized in medical devices for localized drug delivery and reducing systemic side effects.

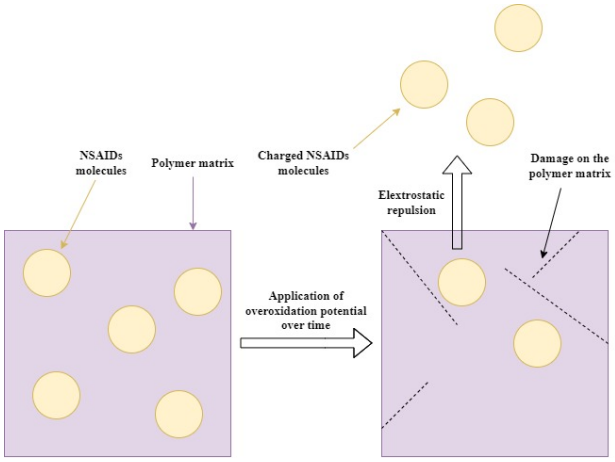


Fig. 1. NSAIDs deposition and release from conductive polymer matrix.

Acknowledgements
This project has received funding from the Research Council of Lithuania (LMTLT), project No P-PD-24-159.

CO-PRECIPITATION SYNTHESIS AND CHARACTERISATION OF Mg/Al-LAYERED DOUBLE HYDROXIDES (LDH)

Gabija Navašinskaitė[1], Denis Sokol[1], Gabrielė Klydžiūtė[1], Aivaras Kareiva[1]

[1]Institute of Chemistry, Faculty of Chemistry and Geosciences, Vilnius University, Naugarduko st. 24, LT – 30225, Vilnius, Lithuania
gabija.navasinskaite@chgf.stud.vu.lt

Layered double hydroxides (LDH) are a class of synthetic clays that contain cationic layers similar to brucite [$Mg(OH)_2$]. An anion in the interlayer provides charge balance. Layered hydroxides are highly susceptible to modification in both the cationic and anionic layers, and their synthesis offers the possibility of obtaining materials with desired properties. The objective of this study is to synthesize $Mg_3Al_1(OH)_Y$, $Mg_{3-X}Ag_XAl_1(OH)_Y$, and $Mg_3Al_{1-X}Cr_X(OH)_Y$ and to investigate the structure and properties of the resulting materials.

Mg/Al LDHs are synthesized by the co-precipitation method. Metal nitrate solutions, mixed in the required proportions, are slowly dropped into a sodium carbonate solution at the required pH which is adjusted with sodium hydroxide solution, followed by aging of the synthesised material at 80 °C. LDH with Cr is synthesised in the same manner, only replacing part of the aluminium nitrate with a solution of $Cr(NO_3)_3$ or CrO_3. The synthesis of LDH with Ag is carried out using pre-made Mg/Al LDH, which is submerged in $AgNO_3$ solution and stirred at temperatures ranging from 80 to 100 °C for 15 minutes. The temperature is maintained by a hydrothermal reactor and a hot plate.

The substitution of Al^{3+} ions by Cr^{3+} ions in the cationic layer was successful, as evidenced by XRD data showing that no additional phases were formed during the reaction, regardless of the Cr source. Conversely, the substitution of Mg^{2+} ions by Ag^+ ions proved unsuccessful, as silver failed to incorporate into the structure and instead precipitated as elemental silver.

TRIMETALLIC CoMoW ELECTROCATALYSTS FOR HYDROGEN GENERATION

Raminta Šakickaitė[1], Zita Sukackienė[1], Loreta Tamašauskaitė-Tamašiūnaitė[1]

[1]Center for Physical Sciences and Technology (FTMC), Saulėtekio ave. 3, LT10257 Vilnius, Lithuania
raminta.sakickaite@ftmc.lt

In 2021, the European Union introduced policies in support of the European Green Deal and the EU Hydrogen Strategy, with the objective of achieving climate neutrality by 2050 [1]. Hydrogen is regarded as a promising clean energy carrier, playing a crucial role in the transition towards a more sustainable and low-carbon economy. Among the various hydrogen production methods, the catalytic hydrolysis of sodium borohydride ($NaBH_4$) has attracted significant attention due to its high gravimetric hydrogen storage capacity (GHSC) of 10.8 wt.%, the elimination of external electrical energy input, and the ability to be stored in a chemically stable solid state until activation [2]. $NaBH_4$ hydrolysis can generate hydrogen under mild temperature and pressure conditions, making it a viable candidate for portable devices and on-demand hydrogen applications.

In this study, trimetallic Cobalt-Molybdenum-Tungsten (CoMoW) catalysts were developed via the electroless plating method using morpholine borane ($C_4H_{12}BNO$) as the reducing agent. The structural and compositional properties of the CoMoW catalysts were characterized using scanning electron microscopy (SEM) and energy-dispersive X-ray spectroscopy (EDX), while their catalytic performance was evaluated in $NaBH_4$ hydrolysis using a 5 wt.% $NaBH_4$ + 0.4 wt.% NaOH solution across a temperature range of 30 – 70 °C.

[1] European Comission. Energy, Climate change, Environment. Hydrogen. Website: https://energy.ec.europa.eu/topics/eus-energy-system/hydrogen_en
[2] Muir, S. S., & Yao, X. (2011). Progress in sodium borohydride as a hydrogen storage material: Development of hydrolysis catalysts and reaction systems. International Journal of Hydrogen Energy, 36(10), 5983-5997.

INVESTIGATION OF SUPERCAPACITIVE BEHAVIOR OF COPPER-OXIDE BASED NANOSTRUCTURED FILMS

Gintautas Jonkus[1], Henrikas Cesiulis[1], Ramunas Levinas[2], Natalia Tsyntsaru[1,3]

[1]Faculty of Chemistry and Geosciences, Vilnius University, 03225 Vilnius, Lithuania
[2]State Research Institute, Center for Physical Sciences and Technology, 10257 Vilnius, Lithuania
[3]Institute of Applied Physics, Moldova State University, 2028 Chisinau, Moldova
gintautas.jonkus@gmc.stud.vu.lt

Nowadays the field of renewable energy is rapidly booming one of such example would be the European Union Green Deal whose goal is to make the European Union the first climate-neutral region in the world by 2050[1]. Although renewable energy provides many advantages it also comes with the obstacles such as non-continuity of energy production thus emphasising the necessity for cost-effective energy storage solutions. Copper, an abundant metal, offers solution, especially copper oxides. They do have an extremely high theoretical capacitance: Cu_2O 2247.6 F/g [2], CuO – 1783 F/g [3]. In our study, we have used cyclic voltammetry to anodize copper-oxide based thin-films on both porous and non-porous electrodes and electrochemical impedance spectroscopy (EIS) to characterize occurring electrochemical processes in 1M NaOH . We obtained their phase purity with the X-ray diffraction (XRD) method and surface morphology using scanning electron microscopy (SEM). It was observed that different oxide and hydroxide phases could be synthesized by tuning the upper vertex potential of the cycle (Fig. 1). The capacitance of electrodes was measured by cyclic voltammetry at different scan rates. The highest specific capacitance of 1380 mF/cm was obtained at the film synthesised on copper foam, vertex potentials: -1:0.65 V, at 5 mV/s scan rate. Therefore, the investigated methodology offers insights into the tunable synthesis of nanostructured copper oxide supercapacitors.

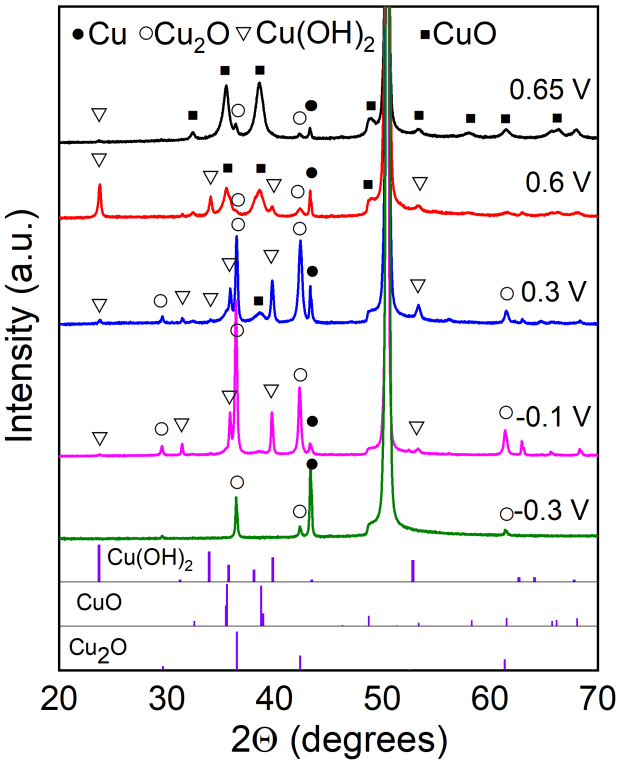


Fig. 1. X ray diffraction data of films synthesized on Copper foil.

[1] Delivering the European Green Deal. Https://Commission.Europa.Eu/Strategy-and-Policy/Priorities-2019-2024/European-Green-Deal/Delivering-European-Gr 2025.
[2] X Panpan, L. Jijun et. al., RSC Adv., 6, 28270-28278 (2016).
[3] B. Kr Singh, A. Shaikh, et. al., J. of Energy Storage, 31, 101631 (2020).

FABRICATION OF MODIFIED HEXAGONAL BORON NITRIDE 3D PHOTOCATALYSTS BY COMBINING STEREOLITHOGRAPHY AND PYROLYSIS

Robertas Virkėtis[1], Vaidas Klimkevičius[1], Greta Merkininkaitė[1], Simas Šakirzanovas[1]

[1]Institute of Chemistry, Faculty of Chemistry and Geosciences, Vilnius University, Vilnius LT-03225, Lithuania
robertas.virketis@chgf.vu.lt

Additive manufacturing has garnered significant attention in both industrial and commercial applications. One of its key techniques, stereolithography, utilizes UV light to fabricate complex 3D structures from UV-curable photoresins. For this process, homogeneous resins are preferred over multiphase resins, as the latter can lead to sedimentation and light scattering, compromising the uniformity of the printed objects. Ensuring uniformity enhances mechanical properties, improves surface finish, and minimizes defects during polymerization and subsequent heat treatment. Moreover, combining stereolithography with pyrolysis—a high-temperature treatment in a non-oxidizing atmosphere—enables the fabrication of ceramic 3D objects.

Hexagonal boron nitride (h-BN) is known for its chemical inertness, corrosion resistance, low density, and high thermal stability. Incorporation carbon into the h-BN lattice reduces its bandgap, making it a semiconductor with potential applications in photocatalysis [1]. When exposed to light, semiconductor materials accelerate photoreactions, a process known as photocatalysis, which can be applied to water treatment by degrading non-biodegradable organic pollutants. Unlike conventional methods, this photocatalytic approach eliminates the need for an additional purification step to remove reactants and by-products after treatment.

In this study, the boron-containing organic monomer 2-(5,5-dimethyl-1,2,3-dioxaborinan-2-yloxy)ethyl methacrylate (BoMA) was synthesized via esterification reaction as described in [2]. The successful synthesis of BoMA was confirmed by proton nuclear magnetic resonance analysis, achieving a product yield of approximately 70%. Subsequently, BoMA was employed in the fabrication of 3D-printed objects using UV-based stereolithography system Zortrax Inkspire. The printed 3D objects were then subjected to pyrolysis at 1000 °C in vacuum and later at 1700 °C in N_2 atmosphere. X-ray diffraction (XRD) analysis confirmed the formation of the h-BN phase (Figure 1a). Additionally, the photocatalytic activity of the fabricated ceramic structures was evaluated through rhodamine B degradation under halogen lamp simulating sunlight, confirming their efficiency as photocatalysts (Figure 1b).

This study demonstrates that the combination of organoboron methacrylate synthesis, stereolithography, and pyrolysis provides a viable approach for fabricating photocatalysts capable of degrading organic pollutants in water under solar irradiation.

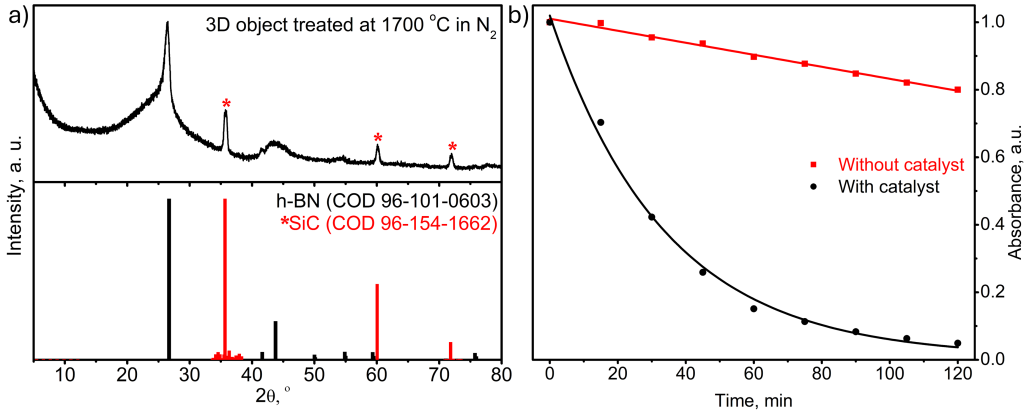


Fig. 1. a) XRD pattern of 3D object treated at 1700 °C in N_2 atmosphere, b) absorbance change of rodamine B during photocatalysis using 3D object treated at 1700 °C in N_2 atmosphere.

Acknowledgements
Research funded by Vilnius University Research Promotion Fund (project No. MSF-JM-10/2024)

[1] N. S. Mishra et. al., LED-light-activated photocatalytic performance of metal-free carbon-modified hexagonal boron nitride towards degradation of methylene blue and phenol, Beilstein Journal of Nanotechnology. 13 (2022) 1380-1392. doi: https://doi.org/10.3762/bjnano.13.114
[2] N. Aliyeva et. al., Synthesis and characterization of boron-acrylate/Santa Barbara Amorphous-15 polymer composite, Journal of Applied Polymer Science. 138 (2021) 50445. doi: https://doi.org/10.1002/app.50445

SYNTHESIS AND INVESTIGATION OF AROMATIC ELECTRON-TRANSPORTING PHOSPHINE OXIDE COMPOUNDS

Andrius Stankus[1], Mantas Marčinskas[1]

[1]Kaunas University of Technology, Faculty of Chemical Technology, Department of Organic Chemistry
andrius.stankus@ktu.edu

Perovskite solar cells are among the most promising and rapidly advancing solar cell technologies. Over the past decade, they have undergone significant performance improvements. By adjusting the composition of the perovskite layer, it is possible to optimize its electrochemical properties to achieve maximum efficiency. However, the primary drawback of perovskite solar cells is their sensitivity to moisture and oxygen, which can lead to the degradation of the perovskite layer and the formation of defects in its crystalline structure. These defects can also occur during the crystallization process, leading to a decrease in the longevity and efficiency of the final device [1,2].

Charge-transporting materials are crucial in determining the effectiveness and stability of perovskite solar cells. The presence of incompatible functional groups or electrochemically unstable compounds can negatively impact device performance. However, certain functional groups have the opposite effect—they can passivate existing defects in the perovskite layer and prevent the formation of new imperfections. One of the most effective functional groups for passivating the perovskite layer is the phosphine oxide fragment, which easily coordinates with free lead ions in the crystal. Such passivating compounds are often used to form interlayers, as they typically exhibit poor electron-transporting properties [3].

Currently, the most commonly used electron-transporting materials are fullerenes and their modified derivatives, such as $PC_{61}BM$ and $PC_{71}BM$. These compounds possess excellent electrochemical properties, demonstrate high performance in solar cells, and can effectively passivate the perovskite layer's surface. However, fullerenes have several drawbacks, including expensive and complex synthesis and low solubility in most organic solvents. The availability of suitable alternatives is limited, and most existing alternatives perform worse than fullerenes in solar cells [4].

The aim of this work was to synthesize aromatic phosphine oxide compounds capable of both transporting electrons and passivating the surface of the perovskite crystal. The synthesized compounds were characterized by investigating their thermal stability, ability to sublimate under vacuum, and performance in triple halide 1.68 eV perovskite solar cells of a p-i-n architecture. These compounds were tested both as an interlayer along with fullerene and as a standalone electron-transporting layer.

[1] A. Seitkhan et al. Adv. Funct. Mater., 2020, 30, 2004273.
[2] X. Chen et al. Chem, 2023, 9 (3), 562-575.
[3] S.O. Jeon et al. J. Mater. Chem., 2012, 22, 4233-4243
[4] B.G. Krishna et al Chemistry of Inorganic Materials, 2023, 1, 100026

$GdPO_4$:Cr^{3+} AND VPO_4:Cr^{3+} SYNTHESIS BY SOLID-STATE REACTION

Miglė Minalgaitė[1], Ramūnas Skaudžius[1]

[1]Department of Inorganic Chemistry, Vilnius University, Lithuania
migle.minalgaite@chgf.stud.vu.lt

Near-infrared (NIR) light possesses the ability to penetrate biological tissues. Consequently, it is used as a bioimaging and biosensing tool to monitor human health. Due to Cr^{3+} ions' ability to easily emit broadband NIR light varying from 600 to 1300 nm, Cr^{3+} ions are often used as NIR-emitting activators[1]. Successful Cr^{3+} insertion can also be used in the garnet structure to enhance NIR region emission[2].

In the present study, the $GdPO_4$ and VPO_4 are chosen for doping with different concentrations of Cr^{3+} onto the pentagonal Gd^{3+} and octahedral V^{5+} sites ($GdPO_4$:0.01%Cr^{3+}, $GdPO_4$:1%Cr^{3+}, VPO_4:0.01%Cr^{3+}, and VPO_4:1 %Cr^{3+}).

In the experimental procedure, powders of $GdPO_4$:Cr^{3+} and VPO_4:Cr^{3+} were prepared by solid-state reaction using stoichiometric amounts of analytical grade nitrates, phosphate, and oxide, viz. $Gd(NO_3)_3{\cdot}6H_2O$, $Cr(NO_3)_3{\cdot}9H_2O$, $(NH_4)_2HPO_4$, V_2O_5. During $GdPO_4$ synthesis, the ratio of cations to the P source was 1:1. During VPO_4 synthesis, it was 1:10 and 1:1. The mashed powders were then placed in a furnace and annealed. The obtained materials were characterized by X-ray diffraction, and luminescence properties were investigated. Experimental results confirmed that chromium is not optically active in the pentagonal position, and VPO_4 was not synthesized under chosen conditions.

[1] Y. Wei, P. Dang, Z. Dai, G. Li, and J. Lin, 'Advances in Near-Infrared Luminescent Materials without Cr3+: Crystal Structure Design, Luminescence Properties, and Applications', Chemistry of Materials, vol. 33, no. 14, pp. 5496−5526, Jul. 2021, doi: 10.1021/ACS.CHEMMATER.1C01325/ASSET/IMAGES/LARGE/CM1C01325_0013.JPEG.

[2] M. Norkus and R. Skaudžius, 'Enhanced NIR region emission of chromium by changing the chromium concentration in yttrium aluminum garnet (YAG) host matrix', J Alloys Compd, vol. 908, p. 164601, Jul. 2022, doi: 10.1016/J.JALLCOM.2022.164601.

SYNTHESIS AND APPLICATION OF ISOTHIOURONIUM MOIETY CONTAINING CARBOXYLIC OR PHOSPHONIC ACIDS IN PEROVSKITE SOLAR CELLS

Justina Mikučiūnaitė[1], Kasparas Rakštys[1]

[1]Department of Organic Chemistry, Kaunas University of Technology, Lithuania
justina.mikuciunaite@ktu.edu

Solar energy is one of the most widespread types of renewable energy, and much attention is currently being paid to the development of perovskite solar cells. Perovskite solar cells are a rapidly developing third-generation technology that has already achieved higher energy conversion efficiency than silicon solar cells [1]. The production of perovskite solar cells is simpler, the cells themselves are light and flexible, which increases their industrial application possibilities. Despite these advantages, perovskites are very sensitive to environmental factors, and various crystal lattice defects are formed during production. Most often, chemical passivation of the perovskite surface with organic salts is used to reduce or eliminate these defects [2].

It was found that the isothiouronium group interacts well with the perovskite layer, so compounds containing this functional group are suitable for perovskite passivation. The interface between hole transport layer and perovskite is also important to ensure the highest possible efficiency of the solar cell. The efficiency of fabricated perovskite solar cells has been improved when organic isothiouronium compounds with a phosphonic or carboxylic acid anchoring groups are used for the bottom passivation of perovskite solar cells [Fig. 1]. Phosphonic or carboxylic acid anchoring groups interacting with hole transport layer ensure fast charge transportation improving overall performance of perovskite solar cells [3]. In this work, bifunctional passivation agents combining isothiouronium ionic head and phosphonic or carboxylic acid fragments were compared and the effect of the resulting compounds on perovskite solar cells is evaluated.

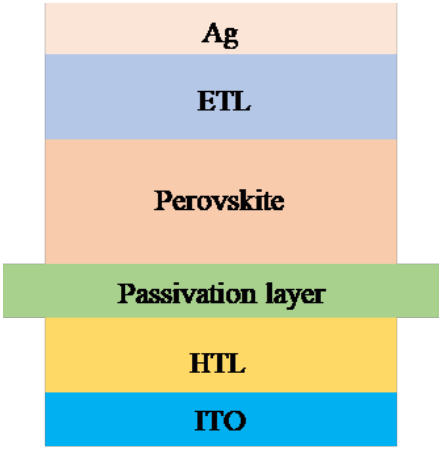


Fig. 1. Scheme of perovskite solar cell with bottom passivation

Acknowledgements
This project has received funding from the Research Council of Lithuania, agreement No [S-ST-24-19].

[1] T. A. Chowdhury, Md. A. Bin Zafar, Md. Sajjad-Ul Islam, M. Shahinuzzaman, M. A. Islam, and M. U. Khandaker, “Stability of perovskite solar cells: issues and prospects,” RSC Advances, vol. 13, no. 3, pp. 1787–1810, 2023, doi: https://doi.org/10.1039/d2ra05903g.
[2] X. Yu, X. Sun, Z. Zhu, and Z. Li, “Stabilization Strategies of Buried Interface for Efficient SAM-based Inverted Perovskite Solar Cells,” Angewandte Chemie International Edition, Nov. 2024, doi: https://doi.org/10.1002/anie.202419608.
[3] K. Du et al., “The Synergistic Effect of Phosphonic and Carboxyl Acid Groups for Efficient and Stable Perovskite Solar Cells,” Materials, vol. 16, no. 23, p. 7306, Nov. 2023, doi: https://doi.org/10.3390/ma16237306.

INVESTIGATION OF ZINC HEXACYANOFERRATE FOR AQUEOUS ZINC ION BATTERIES

Dovilė Škarnulytė[1], Jurgis Pilipavičius[1,2], Linas Vilčiauskas[1,2]

[1]Centre for Physical Sciences and Technology, Sauletekio av. 3, LT-10257, Vilnius, Lithuania
[2]Institute of Chemistry, Vilnius University, Naugarduko 24, LT-03225, Vilnius, Lithuania
dovile.skarnulyte@chgf.vu.lt

The Prussian blue analogue zinc hexacyanoferrate ($Zn_3[Fe(CN)_6]_2$), which is the focus of this research, has an open-channel framework. The unique structure makes this material suitable for the storage of ions and even small molecules [1]. Moreover, due to the abundance of zinc and iron in the world, and the simplicity of the co-precipitation synthesis method, used to obtain this compound, ZnHCF has become one of the potential candidates for being utilized for the use as cathode in aqueous zinc-ion batteries [2]. Aqueous electrolytes, despite having a narrower electrochemical stability window, provide a safer environment compared to the commonly used organic electrolytes [3]. In addition, the reduction potential of Zn (-0.76 V vs. standard hydrogen electrode, SHE) makes it a significantly safer choice for ambient conditions than alkaline or alkali earth metal compounds [4].

In this work, we have used structural characterisation methods to analyse the dependence of the final phase obtained to changes in the synthesis procedure. In addition, the electrochemical performance of the samples was investigated as well as the relationship between said performance and structural characteristics of the material.

[1] Cartraud, P., Cointot, A. & Renaud, A. Zeolitic properties of mixed hexacyanoferrate (II): K2Zn3[Fe (CN)6]2 x H2O. Journal of the Chemical Society, Faraday Transactions 1: Physical Chemistry in Condensed Phases 77, 1561–1567 (1981).
[2] Zhang, L., Chen, L., Zhou, X. & Liu, Z. Towards High-Voltage Aqueous Metal-Ion Batteries Beyond 1.5 V: The Zinc/Zinc Hexacyanoferrate System. Adv Energy Mater 5, (2015).
[3] Kundu, D., Adams, B. D., Duffort, V., Vajargah, S. H. & Nazar, L. F. A high-capacity and long-life aqueous rechargeable zinc battery using a metal oxide intercalation cathode. Nat Energy 1, 1–8 (2016).
[4] Wang, Q., Li, J., Jin, H., Xin, S. & Gao, H. Prussian-blue materials: Revealing new opportunities for rechargeable batteries. InfoMat 4, e12311 (2022).

IMPACT OF CAPSULAR POLYSACCHARIDES ON ACINETOBACTER BAUMANNII SURVIVAL UNDER ANTIBIOTIC-INDUCED STRESS

Dominykas Grigorjevas[1], Jūratė Skerniškytė[1]

[1]Institute of Biosciences, Life Sciences Center, Vilnius University, Vilnius, Lithuania
dominykas.grigorjevas@gmc.stud.vu.lt

The development of antibiotics ushered in a new era of medicine in which bacterial infections could be easily treated. However, the emergence of antibiotic-resistant bacteria has rendered these drugs ineffective. Almost 5 million deaths were associated with drug-resistant infections in 2019 [1]. *Acinetobacter baumannii* is a multidrug-resistant opportunistic pathogen that causes various infections with a mortality rate of up to 44% [2]. Due to limited treatment options and a high mortality rate, the World Health Organization designated *A. baumannii* as a critical priority for new antibiotic development [2]. Although this pathogen is clinically relevant there is a lack of understanding about its virulence [3]. It is known that polysaccharide capsule plays a role in *A. baumannii's* ability to survive desiccation, evade the host immune system and resist antibiotics [4]. Therefore, it is important to evaluate the impact of capsular polysaccharides on *A. baumannii* resistance to antibiotics.

This study aimed to compare the resistance of *A. baumannii* wild-type isolate and its capsule-deficient mutant (*ΔgalU*) to different classes of antibiotics. This was achieved by assessing antibiotic minimal inhibitory concentrations in a liquid medium by microdilution. Bacteria were incubated for 24 hours at 37 °C with antibiotics and then the bacterial growth in different antibiotic concentrations was evaluated.

In this research, 13 antibiotics (tetracycline, colistin, gentamicin, ciprofloxacin, ampicillin, kanamycin, streptomycin, chloramphenicol, imipenem, meropenem, cefazolin and a mixture of sulfamethoxazole/trimethoprim) were used. It was found that wild-type strain and *ΔgalU* mutant displayed different growth profiles when tetracycline, colistin and gentamicin were applied. Further research is required to investigate how the genes responsible for capsule production are regulated in response to these antibiotics.

[1] Md. A. Salam et al., "Antimicrobial resistance: a growing serious threat for global public health," Healthcare, vol. 11, no. 13, p. 1946, Jul. 2023, doi: 10.3390/healthcare11131946.

[2] D. Alrahmany, A. F. Omar, A. Alreesi, G. Harb, and I. M. Ghazi, "Acinetobacter baumannii Infection-Related Mortality in Hospitalized Patients: Risk Factors and Potential Targets for Clinical and Antimicrobial Stewardship Interventions," Antibiotics, vol. 11, no. 8, p. 1086, Aug. 2022, doi: 10.3390/antibiotics11081086.

[3] C. M. Harding, S. W. Hennon, and M. F. Feldman, "Uncovering the mechanisms of Acinetobacter baumannii virulence," Nature Reviews Microbiology, vol. 16, no. 2, pp. 91–102, Dec. 2017, doi: 10.1038/nrmicro.2017.148.

[4] Geisinger, E., Huo, W., Hernandez-Bird, J., & Isberg, R. R. (2019). Acinetobacter baumannii: Envelope determinants that control drug resistance, virulence, and surface variability. Annual Review of ME. Geisinger, W. Huo, J. Hernandez-Bird, and R. R. Isberg, "Acinetobacter baumannii: Envelope Determinants That Control Drug Resistance, Virulence, and Surface Variability," Annual Review of Microbiology, vol. 73, no. 1, pp. 481–506, Jun. 2019, doi: 10.1146/annurev-micro-020518-115714.icrobiology, 73(1), 481–506. doi:10.1146/annurev-micro-020518-115714

PHENOTYPIC CHARACTERIZATION OF ACTINOBACTERIA ISOLATED FROM APHIDS ADELGES (APHRASTASIA) PECTINATAE (HEMIPTERA: ADELGIDAE)

Gustė Tamošiūnaitė[1], Jekaterina Havelka[2], Nomeda Kuisienė[1]

[1]Department of Microbiology and Biotechnology, Vilnius University, Lithuania
[2]Department of Zoology, Vilnius University, Lithuania
guste.tamosiunaite@gmc.stud.vu.t

Actinobacteria are Gram-positive bacteria with high guanine and cytosine content in their genetic structure [1]. Their metabolic versatility enables them to form diverse symbiotic relationships, including defensive associations with arthropods such as ants, beetles, and wasps, where they produce secondary metabolites that protect against pathogenic microorganisms [2]. Beyond their role in arthropod defense, they also contribute to plant health by colonizing surfaces or forming close symbiotic associations as rhizosphere or endophytic bacteria. Through the production of bioactive compounds like herbicides, fungicides, and biofertilizers, they promote plant growth and enhance resistance to diseases. This study investigates the phenotypic characterization of Actinobacteria isolated from aphids of the genus Adelges Vallot, 1836, sap-feeding pests that infect conifers of the family Pinaceae. Aphids maintain close associations with microorganisms through various interactions, including symbiotic relationships, the transmission of pathogens, and the dispersal of bacteria. The isolation of Actinobacteria began with the preparation of an aphid suspension, where aphids were crushed and plated on a microbiological medium. Based on their distinctive colony morphologies, five strains were subsequently isolated. These strains were designated C1, D8, D11, D15, and LB2. The 16S rRNA genes of the isolates were PCR-amplified and sequenced. Subsequent BLAST analysis confirmed their classification within the genus Frigoribacterium. Moreover, further examination of the 16S rRNA region revealed that these isolates share the greatest sequence similarity with Frigoribacterium faeni, indicating a close evolutionary relationship. Currently, delineation of prokaryotic taxa based on 16S rRNA gene sequence similarity stands at 98.7% for species and 94.5% for genera. The ultimate finding suggests that LB2 may belong to a particular species (sequence similarity 98.35%), whereas other strains (sequence similarity 95.95-96.43%) might potentially represent a novel species, however, additional genome analysis is needed. To further characterize these isolates, we conducted a phenotypic analysis, which included assessments of optimal growth temperature, pH tolerance, and salt tolerance. Additionally, motility tests as well as enzymatic activity assays, were performed, including catalase, gelatin hydrolysis, starch degradation, lipase, chitinase, and cellulase activity tests. Furthermore, glucose and ornithine fermentation, ability to reduce thiosulphate to sulphide tests, along with Biolog GEN III MicroPlate and API assays, were conducted to gain deeper insights into the metabolic properties of these bacterial strains. These assays assess the utilization of various carbon and nitrogen sources, enzymatic activities, and overall metabolic capabilities under standardized conditions.

[1] Barka, E. A., P. Vatsa, L. Sanchez, N. Gaveau-Vaillant, C. Jacquard, J. P. Meier-Kolthoff, H. P. Klenk, C. Clément, Y. Ouhdouch, and G. P. van Wezel, "Taxonomy, physiology, and natural products of Actinobacteria," Microbiol. Mol. Biol. Rev., vol. 80, no. 1, pp. 1–43, Nov. 2015, doi: 10.1128/MMBR.00019-15. Erratum in: Microbiol. Mol. Biol. Rev., vol. 80, no. 4, p. iii, Nov. 2016, doi: 10.1128/MMBR.00044-16.

[2] C. Olano and M. Rodríguez, "Actinomycetes Associated with Arthropods as a Source of New Bioactive Compounds," Curr. Issues Mol. Biol., vol. 46, no. 5, pp. 3822-3838, Apr. 2024, doi: 10.3390/cimb46050238.

MUTATIONAL ANALYSIS OF A NOVEL BACTERIAL DEFENSE SYSTEM

Vakarė Gavėnaitė[1], Tomas Šinkūnas[1], Inga Songailienė[1,2]

[1]Institute of Biotechnology, Life Sciences Center, Vilnius University, Lithuania
[2]University of Copenhagen, Novo Nordisk Foundation Center for Protein Research, Faculty of Health and Medical Sciences
vakare.gavenaite@gmc.stud.vu.lt

The ongoing cycle of co-evolution between bacteria and bacteriophages has led to the development of complex defense mechanisms in bacteria. For example, restriction-modification and the adaptive CRISPR-Cas systems target bacteriophage nucleic acids, helping to combat infection in its early stages. Additionally, small molecule defenses, such as prokaryotic viperins, produce modified nucleotides that inhibit viral transcription. Finally, abortive infection systems, like CBASS, act in later stages of infection by halting phage replication, slowing cell metabolism, or triggering programmed cell death. These are just a few examples of anti-phage systems with elucidated mechanisms of action. A recent discovery that genes encoding defense systems in prokaryotes tend to cluster in genomic regions called defense islands has led to the identification of numerous novel, previously unknown antiviral systems [1]. QatABCD is one of these newly discovered defense systems that can restrict P1, λ, and T3 dsDNA bacteriophages in *E. coli* [2]. Additionally, our data has shown that it can protect against Bas18 and Bas24 phages. However, the precise molecular mechanism of its action remains elusive.

Bioinformatic analysis of the proteins in this system revealed active sites typical of ATPases (QatA), 7-cyano-7-deazaguanine ($PreQ_0$) synthase (QatC), and TatD nuclease (QatD). It is hypothesized that a small molecule, 7-cyano-7-deazaguanine ($PreQ_0$), may be required for the system's activity and could act as a signaling molecule. In this study, we tested the influence of separate gene deletions and mutations in the putative active sites for the QatABCD defence against different bacteriophages.

[1] Doron, S. et al. Systematic discovery of antiphage defense systems in the microbial pangenome. Science 359, eaar4120 (2018).
[2] Gao, L. et al. Diverse enzymatic activities mediate antiviral immunity in prokaryotes. Science 369, 1077–1084 (2020).

INACTIVATION OF THE OPPORTUNISTIC PATHOGEN STENOTROPHOMONAS MALTOPHILIA BY 5-AMINOLEVULINIC ACID-BASED PHOTODYNAMIC THERAPY

Gabija Gervinskytė[1], Irina Buchovec[2]

[1]Institute of Biosciences, Department of Biochemistry and Molecular Biology, Life Sciences Center, Vilnius University, Lithuania
[2]Institute of Photonics and Nanotechnology, Faculty of Physics, Vilnius University, Lithuania
gabija.gervinskyte@gmc.stud.vu.lt

Antibiotics are the primary treatment for bacterial infections. However, the misuse and overuse of antibiotics have led to a global rise in multidrug-resistant (MDR) pathogens, posing a severe public health challenge. *Stenotrophomonas maltophilia* is an emerging opportunistic pathogen responsible for nosocomial infections. Due to its strong biofilm- forming ability and extensive antimicrobialg resistance, alternative inactivation strategies are needed [1]. One promising approachs is antimicrobial photodynamic therapy (aPDT), which utilizes a photosensitizer (PS), light and molecular oxygen to generate cytotoxic reactive oxygen species (ROS), leading to microbial cell damage and inactivation [2]. Porphyrins are widely used as a PS due to their high ROS generation efficiency, particularly singlet oxygen($^1O_2$), and broad absorption spectrum [3]. 5-aminolevulinic acid (ALA) serves as a precursor in the heme biosynthesis pathway, leading to the production of various endogenous porphyrins (protoporphyrin IX, uroporphyrin, coproporphyrin and metalloporphyrins) [4].

The study aimed to evaluate the endogenous porphyrin synthesis in different biofilm-forming and multi-drug resistant clinical isolates of *S. maltophilia* (SM3 and SM21) and assess the inactivation efficiency of ALA-based aPDT against them. *S. maltophilia* isolates were incubated with 0.5, 1, and 5 mM ALA in the dark at 37°C for up to 24 h. At different incubation periods, porphyrin fluorescence intensity was measured using excitation wavelengths within the Soret band (390 nm, 405 nm and 420 nm). Fluorescence excitation and emission spectra were recorded using an LS55 fluorescence spectrophotometer (PerkinElmer, USA), with excitation and emission slits set to 5 nm and 7.5 nm, respectively.

The results indicate that compared to the SM3 isolate, the SM21 clinical isolate synthesized a higher amount of porphyrins. These findings suggest that differences in porphyrin production among *S. maltophilia* isolates could influence their susceptibility to ALA-based aPDT. Further results, including aPDT inactivation efficiency and porphyrin quantification, will be presented in the poster session.

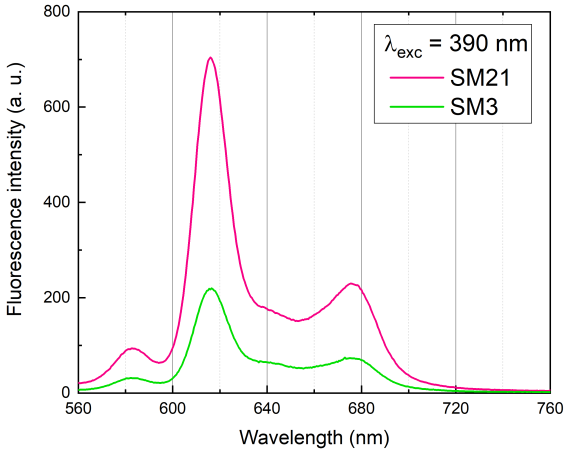


Fig. 1. Fluorescence emission spectra of *S. maltophilia* clinical isolates SM21 and SM3, excited at 390 nm after 24-hour incubation with 0.5 mM ALA.

Keywords: antimicrobial photodynamic therapy, *Stenotrophomonas maltophilia*, 5-aminolevulinic acid, porphyrin synthesis, multidrug resistance, fluorescence spectroscopy

[1] Pompilio, A. et al. Microorganisms vol. 9,1 49. 27 Dec. 2020, doi:10.3390/microorganisms9010049
[2] Polmickaitė-Smirnova, E. et al. Photochemical & photobiological sciences; vol. 18,11 (2019): 2730-2739. doi:10.1039/c9pp00200f
[3] Yang, F. et al. Biomedicine & pharmacotherapy = Biomedecine & pharmacotherapie; vol. 164 (2023): 114933. doi:10.1016/j.biopha.2023.114933
[4] Amos-Tautua, B. M. et al. Molecules (Basel, Switzerland); vol. 24,13 2456. 4 Jul. 2019, doi:10.3390/molecules24132456

STRUCTURAL INVESTIGATION OF A BACTERIAL ANTI-PHAGE SYSTEM

Miglė Paulikaitė[1], Monika Jasnauskaitė[1], Dr. Patrick Pausch[1]

[1]LSC-EMBL Institute for Genome Editing Technologies, Vilnius University, Lithuania
migle.paulikaite@gmc.stud.vu.lt

Bacteriophages (phages) pose a constant threat to bacteria, driving the evolution of diverse anti-phage defense mechanisms. Among these defense strategies, recently identified anti-phage systems involve protein components of eukaryotic ubiquitination pathways. Structural characterization of these proteins is essential for elucidating their role in bacterial immunity and phage evasion strategies.

In this study, we focus on the structural and mechanistic characterization of key proteins from a bacterial anti-phage system. Using recombinant expression strategies and a multi-step purification protocol involving affinity and size-exclusion chromatography, we successfully purified all system proteins with high yield and purity. This accomplishment ensures the samples are well-suited for further structural analysis. We intend to use cryo-electron microscopy (cryo-EM) to gain a deeper understanding of their three-dimensional organization. This approach will enable high-resolution imaging of protein complexes, providing important insights into their structural organization and conformational dynamics. A deeper understanding of bacterial anti-phage systems could contribute to improving the stability of bacterial cultures, benefiting applications such as fermentation and probiotic production.

MOLECULAR MECHANISMS DIFFERENTLY AFFECTING THE ATRIAL CELLS UNDER NORMOXIA AND HYPOXIA

Liepa Gedvilaitė[1], Dr. Rokas Mikšiūnas[1], Dr. Daiva Bironaitė[1]

[1]Department of Regenerative Medicine, State Research Institute Centre for Innovative Medicine
daibironai@gmail.com

Atrial disorders are often asymptomatic but can lead to serious complications, such as heart failure. One of the most common atrial disorders is arrhythmia, a condition characterized by an irregular heartbeat that impairs blood circulation and reduces oxygen supply to tissues.

In this study, an in vitro model of atrial disorders was established using the immortalized HL-1 mouse atrial cardiomyocyte cell line. The response of these cells to the cardiotoxic anticancer drug doxorubicin (Dox) was evaluated in combination with the antioxidant N-acetylcysteine (NAC) and the HIF-1α inhibitor PX-478 under normoxic and hypoxic (1 % oxygen) conditions. The effects of these compounds on cell viability were assessed spectrophotometrically using Alamar Blue staining, while HIF-1α expression was evaluated via real-time PCR.

The findings indicate that the cytotoxic effects of Dox on HL-1 cells were similar under both normoxic and hypoxic conditions. The HIF-1α inhibitor PX-478 enhanced Dox-induced cytotoxicity under hypoxia, while the antioxidant NAC protected cell viability in both oxygen conditions. Under normoxia, NAC exerted its protective effect by inhibiting reactive oxygen species (ROS) formation, whereas under hypoxia, its effect was linked to the stabilization of HIF-1α and the subsequent activation of cell survival pathways.

Acknowledgements
ElectroMechanoActive Polymer-based Scaffolds for Heart-on-Chip (EMAPS – Cardio)

PHENOLOXIDASE ACTIVITY OF MICROSCOPICFUNGI FOUND IN OLD-GROWTH FORESTS: DIVERSITY AND LIGNIN DEGRADATION POTENTIAL

Ieva Sokė[1,2], Dovydas Petlinskas[1,2], Daiva Burokienė[1]

[1]Laboratory of Plant Pathology, Nature Research Centre, Lithuania
[2]Life Sciences Center, Vilnius University, Lithuania
ieva.soke@gamtc.lt

Lignin is natural aromatic heteropolymer that is difficult to degrade due to its complex structure. The main sources of lignin as a by-product include pulp and paper production, agriculture and biorefineries. In these areas, physical and chemical methods are generally used to remove it. However, these approaches are costly, energy-intensive and environmentally harmful due to the formation of toxic products. An alternative method for lignin degradation is biological processes carried out by microorganisms that produce lignin oxidizing enzymes known as phenoloxidases.

Despite the ecological significance of lignin degradation, the diversity and characteristics of microscopic fungi in Punios Šilas Strict Nature Reserve and Plokštinė Strict Nature Reserve have not yet been studied. To fill this gap, we investigated the phenoloxidase activity of fungi colonizing four tree species – *Pinus sylvestris*, *Picea abies*, *Betula pendula*, *Quercus robur* – in two old forests of Lithuania.

In the summer of 2023, a total of 311 fungal cultures were obtained from the wood of two coniferous and two deciduous tree species. After dividing the isolates into 84 morphological groups, their phenoloxidase activity was determined [1]. According to the enzymatic activity index, the isolates were divided into strong, medium and weak activity groups [2]. It was also found that 0.2 % gallic acid had different effects on fungal growth. Insome cases, it promoted growth, while in others it inhibited it or had no significant effect. These results contribute to a better understanding of fungal diversity and their possible role in lignin degradation in the protected forest ecosystems of Lithuania.

[1] Bridžiuvienė D., Raudonienė V., 2013. Fungi surviving on treated wood and some of their physiological properties. Materials science, 19 (1): 43-50. https://doi.org/10.5755/j01.ms.19.1.3824

[2] Saroj P., Manasa P., Korrapati N., 2018. Characterization of thermophilic fungi producing extracellular lignocellulolytic enzymes for lignocellulosic hydrolysis under solid-state fermentation. Bioresources and bioprocessing, 5 (1): 1-14. https://doi.org/10.1186/s40643-018-0216-6

EXPLORING GENETIC BIOMARKERS IN PLASMA SAMPLES FROM CLEAR CELL RENAL CELL CARCINOMA PATIENTS

Milda Urbonaitė[1], Ieva Vaicekauskaitė[1,2], Algirdas Žalimas[3], Rasa Sabaliauskaitė[1,2]

[1]Institute of Biosciences, Life Sciences Center, Vilnius University, Vilnius, Lithuania
[2]National Cancer Institute, Vilnius, Lithuania
[3]National Cancer Center, Vilnius University Hospital Santaros Klinikos, Vilnius, Lithuania
milda.urbonaite@gmc.stud.vu.lt

Clear cell renal cell carcinoma (ccRCC) is the most common type of kidney cancer, constituting 70-80% of all renal malignancies [1]. Today, the diagnosis and prognosis of ccRCC rely heavily on tissue biopsy, an invasive procedure that may endanger patients and is limited in its ability to capture the heterogeneity of the tumor. Moreover, tissue biopsies are often performed only after the disease has progressed to an advanced stage, limiting opportunities for early intervention [2]. In contrast, using liquid biopsy – blood plasma, urine, or other biofluids – provides a minimally invasive, repeatable alternative that provides real-time insights into tumor dynamics. Tumor-derived biomarkers detectable in plasma, such as circulating DNA, RNA, or proteins, become powerful tools in this context [3].

The WNT and MYC pathways are important in tumorigenesis because they regulate essential cellular processes that are often dysregulated in cancer. The WNT pathway key gene is *CTNNB1* and *C-MYC* is the main gene in MYC. This *C-MYC* and *CTNNB1* are of particular interest due to their known roles in cell proliferation, metabolic reprogramming, and tumor progression in ccRCC [4][5].

The use of liquid biopsy-based methodologies for detecting ccRCC could revolutionize diagnostic protocols by providing a rapid and cost-efficient way of identifying malignant renal tumors. This study investigates the potential of *C-MYC* and *CTNNB1* as non-invasive biomarkers for the diagnosis of ccRCC.

In this study, RNA was isolated from 53 ccRCC patients and 26 individuals with benign renal tumors, of which 8 were angiomyolipomas and 18 were oncocytomas. Quantitative reverse transcription PCR (RT-qPCR) method was used for the analysis. ROC analysis was used to determine the diagnostic potential of the *C-MYC* and *CTNNB1* genes, with *GAPDH* serving as the reference gene.

The results' analysis demonstrated differential expression of the *C-MYC* and *CTNNB1* genes in ccRCC cases compared to control samples. Both *CTNNB1* and *C-MYC* effectively distinguished ccRCC cases from angiomyolipomas, with an AUC of 0.69. However, their ability to distinguish ccRCC from oncocytomas was lower, with *CTNNB1* achieving an AUC = 0.58 and *C-MYC* an AUC = 0.54. Furthermore, *CTNNB1* expression correlated with tumor diameter in the ccRCC patient group.

Changes in *C-MYC* and *CTNNB1* gene expressions detected in blood plasma samples may be useful for the early detection and prognosis of ccRCC. However, additional investigations are required to validate *CTNNB1* and *C-MYC* as reliable non-invasive biomarkers for ccRCC.

[1] K. L. Holbrook et al., "Detection and Validation of Organic Metabolites in Urine for Clear Cell Renal Cell Carcinoma Diagnosis," Metabolites, vol. 14, no. 10, p. 546, Oct. 2024, doi: https://doi.org/10.3390/metabo14100546.
[2] C. Mannelli, "Tissue vs Liquid Biopsies for Cancer Detection: Ethical Issues," Journal of Bioethical Inquiry, vol. 16, no. 4, pp. 551–557, Nov. 2019, doi: https://doi.org/10.1007/s11673-019-09944-y.
[3] I. Martins et al., "Liquid Biopsies: Applications for Cancer Diagnosis and Monitoring," Genes, vol. 12, no. 3, p. 349, Feb. 2021, doi: https://doi.org/10.3390/genes12030349.
[4] C. Yang, S. Ji, Y. Li, L. Fu, T. Jiang, and F. Meng, "β-Catenin promotes cell proliferation, migration, and invasion but induces apoptosis in renal cell carcinoma," OncoTargets and therapy, vol. 10, pp. 711–724, Feb. 2017, doi: https://doi.org/10.2147/OTT.S117933.
[5] D. M. Miller, S. D. Thomas, A. Islam, D. Muench, and K. Sedoris, "c-Myc and Cancer Metabolism," Clinical Cancer Research, vol. 18, no. 20, pp. 5546–5553, Oct. 2012, doi: https://doi.org/10.1158/1078-0432.ccr-12-0977.

STUDY OF POTENTIAL NEW DRUG COMBINATIONS FOR TREATMENT OF ENDOMETRIAL CANCER CELLS

Aistė Jarašūnaitė[1], Veronika Viktorija Borutinskaitė[1]

[1]Vilnius University, Department of Molecular Cell Biology
aiste.jarasunaite@chgf.stud.vu.lt

Endometrial cancer is the most common gynaecological pathology and is the sixth most common cancer in women worldwide, with an estimated 417,000 diagnoses in 2020. The disease incidence has increased by 132 percent over the last 30 years and is speculated to rise due to an ageing population and surging worldwide prevalence of obesity and diabetes. [1] Most notably, the 5-year survival rate has declined significantly over the past 30 years, this makes endometrial cancer one of only two cancers with rising mortality rates. [2] For patients with early-stage disease, hysterectomy is considered a definitive treatment. In contrast, advanced-stage and high-grade endometrial cancers are fatal. This is due to chemotherapy resistance and metastasis. Nevertheless, new therapies are being tested, aiming to improve treatment efficacy and patient outcomes, such as targeted therapies, immunotherapy, and hormone therapy, either alone or in combination. [3]

The aim of this study was to investigate the combination of epigenetic inhibitors and cannabidiol potential for endometrial cancer treatment in comparison to standard chemotherapy. The endometrium KLE cell line was treated with sodium butyrate, EGCG, BML-210, zebularine, cannabidiol, paclitaxel and cisplatin. We prepared cell growth analysis with Trypan Blue, apoptosis and cell cycle analysis with Propidium Iodide, gene expression analysis with quantitative Polymerase Chain Reaction, and protein analysis with Western Blot. We observed that combination of cannabidiol with HDACi or DNMTi reduced viability of the cells and increased apoptosis. Moreover, we discovered changes in the expression of genes responsible for actin cytoskeleton regulation, cell cycle, apoptosis, decidualization, genes critical in epigenetic regulation (DNMT1, DNMT3A, DNMT3B, HDAC1, EED, SUZ12, EHMT2) and in immune response.

In conclusion, the combination of epigenetic inhibitors and cannabidiol increases apoptosis and reduces proliferation. These findings provide new insights into the potential of combining cannabinoids with epigenetic therapy as an alternative approach for endometrial cancer treatment, warranting further investigation into its clinical applicability.

[1] Baker-Rand, H., & Kitson, S. J. (2024). Recent Advances in Endometrial Cancer Prevention, Early Diagnosis and Treatment. Cancers, 16(5), 1028. https://doi.org/10.3390/cancers16051028

[2] Leslie, K. K., Thiel, K. W., Goodheart, M. J., De Geest, K., Jia, Y., & Yang, S. (2012). Endometrial cancer. Obstetrics and gynecology clinics of North America, 39(2), 255–268. https://doi.org/10.1016/j.ogc.2012.04.001

[3] Tronconi, F., Nero, C., Giudice, E., Salutari, V., Musacchio, L., Ricci, C., Carbone, M. V., Ghizzoni, V., Perri, M. T., Camarda, F., Gentile, M., Berardi, R., Scambia, G., & Lorusso, D. (2022). Advanced and recurrent endometrial cancer: State of the art and future perspectives. Critical reviews in oncology/hematology, 180, 103851. https://doi.org/10.1016/j.critrevonc.2022.103851

ELECTROCHEMICAL INVESTIGATION OF CHO CELLS WITH VARIOUS REDOX MEDIATORS

Domantas Barkauskas[1,2], Tomas Mockaitis[2], Inga Morkvėnaitė- Vilkončienė[2,3], Ingrida Bružaitė[1,2]

[1]Faculty of Fundamental Sciences, Department of Chemistry and Bioengineering, Vilnius TECH, Lithuania
[2]Laboratory of Bioelectrochemical Technologies, Department of Nanotechnology, State Research Institute Centre for Physical Sciences and Technology, Vilnius 10257, Lithuania
[3]Department of Electrical Engineering, Vilnius Gediminas Technical University, Vilnius 10223, Lithuania
Domantas.barkauskas@stud.vilniustech.lt

Redox processes occurring in eukaryotic cells are crucial for understanding cellular metabolism and viability. Electrochemical methods enable the study of these processes, their accuracy and sensitivity also depend on the mediators used. When assessing the redox state of cells, it is important to observe how mediators influence electron transfer and adjust research outcomes. Studying cells using electrochemical methods without mediators, there is a risk that redox processes may not be detected at all. Additionally, improper selection of mediators can lead to cell death. Chinese hamster ovary (CHO) cells are widely used in the field of biotechnology due to their ability to easily adapt to changing environmental conditions, high productivity, and capability to perform various human-like modifications [1]. CHO cells are also valuable in electrochemical studies because the purine group metabolites in their structure, such as xanthine and guanine, can generate specific electrochemical signals, enabling the determination of cell viability and ongoing intracellular processes [2]. Scanning electrochemical microscope (SECM) studies will provide deeper insights into electrochemical methods and their application in studying living cells using mediators. The obtained results will also help determine whether mediators are necessary at all. This will contribute to future electrochemical cell studies aimed at more accurately assessing cell viability and redox processes using mediators [3]. This study aims to analyze behavior of CHO cells using SECM with two redox mediators, one lipophilic and one hydrophilic.

Acknowledgements

I would like to thank my lecturer, Inga Morkvėnaitė-Vilkončienė, for providing me with the opportunity to conduct my final thesis and internship under her supervision. I also extend my gratitude to Tomas Mockaitis for his immense help and advice on both practical and theoretical matters, as well as to Ingrida Bružaitė for her assistance in cell cultivation.

[1] P. Tang et al., Crit. Rev. Biotechnol., vol. 40, no. 3, pp. 1–15, (2020).
[2] W. Wang et al., J. Pharmacol. Toxicol. Methods, vol. 100, 106625, (2019).
[3] J. Petronienė et al., Electrochim. Acta, vol. 360, 136956, (2020).

REDOX PROPERTIES OF CHLOROBACULUM TEPIDUM FERREDOXIN:NADP$^+$ OXIDOREDUCTASE: POTENTIOMETRIC CHARACTERISTICS AND REACTIONS WITH PROOXIDANT XENOBIOTICS

Dominykas Laibakojis[1], Daisuke Seo[2], Mindaugas Lesanavičius[1], Narimantas Čėnas[1]

[1]Department of Xenobiotics Biochemistry, Institute of Biochemistry, Life Sciences Center, Vilnius University, Lithuania
[2]Division of Materials Science, Graduate School of Natural Science and Technology, Kanazawa University, Japan
dominykas.laibakojis@chgf.stud.vu.lt

Chlorobaculum tepidum ferredoxin:NADP$^+$ oxidoreductase (*Ct*FNR) is a thioredoxin reductase (TrxR)-type FNR with scarcely characterized redox properties and reactivity with nonphysiological electron acceptors. The enzyme employs a noncovalently bound FAD and acts in transforming between one- and two-electron transfer with its native substrates NADP(H) and low molecular weight protein ferredoxin (Fd). The TrxR-type FNRs exhibit a homodimeric structure with their NADP(H)-binding domain being inserted between two segments of FAD-binding domains. The domains are mobile during catalysis, as the distance between the bound NADP(H) and FAD is 15 Å, too great for efficient electron transfer [1,2].

In this study, we combined steady-state and presteady-state kinetic methods to examine the potentiometric characteristics of *Ct*FNR and its reactions with prooxidant xenobiotics. On the basis of redox reactions with 3-acetylpyridine adenine dinucleotide phosphate, the two-electron reduction midpoint potential of FAD cofactor was estimated to be –0.275 V, and photoreduction using 5-deazaFMN as a photosensitizer revealed that the difference in the redox potentials between the first and second single-electron transfer steps was 0.042 V. The enzymatic reaction proceeds via the *ping-pong* mechanism and exhibits the expected inhibition patterns by the reaction product NADP$^+$, namely competitive inhibition towards NADPH and uncompetitive inhibition towards a quinone. The reactivity of quinones and nitroaromatics towards *Ct*FNR increases with their increasing single-electron reduction midpoint potentials; however, the reactivity of nitroaromatics was lower due to their lower electron self-exchange rate. The reduction reaction of quinones proceeds in a mixed single- and two-electron way, and nitroaromatics are reduced via the single-electron reaction. The experiments with varied ionic strength of the buffer exhibit a trend similar to that seen in other TrxR-type FNRs from *Bacillus subtilis* and *Rhodopseudomonas palustris*: the k_{cat}/K_m of a noncharged electron acceptor remains constant, while it increases for the negatively charged FeEDTA$^-$ and decreases for the positively charged benzyl viologen upon increasing the ionic strength, thus giving insight into the role of charged amino acid residues in the vicinity of enzyme-bound FAD [3,4].

The obtained results are generally similar to those obtained with *Rp*FNR and *Bs*FNR and further expand our understanding of the novel TrxR-type FNRs and their catalysis.

[1] Hammerstad, M., Hersleth, H. P. (2021). Overview of structurally homologous flavoprotein oxidoreductases containing the low Mr thioredoxin reductase-like fold—A functionally diverse group. Arch. Biochem. Biophys., 702, 108826.
[2] Muraki, N., Seo, D., Shiba, T., Sakurai, T., Kurisu, G. (2010). Asymmetric dimeric structure of ferredoxin-NAD(P)+ oxidoreductase from the green sulfur bacterium Chlorobaculum tepidum: Implications for binding ferredoxin and NADP+. J. Mol. Biol., 401, 403–414.
[3] Lesanavičius, M., Seo, D., Čėnas, N. (2024). Thioredoxin Reductase-Type Ferredoxin: NADP+ Oxidoreductase of Rhodopseudomonas palustris: Potentiometric Characteristics and Reactions with Nonphysiological Oxidants. Antioxidants, 11(5), 1000.
[4] Lesanavičius, M., Seo, D., Maurutytė, G., Čėnas, N. (2024). Redox Properties of Bacillus subtilis Ferredoxin:NADP+ Oxidoreductase: Potentiometric Characteristics and Reactions with Pro-Oxidant Xenobiotics. Int. J. Mol. Sci., 25(10), 5373.

APPLICATION OF MICROFLUIDIC TECHNOLOGY TO α-SYNUCLEIN LIQUID-LIQUID PHASE SEPARATION STUDY

Saulė Rapalytė[1], Dominykas Veiveris[1], Karolis Goda[2], Mantas Žiaunys[1], Vytautas Smirnovas[1], Darius Šulskis[1]

[1]Sector of Amyloid Research, Institute of Biotechnology, Life Sciences Centre, Vilnius University
[2]Sector of Microtechnologies, Institute of Biotechnology, Life Sciences Centre, Vilnius University
saule.rapalyte@chgf.stud.vu.lt

α-Synuclein (α-Syn) is an intrinsically disordered protein associated with the pathogenesis of neurodegenerative diseases, including Parkinson's disease, dementia with Lewy bodies, and multiple system atrophy. α-Syn aggregates into amyloid fibrils, a major component of Lewy bodies, which is a marker for neuronal degeneration [1]. The aggregation of α-Syn can be initiated through liquid-liquid phase separation (LLPS) – a biophysical process involved in the formation of membraneless organelles [2]. Imitating intracellular environment requires precise control, therefore, our goal is to apply microfluidic technology for an in-depth LLPS study of α-Syn aggregation.

For this study we constructed and purified α-Syn with four fluorescent protein tags – eGFP, mCherry, mOrange, mCerulean. Initially, fluorescence microscopy was used to observe the LLPS process of each fluorescently tagged protein with wild type α-Syn. Then, we applied microfluidic technology that enables the study of rapidly generated subnanoliter volume droplets within microchannel systems [3]. We formed droplets containing α-Syn fibrils mixed with α-Syn monomer, suspended in a buffer solution, as well as with the molecular crowder polyethylene glycol (PEG), which induces LLPS. The resulting droplets were then analyzed using fluorescence microscopy.

Our study demonstrates that applying microfluidic technology to generate droplets containing α-Syn fibrils and monomers in the presence of PEG concentrates protein aggregates at the center of the droplets, compared to mixtures without a crowding agent. After separating aggregates from the droplets and using them as a seed for aggregation, the fibrils formed under LLPS conditions showed weaker aggregation compared to control and α-Syn fibrils formed without PEG in droplets. In the further steps, we will investigate the structures of α-Syn fibrils and optimize the application of microfluidic technology.

[1] Wakabayashi, K., Tanji, K., Mori, F. and Takahashi, H. (2007), The Lewy body in Parkinson's disease: Molecules implicated in the formation and degradation of α-synuclein aggregates. Neuropathology, 27: 494-506. https://doi.org/10.1111/j.1440-1789.2007.00803.x

[2] Ray, S., Singh, N., Kumar, R. et al. α-Synuclein aggregation nucleates through liquid–liquid phase separation. Nat. Chem. 12, 705–716 (2020). https://doi.org/10.1038/s41557-020-0465-9

[3] Ding, Y., Howes, P. D., & deMello, A. J. (2019). Recent advances in droplet microfluidics. Analytical Chemistry, 92(1), 132–149. https://doi.org/10.1021/acs.analchem.9b05047

WILD BEES AND WASPS (HYMENOPTERA: ACULEATA) IN RESTORED INLAND SAND DUNES IN SOUTHEASTERN LITHUANIA

Dominykas Slančiauskas[1]

[1]Institute of Bioscience, Life Sciences Center, Vilnius University, Lithuania
dominykas.slanciauskas@gmc.stud.vu.lt

One of the greatest threats to biodiversity is habitat loss. Xerothermic habitats associated with a high diversity of Hymenoptera insects are rapidly disappearing. [1]. Bees and wasps (Aculeata) are important in arthropod population management and plant pollination. [2]. Restoration of natural habitats can be important in restoring and preserving the Hymenoptera insect community. The Hymenoptera community depends on a relatively large diversity of ecosystem resources and can be an important biological indicator of ecosystem health. Therefore studies of this community may be important in assessing habitat quality and necessary conservation actions. [3]. The aim of the study was to assess the diversity of Hymenoptera in newly restored inland dunes in southeastern Lithuania.

The research was conducted in Dzūkija National Park, in the Alkūnės Kampas, Marcinkonys, and Dravių Kampas geomorphological reserves. In these areas, the LIFE integrated project ”Optimizing the Management of the Natura 2000 Network in Lithuania” was implemented, and in 2023 - 2024 three continental dune plots were opened for the restoration of habitats of European Community importance. Insects were caught in 2023 and 2024 from June to August. Ten yellow and white pan (Moericke) traps were used in open dune plots and surrounding forests (control samples) (Fig. 1). The collected insects were identified in the laboratory based on morphological characteristics to the species level.

During the study, 667 individuals of the order Hymenoptera from 103 species, 17 families, and 5 superfamilies were identified. The largest number of families was from the Apoidea superfamily (13), with the family Sphecidae having the largest number of individuals (220). The most species-rich family was Pompilidae (29). Of the identified species, 51 species were captured only in open inland dunes and 24 species were captured only in forest habitats. *Scolia hirta* (Schrank, 1781), which is listed in the Lithuanian Red Book, was caught in a trap in open dunes. 28 species were captured in both forest and open continental dune habitats, with the majority of species being relatively more abundant in the dunes. The average number of individuals per trap per day was higher in open continental dune habitats.

The study found that insect species associated with open sandy areas (bees and wasps), which provide important ecosystem services, increased in the open dunes. Inland dune restoration is still ongoing in the restoration project areas, so further research is important to assess the importance of such projects.

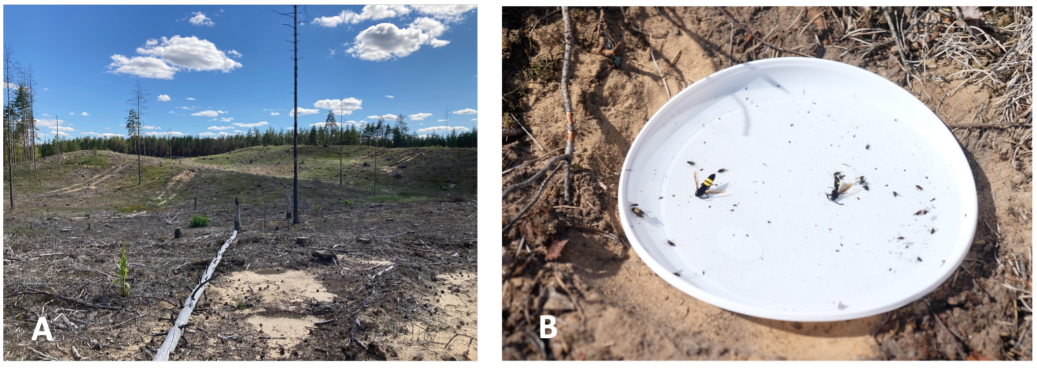


Fig. 1. (A) View of open inland dunes; (B) Pan (Moericke) trap in inland dune habitat.

Acknowledgements

I would like to thank Dr. Eduardas Budrys, Dr. Svetlana Orlovskytė, Miglė Lazauskaitė, Simonas Slančiauskas for their assistance in collecting research material and identifying insects.

[1] Exeler, N., Kratochwil, A., & Hochkirch, A. (2009). Restoration of Riverine Inland Sand Dune Complexes: Implications for the Conservation of Wild Bees. Journal of Applied Ecology, 46(5), 1097–1105.
[2] Brock, R.E., Cini, A., & Sumner, S. (2021). Ecosystem services provided by aculeate wasps. Biological Reviews, 96(4), 1645–1675.
[3] Buschini, M.L.T., Woiski, T.D. (2008). Alpha-beta diversity in trap-nesting wasps (Hymenoptera: aculeata) in Southern Brazil. Acta Zoologica, 89(4), 351–358.

HYMENOPTERA (INSECTA) IN LARGE DIAMETER DEAD TREE TRUNKS OF DECIDUOUS TREE SPECIES IN LITHUANIA

Simonas Slančiauskas[1]

[1]Institute of Biosciences, Life Sciences Center, Vilnius University
simonas.slanciauskas@gmc.stud.vu.lt

Large-diameter dead wood is an important component of the forest ecosystem and an indicator of sustainable forestry, which supports ecosystem diversity by providing natural habitats for many species of organisms [1]. Insects of the order Hymenoptera are extremely diverse in dead wood. This group is particularly rich in parasites, decomposers, and predators. They play an important role in the wood decay process and in controlling forest pest populations [2]. In the past, Hymenoptera associated with dead wood are rarely studied in Lithuania. Therefore, in order to preserve these insects, it is important to study the habitats in which they live. The aim of the study was to assess the diversity of Hymenoptera in the dead wood of four species of deciduous trees of the second decay class in unmanaged forests in Lithuania.

The study was conducted in old-growth forests of Lithuania: Būda Botanical-Zoological Reserve; Dubrava Reserve Area; Punios Šilas Strict Nature Reserve. These areas are part of the „Natura 2000“ ecological network of European importance. Insects were caught in 2021 from May to September. 18 trunk-emergence-type traps were installed on 4 tree species *(Alnus glutinosa, Betula sp., Populus tremula, Quercus robur)* of large-diameter deadwood trunks of the second decay class, covering a 1-meter section of deadwood (Fig. 1, B). The collected insects were described in the laboratory based on morphological characteristics to the family or subfamily level.

During the study, 1157 individuals of the order Hymenoptera from 12 superfamilies and 24 families were identified. The Aculeata group consisted of 231 individuals, most of which belonged to the family Formicidae (208), the Parasitica group consisted of 926 individuals with the most abundant family Ichneumonidae (191) (Fig. 1, A). On average, the largest number of individuals were caught from *Q. robur* trunks. The least number of different taxa (families) was captured on average from *A. glutinosa*, while the average number of different taxa was similar in other trees. Individuals from 12 families were caught from all tree species, and 7 from the wood of only one tree species. The family Ichneumonidae consisted of 14 different subfamilies. The highest average number of Ichneumonidae individuals caught was from *Q. robur*, and the lowest was from *P. tremula*.

The results of the study show that dead wood of deciduous trees is characterized by an extremely high diversity of Hymenoptera insects, especially parasitic wasps. Further research is needed to more fully assess the diversity of Hymenoptera in dead wood. By studying their habitat needs, these indicators could be used in protective habitat management.

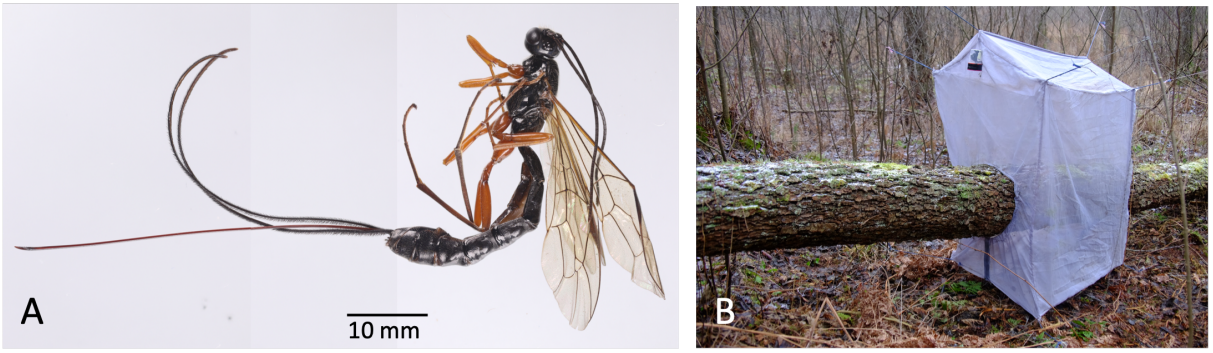


Fig. 1. (A) Pimplinae (Ichneumonidae), Canon EOS 80D camera, Canon Mp E 65 mm Macro Lens; (B) trunk-emergence-type trap on *A. glutinosa* trunk

Acknowledgements

I would like to thank Prof. Virginija Podėnienė for her help, Dr. Aistė Lekoveckaitė and Dr. Ina Gorban for collecting the research material, Dominykas Slančiauskas for his help in identifying the insects.

[1] Lier, M., Köhl, M., Korhonen, K. T., Linser, S., & Prins, K. (2021). Forest relevant targets in EU policy instruments-can progress be measured by the pan-European criteria and indicators for sustainable forest management?. Forest Policy and Economics, 128, 102481.

[2] Ulyshen, M. D., & Šobotnik, J. (2018). An introduction to the diversity, ecology and conservation of saproxylic insects. In: Ulyshen, M. D. (ed.), Saproxylic Insects: Diversity, Ecology and Conservation. Springer, 1–47.

RESEARCH OF MULTIENZYMATIC FLAVIN ADENINE DINUCLEOTIDE BIOSENSOR PLATFORM

Agnė Vanagaitė[1], Eimantas Ramonas[1]

[1]Department of Bioanalysis, Institute of Biochemistry, Life Sciences Center, Vilnius University, Saulėtekio av. 7, LT-10257 Vilnius, Lithuania
agne.vanagaite@gmc.stud.vu.lt

Flavin adenine dinucleotide (FAD) is a crucial redox cofactor involved in various metabolic and enzymatic processes. Accurate detection of FAD is essential for biomedical and biochemical applications, but current FAD detection techniques face challenges such as high costs and require specialized equipment, such as microplate readers. A more affordable and user-friendly biosensing approach is needed to improve FAD monitoring.

In this study, an enzymatic biosensor platform was developed incorporating horseradish peroxidase (HRP), PQQ-dependent glucose dehydrogenase (GDH), and apo-glucose oxidase (apo-GOx) for FAD detection. The biosensor works through a three-enzyme cascade, where FAD reconstitutes apo-GOx into its active form, enabling glucose oxidation and production of gluconolactone and hydrogen peroxide, which is used by HRP and results oxidized guaiacol (oxGUA) production [1]. GDH independently oxidizes glucose, and the electrochemical signal is generated through oxGUA, which serves as a mediator [2]. The biosensors performance was tested using electrochemical techniques, including chronoamperometry and cyclic voltammetry.

This research offers an innovative method for FAD detection, with potential applications in biomedical diagnostics and biochemical research.

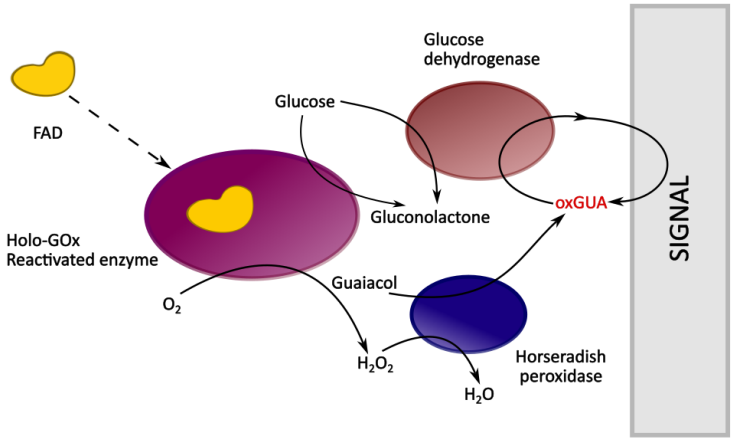


Fig. 1. Schematic representation of this biosensor.

[1] A. Gee, J. A. Grennell, S. Sitaula, J. Jayawickramarajah, and M. F. Ali, "Flavin Binding Allosteric Aptamer with Noncovalent Labeling for miR Sensing," Bioconjugate Chem., vol. 30, no. 11, pp. 2822–2827, Nov. 2019, doi: 10.1021/acs.bioconjchem.9b00561.

[2] M. Gandhi, D. Rajagopal, and A. Senthil Kumar, "Facile Electrochemical Demethylation of 2-Methoxyphenol to Surface-Confined Catechol on the MWCNT and Its Efficient Electrocatalytic Hydrazine Oxidation and Sensing Applications," ACS Omega, vol. 5, no. 26, pp. 16208–16219, Jul. 2020, doi: 10.1021/acsomega.0c01846.

MOLECULARLY IMPRINTED POLYMER BASED BIOSENSOR FOR SELECTIVE DETECTION OF THE SARS-COV-2 SPIKE PROTEIN.

Artem Yerniiazov[1], Sharunas Zukauskas[1,2], Arunas Ramanavicius[1]

[1]Vilnius University
[2]Fizinių ir technologijos mokslų centras
artem.yerniiazov@chgf.stud.vu.lt

There is a need for a cheaply available and sensitive Molecularly Imprinted polymer (MIP) based biosensor for SARS-CoV-2 spike protein detection.

MIP biosensor for selective detection of the SARS-CoV-2 spike protein in aqueous solutions via electrochemical impedance spectroscopy (EIS) of polydopamine (PDA)-based biosensor on a glassy carbon (GC) is promising in an aqueous solution via outer-sphere electron transfer from redox Fe(CN)6.

A sandwich-like architecture (GC electrode → PPy → PDA-MIP doped with AuNP → secondary PPy interconnecting layer) forming a conductive hybrid polymer nanostructure which is required for the MIPs EIS measurement upon binding of the target. Initially Ppy is electropolymerized on top of the electrode for continuous coverage of PDA-MIP. The PDA-MIP layer is applied via drop-casting, the MIP is fabricated via pH shift polymerization of dopamine in the presence of the spike pr otein template and AuNP dopant, ensuring non-denaturing conditions of the spike protein. Followed by a secondary PPy layer polymerized via cyclic voltammetry (CV), interconnecting the PDA-MIPs on the surface.

MIP biosensor exploits the conductive properties of PDA, PPy, and AuNPs, providing a platform for SARS-CoV-2 spike protein detection with high sensitivity and low limit of detection.

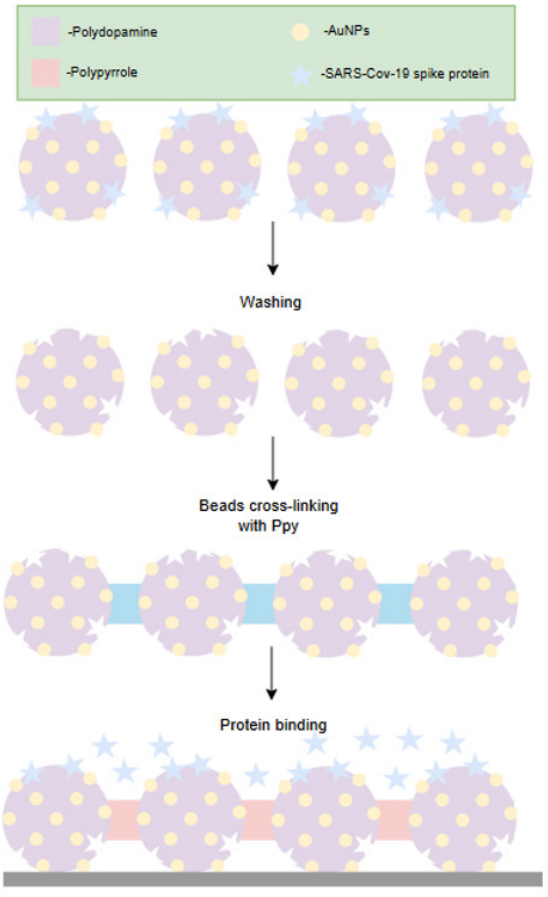


Fig. 1. Fabrication workflow of SARS-CoV-2 spike protein biosensor

Acknowledgements
Fizinių ir technologijos mokslų centras (FTMC), Vilnius Univesity (VU)

ANALYSIS OF DOPED BARIUM BORATE

Marius Dzvinka[1], Martynas Misevičius[1]

[1] Institute of Chemistry, Vilnius University
marius.dzvinka@chgf.stud.vu.lt

β-Barium borate is an important material commonly used in lasers due to nonlinear optical properties. This work concentrates on analyzing properties of lanthanide-doped β-barium borate.

The samples were produced using solid-state synthesis. The precursors included barium carbonate, boric acid, europium (III) oxide. Before the synthesis, stoichiometric amounts of reagents were mixed in agate mortar. After that the powders were sintered two times for 1 hour in 800 °C temperature in air.

The produced samples were firstly analyzed using X-ray diffractometer to check the purity of the powders. Only the specimen doped with 16% europium showed impurities which were identified as α-barium borate. The crystal unite cell of β-barium borate was refined using Rietveld method (Fig. 1). The optical properties of the europium-doped samples were checked using photoluminescence spectrometer. Europium(III)-doped samples exhibited expected phosphorence in the red part of the visible spectrum with strongest emission in 702 nm wavelength when excited by 393 nm wavelength light.

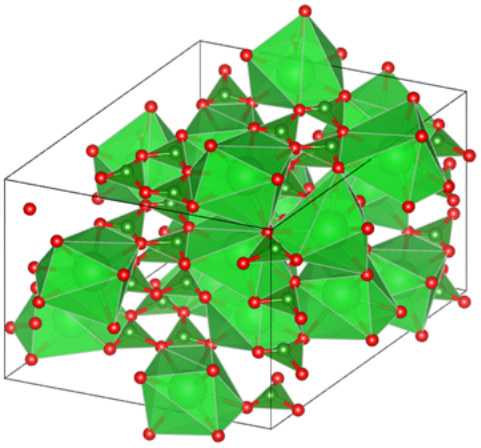


Fig. 1. Refined model of β-barium borate crystal unit cell

BISMUTH SULFIDE THIN FILM SYNTHESIS AND DEPOSITION ON FTO GLASS

Aistis Melnikas[1], Skirma Žalenkienė[1]

[1]Department of Physical and Inorganic Chemistry of Kaunas University of Technology, Lithuania
aistis.melnikas@ktu.edu

Bismuth sulfide is a prominent non-toxic n-type semiconductor, known for its band gap energy of 1.3 eV [1]. When paired with FTO glass, it emerges as an ideal choice for optoelectronic devices, especially suited for solar cells. Its excellent light absorption properties and simple synthesis contribute to its growing significance in next-generation photovoltaic systems.

Pre-patterned FTO (fluorine-doped tin oxide) substrates were cleaned thoroughly before deposition. The first approach to bismuth sulfide thin film synthesis was a chemical bath deposition method, using $Bi(NO_3)_3 \cdot 5H_2O$, L-cysteine, and $EDTA - Na_2$ as a chelating agent, whereas bismuth ions coordinate with it, forming stable $[Bi - EDTA]^-$ structures, which inhibits the direct bonding with S^{2-} ions. After the complete dissolution of all reagents, FTO substrates were inserted into the solution, all while keeping the bath at 90 °C for at least 8 hours to produce Bi_2S_3 thin films.

The other approach to this reaction is to utilize an autoclave, which differs significantly in reaction conditions and final product characteristics. Unlike the first method, synthesis using an autoclave occurs under a high temperature and pressure. This method results in better-defined with improved purity crystals.

All samples were analyzed by X-ray diffraction analysis on the Bruker D8 Advance diffractometer. Precipitate was scanned over the range 2θ = 3-70° at a scanning speed of 1° min^{-1} using a coupled two theta/theta scan type. This test determined structural characterization of the obtained materials. In addition, crystallite size of obtained Bi_2S_3 product was calculated using the Scherer equation. The acquired results were compared and discussed.

[1] Ajiboye, T. O., & Onwudiwe, D. C. (2021). Bismuth sulfide based compounds: Properties, synthesis and applications. In Results in Chemistry (Vol. 3). https://doi.org/10.1016/j.rechem.2021.100151

INVESTIGATION OF TIME-OF-FLIGHT RELIABILITY IN EVALUATING BIMOLECULAR RECOMBINATION IN BULK HETEROJUNCTION DEVICES

Martynas Stonkus[1], Kristijonas Genevičius[1], Romualdas Jonas Čepas[1]

[1] Institute of Chemical Physics, Faculty of Physics, Vilnius University, Lithuania
martynas.stonkus@ff.stud.vu.lt

Due to low charge carrier mobilities in disordered organic materials, compared to crystalline semiconductors, the concentration of charge carriers in third generation organic thin film solar cells must be much higher to achieve comparable efficiencies to their non-organic counterparts. Previous studies have demonstrated that for these low-mobility organic materials, the primary mechanism limiting current density is Langevin-type bimolecular recombination. This type of recombination can be reduced by taking advantage of the morphology of bulk heterojunctions (BHJ), which is comprised of bicontinuous interpenetrating networks of acceptor and donor materials, where carriers are spatially separated. This makes the encounter probability for the carriers less likely and reduces Langevin recombination. This in turn makes the reduction factor an important testing parameter to achieve high efficiency organic thin film solar cells.

There are several methods to measure the bimolecular recombination coefficients in BHJ, including Transient Photovoltage (TPV), Transient Photocurrent (TPC) and integral mode Time-Of-Flight (Q-TOF) techniques. TPV and TPC techniques provide valuable insights into charge carrier dynamics by analyzing voltage and current decay after a small perturbation, however their reliance on low-intensity probing makes them susceptible to noise, and their applicability is restricted to open-circuit and short-circuit conditions [1]. Additionally, in multilayered devices, distinguishing capacitance contributions from different layers complicates the analysis, potentially leading to inaccuracies. In contrast, the Q-TOF technique, introduced in [2], can offer more direct measurements of charge transport and recombination in operational multilayered devices under applied electric field that are less affected by multilayer capacitance contributions, making it a more robust method for characterizing carrier dynamics in complex device architectures. In this study we are investigating the necessary experiment conditions introduced in the original paper, including high load resistance, high light intensity and bulk charge carrier generation ($\alpha d \leq 1$), as well as the effect of diffusion and carrier mobility ratio on the calculated bimolecular recombination coefficient value.

In order to better assess the reliability of Q-TOF technique the experiment was numerically modelled as a one-dimensional system by solving Poisson and current continuity equations utilizing the finite difference method. Using these numerical calculations, working limits for Q-TOF technique were set.

Obtained results demonstrated that diffusion lowers the accuracy of the method by approximately 20%, while photogeneration profile had negligible impact on the techniques accuracy (up to $\alpha d = 10$). In addition, different carrier mobility ratios introduce a deviation in calculated bimolecular recombination values.

[1] J. Vollbrecht, N. Tokmoldin, B. Sun, V. V. Brus, S. Shoaee, and D. Neher, “Determination of the charge carrier density in organic solar cells: A tutorial,” J Appl Phys, vol. 131, no. 22, p. 221101, Jun. 2022, doi: 10.1063/5.0094955/2836979.

[2] A. Pivrikas et al., “Bimolecular recombination coefficient as a sensitive testing parameter for low-mobility solar-cell materials,” Phys Rev Lett, vol. 94, no. 17, May 2005, doi: 10.1103/PHYSREVLETT.94.176806.

MOLTEN SALT SYNTHESIS AND INVESTIGATION OF RADIOCHROMIC BARIUM APATITE

Simona Bendziute[1], Aleksej Zarkov[1]

[1]Institute of Chemistry, Faculty of Chemistry and Geosciences, Vilnius University, Naugarduko 24, LT-03225 Vilnius, Lithuania
simona.bendziute@chgf.stud.vu.lt

Recently, optical materials and their luminescent properties have become a highly relevant topic. There are inorganic materials that exhibit the radiochromic/photochromic effect — a reversible color change that occurs due to formation of defects in the materials crystal structure, leading to different absorption spectra. Due to the favorable crystalline structure for the photochromic effect, apatite-type compounds are the most dominant in scientific research. One of such promising compounds is barium chlorapatite ($Ba_5(PO_4)_3Cl$), which undergoes a color change that persists for a certain period of time, when exposed to X-ray radiation. Such materials are promising for the development of information technologies, medicine, the military industry and everyday life.

This study focuses on the impact of synthesis conditions on the intensity of the radiochromic effect and the persistence of the altered color in $Ba_5(PO_4)_3Cl$. The first part of the research involves optimizing the synthesis conditions, taking into account the synthesis temperature. In the next research stage, color changes are monitored over time. Results show tendencies that there is a particular optimal temperature for the most intense color change as well as slow, gradual color fading as the time passes. The phase purity and crystal structure of the synthesis products were analyzed using powder X-ray diffraction (XRD) and Fourier-transform infrared spectroscopy (FTIR). Morphological properties were observed using a scanning electron microscope (SEM).

EPR INVESTIGATION OF ENCAPSULATED ATOMIC HYDROGEN IN POSS CAGES FOR QUANTUM TECHNOLOGIES

Justinas Turčak[1], Gediminas Usevičius[1], Vidmantas Kalendra[1], Jūras Banys[1], George Mitrikas[2], Mantas Šimėnas[1]

[1]Faculty of Physics, Vilnius University, Sauletekio 9, LT-10222 Vilnius, Lithuania
[2]Institute of Nanoscience and Nanotechnology, NCSR Demokritos, Athens 15310, Greece
justinas.turcak@ff.vu.lt

Electron spins in solid-state matrices are among the most studied platforms for quantum technologies, offering sufficiently long coherence times. Various spin systems have been extensively explored – some excel in isolation (e.g., donor spins [1]), while others provide better control (e.g., quantum dots [2]). A novel promising candidate for a spin-based spin qubit platform is an encapsulated atomic hydrogen in polyhedral oligomeric silsesquioxane (POSS) cages [3, 4]. This system exhibits a clock transition, making it insensitive to first-order external magnetic field fluctuations, a property that can be leveraged to increase coherence time. Here, we employ electron paramagnetic resonance (EPR) spectroscopy to study the coherence and relaxation properties of encapsulated atomic hydrogen in POSS cages at low temperature and at both X-band ($\sim$ 9.5 GHz) and at the famous 1420 MHz hydrogen line. Additionally, we describe the specialized equipment developed for this study: a custom L-band (1 – 2 GHz) EPR probe with low noise amplifiers cooled in closed-cycle He cryostat [5] and employment of a home-built EPR spectrometer capable of operating up to 12 GHz frequencies.

[1] G. Wolfowicz et al., "Atomic clock transitions in silicon-based spin qubits," Nature Technology, vol. 8, pp. 561-564, 2013.
[2] D. Loss and D. P. DiVincenzo, "Quantum Computing with Quantum Dots", Physical Review A, vol. 57, no. 1, pp. 120–126, 1998.
[3] G. Mitrikas and S. Menenakou, "Electron spin relaxation properties of atomic hydrogen encapsulated in octavinyl POSS cages," Physical Chemistry Chemical Physics, vol. 22, no. 28, pp. 15751–15758, 2020.
[4] G. Mitrikas, "Encapsulated Atomic Hydrogen in Octamethyl-POSS Cages: A Pulsed EPR Study," ChemPlusChem, vol. 89, no. 11, p. e202400146, 2024.
[5] M. Šimėnas et al., "A sensitivity leap for X-band EPR using a probehead with a cryogenic preamplifier," Journal of Magnetic Resonance, vol. 322, p. 106876, 2021.

IMPACT OF STARTING MATERIALS AND Ba^{2+} DOPING CONCENTRATION ON THE MICROSTRUCTURE AND PHASE FORMATION OF La_2 Mo_2O_9

Ugnė Vazgelevičiūtė[1], Artūras Žalga[1], Giedrė Gaidamavičienė[1]

[1]Faculty of Chemistry and Geosciences, Institute of Chemistry, Vilnius University, Naugarduko str. 24, LT-03225 Vilnius, Lithuania
ugne.vazgeleviciute@chgf.stud.vu.lt

In the past decades, fast oxide-ion conductors have garnered significant attention due to their promising applications in high-temperature electrochemical devices, such as solid oxide fuel cells (SOFCs), oxygen sensors and other related technologies [1]. Oxide-ion conductors play a vital role in solid oxide fuel cells, and yttria-stabilized zirconia is a widely used electrolyte because it offers high ionic conductivity at around 1000 °C. Another promising candidate is $La_2Mo_2O_9$. However, lanthanum molybdate undergoes a phase transition from high-temperature cubic β-phase to low-temperature monoclinic α-phase at 580 °C, resulting a sudden drop in conductivity. Substituting lanthanum or molybdenum sites with appropriate dopants can suppress this phase transition, stabilizing the β-phase and ensuring high ionic conductivity at lower temperatures [2].

Several physical, structural, and morphological properties are essential for SOFC performance. The microstructural characteristics of SOFC electrolytes are critical for their performance and durability. Key properties include high density, absence of cracks and large pores, and uniform grain distribution. A dense ceramic structure prevents gas mixing between the fuel and oxidant, ensuring efficient operation, while the elimination of cracks and excessive porosity enhances both mechanical stability and ionic conductivity. Additionally, a homogeneous grain structure reduces grain boundary resistance, optimizing ion transport [3]. These properties are highly influenced by the nature of the starting materials, which is why it is very important to choose the right precursors to achieve maximum efficiency.

In this study, the effects of precursor selection and Ba^{2+} doping concentration on the microstructure and phase formation of $La_2Mo_2O_9$ ceramics were investigated. $La_{2-x}Ba_xMo_2O_{9-y}$ ceramics were synthesized using aqueous sol-gel method. X-ray diffraction (XRD) analysis was used to determine the crystal structure, assess solubility limit of barium, and detect any impurity phases of the annealed ceramics. Additionally, scanning electron microscopy (SEM) and energy dispersive X-ray spectroscopy (EDX) analyses enabled the evaluation of the influence of starting materials on the surface morphology and homogeneity of the final $La_{1.9}Ba_{0.1}Mo_2O_{8.95}$ ceramics.

[1] D. Zhang, et al., Electrical properties and microstructure of nanocrystalline La2−xAxMo2O9−Y (A = Ca, Sr, Ba, K) films, Solid State Ionics, 181, 1510-1515, 2010.
[2] Shao, Lingbo, et al. Synthesis and characterization of tungsten and barium co-doped La2Mo2O9 by sol-gel process for solid oxide fuel cells, Journal of Rare Earths, 37.9, 984-988, 2019.
[3] Marrero-López, D., et al. Synthesis and transport properties in La2−xAxMo2O9-δ (A= Ca2+, Sr2+, Ba2+, K+) series, Electrochimica acta, 52, 5219-5231, 2007.

SUBSTRATE SPECIFICITY STUDY OF AI-GENERATED BOS TAURUS TERMINAL DEOXYNUCLEOTIDE TRANSFERASE VARIANTS

Simona Lukšytė[1], Roberta Statkevičiūtė[1], Andrius Burdulis[2], Taisija Dėmčėnko[2], Linas Zakrys[2], Skaistė Valinskytė[2], Rolandas Meškys[1]

[1]Department of Molecular Microbiology and Biotechnology, Institute of Biochemistry, Life Sciences Center, Vilnius University, Saulėtekio av. 7, Vilnius, Lithuania
[2]Biomatter Designs UAB, Business Stadium West, Rinktines str. 5-101, Vilnius, Lithuania
simona.luksyte@gmc.stud.vu.lt

Terminal deoxynucleotidyl transferase (TdT) is a unique DNA polymerase that catalyses the addition of nucleotides to the 3' terminus of a DNA molecule without the need for a template. The ability of TdT to incorporate modified nucleotides has potential applications in creating functionalized DNA for diagnostic tools, therapeutics, and advanced materials for DNA origami and biosensors [1]. Due to the mesophilic nature of wild-type TdT, its efficiency is limited in vitro, particularly when working with modified nucleotides or structured DNA templates, as the enzyme's activity decreases at elevated temperatures needed for substrate accessibility and reduced secondary structure formation [2].

This study aims to evaluate the efficiency of novel AI-generated TdT variants with enhanced thermostability and the ability to incorporate various modified nucleotides and ribonucleotides into oligonucleotide chains, comparing their performance to that of the wild-type enzyme.

AI-designed TdT variants and N-terminal truncated protein variants were produced in *Escherichia coli* KRX strain. The recombinant proteins were purified using a two-step chromatography approach and used for enzymatic primer extension reactions by incorporation of various unnatural nucleotides such as alkyne-modified nucleotides (5-propargylamino-dUTP, C8-alkyne-dUTP, 5-ethynyl-UTP/dUTP) and thio-modified nucleotides (4-thio-UTP, 6-thio-GTP/dGTP) at various temperatures.

The AI-generated TdT variants demonstrated similar or better activity in extending ssDNAs with all used nucleoside triphosphates by incorporating one to several nucleotides onto the 3′-end of the primer compared to the wild-type enzyme. Among the tested variants, TdT-P15 showed no reduction in enzymatic activity even at 70 °C, which is 25 degrees above the thermostability limit of the wild-type enzyme. However, TdT-P15 variant possessed diminished thermostability after N-terminus truncation. This suggests that N-terminus may be also responsible for protein thermostability.

The successful development of TdT variants with enhanced thermostability and ability to incorporate modified nucleotides opens new paths for enzymatic DNA synthesis and modification applications.

[1] J. Ashley, I. G. Potts, and F. J. Olorunniji, "Applications of Terminal Deoxynucleotidyl Transferase Enzyme in Biotechnology," Nov. 2022
[2] S. Barthel, S. Palluk, N. J. Hillson, J. D. Keasling, and D. H. Arlow, "Enhancing Terminal Deoxynucleotidyl Transferase Activity on Substrates with 3′ Terminal Structures for Enzymatic De Novo DNA Synthesis," Genes, vol. 11, no. 1, p. 102, Jan. 2020

INFLUENCE OF PROCESS CONDITIONS ON THE PYROLYTIC CONVERSION OF PLASTICS: FOCUS ON THE REACTION KINETICS AND PRODUCT DISTRIBUTION

Ieva Kiminaitė[1], Simon Schuler[2], Clara Leonie Brigitte Eckert[2], Vilmantė Kudelytė[1]

[1]Lithuanian Energy Institute
[2]Technical University of Munich
ieva.kiminaite@lei.lt

Plastic waste is one of the greatest challenges facing the world today. Mechanical recycling is still highly limited in efficiently recycling plastic waste – secondary plastics lose their mechanical properties due to thermo-oxidative degradation during the process. Also, the process requires homogeneous and clean streams. Consequently, the main treatment method in Europe remains incineration for heat energy recovery, which emits large amounts of CO2, accelerating global warming. In the present research a low carbon footprint process – pyrolysis of plastic packaging waste was investigated, estimating the product distribution dependence on pyrolysis conditions along with conversion rates determination by Arrhenius approach and a single first-order reaction model. The temperature influence was investigated to up to 1400 °C maintaining the samples for 0.5–420 s to estimate the decomposition rate, measuring the weight changes in a lower scale (wire mesh reactor) and a higher scale – fixed bed reactor with a high-temperature furnace. The gaseous products evolved were analysed by mass spectrometry and a solid product by Raman spectroscopy and scanning electron microscopy. The influence of the slow heating rate was estimated by carrying thermogravimetric analysis combined with Fourier transform infrared spectroscopy (FTIR) and gas chromatography-mass spectrometry (GC–MS), which results are illustrated in Figure 1. The main components of the plastic packaging feedstock were polypropylene and polyethylene terephthalate, established by simultaneous thermal analysis. Pyrolysis conditions determined the conversion process and the composition of pyrolysis volatile organic compounds and reaction kinetics. Pyrolysis temperature elevation positively influenced the yields of lower molecular weight hydrocarbons and hydrogen gas and reaction rate with varying effect. Additionally, the formation of carbon black, an industrially valuable product was confirmed during flash pyrolysis carried out in a high-temperature tube reactor. Overall, this research enhances the understanding and development of plastic waste upcycling via pyrolysis targeting high-value products recovery, aligning with circular economy principles.

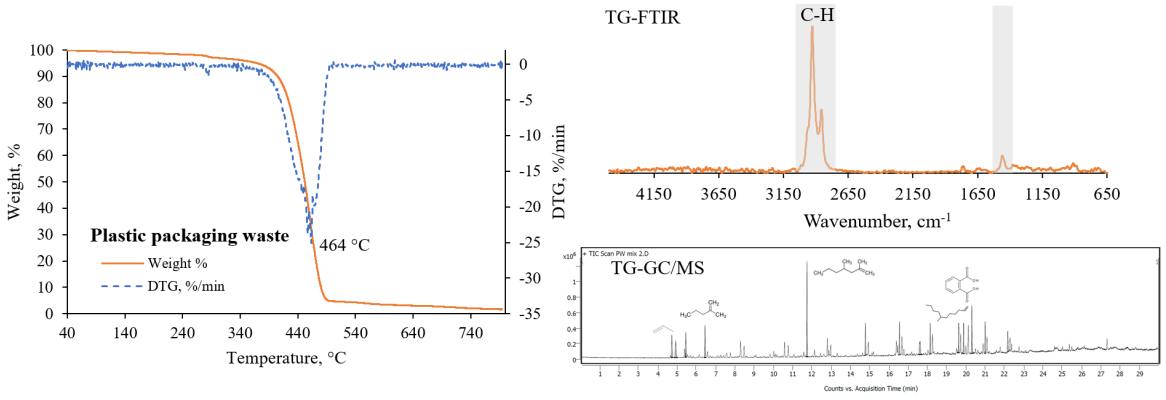


Fig. 1. TG-FTIR-GC/MS analysis results of plastic packaging waste pyrolysis in heating rate of 15 °C/min

Acknowledgements

The corresponding author sincerely acknowledges Prof. Hartmut Spliethoff and Dr. Sebastian Fendt for their support during the scientific internship, which greatly contributed to the generation of valuable results and the deepening of knowledge. Special appreciation is extended to M. Sc. Sebastian Wilhelm for his expertise in reaction kinetics and his guidance throughout the course of this research.

[1] Plastics Europe. The Circular Economy for Plastics – A European Analysis 2024. 2024.
[2] Jin H, Gonzalez-Gutierrez J, Oblak P, Zupančič B, Emri I. The effect of extensive mechanical recycling on the properties of low density polyethylene. Polym Degrad Stab 2012;97:2262–72. https://doi.org/10.1016/j.polymdegradstab.2012.07.039.
[3] Papari S, Bamdad H, Berruti F. Pyrolytic conversion of plastic waste to value-added products and fuels: A review. Materials (Basel) 2021. https://doi.org/10.3390/ma14102586.
[4] Karaduman A, Şimşek E., Çiçek B, Bilgesü A. Flash pyrolysis of polystyrene wastes in a free-fall reactor under vacuum. J Anal Appl Pyrolysis 2001;60:179–86. https://doi.org/10.1016/S0165-2370(00)00169-8.
[5] Bortoluzzi JH, Cristiano R, Gallardo HA, Carasek E, Soldi V. Use of the SPME-GC-MS technique to study the thermal degradation of isotactic polypropylene: Effects of temperature and reaction time, and analysis of the reaction mechanism. E-Polymers 2008;8. https://doi.org/10.1515/epoly.2008.8.1.193.

VIBRATIONAL SPECTROSCOPY STUDY OF ANCHOR MOLECULE STRUCTURE FOR MODEL LIPID MEMBRANES

Kamilla Kalmykova[1], Vaidas Pudžaitis[1], Martynas Talaikis[1]

[1]Department of Organic Chemistry, Center for Physical Sciences and Technology, Vilnius, Lithuania
kamilla.kalmykova@stud.vilniustech.lt

Tethered bilayer lipid membranes (tBLMs) are artificial structured membranes that are used to imitate natural cell membranes, which helps us to analyze how biological membranes work. tBLMs are constructed of a lipid bilayer that is anchored to the solid support, which is typically to a gold surface, by the self-assembled monolayer (Figure 1).

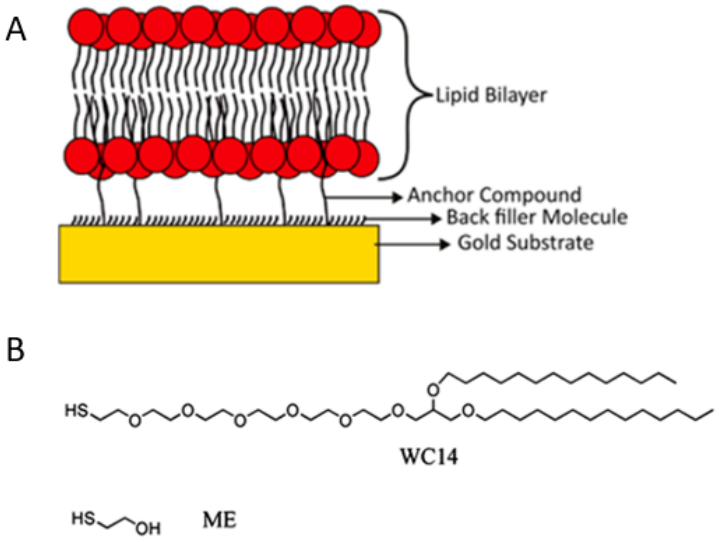


Fig. 1. (A) Cartoon of tBLM architecture [1]. (B) Structures of WC14 and β-mercaptoethanol [2].

Self-assembled monolayer consists of anchor thiol WC14 (20-tetradecyloxy-3,6,9,12,15,18,22-heptaoxahexatricontane-1-thiol) and back-filler β-mercaptoethanol molecules. The WC14 molecule is composed of three structural segments: the thiol group that attaches the molecule to the surface, the ethylene glycol that acts as a spacer, and two alkyl chains that immobilize the lipid bilayer. The structure and surface concentration of the anchor molecules significantly affect the biophysical properties of the tBLMs, such as integrity and fluidity. These parameters directly affect sensitivity to membrane-damaging agents such as pore-forming toxins.

In this work, we intended to study how the structure and orientation of anchoring molecules change on the gold surface when employing different WC14 homologs and concentrations. For that, we analyzed two different chain lengths of anchor molecules: WC14 with 6 and 4 ethylene glycol segments. By using spectral markers of surface-enhanced infrared absorption spectroscopy (SEIRAS), we found that the lower concentrations of WC14 anchor molecule and the shorter ethylene glycol segment lead to more flexible and distorted spacer segment [3].

[1] Shivabalan, A. P., Ambrulevicius, F., Talaikis, M., Pudzaitis, V., Niaura, G., & Valincius, G. (2023). Effect of pH on Electrochemical Impedance Response of Tethered Bilayer Lipid Membranes: Implications for Quantitative Biosensing. Chemosensors, 11(8). https://doi.org/10.3390/chemosensors11080450

[2] Talaikis, M., Eicher-Lorka, O., Valincius, G., & Niaura, G. (2016). Water-induced structural changes in the membrane-anchoring monolayers revealed by isotope-edited SERS. Journal of Physical Chemistry C, 120(39), 22489–22499. https://doi.org/10.1021/acs.jpcc.6b07686

[3] Penkauskas, T., Jankunec, M., & Valincius, G. Tethered bilayer lipid membranes for picomolar detection of pore-forming toxins. OpenReadings, 2017, conference abstract

POSTER SESSION 3

Biochemistry, Biophysics and Biotechnology
Biology, Genenetics and Biomedical Sciences

THE EFFECT OF NOVEL HYDRAZONE DERIVATIVES ON HUMAN BRAIN, TRIPLE-NEGATIVE BREAST, AND SKIN CANCER CELL LINES

Tomas Ragauskas[1], Juozas Kiltinavičius[2], Ingrida Tumosienė[2], Kristina Kantminienė[3], Vilma Petrikaitė[1]

[1]Department of Drug Targets Histopathology, Institute of Cardiology, Lithuanian University of Health Sciences, Lithuania
[2]Department of Organic Chemistry, Kaunas University of Technology, Lithuania
[3]Department of Physical and Inorganic Chemistry, Kaunas University of Technology, Lithuania
tomas.ragauskas@stud.lsmu.lt

Triple-negative breast cancer accounts for 10–15% of all new cases of breast cancer but has a poor prognosis and aggressive behavior [1]. Melanoma accounts for 1.7% of global cancer diagnoses and is the fifth most common cancer in the US [2]. The global incidence of glioblastoma is considered rare but with poor prognosis and a survival rate of 14–15 months [3]. Targeted drugs have made remarkable progress in the treatment of cancer. Therefore, potential kinase inhibitor hydrazone derivatives are expected to contribute to the efficacy of treatment. The aim of our research was to evaluate the anticancer activity of hydrazone derivatives synthesized at Kaunas University of Technology (Lithuania) in human triple-negative breast, melanoma, and glioblastoma cell lines.

In our study, we investigated the activity of 22 hydrazone derivatives bearing substituted aromatic and different heterocyclic moieties on triple-negative breast cancer cell line MDA-MB231, melanoma cell line IGR39, and glioblastoma cell line U87. The effect on cell viability was determined by the MTT assay at 50 μM of compounds after 72 hours of incubation. Compounds with significant cell viability-reducing capabilities were chosen for further studies and the EC_{50} values were established.

Compounds IT199, IT207, IT224, IT227, and IT231 reduced the viability of at least one cell line by up to appr. 20–25%. Evaluation of the selectivity of the compounds for cancer cells showed that compound IT224 is selective to IGR39 and IT231 is selective to MDA-MB231 cell line, compound IT199 is selective to IGR39 and MDA-MB231 and IT207 is selective to IGR39 and U87 cell lines while the compound IT227 significantly reduced all three cell lines investigated in this study. These compounds were selected for the determination of EC_{50} values, which would be used for further studies on cell migration and the activity on 3D cell cultures. Based on estimated EC_{50} values, IT207 and IT227 reduced the viability of IGR39 cell line about 50% stronger than sunitinib. Compound IT227 reduced the viability of MDA-MB231 cell line 2 times stronger than sunitinib. Compounds IT199, IT207 and IT227 reduced the viability of U87 cell line from 3 to 9 times.

In conclusion, compounds IT199, IT207, IT224, IT227, and IT231 showed a significant reduction of cell viability by MTT assay and were chosen as potent candidates for further anticancer activity studies.

[1] A. M. Karim et al., „Triple-negative breast cancer: epidemiology, molecular mechanisms, and modern vaccine-based treatment strategies“, Biochemical Pharmacology, t. 212, p. 115545, Jun. 2023, doi: 10.1016/j.bcp.2023.115545.
[2] K. Saginala, A. Barsouk, J. S. Aluru, P. Rawla, and A. Barsouk, ‘Epidemiology of Melanoma’, Med Sci (Basel), vol. 9, no. 4, p. 63, Oct. 2021, doi: 10.3390/medsci9040063.
[3] F. Hanif, K. Muzaffar, K. Perveen, S. M. Malhi, and S. U. Simjee, ‘Glioblastoma Multiforme: A Review of its Epidemiology and Pathogenesis through Clinical Presentation and Treatment’, Asian Pac J Cancer Prev, vol. 18, no. 1, pp. 3–9, 2017, doi: 10.22034/APJCP.2017.18.1.3.

STUDY OF INNATE RESISTANCE OF HUMAN COLORECTAL CANCER CELLS

Ieva Norkaitytė[1], Eglė Žalytė[1]

[1]Department of Biochemistry and Molecular Biology, Institute of Biosciences, Vilnius University Life Sciences Center, Lithuania
ieva.norkaityte@gmc.stud.vu.lt

Colorectal cancer is the third most frequently diagnosed cancer, and the second most common cause of cancer-related deaths worldwide [1]. Many chemotherapy drugs are used to treat this cancer, but in many cases the effectiveness of the drug treatment is impaired by the tumour's innate or acquired resistance to chemotherapy treatment. Innate resistance can be caused by tumour heterogeneity, where the tumour is composed of sub-populations with different sensitivities, which makes eradication of the cancer extremely difficult.

To investigate the heterogeneity of DLD-1 human colorectal cancer cells, this cell line was cloned by seeding the cells one at a time in separate plates and waiting for the formation of separate clonal populations. From the 26 clones produced, those with a different sensitivity to chemotherapeutic drugs oxaliplatin and cisplatin compared to the parental line were selected. The viability of the parental DLD-1 line and its clones K, M, Z, X, K after exposure to the ferroptosis inducer RSL3 was further investigated using flow cytometry. RSL3 was chosen for the heterogeneity assay because resistant tumour cells may be sensitive to a newly discovered type of cell death – ferroptosis [2]. This form of death is characterized by an iron-dependent accumulation of reactive oxygen species (ROS) in the cell [3]. The results showed an increased resistance of clone K and sensitivity of clone Z to RSL3 treatment, compared to the parental line.

In conclusion, our results indicate that subpopulations of colorectal cancer cells DLD-1 have different sensitivity to ferroptosis inducer RSL3.

[1] Dixon, S. J., & Stockwell, B. R. (2019). The Hallmarks of Ferroptosis. Annual Review of Cancer Biology, 3(1), 35–54. https://doi.org/10.1146/annurev-cancerbio-030518-055844.

[2] Duan, B., Zhao, Y., Bai, J., Wang, J., Duan, X., Luo, X., Zhang, R., Pu, Y., Kou, M., Lei, J., & Yang, S. (2022). Colorectal Cancer: An Overview. In Gastrointestinal Cancers (pp. 1–12). Exon Publications. https://doi.org/10.36255/exon-publications-gastrointestinal-cancers-colorectal-cancer.

[3] Sui, X., Zhang, R., Liu, S., Duan, T., Zhai, L., Zhang, M., Han, X., Xiang, Y., Huang, X., Lin, H., & Xie, T. (2018). RSL3 Drives Ferroptosis Through GPX4 Inactivation and ROS Production in Colorectal Cancer. Frontiers in Pharmacology, 9. https://doi.org/10.3389/fphar.2018.

POTENTIAL BIOMARKERS FOR PREDICTING PROGNOSIS AND TREATMENT RESPONSE IN TRIPLE-NEGATIVE BREAST CANCER (TNBC)

Domas Stitilis[1,2], Adomas Vasiliauskas[1,2], Linas Kunigenas[1,3], Monika Drobniene[1,3], Egle Strainiene[1,2], Kestutis Suziedelis[1,3]

[1]National Cancer Institute, LT-08660 Vilnius, Lithuania.
[2]Vilnius Gediminas Technical University, Department of Chemistry and Bioengineering, LT-10223 Vilnius, Lithuania.
[3]Vilnius University, LT-08412 Vilnius, Lithuania.
adomas.vasiliauskas@stud.vilniustech.lt

Breast cancer remains the most prevalent malignancy and a leading cause of cancer-related mortality among women worldwide. Among its subtypes, triple-negative breast cancer (TNBC) is the most aggressive, characterized by the absence of estrogen receptor (ER), progesterone receptor (PR), and human epidermal growth factor receptor 2 (HER2). Due to its heterogeneity and lack of targeted therapies, TNBC is associated with poor prognosis and high recurrence rates. Recent research has highlighted microRNAs (miRNAs) as regulators of TNBC progression and development by targeting key genes and modulating signaling pathways involved in tumor growth, metastasis, and treatment resistance [1, 2].

This study aims to provide insights into the role of miRNAs and their target genes in assessing cancer cell resistance to chemotherapy. Bioinformatic case study analysis of the cancer genome atlas (TCGA) datasets revealed 195 differentially expressed miRNAs targeting 57 genes linked to the platinum drug resistance pathway. Analysis of patient survival data showed 13 of those to be directly related to patient survival rate.

Based on these findings, we focused on selected miRNA expression levels in TNBC patient blood samples before and after neoadjuvant chemotherapy and their association with disease or residual cancer burden (RCB). We discovered that miR-340-5p expression is higher in the healthy control group compared to cancer patient samples before and after treatment. A notable increase in miR-340-5p expression levels was noted in the RCB-0-I group, comparing patient samples before and after chemotherapy, with levels rising post-chemotherapy. For miR-22-3p, expression levels were lower in patient samples compared to controls, and expression increased after chemotherapy in both RCB patient groups. These results underscore the potential tumor-suppressive roles of miR-340-5p and miR-22-3p. Additionally, we analyzed changes in the expression of target genes of these miRNAs in blood samples. Specifically, we focused on the expression of the miR-340-5p target genes DNMT3A, RHOA, and IGF1R, with IGF1R being a common target of both miR-340-5p and miR-22-3p. Furthermore, we performed KEGG pathway enrichment analysis to identify the signaling pathways influenced by these miRNA-regulated genes.

Gaining insights into the network of miRNA-target interactions and their role in TNBC-associated pathways offers new opportunities for therapeutic interventions and potential use as biomarkers for TNBC prognosis and treatment response.

[1] Sabit, H., Cevik, E., Tombuloglu, H., Abdel-Ghany, S., Tombuloglu, G., & Esteller, M. (2021). Triple negative breast cancer in the era of miRNA. Critical reviews in oncology/hematology, 157, 103196.
[2] Balkrishna, A., Mittal, R., Bishayee, A., Kumar, A. P., & Bishayee, A. (2024). miRNA signatures affecting the survival outcome in distant metastasis of triple-negative breast cancer. Biochemical Pharmacology, 116683.

MOLECULAR AND MORPHOLOGICAL DETECTION OF SARCOCYSTIS HALIETI IN MUSCLES OF RAPTORS FROM LITHUANIA

Evelina Juozaitytė-Ngugu[1], Tautvilė Šukytė[1], Dalius Butkauskas[1], Petras Prakas[1]

[1]Nature Research Centre, Akademijos St. 2, Vilnius, LT-08412, Lithuania
juozaityt.evelina@gmail.com

The genus Sarcocystis comprises a diverse group of apicomplexan parasites infecting reptiles, birds, and mammals. These parasites are characterized by the formation of sarcocysts in the muscles of the intermediate host (IH) and the development of sporocysts in the intestines of the definitive host (DH). Raptors have been confirmed to be DH for numerous Sarcocystis species, however, there is a lack of studies on Sarcocystis spp. in the muscles of raptorial birds. In the period of 2014-2024, we analysed muscle samples from 90 raptorial birds belonging to orders Accipitriformes, Falconiformes, and Strigiformes collected in different regions of Lithuania for the presence of Sarcocystis spp. The infection rate of Sarcocystis spp. was established by examining methylene blue-stained muscle samples. Sarcocysts in fresh squashed samples were morphologically characterized under the light microscope (LM). Sarcocystis species identification was performed using the internal transcribed spacer 1 (ITS1) region analysis. By LM, one morphological type of sarcocyst was distinguished. Sarcocysts were detected in 8.9% (8/90) of muscles of Lithuanian raptors examined. In addition, Sarcocystis sp. were found in the leg muscles of five raptors 9.3% (5/54). Sarcocysts were present in 5.7% (3/53) of the neck muscles of three raptors studied. Furthermore, Sarcocystis sp. have been observed in the thoracic muscles of one rough-legged buzzard (Buteo lagopus). No sarcocysts were observed in the hearts of birds examined. Overall, of the 243 muscle samples stained with methylene blue, sarcocysts were found in nine of them (3.7%). Only two sarcocysts were excised from fresh samples. In methylene blue-stained samples, sarcocysts were microscopic, looked like tiny threads, had smooth and thin (about 1 μm) cyst wall, and contained banana-shaped bradyzoites. Representatives of one Sarcocystis species, S. halieti were molecularly identified in seven birds. This is the first study to report five new IHs for S. halieti, common buzzard (Buteo buteo), Eurasian goshawk (Accipiter gentilis), rough-legged buzzard, long-eared owl (Asio otus), and tawny owl (Strix aluco). Further investigations are needed to assess the possible pathogenicity of S. halieti in extra-intestinal organs of raptors.

Acknowledgements

The authors are grateful to Kaunas T. Ivanauskas Zoology Museum for providing bird samples used in the study.

P62 PROMOTES COLORECTAL CANCER CELL SURVIVAL AND CHEMORESISTANCE

Guoda Vaitiekaitė[1], Andrius Jasinevičius[1], Aušra Sasnauskienė[1], Vilmantė Žitkutė[1]

[1]Department of Biochemistry and Molecular Biology, Institute of Biosciences, Life Sciences Centre, Vilnius University, Vilnius, Lithuania
guoda.vaitiekaite@gmc.stud.vu.lt

Colorectal cancer (CRC) is the third most common diagnosed and second leading cause of cancer death worldwide. According to the latest statistical data, the number of new cases of CRC and the mortality rate are expected to increase annually [1]. Advanced CRC is treated with a combination of chemotherapeutic agents 5-fluorouracil (5-FU) and oxaliplatin (OxaPt), which cause DNA damage and induce cell death. During chemotherapy, cancer cells can acquire resistance to chemotherapeutic drugs, which reduces the effectiveness of cancer treatment [2]. The underlying mechanisms of chemoresistance, including the role of specific factors and proteins, are poorly understood.

One possible cause of chemoresistance is the multifunctional protein selective autophagy receptor p62. Higher levels of p62 protein are detected in the cancerous tissues of CRC patients compared to healthy tissues. Increased levels of p62 in CRC patients predict poor survival prognosis [3]. p62 is an autophagic receptor that targets ubiquitinated organelles or proteins to autophagosomes for degradation. Also, p62 plays a role in tumorigenesis by regulating NF-κB signalling pathways, inflammation, cell proliferation, viability, survival, angiogenesis, and cytokine expression in the tumour environment [4]. The impact of p62 on the molecular causes of chemoresistance in CRC cells is insufficiently analysed.

The aim of our study was to investigate the role of p62 in resistance to 5-FU and OxaPt in human CRC cell lines. As an *in vitro* model, we used colorectal carcinoma cell line HCT116 and its chemoresistant sublines HCT116/FU and HCT116/OXA, which had acquired resistance to 5-FU and OxaPt. Cells were transfected with p62-specific siRNA and they were treated with 5-FU or OxaPt. Then, we evaluated the effects of p62 silencing on cell viability (crystal violet test), apoptosis (flow cytometry), active caspase-3 levels (western blot) and cytokine interleukin-8 (IL-8) (ELISA) amount in HCT116 cells and their chemoresistant sublines. Our data revealed that the silencing of p62 decreased HCT116, HCT116/FU and HCT116/OXA cells viability, and increased their sensitivity to 5-FU and OxaPt treatment. The downregulation of p62 reduced the activation of caspase-3 and did not affect the fraction of apoptotic cells but reduced the amount of IL-8 protein.

Our results revealed that p62 is an important factor in chemoresistance by stimulating pro-survival molecules.

[1] E. Morgan et al., “Global burden of colorectal cancer in 2020 and 2040: incidence and mortality estimates from GLOBOCAN,” Gut, vol. 72, no. 2, pp. 338–344, 2023.
[2] Q. Wang, X. Shen, G. Chen, and J. Du, “Drug resistance in colorectal cancer: from mechanism to clinic,” Cancers, vol. 14, no. 12, p. 2928, Jun. 2022.
[3] F. Ren et al., “Knockdown of p62/sequestosome 1 attenuates autophagy and inhibits colorectal cancer cell growth,” Molecular and Cellular Biochemistry, vol. 385, no. 1–2, pp. 95–102, Sep. 2013.
[4] A. V. Kumar, J. Mills, and L. R. Lapierre, “Selective Autophagy Receptor p62/SQSTM1, a Pivotal Player in Stress and Aging,” Frontiers in Cell and Developmental Biology, vol. 10, Feb. 2022.

SCREENING FOR NOVEL ENZYMES USING MODIFIED PURINES

Daniil Kaminskyi[1], Ieva Petkevičiūtė[1], Jaunius Urbonavičius[1], Daiva Tauraitė[1]

[1]Department of Chemistry and Bioengineering, Vilnius Gediminas Technical University, Lithuania
daniil.kaminskyi@stud.vilniustech.lt

Ribonucleic acids are essential to many processes of life and, to fulfil their functions, they have numerous chemical modifications. Most of such modifications are found in tRNA, where they affect metabolism, structure, stability, localisation and transport. Modified purine base derivatives are critical in various biological process regulation across both prokaryotic and eukaryotic organisms. These modifications affect gene expression, the stability of RNA, and protein interactions, which are crucial for cellular differentiation, development, and reactions to environmental factors. In order to use modified purine base as drugs or as other medicval tools, it is crucial to know and understand their metabolic pathways. This is why investigation of enzymes that play part in modified purine base metabolism are highly significant for basic research and translational applications [1].

In this study, modified purine heterocyclic bases, such as N2-methylguanine, N6-methylguanine, N6-methyladenine, N6,N6-dimethyladenine etc., were synthesized and purified by flash column chromatography. The structure and the purity of synthesized derivatives were proven by UV/Vis, NMR spectroscopy, TLC and HPLC-MS analysis. The synthesized methylated compounds and some other commercially available modified purines were used as substrates to select enzymes involved in the catabolism of the modified heterocyclic bases. For this purpose, purine auxotrophy-based selection systems, similar to previously described [2], were used. These systems allow the selection of enzymes that convert modified respective purines into unmodified counterparts. Also, new metagenomic libraries, created by isolating DNA from the environmental samples, sharing and cloning into the multicopy cloning vectors, were used for selection of genes involved in metabolism of modified heterocyclic bases. Several candidate DNA fragments were obtained during the screening procedure and are currently under the investigation.

[1] Delaunay, S., Helm, M. & Frye, M. (2024). RNA modifications in physiology and disease: towards clinical applications. Nature Reviews Genetics, 25, 104-122

[2] Aučynaitė, A., Rutkienė, R., Tauraitė, D., Meškys, R. & Urbonavičius, J. (2018). Discovery of bacterial deaminases that convert 5-fluoroisocytosine into 5-fluorouracil. Frontiers in Microbiology, 9, 2375.

DESIGN AND MOLECULAR DOCKING STUDIES OF PYRIDINE-1,2,4-TRIAZOLE-3-THIONE DERIVATIVES AS POTENTIAL ANTICANCER DRUG CANDIDATES

Aida Šermukšnytė[1], Maryna Stasevych[2], Olena Komarovska-Porokhnyavets[2], Viktor Zvarych[3], Juozas Kiltinavičius[1], Simona Talačkaitė[1], Ingrida Tumosienė[1], Kristina Kantminienė[4]

[1]Department of Organic Chemistry, Kaunas University of Technology, Lithuania
[2]Department of Technology of Biologically Active Substances, Pharmacy, and Biotechnology, Lviv Polytechnic National University
[3]Department of Automated Control Systems, Lviv Polytechnic National University
[4]Department of Physical and Inorganic Chemistry, Kaunas University of Technology
aida.sermuksnyte@ktu.edu

Cancer is a complex and heterogenous disease characterized by uncontrolled cell proliferation, leading to the formation of abnormal tissue masses – tumors. While cytotoxic agents remain a cornerstone of cancer treatment, their therapeutic potential is restricted by limited selectivity and permeability. As a result, the search for novel, highly specific anticancer compounds is crucial to enhance treatment precision and minimize the adverse effects associated with conventional therapies. The current study focuses on designing molecules that exploit cancer cell vulnerabilities, including inhibiting key signaling pathways involved in tumor progression. Hydrazone derivatives have demonstrated promising anticancer activity by acting as protein kinase inhibitors [1].

This work's objective was to synthesize variously substituted pyridine-1,2,4-triazole-3-thione-hydrazones and evaluate their binding affinity towards four protein kinase sites.

The reaction of 2-aminopyridine and 2-amino-5-chloropyridine with acrylic acid in toluene under reflux conditions resulted in the formation of the corresponding β-alanines in good yields [2]. The obtained compounds were melted with thioacetohydrazide at 200 °C to provide 4-amino-1,2,4-triazole-3-thione and chloro-substituted 4-amino-1,2,4-triazole-3-thione in 74% and 76% yields, respectively. 4-Substituted-5-(2-(pyridine-2-yl-amino)ethyl)-2,4-dihydro-3*H*-1,2,4-triazole-3-thiones and their chloro analogs were synthesized in 53-85% yield by reacting 4-amino-1,2,4-triazole-3-thiones with the corresponding aldehydes in methanol in the presence of a catalytic amount of hydrochloric acid under reflux conditions. The novel compounds' structures were confirmed by ^{1}H and ^{13}C nuclear magnetic resonance (NMR), and mass spectrometry (MS).

Molecular docking studies of three newly synthesized compounds, which demonstrated significant cytotoxicity against MDA-MB-231 and U-87 cancer cell lines, were conducted to explore potential anticancer mechanisms. Kinase inhibitors have shown efficacy in treating breast cancer and glioblastoma [3], prompting the modeling of interactions between the 1,2,4-triazole-3-thione bearing pyridine-3-methylene moiety, its chloro analog, chloro-substituted 1,2,4-triazole-3-thione, bearing methylthio substituent and selected receptor protein kinases. The standard ligands dasatinib, sorafenib, and vemurafenib were used for comparison. All three compounds showed strong binding affinity to four kinase sites, with binding scores ranging from –9.103 to –10.122 kcal/mol, superior to the standard ligands.

Overall, the three selected compounds showed promising potential as anticancer agents. They have demonstrated strong binding affinity to the four protein kinase sites and likely exert their effects by targeting the MAPK pathway, inhibiting the BRAF and MEK serine-threonine protein kinases.

[1] R.E. Ferraz de Paiva et. al., Front. Mol. Biosci. 7, 627272 (2021).
[2] Z.J. Beresnevichyus et. al., Chem. Heterocycl. Compd. 28, 71–75 (1992).
[3] H.K. Brar et. al., Pharmaceutics 15, 59 (2022).

HETEROLOGOUS EXPRESSION OF A CLASS II LANTHIPEPTIDE FROM PAENIBACILLUS SP. 23TSA30-6 STRAIN IN LACTOCOCCUS LACTIS

Kamilė Pozniakaitė[1,2], Nomeda Kuisienė[1,2], Rūta Kananavičiūtė[1,2]

[1]Vilnius University, Department of Microbiology and Biotechnology
[2]Institute of Biosciences, Life Sciences Center
kamile.pozniakaite@gmail.com

Recent genome mining studies have demonstrated that unexplored habitats hold significant potential for discovering novel nonribosomal peptides (NRPs) and ribosomally synthesized and post-translationally modified peptides (RiPPs). Lanthipeptides are a class of RiPPs that contain lanthionine and methyllanthionine cross-links. These modifications give lanthipeptides unique structural stability and bioactivity, often resulting in potent antimicrobial properties [1-2].

Paenibacillus sp. 23TSA30-6 is an endospore-forming strain isolated from the deep oligotrophic Krubera-Voronja Cave. This strain is highly active against both Gram-positive and Gram-negative bacteria and was shown to encode 21 biosynthetic gene clusters (BGCs). One of these BGC code for a RiPP that belong to class II lanthipeptides [3]. The goal of this work is to produce class II lanthipeptide of 23TSA30-6 strain heterologously in *Lactoccocus lactis* and to determine its antibacterial activity.

For this purpose, genes of predicted BGC, responsible for synthesis of class II lanthipeptide (LanT, LanA, LanM) were cloned into the *L. lactis* expression vector, pNZ8048. The resulting plasmid were transferred to *L. lactis* cells by electroporation. The recombinant gene expression was tested by determining the antimicrobial activity against Gram-positive and Gram-negative bacteria. After determining its activity, the peptide will be later purified and characterised. Initial observations indicate that expression in *L. lactis* may support the production of a class II lanthipeptide, with further studies required to determine its properties and activity.

In conclusion, this study aimed to heterologously express the class II lanthipeptide and to determine its antimicrobial activity (separately from other bioactive compounds secreted by *Paenibacillus* sp. 23TSA30-6). The obtained results will contribute to discovering novel antimicrobials, which could be applied in the development of new therapeutic agents.

[1] C. Wang, J. Wambui, M. V. Fernandez-Cantos, S. Jurt, J. Broos, R. Stephan, and O. P. Kuipers, "Heterologous expression and characterization of Estercin A, a class II lanthipeptide derived from Clostridium estertheticum CF016, with antimicrobial activity against clinically relevant pathogens," J. Nat. Prod., advance online publication, 2025

[2] P. Arias-Orozco, Maartje Inklaar, J. Lanooij, Rubén Cebrián, and O. P. Kuipers, "Functional Expression and Characterization of the Highly Promiscuous Lanthipeptide Synthetase SyncM, Enabling the Production of Lanthipeptides with a Broad Range of Ring Topologies," ACS Synthetic Biology, vol. 10, no. 10, pp. 2579–2591, Sep. 2021

[3] J. Lebedeva, G. Jukneviciute, R. Čepaitė, V. Vickackaite, R. Pranckutė, and N. Kuisiene, "Genome Mining and Characterization of Biosynthetic Gene Clusters in Two Cave Strains of Paenibacillus sp.," Frontiers in Microbiology, vol. 11, Jan. 2021

SYNTHESIS OF RECOMBINANT APIS MELLIFERA ALLERGENS API M 7 AND APIM 10 IN ESCHERICHIA COLI

Aistis Navickas[1], Laima Čepulytė[1], Vytautas Rudokas[2], Rasa Petraitytė-Burneikienė[1]

[1]Department of Eukaryote Gene Engineering, Institute of Biotechnology, Life Sciences Center, Vilnius University, Lithuania
[2]Department of Immunology, Institute of Biotechnology, Life Sciences Center, Vilnius University, Lithuania
aistis.navickas@gmc.stud.vu.lt

Between 30% and 40% of the world's population suffers from allergies [1]. Allergies can cause a range of symptoms, from mild to moderate, such as itching or vomiting, to severe reactions like anaphylaxis [2]. Anaphylaxis is dangerous because it can be life-threatening if the allergic person cannot receive timely treatment, such as an epinephrine injection [3]. Various allergens, including foods, pollen, and dust mites, can trigger allergic reactions. Among these, the venoms of hymenopteran insects, such as bees and wasps, are one of the most common causes of anaphylactic shock [2, 3].

Allergy diagnostic methods are rapidly improving. This is evident by the shift towards using specific allergens in *in vitro* tests, which are replacing the traditional use of allergen extracts in *in vivo* tests, as well as expanding the diagnostic capabilities of *in vitro* testing. This change has several advantages for the following reasons. Firstly, allergen extracts can lead to inaccurate results due to their varying compositions. Secondly, since these extracts come from natural sources, there is a risk of cross-reactivity. Finally, conducting allergy tests *in vitro*, rather than *in vivo*, eliminates the risk of triggering allergic reactions in patients. This is highly beneficial when working with potentially dangerous allergens, such as the aforementioned hymenopteran insect venoms that can cause anaphylactic shock [4].

Recombinant Api m 7 and Api m 10 allergens, naturally found in European honey bees (*Apis mellifera*), were synthesized during this study. European honey bees are the most common and the most studied species of bees [5]. Up to 80% of individuals allergic to honey bee venom are sensitive specifically to the 7^{th} allergen, and between 49% to 62% are sensitized to the 10^{th} of the 12 known Api m allergens [6]. In this study, the synthesis of recombinant Api m 7 and Api m 10 allergens was induced in different *E. coli* strains and under different temperatures to optimize the synthesis.

Acknowledgements
The research was funded by the Vilnius University Science Promotion Fund, project code MSF-JM-14/2023.

[1] R. Pawankar, G. W. Canonica, S. T. Holgate, and R. F. Lockey, White book on allergy: Executive summary 2011–2012. World Health Organization, 2011.
[2] V. Cardona et al., "World Allergy Organization Anaphylaxis Guidance 2020," World Allergy Organization Journal, vol. 13, no. 10, p. 100472, 2020. doi: 10.1016/j.waojou.2020.100472.
[3] D. Fischer, T. K. V. Leek, A. K. Ellis, and H. Kim, "Anaphylaxis," Allergy, Asthma, and Clinical Immunology, vol. 14, Suppl. 2, p. 54, 2018. doi: 10.1186/s13223-018-0283-4.
[4] R. Valenta et al., "Allergen Extracts for In Vivo Diagnosis and Treatment of Allergy: Is There a Future?," J. Allergy Clin. Immunol. Pract., vol. 6, no. 6, pp. 1845–1855.e2, 2018. doi: 10.1016/j.jaip.2018.08.032.
[5] J. Gould, "Meet our prime pollinators," Nature, vol. 521, pp. S48–S49, 2015. doi: 10.1038/521S48a.
[6] M. Burzyńska and D. Piasecka-Kwiatkowska, "A Review of Honeybee Venom Allergens and Allergenicity," Int. J. Mol. Sci., vol. 22, no. 16, p. 8371, 2021. doi: 10.3390/ijms22168371.

PRODUCTION AND FUNCTIONAL ANALYSIS OF CYSTEINE-MUTATED RECOMBINANT HUMAN MITOCHONDRIAL CARBONIC ANHYDRASES CAVA AND CAVB

Austėja Frederaitė[1], Tautvydas Kojis[1], Aurelija Mickevičiūtė[1], Lina Baranauskienė[1]

[1]Department of Biothermodynamics and Drug Design, Institute of Biotechnology, Life Sciences Centre, Vilnius University
austeja.frederaite@gmc.stud.vu.lt

Carbonic anhydrases (CA) are ubiquitous enzymes that catalyze the reversible hydration of carbon dioxide into bicarbonate ($CO_2 + H_2O \rightleftharpoons H_2CO_3$).These enzymes play a vital role in physiological functions such as pH regulation and calcification. Among the fifteen human CAs, we focused on CA VA and CA VB, the only mitochondrial isozymes that provide bicarbonate ions during gluconeogenesis and lipogenesis[1].

The investigation of carbonic anhydrases is crucial for drug design due to their links with various pathological conditions, including cancer and obesity[2]. Our research aimed to produce recombinant proteins for human mitochondrial carbonic anhydrases CA VA and CA VB. In previous efforts to produce recombinant functional CA VA and CA VB, we encountered low solubility and aggregation challenges. To improve recombinant protein stability, we hypothesized that removing cysteine residues from the protein sequences would be beneficial. Using targeted mutagenesis, we replaced each cysteine with serine or alanine.

After completing the mutagenesis, we expressed the target proteins in *Escherichia coli* and purified them. We then evaluated the CO_2 hydratase activity of the recombinant CA VA and CA VB proteins by stopped-flow method and inhibitor binding using fluorescence thermal shift assay, as illustrated in Figure 1.

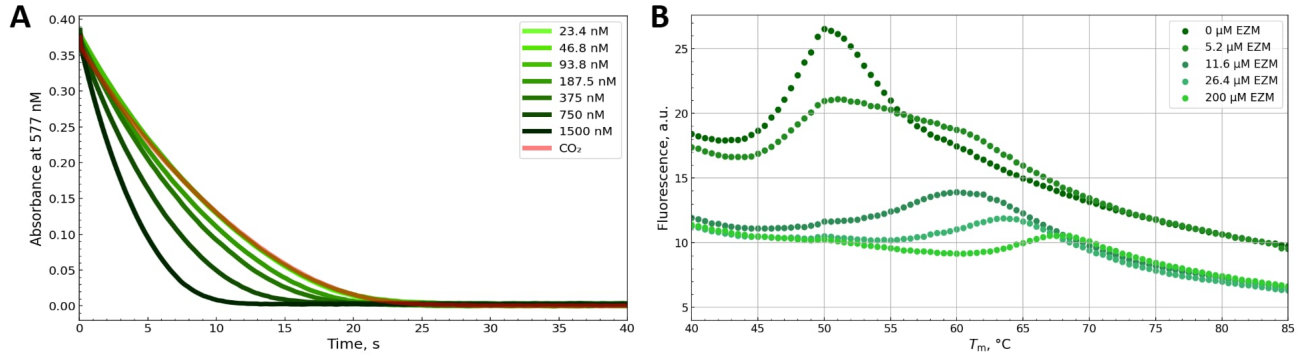


Fig. 1. A – CO_2 hydration activity of CA VB by stopped-flow analysis. Initial experimental curves for the determination of enzymatic activity, showing the changes in the absorption of the pH indicator over time depending on the concentration of CA VB, B – Ligand binding by fluorescence thermal shift assay: pure protein CA VB and protein with different concentrations of CA inhibitor ethoxzolamide (EZM).

[1] Aspatwar, A., Supuran, C.T., Waheed, A., Sly, W.S., Parkkila, S., 2023. Mitochondrial carbonic anhydrase VA and VB: properties and roles in health and disease. The Journal of Physiology 601, 257–274. https://doi.org/10.1113/JP283579

[2] Lomelino, C.L., Andring, J.T., McKenna, R., 2018. Crystallography and Its Impact on Carbonic Anhydrase Research. International Journal of Medicinal Chemistry 2018, 1–21. https://doi.org/10.1155/2018/9419521

DEVELOPMENT OF A RAPID METHOD FOR FUNCTIONAL SELECTION OF URETHANASES FROM METAGENOMIC LIBRARIES

Kristupas Volbikas[1], Nina Urbelienė[1], Rolandas Meškys[1]

[1]Department of Molecular Microbiology and Biotechnology, Institute of Biochemistry, Life Science Centre, Vilnius University
kristupas.volbikas@gmc.stud.vu.lt

In recent decades biocatalysis has become indispensable as a more selective, ecological and ultimately more efficient alternative to some traditional chemical routes. The use of enzymes or microorganisms is especially advantageous when stereo- and/or regio- selectivity and mild reaction conditions are required [1].

Although biocatalysis provides profound benefits, achieving desired biocatalytic activity comes with its own set of challenges. Naturally occurring enzymes do not often possess synthetically relevant catalytic activity [2]. Enzyme engineering is an approach which utilizes known enzyme structural and functional motifs to create proteins that can catalyze a desired reaction. However, these methods require vast knowledge of enzymes possessing similar to desired catalytic activity. To this extent, high-throughput functional screening methods, which enable the discovery of enzymes with novel catalytic activities from metagenomic libraries, are necessary [2].

Urethanes are mostly encountered in the form of a polymer – many household items such as mattresses, sponges, glues and many others are made from polyurethane (PU). PU composes 8% of all annual plastic production, which brings forth the question of PU waste management [3]. Several methods of chemical PU recycling exist, but none are practically used because of their high costs and inability to effectively separate and utilize the products of these processes. The use of urethanases can counter several of these problems, making PU recycling a reality [4]. Furthermore, urethanes are used in their monomeric form in synthetic chemistry as protecting groups and in the pharmaceutical [5] and agricultural industries [6] as drugs and pesticides. It is possible to use urethanases for selective and mild condition synthesis of these compounds [7].

No high-throughput methods for the selection of urethanases from metagenomic libraries have been reported. To this end, our team is developing such methods based on E. coli uridine auxotrophs. Genes from metagenomic libraries are transferred into E. coli uridine auxotrophs, which are then grown on minimal media supplemented with different uridine analogs containing urethane fragments. Based on previous achievements, such selection method is expected to be highly efficient [8][9]. The first step in the development of such approach is the synthesis of the appropriate 5'-carbamoyluridine analogs (Fig. 1). The synthesis of 2',3'-isopropyledeneuridines with different 5'-carbamoyl groups (**4-8**) has been achieved with varying total yields (41%-46%) as well as the 2',3' deprotection of 5'-butylcarbamoyluridine (**9**) with a yield of 95%.

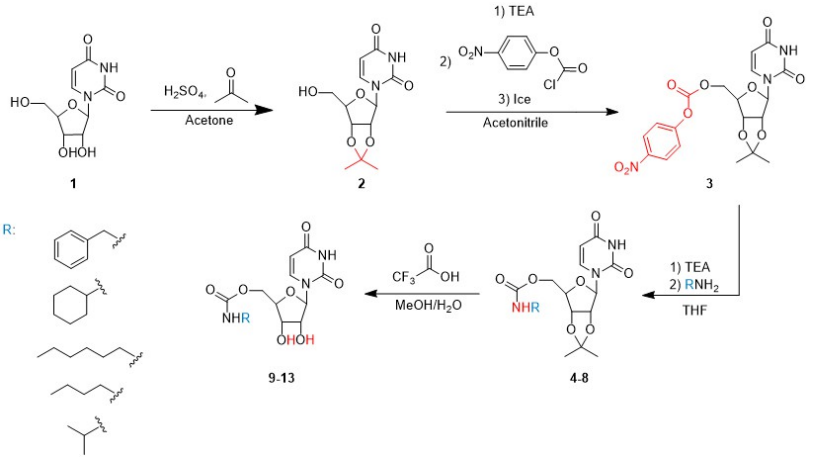


Fig. 1. Synthesis of 5'-carbamoyluridines

[1] Buller Et al. Science 2023, 382, (6673).
[2] Leveson-Gower Et al. Nat. Rev. Chem. 2019, 3, 687.
[3] Kemona Et al. Polymers 2020, 12, 1752.
[4] Branson Et al. Angew Chem. Int. Ed. 2023, 62.
[5] Ghosh Et al. J. Med. Chem. 2015, 58, 2895.
[6] Gupta Et al. In Encyclopedia of Toxicology; Elsevier, 2014; pp 661.
[7] Meinert Et al. Angew. Chem. Int. Ed. 2024, 63.
[8] Urbelienė Et al. Microb. Biotechnol. 2019, 12, 148.
[9] Urbelienė Et al. Catalysts 2020, 10, 445.

APPLICATION OF SYNTHESISED GLUCOSE-6-ESTERS FOR DETERMINATION OF ESTERASE ACTIVITY

Gustė Pikturnaitė[1], Marius Butkevičius[1]

[1]1Department of Bioanalysis, Institute of Biochemistry, Life Sciences Center, Vilnius University, Saulėtekio av. 7, LT-10257 Vilnius, Lithuania
guste.pikturnaite@gmc.stud.vu.lt

Esterases are enzymes that hydrolyses esters into acid and alcohol. Since esterases are involved in the regulation of many physiological processes such as immune system and inflammatory reactions, they are often associated with neurodegenerative and digestive diseases and inflammatory processes. During inflammatory processes in the body, immune cells are activated and the enzymes they secrete, including esterases, help fight infection. Early detection of esterase activity changes in urine or blood can lead to faster identification of inflammation and more effective treatment. In this study, esterase activity was measured using synthesized glucose-6-esters to assist in identifying inflammatory processes in diagnostic medicine. Glucose-6-esters were synthesized via a transesterification reaction catalysed by *Candida antarctica* lipase B (CalB). In transesterification reaction, alcohol is displaced from an ester by another alcohol. [1] In this case, the synthesis involves the exchange of the primary hydroxyl group of glucose with an ester group from a short vinyl ester, which serves as the substrate for the reaction. Since glucose has only one primary hydroxyl group, it is the best choice for the synthesis of new esters due to high selectivity of CalB for primary alcohols. [2] The idea of the work is to use synthesized glucose-6-esters and amperometric glucose biosensors to determine the esterase activity. The idea is based on the fact that glucose oxidase is used to construct the amperometric glucose sensor, which is a very specific enzyme and should not react to glucose-6-esters. In the presence of esterase in the solution and catalyzing the hydrolysis of glucose-6-esters, glucose is formed, the increase in glucose concentration is recorded by an amperometric biosensor. The rate of glucose increase is equated to esterase activity. Seven different short vinyl esters were used in the study: vinyl acetate, vinyl propionate, vinyl propionate, vinyl methacrylate, vinyl pivalate, vinyl 4-tert-butylbenzoate and vinyl benzoate. A first-generation amperometric glucose biosensor and a dinitrosalicylic acid-based method for determining reducing sugars were used to assess the efficiency of glucose-6-ester synthesis. As glucose is consumed during synthesis, the reduction in glucose detected by the glucose biosensor can be correlated with the amount of product formed. The study also found an optimum synthesis time of 24 hours and tested few glucose-short vinyl ester concentration ratios. Also, in order to verify the operation of the idea, an attempt was made to determine the activity of two esterases (Carboxyl esterase from porcine liver and acetylcholinesterase from *Electrophorus electricus*) using the synthesized new esters. In this work, the results obtained by the different methods were compared with each other and different synthesis conditions were tested, to obtain the highest yield.

[1] [1] M. A. Sundaramahalingam, C. Amrutha, P. Sivashanmugam, and J. Rajeshbanu, 'An encapsulated report on enzyme-assisted transesterification with an allusion to lipase', 3 Biotech, vol. 11, no. 11, p. 481, Nov. 2021, doi: 10.1007/s13205-021-03003-3.

[2] [2] H. A. El-Baz et al., 'Enzymatic Synthesis of Glucose Fatty Acid Esters Using SCOs as Acyl Group-Donors and Their Biological Activities', Appl. Sci., vol. 11, no. 6, p. 2700, Mar. 2021, doi: 10.3390/app11062700

BIOCOMPATIBILITY EVALUATION OF POLYCAPROLACTONE-MXENE SCAFFOLDS USING HUMAN UMBILICAL VEIN ENDOTHELIAL CELLS

Rusnė Uzielaitė[1], Rokas Mikšiūnas[1,2], Simonas Ramanavičius[3], Antanas Zinovičius[4,5], Inga Morkvėnaitė-Vilkončienė[4,6], Maksym Pogorielov[7], Viktoriia Korniienko[8], Arūnas Ramanavičius[2,9]

[1]Department of Regenerative Medicine, State Research Institute Centre for Innovative Medicine, Vilnius, Lithuania
[2]Laboratory of Nanotechnology, Center for Physical Sciences and Technology, Vilnius, Lithuania
[3]Department of Electrochemical Material Science, Centre for Physical Sciences and Technology, Vilnius, Lithuania
[4]Bioelectrochemical Technologies Laboratory, Centre for Physical Sciences and Technology, Vilnius, Lithuania
[5]Department of Mechatronics, Robotics, and Digital Manufacturing, Vilnius Tech, Vilnius, Lithuania
[6]Department of Electrical Engineering, Vilnius Tech, Vilnius, Lithuania
[7]Biomedical Research Centre, Medical Institute, Sumy State University, Sumy, Ukraine
[8]Institute of Atomic Physics and Spectroscopy, University of Latvia, Riga, Latvia
[9]Department of Physical Chemistry, Institute of Chemistry, Faculty of Chemistry and Geosciences, Vilnius University, Vilnius, Lithuania
rusne.uzielaite@gmc.stud.vu.lt

Tissue engineering methods and regenerative medicine innovations rely on scaffold materials and their fabrication methods [1]. Scaffolds should be biocompatible, biodegradable, and possess mechanical properties suitable for tissue engineering while mimicking the natural tissue structure [2].

This study explores combining polycaprolactone (PCL) with MXenes for regenerative medicine. While PCL is a biodegradable polyester with biomedical potential, its low stiffness, conductivity, cell affinity, and hydrophobicity limit its applications. MXenes, 2D nanomaterials with antibacterial, conductive, and hydrophilic properties, offer a solution. However, further research is needed to evaluate their biocompatibility, biodegradability, and cytotoxicity.

Conventional electrospinning was performed using a positively charged needle electrode (25 kV) at 180 mm distance, and a 12 mL/h feed rate in a controlled atmospheric chamber. MXenes were synthesized via a minimally intensive layer delamination method using a Ti_3AlC_2 MAX-phase precursor, selectively etched within situ-formed hydrofluoric acid, delaminated in LiCl solution, and centrifuged to obtain single-layer flakes. PCL membranes (Ø 5 mm) were treated with NaOH to enhance hydrophilicity, then immersed in an MXene colloid, sonicated, and left for 3 hours to immobilize MXene, with the process repeated up to four times for varying layer thicknesses. HUVEC cells were seeded on PCL-MXene scaffolds, cell viability and proliferation were evaluated.

The results will allow us to evaluate the biocompatibility of PCL-Mxene scaffolds with HUVECs for further applications in regenerative medicine.

Acknowledgements

This research has received funding from the Research Council of Lithuania post-doc project No. S-PD-24-41

[1] Farag MM. 2023. Recent trends on biomaterials for tissue regeneration applications: review. Journal of Materials Science 58 527–558.
[2] Kazemzadeh G, Jirofti N, Mehrjerdi HK, Rajabioun M, Alamdaran SA, Mohebbi-Kalhori D, Mirbagheri MS, Taheri R. 2022. A review on developments of in-vitro and in-vivo evaluation of hybrid PCL-based natural polymers nanofibers scaffolds for vascular tissue engineering. Journal of Industrial Textiles 52

ANALYSIS OF CANCER CELL MIGRATION ON COLLAGEN SCAFFOLDS

Jorė Rutkauskaitė[1,2], Ilona Uzielienė[3], Tadas Jelinskas[4], Martynas Gavutis[4], Alėja Marija Daugėlaitė[1], Džiugas Jurgutis[1], Ričardas Rotomskis[1]

[1]Biomedical Physics Laboratory, National Cancer Institute, Lithuania
[2]Faculty of Chemistry and Geosciences, Vilnius University, Lithuania
[3]Department of Regenerative Medicine, State Research Institute Centre for Innovative Medicine, Lithuania
[4]Department of Nanoengineering, Center for Physical Sciences and Technology, Lithuania
jore.rutkauskaite@chgf.stud.vu.lt

Cancer metastasis, the migration of cancer cells from a primary tumor to other parts of the body, is a leading cause of death and complications in oncology. Tumor cell migration through the extracellular matrix (ECM) and basal membrane is crucial for the formation of metastases, making accurate and precise measurements of cancer cell migration essential for studying metastatic potential [1]. While traditional migration assays, such as the scratch test, are widely used, they rely on plastic surfaces that fail to replicate the natural tumor environment.

One of the ways to better help simulate the natural environment is the use of collagen hydrogel scaffolds. Collagen is abundant in the ECM, which makes these scaffolds more closely resemble the *in vivo* conditions the cells experience [2]. For this reason, collagen scaffolds have found widespread use in multiple tissue engineering fields [3]. Their ability to better mimic *in vivo* conditions compared to 2D cell cultures can help more accurately study cell migration and motility.

In this study, type I porcine skin collagen hydrogel scaffolds were synthesized and characterized using atomic force microscopy. The migration of two human breast cancer cell lines —highly metastatic MDA-MB-231 and less aggressive MCF-7—was compared on plastic surfaces and collagen hydrogel scaffolds using a HoloMonitor live-cell imaging system. Additionally, cell migration within the scaffolds was assessed using laser-scanning confocal microscope.

Our results show that the more aggressive, triple-negative breast cancer cells – MDA-MB-231 exhibited significantly higher motility and migration on collagen scaffolds than on plastic, whereas MCF-7 cells remained relatively immobile in both conditions. Confocal imaging suggests that MDA-MB-231 cells may penetrate the collagen scaffold, while MCF-7 cells remained on the surface. These findings indicate that collagen hydrogel scaffolds provide an effective matrix for studying cancer cell migration, better mimicking the tumor microenvironment.

[1] J. Wu, J. Jiang, B. Chen, K. Wang, Y. Tang, and X. Liang, “Plasticity of cancer cell invasion: Patterns and mechanisms,” Translational Oncology, vol. 14, no. 1, p. 100899, Jan. 2021.
[2] E. E. Antoine, P. P. Vlachos, and M. N. Rylander, “Review of Collagen I Hydrogels for Bioengineered Tissue Microenvironments: Characterization of Mechanics, Structure, and Transport,” Tissue Engineering Part B: Reviews, vol. 20, no. 6, pp. 683–696, Dec. 2014.
[3] S. Dinescu, M. Albu Kaya, L. Chitoiu, S. Ignat, D. A. Kaya, and M. Costache, “Collagen-Based Hydrogels and Their Applications for Tissue Engineering and Regenerative Medicine,” Polymers and Polymeric Composites: A Reference Series, pp. 1643–1664, 2019.

MODIFICATION OF COLLAGEN BY REPLACING PROLINE OR HYDROXYPROLINE WITH A 2-AZABICYCLOALKANE FRAGMENT

Volodymyr Lyakh[1], Radosław Gaida[1], Elżbieta Wojaczyńska[1]

[1]Faculty of Chemistry, Wroclaw University of Science and Technology, Poland
volodimirlah@gmail.com

Collagen is a key protein of the extracellular matrix, responsible for the mechanical strength of tissues and their structural integrity. The stability of the collagen triple helix largely results from the presence of proline and hydroxyproline, which determine the conformational flexibility of the peptide chain. However, natural variants of collagen exhibit limited thermal stability, which poses a significant challenge in the context of biomedical applications, such as tissue engineering or materials for tissue regeneration.

This study focuses on the modification of collagen by replacing proline or hydroxyproline with a chiral bicyclic 2-azabicycloalkane fragment or its mono- or dihydroxylated derivative. This approach aims to enhance the thermal stability and structural integrity of collagen while preserving its biological functionality. By systematically investigating the effects of these modifications, we hope to develop collagen-based materials that can better withstand physiological conditions and improve outcomes in regenerative medicine.

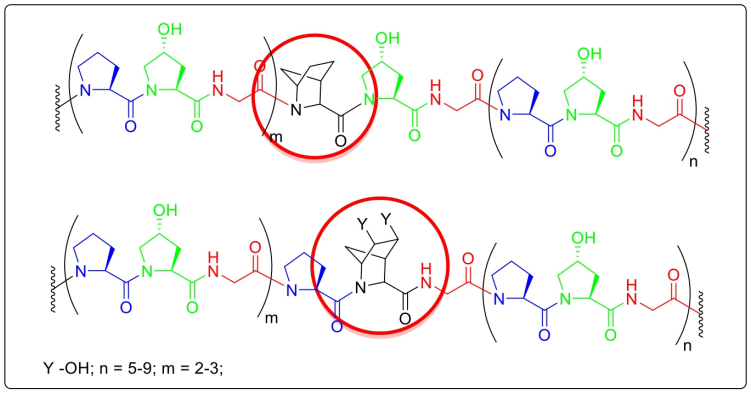


Fig. 1. Scheme of proline or hydroxyproline replacement with a bicyclic 2-azabicycloalkane analogue.

This modification aims to enhance the stability and functionality of collagen-based materials for various biomedical applications. By analyzing the structural and mechanical properties of these modified collagens, researchers hope to uncover new potential uses in tissue engineering and regenerative medicine. Replacing proline with a slightly larger 2-azabicycloalkane system may significantly increase the stability of the collagen triple helix. 2-Azabicycloalkane systems are structurally more rigid than proline, which may lead to better preorganization of collagen chain conformations and increased stability of the helical structure [1]. This stabilization may result from the limited conformational flexibility of the pyrrolidine ring and its influence on the *trans/cis* equilibrium of the peptide bond, potentially reducing the tendency of helix dissociation at higher temperatures [1].

Additionally, if instead of hydroxyproline, a bicyclic 2-azabicycloalkane analogue with one or two hydroxyl groups is introduced, additional hydrogen bonding between adjacent chains in the triple helix will be provided, which may further stabilize the entire structure. Hydroxyl groups in 2-azabicycloalkane systems can participate in the formation of hydrogen bond networks similarly to hydroxyproline while simultaneously contributing to greater control over structural preorganization.

The proposed strategy for collagen modification may lead to the development of materials with enhanced thermal and mechanical stability, making them attractive for biomedical applications such as implants, regenerative materials, or tissue engineering.

[1] C. Jenkins, G. Lin, J. Duo, D. Rapolu, I. Guzei, R. Raines, and G. Krow, "Substituted 2-azabicyclo[2.1.1]hexanes as constrained proline analogues: implications for collagen stability," J. Org. Chem., vol. 69, pp. 8565-8573, 2004, doi: 10.1021/JO049242Y.

INFLUENCE OF CELL SHAPE ON MICROVISCOSITY OF LIPID DROPLETS AND PLASMA MEMBRANE IN MESENCHYMAL STEM CELLS

Jekaterina Skibickaja[1,2], Džiugas Jurgutis[1,3], Airina Mazėtytė-Godienė[4], Martynas Gavutis[4], Jelena Dodonova-Vaitkūnienė[2], Ramūnas Valiokas[4], Vitalijus Karabanovas[1,5]

[1]National Cancer Institute, Biomedical Physics Laboratory, P. Baublio str. 3b, 08406 Vilnius, Lithuania
[2]Faculty of Chemistry and Geosciences, Vilnius University, Naugarduko str. 24, Vilnius, 03225, Lithuania
[3]Life Sciences Center, Vilnius University, Saulėtekio Ave. 7, 10257 Vilnius, Lithuania
[4]Center for Physical Sciences and Technology, Department of Nanoengineering, Savanorių 231, 02300 Vilnius, Lithuania
[5]Vilnius Gediminas Technical University, Department of Chemistry and Bioengineering, Saulėtekio Ave. 11, 10223 Vilnius, Lithuania
jekaterina.skibickaja@chgf.stud.vu.lt

The intracellular environment's physical properties, particularly microviscosity, regulate molecular diffusion and cell function. Microviscosity varies across organelles, changes under pathological conditions, and shifts during mesenchymal stem cell (MSC) differentiation [1]. MSCs are highly plastic, adapting their shape to biomechanical cues, which influence differentiation, proliferation, and organisation of intracellular structures. However, it remains unknown how MSC shape affects microviscosity in different organelles.

In this study, we used fluorescence lifetime imaging microscopy (FLIM) with two viscosity-sensitive fluorophores, BDP-H (Fig. 1A) and BODIPY-PM (Fig. 1B), to measure microviscosity in MSCs. Both BDP-H and BODIPY-PM change their fluorescence lifetime in response to microviscosity changes, displaying biexponential fluorescence decays in lipid droplets and plasma membrane, respectively [2-3].

The aim of our research was to measure the microviscosity of lipid droplets and plasma membranes in human skin-derived MSCs cultured on adhesive micropatterns of varying shapes and sizes.

MSCs were grown on polyethylenglycol hydrogel with covalently immobilized adhesion promoting fibronectin micropatterns shaped like circles, drops and triangles, each available in three sizes: 710 μm^2, 1260 μm^2, 2000 μm^2. Live-cell imaging was conducted using a laser-scanning confocal microscope, and fluorescence lifetimes were measured using time-correlated single photon-counting based FLIM.

Our results show that the fluorescence lifetime of BDP-H remained unchanged across different micropatterns, indicating that lipid droplet microviscosity is unaffected by cell shape or size. In contrast, BODIPY-PM fluorescence lifetime varied significantly with cell geometry and size, demonstrating that plasma membrane microviscosity is highly dynamic and responsive to morphological changes. Taken together, our findings suggest that organelles respond differently to morphological changes, with manipulation of cell geometry through adhesive micropatterns specifically altering plasma membrane microviscosity but not lipid droplet microviscosity.

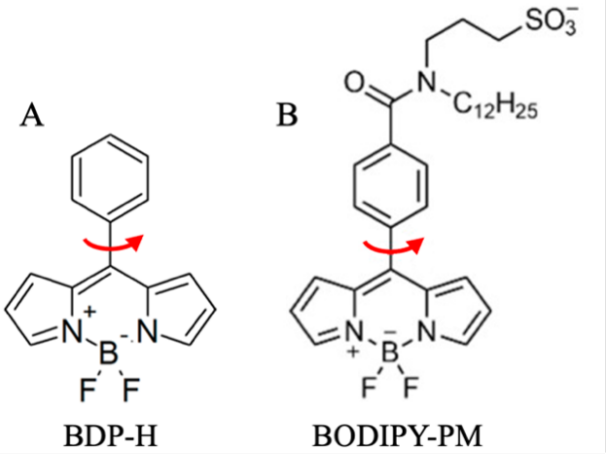


Fig. 1. Fig. 1. The structures of BDP-H (A) and BODIPY-PM (B) viscosity-sensors used in this work. [2-3]

[1] M. Paez-Perez and M. K. Kuimova, Angew. Chem. Int. Ed., 63(6): e202311233 (2024).
[2] D. Jurgutis et al., Int. J. Mol. Sci., 23, 5687 (2022).
[3] A. Polita et al., RSC Adv., 13(28): 19257-19264 (2023).

ASSOCIATIONS OF MIR-146A-5P AND MIR-31-5P WITH NEUROINFLAMMATORY DISEASES

Ugnė Zubrickaitė[1], Edita Kuncevičienė[2,3], Laura Šauklytė[1], Evelina Gružauskienė[4], Paulina Vaitkienė[2]

[1]Medical Faculty, Lithuanian University of Health Sciences, A. Mickeviciaus g. 9, LT-44307 Kaunas, Lithuania
[2]Laboratory of Molecular Neurobiology, Neuroscience Institute, Lithuanian University of Health Sciences, Eiveniu 4, LT-50161 Kaunas, Lithuania
[3]Institute of Biology Systems and Genetic Research, Lithuanian University of Health Sciences, Eiveniu Street 4, LT-50161 Kaunas, Lithuania
[4]Department of Neurology, Lithuanian University of Health Sciences, Eiveniu 2, LT-50161 Kaunas, Lithuania
ugne.zubrickaite@stud.lsmu.lt

Aim: To evaluate the expression changes of miR-146a-5p and miR-31-5p molecules in the blood of patients with inflammatory polyneuropathy.

Methods and Subjects: The expression of miR-146a-5p and miR-31-5p molecules was determined in the blood of patients with chronic inflammatory demyelinating polyneuropathy (CIDP, n = 13) and multifocal motor neuropathy (MMN, n = 10) and compared to a control group (n = 40). Blood samples for miRNA expression analysis were collected in specialized “Tempus™ Blood RNA Tubes.” RNA was purified from whole blood using the “mirVana™ miRNA Isolation Kit.” Complementary DNA (cDNA) synthesis was performed using the “TaqMan® Advanced miRNA cDNA Synthesis Kit.” The expression of microRNA molecules was determined by real-time PCR (RT-PCR), and the data were analyzed using the “ThermoFisher Cloud” platform. Statistical analysis was performed using the “IBM SPSS 29.0” software.

Results: The ΔCT values of miR-146a-5p and miR-31-5p were compared between the inflammatory polyneuropathy (IPN) and control groups. It was found that the expression of miR-146a-5p significantly differed between the IPN and control groups ($p = 0.014$). The control group showed higher expression of miR-146a-5p (mean $-\Delta Ct = -9.088$) compared to the IPN group (mean $-\Delta Ct = -9.588$). Additionally, the ΔCT values of miR-146a-5p and miR-31-5p were compared among the two diseases: CIDP, MMN, and the control group. Analysis of the obtained data confirmed that the ΔCT values of miR-146a-5p significantly differed between the groups ($p = 0.047$).

Conclusion: The expression of miR-146a-5p and miR-31-5p molecules was statistically significantly lower compared to the control group.

DETERMINATION OF QUANTITATIVE COMPOSITION OF PHLORIDZIN AND CHLOROGENIC ACID IN ORNAMENTAL APPLE FRUIT SAMPLES

Samanta Petrauskaitė[1], Darius Ryliškis[2], Mindaugas Liaudanskas[1,3], Valdimaras Janulis[1]

[1]Department of Pharmacognosy, Faculty of Pharmacy, Lithuanian University of Health Sciences, Kaunas, Lithuania
[2]Botanical Garden of Vilnius University, Vilnius, Lithuania
[3]Institute of Pharmaceutical Technologies of the Faculty of Pharmacy of Lithuanian University of Health Sciences, Kaunas, Lithuania
samanta.petrauskaite@stud.lsmu.lt

Apples are a rich source of biologically active compounds, particularly phenolic compounds such as phloridzin and chlorogenic acid. Phloridzin is found in both the peel and flesh of apples, but their concentration is much higher in the peel, while chlorogenic acid is more abundant in the flesh than in the peel, highlighting their distinct distribution within the fruit. These phenolic compound can inhibit cancer cell proliferation, decrease lipid oxidation and lower cholesterol, providing potential health benefits, including the prevention of chronic diseases such as diabetes, asthma, cancer, neurodegenerative disorders and chronic cardiovascular conditions [1,2]. The aim of this research was to determine the quantitative composition of phloridzin and chlorogenic acid in ornamental apple fruit samples.

Fruit samples of 19 ornamental apple cultivars were used for this research. An amount of 2.5 g of lyophilized apple powder (exact weight) was weighed, added to 30 mL of ethanol (70 %, v/v) and extracted in ultrasonic bath for 20 minutes at 40∘C using 1130 W of ultrasonic power at a frequency of 80 kHz. The apple lyophilizate on the filter was washed twice with 10 mL of ethanol (70%, v/v) in a 50 mL flask. The extract was filtered through a membrane filter with a pore size of 0.22 µm (Carl Roth GmbH, Karlsruhe, Germany). The qualitative and quantitative determination of phloridzin and chlorogenic acid was performed using Liaudanskas et al. developed and validated technique [3]. The results were analyzed using MS Excel 2023 (Microsoft, Redmond, WA, USA) and SPSS Statistics 21 (IBM, Chicago, IL, USA). In this research, phloridzin and chlorogenic acid contents in apple cultivars were determined. The highest amount (7640.82 µg/g) of chlorogenic acid was determined in Malus domestica Borkh. cultivar 'Rylio' fruit sample while the lowest amount (135.48 µg/g) was determined in Malus '173224' fruit sample. The highest concentration of phloridzin (5041.40 µg/g) was ascertained in the Malus baccata (L.) Borkh. cultivar 'Vaja' fruit sample. In contrast, the lowest amount (245.71 µg/g) was determined in the Malus '144845' fruit sample. Chlorogenic acid amount in the tested apple fruit samples varied widely, with a calculated coefficient of variation of 82.73% Similarly, phloridzin amount in the tested apple fruit samples also showed significant variation, with a calculated coefficient of variation of 88.96 %.

This research evaluated the qualitative and quantitative composition of samples from different ornamental apple cultivars, revealing significant variations in chlorogenic acid and phloridzin amounts. M. baccata cultivar 'Vaja' fruit samples had the highest phloridzin amount, while the chlorogenic acid amount was highest in M. domestica cultivar 'Rylio' fruit samples.

[1] Patocka, J., Bhardwaj, K., Klimova, B., Nepovimova, E., Wu, Q., Landi, M., Kuca, K., Valis, M., & Wu, W. (2020). Malus domestica: A Review on Nutritional Features, Chemical Composition, Traditional and Medicinal Value. Plants, 9(11), 1408.

[2] Butkevičiūtė, A., Liaudanskas, M., Kviklys, D., Gelvonauskienė, D., & Janulis, V. (2020). The Qualitative and Quantitative Compositions of Phenolic Compounds in Fruits of Lithuanian Heirloom Apple Cultivars. Molecules, 25(22), 5263.

[3] Mindaugas Liaudanskas, Pranas Viškelis, Valdas Jakštas, Raimondas Raudonis, Kviklys D, Arvydas Milašius, et al. Application of an Optimized HPLC Method for the Detection of Various Phenolic Compounds in Apples from Lithuanian Cultivars. Journal of Chemistry. 2014 Jan 1;2014:1–10.

STRUCTURE OF MOLLUSC COMMUNITIES OF IN THE SITES OF VERTIGO MOULINSIANA (DUPUY, 1849)

Guoda Petraitytė[1], Benediktas Jukonis[1], Jekaterina Havelka[1], Grita Skujienė[1]

[1]Department of Zoology, Institute of Biosciences, Life Sciences Centre, Vilnius University, Lithuania
guoda.petraityte@gmc.stud.vu.lt

Desmoulin's Whorl Snail Vertigo moulinsiana has most recently been assessed for The IUCN Red List of Threatened Species in 2011 and is listed as Vulnerable under criteria A2ac. It has been in decline throughout much of its range and has been protected in Lithuania since 2003 and was categorized as a rare species in the Lithuanian Red Data Book. 50 reference areas were randomly selected to assess the distribution of V. moulinsiana in 2024 August and the characteristics of mollusc communities (Fig. 1).

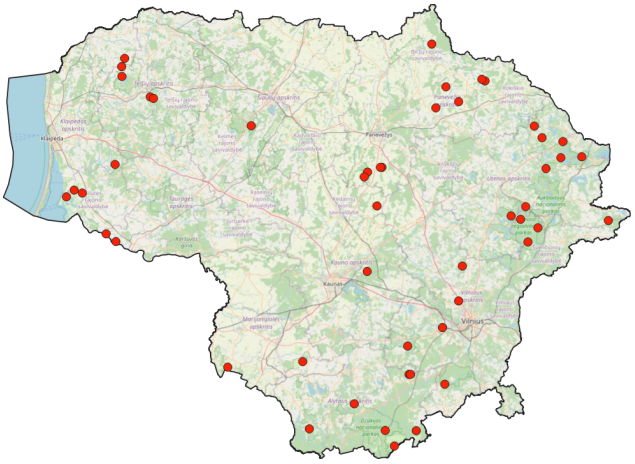


Fig. 1. Monitoring of sites and habitat for Vertigo moulinsiana - Annex II species

The species was found in only three of the fifty selected localities, so data from previous studies were added for analysis [1]. The occurrence of V. moulinsiana were strongly associated with local hydrological conditions. In the habitats of V. moulinsiana, aquatic and terrestrial molluscs were found together with V. moulinsiana, their distribution varied between the different study sites.

Acknowledgements
We thank Rokas Zalūba for his active assistance in conducting the research.

[1] Skujienė G, Kuznecova V, Jukonis B, Juzėnas S. 2020. New records of rare Vertiginidae (Mollusca: Gastropoda) in Lithuania. Bull Lithuanian Entomol Soc 4:132–140.

LINE-1 PROMOTER ORF2 EXPRESSION AS A PREDICTIVE BIOMARKER FOR DIAGNOSING SERRATED ADENOMAS IN MALES

Rima Miknaite[1], Ryte Rynkeviciene[2], Inga Kildusiene[3,4], Auguste Kaceniene[3], Kestutis Suziedelis[1,2], Giedre Smailyte[3,5]

[1]Life Sciences Center, Vilnius University, Lithuania
[2]Laboratory of Molecular Oncology, National Cancer Institute, Lithuania
[3]Laboratory of Cancer Epidemiology, National Cancer Institute, Lithuania
[4]Department of Abdominal and General Surgery and Oncology, National Cancer Institute, Lithuania
[5]Department of Public Health, Institute of Health Sciences, Vilnius university, Lithuania
rima.miknaite@gmc.stud.vu.lt

Colorectal cancer (CRC) ranks as the second leading cause of cancer-related fatalities and is the third most commonly diagnosed cancer in Lithuania and worldwide [1]. The first sign of colorectal cancer is the formation of hyperplastic polyps on the lining of the intestine. As a result of new mutations and changes in genome methylation patterns, traditional adenomas or serrated lesions can develop and later become adenocarcinomas – a type of cancer [2]. Currently, cancer risk is assessed based on lesion size and histological features, thus distinguishing serrated adenomas from other lesions is challenging. However, recent research suggests that the pathways leading to colorectal cancer may vary between genders [3]. Adenocarcinoma development is 1.5 times higher in males than females due to different sex hormones and microbiota. Also, genome-wide methylation analysis revealed the different methylation patterns in colon tissue between males and females [4]. However, the differences in LINE-1 promoter expression in colon cancer and adenomas between genders are unclear.

The present study aimed to assess LINE-1 promoter ORF1 and ORF2 expression in tubular adenomas, adenocarcinomas, and serrated lesions, analyzing male and female cohorts separately. Adenocarcinoma samples (9 male, 11 female), tubular adenoma samples (18 male, 13 female), and serrated adenoma samples (7 male, 9 female) were collected (NCI). Quantitative analysis of LINE-1 promoter ORF1 and ORF2 expression was conducted using qPCR, the data was analyzed using Mann-Whitney and Kruskal-Wallis tests with GraphPad v.9.

The LINE-1 expression analysis results reveal statistically significant differences in ORF2 expression levels between males and females in serrated adenoma tissue samples. Also, LINE-1 ORF-2 expression in serrated adenoma was significantly lower than in tubular adenoma and adenocarcinoma in the male cohort. Receiver operating characteristic (ROC) curves for methylation levels of serrated and tubular adenoma displayed that LINE-1 ORF2 expression had reliable predictive accuracy across the test cohort, with AUC values of 0.84. The AUC value for the methylation level of serrated adenoma and adenocarcinoma also was 0.84. These results indicated that LINE-1 ORF2 expression could serve as a potential biomarker to differentiate serrated adenoma from tubular adenoma and adenocarcinoma in the male cohort.

[1] '31316f70-en.pdf'. Accessed: Feb. 09, 2025. [Online]. Available: https://www.oecd.org/content/dam/oecd/en/publications/reports/2023/02/eu-country-cancer
[2] A. Aiderus, N. Barker, and V. Tergaonkar, 'Serrated colorectal cancer: preclinical models and molecular pathways', Trends in Cancer, vol. 10, no. 1, pp. 76–91, Jan. 2024, doi: 10.1016/j.trecan.2023.09.011.
[3] B. J. Harvey and H. M. Harvey, 'Sex Differences in Colon Cancer: Genomic and Nongenomic Signalling of Oestrogen', Genes (Basel), vol. 14, no. 12, p. 2225, Dec. 2023, doi: 10.3390/genes14122225.
[4] A. M. Kaz, C.-J. Wong, S. Dzieciatkowski, Y. Luo, R. E. Schoen, and W. M. Grady, 'Patterns of DNA methylation in the normal colon vary by anatomical location, gender, and age', Epigenetics, vol. 9, no. 4, pp. 492–502, Apr. 2014, doi: 10.4161/epi.27650.

GENETIC MAPPING OF BARLEY TWEAKY SPIKE MUTATION

Miglė Remeikytė[1], Vėjūnė Pukenytė[1], Virginija Vaitkūnienė[1,2], Sigita Jurkonienė[1,3], Raimondas Šiukšta[1,3]

[1]Institute of Biosciences, Life Sciences Center, Vilnius University, Saulėtekis Ave. 7, LT-10257, Vilnius, Lithuania
[2]Botanical Garden of Vilnius University, Kairėnai St. 43, LT-10239, Vilnius, Lithuania
[3]Nature Research Centre, Akademijos St. 2, LT-08412 Vilnius, Lithuania
migle.remeikyte@gmc.stud.vu.lt

Barley (*Hordeum vulgare*) ranks as the world's fourth most widely cultivated cereal crop, making it a valuable object for genetic research [1]. Understanding barley inflorescence development is crucial for improving grain yield and creating new varieties [2]. During the pinnacle of mutational breeding, a large collection of mutants that have no direct economic value but are interesting as a source for genetic mapping and gene function identification were created [3]. About 50 years ago, a series of barley developmental mutants were created using chemical mutagenesis at Vilnius University Department of Botany and Genetics. These mutants feature gradient inflorescence development and spikelet-free gaps in spikes, hyperdeveloped spike tips, and the most interesting feature is genome instability in the remote generations [4]. Genetic mapping of *tw* (*tweaky spike*) mutants can offer new insights into barley inflorescence development.

This study aimed to explore the genetic background of barley *tw* phenotype by creating two F_2 recombinant populations possessing the *tw* phenotype, *tw x WT* (*tw*-rF_2) and tw_2 *x WT* (tw_2-rF_2). Segregation analysis revealed *tw* mutation to be monogenic. To identify candidate genes responsible for the *tw* phenotype, whole genome sequencing was performed on *WT, tw*-rF_2 and tw_2-rF_2. SNP ratio analysis determined the same non-recombinant region in both populations, *tw*-rF_2 had 65 genes with deleterious mutations, whereas tw_2-rF_2 had 27 genes. 7 genes with deleterious mutations were common between both populations: 2 of them were already annotated, 3 – SIFT [5] algorithm predicted as tolerated substitutions, 1 gene with exon deletion (candidate gene 1) and 1 gene with whole gene deletion (candidate gene 2). Two candidate genes were later investigated in other *tw* allelic mutants (tw_1, tw_4, tw_5, tw_6, tw_8, tw_9, tw_{10}) using Sanger sequencing. Only one candidate gene (2) had disrupted gene function in all allelic mutants, making it responsible for the *tw* phenotype. This hypothesis will be validated by creating gene knockout in *WT* later on.

Acknowledgements

This research was was supported by the Research Council of Lithuania (LMTLT) under grant No. P-MIP-24-109 "Genetic mapping and characterization of barley developmental flower/inflorescence tweaky spike (tw) mutation"

[1] Sreenivasulu, N., Graner, A., & Wobus, U. (2008). Barley genomics: an overview. International journal of plant genomics, 2008(1), 486258.
[2] Terzi, V., Tumino, G., Pagani, D., Rizza, F., Ghizzoni, R., Morcia, C., & Stanca, A. M. (2017). Barley developmental mutants: The high road to understand the cereal spike morphology. Diversity, 9(2), 21.
[3] Hansson, M., Youssef, H. M., Zakhrabekova, S., Stuart, D., Svensson, J. T., Dockter, C., ... & Franckowiak, J. (2024). A guide to barley mutants. Hereditas, 161(1), 11.
[4] Rančelis, V. (2001). Miežių tweaky spike tipo mutantų ypatybės. Mokslas Gamtos mokslų fakultete (p. 43-48)
[5] Ng PC, Henikoff S. Predicting deleterious amino acid substitutions. Genome Res. 2001 May;11(5):863-74. doi: 10.1101/gr.176601. PMID: 11337480; PMCID: PMC311071.

EPITRANSCRIPTOMIC MODIFICATIONS AS THERAPEUTIC TARGETS IN GLIOMA

Kamilė Milkintaitė[1,2], Urbanavičiūtė-Orentė Rūta[2]

[1]Faculty of Medicine, Lithuanian University of Health Sciences, Lithuania
[2]Neuroscience Institute, Laboratory of Molecular Neurooncology, Lithuanian University of Health Sciences, Lithuania
k.milkintaite1@gmail.com

Introduction. Glioblastoma (GBM), the most widespread and aggressive primary brain tumor with survival time typically less than two years [1]. Therefore, a deeper understanding of the molecular processes underlying the onset and progression of GBM is also required to identify more effective therapeutic and diagnostic strategies. RNA methylation, a post-transcriptional modification, has emerged as a crucial regulator of gene expression, RNA stability, and protein translation, thus influencing cellular processes, including those implicated in oncogenesis [2]. This study focuses on several modifications: m6A and m7G, dynamically controlled by methyltransferases (”writers”), demethylases (”erasers”), and “readers”. Furthermore, the transcription factor SOX2, essential for stem cell maintenance and implicated in tumor initiation and progression, is frequently overexpressed in gliomas [3,4]. Investigating a modified form lacking the C-terminal domain provides insights into SOX2’s effects on glioma cell survival and proliferation. This study explores the potential of RNA methylation regulators and SOX2 as novel targets in glioma diagnosis and therapy.

Aim. To investigate the expression and functional significance of specific RNA methylation regulators as well as modified SOX2 variant in glioma, evaluating their potential as diagnostic and therapeutic biomarkers.

Methods. Gene expression levels were quantified in both tumor tissue samples from 54 glioma patients and U87 and U87 SOX2ΔC glioblastoma cell lines using qRT-PCR. Cell migration was assessed using a wound-healing assay. Publicly available RNA sequencing data from experiments involving ALKBH5 knockdown were analyzed bioinformatically to identify differentially expressed genes and affected biological pathways.

Results. Analysis of patient tumor samples revealed significantly reduced expression of ALKBH5 ($p<0.01$), FTO ($p<0.0001$), and BUD23 ($p<0.002$) in higher-grade gliomas. In contrast, increased expression of these RNA methylation regulators was positively associated with patient survival (ALKBH5 $p<0.02$; FTO $p<0.001$ BUD23, $p<0.003$), suggesting their potential as valuable prognostic biomarkers. In modified U87 cell line, SOX2ΔC overexpression led to a significant increase in ALKBH5 expression ($p=0.03$) and a decrease in BUD23 expression ($p=0.03$), demonstrating a regulatory link between SOX2 and these methylation regulators. Over 53% of transcripts showed significant transcriptome changes as a result of ALKBH5 knockdown, including genes essential for cell division, and DNA replication and repair. Notably, some of these dysregulated genes, such as TOP2A are established targets in other cancer therapies, suggesting their potential repurposing for glioma treatment.

Conclusions. ALKBH5, FTO, and BUD23 are promising prognostic biomarkers. Targeting these methylation regulators and SOX2 offers potential for improved glioma treatment and early diagnosis.

[1] Tamimi, A. F. & Juweid, M. Epidemiology and Outcome of Glioblastoma. Glioblastoma 143–153 (2017).
[2] Han, X. et al. RNA methylations in human cancers. Semin Cancer Biol 75, 97–115 (2021).
[3] Lopez-Bertoni, H., Johnson, A., Rui, Y. et al. Sox2 induces glioblastoma cell stemness and tumor propagation by repressing TET2 and deregulating 5hmC and 5mC DNA modifications. Sig Transduct Target Ther 7, 37 (2022).
[4] Mansouri S, Nejad R, Karabork M, Ekinci C, Solaroglu I, Aldape KD, Zadeh G. Sox2: regulation of expression and contribution to brain tumors. CNS Oncol 159-73 (2016).

DETECTION OF MEASLES VIRUS ANTIBODIES USING ENZYME-LINKED IMMUNOSORBENT ASSAY

Justina Dagytė[1], Indrė Lipatova[1], Algimantas Paulauskas[1]

[1]Vytautas Magnus University, Lithuania
justina.dagyte@vdu.lt

Measles is an acute and extremely contagious infection that affects all age groups. The disease can be particularly severe for children and adults with weakened immune systems, often leading to serious complications [1]. Measles outbreaks have risen in recent years [2], despite broad vaccination initiatives. From 2013 to 2018, the World Health Organization reported a total of 899,800 cases of measles. This indicates that some individuals are either unvaccinated or have received only a single vaccine dose, despite the recommendation of two doses for full immunity. This study aimed to assess the presence of IgG antibodies against the measles virus in adults and to identify individuals at risk of measles infection in Lithuania. The enzyme-linked immunosorbent assay was used to detect measles IgG antibodies in 88 participants. The results showed that 80.69% (71 out of 88) of individuals had immunity to measles, 7.95% (7 out of 88) had borderline results, and 11.36% (10 out of 88) lacked immunity to measles. The findings confirmed that individuals without protective antibody levels were most frequently found in the 1976–1981 and 1982–1987 age groups. Individuals who tested negative either had an unknown vaccination status or had received just one vaccine dose, with a similar distribution of negative results between sexes. These findings emphasize the importance of enhancing vaccination coverage, especially among individuals with incomplete vaccination histories, to prevent future measles outbreaks.

[1] Moss, W. J. (2017). Measles. The Lancet, 390(10111), 2490–2502. https://doi.org/10.1016/S0140-6736(17)31463-0
[2] Patel, M. K., Antoni, S., Nedelec, Y., Sodha, S., Menning, L., Ogbuanu, I. U., ir Gacic Dobo, M. (2020). The Changing Global Epidemiology of Measles, 2013–2018. The Journal of Infectious Diseases, 222(7), 1117–1128. https://doi.org/10.1093/infdis/jiaa044

REPROGRAMMING STRATEGIES: COMPARING THE EFFECTIVENESS OF MONOLAYER AND NEUROSPHERE TECHNIQUES IN MESENCHYMAL STEM CELLS DEDIFFERENTIATION INTO NEURAL STEM CELLS

Greta Žvinakytė[1,2], Vitoldas Šalašidi[3], Giedrius Steponaitis[2]

[1]Faculty of Medicine, Medical Academy, Lithuanian University of Health Sciences Lithuanian University of Health Sciences, Kaunas, Lithuania
[2]Laboratory of Molecular Neurooncology, Neuroscience Institute, Lithuanian University of Health Sciences, Kaunas, Lithuania
[3]ArtDenistry by Privati Praktika, Vilnius, Lithuania
greta.zvinakyte@lsmu.lt

The remarkable plasticity of human dental pulp mesenchymal stem cells (hDPSCs) has paved the way for significant advancements in regenerative medicine, particularly in addressing challenges related to neural repair, neurodegenerative diseases, and glioblastoma (GBM) research [1]. GBM are highly aggressive brain tumors with limited treatment options and poor survival rates [2]. A major factor driving their progression and recurrence is the presence of glioblastoma stem cells (GSCs), which share molecular and functional traits with neural stem cells (NSCs) (3). These similarities complicate therapeutic strategies, as distinguishing between GSCs and normal NSCs is critical for developing precise and effective treatments. Additionally, NSCs interact with the tumor microenvironment, influencing GBM behavior and its response to therapies [3,4]. Despite their potential, sourcing NSCs for research and therapeutic purposes is often hindered by ethical and technical challenges [4,5]. To address this, researchers have turned to the dedifferentiation of hDPSCs into NSCs, offering a scalable, ethical, and reliable alternative [5]. These dedifferentiated hDPSC-derived NSCs are invaluable for refining glioblastoma models, enabling researchers to better understand the interactions between GSCs and the neural microenvironment [5,6].

The aim of this research is to identify the most effective method for dedifferentiating human dental pulp mesenchymal stem cells into neural stem cells that closely resemble commercial NSC lines.

In total, five different cell lines derived from human dental pulp were previously validated as mesenchymal stem cells. For the induction of hDPSCs to dedifferentiate into NSCs were used DMEM/F12 conditioning media supplemented with B27, N2, and bFGF and EGF factors. Dedifferentiation was perfomed in two different ways: culturing the cells in neurospheres within low-adhesion dishes and by dedifferentiating them in a monolayer format. After 8 hours, 1 and 2 weeks of dedifferentiation, all cells were collected to assess changes in gene expression. RNA was extracted from the cell pellets using TRIzol reagent and then converted into complementary DNA (cDNA) with the High-Capacity RNA-to-cDNA kit. The expression levels of specific markers associated with neural stem cells were analyzed using reverse transcription quantitative polymerase chain reaction (RT-qPCR) which revieled mRNA changes, compared to the control.

Validated cells were dedifferentiated into neural stem cells, which after 8 hours, 1 and 2 weeks showed morphological changes in the cells and mRNA changes in the genes CDK5R1, MAP2 and MSI1. A comparative analysis of the two methods revealed that the method of dedifferentiating cells with neurospheres was more effective than dedifferentiation in monolayer. Nevertheless, the expression of these markers did not reach NSC values, which suggests that dedifferentiation occurred, but the efficiency was low.

[1] Yoshida S, Tomokiyo A, Hasegawa D, Hamano S, Sugii H, Maeda H. Insight into the Role of Dental Pulp Stem Cells in Regenerative Therapy. Biology 2020, Vol 9, Page 160. 2020;9(7):160.
[2] Hanif F, Muzaffar K, Perveen K, Malhi SM, Simjee SU. Glioblastoma Multiforme: A Review of its Epidemiology and Pathogenesis through Clinical Presentation and Treatment. Asian Pac J Cancer Prev. 2017;18(1):3.
[3] Bao S, Wu Q, McLendon RE, Hao Y, Shi Q, Hjelmeland AB, et al. Glioma stem cells promote radioresistance by preferential activation of the DNA damage response. Nature 2006 444:7120;444(7120):756–60.
[4] Bakhshinyan D, Savage N, Salim SK, Venugopal C, Singh SK. The Strange Case of Jekyll and Hyde: Parallels Between Neural Stem Cells and Glioblastoma-Initiating Cells. Front Oncol. 2021;10:603738.
[5] Nielen MG, De Vries SA, Geijsen N. European stem cell research in legal shackles. EMBO J. 2013 32(24):3107.
[6] Rafiee F, Pourteymourfard-Tabrizi Z, Mahmoudian-Sani MR, Mehri-Ghahfarrokhi A, Soltani A, Hashemzadeh-Chaleshtori M, et al. Differentiation of dental pulp stem cells into neuron-like cells. International Journal of Neuroscience. 2020;130(2):107–16.

UNLOCKING THE ANTIOXIDANT POTENTIAL OF GREEN WASTE THROUGH SOLID-STATE KOMBUCHA FERMENTATION

Taisa Vashkevich[1], Vilma Kaškonienė[1], Audrius Sigitas Maruška[1]

[1] Instrumental Analysis Open Access Center, Vytautas Magnus University, Lithuania
taisa.vashkevich@stud.vdu.lt

Radical scavenging species can accumulate in human body, cause oxidation of macromolecules, which can potentially lead to the development of cancer and cardiovascular diseases [1]. To counteract the effect of radical scavenging species, plants produce phenolic, carotenoid, chlorophyll, and flavonoid compounds, which can also have anti-cancer and anti-inflammatory properties [2,3]. The aim was to analyze and compare total content of antioxidant compounds in selected plant materials, with particular focus on underutilized green waste which is discarded instead of repurposing for extraction of phytochemicals: red radish leaves belonging to *Raphanus* genus, strawberry *(Fragaria × ananassa)* calyxes, and Scottish thistle *(Onopordum acanthium)* flowers and leaves. The novelty of this research lies in analyzing these compounds both before and after solid-state kombucha fermentation with spectrophotometric methods, as fermentation can enhance phytochemical bioavailability [4]. Results showed that strawberry calyxes contained the highest phenolic and flavonoid contents, with an increase of approximately 45.2% and 19.0% after fermentation, respectively, as well as the highest antioxidant capacity (DPPH assay) pre- and post-fermentation (127.31 and 82.18 mg/g, expressed as rutin equivalents), while interestingly exhibiting anti-inflammatory properties only after the fermentation. Red radish leaves exhibited the highest carotenoid (2.77 mg/g) and chlorophyll a and b (3.27 and 2.18 mg/g) concentrations.

Acknowledgements
This project has received funding from the Research Council of Lithuania (LMTLT), agreement No. S-ST-24-61.

[1] Yashin, A., Yashin, Y., Wang, J., & Nemzer, B. (2013). Antioxidant and Antiradical Activity of Coffee. Antioxidants, 2(4), 230–245. https://doi.org/10.3390/antiox2040230
[2] Ciupei, D., Colişar, A., Leopold, L., Stănilă, A., & Diaconeasa, Z. M. (2024). Polyphenols: From Classification to Therapeutic Potential and Bioavailability. Foods, 13(24), 4131. https://doi.org/10.3390/foods13244131
[3] Crupi, P., Faienza, M. F., Naeem, M. Y., Corbo, F., Clodoveo, M. L., & Muraglia, M. (2023). Overview of the Potential Beneficial Effects of Carotenoids on Consumer Health and Well-Being. Antioxidants, 12(5), 1069. https://doi.org/10.3390/antiox12051069
[4] Leonard, W., Zhang, P., Ying, D., Adhikari, B., & Fang, Z. (2021). Fermentation transforms the phenolic profiles and bioactivities of plant-based foods. Biotechnology Advances, 49, 107763. https://doi.org/10.1016/j.biotechadv.2021.107763

MICROBIAL DIVERSITY IN FERMENTED FOOD SYSTEMS USING SHOTGUN METAGENOMIC ANALYSIS WITH SEABUCKTHORN SECONDARY RAW MATERIALS

Juozas Girtas[1], Ingrida Mažeikienė[1,2], Antanas Šarkinas[1], Karolina Almonaitytė[1]

[1]Food Institute, Kaunas University of Technology, Radvilenu Rd.19 C, Kaunas, Lithuania
[2]Lithuanian Research Centre for Agriculture and Forestry, Institute of Horticulture, Akademija, LT-58344 Kedainiai Distr., Lithuania
juozas.girtas@ktu.edu

Valorisation of sea buckthorn by-products using different extraction methods could help preserve bioactive compounds and apply them for food with increased nutritional value In recent studies it is suggested that sea buckthorn biomass can be implied as a substrate for fermentation resulting in a production of novel sea buckthorn beverage, such as kombucha, which can be refreshing and healthy [1]. Although various teas and additives have been used to make kombucha [2], knowledge about the use of sea buckthorn secondary raw material extract is lacking . Considering the requirements of EFSA and the lack of scientific publications, it is important to evaluate the genetic parameters of sea buckthorn secondary raw material and fermented products. The aim of this study is to optimize the extraction of bioactive compounds from sea buckthorn by-products formed after harvesting berries and using an innovative solid-phase extraction methods, based on the creation of a pressure gradient between solid and liquid matrices. The compounds extracted were evaluated and applied to the production of kombucha. The study includes shotgun sequencing for comparative metagenomic analysis of the *Medusomyces gisevii* used in kombucha to understand their effects on fermentation and product quality. Kombucha was characterized by a greater diversity of microorganisms due to the addition of plant endophytes (Table.1). Its overall activity according to carbohydrate-active enzymes also increased. Virulence factors of pathogenic bacteria were also more abundant in the fermented product.

Table.1 Number of microorganism species in *Medusomyces gisevii* and kombucha of sea buckthorn leaves (FP).

	Medusomyces gisevii		FP	
Kingdom	**Number**	**%**	**Number**	**%**
Bacteria	227	81.07	318	82.60
Eucaryote	44	15.72	38	9.87
Virus	9	3.21	28	7.28
Archaea	0	0	1	0.26
Total	**280**		**385**	

Considering obtained results the secondary raw materials such as sea buckthorn are not only nutritional material but also could be used as bioactive compound source. This approach highlights the potential for utilizing underappreciated biomass in creating functional foods that contribute to a more sustainable and circular economy.

Acknowledgements

This research was supported by Lithuanian Rural Development Program 2014- 2020 under activity “Support for the creation and development of EIP activity groups” project Circular manufacturing model for producing biologically active material No. 35BV-KK-22-1-05005-PR001

[1] A. Chen, X. Feng, B. Dorjsuren, C. Chimedtseren, T.-A. Damda, and C. Zhang, “Traditional food, modern food and nutritional value of Sea buckthorn (Hippophae rhamnoides L.): a review,” vol. 3, no. 3, pp. 191–205, Sep. 2023

[2] K. Jakubczyk, K. Melkis, D. Maciejewska-Markiewicz, A. Muzykiewicz-Szymańska, A. Nowak, and K. Skonieczna-Żydecka, “Innovative approaches to enhancing kombucha through flavour additives: a phytochemical and antioxidant analysis,” vol. 16, no. 4, pp. 1442–1457, Feb. 2025

IDENTIFICATIONOF BIOFILM FORMATION FACTORS IN CLINICAL METHICILLIN RESISTANT STAPHYLOCOCCUSAUREUS (MRSA) ISOLATES

Dorota Demjanko[1], Agnė Kirkliauskienė[2], Greta Vizujė[3], Jolanta Miciulevičienė[4], Tatjana Kirtikliené[1]

[1]Department of Microbiology and Biotechnology, Vilnius University, Lithuania
[2]Faculty of Medicine, Institute of Biomedical Science, Vilnius University, Vilnius, Lithuania
[3]Microbiology Laboratory, Republican Vilnius University Hospital, Vilnius, Lithuania
[4]Vilnius City Clinical Hospital Vilnius, Lithuania
dorota.demjanko@mf.stud.vu.lt

Methicillin-resistant Staphylococcus aureus (MRSA) is a significant pathogen capable of forming biofilms, which enhance its resistance to antibiotics and host immune responses [1]. Various genes regulate biofilm formation, including fnbA, fnbB, clfA, icaD, icaR, spa, and bap [2]. The aim of this study was to evaluate the relationship between biofilm formation strength and the presence of biofilm-associated genes in clinical MRSA isolates. Understanding the prevalence and combination of these genes in clinical isolates can provide insights into MRSA biofilm development and its potential impact on pathogenicity.

This study analyzed the biofilm-associated genes (fnbA, fnbB, clfA, icaD, icaR, spa, bap) in 95 clinical MRSA isolates from two hospitals in Vilnius, using PCR. Isolates were categorized as strong or moderate biofilm formers based on a quantitative biofilm assay using microtiter plates method. The optical density of the stained biofilms was measured spectrophotometrically to determine the biofilm formation strength. The most frequent genes and their combinations were identified, and their distributions among the biofilm-forming groups were statistically assessed.

All the MRSA isolates demonstrated the ability to form biofilms. 72% produced strong biofilms and 28% produced moderate biofilms. The most prevalent genes in the isolates were fnbA (94.74%), icaR (96.84%), and icaD (84.21%). The spa gene was present in all the MRSA clinical isolates (100%), suggesting its ubiquitous role in these strains. bap was absent in all the isolates. Statistical analysis revealed no significant differences in the prevalence of individual genes between the two biofilm-forming groups ($p > 0.05$). The most common gene combination, detected in 44% of all isolates, included icaD, spa, fnbA, clfA and icaR. While gene combinations did not significantly differ between strong and moderate biofilm formers ($p > 0.05$), one specific combination (icaD, fnbA, fnbB, clfA, icaR and spa), which included all the investigated genes, was found exclusively in strong biofilm formers (5.89%).

This study identified the dominant genetic profile of the biofilm-forming MRSA isolates. All the tested genes were present only in strong biofilm producers, suggesting that an expanded genetic repertoire may enhance biofilm formation. Further research is required to identify additional biofilm-associated gen

SEARCH AND ANALYSIS OF PYRETHROID-DEGRADING MICROBIAL LIPOLYTICENZYMES

Ugnė Rickevičiūtė[1], Alisa Gricajeva[1]

[1]Department of Microbiology and Biotechnology, Institute of Biosciences, Life Sciences Center, Vilnius University, Lithuania
ugne.rickeviciute@gmc.stud.vu.lt

Pyrethroids are ester-containing synthetic compounds derived from natural pyrethrins. They are widely used as insecticides in agriculture, animal husbandry, and homes, but their persistence poses risks to non-target organisms and natural habitats [1;2]. Microbial lipolytic enzymes (e.g., carboxylesterases EC 3.1.1.1, lipases EC 3.1.1.3) offer potential for pyrethroid degradation due to their broad substrate specificity, thermo-, pH and other attractive characteristics can be a new and effective means of removing pyrethroids from the environment. Bacteria such as Bacillus sp., Pseudomonas sp., Serratia sp., Micrococcus sp., Sphingomonas sp., and Staphylococcus sp. produce lipolytic enzymes capable of breaking ester bonds in compounds like cypermethrin, permethrin, and deltamethrin [1].

In this study, plant growing substrate samples from three Lithuanian farmlands were investigated using conventional methods to identify pyrethroid-degrading bacteria. To isolate bacteria capable of degrading pyrethroids, an enrichment culture was used with permethrin as the sole carbon source. The selected bacterial isolates were identified through 16S rRNA gene sequencing and phylogenetic analysis. After identifying the target bacteria, 12 cultures from the genera Pseudomonas, Staphylococcus, Micrococcus, Bacillus, Peribacillus and Paenibacillus sp. were assessed based on the hydrolysis zones around their colonies in solid minimal salts media supplemented with permethrin. Further, target proteins were purified from both intracellular and extracellular fractions of the most active bacterial strains and analyzed using zymographic analysis. For the latter, tributyrin and permethrin were used as substrates. Lipolytic activity of partially purified enzymes was also tested using para-nitrophenyl butyrate (p-NPB) substrate.

In four bacterial strains, which according to the phylogenetic analysis most likely belong to Pseudomonas knackmussii, Staphylococcus warneri, Micrococcus aloeverae and Solibacillus sp., 55-70 kDa lipolytic enzymes active towards tributyrin and permethrin in the zymogram gels, were determined. In the partially purified fractions of other studied bacterial strains enzymes (20-100 kDa) active towards only the tributyrin were determined.

[1] Zhan, H., Huang, Y., Lin, Z., Bhatt, P., & Chen, S. (2020). New insights into the microbial degradation and catalytic mechanism of synthetic pyrethroids. Environmental Research, 182, 109138.

[2] Liu, Y., Tang, S., Wang, X., Wang, X., Tang, X., Wu, Q., ... & Ding, J. (2023). A novel thermostable and salt-tolerant carboxylesterase involved in the initial aerobic degradation pathway for pyrethroids in Glycomyces salinus. Journal of Hazardous Materials, 451, 131128.

SYNTHESIS,CHARACTERIZATION, AND PROPERTY PREDICTION OF 1-(5-CHLOROPYRIDIN-2-YL)-N-(4-SUBSTITUTED BENZYLIDENE)-5-OXOPYRROLIDINE-3-CARBOHYDRAZIDES

Simona Talačkaitė[1], Aida Šermukšnytė[1], Kristina Kantminienė[1], Ilona Jonuškienė[1], Ingrida Tumosienė[1]

[1]Kaunas University of Technology
simona.talackaite@ktu.edu

Approx. 75% of modern low-molecular-mass pharmaceutical agents contain heterocyclic fragments. 5-Chloropyridine and its derivatives have been investigated for their potential antimicrobial, anticancer, anti-inflammatory, and antiviral properties. Pyridine moiety is often found in therapeutic agents due to its ability to effectively interact with biological targets. The prediction of ADMET parameters is a crucial aspect of drug discovery and development; it plays a significant role in optimizing the pharmacokinetic properties of novel drug candidates. This work aimed to synthesize biologically active compounds bearing 2-aminopyridine moiety and evaluate them as potential drug candidates based on their ADMET properties [1].

Reaction of 2-amino-5-chloropyridine with itaconic acid in water resulted in formation of 1-(5-chloropyridin-2-yl)-5-oxopyrrolidine-3-carboxylic acid, which subsequent reaction with hydrazine hydrate in DMF provided hydrazide 1. Hydrazide 1 reacted with various aldehydes to provide hydrazones 2–7 [2,3]. To assess their drug-likeness and pharmaceutical properties, pharmacokinetic profiles were calculated using in silico software AdmetLab 2.0. The molecular weight (MW) of all compounds falls within an acceptable range for oral bioavailability (346.1–420). Log P values for compounds 2-5 are in the range of 3.5–4.17 indicating moderate lipophilicity suitable for absorption, while they are slightly lower for 6, 7 suggesting an improved water solubility. Total polar surface area (TPSA) values range from 57.59 to 117.8. Lower TPSA values for 2, 3, and 7 suggest better permeability, while 5 and 6 may face challenges in intestinal absorption due to higher TPSA. Blood-brain barrier (BBB) permeability is the highest for 2, 5, and 7 (>0.9) suggesting potential for CNS-targeting, while 6 is unlikely to penetrate the BBB. Compound 6 shows the highest value (0.01) for human intestinal absorption (HIA).

Thus, six new compounds, bearing 2-amino-5-chloropyridine and hydrazone moieties, were synthesized. Evaluation of their ADMET properties has suggested that compound 5, bearing dimethylamino substituent, exhibits the most balanced pharmacokinetic profile with high blood-brain barrier permeability and moderate intestinal absorption, making it a promising candidate for further development. Its favorable lipophilicity and permeability suggest strong potential for both systemic and CNS targeting.

[1] A. Šermukšnytė et al., Biomolecules 14, 1529 (2024).
[2] I. Tumosienė et al., Monatsh. Chem. 149, 577-594 (2018).
[3] A. Šermukšnytė et al., Pharmaceuticals 15, 1026 (2022).

MULTIPLEXED EPIGENETIC PROFILING WITH Mx-TOP: A NOVEL METHOD FOR CHROMATIN AND DNA MODIFICATION ANALYSIS

Kotryna Kvederavičiūtė[1], Kotryna Skardžiūtė[1], Inga Pečiulienė[1], Janina Ličytė[1], Milda Narmontė[1], Saulius Klimašauskas[1], Edita Kriukienė[1]

[1]Department of Biological DNA Modification, Institute of Biotechnology, Life Sciences Center, Vilnius University, 10257 Vilnius, Lithuania
kotryna.kvederaviciute@mif.vu.lt

Epigenetic regulation is fundamental to gene expression control and cellular differentiation, with chromatin accessibility, DNA methylation, and hydroxymethylation serving as key transcriptional modulators. These regulatory layers function in a highly dynamic and interdependent manner, shaping the epigenomic landscape that underlies cell fate decisions. However, current approaches often require separate assays to investigate each of these regulators, increasing experimental and analytical costs while limiting insights into their interrelation. To address this, we developed Mx-TOP [1], a novel multiomic method that enables simultaneous profiling of chromatin accessibility, general DNA modification, and hydroxymethylation from a single sequencing library.

Mx-TOP is based on a chemo-enzymatic covalent tagging strategy to selectively label unmodified CG sites, hydroxymethylated cytosines (5hmC), and GC sites within chromatin, preserving base-resolution information through tag-selective TOP-seq [2] sequencing. This integrated approach enhances epigenetic profiling resolution while reducing experimental complexity. To identify open chromatin regions, we applied two peak-calling strategies: seed-and-extend and hidden Markov models, enabling robust detection of accessible genomic loci. Both strategies delineate chromatin accessibility patterns and their interplay with DNA modifications, offering deeper insights into transcriptional regulation.

We validated Mx-TOP through extensive benchmarking, demonstrating its high sensitivity in capturing chromatin accessibility and DNA modification dynamics in mouse embryonic stem cells. We then applied it to study chromatin remodeling and DNA demethylation during in vitro neuronal differentiation, a process characterized by extensive epigenetic reprogramming. Our results revealed decoupling between promoter accessibility and transcription, with gene body 5hmC emerging as a key gene expression modulator. Specifically, higher 5hmC levels within gene bodies correlated with transcriptional activity, even when promoter accessibility remained unchanged or decreased. Additionally, we identified developmentally regulated open chromatin loci resistant to global 5hmC erasure during epigenome reprogramming, suggesting that 5hmC in open chromatin plays a critical role in differentiation.

These findings provide new insights into gene body 5hmC's functional role in transcriptional regulation and chromatin remodeling, particularly in neuronal lineage commitment. By offering a high-resolution, multi-dimensional view of epigenetic landscapes, Mx-TOP serves as a powerful tool for studying complex gene regulatory networks. Its ability to integrate multiple epigenetic layers within a single framework holds great potential for developmental biology, neuroepigenetics, and disease-related epigenetic reprogramming.

[1] K. Skardžiūtė et al., "One-pot trimodal mapping of unmethylated, hydroxymethylated, and open chromatin sites unveils distinctive 5hmC roles at dynamic chromatin loci," Cell Chemical Biology, vol. 31, no. 3. Elsevier BV, pp. 607-621.e9, Mar. 2024. doi: 10.1016/j.chembiol.2023.12.003.

[2] Z. Staševskij, P. Gibas, J. Gordevičius, E. Kriukienė, and S. Klimašauskas, "Tethered Oligonucleotide-Primed Sequencing, TOP-Seq: A High-Resolution Economical Approach for DNA Epigenome Profiling," Molecular Cell, vol. 65, no. 3. Elsevier BV, pp. 554-564.e6, Feb. 2017. doi: 10.1016/j.molcel.2016.12.012.

CONSTRUCTION OF BACTERIOPHAGE GENOMIC DNA FRAGMENT LIBRARIES

Miglė Plioplytė[1], Jonas Juozapaitis[1], Giedrius Sasnauskas[1]

[1]Department of Protein - DNA Interactions, Vilnius University Life Sciences Center, Lithuania
migle.plioplyte@gmc.stud.vu.lt

The arms race between bacteria and their viruses (bacteriophages) is a millions-of-year-long struggle that has led to the mutual evolution of microorganisms [1]. One of the defense strategies used by bacteria against bacteriophages is abortive infection (Abi). Abi is a group of different systems that work by the same mechanism, where phage infection initiates cell death or metabolic slowdown to prevent the completion of phage replication cycle and infection of neighboring cells [2]. Many mechanisms of defense systems underlying abortive infection remain poorly understood and identifying the factors that activate abortive infection remains a major challenge [3]. So far, one approach to identifying genes that activate abortive infection has been the isolation and sequencing of bacteriophage mutants that escape the effects of defense systems. However, isolation of such phage mutants is successful only for a smaller part of the systems, and other assays are slower and of low-throughput [4]. Our study seeks to overcome the limitations of phage mutant assays and introduce a faster method based on high-throughput phage genes testing. This method is based on the construction of bacteriophage genomic DNA fragment libraries. To construct these phage libraries, first we amplified phage genomic DNA using Oxford Nanopore PCR Barcoding Kit, which allowed us to obtain 3000 kb and longer DNA fragments. These DNA fragments were then cloned into high-copy and low-copy cloning vectors to test whether toxic phage genes are better retained in the low-copy vector. As expected, the number of colonies differed between high-copy plasmid and low-copy plasmid phage libraries. The quality of constructed libraries was then assessed using the Oxford Nanopore sequencing method. The sequences of the phage library were then aligned to the reference phage genome. The reference phage genome was almost completely and evenly overlaid, which showed that the phage libraries were constructed successfully. The libraries will be further screened in cells, coding Abi systems of interest. The constructed phage library is transformed together with the Abi system, and library genes lost due to activated Abi proteins potentially encoding activators would be identified by sequencing.

[1] Wang, X., & Leptihn, S. (2024). Defense and anti-defense mechanisms of bacteria and bacteriophages. Journal of Zhejiang University-SCIENCE B, 25(3), 181–196. https://doi.org/10.1631/jzus.B2300101.

[2] Lopatina, A., Tal, N., & Sorek, R. (2020). Abortive Infection: Bacterial Suicide as an Antiviral Immune Strategy. Annual Review of Virology, 7(1), 371–384. https://doi.org/10.1146/annurev-virology-011620-040628.

[3] Aframian, N., & Eldar, A. (2023). Abortive infection antiphage defense systems: separating mechanism and phenotype. Trends in Microbiology, 31(10), 1003–1012. https://doi.org/10.1016/j.tim.2023.05.002.

[4] Stokar-Avihail, A., Fedorenko, T., Hör, J., Garb, J., Leavitt, A., Millman, A., Shulman, G., Wojtania, N., Melamed, S., Amitai, G., & Sorek, R. (2023). Discovery of phage determinants that confer sensitivity to bacterial immune systems. Cell, 186(9), 1863-1876.e16. https://doi.org/10.1016/j.cell.2023.02.029.

INTERACTION SURFACES WITHIN THE TYPE I-F CRISPR-CAS EFFECTOR COMPLEX

Toma Liegutė[1], Inga Songailienė[1,2], Tomas Šinkūnas[1]

[1]Vilnius University, Life Sciences Center, Department of Protein-DNA Interactions
[2]University of Copenhagen, Novo Nordisk Foundation Center for Protein Research, Faculty of Health and Medical Sciences
toma.liegute@gmc.stud.vu.lt

Prokaryotes have a wide range of defense mechanisms against invading nucleic acids. CRISPR-Cas is by far the most extensively studied and successfully applied anti-phage system. The vast diversity of CRISPR-Cas systems is divided into two classes and six types with different modes of action. The focus of this study is the type I-F CRISPR-Cas defense system found in *A. actinomycetemcomitans* bacteria[1]. This system encodes four different proteins (Cas5, Cas6, Cas7, Cas8), which together with crRNA form the ribonucleoprotein effector complex called Cascade (Csy), as well as Cas2/3 nuclease-helicase[2]. Cascade binds to the invading DNA site that is complementary to the crRNA, forming the R-loop structure. The R-loop triggers the Cas2/3 to degrade the foreign DNA eliminating the infection[3].

We have recently solved the cryo-EM structure of Cas2/3 bound to the Cascade-DNA complex and determined the interaction surfaces of Cas2/3 with Cascade. Here, using *in vitro* biochemical methods we analyse the importance of these surfaces for the DNA interference in the type I-F system.

[1] Donata Tuminauskaite et al., “DNA interference is controlled by R-loop length in a type I-F1 CRISPR-Cas system,” vol. 18, no. 1, Jun. 2020
[2] C. Xue and D. G. Sashital, “Mechanisms of Type I-E and I-F CRISPR-Cas Systems in Enterobacteriaceae,” EcoSal Plus, vol. 8, no. 2, Sep. 2019
[3] M. F. Rollins et al., “Cas1 and the Csy complex are opposing regulators of Cas2/3 nuclease activity,” Proceedings of the National Academy of Sciences, vol. 114, no. 26, Apr. 2017

HETEROLOGOUS EXPRESSION OF GRTB, A PREDICTED COLLAGEN-LIKE PROTEIN OF GRANULICELLA TUNDRICOLA MP5ACTX9T

Rosita Kavaliauskaitė[1], Rūta Kananavičiūtė[2]

[1] 1Institute of Biosciences, Life Sciences Center
kavaliauskaiterosita@gmail.com

Bacterial collagen-like proteins (CLP) contain $[G\text{-}X\text{-}Y]_n$ amino acid repeats and form collagen helix – a hallmark of mammalian collagen [1]. Bacterial CLP differ from the mammalian collagen in amino acid composition at X and Y positions, lack of post-translational modifications, and ability to form superstructures. Nevertheless, CLP offer many potential applications as alternatives to mammalian collagen. Moreover, comparing with animal collagens, bacterial CLP could be more easily engineered that makes them a promising candidates for unique biomaterial applications.

In this study, we focused on the GrtB putative collagen-like protein encoded by *Granulicella tundricola* MP5ACTX9T. *G. tundricola* is acidophilic bacterium, growing in environments with a pH range of 3.5 to 6.5 . Bioinformatic analysis of GrtB protein revealed that it contains $[G\text{-}X\text{-}Y]_n$ repeat region followed by the C-terminal domain related to SGNH hydrolase superfamily. The predicted function of this domain is related to GDSL-lipase activity. To date, only one CLP with an enzymatic domain has been described, making this a novel target for investigation [2].

The aim of this study was to express several constructs of the GrtB protein for characterisation of this unique protein. Different constructs where design, including: 1) Full length protein fused to His-tag, 2) N-terminal domain of the protein, containing collagenous repeats, 3) C-terminal domains, containing lipase domain. To achieve this, genes encoding distinct protein variants were amplified by PCR and cloned into pCoofy or pColdI vectors by restriction-ligation cloning or by ligation independent cloning, respectively. Recombinant plasmids were then transferred into *E. coli* cells for expression.

In conclusion, the designed and expressed different GrtB protein constructs enable further investigation into the structural and functional properties of this unique putative collage-like protein. Moreover, the obtained results will provide substantial insights into the novel properties of bacterial collagen-like proteins with enzymatic domains, which could have potential applications in drug delivery, tissue engineering, and the development of bioactive materials.

[1] Y. Qiu, C. Zhai, L. Chen, X. Liu, & J. Yeo, Current Insights on the Diverse Structures and Functions in Bacterial Collagen-like Proteins. ACS Biomaterials Science & Engineering, (2021) acsbiomaterials.1c00018. https://doi.org/10.1021/acsbiomaterials.1c00018.

[2] R. Kananavičiūtė, K. Kvederavičiūtė, D. Dabkevičienė, G. Mackevičius, & N. Kuisienė, Collagen-like sequences encoded by extremophilic and extremotolerant bacteria. Genomics, 112 (2020) 2271–2281. https://doi.org/10.1016/j.ygeno.2019.12.023.

STUDY OF TYPE IV-A2 CRISPR-CAS SYSTEMS

Gintarė Žvejytė[1], Rimvydė Čepaitė[1], Patrick Pausch[1]

[1]Life Sciences Center - European Molecular Biology Laboratory (LSC-EMBL) Partnership Institute for Genome Editing Technologies, Vilnius University, Vilnius, Lithuania
gintare.zvejyte@gmc.stud.vu.lt

CRISPR-Cas systems assure adaptive immunity against invading mobile genetic elements in bacteria and archaea. Among them, type IV-A CRISPR-Cas systems stand out due to their distinct mechanism. Type IV-A systems lack the typical DNA/RNA nuclease activity, instead, these multisubunit systems employ a helicase DinG, which unwinds the DNA rather than cleaving it, thus causing transcriptional interference [1][2]. While subtypes IV-A1 and IV-A3 have been thoroughly characterized through structural and biochemical studies, subtype IV-A2 remains largely unexplored. This is mainly because type IV-A2 systems diverge from other subtypes with the absence of a Cas8 homologous protein, which in type IV-A1 and A3 systems, together with Cas5, is responsible for protospacer adjacent motif (PAM) recognition [1][3][4]. However, in our study using a bioinformatic guilt-by-association approach, it was discovered that CRISPR-Cas type IV-A2 systems co-occur with a small, conserved gene near the *cas* operon, which is transcribed in the opposite direction. Investigating the function of the protein encoded by this gene will not only deepen the understanding of type IV-A2 mechanisms but also lead to their potential applications in gene editing in the future. Here, we present the preparatory studies laying the groundwork for the structural and functional characterization of one of type IV-A2 systems.

[1] R. Pinilla-Redondo et al., “Type IV CRISPR–Cas systems are highly diverse and involved in competition between plasmids”, Nucleic Acids Res., vol. 48, no. 4, pp. 2000–2012, Dec. 2019. Accessed: Feb. 16, 2025. [Online]. Available: https://doi.org/10.1093/nar/gkz1197

[2] V. M. Crowley et al., “A Type IV-A CRISPR-Cas System in Pseudomonas aeruginosa Mediates RNA-Guided Plasmid Interference In Vivo”, CRISPR J., vol. 2, no. 6, pp. 434–440, Dec. 2019. Accessed: Feb. 16, 2025. [Online]. Available: https://doi.org/10.1089/crispr.2019.0048

[3] N. Cui et al., “Type IV-A CRISPR-Csf complex: Assembly, dsDNA targeting, and CasDinG recruitment”, Mol. Cell, Jun. 2023. Accessed: Feb. 16, 2025. [Online]. Available: https://doi.org/10.1016/j.molcel.2023.05.036

[4] R. Čepaitė et al., “Structural variation of types IV-A1- and IV-A3-mediated CRISPR interference”, Nature Commun., vol. 15, no. 1, Oct. 2024. Accessed: Feb. 16, 2025. [Online]. Available: https://doi.org/10.1038/s41467-024-53778-1

DEVELOPMENT OF HYPOALLERGENIC VARIANTS OF COMMON MUGWORT ALLERGEN COMPONENT ART V 3

Eva Kupetytė[1], Laima Čepulytė[1], Rasa Petraitytė-Burneikienė[1]

[1]Department of Eukaryote Gene Engineering, Institute of Biotechnology, Life Sciences Center, Vilnius University, Lithuania
eva.kupetyte@gmc.stud.vu.lt

Allergic diseases are a common health issue that affects all of humanity. Over 20% of the population suffers from allergic diseases such as allergic rhinitis and allergic asthma [1]. Allergies occur when the immune system overreacts to substances that are harmless to most individuals, such as pollen, dust mites, certain foods, and pharmaceuticals. In response, the immune system produces antigen-specific immunoglobulin E (sIgE), leading to symptoms like sneezing, coughing, skin rashes, and runny nose. Symptom control can be achieved by allergen avoidance and pharmaceuticals. Still, allergen-specific immunotherapy (ASIT) is currently the only therapeutic approach that can modify the immune response and prevent the development of allergic diseases [2]. However, ASIT relies on natural allergen extracts and has some limitations, including the potential to cause side effects or sensitization to new allergens. Recombinant allergens with modified IgE epitopes are known as hypoallergens. Hypoallergens are less likely to induce an allergen-specific IgE response and cause side effects but can elicit the T-cell response. Using hypoallergens in allergen-specific immunotherapy may help modulate the immune response to the target allergen and induce immune tolerance to it. Also, the use of hypoallergens in therapy reduces the risk of side effects such as allergy symptoms or even anaphylactic shock [3].

Airborne pollen is a common trigger of respiratory allergies, affecting many people worldwide [4]. Common mugwort *(Artemisia vulgaris)* is a highly allergenic plant that produces large amounts of wind-borne pollen. It is a major cause of allergic reactions in Europe, affecting 10% to 15% of pollinosis patients during its long-lasting flowering period [5]. One of the six allergen components of the common mugwort, Art v 3, was approved in 2003. However, its IgE epitopes, important for developing hypoallergens, remain unidentified [6].

This research aimed to create mutant variants of the allergen component Art v 3 and to conduct a primary antigenicity assay. Based on the literature review and bioinformatic analysis, amino acids potentially involved in IgE-binding epitope formation were identified and mutant variants of Art v 3 were generated by site-directed mutagenesis. Proteins were synthesized in *E. coli* and purified using Ni^{2+} affinity chromatography. Primary antigenicity tests were performed to assess whether the reactivity of the recombinant proteins with sIgE was reduced. The identification of IgE epitopes is important for the synthesis of hypoallergens, and antigenicity assays of these mutants will provide valuable insights into their therapeutic applications.

Acknowledgements
The research is funded by the Research Council of Lithuania (LMTLT), agreement No S-MIP-24-41.

[1] O. Pfaar et al., "Comparison of allergen immunotherapy practice patterns in inhalant allergies in the United States of America and Europe: Similarities and differences 2023," World Allergy Organ. J., vol. 16, no. 5, p. 100766, 2023.
[2] J. Wang et al., "Pathogenesis of allergic diseases and implications for therapeutic interventions," Signal Transduct. Target. Ther., vol. 8, no. 1, p. 138, 2023.
[3] O. Akinfenwa, A. Rodríguez-Domínguez, S. Vrtala, R. Valenta, and R. Campana, 'Novel vaccines for allergen-specific immunotherapy', Current Opinion in Allergy & Clinical Immunology, vol. 21, no. 1, pp. 86–99, 2021.
[4] J.-W. Oh, 'Pollen Allergy in a Changing Planetary Environment', Allergy Asthma Immunol Res, vol. 14, no. 2, pp. 168–181, 2022.
[5] N. Wopfner et al., 'The Spectrum of Allergens in Ragweed and Mugwort Pollen', Int Arch Allergy Immunol, vol. 138, no. 4, pp. 337–346, 2005.
[6] G. Gadermaier, M. Hauser, and F. Ferreira, 'Allergens of weed pollen: An overview on recombinant and natural molecules', Methods, vol. 66, no. 1, pp. 55–66, 2014.

THE SPECIFICITY OF THE STREPTOCOCCUS PNEUMONIAE TOXIN PNEUMOLYSIN FOR LIPID BILAYER COMPOSITION

Adelė Unikauskaitė[1], Tadas Ragliauskas[1]

[1] Institute of Biochemistry, Life Sciences Center, Vilnius University
adele.unikauskaite@gmc.stud.vu.lt

The cell membrane is a crucial barrier, protecting cellular contents from the external environment while maintaining interactions with surrounding molecules. However, bacterial toxins, such as pneumolysin (PLY) [1], a cholesterol-dependent cytolysin from Streptococcus pneumoniae, can bind to membranes, form pores, and disrupt cellular homeostasis. The main objective is to investigate how variations in lipid bilayer composition influence PLY binding and pore formation, providing insights into the toxin's membrane selectivity.

Cholesterol is the major contributor to promoting PLY binding to lipid membranes and induction of ion-defect formation. However, the levels of cholesterol needed may vary on surrounding lipids. Also, the size and charge of the lipid headgroup interplay with the protein's access to cholesterol within the membrane; potentially, other physical properties of the lipid bilayer are affected. In this work, we use electrochemical impedance spectroscopy (EIS) to analyze the electrical properties of membranes, such as electric conductivity and capacitance. We use tethered lipid bilayers (tBLMs) [2] composed of unsaturated lipids with various headgroups (choline, ethanolamine, glycerol) and cholesterol. Permeability is determined by the minimum frequency, which reflects membrane resistance and capacitance changes, indicating protein binding and further pore formation.

The primary findings indicate that in two-lipid systems (cholesterol and zwitterionic lipid), the threshold of detection of pneumolysin activity requires at least 40 mol% of cholesterol. In more complex systems with the addition of other zwitterionic lipids, which affect bilayer packing, pneumolysin induces similar damage to the membranes but with lower cholesterol levels.

[1] Rubins and Janoff, 1998. Pneumolysin: a multifunctional pneumococcal virulence factor. Journal of Laboratory and Clinical Medicine, vol. 131, iss. 1, p. 21-27.

[2] Ragaliauskas et al. 2017. Fast formation of low-defect-density tethered lipid bilayers by fusion of multilamellar vesicles. BBA Biomembranes, vol. 1859, iss. 5, p. 669-678.

SINGLE-CELL HIGH-THROUGHPUT RT-PCR ANALYSIS OF PFA FIXED PROKARYOTIC SAMPLES

Laura Kuliešytė[1], Greta Leonavičienė[1], Linas Mažutis[1]

[1]Department of Single Cell Analytics, Institute of Biotechnology, Life Sciences Center, Vilnius University, Vilnius, Lithuania
laura.kuliesyte@gmc.stud.vu.lt

The field of transcriptomics examines cellular RNA content and provides functional insight into organisms, their regulatory mechanisms and responses to changing environmental conditions. Initial methods for transcriptomic analysis required high amount of input material and provided an averaged-out, population level readout. However, biological systems are inherently heterogenous. To probe this heterogeneity, single-cell transcriptomic technology was developed [1]. The technology became inseparable in the fields of cancer and developmental biology among many others, however, its' application in the prokaryotic research remained relatively constrained [2].This is due several limitations: most prokaryotes possess a rigid cell wall, complicating the cell lysis, the amount of bacterial messenger RNA (mRNA) is low compared to eukaryotes, molecules have a shorter lifespan, usually lasting only few minutes, and lack a poly-A tail, required for barcoding. Cellular fixation overcomes some of these hurdles, however, to enable efficient transcriptomic studies, bacterial RNA must be successfully barcoded, reverse transcribed and amplified. In this work, fixation reagents: formaldehyde, glutaraldehyde and paraformaldehyde (PFA) were evaluated and optimal concentrations and fixation durations determined. What is more, several approaches to reverse transcribe bacterial mRNA were explored, including polyadenylation prior reverse transcription (RT) versus the use of random hexamer primers.

To this end, PFA fixed bacterial samples underwent isolation in semi-permeable microcapsules, lysis, polyadenylation, reverse transcription, PCR and fluorescent imaging.

[1] J. Tang, Y. C. Barbacioru, X. Wang, et al., "mRNA-Seq whole-transcriptome analysis of a single cell," Nature Methods, vol. 6, no. 5, pp. 377–382, 2009. doi: 10.1038/nmeth.1315.

[2] S. B. Blattman, W. Jiang, P. Oikonomou, and S. Tavazoie, "Prokaryotic single-cell RNA sequencing by in situ combinatorial indexing," Nat. Microbiol., vol. 5, no. 10, pp. 1192–1201, 2020, doi: 10.1038/s41564-020-0729-9.

OLOKUN - A NOVEL PROKARYOTIC ANTIPHAGE DEFENSE SYSTEM

Vincentas Raudys[1], Viktorija Rainytė[1], Edvinas Jurgelaitis[1], Paulius Toliušis[1], Mindaugas Zaremba[1]

[1]Department of Protein-DNA Interactions, Institute of Biotechnology, Life Sciences Center, Vilnius University
vincentas.raudys@gmc.vu.lt

The long ongoing fight between bacteria and bacteriophages has led to bacteria evolving and/or acquiring diverse defense mechanisms. Many of these have become irreplaceable tools in molecular biology and biochemistry. CRISPR-Cas systems for genome editing and restriction-modification systems (RM) for manipulating nucleic acids are all derived from prokaryotic antiviral defense systems[1]. However, there is always a need for new tools to be discovered. Fortunately, recent bioinformatics approaches have identified “defense islands” (DIs), genomic regions enriched in defense-related genes, leading to the identification of numerous novel and uncharacterized defense systems[2, 3].

This study aims to characterize the novel prokaryotic antiviral defense system - Olokun, discovered in the *E.coli* UMB0934 strain. To better understand the underlying mechanism of Olokun, site-specific mutagenesis targeting the predicted active centers has been carried out. Following mutagenesis, Western blotting was used to confirm the expression of the defense system mutants. At the same time, phage plaque assays were employed to determine the effect of these mutations on the system’s ability to protect bacteria from bacteriophage infection *in vivo*. The purified mutant protein was also subjected to biochemical assays to investigate its nucleolytic activity *in vitro*.

This work contributes to a deeper understanding of prokaryotic antiphage defense and its potential applications in biotechnology.

[1] Georjon, H., & Bernheim, A. (2023). The highly diverse antiphage defence systems of bacteria. Nature Reviews Microbiology, 21(10), 686–700. https://doi.org/10.1038/s41579-023-00934-x

[2] Millman, A., Melamed, S., Leavitt, A., Doron, S., Bernheim, A., Hör, J., Lopatina, A., Ofir, G., Hochhauser, D., Stokar-Avihail, A., Tal, N., Sharir, S., Voichek, M., Erez, Z., Ferrer, J. L. M., Dar, D., Kacen, A., Amitai, G., & Sorek, R. (2022). An expanding arsenal of immune systems that protect bacteria from phages. bioRxiv (Cold Spring Harbor Laboratory). https://doi.org/10.1101/2022.05.11.491447

[3] Vassallo, C., Doering, C., Littlehale, M. L., Teodoro, G., & Laub, M. T. (2022). Mapping the landscape of anti-phage defense mechanisms in the E. coli pangenome. bioRxiv (Cold Spring Harbor Laboratory). https://doi.org/10.1101/2022.05.12.491691

DEVELOPMENT OF THE BACTERIAL AMIDOHYDROLASE YQFB TO IMPROVE ITS BIOTHERAPEUTIC APPLICATIONS

Kamilė Dzisevič[1], Viktorija Preitakaitė[1], Rolandas Meškys[1]

[1]Department of Molecular Microbiology and Biotechnology, Institute of Biochemistry, Life Sciences Center, Vilnius University, Saulėtekio av. 7, Vilnius, Lithuania
kamile.dzisevic@gmc.stud.vu.lt

Amidohydrolases are a large class of enzymes catalyzing the hydrolysis of a wide range of substrates bearing amide or ester functional groups at the carbon and phosphorus centers. Due to their functionality, amidohydrolases are applicable in various fields, starting from research assaying their role in metabolic pathways, such as the metabolism of certain amino acids and nucleotides, and ending with the usage of these enzymes in chemical synthesis, food, and cosmetic industry. Nevertheless, a remaining conundrum regarding the application of amidohydrolases in biotherapy is the targeted delivery of these enzymes to malignant cells or affected tissues. Therefore, the aim of this study was to develop modified variants of YqfB amidohydrolase which possess alterations in the amino acid sequence not interfering with its catalytic activity, but providing improved biotherapeutic applications.

Firstly, targeted mutagenesis of the sequence encoding YqfB amidohydrolase was performed by PCR using synthetic primers. Next, the mutant sequences were transformed into an *Escherichia coli* strain (*HMS174ΔpyrFΔyqfB*), in which the protein expression was later induced using IPTG at 20 °C for 22 hours. The bacterial biomass was collected and lysed. The final steps included the collection of the soluble protein extract via centrifugation and the verification of enzyme activity by thin-layer chromatography using the soluble protein extract and N^4-acetylcytosine as a substrate.

The results showed that modifications that were tested in the amino acid sequence of YqfB did not interfere with its enzymatic activity towards N^4-acetylcytosine. This not only indicated sites in the protein's amino acid sequence amenable to modification without compromising enzymatic activity, but also opened up the possibility of more efficient application of modified YqfB variants in biotherapy, which requires further research.

SINGLE-CELL ISOLATION USING SEMI-PERMEABLE CAPSULES: MARKER GENE DETECTION AND CELL CULTIVATION ANALYSIS

Aina El Ravvas[1], Linas Mažutis[1]

[1]Department of Single Cell Analytics, Institute of Biotechnology, Life Sciences Centre, Vilnius University
aina.el@gmc.vu.lt

Single-cell isolation from heterogeneous populations enables detailed characterization of individual cells. While high-throughput microfluidic techniques are commonly used [1], conventional methods often struggle to support multi-step biochemical reactions while maintaining genetic integrity. To address this, we explore a semi-permeable capsule-based approach in which the capsules retain genetic material while allowing the diffusion of small molecules [2], [3]. A representative image of a microcapsule hosting a cell is shown in Figure 1A. This method is particularly appealing for analyzing biological systems in a cost-effective manner.

We applied capsule-based technology to perform (i) single-cell marker gene analysis and (ii) 3D cell cultivation. Marker gene expression was assessed using cDNA synthesis, PCR, and fluorescent *in situ* hybridization (*FISH*) for housekeeping genes, with further optimization needed for specific markers. Additionally, we demonstrated that the capsules support long-term cell growth. For example, suspension cells (K562) proliferated within the capsules for 18 days, eventually filling the entire capsule volume and also expanding the capsule. Adhesive (HeLa) cells adhered to the inner surface of the capsules and remained there long-term, indicating a supportive microenvironment.

This work shows that semi-permeable capsule technology represents a promising tool for single-cell gene expression analysis and controlled growth in 3D microenvironment, with broader potential applications in spheroid formation, drug screening, and high-throughput single-cell studies.

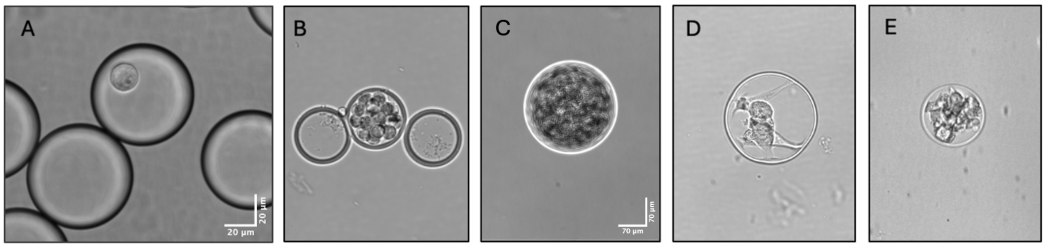


Figure 1. A Bright-field image of a semi-permeable microcapsule containing a single cell.
B Single-cell derived suspension cell (K562) clump after 4 days of growth.
C Single-cell derived suspension cell (K562) spheroid after 18 days of growth.
D Single-cell derived adherent cells (HeLa) after 4 days of growth.
E Single-cell derived adherent cells (HeLa) after 7 days of growth.

[1] Klein, A. M., Mazutis, L., Akartuna, I., Tallapragada, N., Veres, A., Li, V., Peshkin, L., Weitz, D. A., & Kirschner, M. W. (2015). Droplet barcoding for single-cell transcriptomics applied to embryonic stem cells. Cell, 161(5), 1187–1201.
[2] Leonaviciene, G., Leonavicius, K., Meskys, R., & Mazutis, L. (2020). Multi-step processing of single cells using semi-permeable capsules. Lab on a Chip, 20(21), 4052–4062.
[3] Leonaviciene, G., & Mazutis, L. (2023). RNA cytometry of single-cells using semi-permeable microcapsules. Nucleic Acids Research, 51(1), e2.

RECOMBINANT β-CARBONIC ANHYDRASE PROTEINS PRODUCTION

Eglė Lukauskaitė[1], Tautvydas Kojis[1], Justinas Babinskas[2], Ieva Gaubė[2], Lina Baranauskienė[1], Inga Matijošytė[2]

[1]Department of Biothermodynamics and Drug Design, Institute of Biotechnology, Life Sciences Centre, Vilnius University, Vilnius, Lithuania
[2]Sector of Applied Biocatalysis, Institute of Biotechnology, Life Sciences Centre, Vilnius University, Vilnius, Lithuania
eglelukauskaite04@gmail.com

Carbonic anhydrase (CA) is an enzyme responsible for carbon dioxide's reversible reaction to bicarbonate ($CO_2 + H_2O \rightleftharpoons HCO_3^- + H^+$). While this chemical reaction can occur spontaneously, its rate is often insufficient to meet living organisms' needs. To address this issue, most organisms have evolved one or more forms of CA to enhance the reaction rate [1].

There are currently eight distinct evolutionary unrelated classes of CAs found, denoted by Greek letters: α, β, γ, δ, ζ, η, θ, and ι. Among these classes, four – α, β, γ, and ι – can be found in bacteria and fungi. In these organisms, enzymes play a vital role, including the transport of bicarbonate and CO_2, pH regulation, ion and water transport, and carbon fixation in photosynthetic bacteria [2].

Microorganisms that produce β-carbonic anhydrases (β-CAs) can thrive in extreme environments, such as those with high salt levels, acidity, or alkalinity. This ability makes these enzymes very useful in biotechnology. Recent studies have demonstrated that β-CAs can be applied in biomedical research and drug development [3]. They are also being explored for their role in carbon capture technologies, where they help convert CO_2 emissions into valuable products [4]. Furthermore, they can serve as biocatalysts in industrial processes, often under harsh conditions. As more enzymes that can withstand extreme environments are discovered, the future for β-CAs looks promising.

With this study, we aim to produce recombinant β-CAs and establish the technology for the enzymatic synthesis of cyclic carbonates (Fig. 1).

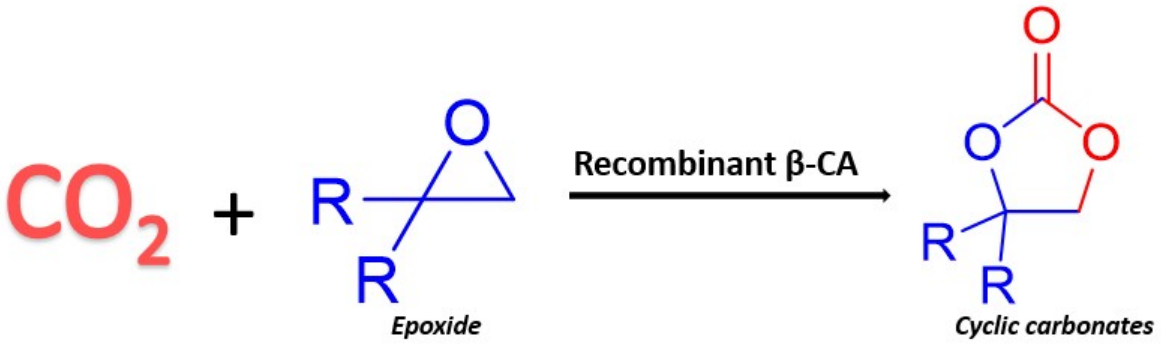


Fig. 1. Schematic representation of using β-CAs for producing cyclic carbonate.

This project has received funding from the Research Council of Lithuania (LMTLT), agreement No S-MIP-24-49.

[1] Chegwidden W.R. (2021) The Carbonic Anhydrases in Health and Disease. In: Chegwidden W.R., Carter N.D. (eds) The Carbonic Anhydrases: Current and Emerging Therapeutic Targets. Progress in Drug Research, vol 75. Springer, Cham.
[2] Capasso, C., & Supuran, C. T. (2024). Overview of bacterial carbonic anhydrase genetic families. In C. T. Supuran (Ed.), The enzymes (Vol. 55, pp. 1-29). Academic Pres.
[3] Capasso, C., & Supuran, C. T. (2024). Biomedical applications of prokaryotic carbonic anhydrases: an update. Expert opinion on therapeutic patents, 34(5), 351–363. https://doi.org/10.1080/13543776.2024.236540
[4] Talekar, S., Jo, B. H., Dordick, J. S., & Kim, J. (2022). Carbonic anhydrase for CO2 capture, conversion, and utilization. Current Opinion in Biotechnology, 74, 230–240.

EXPANDING THE ARSENAL: FIRST PEEK AT A NOVEL TYPE III CRISPR-CAS EFFECTOR

Marija Duchovskyte[1], Dalia Smalakyte[1], Irmantas Mogila[1], Gintautas Tamulaitis[1]

[1] Institute of Biotechnology, Life Sciences Center, Vilnius University, Lithuania
marija.duchovskyte@gmc.stud.vu.lt

Clustered Regularly Interspaced Short Palindromic Repeats (CRISPR) loci and CRISPR-associated proteins (Cas) defend bacteria and archaea from bacteriophages by specifically targeting viral nucleic acids. Among these defense mechanisms, type III CRISPR-Cas systems provide an additional layer of protection through a distinct signaling pathway. When the type III CRISPR-Cas interference complex recognizes a foreign transcript, the Cas10 subunit starts to synthesize cyclic oligoadenylates. These signaling molecules bind to the sensory domains of ancillary effector proteins, triggering the activation of their effector domains. Once activated, these effectors can degrade RNA or DNA, inhibit translation, or disrupt membrane integrity, thus preventing viral replication or killing infected cells [1], [2].

Recent systematic analyses of previously uncharacterized genes within CRISPR-Cas operons have identified a wider range of effector proteins [3] with predicted biochemical activities not previously linked to CRISPR-Cas immunity. However, the precise functions of these novel effectors in type III CRISPR-Cas immunity remain unknown. In this study, we present the initial studies on novel putative type III CRISPR-Cas effectors demonstrating their activity in the heterologous *E. coli* host.

[1] I. Mogila et al., “Ribosomal stalk-captured CARF-RelE ribonuclease inhibits translation following CRISPR signaling,” Science, vol. 382, no. 6674, pp. 1036–1041, 2023.
[2] G. Stella and L. Marraffini, “Type III CRISPR-Cas: beyond the Cas10 effector complex,” Trends in Biochemical Sciences, vol. 49, no. 1, pp. 28–37, 2024.
[3] H. Altae-Tran et al., “Uncovering the functional diversity of rare CRISPR-Cas systems with deep terascale clustering,” Science, vol. 382, no. 6673, 2023.

DISASSEMBLY AND REASSEMBLY OF L-A VIRUS-LIKE PARTICLES PURIFIED FROM SACCHAROMYCES CEREVISIAE

Kamilė Vaišaitė[1], Enrika Celitan[1], Saulius Serva[1]

[1]Vilnius university, Life Sciences Center, Vilnius, Lithuania
kamile.vaisaite@gmc.vu.lt

L-A virus is a dsRNA virus of the *Totiviridae* family found in *Saccharomyces cerevisiae* yeast [1]. With evidence that the native L-A host, *S. cerevisiae*, is abundant in the natural human environment [2], it is expected that the capsids of this virus could be adapted for immune response-neutral nanodelivery of biomolecules into mammalian cells. To this end, our previous studies have developed a system for the synthesis of L-A virus capsids in *S. cerevisiae* yeast. Such particles, consisting of recombinant viral capsid proteins and resembling native virions in structure, yet lacking of genetic material, are more commonly known as virus-like particles (VLPs). VLPs are becoming an increasingly popular object for drug nanodelivery studies due to their biocompatibility, safety, monodispersity, natural tissue tropism, and the possibility of easy chemical and genetic modification of the inner and outer surface [3].

One of the key steps in the application of VLPs to nanocarrier applications is disassembly-reassembly studies. This method helps to get rid of cellular proteins and other molecules that are encapsulated during self-assembly in the cell, often increases the stability of the reassembled particles, and is a popular method for encapsulating larger cargoes such as proteins or nucleic acids [3]. Therefore, in order to apply the L-A VLPs synthesized by *Saccharomyces cerevisiae* to nanocarrier applications, the main objective of this study was to find the conditions for both their disassembly and reassembly.

Particle disassembly was examined under different conditions: high ionic strength, basic and acidic pH, and reducing and denaturing reagents (β-mercaptoethanol, dithiothreitol, urea). Following the overnight treatment, dynamic light scattering (DLS) method was used to assess the particle size. Small structures of 14–18 nm were only detected in samples containing urea, suggesting that the L-A VLPs had disassembled. Consequently, further reassembly experiments were conducted using particles that had been disintegrated using 2 M urea. The disassembled particles were dialyzed overnight in Tris-HCl-based buffers with different ionic strengths and Tween 80, and then reassembled particles were precipitated by ultracentrifugation through sucrose cushion. As evidenced by the initial experiments, L-A VLPs did reassemble during dialysis, regardless of the buffer solution. Future research will be conducted to determine the efficiency of the reassembly, as well as the prospects of cargo encapsulation.

[1] R.B. Wickner, T. Fujimura, & R. Esteban (2013). Viruses and prions of Saccharomyces cerevisiae, Advances in Virus Research, 86(1).
[2] J. F. Garcia-Mazcorro, italic et al. (2020). Are there indigenous Saccharomyces in the digestive tract of livestock animal species? Implications for health, nutrition and productivity traits. Animal, 14:22–30.
[3] S. Nooraei, et al. (2021). Virus-like particles: preparation, immunogenicity and their roles as nanovaccines and drug nanocarriers. Journal of Nanobiotechnology, 19(1), 1-27.

SYNTHESIS OF RECOMBINANT ARTEMISIA VULGARIS ALLERGEN ART V 3 IN DIFFERENT YEAST EXPRESSION SYSTEMS

Emilija Dobrovolskytė[1], Laima Čepulytė[1], Paulius Lukas Tamošiūnas[1], Rasa Petraitytė-Burneikienė[1]

[1]Department of Eukaryote Gene Engineering, Institute of Biotechnology, Life Sciences Center, Vilnius University, Lithuania
emilija.dobrovolskyte@gmc.stud.vu.lt

Allergies are a prevalent health issue that affects many people regularly. The prevalence of allergies varies between 20% and 40% of the population in each country. However, these numbers are underestimated because many individuals do not seek medical advice or are incorrectly diagnosed [1]. Allergy is an overactive response of the immune system to substances that are typically harmless to most people [2]. These substances, known as allergens, are molecules from animal fur, dust, pollen, etc., which can trigger allergic reactions. People with allergies can experience various symptoms, including swollen tongue, itchy and/or watery eyes, etc. Allergies could also lead to chronic conditions like eczema and allergic asthma [3]. Whole-allergen extracts from natural sources are still widely used for allergy diagnostics and immunotherapy. However, the use of natural extracts, which are difficult to standardize, is limited by many factors. A varying number of different allergens, their biological activity, and contaminants in extracts can lead to false positive or negative results and ineffective immunotherapy. Single recombinant allergen molecules could be used to overcome these problems [4].

Yeasts are commonly used for the synthesis of recombinant proteins because they combine the advantages of both prokaryotic and eukaryotic cells. Yeast can perform post-translational modifications, such as disulfide bond formation and glycosylation. Additionally, yeast cultivation is cost-effective, simple, and allows for producing recombinant proteins in high yields. Nevertheless, a significant drawback of using yeast is the hyperglycosylation of proteins, which can impact protein antigenicity. Therefore, testing different yeast species and strains can benefit recombinant protein production, as their distinct glycosylation profiles may help reduce the effects of hyperglycosylation [5].

In this study, recombinant allergen Art v 3 from *Artemisia vulgaris* (common mugwort) was analyzed. *A. vulgaris* is prevalent in Europe, North America, and Asia. During the pollen season in late summer and fall, common mugwort is one of the main causes of pollinosis [6]. In Europe, *A. vulgaris* accounts for approximately 10% to 14% of all cases of pollinosis [7]. *Artemisia vulgaris* has six different allergens (Art v 1-6), and up to 70% of individuals allergic to common mugwort can be sensitized to Art v 3. Art v 3 belongs to the family of non-specific lipid transfer proteins. [6]. During this study, recombinant Art v 3 protein synthesis experiments were conducted using three different yeast species: *Saccharomyces cerevisiae*, *Kluyveromyces lactis*, and *Pichia pastoris*. The recombinant allergen proteins were purified, and primary antigenicity experiments were carried out.

Acknowledgements
The research is funded by the Research Council of Lithuania (LMTLT), agreement No S-ST-24-73.

[1] D. Boehmer, B. Schuster, J. Krause, U. Darsow, T. Biedermann, and A. Zink, “Prevalence and treatment of allergies in rural areas of Bavaria, Germany: a cross-sectional study,” World Allergy Organization Journal, vol. 11, pp. 36–36, Jan. 2018, doi: 10.1186/s40413-018-021 8-z.
[2] J. M. Dougherty, K. Alsayouri, and A. Sadowski, “Allergy,” PubMed, 2023. https://pubmed.ncbi.nlm.nih.gov/31424821/
[3] Van R. Ree, and C. R. Aalberse, “Allergens and the allergenic composition of source materials,“ in Molecular Allergology User’s Guide 2.0, K. Hoffmann, C. Hilger, A. Santos, L. de las Vecillas and S. Dramburg, Eds. Switzerland: John Wiley & Sons, 2022, pp-25-37.
[4] R. Valenta, A. Karaulov, V. Niederberger, Y. Zhernov, O. Elisyutina, R. Campana, M. Focke-Tejkl, M. Curin, L. Namazova-Baranova, J. Y. Wang, R. Pawankar and M. Khaitov, “Allergen Extracts for In Vivo Diagnosis and Treatment of Allergy: Is There a Future?,” The Journal of Allergy and Clinical Immunology: In Practice, vol. 6, no. 6, pp. 1845-1855.e2, Nov. 2018, doi: 10.1016/j.jaip.2018.08.032.
[5] A. Schütz F. Bernhard, N. Berrow, J. F. Buyel, F. Ferreira-da-Silva, J. Haustraete, J. van den Heuvel, J. E. Hoffmann, A. de Marco, Y. Peleg, S. Suppmann, T. Unger, M. Vanhoucke, S. Witt and K. Remans, “A concise guide to choosing suitable gene expression systems for recombinant protein production,” STAR Protocols, vol. 4, no. 4, pp. 102572–102572, Dec. 2023, doi: https://doi.org/10.1016/j.xpro.2023.102572.
[6] M. Hauser, J. M. Davies, T. Hawranek, and G. Gadermaier, “Weed pollen allergy,“ in Molecular Allergology User’s Guide 2.0, K. Hoffmann, C. Hilger, A. Santos, L. de las Vecillas and S. Dramburg, Eds. Switzerland: John Wiley & Sons, 2022, pp-201-215.
[7] I. Pablos, M. Egger, E. Vejvar, V. Reichl, P. Briza, D. Zennaro, C. Rafaiani, W. Pickl, B. Bohle, A. Mari, F. Ferreira, G. Gadermaier, “Similar Allergenicity to Different Artemisia Species Is a Consequence of Highly Cross-Reactive Art v 1-Like Molecules,” Medicina, vol. 55, no. 8, pp. 504–504, Aug. 2019, doi: 10.3390/medicina55080504.

CLONING, EXPRESSION AND FUNCTIONAL ANALYSIS OF RECOMBINANT LIPOXYGENASE

Vytautė Blekaitytė[1], Dovilė Daunoraitė[1], Inga Matijošytė[1]

[1]Sector of Applied Biocatalysis, Institute of Biotechnology, Life Sciences Center, Vilnius University, Lithuania
vytauteblekaityte@gmc.stud.vu.lt

The heterologous production of enzymes has been a central focus of modern biotechnology for several decades, driven by the increasing demand for industrial enzymes due to their ecological and economic advantages. Lipoxygenases (LOX) catalyse the peroxidation of unsaturated fatty acids into fatty acid hydroperoxides, which are of particular interest due to their ability to be readily transformed into various valuable compounds. These compounds can be used across a broad spectrum of applications, ranging from the production of oleochemicals to the creation of flavour compounds, the synthesis of signalling compounds, and their use as food additives. Although lipoxygenases are present in almost every living organism, they differentiate by the type of substrate they utilise. Furthermore, bacterial LOXs may possess improved thermostability and activity over a broader pH range compared to their eukaryotic counterparts [1]. *Pseudomonas aeruginosa* lipoxygenase (PaLOX) is a resilient enzyme that exhibits considerable activity at elevated temperatures and can peroxidize not only linoleic and linolenic acids but also arachidonic acid and oleic acid, demonstrating a diverse range of substrates [2]. This versatility highlights its potential as an eco-friendly biocatalyst for a wide range of industrial applications.

The aim of this study is to produce an active recombinant *P. aeruginosa* lipoxygenase employing the yeast *Pichia pastoris* as the expression system. The *palox* gene was fused with a C- or N-terminal histidine tag to facilitate purification by immobilised metal affinity chromatography (IMAC) and cloned into the pPic9K shuttle vector. The construct ensures methanol-induced protein expression and secretion. The recombinant plasmid was then introduced into *P. pastoris* GS115. Transformed cells were screened and cultivated in BMMY medium to induce expression. SDS-PAGE and lipoxygenase activity assay were used to verify the successful expression of PaLOX. The detailed presentation of the findings will be showcased at the poster session.

[1] R. Chrisnasari, M. Hennebelle, J.-P. Vincken, W. J. H. Van Berkel, and T. A. Ewing, “Bacterial lipoxygenases: Biochemical characteristics, molecular structure and potential applications,” Biotechnology Advances, vol. 61, p. 108046, Oct. 2022, doi: 10.1016/j.biotechadv.2022.108046.

[2] C. Hashem, H. Stolterfoht, C. Rinnofner, S. Steinberger, M. Winkler, and H. Pichler, “Secretion ofPseudomonas aeruginosaLipoxygenase byPichia pastorisupon Glycerol Feed,” Biotechnology Journal, vol. 15, no. 11, Aug. 2020, doi: 10.1002/biot.202000089.

BIOCHEMICAL CHARACTERIZATION OF ARGONAUTE PROTEINS XAUSPARDA AND EAESPARDA CONTAINING NUCLEASE EFFECTOR DOMAIN

Edvinas Jurgelaitis[1], Arunas Silanskas[1], Mindaugas Zaremba[1]

[1]Vilnius University
edvinas.jurgelaitis@gmc.vu.lt

Prokaryotic Argonautes (pAgos) are divided into long and short Agos. The majority (60%) are short pAgos containing only MID and catalytically inactive PIWI domains. Short pAgos have a guide-mediated target recognition function, while various effector domains (Sir2, TIR, DREN, fig. 1) of their associated APAZ proteins execute enzymatic reactions to kill the host cell, thus, preventing spread of the invader [1-4]. It has been demonstrated that short prokaryotic Argonaute associated with DNase/RNase effector nuclease (DREN-APAZ) (SPARDA) proteins using RNA guides (gRNA) recognize their DNA targets (tDNA), leading to nonspecific collateral cleavage of DNA and RNA [4-5]. However, the detailed SPARDA activation mechanism remains unknown. Here we present the in vitro study of previously uncharacterized SPARDA systems. Firstly, we determined the specificity of XauSPARDA and EaeSPARDA for gRNA and tDNA with a dsDNA substrate. Then we analysed collateral cleavage activity of XauSPARDA and EaeSPARDA with various substrates. Next, we purified 4 different active site mutants for XauSPARDA and measured their DNase activity. Finally, by varying different bases in guide RNA and target DNA sequences we determined key base pair positions responsible for activating each protein's enzymatic activity.

[1] Zaremba, M., Dakineviciene, D., Golovinas, E. et al. Short prokaryotic Argonautes provide defence against incoming mobile genetic elements through NAD+ depletion. Nat Microbiol 7, 1857–1869 (2022).
[2] Garb, J., Lopatina, A., Bernheim, A. et al. Multiple phage resistance systems inhibit infection via SIR2-dependent NAD+ depletion. Nat Microbiol 7, 1849–1856 (2022).
[3] Koopal, Balwina et al. Short prokaryotic Argonaute systems trigger cell death upon detection of invading DNA Cell, Volume 185, Issue 9, 1471 - 1486.e19
[4] Xueling Lu, Jun Xiao, Longfei Wang, Bin Zhu, Fengtao Huang, The nuclease-associated short prokaryotic Argonaute system nonspecifically degrades DNA upon activation by target recognition, Nucleic Acids Research, Volume 52, Issue 2, 25 January 2024, Pages 844–855,
[5] Prostova, M., Kanevskaya, A., Panteleev, V. et al. DNA-targeting short Argonautes complex with effector proteins for collateral nuclease activity and bacterial population immunity. Nat Microbiol 9, 1368–1381 (2024). https://doi.org/10.1038/s41564-024-01654-5

CHARACTERIZATION OF HYBRID CLASS 1 AND CLASS 2 CRISPR-CAS SYSTEMS

Brigita Duchovska[1], Tomas Šinkūnas[1], Tautvydas Karvelis[1]

[1]Department of Protein-DNA Interactions, Institute of Biotechnology, Vilnius University, Lithuania
brigita.duchovska@gmc.stud.vu.lt

CRISPR-Cas systems are diverse microbial RNA-guided adaptive immune systems that protect bacteria from viruses and other mobile genetic elements by using guide RNAs to recognize and target them. These systems have also served as the foundation for several molecular technologies, most notably programmable genome editing. CRISPR-Cas systems are classified into two classes. In class 1 CRISPR-Cas, the effector complex consists of several different Cas proteins to recognize foreign DNA, while a separate component – Cas3 – is responsible for cutting the target DNA. Although Class 1 systems have been used to induce targeted deletions in genomic DNA, the number and size of their constituent components limit their wider application in the genome editing field [1]. In class 2 CRISPR-Cas systems, the effector complex comprises a single protein responsible for both target recognition and cleavage. Because of this feature, the class 2 RNA-programmed Cas9 and Cas12 effector proteins have been widely adapted to cut genomic DNA, which can be exploited to introduce precise changes in the genome [2].

A recent study has identified previously unknown associations with core CRISPR effector modules [3]. One of the associations included hybrid Cas12m-Cas3 systems, where Cas3 nuclease-helicase, characteristic of class 1 CRISPR-Cas systems, is located in the same genomic locus as class 2 Cas12m proteins. Interestingly, the compact Cas12m proteins of this type cannot cut DNA but can strongly bind it in a PAM (short motif adjacent to the DNA target recognized by the Cas effector complex) dependent manner [4]. The Cas12-Cas3 system is a putative class 1-class 2 hybrid system in which a Cas12m may have associated with a Cas3 helicase-nuclease that might enact an interference mechanism beyond DNA binding.

This project aims to biochemically characterize Cas12m-Cas3 hybrid systems to gain a better understanding of their molecular mechanisms and function. The successful implementation of this project could lead to novel tools with additional functionalities for biotechnological applications.

[1] Dolan, A. E., Hou, Z., Xiao, Y., Gramelspacher, M. J., Heo, J., Howden, S. E., Freddolino, P. L., Ke, A., & Zhang, Y. (2019). Introducing a spectrum of long-range genomic deletions in human embryonic stem cells using type i crispr-cas. Molecular Cell, 74(5), 936-950.e5. https://doi.org/10.1016/j.molcel.2019.03.014

[2] Wang, J. Y., & Doudna, J. A. (2023). CRISPR technology: A decade of genome editing is only the beginning. Science, 379(6629), eadd8643. https://doi.org/10.1126/science.add8643

[3] Altae-Tran, H., Kannan, S., Suberski, A. J., Mears, K. S., Demircioglu, F. E., Moeller, L., Kocalar, S., Oshiro, R., Makarova, K. S., Macrae, R. K., Koonin, E. V., & Zhang, F. (2023). Uncovering the functional diversity of rare CRISPR-Cas systems with deep terascale clustering. Science, 382(6673), eadi1910. https://doi.org/10.1126/science.adi1910

[4] Bigelyte, G., Duchovska, B., Zedaveinyte, R., Sasnauskas, G., Sinkunas, T., Dalgediene, I., Tamulaitiene, G., Silanskas, A., Kazlauskas, D., Valančauskas, L., Madariaga-Marcos, J., Seidel, R., Siksnys, V., & Karvelis, T. (2024). Innate programmable DNA binding by CRISPR-Cas12m effectors enable efficient base editing. Nucleic Acids Research, 52(6), 3234–3248. https://doi.org/10.1093/nar/gkae016

STUDY OF SPLIT pAGOS AND THE ACTIVITY OF THEIR ASSOCIATED HEPN EFFECTORS IN E. COLI

Rokas Bružaitis[1], Edvardas Golovinas[1], Mindaugas Zaremba[1]

[1]Department of Protein-DNA Interactions, Institute of Biotechnology, Vilnius University
rokas.bruzaitis@gmc.stud.vu.lt

As genome editing technologies progress, the scientific community is committed to enhancing the tools that facilitate this development. Presently, CRISPR-Cas systems lead the way in genome editing technologies, while limited research has been dedicated to their connection with the HEPN domain and its interactions. Nonetheless, recent discoveries regarding Argonaute protein research suggest that the HEPN domain is also vital for the function of certain Argonaute systems.

This research explores the potential interaction between prokaryotic Argonautes (pAgos) and a HEPN domain-containing effector protein, examining its influence on the functionality of Argonaute proteins and its effects on *E. coli*. In pAgos, the catalytic center is found within the PIWI domain, where the conserved DEDX tetrad facilitates the cleavage of target nucleic acids [1]. In the Argonaute-HEPN systems analyzed, the PIWI domain is inactive, with the HEPN domain predicted to serve as the primary effector responsible for cleavage. Through the investigation of various homologous Argonaute–HEPN systems, we aim to explore the role and mechanism of the pAgo-HEPN interaction in bacterial defense. This research not only lays the groundwork for future studies but also possesses significant potential for programmable DNA targeting in the field of biotechnology [2].

Investigating bacterial defense mechanisms broadens our comprehension of the intricate ways in which bacteria safeguard themselves against foreign DNA while also creating opportunities for advancements in biotechnology and genome editing tools

[1] Wang, C., Shen, Z., Yang, X., & Fu, T. (2024). Structures and functions of short argonautes. RNA Biology, 21(1), 1–7. https://doi.org/10.1080/15476286.2024.2380948

[2] Agapov, A., Panteleev, V., Kropocheva, E., Kanevskaya, A., Esyunina, D., & Kulbachinskiy, A. (2024). Prokaryotic Argonaute nuclease cooperates with co-encoded RNase to acquire guide RNAs and target invader DNA. Nucleic Acids Research, 52(10), 5895–5911. https://doi.org/10.1093/nar/gkae345;

OPTIC NEURITIS: EXPLORING GENETIC ASSOCIATIONS OF EXOC3L1 AND TNF IN THE LITHUANIAN POPULATION

Auguste Simanonyte[1], Rusne Lapienyte[1], Kriste Kaikaryte[1], Rasa Liutkeviciene[1,2]

[1]Lithuanian University of Health Sciences, Laboratory of Ophthalmology, Neuroscience Institute, Medical Academy, Kaunas, Lithuania
[2]Lithuanian University of Health Sciences, Department of Ophtalmology, Medical Academy, Kaunas, Lithuania
auguste.simanonyte@stud.lsmu.lt

Optic neuritis (ON) is a common cause of acute optic nerve damage in adults [1]. It is characterized by optic nerve inflammation, demyelination and secondary axonal damage, leading to retinal ganglion cell (RGC) apoptosis [2]. ON typically manifests around the age of 36 and is classified as either typical or atypical [3]. Typical ON is often associated with optic nerve demyelination and may occur in isolation or as part of multiple sclerosis (MS). In contrast, atypical ON is linked to infections, autoimmune disorders, or neuromyelitis optica spectrum disorders (NMOSD) [4].

Tumor Necrosis Factor (TNF) is a key pro-inflammatory cytokine involved in immune system regulation and various pathological conditions, including inflammation and tumorigenesis [5,6]. Single nucleotide polymorphisms (SNPs) in the *TNF-α* promoter region are associated with susceptibility to infectious and inflammatory diseases [7]. The *EXOC3L1* gene is implicated in insulin secretion, protein exocytosis following brain injury, spontaneous apoptosis induction, and high-density lipoprotein regulation. However, it is precise biological functions remain unclear [8].

In this study we investigated the associations between *TNF*, *EXOC3L1* gene polymorphisms and the occurrence of ON.

A total of 82 patients with ON and 160 healthy controls were included in the study. DNA was extracted from peripheral blood leukocytes using the DNA salting-out method. Genotyping was performed using the real-time polymerase chain reaction (RT-PCR) method. Statistical data analysis was performed with ”IBM SPSS Statistics 29.0”.

Our analysis revealed statistically significant differences in the distribution of genotypes and alleles for *EXOC3L1* rs868213. The *EXOC3L1* rs868213 G allele was significantly less frequent in patients with ON compared to the control group (1.2% vs. 5.6%, respectively, $p = 0.021$). In contrast, statistical analysis of *TNF* rs2229094 showed no significant differences. Binary logistic regression also showed no significant differences.

Our study identifies an association between *EXOC3L1* rs868213 and the occurrence of optic neuritis in the Lithuanian population.

[1] Bennett JL. Optic neuritis. Continuum (Minneap Minn). 2019 Oct;25(5):1236-64.
[2] Del Negro I, Pauletto G, Verriello L, Spadea L, Salati C, Ius T, et al. Uncovering the genetics and physiology behind optic neuritis. Genes (Basel). 2023 Dec 9;14(12).
[3] Wilhelm H, Schabet M. The diagnosis and treatment of optic neuritis. Dtsch Arztebl Int. 2015 Sep 11;112(37):616-25; quiz 626.
[4] Phuljhele S, Kedar S, Saxena R. Approach to optic neuritis: an update. Indian J Ophthalmol. 2021 Sep;69(9):2266-76.
[5] Holbrook J, Lara-Reyna S, Jarosz-Griffiths H, McDermott M. Tumour necrosis factor signalling in health and disease. F1000Res. 2019;8.
[6] Wang X, Lin Y. Tumor necrosis factor and cancer, buddies or foes? Acta Pharmacol Sin. 2008 Nov;29(11):1275-88.
[7] Acar L, Atalan N, Karagedik EH, Ergen A. Tumour necrosis factor-alpha and nuclear factorkappa B gene variants in sepsis. Balkan Med J. 2018 Jan 20;35(1):30-5.
[8] Zhang ZF. A comprehensive prognostic and immune infiltration analysis of EXOC3L1 in pancancer. Front Genet. 2022;13:1044100.

STUDIES ON ANTIOXIDANT ACTIVITY AND PHYTOCHEMICAL COMPOUNDS IN FLAX (LINUM USITATISSIMUM L.) CALLUS CULTURES IN VITRO

Judita Zeiderytė[1]

[1]Department of Chemical Technology, Kaunas University of Technology, Lithuania
judita.zeideryte@ktu.edu

Flax (Linum usitatissimum L.) is a valuable medicinal plant rich in bioactive compounds, including lignans and flavonoids, which contribute to its antioxidant properties. In vitro callus cultures provide a controlled system for the production of secondary metabolites, yet their antioxidant potential remains largely unexplored. This study aims to evaluate the phytochemical composition and antioxidant activity of flax callus cultures [1]. Callus was induced from seeds on Murashige and Skoog (MS) medium supplemented with auxin 1-naphthylactic acid and cytokinin 6-benzylaminopurine. By adding the amino acids L-phenylalanine and L-tryptophan. For comparison, flax grown in a nutrient medium without growth regulators was studied (Figure 1).

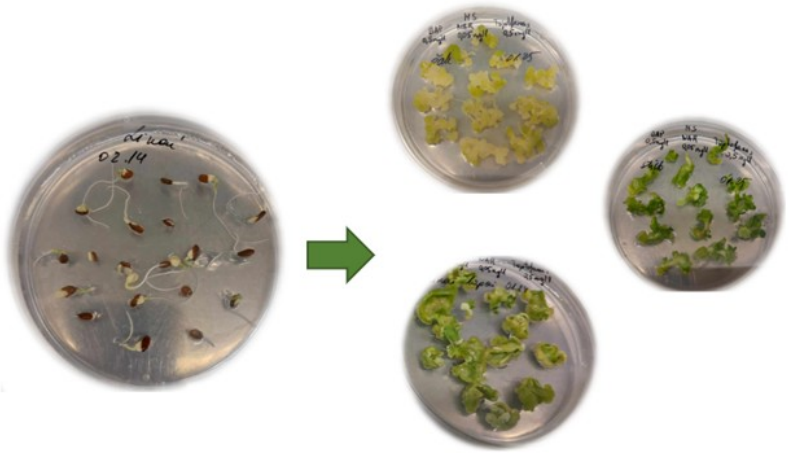


Fig. 1. Flax (Linum usitatissimum L.) Callus Cultures In Vitro

The antioxidant activity of extracts was assessed using DPPH, FRAP, ABTS assays, while total phenolic, flavonoid and protein content was quantified spectrophotometrically. Additionally, antioxidative enzyme activity were analyzed to further evaluate the biochemical properties of the extracts. Preliminary results indicate that antioxidative activity, flavonoid, and phenolic content showed significant enhancement with the addition of L-tryptophan, while protein content reached its highest levels when supplemented with L-phenylalanine. These findings emphasize the potential of flax callus cultures as a sustainable source of bioactive compounds, particularly for pharmaceutical and cosmetic applications. Future research will focus on optimizing culture conditions to further enhance the accumulation of these valuable metabolites.

[1] Asad, B.; Khan, T.; Gul, F.Z.; Ullah, M.A.; Drouet, S.; Mikac, S.; Garros, L.; Ferrier, M.; Bose, S.; Munsch, T.; et al. Scarlet Flax Linum grandiflorum (L.) In Vitro Cultures as a New Source of Antioxidant and Anti-Inflammatory Lignans. Molecules. 2021, 26, 4511. https://doi.org/10.3390/molecules26154511

ASSOCIATIONS BETWEEN COPY NUMBER VARIATIONS OF α-AMYLASE AND TEETH LOSS IN INDIVIDUALS WITH INTELLECTUAL DISABILITY

Neringa Meilutė[1], Indrė Stankevičienė[1], Kristina Daniūnaitė[2]

[1]Institute of Dentistry, Faculty of Medicine, Vilnius University, Vilnius, Lithuania
[2]Institute of Biosciences, Life Sciences Center, Vilnius University, Vilnius, Lithuania
neringa.meilute@mf.stud.vu.lt

Caries is a widespread chronic disease. It is thought that changes in composition of salivary proteins could influence oral health [1]. One of such proteins is α-amylase enzyme, which metabolizes starch and may be related to the development of dental caries [2]. The aim of this study was to evaluate the association between *AMY1* copy number variation (CNV) and tooth loss in individuals with intellectual disabilities.

This pilot study included 38 individuals (14 males and 21 females) with mental disability, who underwent oral treatment under general anesthesia at the Zalgiris Clinic, a branch of Vilnius University Hospital Santaros Clinics, Vilnius. The mean age (±SD) of participants was 32±9 for males and 29±7 for females. The missing teeth number was assessed by one trained clinician. Participants were referred to one of three study groups: a group with no missing teeth, a group with 1-2 missing teeth, and a group with ≥3 missing teeth. Molecular analysis was performed from buccal swabs collected during dental examination. The MagMAX Nucleic Acid Isolation Kit and KingFisher Flex automated extraction system were used for DNA purification. *AMY1* CNV values were determined using droplet PCR assays with the QuantStudio Absolute Q Digital PCR System (Thermo Fisher Scientific). Statistical analysis was conducted using IBM SPSS 27.0 software, assessing possible trends in the correlation between *AMY1* CNV and tooth loss.

The mean *AMY1* CNV value was 12 and ranged from 1 to 38 (Fig. 1), while the mean number of missing teeth was 4 and ranged from 0 to 14. A trend toward a negative correlation between *AMY1* CNV and tooth loss was observed: the mean *AMY1* CNV was 15±9 in individuals with no missing teeth, 11±4 in those with 1–2 missing teeth, and 11±6 in individuals with ≥3 missing teeth. There were no significant associations between *AMY1* CNV values and age, and no notable differences were found between males and females.

This pilot study indicates a possible association between lower *AMY1* copy numbers and higher tooth loss in individuals with intellectual disabilities. However, further large-scale studies are required to validate these findings.

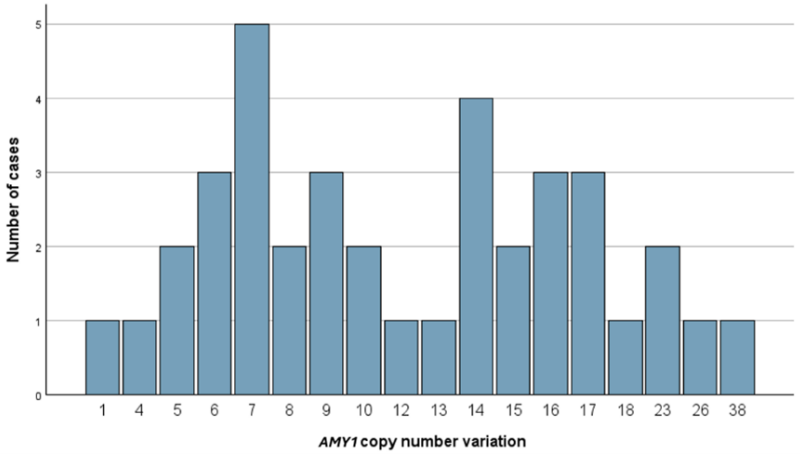


Fig. 1. Distribution of copy number variation (CNV) values of *AMY1* gene locus in individuals with intellectual disabilities who underwent dental examination.

[1] Hemadi, A. S., Huang, R., Zhou, Y., & Zou, J. (2017). Salivary proteins and microbiota as biomarkers for early childhood caries risk assessment. International Journal of Oral Science, 9(11), e1–e1. https://doi.org/10.1038/ijos.2017.35

[2] Padmanabhan, V., Islam, M. S., Rahman, M. M., Goud, M. B. K., Alshehhi, L. M. S. A., Hamed, H. M. A., Haridas, S., & Sharma, D. (2025). Salivary alpha-amylase activity and its association with early childhood caries and rampant caries experience: a cross-sectional study. Frontiers in Medicine, 11. https://doi.org/10.3389/fmed.2024.1480139

DNA ISOLATION FROM HERBARIUM SPECIMENS: A COMPARISON OF DIFFERENT METHODS

Viktorija Dolotova[1], Jurgita Butkuvienė[1]

[1]Life Sciences Center, Vilnius University, Sauletekio Ave. 7, 10222 Vilnius, Lithuania
viktorija.dolotova@gmc.stud.vu.lt

Herbarized plants are a very valuable source of DNA, allowing the development of paleogenomics, the determination of evolutionary and phylogenetic relationships, and the determination of current ecosystem and global environmental changes. Plant cells differ from other organisms' cells in a much more complex cellular structure and molecular composition. The cell wall in plants, consisting of polysaccharides, is challenging to break down, and secondary metabolites, proteins, and RNA are difficult to remove. An even greater amount of these substances is found in herbarium plants. Therefore, DNA isolated from herbarium plants has a much lower yield and higher contamination. For this reason, it is important to properly select the methodology for isolating DNA from herbarium plants, modify existing protocols, and optimize the DNA isolation process. Many methods exist for isolating DNA from herbarium plants, but it is still impossible to single out one of the most suitable ones. This work evaluated the suitability of several selected DNA extraction methods for DNA isolation from different herbarium plant species.

DNA from 6 different herbarium aquatic plants was isolated by 3 different methods: a modified CTAB method, Qiagen "Dneasy Plant Mini Kit," and Thermo Fisher "GeneJET Plant Genomic DNA Purification Mini Kit." Further modifications of the CTAB buffer were also performed: in one case, the amount of β-mercaptoethanol was doubled; in the second – the amount of PVP-40 was doubled. A Nanodrop spectrophotometer assessed the quality and concentration of the isolated DNA. ISSR-PCR amplification was performed with 4 selected primers (I-32, I-18, I-28, and Arcade-2) and visualized by agarose gel electrophoresis.

When comparing the three different methods, the highest DNA concentration was obtained by the CTAB method (CTAB – 249.04 ng/µL, Qiagen - 40.00 ng/µL, Fisher - 46.66 ng/µL), the absorbance ratios did not show significant differences.

ISSR-PCR amplification also did not show significant differences. After performing CTAB buffer modifications, higher DNA concentrations were obtained in most samples (β-mercaptoethanol – 222.15 ng/µL, PVP-40 336.78 ng/µL) and better A260/280 absorbance ratios (β-mercaptoethanol 1.97 ± 0.11, PVP-40 2.00 ± 0.06), and after performing ISSR-PCR amplification, sharper and clearer amplicon profiles were obtained.

The modifications made to the CTAB buffer improved the quality of DNA, increased its concentration, and allowed for higher-quality ISSR-PCR amplification results.

HEAVY METAL BIOACCUMULATION CAPACITY IN PROTOZOA - TETRAHYMENA TERMOPHILA

Mindaugas Matijūnas[1], Remigijus Ivanauskas[1]

[1]Department of physical and inorganic chemistry. Kaunas University of Technology
mindaugas.matijunas@ktu.edu

Dissolved heavy metals in wastewater represent a significant threat to environmental and public health due to the persistent toxicity of these pollutants [1]. Traditional treatment methods, such as chemical precipitation and membrane ultrafiltration are energy-intensive and may not be sustainable over the long term [2]. In contrast, biological processes offer a promising alternative by harnessing the inherent capabilities of microorganisms to capture heavy metals, using methods, such as bioprecipitation, biosorption, and bioaccumulation [3]. In this study, we examine the heavy metal bioaccumulation capacity of the protozoan Tetrahymena thermophila.

Tetrahymena thermophila was selected for this study because of its extensive documentation in literature, its complex metallothionein systems, rapid growth rate, and minimal ethical concerns; all of which underscore its potential for large-scale heavy metal treatment applications [4].

We evaluated the bioaccumulation capacity of Tetrahymena thermophila in saturated cultures exposed to zinc (Zn^{2+}), molybdenum (Mo^{2+}), copper (Cu^{2+}), trivalent chromium (Cr^{3+}), and hexavalent chromium (Cr^{6+}) over a three-day period with concentrations chosen to match similar toxicity levels. The results demonstrated that T. thermophila maintained growth, altered its metabolic pathways, and displayed significant bioaccumulation capabilities under heavy metal exposure. However, prolonged resistance was not achieved, and the cultures eventually succumbed to toxicity. Notably, chromium exposure indicated the presence of a reversible ion-binding mechanism.

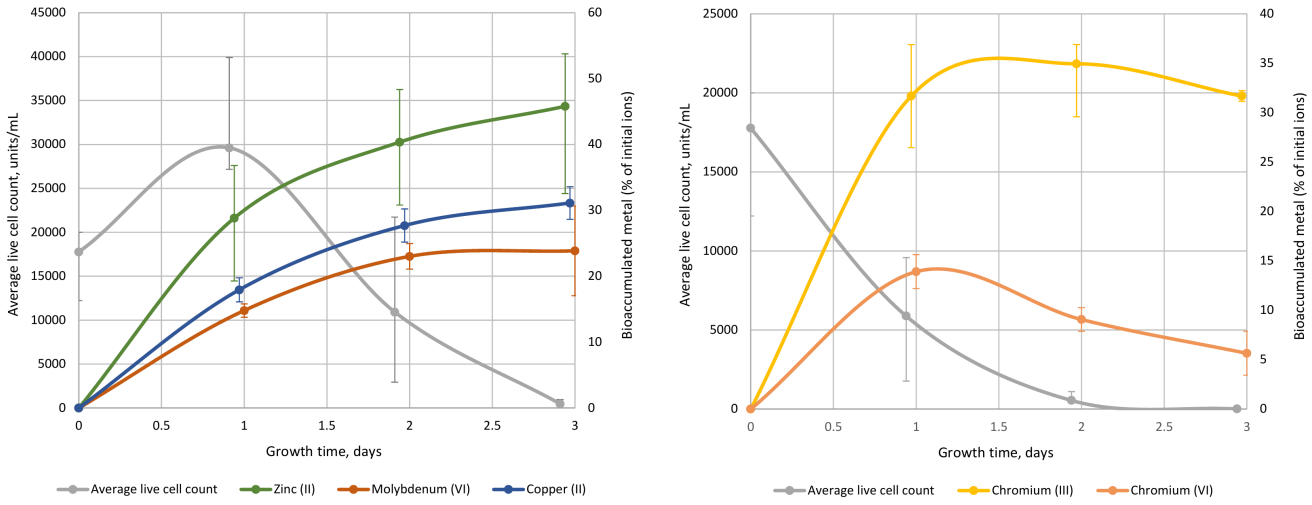


Fig. 1. Bioaccumulation capacity in T. Thermophila over time, when initial ion concentration is: Zn^{2+} - 63.33 µM, Mo^{6+} - 46.0 µM, Cu^{2+} - 47.50 µM, Cr^{3+} - 37.05 µM, Cr^{6+} - 38.80 µM. Nutrient media contains 2% casein peptone, 0.2% D-glucose, 0.05 M NaH_2PO_4/Na_2HPO_4 (pH 7.0) buffer and 6.55 µM $FeCl_3$. Growth is conducted at 35 °C

These results suggest that T. thermophila is effective at reducing heavy metal concentrations through bioaccumulation. When integrated with sustainably sourced nutrients, this biological treatment approach has the potential to significantly lower the energetic demands associated with conventional treatment processes.

[1] K. Vikas, Heavy Metal Ions in Wastewater: A Review on Detection and Toxicity. SciMed Central, Chemical Engineering & Process Techniques. 8(3): 1082 (2023)
[2] N. A. A. Qasem, R. H. Mohammed, D. U. Lawal, Removal of heavy metal ions from wastewater: a comprehensive and critical review. npj Clean Water 4, 36 (2021)
[3] P.R. Sreedevi, K. Suresh, G. Jiang, Bacterial bioremediation of heavy metals in wastewater: A review of processes and applications, Journal of Water Process Engineering, Volume 48, (2022)
[4] B. Francesco, S. Gianfranco, G. Jacek, W. Dorota, C. H. Donna, C. G. Theodore, P. Ester. Metallothionein gene from Tetrahymena thermophila with a copper-inducible-repressible promoter. Eukaryotic cell, Volume 5, issue 2, P. 422-425 (2006)

EXPLORING ENZYMATIC POLYURETHANE DEGRADATION BY A URETHANE BOND HYDROLYSING ENZYME FROM LYSINIBACILLUS SP.

Eglė Gečaitė[1], Jokūbas Krutkevičius[1], Inga Matijošytė[1]

[1]Vilnius University, Life Sciences Center, Institute of Biotechnology, Sector of Applied Biocatalysis
egle.gecaite@gmc.stud.vu.lt

Plastic pollution is one of the most significant environmental concerns in the contemporary world. Polyurethane (PU), the 6th most widely used plastic, contributes to 675,000 tonnes of waste per year in Europe [1]. Conventional waste treatment methods, such as landfilling and incineration, present a threat to the environment. Moreover, mechanical or chemical recycling methods require significant energy consumption and can result in recycled products of inferior quality.

A viable alternative solution for the management of PU waste is microbiological or enzymatic treatment, since the reaction conditions are mild and the degradation products can be used in the production of new PU materials. PU is a suitable candidate for this type of recycling, since it possesses bonds susceptible to hydrolysis, such as ester and urethane bonds. The urethane bond exists in all types of PU, and therefore represents an effective target for the creation of a universal PU recycling method. The cleavage of this bond is performed by urethanases (EC 3.5.1.75) [2]. However, research on these enzymes specifically for PU degradation is currently limited.

The present study is based on a *Lysinibacillus* sp. urethanase (UTH, GenBank: QCW12854.1), derived from soil collected in Lithuania. The *uth* gene was expressed in the *Escherichia coli* expression system. The enzyme was then purified by immobilised metal affinity chromatography and its application in PU degradation was investigated. The products were determined by gas chromatography and liquid chromatography-mass spectrometry. Further details of the study will be presented during the poster session.

[1] "LIFE 3.0," LIFE Project Public Page, 2020. https://webgate.ec.europa.eu/life/publicWebsite/project/LIFE16-ENV-ES-000254/recovery-of-polyurethane-for-re
[2] A. Raczyńska, A. Góra, and I. André, "An overview on polyurethane degrading enzymes," Biotechnology Advances, vol. 77, p. 108439, Sep. 2024, doi: 10.1016/j.biotechadv.2024.108439.

FORMULATION OF BIOMIMETIC LIPID BASED NANOPARTICLES FOR CRISPR/CAS9 DELIVERY

Kamilė Bužinskytė[1], Evelina Jankaitytė[1,2], Rima Budvytytė[1,2]

[1]Life Sciences Center, University of Vilnius, Vilnius, Lithuania
[2]Institute of Biochemistry, Department of Bioelectrochemistry and Biospectroscopy, Life Sciences Center
kamile.buzinskyte@gmc.stud.vu.lt

For the past years, the CRISPR-cas9 system has been studied as a new genome editing tool that could lead to new gene therapy strategies and improve human health. However, the delivery of such a system to a cell has remained a challenge.

Lipid-based nanoparticles (LNPs) are versatile, have low immunogenicity, and are easy to manufacture – all these characteristics make liposomes an attractive potential delivery vector for CRISPR/Cas9 transportation through cell membranes [1]. This research project investigated stability and protein encapsulation efficiency of different liposome sizes and compositions.

Based on previous studies there were chosen 4 different LNP compositions [2]. All LNPs were made using these lipids: Dipalmitoylphosphatidylcholine (DOPC), dioleoylphosphatidylethanolamine (DOPE), cholesterol, 1,2-dioleoyl-3-trimethylammonium propane (DOTAP), 1,2-dioctadecenoyl-sn-glycero-3- Phosphoserine (DOPS), PEG-lipids and ALC-0315 [2]. The size and stability of LNPs were measured using the dynamic light scattering technique (DLS, ZetaSizer). Then, different sizes of LNPs were prepared using membranes with 40nm, 200nm, and 400nm pores [3]. The encapsulation efficiency of these LNPs was investigated by measuring the fluorescence intensity of encapsulated model protein BSA- Alexa Fluor 488 or Cas9 – GFP protein by Fluorometer (Spectrofluorometer FS5) and HPLC.

The results showed that the concentration of PEG and cholesterol changes the stability and size of LNPs. Composition DOPC/DOPE/chol/DOTAP/ALC-0315/DMG-PEG 20/10/20/15/5 was determined as the most stable one. LNPs prepared with 200nm pores showed the best encapsulation efficiency – 70% and had the smallest polydispersity index.

[1] Walther, J., Porenta, D., Wilbie, D., Seinen, C. W., Benne, N., Yang, Q., De Jong, O. G., Lei, Z., & Mastrobattista, E. (2024). Comparative analysis of lipid Nanoparticle-Mediated delivery of CRISPR-Cas9 RNP versus mRNA/sgRNA for gene editing in vitro and in vivo. European Journal of Pharmaceutics and Biopharmaceutics, 196, 114207

[2] Eoh, J., & Gu, L. (2019). Biomaterials as vectors for the delivery of CRISPR–Cas9. Biomaterials Science, 7(4), 1240–1261

[3] Song Zhang, Jiangtao Shen, Dali Li, Yiyun Cheng (2021) Strategies in the delivery of Cas9 ribonucleoprotein for CRISPR/Cas9 genome editing. Theranostics 11(2): 614-648

SCREENING AND CHARACTERIZATION OF PSYCHROPHYLIC XYLANOLYTIC BACTERIA

Kamilia Mikelevič[1], Nomeda Kuisienė[1]

[1]Department of Microbiology and Biotechnology, Institute of Biosciences, Life Sciences Center, Vilnius University
kamilia.mikelevic@gmc.stud.vu.lt

Temperature is the most significant parameter that plays a key role in the distribution of microorganisms on our planet. Psychrophilic microorganisms are the most prominent inhabitants of the cold ecosystems, producing cold-adapted enzymes, particularly useful due to their high catalytic activity at low temperatures, offering energy-saving advantages, this feature makes them more appealing and attractive in biotechnology [1]. Xylanolytic microorganisms, especially bacteria, have been reported from various extreme environments, such as marine habitats or Antarctic regions. They breakdown a xylan, the second most abundant naturally occurring renewable polysaccharide available on earth. The complete hydrolysis of xylan is challenging due to its heterogeneous structure, it requires a complex of several cooperatively acting enzymes collectively known as xylanases. The suitability of xylanases for its application in food and feed, paper and pulp, textile, pharmaceuticals, and lignocellulosic biorefinery has led to an increase in demand of xylanases globally. Although cold-adapted xylanases are not very common, some bacteria have been reported to produce them [2,3]. The objective of this study was to search and characterize psychrophylic xylanolytic bacteria, isolated from the compost sample in Vilnius. Ten isolated cultures were selected and genotyped using BOX-PCR. Our analysis showed that these 10 isolates belong to 10 different strains. 16S rRNA genes of these isolates were amplified and sequenced. BLAST analysis showed that the strains could be assigned to the genera Rhodococcus, Flavobacterium, Arthrobacter, Sporosarcina, Sphingobacterium and Pseudomonas. One of these strains (S31) was selected for further work due to its lowest 16S rRNA gene similarity (93.99%). The S31 strain was grown in a medium, where xylan was the only carbon source; cultivation was carried out in a cold room at 6 °C. The Congo red staining method was used to show the activity of xylanases. According to 16S rRNA gene sequence analysis as well as Oxford Nanopore PromethION and Illumina NovaSeq sequencing results, the S31 strain was identified as Pseudomonas bubulae S31 strain. The genome was submitted to the Genbank, acc. No. CP178394-CP178396. The genome consists of 3 contigs – chromosome and two plasmids. In the genome, 106 CAZY protein genes have been identified, 22 of which were supposed to be secreted. Three secreted protein genes have been identified that could potentially be involved in xylan degradation.

[1] Hamid, B., et al. (2022). Cold-Active Enzymes and Their Potential Industrial Applications—A Review. Molecules, 27, 5885.
[2] Moreira, L. R. S., Filho E. X. F.. (2016). Insights into the mechanism of enzymatic hydrolysis of xylan. Applied Microbiology and Biotechnology, 100: 5205–5214.
[3] Chakdar, H., et al. (2016). Bacterial xylanases: biology to biotechnology. 3 Biotech, 6:150.

THE IMPACT OF DIFFERENT ORIGINS AND CONCENTRATIONS MICROPLASTICS ON SOIL AND BUCKWHEAT (FAGOPYRUMESCULENTUM L.) CARBON AND NITROGEN

S. Dreskinienė[1], M. Vilkienė[1], K. Barčauskaitė[1]

[1]Lithuanian Research Centre for Agriculture and Forestry
skaiste.dreskiniene@lammc.lt

Microplastic pollution is a well-documented issue in aquatic ecosystems and is increasingly being studied in agroecosystems. Recent research has demonstrated that microplastics can affect plant growth and soil properties, posing a potential threat to agricultural production and crop quality. Buckwheat has been identified as a promising model crop for assessing plant responses to harmful substances, as it can thrive in poor soil conditions and exhibits strong reactions to environmental stressors such as microplastics. However, limited information is available on how different types and concentrations of microplastics impact buckwheat.

This laboratory experiment examined how different concentrations (0.05%; 0.1%; 0.3%; 0.5%) of polyethylene (PE) and polypropylene (PP) microplastic particles in soil affect the soil and the grown buckwheat. The control was grown in soil without any microplastic. The experiment was done under controlled conditions and any secondary contamination with microplastics was avoided. After the experiment, soil and buckwheat samples were analyzed. Results showed that no significant changes in total carbon and total nitrogen were determined in all analyzed groups. These findings suggest that buckwheat responds to microplastic-induced stress. However, further in-depth research is needed to better understand the interaction between microplastic exposure and the plant's defense mechanisms.

Keywords: microplastics, buckwheat, polyethylene (PE), polypropylene (PP)

SERCH, PURIFICATION AND ANALYSIS OF PYRETHROIDS-DEGRADING AND OTHER BIOTECHNOLOGICALLY APPLICABLE LIPOLYTIC ENZYMES

Jūratė Udraitė[1], Ugnė Rickevičiūtė[1], Alisa Gricajeva[1]

[1]Department of Microbiology and Biotechnology, Institute of Biosciences, Life Sciences Center, Vilnius University, Vilnius, Lithuania
jurate.udraite@gmc.stud.vu.lt

Pyrethroids are synthetic pesticides widely used for pest control in agricultural and public settings, but their high insecticidal potency, persistence, and slow degradation can harm non-target organisms and contaminate natural habitats [1]. Bacteria produce different lipolytic enzymes - carboxylesterases and true lipases which are multifunctional biological catalysts and have been the subject of research for a long time. Although lipolytic enzymes are mainly known as enzymes catalyzing the hydrolysis (and other transformations) of ester-bonded lipid substrates, it has been discovered more recently that they are also capable of breaking down the ester linkages of pyrethroids and can thus serve as an efficient and eco-friendly method for their removal [1,2].

In this study, plant growing substrate samples from two Lithuanian farmlands were used to isolate pyrethroid-degrading bacteria through enrichment culture with pyrethroid (permethrin) as the sole carbon source. Isolated cultures were selected and identified employing 16S rDNA analysis. After identification of target bacteria, 7 bacterial cultures belonging to the *Pseudomonas* spp. (II1; II3; II10; IIB; IIC), *Rhodanobacter* sp. (II14), *Priestia* sp. (III3) genus, were selected for further study based on their lipolytic and pyrethroid-degrading activity (Fig. 1). The lipolytic enzymes located in extracellular media were salted out using ammonium sulphate and gel filtrated. Intracellular proteins were derived from bacteria via sonication. Lipolytic activity of both partially purified protein fractions was determined using *p*-NPB assay.

Partially purified proteins from the extracellular medium of *Pseudomonas* spp. (II1; II3; IIB) and *Rhodanobacter* sp. (II14), as well as intracellular proteins of *Pseudomonas* sp. (II10) and Rhodanobacter sp. (II14), formed hydrolysis zones in permethrin (tested by agar diffusion method). To determine the size of target proteins a zymography was used. Zymography analysis showed that all tested protein fractions formed tributyrin hydrolysis zones, *Pseudomonas* sp. (IIB) total cell protein (TCP) fraction was active toward both tributyrin and permethrin in the zymography gels.

Enzymes, partially purified from the extracellular and cell's intracellular fractions, were used for the synthesis of *2*-phenylethyl butyrate (*2*-PEB). This method was chosen to evaluate the ability of the obtained protein solutions to perform esterification reactions, resulting in the production of *2*-PEB, an ester widely used in the fragrance and flavor industry (Fig. 1).

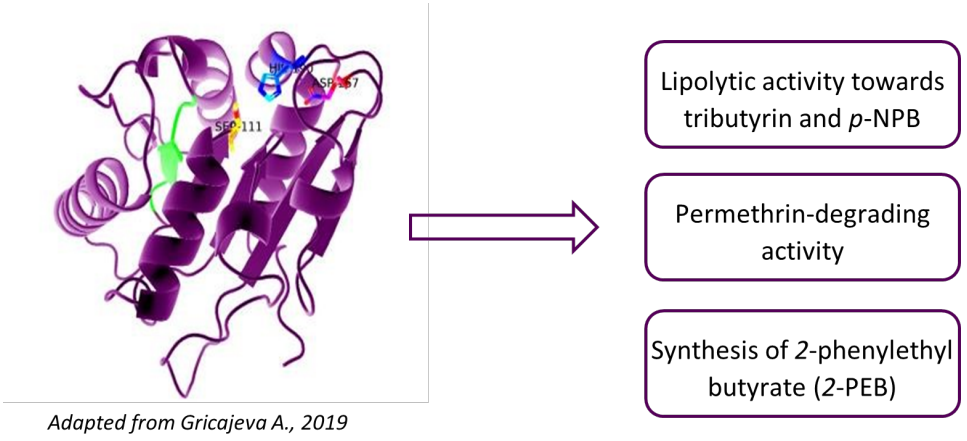


Fig. 1. A simplistic protein model with functional annotations.

[1] Liu, H., Chen, W.-J., Xu, Z., Chen, S.-F., Song, H., Huang, Y., Bhatt, K., Mishra, S., Ghorab, M. A., Zhang, L.-H., & Chen, S. (2025). Unraveling the degradation mechanism of multiple pyrethroid insecticides by Pseudomonas aeruginosa and its environmental bioremediation potential. Environment International, 195, 109221.

[2] Gricajeva, A., & Kalėdienė, L. (2023). Investigation of amino acids related to Staphylococcus saprophyticus AG1 EstAG1 carboxylesterase catalytic function revealed a new family of bacterial lipolytic enzymes. International Journal of Biological Macromolecules, 235, 123791.

CYANOPHAGE-INDUCED TRANSCRIPTIONAL CHANGES IN RAPHIDIOPSIS RACIBORSKII

Vaiva Slatkevičiūtė[1,2,3], Barbara Klimczak[4], Gediminas Azlbutas[2], Adam Antosiak[4], Petras Venckus[5], Hanna Zkukava[1], Natalija Kazlauskienė[1], Sarit Avrani[6], Dariusz Dziga[4], Sigitas Šulčius[1,2]

[1]Laboratory of Algology and Microbial Ecology, Nature Research Centre, Lithuania
[2]Bioinformatics Department, Nature Research Centre, Lithuania
[3]Institute of Biotechnology, Life Science Center, Vilnius University, Lithuania
[4]Laboratory of Metabolomics, Faculty of Biochemistry, Biophysics and Biotechnology, Jagiellonian University, Poland
[5]Institute of Biosciences, Life Sciences Center, Vilnius University, Lithuania
[6]Aquatic Microbial Interactions Lab, Department of Evolutionary and Environmental Biology, Faculty of Natural Sciences, University of Haifa, Israel
sigitas.sulcius@gamtc.lt

Raphidiopsis raciborskii is a nitrogen-fixing freshwater cyanobacterium that recently gained attention due to its high invasiveness potential, toxicity, and harmful blooms, which can negatively impact biodiversity, ecosystem functions, and water quality. Despite its ecological significance, factors controlling this species' occurrence and bloom dynamics remain poorly understood. Cyanophages, viruses that infect cyanobacteria, may play a crucial role in microbial population and community dynamics through host lysis, horizontal gene transfer, and metabolic reprogramming [1,2]. Understanding these interactions in freshwater ecosystems is essential for advancing our knowledge of cyanophage ecology and may provide insights into the mechanisms by which viruses regulate cyanobacterial activity, growth, and transcription. Investigations into transcriptional regulation of host cyanobacteria by viral infection are also crucial for the assessment and development of phage-based technologies for the mitigation of harmful algal blooms.

To investigate the transcriptional response of *R. raciborskii* to cyanophage infection as well as to establish a transcriptional scheme for cyanophage, we used *R. raciborskii* strain KLL07 and its lytic cyanophage Cr-LKS4 as a model virus-host system. In this study, control and infection treatments were established by adding either filter-sterilized growth medium or cyanophage suspensions at the multiplicity of infection of three (MOI = 3) in four biological replicates to unialgal yet non-axenic cultures. The experiment lasted 120 hours, with samples collected every 4-8 hours for cell and phage abundance measurements, DNA and RNA sequencing, and proteomic analysis.

We will present results on cyanobacterial and cyanophage dynamics during the infection experiment along with differential gene expression analysis during different infection stages (adsorption, DNA replication and lysis) of *R. raciborskii*. Additionally, changes in *R. raciborskii* microbiome composition induced by the cyanophage-mediated lysis of the photosynthetic host will be presented. These findings will contribute to a better understanding of the ecological significance of freshwater cyanophages and their impact on cyanobacteria growth and succession.

[1] D. Kolan et al., "Tradeoffs between phage resistance and nitrogen fixation drive the evolution of genes essential for cyanobacterial heterocyst functionality," The ISME Journal, vol. 18, no. 1, Jan. 2024, doi: 10.1093/ismejo/wrad008.
[2] D. Morimoto, S. Šulčius, and T. Yoshida, "Viruses of freshwater bloom-forming cyanobacteria: genomic features, infection strategies and coexistence with the host," Environmental Microbiology Reports, vol. 12, no. 5, pp. 486–502, Aug. 2020, doi: 10.1111/1758-2229.12872.

REMOTE SENSING ANALYSIS OF VEGETATION COVER DYNAMICS AS AN INDICATOR OF EVOLUTIONARY TRENDS OF THE SUKHA SPIT (KINBURN PENINSULA, BLACK SEA, UKRAINE)

Yuliia Shevchuk[1], Oleksiy Davydov[1,2]

[1]Laboratory of Geoenvironmental Research, Nature Research Centre, Vilnius, Lithuania
[2]National Park «Biloberezhzhia Svyatoslava»
julija.shevchuk@gamtc.lt

The Sukha Spit is a young coastal accumulative landform located in the southwestern part of the Kinburn Peninsula (Black Sea). The formation of the spit began in the early 1980s under the influence of several natural factors, including the accumulation of coastal and marine sediments, the impact of aeolian processes, and the stabilization of the spit's surface by vegetation cover.

This study aims to analyze the morphodynamic and spatiotemporal parameters of the Sukha Spit's development, as well as to determine the characteristics of its surface stabilization by vegetation cover.

The research utilizes regional aerial photographs from 1983–1984, satellite images from Landsat (1975–2010) and Sentinel (2016–2025), as well as data from hydrometeorological databases. Spatial analysis was conducted in ArcGIS using classification methods (water, sand, vegetation), indexing (NDVI), shoreline vectorization, and the calculation of accumulation rates based on time-series data.

Over its 45-year evolution, the total length of the Sukha Spit has reached approximately 4.5 km, indicating its continuous progradation in a southeastern direction. However, retrospective remote sensing analysis suggests that the spit's development follows a staged process, influenced by the hydrodynamic conditions of the adjacent water bodies.

Vegetation cover began forming a few years after the stabilization of the spit's basal sandy deposits, initially concentrating in the most sheltered areas on the leeward side of the spit, particularly on the surface of aeolian landforms. NDVI analysis revealed a gradual increase in vegetation biomass since the 1990s (Fig. 1).

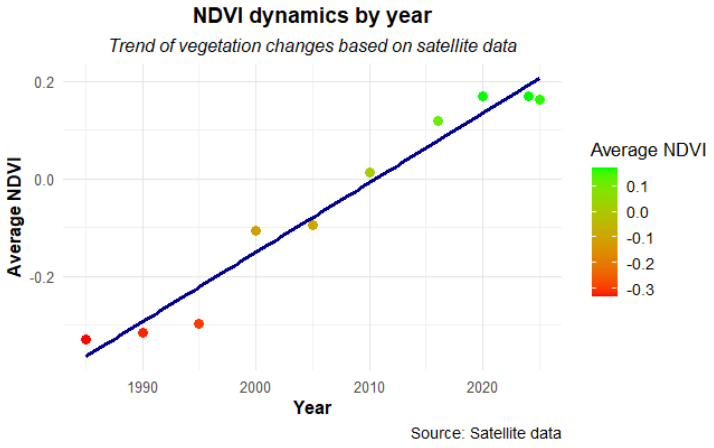


Fig. 1. Temporal trends in vegetation cover changes based on satellite analysis results.

The correlation between morphodynamic trends and vegetation cover formation patterns suggests the stability of the Sukha Spit and its continued evolution, progressing along the surface of the underwater bar in a southeastern direction.

[1] Krivulchenko, A. 2016. Kinburn: landscapes, current state and significance: Monograph. Kropyvnytskyi: Central Ukrainian Publishing House. 416.
[2] Babiichuk S. M. 2022 Fundamentals of Remote Sensing: Practice Book. Part 1 . Kyiv: The Junior Academy of Sciences of Ukraine, National Center. 120 p.
[3] Davydov, O.V., Chaus, V.B., Kasyanov, E.O., Pavlik, A.O. 2023. Dynamics of the coastline of Sukhoi Spit, based on the results of GPS survey. Theory and practice of coastal science and nature management: Collection of materials. II All-Ukrainian Scientific and Practical Online Conference (Odesa, May 29-31, 2023). 24 - 29.

REGULATION OF LARGE TERMINASESUBUNIT NUCLEASE ACTIVITY BY THE PORTAL PROTEIN IN NOVEL JUMBO PHAGE KLEB27-3

Miglė Šarpilo[1], Ayush Kumar Ganguli[1], Algirdas Toleikis[1]

[1] Institute of Biotechnology, Life Sciences Center, Vilnius University, 7 Saulėtekio Ave, LT- 10257 Vilnius
migle.sarpilo@gmc.vu.lt

The study of bacteriophages, viruses that infect bacteria, has greatly advanced molecular biology and biotechnology. Among these, jumbo phages, with genomes over 200 kilobases, stand out for their genomic complexity and partial independence from host machinery. Jumbo phages have a broad host range, infecting diverse bacterial species, including multidrug-resistant pathogens [1]. They play key roles in microbial ecosystems by regulating pathogenic populations, making them valuable for environmental and clinical applications. Given the growing threat of antibiotic resistance, jumbo phages hold promise as therapeutic agents.

Within the Podoviridae family, the jumbo phage KLEB 27-3, a double-stranded DNA (dsDNA) virus, provides an intriguing model for studying viral assembly and genome packaging [2]. A critical step in this process is the packaging of viral genomes into preformed capsids, facilitated by the terminase complex (TerC) and regulated by the portal protein. The large terminase subunit performs ATP-dependent genome translocation and cleavage, yet how the portal protein regulates the large subunit‘s nuclease function remains unclear.

This study investigates the portal protein of KLEB 27-3 aiming to identify amino acid residues responsible for regulating TerL nuclease activity. Using AlphaFold3 structural modeling, mutagenesis, and DNA curtains it aims to uncover the molecular mechanisms governing this regulation, offering insights into jumbo phage biology and genome packaging dynamics.

[1] Harding, K. R., Kyte, N., & Fineran, P. C. (2023). Jumbo phages. Current Biology, 33(14), R750–R751. https://doi.org/10.1016/j.cub.2023.05.056

[2] Duda, R. L. (2008). Icosahedral tailed dsDNA bacterial viruses. In Encyclopedia of virology (pp. 30–37). Elsevier. https://doi.org/10.1016/B978-012374410-4.00754-8

FUNCTIONAL ANALYSIS OF SMALL REGULATORY RNA SLLM1238 IN LACTOCOCCUS LACTIS

Naglis Mykolas Pakštys[1], Oskaras Safinas[1], Kotryna Kvederavičiūtė[1], Milda Mickutė[1], Janina Ličytė[1], Giedrius Vilkaitis[1]

[1]Department of Biological DNA Modification, Life Sciences Center, Vilnius University, Lithuania
mykolas.pakstys@chgf.stud.vu.lt

Lactococcus lactis are Gram-positive, immobile, facultatively anaerobic, non-spore-forming lactic acid bacteria that have become an important model organism due to their industrial role as primary components of dairy starter cultures and their impact on public health due to their probiotic properties [1]. In order to maintain and improve these properties it is important to understand how these microorganisms adapt to environmental changes, especially when subjected to stress conditions caused by temperature changes, nutrient availability or other stress inducing factors.

Small regulatory RNAs (sRNAs) are amongst the most abundant gene-regulating RNAs, serving as key post-transcriptional regulators essential for bacterial adaptation to environmental changes [2]. These sRNAs regulate gene expression by base pairing with target mRNAs influencing its translation or by directly interacting with proteins and affecting their activity [3]. Gaining deeper insight into the role of regulatory RNAs in controlling stress responses and metabolic processes in *Lactococcus lactis* could potentially lead to innovative practical industrial applications [4]. In the Department of Biological DNA Modification, it was shown that transcription of several small regulatory RNAs is observed in a region of the *L. lactis* genome, which we have named the sLLM1238 system.

The aim of this study is to determine the mechanism of action of *L. lactis* sLLM1238 sRNAs. Firstly, we determined different forms of sRNAs by Northern blotting. Afterwards, to facilitate overexpression of sRNAs, we created a vector with a sLLM1238 gene and an empty one for control and electroporated them into *L. lactis*. In order to see expression changes of genes possibly regulated by sLLM1238, we performed total RNA sequencing analysis of *L. lactis* electroporated with these vectors. Furthermore, we analysed how *L. lactis* with and without overexpression of sRNAs responds when grown on agar plates with different concentrations of lysozyme. In addition, we extracted total RNA samples from *L. lactis* subjected to lysozyme in order to observe sRNA expression changes.

The obtained results will help to understand the mechanisms of action of sRNAs in *L. lactis* and their role in gene regulation as well as response to environment changes.

Acknowledgements

This work was supported by funding from Research Council of Lithuania [MIP-22-11 to GV].

[1] Khemariya, P., Singh, S., Nath, G., & Gulati, A. K. (2017). Probiotic Lactococcus lactis: A Review. Turkish Journal of Agriculture - Food Science and Technology, 5(6), 556–562.

[2] Storz, G., Vogel, J., & Wassarman, Karen M. (2011). Regulation by Small RNAs in Bacteria: Expanding Frontiers. Molecular Cell, 43(6), 880–891.

[3] Jørgensen, M. G., Pettersen, J. S., & Kallipolitis, B. H. (2020). sRNA-mediated control in bacteria: An increasing diversity of regulatory mechanisms. Biochimica et Biophysica Acta (BBA) - Gene Regulatory Mechanisms, 1863(5), 194504.

[4] van der Meulen, S. B., de Jong, A., & Kok, J. (2016). Transcriptome landscape of Lactococcus lactis reveals many novel RNAs including a small regulatory RNA involved in carbon uptake and metabolism. RNA Biology, 13(3), 353–366.

HIGH-THROUGHPUT KINETIC PROFILING OF RNA-GUIDED NUCLEASES FOR PRECISION GENOME EDITING

Marius Vinogradovas[1], Gytis Druteika[2], Lina Krikščikaitė[1], Arūnas Šilanskas[2], Tautvydas Karvelis[2], Stephen Knox Jones Jr.[1]

[1]Life Sciences Center, EMBL Partnership Institute, Vilnius University, Lithuania
[2]Life Sciences Center, Institute of Biotechnology, Vilnius University, Lithuania
marius.vinogradovas@gmc.vu.lt

Genome editing tools enabling precise DNA cleavage have rapidly advanced since the discovery and engineering of programmable RNA-guided nucleases, like CRISPR-Cas9. However, it is still challenging to comprehend the mechanisms and benchmark the specificity of these nucleases. Specificity describes a nucleases ability to distinguish a programmed target from all other DNA. The recently discovered TnpB nuclease, derived from a transposon system, represents a compact genome editing tool with high potential. However, its functionality, kinetics, and editing capabilities are not fully understood [1].

This study aims to profile TnpB's target specificity and kinetics with NucleaSeq, a high-throughput kinetic profiling platform [2].

To investigate TnpB's RNA-guided DNA cleavage mechanism, functional assays and bioinformatical analysis of NGS data were performed. Using NucleaSeq we investigated the time-resolved cleavage rates, cleavage patterns, and specificities for thousands of DNAs that mispair with TnpB's RNA guide but are nonetheless cut by TnpB.

Distinct patterns of cleavage and kinetic rates were observed, driven by DNA mismatches and target modifications. Cleavage analysis of TnpB has shown similar trends to those of previously published data – TnpB works less specifically when compared to more widely studied Cas9 [1]. When a mismatch is introduced in the seed region (close to PAM), it has been observed to have a greater impact on the cleavage rate when compared to the other positions in the target.

This research expands on the knowledge about the specificity of TnpB, presenting it as a possible compact alternative to more widely used CRISPR systems.

[1] Karvelis, T. et al. (2021) 'Transposon-associated TnpB is a programmable RNA-guided DNA endonuclease', Nature, 599(7886), pp. 692–696. doi:10.1038/s41586-021-04058-1.

[2] Jones, S.K. et al. (2020) 'Massively parallel kinetic profiling of natural and engineered CRISPR nucleases', Nature Biotechnology, 39(1), pp. 84–93. doi:10.1038/s41587-020-0646-5.

CHARACTERIZATION OF A NOVEL PROTEIN OF THE BACTERIAL ANTIVIRAL DEFENSE SYSTEM THOERIS

Ugnė Andrijauskaitė[1], Arūnas Šilanskas[1], Giedrė Tamulaitienė[1]

[1]Department of Protein-Nucleic Acid Interactions, Institute of Biotechnology, Life Sciences Center, Vilnius University, 7 Saulėtekio Ave, LT- 10257 Vilnius
ugne.andrijauskaite@gmc.vu.lt

Application of bacterial antiviral defense CRISPR-Cas system as a genome editing tool and recent developments in bioinformatics tools, advances in genomic sequencing techniques and experimental progress have sparked a breakthrough in the study of bacterial antiviral defense systems, resulting in the identification of more than 100 new prokaryotic antiviral defense systems [1]. Despite significant progress, many of these newly found systems remain poorly understood, and further research continues to uncover novel features of known defense systems.

Thoeris is an abortive bacterial antiviral defense system that can be classified into 4 types. The system consists of two genes – *thsA* and *thsB*. ThsB protein contains Toll/interleukin-1 receptor (TIR) domain in all Thoeris types while ThsA proteins are different [2-4]. Thoeris mechanism of action is based on intracellular signaling: the ThsB protein detects phage infection and produces a signaling molecule, which is recognized by the effector protein ThsA, leading to its activation. Upon bacteriophage infection, Thoeris type I ThsB produces a signaling molecule 1'-3'gcADPR, which is bound by ThsA SLOG domain [5,6]. Activated ThsA forms helical filaments, enabling SIR2 NAD^+ hydrolase activity and resulting in NAD^+ depletion and host cell death [7]. Type II Thoeris active ThsB produces a different signaling molecule His-ADPR, which is bound by ThsA Macro domain, followed by ThsA oligomerization and presumably cell membrane perturbation [8]. Type IV Thoeris active ThsB synthesizes N7-cADPR, which activates a caspase-like effector that nonspecifically degrades intracellular and potentially bacteriophage proteins [4]. Type III Thoeris mechanism is unknown [3].

Here, we characterize a new Thoeris protein by biochemical analyses. We also performed in vivo experiments to study the impact of this protein for phage defense. These results will provide a deeper understanding of the bacterial immunity.

[1] S. J. Hobbs and P. J. Kranzusch, "Nucleotide Immune Signaling in CBASS, Pycsar, Thoeris, and CRISPR Antiphage Defense," Annu. Rev. Microbiol., vol. 78, no. 1, pp. 255–276, Nov. 2024, doi: 10.1146/annurev-micro-041222-024843.
[2] S. Doron et al., "Systematic discovery of antiphage defense systems in the microbial pangenome," Science, vol. 359, no. 6379, p. eaar4120, Mar. 2018, doi: 10.1126/science.aar4120.
[3] D. F. Van Den Berg et al., "Bacterial homologs of innate eukaryotic antiviral defenses with anti-phage activity highlight shared evolutionary roots of viral defenses," Cell Host Microbe, vol. 32, no. 8, pp. 1427-1443.e8, Aug. 2024, doi: 10.1016/j.chom.2024.07.007.
[4] F. Rousset et al., "TIR signaling activates caspase-like immunity in bacteria," Science, vol. 387, no. 6733, p. eadu2262, Jan. 2025, doi: 10.1126/science.adu2262.
[5] M. K. Manik et al., "Cyclic ADP ribose isomers: Production, chemical structures, and immune signaling," Science, vol. 377, no. 6614, p. eadc8969, Sep. 2022, doi: 10.1126/science.adc8969.
[6] A. Leavitt et al., "Viruses inhibit TIR gcADPR signalling to overcome bacterial defence," Nature, vol. 611, no. 7935, pp. 326–331, Nov. 2022, doi: 10.1038/s41586-022-05375-9.
[7] G. Tamulaitiene et al., "Activation of Thoeris antiviral system via SIR2 effector filament assembly," Nature, vol. 627, no. 8003, pp. 431–436, Mar. 2024, doi: 10.1038/s41586-024-07092-x.
[8] D. Sabonis et al., "TIR domains produce histidine-ADPR conjugates as immune signaling molecules in bacteria," bioRxiv, Jan. 03, 2024. doi: 10.1101/2024.01.03.573942.

STUDY OF INTERACTION BETWEEN SHORT PAGOS AND RNA CHAPERONE HFQ USING NAD$^+$ DETECTION

Jokūbas Šiaučiūnas[1], Evelina Zagorskaitė[1], Edvinas Jurgelaitis[1], Mindaugas Zaremba[1]

[1]Vilnius University, Department of Biotechnology
jokubas.siauciunas@gmc.stud.vu.lt

Throughout recent years antiviral defense systems in bacteria have received worldwide focus as they unveil biology of various prokaryotes and potential advancement in antibacterial therapy and genome editing. The sheer number of these systems and their intricacy demand thorough studies regarding their unique mechanisms [1].

It has been demonstrated that short prokaryotic Argonaute associated with Toll-Interleukin Receptor (TIR) effector (SPARTA) proteins using RNA guides (gRNA) recognize their DNA targets (tDNA), leading to nicotine adenine dinucleotide (NAD+) depletion. Whereas Hfq protein up until now has been shown to be responsible for numerous functions involved with RNA such as RNA matchmaking that promotes the base-pairing between sRNAs and mRNAs, Hfq associates not only with rRNAs, affecting rRNA processing, ribosome biogenesis and translation fidelity but also with tRNAs, affecting its maturation [2]. However, Hfq has never been shown to co-regulate immune response with pAgos. The aim of this study is to explore the interaction between a ubiquitous bacterial RNA chaperone Hfq and short prokaryote Argonautes (pAgos). By observing the interactions of Hfq protein and multiple homologous SPARTA and the effect the RNA chaperone has on the NADase activity of the defense system, we seek to reveal a clearer picture on SPARTA activity and its dependence on other molecules.

Examining antiviral defense systems and their interactions with other molecules not only enables a greater insight into the interrelationship between bacteria and phages but also unlocks new pathways for research in the field of biotechnology and gene engineering.

[1]] Loureiro A, da Silva GJ. CRISPR-Cas: Converting A Bacterial Defence Mechanism into A State-of-the-Art Genetic Manipulation Tool. Antibiotics (Basel). 2019 Feb 28;8(1):18. doi: 10.3390/antibiotics8010018. PMID: 30823430; PMCID: PMC6466564.

[2] R. F.dos Santos, C. M. Arraiano, J. M. Andrade. New molecular interactions broaden the functions of the RNA chaperone Hfq. Springer Nature Link. 2019 May 18; Volume 65, pages 1313–1319, (2019)

UNCOVERING NEW PROKARYOTIC ANTIVIRAL DEFENSE SYSTEMS: PD-T4-1, PD-T7-1, AZACA AND MOKOSH I

Viktorija Rainytė[1], Paulius Toliušis[1], Mindaugas Zaremba[1]

[1]Department of Protein-DNA Interactions, Institute of Biotechnology, Life Sciences Center, Vilnius University
viktorija.rainyte@gmc.vu.lt

The ongoing evolutionary battle between bacteria and bacteriophages has led to the emergence of diverse prokaryotic antiviral defense systems. Historically, research focused on well-known defense mechanisms like restriction-modification (RM), abortive infection (Abi) systems and the widely-recognized CRISPR-Cas system. However, recent advancements in exploring the vast bacterial pangenome, the collective genetic pool of a species, are revealing a hidden arsenal of previously unknown defense systems clustered in ”defense islands” [1, 2].

In this study, we explore the molecular mechanisms and functional optimization of four novel defense systems: PD-T4-1, PD-T7-1, Azaca and Mokosh I. Our research starts by testing whether the defence systems are able to protect against bacteriophages. We have tested the defence systems against bacteriophages from the BASEL collection and have shown that they are active and able to defend against some of the bacteriophages in the collection. We were also able to isolate several bacteriophage mutants (escapers). In future studies, the genomic DNA information isolated from these bacteriophage mutants will provide a more detailed understanding of the defence systems we are studying. Subsequently, we purified wild-type and mutant proteins from the Azaca, PD-T4-1, and PD-T7-1 systems and conducted nuclease activity assays using various DNA substrates. These experiments revealed the specificities and efficiencies of the nucleases, highlighting key functional domains and residues. Finally, we performed optimization studies to determine the optimal conditions for the nuclease activity of the wild-type proteins, enhancing our understanding of their biochemical properties and potential applications.

This work not only advances our knowledge of prokaryotic antiviral defense mechanisms but also lays the groundwork for the development of novel biotechnological tools and therapeutic strategies.

[1] Vassallo, C.N. et al. (2022) “A functional selection reveals previously undetected anti-phage defence systems in the E. Coli pangenome,” Nature Microbiology, 7(10), pp. 1568–1579.
[2] Millman, A. et al. (2022) “An expanded arsenal of immune systems that protect bacteria from phages,” Cell Host & Microbe, 30(11).

COMPREHENSIVE ANALYSIS OF M6A AND M5C RNA METHYLATION PROFILES IN GLIOMAS

Samanta Tamašuitytė[1], Rūta Urbanavičiūtė-Orentė[1]

[1]Faculty of Medicine Medical Academy, Institute of Neuroscience, Lithuanian University of Health Sciences, Kaunas, Lithuania
tamasuityte.samanta@gmail.com

Gliomas are aggressive primary brain tumors with high morbidity and mortality [1]. Despite advances in oncology, their complex biology limits effective treatment options, making gliomas a key focus of cancer research. Epigenetic modifications, including RNA methylation (m6A and 5mC), have been implicated in tumor progression, yet their specific roles in gliomas remain unclear [2]. This study investigates m6A and 5mC RNA methylation profiles in gliomas and their potential as biomarkers for tumor malignancy and clinical outcomes.

Methods: Total RNA was extracted from glioma tissue samples (n = 30; grade II = 20, grade IV = 8) and cell cultures (n = 8; commercial glioblastoma cell lines = 4, glioma stem cell cultures = 2, neural stem cell cultures = 3) using TRIzol reagent. Poly(A) RNA was isolated with magnetic oligo(dT) beads, and m6A/5mC modifications were quantified via ELISA-based colorimetric and fluorometric assays. Statistical analyses, including Kolmogorov-Smirnov, unpaired t-test, Mann-Whitney U test, and Kaplan-Meier survival analysis, assessed correlations between methylation levels, tumor grade, and clinical characteristics.

Results: m6A levels were significantly lower in grade II gliomas and neural stem cell lines and highest in grade IV gliomas and GBM cell lines ($p < 0.05$). Female patients exhibited significantly higher m6A levels compared to males ($p = 0.011$), but no association with survival was observed. 5mC levels were significantly higher in tumor samples than in cell lines ($p < 0.05$), and elevated 5mC was correlated with shorter survival in grade IV gliomas ($p = 0.0299$).

Conclusion: Distinct m6A and 5mC RNA methylation profiles were observed in gliomas, suggesting their involvement in tumor progression. The association between 5mC levels and survival highlights its potential prognostic value, warranting further investigation into RNA methylation as a biomarker for glioma malignancy.

[1] Ludwig K, Kornblum HI. Molecular markers in glioma. T. 134, Journal of Neuro-Oncology. Springer New York LLC; 2017. p. 505–12.
[2] Xu J, Liu F, Li Y, Shen L. A 1p/19q Codeletion-Associated Immune Signature for Predicting Lower Grade Glioma Prognosis. Cell Mol Neurobiol; 42(3):709–22.

CHARACTERIZATION OF DesR-DEPENDED VANILLIC AND SYRINGIC ACIDS-INDUCIBLE SYSTEM FROM SPHINGOBIUM SP.SYK-6

Miglė Loveikytė[1], Naglis Malys[1], Ernesta Augustienė[1]

[1]Bioprocess Research Centre, Faculty of Chemical Technology, Kaunas University of Technology, Radvilėnų pl. 19, Kaunas LT-50254, Lithuania
migle.loveikyte@ktu.edu

Phenolic acids are bioactive compounds commonly found in seeds, fruit peels, and leafy vegetables, were they exist as conjugates or in a free form. Syringic acid, a derivative of hydroxybenzoic acid, exhibits a range of bioactivities including antioxidant, anti-inflammatory, antimicrobial, and even anticancer properties, highlighting its significance in biomedical and industrial applications. Furthermore, syringic acid acts as a precursor for syringyl derivatives, important in food and pharmaceutical industries. Over the past decades, the aerobic alphaproteobacterium Sphingobium sp. SYK-6 has emerged as a model system for lignin-derived aromatic compound catabolism [1,2]. This Gram-negative bacterium, originally isolated from kraft pulp mill effluent, utilizes diverse biaryl and monoaryl lignin derivatives as sole carbon and energy sources. Syringic acid is converted to 3-methylgallic acid by gallate dioxygenase, and which is metabolized via gallate cleavage pathway. Inducible gene expression systems, composed of transcription factors (TFs) and inducible promoters, regulate gene expression in response to environmental conditions, including small molecules. These systems regulate gene expression by either repressing or activating transcription, depending on whether the TF inhibits or promotes RNA polymerase binding to the promoter. Genetically encoded biosensors, based on these systems, are powerful analytical tools for detecting specific chemical compounds in biological samples. TF-based whole-cell biosensors have been applied in synthetic biology for strain screening, target molecule detection, or monitoring biopolymer degradation processes. Although biosensors for various phenolic acids have been developed, a syringic acid-specific biosensor remains a challenge [3]. In this study, we characterized and parameterized the DesR-depended vanillic and syringic acids-inducible gene expression system from Sphingobium sp. SYK-6 that can potentially be used for developing transcription factor-based biosensor.

Acknowledgements

This work was supported by the EU funds investment programme 2021–2027 [Project No. 10-038-T-0062] under grant agreement with the Central Project Management Agency.

[1] 1. Araki, T. et al., 2019. Regulation of vanillate and syringate catabolism by a MarR-type transcriptional regulator DesR in Sphingobium sp. SYK-6. Scientific Reports, 9(1), p. 18036. 2. Kamimura, N. et al., 2017. Bacterial catabolism of lignin-derived aromatics: New findings in a recent decade. Environ. Microbiol. Rep., 9(6), pp. 679-705. 3. Au

[2] 2. Kamimura, N. et al., 2017. Bacterial catabolism of lignin-derived aromatics: New findings in a recent decade. Environ. Microbiol. Rep., 9(6), pp. 679-705.

[3] 3. Augustiniene, E. et al., 2023. Transcription factor-based biosensors for detection of naturally occurring phenolic acids. New Biotechnology, Volume 78, pp. 1-12.

EXPLORING SOYBEAN-MICROORGANISM INTERACTIONS THROUGH STABLE ISOTOPE ANALYSIS

Raminta Skipitytė[1,2], Rūta Barisevičiūtė[2], Monika Toleikienė[1]

[1]Lithuanian Research Centre for Agriculture and Forestry, Department of Plant Nutrition and Agroecology, Lithuania
[2]Center for Physical Sciences and Technology, Department of Nuclear Research, Lithuania
raminta.skipityte@lammc.lt

Soybean (*Glycine max*) is a leguminous crop highly valued for its rich protein content, natural ability to fix atmospheric nitrogen, and diverse applications in food, feed, and industry, making it a key component of global agriculture and sustainability initiatives. In the Nordic and Baltic regions, efforts are increasingly directed toward boosting local protein production and reducing reliance on imports, with soybean cultivation emerging as a viable solution. However, successful cultivation in soils lacking native *Bradyrhizobium* strains—essential for biological nitrogen fixation (BNF) through nodule formation—remains a challenge. This study investigated soybean N_2-fixation potential using inoculants containing *Bradyrhizobium japonicum* strains, aiming to enhance BNF through seed inoculation, a standard practice that serves as an alternative to mineral nitrogen fertilizers.

Field experiment was carried out in Lithuanian Research Centre for Agriculture and Forestry (LAMMC) in Akademija (55°24′ N, 23°51′ E), Kėdainiai district. Field trials were performed in organic fields, which have been managed organically for many years, with no additional irrigation, pesticides, or chemical inputs. BNF efficiency was evaluated measuring nitrogen stable isotope ratios in bean, shoot and stem samples using Thermo Flash EA 1112 elemental analyser connected to Thermo Scientific Delta V Advantage isotope ratio mass spectrometer (EA-IRMS) in Center for Physical Sciences and Technology (FTMC). Various biological parameters, such as yield, plant height, nodule number and mass, as well as protein and lipid contents, were analyzed.

The number of nodules per plant affected both the nitrogen isotopic ratio and nitrogen content in soybean samples. Higher biomass displayed a slight correlation with the nitrogen isotopic ratio. Seed yield was linked to nodule weight and nitrogen content in seeds, while protein content correlated with the number of nodules per plant. Tendencies in nitrogen isotopic values and nitrogen contents in different plant parts of soybean inoculated and not inoculated with *Bradyrhizobium japonicum* are shown in Fig. 1. The study demonstrated that soybean inoculation can be an effective technique for enhancing atmospheric nitrogen fixation and improving yield quality.

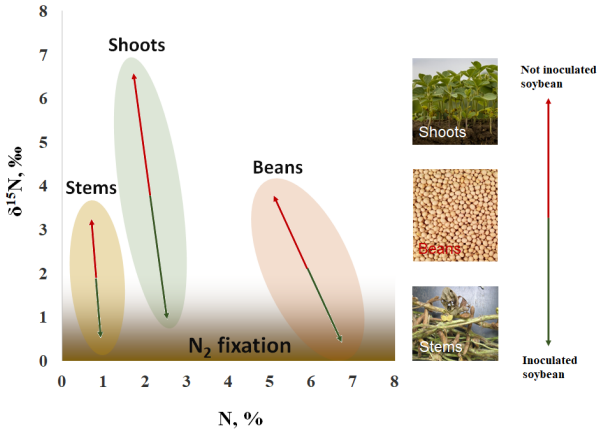


Fig. 1. Tendencies in nitrogen isotopic values and nitrogen content across different soybean plant parts, comparing inoculated and non-inoculated soybeans.

Acknowledgements

This study was conducted as part of postdoctoral research funded by the Research Council of Lithuania No. S-PD-24-45.

DETERMINATION OF QUANTITATIVE COMPOSITION OF α-AMYRIN AND MASLINIC ACID IN PRUNUS DOMESTICA L. FRUIT SAMPLES

Augustė Adomaitytė[1], Mindaugas Liaudanskas[1,2], Rima Šedbarė[2], Juozas Lanauskas[3], Darius Kviklys[3,4], Jonas Viškelis[3], Pranas Viškelis[3], Valdimaras Janulis[2]

[1]Institute of Pharmaceutical Technologies, Faculty of Pharmacy, Lithuanian University of Health Sciences, Kaunas, Lithuania
[2]Department of Pharmacognosy, Faculty of Pharmacy, Lithuanian University of Health Sciences, Kaunas, Lithuania
[3]Lithuanian Research Centre for Agriculture and Forestry, Institute of Horticulture, Kauno str. 30, Babtai, Kaunas distr., Lithuania
[4]Department of Horticulture, Norwegian Institute of Bioeconomy Research—NIBIO Ullensvang, Ullensvangvegen, Lofthus, Norway
auguste.adomaityte@stud.lsmu.lt

Triterpenic compounds are widely distributed in edible and medicinal plants, and consequently, they are an integral part of the human diet. Although triterpenic compounds were considered to be biologically inactive for a long period of time, accumulating evidence on their broad spectrum pharmacological activities coupled with a low toxicity profile has sparked renewed interest with regard to human health. Triterpenic compounds have been shown to possess numerous biological activities such as antidiabetic, hypolipidemic and cholesterol-lowering, anticarcinogenic, hepatoprotective, antiatherosclerotic, wound-healing, anticoagulant, antioxidant, anti-inflammatory, and antimicrobial. [1-3]

The aim of this research was to determine the quantitative composition of α-amyrin and maslinic acid in P. domestica fruit samples. 1 g of lyophilized Prunus domestica L. fruit powder was placed in dark glass bottles and covered with 10 ml 100% (v/v) acetone. The bottles are placed in an ultrasonic bath (Elmasonic P, Singen, Germany) for extraction performed for 10 minutes. The ultrasonic bath operates at a frequency of 80 kHz and a power of 1130 W. Following the extraction, the solution was filtered and the filter rinsed with 100% (v/v) acetone. The filtrate is subsequently transferred into a 10 ml volumetric flask and diluted to the calibration mark with 100% (v/v) acetone. [4] The UHPLC analysis of triterpenic compounds was performed according to Sedbare et al. [5] The results were analyzed using 'MS Excel 2023' (Microsoft, Redmond, WA, USA) and 'SPSS Statistics 21' (IBM, Chicago, IL, USA). α-Amyrin contents in the tested P. domestica fruit samples varied from 51.56 µg/g to 148.73 µg/g. The calculated average amount of α-Amyrin was 96.40 µg/g, and the coefficient of variation was 40.82 %. The highest amount (148.73 µg/g) of α-amyrin was determined in P. domestica cultivar 'Renklod Rannij Doneckij' fruit sample. The lowest amount (51.56 µg/g) of α-amyrin was determined in P. domestica cultivar 'Dambrovicų vengrinė' fruit sample. The amount of maslinic acid found in P. domestica fruit samples varied from 4.37 µg/g to 48.46 µg/g. The average amount of maslinic acid calculated was 20.32 µg/g, with a coefficient of variation of 85.43 %. The highest amount (48.46 µg/g.) of maslinic acid was determined in P. domestica cultivar 'Renklod Rannij Doneckij' fruit sample. The lowest amount (4.37 µg/g) of maslinic acid was determined in P. domestica cultivar 'Opal' fruit sample.

This research revealed the significant variations of α-amyrin and maslinic acid amounts in P. domestica samples. Among the tested cultivars, the fruit sample of 'Renklod Rannij Donetskij' cultivar had the highest amounts of α-amyrin and maslinic acid, therefore the plum fruits of this cultivar could be promising for the further researches.

[1] Szakiel, A., Pączkowski, C., Pensec, F., & Bertsch, C. (2012). Fruit cuticular waxes as a source of biologically active triterpenoids. Phytochemistry Reviews, 11(2-3), 263–284. https://doi.org/10.1007/s11101-012-9241-9
[2] Sandeep, & Ghosh, S. (2020). Triterpenoids: Structural diversity, biosynthetic pathway, and bioactivity. Bioactive Natural Products, 411–461. https://doi.org/10.1016/b978-0-12-819483-6.00012-6
[3] Bishayee, A. (2011). Triterpenoids as potential agents for the chemoprevention and therapy of breast cancer. Frontiers in Bioscience, 16(1), 980. https://doi.org/10.2741/3730
[4] Butkevičiūtė, A., Liaudanskas, M., Kviklys, D., Zymonė, K., Raudonis, R., Viškelis, J., Uselis, N., & Janulis, V. (2018). Detection and analysis of triterpenic compounds in apple extracts. International Journal of Food Properties, 21(1), 1716–1727. https://doi.org/10.1080/10942912.2018.1506478
[5] Sedbare, R.; Raudone, L.; Zvikas, V.; Viskelis, J.; Liaudanskas, M.; Janulis, V. Development and validation of the UPLC-DAD methodology for the detection of triterpenoids and phytosterols in fruit samples of Vaccinium macrocarpon Aiton and Vaccinium oxycoccos L. Molecules 2022, 27, 4403.

BIOCONTROL CAPABILITIES OF ENDOPHYTIC FUNGI DERIVED FROM SCOTS PINE AGAINST NEEDLE CAST

Milana Šilanskienė[1], Dorotėja Vaitiekūnaitė[1], Vaida Sirgedaitė-Šėžienė[1]

[1]Lithuanian Research Center for Agriculture and Forestry
milana.silanskiene@lammc.lt

Scots pine (*Pinus sylvestris*) is one of the most common and highly valued tree species in the Baltics. Nurseries and young stands of Scots pine are highly susceptible to needle cast disease caused by fungi *Lophodermium seditiosum* Minter, Staley and Millar, which affects the growth and survival of saplings negatively and makes them more prone to other biotic factors [1].

Research was conducted to find an environmentally safe way to protect younger Scots pine saplings from premature needle cast caused by *L.seditiosum*. For this purpose, endophytic fungi were isolated from mature Scots pine trees located in Juodkrantė Forest, and their antagonistic potential was tested under in vitro conditions. In total, 62 endophytic fungi were extracted by using five different growth mediums to achieve maximum diversity of fungi. To check if endophytes were natural antagonists of needle cast, an in vitro dual culture study was conducted: a pathogen and possible antagonist were placed in a Petri dish and their interaction was observed [2] for 5 weeks (Fig. 1). It was found that only 13% of fungi slowed down or completely stopped the growth of *L.seditiosum* by 30% during all 5 weeks of the experiment. Six endophytic fungi were discovered to inhibit the growth of the pathogen by 60% or more, and they will be chosen for further investigations in field experiments, where Scots pine saplings will be treated with antagonists to prevent the needle cast disease.

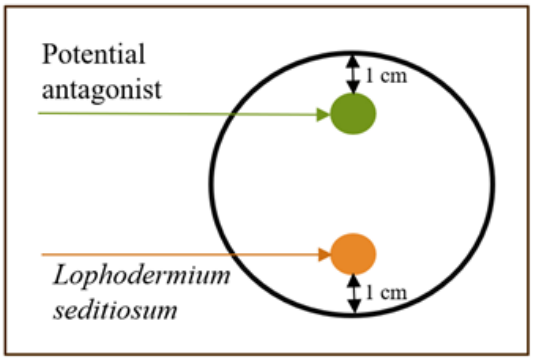


Fig. 1. Experimental setting of dual culture on Malt extract agar. Measurements of fungi radius were taken for 5 weeks to calculate *L. seditiosum* growth inhibition percentage.

[1] Jansons, A., Zeltiņš, P., Donis, J., & Neimane, U. (2020). Long-Term Effect of Lophodermium Needle Cast on The Growth of Scots Pine and Implications for Financial Outcomes. Forests, 11, 718. https://doi.org/10.3390/f11070718

[2] Vaitiekūnaitė, D., Striganavičiūtė, G., Beniušytė, E., Sirgedaitė-šėžienė, V., & Augustauskaitė, M. (2023). Putative biocontrol agents for European forest pathogens found in English oak (Quercus robur L.) endosphere. Zemdirbyste, 110(1), 79–86. https://doi.org/10.13080/z-a.2023.110.011

DIVERSITY OF INSECTS (INSECTA) IN DECAYING DEAD WOOD PARTIALLY SUBMERGED IN WATER

Austėja Černiauskaitė[1], Virginija Podėnienė[1], Jekaterina Havelka[1]

[1] Institute of Biosciences, Life Sciences Center, Vilnius University, Lithuania
austeja.cerniauskaite@gmc.stud.vu.lt

Dead decaying wood in freshwater ecosystems plays a significant role: it maintains balance in food webs and regulates shape, width, and stream flow in rivers and streams. The most important function of dead wood, partially submerged in water, is creating unique habitats for specialized but vulnerable insect species. Those insects that live in dead wood are often called saproxylic insects because they must spend part of their life cycle in decaying dead wood. No research about insect diversity in dead, partially submerged wood in water has been done in Lithuania – this work is the first. The primary purpose of this work is to find out which families, genera, and species choose to live in dead wood, partially submerged in water in Lithuania [1-3].

Organisms were collected from dead, partially submerged wood by hand in May, June, September, and October 2024 using measuring tapes, knife, tweezer, and small jars filled with 70 % alcohol. Collected organisms were identified by their morphological features using a few identification sources with characterization keys. Molecular methods like DNA extraction, polymerase chain reaction (PCR), DNA electrophoresis, and purification of PCR products were used for organisms with questionable identification. Samples were sent for sequencing to BaseClear B.V Leiden, Netherlands. DNA sequence fragments were analyzed using BioEdit and MEGA software. The analyzed sequences were compared with those published in the GenBank and BOLD systems databases.

300 pieces of dead wood from 4 sites and 12 points in Varėna and Trakai districts were examined. 1719 insects were collected (1684 larvae, 22 pupae, 4 puparia, 9 adults). 35 families were identified, of which family Limoniidae was the most abundant (1229) (Fig. 1). Collected insects belonged to 6 orders, of which the most extensive taxonomical diversity was in the order Diptera (16 families). The most diverse families of this order were Chironomidae and Limoniidae (both had 12 genera). The most abundant genus was *Lipsothrix* Loew, 1873 (1136 individuals) from family Limoniidae.

The results show that there is quite a high insect diversity in dead decaying wood, partially submerged in water with the highest diversity in order Diptera.

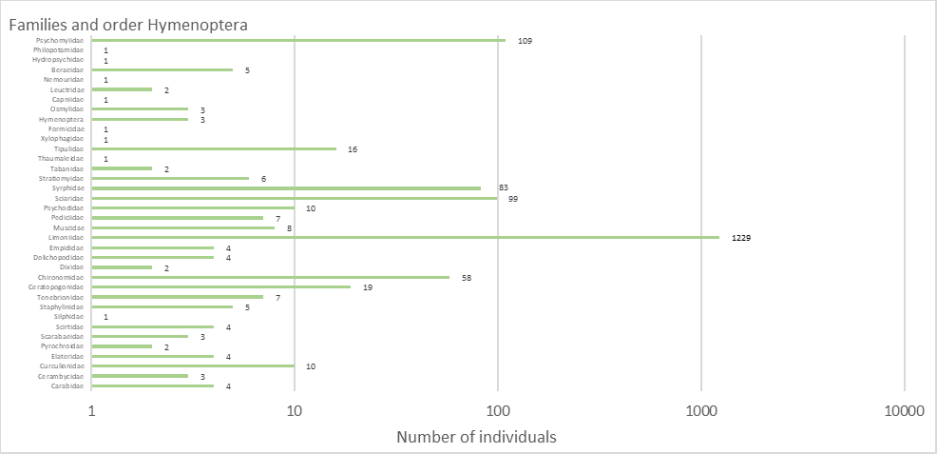


Fig. 1. Insect family diversity and abundance in decaying, partially submerged wood.

[1] S. J. Grove, "Saproxylic Insect Ecology and the Sustainable Management of Forests," Annual Review of Ecology and Systematics, vol. 33, no. 1, pp. 1–23, Nov. 2002, doi: https://doi.org/10.1146/annurev.ecolsys.33.010802.150507.

[2] A.M. Gurnell, "9.11 Wood in Fluvial Systems," Elsevier eBooks, pp. 163–188, Jan. 2013, doi: https://doi.org/10.1016/b978-0-12-374739-6.00236-0.

[3] M. Venarsky, K. S. Simon, Mattia Saccò, Clémentine François, L. Simon, and C. Griebler, "Groundwater food webs," Elsevier eBooks, pp. 241–261, Jan. 2023, doi: https://doi.org/10.1016/b978-0-12-819119-4.00010-x.

DETERMINATION OF QUALITATIVEAND QUANTITATIVE COMPOSITION OF PHENOLIC COMPOUNDS IN RAPESEED HONEY SAMPLES

Ernesta Zaksaitė[1], Mindaugas Liaudanskas[1,2], Sonata Trumbeckaitė[1], Vaidotas Žvikas[1,2]

[1]Department of Pharmacognosy, Faculty of Pharmacy, Lithuanian University of Health Science, Lithuania
[2]Institute of Pharmaceutical Technologies of the Faculty of Pharmacy of Lithuanian University of Health Science, Lithuania
ernesta.zaksaite@stud.lsmu.lt

Honey is one of the oldest sweeteners in the world. Researchers discovered that different types of honey contain around 200 dissimilar substances. One of them is phenolic compounds, that are responsible for antioxidant activity, and it is important for human health due to the antioxidant and anti-inflammatory properties. [1] Therefore, it is important to investigate the phytochemical composition and biological properties of honey samples obtained from different regions of Lithuania. In this work, is important to determine the qualitative and quantitative composition of phenolic compounds in rapeseed honey samples, collected in different regions of Lithuania.

Rapeseed honey samples were collected in 2023 from six different apiaries. They were in Kloniniai Mijaugonys, Šeduva, Mažeikiai, Šilutė, Biržai and Kėdainiai districts. 1 g honey was dissolved in 10 ml 70 % ethanol. Then samples were extracted by ultrasound 20 min. in an ultrasonic bath. Before analysis, extracts were filtered through a 0.22 µm membrane filter. All samples contained flavonoids: quercetin, isorhamnetin, hyperoside and hydroxycinnamic acids – p-coumaric acid. Quercetin determined in rapeseed honey samples ranged between 2.12 µg/g and 6.36 µg/g. The highest quercetin content was detected in a sample from Šeduva (6.36 µg/g). The lowest quercetin content was found in a sample from Kėdainiai (2.12 µg/g). The coefficient of variation (CV) was 34.58%, this indicates a significant variability of quercetin content in the rapeseed honey samples. Isorhamnetin determined in rapeseed honey samples varied between 1.25 µg/g and 8.96 µg/g. The highest isorhamnetin content was detected in a sample from Šeduva (8.96 µg/g). The lowest isorhamnetin content was found in a sample from Šilutė (1.25 µg/g). The CV% was 87.18%, which indicates a very significant variability of isorhamnetin content in the rapeseed honey samples. Hyperoside determined in rapeseed honey samples ranged between 2.64 µg/g and 10.85 µg/g. In rapeseed honey sample from Šeduva district was evaluated the highest hyperoside content (10.85 µg/g). Rapeseed honey from Kloniniai Mijaugonys district ascertained the lowest hyperoside content (2.64 µg/g). The CV was 43.94%. p-Coumaric acid determined in rapeseed honey samples varied between 1.92 µg/g and 10.57 µg/g. The highest p-coumaric acid content was evaluated in a sample from Šilutė (10.57 µg/g). The lowest p-coumaric acid content was ascertained in a sample from Kėdainiai (1.92 µg/g). The CV% was 75.53%, which also indicates significant variability of p-coumaric acid content in rapeseed honey samples.

The results of our research have shown that all investigated samples of rapeseed honey contains flavonoids: quercetin, isorhamnetin, hyperoside and hydroxycinnamic acids – p-coumaric acid. Rapeseed honey sample from Šeduva region had the highest amount of quercetin, isorhamnetin and hyperoside. The highest p-coumaric amount was evaluated in a sample from Šilutė region.

[1] Cheung, Y., Meenu, M., Yu, X., & Xu, B. (2019). Phenolic acids and flavonoids profiles of commercial honey from different floral sources and geographic sources. International Journal of Food Properties, 22(1), 290–308. https://doi.org/10.1080/10942912.2019.1579835

ENVIRONMENTAL IMPLICATIONS OF DIVERSE RHIZOSPHERIC COMMUNITIES OF BACTERIA FOR NATURAL WEED SUPPRESSION ALONGSIDE CROP GROWTH STIMULATION

Tasawar Abbas[1]

[1]Kaunas University of Technology
tasawar.abbas@ktu.edu

Diverse communities of bacteria inhabiting the rhizosphere of plants are known for possessing complex mechanisms which impart implications on the growth and economic performance of plants. Present work is the key to the interest of researchers to maneuver these mechanisms to the benefit of mankind and resolve present day grave challenges of food security and environment. A large collection of rhizobacterial strains has undergone exhaustive screening process of their testing for the extracellular production of known plant growth inhibitory as well as stimulatory substances. The best candidate strains from the metabolite tests were applied under in vivo studies to plants which included three most noxious weeds of wheat (wild oat, littleseed canary grass and broadleaved dock) and wheat crop. The strains with maximum weed inhibition activities alongside non-deleterious or stimulatory effects on wheat were selected to be further tested in multiple field experiments. In weed control field trials, biomass of wild oat was inhibited from 14.3 to 52.1 percent, that of littleseed canary grass from 43.8 to 52.2 percent, and that of broadleaved dock was restricted from 17.9 to 44.0 percent where attack of these weeds, respectively, caused 60.8, 59.9 and 86 percent loss of grain yield of wheat. In crop growth testing trials, three of the five applied strains remained non-inhibitory as well as non-stimulatory to the wheat crop whereas two strains stimulated growth, yield and physiology of wheat. They increased the grain yield of wheat up to 34.3 and 40.3 percent. 16s rRNA sequencing technique identified all these strains to be pseudomonads. This work forms the framework of biobased products for control of weeds and higher production of wheat. This work promotes non-chemical natural means of food production indicating a multitude of benefits ranging from sustainability of the environment to healthy foods and enriched biodiversity.

Acknowledgements

1. University of Agriculture Faisalabad, Pakistan, 2. Higher Education Commission, Islamabad, Pakistan

EFFECT OF AGING ON THE STRUCTURAL PARAMETERS OF A BIODEGRADABLE SENSOR MADE FROM SEAWEED

Ujjawal Malani[2], Uldis Zaimis[1], Jurate Jolanta Petroniene[2], Andrius Dzedzickis[2], Vytautas Bucinskas[2]

[1]Institute of Science and Innovative Technology, Liepaja University, LV-3401 Liepaja, Latvia
[2]Department Of Mechatronics, Robotics and Digital Manufacturing, Vilnius Gediminas Technical University, LT-10105 Vilnius, Lithuania
ujjawal.malani@stud.vilniustech.lt

With increasing emphasis on sustainability and human safety, biodegradable materials are being explored for modern sensor applications. This study investigates the effect of aging on the structural parameters of sensors made using ***κ-Carrageenan hydrogel***, ferric oxide, and glycerol. *κ-Carrageenan* is a sulfated polysaccharide extracted from ***Furcellaria lumbricalis***, a red edible seaweed. Hydrogels are flexible and stretchable polymers, with high moisture retention capacity, making them similar to biological tissue.

A testing sample was prepared using two *aluminum electrodes* and a one-year-aged sensor film *(made using the procedure listed in [1])*. Each electrode was connected to opposite sides and opposite ends of the sensor, leaving a 10 x 10 mm sensing area between them. The electrodes were then connected to a *multimeter* and a *tension-compression bench* to record the force, elongation, and resistance of the prepared sample.

In the performed study, we observed that the electrons have a clear path to travel through the material, leading to an increase in conductivity. The initial conductivity of the sample was *1.96E-4*, increasing to *0.0852E-4* at rupture (9 mm elongation), with a maximum recorded force of *4.612 N*. This structural change suggests that the aging process may have enhanced the mobility of charge carriers, contributing to the observed increase in conductivity. These findings highlight the need for a more stable composition to ensure the long-term reliability of the sensor.

[1] Žaimis, U., Petronienė, J. J., Dzedzickis, A., & Bučinskas, V. (2024). Stretch Sensor: Development of Biodegradable Film. Sensors, 24(2), 683

THE EFFECT OF LACTICASEIBACILLUS CASEI CELL-FREE SUPERNATANT ON DECIDUALIZATION OF ENDOMETRIUM STROMAL CELLS

Saulė Dominyka Bučiūnaitė[1], Elvina Valatkaitė[1], Rūta Navakauskienė[1]

[1]Department of Molecular Cell Biology, Institute of Biochemistry, Life Sciences Center, Vilnius University, Lithuania
saule.buciunaite@gmc.stud.vu.lt

Various factors can cause female infertility most of which fall in the category of female reproductive system disorders, however, a growing number of studies show that infertility can be caused by the composition of female reproductive system microbiota. Recent studies on female reproductive organ microbiota showed that the most abundant bacteria genus is *Lactobacillus*, and that bacteria of this genus can have a positive impact on the function of female reproductive system organs [1].

The human endometrium - inner layer of the uterus - is a dynamic tissue, which experiences cyclic changes throughout the woman's reproductive years [2]. Endometrium decidualization refers to a process that occurs during every menstrual cycle when endometrium stromal cells (EnSCs) differentiate into specialised secretory cells in order to form the decidual lining into which the blastocyst later implants. Improper decidualization response could be a cause of several pregnancy complications, not only in early but also in advanced gestation [3,4]. This demonstrates the importance of proper decidualization process for female reproductive health.

The goal of this study was to determine the effect of the supernatant of *Lactobacillus casei* on decidualized and non-decidualized EnSCs by studying cell proliferation and changes in gene expression. EnSCs were isolated from endometrial tissue obtained from female patients undergoing *in vitro* fertilization (IVF). EnSC decidualization was induced with 8-bromo-cAMP and MPA inductors and cells were treated with 5X, 20X, 50X and 100X *L. casei* supernatant dilutions for 72 hours. To assess EnSC proliferation, XTT assay, a colorimetric method that detects the cellular metabolic activity was used. Using RT-qPCR, changes in *IGFBP1* and *PRL* gene expression of control and decidualized EnSCs treated with the supernatant of *L. casei* were analysed. Lastly, we plan to perform western blot analysis to examine decidualization related protein expression in EnSCs.

In both pregnant and non-pregnant patient cell lines it was shown that the 5X *L. casei* supernatant dilution reduced EnSC proliferation by approximately 60% compared to untreated cells. However, in the case of higher supernatant dilutions such as 50X and 100X, EnSCs were not affected as much by the supernatant and proliferation activity was closer to the one seen in control cells. RT-qPCR results revealed that EnSC decidualization was successfully induced, as visible by upregulation of *IGFBP1* and *PRL* expression levels in cells after the induction of decidualization. Furthermore, the highest gene expression levels of decidualization related gene-markers were reached in cells treated with 20X dilution of the supernatant of *L. casei*, showing the possible significance of *L. casei* metabolites for gene expression regulation during decidualization.

[1] Tomaiuolo, R., Veneruso, I., Cariati, F., & D'Argenio, V. (2020). Microbiota and Human Reproduction: The Case of Female Infertility. High-Throughput, 9(2), 12.

[2] Azizi, R., Aghebati-Maleki, L., Nouri, M., Marofi, F., Negargar, S., & Yousefi, M. (2018). Stem cell therapy in Asherman syndrome and thin endometrium: Stem cell- based therapy. Biomedicine & Pharmacotherapy = Biomedecine & Pharmacotherapie, 102, 333–343.

[3] Okada, H., Tsuzuki, T., & Murata, H. (2018). Decidualization of the human endometrium. Reproductive Medicine and Biology, 17(3), 220–227.

[4] Ng, S.-W., Norwitz, G. A., Pavlicev, M., Tilburgs, T., Simón, C., & Norwitz, E. R. (2020). Endometrial Decidualization: The Primary Driver of Pregnancy Health. International Journal of Molecular Sciences, 21(11), 4092.

TIME-DEPENDENT EFFECTS ON MITOCHONDRIAL FUNCTIONS INDUCED BY PSORIASIS-LIKE INFLAMMATION IN HUMAN KERATINOCYTES AND FIBROBLASTS

Martyna Uldukytė[1], Gabrielė Kulkovienė[1,2], Ramunė Morkūnienė[2], Aistė Jekabsone[1,3]

[1]Laboratory of Pharmaceutical Sciences Institute of Pharmaceutical Technologies, Lithuanian University of Health and Sciences, Kaunas, Lithuania
[2]Department of Drug Chemistry, Faculty of Pharmacy, Lithuanian University of Health and Sciences, Kaunas, Lithuania
[3]Preclinical Research Laboratory for Medicinal Products Institute of Cardiology, Lithuanian University of Health and Sciences, Kaunas, Lithuania
martyna.uldukyte@stud.lsmu.lt

Psoriasis is a chronic inflammatory skin disease driven by excessive keratinocyte proliferation, psoriatic fibroblasts, and key cytokines such as TNF-α, IL-17, and IL-22 [1]. *In vivo* studies have shown that mitochondrial dysfunction, marked by increased ROS production and metabolic alterations, plays a critical role in psoriasis progression [2]. It has been discovered that skin cells exhibit different sensitivities to psoriasis inflammation, with keratinocytes showing a more immediate and intense response than fibroblasts [3]; however, the underlying mechanisms of these mitochondrial responses remain insufficiently investigated.

The aim of this study is to examine the impact of psoriasis-like inflammation (PLI) on mitochondrial functions in human keratinocytes and fibroblasts over 24, 48, and 72 hours, specifically assessing mitochondrial membrane potential, mtROS production, and cellular respiration.

PLI was induced by treating keratinocytes and fibroblasts with a cytokine mixture consisting of TNF-α, IL-17, and IL-22. Mitochondrial membrane potential and mtROS levels were assessed at 24, 48, and 72 hours using TMRM and MitoSox Red staining, respectively, with fluorescence microscopy performed on an Olympus APX100 microscope and image analysis conducted via Fiji software. Cellular respiration was measured at 24 and 72 hours using the Seahorse XFp Analyzer and Mito Stress Test Kit, with data normalized to total protein content using the Bradford assay and analyzed with the Infinite 200 Pro Nano Plex reader.

The results demonstrated that keratinocytes exposed to PLI exhibited a transient increase in mitochondrial membrane potential at 24 and 48 hours, accompanied by a peak in mtROS production at 24 hours that remained stable thereafter. These mitochondrial alterations were linked to significant reductions in cellular respiration, and glycolytic activity at 24 hours, all of which returned to baseline levels by 72 hours. In PLI-treated fibroblasts, mitochondrial membrane potential increased at 24 hours but normalized by 72 hours, alongside a progressive rise in mtROS production that reached its peak at 72 hours. Unlike keratinocytes, fibroblast cellular respiration and glycolysis remained stable initially but showed a decline in respiration and an increase in glycolytic efficiency at 72 hours.

This study reveals that PLI induces distinct time-dependent mitochondrial responses in keratinocytes and fibroblasts, with rapid dysfunction in keratinocytes and delayed impairment in fibroblasts, providing insights into mitochondrial mechanisms in psoriatic skin cells and potential therapeutic targets for restoring mitochondrial homeostasis.

[1] Sieminska, I., Pieniawska, M., & Grzywa, T. M. (2024). The Immunology of Psoriasis—Current Concepts in Pathogenesis. Clinical Reviews in Allergy & Immunology, 66(2), 164–191.
[2] Mizuguchi, S., Gotoh, K., Nakashima, Y., Setoyama, D., Takata, Y., Ohga, S., &
[3] Kulkovienė, G., Uldukytė, M., Haluts, S., Kairytė, M., Šoliūnas, J., Šalčiūtė, V., Morkūnienė, R., & Jekabsone, A. (2024). Psoriasis-like inflammation induces mitochondrial function and structure changes in human keratinocytes and fibroblasts. bioRxiv (Cold Spring Harbor Laboratory).

MATERNAL HIGH-FAT DIET EFFECT ON THE OFFSPRINGS RETINAL INFLAMMATORY RESPONSE

Patricija Čepauskytė[1], Gintarė Urbonaitė[1], Neda Ieva Biliūtė[1], Guoda Laurinavičiūtė[2], Urtė Neniškytė[1,3]

[1]Institute of Biosciences, Life Sciences Center, Vilnius University, Lithuania
[2]Institute of Biomedical Sciences, Faculty of Medicine, Vilnius University, Lithuania
[3]VU-EMBL Partnership Institute, Life Sciences Center, Vilnius University, Lithuania
patricija.cepauskyte@gmc.stud.vu.lt

Aim: Increased high-fat content in today's society's diet is one of the leading factors contributing to the rising obesity rates. Research studies show that maternal high-fat diet (mHFD) can be the cause of neurodevelopmental disorders in the offspring due to induced systemic inflammation [1, 2, 3]. Moreover, inflammatory response changes throughout different pahses of female mice estrous cycle [4, 5, 6]. Proteins such as CD68 and TSPO can be used as dependable biomarkers for detecting microglia phagocytic and metabolic activation, and identifying inflammatory response in the central nervous system, which also includes the retina [7,8]. Although some studies show HFD effect on the retina, little research has been done to investigate its impact on the offspring retina [9]. This study aims to evaluate maternal diet induced changes of microglial CD68 and TSPO area and Müller cell activity in the peripheral retina of the offspring and assess how they depend on the mice female estrous cycle phases.

Methods: Female C57Bl/6J mice, from weaning and during pairing, pregnancy and lactation, were fed with either control diet (CD, 10% fat) or high-fat diet (HFD, 60% fat). The offspring were weaned to normal rodient diet. Collected eyeballs of the offspring were fixed with 4% PFA, cryoprotected, and sliced using cryotome. Microglia, Müller cells, CD68 and TSPO proteins in microglia were labeled immunohistochemically using anti-RFP, anti-GFAP, anti-CD68, and anti-TSPO antibodies, respectively. Before tissue collection, the estrous cycle phases were determined by vaginal cytology of 22-week-old female offspring.

Results: We evaluated mHFD effect on offspring Müller cells, microglia cells, CD68 and TSPO area in microglia cells in peripheral retina. Our results revealed that mHFD significantly increased the area of microglia, Müller cells, CD68 and TSPO in both male and female offspring's peripheral retina. However, we observed a more subtle mHFD effect on female offspring retina. Further research confirmed that these different mHFD alterations could be due to female hormone changes during female estrous cycle.

Conclusion: Our findings demonstrated that mHFD had an effect on both male and female offspring peripheral retina, and that the inflammatory response of the retina could be dependent on reproductive hormones.

Funding: This work was supported by the Science Promotion Fund of Vilnius University.

[1] M. Maes, R. Verkerk, S. Bonaccorso, W. Ombelet, E. Bosmans, and S. Scharpé, 'Depressive and anxiety symptoms in the early puerperium are related to increased degradation of tryptophan into kynurenine, a phenomenon which is related to immune activation', Life Sciences, vol. 71, no. 16, pp. 1837–1848, Sep. 2002.

[2] R. D. Oades, A.-M. Myint, M. R. Dauvermann, B. G. Schimmelmann, and M. J. Schwarz, 'Attention-deficit hyperactivity disorder (ADHD) and glial integrity: an exploration of associations of cytokines and kynurenine metabolites with symptoms and attention', p. 19, 2010.

[3] S. S. Kang, A. Kurti, D. A. Fair, and J. D. Fryer, 'Dietary intervention rescues maternal obesity induced behavior deficits and neuroinflammation in offspring', p. 12, 2014.

[4] Villa A, Vegeto E, Poletti A, Maggi A. Estrogens, Neuroinflammation, and Neurodegeneration. Endocr Rev. 2016 Aug;37(4):372-402. doi: 10.1210/er.2016-1007. Epub 2016 May 19. PMID: 27196727; PMCID: PMC4971309.

[5] Crespo-Castrillo, A., & Arevalo, M. A. (2020). Microglial and Astrocytic Function in Physiological and Pathological Conditions: Estrogenic Modulation. International journal of molecular sciences, 21(9), 3219. https://doi.org/10.3390/ijms21093219.

[6] Benlloch-Navarro, S., Trachsel-Moncho, L., Fernández-Carbonell, Á., Olivar, T., Soria, J. M., Almansa, I., & Miranda, M. (2019). Progesterone anti-inflammatory properties in hereditary retinal degeneration. The Journal of steroid biochemistry and molecular biology, 189, 291–301. https://doi.org/10.1016/j.jsbmb.2019.01.007.

[7] Fu R, Shen Q, Xu P, Luo JJ, Tang Y. Phagocytosis of microglia in the central nervous system diseases. Mol Neurobiol. 2014 Jun;49(3):1422-34. doi: 10.1007/s12035-013-8620-6. Epub 2014 Jan 7. PMID: 24395130; PMCID: PMC4012154.

[8] Hector, M., Langmann, T., & Wolf, A. (2024). Translocator protein (18 kDa) (Tspo) in the retina and implications for ocular diseases. Progress in retinal and eye research, 100, 101249. https://doi.org/10.1016/j.preteyeres.2024.101249.

[9] D. A. Clarkson-Townsend, A. J. Douglass, A. Singh, R. S. Allen, I. N. Uwaifo, and M. T. Pardue, 'Impacts of high fat diet on ocular outcomes in rodent models of visual disease', Experimental Eye Research, vol. 204, p. 108440, Mar. 2021, doi: 10.1016/j.exer.2021.108440.

MICROGRAVITY AND YEAST RESISTANCE TO MANDELIC ACID: EXPLORING THE CONNECTION WITH TELOMERE LENGTH

Ugnė Juodviršytė[1], Eglė Lastauskienė[1]

[1] Institute of Biosciences, Life Sciences Center, Vilnius University,
ugne.juodvirsyte@gmc.stud.vu.lt

The effects of microgravity on biological systems pose a significant challenge for long-term space missions, as it influences cellular aging, immune function, and stress resistance. One of the key cellular changes in microgravity is the alteration of telomere length—specialized repetitive DNA sequences at the ends of chromosomes that protect genetic information from degradation during cell division. Telomere length changes are associated with genomic instability and premature cellular aging. In microgravity, telomeres tend to lengthen, but upon return to Earth's gravity, they become even shorter. These changes could have significant implications not only for astronaut health but also for biotechnological applications in space.

This study investigated the effects of microgravity on the resistance of *Saccharomyces cerevisiae* yeast to mandelic acid, a widely used cosmetic compound known for its antibacterial and exfoliating properties. Using yeast strains with different telomere lengths, minimum inhibitory concentrations (MICs) were determined through a drop assay, and growth was analyzed at various MIC concentrations (1 MIC, 0.5 MIC, 0.25 MIC) under different gravity conditions to assess growth dynamics.

Results from the drop test revealed that microgravity had only a slight impact, increasing the sensitivity of yeast with normal telomere length by 1.2 times. It was also observed that telomere length did not affect MIC values. Growth curve analysis showed that exposure to mandelic acid resulted in a lower final optical density (OD_{600}) in all tested samples compared to the control group, regardless of telomere length or gravity conditions. Additionally, a 1.3-fold extension of the lag phase was observed in all strains when 0.25 MIC of mandelic acid was added to the medium, indicating that mandelic acid prolongs adaptation and delays the growth of yeast cells. When 0.5 MIC of mandelic acid was introduced, a statistically significant effect of microgravity was observed only in the strain with short telomeres. Under microgravity conditions, this strain exhibited a higher OD_{600} than under normal gravity, suggesting improved survival or faster recovery from mandelic acid-induced stress.

To conclude, these findings suggest that microgravity influences yeast susceptibility to mandelic acid, particularly in strains with short telomeres. The observed changes in growth dynamics, including increased sensitivity and extended lag phase, highlight the potential impact of microgravity on cellular stress responses. Further research is needed to explore the molecular mechanisms underlying these effects and to determine whether similar responses occur in other eukaryotic models. Understanding these interactions could provide valuable insights for both space biology and the development of biotechnological applications in microgravity environments.

INVESTIGATION OF THE EFFECTS OF TRANSCRANIAL MAGNETIC STIMULATION IN A DIFFERENTIATED SH-SY5Y CELL MODEL

Deimilė Asipavičiūtė[1], Aistė Zentelytė[2], Vladas Valiulis[3], Rūta Navakauskienė[4], Giedrė Valiulienė[5]

[1]Life Sciences Center, Institute of Biochemistry, Vilnius University
deimile.asipaviciute@gmc.stud.vu.lt

This study investigates the effects of transcranial magnetic stimulation (TMS) on cellular energetics using a differentiated SH-SY5Y neural cell model.

To explore this, SH-SY5Y neuroblastoma cells were differentiated into a more mature neural phenotype using BrainPhys™ neuronal medium supplemented with Penicillin/Streptomycin, a serum- and antioxidant-free B-27™ supplement, 50 ng/ml BDNF, and 10 µM retinoic acid. Following differentiation of 7 days, cells were seeded in 35 mm Petri dishes and placed 1 cm below the center of a TMS coil. The stimulation parameters were applied as described by Thomson and colleagues (2020), with stimulation at 100% Maximum Stimulator Output. Intermittent theta-burst stimulation (iTBS) consisted of 50 Hz triplets repeated in a 5 Hz rhythm in 2-second trains with 8-second inter-train intervals, while continuous theta-burst stimulation (cTBS) was applied as a continuous train, both for 600 pulses.

To assess the effects of iTBS and cTBS on mitochondrial respiration, the Agilent Seahorse Cell Mito Stress Test kit was used. The results indicated that cTBS had no significant effects on oxygen consumption rate (OCR), while iTBS stimulation led to an increase in maximal respiration and spare capacity values. Additionally, reactive oxygen species (ROS) production was evaluated using the DCFDA/H2DCFDA Cellular ROS Assay Kit (Abcam). The results showed a 1.5-fold downregulation of ROS levels following iTBS stimulation. These findings suggest that iTBS enhances mitochondrial function and reduces oxidative stress in the SH-SY5Y neural cell model, whereas cTBS does not significantly affect these parameters. Further research is needed to understand the molecular mechanisms behind these changes and their potential therapeutic applications.

RESEARCH OF ANEXIN A4 INFLUENCE ON PLASMA MEMBRAIN PERMABILIZATION DYNAMICS AND CELL VIABILITY AFTER ELECTROPORATION

Augustinas Andziuslis[1], Baltramiejus Jakštys[2], Saulius Šatkauskas[2]

[1]Biochemistry Cathedral, Faculty of Natural Sciences, Vytautas Magnus University, Kaunas, Lithuania
[2]Cell and Tissue Biotechnology Research Group, Research Institute of Natural and Technological Sciences, Vytautas Magnus University, Kaunas, Lithuania
augustinas.andziulis@vdu.lt

When mammalian cells are exposed to induced electric fields (IEFs), the outer plasma membrane (PM) potential increases, reaching a critical value of 0.2–1 V [1]. This enhances PM permeability to molecules and electrical current [2], a process termed electroporation (EP) or electropermeabilization. EP research has expanded into medical applications, including electrochemotherapy (ECT), gene electrotransfer (GET), and tissue ablation. Reversible EP (RE) is used in ECT and GET, while irreversible EP (IRE) is applied in ablation. Improving the safety and efficacy of these methods requires a deeper understanding of cellular responses to EP, including membrane integrity restoration and homeostasis recovery. Electropermeabilization activates repair mechanisms like exocytosis, pore sealing, and membrane shedding [3]. However, the role of Annexin A4 in pore sealing remains understudied. Annexins, a multifunctional protein superfamily, regulate apoptosis (via PS externalization and Ca^{2+} signaling [4]) and necrosis (via membrane repair and inflammatory responses [5]). Despite their importance, studies on Annexin A4's role in post-EP membrane repair are limited. Thus, we investigated Annexin A4's significance in electropermeabilization efficacy, PM integrity recovery, and cell viability after EP.

In this study, we used wild-type MCF7-WT (WT) and MCF7-ANXA4- (KO) cells, in which Annexin A4 protein expression was knocked out using the CRISPR/Cas9 system. The efficiency of electrotransfer and the dynamics of pore resealing were assessed using flow cytometry by evaluating propidium iodide uptake, while cell viability was determined using the MTS assay.

Our findings demonstrate that WT cells exhibit higher viability than KO cells under equivalent pulse intensities. Furthermore, KO cell line demonstrated greater permeabilization levels. However, compared to the WT cell line, KO cell pore closure efficiency had significantly decreased. Additionally, it was observed that the presence of $CaCl_2$ in the EP medium did not affect electropermeabilization efficiency but negatively impacted the ability of both WT and KO cells to repair plasma membrane and reduced cell viability within the tested parameter range. Notably, KO cells were more sensitive to EP exposure, despite WT cells being morphologically larger. Based on the Shwan equation, larger cells are more susceptible to electric pulses and suggest that the WT cell line should have been more sensitive than the KO line. The increased sensitivity of KO cells to EP indicates that the role of the ANX A4 protein in membrane recovery and maintaining cell viability process after EP is far more significant than previously thought. In summary, this study demonstrated the importance of the Annexin A4 protein in plasma membrane recovery and cell viability maintenance after electroporation.

[1] Weaver, J. C. (2000). Electroporation of cells and tissues. IEEE transactions on plasma science, 28(1), 24-33.
[2] Teissie, J., Golzio, M., & Rols, M. P. (2005). Mechanisms of cell membrane electropermeabilization: a minireview of our present (lack of?) knowledge. Biochimica et Biophysica Acta (BBA)-General Subjects, 1724(3), 270-280
[3] Cooper, S. T., & McNeil, P. L. (2015). Membrane repair: mechanisms andathophysiology. Physiological reviews, 95(4), 1205-1240
[4] Gerke, V., Creutz, C. E., & Moss, S. E. (2005). Annexins: linking Ca2+ signalling to membrane dynamics. Nature reviews Molecular cell biology, 6(6), 449-461
[5] a Monocytic, S. N. G. (2011). Cleavage of Annexin A1 by ADAM10 during.

OXIDATION AND CROSS-INTERACTIONS AS KEY MODULATORS OF S100A1 PROTEIN AGGREGATION

Viktorija Karalkevičiūtė[1], Ieva Baronaitė[1], Vytautas Smirnovas[1], Darius Šulskis[1]

[1]Institute of Biotechnology, Life Sciences Center, Vilnius University, Vilnius, Lithuania
viktorija.karalkeviciute@gmc.stud.vu.lt

The S100 protein family consists of structurally similar calcium-binding proteins that play diverse roles in regulating calcium homeostasis, cell growth, differentiation, cytoskeleton dynamics and response to inflammation[1]. In recent years, several members have been found to play significant roles in neurodegeneration by facilitating neuroinflammatory signalling and forming amyloid fibrils[2]. Furthermore, it has been shown that some S100 proteins can interact with Hsp70/Hsp90 multichaperone complex with S100A1 exhibiting the strongest interaction[3]. Another common feature of all S100 proteins is their ability to form homo- and heterodimers[2]. A potential candidate for this type of interaction with S100A1 is S100A8, since both proteins are found within amyloid plaques or astrocytes and play a role in the Alzheimer's disease (AD) cascade by transmitting neuroinflammatory signals[2].

Another characteristic of AD pathogenesis is oxidative stress, caused by reactive oxygen species (ROS) and liquid-liquid phase separation (LLPS), during which proteins form membraneless organelles[4]. ROS can lead to structural modifications of proteins and cause cellular damage[5]. While it is known that ROS can impair the functionality of S100 proteins[6], how it affects S100 aggregation is not known. In addition, LLPS is an emerging area of research exploring the relationship between phase transitions and neurological disease. LLPS is linked to redox imbalance in cells[4], but currently, there are no available LLPS studies of S100 proteins. Therefore, we decided to investigate how these cross-interactions, ROS and LLPS, affect S100A1 protein.

We monitored the aggregation of S100A1, S100A8 and S100A1/A8 proteins using amyloid-specific dye Thioflavin T (ThT) fluorescence and the resulting aggregates were analysed via Atomic Force (AFM) and Transmission electron (TEM) microscopies. A lysozyme chaperone activity test was performed to investigate whether S100A1 exhibits aggregation-inducing properties. Furthermore, we explored the aggregation of S100A1 under conditions of liquid-liquid phase separation (LLPS) and oxidation by measuring ThT fluorescence and turbidity.

Our research demonstrated that S100A1 and S100A8 form fibrillar aggregates in the presence of each other – a process chaperoned by calcium ions. AFM and TEM imaging confirmed that the interaction between these proteins led to the formation of worm-like fibrils. The lysozyme chaperone activity test revealed induction of lysozyme aggregation by S100A1 at low concentrations of calcium ions. These findings suggest that S100A1, when mixed with S100 or other proteins, can promote their aggregation. Finally, we showed that the highly stable S100A1 protein can form worm-like fibrils in the presence of crowding and oxidizing agents.

[1] Donato, R.; Cannon, B. R.; Sorci, G.; Riuzzi, F.; Hsu, K.; Weber, D. J.; Geczy, C. L. Functions of S100 Proteins. Curr. Mol. Med. 2013, 13 (1), 24–57.
[2] Cristóvão, J. S.; Gomes, C. M. S100 Proteins in Alzheimer's Disease. Front. Neurosci. 2019, 13.
[3] Okada, M.; Hatakeyama, T.; Itoh, H.; Tokuta, N.; Tokumitsu, H.; Kobayashi, R. S100A1 Is a Novel Molecular Chaperone and a Member of the Hsp70/Hsp90 Multichaperone Complex *. J. Biol. Chem. 2004, 279 (6), 4221–4233. https://doi.org/10.1074/jbc.M309014200.
[4] Saito, Y.; Kimura, W. Roles of Phase Separation for Cellular Redox Maintenance. Front. Genet. 2021, 12. https://doi.org/10.3389/fgene.2021.691946.
[5] Tramutola, A.; Lanzillotta, C.; Perluigi, M.; Butterfield, D. A. Oxidative Stress, Protein Modification and Alzheimer Disease. Brain Res. Bull. 2017, 133, 88–96. https://doi.org/10.1016/j.brainresbull.2016.06.005.
[6] Yamaguchi, F.; Tsuchiya, M.; Shimamoto, S.; Fujimoto, T.; Tokumitsu, H.; Tokuda, M.; Kobayashi, R. Oxidative Stress Impairs the Stimulatory Effect of S100 Proteins on Protein Phosphatase 5 Activity. Tohoku J. Exp. Med. 2016, 240 (1), 67–78. https://doi.org/10.1620/tjem.240.67.

PRODUCTION OF THEORETICAL TTV CAPSID PROTEIN IN E. COLI

Gabija Klimavičiūtė[1], Uršulė Simonaitytė[1], Martynas Simanavičius[1]

[1]Department of Immunology, Institute of Biotechnology, Life Sciences Center, Vilnius University
gabja.klimaviciute@gmc.stud.vu.lt

Torque teno virus (TTV) is a part of human virome. TTV is under active investigation as a marker of immunocompetence. After a solid organ transplant (SOT), patients are treated with immunosuppressants to reduce the immune response. However, if immunosuppression is not optimal, the risk of infection or organ rejection is higher, and the patient's health could be at risk. Therefore, a reliable molecular marker of immunosuppression is needed. Previous studies in this area have reported that TTV levels are elevated in the blood of SOT patients, making it a potential marker for monitoring the level of immunosuppression [1].

TTV is a small, non-enveloped, single-stranded DNA virus of the Anelloviridae family. The TTV genome consists of at least 6 open reading frames (ORFs), of which ORF1 is the longest [2]. It encodes the putative TTV capsid protein ORF1, which exposes antigenic peptides in its C-terminus and is recognized by antibodies [3]. The aim of this study is to achieve the bacterial synthesis of recombinant putative TTV capsid protein. A gene sequence was selected and the gene encoding the required protein was acquired based on the epitopes identified in the literature. The gene construct was chosen for its ability to allow gene expression in bacteria, followed by potentially soluble protein synthesis [3][4]. A gene expression vector was selected, and protein synthesis was confirmed by Western blot.

In conclusion, the synthesis of a putative TTV capsid protein has been achieved. Future plans include protein purification, mice immunization, and the development of monoclonal antibodies specific to this protein as universal tools for detection of TTV in patient samples.

[1] van Rijn, A., Roos, R., Dekker, F., Rotmans, J., & Feltkamp, M. (2023). Torque teno virus load as marker of rejection and infection in solid organ transplantation – A systematic review and meta-analysis. Reviews in Medical Virology, 33(1), e2393. https://doi.org/10.1002/rmv.2393

[2] Rezahosseini, O., Drabe, C. H., Sørensen, S. S., Rasmussen, A., Perch, M., Ostrowski, S. R., & Nielsen, S. D. (2019). Torque-Teno virus viral load as a potential endogenous marker of immune function in solid organ transplantation. Transplantation Reviews (Orlando, Fla.), 33(3), 137–144. https://doi.org/10.1016/j.trre.2019.03.004

[3] Venkataraman, T., Swaminathan, H., Arze, C. A., Jacobo, S. M., Bhattacharyya, A., David, T., Nawandar, D. M., Delagrave, S., Mani, V., Yozwiak, N. L., & Larman, H. B. (2022). Comprehensive profiling of antibody responses to the human anellome using programmable phage display. Cell Reports, 41(12), 111754. https://doi.org/10.1016/j.celrep.2022.111754

[4] Kakkola, L., Bondén, H., Hedman, L., Kivi, N., Moisala, S., Julin, J., Ylä-Liedenpohja, J., Miettinen, S., Kantola, K., Hedman, K., & Söderlund-Venermo, M. (2008). Expression of all six human Torque teno virus (TTV) proteins in bacteria and in insect cells, and analysis of their IgG responses. Virology, 382(2), 182–189. https://doi.org/10.1016/j.virol.2008.09.012

ELECTROCHEMICAL ANALYSIS OF ENSIFER MELILOTI USING DIVERSE REDOX MEDIATORS FOR MFC APPLICATIONS

Asta Bubnelytė[1,2], Tomas Mockaitis[2], Ingrida Bružaitė[1,2], Inga Morkvėnaitė-Vilkončienė[2,3]

[1]Department of Chemistry and Bioengineering, Faculty of Fundamental Sciences, Vilnius Gediminas Technical University, Vilnius 10223, Lithuania
[2]Laboratory of Bioelectrochemical Technologies, Department of Nanotechnology, State Research Institute Centre for Physical Sciences and Technology, Vilnius 10257, Lithuania
[3]Department of Electrical Engineering, Vilnius Gediminas Technical University, Vilnius 10223, Lithuania
tomas.mockaitis@ftmc.lt

As climate change intensifies and greenhouse gas emissions increase, there is growing global interest in finding sustainable solutions. A microbial fuel cell (MFC) is a bioelectrochemical system that can transform chemical energy into electrical energy, contributing to the reduction of pollution caused by harmful chemical compounds. This method emerged as a promising technology to address energy and environmental challenges by generating renewable energy [2].

Ensifer meliloti is a nitrogen-fixing bacterium that forms a symbiotic relationship with plants. The process begins when plant releases betaines and flavonoids that attract *E. meliloti* to root hairs. The bacteria then penetrate the root, forming nodules where they can develop into bacteroids, only then nitrogen fixation occur. Leghemoglobin, produced by the plant, regulates oxygen levels to maintain nitrogenase activity. These natural mechanisms could be adapted for microbial fuel cell [1]. MFCs utilize microbial catalysis to facilitate electron transfer, enhancing their efficiency in energy production. The use of redox mediators, such as quinones, is particularly significant, as they help improve electron flow between microbes and electrodes, advancing MFC performance. This mechanism makes MFCs a viable solution for clean energy generation while simultaneously addressing environmental concerns and reducing of pollutants [3].

This research aims to investigate the electrochemical behavior of *Ensifer meliloti* in microbial fuel cell while determining the efficiency of electron transfer and assessing its interaction with redox mediators, including various quinones and a $K_3[Fe(CN)_6]$ solution.

[1] S. Bendinskaite, I. Bruzaite, J. Rožėnė, T. Mockaitis, I. Morkvenaite-Vilkonciene, A. Ramanaviciene, A. Zinovicius, & A. Ramanavicius. Microbial Fuel Cell Based on Ensifer meliloti. Journal of the Electrochemical Society, 171(10), (2024). https://doi.org/10.1149/1945-7111/ad8037.

[2] V. Reinikovaite, S. Zukauskas, R. Zalneravicius, V. Ratautaite, S. Ramanavicius, V. Bucinskas, M. Vilkiene, A. Ramanavicius, U. Samukaite Bubniene. Assessment of Rhizobium anhuiense Bacteria as a Potential Biocatalyst for Microbial Biofuel Cell Design. Biosensors, 13(1), (2023) https://doi.org/10.3390/bios13010066.

[3] S. Ramanavicius, A. Ramanavicius, Charge Transfer and Biocompatibility Aspects in Conducting Polymer-Based Enzymatic Biosensors and Biofuel Cells. Nanomaterials, 11(2), (2021) https://doi.org/10.3390/nano11020371.

ISOLATION AND PURIFICATION OF ASCORBATE OXIDASE FROM THE APPLE.

Patrycija Kostiukevič[1], Jolanta Sereikaitė[1]

[1]Faculty of chemistry and bioengineering, Vilnius Tech, Vilnius, Lithuania
patrycija.kostiukevic@stud.vilniustech.lt

Effective waste management and reuse are key challenges in achieving sustainable development and implementing zero waste policies. Approximately 44% of all waste consists of food and other biomass waste, a significant portion of which is generated by the fruit and vegetable processing industry. Juice production alone creates about 4–5 million tons of apple pomace annually, and its effective utilization is still underdeveloped [1]. In line with circular economy principles, this pomace should be reused, particularly for extracting biologically active compounds that could be applied in the food industry or biotechnology fields.

The aim of this study was to purify ascorbate oxidase from apple pomace and evaluate its potential for use. This enzyme is significant for the food industry and biotechnology, particularly in the development of biosensors [2]. To confirm the presence of ascorbate oxidase in apples, its activity was investigated in both fresh juices and pomace. ”Golden Delicious” variety apple pomace and juice were processed with two different buffer solutions: 25 mM phosphate buffer (pH 7) and 25 mM acetate buffer (pH 4). Ascorbate oxidase activity was measured using two substrates—L-ascorbic acid and catechol—in different pH buffers solutions. The enzyme was precipitated with ammonium sulfate at 60% saturation, and further purification was performed using chromatographic methods. The purity of the sample was analyzed by protein electrophoresis method.

[1] Golebiewska E., Kalinowska M., Yildiz G. Sustainable use of apple pomace (AP) in different industrial sectors. Materials, 2022, 15, 1788.
[2] Wang X., Dong S., Wei H. Recent Advances on Nanozyme-based Electrochemical Biosensors. Electroanalysis, 2023, 35, e202100684.

STUDY OF XYLOSE TRANSPORT IN MODIFIED OGATAEA POLYMORPHA YEAST DURING ALCOHOLIC FERMENTATION

Tomas Stanevičius[1], Tomas Nenartavičius[1], Andryi Sibirny[3], Rimantas Daugelavičius[1,2]

[1]Department of Biochemistry, Vytautas Magnus University, Kaunas, Lithuania
[2]Research Institute of Natural and Technological Sciences, Vytautas Magnus University, Kaunas, Lithuania
[3]Department of Molecular Genetics and Biotechnology, Institute of Cell Biology, NAS of Ukraine, Lviv, Ukraine
tomas.stanevicius1@vdu.lt

The growing concerns about the depletion of fossil fuels and their environmental impact are the driving forces to find alternative energy sources. Bioethanol produced from renewable materials offers a promising alternative fuel, as its combustion releases fewer nitrogen oxides and solid particles into the environment. In particular, second-generation bioethanol, made from lignocellulosic biomass, derived from agricultural and forestry waste, makes it a more sustainable option since it utilizes non-food raw materials [1].

Xylose, the second most abundant monosaccharide after glucose and the most prevalent pentose sugar, is a key component of hemicelluloses. More than half of the world's agricultural plant biomass consists of lignocellulosic crop residues [2]. By utilizing xylose, the bioethanol yield from raw materials can be increased, and maximizing xylose uptake by yeast cells is crucial for improving its use in lignocellulosic bioethanol production.

This *Ogataea polymorpha*, a thermotolerant methylotrophic yeast, is capable of fermenting xylose at elevated temperatures. However, transporting xylose into yeast cells in the presence of both glucose and xylose remains a challenge for efficient lignocellulosic ethanol production. In xylose-utilizing wild-type yeast cultures, xylose consumption begins only after glucose is depleted, leading to longer fermentation periods and incomplete sugar conversion from lignocellulose hydrolysates [3]. This issue arises because transporters responsible for xylose uptake have a stronger affinity for glucose than for xylose. Moreover, some potential xylose transporters are removed from the yeast plasma membrane when glucose levels are low, making it essential to modify these transporters to enhance their stability [4]. For this reason, transporters found in *Saccharomyces cerevisiae* Gal2 and Hxt7 or *O. polymorpha* Hxt1 are seen as potential xylose carriers, and mutagenesis could improve xylose uptake and its utilization in alcoholic fermentation. This research project aims to investigate the importance of the *O. polymorpha* Hxt1 transporter and heterologous modifications of the *S. cerevisiae* Gal2 or Hxt7 transporters in *O. polymorpha* yeast, particularly for high-temperature alcoholic fermentation. Registration of the activity of energy metabolism (respiration, glycolysis, ATP synthesis) allows to determine the rate of glucose and xylose uptake into the cells.

In our experiments, respiration and glycolysis of *O. polymorpha* cells were evaluated in different environmental conditions, such as reduced or increased sugar concentrations, different temperatures, in salt buffers and/or the growth media. Results of the experiments showed that a high concentration of one sugar (glucose or xylose) inhibited the entry of the other sugar into *O. polymorpha* cells.

[1] Li, B., Xie, C.-Y., Yang, B.-X., Gou, M., Xia, Z.-Y., Sun, Z.-Y., & Tang, Y.-Q. (2020). The response mechanisms of industrial Saccharomyces cerevisiae to acetic acid and formic acid during mixed glucose and xylose fermentation. Process Biochemistry, 91, 319-329. https://doi.org/https://doi.org/10.1016/j.procbio.2020.01.002

[2] Sibirny, A. A. (2023). Metabolic engineering of non-conventional yeasts for construction of the advanced producers of biofuels and high-value chemicals. BBA Advanc3es, 3, 100071. https://doi.org/https://doi.org/10.1016/j.bbadva.2022.100071

[3] Vasylyshyn, R., Kurylenko, O., Ruchala, J., Shevchuk, N., Kuliesiene, N., Khroustalyova, G., . . . Sibirny, A. (2020). Engineering of sugar transporters for improvement of xylose utilization during high-temperature alcoholic fermentation in Ogataea polymorpha yeast. Microbial Cell Factories, 19(1), 96. https://doi.org/10.1186/s12934-020-01354-9

[4] Sharma, N. K., Behera, S., Arora, R., Kumar, S., & Sani, R. K. (2018). Xylose transport in yeast for lignocellulosic ethanol production: Current status. Journal of Bioscience and Bioengineering, 125(3), 259-267. https://doi.org/https://doi.org/10.1016/j.jbiosc.2017.10.006

THE POTENTIAL OF WASTE VEGETABLE OIL IN GHANA FOR BIODIESEL PRODUCTION

Felix Nkansah Buabeng[1]

[1]KWAME NKRUMAH UNIVERSITY OF SCIENCE AND TECHNOLOGY
felixnkansahb@gmail.com

The gradual depletion of world petroleum reserves and the impact of environmental pollution of increasing exhaust emissions have stimulated the search for alternative sources for petroleum-based fuel, including diesel fuels. Biodiesel, an alternative diesel fuel, is made from renewable biological sources such as vegetable oils and animal fats. The production of biodiesel from waste vegetable oil offers a triple-facet solution: economic, environmental and waste management.

The objective of this project was to determine the various properties of biodiesel produced from waste vegetable oils of different stocks in Ghana and the effects of blending on these properties. Five waste vegetable oil samples from five major cities in Ghana and of different stocks were processed into biodiesel and were later blended with fossil diesel. The samples were the 'Ghana sample', 'Accra sample', 'filtered sample', 'coconut oil' and 'palm kernel oil'.

Tests were carried out on the various physicochemical properties of the raw biodiesels and its blends and the data obtained were analyzed and compared to fossil diesel. The minimum and maximum cetane numbers recorded by the biodiesel blends were 45.95 and 50.44 respectively, which was within ASTM's required standard. The B100 biodiesels also recorded low sulphur contents which were 0.0040%wt, 0.0054%wt, 0.0059%wt, 0.0071%wt and 0.0082%wt for Accra sample, filtered sample, Ghana sample, palm kernel oil and coconut oil respectively. The biodiesel blends again obtained colours of 1.0 which is seen by ASTM as the best.

From the results it was clear that, the measured properties of produced raw biodiesel fuels were within ASTM recommended standards and the physicochemical properties also improved when blending was done with regards to fossil diesel.

PHYSICOCHEMICAL PROPERTIES OF NISIN AND K2 TOXIN-LOADED FUCOIDAN PARTICLES

Aistė Galinskaitė[1], Rūta Gruškienė[1], Tatjana Kavleiskaja[2], Jolanta Sereikaitė[1]

[1]Department of Chemistry and Bioengineering, Vilnius Gediminas Technical University, Vilnius, Lithuania
[2]Department of Polymer Chemistry, Vilnius University, Vilnius, Lithuania
aiste.galinskaite@vilniustech.lt

Nisin is a cationic antimicrobial peptide, that has activity against gram-positive bacteria [1]. K2 toxin is an antimicrobial protein produced by Saccharomyces cerevisiae that is active against other yeasts [2]. Both of these compounds are of protein origin. This means that their activity could be reduced by environmental stresses, proteolysis, and undesirable interactions with food components [1]. Encapsulation is often used to overcome this problem. It also provides controlled release which is important to ensure food safety and to extend the shelf life [1]. In this study, fucoidan was used for the encapsulation of the components.

Fucoidan is an anionic, sulfated polysaccharide that is produced by brown seaweeds. It also has excellent anti-inflammatory, anticoagulant, antithrombotic, antitumor, and antioxidant activities, which could also provide additional beneficial properties for food products [3].

This study researched physicochemical properties of K2 toxin-fucoidan and K2 toxin-nisin-fucoidan particles. Particles were synthesized using two fucoidan concentrations (0.1 and 0.4 mg/mL), two pH values (pH 4.0 and 5.0). K2 toxin was purified by ion exchange chromatography and the concentration in the particles was 3.6 µg/mL and the nisin concentration was 0.1 mg/mL. Control fucoidan samples without K2 toxin and nisin were also prepared. The size and zeta potential of the particles were measured at the initial moment and after 4 weeks of storage at 4 ^{0}C using Zetasizer NanoZS device.

When a lower concentration of fucoidan was used, the particles were much larger than those obtained using higher concentration of fucoidan. This difference is clear when comparing K2 toxin-nisin-fucoidan and nisin-fucoidan particles. The size of these particles is also pH dependent. When a lower concentration of fucoidan was used, smaller particles were formed, when the pH of the sample was 4.0. K2 toxin-fucoidan particles were the smallest and their size was close to 200 nm at pH 5.0 and from 100 to 300 nm at pH 4.0. When a higher concentration of fucoidan was used, the size of all the particles was always similar. The results show that control fucoidan and the particle samples differ in size. This confirms, that the components interact and particles are truly formed. When comparing particle size at the initial moment and after 4 weeks, it can be seen that there is not much of a difference. This means, that the particles are stable and do not change significantly after 4 weeks of storage.

The zeta potential of the samples was also measured. The results show that there is not much of a difference depending on fucoidan concentration and pH. The particles had a zeta potential between -18 and -35 mV. K2 toxin-nisin-fucoidan particles may be more stable compared to K2 toxin-fucoidan particles. The results show, that the zeta potential of the particles does not change significantly after 4 weeks. This could also mean that the particles remain stable during this time.

[1] A. Bahrami, R. Delshadi, S. M. Jafari et al., Nanoencapsulated nisin: An engineered natural antimicrobial system for the food industry, Trends in Food Science & Technology 94, 20-31 (2019).
[2] Lukša, J., Serva, S., & Serviene, E. (2016). Saccharomyces cerevisiae K2 toxin requires acidic environment for unidirectional folding into active state. Mycoscience, 57(1).
[3] J. Venkatesan, S. Anil, S. K. Kim, M. S. Shim. Seaweed polysaccharide-based nanoparticles: Preparation and Applications for Drug Delivery, Polymers 8 (2016).

THE INFLUENCE OF THE MEDIUM PH ON THE EFFICIENCY OF NYSTATIN ON CANDIDA YEAST

Eglė Vansevičiūtė[1], Tomas Stanevičius[1], Rimantas Daugelavičius[1,2]

[1]Department of Biochemistry, Vytautas Magnus University, Kaunas
[2]Research Institute of Natural and Technological Sciences, Vytautas Magnus University, Lithuania
egle.vanseviciute@vdu.lt

Candida albicans and *Candida glabrata* yeast are successful commensals and opportunistic pathogens of humans that cause superficial or disseminated infections in immunocompromised and hospitalized individuals. These yeasts are only sensitive to four classes of antifungals, but the cells can acquire multidrug resistance [1]. Therefore, it is necessary to find ways to strengthen the efficiency of already-known drugs to fight against *Candida* infections.

This study aimed to evaluate the efficiency of nystatin – antifungal polyene drug which creates pores in the cell envelope, increasing the plasma membrane permeability and osmotic disbalance [2] - on *C. albicans* and *C. glabrata* cells in salt buffers and growth media of various acidity. The effects of nystatin on *Candida* yeast were followed using real-time methods, such as registering lipophilic anion binding to the cells, the cell respiration rate, and the cells' ability to keep a K^+ gradient. These methods allowed us to monitor different antifungals' effects in tenths of minutes. This was much faster compared to the traditional assays using agar or immunological plates, which usually require incubation for more than 18 hours. After evaluating the effects of nystatin on the cell suspensions in the growth media - RPMI and YPD - or citrate-phosphate buffer of different pH, it was observed that both *C. albicans* and *C. glabrata* cells bind the highest amount of PCB^- at acidic conditions. A quicker and stronger inhibition of the respiration of *C. albicans* and *C. glabrata* cells by nystatin was also observed when the incubation medium pH was as low as 3. Our findings suggest that the antifungal drug nystatin could be more effective in an acidic environment, but further research is still needed.

[1] Arendrup, M.C. & Patterson, T. F. 2017. Multidrug-Resistant Candida: Epidemiology, Molecular Mechanisms, and Treatment. The Journal of Infectious Diseases. 216(15). S445-S451.

[2] Esfahani, A. N., Golestannejad, Z., Khozeimeh, F., Dehghan, P., Maheronnaghsh, M. & Zarei, Z. (2019). Antifungal effect of Atorvastatin against Candida species in comparison to Fluconazole and Nystatin. Medicine and Pharmacy Reports, 92(4), 368–373

PROTEOLYTIC STABILITY OF NISIN DELIVERY SYSTEMS AGAINST PROTEASE FROM RHIZOPUS CHINENSIS

Agnė Česnulevičiūtė[1], Rūta Gruškienė[1]

[1]Department of Chemistry and Bioengineering, Vilnius Gediminas Technical University, Lithuania
agne.cesnuleviciute@stud.vilniustech.lt

Nisin is an antimicrobial peptide with a molecular weight of 3.5 kDa derived from Lactococcus lactis, and it is a potential natural substitute for traditional antimicrobial additives. Its broad-spectrum activity against Gram-positive bacteria makes this peptide a promising candidate for applications in food preservation, pharmaceuticals, and healthcare [1]. However, due to its protein nature, nisin is sensitive to proteolytic degradation, which creates a barrier to its effective use in various applications. Encapsulation methods can be used to mitigate this problem. Among the eco-friendly materials, biopolymers (mainly polysaccharides) are an excellent choice due to their natural availability from plants and animals or microbes. Negatively charged polysaccharides can interact with positively charged peptides to form nanospheres.

The aim of this study is to prepare nisin-loaded particles and compare their proteolytic stability with free nisin when exposed to protease from Rhizopus chinensis. Members of the genus Rhizopus produce subtilisin-type serine proteases with very high proteolytic activity. These enzymes frequently attack and spoil functional peptides, resulting in a loss of functional stability in food and pharmaceutical systems [2]. On the other hand, bioencapsulation in biopolymer matrices is a way out of this problem, since the primary effect is shielding both physical and electrostatic.

Nisin Z was encapsulated using four different biopolymers: fucoidan, low and high esterified pectins, and pectic acid. The preparation of nisin-loaded particles was based on electrostatic interactions. The final concentration of nisin and the carriers in all particle samples was 0.4 mg/ml, and the pH was 4. The proteolysis was performed at pH 4 for 2 hours at 37 ^{0}C, and the final enzyme concentration was 0.3 mg/ml. Capillary electrophoresis and determination of free amino groups by the TBNS (2,4,6-trinitrobenzenesulfonic acid) assays were used to study proteolysis.

The study showed that nisin in particles is more protected from proteolytic action compared to free nisin. It was also found that fucoidan used for nisin encapsulation provided better protection against protease from Rhizopus chinensis than pectins, regardless of their degree of esterification.

[1] Delves-Broughton, J., & Weber, G. (2011). Nisin, natamycin and other commercial fermentates used in food biopreservation. In Elsevier eBooks (pp. 63–99). https://doi.org/10.1533/9780857090522.1.63

[2] Fukumoto, J., Tsuru, D., & Yamamoto, T. (1967). Studies on mold protease. Agricultural and Biological Chemistry, 31(6), 710–717. https://doi.org/10.1080/00021369.1967.10858863

ENGINEERING YEAST SURFACE DISPLAY SYSTEM FOR EXPRESSION OF ESTERASE FROM GEOBACILLUS STEAROTHERMOPHILUS

Viktorija Kurpickaja[1], Arūnė Verbickaitė[1], Rasa Petraitytė-Burneikienė[1]

[1]Department of Eukaryote Gene Engineering, Institute of Biotechnology, Life Sciences Center, Vilnius University, Lithuania
viktorija.kurpickaja@gmc.stud.vu.lt

Yeast surface display system is a widely used protein engineering technology that enables the anchoring of recombinant proteins to the yeast cell wall. Our technique uses the a-agglutinin system, where the Aga1 and Aga2 subunits form disulfide bridges. By fusing the target protein with the Aga2 subunit, it can be effectively exposed on the yeast surface [1]. This approach has broad applications in biotechnology, including enzyme immobilization, biocatalysis, and industrial processes. It simplifies substrate accessibility and allows continuous enzymatic reactions. Moreover, this system reduces the risk of enzyme contamination in the final product, as the enzymes remain immobilized on yeast cells and are not released into the reaction mixture.

This study aimed to express and display the extremoenzyme esterase from *Geobacillus stearothermophilus* [2] on the surface of *Saccharomyces cerevisiae* using five distinct yeast expression vectors. Previously developed with different linker peptides between Aga2 and the target protein [3], these vectors were designed to optimize protein synthesis and enzymatic activity. Previous studies have demonstrated that lipase from mesophilic bacteria was successfully displayed on the yeast surface and had enzymatic activity [4]. These findings suggest that the yeast surface display system could be an effective platform for esterase displaying as well, since lipases and esterases belong to the same enzyme class. The constructed plasmids will be tested in further research to evaluate their enzyme display and activity efficiency. This study contributes to expanding the application of yeast display in biocatalysis and industrial enzyme production.

[1] Piraine, R. E. A., Gonçalves, V. S., dos Santos Junior, A. G., Cunha, R. C., de Albuquerque, P. M. M., Conrad, N. L., & Leite, F. P. L. (2021). Expression cassette and plasmid construction for Yeast Surface Display in Saccharomyces cerevisiae. Biotechnology Letters, 43(8), 1649–1657.

[2] Gudiukaite, R., Sadauskas, M., Gegeckas, A., Malunavicius, V., & Citavicius, D. (2017). Construction of a novel lipolytic fusion biocatalyst GDEst-lip for industrial application. Journal of Industrial Microbiology and Biotechnology, 44(6), 799–815.

[3] Šapronytė I. (2024). Acinetobacter baumannii Blp1 baltymo C-galinio fragmento eksponavimo mielių Saccharomyces cerevisiae ląstelių paviršiuje tyrimai. Vilnius University.

[4] Verbickaitė A., Krutkevičius J., Matijošytė I., Petraitytė-Burneikienė R. (2024). Surface display of lipase from Serratia sp. on yeast Saccharomyces cerevisiae. Vilnius University

SYNTHESIS OF HYDRAZONES FROM 3-(4-ETHOXYPHENYL)AMINOPROPANEHYDRAZIDE AND EVALUATION OF THEIR BIOLOGICAL ACTIVITY IN SILICO

Juozas Kiltinavičius[1], Aida Šermukšnytė[1], Kristina Kantminienė[2], Ilona Jonuškienė[1], Ingrida Tumosienė[1]

[1]Department of Organic Chemistry, Kaunas University of Technology, Lithuania
[2]Department of Physical and Inorganic Chemistry, Kaunas University of Technology, Lithuania
juozas.kiltinavicius@ktu.edu

Antimicrobial resistance (AMR) has become one of the main challenges of the 21st century public health systems that threatens effective prevention and treatment of infectious diseases. The rise of AMR has led to an increasing number of infections caused by bacteria, parasites, viruses, and fungi that are no longer susceptible to conventional antimicrobial drugs. This growing resistance causes threat to the efficacy of treatments for common and life-threatening infections, complicating clinical management and leading to higher mortality rates. Since the pace of discovering novel drugs has drastically slowed in recent decades, insufficient development and availability of new antimicrobial agents for the treatment of life-threatening infections caused by resistant pathogens is behind the growing demand, making the synthesis of such compounds and analysis of their properties one of the most important research areas in medicinal chemistry [1].

Hydrazones are important intermediate compounds in the synthesis of pharmacological substances, especially in the development of prodrugs, which is an important aspect of the pharmaceutical industry, as it provides the opportunity to improve the efficacy of drugs, reduce side effects and/or improve their bioavailability [2]. Therefore, this work has aimed to contribute to the solution of the antimicrobial resistance problem.

Novel hydrazones bearing various heterocyclic moieties were synthesized from 3-[(4-ethoxyphenyl)amino]propanehydrazide. The primary screening of the biological activity of the target compounds was performed in silico by analyzing their predicted properties according to ADMET. All synthesized hydrazones are characterized by good absorption, and a significant part of the compounds should cross the blood-brain barrier. A difference in pharmacological properties has been observed as the carbon chain of the radicals lengthened. The predicted toxicity of these compounds is low and acceptable compared to pharmaceutical requirements and existing commercial drugs, making them good candidates for the development of new antimicrobial agents. Further studies will be carried out in vitro by specific conventional methods.

[1] M.A. Salam, et al. Antimicrobial Resistance: A Growing Serious Threat for Global Public Health. Healthcare 11, 1946 (2023).
[2] I. Tumosienė, et al. Antioxidant and Anticancer Activity of Novel Derivatives of 3-[(4-Methoxyphenyl)amino]propanehydrazide. Molecules 25, 2980 (2020).

CYTOTOXICITY OF ANTIBACTERIAL TUNGSTEN TRIOXIDE NANOPARTICLE-COATED TEXTILES ON HUMAN UMBILICAL VEIN ENDOTHELIAL CELLS (HUVEC) IN VITRO

Laura Kairytė[1,2], Raminta Rodaitė[1], Agnė Giedraitienė[3], Modestas Ružauskas[3], Rita Šiugždinienė[3], Šarūnas Varnagiris[1], Darius Milčius[1]

[1]Lithuanian Energy Institute, Breslaujos str. 3, 44403 Kaunas, Lithuania
[2]Vytautas Magnus University, Universiteto str. 10, 53361 Akademija, Lithuania
[3]Lithuanian University of Health Sciences, Mickeviciaus str. 9, 44307 Kaunas, Lithuania
laura.kairyte@vdu.lt

Nanotextiles could be an innovative way to stop the spread of antibiotic-resistant pathogenic microorganisms [1]. Since it is known that nonorganic nanoparticles can enter the human body through the respiratory and digestive systems, as well as via skin contact [2], studying their toxicity is essential.

This study aims to assess the potential cytotoxicity of an antibacterial nanotextile, created by depositing WO_3 nanoparticles onto a textile surface through low-temperature glow discharge plasma sputtering in a pure oxygen atmosphere. The properties of the deposited thin films were evaluated using Scanning Electron Microscopy (SEM), and X-ray Photoelectron Spectroscopy (XPS). Using human endothelial HUVEC cells, the cytotoxic characteristics of the textile modified with WO3 nanoparticles were evaluated *in vitro* by MTT assay and by assessing cell viability with the live-cell fluorescent dye calcein-AM. No indication of either short-term (24-hour exposure) or long-term (72-hour exposure) toxicity was observed in textiles treated with WO3 nanoparticles, as cell viability remained above 70 %.

This study highlights the potential of WO_3 nanoparticle-modified textiles as a biocompatible alternative to conventional antimicrobial treatments, offering a promising global solution for combating microbial infections.

[1] Vakayil, R. et al. Process Biochem., vol. 111, pp. 1–8, (2021).
[2] He, M. et al. Toxics, vol. 10, no. 3, p. 144 (2022).

INVESTIGATION OF INFLAMMATORY RESPONSE PATHWAY - INFLAMMASOME ACTIVATION

Viltė Mataraitė[1], Milda Norkienė[1], Asta Lučiūnaitė[1]

[1]Institute of Biotechnology, Life Sciences Center, Vilnius University
vilte.mataraite@gmail.com

The innate immune response is the first mechanism for host defense and is intended to prevent infection and remove the invading pathogens. Activation of the inflammasome is one of the inflammation-related pathways mediated by the innate immune system. Inflammasomes are responsible for producing inflammatory molecules and causing inflammatory cell death - pyroptosis [1]. There are a few inflammasome types, but they all have a common adapter protein – apoptosis-associated speck-like protein containing a CARD, ASC [2]. ASC is necessary for the inflammasome complex assembly and activation. During inflammasome activation, ASCs oligomerize to about 1 μM size particles called ASC specks, which are released to extracellular space and can further trigger inflammation [3]. Inflammasomes are linked to a variety of autoimmune and neurodegenerative diseases [4]. Thus, ASC proteins can be used as targets to inhibit the inflammatory response. This research aimed to investigate how ASC specks affect macrophage activation by viral antigens.

We prepared ASC speck fractions using the THP1-ASC-GFP cell line. We settled on an optimal technique to gather ASC specks using various cell lysis methods and centrifugation steps. THP-1 macrophage-like cells were treated with ASC specks and viral antigens – human KI polyomavirus virus-like particles (KIPyV VLPs). We assessed cell viability and inflammatory response via cytokine secretion to analyze the effect of ASC specks and KIPyV VLPs on macrophages. Cell viability was evaluated by lactate dehydrogenase (LDH) assay. Enzyme-linked immunosorbent assay (ELISA) was applied to measure the release of cytokines, including IL-8, IL-1β and CCL2.

Our results demonstrated that ASC specks and a mixture of ASC specks with KIPyV VLPs significantly increased LDH release in macrophages. We also observed the tendency - the higher the concentration of ASC specks used for macrophage activation, the higher the LDH concentration in the cell medium. Macrophages treated with KIPyV VLPs released a higher LDH concentration than the control group, but it was insignificant. We also found that KIPyV VLPs induced a higher IL-8 and CCL2 secretion in macrophages than ASC specks. However, macrophages treated with ASC specks released more IL-1β than viral antigen-activated cells. Interestingly, ASC specks significantly reduced the KIPyV VLPs-induced effect on macrophages regarding CCL2 secretion. A mixture of ASC specks and KIPyV VLPs induced different secretion of CCL2 and IL-1β than KIPyV VLPs alone. However, the opposite effect was observed in the case of IL-8 secretion - ASC specks alone had less impact on IL-8 secretion than the mixture of KIPyV VLPs and ASC specks.

Our results suggest that ASC specks induce inflammasome assembly and promote pyroptosis in macrophages. The specks also modulate KIPyV VLP-induced release of pro-inflammatory cytokines. In conclusion, ASC specks can affect viral antigen-mediated inflammatory response in macrophages.

[1] Y. Tan et al., “Pyroptosis: a new paradigm of cell death for fighting against cancer,” Journal of Experimental & Clinical Cancer Research, vol. 40, no. 1, May 2021, doi: https://doi.org/10.1186/s13046-021-01959-x.

[2] Y. Yang, H. Wang, M. Kouadir, H. Song, and F. Shi, “Recent advances in the mechanisms of NLRP3 inflammasome activation and its inhibitors,” Cell Death & Disease, vol. 10, no. 2, Feb. 2019, doi: https://doi.org/10.1038/s41419-019-1413-8.

[3] J. G. Souza, N. Starobinas, and O. C. M. Ibañez, “Unknown/enigmatic functions of extracellular ASC,” Immunology, vol. 163, no. 4, pp. 377–388, Jun. 2021, doi: https://doi.org/10.1111/imm.13375.

[4] Y.-Q. Chen et al., “CRID3, a Blocker of Apoptosis Associated Speck Like Protein Containing a Card, Ameliorates Murine Spinal Cord Injury by Improving Local Immune Microenvironment,” SSRN Electronic Journal, Jan. 2020, doi: https://doi.org/10.2139/ssrn.3569817.

EVALUATION OF PHYTOCHEMICALS AND BIOACTIVITY IN BROCCOLI (BRASSICA OLERACEA VAR. ITALICA) CALLUS CULTURES IN VITRO

Paulina Lukošiūtė[1]

[1]Department of Chemical Technology, Kaunas University of Technology, Lithuania
paulina.lukosiute@ktu.edu

Broccoli (Brassica oleracea var. italica) is an annually cultivated plant from the Brassicaceae family, closely related to Brussels sprouts, cabbage, cauliflower, and kale. It is well known for its rich nutritional profile, providing essential nutrients such as minerals, vitamins, dietary fiber, and phytochemicals such as glucosinolates and phenolic compounds. In recent years, its bioactive components, particularly glucosinolates and their metabolites, have gained increasing interest. Numerous studies have highlighted the health benefits of broccoli and its derivatives, including antioxidant, anti-inflammatory, anti-cancer, antimicrobial, metabolic-regulating, and neuroprotective properties. As a result, broccoli is regarded as a functional food with significant health potential. The global nutraceutical market is expanding, particularly in emerging economies, creating a promising opportunity to develop broccoli into value-added products. Understanding the nutritional benefits and health effects of different parts of broccoli provides a foundation for further research and utilization [1].

The aim of the study: to explore the potential of broccoli (Brassica oleracea var. italica) callus cultures as an alternative source of bioactive phytochemicals under in vitro conditions. The main objectives are to assess the efficiency of callus induction, analyze its phytochemical composition, and evaluate the bioactivity (antioxidant and antibacterial properties) of callus-derived extracts in comparison to a nutrient medium without growth regulators.

Material and methods of research. Broccoli explants (leaves, stems and roots) were cultured on Murashige and Skoog (MS) medium supplemented with cytokinin 6-benzylaminopurine (BAP) and auxin 2,4-dichlorophenoxyacetic acid (2,4-D). Additionally, the amino acids L-methionine and L-tryptophan were added. Antioxidant assays using 2,2-diphenyl-1-picrylhydrazyl (DPPH) radical scavening, ferric ion reducing antioxidant power (FRAP), and ABTS were performed. The concentrations of antioxidant phytochemicals, i.e. carotenoids, total phenolics, phenolic acids were determined, the activity of antioxidant enzymes of the superoxide dismutase (SOD) were evaluated.

Results. Results indicates antioxidative activity according DPPH, FRAP assays was in callus culture of Brassica oleracea var. italica induced on Murashige and Skoog (MS) medium containing cytokinin 6-benzylaminopurine and auxin 2,4-dichlorophenoxyacetic acid and supplemented with L-tryptophan and L-methionine. The results highlight the potential of broccoli callus cultures to produce valuable phytochemicals with promising bioactivities. Future studies will focus on optimizing culture conditions to enhance metabolite accumulation.

Conclusions. Phytochemical tests have confirmed the presence of bioactive secondary metabolites in callus cultures of broccoli. These cultures have the potential to produce valuable phytochemicals with promising bioactivities.

[1] Hang Li, Yu Xia, Hong-Yan Liu, Huan Guo, Xiao-Qin He, Yi Liu, Ding-Tao Wu, Ying-Hui Mai, Hua-Bin Li, Liang Zou, Ren-You Gan. Nutritional values, beneficial effects, and food applications of broccoli (Brassica oleracea var. italica Plenck). Trends in Food Science & Technology. 2022, Vol. 119, 288–308. doi.org/10.1016/j.tifs.2021.12.015

Poster Session 4

Chemistry and Chemical Physics

EXPLORING THE SYNTHESIS OF NOVEL BENZIMIDAZOTHIAZINES AS POTENTIAL AMYLOID AGGREGATION MODULATORS

Urtė Milerytė[1], Rita Bukšnaitienė[1], Ieva Žutautė[1]

[1] Institute of Chemistry, Faculty of Chemistry and Geosciences, Vilnius University, Naugarduko str. 24, Vilnius, Lithuania
urte.mileryte@chgf.vu.lt

Amyloids are protein aggregates with an insoluble, fibrillar structure formed by improper β-sheet folding. These aggregates can accumulate in various organs, leading to amyloidosis, which includes Alzheimer's disease, Parkinson's disease, and type II diabetes mellitus. Recent studies highlight liquid–liquid phase separation (LLPS) as a key step in amyloid formation. While LLPS plays a crucial role in cellular organization, its dysregulation can contribute to neurodegenerative and oncological diseases. Increased protein concentration during LLPS may trigger changes that promote fibril formation. Researchers are exploring small-molecule compounds such as bis-ANS, ATP, polyphosphates, RNA, heparin, and specific chaperones to regulate this process, although their mechanisms remain partially understood [1].

Recent studies indicate that the imidazo[2,1-*b*][1,3]thiazine scaffold represents a promising pharmacophore for inhibiting amyloid protein aggregation. Its capacity to interact with biological macromolecules suggests that imidazo[2,1-*b*][1,3]thiazine-based derivatives are potential candidates for modulating phase separation processes implicated in neurodegenerative diseases [2].

This study aims to synthesize various benzimidazo[2,1-*b*][1,3]thiazines with potential amyloid aggregation inhibitory properties. The newly developed compounds feature a substituent at the C_2 position adjacent to the double bond, representing a novel structural modification. Given the novelty of these compounds, it is crucial to first establish the most efficient synthetic pathway.

The synthesis of the starting compound, 1-(3-phenylprop-2-yn-1-yl)-1,3-dihydro-2*H*-benzo[*d*]imidazole-2-thione, was achieved via the alkylation of 1,2-diaminobenzene with (3-bromoprop-1-yn-1-yl)benzene, followed by the condensation of the resulting intermediate with thiocarbonyldiimidazole. Optimization of the cyclization reaction conditions is currently underway to enhance reaction selectivity by employing various coinage catalysts.

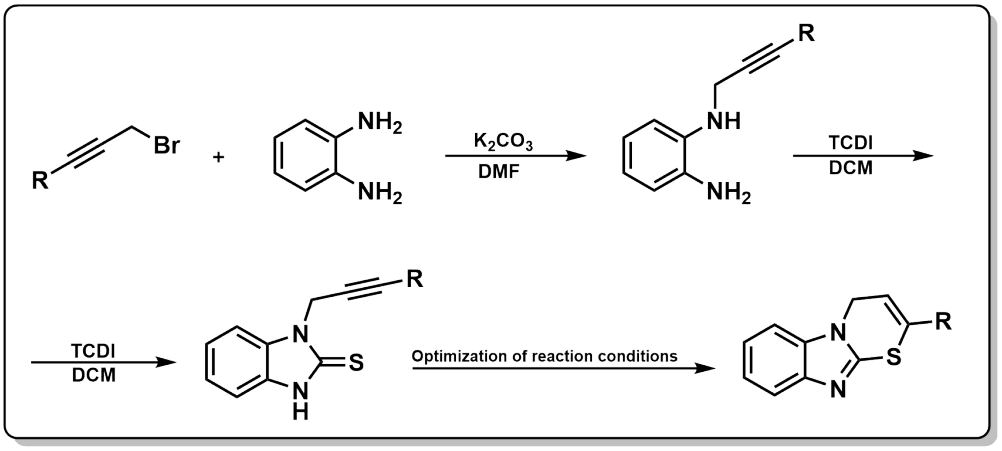


Fig. 1. General scheme of reactions

[1] M. Ziaunys et al., "Liquid–liquid phase separation of alpha-synuclein increases the structural variability of fibrils formed during amyloid aggregation," FEBS J., vol. 291, no. 20, pp. 4522–4538, Oct. 2024, doi: 10.1111/febs.17244.

[2] I. Misiūnaitė et al., "Imidazo[2,1- b][1,3]thiazine Derivatives as Potential Modulators of Alpha-Synuclein Amyloid Aggregation," ACS Chem. Neurosci., vol. 15, no. 24, pp. 4418–4430, Dec. 2024, doi: 10.1021/acschemneuro.4c00451.

SYNTHESIS AND BIOLOGICAL EVALUATION OF NOVEL SULFANILAMIDE DERIVATIVES

Valdas Vainauskas[1], Vytautas Mickevičius[1], Birutė Grybaitė[1]

[1]Kaunas University of Technology, Department of Organic Chemistry
valdas.vainauskas@ktu.edu

Benzenesulfonamides are widely explored due to their wide range of potential pharmaceutical uses as anticancer, antibacterial and antifungal drugs [1]. As well as alkylated imidazoles which bear anticancer activity and ketoximes which garnered attention for their potent antibacterial properties [2, 3].

In this present study, α-aminoketone **2** was obtained by reacting the primary amine **1** with bromoacetophenone in H_2O and 1,4-dioxane mixture. 3,5-dichloro-4-((2-oxo-2-phenylethyl)amino)benzenesulfonamide (**3**) was synthesized by chlorination of compound **2** with HCl in a presence of hydrogen peroxyde. Ketoximes **4** and **5** were synthesized by treating α-aminoketones **2**,**3** with hydroxylamine hydrochloride in methanol using sodium acetate as base. Oxoimidazole **6** was yielded by treating α-aminoketone **2** with sodium cyanate in glacial acetic acid, and mercaptoimidazole **8** - by treating α-aminoketone **2** with potassium thiocyanate in hydrochloric acid. The alkylation reactions of the synthesized imidazole derivatives **6** and **8** with ethyl iodide were investigated and it was found that by varying the reaction conditions, *N*-, *S*- and *N*,*S*-alkyl derivatives **7**,**9**-**11** could be synthesized. Molecular structures were confirmed via FT-IR, NMR spectra and elemental analysis.

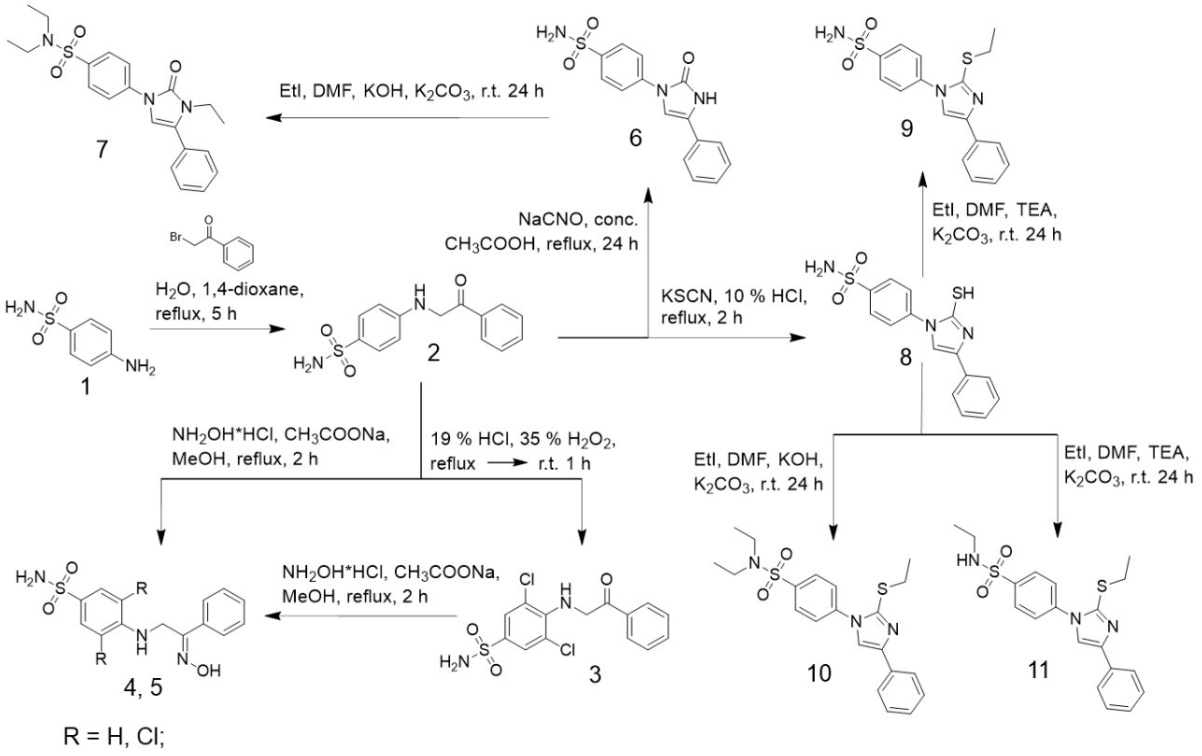


Fig. 1. Synthesis of compounds **2**-**11**

Synthesized compounds were evaluated against H69 human lung carcinoma cells and *C. albicans*, *C. auris* cultures bearing promising results.

[1] M. T. M. Nemr, A. M. AboulMagd, H. M. Hassan, A. A. Hamed, M. I. A. Hamed, and M. T. Elsaadi, "Design, synthesis and mechanistic study of new benzenesulfonamide derivatives as anticancer and antimicrobial agents via carbonic anhydrase IX inhibition," RSC Advances, vol. 11, no. 42. Royal Society of Chemistry (RSC), pp. 26241–26257, 2021.

[2] B. Balandis, V. Mickevičius, and V. Petrikaitė, "Exploration of Benzenesulfonamide-Bearing Imidazole Derivatives Activity in Triple-Negative Breast Cancer and Melanoma 2D and 3D Cell Cultures," Pharmaceuticals, vol. 14, no. 11. MDPI AG, p. 1158, Nov. 13, 2021.

[3] P. Gayathri et al., "Bio-potent aryl ketoximes," Ovidius University Annals of Chemistry, vol. 35, no. 2. Walter de Gruyter GmbH, pp. 146–153, Jul. 01, 2024.

SYNTHESIS AND BIOLOGICAL ACTIVITY OF 2-SUBSTITUTED-N-HETEROARYLACETAMIDES

Gabrielė Juraitytė[1], Austėja Šakalytė[2], Algirdas Šačkus[1], Ingrida Šatkauskienė[2], Vida Malinauskienė[1]

[1]Kaunas University of Technology, Kaunas, Lithuania
[2]Vytautas Magnus University, Kaunas, Lithuania
gabriele.juraityte@ktu.edu

Artificial intelligence systems are progressively utilized to forecast the structure of prospective pharmaceutical active compounds, yet their effectiveness is still doubtful. The classical way of generating new potentially biologically active substances by merging various fragments that have previously demonstrated comparable activity continues to be significant. After initial evaluations of such compounds, additional adjustments can be done based on the outcomes of biological testing.

Different 2-arylacetamides [1] and pyridine compounds [2] have been identified to possess antibacterial properties. The amide bond serves as a crucial component in the structure of antibacterial active compounds. Recent studies have shown that N-heteroarylphenylacetamides were also reported as trypanosomacides [3].

The aim of this research was to synthesize new 2-aryl-N-(heteroaryl)acetamides and assess their biological activity.

To fulfill this objective, aminopyridine acylation different reaction conditions were experimentally tested. The chosen conditions for this acylation reaction were applied for the preparation a set of 2-(chlorophenyl)-N-(heteroaryl)acetamides. The structures of these synthesized products were verified using mass spectrometry, nuclear magnetic resonance, and infrared spectroscopy techniques.

Evaluation of 2-(chlorophenyl)-N-(pyridine)acetamides antibacterial properties was carried out against the E.Coli dh5α bacterial line aiming to define possible direction of compound library expansion. Additionally primary antiprotozoal activity testing was carried out.

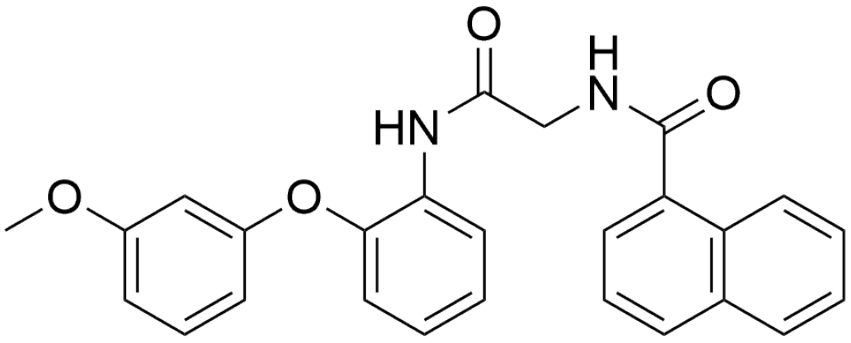
[1] Kumari, S. et al. J. Med. Chem. 2020, 63, p. 12290.
[2] Aatif, M. et al. Antibiotics. 2022, 11, p. 1750
[3] Rezende Júnior, C. O. et al. Eur. J. Med. Chem. 2023, 246, p. 114925.

SYNTHESIS OF POTENTIAL PROLIFERATING CELL NUCLEAR ANTIGEN INHIBITORS

Simona Jonušienė[1], Mantas Jonušis[2], Denis Sokol[1]

[1]Institute of Chemistry, Faculty of Chemistry and Geosciences, Vilnius University
[2]Laboratory of Bioorganic Compounds, Institute of Biochemistry, Vilnius University Life Sciences Centre
simona.jonusiene@gmc.vu.lt

According to WHO (World Health Organization) various types of cancer is the second leading cause of death globally. Despite the fact that cancer has no universal cure, it has many targets for possible treatment. In 2023 City of Hope National Medical Center published preclinical research on a targeted chemotherapy using novel small molecule - AOH1996 that appears to suppress tumor growth without causing adverse effects. Our group of scientists developed new synthesis pathway for obtaining N-(2-((2-(3-methoxyphenoxy)phenyl)amino)-2-oxoethyl)-1-naphthamide (AOH-1996)[1] in sub kilogram quantities. New method is superior to previously published in scientific literature because of easily accessible materials and classic techniques are used which allows to significantly reduce production cost while maintaining product quality. In addition, our method does not use chromatographic purification, which further reduces production costs. Synthesis starts from mono methylation of resorcinol with dimethyl sulfate in anisole as a solvent. Obtained 3-methoxyphenol is converted to substituted diphenyl ether by Ullmann reaction with 2-chloronitrobenzene. Nitro derivative is reduced with hydrazine hydrate and Raney nickel as a catalyst. Further, reaction with chloroacetyl chloride and sodium azide followed by reduction with hydrogen gas and palladium on carbon catalyst gives glycine derivative. Finally, reaction with alpha naphthoic acid chloroanhydride gives desired AOH-1996. Moreover, we have synthesized series of compounds similar to AOH-1996 in the expectation that they will also behave as proliferating cell nuclear antigen inhibitors. Synthesized series includes: N substituted glycine derivatives, triazoles formed from intermediate azide and various terminal acetylenes, compounds with other than naphthoyl substituents, attached strained heterocycles such as aziridine and azetidine, nitrogen mustards, etc. To conclude, our group has developed new, efficient and chromatography free synthesis pathway for AOH-1996 and created series of structurally similar compounds for near future studies on cancer cell lines.



AOH-1996

Fig. 1. Chemical structure of AOH-1996

[1] L. Gu, M. Li, C. M. Li, P. Haratipour, R. Lingeman, J. Jossart, M. Gutova, L. Flores, C. Hyde, N. Kenjić, et al., Cell Chem. Biol. 2023, 30, 1235-1247.e6.

5-HETEROARYL-1,3,4-OXADIAZOL-2-THIOLS:SYNTHESIS, ALKYLATION, ACYLATION AND BIOTESTING

Roberta Kuneikytė[1], Ieva Bartkevičiūtė[1], Algirdas Šačkus[1], Vilija Kederienė[1], Vida Malinauskienė[1], Asta Žukauskaitė[2]

[1]Kaunas University of Technology, Kaunas, Lithuania
[2]Palacký University, Olomouc, Czech Republic
roberta.kuneikyte@ktu.edu

The synthesis and study of novel heterocyclic compounds is of ongoing relevance as scientists continuously strive to improve the efficiency and accuracy of drugs. The development of new active substances for drugs is constantly challenged by the need to design a drug that is effective and binds selectively to the drug target. On the other hand, the substance should be as non-toxic as possible to humans and not cause side effects. Although theoretical computational programmes are increasingly being used for this purpose, they are not a sufficient substitute for testing the actual compounds in laboratories. Comparison of the results of theoretically calculated activity with the activity of the compounds actually tested is still very relevant. In this way, knowledge is being built up and algorithms for such calculation programmes are being improved.

It has been observed that derivatives with two or more heterocycles are safer, cause fewer side-effects. The inclusion of target functional groups enables the development of specificity. The aim of this project was to obtain 1,3,4-oxadiazole analogues capable of acting on the enzyme succinate dehydrogenase (SDH). Mutations in succinate dehydrogenase are believed to be responsible for the progression of some cancers, as excessive amounts of succinate accumulate in the cytosol and intracellular fluid of cells leading to tumour formation.

In collaboration with researchers at Palacký University, an initial theoretical library of 2-(heteroaryl)-5-(alkylthio)-1,3,4-oxadiazole derivatives has been developed and a theoretical in-silico study of their interaction with SDH has been performed. The most selective compounds were selected, synthesis of them was performed and in-vitro studies were carried out by Palacký University scientists.

Preliminary results of the bioassays show that a correlation between the theoretical calculations and the experimental results can be observed. In order to reach reliable conclusions, the library of compounds was extended by the synthesis of 2-heteroaryl-5-(acylthio)-1,3,4-oxadiazole derivatives.

SYNTHESIS AND INVESTIGATION OF CONDENSED SYSTEMS WITH PYRAZOLE SCAFFOLD

Povilas Viltrakis[1], Eglė Arbačiauskienė[1], Algirdas Šačkus[1], Vilija Kederienė[1]

[1]Department of Organic Chemistry, Kaunas University of Technology, Lithuania
povilas.viltrakis@ktu.edu

Pyrazole derivatives are widely studied due to their broad biological activities, such as anticancer, antioxidant, antimicrobial, antidepressant, antiviral and various other activities [1]. Meanwhile, benzimidazole derivatives, like compounds containing a pyrazole fragment, also exhibit a diverse spectrum of biological activities and are widely used in the production of pharmaceuticals, such as Omeprazole or Pimozide [2]. Combining these two bioactive fragments allows new, potentially biologically active compounds to be created, which could be applied in the developing new pharmaceuticals. Recent studies have shown, novel pyrazole-benzimidazole derivatives, has exceptional anti-proliferative activity and could significantly induce cancer cell cycle arrest and apoptosis [3]. Other identified biological activities in pyrazole-benzimidazole compounds are analgesic, antimicrobial, antioxidant and antiulcer [4].

The aim of this work is to synthesize new cyclic potential active pyrazole derivatives by applying alkylation and cyclocondensation reactions.

A multi-step synthesis obtained the starting compound 3-hydroxy-1-phenyl-1H-pyrazole-4-carbaldehyde. To synthesize the carbaldehyde, a benzyl protecting group was first attached to the hydroxy group. An alkylation reaction of 1-phenyl-1H-pyrazol-3-ol was carried out using benzyl bromide as an alkylating agent and sodium hydride as a base. In the next step, 3-(benzyloxy)-1-phenyl-1H-pyrazole, an aldehyde group, was introduced into the pyrazole ring using a Vilsmeier-Hack reaction. After obtaining 3-(benzyloxy)-1-phenyl-1H-pyrazole-4-carbaldehyde, the benzyl group was removed in a reaction using trifluoroacetic acid in toluene. The intermediate pyrazole derivative was synthesized in good yield. The desired products were obtained by amination reaction and then by cyclisation reaction. The resulting functionalized cyclic pyrazole derivatives were investigated for their biological activity.

Acknowledgements

Part of this work has received funding from the Research Council of Lithuania (LMTLT), agreement No. S-SV-24-167.

[1]] FARIA, J.V., et al. Recently Reported Biological Activities of Pyrazole Compounds,. Bioorganic & Medicinal Chemistry, vol. 25, 2017, nr. 21. pp. 5891-5903.

[2] EBENEZER, O., OYETUNDE-JOSHUA, F., OMOTOSO, O.D. and SHAPI, M. Benzimidazole and its Derivatives: Recent Advances (2020–2022). Results in Chemistry, vol. 5, 2023. pp. 100925.

[3] REN, B., et al. Design, Synthesis and in Vitro Antitumor Evaluation of Novel Pyrazole-Benzimidazole Derivatives. Bioorganic & Medicinal Chemistry Letters, vol. 43, 2021. pp. 128097.

[4] Marinescu M. Synthesis of Antimicrobial Benzimidazole-Pyrazole Compounds and Their Biological Activities. Antibiotics (Basel). 2021 Aug 19;10(8):1002. doi: 10.3390/antibiotics10081002. PMID: 34439052; PMCID: PMC8389006.

SYNTHESIS OF NEW 4-PHENYL-1-(3,4,5-TRIMETHOXYPHENYL)-1H-IMIDAZOLE-2-THIOLDERIVATIVES

B. Grybaitė[1], A. Starkauskaitė[1], V. Mickevičius[1]

[1]Kaunas University of Technology, Department of Organic Chemistry, Radvilėnų pl. 19, 50254 Kaunas, Lithuania
birute.grybaite@ktu.lt

Imidazoles are a large group of compounds that play important role in organic and medicinal chemistry. The specific structure of the imidazole ring with desirable electrophilicity makes its compounds very versatile for many biological applications. Derivatives of imidazoles attract considerable interest in the field of organic synthesis due to their wide spectrum of biological activity – these compounds contribute to various catalysis in enzymatic and endocytosis processes also this structures are known to have a wide variety of biological activities including antidiabetic, antioxidant, anti-amoebic, antihelmintic antibacterial, antimycobacterial, anti-inflammatory, antitumor, antidiabetic, antiviral, and antifungal activities [1–3].

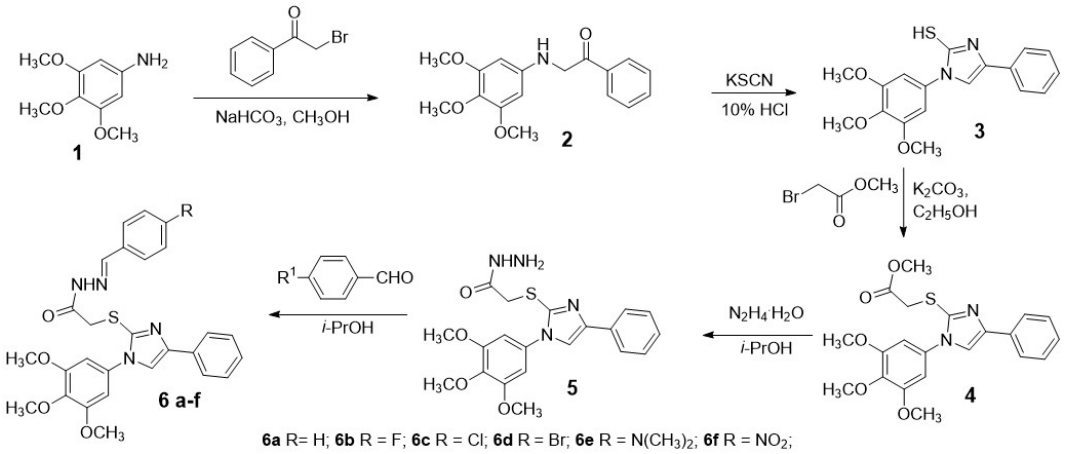


Fig. 1. Synthesis of compounds **2–6.**

In this study, 3,4,5-trimethoxyaniline (**1**) upon reaction with phenacyl bromide in methanol at room temperature for 2h formed the target 1-phenyl-2-((3,4,5-trimethoxyphenyl)amino)ethan-1-one (**2**). To obtain compound **3**, *α*-amino ketone **2** reacted with potassium thiocyanate in diluted HCl. The reactions afforded imidazole-2-thione **3**, which can exist in the tautomeric form.We found that the reaction of compound **3** with methyl bromoacetate in ethanol, in the presence of potassium carbonate, occurred uniquely to give the product of *S*-alkylation – methyl 2-((4-phenyl-1-(3,4,5-trimethoxyphenyl)-1*H*-imidazol-2-yl)thio)acetate (**4**). The obtained methyl ester **4** was transformed into hydrazide **5** using hydrazine monohydrate in 2-propanol (Fig. 1). Condensation of compound **5** with aromatic aldehydes in propan-2-ol led to the formation of *N*'-benzylidene hydrazides **6a-f**. The structures of the obtained compounds **6a-f** were confirmed by the data of the ^{1}H, ^{13}C NMR and FT-IR spectroscopy and elemental analysis.

[1] Du, J. et al., Eur. J. Med. Chem. 246, 114956 (2023).
[2] Liu, Y.C. et al., Bioorganic Med. Chem. 65, 116757 (2022).
[3] Gurjar, A.S. et al., Bioorg Med Chem. 26, 1511–1522 (2018).

SYNTHESIS OF PHOSPHORUS-CONTAINING POLYESTERS OF L-GLUTAMIC ACID AND THEIR COMPLEXES WITH ANTIBIOTICS

Yaryna Kuryshchuk[1], Diana Varchuk[1], Zoriana Nadashkevych[1], Anna Stasiuk[1]

[1]Department of Organic Chemistry, Lviv Polytechnic National University, Ukraine
yaryna.kuryshchuk.mkhtkhd.2024@lpnu.ua

Health is a top priority in the modern world, and achieving it relies on effective pharmaceutical treatments. However, the excessive and improper use of antibiotics has led to a growing threat of pathogenic microbial resistance. The World Health Organization (WHO) has classified ESKAPE pathogens (*Enterococcus faecium, Staphylococcus aureus, Klebsiella pneumoniae, Acinetobacter baumannii, Pseudomonas aeruginosa* and *Enterobacter* spp.) as high-priority threats due to their resistance to certain antibiotics [1]. Therefore, developing novel methods for antibiotic delivery with enhanced properties is crucial to ensuring their effectiveness, preventing degradation by protective enzymes in the body, and avoiding the induction of further resistance mechanisms.

One promising approach to enhancing antibiotic efficiency is the formation of complexes with transport carriers, particularly phosphorus-containing polyesters. Such complexes are expected to facilitate the rapid penetration of active pharmaceutical ingredients across cell membranes.

Phosphorus-containing polyesters were synthesized using the Steglich esterification reaction, involving the interaction of N-stearoylglutamic acid with dipolyethylene glycol ethyl phosphate. The ester bonds within these macromolecules impart biodegradability, while the polymer structure, based on polyethylene glycols and amino acids, ensures the absence of cytotoxic and organotoxic properties. The presence of phosphate groups in the polyester structure allows for the conjugation of biologically active compounds, maintaining their essential pharmacological properties. Antibiotics are a notable example of such compounds.

The synthesized phosphorus-containing polyesters form dispersions in aqueous and physiological solutions, with nanometric-sized dispersed phases. It has been demonstrated that these aqueous dispersions exhibit surface-active properties, enabling self-stabilization and the solubilization of poorly water-soluble compounds.

Furthermore, it has been established that phosphorus-containing polyesters can bind and form complexes with antibiotics, including amoxicillin, oxytetracycline, benzylpenicillin, and doxycycline.

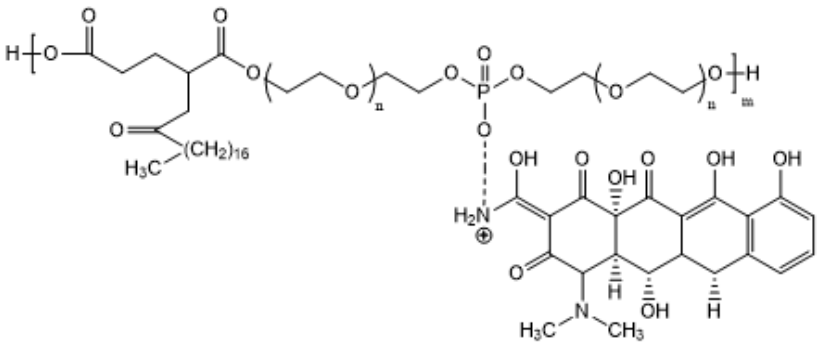


Fig. 1. Schematic representation of the complex formation between phosphorus-containing polyesters and doxycycline

The antibacterial activity of these complexes was studied against *Escherichia coli* and *Staphylococcus aureus*. The minimum inhibitory concentration (MIC) of polyester-antibiotic complexes was found to be 4 to 5 times lower than that of the pure antibiotics.

The results indicate that these polyester-antibiotic complexes are highly effective, allowing for a reduced antibiotic concentration compared to pure drugs, which could help mitigate antibiotic resistance.

Acknowledgements

The presented research findings were obtained with financial support from the National Research Foundation of Ukraine under the competition “Research Infrastructures for Conducting Advanced Scientific Studies” within the framework of project 2023.05/0015, titled “Development of Hydrogel-Based Emergency Care Solutions for Penetrating Abdominal Wounds as Part of the Establishment of a Research Center for Novel Polymer Materials for Medicine.”

[1] Aggarwal, R., Mahajan, P., Pandiya, S., Bajaj, A., Verma, S. K., Yadav, P., ... Johri, A. K. (2024). Antibiotic resistance: a global crisis, problems and solutions. Critical Reviews in Microbiology, 50(5), 896–921. https://doi.org/10.1080/1040841X.2024.2313024

SYNTHESIS OF NEW 3-SUBSTITUDED-6-BROMOBENZOXAZOLIN-2-ONE DERIVATIVES

Monika Bertašiūtė[1], Vytautas Mickevičius[1], Birutė Grybaitė[1]

[1]Department of Organic Chemistry, Faculty of Chemical technology, Kaunas University of Technology, Lithuania
monika.bertasiute@ktu.edu

Benzoxazole-based structures play a significant role in medicinal chemistry due to their broad spectrum of biological activities. These fused oxazole-benzene systems exhibit promising antifungal, antibacterial, anti-inflammatory, and anticancer properties.[1, 2, 3] This study focuses on the synthesis of novel benzoxazolinone derivatives with potential biological activity.

The precursor acid **2** was synthesized via bromination of 3-(2-oxobenzo[d]oxazol-3(2*H*)-yl)propanoic acid **1** in the presence of acetic acid (**Fig. 1**). The molecular structures of benzimidazole-containing compounds **3–6** were obtained through the Phillips reaction. Compound **7** was synthesized from precursor **2** using polyphosphoric acid (PPA). To achieve the target acid hydrazide **9**, a standard synthetic pathway - acid to ester to hydrazide - was employed. Finally, hydrazide **9** was condensed with various aromatic aldehydes to introduce the hydrazone moiety **10–18**.

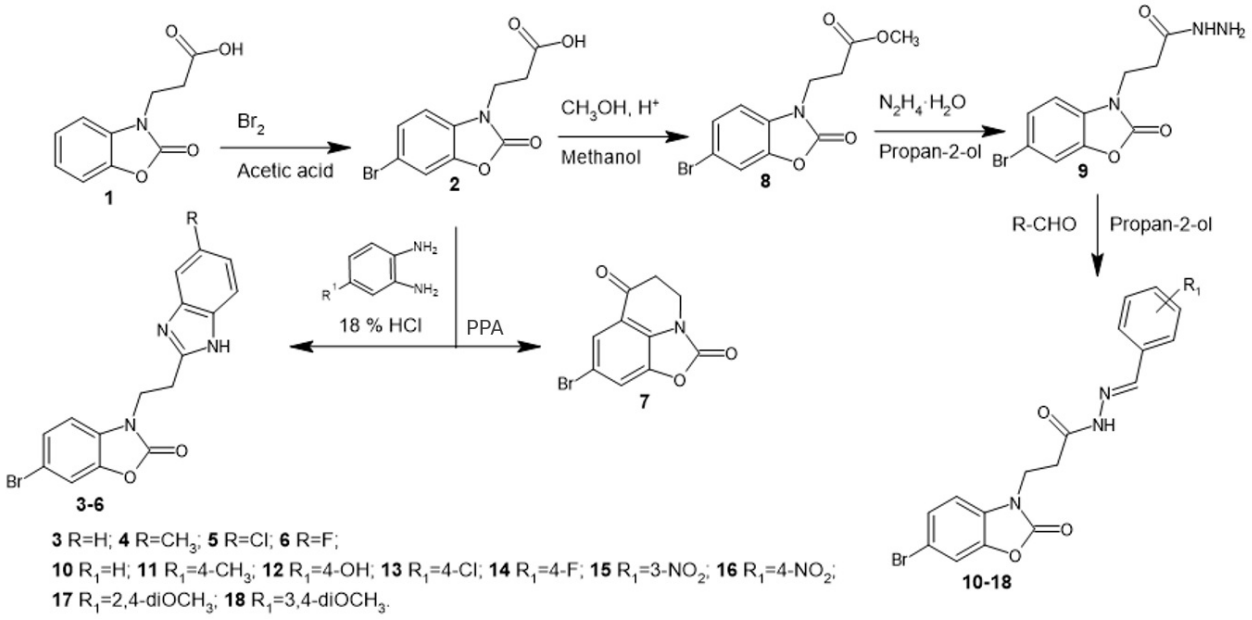


Fig. 1. Synthesis of compounds 2-18

The structure of the synthesized compounds was characterized by spectral data (IR, NMR spectra, and elemental analysis). The spectra showed good agreement with the assigned molecular structures.

[1] GHOSHAL, T., Patel, T.M. Anticancer activity of benzoxazole derivative: a review. Futur J Pharm Sci 6, 94 (2020). DOI:10.1186/s43094-020-00115-0.

[2] AGGARWAL Nupur, et al. Biologically active Benzoxazole: A comprehensive review. Int. J. Pharm. Sci. Res, 2017, 2.2: 1-5, ISSN: 2455-4685.

[3] SAMIA M. Rida et al. Synthesis of some novel benzoxazole derivatives as anticancer, anti-HIV-1 and antimicrobial agents, European Journal of Medicinal Chemistry, Volume 40, Issue 9, 2005, Pages 949-959. DOI: 10.1016/j.ejmech.2005.03.023.

SYNTHESIS OF TARGETED 4-(7H-IMIDAZO(2,1-b)(1,3)THIAZIN-5-YL)ANILINE DERIVATES

Polina Pylskaja[1], Martyna Paulauskaitė[1], Ieva Žutautė[1]

[1]Institute of Chemistry, Faculty of Chemistry and Geosciences, Vilnius University, Vilnius, Lithuania
polina.pylskaja@chgf.stud.vu.lt

Interest in the study of protein aggregation and amyloid formation is growing, mainly due to their links to various neurodegenerative and systemic diseases such as Alzheimer's disease, Parkinson's disease, and type II diabetes [1]. Amyloid fibril formation is a defining feature of these conditions, making the quest for effective inhibitors of this process critically necessary, scientifically and medically [2]. Recent research has indicated that imidazo[2,1-b][1,3]thiazine derivatives may be promising modulators of amyloid aggregation [3]. In this study, we focus on the synthesis and characterization of 4-(7H-imidazo[2,1-b][1,3]thiazin-5-yl)aniline, along with its carbamate and amide derivatives. These modified compounds are intended to enhance bioavailability, stability, and interactions with amyloidogenic proteins.

Our synthetic approach involves the cyclization reaction of starting 2-alkynylthioimidazoles to yield corresponding 4-(7H-imidazo[2,1-b][1,3]thiazin-5-yl)aniline. The second step entails functionalizing the aniline group through carbamation and amidation reactions, utilizing appropriate electrophilic reagents. The results of this study will provide insights into the structure-activity relationships of imidazo[2,1-b][1,3]thiazine-based inhibitors and contribute to the development of new therapeutic strategies for amyloid-related diseases.

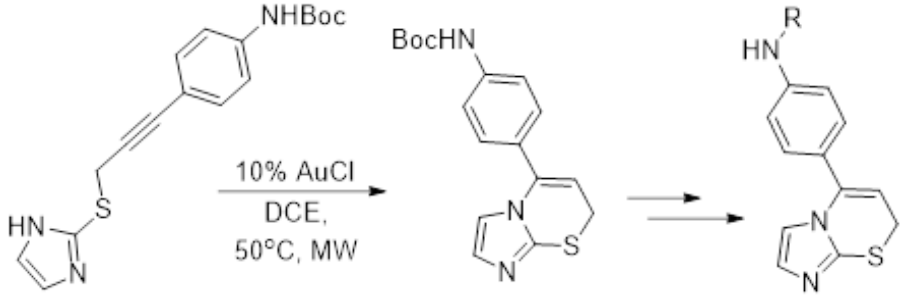


Fig. 1. Synthesis of 4-(7H-imidazo[2,1-b][1,3]thiazin-5-yl)aniline derivatives.

[1] M. G. Iadanza, et. al., "A new era for understanding amyloid structures and disease," Nat. Rev. Mol. Cell Biol., 2018, 19, 755–773.
[2] X. Zhang, et. al., "How the imidazole ring modulates amyloid formation of islet amyloid polypeptide: A chemical modification study," Prog. Biophys. Mol. Biol., 2016, 124, 1–9.
[3] I. Misiūnaitė, et. al., "Imidazo[2,1-b][1,3]thiazine Derivatives as Potential Modulators of Alpha-Synuclein Amyloid Aggregation," ACS Chem. Neurosci., 2024.

SYNTHESIS AND MODIFICATION OF ETHYL 2-(2-(-7H-IMIDAZO(2,1-b)(1,3)THIAZIN-5-YL)PHENOXY)ACETATE FOR AMYLOID AGGREGATION INHIBITION

Fausta Kairytė[1], Indrė Misiūnaitė-Vaškevičienė[1], Ieva Žutautė[1]

[1]Institute of Chemistry, Faculty of Chemistry and Geosciences, Vilnius University, Vilnius, Lithuania
fausta.kairyte@chgf.stud.vu.lt

Amyloid fibril formation is a hallmark of numerous neurodegenerative and systemic diseases, including Alzheimer's disease, Parkinson's disease, and type II diabetes. The aggregation of misfolded proteins into amyloid plaques has been identified as a key pathological process contributing to cellular dysfunction and toxicity[1]. The urgency of identifying effective inhibitors of amyloid aggregation has led to extensive research into small-molecule modulators capable of disrupting fibril formation or stabilizing non-toxic conformations of amyloidogenic proteins[2]. Among these small molecules, imidazole-based compounds have emerged as promising candidates due to their unique electronic properties and ability to interact with protein aggregation pathways[3]. The imidazo[2,1-b][1,3]thiazine scaffold, in particular, has garnered interest for its bioactive potential, as derivatives of this core structure have demonstrated anti-amyloidogenic properties[4].

Following previous research, ethyl 2-(2-(7H-imidazo[2,1-b][1,3]thiazin-5-yl)phenoxy)acetate was chosen for functional group position evaluation in the core structure of 5-arylimidazo[2,1-b][1,3]thiazine. The desired compound was synthesized with a cyclization reaction of appropriate 2-alkynylthioimidazole. Further modification of the ester group led to a purposive group of compounds required for further structural-activity relationship investigation on inhibition of alpha-synuclein aggregation.

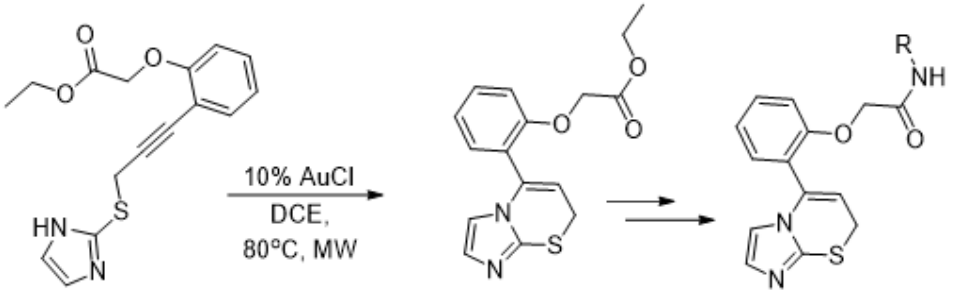


Fig. 1. Ethyl 2-(2-(7H-imidazo[2,1-b][1,3]thiazin-5-yl)phenoxy)acetate synthesis and its further modification.

[1] M. G. Iadanza, M. P. Jackson, E. W. Hewitt, N. A. Ranson, S. E. Radford, "A new era for understanding amyloid structures and disease," Nat. Rev. Mol. Cell Biol., 2018, 19, 755-773

[2] Fabrizio Chiti, Christopher M. Dobson, "Protein Misfolding, Amyloid Formation and Human Disease: a Summary of Progress Over the Last Decade," Ann. Rev. Biochem., 2017, 86, 28-38.

[3] X. Zhang, J. Liu, L. Huang, X. Yang, R. B. Petersen, Y. Sun, H. Gong, L. Zheng., K. Huan, "How the imidazole ring modulates amyloid formation of islet amyloid polypeptide: A chemical modification study," Prog. Biophys. Mol. Biol., 2016, 124, 1-9.

[4] I. Misiūnaitė, K. Mikalauskaitė, M. Paulauskaitė, R. Sniečkutė, V. Smirnovas, A. Brukštus, M. Žiaunys, I. Žutautė, "Imidazo[2,1-b][1,3]thiazine Derivatives as Potential Modulators of Alpha-Synuclein Amyloid Aggregation," ACS Chem., Neurosci., 2024, 24, 4418-4430.

SYNTHESIS OF A NEW GENERATIONOF HSP90 INHIBITORS CONTAINING A BENZIMIDAZOLE-RESORCINOL MOIETY

Vilius Petraška[1], Ieva Žutautė[1], Algirdas Brukštus[1]

[1]Faculty of Chemistry and Geosciences, Vilnius University, Lithuania
vilius.petraska@chgf.vu.lt

Hsp90 (Heat Shock Protein 90) is a chaperone protein classified under the heat shock protein family, with an approximate molecular mass of 90 kDa. It is widely distributed across various animal kingdoms and constitutes 1-2% of the total protein content in human cells. Hsp90 ensures proper protein folding, stabilizes proteins under heat stress, and facilitates their degradation [1]. In cancer cells, Hsp90 levels are significantly elevated, supporting key processes such as migration, metastasis, proliferation, and other aspects of tumor progression. According to data published by the World Health Organization in 2022, cancer is a leading cause of death worldwide, accounting for approximately 10 million fatalities each year [3]. As a result, Hsp90 has been extensively investigated over the past decade as a potential therapeutic target for both anti-cancer and anti-neurodegenerative treatments [2].

Studies on radicicol, a natural compound that competitively binds to Hsp90, have demonstrated that the resorcinol fragment and its hydroxyl groups are essential for inhibiting the protein's N-terminal domain, which contains the crucial ATP binding pocket. Further research has indicated that for a drug to effectively bind to Hsp90's active site, it must feature an aromatic ring near the resorcinol moiety [4].

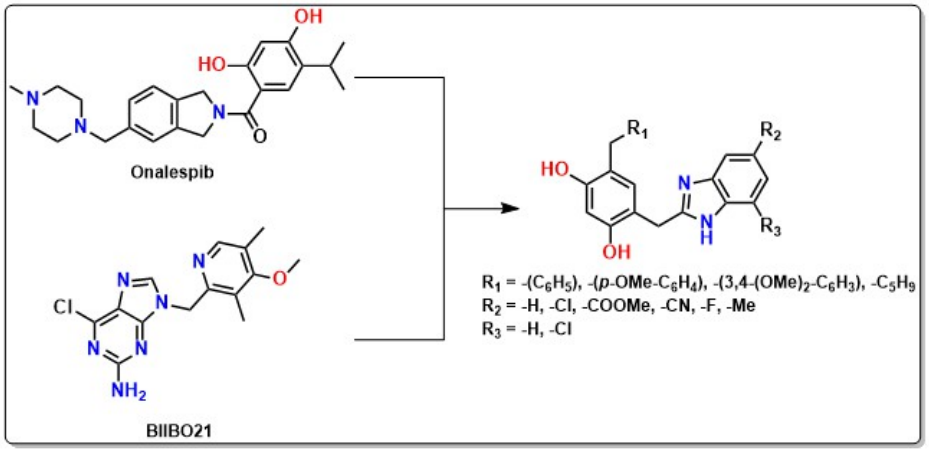


Fig. 1. Onalespib, BIIBO21, and target structures

This work aimed to synthesize a range of Hsp90 inhibitors containing a benzimidazole-resorcinol moiety and explore their application in developing potential resorcinol-based Hsp90 inhibitors featuring a benzimidazole moiety. Onalespib, a drug that has already completed phase II clinical trials, as well as structures of other resorcinol-based Hsp90 inhibitors (like BIIBO21), were used as a reference in this work [5]. The presentation will cover the ten-step synthesis process, its challenges, and results.

[1] Tsutsumi, S. et al. Charged linker sequence modulates eukaryotic heat shock protein 90 (Hsp90) chaperone activity. Proceedings of the National Academy of Sciences of the United States of America, 109(8), 2937–2942 (2012).
[2] World Health Organization (2022, February 3). Cancer. Retrieved from https://www.who.int/news-room/fact-sheets/detail/cancer.
[3] Neckers, L., & Neckers, K. Heat-shock protein 90 inhibitors as novel cancer chemotherapeutics - an update. Expert Opinion on Emerging Drugs, 10(1), 137–149 (2005).
[4] Ardestani, M. et al. Heterocyclic Compounds as Hsp90 Inhibitors: A Perspective on Anticancer Applications. Pharmaceutics, 14(10) (2022).
[5] Clinical trials.gov. [Date accessed: 2025-02-10] Available:https://clinicaltrials.gov/

SYNTHESIS OF NEW 1-(NAPHTHALEN-1-YL)-4-PHENYL-1H-IMIDAZOLE-2-THIOL DERIVATIVES

Aistė Starkauskaitė[1], Birutė Grybaitė[1], Vytautas Mickevičius[1]

[1]Kaunas University of Technology, Department of Organic Chemistry, Lithuania
aiste.starkauskaite@ktu.edu

Hydrazones are organic compounds containing the azomethine (-C=NNH-) functional group, which have gained significant attention in recent years due to their anticancer activity [1,2]. Similarly, imidazole derivatives exhibit a wide range of biological activities, including antifungal, antioxidant, and anticancer effects, making them valuable candidates in drug discovery [3].

The starting compound **2** was prepared by the reaction of 1- naphthylamine (**1**) and 2-bromo-1-phenylethan-1-one at room temperature. Compound **3** was yielded by the reaction between aminoketone **2** and KSCN in 10% HCl at reflux.

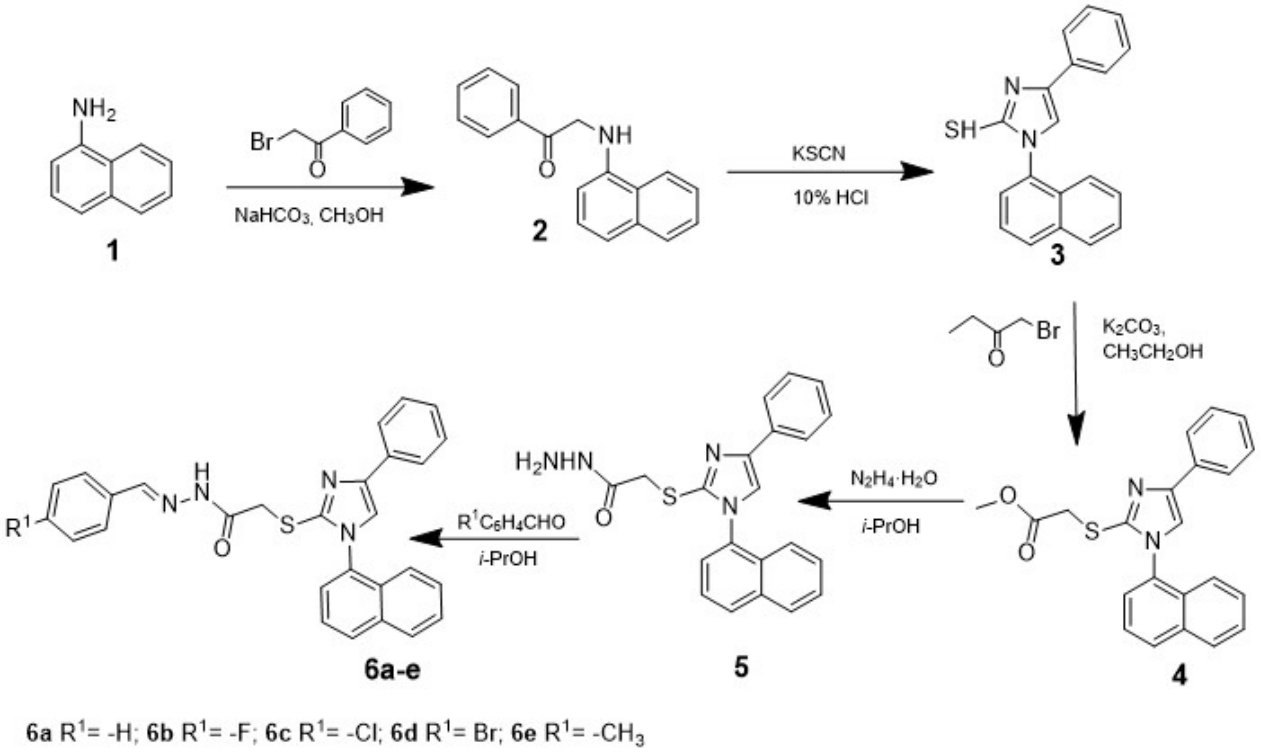


Fig. 1. Synthesis of compounds (**2-6**).

Compound **3** interaction with methyl bromoacetate gave imidazole analog **4**. The obtained methyl ester **4** was transformed into hydrazide **5** using hydrazine monohydrate in propan-2-ol (Fig. 1). Condensation of compound **5** with aromatic aldehydes in propan-2-ol led to the formation of *N*'-benzylidene hydrazides **6a-e**. The structures of the obtained compounds **2-6** were confirmed by the data of the ^{1}H, ^{13}C NMR and FT-IR spectroscopy and elemental analysis.

[1] S. Murugappan, S. Dastari, K. Jungare, N. M. Barve, and N. Shankaraiah, "Hydrazide-hydrazone/hydrazone as enabling linkers in anti-cancer drug discovery: A comprehensive review," Journal of Molecular Structure, vol. 1307, p. 138012, Mar. 2024, doi: https://doi.org/10.1016/j.molstruc.2024.138012.

[2] Yağmur Biliz et al., "Novel N-Acyl Hydrazone Compounds as Promising Anticancer Agents: Synthesis and Molecular Docking Studies," ACS omega, vol. 8, no. 22, pp. 20073–20084, May 2023, doi: https://doi.org/10.1021/acsomega.3c02361.

[3] I. Ali, M. N. Lone, and H. Y. Aboul-Enein, "Imidazoles as potential anticancer agents," MedChemComm, vol. 8, no. 9, pp. 1742–1773, Sep. 2017, doi: https://doi.org/10.1039/C7MD00067G.

COMPUTATIONAL STUDY OF ELECTRONIC SPECTRA AND STRUCTURE OF RETINOIDS

Julius Ažukas[1], Žyginta Murnikova[1], Kęstutis Aidas[1]

[1] Institute of Chemical Physics, Faculty of Physics, Vilnius University
julius.azukas@ff.stud.vu.lt

Retinoids are a group of compounds chemically related to vitamin A and found all throughout the human body. Our visual system, for instance, is largely dependent on the isomerization of 11-*cis*-retinal to all-*trans*-retinal, and the following replenishment of 11-*cis*-retinal during the retinoid cycle [1]. Understanding the structure of such compounds is an important part of broadening the field of applications, and spectroscopic methods are often used for such tasks. While experimental methods provide us with accurate results, theoretical calculations may offer insights into molecular level of the compounds being investigated. Although similar compounds, such as various carotenoids, were successfully studied computationally in terms of vibrational and electronic spectra using density functional theory (DFT) [2], the same success has not yet been reproduced for retinoids in common solvents, especially regarding different *cis-trans* isomers, despite existing experimental results [3].

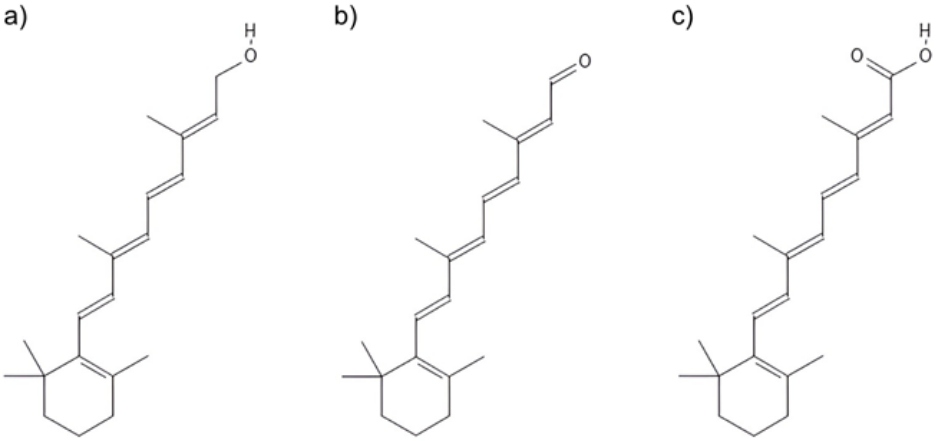


Fig. 1. Structural formulas of retinoids a) all-*trans*-retinol, b) all-*trans*-retinal, c) all-*trans*-retinoic acid.

The primary goal of this study was to properly evaluate the electronic absorption spectra of retinoids in organic solvents for different *cis-trans* isomeric forms, as the absorption maxima of retinoids vary depending on the molecule's configuration and the solvent used. Quantum mechanics/molecular mechanics (QM/MM) calculations, as well as DFT methods, were used in this work in order to investigate the systems more closely. The results provide more clarity about the electronic structure of retinoid molecules.

Acknowledgements

Computations were performed using the resources provided by the High-Performance Computing Center "HPC Saulėtekis" at Vilnius University, Lithuania.

[1] E. H. Choi, A. Daruwalla, S. Suh, H. Leinonen, K. Palczewski, "Retinoids in the visual cycle: role of the retinal G protein-coupled receptor", Journal of Lipid Research 62, 100040 (2021)

[2] M. Macernis, J. Sulskus, S. Malickaja, B. Robert, L. Valkunas, "Resonance Raman Spectra and Electronic Transitions in Carotenoids: A Density Functional Theory Study", The Journal of Physical Chemistry A 118, 1817-1825 (2014)

[3] M. A. Kane and J. L. Napoli, "Quantification of physiological levels of retinoic acid", Methods in Enzymology 123, 112-124 (1986)

SYNTHESIS OF MODULAR AND FUNCTIONALIZABLE SUPRAMOLECULAR CAVITANDS

Nojus Radzevičius[1], Eivydas Trioška[1], Edvinas Orentas[1]

[1] Institute of Chemistry, Faculty of Chemistry and Geosciences, Vilnius University, Naugarduko str. 24, Vilnius, Lithuania
nojus.radzevicius@chgf.vu.lt

Cavitands are a class of macrocyclic molecules possessing an intrinsic internal cavity that is capable of reversible binding to various guest molecules through various non-covalent interactions. Such (often selective) host-guest binding allows for various potential applications - molecular recognition for sensors [1], encapsualtion of hydrophilic molecules for drug delivery [2], or catalysis through proximity effect (to other molecules or reactive groups of the cavitand itself) [3]. However, currently available cavitands (such as cyclodextrins and calixarenes) have very limited potential due to the small range of variation for their size and geometry, poor functionalization capabilities and large symmetry enforced by their synthesis methods.

In this work, a novel supramoelcular tetrameric cavitand possessing a large cross-shaped cavity was prepared. It consists of the monomers **7**, which can form quadruple self-complementary hydrogen bonds via the ureidopyrimidinone structures placed at the terminuses. The rigid structure of the monomer, resulting from the enantiomerically pure bicyclo[3.3.1]nonane derivatives **(-)-1** and **(+)-5** fused with aromatic linkers **2**, forces a spatial arrangement that allows for the formation of cyclic cross-shaped tetramers through the ureidopyrimidinone hydrogen bonding. The presence of large discrete oligomeric structures in $CDCl_3$ was confirmed by diffusion-ordered NMR spectroscopy (DOSY).

The synthesis procedure is also highly modular, potentially allowing for easy modification of cavity shape and size (e.g. by using different sized aromatic linkers, or completely changing the geometry with different bicyclo[3.3.1]nonane enantiomers). The procedure also allows for very versatile functionalization through multiple sites, such as Michael addition to unsaturated β-keto ester (succesfully performed with organocopper nucleophiles, alkynes & arylboronic acids) or formation of the ureidopyrimidinone with isocytosines derived from various amines. Future research includes the synthesis of more diverse cavitands based on this system, along with host-guest binding tests.

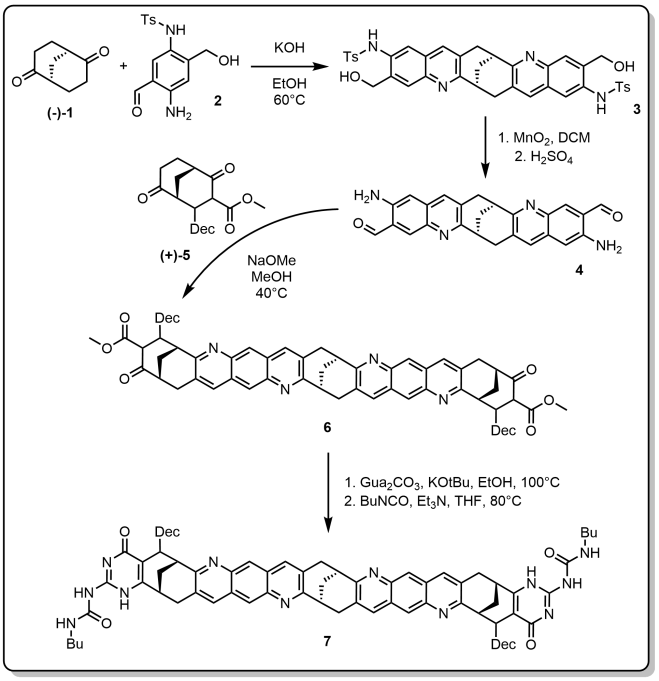


Fig. 1. Synthesis of cavitand monomer **7**.

[1] T. L. Mako, J. M. Racicot, and M. Levine, "Supramolecular Luminescent Sensors," Chem. Rev., vol. 119, no. 1, pp. 322–477, Jan. 2019.
[2] M. J. Webber and R. Langer, "Drug delivery by supramolecular design," Chem. Soc. Rev., vol. 46, no. 21, pp. 6600–6620, Oct. 2017.
[3] M. Morimoto, S. M. Bierschenk, K. T. Xia, R. G. Bergman, K. N. Raymond, and F. D. Toste, "Advances in supramolecular host-mediated reactivity," Nat Catal, vol. 3, no. 12, pp. 969–984, Dec. 2020.

STUDY OF THE OPTICAL PROPERTIES OF THE COMPLEX OF CARBON-BASED QUANTUM DOTS AND COMPOUNDS WITH ANTICANCER PROPERTIES

Martynas Zalieckas[1,2], Nikita Belko[3], Hanna Maltanava[3], Polina Kuzhir[3], Renata Karpicz[2]

[1]Faculty of Fundamental Sciences, Vilnius Gediminas Technical University, Saulėtekio Ave. 11, LT-10223 Vilnius, Lithuania
[2]Center for Physical Sciences and Technology, Saulėtekio Ave. 3, LT-10257 Vilnius, Lithuania.
[3]Department of Physics and Mathematics, University of Eastern Finland, FI-80100 Joensuu, Finland.
martynas.zalieckas@stud.vilniustech.lt

Quinone-based drugs such as doxorubicin (DOX), daunorubicin, etc. are widely used in cancer chemotherapy. Their use has adverse side effects such as dilated cardiomyopathy and heart failure [1,2]. This has led to the development of controllable nanocarrier-based drug delivery systems that allow for the targeted release of drugs at specific locations. Potential candidates for the development of such systems, heavy metal-free carbon-based quantum dots, such as: graphene quantum dots (GQD), carbon quantum dots (CQD), carbon nitride quantum dots (CNQD), are receiving increasing attention. Carbon-based quantum dots, with advanced surface functionalization and luminescent properties that allow the control of the intracellular location of nanocarrier-drug complexes, are a promising nanostructured material for theranostics, as they can simultaneously provide imaging and therapeutic effects [3]. Theranostic agents must meet several requirements. The most important condition is that it delivers the medicine to the target. To do this, it must be soluble in water and stable under physiological conditions. The nanocomplex must be biocompatible. It is highly desirable that it can be tracked optically to monitor its pharmacodynamics and accumulation in cancer tissue.

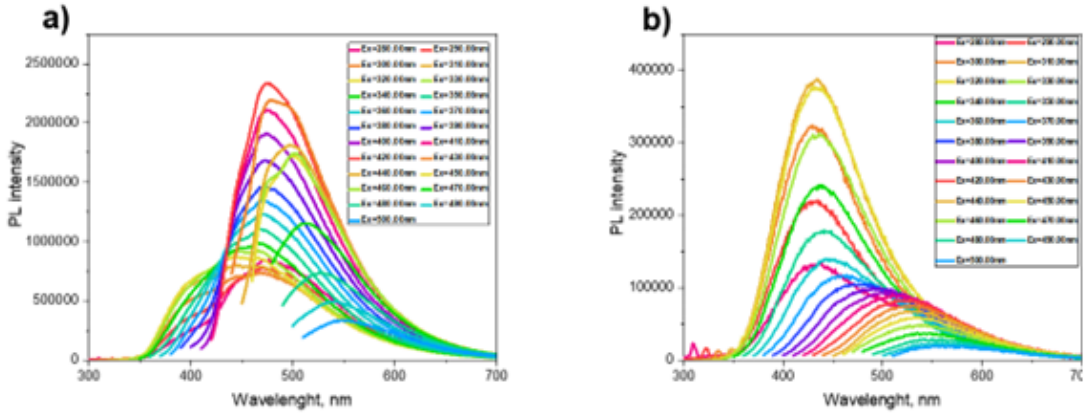


Fig. 1. Excitation wavelength-dependent emission of a) urea and b) thiourea derived CNQDs

In this study, we focus to investigate the stability and optical properties of carbon nitride quantum dots (CNQD) and compounds with anticancer properties using spectroscopic methods. CNQDs were synthesized using hydrothermal synthesis from urea/thiourea and citric acid. Currently the obtained samples were characterized by measuring absorption and fluorescence spectra, fluorescence decay times and Fourier transform infrared (FT-IR) spectra. The interaction of these quantum dots with doxorubicin and other studies will be optically investigated in the future.

[1] Kaushik, N., Borkar, S. B., Nandanwar, S. K., Panda, P. K., Choi, E. H., & Kaushik, N. K. (2022). Nanocarrier cancer therapeutics with functional stimuli-responsive mechanisms. In Journal of Nanobiotechnology (Vol. 20, Issue 1, p. 152). BioMed Central Ltd. https://doi.org/10.1186/s12951-022-01364-2
[2] Kciuk, M., Gielecí Nska, A., Mujwar, S., Kołat, D., Kałuzí Nska-Kołat, Z., Celik, I., & Kontek, R. (2023). Doxorubicin-An Agent with Multiple Mechanisms of Anticancer Activity. https://doi.org/10.3390/cells12040659
[3] 3. Azam, N., Ali, N., & Khan, T. J. (n.d.). Carbon Quantum Dots for Biomedical Applications: Review and Analysis. https://doi.org/10.3389/fmats.2021.700403

ACOST-EFFECTIVE NiZn/Ti EIECTROCATALYST FOR EFFICIENT HYDROGEN EVOLUTION AND OXYGEN EVOLUTION REACTIONS

Tripura Ganti[1], Aldona Balčiūnaitė[1], Jūrate Vaičiūnienė[1], Loreta Tamašauskaitė-Tamašiūnaitė[1], Eugenijus Norkus[1]

[1]Department of Catalysis, Center for Physical Sciences and Technology (FTMC),10257,Vilnius, Lithuania.
tripura.ganti@ftmc.lt

Though fossil fuels are efficient sources of energy, their harmful pollution necessitates the transition to environmentally friendly alternatives like hydrogen. With high energy density, hydrogen can store, transport, and deliver energy produced from renewable sources. Water electrolysis, a simple and efficient method, is increasingly being explored for producing hydrogen with zero carbon footprint, making it a clean and sustainable alternative for fuel production. To overcome the sluggish kinetics of HER and OER, noble metal catalysts typically offer low overpotentials and high current densities. However, their high cost and scarcity limit their practical application. Therefore, in this work, the cost-effective, non-noble NiZn/Ti electrocatalyst was synthesized via a single-step electrodeposition technique on a titanium substrate. The composition and surface structure of the NiZn/Ti catalyst were precisely optimized to enhance its catalytic performance. Detailed characterizations were conducted to investigate the catalysts' morphology, structure, and composition using Scanning Electron Microscopy (SEM) and Inductively Coupled Plasma Optical Emission Spectroscopy (ICP-OES). The catalytic activity was evaluated using Linear Sweep Voltammetry (LSV) in alkaline medium (1 M KOH) at a scan rate of 10 mV s^{-1}. Electrochemical tests in alkaline medium showed that the NiZn/Ti catalyst had improved catalytic activity, making it a cost-effective electrocatalyst for water splitting applications.

NICKEL COBALT CATALYSTS FOR HYDROGEN GENERATION

Gitana Valeckytė[1], Zita Sukackienė[1], Jūratė Vaičiūnienė[1], Loreta Tamašauskaitė-Tamašiūnaitė[1], Eugenijus Norkus[1]

[1]Center for Physical Sciences and Technology
gitana.valeckyte@ftmc.lt

Hydrogen can be regarded as a viable alternative to conventional fossil fuels, such as coal, oil and natural gas [1]. The necessity for the replacement of these fuels arises from their perpetual depletion, the concomitant pollution of the environment and the promotion of the greenhouse effect, thus contributing to climate change when burned. Although the majority of hydrogen is currently produced from natural gas (62%), coal (19%) or naphtha reforming (18%), there is potential for change. The borohydride hydrolysis reaction is a process that yields hydrogen in an extremely pure form, which can be utilised directly as a hydrogen fuel cell. Moreover, fuel cells that employ pure hydrogen emit minimal pollutants other than water [2].

In the present study, the synthesis of NiCo(10)/Cu, NiCo(20)/Cu, and NiCo(80)/Cu catalysts was accomplished through the chemical method of metal deposition. The surface morphology, internal structure and chemical composition of the obtained catalysts were analysed using scanning electron microscopy (SEM) and induced plasma optical emission spectroscopy (ICP-OES). It was determined that the prepared coating particles consist of oval-shaped agglomerates. The composition of the catalysts was analysed, showing Ni loading ranging from 179.4 to 789 μg/cm^3 and Co ranging from 88.2 to 614 μg/cm^3. The catalytic properties of the formed catalysts for sodium borohydride hydrolysis reaction were investigated, revealing the two-component NiCo(80) coating as the most active. The activation energy of this catalyst was determined to be 56.4 kJ/mol and its hydrogen evolution rate was found to be 1.24 ml/min at 30 °C and 14.59 ml/min at 70 °C.

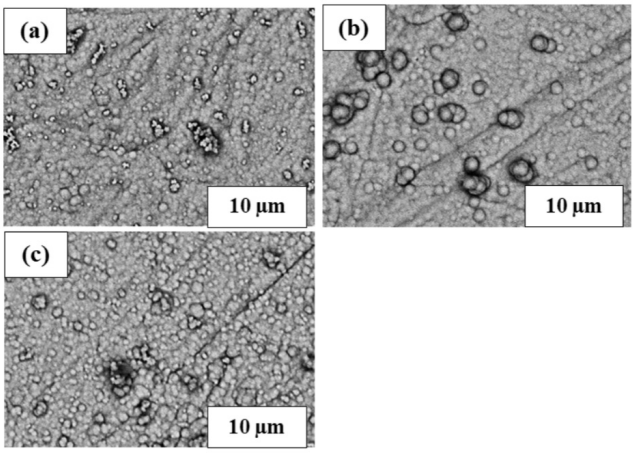


Fig. 1. SEM images of prepared NiCo(10)/Cu (a), NiCo(20)/Cu (b), NiCo(80)/Cu (c).

[1] Alasali F. et al., Energy Science and Engineering, vol 12, 1934-1968 (2024).
[2] Hoecke Van L. et al., Energy and Environmental Science, vol 14, 815-843 (2021).

NON-PRECIOUS METAL ELECTROCATALYSTS FOR THE OVERALLWATER SPLITTING: SYNTHESIS, CHARACTERIZATION AND PROPERTIES

Huma Amber[1], Aldona Balčiūnaitė[1], Loreta Tamašauskaitė-Tamašiūnaitė[1], Jūratė Vaičiūnienė[1], Eugenijus Norkus[1]

[1]Department of Catalysis, Center for Physical Sciences and Technology (FTMC), Sauletekio Ave. 3, Vilnius, Lithuania
huma.amber@ftmc.lt

Developing highly efficient and stable electrocatalysts from inexpensive and earth-abundant elements represents a significant advancement in the overall water splitting (OWS) process. This study investigates the synthesis, characterization, and electrocatalytic properties of four different electrocatalysts: cobalt-phosphorus (CoP), cobalt-iron-phosphorus (CoFeP), palladium-cobalt-phosphorus (PdCoP), and palladium-cobalt-iron-phosphorus (PdCoFeP). The CoP and CoFeP coatings were synthesized using the electroless deposition method, ensuring uniform deposition of metal and phosphorus components on the copper surface. Sodium hypophosphite (NaH_2PO_2) was utilized as the reducing agent. In addition, Pd crystallites were incorporated onto the CoP and CoFeP coatings via the galvanic displacement method, which resulted in a significant enhancement of the catalytic properties. The electrocatalysts were comprehensively characterized through techniques such as scanning electron microscopy (SEM), energy-dispersive X-ray spectroscopy (EDS), X-ray diffraction (XRD), and inductively coupled plasma optical emission spectroscopy (ICP-OES). These methods were employed to investigate the surface morphology, structure, and composition of the catalytic materials. The electrocatalytic performance for the hydrogen evolution reaction (HER) and oxygen evolution reaction (OER) was evaluated in 1 M KOH using a three-electrode setup. Meanwhile, the OWS performance was measured in a two-electrode system. It was found that Pd-modified CoP and CoFeP coatings exhibited superior bifunctional catalytic activities in comparison with CoP and CoFeP, with low overpotentials and high current densities for both HER and OER. The PdCoFeP catalyst demonstrated the lowest overpotential of 180 mV for HER at a current density of 10 mA cm^{-2} and 398 mV for OER at the same current density, thus exhibiting superior performance in comparison to other compositions. The enhanced performance of PdCoFeP can be attributed to the synergistic effect between Pd, Co, and Fe, which has been shown to enhance charge transfer kinetics and increase the density of active sites. Furthermore, when PdCoFeP electrodes are employed as both the anode and the cathode for water splitting, a low cell voltage of 1.70 V at 10 mA cm^{-2} is observed. The findings of this study highlight the potential of these phosphide-based materials as promising candidates for sustainable hydrogen production through overall water splitting.

Acknowledgements
This research was funded by a grant (No. P-MIP-23-467) from the Research Council of Lithuania.

APPLICATION OF FLEXIBLE NICKEL-IRON CATALYSTS FOR WATER SPLITTING REACTIONS

Dmytro Shyshkin[1,2], Loreta Tamasauskaite-Tamasiunaite[2], Aldona Balciunaite[2]

[1]Vilnius University, Naugarduko str. 24, LT-03225 Vilnius, Lithuania
[2]Center for Physical Sciences and Technology (FTMC), Saulėtekio ave. 3, LT-10257 Vilnius, Lithuania
dmytro.shyshkin@chgf.stud.vu.lt

Electrolysis of water is one of low-cost green hydrogen production technologies. The challenge is designing and developing low-cost and high-activity catalysts. Herein, we present a strategy to fabricate flexible electrocatalysts based on nickel-iron (NiFe) alloy coatings. NiFe coatings were plated on the flexible copper-coated polyimide surface (Cu/PI) using the low-cost and straightforward electroless metal plating method and morpholine borane as a reducing agent. It was found that Ni90Fe10, Ni80Fe20, Ni60Fe40, and Ni30Fe70 coatings were deposited on the Cu/PI surface, then the concentration of Fe2+ in the plating solution was 0.5, 1, 5, and 10 mM, respectively. Morphology, structure, and composition of NixFey/Cu/PI catalysts have been examined using scanning electron microscopy (SEM), energy dispersive X-ray spectroscopy (EDX), X-ray diffraction (XRD), and inductively coupled plasma optical emission spectroscopy (ICP-OES), whereas their activity has been investigated for hydrogen evolution (HER) and oxygen evolution (OER) reactions in 1 M KOH using linear sweep voltammetry (LSVs). It was found that the Ni80Fe20/Cu/PI catalyst exhibited the lowest overpotential value of 202.7 mV for the HER to obtain a current density of 10 mA cm−2 compared to Ni90Fe10/Cu/PI (211.9 mV), Ni60Fe40/Cu/PI (276.3 mV), Ni30Fe70/Cu/PI (278.4 mV), and Ni (303.4 mV). On the other hand, the lowest OER overpotential of 344.7 mV was observed for the Ni60Fe40/Cu/PI catalyst to obtain a current density of 10 mA cm−2 as compared with the Ni35Fe65/Cu/PI (369.9 mV), Ni80Fe20/Cu/PI (450.2 mV), Ni90Fe10/Cu/PI (454.2 mV), and Ni/Cu/PI (532.1 mV) catalysts. The developed Ni60Fe40/Cu/PI catalyst exhibit a cell potential of 1.85 V at 10 mA cm−2. The obtained catalysts seem to be suitable flexible catalysts for HER and OER in alkaline media.

ADVANCED 3D BIMETALLIC NICKEL-IRON/TITANIUM BIFUNCTIONAL ELECTROCATALYSTS FOR EFFECTIVE HYDROGEN EVOLUTION REACTION IN ACIDIC MEDIA

Shahid Nawaz[1], Aldona Balčiūnaitė[1], Loreta Tamašauskaitė-Tamašiūnaitė[1], Eugenijus Norkus[1]

[1]Department of catalysis, Center for Physical Sciences and Technology, Saulėtekio av. 3, LT-10257 Vilnius
shahid.nawaz@ftmc.lt

Owing to their pivotal role in scientific and technological advancements, the development of cost-effective, highly efficient, and durable electrocatalysts for the hydrogen evolution reaction (HER) has remained a longstanding research objective. However, achieving catalysts with both high activity and low cost remains a significant challenge. In this study, iron-nickel (Fe-Ni) bimetallic coatings were investigated as electrocatalysts for HER in acidic (0.5 M H_2SO_4) media. The catalysts were deposited onto titanium substrates (1 × 1 cm) using a cost-effective and straightforward electrochemical deposition process, specifically the dynamic hydrogen bubble template method. The electrocatalytic activity of the synthesized catalysts for HER was evaluated at 25 °C using linear sweep voltammetry (LSV). The surface morphology and composition were further characterized using scanning electron microscopy (SEM) and inductively coupled plasma optical emission spectroscopy (ICP-OES). The synthesized Fe-Ni/Ti-1 and Fe-Ni/Ti-2 electrocatalysts exhibited remarkable HER activity in acidic media, requiring overpotentials of only 106 mV and 247 mV, respectively, to achieve a current density of 10 mA cm^{-2}. Both catalysts demonstrated excellent long-term stability, maintaining consistent performance for two and ten hours at constant potentials and a constant current density of 10 mA cm^{-2}, underscoring their robustness and durability.

A COMPARATIVE STUDY OF HYDROGEN EVOLUTION REACTION PERFORMANCE BY NON-NOBLE TRANSITION METAL-BASED 3D ELECTROCATALYSTS TOWARDS ALKALINE WATER SPLITTING

Sukomol Barua[1], Aldona Balčiūnaitė[1], Jūratė Vaičiūnienė[1], Loreta Tamašauskaitė-Tamašiūnaitė[1], Eugenijus Norkus[1]

[1]Department of Catalysis, Center for Physical Sciences and Technology (FTMC), Vilnius, Lithuania
sukomol.barua@ftmc.lt

In this comparative study, we investigated the facile and cost-effective fabrication of non-noble transition metal-based bimetallic and trimetallic 3D coatings as highly efficient and sustainable electrocatalysts for the hydrogen evolution reaction (HER) in alkaline media (pH ≈ 14). These coatings were fabricated on thin titanium substrates (0.127 mm thickness, 1×1 cm^2) using an electrochemical deposition method through a dynamic hydrogen bubble template technique. The as-fabricated bimetallic NiMo/Ti catalyst exhibited a unique cedar leaf-like surface morphology while the NiMn/Ti catalyst demonstrated a nodule-like structure. In contrast, the trimetallic NiCoMn/Ti electrocatalyst displayed a unique cauliflower curd-shaped micro-sized nodular architecture. The HER activity of these fabricated catalysts was investigated by using Linear Sweep Voltammetry (LSV) in the alkaline environment at different temperatures. Also, the electrocatalysts were characterized by scanning electron microscopy (SEM) and inductively coupled plasma optical emission spectroscopy (ICP-OES).

From a comparative point of view, the as-prepared NiCoMn/Ti electrocatalyst exhibits excellent HER activity in alkaline media with a low overpotential of 139 mV to reach a current density of 10 mA cm^{-2}, whereas this benchmark current density was attained by NiMn/Ti and NiMo/Ti electrocatalysts with higher overpotentials of 220.3 mV and 288 mV, respectively. The current densities increased with an increase in temperatures from 25 °C to 75 °C for all three electrocatalysts. These non-noble metal-based catalysts have displayed excellent long-term stability at a constant potential of -0.232 V (vs. RHE) and a constant current density of 10 mA cm^{-2} and a multi-step chronopotentiometry test with current densities ranging from 20 mA cm^{-2} to 100 mA cm^{-2}, indicating sustainable durability and suitability for practical alkaline water splitting applications.

SUSTAINABLE NICKEL-DOPED NITROGEN-ENRICHED BIOMASS-DERIVEDCARBON CATALYSTS FOR HYDRAZINE FUEL CELLS

Virginija Ulevičienė[1], Aldona Balčiūnaitė[1], Daina Upskuvienė[1], Galina Dobele[2], Aleksandrs Volperts[2], Ance Plavniece[2], Aivars Zhurinsh[2], Loreta Tamašauskaitė-Tamašiūnaitė[1], Eugenijus Norkus[1]

[1]Department of Catalysis, Center for Physical Sciences and Technology, Sauletekio Ave. 3, LT-10257 Vilnius, Lithuania
[2]Latvian State Institute of Wood Chemistry, Dzerbenes Str. 27, LV-1006 Riga, Latvia
virginija.uleviciene@ftmc.lt

The growing demand for sustainable and efficient energy conversion technologies has led to increasing interest in biomass-derived carbon materials as cost-effective and environmentally friendly catalysts [1,2]. Biomass-based carbons, unlike traditional carbon materials, provide a renewable and abundant alternative enriched with inherent heteroatoms (e.g., N, P, S), which contribute to enhanced catalytic performance. In particular, nitrogen-doped carbon materials have demonstrated significant potential for electrochemical applications due to their improved conductivity and active sites. The incorporation of transition metals (Co, Cu, Ni, Fe, etc.) can further enhance catalytic activity, making these materials suitable for direct hydrazine fuel cells (DHFCs) [3-5]. Hydrazine (N_2H_4) is a promising liquid fuel for fuel cells due to its high energy density and carbon-free oxidation, offering a clean and efficient power source for next-generation energy systems.

In this study, we present a straightforward synthesis of non-noble metal-doped nitrogen-enriched biomass-based activated carbon catalysts for alkaline fuel cell applications. Activated wood carbon (AWC) was derived from birch wood and doped with Ni and nitrogen in a one-step synthesis using 10 % Ni^{2+} ions relative to AWC, along with dicyandiamide (DCDA) in dimethylformamide (DMF). After solvent evaporation, the mixture was subjected to pyrolysis at 800 °C for 60 minutes. The obtained catalysts were comprehensively characterized using ICP-OES for elemental composition, XRD for crystalline structure, XPS for surface chemistry, SEM-EDS for morphology and elemental distribution, BET analysis for surface area, and Raman spectroscopy for structural integrity. The AWC-Ni-N catalyst contained 1.12 at. % Ni and 98.88 at. % C. The catalytic performance of the AWC-Ni-N catalyst was assessed in DHFCs operating with 1 M N_2H_4 + 1 M KOH as the fuel and 5 M H_2O_2 + 1.5 M HCl as the oxidant, employing AWC-Ni-N as both the anode and cathode catalyst. Peak power densities of up to 10.8 mW cm^{-2} were achieved at 25 °C with the AWC-Ni-N catalyst. The AWC-Ni-N catalyst demonstrated excellent electrocatalytic activity, stability, and power output, highlighting its potential as an efficient electrode material for sustainable fuel cell technologies.

[1] X. Zhang et al. Appl. Catal. B: Environ. Energy vol. 363, p. 124783 (2025).
[2] Z. Zhu et al. eSci., vol. 4(5), 100249 (2024).
[3] G.M. Pereira et al. Mater. Chem. Phys., 307, 128102 (2023).
[4] S. Song et al. J. Electroanal. Chem., 906, 115986 (2022).
[5] S. Taghaddosi et al. J. Electroanal. Chem., 873, 114437 (2020).

CATHODE CATALYST SELECTION FOR ENHANCING OXYGEN REDUCTION REACTION OF FUEL CELLS: GR/Cu, Co_3 O_4-NC/GR/Cu, AND Co_3O_4-Cr_2O_3-NC/GR/Cu

Karina Vjūnova[1,2], Loreta Tamašauskaitė-Tamašiūnaitė[1]

[1]Center for Physical Sciences and Technology (FTMC)
[2]Vilnius University
karinavjunova@gmail.com

Since the oxygen reduction reaction (ORR) in fuel cells needs to be catalyzed heterogeneously, conductive substrates such as carbon materials are always needed in the construction of electrocatalysts. In order to increase the conductivity and improve the substrate-loading interaction, a graphene film was electrodeposited on the copper (Cu) substrate from the stable aqueous dispersion of graphene (GR) and the surfactant sodium dodecylbenzene sulfonate (SDBS). Then, the N-doped carbon supported Co_3O_4 or Co_3O_4-Cr_2O_3 particles (denoted as Co_3O_4-NC or Co_3O_4-Cr_2O_3-NC) were grown on the prepared GR/Cu electrodes. The hydrothermal method was applied to synthesize the Co_3O_4 or Co_3O_4-Cr_2O_3 particles. The resulting materials were characterized by X-ray diffraction (XRD), scanning electron microscopy (SEM), energy dispersive spectroscopy (EDS), and X-ray photoelectron spectroscopy (XPS), while the electrocatalytic activity for ORR was investigated by cyclic voltammetry (CV) and linear sweep voltammetry (LSV) in an O_2-saturated 0.1 M KOH solution. The data for ORR on the GR/Cu, Co_3O_4-NC/GR/Cu, and Co_3O_4-Cr_2O_3-NC/GR/Cu catalysts in an alkaline medium are compared and discussed based on the electrochemical data.

Acknowledgements
This research was funded by a grant (No. P-ST-24-380) from the Research Council of Lithuania.

SYNTHESIS OF PHENOTHIAZINE DERIVATIVES EXHIBITING VERY LONG ROOM TEMPERATURE PHOSPHORESCENCE

Paulius Vaickūnas[1], Jonas Žurauskas[1], Vilius Stankevičius[2], Steponas Raišys[2], Karolis Kazlauskas[2], Edvinas Orentas[1]

[1]Department of Organic Chemistry, Vilnius University, Vilnius, Lithuania
[2]Institute of Photonics and Nanotechnology, Vilnius University, Vilnius, Lithuania
edvinas.orentas@chf.vu.lt

Room-temperature phosphorescence (RTP) in organic compounds is an uncommon yet highly intriguing phenomenon with significant applications in various fields, including bioimaging[1,2], data encryption[1,2], and digital displays[1,2]. However, inducing phosphorescence in organic compounds presents considerable challenges, often necessitating cryogenic temperatures and an inert atmosphere[1]. In this study, we have developed a series of S,S-dioxophenothiazine derivatives capable of exhibiting long-lasting RTP. Through systematic structural modifications, we aim to elucidate the correlation between molecular architecture and phosphorescent properties, ultimately advancing the design of organic compounds that demonstrate stable and prolonged phosphorescence under ambient conditions, with observed lifetimes reaching up to 700 milliseconds. The synthesized crystalline structures were characterized using X-ray diffraction, while fluorescence spectrophotometry was employed to measure the phosphorescence lifetimes of each compound. These findings contribute to the growing class of fully organic phosphorescent materials with extensive application potential. S,S-dioxophenothiazine serves as a versatile molecular scaffold, offering high tunability and synthetic accessibility—both of which are crucial attributes in the development of phosphorescent materials. While this research is ongoing, it provides valuable insights for the future advancement of organic phosphorescent systems.

[1] 1. Kenry, Chen, C. & Liu, B. Enhancing the performance of pure organic room-temperature phosphorescent luminophores. Nat. Commun. 10, 2111 (2019).
[2] Wright, I. A., Etherington, M. K., Batsanov, A. S., Monkman, A. P. & Bryce, M. R. Oxidation State Tuning of Room Temperature Phosphorescence and Delayed Fluorescence in Phenothiazine and Phenothiazine-5,5-dioxide Dimers. Chem. – Eur. J. 29, e202300428 (2023).

INVESTIGATION OF CHROMIUM EMISSION IN THE NIR REGION OF YAG AND YLuAG BY CHANGING Cr^{3+} CONTENT IN THE HOST MATRIX

Nerija Ričkutė[1], Greta Inkrataitė[1]

[1]Institute of Chemistry, Faculty of Chemistry and Geosciences, Vilnius University, Vilnius, Lithuania
nerija.rickute@chgf.stud.vu.lt

Yttrium aluminium garnet (YAG) and yttrium lutetium aluminium garnet (YLuAG) are synthetic materials that belong to the garnet group. Synthetic garnet was first discovered in the 1950s, and since then the electronics industry has seen a rapid development of technologies using synthetic compounds with a garnet structure. YAG and YLuAG have good mechanical and optical properties. This matrix allows incorporation in solid solution of luminescent ions such as transition metals (Cr^{3+}). Chromium doped YAG and YLuAG have different luminescence properties due to their structural differences and effect on crystal field, they are both widely used in luminescent systems. YAG is an excellent host for high power solid-state lasers due to its high density, high thermal stability, relatively efficient luminescence processes and high quantum efficiency. YLuAG, on the other hand, is often used in phosphor-converted LEDs and scintillators due to its great optical properties. However, garnets doped with different amounts of chromium show different results in luminescence properties. The measurements showed that even a small amounts of chromium incorporated in garnets indicate luminescent properties such as emission in NIR region, which is highly significant for applications in NIR-LED construction, horticulture and theranostics. This enables excellent results in luminescence with only a small amount of Cr^{3+}.

In the present work, garnets doped with different amounts of chromium have been synthesised and their structural and luminescence properties were studied. Cr^{3+} doped YAG and YLuAG were synthesized by the sol-gel method. The phase purity of the samples was analysed by means of X-ray diffraction. The morphology of the compounds was evaluated by using scanning electron microscopy. Elemental analysis was carried out using inductively coupled plasma optical emission spectrometry. Photoluminescence properties such as emission and excitation spectra, decay curves, quantum efficiency have been investigated.

SPECTROSCOPIC STUDY OF FREE-BASE MESO-TETRAPHENYLPORPHYRIN AND HEXAGONAL BORON NITRIDE VAN DER WAALS COMPLEX

Jelizaveta Fedotova[1,2], Ivan Halimski[1], Martynas Talaikis[1], Renata Karpicz[1], Jevgenij Chmeliov[1,2], Patrizia Lamberti[3], Maksim Shundalau[3]

[1]Center for Physical Sciences and Technology, Lithuania
[2]Faculty of Physics, Vilnius University, Lithuania
[3]Department of Information and Electrical Engineering and Applied Mathematics, University of Salerno, Italy
jelizaveta.fedotova@ff.stud.vu.lt

Development of functional nanomaterials requires a deep understanding of how organic molecules interact with solid surfaces. Understanding the interaction between organic molecules and nanomaterials is essential for advancing applications in optoelectronics, biomedical imaging, and nanophotonics. For example, weak non-covalent interactions that are often overlooked can nevertheless significantly influence optical properties and molecular behavior [1,2], making them crucial for the mentioned applications. The combination of vibrational (Raman scattering and IR absorption) and electronic spectroscopy (steady-state and time-resolved fluorescence) techniques was recently shown to be a useful tool for investigating such types of intermolecular interactions [3].

This study explores the formation of a weak van der Waals (vdW) complex between free-base meso-Tetraphenylporphyrin (TPP; molecular formula is $C_{44}H_{30}N_4$) and hexagonal boron nitride (hBN) (see Fig 1, a) through Raman (Fig. 1, b), FTIR, steady-state and time-resolved fluorescence. We observe red shifts (avg. 4 cm^{-1}) in the TPP Raman lines corresponding to macrocycle vibrations and blue shifts (avg. 3 cm^{-1}) in those corresponding to phenyl rings. These experimental results are confirmed by density functional theory calculations using all-electron Gaussian-type basis sets with dispersion correction (to take vdW interactions into account) included in the BPW91+d exchange-correlation functional. Additionally, both steady-state and time-resolved fluorescence exhibit changes that can be attributed to vdW interactions between TPP and hBN surface.

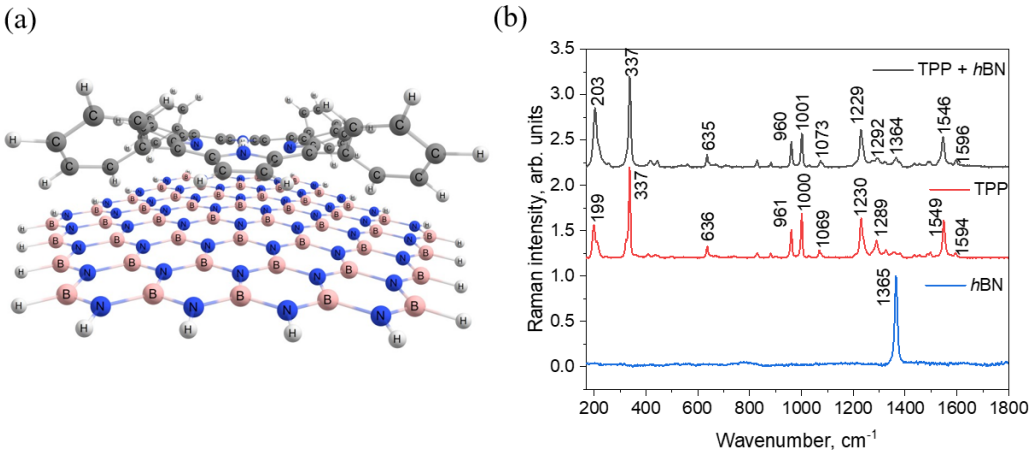


Fig. 1. a) Optimized geometry of TPP + hBN complex and b) Raman spectra of TPP + hBN, TPP and hBN

Acknowledgements

This work was supported by the Horizon 2020 RISE DiSeTCom project (GA 823728), the Horizon Europe FLORIN project (No. 101086142), and the Research Council of Lithuania (Grant No. S-MIP-23-70).

[1] V. V. Korolkov et al., ACS Nano 9(10), 10347 – 10355, 2015.
[2] A.-C. Nellissen et al., ACS Omega 8(39), 35638 – 35652, 2023.
[3] I. Halimski et.al., Under review in Langmuir.

LUMINESCENT PROPERTIES OF RARE-EARTH DOPED $NaAlGeO_4$ PHOSPHORS

Gabija Janušauskaitė[1], Martynas Misevičius[1,2]

[1]Institute of Chemistry, Faculty of Chemistry and Geosciences, Vilnius University, Lithuania
[2]Centre for Physical Sciences and Technology, Vilnius, Lithuania
gabija.janusauskaite@chgf.stud.vu.lt

Photoluminescent (PL) phosphors rely on a host material and an emitter, with rare-earth ions often used as activators due to their excellent luminescent properties. Germanates have gained attention as promising host materials because of their high thermal stability, low synthesis temperatures, and tunable optical properties. Despite extensive research on various germanate-based phosphors, the luminescent properties of $NaAlGeO_4$ remain largely unexplored. This study aims to investigate the luminescence properties of $NaAlGeO_4$ phosphors doped with Dy^{3+}, Eu^{3+}, Pr^{3+}, Sm^{3+}, and Tb^{3+}. By analysing their emission spectra, decay lifetimes, and quantum yields, we seek to evaluate their potential as efficient phosphors for optoelectronic applications.

$NaAlGeO_4$ phosphors were synthesized using a high-temperature solid-state method with different doping concentrations. The phase purity of the samples was confirmed using X-ray diffraction (XRD), while their photoluminescence properties were characterized through excitation and emission spectroscopy. Luminescence decay times and quantum efficiencies were also measured to assess the performance of the doped phosphors. XRD analysis revealed that most doped samples remained single-phase up to 1 % dopant concentration, with impurity phases emerging at higher concentrations. Photoluminescence measurements demonstrated distinct emission characteristics for each dopant: red emission from Eu^{3+}, yellow from Dy^{3+}, orange from Pr^{3+}, orange-red from Sm^{3+}, and green from Tb^{3+} (Fig 1).

$NaAlGeO_4$ doped with rare-earth ions demonstrates promising luminescent properties, making it a viable candidate for applications in light-emitting devices and persistent luminescence materials. The ability to fine-tune emission wavelengths by varying dopant concentrations highlights the versatility of this host for future optoelectronic applications.

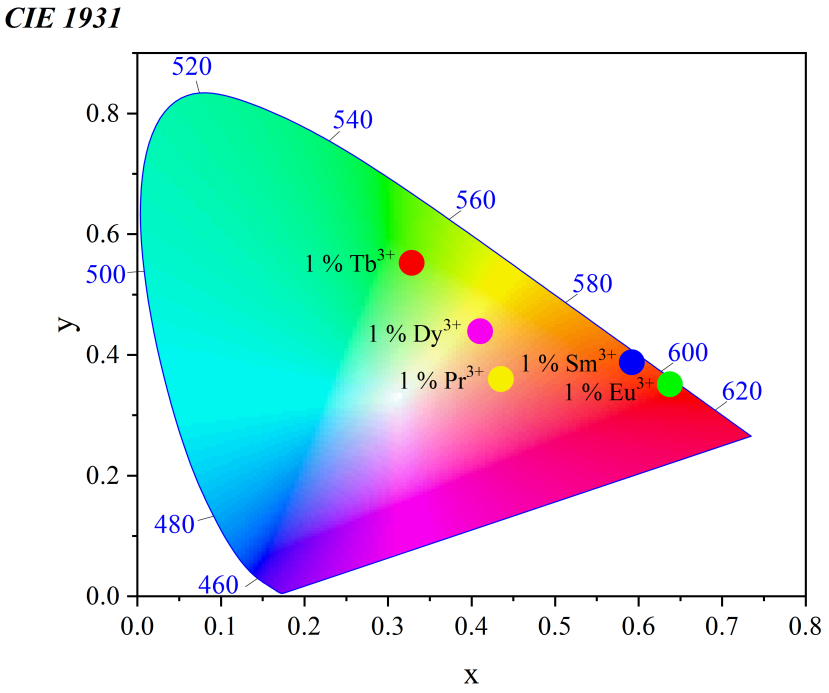


Fig. 1. CIE 1931 chromaticity diagram of 1 % Dy, Eu, Pr, Sm, Tb^{3+}-doped $NaAlGeO_4$

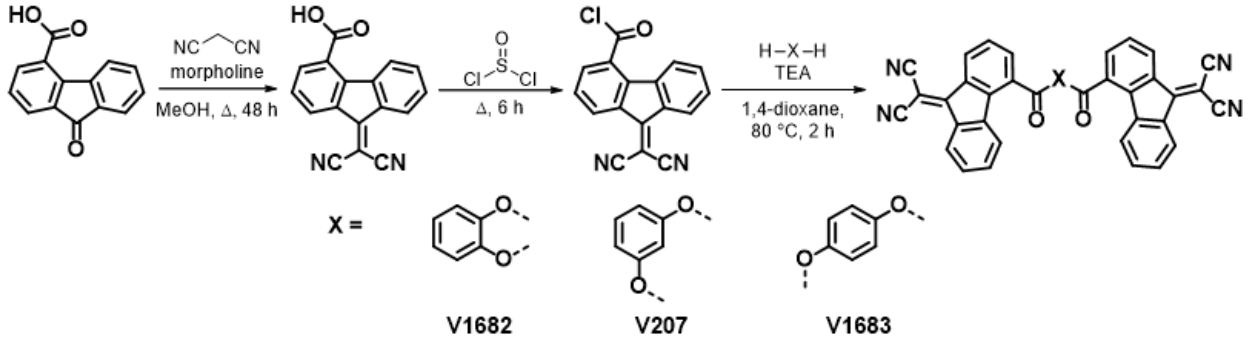
SYNTHESIS AND PROPERTIES OF (9-FLUORENYLIDENE)MALONONITRILE DERIVATIVES AS ELECTRON TRANSPORTING MATERIALS

Julius Petrulevičius[1], Marytė Daškevičienė[1], Giedrė Bubnienė[1], Giedrius Juška[2], Vygintas Jankauskas[2], Vytautas Getautis[1]

[1]Department of Organic Chemistry, Kaunas University of Technology, Lithuania
[2]Institute of Chemical Physics, Vilnius University, Lithuania
julius.petrulevicius@ktu.lt

As a result of increasing global warming, renewable energy sources are gaining more interest as an alternative to fossil fuels. One of these alternatives is the Sun, which is an infinite resource of energy. Solar cells (SC), also known as photovoltaic devices, are used for the conversion of solar energy into electricity. Nowadays, silicon solar cells (first-generation photovoltaic technology) still dominate the photovoltaic market due to high efficiency and high device stability, despite having several disadvantages such as high cost, inflexibility, and opacity, which limit their future development prospects. Fortunately, perovskite solar cells (PSCs) have undoubtedly become the super star in the photovoltaic field, and now the certified power conversion efficiency (PCE) has reached a very high level of 27.0%, which is comparable to that of crystalline silicon solar cells [1].

Due to low cost and straightforward synthesis, organic electron transport materials (ETMs) have recently attracted much attention as an alternative to fullerene C60. ETMs are an important component of photovoltaic devices, facilitating the transport of photogenerated electrons from the photoactive layer to the cathode. One of the advantages of using organic semiconductors is the possibility of constructing lightweight and flexible devices [2, 3].



Scheme 1. Synthesis of ETMs **V1682**, **V207**, and **V1683**

Table 1. The electron drift mobility of new ETMs

ETM	*d* [μm][a]	*μ*(0) [cm²/Vs][b]	*μ*(1·10⁶ V/cm) [cm²/Vs][c]
V1682	2.4	$1.5 \cdot 10^{-6}$	$9.6 \cdot 10^{-4}$
V207	2.4	$1.3 \cdot 10^{-6}$	$6.9 \cdot 10^{-4}$
V1683	3.2	-	$\sim 7 \cdot 10^{-6}$

[a]Thickness of the evaporated semiconductor. [b]Electron drift mobility in zero field. [c]Electron drift mobility at an electric field of $1 \cdot 10^6$ V/cm.

In this work, new ETMs **V1682**, **V207** and **V1683** were obtained by a three-step synthesis (**Scheme 1**). The thermal, optical, and photoelectric properties of these materials were investigated. Measurements of the electron drift mobility of the new organic semiconductors **V1682**, **V207** and **V1683** have revealed that mobility decreases with increasing distance between two (9-fluorenylidene)malononitrile chromophores in the molecule (**Table 1**).

[1] National Renewable Energy Laboratory: best research-cell efciencies chart. Available at https://www.nrel.gov/pv/cell-efficiency.html.
[2] Lian, J. et al. Electron-Transport materials in perovskite solar cells. Small Methods, 2(10), (2018).
[3] Zhang, S. et al. GraphDiyne: Bridging SNO2 and perovskite in Planar solar cells. Angewandte Chemie International Edition, 59(28), 11573–11582, (2020).

SYNTHESIS AND OPTICAL PROPERTIES OF Mn^{5+} -DOPED $Sr_5(PO_4)_3F$

Jonas Stadulis[1], Arturas Katelnikovas[1], Aleksej Zarkov[1]

[1]Institute of Chemistry, Faculty of Chemistry and Geosciences, Vilnius University, Naugarduko 24, LT-03225 Vilnius, Lithuania
jonas.stadulis@chgf.stud.vu.lt

As technologies are advancing, demand for new chemical materials is increasing. Part of the materials of interest are optically active materials, which usually consist of host matrix and dopant – optically active ion. For example, these materials can be used for a wide range of applications, including luminescence thermometers or manometers, lasers, LEDs, or even biomedicine, etc. One of the suitable host materials can be strontium fluorapatite ($Sr_5(PO_4)_3F$; SFAp). Because of alkaline strontium properties and the presence of P^{5+} ions in the structure, SFAp can adopt and stabilize optically active Mn^{5+} ions, which are usually unstable under normal conditions. Mn^{5+} ions have a wide excitation range, including the NIR-I region as well as intense emission in the NIR-II range. Due to the mentioned properties, Mn^{5+}-doped strontium fluorapatite is a promising material to use in many applications such as luminescent thermometry, NIR lasers, or biomedicine.

The main goal of the present work was to synthesize Mn^{5+}-doped SFAp powders and investigate their optical properties. Synthesis was performed in two steps. Firstly, strontium nitrate ($Sr(NO_3)_2$), diammonium hydrogen phosphate ($(NH_4)_2HPO_4$) and ammonia ($NH_{3(aq)}$) were used for wet-precipitation synthesis of strontium phosphate ($Sr_3(PO_4)_2$). Secondly, $Sr_5(PO_4)_3F$ powders doped with various amounts of Mn^{5+} ions were obtained by molten salts method using $Sr_3(PO_4)_2$, strontium fluoride (SrF_2), sodium fluoride (NaF) and manganese (II) nitrate tetrahydrate ($Mn(NO_3)_2 \bullet 4H_2O$) as starting materials. Phase purity and crystal structure of synthesized samples were studied by powder X-ray diffraction (XRD), infrared (FTIR) and Raman spectroscopies. Morphological features of synthesized materials were investigated by scanning electron microscopy (SEM). The chemical composition of the samples was determined by inductively coupled plasma optical emission spectrometry (ICP-OES). Optical properties were investigated by means of photoluminescence measurements: reflectance spectra, excitation spectra, emission spectra, and decay times were measured. Temperature-dependent measurements were performed as well.

THE SOL-GEL SYNTHESIS AND CHARACTERIZATION OF $Y_{2.97-x}$ $Na_x$$Tb_{0.03}$$Al_5O_{12}$ garnets

Diana Vistorskaja[1], Arturas Katelnikovas[1], Gintautas Tamulaitis[2], Aivaras Kareiva[1]

[1]Institute of Chemistry, Faculty of Chemistry and Geosciences, Vilnius University, Naugarduko st. 24, LT-03225 Vilnius, Lithuania
[2]Institute of Photonics and Nanotechnology, Faculty of Physics, Vilnius University, Sauletekis av. 3, LT-10257 Vilnius, Lithuania
diana.vistorskaja@chgf.vu.lt

In recent years, inorganic luminescent materials have become essential components in various lighting systems, significantly influencing the functionality of these devices [1]. These luminescent materials typically consist of two components: a crystalline matrix and an activator [2]. When searching for and developing new luminescent materials, it is crucial to select an appropriate optically active ion and a suitable crystalline host for its embedding [3]. Among many hosts, garnet crystal structure compounds are recognized as particularly important optical host materials [4]. Yttrium aluminium garnet (YAG) is a prominent synthetic garnet known for its impressive characteristics, such as broad optical transparency spectrum range, high chemical stability and the capacity to incorporate big amounts of dopants (Ln^{3+}) substituting for Y^{3+}. YAG doped with lanthanides or transition metal ions has found use in a wide range of applications including all-color phosphors, solid-state lasers, scintillators, and vacuum fluorescent displays [3-6]. For example, YAG:Tb is a green phosphor that stands out for its thermal stability. Additionally, the emission color of this luminescent material can change from violet/blue to green, depending on the concentration of terbium. Due to these characteristics, YAG:Tb is used in plasma screens and cathode ray tubes [2]. It is well known that the optical properties of luminescent materials are influenced by both the doping ions and their concentrations, as well as the crystal structure and chemical composition of the phosphor host material. In this study, the YAG matrix was modified by substituting yttrium with sodium and terbium. The primary objective was to synthesize novel garnet-type luminescent materials and investigate their structural and morphological features, as well as to study their optical properties. All the obtained products were characterized by using XRD, FTIR, and SEM methods. Also, the emission and excitation spectra were recorded, the colour coordinates, the decay times and quantum efficiencies were obtained.

Acknowledgements

This research has been carried out in the framework of the „Universities' Excellence Initiative" programme by the Ministry of Education, Science and Sports of the Republic of Lithuania under the agreement with the Research Council of Lithuania (project No. S-A-UEI-23-6).

[1] S. Ye, F. Xiao, Y.X. Pan, Y. Y. Ma, Q. Y. Zhang, Phosphors in phosphor-converted white light-emitting diodes: Recent advances in materials, techniques and properties (Mat. Sci. Eng. R., 71 (2010) 1-34)
[2] J. C. A. Santos, E. P. Silva, N. R. S. Souza, Y. G. S. Alves, D. V. Sampaio, C. Kucera, L. G. Jacobsohn, J. Ballato, R. S. Silva, Laser sintering and photoluminescence study of Tb-doped yttrium aluminum garnet ceramics (Ceram. Int., 45 (2019) 3797-3802)
[3] E. Hertle, L. Chepyga, M. Batentschuk, S. Will, L. Zigan, Temperature-dependent luminescence characteristics of Dy3+ doped in various crystalline hosts (J. Lumin., 204 (2018) 64–74)
[4] A. Jain, P. Sengar, G. A. Hirata, Rare-earth-doped Y3Al5O12 (YAG) nanophosphors: synthesis, surface functionalization, and applications in thermoluminescence dosimetry and nanomedicine (J. Phys. D Appl. Phys., 51 (2018) 303002 1–62)
[5] C. Liao, F. Liu, H. Wu, H. Wu, L. Zhang, G. Pan, Z. Hao, X. Wang, J. Zhang, Creating Deep Traps in Yttrium Aluminum Garnet for Long-Term Optical Storage and Afterglow-Intensity-Ratio-Based Temperature Sensing (Laser Photonics Rev., (2024) 2300924)
[6] Y. K. Li, Y. F. Liu, Z. H. Luo, Z. H. Liu, S. Hanson, C. H. Pang, H. Lin, H. M. Qin, J. Jiang, Ce/Mn/Cr: Y3Al5O12 phosphor ceramics for white LED and LD lighting with a high color rendering index (Ceram. Int., 49 (2023) 24703-24711)

CHARACTERIZATION OF OPTICAL AND MECHANICAL PROPERTIES OF $Ti_3C_2T_x$ MXENE THIN FILMS

Miglė Stančiauskaitė[1], Justina Anulytė[2], Simonas Ramanavičius[2], Ernesta Bužavaite-Vertelienė[2], Zigmas Balevičius[2], Ieva Plikusienė[1]

[1]NanoTechnas - Center of Nanotechnology and Materials Science, Faculty of Chemistry and Geosciences, Vilnius University, Naugarduko Str. 24 Vilnius, Lithuania
[2]State Research Institute Center for Physical and Technological Sciences, Sauletekio ave. 3 Vilnius, Lithuania
migle.stanciauskaite@chgf.stud.vu.lt

MXenes are a family of two-dimensional transition metal carbides and nitrides with a general formula $M_{n+1}X_nT_x$ (where M is an early transition metal, X is C or N, Tx represents surface terminations). The plasmonic behavior in the infrared, broadband absorbance, and high refractive index of MXenes make them promising candidates for optical biosensing platforms [1]. MXenes exhibit high surface area and tunable surface chemistry, making them a viable biosensing platform.

In this study, we explore the optical and mechanical properties of spin-coated multilayered MXene films alongside the chemical stability of single-layer coatings, offering critical insights into their potential applications in diverse sensing environments. Multilayer MXene films were spin-coated onto BK7 glass substrates to systematically study the relationship between layer thickness and optical properties. Ellipsometric measurements revealed uniform thickness growth, demonstrating controlled layer deposition.

Single-layer MXene was deposited onto a QCM-D electrode to evaluate its stability and mechanical properties under acidic pH conditions. Frequency and dissipation monitoring provided real-time data on mass changes and viscoelastic responses. The MXene layer exhibited uniform stability across 3 different acetate buffer pH values, revealing the minimal impact of short-term environmental changes on film integrity.

Together, these findings offer a dual perspective on MXene thin films highlighting the relationship between deposition method and structural properties, emphasizing their potential for integration into optical and acoustic sensing devices.

[1] K. Chaudhuri, M. Alhabeb, Z. Wang, V. M. Shalaev, Y. Gogotsi, and A. Boltasseva, “Highly Broadband Absorber Using Plasmonic Titanium Carbide (MXene),” ACS Photonics, vol. 5, no. 3, pp. 1115–1122, Mar. 2018, doi: 10.1021/acsphotonics.7b01439.

PHYSICAL AND CHEMICAL CHARACTERISTICS OF MICROPLASTIC PARTICLES IN LITHUANIANS SCHOOLS PREMISES

Tomas Stonkus[1], Ieva Uogintė[2], Steigvilė Byčenkienė[3]

[1]Center for Physical Sciences and Technology, Department of Environmental Research
tomas.stonkus@ftmc.lt

Plastic has become one of the most widely used materials since its invention as a phenol-formaldehyde resin. It was originally created to make life easier, but today it poses a serious threat to the environment and human health [1]. In recent decades, the increasing use of synthetic polymers in various industries has led to a rise in microplastic pollution in the air. These tiny particles, often smaller than 5 millimeters, come from different sources. Primary microplastics, like microbeads in personal care products, and secondary microplastics, which form when larger plastic items break down, spread through the atmosphere. Once in the air, they can travel long distances and pose risks to both the environment and human health [2]. It is important to analyze microplastic particles in the indoor air, since about 90 % of our time is spent indoors [3]. Not only that, microplastic particles concentrations are 1.8 times larger compared to outdoor air [4].

In this study indoor microplastic particles were collected by teachers using 5,5 cm paper filter left out in the school premises for a week. In the laboratory paper filters are washed with filtered distilled water. Samples then go through chemical processing with concentrated hydrogen peroxide for 24h and concentrated hydrochloric acid for 1h. For separating microplastics from denser impurities such as dirt or sand, zinc chloride solution is used for 1h. After chemical processing samples are transferred to fiberglass filter for optical analysis and aluminum dioxide filter for chemical composition using FTIR spectroscopy.

This study aims to analyze microplastic particles found in the air across Lithuania schools' premises, focusing on their size, color, shape, and chemical composition. This research will help expand knowledge about microplastic contamination in the air and its potential negative effects.

Acknowledgements

We would like to thank the schools, teachers, and students who helped to collect data on indoor microplastic particles in Lithuanian school's premises

[1] Hassan Khalid Ageel, Stuart Harrad, Mohomed Abou-Elwefa Abdallah, Environmental Pollution, volume 362, Microplastics in indoor air from Birmingham, UK: Implications for inhalation exposure, 2024, https://doi.org/10.1016/j.envpol.2024.124960

[2] Adel Mokammel, Kazem Naddafi, Mohammad Sadegh Hassanv and and others, Emerging Contaminants 11, Airborne microplastics pollution in municipal solid waste processing and disposal complex: Concentration, characterization, and composition, 2025, https://doi.org/10.1016/j.emcon.2024.100459

[3] Hassan Khalid Ageel, Stuart Harrad and Mohamed Abou-Elwafa Abdallah, Environmental Science: Processes & Impacts, Occurrence, human exposure, and risk of microplastics in the indoor environment, 2022

[4] Muhammad Jahanzaib, Shambhavi Sharma, Duckshin Park, Emerging Contaminants 11, Microplastics comparison of indoor and outdoor air and ventilation rate effect in outskirts of the Seoul metropolitan city, 2025, https://doi.org/10.1016/j.emcon.2024.100408

POTENTIAL APPLICATION OF BUCKWHEAT HULL FOR EFFICIENT BIOSORPTION OF CADMIUM FROM AQEUOUS MEDIA: AN INSIGHT INTO THE SORPTION KINETIC, EQUILIBRIUM AND THERMODYNAMIC STUDIES

Tayyab Tahir[1], Rūta Druteikienė[1], Zita Žukauskaitė[1], Jūratė Vaičiūnienė[2]

[1]Center for Physical Sciences and Technology, Department of Nuclear Research Savanorių ave. 231, LT-02300 Vilnius, Lithuania
[2]Center for Physical Sciences and Technology, Department of Catalysis Saulėtekio av. 3, LT-10257 Vilnius, Lithuania
tayyab.tahir@ftmc.lt

Water pollution by heavy metals is a serious global issue due to their high toxicity, non-biodegradability, and persistence in the environment. Human activities such as mining, metal production, electronics electroplating, agriculture, and metallurgical waste disposal are the main contributors to the increased concentrations of hazardous metals. Long-term exposure to hazardous heavy metals can cause irreversible damage to various biological systems [1]. Among these, cadmium (Cd) is a toxic heavy metal that can contaminate water systems due to its higher solubility compared to other heavy metals. Therefore, according to the Environmental Protection Agency and the World Health Organization, the level of cadmium concentration in water should be in the range of 4.0-10.0 mg/L. Excessive exposure to cadmium can cause health problems. In many regions, cadmium levels are above safe limits. That's why it's important to detect and then remove Cd(II) ions from industrial wastewater [2].

Technologies such as ion exchange, solvent extraction, membrane-based processes, and precipitation are used for heavy metal removal from industrial effluents. However, all of these methods have some limitations in term of technical and economic feasibility. This has led environmentalists to focus on developing better, cheaper, and more effective removal techniques that use biological materials. Biosorption is an alternative method for heavy metals removal from water, replacing the above-discussed techniques [3].

The aim of this study is to provide an alternative to existing techniques in terms of efficiency, economy, and sustainability. In this study, buckwheat hulls, have been used for the efficient removal of Cd(II) from aqueous media. The sorption capacity and removal percentage of Cd(II) on buckwheat hulls were examined using batch sorption experiments with different parameters such as contact time, solution pH, biosorbent dose, temperature, and initial Cd(II) concentration. The results obtained were examined for isotherm, kinetic, and thermodynamic study. SEM, EDX, FTIR, and pH of point of zero charge confirmed the favorable biosorption surface characteristics. The maximum Cd(II) sorption by buckwheat hulls was 97.5% at pH 5, initial Cd(II) concentration of 10 mg/L, contact time for 180 min, sorbent dose of 0.1 g, temperature of 25 °C, and agitation speed 150 rpm. A kinetic study shows that the pseudo-second-order (R^2=0.999) is suitable for this sorption process. The isotherm study shows that the Langmuir model (R^2=0.998) is the best to explain experimental data, with a maximum sorption capacity of 44.44 mg/g. The thermodynamic parameter shows that the removal of Cd(II) by buckwheat hulls is an exothermic and non-spontaneous process.

These results showed that buckwheat hulls are suitable for the effective removal of metals from the aqueous media.

[1] Kaleem, M., et al., Molecules, 28(5): p. 2292 (2023).
[2] Alamrani, N., et al., Materials Today Chemistry, 30: p. 101547 (2023).
[3] Pérez-Marín, A.B., et al., Processes, 12(1): p. 148 (2024).

A MACHINE LEARNING FRAMEWORK FOR AIR POLLUTION MODELING USING SATELLITE DATA AND URBAN SPATIAL FEATURES IN VILNIUS

Mehri Davtalab[1], Steigvilė Byčenkienė[1]

[1]SRI Center for Physical Sciences and Technology (FTMC), LT-10257 Vilnius, Lithuania
mehri.davtalab@ftmc.lt

Urban air pollution remains a critical challenge for public health and environmental management, particularly in regions where ground-based monitoring stations are sparse. Previous studies have primarily examined individual pollutants [1,2], while simultaneous contamination by multiple pollutants has received less attention. Effective modeling of multi-pollutant air pollution requires integrating diverse data sources and addressing the spatial heterogeneity of urban areas. Existing approaches often fail to achieve high accuracy in urban settings due to limited data coverage and the complex interplay among built-up areas, green spaces, and pollutant dispersion. This study presents a machine learning-based framework utilizing a Random Forest (RF) model to estimate the multi-pollutant concentrations (NO_2, SO_2, CO) distribution in Vilnius (Fig1).

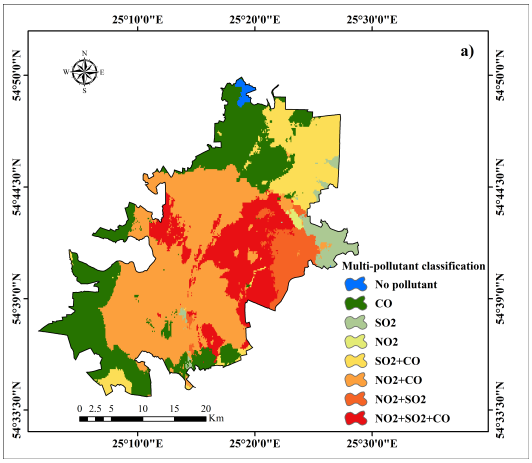


Fig. 1. Spatial distribution of multi-pollutants in Vilnius using RF model

It integrates diverse data sources, including satellite retrievals, sparse ground station measurements, meteorological data, urban built-up density, green space metrics, and geographical classification maps, to address urban heterogeneity. Evaluation of the RF model across the study area yielded robust performance metrics: Accuracy = 0.900, Precision = 0.895, Recall = 0.897, and F1 Score = 0.896. This work demonstrates that combining machine learning with multi-source data and urban spatial features provides scalable and accurate multi-pollutant air pollution modeling, offering valuable insights for urban environmental planning and public health interventions.

Acknowledgements

This research was funded by the Lithuanian Research Council LMT and is implemented under the Postdoctoral Fellowship agreement Nr. S-PD-24-137

[1] Dong J, Cai X, Tian L, Chen F, Xu Q, Li T, et al. (2023); Satellite-based estimates of daily NO2 exposure in urban agglomerations of China and application to spatio-temporal characteristics of hotspots. Atmospheric Environment ; 293: 119453

[2] Karppinen T, Sundström A-M, Lindqvist H, Hatakka J, Tamminen J. (2024); Satellite-based assessment of national carbon monoxide concentrations for air quality reporting in Finland. Remote Sensing Applications: Society and Environment ; 33: 101120.

SOURCE APPORTIONMENT OF AEROSOL PARTICLES BY POSITIVE MATRIX FACTORIZATION IN URBAN BACKGROUND ENVIRONMENT (VILNIUS, LITHUANIA)

Viachaslau Alifirenka[1], Vitalij Kovalevskij[1], Mindaugas Gaspariūnas[1], Mindaugas Bernatonis[2], Steigvilė Byčenkienė[1]

[1]SRI Center for Physical Sciences and Technology (FTMC), Saulėtekio ave. 3, LT-10257 Vilnius, Lithuania
[2]Environmental Protection Agency, A. Juozapavičiaus str. 9, LT-09311 Vilnius, Lithuania
viachaslau.alifirenka@ftmc.lt

An aerosol is defined as a suspension of a liquid or solid particles suspended in a gas. Aerosols are a key contributor to environmental issues such as global warming, photochemical smog, and poor air quality. The health risks of aerosol exposure in urban areas pose a significant health concern. Awareness of the potential health impacts from aerosol anthropogenic sources particularly those associated with fine particles has increased only in recent years. The problem of environmental pollution in cities is relevant and the need to know the sources of pollution is a very important aspect for monitoring and reducing pollution [1]. The aim of this study was to determine the sources of aerosol particles using positive matrix factorization in an urban background environment. Measurements were performed from January 2 to December 21, 2019 at the urban background site located at the Vilnius. 100 samples of PM2.5 were collected on polytetrafluoroethylene filters and investigated by broad-beam particle-induced X-ray emission (PIXE) using 1.9 MeV protons. A proton beam, accelerated using a Tandetron 4110A ion accelerator and collimated to a diameter of 5 mm, was used to irradiate the samples. A single spectrum was measured for each PM2.5 sample, and the ppm (ng/cm3) levels were evaluated by assuming homogeneous deposition of PM on the filters. X-ray spectra are recorded using a Canberra SL30165 Si(Li) detector with 165 eV energy resolution at 5.894 keV and Canberra DSA1000 MCA. The distance between the sample and the detector was 59.5 mm (8.5 msr). X-ray spectra were fitted using the GupixWin software package for quantitative elemental analysis. The NIST-2783 standard reference material (PM2.5 deposited on the filter) was used to calibrate the X-ray yield. Eleven elements (Al, Si, K, Ca, Cr, Mn, Fe, Co, Ni, Cu, and Zn) were identified in the analysed samples. Figure 1 shows the distribution of concentrations of 11 identified elements and their presence in the factors.

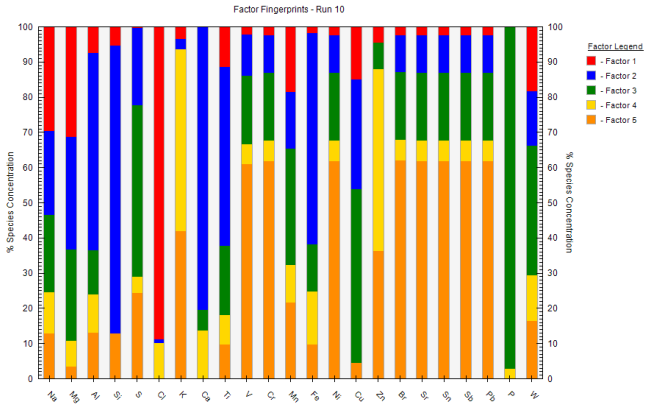


Fig. 1. PM2.5 factors(sourses) profile for Vilnius urban background area from 2 January to 21 December 2019

Positive matrix factorization method was applied to assess the source apportionment of aerosol particles. The analysis revealed five factors (sources): factor 1 – coal and oil combustion, factor 2 – traffic, factor 3 – industrial emission, factor 4 – soil, factor 5 – biomass burning.

[1] Aerosol science: Technology and applications. Ian Colbeck, Mihalis Lazaridis, 2014

SYNTHESIS AND APPLICATION OF $Ti_3C_2T_X$ MXENES FOR DRINKING WATER QUALITY ASSESSMENT

Kristina Sobol[1,2], Almira Ramanaviciene[1], Simonas Ramanavicius[2]

[1]NanoTechnas – Center of Nanotechnology and Materials Science, Institute of Chemistry, Faculty of Chemistry and Geosciences, Vilnius University, Naugarduko St. 24, LT-03225, Vilnius, Lithuania
[2]Center for Physical Sciences and Technology, Department of Electrochemical Material Science, Sauletekio av. 3, LT-10257, Vilnius, Lithuania
kristina.sobol@chgf.vu.lt

Water pollution remains a pervasive problem, leading to 1.8 million deaths each year and posing significant threats to human, animal, and plant health. The main sources of water contamination include industrial and agricultural waste, maritime traffic, and fuel spillages, releasing millions of tons of pollutants into the water worldwide [1]. The challenges in detecting and removing certain pollutants highlight the necessity of innovative solutions for environmental applications.

MXenes is a novel family of two-dimensional (2D) inorganic nanomaterials, first discovered in 2011 at Drexel University's College of Engineering. The MXene family, with the general structure of $M_{n+1}X_nT_x$, where M is a transition metal, X is C and/or N, and T_x is the surface functional group, consists of transitional metal carbides, nitrides, and carbonitrides [2]. Due to their large surface area, simple surface functionalization, tunable hydrophilicity, biocompatibility, and high adsorption capacity of both organic and inorganic materials, MXenes hold great promise in various fields, including electronics, energy storage, energy conversion, and biotechnology. In particular, MXenes could be a promising solution for assessing drinking water quality and pollutant removal [3].

In this study, we successfully synthesized and applied spherical and layered $-SO_4$ and -F functionalized $Ti_3C_2T_x$ MXenes to detect water pollutants of various origins. Our findings demonstrate the effectiveness of the synthesized MXenes in detecting different chemical compounds, offering valuable insights into the potential application of $-SO_4$ and -F functionalized $Ti_3C_2T_x$ MXenes in wastewater treatment.

Acknowledgements
This project received funding from the Research Council of Lithuania (LMTLT), agreement No. S-MIP-24-14.

[1] P.M.Boersenberger D. Bury, M, Jakubczak, R. Kumar, D. Sciezynska, B.Jan, P. Marcinowski, A. M. Jastrzebska, Cleaning the environment with MXenes, MRS Bulletin, 48, 10.1557/s43577-023-00507-6 (2023).
[2] S. Adomaviciute-Grabusove, A. Popov, S. Ramanavicius, V. Sablinskas, K. Schevchuk, O. Gogotsi, I. Baginskiy, Y. Gogotsi, A. Ramanavicius, Monitoring Ti‘3C‘2Tx MXene Degradation Pathways Using Raman Spectroscopy, ACS Nano, 18, 20, 13184-13195 (2024).
[3] S. Zukauskas, A. Rucinskiene, S. Ramanavicius, A. Popov, G. Niaura, I. Baginskiy, V. Zahorodna, S. Dukhnovskiy, O. Gogotsi, A. Ramanavicius, Electrochemical real-time sensor for the detection of Pb(II) ions based on Ti3C2Tx MXene, Science of The Total Environment, Volume 950, 175190 (2024).

EXPLORING THE INFLUENCE OF BIOMASS BURNING ON ATMOSPHERIC AEROSOLS THROUGH ISOTOPIC ANALYSIS

Durre Nayab Habib[1], Andrius Garbaras[2], Agnė Mašalaitė-Nalivaikė[3]

[1]State research institute, Center for Physical Sciences and Technology, Vilnius, LT-10257, Lithuania
durre.nayab@ftmc.lt

Keywords: biomass burning, aerosol, isotopic fractionation.

Biomass burning is a major contributor to atmospheric aerosols, releasing a variety of particles and gases that have significant environmental impacts. These aerosols not only affect local and regional air quality but also can be transported globally, influencing climate and atmospheric conditions in distant areas. This study investigates the aerosols produced from 17 different wood species and coal, focusing on their isotopic signatures of total carbon, elemental carbon, and organic carbon at varying combustion temperatures. The experimental setup was designed to replicate typical domestic heating practices in Lithuania during the winter months. Our findings reveal a wide range of isotopic variations in the carbon isotopes (δ13C) across the biomass fuels used in the burning experiments. Lower temperature combustion (below 350 °C) showed more diverse isotopic signatures compared to higher temperature stages (350 °C and 650 °C). Notably, distinct isotopic patterns emerged between C3 and C4 plants, with C4 species like corn exhibiting less negative δ13C values (-12‰), whereas C3 species, such as willow and oak, presented more negative values (-29‰ to -31‰). Elemental carbon (EC) consistently displayed more negative δ13C values compared to total carbon (TC) across most plant species, suggesting isotopic fractionation during EC formation. Additionally, the fractionation factor (ε) analysis revealed that, while most biomass materials showed ε values close to zero (indicating minimal fractionation), coal displayed unique isotopic behaviour with noticeably higher positive ε values. Overall, our study underscores the distinct isotopic signatures of different biomass fuels and coal, contributing to a deeper understanding of biomass burning aerosols and their environmental effects.

STUDY ON THE KINETICS AND ISOTHERMS OF SORPTION OF MICROPLASTICS AND LIGNIN NANOMATERIALS

Austėja Burbulytė[1], Ieva Uogintė[1]

[1]Center for Physical Sciences and Technology, Department of Environmental Research Saulėtekio av. 3, LT-10257 Vilnius
austeja.burbulyte@ftmc.lt

The global production of plastics began in the 1950s with the aim of improving daily life. Various plastic products, such as packaging, disposable dishes, and device components, have become increasingly useful. However, most plastic products through out in the environment after use, either through wastewater discharge or improper disposal (Pham et al., 2021). Also, in the environment can be found microplastics, which are particles smaller than 5 mm. These particles are found in water, soil, and the atmosphere. Every year, tons of primary and secondary microplastics are released into aquatic ecosystems, including oceans, seas, rivers, and lakes (Henderson & Green, 2020). Due to their widespread distribution and potential toxicity to living organisms, it is crucial to explore effective methods for removing these particles from water. One way is to apply the sorption process by using natural materials from nature.

This study investigates the sorption of microplastic particles using lignin and lignin-magnetite nanomaterials. One of the most important sorption parameters are time and sorbent concentration. In order to understand the sorption behavior and mechanism, it is essential to analyze the kinetics and isotherms. Two kinetic models, the pseudo-first order and pseudo-second order models, were applied in this study. Additionally, Langmuir and Freundlich isotherms were used to examine the impact of sorbent concentration on the sorption.

The results showed that the sorption of both lignin and lignin-magnetite nanomaterials is best described by the pseudo-second-order kinetic model, as correlation coefficient (R^2) values close to 1. The rate constants showed that the sorption reaction of lignin-magnetite in water occurs faster than that of lignin. Furthermore, theoretical sorption capacity values were found to be consistent with the experimental results. Sorption isotherms revealed the relationship between lignin and lignin-magnetite concentrations and their sorption capacities. The dominated sorption mechanism of both nanomaterials is chemisorption.

[1] Henderson, L., & Green, C. (2020). Making sense of microplastics? Public understandings of plastic pollution. Marine Pollution Bulletin, 152. https://doi.org/10.1016/j.marpolbul.2020.110908

[2] Pham, T. H., Do, H. T., Phan Thi, L. A., Singh, P., Raizada, P., Chi-Sheng Wu, J., & Nguyen, V. H. (2021). Global challenges in microplastics: From fundamental understanding to advanced degradations toward sustainable strategies. Chemosphere, 267. https://doi.org/10.1016/j.chemosphere.2020.129275

REMOVAL OF MICROPLASTICS FROM WATER USING A CATIONIC STARCH FLOCCULANT

Klaudija Cerkaite[1], Joana Bendoraitiene[2]

[1]Department of Polymer Chemistry and Technology, Kaunas University of Technology, Lithuania
klaudija.cerkaite@ktu.edu

Microplastics (MP) that are widespread in aquatic environments around the world is one of the biggest environmental problems and poses a major threat not only to the aquatic ecosystem but also to humans [1]. Flocculation is one of the ways of removing microplastics from water. The flocculants currently used are synthetic and therefore not only contribute to environmental pollution but also can be toxic [2]. Therefore, the main objective of this work was to synthesize cationic starches and to explores them use as flocculants for the removal of microplastics from water.

Sixteen cationic starch derivatives were synthesized by the etherification reaction of potato starch and various amounts of (3-chloro-2-hydroxypropyl)trimethylammonium chloride (CHTAC) as a cationization agent (CA) in aqueous medium with or without CaO and $CaCl_2$ additives. The cationic starch selected for the flocculation study was obtained at the molar ratio of starch : CHTAC : $CaO/CaCl_2$: NaOH : H_2O of 1 : 0.21 : 0.04/0.1 : 0.31 : 3.1, at a temperature of 45 °C, and the reaction duration of 16 hours.

The flocculation properties of synthesized cationic starch were tested using two aqueous model systems, namely, those of kaolin and industrially produced polyethylene (PE) microparticles as well as an aqueous microdispersions of artificially obtained polystyrene (PS) and polypropylene (PP) particles. The amount of microplastic particles in water ranged from 500 to 1500 mg/l and the optimum amounts of cationic starch required to destabilize the tested suspensions were established. In was determined that cationic starch concentration of 0.6, 1, 1, and 7.5 mg/l was required to destabilize the aqueous suspensions of PE, PP, PS and kaolin, respectively. The performed studies have shown that cationic starches have suitable properties to be applied as biopolymer-based flocculants for removing microplastics from water.

[1] W. Gao, Y. Zhang, A. Mo, J. Jiang, and Y. Liang. Removal of microplastics in water: Technology progress and green strategies. Green Analytical Chemistry, Vol. 3, 2022. [Online]. Available: https://doi.org/10.1016/j.greeac.2022.100042. [Accessed Feb. 08, 2025].

[2] L. Dayal, K. Yadav, U. Dey, K. Das, and P. Kumari. Recent advancement in microplastic removal process from wastewater - A critical review. Journal of Hazardous Materials Advances, Vol. 16, 2024. [Online]. Available: https://doi.org/10.1016/j.hazadv.2024.100460. [Accessed Feb. 08, 2025].

APPLICATION OF MAGNETIC BIOPOLYMERS FOR WATER PURIFICATION RADIONUCLIDES AND HEAVY METALS

Sergej Šemčuk[1,7], Galina Lujanienė[1], Kęstutis Jokšas[2], Karina Kuzborskaja[1], Vidas Pakštas[3], Kęstutis Mažeika[4], Martynas Talaikis[5], Jonas Mažeika[6], Živilė Jurgelėnė[7]

[1]Department of Environmental Research, Center for Physical Sciences and Technology, Vilnius, Lithuania
[2]Laboratory of Geoenvironmental Research, Nature Research Centre, Vilnius, Lithuania
[3]Dep. of Characterisation of Materials Structure, Center for Physical Sciences and Technology, Vilnius, Lithuania
[4]Department of Nuclear Research, Center for Physical Sciences and Technology, Vilnius, Lithuania
[5]Department of Organic Chemistry, Center for Physical Sciences and Technology, Vilnius, Lithuania
[6]Laboratory of Nuclear Geophysics and Radioecology, Nature Research Centre, Vilnius, Lithuania
[7]Laboratory of Ecotoxicology, Nature Research Centre, Vilnius, Lithuania
karina.kuzborskaja@ktu.edu

Pollution of the environment with heavy metals has consequences for public health due to their toxicity, their longevity, their rapid migration in aquatic ecosystems and their ability to bioaccumulate in organisms entering the food chains [1]. Various technologies are used to purify polluted water, such as sedimentation, flocculation, evaporation, membrane technology, etc. However, the most promising is still the adsorption method using various sorbents, such as activated carbon, zeolites, polymers, functionalized silicon, clay, etc., since it is considered one of the most effective and simplest. Among them, biopolymers such as chitosan and cellulose are particularly in demand due to their non-toxicity and biodegradability, their widespread use and natural origin, regenerability and modifiability, low-cost and biocompatibility [2-3]. This work aims to study the sorption capabilities of synthesised magnetic chitosan (MCN) in various aqueous media.

Synthesised MCNs were characterised using the XRD, SEM, FT-IR and Mössbauer methods to verify the composition, morphology and magnetic properties. Experiments were carried out to investigate the dependence of the adsorption of Cu (II), Ni (II) and Cr (II) on the concentration, removal efficiency (Fig. 1), pH value and contact time. In addition, the sorption potential of MCNs was tested on water samples from different aquatic ecosystems (Baltic Sea, Balsys Lake and Neris River) using the trace radionuclides (^{152}Eu and ^{60}Co). A gamma-spectrometer was used for concentration determination in the traced samples and ICP-OES for heavy metals. The sorption data obtained were analyzed with the isothermal studies, and sorption kinetic parameters for MCNs were calculated.

The results obtained indicate that the MCN adsorbent can be considered quite effective for the removal of heavy metals. It can be used for the pre-concentration of radionuclides and can be easily separated from the medium/sample using a magnet.

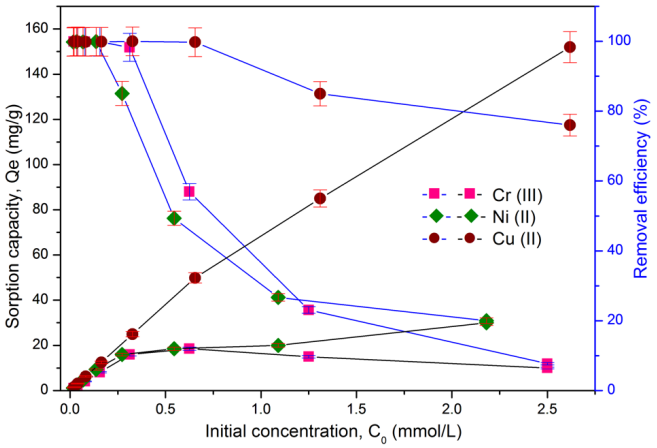


Fig. 1. Sorption capacity and removal efficiency of MCN for Cr (III), Ni (II) and Cu (II).

Acknowledgements
This work was funded by the Research Council of Lithuania, Projects No. P-SV-24-772 and S-PD-24-44.

[1] Saikat Mitra et al., J. of King Saud Uni. Vol.34, I.3, 101865 (2022).
[2] Mohammad Shahadat et al., Polymer 254, 124975 (2022).
[3] Camilo Zamora-Ledezma et al., Env. Techn. & Inn. 22, 101504 (2022).

THE IMPACT OF ISOPROPANOL TREATED SPENT COFFEE GROUNDS ON VARIOUS PROPERTIES OF BUILDING GYPSUM

Neringa Matutytė[1], Nora Kybartienė[1]

[1]Department of Silicate Technology, Kaunas University of Technology, Lithuania
neringa.matutyte@ktu.edu

Till this day coffee is the most consumed beverage worldwide. As a result, plenty of waste is being generated during the coffee brewing process. It was estimated that from 1 ton of green coffee beans, 650 kg of spent coffee grounds (SCG) are generated, making the SCG a major threat to the environment [1]. This type of biomass is rarely used somewhere else, therefore most of the time SCG end up in landfills. Due to their decomposition, spent coffee grounds emit environmentally harmful carbon dioxide and methane gases, which contribute to the faster global warming [2]. Moreover, SCG are rich in various chemical compounds, which can be extracted to make higher value products. For example, the oil content in SCG makes around 15-20 % and later can be used for biodiesel production [3]. Unfortunately, the information about what happens with SCG after oil extraction and where they can be further utilized, instead of ending up in the landfills again, is rather scarce.

The aim of the present study was to determine the impact of solvent treated spent coffee grounds on the building gypsum properties. In this research Arabica spent coffee grounds were treated with isopropanol for 0.5 and 2 hours. Gypsum and SCG were characterized using STA, XRF, XRD and FTIR analysis methods. Various properties, such as water/gypsum ratio (W/G), setting time, compressive strength, density, water absorption and open porosity of gypsum samples with 5 wt.% spent coffee grounds were determined.

When treated SCG were used it was found that the W/G ratio of gypsum paste decreased, setting time shortened, compressive strength of the samples increased, open porosity and water absorption values decreased compared to the samples with untreated SCG. However, the treatment duration of SCG, whether it was 0.5 or 2 hours, had just a minor difference on the obtained results. Additionally, the FTIR spectrum showed, that the lipids content in SCG decreased after the treatment.

All things considered, there is not a big difference in SCG treatment time between 0.5 and 2 hours. However, research results showed that by using isopropanol treated SCG, gypsum samples had good properties. And this kind of SCG application could be one of the solutions on how to reduce the large amount of spent coffee grounds in the landfills.

[1] M. Lauberts, et al., “Spent Coffee Grounds Valorization in Biorefinery Context to Obtain Valuable Products Using Different Extraction Approaches and Solvents”, Plants, 12, 30, 2023.
[2] W. Sidło and J. Latosińska, “Reuse of Spent Coffee Grounds: Alternative Applications, Challenges, and Prospects—A Review”, Applied Sciences, 15, 137, 2025.
[3] A.E. Atabani, et. al., ”Valorization of spent coffee grounds into biofuels and value-added products: Pathway towards integrated bio-refinery“, Fuel, 54, 115640, 2019.

ONE-POT APTES GRAFTED SILICA SYNTHESIS AND MODIFICATION WITH AGNP

Gerardas Laurinavičius[1], Vilius Poškus[1]

[1]Vilnius University, Faculty of Chemistry and Geosciences
gerardas.laurinavicius@chgf.stud.vu.lt

Mesouporous materials plays an important role in material science, especially in sample preparation techniques like solid phase extraction and solid phase microextraction. Mesoporous materials, compared with other two types of porous materials (micro and macroporous), comes with a big advantages: narrow pore size distribution and high surface area, can be made with different materials such as silica or various metal oxides, have biocompatibility and low toxicity.

Silica is a perfect candidate for mesoporous sorbents – it can be easily modified and has a rather good chemical stability against organic solvents. Usually, the synthesis of mesoporous silica sorbent starts with a silica source (typically TMOS or TEOS orthosilicates) porogen and a catalyst. The latter steps involves porogen removal and surface modification with the desired functional groups or nanoparticles.

In this study we synthesized two types of silver nanoparticles (AgNP) modified silicas with different porogens (CTAB and P123) and TMOS and APTES as a silica sources. AgNP presence was confirmed with EDX and SEM analyses, porosity and surface area were assessed with nitrogen sorption desorption analysis. FT-IR analysis was also performed on synthesized silica samples. AgNP load (compared to silicon) was around 40-50 % for both silicas. BET surface areas: 344.6 and 8.8 m^2/g for silicas, synthesized using CTAB and P123 as a porogens. Nitrogen sorption-desorption analysis showed better porosity for CTAB silica with mesopores, ranging from 2 to 45 nm in size.

ASSUMPTIONS FOR MODELING NITROGEN BIOFERTILIZER GRANULATION

Dovilė Oksaitė[1], Rasa Šlinkšienė[1]

[1]Kaunas University of Technology
dovile.oksaite@ktu.edu

Nitrogen fertilizers, especially urea, are widely used to increase crop yield and ensure optimal plant growth conditions. Enough nitrogen positively influences harvest quality, enhances plant resistance to diseases and environmental factors such as temperature fluctuations [1]. However, despite its agronomic advantages, the use of nitrogen fertilizers raises environmental concerns. Due to leaching, nitrogen compounds, particularly nitrates, can infiltrate groundwater, promoting eutrophication and degrading soil quality [2]. To reduce the negative impact, innovative solutions are being explored, including the incorporation of bioactive substances into fertilizer. One such substance is algae, which act as natural bio-stimulants. Algae stimulate plant growth, enhance nutrient uptake [3]. Granular fertilizers are usually produced and used. Granulation can be performed using various methods, with wet granulation being one of the most effective, typically carried out with a drum granulator. During this process, granules form through primary particle agglomeration, progressing to fully developed and stabilized granules. As granulation is a multi-stage and complex process, its optimization in industrial applications is crucial [4]. Due to the complexity of the granulation process, mathematical models are increasingly used in the industry to optimize production conditions and reduce the number of experimental trials. One of the modelling techniques is the Discrete Element Method (DEM), which enables the analysis of individual particle interactions and the prediction of granule formation [5]. However, to successfully implement DEM modelling, it is essential to collect accurate data on particle properties. Therefore, in this work, to model the granulation process of crystalline urea and algae, experimental granulation was performed and the following mechanical and physical characteristics were investigated: inter-particle adhesion forces, friction coefficients, angle of refraction etc.

[1] M. Farhan, M. Sathish, R. Kiran, A. Mushtaq, A. Baazeem, A. Hasnain, F. Hakim, S. A. H. Naqvi, M. Mubeen, Y. Iftikhar, A. Abbas, M. Z. Hassan, and M. Moustafa, Plant Nitrogen Metabolism: Balancing Resilience to Nutritional Stress and Abiotic Challenges (Phyton-International Journal of Experimental Botany, 2024), vol. 93, no. 3, pp. 581–609.

[2] P. Vejan, T. Khadiran, R. Abdullah, and N. Ahmad, Controlled Release Fertilizer: A Review on Developments, Applications and Potential in Agriculture (Journal of Controlled Release, 2021), vol. 339, pp. 321–334.

[3] E. E. Ammara, A. A. A. Aioub, A. E. Elesawy, A. M. Karkour, M. S. Mouhamedd, A. A. Amer, and N. A. EL-Shershaby, Algae as Bio-fertilizers: Between Current Situation and Future Prospective (Saudi Journal of Biological Sciences, 2022), vol. 29, pp. 3083–3096

[4] V. De Simone, D. Caccavo, G. Lamberti, M. d'Amore, and A. A. Barba, Wet-Granulation Process: Phenomenological Analysis and Process Parameters Optimization (Powder Technology, 2018), pp. 411–419

[5] H. Nakamura, T. Baba, S. Ohsaki, S. Watano, K. Takehara, and T. Higuchi, Numerical Simulation of Wet Granulation Using the DEM–PBM Coupling Method with a Deterministically Calculated Agglomeration Kernel (Chemical Engineering Journal, 2022), vol. 450, no. 3

THE USE OF COFFEE SILVERSKIN PARTICLES AS FILLERS IN CELLULOSE ACETATE BASED BIOPLASTICS

Laurynas Lukomskis[1], Laura Peciulyte[1], Ramune Rutkaite[1]

[1]Department of Polymer Chemistry and Technology, Kaunas University of Technology, Kaunas, Lithuania
laurynas.lukomskis@ktu.edu

With the increasing production of synthetic polymers, waste management has become a global issue, posing an enormous threat to the natural environment [1]. Cellulose diacetate, a modified natural polymer, serves as an excellent alternative to synthetic plastics. By incorporating plasticizers, such as polyethylene glycol, triacetin and triethyl citrate, this polymer can withstand extrusion parameters and be formed into various products [2]. Additionally, agriculture and food production waste can be utilised as fillers to adjust product mechanical, thermal and/or hydrophobicity properties and reduce manufacturing cost. Thus, in this study, compositions of thermoplastic cellulose diacetate were obtained using ecofriendly plasticizer – triacetin and coffee silverskin filler which is by-product of food industry. Additionally, incorporating waste materials—such as agricultural or food industry waste—into compositions helps address waste utilization challenges while reducing production costs. By varying the particle size and amounts of filler, a set of thermoplastic mixtures was prepared and thermally processed using twin-screw extrusion. By the means of injection moulding and 3D printing the samples of novel bioplastics were obtained to investigate their properties. The properties of the resulting composites were evaluated by determining the melt flow index, hardness, mechanical properties, and contact angle.

It has been found that increasing particle size and concentration of coffee silverskin in composition decreases melt flow index. Hardness values increased with higher coffee silverskin content, while particle size had minimal influence on hardness. Mechanical properties analysis revealed that tensile strength and elongation at break decreased with increasing coffee silverskin content and particle size. The tensile modulus increased with higher coffee silverskin content but decreased when using larger size particles. The influence of coffee silverskin content and particle size on the hydrophobicity of the composites was minimal.

[1] R. Geyer. Chapter 2 – Production, use, and fate of synthetic polymers. Plastic Waste and Recycling. 13-32 (2020)
[2] R. Erdmann, S. Kabasci, H. Heim. Thermal Properties of Plasticized Cellulose Acetate and Its β-Relaxation Phenomenon. Polymers. 13. 1356 (2021)

INFLUENCE OF RAW MATERIAL ORIGIN ON THE CONCENTRATION OF NITROGEN, PHOSPHORUS AND POTASSIUM IN BULK ORGANIC FERTILIZERS

Gabija Aleksaitytė[1], Odeta Pocienė[1], Rasa Šlinkšienė[1]

[1]Kaunas University of Technology
gabija.aleksaityte@ktu.edu

It is generally accepted that the unbalanced use of mineral fertilizers in pursuit of the highest possible yield has a negative effect on the ecosystem. Therefore, recently, ways have been sought to replace at least part of mineral fertilizers with organic ones, which have a number of advantages over mineral fertilizers, especially in the long term. Organic fertilizers improve soil structure, increase its aeration, promote the accumulation of humus, which increases the soil's ability to retain moisture and nutrients, while helping to maintain a healthy soil ecosystem, help accumulate carbon in the soil, reducing the amount of CO_2 in the atmosphere and contributing to climate change mitigation. They also feed beneficial microorganisms that help decompose organic matter and release nutrients for plants. Unlike mineral fertilizers, which often dissolve quickly and can be washed away by rain or irrigation, organic fertilizers release nutrients gradually, ensuring a long-term supply to plants, reducing the risk of nitrogen compounds and phosphorus entering water bodies and causing eutrophication. Organic fertilizers are usually produced from renewable sources, therefore contributing to the circular economy and waste recycling.

However, the concentration of nitrogen, phosphorus and potassium in organic fertilizers can vary greatly depending on their origin, composition and processing method and is more difficult to control than in mineral fertilizers, where these nutrients are provided in pure compounds and precisely dosed. The composition of organic fertilizers depends on: the type of raw material, the processing method, the degree of maturity. Typically, the most nitrogen is found in poultry manure (4–6% N), phosphorus is found in bone meal (12–30% P_2O_5), and potassium is found in ash (10–35% K_2O). In this work, granular organic fertilizers from various waste: uncleaned buckwheat biomass (UBM), buckwheat husks (BH), buckwheat husk ash (BHA), bone meal (BM), molasses solution (MS), and beaten eggs (BE) were produced using different dry and liquid raw materials. By changing their ratio, the aim was to create organic fertilizers of various compositions (Fig.1.) that would be suitable for use in different periods of plant vegetation.

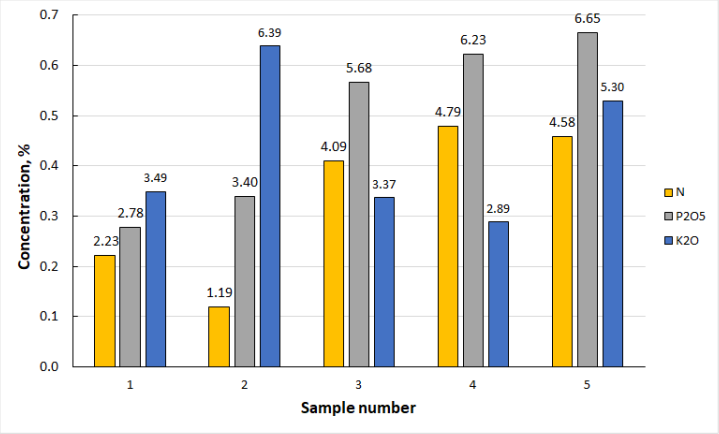


Fig. 1. Nitrogen, phosphorus and potassium concentrations in bulk organic fertilizers: 1 – 20% BHA + 40% BH + 40% UBM + BE; 2 – 40% BHA + 30% BH + 30% UBM + MS; 3 – 20% BHA + 20% BH + 20% UBM + 40% BM + MS; 4 – 20% BHA + 20% BH + 20% UBM + 40% BM + BE; 5 – 40% BHA + 10% BH + 10% UBM + 40% BM + BE.

LIQUID NITROGEN-CALCIUM-MAGNESIUM FERTILIZER WITHEXTRACT FROM BIODEGRADABLE MATERIALS

Eglė Didžiulytė[1], Rasa Šlinkšienė[1]

[1]Department of Physical and Inorganic Chemistry, Faculty of Chemical Technology, Kaunas University of Technology, Kaunas, Lithuania
egle.didziulyte@ktu.lt

Liquid fertilizers - a solutions that not contain any undissolved substances gaining in popularity over the last few years owing to their ease of use and fast results. Different liquid grades of fertilizer can be produced using a variety of chemicals for grades obtained through the solving process of salts, mineral fertilisers or the special mixing of aqueous solutions [1]. Since they are readily available to the plant, they are immediately absorbed or, if there is an excess, washed away by rain. Since liquid fertilizers do not remain in the soil for long, they will need to be fertilized several times during the growing season. Such intensive and chemical farming is very harmful to the natural ecosystem [2]. This issue raises concerns about soil conservation, soil quality improvement, human health, and environmental protection, driving the search for alternative farming methods. One way to reduce the negative impact on the environment is to use as many biodegradable materials as possible, which not only enrich plants with essential nutrients but also help mitigate various environmental, economic, and social problems [3].

At the beginning of the study, liquid nitrogen-calcium-magnesium fertilisers were developed based on dolomite. The digestion process used 45% nitric acid with a 40% excess of nitric acid, following the stoichiometry of the chemical reaction. The reaction proceeded rapidly, achieving a maximum free decomposition of dolomite (80%) within 50 minutes. The resulting dolomite decomposition solution was then neutralised, and nitrogenous components (urea, ammonium nitrate, potassium nitrate) were added to the composition. These studies on calcium-magnesium-nitrogen fertilisers led to the development liquid fertilisers, whose chemical composition and physicochemical properties were analysed. In response to environmental goals, organic matter extract from biodegradable material, digestate was added to nitrogen-calcium-magnesium fertilizers and physicochemical properties of liquid biofertilizers analysed.

[1] Falls J. H. Encyclopeadia of Analytical Science (Second Edition), Liquid fertilizers. 2005, 1–8.
[2] Parikh, S. J. et al. Soil: The Foundation of Agriculture. Nature Education Knowledge. 2012, 3(10):2.
[3] Paull, J. Attending the First Organic Agriculture Course: Rudolf Steiner's Agriculture Course at Koberwitz, 1924. European Journal of Social Sciences. 2011, 21(1).

SYNTHESIS ANDSTUDY OF THE PROPERTIES OF POLYMER HYDROGEL AS A COMPONENT OF FIRE-RESISTANT POLYMER-MINERAL (HYBRID) HYDROGEL

Diana Varchuk[1], Serhiy Tsykunkov[1], Olha Maikovych[1], Nataliya Nosova[1], Serhiy Varvarenko[1]

[1]Department of Organic Chemistry, Lviv Polytechnic National University, Ukraine
diana.varchuk.mkhtkhd.2024@lpnu.ua

The creation of a new generation of transparent hybrid fire-resistant hydrogel materials in particular refractory glass structures on polymer-mineral basis has great social significance as well as their production establishment and implementation in practice. This class of material allow to increase the time for evacuation and save the most valuable thing – human life – in the event of a fire.

This study proposes the formation of fire-resistant glass units using polymer-mineral (hybrid) hydrogel. Under the influence of extremely high temperatures (above 100°C), this material changes its structure, forming a porous layer that prevents glass deformation and the appearance of fractures. This technology effectively inhibits the spread of fire and high temperatures, providing a reliable level of fire protection and meeting modern safety standards.



Fig. 1. Effect of fire on the structure of hydrogel

The technology for obtaining the fire-resistant layer is based on the hybrid hydrogel synthesis that combines the properties of mineral polysilicate hydrogel and polymer hydrogel (polyacrylamide copolymer crosslinked with poly-N-(hydroxymethyl)acrylamide-co-acrylic acid-co-N,N-methylenebisacrylamide).

A method for the controlled synthesis of branched copolymers of acrylamide, acrylic acid and N,N-methylenebisacrylamide has been developed, the aqueous solutions of which in a wide range of concentrations (up to 30%) obey the laws of flow of Newtonian liquids, which makes it possible to create low-viscosity pouring compositions based on them. The obtained copolymers have been characterized by IR and PMR spectroscopy methods and it has been established that copolymers containing no more than 15 mol% of acrylic acid units are suitable for obtaining transparent solutions in the presence of polyvalent metals (magnesium, aluminum) cations. On the basis of the selected copolymers using polymer reactions of transformations and intermolecular structuring, polymeric hydrogels of various compositions were obtained, the regularities of their synthesis were investigated and the obtained material was characterized. Correlation analysis of experimental data (crosslinking density, light transmittance, swelling behavior, gel fraction, mechanical properties) was carried out. Graphical and mathematical relationships describing polycondensation reactions in the selected system and properties of polymer hydrogels were obtained.

The conditions for obtaining polymer hydrogels with optimal properties have been determined for their use as a component of the polymer part of a hybrid hydrogel composition in the production of fire-resistant glazing units. Testing of the obtained fire-resistant glazing units filled with hybrid hydrogel demonstrates an increase in fire resistance properties compared to existing analogs.

APPLICATION AND OPTIMIZATION OF LIQUIDCHROMATOGRAPHY METHOD FOR THE STUDY OF CORDYCEPIN AND ITS DERIVATIVES

Ąžuolas Ivickas[1,2], Evaldas Naujalis[1,2], Simonas Balčiūnas[1,2]

[1]Vilnius University
[2]State research institute Center for Physical Sciences and Technology
azuolas.ivickas@ftmc.lt

Cordycepin is a bioactive derivative of the nucleoside adenosine and is one of the primary bioactive components identified in *Cordyceps militaris* species of fungus [1]. Cordycepin has gained significant attention for its pharmacological properties, including antineoplastic, antioxidant, and anti-inflammatory activities [2].

It was extensively used in China of many ears but has recently grown in popularity in the west as a herbal alternative to prescribed medication [3, 4]. However, accurate quantification of cordycepin and its derivatives in food products remains challenging due to matrix complexity and variability in formulation. Particularly worrisome are dietary supplements as they are largely unregulated, making it unclear whether the product contains the advertised dose or even the correct compound. Therefore, the aim of this study was to develop and optimize a liquid chromatography method for the precise analysis of cordycepin and adenosine in commercial supplements, ensuring reliable detection and quantification.

A high-performance liquid chromatography (HPLC) method was developed and validated to enhance sensitivity and selectivity. In addition, a time-of-flight mass spectrometer (TOF) was used to ensure the correct analytes were detected. The method was optimized for column selection, mobile phase composition, flow rate, and detection wavelength to achieve optimal separation and resolution. Sample preparation techniques and dilution strategies, were evaluated to improve analyte recovery and reduce matrix interference. Using the optimized conditions, results were obtained for several dietary supplements produced both locally and abroad. All samples contained significant amounts of cordycepin and adenosine, confirming the sellers' claims.

Preliminary results demonstrate that the optimized HPLC method successfully quantifies cordycepin and adenosine with high accuracy, precision, and reproducibility. The method exhibits excellent linearity, limit of detection (LOD), and limit of quantification (LOQ) within the expected ranges found in supplements. Additionally, recovery rates confirm the method's effectiveness in minimizing matrix effects.

These findings provide a robust analytical framework for quality control and standardization of cordycepin-containing supplements. The optimized chromatography method enhances the reliability of bioactive compound analysis and can be applied in regulatory and research settings to ensure product consistency and efficacy.

[1] Cunningham, K. G., et al. "Cordycepin, a metabolic product isolated from cultures of Cordyceps militaris (Linn.) Link." Nature 166.4231 (1950): 949-949.
[2] Radhi, Masar, et al. "A systematic review of the biological effects of cordycepin." Molecules 26.19 (2021): 5886.
[3] Tan, Lu, et al. "Anti-inflammatory effects of cordycepin: A review." Phytotherapy Research 35.3 (2021): 1284-1297.
[4] Choi, Jungwon, et al. "Quantitative analysis of cordycepin in Cordyceps militaris under different extraction methods." Journal of Applied Biological Chemistry 64.2 (2021): 153-158.

OPTIMIZATION OF SOLID-PHASE EXTRACTION FOR THE ANALYSIS OF SEDATIVE-HYPNOTIC DRUGS IN BIOLOGICAL SAMPLES

Nerijus Karlonas[1]

[1]The State Forensic Medicine Service, Toxicology Laboratory, Didlaukio 86E, LT-08303 Vilnius, Lithuania
nerijus.karlonas@vtmt.lt

Sample preparation is one of the most important steps in most analytical procedures to determine trace sedative-hypnotic drugs in biological samples with complex matrices. An ideal biological sample preparation technique should be simple, inexpensive, efficient, selective, and compatible with various analytical techniques. It should give a recovery as high as possible, use the minimum amount of solvent, and be environmentally friendly. Therefore, researchers are making great efforts to develop rapid, accurate, precise, and sensitive methods for the determination of sedative-hypnotic drugs in real biological samples [1].

The main aim of my study was the development of a new sensitive and specific method based on fast gas chromatography with negative-ion chemical ionization mass spectrometry (GC/NICI-MS) using a mixed-mode solid phase extraction for the quantification of sedative-hypnotic drugs in biological samples.

One of the greatest challenges with a residue analysis of sedative-hypnotic drugs is the selection of a sorbent suitable to achieve an acceptable sensitivity to all compounds characterized by different physicochemical properties. In this research, a mixed-mode polymeric sorbent with ion-exchange properties was applied. This sorbent is capable of hydrophilic-lipophilic and ion-exchange interactions [2-4], and therefore it is suitable for achieving an efficient extraction of all herein-investigated analytes by a single extraction step. For that reason, biological sample preparation conditions including a selection of the solvent for washing and elution steps, pH values were optimized. To the best of my knowledge, this method has been used for the first time for the optimization of sample preparation at pH 1.0.

The developed method for the determination of sedative-hypnotic drugs in biological samples was validated following the recommendations for new methods [2,5,6]. The linear relationships with the correlation coefficients (r2) better than 0.996 were evaluated. It was determined that extraction efficiency ranged from 82.9 (±6.2) % to 94.6 (±3.4) %. The precision (RSD) for analytes was 4.08-9.52 %, while the accuracy was in the range of 93.0-106.3 %. Moreover, this method has several advantages: elimination of interferences, low volume of samples (0.2 mL), a multi-residue analysis, and very fast chromatographic separation of analytes (3.9 min). According to the results, the developed method is accurate, precise, effective, selective, sensitive, and specific enough to detect analytes after a long time of use of a single oral administration of some psychoactive substances. Furthermore, this method enables reaching the highest specificity for major analytes and meets the requirements of good laboratory practice, especially when applied to pharmacodynamic investigations. Ultimately, the developed method has been applied in routine toxicological analysis during the investigation of both clinical and forensic cases.

Acknowledgements
This research was supported by the State Forensic Medicine Service, Lithuania

[1] A. Y. Simão, M. Antunes, H. Marques, T. Rosado, S. Soares, J. Gonçalves, M. Barroso, M. Andraus, et al. Bioanalysis 12, 1557-1595 (2020)
[2] N. Karlonas, A. Padarauskas, A. Ramanavicius, A. Ramanaviciene. Journal of Separation Science 36, 1437-1445 (2013)
[3] N. Fontanals, F. Borrull, R. M. Marcé. Journal of Chromatography A 1609, 460531 (2020)
[4] N. Karlonas, A. Ramanavicius, A. Ramanaviciene. Journal of Separation Science 37, 551-557 (2014)
[5] N. Karlonas, A. Padarauskas, A. Ramanavicius, Z. Minkuviene, A. Ramanaviciene. Chemija 23, 91-99 (2012)
[6] J. Pum. Advances in Clinical Chemistry 90, 215-281 (2019)

STUDY OF WUPyV VIRUS-LIKE PARTICLES IMMUNE COMPLEX FORMATION WITH MONOCLONAL ANTIBODIES BY SPECTROSCOPIC ELLIPSOMETRY AND QUARTZ CRYSTAL MICROBALANCE WITH DISSIPATION

Silvija Juciutė[1], Asta Lučiūnaitė[2,3], Vincentas Mačiulis[1,2], Ieva Plikusienė[1,2]

[1]Faculty of Chemistry and Geosciences, Institute of Chemistry, Vilnius University
[2]State Research Institute Centre for Physical Sciences and Technology
[3]Life Sciences Center, Vilnius University
silvija.juciute@chgf.stud.vu.lt

Viral infections can cause severe inflammations. Antibodies, produced during these infections or after vaccination, form immune complex with antigens as a response of immune system. Formed immune complex can also participate in inflammation processes. Overactivation and induced inflammation during viral infections or vaccination can cause unwelcome effects to human organism. In order to avoid overactivation, it is of great significance to understand immune cells' response to immune complex.

In our study, we investigated differences between immune complex formations of recombinant virus-like particles (VLPs) derived from the major capsid protein VP1 of human Washington University (WU) human polyomavirus (PyV), self-assembling to spherical nanoparticles, and a set of VLP-specific monoclonal antibodies (mAbs). We used a collection of mAbs IgG1, IgG2a and IgG2b subclass [1].

For this investigation we utilized two surface-sensitive methods: spectroscopic ellipsometry (SE) and quartz crystal microbalance with dissipation (QCM-D). SE is an optical technique, which can provide valuable information about sensing surfaces' dielectric properties, such as refractive index or thickness. QCM-D is an acoustic method, based on sound waves, and it gives knowledge about mechanical and viscoelastic characteristics of the layer. SE and QCM-D combination is highly suitable for the real-time detection of protein-protein interactions, as it does not require labelling of proteins and it is non-invasive and non-destructive to analytes.

From data, obtained during SE measurements, the equilibrium dissociation and association constants, dissociation and association rate constants were calculated by applied mathematical model based on encounter theory. All tested mAbs were determined to be from medium to very high affinity to VLPs. Simultaneously, data from QCM-D measurements revealed different viscoelastic properties of mAbs and immune complexes layers and possible mechanisms for mAbs binding to VLPs.

[1] Lučiūnaitė, A., Mašalaitė, K., Plikusiene, I. et al. Structural properties of immune complexes formed by viral antigens and specific antibodies shape the inflammatory response of macrophages. Cell Biosci 14, 53 (2024). https://doi.org/10.1186/s13578-024-01237-1

EFFECT OF ELECTRODE POTENTIAL ON ELECTROCHEMICAL IMPEDANCE SPECTRA OF TETHERED-BILAYER LIPID MEMBRANES ON FLUORINE-DOPED TIN OXIDE

Narvydas Dėnas[1,2], Kipras Eigminas[1], Aušra Valiūnienė[1,2]

[1]Vilnius university, Institute of Chemistry, Naugarduko str. 24, LT-03225, Vilnius, Lithuania
[2]State Research Institute Center for Physical Sciences and Technology, Sauletekio Ave. 3, LT-10257
narvydas.denas@chgf.stud.vu.lt

Tethered-bilayer lipid membranes (tBLMs) are membranes supported on a solid surface in which the inner layer of the lipid bilayer is covalently attached to the surface through a spacer group, which covers minor surface irregularities and forms an aqueous reservoir with the functional properties of the cytoplasm [1]. tBLMs can simulate cell membranes as accurately as possible and recreate the basic functions of cell membranes [2, 3].

tBLMs are suitable for the systematic study of different types of membrane-associated processes, provide the lipid environment needed to study membrane-associated proteins and can be used for biosensing applications [4]. Surface-sensitive techniques such as electrochemical impedance spectroscopy (EIS) are commonly used to study tBLMs and their interactions with proteins. However, the EIS response of tBLMs on the gold surface is strongly dependent on the potential, so a three-electrode system must be used for measurements [5]. Furthermore, EIS signal on gold surface highly depends on the composition of the tBLMs spacer group [6]. The problems mentioned above lead to some difficulties in the practical application of tBLM-based sensors on gold surfaces. Metal oxide substrates, such as fluorine-doped tin oxide (FTO) or others, can offer significant advantages as solid supports due to their lower fabrication cost and strong Si-MeO covalent bond, which avoids clustering of molecular anchors and provides regeneration capabilities [7].

In this work, tBLMs were formed on FTO-coated glass surfaces using different compositions of molecular anchors and EIS measurements were performed to determine the sensitivity of tBLM-based sensors to pore-forming toxin at different electrode potentials. The potential range used for the measurements was 0V to 1V vs Ag|AgCl, $KCl_{sat.}$ which is the ideal polarisation range of the system under investigation. The tBLM-based sensors on the FTO surface were investigated using fast Fourier Transform Electrochemical Impedance Spectroscopy (FFT-EIS), which allows a single EIS spectrum to be obtained in 3 s in the frequency range from 0.2 Hz to 10 kHz.

[1] S. Rebaud, O. Maniti, and A. P. Girard-Egrot, “Tethered bilayer lipid membranes (tBLMs): interest and applications for biological membrane investigations,” Biochimie, vol. 107 Pt A, no. Part A, pp. 135–142, 2014, doi: 10.1016/J.BIOCHI.2014.06.021.
[2] I. Zawisza, R. Bilewicz, M. Rosa Moncelli, and R. Guidelli, “Electrochemistry of Langmuir–Blodgett and self-organized monolayers of an azocrown ether, both pure and mixed with a phospholipid,” Journal of Electroanalytical Chemistry, vol. 509, no. 1, pp. 31–41, Aug. 2001, doi: 10.1016/S0022-0728(01)00380-1.
[3] R. Naumann et al., “Tethered Lipid Bilayers on Ultraflat Gold Surfaces,” Langmuir, vol. 19, no. 13, pp. 5435–5443, Jun. 2003, doi: 10.1021/LA0342060.
[4] J. A. Jackman, W. Knoll, and N. J. Cho, “Biotechnology Applications of Tethered Lipid Bilayer Membranes,” Materials 2012, Vol. 5, Pages 2637-2657, vol. 5, no. 12, pp. 2637–2657, Dec. 2012, doi: 10.3390/MA5122637.
[5] V. Liustrovaitė, A. Valiūnienė, G. Valinčius, and A. Ramanavičius, “Electrochemical Impedance Spectroscopy Based Evaluation of Chlorophyll a Reconstitution within Tethered Bilayer Lipid Membrane,” J Electrochem Soc, vol. 168, no. 6, p. 066506, Jun. 2021, doi: 10.1149/1945-7111/AC0262.
[6] D. J. McGillivray et al., “Molecular-scale structural and functional characterization of sparsely tethered bilayer lipid membranes,” Biointerphases, vol. 2, no. 1, pp. 21–33, Mar. 2007, doi: 10.1116/1.2709308.
[7] I. Gabriunaite, A. Valiūnienė, and G. Valincius, “Formation and properties of phospholipid bilayers on fluorine doped tin oxide electrodes,” Electrochim Acta, vol. 283, pp. 1351–1358, Sep. 2018, doi: 10.1016/J.ELECTACTA.2018.04.160.

MICROFLUIDIC CHIP FABRICATION FOR THE DEVELOPMENT OF A NERVE-ON-CHIP MODEL

Kamilė Kasperavičiūtė[1], Arūnas Stirkė[1], Wanessa Melo[1], Eivydas Andriukonis[1]

[1]Laboratory of Bioelectrics, Center for Physical Sciences and Technology, Saulėtekio av. 3, Vilnius, Lithuania
kamile.kasperaviciute@ftmc.lt

Organ-on-a-chip (OOC) devices, referred to as “tissue-chips,” or “micro-physiological systems” (MPS), are microfabricated devices that mimic the properties and physiological functions of complex tissues or specific organs in vitro [2]. Additionally, microfluidics has significant advantages over working on a macro scale, including increased efficiency, lower cost, and increased control of volume and other experimental parameters [1]. Extensive research has demonstrated the potential of microfluidic platforms in recreating tissue-specific microenvironments, enabling precise manipulation of cellular processes, and providing valuable insights into disease mechanisms and drug responses. Building on these advancements, the development of novel microfluidic systems tailored for neural applications has gained increasing attention. To address this need, a microfluidic chip featuring a two-channel design has been fabricated to facilitate controlled cell culture conditions and dynamic fluid flow, essential for replicating neural tissue environments. The chip is produced using soft lithography techniques with polydimethylsiloxane (PDMS), a material known for its biocompatibility and design flexibility. The fabrication process consists of several key stages, including photolithography to create a master mold, PDMS casting and curing, plasma bonding for channel sealing, and surface treatment to improve hydrophilicity. Each stage is meticulously optimized to ensure reproducibility and dimensional accuracy in the final device. Current efforts are directed towards refining the chip’s surface properties to enhance cell adhesion and viability, paving the way for future biological applications. This research contributes to the advancement of in vitro neurological models, with potential applications in neurodegenerative disease studies and personalized medicine. The integration of microfluidic technology with nerve cell models offers a promising platform for investigating neural dynamics and therapeutic strategies.

[1] Farhang Doost, Negar, and Soumya K Srivastava. 2024. “A Comprehensive Review of Organ-on-a-Chip Technology and Its Applications.” Biosensors 14 (5): 225. https://doi.org/10.3390/bios14050225.

[2] R, Nithin, Ayushi Aggarwal, Anne Boyina Sravani, Pooja Mallya, and Shaila Lewis. 2023. “Organ-On-A-Chip: An Emerging Research Platform.” Organogenesis 19 (1): 2278236. https://doi.org/10.1080/15476278.2023.2278236.

DEVELOPMENT AND INVESTIGATION OF IN-SITU NMR PROBE

Aurimas Dubauskas[1], Jurgis Pilipavičius[2,3], Linas Vilčiauskas[2,3], Vytautas Klimavičius[1]

[1]Institute of Chemical Physics, Faculty of Physics, Vilnius University, Lithuania
[2]Institute of Chemistry, Vilnius University, Lithuania
[3]Center for Physical Sciences and Technology (FTMC), Lithuania
aurimas.dubauskas@ff.stud.vu.lt

Transition towards sustainable and renewable energy requires development of energy storage technologies such as Na-ion based batteries. Promising sodium ion batteries (SIB) are aqueous NASICON (Na Super Ionic CONductor) based batteries. NASICON materials feature a stable three-dimensional crystal structure, good ionic conductivity, and thermal stability. NASICON can be used as anodes, cathodes, solid electrolytes, or electrode coating materials [1] in battery development. To efficiently and successfully use these technologies, it is necessary to understand the chemical processes that limit the effective usage time of the batteries. Solid-state Nuclear Magnetic Resonance (NMR) spectroscopy is a powerful method that can assist in the study of these processes. NMR spectroscopy is already used in battery research, but most of the applied methods are *ex-situ* experiments, during which the batteries are disassembled, and the environment of the materials under study is altered. To avoid this, *in-situ* NMR methods can be applied, where measurements are carried out without disassembling the electrochemical device.

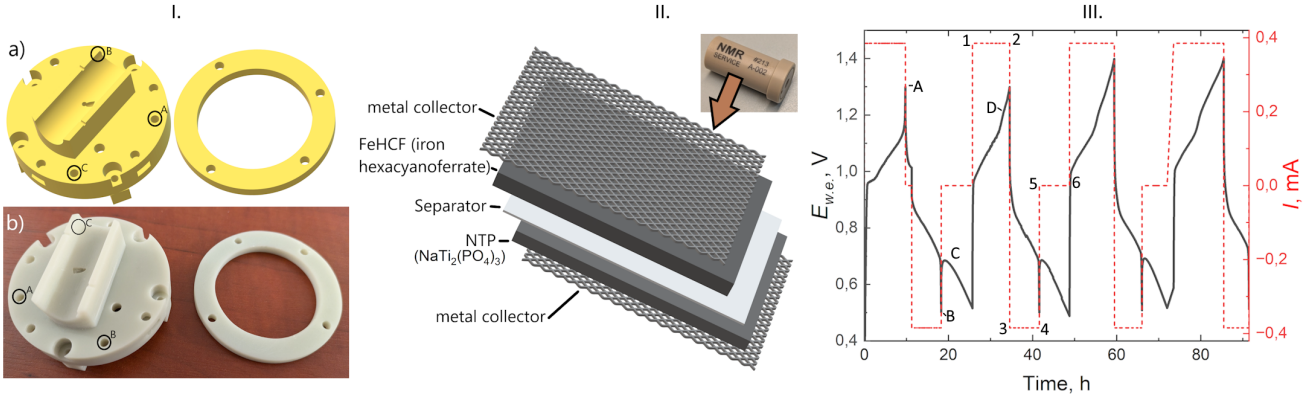


Fig. 1. I. In situ cell and NMR coil housing, A, B, C – electrochemical channels. It was designed using OpenSCAD program (a), produced by stereolithography method (b). II. Creation of battery cell. III. Time dependent working electrode voltage (black) and output current (red) during charge discharge cycling. 1-2 (I>0) battery is charging, 3-4 (I<0) discharging, 5-6 (I=0) pause during which the NMR spectrum is measured. A – fully charged battery, B – discharged battery, C – self-discharge of by-products, D – a parasitic oxygen evolution reaction is taking place.

We modified the commercial 5 mm wideline NMR probe that 11 mm *in-situ* cell is compatible and tuned the NMR probe to ^{31}P and ^{23}Na resonances. Two NMR probe setups with distinct electrical circuits for impedance matching were created: shunt inductive and series capacitive matching circuits. Three additional channels were introduced for charging and discharging (cycling) the battery. Nutation curves and spectra were registered for the purpose of NMR probe setups comparison. Shunt inductive NMR probe setup was tested by measuring ^{31}P spectra of aqueous NASICON based battery during charge–discharge cycling. Registered working electrode spectra of time dependant voltage showed when parasitic competing oxygen evolution reaction becomes significant. By examining NTP ($NaTi_2(PO_4)_3$) ^{31}P spectra of different cell configurations, and by comparing nutation curves of different NMR probe setups adequate NMR probe and cell configurations were determined for aqueous NASICON battery in-situ research.

[1] J. Xiao, B. Zhang, J. Liu, X. He, et al. "NaSICON-type materials for lithium-ion battery applications: Progress and challenges," Nano Energy, vol. 127, 109730, Aug 2024.

SHROOM CLUES: WHAT STABLE ISOTOPES REVEAL ABOUT FUNGI

Justina Stonytė[1], Aistė Tuzinaitė[2], Giedrė Keen Motuzaitė Matuzevičiūtė[3], Rasa Pauliukaitė[1]

[1]Department of Nanoengineering, Center for Physical Sciences and Technology, Vilnius, Lithuania
[2]Department of Nuclear Research, Center for Physical Sciences and Technology, Vilnius, Lithuania
[3]Department of Archaeology, Faculty of History, Vilnius University, Vilnius, Lithuania
justina.stonyte@ftmc.lt

Fungi have played a significant role in human diets, yet their presence in archaeological contexts remains underexplored. Evidence of mushroom consumption has been found in human dental calculus, tombs, and sacks found in burrial grounds [1,2,3]. This study investigates whether stable isotope analysis can reveal fungal contributions to past diets, focusing on Lithuania, where mushroom foraging is a long-standing cultural tradition.

By synthesizing data from the literature and our analyses, we explore the isotopic variability of fungi and its implications for dietary reconstructions while considering the soil in which the mushrooms grew. Our findings indicate that fungi exhibit highly variable carbon and nitrogen isotope values, which can complicate traditional interpretations of nutritional sources. Notably, substantial mushroom ingestion may contribute to isotopic signatures resembling those of high meat consumption. This effect is particularly relevant in archaeological human and animal remains displaying 'terrestrial' carbon isotope ratios and elevated nitrogen isotope values.

Given Lithuania's deep-rooted history of mushroom foraging, our research highlights the importance of considering fungi as a dietary factor in stable isotope studies. Factoring fungi into these studies will provide us with a better understanding of what people ate in the past and how their surroundings influenced their diets.

Acknowledgements

Great thanks to dr. Olga Jefanova and prof. habil. dr. Jonas Mažeika from the Laboratory of Nuclear Geophysics and Radioecology, Nature Research Centre, for the mushroom sample lyophilization.

[1] Power, R.C., Salazar-García, D.C., Straus, L.G., Gonzalez Morales, M.R., Henry, A.G., 2015. Microremains from El Miron Cave human dental calculus suggest a mixed plant-animal subsistence economy during the Magdalenian in northern Iberia. J. Archaeol. Sci. 60, 39e46.
[2] Peintner, U., Pöder, R., & Pümpel, T. (1998). The iceman's fungi. Mycological Research, 102(10), 1153–1162. https://doi.org/10.1017/S0953756298006546
[3] Borhegyi SF de. Miniature Mushroom Stones from Guatemala. American Antiquity. 1961;26(4):498-504. doi:10.2307/278737

SURFACE PLASMON RESONANCE IMMUNOSENSOR FOR DETECTION OF SARS-COV-2 ANTI-RBD ANTIBODIES

Agne Giniunaite[1], Almira Ramanaviciene[1], Asta Kausaite-Minkstimiene[1]

[1]NanoTechnas – Center of Nanotechnology and Materials Science, Institute of Chemistry, Faculty of Chemistry and Geosciences, Vilnius University, Naugarduko St. 24, LT-03225, Vilnius, Lithuania
agne.giniunaite@chgf.stud.vu.lt

The SARS-CoV-2 virus, which originated in Wuhan in late 2019, caused a global coronavirus pandemic. To assess acquired immunity to this virus, diagnostic tools are needed that can quickly, efficiently, and accurately detect antibodies against it. The SARS-CoV-2 structure is composed of four essential proteins: spike (S), envelope, membrane, and nucleocapsid. The S protein contains a short immunogenic fragment called the receptor binding domain (RBD) (SARS-CoV-2-RBD), which plays a crucial role in initiating the infection. Among the various diagnostic methods, surface plasmon resonance (SPR) immunosensors are widely used for detecting various viral and bacterial pathogens and are promising for the quantitative detection of SARS-CoV-2 antibodies. SPR immunosensors operating in a label-free direct detection format are very attractive, but often lack sufficient sensitivity. To improve sensitivity, an indirect detection format and signal amplification using nanomaterials as high-mass labels are often used. Although various nanomaterials such as carbon nanotubes, magnetic nanoparticles, or quantum dots can be applied, noble metal nanoparticles, especially gold (AuNDs), are most commonly used. Due to significantly higher mass compared to conventional molecules, nanomaterials cause a much larger change in refractive index and significantly increase the sensitivity of the immunosensor.

This research will introduce the SPR immunosensor for the quantitative analysis of antibodies against the SARS-CoV-2-RBD (anti-RBD). The immunosensor, operating in a direct detection format, was able to detect anti-RBD concentrations in the range of 0.27 – 66.60 nM, with a LOD of 0.27 nM and a LOQ of 0.47 nM. By adopting an indirect sandwich-type detection format and conjugates of biotinylated secondary antibodies against IgG and streptavidin-modified AuNDs, the immunosensor was able to detect anti-RBD antibodies in the concentration range of 0.043 – 10.66 nM, with LOD of 0.043 nM, and LOQ of 0.057 nM. It also demonstrated excellent repeatability, reproducibility, and operational stability. Finally, the immunosensor's suitability for real sample analysis was confirmed through the quantitative determination of anti-RBD antibodies in human serum samples.

Acknowledgements

This research has received funding from the Research Council of Lithuania (LMTLT), agreement No. S-MIP-22-46.

ELECTROCHEMICAL FORMATION AND EVALUATION OF POLYPYRROLE LAYER FOR DEVELOPMENT OF MOLECULARLY IMPRINTED POLYMER

Domas Pirstelis[1,2], Ernestas Brazys[2], Vilma Ratautaite[1], Arunas Ramanavicius[1,2]

[1]Department of Nanotechnology, State Research Institute Center for Physical Sciences and Technology, Sauletekio Ave. 3, Vilnius LT-10257, Lithuania
[2]Department of Physical Chemistry, Institute of Chemistry, Faculty of Chemistry and Geosciences, Vilnius University, Naugarduko str. 24, Vilnius LT-03225, Lithuania
domas.pirstelis@ftmc.lt

Electrically conductive polymers, such as polypyrrole (Ppy), have been widely utilized in the field of molecular imprinting‘ for use in biosensors [1, 2] and drug delivery systems [3]. Herein, we demonstrate electrochemical synthesis and in situ monitoring of a polypyrrole film for its application as a molecularly imprinted polymer (MIP)-based electrochemical sensor.

In this study, the Ppy film was deposited on a glass slide coated with a layer of fluorine-doped tin oxide (FTO) from an aqueous acetate buffer solution. The polymer was electrochemically synthesized using the pulsed chronoamperometry (PCA) method. The formation and changes to the Ppy layer were monitored in situ utilizing fast Fourier transform electrochemical impedance spectroscopy (FFT-EIS). Changes in cumulative charge Q and constant phase element admittance Y_{CPE} were observed during the formation of the layer.

The results demonstrate the viability of synthesizing Ppy films in an acetate buffer. The possibility of closely monitoring and controlling their characteristics is also demonstrated.

Acknowledgements

This project has received funding from the Research Council of Lithuania (LMTLT), agreement No. [S-MIP-24-111].

[1] V. Liustrovaite, V. Ratautaite, A. Ramanaviciene, and A. Ramanavicius, “Detection of the SARS-CoV-2 nucleoprotein by electrochemical biosensor based on molecularly imprinted polypyrrole formed on self-assembled monolayer,” Biosens Bioelectron, vol. 272, p. 117092, Mar. 2025, doi: 10.1016/J.BIOS.2024.117092.

[2] V. Ratautaite, E. Brazys, A. Ramanaviciene, and A. Ramanavicius, “Electrochemical sensors based on L-tryptophan molecularly imprinted polypyrrole and polyaniline,” Journal of Electroanalytical Chemistry, vol. 917, Jul. 2022, doi: 10.1016/j.jelechem.2022.116389.

[3] J. Sarvutiene, U. Prentice, S. Ramanavicius, and A. Ramanavicius, “Molecular imprinting technology for biomedical applications,” Mar. 01, 2024, Elsevier Inc. doi: 10.1016/j.biotechadv.2024.108318.

PEI-DERIVED LASER-INDUCED GRAPHENE FOR ZINC ELECTROCHEMICAL SENSING: EFFECT OF LASER WAVELENGTH ON MORPHOLOGY AND ELECTROCHEMICAL PERFORMANCE

Pamela Rivera[1], Šarūnas Mickus[2], Aivaras Sartanavičius[2], Romualdas Trusovas[2], Rasa Pauliukaite[1]

[1]Department of Nanoengineering
[2]Department of Laser Technology, Center for Physical Sciences and Technology (FTMC), Savanoriu ave. 231, LT-02300 Vilnius
pamela.rivera@ftmc.lt

Zinc is an essential micronutrient for plants, playing a crucial role in metabolic and physiological processes, enzyme activation, and ion homeostasis [1]. Zn deficiency disrupts plant metabolism, leading to stunted growth and impaired nutrient uptake, which can ultimately contribute to Zn deficiency in the human diet. Conversely, excessive Zn exposure reduces germination vigor and biomass, decreasing crop yield and quality [2]. To ensure optimal Zn fertilization, precise monitoring of Zn levels in plant tissues and growth substrates is necessary to enhance fertilization efficiency and prevent overapplication.

Currently, Zn determination in plant tissues relies on atomic spectroscopy techniques after acid digestion [3], [4], a method that requires specialized personnel, laboratory analysis, and lengthy processing times. Electrochemical sensors offer a promising alternative, enabling rapid, accurate, and on-site Zn measurement, thereby improving data availability for real-time fertilization management.

In this study, we investigate polyethylenimine-derived laser-induced graphene (PEI-LIG) as an electrode material for trace-level Zn^{2+} detection using square wave anodic stripping voltammetry (SWASV). PEI-LIG is fabricated using two different laser sources: a 532 nm laser and a CO_2 laser (10.6 µm). We assess how the laser wavelength influences the morphology, surface chemistry, and electrochemical performance of the resulting LIG. Raman spectroscopy is used to evaluate graphene quality, while X-ray photoelectron spectroscopy (XPS) provides insights into surface chemistry modifications. Morphology and elemental composition are examined through scanning electron microscopy with energy-dispersive spectroscopy (SEM-EDS). Furthermore, the electrochemical properties of PEI-LIG are characterized using cyclic voltammetry (CV) and electrochemical impedance spectroscopy (EIS). Finally, the developed sensing material is applied for the detection of Zn2+ using SWASV.

[1] M. Yang et al., “A high activity zinc transporter OsZIP9 mediates zinc uptake in rice,” The Plant Journal, vol. 103, no. 5, pp. 1695–1709, Aug. 2020, doi: 10.1111/tpj.14855.
[2] H. Kaur and N. Garg, “Zinc toxicity in plants: a review,” Planta, vol. 253, no. 6, p. 129, Jun. 2021, doi: 10.1007/s00425-021-03642-z.
[3] C. Wei et al., “Hormetic effects of zinc on growth and antioxidant defense system of wheat plants,” Science of The Total Environment, vol. 807, p. 150992, Feb. 2022, doi: 10.1016/j.scitotenv.2021.150992.
[4] M. B. Hassanpouraghdam, L. V. Mehrabani, and N. Tzortzakis, “Foliar Application of Nano-zinc and Iron Affects Physiological Attributes of Rosmarinus officinalis and Quietens NaCl Salinity Depression,” J Soil Sci Plant Nutr, vol. 20, no. 2, pp. 335–345, Jun. 2020, doi: 10.1007/s42729-019-00111-1.

Au-MXENE HETEROSTRUCTURE FOR THE COLORIMETRIC SENSING OF BIOMOLECULES

Saqib Ali[1], Veronika Zahorodna[2], Oleksiy Gogotsi[2], Arunas Ramanavicius[3], Simonas Ramanavicius[1]

[1]Department of Electrochemical Material Science, State Research Institute Center for Physical Sciences and Technology, Sauletekio av. 3, LT-10257 Vilnius, Lithuania
[2]Materials Research Center, Krzhizhanovskogo street, 3, 03680, Kyiv, Ukraine
[3]Department of Nanotechnology, State Research Institute Center for Physical Sciences and Technology, Sauletekio av. 3, LT-10257 Vilnius, Lithuania
saqib.ali@ftmc.lt

Colorimetric sensors are gaining significant interest in various sensing applications for biological and environmental fields, because to their high selectivity, high sensitivity, cost effectiveness, simplicity of use, rapid analysis, ease of use, and visibility to the naked eye. Researchers have developed a variety of colorimetric sensors to detect both organic and inorganic species. Some key areas of application for colorimetric sensors are the detection of organic species, e.g., proteins, amino acids, DNA/RNA, and microorganisms like viruses and bacteria, as well as their widespread exploration for water quality sensing, which is also in the mainstream, e.g., reactive oxygen species, acidity/base and heavy metal ions detections, and use as biomarkers in clinical diagnostics [1][2]. The working principle of colorimetric sensors is based on record of changes in color in the presence of the target analyte, providing real-time detection and highly sensitive direct identification of target analyte. However, existing technologies are limited due to low extinction coefficients and low accuracy of colorimeter due to material limitations [3]. Advanced nanomaterials, such as 2D materials, metal and metal oxide nanoparticles and quantum dots, have significantly aided the development of colorimetric sensors [4]. MXenes are the newest member of 2D material family, discovered in 2011, since then MXenes are under spotlight for their numerous applications due to their high surface area and surface functionality [5]. Herein we demonstrate the Au nanoparticles-decorated, functionalized MXene-based colorimetric sensor prepared at room temperature for colorimetric detection of trace amounts of glycolic acid and thiol glycolic acid in water. In this study, L-Cystine functionalized MXene shows the prominent Au nanocluster growth evident in the 375 nm Au plasmonic peak. This work shows high detection sensitivity and selectivity for glycolic acid and thioglycolic acid in water. Furthermore, this work expands the application of MXene in colorimetric sensors technology and provides a simple analyte sensing platform to open a new avenue for highly sensitive colorimetric sensors for future applications.

[1] S. Zukauskas et al., “Electrochemical real-time sensor for the detection of Pb(II) ions based on Ti3C2Tx MXene,” Sci. Total Environ., vol. 950, p. 175190, Nov. 2024, doi: 10.1016/J.SCITOTENV.2024.175190
[2] I. Navitski, A. Ramanaviciute, S. Ramanavicius, M. Pogorielov, and A. Ramanavicius, “MXene-Based Chemo-Sensors and Other Sensing Devices,” Nanomater. 2024, Vol. 14, Page 447, vol. 14, no. 5, p. 447, Feb. 2024, doi: 10.3390/NANO1405044
[3] J. Zhou et al., “Recent Advances in Design and Application of Nanomaterials-Based Colorimetric Biosensors for Agri-food Safety Analysis,” ACS Omega, vol. 8, no. 49, pp. 46346–46361, Dec. 2023, doi:10.1021/ACSOMEGA.3C06409/ASSET/IMAGES/LARGE/AO3C06409_0007.JPEG
[4] Y. Wu, J. Feng, G. Hu, E. Zhang, and H. H. Yu, “Colorimetric Sensors for Chemical and Biological Sensing Applications,” Sensors 2023, Vol. 23, Page 2749, vol. 23, no. 5, p. 2749, Mar. 2023, doi: 10.3390/S23052749.
[5] M. Naguib et al., “Two-Dimensional Nanocrystals Produced by Exfoliation of Ti3AlC2,” Adv. Mater., vol. 23, no. 37, pp. 4248–4253, Oct. 2011, doi: 10.1002/ADMA.201102306.

DEVELOPMENT OF GLUCOSE BIOSENSORS USING GLUCOSE OXIDASE AND NANOPARTICLE-MODIFIED ELEKCRTRODES

Rugilė Blauzdžiūnaitė[1], Antanas Zinovičius[1,2]

[1]Vilnius Tech, Faculty of Fundamental Sciences
[2]Center for Physical Sciences and Technology, Department of Nanotechnology
rugile.blauzdziunaite@stud.vilniustech.com

Diabetes mellitus is a global health issue marked by insulin deficiency and high blood sugar, leading to complications like heart disease, kidney failure, and even death. Tight glucose control reduces health risks, making regular monitoring essential and positioning glucose as the most tested analyte, with biosensors covering 85% of the market. This demand for reliable glycaemic control drives continuous research into advanced detection technologies [1].

Amperometric enzyme electrodes, in particular glucose oxidase (GOx) enzyme-based electrodes, have helped to simplify the detection of blood sugar levels and are expected to contribute to the advancement of continuous glucose control [2]. Second-generation enzymatic glucose biosensors use artificial redox mediators instead of oxygen for electron transfer. These small, soluble mediators transfer electrons from the enzyme's FAD center to the electrode, lowering the sensor's operational potential and reducing interference [1]. Common mediators include ferrocene derivatives, ferricyanide, quinones, transition metal complexes, and phenothiazine [3].

In this work, a second-generation glucose biosensor was designed, and its performance characteristics were evaluated. The biosensor design incorporated metal and hybrid/composite nanomaterials for electrode modification, aiming to enhance the detection mechanism and electrochemical performance of enzymatic glucose biosensors. The results were compared to those of a conventional second-generation glucose biosensor.

[1] Mohamad Nor N, Ridhuan NS, Abdul Razak K. Progress of Enzymatic and Non-Enzymatic Electrochemical Glucose Biosensor Based on Nanomaterial-Modified Electrode. Biosensors. 2022 Dec 6;12(12):1136.
[2] Hosseinikebria S, Khazaei M, Dervisevic M, Judicpa MA, Tian J, Razal JM, et al. Electrochemical biosensors: The Beacon for food safety and quality. Food Chem. 2025 Feb;143284.
[3] Cass AEG, Davis Graham, Francis GD, Hill HAO, Aston WJ, Higgins IJohn, et al. Ferrocene-mediated enzyme electrode for amperometric determination of glucose. Anal Chem. 1984 Apr 1;56(4):667–71.

APPLICATION OF PtCo NANOZYMES IN THE DEVELOPMENT OF AN AMPEROMETRIC GLUCOSE BIOSENSOR

Aistė Krikštaponytė[1], Asta Kaušaitė-Minkštimienė[2]

[1]NanoTechnas - Center of Nanotechnology and Materials Science, Institute of Chemistry, Faculty of Chemistry and Geosciences, Vilnius University, Naugarduko St. 24, LT-03225 Vilnius, Lithuania.
aiste.krikstaponyte@chgf.vu.lt

Determination of glucose concentration is very important for people with diabetes. By monitoring blood glucose levels, these individuals can make informed decisions about medication, diet and lifestyle, thereby reducing the risk of diabetes complications. There are many ways to determine the concentration of glucose, but amperometric biosensors, whose operation is usually based on the oxidation of glucose catalyzed by immobilized glucose oxidase (GOx), are the most common object of research due to their extremely simple operating principle. In addition, they are highly sensitive and selective for glucose, have a short response time, and do not require additional sample preparation.

In order to increase the sensitivity and selectivity of biosensors and reduce the effect of interfering substances on the analytical signal, nanomaterials are being implemented. Currently, nanozymes - nanomaterials imitating the catalytic activity of enzymes - are attracting a lot of attention from scientists. Unlike natural enzymes, they are resistant to denaturation and are less sensitive to environmental changes such as temperature or pH. Nanozymes provide greater catalytic stability, easy modification, and lower production costs because they can be synthesized in simpler ways than natural enzymes, which often require extraction and purification. In addition, nanozymes also have properties characteristic of nanomaterials. Among the first nanozymes to be used in the construction of biosensors were Prussian blue nanoparticles that play the role of ”artificial peroxidase” and catalyze the reduction of hydrogen peroxide.

In this work, seven different nanozymes were investigated and an amperometric glucose biosensor was developed using PtCo nanoparticles and GOx. The developed biosensor had a linear range of 0,04 – 2,18 mM glucose, a sensitivity of 1,42 μA/mM, and a detection limit of 0,032 mM. The biosensor was selective for glucose and its performance was not affected by interfering substances commonly found in biological samples. Thus, the obtained results suggest that the developed biosensor has potential to be used for glucose analysis, without interference from other substances. In addition, it had good stability over a period of 14 days.

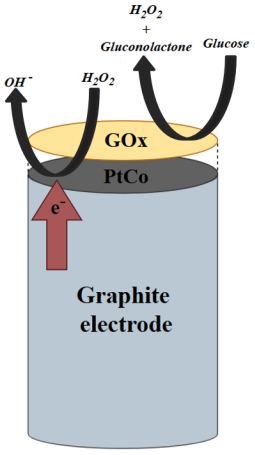


Fig. 1. A schematic representation of the amperometric glucose biosensor based on PtCo nanozyme and GOx

Acknowledgements

This research has received funding from the Research Council of Lithuania (LMTLT), agreement No. S-MIP-24-7.

DOSY INVESTIGATION OF BIOACTIVE IONIC LIQUIDS

Lukas Mikalauskas[1], Vytautas Klimavičius[1]

[1] Institute of Chemical Physics, Faculty of Physics, Vilnius University
lukas.mikalauskas@ff.stud.vu.lt

Bioactive room temperature ionic liquids (b-RTILs) are room temperature-molten salts compatible with living organisms. RTILs are becoming more popular in the scientific community due to the high number of ion combinations and tunability. Specifically, b-RTILs are applied in the medical field in drug delivery systems and to increase non-soluble drug solubility in water [1]. One of the important parameters of ILs is diffusion because it gives us information about the size or structure of molecules and how molecules interact with each other due to the change in concentration [2]. The main objective is to investigate diffusions of two b-RTILs: choline lysinate ([Ch][Lys]) and choline tryptophanate ([Ch][Trp]) in a water mixture using DOSY. [Ch] cation is involved in the metabolism process while [Trp] and [Lys] anions are involved in protein biosynthesis.

DOSY (Diffusion-Ordered Spectroscopy) is a powerful NMR (Nuclear Magnetic Resonance) tool for measuring the diffusion coefficient of a specific proton. The gradient of a magnetic field is applied to the sample. Due to magnetic field inhomogeneity, the magnetic spin orientation of protons across the sample differs. Also, due to the constant movement of molecules, the intensity of the spectra is lower than with a homogenous magnetic field across the sample. The change in the intensity also depends on the size of the molecule. Using the DOSY method, it was found that there are two diffusion regimes in [Ch][Lys]. 1 fig. shows how the diffusion of water changes according to the change in IL concentration. The same applies to [Ch] and [Lys] ions. The diffusion gradually decreases to the concentration χ_{RTIL} = 0.1 mol. frac. From that concentration, the diffusion coefficient decreases more slowly, meaning that the regime of diffusion changes. It's also corresponding to the chemical shift minima seen in [Ch][Lys] protons. The regime change can be due to a change in the interaction of the water molecules between themselves and the protons of [Ch][Lys]. The change of regimes cannot be seen in [Ch][Trp] where the [Ch][Trp] and water diffusion coefficients gradually decrease with increasing IL concentration.

The results can be used to analyse how molecules behave at the higher IL concentration, especially around from χ_{RTIL} = 0.1 to 0.15 mol. frac.

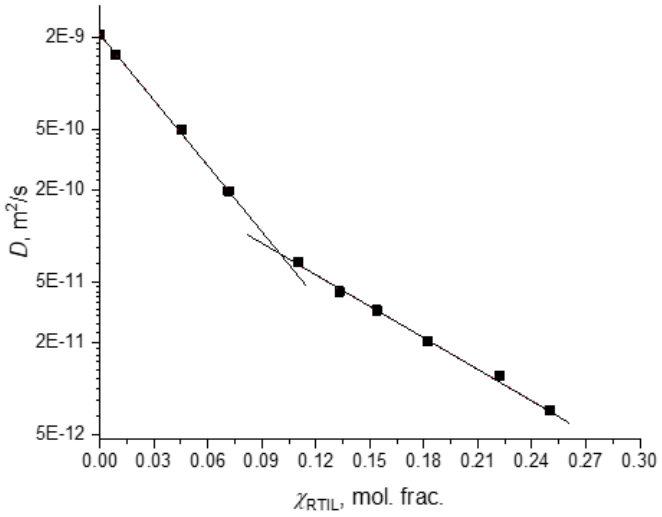


Fig. 1. H_2O diffusion coefficient dependency from molar concentration of [Ch][Lys]

[1] Y. Zhuo, H.-L. Cheng, Y.-G. Zhao, and H.-R. Cui, "Ionic Liquids in Pharmaceutical and Biomedical Applications: A Review," Pharmaceutics, vol. 16, no. 1, p. 151, Jan. 2024, doi: https://doi.org/10.3390/pharmaceutics16010151.

[2] G. Colafemmina, H. Mateos, and G. Palazzo, "Diffusion NMR studies of complex liquid formulations," Current Opinion in Colloid and Interface Science, vol. 48, pp. 109–120, Aug. 2020, doi: https://doi.org/10.1016/j.cocis.2020.04.006.

SYNTHESIS OF NEW IMIDAZOLE-2-THIOLES CONTAINING CARBAZOLYL MOIETY

Tomas Tutkus[1], Birutė Sapijanskaitė-Banevič[1]

[1]Department of Organic Chemistry, Kaunas University of Technology, Lithuania
tomtut@ktu.lt

The imidazole scaffold can often be found in a wide variety of bioactive compounds, it serves as the fundamental core of numerous natural products, including histidine, purine, histamine and DNA-base structures[1]. Imidazole derivatives have garnered significant attention in medicinal chemistry due to their diverse biological activities, such as antifungal properties. Clinically, imidazole-based compounds, particularly Miconazole, Econazole, Ketoconazole and Clotrimazole, are widely used to treat yeast and fungal infections[2].

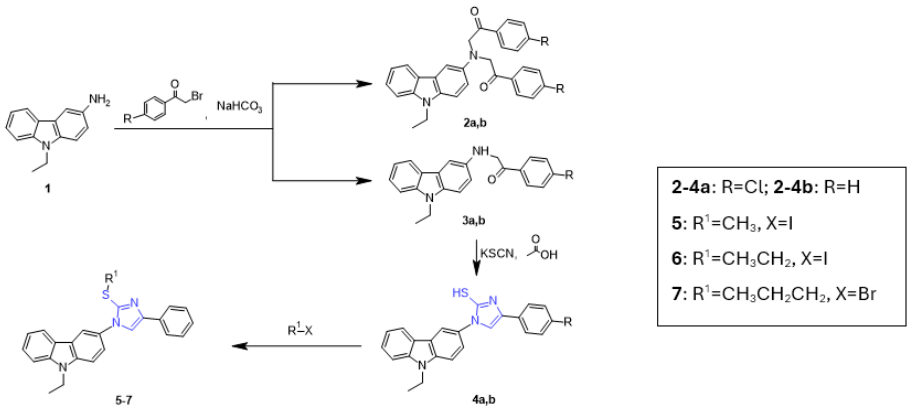


Fig. 1. Synthesis of imidazole-2-thioles containing carbazolyl moiety

In this work, we investigated reactions of 3-amino-9-ethylcarbazole with α-haloketones. The reaction of 3-amino-9-ethylcarbazole **1** with *α*-haloketones in methanol at room temperature in the presence of sodium bicarbonate resulted in formation of mixture of mono- and bis-addition products. The yields of the formed compounds **2a,b** and **3a,b** depended on the duration of the reaction. Subsequently, 1-(4-chlorophenyl)-2-((9-ethyl-9*H*-carbazol-3-yl)amino)ethan-1-one **3a** and 2-((9-ethyl-9*H*-carbazol-3yl)amino)-1-phenylethan-2-one **3b** have been cyclized to imidazolethiols **4a,b** during the reaction with potassium thiocyanate in glacial acetic acid. Obtained compound **4b** have been alkylated with various haloalkanes resulting in formation of compounds **5-7**.

The structures of compounds **2-4a,b** and **5-7** have been confirmed by elemental analysis, ^{1}H and ^{13}C NMR spectral data.

[1] Benas Balandis, Povilas Kavaliauskas, Birutė Grybaitė, Vidmantas Petraitis, Rūta Petraitienė, Ethan Naing, Andrew Garcia, Ramunė Grigalevičiūtė, Vytautas Mickevičius // Microorganisms, 2023, 11,935, doi:10.3390, 1-14.

[2] D. Serdaliyeva, T. Nurgozhin, E. Satbayeva, M. Khayitova, A. Seitaliyeva, and L. Ananyeva, "Journal of Clinical Medicine of Kazakhstan," J. Clin. Med. Kazakhstan, vol. 19, no. 3, pp. 11–15, 2022, doi:10.23950/jcmk/12117.

MAGNETIC-CONTROLLED HYDROGELS BASED ON POLYESTER-TYPE PSEUDO-POLYAMINOACIDS

Yuliia Kyrychuk[1], Roman Taras[1], Volodymyr Samaryk[1], Yaryna Kuryshchuk[1]

[1]Department of Organic Chemistry, Lviv Polytechnic National University, Ukraine
yuliia.kyrychuk.mkhtkhd.2024@lpnu.ua

Nowadays, hydrogels are widely used as carriers of drugs and biologically active substances. A separate application of hydrogels is their use as components for drug delivery devices. In tissue engineering, hydrogels are used as implants, for the manufacture of biosensors and in cancer therapy. To control hydrogels within the body and facilitate their removal, systems incorporating magnetically controlled particles - such as Fe_3O_4 and $CoFe_2O_4$ and others- are actively being developed. Magnetically controlled hydrogels are obtained by three different methods: mixing, precipitation and grafting to the surface [1]. In this work, magnetite was used to graft the polymer matrix, the surface of which was modified with 3-aminopropyltriethoxysilane (APTES) to localize reactive amino groups on the surface of magnetite. A schematic representation of magnetite surface modification is shown in Fig. 1a.

Surface-modified magnetite was used for grafting N-stearoylglutamic acid polyester along with oxyethylene and oxypropylene diols in the presence of glycerol via the Steglich reaction at 15°C. The principle scheme of grafting polyester to the surface of magnetite is shown in Fig. 1b. The polyester components were chosen primarily for their non-toxicity, as well as for the non-toxicity of their biodegradation products.

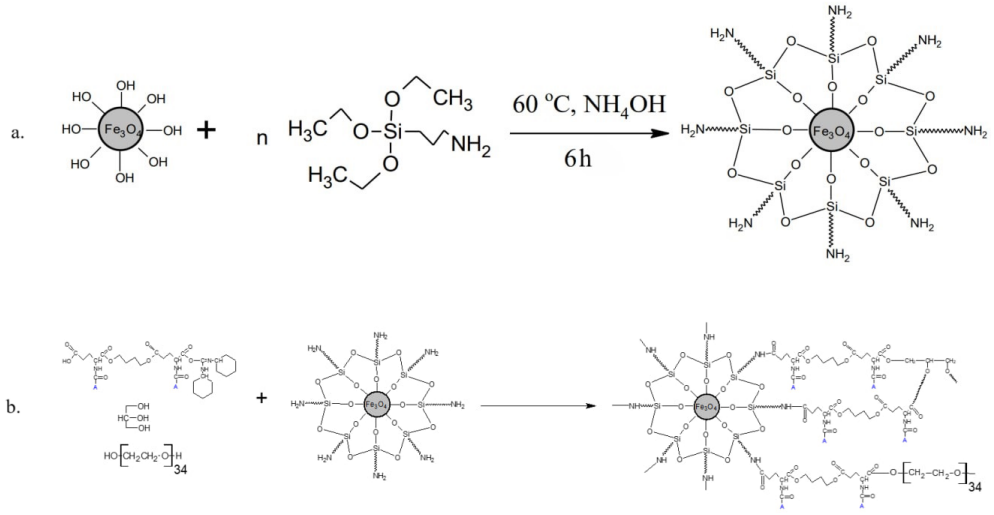


Fig. 1. a. Grafting APTES to the surface of magnetite. b. Scheme of grafting polyester to the surface of magnetite

The degree of Fe_3O_4/APTES surface modification was estimated using IR spectra at different molar ratios of the modifier to magnetite. Based on the obtained spectra, it can be concluded that a ratio of 13:1 (APTES/Fe_3O_4)) is the minimal sufficient amount for surface modification. The formation of a cross-linked monomolecular layer of polyester on the surface of modified magnetite occurs at a ratio of 41:44 (APTES/Fe_3O_4), ensuring 31.8% grafting of polyester to the magnetite surface. The obtained magnetically controlled polyesters were used for sorption of α-amylase into the grafted polyester matrix as a model sample. The incorporation of the enzyme preparation into the grafted polyester matrix was confirmed using thermogravimetric analysis. The activity of the enzyme preparation immobilized in the polyester matrix grafted to the magnetite surface was carried out according to the classical method.

[1] Huang Y. Magnetic hydrogels and their potential biomedical applications / Y. Li. G. Huang et al. // Adv. Funct. Mater. -2013. -№23. -p.660-672.

SYNTHESIS AND CHARACTERIZATION OF CROSS-LINKED COPOLYMERS BASED ON DEXTRIN AND POLY(N-ISOPROPYLACRYLAMIDE)

Emilija Morkvėnaitė[1], Miglė Savickė[1], Dovilė Liudvinavičiūtė[1], Ramunė Rutkaitė[1]

[1]Department of Polymer Chemistry and Technology, Kaunas University of Technology, Lithuania
emilija.morkvenaite@ktu.edu

Thermo-responsive polymers have gained significant attention due to their ability to undergo reversible phase transitions in response to temperature changes. These materials are widely explored in biomedical applications, particularly drug delivery, tissue engineering, and stimuli-responsive systems. However, developing effective thermo-responsive polymeric matrices with controlled swelling and phase transition behavior remains a challenge [1]. This study addresses this gap by synthesizing and characterizing cross-linked dextrin-based copolymers with tunable thermo-responsive properties.

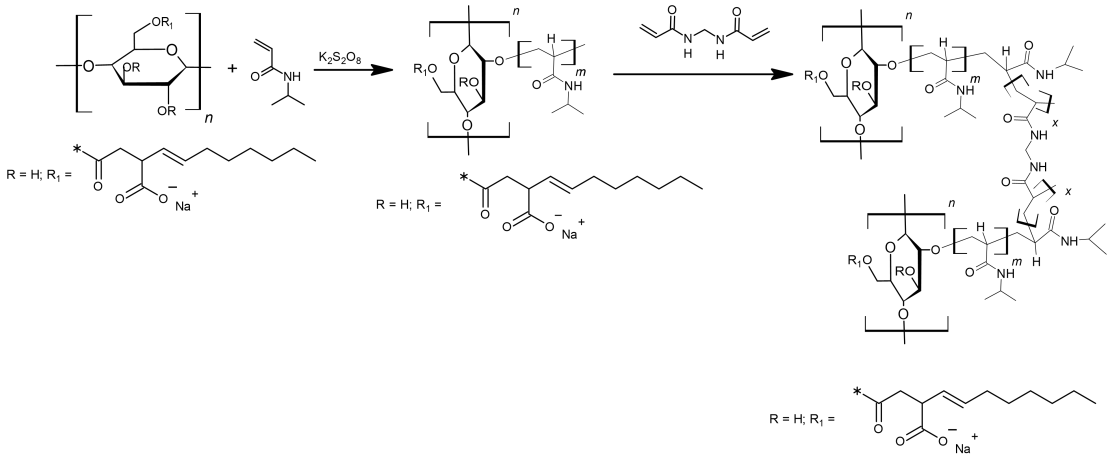


Fig. 1. Reaction scheme for synthesis of dextrin octenylsuccinate, dextrin octenylsuccinate-graft-poly(*N*-isopropylacrylamide) and cross-linked derivatives

Four dextrin octenylsuccinates (OSA) were synthesized by varying the content of OSA (4.37 %, 6.82 %, 8.05 %, and 10.67 %). Further, dextrin octenylsuccinate-graft-poly(*N*-isopropylacrylamide) copolymers were obtained via free-radical polymerization and crosslinked with *N*, *N'*-methylenebisacrylamide. Characterization techniques included FTIR, thermogravimetric analysis, DSC and dynamic light scattering to assess chemical structure, thermal stability, and thermoresponsive properties of synthesized derivatives.

The synthesized cross-linked grafted dextrin copolymers exhibited thermo-responsive behavior in water, with phase separation occurring at 31–33 °C. Moreover, a 10-hour swelling study was conducted in simulated gastric fluid (pH 1.2), intestinal fluid (pH 6.8), and blood plasma (pH 7.4) at 25 °C and 37 °C. Swelling increased with temperature, particularly in the gastric environment, due to enhanced water diffusion. Intestinal swelling was moderate, while the lowest swelling was observed at neutral pH conditions. Higher OSA content resulted in faster and greater swelling, with equilibrium reached within 400–500 minutes, and also higher thermal stability.

In this study thermo-responsive dextrin-based copolymers with tailored swelling properties and controlled phase transition in aqueous media were successfully developed, supporting their potential for controlled drug release and drug delivery applications.

[1] M. Sponchioni, U. Capasso Palmiero, and D. Moscatelli, “Thermo-responsive polymers: Applications of smart materials in drug delivery and tissue engineering,” Materials Science and Engineering: C, vol. 102, pp. 589–605, Sep. 2019.

THE CREATION OF POROUS HYDROGELS USING PEROXIDES

Yuliia Cherkas[1], Nataliia Bukartyk[1], Solomiia Kapatsila[1], Serhiy Tsykunkov[1], Volodymyr Samaryk[1]

[1]Department of Organic Chemistry, Lviv Polytechnic National University, Ukraine
yuliia.cherkas.kht.2022@lpnu.ua

Polymer hydrogels are hydrophilic structured systems that swell well but are insoluble in water. Typically, they are obtained by polymerising water-soluble unsaturated compounds in the presence of a bifunctional cross-linking agent or by cross-linking pre-prepared polymers. Hydrogels are widely used as drug delivery devices, immobilised biologically active compound carriers, and implants. In recent years, hydrogels with nano-, micro-, and macroporous structures have been researched and synthesised. They have been widely used in tissue engineering, for protein separation, and purification. A significant disadvantage of known hydrogels, in particular porous hydrogels, is their low physical and mechanical characteristics.

The main purpose of the research was to improve the mechanical properties of a porous gel by chemically reinforcing the pore walls. The imparting of adjustable physical and mechanical properties to porous hydrogels was achieved by using a filler with a specifically modified surface. This process includes the following steps: 1. Peroxidation of the silica surface by adsorption of heterofunctional polyperoxide; 2. Grafting polyacrylamide chains to the peroxidised surface; 3. Formation of a three-dimensional gel network using a filler with a reactive surface; 4. Creation of a porous system by removing the mineral component of the filler.

Peroxidation of the mineral filler surface with a subsequent graft polymerisation from the acrylamide surface makes it possible to obtain silica particles containing grafted polyacrylamide chains on the surface. The use of modified silica as a reactive filler in the formation of hydrogels leads to the establishing of a three-dimensional mesh with the involvement of grafted polyacrylamide chains in it.

The grafting of polyacrylamide to the surface of silica was confirmed by FTIR multiple reflection spectroscopy and thermogravimetric analysis.

Thus, when using the modified filler, a more uniform distribution of the filler in the polymer matrix was observed, and after the removal of silica, the walls of the obtained porous hydrogels were less damaged compared to the use of unmodified filler, which has a positive effect on the physical and mechanical properties of the hydrogel (Fig. 1).

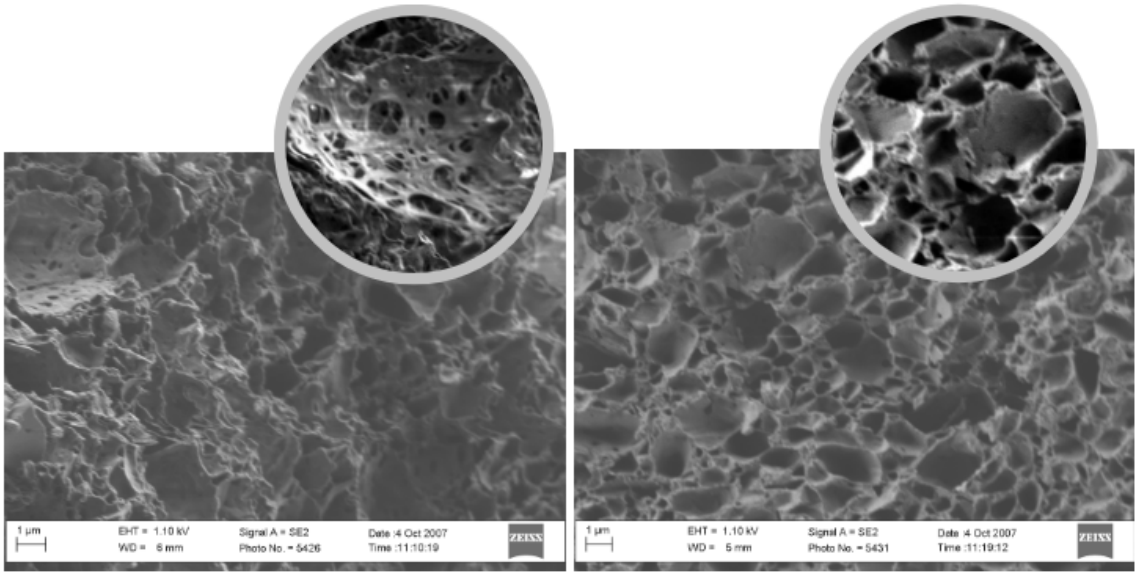


Fig. 1. SEM micrographs of porous gels obtained using filler (SiO_2): a) unmodified, b) modified. The degree of filling is 65%.

Thus, for the first time, a method for the porous hydrogels preparation using peroxidised filler particles to form a filled polymeric hydrogel framework allows creating porous hydrogels with adjustable mechanical properties at a higher degree of porosity when removing the filler.

EFFECT OF CALCIUM IONS STRUCTURING METHODS ON THE PHYSICAL AND MECHANICAL PROPERTIES OF ALGINATE HYDROGELS

Solomiia Kapatsila[1], Yuliia Kyrychuk[1], Yuliia Cherkas[1], Volodymyr Samaryk[1]

[1]Lviv Polytechnic National University
solomiia.m.kapatsila@lpnu.ua

Sodium alginate is widely used in the polymer research field due to its properties in forming three-dimensional hydrogel structures. This type of hydrogel is likewise actively used in the cosmetic, food, and biomedical fields [1]. Sodium alginate, which is a polymer of natural origin, can be structured with polyvalent metal ions, resulting in the creation of a crosslinked polymer network. Such crosslinkers are often inorganic salts of aluminum, calcium, strontium, barium, copper, and others [2]. In this case, the composition of the hydrogel will contain impurities of low-molecular acid residues, such as hydrochloric, acetic, nitric, or other acids.

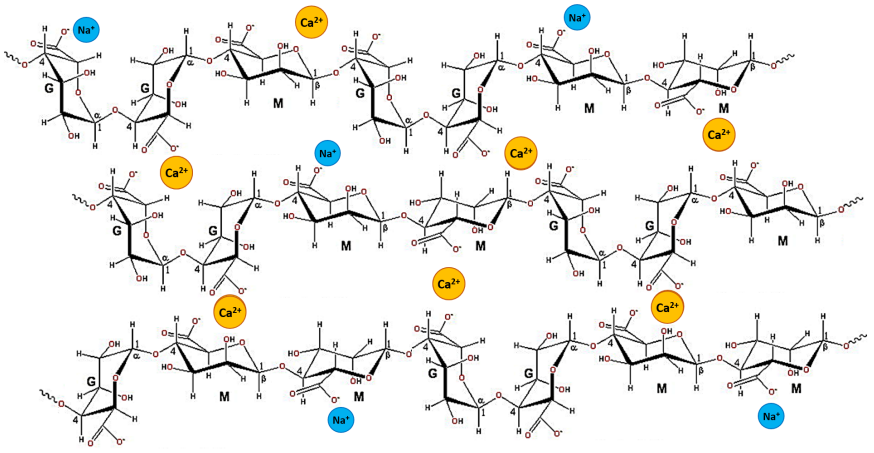


Fig. 1. Schematic representation of a sodium alginate hydrogel crosslinked with calcium ions

Other structuring methods are also possible without the use of inorganic and low-molecular calcium salts. The method of crosslinking alginate hydrogels with calcium ions from a compound with polyacrylic acid is noteworthy. Calcium polyacrylate can be obtained by the action of calcium oxide on both specifically structured and branched polyacrylic acid. The introduction of a structuring agent in the form of polyelectrolyte salts has a significant impact on the morphology and physicochemical properties of the hydrogel due to the introduction of a high-molecular component into the system.

The work carried out a full-factorial analysis of the dependence of physicomechanical properties on the ratio between the reagents, their concentrations in the initial solutions, and the method of obtaining such compositions. The dependence of the sol-gel fraction, the degree of swelling in distilled water and a model body fluid, the physicomechanical properties of these hydrogels on the method, and the degree of structuring were analyzed. During the study, a rotational rheometer was used for oscillatory, axial, and other loads on the samples.

The introduction of a crosslinker for alginate hydrogel in the form of polyelectrolyte salts has a number of advantages in assessing such indicators as physicomechanical properties and swelling in model fluids at different temperatures.

[1] G. Alkhayer, “Alginate metal complexes and their application,” in IntechOpen eBooks, 2021. doi: 10.5772/intechopen.98885.
[2] Y. Wang et al., “Progress in research on metal ion crosslinking Alginate-Based gels,” Gels, vol. 11, no. 1, p. 16, Dec. 2024, doi: 10.3390/gels11010016.

PREPARATION AND INVESTIGATION OF ARTHROSPIRA PLATENSIS EXTRACT ENCAPSULATED IN MODIFIED STARCH USING DIFFERENT TECHNIQUES

Dovilė Liudvinavičiūtė[1], Vesta Navikaitė-Šnipaitienė[1], Vaida Kitrytė-Syrpa[2], Michail Syrpas[2], Ramunė Rutkaitė[1]

[1]Department of Polymer Chemistry and Technology, Faculty of Chemical Technology, Kaunas University of Technology, Kaunas, Lithuania
[2]Department of Food Science and Technology, Faculty of Chemical Technology, Kaunas University of Technology, Kaunas, Lithuania
dovile.liudvinaviciute@ktu.lt

Arthrospira platensis is one of the most significant cultivated microalgae species, recognized for its high protein content (60–70% based on dry weight) and a wide range of bioactive compounds e.g. vitamins, minerals, unsaturated fatty acids especially gamma-linolenic acid [1-2]. *Arthrospira platensis* is renowned for its pharmacological properties, with phycocyanin (pigment-binding protein) being one of the most effective compounds, showing antioxidant, anticancer, antidiabetic, antibiotic and immune-enhancing effects. Sensitivity of phycocyanin is influenced by various factors such as temperature, pH, moisture, light, and oxygen. To mitigate these challenges, several effective methods have been developed to enhance and protect the bioactivity of these compounds. Encapsulation of phycocyanin into various matrices could help improve resistance to environmental factors, prevent interactions with other compounds, and have controlled release in different media. Encapsulated materials could be applied as nutraceuticals, in food industry, also in biomedical products.

In this study, a crude *Arthrospira platensis* extract was obtained by employing freeze-thaw method. A biomass suspended in distilled water was subjected to three freezing (-20 °C, 12 h) and thawing (25 °C, 12 h) cycles, the cell debris were removed by centrifugation at 8000 rpm for 5 min and filtration through a 160 µm glass filter. Obtained liquid extract was frozen and freeze-dried. For the encapsulation of Arthrospira platensis extract, firstly aqueous formulations containing 10 % (w/w) of starch sodium octenyl succinate and 1 or 5 % w/w of *Arthrospira platensis* extract were prepared by homogenizing at 12,000 rpm for 5 min. Encapsulated extract in the form of solid particles were obtained utilizing freeze-drying, as well as conventional and nanospray-drying techniques. SEM analysis of encapsulated *Arthrospira platensis* extract was performed. Also, the release of phycocyanins into saliva medium was studied. Moreover, thermal characteristics, antioxidant activity and total phenolic content of the particles were determined and assessed.

Acknowledgements
This project has received funding from the Research Council of Lithuania (LMTLT), agreement No S-MIP-23-78.

[1] G. Özyurt, L. Uslu, M. Durmuş, Y. Sakarya, T. Uzlaşir, E. Küley. Chemical and physical characterization of microencapsulated Spirulina fermented with Lactobacillus plantarum. Algal Research 73, 103149, (2023).
[2] S. Yagoubi, A. Shahidi, F. Mohebbi, et al. Preparation, characterization and evaluation of physicochemical properties of phycocyanin-loaded solid lipid nanoparticles and nanostructured lipid carriers. Food Measure 12, 378–385, (2018).

DEVELOPMENT OF BIOACTIVE 3D-PRINTED POLYLACTIC ACID AND HYDROXYAPATITE SCAFFOLDS FOR BONE TISSUE ENGINEERING

Jokūbas Lukošiūnas[1], Martyna Sabaitė[1], Odeta Baniukaitienė[1]

[1]Department of polymer chemistry and technology, faculty of chemical technology, Kaunas university of technology
jokubas.lukosiunas@ktu.edu

Tissue engineering is a rapidly evolving field aimed at developing biomimetic scaffolds to restore or replace damaged tissues. Three-dimensional (3D) printing offers precise control over scaffold architecture, facilitating the creation of structures that support cellular attachment, proliferation, and differentiation. This study focuses on the fabrication and characterization of poly(lactic acid) (PLA) scaffolds reinforced with hydroxyapatite (HAP) to enhance their bioactivity and mechanical properties for bone tissue engineering applications.

Initially, PLA-HAP filaments containing varying amounts of inorganic material were fabricated using extrusion technology. Subsequently, 3D scaffold modeling was performed using the Z-Suite computer software, followed by 3D printing of various scaffold designs with different structural parameters using the Zortrax M200 Plus 3D printer.

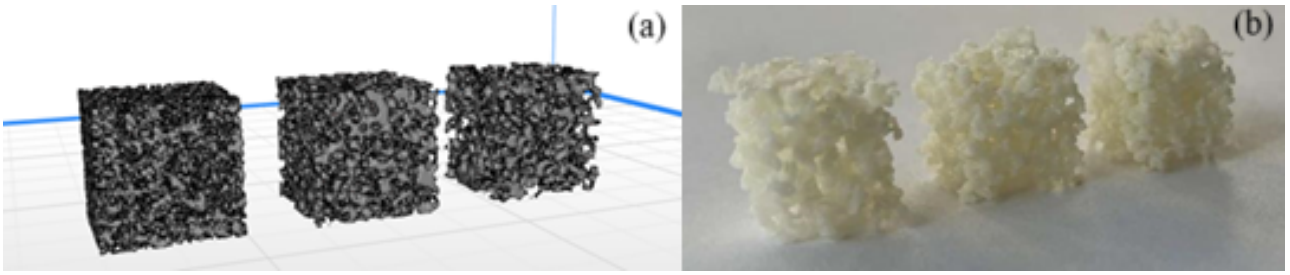


Fig. 1. Composite 3D models (a) and printed prototypes (b)

The results indicate that the composition of the PLA-HAP filament significantly influences the 3D printing process, layer adhesion, and structural integrity. Furthermore, the mechanical properties of the printed scaffolds directly correlate with the concentration of HAP within the filament.

SYNTHESIS OF 6-CHLORORESORCINOLS MODIFIED WITH CYCLIC AMINES AND AMIDES IN THE FOURTH POSITION

Ugnius Popovas[1], Ieva Žutautė[1]

[1] Institute of Chemistry, Faculty of Chemistry and Geosciences, Vilnius University
ugnius.popovas@chgf.stud.vu.lt

Hsp90 (Heat Shock Protein 90) is one of the most essential molecular chaperones involved in the maturation regulation of over 300 client proteins. Many of these proteins are closely related to hard-to-treat diseases such as cancer, neurodegenerative, and infectious diseases. For this reason, Hsp90 is a significant target in the search for synthetic inhibitors of this protein. One of its key pharmacophores is the resorcinol fragment, which inhibits Hsp90 activity due to hydrogen bonding between its hydroxyl groups and the Asp93 amino acid in the N-terminal domain of the protein. Consequently, compounds containing this structure are widely used to develop second-generation inhibitors [1].

To discover new structures that could enhance the inhibitory properties of resorcinol derivatives, it was decided to synthesize amides and amines containing the resorcinol fragment. The chosen base structure was 4-chlororesorcinol.

In the first step, an aldehyde group was introduced at the sixth position of 4-chlororesorcinol. In the second step, considering the subsequent synthetic steps, the hydroxyl groups in 4-chlororesorcinol were blocked using methyl iodide. In the third step, the synthesis diverges slightly: the aldehyde was oxidized to a carboxylic acid using a potassium permanganate, followed by condensation with target amines to produce amides. Another route involved the reduction of the aldehyde to alcohol, which was then brominated using phosphorus tribromide in a two-step reaction, immediately followed by nucleophilic substitution with target amines.

To complete this research, the only remaining step is to unblock the hydroxyl groups, which is currently in progress, and to investigate whether the compounds are suitable for Hsp90.

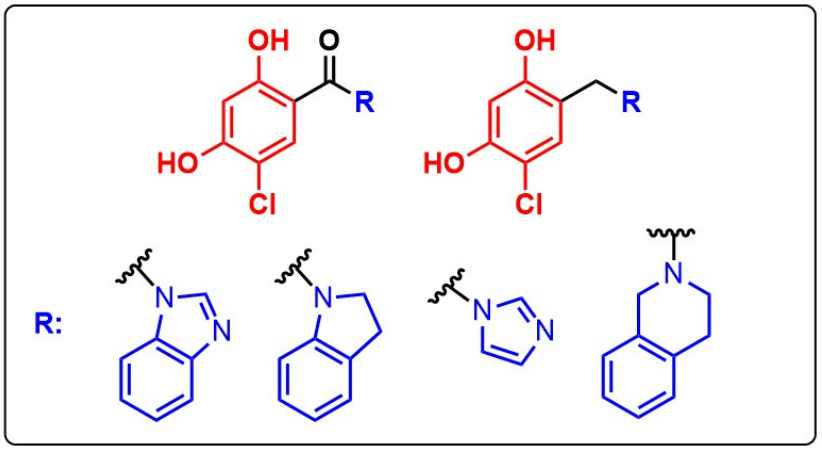


Fig. 1. Scheme of synthesized compounds containing resorcinol fragments and cyclic amines.

[1] L. Li, L. Wang, Q. You, and X. Xu, "Heat Shock Protein 90 Inhibitors: An Update on Achievements, Challenges, and Future Directions," Journal of Medicinal Chemistry, vol. 63, no. 5, pp. 1798–1822, 2019.

MODIFICATION OF CORN STARCH VIA SUCCINYLATION AND ACETYLATION

Muhammad Nasif[1], Ayodeji Amobonye[1], Joana Bendoraitiene[1], Laura Peciulyte[1], Remo Merijs Meri[2], Shu-Kai Yeh[3], Ramune Rutkaite[1]

[1]Department of Polymer Chemistry and Technology, Kaunas University of Technology, Lithuania
[2]Institute of Chemistry and Chemical Technology, Riga Technical University, Latvia
[3]Department of Materials Science and Engineering, National Taiwan University of Science and Technology, Taiwan
muhammad.nasif@ktu.edu

For the replacement of conventional plastics, the bioplastics based on renewable biopolymers such as natural polysaccharides are receiving increasing attention. In order to impart thermoplastic properties to polysaccharides such as starch, they should be chemically modified. Therefore, in this work the double modification of starch with organic anhydrides was investigated and the influence of the degree of substitution (DS) on the properties of modified starches was studied. In this study, we report the double modification of corn starch via succinylation and acetylation. The initial modification was carried out with dodecylsuccinic anhydride to synthesize the modified starches with three different degrees of substitution of dodecylsuccinate groups which were further modified with acetic anhydride, and acetylation reaction conditions were optimized to get highest degree of substitution of acetyl groups. The results show that starches with high degree of substitution have improved thermoplastic behavior and glass transition temperature as compared to those with low degree of substitution which show poor thermal stability. This dual modification method significantly increases the properties and functionality of starches making them promising materials for sustainable plastic alternatives.

Acknowledgements

This work was supported by the Project of Scientific Cooperation Program between Latvia, Lithuania, and Taiwan and received funding from the Research Council of Lithuania (LMTLT), agreement No S-LLT-25-4.

PHOTOREDOX MANIFOLD FOR DEHYDROGENATIVE COUPLING USING PROTONS AS THE SOLE OXIDANTS

Jonas Žurauskas[1], Paulius Vaickūnas[1], Gustautas Snarskis[3], Gediminas Kreiza[2], Steponas Raišys[2], Mantas Šimėnas[2], Vidmantas Kalendra[2], Kęstutis Zakarauskas[4], Barbara Chatinovska[1], Karolis Kazlauskas[2], Edvinas Orentas[1]

[1]Department of Organic Chemistry, Vilnius University; Vilnius, Naugarduko 24, LT-03225, Lithuania
[2]Institute of Photonics and Nanotechnology, Vilnius University, Vilnius, Saulėtekio av. 3, LT-10257, Lithuania
[3]Biomatter, Business Stadium West, Rinktinės g. 5-101, LT-09234 Vilnius, Lithuania
[4]Laboratory of Combustion Processes, Lithuanian Energy Institute, Breslaujos 3, LT-44403, Kaunas, Lithuania
jonas.zurauskas@chgf.vu.lt

We report a metal-free photocatalytic process for arene C-H functionalization that employs an acridinium-type catalyst and produces dihydrogen as the only by-product. Throughout the catalytic cycle, the catalyst acts as an oxidising, a hydrogen atom transfer, and a proton-reducing agent enabling a cross-dehydrogenative transformation without the need for external oxidants. The reaction is conveniently performed using visible light and the high oxidation potential of the catalyst allows to engage even electron-deficient arenes as substrates. The catalytic mechanism disclosed herein has a potential to become a general logic for the development of various cross-dehydrogenative reactions adaptable for use in pharmaceutical and material sciences.

ELECTRON-DEFICIENT PHOSPHINE LIGANDS FOR PALLADIUM CATALYSED C-N CROSS-COUPLING REACTIONS

Jonas Paukštys[1,2], Tomas Paškevičius[1], Linas Labanauskas[1]

[1]Center for Physical Sciences and Technology (FTMC)
[2]Vilnius Unversity
jonas.paukstys@ftmc.lt

Arylamine moiety is widely encountered in pharmaceuticals[1] , N-ligands[2], herbicides and fungicides[3]. Palladium catalysed C-N cross-coupling reactions are often strategically used for the synthesis of such compounds. Despite extensive research in this area, the coupling of heteroaryl compounds remains a challenging task. In 2024, novel O-bound electron deficient phosphine ligands (Figure 1.) were introduced that allegedly have been shown to be resistant to deactivation by many nitrogen containing heteroaromatic compounds.[4] Modification of steric and electronic properties of these ligands may enable chemists to include N-heteroaromatic compounds as coupling partners and thus expand the overall application scope of this reaction.

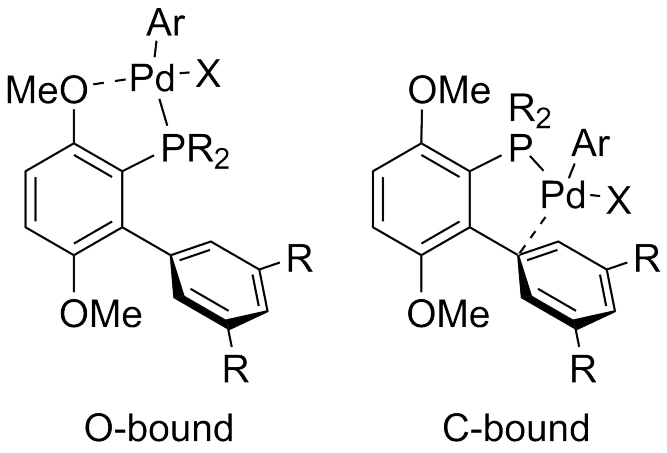


Fig. 1. O-bound and C-bound conformations

In this work, we synthesized the ligand backbones via aryne coupling reactions following iodine quench, iodinated backbones were used in further synthesis. Key step of this synthesis was the coupling of backbones with various di-substituted chlorophosphines, which were prepared from PCl_3 and desired Grignard reagent. Finally, we subjected these ligands to screening procedures to asses their catalytic performance in C-N cross coupling reactions.

[1] Roughley, S. D.; Jordan, A. M. The Medicinal Chemist's Toolbox: An Analysis of Reactions Used in the Pursuit of Drug Candidates. J. Med. Chem. 2011, 54, 3451–3479.
[2] Ruiz-Castillo, P.; Buchwald, S. L. Applications of Palladium-Catalyzed C–N Cross-Coupling Reactions. Chem. Rev. 2016, 116, 12564–12649, DOI: 10.1021/acs.chemrev.6b00512
[3] Devendar, P.; Qu, R.-Y.; Kang, W.-M.; He, B.; Yang, G.-F. Palladium-Catalyzed Cross-Coupling Reactions: A Powerful Tool for the Synthesis of Agrochemicals. J. Agric. Food Chem. 2018, 66, 8914– 8934, DOI: 10.1021/acs.jafc.8b03792
[4] Feng, K.; Elaine Reichert Raguram; Howard, J. R.; Peters, E.; Liu, C.; Sigman, M. S.; Buchwald, S. L. Development of a Deactivation-Resistant Dialkylbiarylphosphine Ligand for Pd-Catalyzed Arylation of Secondary Amines. Journal of the American Chemical Society 2024. https://doi.org/10.1021/jacs.4c09667.

INVESTIGATION OF ELECTROPHILIC CYCLIZATION REACTIONS OF 2-ALKENYLTHIOIMIDAZOLES

Martyna Paulauskaitė[1], Ieva Žutautė[1]

[1]Faculty of Chemistry and Geosciences, Vilnius University, Lithuania
martyna.paulauskaite@chgf.stud.vu.lt

Compounds containing an imidazo[2,1-*b*][1,3]thiazine fragment exhibit a wide range of biological properties, including anti-tuberculosis [1], anti-inflammatory [2], antifungal [3], and amyloid aggregation inhibitory [4] activities. These compounds demonstrate excellent chemical stability and the ability to selectively bind to various biomolecules, making them highly attractive for synthetic and medicinal applications.

Typically, the imidazo[2,1-*b*][1,3]thiazine fragment formation involves nucleophilic substitution or condensation reactions, which often require multiple synthetic steps. A growing approach to synthesizing heterocyclic systems from alkynes is using nucleophilic cyclization reactions promoted by electrophiles [5]. This method allows for the efficient formation of imidazo[2,1-*b*][1,3]thiazine rings and ensures good selectivity and high yields. However, the electrophile-initiated cyclization of 2-alkenylthioimidazoles has been scarcely explored. The heterocycles produced by this reaction are expected to possess novel chemical properties and enhanced biological activity. In this study, 2-cinnamylthiobenzimidazole was chosen as a model compound to investigate the cyclization reaction outcome and optimize its conditions. After applying the best conditions, other 5-arylimidazo[2,1-*b*][1,3]thiazines were synthesized. Formed compounds obtain a readily cleavable group, which can be replaced by other nucleophiles or eliminated by treatment with a base yielding 5-aryl-5*H*-benzimidazo[2,1-*b*][1,3]thiazine.

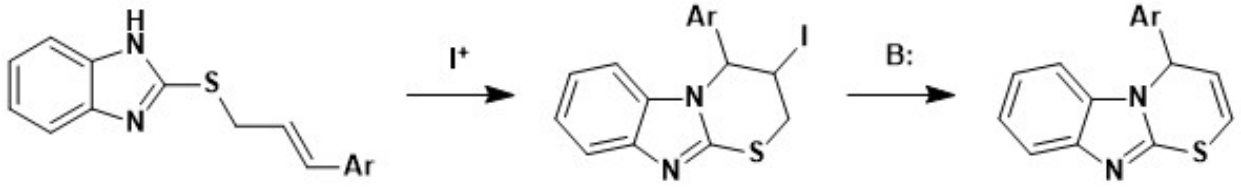


Fig. 1. Synthesis of benzimidazo[2,1-*b*][1,3]thiazine frameworks

[1] J. X. Gong, et al., Synthesis, spectral characterization, and antituberculosis activity of thiazino[3,2-a]benzimidazole derivatives, Phosphorus Sulfur Silicon Relat. Elem. 2016, 191, 1036–1041.
[2] N. Slyvka, et al., Synthesis and anti-inflammatory activity of S-oxides of pyridinyloxy substituted imidazo[2,1-b][1,3]thiazines, Curr. Chem. Lett. 2023, 12 335–342.
[3] M. D. LaFleur, et al., Novel high-throughput screen against Candida albicans identifies antifungal potentiators and agents effective against biofilms, J. Antimicrob. Chemoth. 2011, 66, 820–826.
[4] I. Misiunaite, et al., Imidazo[2,1-b][1,3]thiazine Derivatives as Potential Modulators of Alpha-Synuclein Amyloid Aggregation, ACS Chem. Neurosci. 2024, 15, 4418-4430.
[5] B. Godoi, et al., Synthesis of Heterocycles via Electrophilic Cyclization of Alkynes Containing Heteroatom, Chem. Rev. 2011, 111, 2937-2980.

INVESTIGATION OF SYNTHETIC PATHWAYS FOR REZORCINOL COMPOUNDS WITH SULFUR-CONTAINING NITROGEN HETEROCYCLES

Gabija Griškonytė[1], Ieva Žutautė[1], Rita Bukšnaitienė[1], Algirdas Brukštus[1]

[1]Faculty of Chemistry and Geosciences, Vilnius University, Vilnius, Lithuania
gabija.griskonyte@chgf.stud.vu.lt

Hsp90 is a heat shock protein whose inhibition has excellent potential in cancer treatment. More than 400 client proteins rely on Hsp90 for maturation, activation, and stabilization [1], it is also essential in cell cycle control, protein folding, and degradation [2]. Various diseases, including cancer, are associated with the stability and overexpression of this protein, which influences cancer development. Understanding the link between the overexpression of Hsp90 and cancer is crucial to finding better cancer treatments by exploiting the differences between normal and tumor cells in terms of Hsp90 mRNA and protein induction, protein activation, and the number of post-translational modification (PTM) sites. Clinical trials have been initiated with various Hsp90 inhibitors, but none have yet been approved as monotherapy medication [3]. This work aims to synthesize resorcinol as lead compounds with combined structures that could be potential Hsp90 inhibitors and may fight against cancer.

To investigate benzimidazole's influence on the effectiveness of resorcinol inhibition, we connected these two fragments using different strategies. For this purpose, we selected 2,4-dihydroxybenzaldehyde as the starting compound. The hydroxyl groups of resorcinol were protected by adding methoxy substituents to prevent side reactions. To create the direct connection, we condensed the aldehyde with diaminobenzene. Simultaneously, to form the thiomethylene bridge, we reduced benzaldehyde to an alcohol and introduced a suitable leaving group. The connection between the fragments via sulfur was achieved using the Ullmann reaction involving the appropriate iodobenzene and thiobenzimidazole. We optimized the reaction conditions using analogous, readily available resorcinol derivatives.

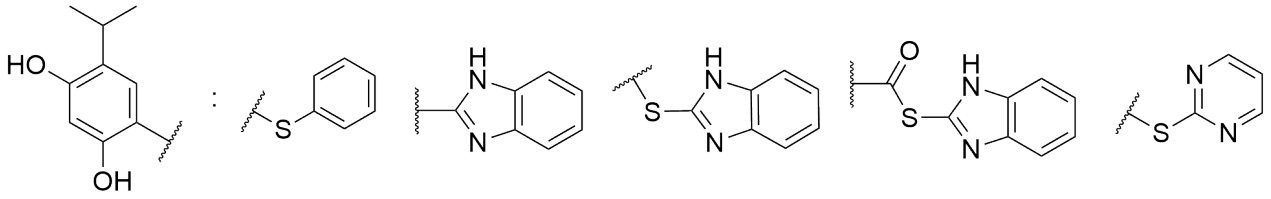


Fig. 1. Structures of targeted compounds

[1] X. Liang, et al., J. Med. Chem., 2024, 67, 15968-15995.
[2] B. Birbo, et al., Int. J. Mol. Sci., 2001, 22 (19), 10317.
[3] Y. Li, et al., Eur. J. Med. Chem., 2024, 275, 116562.

SYNTHESIS OF N-(2,4-DIFLUOROPHENYL)-β-ALANINE DERIVATIVES AND INVESTIGATION OF THEIR PROPERTIES

Guoda Pranaitytė[1], Birutė Grybaitė[1], Vytautas Mickevičius[1]

[1]Department of Organic Chemistry, Kaunas University of Technology, Lithuania
guoda.pranaityte@ktu.edu

Hydrazide derivatives constitute an important part of medicinal chemistry - these compounds are mostly used as organic intermediates in the development of new biologically active molecules. Bound with various heterocyclic fragments, such systems exhibit antimicrobial, anticancer, antiviral, anti-inflammatory, antioxidant activity. Also, introducing hydrazone moiety to organic molecules improve their activity, due to its ability to form hydrogen bonds and create better conditions for interaction with molecular targets [1]. Among heterocyclic compounds, five-membered rings containing nitrogen atoms, such as pyrrole and pyrazole, are often found in medicinal molecules (for example, Sunitinib is used in carcinoma treatment, Celecoxib is anti-inflammatory agent) [2, 3].

In the first step of the synthesis, 3-((2,4-difluorophenyl)amino)propanoic acid (**2**) was prepared by the reaction of 2,4-difluoroaniline (**1**) with acrylic acid in toluene. Later it was transformed into methyl 3-((2,4-difluorophenyl)amino)propanoate (**3**) by an esterification reaction. Propanehydrazide **4** was synthesized by the reaction of hydrazine monohydrate in refluxing 2-propanol. In the further step of the synthesis, reactions with mono- and diketones were investigated. In the case of hydrazones **5** and **6**, acetone and ethyl methyl ketone acted as both reactant and solvent. The desired product **7** was obtained by the reaction of propanehydrazide **4** with 4-aminoacetophenone in 2-propanol at the boiling temperature of the mixture. In analogous reactions with diketones – 2,4-pentanedione and 2,5-hexanedione – cyclic compounds **8**, **9** were synthesized (Fig. 1).

The structure of the compounds has been proven by elemental analysis, ^{1}H NMR, ^{13}C NMR, FT-IR spectroscopy. Investigation of the antimicrobial and anticancer activity of the synthesized compounds are planned.

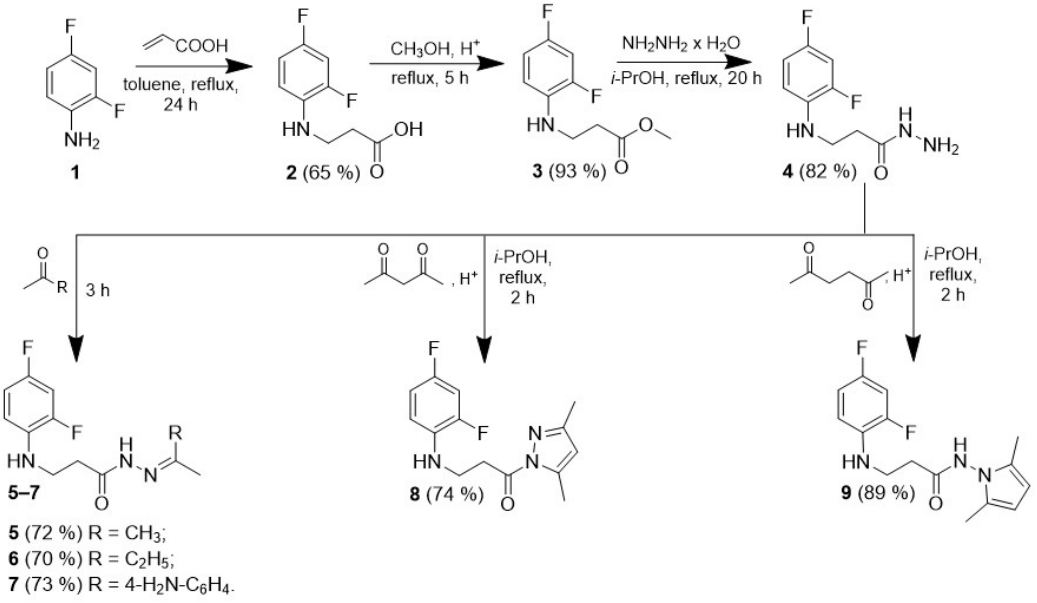


Fig. 1. Synthesis of *N*-(2,4-difluorophenyl)-*β*-alanine derivatives **2–9**

Acknowledgements
This project has received funding from the Research Council of Lithuania (LMTLT), agreement No S-ST-24-23.

[1] Reşit Çakmak, Eyüp Başaran, K. Sahin, Murat Şentürk, and Serdar Durdağı, "Synthesis of Novel Hydrazide–Hydrazone Compounds and In Vitro and In Silico Investigation of Their Biological Activities against AChE, BChE, and hCA I and II," ACS Omega, vol. 9, no. 18, pp. 20030–20041, Apr. 2024, doi: https://doi.org/10.1021/acsomega.3c10182.

[2] B.-C. Ivan et al., "New Pyrrole Derivatives as Promising Biological Agents: Design, Synthesis, Characterization, In Silico, and Cytotoxicity Evaluation," International Journal of Molecular Sciences, vol. 23, no. 16, p. 8854, Jan. 2022, doi: https://doi.org/10.3390/ijms23168854.

[3] O. Ebenezer, M. Shapi, and J. A. Tuszynski, "A Review of the Recent Development in the Synthesis and Biological Evaluations of Pyrazole Derivatives," Biomedicines, vol. 10, no. 5, p. 1124, May 2022, doi: https://doi.org/10.3390/biomedicines10051124.

EFFICIENT TWO-STEP SYNTHESIS OF NOVEL IMIDAZOPYRAZOLOOXAZEPINES

Agnė Užupytė[1], Algirdas Šačkus[1], Eglė Arbačiauskienė[1]

[1]Department of Organic Chemistry, Kaunas University Of Technology
agne.uzupyte@ktu.edu

Heterocyclic compounds play a crucial role in medicinal chemistry due to their diverse biological activities and wide therapeutic applications. Among them, imidazole-pyrazole hybrids have attracted considerable interest for their promising neuroprotective or anticancer potential. Despite advancements in this field, efficient and sustainable synthetic methods for these compounds remain scarce.

This study aims to develop a simple and efficient two-step synthesis of imidazopyrazolooxazepine derivatives from pyrazole-4-carbaldehyde and various diamines, followed by cyclization. The study seeks to evaluate the effectiveness of this synthetic approach in terms of yield and reaction selectivity, as well as to assess the potential biological activity of the resulting compounds. The resulting compounds were characterized using NMR, IR, and mass spectrometry to confirm their structures.

The synthesis and separation of imidazopyrazolooxazepines have shown promising results, highlighting the potential of the developed method for preparing these compounds. However, the separation of regioisomers was not fully efficient, indicating the need for further optimization. Future research will focus on improving the synthesis process and investigating the neuroprotective properties of these compounds, with the aim of exploring their potential for neurological therapies.

FORMATION OF PHOSPOENOLPYRUVATE UNDER PREBIOTIC CONDITIONS

Kajetan Sołtysiak[1], Rafał Szabla[1]

[1]Faculty of Chemistry, Wroclaw University of Science and Technology, Poland
kajetansolo@gmail.com

Phosphoenolpyruvate (PEP) is a important high-energy metabolite in processes such as glycolysis, gluconeogenesis and other relevant metabolic pathways. PEP plays key roles in modern metabolism thus a full understanding of how it was formed is necessary to gain more information about the evolution of the first metabolic processes. Previous studies suggest us that PEP-like compounds may have played a role in primitive phosphorylation pathways, possibly preceding enzymatic catalysis.

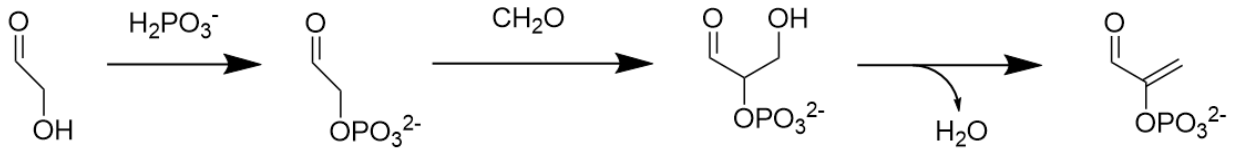


Fig. 1. Fragment of the reaction network leading to PEP [1]

This study focuses on the analysis of the reaction pathway that leads to the formation of phosphoenolpyruvate under prebiotic conditions. The main goal is to calculate the energy barrier, which will allow to calculate the kinetics of these reactions. We focus on reactions such as aldol condensation, elimination and phosphorylation process.

In the research we use computational chemistry methods to model PEP reaction networks. For this purpose we work with the ORCA software and density functional theory (DFT) to determine energy barriers and transition states of reaction. In the calculation we take into account the aqueous phase and different pH values.

The calculations focus on locating transition states for different reaction stages and also on determining energy barriers for the subsequent stages from the PEP reaction network. Preliminary calculations indicate that the aldol condensation of glycolaldehyde to glyceraldehyde proceeds with a moderate energy barrier. The current study extends this approach by investigating the phosphorylation of glycolaldehyde and the subsequent aldol condensation of glycolaldehyde phosphate with formaldehyde to form glyceraldehyde-2-phosphate. Determining the energy barriers for these reactions will provide insights into the feasibility of PEP formation under prebiotic conditions.

A full understanding of the energetic properties of PEP formation under prebiotic conditions contributes to a broader discussion of the evolution of early metabolic pathways. The results of this study may help clarify how quickly phosphoenolpyruvate could be formed and under what conditions it can take place. Future research will additionally focus on including amino acids in the reaction network.

[1] A. F. Magalhaes, M. W. Powner, Prebiotic triose glycolysis promoted by co-catalytic proline and phosphate in neutral water, ChemComm 58, 13519 (2022)

TAILORING THE PROPERTIES OF LANTHANUM-DOPED SrSnO3 LAYERS: THE ROLE OF GAS FLOW RATES

Mindaugas Voznikas[1,2], Milita Vagner[1], Tomas Murauskas[2], Virgaudas Kubilius[2], Valentina Plaušinaitienė[2]

[1]Department of Functional Materials and Electronics, Center for Physical Sciences and Technology, LT-10257 Vilnius, Lithuania
[2]Institute of Chemistry, Faculty of Chemistry and Geosciences, Vilnius University, LT- 03225 Vilnius, Lithuania
mindaugas.voznikas@chgf.stud.vu.lt

Lanthanum-doped SrSnO3 (LSSO) has attracted interest due to its wide band gap, high optical transparency, and relatively low estimated electron mass, which may contribute to higher electron mobility compared to similar materials. However, the orthorhombic crystal structure of LSSO poses challenges for achieving high conductivity, and limited studies have made it difficult to fully understand the factors affecting electron mobility in LSSO layers[1]. This study explores the impact of gas flow rates (ranging from 900 to 1600 ml/min) on the properties of thick LSSO films (550–630 nm) grown using metal-organic chemical vapor deposition (MOCVD). The films were characterized using scanning electron microscopy, X-ray diffraction, and atomic force microscopy. We investigate how varying gas flow rates influence surface structure, morphology, roughness, growth rate, and carrier mobility. The results identify an optimal gas flow rate for achieving improved properties in LSSO layers, offering insights into the factors that affect electron mobility and overall film quality.

[1] Plausinaitiene, V., Murauskas, T., Kubilius, V., Skapas, M., Stanionyte, S., Selskis, A., & Raudonis, R. (2023). Transparent and highly conductive La-doped strontium stannate thin film growth by PI-MOCVD method on LaAlO3 and MgO substrates of (100), (110), (111) orientations. Surfaces and Interfaces, 40, 103035. https://doi.org/10.1016/j.surfin.2023.103035

IMPORTANCE OF DRYING SPEED AND SHRINKAGE COEFFICIENT IN THE SYNTHESIS OF CRACK-FREE SILICA XEROGELS VIA THE SOL-GEL METHOD

Austėja Šernaitė[1], Greta Inkrataitė[1], Ramūnas Skaudžius[1]

[1]Department of Inorganic Chemistry, Faculty of Chemistry and Geosciences, Vilnius University, Naugarduko 24, LT-03225 Vilnius, Lithuania
austeja.sernaite@chgf.stud.vu.lt

Xerogels are highly porous materials that are obtained via the sol-gel process in which the gel is dried in ambient pressure. Due to their noteworthy characteristics such as high surface area, small pore size and low density they can find applications in catalysis and have been established as prospects for thermal and acoustic insulation as well as biomedical applications due to low thermal conductivity and potential biocompatibility respectively [1,2].

However, a prevalent problem impacting the widespread usage of xerogels is their tendency to crack during the drying phase due to high capillary action. The present study hypothesizes that the drying speed and shrinkage coefficient of the gel may serve as reliable indicators of whether the xerogel will end up cracked.

In our experimental design, we varied the filling of gel in the containers (10%; 40%; 50% and 90% visually) and the size of holes in the lids of the containers, drilled to regulate the drying speed. All xerogels were synthesized via the acid catalyzed sol-gel method outlined by Skruodiene et al. with minor adjustment to the drying time [3]. The shrinkage coefficient was calculated by dividing the amount of shrinkage height-wise by the amount of shrinkage width-wise. The experimental results demonstrate that both these variables have an impact, however one more crucial factor for achieving no cracks was found to be the pouring of the gel into the containers and transferring them to the ultrasound bath. It is imperative that there is as little amount of air bubbles as possible. The findings indicate that the most effective method for producing crack-free xerogels is to perforate the lid with a 4 mm wide aperture in the middle and to fill the container with a quantity of gel such that the shrinkage coefficient is approximately equal to any of these numbers: 0.44 (40%), 0.55 (50%), 0.61 (50%), 0.69 (50%), 1.03 (90%).

Acknowledgements

Austėja Šernaitė would like to thank Monika Skruodienė for teaching us this method and Miglė Minalgaitė for occasional help in the laboratory

[1] N. Gizli, S. S. Çok, and F. Koç, “Aerogel, xerogel, and cryogel: Synthesis, surface chemistry, and properties—Practical environmental applications and the future developments,” Advanced Materials for Sustainable Environmental Remediation: Terrestrial and Aquatic Environments, pp. 195–229, Jan. 2022, doi: 10.1016/B978-0-323-90485-8.00021-7.

[2] M. Catauro et al., “Synthesis of SiO2 and CaO rich calcium silicate systems via sol-gel process: Bioactivity, biocompatibility, and drug delivery tests,” J Biomed Mater Res A, vol. 102, no. 9, pp. 3087–3092, Sep. 2014, doi: 10.1002/JBM.A.34978.

[3] M. Skruodiene et al., “Synthesis and Investigation of Novel Optical Active SiO2 Glasses with Entrapped YAG:Ce Synthesized via Sol–Gel Method,” Gels 2023, Vol. 9, Page 488, vol. 9, no. 6, p. 488, Jun. 2023, doi: 10.3390/GELS9060488.

INTERMOLECULAR STRUCTURE ANALYSIS OF CHOLINE TRYPTOPHANATE IONIC LIQUID USING MD AND QM/MM SIMULATIONS

Jonas Vaitiekūnas[1], Lukas Mikalauskas[1], Vytautas Klimavičius[1], Einaras Sipavičius[1], Kęstutis Aidas[1]

[1]Vilnius University
jonas.vaitiekunas@chgf.stud.vu.lt

Ionic liquids (ILs) are normally defined as compounds completely composed of ions with melting point below 100 °C. Generally low melting point is due to one of the ions being an organic molecule whose steric hindrance interferes with the formation of crystal lattice. ILs have a wide range of applications in a variety of fields including but not limited to organic chemistry, materials science and chemical engineering [1]. One of their most attention garnering properties is the capability of increasing the solubility of organic compounds in water. In this research we are studying the change of NMR chemical shift of the choline tryptophanate ([Cho][Trp], Fig. 1) ionic liquid depending on composition of choline tryptophanate and water mixtures.

Two systems were modelled using molecular dynamics (MD) simulations: single ionic pair of [Cho][Trp] dissolved in 4000 molecules of water and 200 ionic pairs dissolved in 1800 molecules of water. Cho^+ and Trp^- structure were initially optimized and RESP charges were calculated using Gaussian 16. General Amber Force Field (GAFF) and TIP4P-Ew model was implemented for ionic species and water respectively. MD simulations were performed in two stages: 1) NPT simulations with decreasing temperature from 400 K to 298 K in order to achieve thermodynamic equilibrium faster and 2) NVT 20 ns equilibration and 20 ns production runs. Radial distribution functions (RDFs) were calculated for choline N and O atoms, tryptophanate O, Nα and mass center of aromatic system and water O atom. Analysis of water clusterization was conducted on both systems. In the case of 1:4000 system distances between the two ions were also analysed in MD trajectory. Finally, QM/MM calculations were performed to obtain NMR shielding constants for Cho^+, Trp^- and water protons in both systems in order to compare with experimental data and validate MD results.

Analysis of distances between ions in the 1:4000 system MD simulation has concluded that the ions were completely solvated for more than 99% of simulation time and did not form an ionic pair. Furthermore, coordination numbers calculated from the RDFs showed that water is the most likely surrounding molecule for Cho^+, Trp^- and other water molecules. Aromatic-aromatic coordination between Trp^- ions is also prevalent in 200:1800 system. The results from water distribution analysis showed that in 200:1800 system water is most likely to belong to clusters of sizes close to 1800 molecules which has led us to believe that the majority of water contained within the system exists as part of a net like structure permeating the whole system. Overall gathered data suggest that various kinds of interactions, including hydrogen bonds and pi stacking, could be very impactful for NMR chemical shifts.

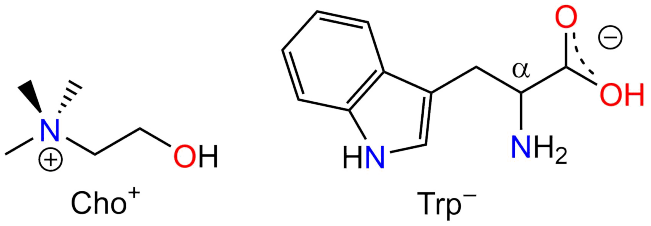


Fig. 1. Chemical structure of choline tryptophanate ionic liquid.

Acknowledgements
HPC „Saulėtekis“ for providing computational resources.

[1] J. P. Hallett, T. Welton, Room-Temperature Ionic Liquids: Solvents for Synthesis and Catalysis, Chem. Rev., 111, 3508-3576, 2011

SYNTHESIS OF REDOX-ACTIVE SUPRAMOLECULAR CAPSULE

Gabija Sergejevaitė[1], Domantas Valčeckas[1], Edvinas Orentas[1]

[1]Department of Organic Chemistry, Vilnius University, Naugarduko 24, LT-03225, Vilnius, Lithuania
gabija.sergejevaite@chgf.stud.vu.lt

The molecular recognition utilizing well-defined molecular constructs is the key subject of supramolecular chemistry. Metal coordination or hydrogen bonds (H-bonds) are usually employed in formation of molecular capsules that are well suited to observe the complexation phenomena and inquire into the nature of non-covalent interactions [1]. Highly flexible building blocks despite their simpler synthesis are rarely used, compared to rigid, preorganized scaffolds, due to absence of entropic penalty reduction when forming molecular aggregates. Modulation of the host-guest chemistry by extending beyond simple covalent adjustment of the cavity size represents a highly sought-after strategy to construct dynamic supramolecular receptors that are reminiscent of enzymes [2]. In nature, induced fit, conformational selection and allosteric control, operating by conformational changes of the host in response to stimuli present, are the principles governing the substrate binding and activation In our report, we present a redox control approach of a simple molecular capsule from tripodal monomer, containing three ureidopyrimidinone (UPy) 4H-bonding units, trimesic acid core and linkers with disulfide moiety (Fig. 1). We have shown that such monomers are capable of forming well-defined dimeric capsules. Furthermore, these capsules are capable of disruption by applying redox conditions that dissociate disulfide links.

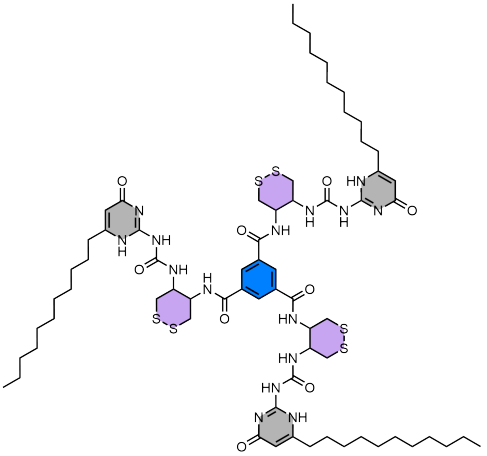


Fig. 1. Chemical structure of the supramolecular monomer

[1] A. Morgan Conn and J. Rebek, Self-assembling Capsules. Chem. Rev., 97, 1647-1668 (1997).
[2] Jozeliunaite et al. Fullerene Complexation in Hydrogen-Bonded Porphyrin Cavitands via Induced-Fit: Cooperative Action of Tautomerization and C-H···π Interactions., J. Am. Chem. Soc., 145 (1), 455-464, (2023).

LAYERED DOUBLE HYDROXIDES: INVESTIGATING SYNTHESIS KINETICS AND THEIR BIOMEDICAL APPLICATIONS

Neringa Gailiūtė[1], Denis Sokol[1]

[1]Institute of Chemistry, Faculty of Chemistry and Geosciences, Vilnius University, Naugarduko st. 24, LT-03225 Vilnius
neringa.gailiute@chgf.stud.vu.lt

Layered double hydroxides (LDH) represent a class of layered compounds, also known as anionic clays or hydrotalcite-like compounds. Interest in LDH compounds has recently increased significantly due to their multifunctional structure, relatively straightforward synthesis, low cytotoxicity, good biocompatibility, and wide range of potential applications. LDHs possess a substantial surface area and the capacity to incorporate a variety of anionic materials, both organic and inorganic, into the interlayer. These modifications make LDHs promising candidates for drug delivery systems, as they can incorporate drug molecules into the interlayer and control their release into the body [1-3].

Over the past decade, research on LDH materials as potential gene and drug carriers has increased substantially, demonstrating successful intercalation of biocatalysts, anti-inflammatory drugs, and anticancer drugs. Such drug delivery systems could potentially aid in the release of poorly soluble or unstable drugs, reduce side effects such as stomach irritation, and minimize the required drug dose [3,4]. However, to develop an efficient LDH-based drug delivery system, it is first necessary to determine the optimal conditions for LDH synthesis and interlayer anion replacement.

The key objective of this research is to investigate LDH compounds synthesized by co-precipitation, with a focus on identifying the optimal synthesis conditions. The formation of LDHs is significantly influenced by the pH value during fabrication, as an inadequate pH can lead to poor purity or even the absence of LDH formation [5]. The syntheses of Zn_2Al_1-CO_3, Mg_2Al_1-CO_3, Cu_2Al_1-CO_3, and Ni_2Fe_1-CO_3 LDHs were conducted via co-precipitation at different pH ranges (from 8 to 12 ± 0.2). The reactions were carried out using appropriate metal nitrate solutions and different bases, depending on the desired pH for synthesis. The resulting crystals were filtered, washed with water until reaching a neutral pH, and dried in an oven at 80 °C for 24 hours.

The crystal structure and morphological properties were analyzed using X-ray diffraction (XRD) and scanning electron microscopy (SEM). Based on the XRD data obtained, the optimal pH values for LDH synthesis were determined as follows: Zn_2Al_1-CO_3 – pH 10-12, Mg_2Al_1-CO_3 – pH 10-12, Cu_2Al_1-CO_3 – pH 8-9, and Ni_2Fe_1-CO_3 – pH 9-10.

[1] V. Rives, M. del Arco, and C. Martín, “Layered double hydroxides as drug carriers and for controlled release of non-steroidal antiinflammatory drugs (NSAIDs): A review,” J. Control. Release, vol. 169, no. 1–2, pp. 28–39, 2013, doi: 10.1016/j.jconrel.2013.03.034.

[2] H.-W. Olfs, L. O. Torres-Dorante, R. Eckelt, and H. Kosslick, “Comparison of different synthesis routes for Mg–Al layered double hydroxides (LDH): Characterization of the structural phases and anion exchange properties,” Appl. Clay Sci., vol. 43, no. 3–4, pp. 464–470, 2009, doi: 10.1016/j.clay.2008.10.009.

[3] K. Ladewig, Z. P. Xu, and G. Q. (Max) Lu, “Layered double hydroxide nanoparticles in gene and drug delivery,” Expert Opin. Drug Deliv., vol. 6, no. 9, pp. 907–922, 2009, doi: 10.1517/17425240903130585.

[4] J.-M. Oh, M. Park, S.-T. Kim, J.-Y. Jung, Y.-G. Kang, and J.-H. Choy, “Efficient delivery of anticancer drug MTX through MTX-LDH nanohybrid system,” J. Phys. Chem. Solids, vol. 67, no. 5–6, pp. 1024–1027, 2006, doi: 10.1016/j.jpcs.2006.01.033.

[5] M. V. Bukhtiyarova, “A review on effect of synthesis conditions on the formation of layered double hydroxides,” J. Solid State Chem., vol. 269, pp. 494–506, 2019, doi: 10.1016/j.jssc.2018.10.018.

MANGANESE COATINGS: TEMPERATURE INFLUENCE ON ELETROCHEMICAL DEPOSITION

Vasaris Statkevičius[1], Nerita Žmuidzinavičienė[1], Egidijus Griškonis[1]

[1]Kaunas University of Technology, Department of Physical and Inorganic Chemistry
vasaris.statkevicius@ktu.edu

Manganese as an element is widely used in a wide range of industries. Its application in steel production has led to attempts to recycle it from batteries or other electronic devices. Electrochemical deposition is a low-energy process, but the electronegativity of manganese limits this process. Supplementing the electrolyte with other materials can improve the efficiency of electrochemical deposition, for example selenium, sulfur and tellurium compounds [1].

Selenium and sulfur compounds are the most widely studied electrolyte additives, and they have a positive effect on the electrodeposition of manganese coatings. Although the use of SeO_2 and H_2SO_3 have proved effective the drawbacks, selenium compound toxicity and sulfurs corrosive properties, leave more to be desired. Research on insertion of tellurium additives in manganese coatings is scarce and by that this research seeks to expand it [2].

The carbon steel (ASTM A283, grade A) plates were used as a substrate for electrodeposition of Mn coatings. NaOH and HCl solutions were used for degreasing and etching the surface of carbon steel plates before electrodeposition process, respectively. After each of these procedures, the rinsing with distilled water was applied. Electrochemical deposition was carried out in aqueous electrolyte containing the mixture of $MnSO_4$ and $(NH_4)_2SO_4$ ($\cdot 5H_2O$). The ammonium complexes in solution inhibit the formation of manganese hydroxides, resulting in denser and thicker manganese coatings [3]. Sodium tellurate ($Na_2TeO_4 \cdot 2H_2O$) was used as electrolyte additive; pH of electrolyte was maintained about 2.32. During electrochemical deposition two lead anodes, coated with lead(IV) oxide (Pb/PbO_2), and polyvinylchloride (PVC) woven membrane, separating the anode and cathode compartments, were used. Deposition lasted for 7 minutes with a cathodic current density of 15 A/dm^2, at four different temperatures: 20, 40, 60, 80 °C. The results of deposition under these conditions are displayed in Table 1.

Table 1. Current yield and thickness of manganese coating in regard to deposition temperature

Deposition temperature, °C	20°C	40°C	60°C	80°C
Current yield, %	42.7 ± 3.5	51.6 ± 1.1	69.7 ± 6.9	80.9 ± 4.6
Mn coating thickness, μm	10.3 ± 0.8	12.4 ± 0.3	12 ± 1.2	13.9 ± 0.8

Further coatings would undergo phosphating process that would further increase anti corrosion properties [4].

[1] J. Lu, D. Dreisinger, and T. Glück, “Manganese electrodeposition — A literature review,” Hydrometallurgy, vol. 141, pp. 105–116, Jan. 2014, doi: 10.1016/J.HYDROMET.2013.11.002.

[2] M. Fernández-Barcia et al., “Electrodeposition of manganese layers from sustainable sulfate based electrolytes,” Surf Coat Technol, vol. 334, pp. 261–268, Jan. 2018, doi: 10.1016/J.SURFCOAT.2017.11.028.

[3] N. Žmuidzinavičienė, E. Griškonis, and A. Šulčius, “The Corrosion of Mn Coatings Electrodeposited from a Sulphate Bath with Te(VI) Additive and Influence of Phosphate Post-Treatment on Corrosion Resistance,” Coatings 2023, Vol. 13, Page 1617, vol. 13, no. 9, p. 1617, Sep. 2023, doi: 10.3390/COATINGS13091617.

[4] P. Kamaraj, “Phosphate Coatings,” Reference Module in Materials Science and Materials Engineering, Jan. 2016, doi: 10.1016/B978-0-12-803581-8.01665-9.

GROWTH OF YB:CALGO CRYSTAL BY OPTICAL FLOATING ZONE METHOD

Domantas Černius[1], Monika Skruodienė[2,3], Anatolijs Šarakovskis[3], Ekaterina Pomjakushina[4], Ramūnas Skaudžius[1]

[1]Department of Inorganic Chemistry, Vilnius University, Naugarduko 24, LT-03225 Vilnius, Lithuania
[2]Department of Chemical Engineering and Technology, Center for Physical Sciences and Technology, Saulėtekio av. 3, LT-10257 Vilnius, Lithuania
[3]Institute of Solid State Physics, University of Latvia, 8 Kengaraga str., LV-1063 Riga, Latvia
[4]Laboratory for Multiscale Materials Experiments, Paul Scherrer Institut, CH-05232 Villiginen PSI, Switzerland
domantas.cernius@chgf.stud.vu.lt

The broad and smooth emission bandwidth of ytterbium-doped calcium gadolinium aluminum oxide (Yb:CaGdAlO4; Yb:CALGO) crystals makes them essential for developing high-power and ultrashort pulse laser technologies. Yb:CALGO is a good material because of exceptionally broad gain bandwidth. This allows to amplify ultrashort, femtosecond pulses. The high thermal conductivity of Yb:CALGO also guarantees efficient heat dissipation during high-power operation, preserving performance stability. Because of these characteristics, Yb:CALGO crystals are perfect for industrial operations requiring a high degree of power and precision, as well as scientific research and medical applications [1–3]. Yb:CALGO powder was synthesized from corresponding metal nitrates using the sol-gel method. The phase purity of the powder samples was confirmed using X-ray diffraction (XRD) analysis. The powder was pressed into rods and then used to grow the crystal by the optical floating zone (OFZ) method. Scanning electron microscopy (SEM) images were taken to determine the morphology of the crystal. SEM images revealed defects on the crystal cut surface. On the other hand, it showed a homogenous element distribution. ICP-OES measurement showed that both the powder and the single-crystal had correct stoichiometry, indicating that the melting process did not alter it. The luminescence properties were also investigated, demonstrating the typical emission and excitation spectrum corresponding to ytterbium electron transitions. This study demonstrated that the OFZ method is suitable for growing Yb:CALGO crystals. However, the crystal exhibited some defects, making it unsuitable for practical use as a laser core. This highlights the need for further research to optimize the crystal growth process.

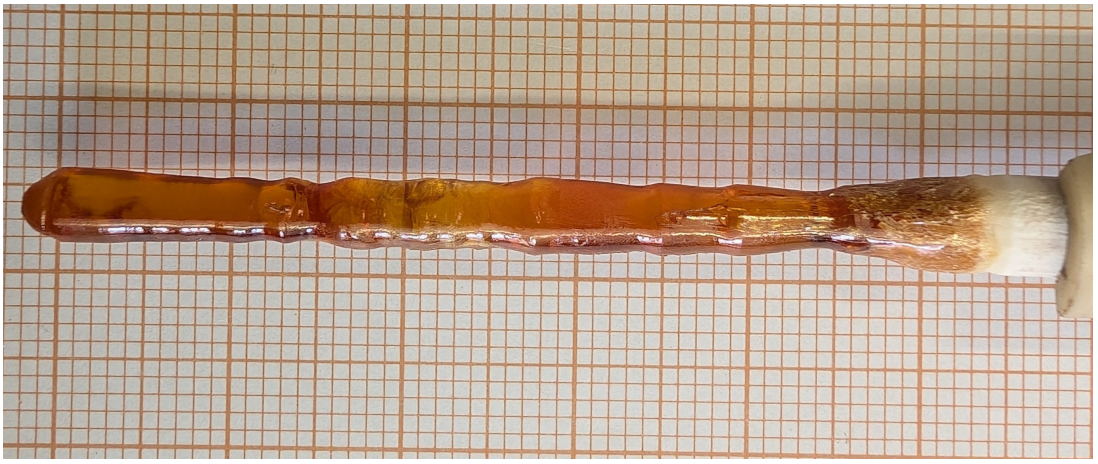


Fig. 1. The crystal grown by optical floating zone method.

[1] J. Yang, Z. Wang, J. Song, R. Lv, X. Wang, J. Zhu, Z. Wei, Diode-pumped 10 W femtosecond Yb:CALGO laser with high beam quality, High Power Laser Science and Engineering 9 (2021).
[2] H. Wang, J. Pan, Y. Meng, Q. Liu, Y. Shen, Advances of Yb:Calgo laser crystals, Crystals (Basel) 11 (2021).
[3] S. Slimi, H. Yu, H. Zhang, C. Kränkel, P. Loiko, R.M. Solé, M. Aguiló, F. Díaz, W. Chen, U. Griebner, V. Petrov, X. Mateos, Growth, structure, spectroscopic, and laser properties of Ho-doped yttrium gallium garnet crystal, Opt. Express 33 (2025) 2529–2541.

FORMATION OF CARBONATED HYDROXYAPATITE UNDER HYDROTHERMAL CONDITIONS

Lidija Turilinaitė[1], Gabrielė Šarapajevaitė[1], Tadas Dambrauskas[1]

[1]Kaunas University of Technology, Faculty of Chemical Technology, Kaunas, Lithuania
lidija.turilinaite@ktu.edu

The rapid ageing of the population is leading to a weakening of the body's ability to regenerate tissues, especially in the bone system. This increases the demand for developing and improving new treatment methods and materials for effective bone substitutes. Hydroxyapatite is the main inorganic component of bone tissue. There are different forms of hydroxyapatite, among which carbonized hydroxyapatite is most similar to natural bone. This form is also characterized by better biocompatibility and activity [1, 2]. Despite these advantages, the scientific literature provides limited data on carbonized hydroxyapatite (CHA) synthesis under hydrothermal conditions, which allow the production of materials with controlled crystallinity and composition.

This study aims to investigate the formation of CHA in a mixture of calcium carbonate and phosphoric acid under hydrothermal conditions. The amount of raw materials used in the experiments corresponds to the stoichiometric Ca/P ratio of CHA (1.67), and the syntheses were carried out at different temperatures (100–200 °C) and durations (4–16 h). To evaluate the outcomes, instrumental techniques, including XRD, STA, FT–IR, and SEM, were employed.

The experimental results showed that, despite the synthesis duration, a lower temperature (100–140 °C) is not suitable for the formation of CHA because other calcium phosphates, such as monetite, were formed. Additionally, a significant amount of unreacted calcium carbonate remained. An increase in synthesis temperature positively affected the formation of CHA, which became the dominant compound after synthesis at 180 °C. Thus, hydrothermal synthesis is a promising method for CHA synthesis in a mixture of calcium carbonate and phosphoric acid.

Acknowledgements

This research was supported by Faculty of Chemical Technology of Kaunas University of Technology (Project BIOCHA).

[1] H. Copete, E. Lopez, C. Baudin. Boletín de la Sociedad Española de Cerámica y Vidrio, 2024 (63), p. 255-267.
[2] K. Benataya, M. Lakrat, L. L. Elansari, E. Mejdoubi. Materials Today: Proceedings, 2020 (31), p. S83- S88.

INFLUENCE OF CU^{2+} IONSON THE FORMATION OF HYDROXYAPATITE UNDER DIFFERENT SYNTHESIS METHODS

Monika Tiskute[1,2], Kęstutis Baltakys[1], Tadas Dambrauskas[1]

[1]Department of Silicate Technology, Faculty of Chemical Technology, Kaunas University of Technology, Radvilenu 19, LT–50254 Kaunas, Lithuania
[2]Animal Science Institute, Lithuanian University of Health Sciences, R. Zebenkos 12, 82317 Baisogala, Lithuania
monika.tiskute@ktu.edu

Human bone naturally contains calcium phosphates with a molar Ca/P ratio of 1.61–1.71, which makes hydroxyapatite (Ca/P – 1.67) extremely valuable in medical applications. Hydroxyapatite which has characterized by chemical stability, biocompatibility, biodegradability, osteoconductivity, and non-toxicity. Unfortunately, pure hydroxyapatite does not exhibit good antimicrobial properties, thus it should be doped with different bacteriostatic ions, like Cu2+ ions, to enhance these properties, stability and sterility [1–5]. The aim of this work was to determine the influence of copper ions on the formation of hydroxyapatite under different synthesis methods.

When preparing the initial mixtures CaCO3-H3PO4-Cu(NO3)2•3H2O-H2O, the molar ratio in the system agree with to 10:6:1. During hydrothermal synthesis, 4 g of CaCO3, 2.736 g of H3PO4 and 0.2396 g of Cu(NO3)2•3H2O were used. Meanwhile for microwave-assisted four times lower amount of raw materials were used. The water to solid ratio was kept 10. Hydrothermal synthesis was carried out without stirring the suspension in a ”Parr instruments” autoclave. The isothermal curing durations were 0 h, 2 h and 8 h, while the target temperature (140 °C) was reached within 2 h. A microwave assisted synthesis was performed in reactor ”Monowave 300” (Anton-Paar). The reaction temperature (100–200 °C) was reached within 3 min, and the mixture was stirred at 200 rpm throughout the reaction.

It has been found that a mixture of calcium phosphates was formed during hydrothermal synthesis, regardless of the duration. XRD data showed that Cu2+ ions were intercalated into the structure of hydroxyapatite (Ca5(PO4)3Cu0.12(OH)0.88) and also formed calcium copper phosphate (Ca10Cu(PO4)7). It should be noted that together with mentioned compounds monetite (CaHPO4) was also formed. Meanwhile during a microwave-assisted synthesis monetite and libethenite (Cu2(PO4)(OH)) were formed. It should be noted that libethenite most often formed from the weathering of phosphate rocks such as apatite [6]. These findings were confirmed by X-ray diffraction (XRD), simultaneous thermal analysis (STA), and Fourier-transform infrared spectroscopy (FT–IR).

The obtained results suggest that the Cu2+ ions strongly affect the formation of phosphate and can be considered potential addition on the modification of calcium phosphates.

[1] A. Szcześ, L. Hołysz, and E. Chibowski. Synthesis of hydroxyapatite for biomedical applications,” Adv Colloid Interface Sci, 2017
[2] Y. Gou, K. Qi, Y. Wei, Z. Gu, and H. Xie, Advances of calcium phosphate nanoceramics for the osteoinductive potential and mechanistic pathways in maxillofacial bone defect repair. Nano TransMed, 2024
[3] A. Nayak and B. Bhushan, Hydroxyapatite as an advanced adsorbent for removal of heavy metal ions from water: Focus on its applications and limitations. Mater Today Proc, 2021
[4] E. Raudonyte-Svirbutaviciene et al., Hydrothermal synthesis of Mn2+- and Cu2+-doped calcium hydroxyapatite: morphological features and importance of EPR insights. Ceram Int, 2024
[5] V. G. DileepKumar et al., A review on the synthesis and properties of hydroxyapatite for biomedical applications. J Biomater Sci Polym Ed, 2022
[6] F. S. Spear and J. M. Pyle, Apatite, Monazite, and Xenotime in Metamorphic Rocks. Rev Mineral Geochem, 2002

COMPUTATIONAL STUDY OF NMR SPECTRA AND STRUCTURAL PROPERTIES OF TETRAPEPTIDE IN IONIC LIQUID MIXTURES WITH WATER

Amina Elkady[1], Žyginta Murnikova[2], Kęstutis Aidas[2]

[1] Institute of Chemistry,Faculty of Chemistry and Geosciences, Vilnius University
[2] Institute of Chemical Physics, Faculty of Physics, Vilnius University
amina.elkady@chgf.stud.vu.lt

Ionic liquids (ILs) have been known as “green” and biocompatible solvents for quite some time and some of their possible biological uses include making them permeate more easily through membranes, changing catalytic activity of enzymes, as well as stabilizing or destabilizing various proteins [1]. The nature of the interactions between ILs and proteins varies and is difficult to evaluate. Therefore, smaller peptides with amino acid sequences common in proteins are often used as model systems to discover how different ILs interact with these peptides and change their structure in aqueous solution. Nuclear magnetic resonance (NMR) spectroscopy is the method best suited for identifying both intermolecular interactions and intramolecular structural changes, since the chemical shifts of atoms, particularly hydrogen, are highly sensitive to changes in the local environment of the central molecule.

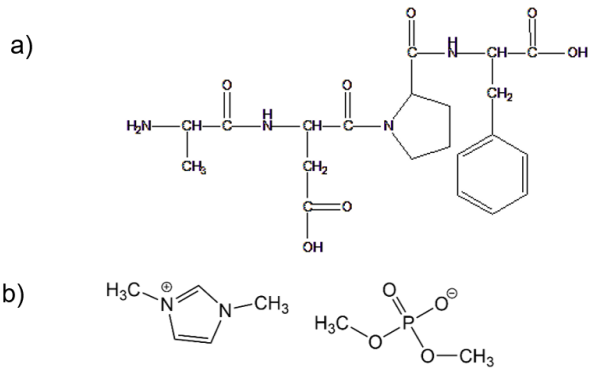


Fig. 1. 1. Structural formulas of a) peptide Ala-Asp-Pro-Phe, b) 1,3-dimethylimidazolium dimethyl phosphate.

In this work, an Ala-Asp-Pro-Phe tetrapeptide was investigated using molecular dynamics (MD) simulations and quantum mechanics/molecular mechanics (QM/MM) calculations under both aqueous conditions and in an IL/water mixture. The chosen ionic liquid (IL) was constituted of the imidazolium-based cation 1,3-dimethylimidazolium and the common IL anion dimethyl phosphate [Mmim][DMP]. Theoretical chemical shift differences of the peptide’s hydrogen atoms were compared with experimental results [2], enabling us to evaluate the various interactions present in peptide/IL/water systems. Meanwhile, trajectories from the MD simulations revealed structural changes in the peptide itself, as well as differences in its immediate surroundings.

Acknowledgements

This study was supported by the Research Council of Lithuania, grant no. S-MIP-22-74. Computations were performed on resources provided by the High-Performance Computing Center “HPC Saulėtekis” at Vilnius University, Lithuania.

[1] Gomes, J. M., Silva, S. S. & Reis, R. L. Biocompatible ionic liquids: fundamental behaviours and applications. Chemical Society Reviews 48, 4317–4335 (2019)

[2] Richardt, A., Mrestani-Klaus, C. & Bordusa, F. Impact of ionic liquids on the structure of peptides proved by HR-MAS NMR spectroscopy. Journal of Molecular Liquids 192, 9–18 (2014).

BIOSYNTHESIS OF SILVER NANOPARTICLES VIA MEDUSOMYCES GISEVII FERMENTATION WITH TILIA CORDATA EXTRACT: ANTIMICROBIAL, ANTIOXIDANT PROPERTIES AND PHYTOCHEMICAL ANALYSIS.

Urte Raubyte[1], Aiste Balciunaitiene[1], Mindaugas Liaudanskas[2], Jonas Viskelis[1]

[1]Institute of Horticulture, Lithuanian Research Centre for Agriculture and Forestry, 54333 Babtai, Lithuania
[2]Department of Pharmacognosy, Faculty of Pharmacy, Lithuanian University of Health Sciences, 50166 Kaunas, Lithuania
urte.raubyte@gmc.stud.vu.lt

Nanotechnology is one of the most advanced fields in the twentieth century, with diverse research areas and applications [1, 2]. Multiple nanoobjects with simultaneous action capability often possess both antioxidant and antimicrobial qualities, in this case emphasizing silver nanoparticles with a size range of 1-100 nm, which exhibit high antimicrobial properties as they interact strongly with low concentrations of microorganisms. Silver ions initiate several mechanisms that disrupt natural cell processes and metabolites, such as the cell's protein structure, the activity of the respiratory chain, cell membrane structure, and deoxyribonucleic acid (DNA) replication. Synthesis of silver nanoparticles (AgNPs) can be achieved through various methods – microwave and biological, photochemical, chemical, physical, and microemulsion. When it comes to biological synthesis, reducing agents often are microorganisms and parts of plants. The therapeutic properties of the flowers and leaves of Tilia species (Linden) contribute to their significance in pharmacogenetic research. Tilia cordata, rich in phenolic compounds, flavonoids, and tiliroside, has been traditionally used for its sedative, diuretic, and antibacterial properties, with its extracts showing potential in treating anxiety, hypertension, respiratory infections, and oxidative stress-related conditions. The goal of our study was to investigate the significance of green nanotechnology in the development of a cost-effective and eco-friendly approach for the biosynthesis of silver nanoparticles utilizing Tilia cordata extract. This process aimed to enhance the antioxidant and antimicrobial activities of the synthesized nanoparticles.

To quantify the total phenolic content (mg GAE/g) in the ethanol extracts of Tilia cordata, the Folin–Ciocâlteu method was used. The highest concentration of phenolic compounds was observed in the composition of fermented T. cordata AgNPs extract. In contrast, a significantly lower phenolic content (18%) was detected in the pure T. cordata herb extract. Furthermore, the data indicate that following the synthesis of silver nanoparticles, the phenolic compound concentration decreased to 206.00±0.59 mg GAE/g (2%). This reduction in phenolic content is likely attributed to the role of phenolic compounds as reducing agents and stabilizers. The pure aqueous extract of T. cordata herb demonstrated antioxidant properties across all applied analytical methods, including Cupric Reducing Antioxidant Capacity (CUPRAC), Ferric Reducing Antioxidant Power (FRAP) assay, and Ultra-High Performance Liquid Chromatography (UHPLC) coupled with mass spectrometry. The surface morphology and chemical composition of AgNPs were analysed using Scanning Electron Microscopy (SEM). SEM micrographs of fermented T. cordata showed uniformly distributed nanoparticles without irregularities or holes. Transmission Electron Microscopy (TEM) images revealed diverse morphologies, predominantly spherical o

Acknowledgements

The authors would like to thank the Research Council of Lithuania, (LMTLT) agreement No. S-MIP-24-56, for the financial support given to achieve this work.

[1] Mashau, M. E.; Mamagau, T.; Foforane, K.; Nethathe, B.; Ramphinwa, M. L.; Mudau, F. N. Biosynthesis of Silver Nanoparticles from Fermented Bush Tea (Athrixia Phylicoides DC) Leaf Extract and Evaluation of Their Antioxidant and Antimicrobial Properties. Fermentation 2023, 9 (7), 648. https://doi.org/10.3390/fermentation9070648.

[2] Balciunaitiene, A.; Januskevice, V.; Saunoriute, S.; Raubyte, U.; Viskelis, J.; Memvanga, P. B.; Viskelis, P. Antimicrobial Antioxidant Polymer Films with Green Silver Nanoparticles from Symphyti Radix. Polymers 2024, 16 (3), 317. https://doi.org/10.3390/polym16030317.

[3] Balciunaitiene, A.; Puzeryte, V.; Radenkovs, V.; Krasnova, I.; Memvanga, P. B.; Viskelis, P.; Streimikyte, P.; Viskelis, J. Sustainable–Green Synthesis of Silver Nanoparticles Using Aqueous Hyssopus Officinalis and Calendula Officinalis Extracts and Their Antioxidant and Antibacterial Activities. Molecules 2022, 27 (22), 7700. https://doi.org/10.3390/molecules27227700.

[4] Ramphinwa, M. L.; Mchau, G. R. A.; Madala, N. E.; Nengovhela, N.; Ogola, J. B. O.; Mudau, F. N. Response of Plant Growth and Development, and Accumulation of Hydroxyl-Cinnamoyl Acid Derivatives to Selected Shade Nets and Seasonality of Field-Grown Bush Tea (Athrixia Phylicoides DC.). HortScience 2022, 57 (1), 87–96. https://doi.org/10.21273/HORTSCI16171-21.

[5] Hashemi, Z.; Mizwari, Z. M.; Mohammadi-Aghdam, S.; Mortazavi-Derazkola, S.; Ali Ebrahimzadeh, M. Sustainable Green Synthesis of Silver Nanoparticles Using Sambucus Ebulus Phenolic Extract (AgNPs@SEE): Optimization and Assessment of Photocatalytic Degradation of Methyl Orange and Their in Vitro Antibacterial and Anticancer Activity. Arab. J. Chem. 2022, 15 (1), 103525. https://doi.org/10.1016/j.arabjc.2021.103525.

[6] Chen, J.; Wang, J.; Zhang, X.; Jin, Y. Microwave-Assisted Green Synthesis of Silver Nanoparticles by Carboxymethyl Cellulose Sodium and Silver Nitrate. Mater. Chem. Phys. 2008, 108 (2–3), 421–424. https://doi.org/10.1016/j.matchemphys.2007.10.019.

[7] Sharma, V. K.; Yngard, R. A.; Lin, Y. Silver Nanoparticles: Green Synthesis and Their Antimicrobial Activities. Adv. Colloid Interface Sci. 2009, 145 (1–2), 83–96. https://doi.org/10.1016/j.cis.2008.09.002.

[8] Zehra, S. H.; Khan, S. A.; Zehra, S. M.; Asad, M. Z. Removal of Cr6+ from Synthetic Polluted Water Using Fe Modified Sugarcane Bagasse & Peanut Shell Powder. J. Chem. Environ. 2023, 2 (2), 1–13. https://doi.org/10.56946/jce.v2i2.146

[9] Ghosh Chaudhuri, R.; Paria, S. Core/Shell Nanoparticles: Classes, Properties, Synthesis Mechanisms, Characterization, and Applications. Chem. Rev. 2012, 112 (4), 2373–2433. https://doi.org/10.1021/cr100449n.

[10] Amith Yadav, H. J.; Eraiah, B.; Kalasad, M.N.; M. Thippeswamy, M.; Rajasreelatha, V. Synthesis, Characterization of ZrO2:Tb3+ (1-9 Mol %) Nanophosphors for Blue Lighting Applications and Antibacterial Property. Biointerface Res. Appl. Chem. 2021, 12 (6), 7147–7158. https://doi.org/10.33263/BRIAC126.71477158.

IMPROVEMENTS OF THE POLYMERS REPRESENTATION IN COD USING QUOTIENT GRAPHS

Yaroslav Rozdobudko[1], Andrius Merkys[1], Antanas Vaitkus[1], Saulius Gražulis[1]

[1]Institute of Biotechnology, Vilnius University, Lithuania
yaroslav.rozdobudko@bti.stud.vu.lt

Coordination polymers and Metal-Organic Frameworks (MOF) are important for chemistry and materials science. A finite representation of these infinite molecules is needed for their understanding and analysis. The theory behind how we can represent infinite molecules was first introduced in [1] through the use of `quotient graph`, which capture translationally equivalent bonds and atoms. However, it is rarely used in crystallographic software. There are no tools that provide standard output that can be used on large databases, and the available software is proprietary. One tool is `cif_molecule` [2], which is part of `cod-tools`, is open source and provides output as a `CIF` [3] file, and can work with a large number of files. However, there was a limitation on how polymers are detected, and the correct detection and stoichiometry of reconstructed molecules cannot be guaranteed. This work focuses on extending existing software `cif_molecule` by introducing `quotient graph`. By using `quotient graphs`, we can always correctly detect infinite molecules, and determine their properties.

The algorithm in `cif_molecule` was modified to use the `quotient graph` to determine ”edge” of a polymer. This allowed us to distinguish polymers correctly, preserve their stoichiometric ratios, determine correct dimensionality, and calculate polymer multiplicity. Output of the `cif_molecule` was extended with `TOPOCIF` data names that represent `quotient graph`, this allows use of `quotient graph` by other programs, and addition of `topol_net` data items allows us to distinguish different nets in the crystal. Programs were developed to convert `quotient graph` in `CIF` to other formats: `cif2qg` converts to `graphviz` format, and to `cgd` format for `Systre` [4] input, `cif_polymer_multiplicity` to calculate polymer multiplicity (number of self-penetrated molecules in the crystal). The calculations were done on the COD [5]. A repository for calculations was created at `svn://databases.crystallography.lt/quotient-graphs`. The repository contains rules defined as Makefiles, and calculations are easily reproducible. A website to search and display the results of the calculations was created in the repository `svn://databases.crystallography.lt/cif-explorer`, available at `http://databases.crystallography.lt:8080/`.

All 511329 structures from COD revision 291294 were processed. The calculations show that 22.7% of structures are polymers. The result of `Systre` [4] identified 56 unique R̂CSR [6] symbols. The most common are `hcb`, `dia` and `kgm` symbols. Multiplicity calculations show that among self-penetrated structures in COD, 2 and 3 multiplicity is the most common. Structures with a higher multiplicity of 27, 25, 18 and 13 were found.

With `quotient graph` we can guarantee finite representation of infinite molecules.

[1] Chung, S. J., Hahn, T., & Klee, W. E. (1984). Nomenclature and generation of three-periodic nets: The vector method. Acta Crystallographica Section A Foundations of Crystallography, 40(1), 42–50. https://doi.org/10.1107/s0108767384000088

[2] Gražulis, S., Merkys, A., Vaitkus, A., & Okulič-Kazarinas, M. (2015). Computing stoichiometric molecular composition from crystal structures. Journal of Applied Crystallography, 48(1), 85–91. https://doi.org/10.1107/s1600576714025904

[3] Hall, S. R., Allen, F. H., & Brown, I. D. (1991). The crystallographic information file (cif): A new standard archive file for crystallography. Acta Crystallographica Section A Foundations of Crystallography, 47(6), 655–685. https://doi.org/10.1107/s010876739101067x

[4] Delgado-Friedrichs, O., & O'Keeffe, M. (2003). Identification of and symmetry computation for crystal nets. Acta Crystallographica Section A Foundations of Crystallography, 59(4), 351–360. https://doi.org/10.1107/s0108767303012017

[5] Gražulis, S., Daškevič, A., Merkys, A., Chateigner, D., Lutterotti, L., Quirós, M., Serebryanaya, N. R., Moeck, P., Downs, R. T., & Le Bail, A. (2011). Crystallography open database (cod): An open-access collection of crystal structures and platform for world-wide collaboration. Nucleic Acids Research, 40(D1), D420–D427. https://doi.org/10.1093/nar/gkr900

[6] O'Keeffe, M., Peskov, M. A., Ramsden, S. J., & Yaghi, O. M. (2008). The reticular chemistry structure resource (RCSR) database of, and symbols for, crystal nets. Accounts of Chemical Research, 41(12), 1782–1789. https://doi.org/10.1021/ar800124u

MACHINE LEARNING FORCE FIELD PARAMETRIZATION AND APPLICATIONS FOR PHOSPHORIC ACID BASED SYSTEMS

Gabrielius Mockus[1], Deimantas Šmigelskas[1], Rokas Šilkinis[1], Linas Vilčiauskas[1]

[1]Department of Chemical Engineering and Technology, Center for Physical Sciences and Technology, Lithuania
gabrielius.mockus@ftmc.lt

Machine learning methods are making their way into computational chemistry. Machine-learned force fields (MLFF) implemented in the Vienna Ab initio Simulation Package (VASP) offer a fast and easy implementation for a wide range of systems. Two major benefits of such force fields is the increased accuracy in comparison to traditional empirical force fields and significant reduction in computational resources and accelerated simulation speed when compared to methods such as Density Functional Theory (DFT).

The objective of this research was to construct a reactive MLFF for phosphoric acid and related systems with the goal of studying the mechanism of proton conductivity. Phosphoric acid is one of the best pure proton conductors therefore a better understanding of such a mechanism could aid in constructing fuel cells, as well as better explain the role of proton conductivity in biological systems.

Our results indicate that MLFFs are a viable option for modeling the molecular dynamics of such systems with a similar accuracy to DFT methods, however at a significantly lower computational cost.

GOLD-NICKEL-RHENIUM-PHOSPHORUS CATALYSTS FOR EFFICIENT SODIUM BOROHYDRIDE OXIDATION

Eimantas Kiseliovas[1], Aušrinė Zabielaitė[1], Aldona Balčiūnaitė[1], Jūratė Vaičiūnienė[1], Loreta Tamašauskaitė-Tamašiūnaitė[1]

[1]Center for Physical Sciences and Technology (FTMC)
EimantasKiseliovas@protonmail.com

Fuel cells are being actively investigated as an attractive alternative energy source for cleaner power generation. One type of fuel cell, the direct borohydride fuel cell (DBFC), is being developed especially for portable power supply. Since sodium borohydride is used as fuel, the development of electrocatalysts with reasonable cost and a high electroactivity towards sodium borohydride oxidation (BOR) is of considerable interest for fuel cells. In this study, gold-nickel-rhenium-phosphorus catalysts deposited on the surface of copper (Au-NiReP/Cu) were investigated as catalysts for the BOR. The Au-NiReP/Cu catalysts were obtained by a two-step process involving the electroless deposition of the NiReP coatings on the Cu surface, followed by the deposition of Au crystallites using the galvanic displacement technique. The morphology, structure and composition of the resulting catalysts were examined by Field Emission Scanning Electron Microscopy (FESEM), Energy Dispersive X-ray Analysis (EDX), and Inductively Coupled Optical Emission Spectroscopy (ICP-OES). Cyclic voltammetry (CV) and chronoamperometry (CA) were used to determine the electrocatalytic activity of the prepared Au-NiReP/Cu catalysts towards the BOR in alkaline medium. It was found that the NiReP coatings deposited on the Cu surface have a typical globular morphology consisting of smaller nodules. The Au crystallites with the size of 10-50 nm were deposited on the as-prepared NiReP/Cu catalysts by immersing them in the 1 mM $HAuCl_4$ + 0.1 M HCl solution at room temperature for 1, 2, and 5 min, respectively. The as-prepared Au-NiReP/Cu catalysts exhibited a higher electrocatalytic activity toward the BOR as compared with that of a bulk Au and NiReP/Cu electrode, and seem to be a promising anodic material for DBFC.

Acknowledgements
This research was funded by a grant (No. P-MIP-23-467) from the Research Council of Lithuania.

SEASONAL CHANGES IN THE VOLATILE PROFILE OF SCOTS PINE (PINUS SYLVESTRIS) NEEDLE EXTRACTS: HYDRODISTILLATION VS. SUPERCRITICAL CO_2 EXTRACTION

Jokūbas Kojelis[1,2], Laura Jūrienė[2], Renata Baranauskienė[2], Ramutė Maždžierienė[2], Petras Rimantas Venskutonis[2]

[1]Vilnius Lyceum
[2]Kaunas University of Technology
jokubas.kojelis@gmail.com

The efficient utilization of by-products from forest thinning and logging operations is a fundamental objective in sustainable forestry. While residual biomass is increasingly used as biofuel, conifer needles—comprising about 20% of a tree's organic matter—are frequently classified as forestry waste. The former, however, is particularly rich in bioactive volatile phytochemicals, including terpenes and terpenoids, whose synthesis fluctuates throughout the year in response to environmental stressors and plant growth cycles. Given that Scots pine (Pinus sylvestris) is one of the most commercially significant forest-forming tree species in Northern Europe, this study explores the optimized use of its foliage with respect to seasonality.

This research investigates the seasonal changes in volatile compounds extracted from pine needles collected from the same trees near Vilnius over six sampling periods between February and December 2024. Various extraction techniques were employed to obtain volatile constituents. Essential oils (EOs) were extracted using a 3-hour hydrodistillation process with a Clevenger-type apparatus, and the resulting water extracts were subsequently freeze-dried. To obtain lipophilic extracts, a novel supercritical fluid extraction (SFE) method utilizing carbon dioxide (40 °C, 15 MPa) was applied, with extraction efficiency assessed through kinetic curve analysis. The chemical composition of volatile compounds in the lipophilic extracts was analyzed using comprehensive two-dimensional gas chromatography coupled with time-of-flight mass spectrometry (GC×GC-TOF/MS) and headspace solid-phase microextraction (HS-SPME). Additionally, gas chromatography with flame ionization detection (GC-FID) was used to characterize the composition of essential oils.

The highest yield of essential oils was recorded in February (0.5%), whereas the maximum yield of water-soluble lyophilized extracts was observed in April (1.4 g/100 ml hydrolat). Similarly, lipophilic fractions exhibited the highest extraction efficiency in February (4.2%). The composition of essential oils was dominated by α-pinene, with its highest concentration occurring in December (27.40%) and the lowest in August (19.43%). In contrast, the composition of lipophilic fractions displayed greater variability - while α-pinene was the primary volatile compound in February (19.92%) and August (14.42%), bornyl acetate was predominant in April (11.77%) and June (10.06%), whereas δ-carene (11.56%) and β-caryophyllene (9.33%) were the most abundant volatiles in October and December, respectively. The concentration of δ-cadinene fluctuated throughout the year. Notably, a peak in secondary plant metabolites in June correlated with the pine pollination period. As one of the highest yields and distributions of the main active volatile components of essential oils and lipophilic fractions were identified in February, this research suggests collecting pine needles in late winter.

EFFICIENT RECOVERY OF ANTIOXIDANT-RICH EXTRACTS FROM BOGBEAN (MENYANTHES TRIFOLIATA L.) LEAVES

Julija Ginkutė[1], Marius Užupis[1], Michail Syrpas[1], Vaida Kitrytė-Syrpa[1]

[1]Department of Food Science and Technology, Faculty of Chemical Technology, Kaunas University of Technology, Radvilėnų Rd. 19, Kaunas, LT 50254, Lithuania
vaida.kitryte@ktu.lt

Bogbean (Menyanthes trifoliata) is a plant belonging to the Menyanthaceae family, growing in peatlands and marshes, and is distributed across Europe, North America, and Asia. Traditionally, it has been used in folk medicine for its antioxidant, antimicrobial, immunomodulatory, antipyretic, sedative, and tonic properties [1]. However, the phytochemical composition, biological activity, and potential applications of this plant remain insufficiently studied. The aim of this study was to extract valuable bioactive compounds from M. trifoliata using conventional (infusion, Soxhlet extraction) and modern (ultrasound-assisted extraction-UAE, pressurized liquid extraction – PLE) methods, employing non-toxic solvents (ethanol and water). The study sought to assess the phytochemical composition, antioxidant properties of the extracts, and optimize the PLE process by varying temperature (40–130 °C), time (15–45 min), and ethanol/water ratio, utilizing central composite design and response surface methodology (CCD-RSM). The dependent variables were extraction yield and antioxidant activity, determined using in vitro assays (CUPRAC and ABTS) as well as total phenolic content (TPC). The results showed that PLE optimization yielded extracts ranging from 8.2 to 45.6 g/100 g dry weight. Compared to Soxhlet extraction (17.7–20.4 g/100 g), infusion (10.2 g/100 g), and UAE (11.3 g/100 g), the PLE method achieved the highest yield in a shorter time. Phytochemical analysis revealed that extracts contained significant amounts of total phenolic compounds (45–56 mg GAE/g extract) and flavonoids (10–11 mg QE/g extract), along with strong antioxidant activity, as determined by TEACABTS (198–206 mg TE/g), TEACCUPRAC (252–294 mg TE/g), and TEACORAC (603–697 mg TE/g) assays. Additionally, the sun protection factor (SPF) was evaluated at different concentrations. The results indicated that all extracts prepared from M. trifoliata leaves exhibited SPF > 6 [2] at ≥ 0.25 mg/ml concentration, demonstrating their potential for use in cosmetic and phytodermatological product formulations, particularly as natural UV-protective agents in sunscreens and skincare products.

[1] T. Kowalczyk, P. Sitarek, E. Skała, P. Rijo, J. M. Andrade, E. Synowiec, J. Szemraj, U. Krajewska, T. Śliwiński, An Evaluation of the DNA-Protective Effects of Extracts from Menyanthes trifoliata L. Plants Derived from In Vitro Culture Associated with Redox Balance and Other Biological Activities (Oxidative Medicine and Cellular Longevity, 2019, 9165784, 13 pages, 2019).

[2] Commission Recommendation of 22 September 2006 on the efficacy of sunscreen products and the claims made relating thereto (2006/647/EC).

MECHANICALLY FRACTIONATED BLACK CURRANT SEEDS AND SKINS AS A VALUABLE SOURCE OF BIOACTIVE COMPOUNDS

Laura Jūrienė[1], Milda Pukalskienė[1]

[1]Department of Food Science and Technology, Faculty of Chemical Technology, Kaunas University of Technology, Kaunas, Lithuania
laura.juriene@ktu.lt

Blackcurrant seeds and skins are residual by-products of berry processing, often overlooked and discarded as waste in the industry. However, recent studies over the past decade have highlighted their potential as a rich source of bioactive compounds. Chemical composition analysis using standard methodologies revealed that seeds are particularly high in fats and proteins, while skins contain greater amounts of minerals and carbohydrates. Notably, a significant portion of the carbohydrates in skins is dietary fiber, averaging approximately 50 g per 100 g, with a lower content in seeds. Supercritical CO_2 extraction yielded a lipophilic extract from seeds with a 16% yield, whereas the yield from skins was considerably lower. The predominant fatty acids in the extracts were identified as unsaturated linoleic, linolenic, and oleic acids. Furthermore, the extract were found to be a rich source of bioactive compounds, including α-tocopherol and β-sitosterol. These findings underscore the potential of blackcurrant seeds and skins as valuable ingredients for sustainable superfood blends or functional food products.

Acknowledgements
This project has received funding from the KTU, grant No INP2025/2.

ANTIOXIDANT ACTIVITY OF DIOSCOREA CAUCASICA AND DIOSCOREA NIPPONICA LEAVES AND ROOTS EXTRACTS OBTAINED BY DIFFERENT EXTRACTION METHODS

Laura Jūrienė[1], Jovita Jovaišaitė[1], Petras Rimantas Venskutonis[1]

[1]Department of Food Science and Technology, Faculty of Chemical Technology, Kaunas University of Technology, Kaunas, Lithuania
laura.juriene@ktu.lt

Dioscorea nipponica Makino and *Dioscorea caucasica Lipsky* plants belong to Dioscoreaceae family. The genus consists of more than 600 species native to Africa, Asia, the Caribbean, South America, and the South Pacific Islands. *Dioscorea* plants are rich in steroids, quinones, cyanides, phenols, diterpenes, diarylheptanoids, and nitrogen-containing compounds. One of the most important bioactive compounds diosgenin possesses various biological effects, including antioxidant, hypoglycemic, hypolipidemic, antimicrobial, inflammatory, antiproliferative, androgenic, estrogenic, and contraceptive properties [1,2]. To sum up, *Dioscorea spp.* are a potential source of bioactive substances for the prevention and treatment of several diseases. However, ultrasound-assisted extraction (UAE) and pressurized liquid extraction (PLE) have not been used to recover bioactive compounds from *D. nipponica* and *D. caucasica* leaves and roots. This study aimed to compare the extracts obtained by PLE and UAE antioxidant activity of *D. nipponica* and *D. caucasica* leaves and roots. The plants were grown in the collection of medicinal plants of the Kaunas Botanical Garden of Vytautas Magnus University. Pressurized liquid extraction (PLE) was accomplished with ethanol (EtOH) and water (H_2O), while ultrasound assisted extraction (UAE) with water. Antioxidant properties of extracts were evaluated by the *in vitro* antioxidant capacity assays. ABTS radical cation scavenging and oxygen radical absorbance capacity (ORAC) were expressed in trolox (synthetic antioxidant) equivalents (TE), while total phenol content (TPC) was determined by Folin-Ciocalteu method and expressed in gallic acid equivalents (GAE). The results showed that *D. nipponica* and *D. caucasica* leaf extracts obtained by two different extraction methods had stronger antioxidant activity, while roots extracts. TPC values of *D. nipponica* and *D. caucasica* extracts obtained by different extraction methods were not significantly different and varied in the range of 205-240 and 219-253 mg GAE/g, respectivelly. In ABTS radical cation scavenging assay *D. caucasica* (836-866 mg TE/g) extract had higher antioxidant capacity than *D. nipponica* (681-686 mg TE/g); however, the differences between extraction methods were not observed. It may be concluded that *D. nipponica* and *D. caucasica* plants extracts are a rich source of various bioactive compounds, which possess strong antioxidant activity and may find applications in nutraceuticals and functional foods.

[1] S-H. Ou-Yang, T. Jiang, L. Zhu, T. Yi, “Dioscorea nipponica Makino: a systematic review on its ethnobotany, phytochemical and pharmacological profiles,” {\Chemistry Central Journal}, vol. 12, no. 1, May, pp 1-18, 2018

[2] A. Adomėnienė, A. Pukalskas, O. Ragažinskienė, P.R. Venskutonis, “Health Beneficial Phytochemicals in Dioscorea caucasica Lipsky Leaves and Tubers and Their Inhibitory Effects on Physiologically Important Enzymes”, {\Plants}, vol. 11, no. 10, 1341, 2022

SYNTHESIS AND INVESTIGATION OF PHOTOPOLYMERS BASED ON NATURAL OIL AND GLYCEROL DERIVATIVES

Vilte Šereikaite[1], Aukse Navaruckiene[1], Aistis Lapinskas[1], Jolita Ostrauskaite[1]

[1]Department of Polymer Chemistry and Technology, Kaunas University of Technology, Radvilenu Rd. 19, LT-50254 Kaunas, Lithuania
vilte.sereikaite@ktu.edu

For more than fifty years, plastic materials have been the most practical and cost-effective choice for both commodity and specialty applications, thanks to their affordability, lightweight nature, corrosion resistance, wide availability, and excellent optical and mechanical properties [1]. The depletion of fossil fuels, along with rising environmental and economic concerns, has driven research toward renewable resource-based polymers with comparable or improved properties [2]. Photopolymerization is a light-induced process that initiates a chemical reaction, efficiently converting liquid resins into solid photopolymer forms, making it a promising and sustainable alternative for material transformation. This reaction is driven by photoinitiators within the resin, which absorb specific wavelengths of light and generate reactive species that start the polymerization process [3]. Photopolymerization is a fast, solvent-free process that minimizes volatile organic compound emissions and supports sustainability using renewable materials. It allows for precise spatial and temporal control, occurring only under light exposure and completing within seconds [4].

In this study, polymers were synthesized by the photopolymerization of resins containing natural oil-based monomers and glycerol-based comonomers, using ethyl-(2,4,6-trimethylbenzoyl)-phenylphosphinate as the photoinitiator.

Using real-time photorheometry, the photocuring process was monitored, revealing the photocuring rate and the effect of monomer content on the resin's properties. The chemical structure of the photopolymers was confirmed by Fourier transform infrared spectroscopy, Soxhlet extraction, and swelling tests. The mechanical properties of the photopolymers were investigated by tensile and compression tests. Fig. 1a illustrates the tensile test characteristics as a function of monomer content in the VS samples. This indicates that both the values of Young's modulus and tensile strength decrease as the monomer content increases, while elongation at break increases. Fig. 1b presents the relationship between the compressive Young's modulus and monomer content, showing a decrease in the values of Young's modulus with higher monomer fragment content.

Results showed that variations in the initial resin composition affected the photocuring rate as well as the rheological and mechanical properties of the photopolymers.

Acknowledgement. This research was funded by the Research Council of Lithuania (project No. S-MIP-23-52).

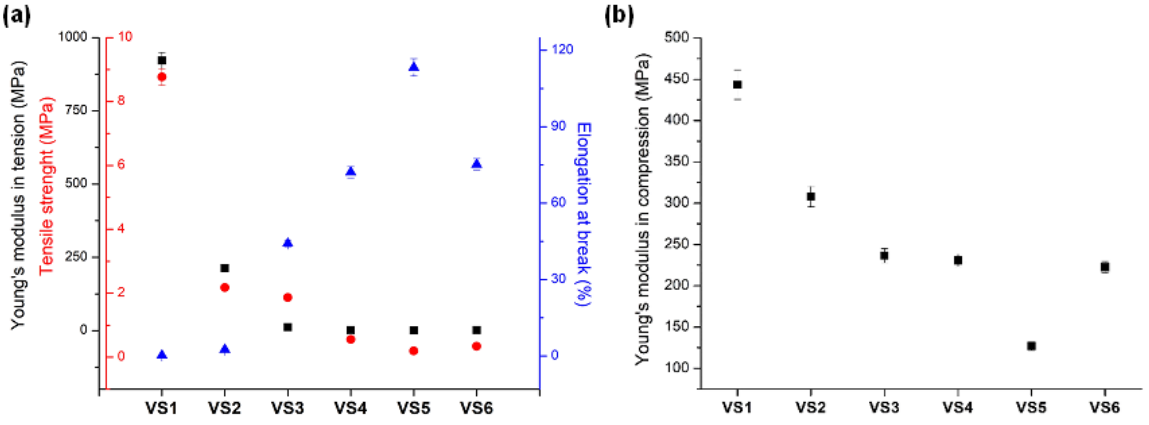


Fig. 1. Mechanical characteristics of polymers VS: (a) Young's modulus in tension (MPa), tensile strength (MPa), elongation at break (%); (b) Young's modulus in compression (MPa).

[1] V. Marturano et al., "Recent advances in bio-based functional additives for polymers," Progress in Materials Science, vol. 139, p. 101186, Oct. 2023.
[2] H. Lai et al., "Renewable Photopolymers: Transformation of Biomass Resources into Value-Added Products Under Light," ACS sustainable chemistry & engineering, vol. 11, no. 46, pp. 16365–16406, Nov. 2023.
[3] J. Xu, et al., "From Soft Lithography to 3D Printing: Current Status and Future of Microfluidic Device Fabrication," Polymers, vol. 17, no. 4, p. 455, Feb. 2025.
[4] N. Giacoletto et al., "Recent Advances in bis-Chalcone-Based Photoinitiators of Polymerization: From Mechanistic Investigations to Applications," Molecules, vol. 26, no. 11, pp. 3192–3192, May 2021.

ORGANIC DYES AS SELF-ASSEMBLED MONOLAYERS FOR PHOTOVOLTAIC DEVICES

Milda Žitinevičiūtė[1], Matas Steponaitis[2]

[1]The Department of Organic Chemistry, Kaunas University of Technology, Lithuania
milda.zitineviciute@ktu.edu

As the global temperature rises, we are approaching tipping points, beyond which the Earth's climate factors can begin to irreversibly decay. This is one of the reasons why renewable energy is rapidly evolving. According to the recent data, solar and wind energy is being developed five times faster than other (hydro, nuclear, hydrogen, etc.) green energy sources combined. Market research suggests that the sun as a sustainable source for electricity is one of the most practical ways for tackling climate change[1].

Perovskite solar cells (PSCs), with their high efficiency and low-cost production are increasingly attracting the attention of researchers and potential manufacturers. PSCs are undergoing rapid development and continue to impress with efficiencies as high as 26% [2]. PSCs still have long term stability issues, however some progress was achieved when self-assembled monolayers were introduced into the structure of PSCs to passivate surface defects that occur between perovskite and metal oxide layers.

Organic dyes have a high potential to be used as self-assembled monolayers. Due to the rich chemistry of dyes, extended π-conjugation system and the ability to strongly bind to the metal oxide, the dyes can be used as stability enhancing materials for perovskite solar cells. With proper optimization of dyes and their functional groups these organic compounds could theoretically act as either electron or hole transporting materials depending on the device configuration. In this work we synthesized and studied triphenylamine based materials that could be applied as charge transporting monolayers for the application in perovskite solar cells.

[1] R. Rüther and A. Blakers. The Fastest Energy Change in History Continues.
[2] H. Chen, et al. Improved charge extraction in inverted perovskite solar cells with dual-site-binding ligands. (Science. New York, 2024)

ELECTROCHEMICAL BEHAVIOUR OF ZIRCONIUM THIN FILMS ON STAINLESS STEEL IN HER

R. Jurgelionytė[1], I. Barauskienė[1,2], G. Laukaitis[2], E. Valatka[1]

[1]Department of Physical and Inorganic Chemistry, Kaunas University of Technology, Lithuania
[2]Department of Physics, Kaunas University of Technology, Lithuania
rugile.jurgelionyte@ktu.lt

With increasing hydrogen demand the ways for carbon-free hydrogen production is sought. In the transition to a net zero emissions energy system, the demand for hydrogen produced from fossil fuels will be replaced by the need for low-emissions hydrogen [1]. In addition, hydrogen energy can be used to generate and store energy and to deal with the intermittent nature of renewable energy sources [2].

A stable and efficient electrocatalyst is required for production of green hydrogen. At this background, transition metal nitrides have raised lots of attention. Their physical properties are similar to those of metallic elements. The inner nitrogens can increase the electron density of d-bands of transition metals, so that the electronic structures of these materials are similar with some precious metals, whose density of states can cross the Fermi level. Therefore, transition metal nitrides have similar conductivities with metals and possess superior electrocatalytic performance. Nanostructured TMNs tend to have relatively large dispersion and more exposed active sites, which have direct improvement for catalytic activity and stability as electrochemical catalysts. [3]. Metallic bonds influence that material have small electrical resistivities and high corrosion resistivity. Covalent bonds influence materials high stress tolerance which gives material high hardness. Ionic bonds points to similar electronic structure to precious metals like Pt and Pd due to contraction of metal d-bands and an expansion of the parent metal lattice [4]. These parameters show high potential for water electrolysis.

The purpose of this work was to synthesize ZrN thin films on AISI 304 type stainless steel, study their structure and electrochemical activity in hydrogen evolution reaction (HER).

Thin films of ZrN were deposited by pulse direct current magnetron sputtering. This method has proved to be fast and efficient way to obtain ZrN coatings of desired thickness of about 250 nm. Coatings were deposited from ZrN target at different conditions by varying the ratio of Ar/N2 in gas atmosphere and applying 200-350 W power. The characterization of prepared electrocatalyst samples was done by scanning electron microscopy and energy-dispersive X-ray spectroscopy (SEM-EDX), Raman spectroscopy, X-ray diffraction spectroscopy, profilometry, and UV-vis spectroscopy. All electrochemical measurements (cyclic voltammetry, chronoamperometry, chronopotentiometry) were performed in 0.1 M KOH electrolyte in a three electrode cell consisting of ZrN/stainless steel substrate as working electrode, Ag,AgCl|KCl(sat) as a reference electrode, and Pt wire as a counter electrode. The experimental results showed that ZrN/stainless steel electrodes are highly stable and active electrocatalysts for hydrogen evolution reaction. Tafel analysis was performed to provide insights into HER mechanism and to evaluate the influence of synthesis conditions on electrocatalytic activity of ZrN thin films.

[1] Global Hydrogen review 2024, International Energy Agency, 2024.
[2] G. AlZohbi. An Overview of Hydrogen Energy Generation. ChemEngineering 8(1), 17. 2024
[3] L. Lin , S. Piao, Y. Choi, L. Lyu, H. Hong, D. Kim, J. Lee, W. Zhang, Y. Piao. Nanostructured Transition Metal Nitrides as Emerging Electrocatalysts for Water Electrolysis: Status and Challenges. EnergyChem Volume 4, Issue 2. 100072. 2022.
[4] J.-P. Glauber, J. Lorenz, J. Liu, B. Müller, S. Bragulla, A. Kostka, D. Rogalla, M. Wark, M. Nolan, C. Harms, A. Devi. A sustainable CVD approach for ZrN as a potential catalyst for nitrogen reduction reaction. Dalton Trans., 53, 15451-15464, 2024.

SYNTHESIS AND INVESTIGATION OF SELF-ASSEMBLED MONOLAYER BENZIMIDAZOLE DERIVATIVES

Gabija Linkaitė[1], dr. Mantas Marčinskas[1]

[1]Kaunas University of Technology
gabija.linkaite@ktu.edu

For over a decade, a large number of researchers have been investigated organic and inorganic perovskites as potential materials for next-generation solar cells. In order to achieve a higher theoretical efficiency and possibly lower the negative attitude of the community towards the usage of lead, during that period scientists started to look into a Pb-less of even Pb-free perovskite materials, which could possess an ideal bandgap in a range of 1.1 to 1.3 eV.

So far, Sn-Pb (1:1) mixed perovskite is one of a few currently existing alternatives, that can be comparable to the regular Pb-based perovskites. Additionally, due to the possible bandgap of 1.25 eV of Sn–Pb perovskites, the development of perovskite/perovskite tandem solar cells was made possible. However, when fully replacing lead and having only Sn^{2+} in the perovskite crystal structure, a number of disadvantages occurs, such as more susceptible surface characteristics, inhomogeneous thin film morphologies, and easy Sn^{2+} oxidation [1]. A number of advancements in surface treatments, precursor design, compositional design, and structural optimization have been done so far, but as the efficiency record of Pb-free PSCs lags behind of Pb-based solar cells (14.81% and 27%, respectively [2]), there is still much more room for further improvement.

Self-assembling monolayer forming compounds have contributed significantly to the development of p-i-n architecture PSCs by increasing the efficiency and stability of the devices. However, when Sn is introduced into the perovskite system, SAMs, which have been found to work optimally in Pb-based perovskites, do not exhibit equally good performance. In succession, carbazole-based SAM material ($BrNH_3$-4PACz) containing ionic groups demonstrated high performance in Pb-Sn mixed PSC because of well-matched energetic alignment between the Pb-Sn perovskite and ITO/$BrNH_3$-4PACz, and perovskite passivation at the buried interface [3]. According to these results, ionic self-assembled monolayers show promising potential for Pb-Sn-mixed PSCs, furthermore, ionic SAMs have the potential to be suitable in lead-free perovskites development.

In this work, we have synthesized and investigated self-assembled monolayer-forming benzimidazole ionic compounds that can be used to construct Sn-based perovskite solar cells.

[1] S. Zhumagali et al., “Efficient Narrow Bandgap Pb-Sn Perovskite Solar Cells Through Self-Assembled Hole Transport Layer with Ionic Head,” Jan. 2025, doi: 10.1002/aenm.202404617.
[2] “Best Research-Cell Efficiency Chart.” Accessed: Feb. 15, 2025. [Online]. Available: https://www.nrel.gov/pv/cell-efficiency.html
[3] H. L. Kim Seok Beom Kang, Sangwook Lee, Kai Zhu, Dong Hoe, “Progress and outlook of Sn–Pb mixed perovskite solar cells,” vol. 5, no. 2, pp. 370–400, 2023, doi: https://doi.org/10.1002/eem2.12211.

FACILE AND LOW-COST DESIGN ALTERNATIVE OF SPIRO-OMETAD AS SEMICONDUCTOR FOR EFFICIENT PEROVSKITE SOLAR CELLS

Šarūnė Daškevičiūtė[1], Yi Zhang[2], Kasparas Rakštys[1], Marytė Daškevičienė[1], Vygintas Jankauskas[3], Mohammad Khaja Nazeeruddin[2], Vytautas Getautis[1]

[1]Department of Organic Chemistry, Kaunas University of Technology, Lithuania
[2]Group for Molecular Engineering of Functional Material, École Polytechnique Fédérale de Lausanne, Switzerland
[3]Institute of Chemical Physics, Vilnius University, Lithuania
sarune.daskeviciute@ktu.lt

Over the recent years, organic-inorganic hybrid perovskite solar cells (PSCs) have been attracting a massive worldwide attention due to their low cost and facile fabrication. HTM is one of the quintessential components required for the efficient and stable PSC devices. The hunt is now on for new organic semiconductors that are prepared by simple, cost-effective, and green chemistry without sacrificing the efficiency [1].

Recently, our research group has focused on tuning the structure by decreasing the number of synthetic steps, thus reducing the synthetic complexity, cost of materials and the environmental impact. This includes reports based on carbazole and fluorene enamines prepared by a facile condensation reaction. In this sense, condensation chemistry is an excellent perspective moving away from palladium-catalyzed reactions since water is the only byproduct and expensive catalysts are not required. Commercially available 3,6-diaminocarbazole (204 Eur/g[2]) and 2,7-diaminofluorene (55 Eur/g[3]) materials were used as starting materials as shown in Figure 1. Those enamines have been successfully applied in PSCs with and without additives, showing excellent efficiency and long-term stability.[4-5]

In this work, we have further explored the potential of enamine HTM family employing 4,4'-diaminodiphenylamine as the central core shown in Figure 1. Two diphenylamine-based HTMs were designed and synthesized from extremely low-cost commercially available 4,4'-diaminodiphenyl amine sulfate hydrate (1.5 Eur/g[6]) condensing with corresponding aldehydes without the use of addition of a catalyst. Their optical, thermal, and electrophysical properties were thoroughly investigated. HTMs V1553 and V1565 were amorphous, thermally stable and showed high hole-drift mobility. The PSC based on the semiconductor V1553 reached the highest power conversion efficiency of almost 23%, which is higher than that of the Spiro-OMeTAD-based device under identical conditions.

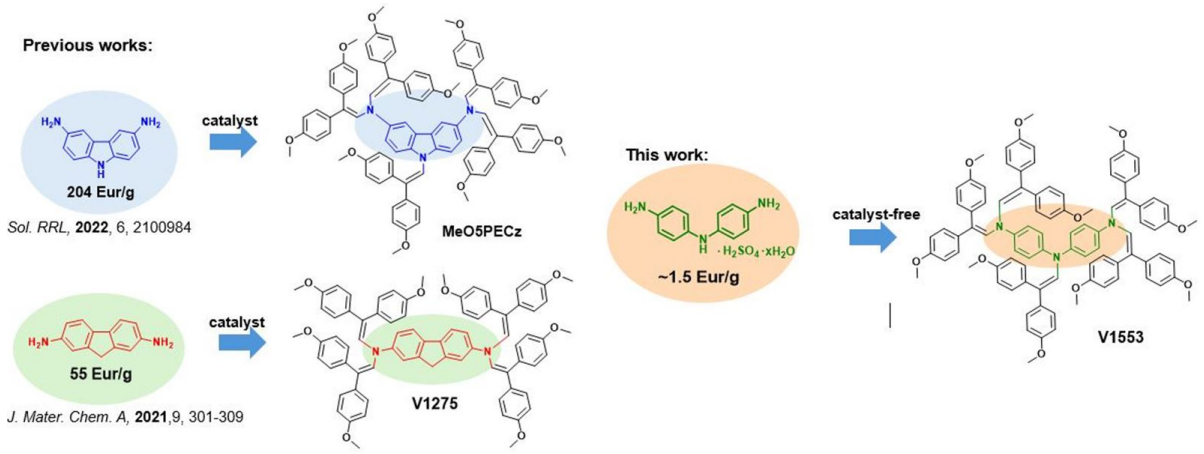


Fig. 1. Design concept comparing previous enamine works with this work.

[1] M. L. Petrus, A. Music, A. C. Closs, J. C. Bijleveld, M. T. Sirtl, Y. Hu, T. J. Dingemans, T. Bein and P. Docampo, J. Mater. Chem. A, 5 (2017) 25200–25210.
[2] TCI Europe. https://www.tcichemicals.com/BE/en/p/D2116.
[3] TCI Europe. https://www.tcichemicals.com/BE/en/p/D0092.
[4] S. Zhou, M. Daskeviciene, M. Steponaitis, G. Bubniene, V. Jankauskas and et. al. Sol. RRL, 6 (2022), 2100984.
[5] S. Daskeviciute; C. Momblona; K. Rakstys; A. A. Sutanto; M. Daskeviciene and et. al J. Mater. Chem. A, 9 (2021) 301–309.
[6] TCI Europe. https://www.tcichemicals.com/BE/en/p/D0041.

BRANCHEDFLUORENYLIDENE DERIVATIVES WITH LOW IONIZATION POTENTIALS AS HOLE-TRANSPORTINGMATERIALS FOR PEROVSKITE SOLAR CELLS

Aistė Jegorovė[1], Jianxing Xia[2], Matas Steponaitis[1], Marytė Daškevičienė[1], Vygintas Jankauskas[3], Alytis Gruodis[3], Egidijus Kamarauskas[3], Mohammad Khaja Nazeeruddin[2], Vytautas Getautis[1]

[1]Department of Organic Chemistry, Kaunas University of Technology, Lithuania
[2]Group for Molecular Engineering of Functional Material, Institute of Chemical Sciences and Engineering, École Polytechnique Fédérale de Lausanne, Switzerland.
[3]Institute of Chemical Physics, Vilnius University, Lithuania
aisilc@ktu.lt

Today, everyday appliances have become an essential part of life, with most of them relying on electricity to function. One of the primary methods of generating electricity is through non-renewable energy sources. However, these sources have significant drawbacks, as their byproducts are often non-biodegradable and can harm the environment. As a result, researchers have been exploring alternative energy generation methods using renewable sources such as wind, solar, and hydropower. Among these, the Sun is considered the most powerful energy source. Solar cells are devices that convert sunlight into electricity, with silicon-based solar cells being the most widely used technology. However, they come with limitations, leading to the development of more efficient alternatives. The evaluation of perovskite solar cell evaluation began more than ten years ago; nevertheless, expensive semiconductors, such as Spiro-OMeTAD are still used as a benchmark for hole-transporting layers. Studies have shown that adopting a similar molecular design can lead to good results in both efficiency and stability. [1,2] There are two main strategies developing materials similar to Spiro-OMeTAD: (1) using spirobifluorene as a central fragment while replacing 4-methoxyphenyl chromophores [3, 4], or (2) mimicking the Spiro-OMeTAD core by carefully selecting central fragments [5, 6]. The first method is generally considered as more reliable, simpler, and more successful in achieving high device performance. However, the second approach has also gained popularity due to its potential to produce more cost-effective and stable compounds. Based on previous study [7], it has been observed that the proper number of carbazolyl fragments can, in some cases, enhance device stability. Therefore, 9-ethyl-N-(4-methoxyphenyl)-9H-carbazol-3-amine was chosen as a side chromophore. In order to maintain similarity to Spiro-OMeTAD, fluorenylidene fragments were introduced into the molecular ”central part” and linked through various aromatic moieties. In this work we synthesized new hole transporting materials that can be divided into two groups: molecules containing two fluorenylidene fragments, and compounds with three fluorenylidene moieties. Thermal and photoelectric properties were investigated and compared with Spiro-OMeTAD. All synthesized hole- transporting materials (HTMs) exhibit good thermal stability. In this study, no additional phase transitions were detected, confirming the complete amorphous nature of the materials. Consequently, these materials are likely to produce high-quality layers. The branched structure compounds were utilized as HTM layer in n-i-p architecture solar cells. The PCE of the most efficient n-i-p PSCs perovskite device containing carbazolyl-terminated Spiro-OMeTAD analogue V1387 has reached 22.13 %. Furthermore, solar cell containing V1387 exhibits good long-term stability and outperforms the device with Spiro-OMeTAD.

Acknowledgements

The project ”Technological and Physical Sciences Excellence Centre (TiFEC)” No. S-A-UEI-23-1 is funded by the Science Council of Lithuania and the Ministry of Education, Science and Sports of the Republic of Lithuania from the state budget under the programme ”University Excellence Initiative”.

[1] XU, Bo; ZHU, Zonglong; ZHANG, Jinbao; LIU, Hongbin; CHUEH. Advanced Energy Materials, vol. 7, nr. 19, pp. 1700683, (2017).
[2] SALIBA, Michael; ORLANDI, Simonetta; MATSUI, Taisuke; AGHAZADA, Sadig; CAVAZZINI, Marco et al. Nature Energy, vol. 1, nr. 2, pp. 15017, (2016).
[3] JEON, Nam Joong; NA, Hyejin; JUNG, Eui Hyuk; YANG, Tae-Youl; LEE, Yong Guk et al. Nature Energy, vol. 3, nr. 8, pp. 682–689, (2018).
[4] JEONG, Mingyu; CHOI, In Woo; YIM, Kanghoon; JEONG, Seonghun; KIM, Minjin et al. Nature Photonics, vol. 16, nr. 2, pp. 119–125, (2022).
[5] RAKSTYS, Kasparas; SALIBA, Michael; GAO, Peng; GRATIA, Paul; KAMARAUSKAS, Egidijus et al. Angewandte Chemie International Edition, vol. 55, nr. 26, pp. 7464–7468, (2016).
[6] RAKSTYS, Kasparas; PAEK, Sanghyun; DREVILKAUSKAITE, Aida; KANDA, Hiroyuki; DASKEVICIUTE, Sarune et al. ACS Applied Materials & Interfaces, vol. 12, nr. 17, pp. 19710–19717, (2020).
[7] JEGOROVĖ, Aistė; MOMBLONA, Cristina; DAŠKEVIČIENĖ, Marytė; MAGOMEDOV, Artiom; DEGUTYTE, Rimgaile ir kt. Solar RRL, vol. 6, nr. 6, pp. 2100990, (2022).

NOTES

NOTES

NOTES

NOTES

NOTES

NOTES

NOTES

NOTES

ORGANIZERS

Faculty of Physics

CENTER FOR PHYSICAL SCIENCES AND TECHNOLOGY

OPTICA Advancing Optics and Photonics Worldwide | STUDENT CHAPTER VILNIUS UNIVERSITY

SPIE. STUDENT CHAPTER VILNIUS UNIVERSITY

EPS Young Minds

SPONSORS

LIGHT CONVERSION

BROLIS

THORLABS

esa BUSINESS INCUBATION CENTRE Lithuania operated by VITP

Toolas

Lithuanian Consortium for Particle Physics

astralight

OPTOMAN

standa

EKSMA OPTICS

LIDARIS LIDT Service

Altechna

DMC Direct Machining Control

OPTOGAMA

MONO SPEKTRA

EVENT FRIEND

Go Vilnius

MEDIA PARTNER

LRT.lt